2.005

Course Notes

Fall 2008

Test 1 Study
Buoyancy / Stability

THERMAL-FLUIDS ENGINEERING

An Integrated Approach to Thermodynamics, Fluid Mechanics, and Heat Transfer

By

Ernest G. Cravalho

Joseph L. Smith, Jr.

John G. Brisson II

Gareth H. McKinley

Department of Mechanical Engineering
Massachusetts Institute of Technology
Cambridge, Massachusetts
02139

MIT/PAPPALARDO SERIES IN MECHANICAL ENGINEERING

Oxford University Press

Acknowledgment

The authors would like to acknowledge Professors Nam P. Suh and Rohan Abeyaratne for their unwavering support and encouragement in this ambitious undertaking. There were many times when it appeared that the odds were against this project ever happening, but Nam and Rohan have done all the right things to make it a reality.

The authors would especially like to thank Neil and Jane Pappalardo who made all this possible. Their commitment to the Department of Mechanical Engineering at MIT, and to this project in particular, has made an enormous positive impact on the education of a new generation of engineers. Because of their support, we can all be confident that the technological future of our society will be in good and knowledgeable hands.

PREFACE

Thermal-fluid systems are amongst the most complicated systems engineers encounter in the practice of the profession. For a variety of reasons, these thermal-fluid systems utilize fluids as the working medium with energy and entropy transfers between the fluid and the surrounding environment occurring by both work transfer and heat transfer processes. System complexity derives largely from the coupling that exists between the thermal and mechanical aspects of system behavior. Since the thermal and mechanical aspects of system behavior cannot be separated in general, more independent parameters are necessary to describe these systems with a concomitant increase in the number of relevant physical phenomena that must be taken into account. In addition, the constitutive relations between these parameters are often non-linear which in some cases leads to system behavior that is counterintuitive.

In the traditional mechanical engineering curriculum, the study of thermal-fluid systems is compartmentalized into three separate subject areas: (1) *thermodynamics* in which we study the basic laws that govern energy and entropy transfers and the ways in these interactions manifest themselves in system behavior; (2) *fluid mechanics* in which we study the complex dynamic behavior of the working fluids that are used as the media to transport energy and entropy from one part of the system to another; and (3) *heat transfer* in which we study the complex physical processes involved in the transport of energy and entropy in these systems.

While this separation of subject matter into three distinct areas of study may be pedagogically convenient, it is not pedagogically sound since it can create the mistaken impression that the design and analysis of thermal-fluid systems can be similarly subdivided. To the contrary, the thermodynamic, fluid dynamic, and heat transfer aspects of thermal-fluid systems are inextricably interconnected. In addition, this artificial separation of the subject matter fails to capitalize on the opportunity to synthesize the material in a way that can lead to improved understanding of the subject matter and superior engineering design of these systems. Furthermore, in the traditional approach, the integration of the subject matter is left ultimately to the student which can be problematical for the beginner.

For these reasons, the faculty of the Department of Mechanical Engineering at MIT have decided to integrate the material of these three subject areas into a single year-long subject. This is not to say that this single subject provides a comprehensive treatment of these subjects in exhaustive detail that would preclude further study in concentrated areas. Rather, the objective is to provide a thorough understanding of thermodynamics, fluid mechanics, and heat transfer at a fundamental, but integrated level that would facilitate sound engineering design and analysis of thermal-fluid systems and point the way to further study and research in these systems.

The specific objectives of this integrated subject are:

(1) To develop the fundamental principles and laws of thermodynamics, fluid mechanics, and heat transfer and the implications of these principles for system behavior.

(2) To formulate the models necessary to study, analyze, and design thermal-fluid systems through the application of these principles.

(3) To develop the problem solving skills essential to good engineering practice in the thermal-fluid systems area.

(4) To develop an understanding of sound engineering design of thermal-fluid systems.

The text material that follows represents an attempt by a small group of faculty to present an organized, integrated approach to the study of thermal-fluids engineering that will exploit the integrated nature of the subject matter as described above. Clearly, in many instances, some elements of the material are necessarily compartmentalized, but in the end that compartmentalization is relaxed as those elements are integrated into the treatment as a whole.

The development of this material has benefitted from the consideration and suggestions from a large group of faculty and many students who have studied this subject matter with the present treatment as a guide. However, in the final analysis, any errors in fact or misdirections in the approach are the sole responsibility of the authors.

TABLE OF CONTENTS

Chapter 9 Viscosity and the Transfer of Momentum in a Fluid

CHAPTER 1

Thermal-Fluids Engineering: A Modern Technology

1.1 Historical Background

Thermal-fluids engineering is that branch of engineering focused on the utilization and deployment of energy resources to produce the goods and services of modern society. The thermal-fluids engineer is particularly concerned with the conversion of energy from one form to another in the most efficient manner practical, usually through the use of a fluid medium. Of necessity, the practice of thermal-fluids engineering draws heavily upon the scientific disciplines of thermodynamics, heat transfer, and fluid mechanics to design, analyze, build, and test the devices that convert or distribute these precious energy resources. Although the terminology "thermal-fluids engineer" is relatively new, individuals engaged in the practice of what we now call thermal-fluids engineering have played an important historical role in the technological advancement of society and will continue to play an even more important role in the future.

While we have come to take for granted the many goods and services that define our modern society, we need look back only a scant 250 years to see the technological developments that have led to our present state. Most historians place the beginning of the industrial revolution at about the year 1750 -- a relatively recent time in the history of the world as we know it. This movement, which persists to this day, is comprised of technological, socioeconomic, and cultural changes that have formed the basis of modern society, but it is the technological changes that are of particular interest to us as engineers. Those advancements regarded as important components of the movement include, among others: (1) the use of new energy sources in the form of fuels, such as coal, natural gas, and petroleum; (2) the development of new energy conversion technologies that utilize these fuels, such as the steam engine, the internal combustion engine, and the "generation" of electricity; (3) the invention of the new methods and machines of manufacturing that have reduced the need for human power while at the same time increasing productivity; and (4) advances in transportation and communication, such as the steam locomotive, steamship, automobile, airplane, telegraph, radio, television, and the Internet. Clearly, most of these advancements were the work of thermal-fluids engineers.

1.2 Modern Thermal-Fluids Engineering

The thermal-fluids engineer is concerned primarily with the mechanical and thermal behavior of matter and the ways in which this behavior can be exploited for the benefit of society. The physical situations of interest to the modern thermal-fluids engineer are many and varied and encompass a huge spectrum of human endeavor. In some applications, the thermal-fluids engineer is concerned only with a single component of a larger, more complex situation. For example, computer technology is constantly seeking ways of increasing the speed of the CPU, the central processing unit that performs the actual operations that constitute computing *per se*. These operations are based on the charged or discharged state of an electrical capacitor that forms the basis of the binary number system (0 or 1) of the computer language. However, each time a capacitor discharges into another capacitor, half the electrical energy stored in the

original capacitor is converted into thermal energy and must be removed by means of thermal-fluids technology to keep the ensemble of capacitors from overheating. As computers increase in complexity, the number of capacitors (on the order of 10^7) increases. As the speed of computers increases, the number of times the capacitor changes state of charge per unit time increases. Thus the rate of energy dissipation has increased to the point that advancements in computer design are dependent upon the advancement of thermal-fluids engineering. For personal computers, the current state-of-the-art is a heat exchanger small enough to fit in the palm of one's hand but effective enough to enable personal computers to run at speeds on the order of 1 GHz (cf. Figure 1.1).

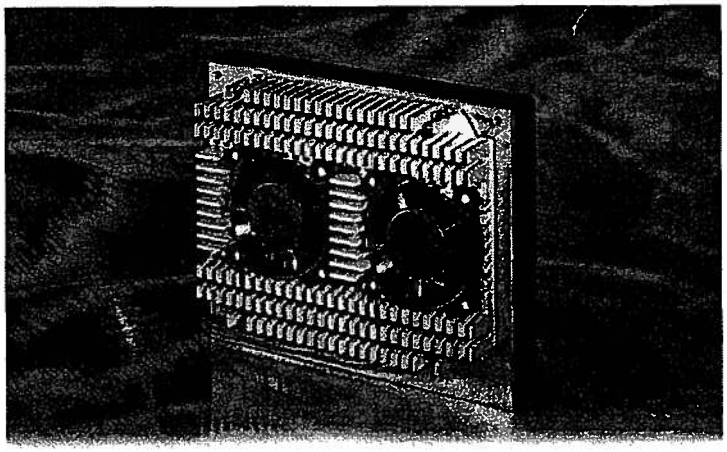

Figure 1.1 Fan-Heat Exchanger Assembly for Intel Xenon© CPU
(Courtesy of PC Power & Cooling, Inc.)

On the other hand, some applications are concerned with a more global perspective. Most energy conversion plants devoted to the conversion of fuel energy to electricity utilize fossil fuels in the form of coal, natural gas, or petroleum. The energy contained in these fuels is released in the form of a heat transfer by means of an oxidation reaction. Carbon dioxide is one of the products of the oxidation reaction. This inert gas is released into the atmosphere thereby increasing the concentration of carbon dioxide. Carbon dioxide gas is relatively transparent to the short wavelength radiation given off by the sun but opaque to the long wavelength thermal radiation emitted by the earth. The energy associated with long wavelength thermal radiation is then trapped in the earth's atmosphere. This is a phenomenon known as the "greenhouse effect" since the glass panes of a greenhouse function in precisely the same manner as gaseous carbon dioxide. The long wavelength thermal radiation trapped inside the greenhouse increases the temperature of the air inside the greenhouse. In a similar manner, the long wavelength thermal radiation trapped in the atmosphere causes an increase in the average temperature of the atmosphere, a phenomenon known as "global warming." In an attempt to reduce carbon dioxide emissions and thereby reduce global warming, thermal-fluids engineers have been developing power generation plants with high energy conversion efficiency. For a given electrical power output, these high efficiency power plants consume less fossil fuel and, therefore, produce less carbon dioxide. The plant currently in service with the highest energy conversion efficiency is the 2,000 MW plant built by General Electric for Korea Electric in Seioinchon, Korea (cf. Figure 1.2). This plant, which operates on a combined Brayton cycle - Rankine cycle, has an energy conversion efficiency in excess of 55 percent.

Figure 1.2 Combined Brayton-Rankine Cycle 2,000 MW Power Plant
Korea Electric Power, Seioinchon, Korea
(Photo courtesy General Electric, Inc.)

In search of ways to reduce the emission of carbon dioxide still further, thermal-fluid engineers have harnessed the energy available in geothermal sources such as geysers. Geysers such as the Old Faithful Geyser located in Napa, California, (cf. Figure 1.3) regularly spout high temperature

Figure 1.3 Old Faithful Geyser of California
(Photo courtesy of Old Faithful Geyser, Calistoga, California.)

(200 C) water and steam tens of meters into the atmosphere. The water and steam originates in reservoirs hundreds of meters below the surface of the earth. By tapping into these reservoirs, thermal-fluid engineers have been able to convert this naturally available geothermal energy into electricity by using plants of the type shown schematically in Figure 1.4. This design

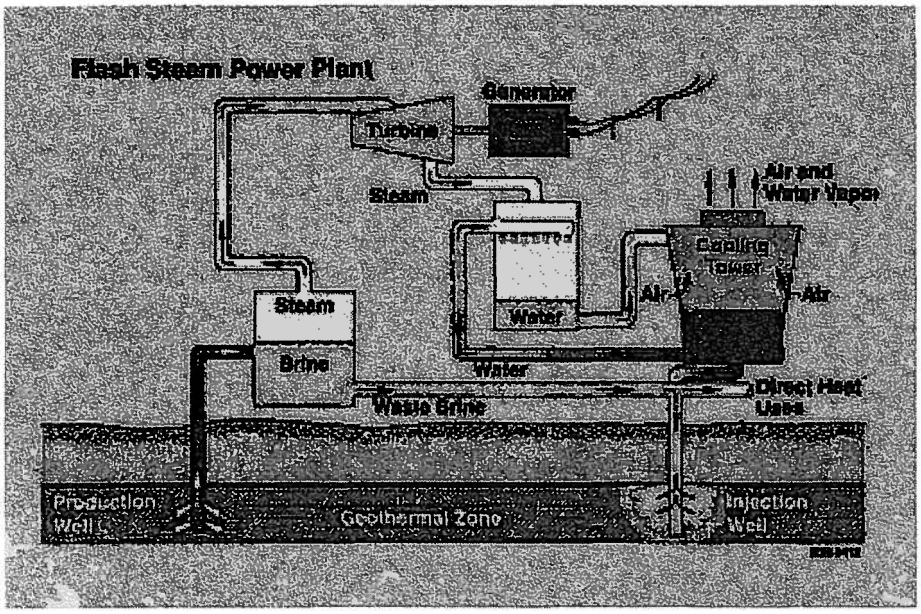

Figure 1.4 Schematic Representation of Geothermal Flash Steam Power Plant
(Diagram courtesy U.S. Department of Energy.)

accomplishes the energy conversion process while producing little or no carbon dioxide. The geyser shown in Figure 1.3 lies in a geographical area that is rich in utilizable geothermal energy.

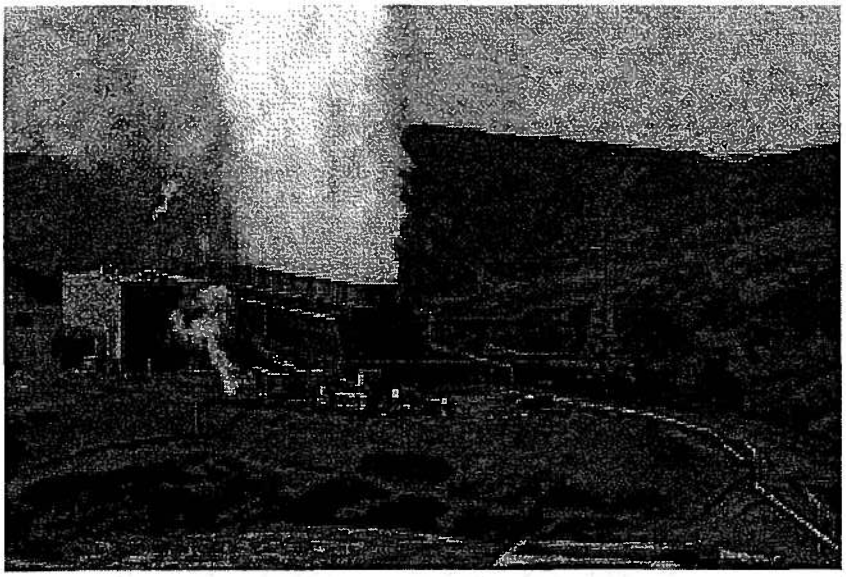

Figure 1.5 Geothermal Power Plant, The Geysers, California
(Photo courtesy of Pacific Gas & Electric Co.)

It is the only steam field that is commercially developed in the United States at the present time (cf. Figure 1.5) and is the largest single source of geothermal power in the world. However, in spite of this impressive display of environmentally sound thermal-fluids engineering, only 2,700 MW of electric power are produced from geothermal sources in the United States each year. This is equivalent to the capacity of a single combined cycle plant of the type described earlier. Unfortunately, geothermal plants suffer from several economic and technical deficiencies that limit their deployment. For example, there is no flexibility with respect to their location since they must be located where the underground geothermal deposits can be found. In addition, the steam produced in these geothermal wells is relatively low in temperature and pressure which reduces the amount of work transfer that can be realized from them. Often these deficiencies are overshadowed by the environmental benefits geothermal sources possess and the fact that they produce power that is approximately one-third the cost to the consumer of that produced from conventional fossil fuel sources. According to present estimates by The U.S. Department of Energy, the geothermal resource base in the United States is approximately 1.5 million quads of thermal energy (cf. Appendix, Chapter 2).

Thermal-fluids engineers play important roles in many other industries as well. For example, in the aircraft industry thermal-fluids engineers are responsible for designing the aerodynamic characteristics of aircraft such as the Boeing 777-300 (cf. Figure 1.6) which is capable of carrying up to 450 passengers a distance of 10,370 km (6,450 miles) while others are

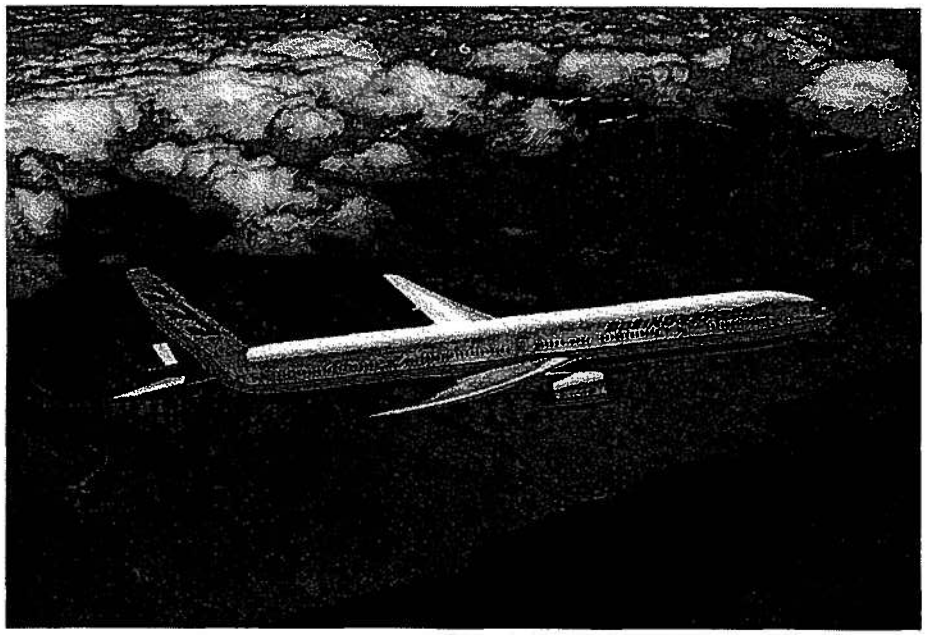

Figure 1.6 Boeing 777-300 Commercial Aircraft
(Photo courtesy of Boeing Aircraft Company, Inc.)

responsible for developing the powerplants (cf. Figures 1.7 and 1.8) that will generate up to 4.36 x 10^5 N (98,000 lbf) of thrust that will accelerate the fully loaded (3 x 10^5 kg) 777-300 to take off speed.

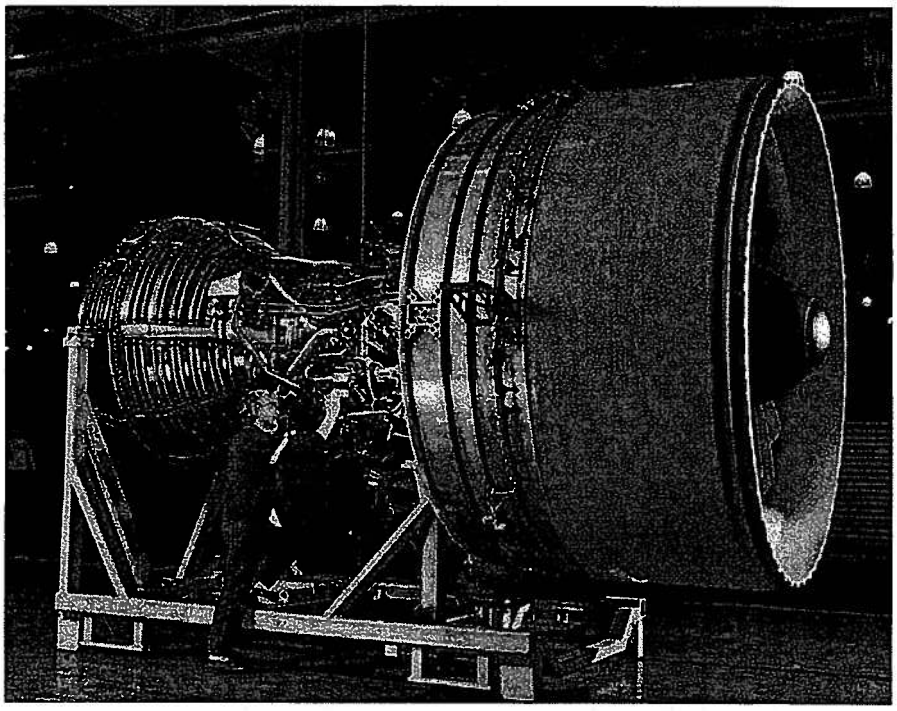

Figure 1.7 Pratt and Whitney PW4000 (112 inch) Turbofan Engine on the Assembly Stand
(Photo courtesy of Pratt and Whitney Division, United Technologies, Inc.)

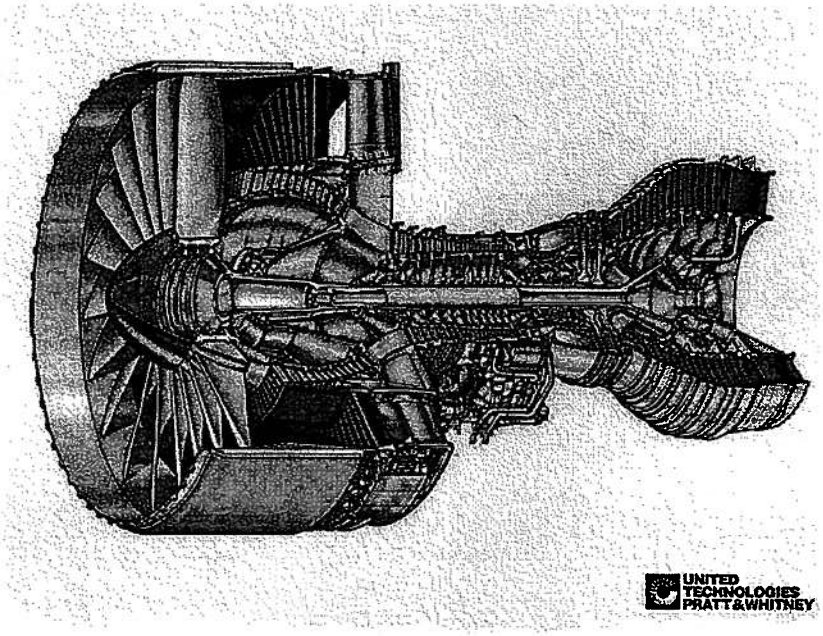

Figure 1.8 Cutaway View of the PW4000 Showing Fan, Compressor, Turbine, and Nozzle
(Photo courtesy of Pratt and Whitney Division, United Technologies, Inc.)

The transportation sector of the economy offers many other opportunities for thermal-fluids engineers. For example, the aerodynamic design of the world's fastest commercial train, the *Train à Grande Vitesse* (TGV) (cf. Figure 1.9), was the work of thermal-fluids engineers in France. This train, which attained the world record speed of 515.47 km/hr (320.3 mi/hr), has a normal operating speed of 299.34 km/hr (186 mi/hr). Since the passenger carrying capability of the train far exceeds that of commercial aircraft designed for local service, the need for air transportation within France itself has been reduced significantly. If the TGV technology were coupled with the combined energy conversion technology developed by GE for Korea Electric and numerous other power plants currently under construction in the United States, a vastly more energy-efficient transportation network could be developed.

Figure 1.9 *Train à Grande Vitesse-Duplex* at Gare de Lyon in Paris
(Photo courtesy Manfred Kalivoda)

Although not the most efficient mode of transportation, certainly one of the most exciting is the top fuel dragster powered by a 4.48 MW (6,000 HP) nitromethane-burning internal combustion engine designed by thermal-fluids engineers. This power plant will accelerate a 1000 kg (2200 lbm) single-passenger vehicle from 0 to 160 km/hr (100 mi/hr) in 1 second (cf. Figure 1.10). While efficiency is not an objective in most racing vehicle designs, other aspects of vehicle performance and thermal-fluids technology have been transferred from racing vehicles to more conventional automotive applications.

As powerful as this vehicle might seem, it pales in comparison to the kind of power plants thermal-fluids engineers design for sea-going vessels. For example, the recently launched Voyager of the Sea, the largest passenger ship ever built at 311 m (1021 ft) in length, has a

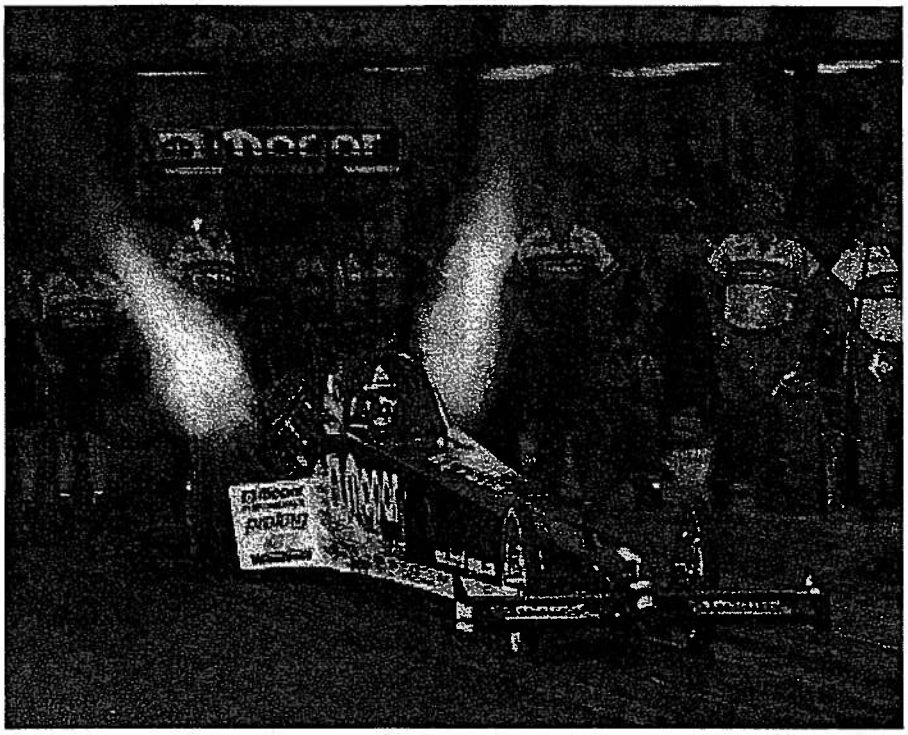

Figure 1.10 Darrell Gwyn's Top Fuel Dragster Driven by Mike Dunn
(Photo courtesy of Mike Dunn Racing.)

power plant rated at 75.6 MW (101,340 HP). A power plant of this size is necessary to not only provide propulsive power for the 142,000 ton ship but also to provide electric power for the many conveniences for the 3100 passengers and 1181 crew members, including an Olympic-size ice rink designed by thermal-fluids engineers (cf. Figure 1.11). Thermal-fluids engineers are also

Figure 1.11 Passenger Ship Voyager of the Seas
(Photo courtesy Kvaerner Masa-Yards, Finland.)

Responsible for designing the systems that maintain the hydrostatic stability of this vessel on the high seas as well as designing the hydrodynamic characteristics of the hull while the vessel is underway.

Thermal-fluids engineers have also led the development of alternative power plant design with the design and construction of nuclear power plants employed on military vessels such as the Nimitz-class aircraft carriers of the U.S. Navy. As shown in Figure 1.12, nuclear

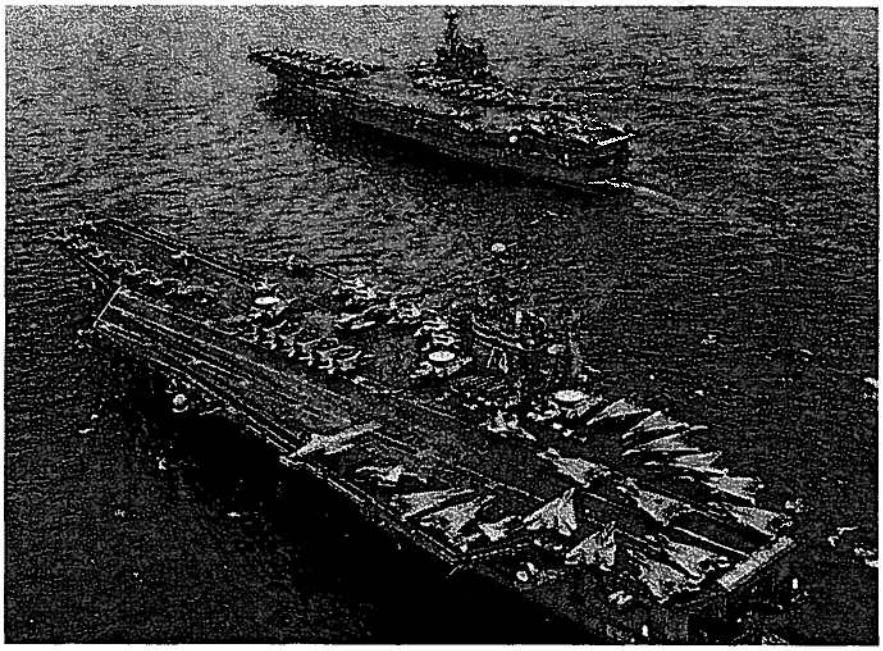

Figure 1.12 US Aircraft Carriers *USS John C. Stennis* (foreground) and *USS Independence* (Photo courtesy of United States Navy.)

power plants eliminate the need for an exhaust stack (Compare the much larger nuclear powered USS *John C. Stennis*, CVN 74, in the foreground with the smaller oil powered USS *Independence*, CV 62, in the background.), but perhaps more importantly, the nuclear powered vessels can go as long as 30 years without refueling, an advantage that is even more important in submarines. These supercarriers also are filled with examples of thermal-fluids engineering ranging from hull hydrostatics and hydrodynamics to steam catapult design to the air conditioning of living spaces for the 6,200 crew members.

Finally, the work of thermal-fluids engineers is not bound by the planet we inhabit. Thermal-fluid engineers design the rocket engines that put astronauts and satellites into space (cf. Figure 1.13) as well as the thermal control systems of the vehicles and the space stations themselves (cf. Figure 1.14).

1.3 The Armamentarium of the Thermal-Fluids Engineer

Whatever the physical situation, whatever the application, wherever it may be located, the thermal-fluids engineer has a very powerful armamentarium that can be brought to bear on the

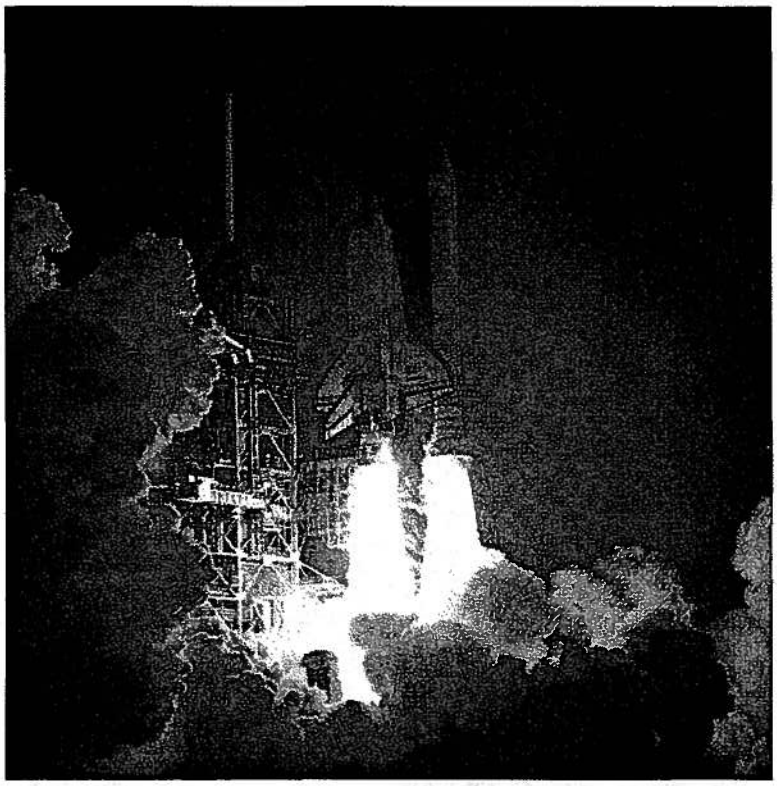

Figure 1.13 Lift-off of Space Shuttle *Discovery*, May 27, 1999
(Photo courtesy of NASA.)

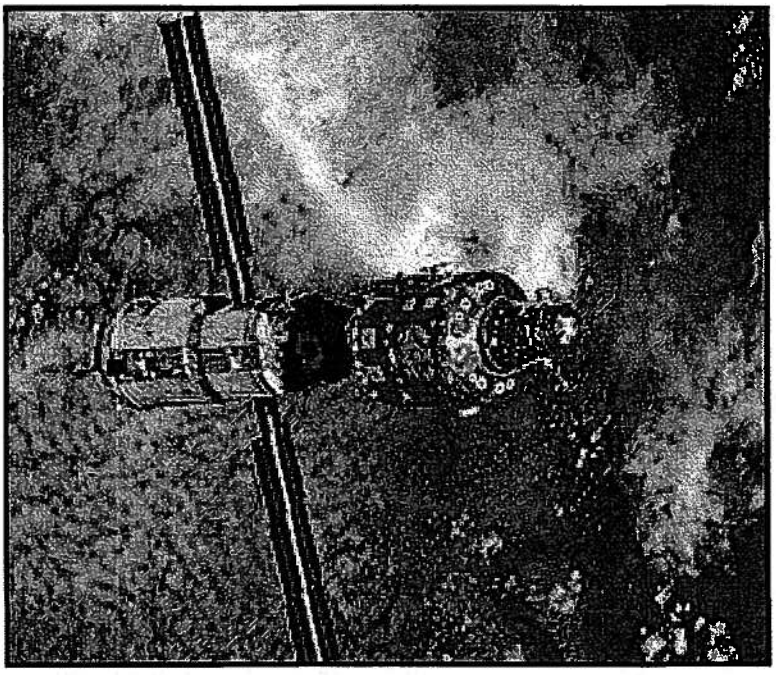

Figure 1.14 International Space Station as Seen from *Discovery*
(Photo courtesy of NASA.)

technical challenges at hand. The tools that comprise this armamentarium are manifold, but derive principally from a rather small but broad set of fundamental principles. Typically, these principles, which we will preview here, are cast in the form of a set of equations that describe the behavior of thermal-fluid *systems*[1] in mathematical terms. The desired information about the physical situation can then be obtained by applying these principles to the situation with the aid of *models* that are idealizations of the relationship amongst the *properties* necessary to describe the *state* of the system.

Not all physical situations require the application of all of these principles, and the forms that these fundamental principles take may vary depending upon the nature of the system under study. Typically, the systems of interest to the thermal-fluid engineer fall into three general categories listed here:

1. **Closed systems** in which the quantity of matter contained within the system *boundary* is fixed for all time.
2. **Open systems** in which matter is allowed to flow across the system boundary.
3. **Cyclic systems** in which the matter contained within the system boundary is subjected to a series of *processes* that produce no net change in the state of the matter but do result in interactions between the system and the *environment*.

The fundamental principles themselves (to be discussed in great detail in subsequent chapters) are essentially a set of phenomenological laws based upon the observation of many physical situations, and they also can be divided into three groups:

1. Those principles that are primarily mechanical in nature:
   a. **Conservation of Mass** that relates the rate of change of mass within the system boundary to the flow of mass into and out of the system across the system boundary.
   b. **Conservation of Linear Momentum** that relates the net force acting on an open system to the net flow of momentum across the system boundary and the rate of change of momentum within the system boundary.
   c. **Conservation of Angular Momentum** that relates the net torque acting on an open system to the net flow of angular momentum across the system boundary and the rate of change of angular momentum within the system boundary.
2. Those principles that are primarily thermal in nature:
   a. **Fourier Conduction Law** that relates the heat transfer flux (rate of flow of energy per unit area normal to the direction of flow) at a point in space by the mechanism of conduction to the local temperature gradient.
   b. **Newton's Law of Cooling** that relates the heat transfer flux at a point on the boundary between a solid and a fluid by the mechanism of convection to the difference in temperature between the fluid and the surface of the solid.
   c. **Stefan-Boltzmann Radiation Law** that relates the energy flux emitted by the mechanism of thermal radiation from an ideally radiating surface to the fourth power of the temperature of the surface.

---

[1] Terms in italic type are defined in section 1.6 of this chapter.

3. Those principles that link together the thermal and mechanical aspects of system behavior:

a. **First law of Thermodynamics** that relates the net change in the stored energy of a system within the system boundary to the net energy interaction across the surface by means of work transfer and heat transfer.

b. **Second Law of Thermodynamics** that relates the net change in the stored entropy of a system within the system boundary to the entropy transfer across the boundary of the system by means of heat transfer and the net entropy generated within the system boundary by means of irreversible processes.

The *models* of system behavior that we employ in the application of these principles to the various categories of systems will be developed in detail later, but they naturally fall into two broad categories:

1. **Uncoupled Systems** in which the thermal and mechanical aspects of system behavior are separate in the absence of dissipation. These include:

a. **Pure conservative mechanical systems** in which work transfer is the only possible energy interaction.

b. **Pure thermal systems** in which heat transfer is the only possible energy interaction.

c. **Pure dissipative systems** in which both heat transfer and work transfer can occur but the energy flow by work transfer is always into the system and the energy flow by heat transfer is always out of the system with no possibility of storing energy within the system boundary.

d. **Incompressible fluid** in which the density of the fluid is always the same value regardless of the interactions that it experiences.

2. **Coupled Systems** in which the thermal and mechanical aspects of system behavior can each be influenced by both work transfer and heat transfer. These include:

a. **Ideal gas** in which there is a single form of stored energy that can be changed by both work transfer and heat transfer interactions and the matter itself can exist only in the gas phase.

b. **Pure substance** in which the single form of stored energy can be changed by both work transfer and heat transfer interactions and the substance can be in any of the three phases: solid, liquid, or vapor.

1.4 The Development of the Subject Matter

The present treatment differs from more traditional approaches to the subject matter in that it attempts to present in an integrated fashion the full spectrum of principles in thermal-fluids engineering. The unifying theme in this approach is the way in which these principles influence the design and performance of the thermal-fluid systems that find widespread utilization in the engineered systems that provide the goods and services of our modern world.

The approach taken here is to develop the underlying principles of thermodynamics first and to then illustrate their applicability through introduction of the simple, but widely used, models for thermal-fluid systems that pervade engineering practice. We then use these models throughout the remainder of the text. We follow this with a development of the methodology for

analyzing the rate processes that describe the various possible modes of heat transfer interactions. We then examine the ways in which the first and second laws of thermodynamics limit the performance of engineering systems at the systems level. Since the physical embodiments of these conceptual system designs depend so heavily upon the dynamic behavior of the working fluids that are literally their life's blood, we develop the principles governing the static and dynamic behavior of fluids. This dynamic behavior includes the details of the convective heat transfer processes that can occur between a moving fluid and the solid surfaces that bound it. We then synthesize this material, i.e., the thermodynamics, the heat transfer, and the fluid dynamics, through a study of the design of thermal-fluid plants based upon the previously developed principles and models. Throughout this treatment, we point out the ways in which the principles of thermal-fluids limit the behavior of the unit processes.

1.5 The Thermal-Fluids Method of Analysis

Two of the most important duties of an engineer are: (1) the design of engineering systems and (2) the analysis of the behavior or performance of these systems. In general, systems vary greatly in their complexity and thermal-fluid systems are no exception. Fortunately, the general techniques for analyzing these systems are much the same regardless of the complexity and can be cast in the form of steps which, if performed in sequence, will provide the information sought. Whether the information is useful depends upon the skill of the individual who asked the questions in the first place. A good analysis will provide the necessary engineering information about the situation within the time available for analysis and with an economy of effort. An analysis which is more complex than necessary is time consuming and wasteful of human and economic resources. The main steps involved in the analysis are:

1. Select the system, system boundary and environment
2. Model possible behavior
   a. System properties and constitutive relations
   b. Possible boundary phenomena and interactions
   c. Environment properties and constitutive relations
3. Model the specific processes of system and environment
   a. Initial and final states
   b. Path of process
   c. Interactions
4. Apply principles of thermal-fluids engineering as appropriate
   a. Space continuity
   b. Conservation of mass
   c. Conservation of linear momentum
   d. Conservation of angular momentum
   e. First law of thermodynamics
   f. Second law of thermodynamics

The first step is an extremely important one. It separates the system of interest from the environment and thereby limits the scope of the analysis. In most cases, this step will establish

the manner in which the principles of thermal-fluids engineering are applied to the system. It should be noted that exercising a little judicious care in the choice of the system boundary can considerably reduce the effort expended in the analysis. A thorough understanding of the information to be gained from such an analysis can often provide insight in the selection of the system boundary. As a general rule, the system boundary should be as global as possible while at the same time consistent with the required details. In many cases, more than one system must be defined and analyzed to obtain the required information.

The second step of the method of analysis models the relevant behavior of the system, the system boundary, and the environment. In formulating this model, the engineer selects the properties of the system which are important in determining the required information. Possible system behavior is thus modeled by the constitutive relations between the relevant properties. Figure 1.15 is a graphical depiction of the models introduced in this text and the conditions under which they apply. It is not a flow chart of the modeling process.

The possible behavior of the system boundary is modeled by specification of the interactions which result in the transfer of mass, momentum, energy, and entropy across the boundary. These interactions produce changes in the state of the system and its environment. The transfer of mass across the system boundary establishes whether the system is a closed system (no mass transfer possible) or an open system (mass transfer possible). The possibility of mass transfer is important because the mass can carry with it momentum (both linear and angular), energy, and entropy as it crosses the boundary. The energy transfer interactions are: heat transfer and various work transfers (these will be discussed in detail in subsequent chapters). Entropy transfer is a consequence of heat transfer.

The possible behavior of the environment is modeled by the constitutive relations amongst the relevant properties of the environment.

The third step of the analysis models the specific processes of the system and the processes of the environment as the system and environment interact and exchange mass, momentum, energy, and entropy. The model for the process includes specification of: the initial state, the path of the processes, the final state, and the interactions across the boundary.

The fourth and final step of the analysis is the application of the principles of thermal-fluids engineering and other relevant physical principles to the model. Continuity of space at a common boundary requires that geometric displacements of the system and the environment are equal in magnitude but opposite in sign at the system boundary. Thus, a volume increase of the system requires an equal volume decrease of the environment. Conservation of mass requires that a closed system have constant mass and that an open system accumulate mass at a rate equal to the difference between the rates of inflow and outflow of mass. Conservation of linear momentum requires that the net force acting on a system be equal to the sum of the rate of change of momentum within the system and the net flow of momentum across the system boundary. Conservation of angular momentum requires that the net torque acting on a system be equal to the sum of the rate of change of angular momentum within the system and the net flow of angular momentum across the system boundary. The first law of thermodynamics relates changes in the energy of the system to the energy transfer via heat transfer and work transfer interactions. The second law relates changes in entropy of the system to the entropy transfer via heat transfer interactions and the generation of entropy within the system boundary.

In formulating the model and executing the analysis, the objective is to idealize the

physical interaction to a level of approximation consistent with the required information. In constructing the model, complex real phenomena are reduced to a simplified description amenable to analysis. It requires skill and ingenuity to accomplish the engineering task of modeling with a minimum expenditure of time and effort. Modeling skill is developed only through experience, but this ability marks excellence in an engineer.

Subsequent chapters of this text are organized to give practice in formulating appropriate thermal-fluid models for increasingly complex physical situations. The basic principles of thermal-fluids engineering are developed by adding phenomena to the thermal-fluid model in steps. The problems associated with each chapter have been selected to illustrate the modeling process and to emphasize the thermal-fluid method of analysis.

1.6 Basic Definitions

Thermal-fluids engineering has its foundations in a set of basic definitions that constitute a lexicon that is unique to this branch of engineering science. Traditionally, these definitions assign precise, technical, meanings to common words, and considerable care must be exercised in stating them in order to minimize any ambiguities. The importance of proper understanding and use of these terms in the study of thermal-fluids engineering cannot be overemphasized.

The definitions will be introduced as the text develops. Many important definitions will be first stated in simple, restricted terms and later generalized as more complex situations are considered.

1.6.1 System

A *system* is defined as any quantity of matter or region of space to which attention is directed for purpose of analysis.

Clearly this is a general definition and can apply to any physical system, thermal-fluids or otherwise. Generally, when attempting to determine the behavior of a system, we would expect to consider all the possible physical phenomena that can involve the system in any way. The task of enumerating all the possibilities is a formidable one and becomes virtually impossible if one is to account for all the coupling which might exist among the phenomena. Fortunately, it is often apparent from the physical situation, that many physical phenomena are of little or no consequence in determining the relevant behavioral aspects of the system. Thus, by judiciously eliminating all nonessential phenomena, we can substantially reduce the effort associated with the analysis of the system's behavior. In fact, this is precisely the point of view employed in the study of mechanical, thermal, and electrical systems.

1.6.2 Boundary

The quantity of matter or region of space which forms the system is delineated by a *boundary.*

The boundary is a surface, real or imaginary, which is prescribed in a rather arbitrary fashion and may possess special features. The most significant among these features is the boundary's ability to permit the transfer of matter into or out of the system. For example, if a system is defined as a particular quantity of matter, the system will always contain the same matter, and there can be no transfer of mass through the boundary. Such a system is called a *closed system* (or a system of fixed mass) and is surrounded by a boundary *impermeable* to mass transfer. However, if a system is defined as a region of space without restriction to mass, it is

enclosed by a boundary *permeable* to mass transfer. Systems of this type are called *open systems.*

Boundaries possess other characteristics in addition to permeability. For example, they can be rigid or deformable. This can influence the nature of mechanical interactions that the system can experience or can restrict the nature of allowable thermal interactions. At this time it is not possible to describe the details of boundary characteristics; however, in each case, the boundary and its characteristics must be carefully specified to avoid ambiguities and misunderstandings.

1.6.3 Environment

Everything outside the system boundary is referred to as the *environment.*

1.6.4 State and Property

The term *state* is used to signify the condition of a system at a specific instant. The state of the system is characterized by a collection of certain observable, macroscopic quantities, called properties. A *property* is one of those observable macroscopic quantities which are definable at a particular instant without reference to the system's history. A complete description of a system's state includes the values of all its properties. The minimum number of these necessary to specify the state of the system constitutes the set of *independent* properties with all others regarded as *dependent* on these.

By definition, the collection of properties that specifies the state does not provide any information regarding the manner in which that state was achieved. In fact, any quantity which depends upon the history of the system is not acceptable as a property. It cannot be used as part of the description for the state of that system.

The concepts of state and property are fundamental to thermal-fluids engineering and the distinction between properties and non-properties is of utmost importance. As an example of this difference, let us consider a system consisting of two vehicles. If the two vehicles, *A* and *B,* are located at given points in two different cities, then the straight line distance from *A* to *B* is a property of the system. This is because the value is fixed only by the location of the vehicles at the specified time and not by the manner in which they arrived in their locations. On the other hand, the distance traveled by vehicle *A* in reaching vehicle *B* depends on how the vehicle *A* travels. The distance traveled is known only if we know the history of the trip, that is, the route followed. Thus, the distance traveled cannot be a property of the system. However, we can say that the distance traveled is greater than or equal to the straight line distance from vehicle *A* to vehicle *B.* We can also compute the straight line distance (a property) from the complete details of the history of the trip (route followed). In thermodynamics we have an analogous situation in which a property (energy) is related to non-properties (heat transfer and work transfer).

As a second example, consider an automobile tire as a system. The depth of the tire tread is a property, but the number of miles traveled is not. There is no direct correlation between the number of miles traveled and the observable condition of the tire at a given time. A tire driven a given number of miles on a rough road at high speed under a heavy load will be in a different condition than one driven the same distance on a smooth road at low speed under a light load.

Some of the common thermal-fluids quantities that are *properties* include: pressure, mass, volume, density, temperature, internal energy, enthalpy, entropy, position, velocity, charge, voltage, and force.[2]

The common quantities in thermal-fluids engineering that are *non-properties* are: heat

---

[2] The precise definitions of these terms in a thermodynamic sense will be given in subsequent chapters.

transfer and work transfer.[3]

In general, properties may be grouped into a number of different categories. For example, properties may be classified as *independent* or *dependent.* A property is independent of another if, for a given system, it varies in an arbitrary fashion without producing any change in the other property. Conversely, one property is dependent upon another if a change in the latter produces a change in the former.

The selection of properties to be taken as independent is somewhat arbitrary; however, the prevailing physical situation usually dictates which properties are the natural choices. Often the choice is related to the ease with which certain properties can be controlled or measured. For example, when gas is being compressed in the cylinder of an automobile engine, the motion of the piston in the cylinder is determined by the crank mechanism so the volume of the gas in the cylinder bounded by the piston is naturally taken as one of the independent properties. In general, should the physical situation be altered in some manner, the set of properties taken to be independent can be transformed into another set of independent properties in much the same manner as one transforms from one set of coordinates to another in mathematics. In any case, a complete set of independent properties is sufficient to establish the state of the system. However, until the system is properly identified, the dependent properties remain unspecified and the description of the state of the system is incomplete.

A system is identified and described by means of mathematical expressions known as the *constitutive relations.* These relations express the dependent properties in terms of the independent properties. The constitutive relations of a system depend upon the characteristics of the physical materials that comprise the system and their geometric arrangement within the system. Hence, for a system with a given set of constitutive relations, the complete state of the system can be described once the values for the independent properties are established.

In the constitutive relation there are often quantities which have the appearance of properties; however, these quantities are not true properties. Rather, they represent certain characteristics of the system and can therefore be used to identify the system. A typical example of this is the spring constant of a linear spring. A linear spring system has two properties: the force on the spring and the relative displacement of its two ends. These properties are sufficient to describe the state of the spring. Since the two properties are related through the constitutive relation, only one of them is independent. However, because the relationship between the two properties is a linear one, a new quantity appears - the spring constant. The spring constant is not a true property. It cannot describe the state of the system in terms of force-displacement behavior and thus serves to identify the system. In fact, for purposes of analysis, the spring constant and the free length are sufficient to define a linear (and massless) spring.

In a geometrical sense, the complete set of independent properties of a given system can be used to form a multidimensional space. In that space, the constitutive relations will form a mathematically defined surface such that every possible state of the system must lie somewhere on the surface. Thus, the independent thermal-fluids properties can be regarded as thermal-fluids coordinates.

1.6.5 Interaction

---

[3] The precise definitions of these terms in a thermodynamic sense will be given in subsequent chapters.

Two systems interact when a change of state in one system causes a change of state in the other. The *interaction* is the phenomenon at the contiguous boundary between the two systems that causes the transfer of mutual influence. In thermal-fluids engineering the mass, momentum, energy, and entropy effects of the interactions are of primary importance. Two systems are in *communication* when interactions are possible, and are *isolated* when interactions are not possible.

1.6.6 Process

A *process* occurs when a system undergoes a change of state with or without interactions with its environment. During the change of state, the system passes through a succession of states which forms the *path* of the process. The complete description of a process requires four specifications: the initial state, the final state, the path, and the interactions between the system and its environment during the change of state.

There exists a special class of processes, known as *cycles,* in which the initial and final states are identical. Quite often the cycle is a series of simple processes that represent changes of states in engineering systems. Thus, a cycle can be regarded as a series of processes that produces no net change of state in the system.

1.6.7 Equilibrium

Consider now two thermal-fluid systems which are free to interact in any possible manner. If the state of one system is changed by some external agent, the two systems will interact with one another. Eventually, they will reach a particular state, known as the *equilibrium* state, determined by the physical situation. In this state, the interaction between systems ceases. Once this state has been established, the two systems cannot be made to interact any further unless the imposed circumstances are altered. In this sense, the two systems are in a state of *mutual equilibrium.* On the other hand, the two interacting systems may actually be part of a larger system. When all subsystems of this larger system reach a state of mutual equilibrium, the composite system is said to be in a state of *internal equilibrium.* That is, any one part of the composite system is in equilibrium with any other part.

It is worth noting that the underlying principle of thermal-fluids engineering is this tendency for all systems to seek the equilibrium state as defined by the particular physical circumstances. On the basis of this principle, it is possible to derive the relations of thermodynamics.[4]

Although it is not specifically mentioned, the variable "time" does play an important role in the definition of equilibrium. Perhaps this point can be clarified by rephrasing the definition:

> When a system is in an equilibrium state, it is impossible for the system to experience a change of state without also experiencing an interaction of some sort.

In a manner of speaking, an equilibrium state is a state of "rest"; nothing is happening. We note, however, that this static nature of the equilibrium state exists only on a macroscopic scale. If we observe any system on a microscopic scale, we see that the system is in a state of constant fluctuation and is far from being at "rest". The magnitudes of these microscopic fluctuations are

---

[4] Hatsopoulos, G. N. and Keenan, J. H., *Principles of General Thermodynamics*, John Wiley & Sons, 1965.

so minute that in most cases they are undetectable on a macroscopic scale. However, the possibility does exist for a large number of these minute fluctuations to "happen" simultaneously so that a spontaneous macroscopic fluctuation is observed. If this possibility exists for every system, then how can we talk about equilibrium states in such absolute terms? This question can be answered by noting that the probability of this spontaneous departure from equilibrium occurring in most systems is so small that the event would probably happen only once during a time period comparable with the age of the universe. Therefore, a system not experiencing any interactions when allowed to do so can be regarded as being in equilibrium.

It is also important to note that this equilibrium is relative rather than absolute. We have just stated (although not explicitly) that if the probability of a system executing a spontaneous change of state is small during the time scale of a typical observation, then the system is assumed to be in equilibrium. We can extend this further by noting that if a system is undergoing a change of state which is "slow" relative to the rate at which the system approaches the equilibrium state, such a system can be treated as though it were in equilibrium.

In the present treatment there are four types of equilibrium that will concern us. These types are characterized by the nature of the interaction which is necessary for the system to reach equilibrium. Accordingly they are called *mechanical equilibrium, thermal equilibrium, chemical equilibrium,* and *diffusion equilibrium.* Detailed definitions of these various types of equilibrium will be presented at the appropriate points in the development of the subject.

Traditionally, classical thermodynamics is a study of the equilibrium states of matter with little regard for the rate processes by which these equilibrium states are established. In the present treatment, we shall take a true thermal-fluids approach and give considerable attention to these rate processes so that we can better model physical situations and thereby obtain a more complete description of the systems involved. In particular, we shall focus on the difference between the rate processes by which mechanical equilibrium is attained (work transfer) and the rate processes by which thermal equilibrium is attained (heat transfer). In general, the former are significantly faster than the latter. With the aid of the material to be presented here, we will soon be able to say how much faster in a given set of circumstances.

1.6.8 Model

A *model* is a mathematical representation that idealizes a complicated physical situation to a greater or lesser degree depending upon the available information and the information being sought.

In our study of thermal-fluid systems, we will develop models for systems, boundaries, the environment, processes, paths, and interactions. While there may be a variety of models for each of these components of thermal-fluid systems, there is only one model in each case that is appropriate for the available information and the information sought. The ability to determine which one is the appropriate one is the hallmark of a good thermal-fluids engineer. One of the objectives here is to develop that skill in each and every one who studies this treatment.

As we progress, we shall elaborate on these definitions and add still others that will eventually form the full lexicon of thermal-fluids engineering. With the aid of this lexicon, which serves as the language of the working thermal-fluids engineer, we will be able to communicate amongst ourselves with far less ambiguity than would be possible otherwise.

Problems

1.1 Based on your experience with the physical world in which you live, list ten examples of thermal-fluid systems. For each example, describe the information that you would need in order to design such a system or to predict the performance of the system.

1.2 Which of the following represent a system? For each system, describe its boundary and decide whether the system is an open system or a closed system.

(a) An explosion
(b) A pump for bicycle tires
(c) Three kilograms of air
(d) A wave on the surface of a lake
(e) A force
(f) An automobile
(g) The volume inside a rigid evacuated container
(h) Ten kilometers of copper wire
(i) A flow through a pipe
(j) The pressure exerted by the atmosphere

1.3 Which of the following are properties of the specified system? Which are not?

(a) *System: The filament of an incandescent lamp*
- the mass
- the diameter
- the number of hours of operation
- the electrical resistance
- the electrical current flowing through it
- the total watt-hours consumed

(b) *System: A dry-cell flashlight battery*
- the volume
- the mass
- the voltage
- the total watt-hours used
- the mass of each chemical compound or element in the battery

(c) *System: A clock spring*
- the torque on the output shaft
- the volume
- the energy transferred to the spring by the input shaft
- the energy transfer required to wind the spring to its present torque from the unwound condition

CHAPTER 2

Energy and The First Law of Thermodynamics

2.1 Introduction

The first law of thermodynamics plays a significant role in the analysis of thermal-fluid systems, and for this reason we shall devote considerable attention to its development. However, it is useful for us to outline briefly the essential features of the first law of thermodynamics as it applies to closed systems. With this information, we will be better prepared to organize and interpret the details of the succeeding development.

In essence, the first law of thermodynamics is a generalization of the observed facts about the energy interactions between a system and its environment. It has been formulated on the basis of our observations of a very large number of systems. Specifically, it relates the various energy interactions between a system and its environment to changes of state experienced by that system during these interactions. All physical experience in the history of humankind has confirmed that in order for any description of a physical situation to be true, the generalizations embodied in the first law of thermodynamics must be satisfied.

The application of the first law to physical situations of interest requires two things: (1) a characterization of the energy interactions between the system and the environment and (2) a means of describing the changes of state, specifically the changes in the stored energy of the system, in terms of the physically observable properties of the system. With a few extraordinary exceptions, all the energy interactions that a system can possibly experience can be grouped into either one of two categories: *work transfer* or *heat transfer*. The changes of state that result from these interactions are described in terms of a set of *constitutive relations* that are the essential element of the model used to describe the system.

2.2 The First Law of Thermodynamics for an Isolated System

There are many ways in which the first law of thermodynamics can be stated, and some rather complex arguments are required to prove the equivalence of these statements. However, the simplest of these statements can be formulated by considering a system that is *isolated*. A system is said to be isolated when all changes within the system produce no changes outside the system. In other words, for an isolated system, there are no interactions between the system and its environment even though there are changes occurring within the system boundary. For such a system, the first law of thermodynamics states that there is no change in the energy stored within the system boundary. When stated in this fashion, the first law is sometimes known as the principle of *conservation of energy*. The mathematical equivalent of this statement is

$$(E_2 - E_1)_{isolated} = 0 \tag{2.1}$$

where E_2 is the energy stored within the system boundary in the second state and E_1 is the energy stored within the system boundary in the first state.

2.3 The Property Energy and Energy Storage Modes

The energy is an *extensive* property which means that it is additive over all subsystems that makeup the system. The value of any extensive property such as the energy of a system can be determined by adding the values of that property for every part of the system. In the case of the stored energy of a system, it has proven useful in engineering practice to categorize the energy according to the various forms, or modes, in which it can be stored. Thus, by virtue of the fact that the energy is an extensive property, the total stored energy of a system is the sum of all the energy stored in its various modes.

In general, the thermal-fluid systems encountered in engineering practice exhibit both mechanical and thermal characteristics, and these characteristics are often manifested in different forms of the stored energy. If in the absence of any dissipative processes such as solid or fluid friction, the thermal and mechanical characteristics remain separate and apart so that the mechanical characteristics can be changed only by work transfers and the thermal characteristics can be changed only by heat transfers, the system is said to be thermodynamically *uncoupled.* On the other hand, if in the absence of dissipative processes the thermal characteristics can be changed by positive work transfers, the system is said to be thermodynamically *coupled.* As we shall soon see, this concept of thermodynamic coupling is an important one since it enables the thermal-fluids engineer to convert the energy stored in fossil fuels such as coal, oil, natural gas, and nuclear fuels into mechanical energy that can be used to power the machines of our modern industrial society.

The significance of the coupling between the thermal and mechanical aspects of system behavior at this point in our discussion is that it enables us to establish two broad classes of energy storage modes: (1) uncoupled energy storage modes, of which there are several, and (2) the coupled energy storage mode, of which there is but one. The distinguishing feature between these two classes of energy storage modes is that in the case of an uncoupled energy storage mode, the stored energy characteristic of that mode can be quantitated in terms of a *single*, measurable property via a single constitutive relation and can be changed only by a *single* type of interaction, *either* a work transfer *or* a heat transfer, between the system and the environment. For a given uncoupled energy storage mode, all the interactions that it can experience must always be of the same type: either work transfer or heat transfer but never a work transfer at one point in time and a heat transfer at some other point in time. The stored energy characteristic of the coupled energy storage mode, on the other hand, can be quantitated, in general, only in terms of two independent measurable properties via a single constitutive relation and can be changed by *either* a work transfer interaction *or* a heat transfer interaction at any point in time *or* by both types of interactions simultaneously.

The energy storage modes that are most frequently encountered in engineering practice are: *kinetic, elastic, gravitational (or potential), thermal, and coupled.* Uncoupled thermal-fluid systems can have *only* uncoupled energy storage modes whereas coupled thermal-fluids systems can have *both* uncoupled and coupled energy storage modes. Thus, for an *uncoupled* system, the stored energy can be written

$$E_{\substack{uncoupled \\ system}} = E_{kinetic} + E_{elastic} + E_{gravitational} + U_{thermal} \tag{2.2a}$$

and for a *coupled* system, the stored energy can be written

$$E_{\substack{coupled \\ system}} = E_{kinetic} + E_{elastic} + E_{gravitational} + U_{thermal} + U_{coupled} \qquad (2.2b)$$

where we have introduced the symbol U to represent any stored energy mode that can have a constitutive relation that depends upon the property temperature. For the beginning student, this notation may be a bit confusing at first, but its use will become clearer in time. The distinction between $U_{thermal}$ and $U_{coupled}$ is that $U_{thermal}$ can be changed only by a heat transfer interaction whereas $U_{coupled}$ can be changed by either a heat transfer or a work transfer or both simultaneously. The utility of this approach will become more apparent when we study the behavior of uncoupled systems in greater detail.

For each energy storage mode, we will develop subsequently a model that enables us to evaluate quantitatively the contribution from that mode to the total stored energy of the system. Each model includes a constitutive relation between the stored energy of that mode and the independent properties that describe the state of the system associated with that mode. Several of these modes are already familiar to us from our previous study of the mechanics of particles and rigid bodies, but the one mode that is unique to thermal-fluid systems is the coupled energy mode also known as the *internal energy*. For this reason, we will devote considerable attention to the models that represent it. As mentioned above, the models representing the uncoupled energy storage modes have simple constitutive relations that describe the particular energy storage mode in terms of a single independent property. For each uncoupled mode, the value of the energy of that mode can be decreased by means of only one specific interaction which is either thermal or mechanical in nature depending upon the energy storage mode. The coupled energy storage mode, however, cannot be described in terms of such simple constitutive relations, and it alone can be decreased (and increased) by both thermal and mechanical interactions acting alone or in concert.

2.4 The First Law of Thermodynamics for a System Interacting with Another System

If a system is not isolated and is therefore free to interact with another system, the first law of thermodynamics states that the net change of energy stored within the system boundary is equal to the net energy transfer across the system boundary. Since there are only two possible ways that we can transfer energy across the system boundary, namely heat transfer, Q, and work transfer, W, we may write the first law of thermodynamics in the following mathematical form

$$E_2 - E_1 = Q_{1-2} - W_{1-2} \qquad (2.3)$$

where the subscripts 1 and 2 indicate the initial and final end states for the process by which the energy is transferred across the system boundary. Note that a positive heat transfer *increases* the stored energy while a positive work transfer *decreases* the stored energy, hence the negative sign on the right-hand side of this expression[1].

---

[1]This is a sign convention established in the eighteenth century when the developments in the science of thermodynamics were driven by the quest for energy conversion devices that could be used to power the machines of the industrial revolution. It was recognized by these early thermodynamicists that the desired result, a work transfer to the machine, could be realized only by converting the energy that could be released by the exothermic reaction resulting from the oxidation of a fossil fuel such as coal. Thus, energy flowed into their energy conversion systems, known as heat engines, by means of heat transfer from the exothermic reaction and out of the heat engine in the form of a work transfer to the machine.

Consider the case of a system A interacting with another system B. The two systems taken together form a composite system $A+B$ that is an isolated system. Thus from equation (2.1), the first law of thermodynamics for the composite system is

$$(E_2 - E_1)_{A+B} = 0 \tag{2.4}$$

and by virtue of the fact that the energy is an extensive property, we have

$$(E_2 - E_1)_{A+B} = (E_2 - E_1)_A + (E_2 - E_1)_B \tag{2.5}$$

From equation (2.3) we have

$$\begin{aligned} (E_2 - E_1)_A &= (Q^{AB})_{1-2} - (W^{AB})_{1-2} \\ (E_2 - E_1)_B &= (Q^{BA})_{1-2} - (W^{BA})_{1-2} \end{aligned} \tag{2.6}$$

In the superscripts on the energy interactions, the first letter indicates the system of interest and the second letter indicates the system that it is interacting with.

For an isolated system consisting of two component subsystems A and B with energy transfer only between A and B, the first law will be satisfied only if

$$\begin{aligned} (Q^{AB})_{1-2} &= -(Q^{BA})_{1-2} \\ (W^{AB})_{1-2} &= -(W^{BA})_{1-2} \end{aligned} \tag{2.7}$$

Figure 2.1 shows a graphical representation of the two interacting systems. Note that the two systems are shown separated with thermal and mechanical interconnections interposed between them. These interconnections, which experience no net change of state themselves, provide the means by which the interactions occur while at the same time insuring that the boundary conditions are appropriate for the particular interaction. In the actual physical situation, the two systems would most likely share a common boundary. Note also in Figure 2.1 that the interactions are shown in the positive sense in each case. Clearly for each of the interactions, one of the systems experiences a positive interaction while the other experiences a negative one. For the system experiencing the negative interaction, the algebraic sign of that interaction is negative which indicates that the energy flows in the opposite direction from that shown in Figure 2.1.

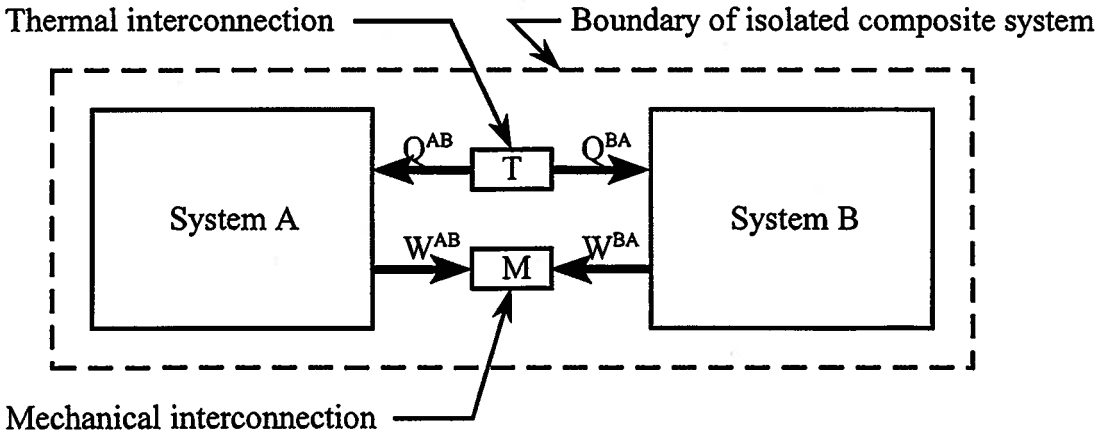

Figure 2.1 Graphical Representation of Two Interacting Systems

For infinitesimal changes of state, the first law of thermodynamics can be written in differential form. In the case of an isolated system experiencing an infinitesimal change of state, the first law becomes

$$dE = 0 \tag{2.8}$$

and for a system with infinitesimal energy interactions, the first law is

$$dE = \delta Q - \delta W \tag{2.9}$$

Note in equations (2.8) and (2.9) that the symbol d indicates that dE is an exact differential. Then since the energy is a property whose value depends only upon the state of the system, it follows that the energy E is a state function and, hence, that dE can be integrated to yield E_2 - E_1 for a finite change of state as long as the states 1 and 2 are known. However, in equation (2.9), the symbol δ indicates that the quantities δQ and δW are infinitesimal interactions for an infinitesimal change of state dE. In order to integrate equation (2.9) for a finite change of state, it is necessary that the process that it represents pass through a series of states for which the values of all the properties are known or can be calculated from the constitutive relations. The interactions, in contrast to the energy, are not state functions and cannot be integrated unless the path (the series of states) is known. In mathematical terms, the path is a specification of the relationship between the various properties necessary to describe the state of the system. It, together with the constitutive relations, must be known to evaluate the line integrals that represent the interactions $Q_{1\text{-}2}$ and $W_{1\text{-}2}$.

The major difficulty in applying the first law to physical situations lies in the determination and formulation of the heat transfers and work transfers. This will soon become apparent as we take the basic concepts of work transfer directly from mechanics and electromechanics, and reformulate them from a thermodynamic point of view. However, as we deal with progressively more complex systems, it may be necessary to extend these definitions of work transfer to avoid any ambiguity. Since heat transfer is unique to thermodynamics, it is not possible to rely on other disciplines for its formulation. In fact, one of the most difficult aspects of the formalism of thermodynamics is a rigorous definition of heat transfer. Therefore, we shall delay its discussion until later in our development. Presently, it is sufficient to regard heat transfer simply as one of the two means of energy interaction, distinct from work transfer, between a system and its environment. The distinction between heat transfer and work transfer is important because, as we shall see subsequently, the work transfer interaction involves the transfer of energy only between a system and its environment, but heat transfer involves the transfer of energy and entropy (a property that we have yet to discuss). The effect on the system for these two interactions is profoundly different and can best be explained through the second law which we shall discuss shortly.

As is evident from the first law of thermodynamics, equation (2.3), energy and work are measured in the same *units*. In 1960, by international agreement, the International System of Units, abbreviated SI from the French "Le Système International d'Unités", was established as the universal system of units for the measurement and specification of physical quantities. The *unit* of work and energy in SI units is the *Newton-meter*, also known as the *Joule*.

(Unfortunately, the United States has lagged behind other countries in the adoption of SI units despite the arguable advantages of SI units. To be sure, in the U.S. there was a large stock of tooling that was designed and built in an earlier era according to a different system of units, but the rest of the world has had to deal with the same issues in changing over to the new system.

The recalcitrance of the U.S. in this area has put the United States at a slight disadvantage not only in the world marketplace, but also in the scientific and engineering communities. As the new millennium begins and the old tooling becomes obsolete, it is appropriate that the U.S. should join its international engineering partners in the adoption of SI units. For this reason, this text will use SI units exclusively, but the authors recognize the need to have conversion factors from one unit system to another conveniently available. Thus, upon the introduction of each new physical quantity, appropriate conversion factors will be presented.)

TABLE 2.1
Equivalent Energy Units

1 Joule (J) = 1 Newton-meter = 1 kg m^2/sec^2 = 10^7 ergs

1 calorie (cal) = 4.1868 Joules

1 electronvolt (eV) = 1.602 x 10^{-19} Joules

1 British thermal unit (Btu) = 1055.056 Joules

1 British thermal unit (Btu) = 778.1693 ft-lbf

1 kilowatt hour (kW-h) = 3.6 x 10^6 Joules

1 foot pound-force (ft-lbf) = 1.356 Joules

2.5 The First Law of Thermodynamics for a System Executing a Cycle

It is now worthwhile for us to consider an alternative statement of the first law of thermodynamics, a statement that will enable us to prove mathematically that the energy is indeed a property. Consider a system that executes a cycle. By definition, the system experiences no net change of state. Therefore, there can be no net energy interaction between the system and its environment. Thus, we may state the first law of thermodynamics in a formal way as:

> The net energy interaction between a system and its environment is zero for a cycle executed by the system.

The mathematical equivalent of this statement is

$$\oint \delta Q = \oint \delta W \tag{2.10}$$

The integral sign indicates the algebraic summation of each infinitesimal heat transfer δQ or work transfer δW over the complete cycle.

We may now use the first law of thermodynamics in the form of equation (2.10) to show that the energy change $E_2 - E_1$ is the change of a property of the system. Consider the situation

depicted in Figure 2.2. The system is one for which two independent properties are adequate to specify the state. Thus, each point in the plane of Figure 2.2 represents a state of the system.

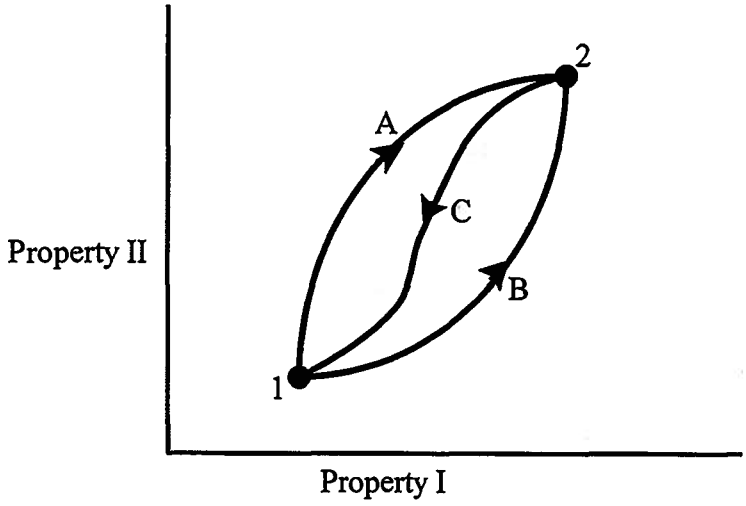

Figure 2.2 States of a System with Two Independent Properties

(Note: our proof is not restricted to systems of this type. We have used this example simply because it is easier to present in graphical form.) The state of the system is changed from state 1 to state 2 by two different processes, *A* and *B* involving heat transfer and work transfer interactions with the environment. From equation (2.3) we have

$$(Q_{1-2} - W_{1-2})_{process\ A} = (E_2 - E_1)_{process\ A} \tag{2.11}$$

and

$$(Q_{1-2} - W_{1-2})_{process\ B} = (E_2 - E_1)_{process\ B} \tag{2.12}$$

Now we can find some other process to return the system from state 2 to state 1, say process *C*, such that

$$(Q_{1-2} - W_{1-2})_{process\ C} = (E_2 - E_1)_{process\ C} \tag{2.13}$$

If we apply the first law of thermodynamics to one cycle consisting of process *A* and process *C* and to a second cycle consisting of process *B* and process *C*, we have from equation (2.10)

$$(Q_{1-2} - W_{1-2})_{process\ A} + (Q_{1-2} - W_{1-2})_{process\ C} = 0 \tag{2.14}$$

and

$$(Q_{1-2} - W_{1-2})_{process\ B} + (Q_{1-2} - W_{1-2})_{process\ C} = 0 \tag{2.15}$$

Thus, from equations (2.14) and (2.15) it follows that the net energy interaction for any two *processes between state 1 and state 2* must have the same value, or

$$(Q_{1-2} - W_{1-2})_{process\ A} = (Q_{1-2} - W_{1-2})_{process\ B} \tag{2.16}$$

Thus, when we substitute the definition of the energy change, equation (2.3), we show that

$$(E_2 - E_1)_{process\ A} = (E_2 - E_1)_{process\ B} \tag{2.17}$$

Since processes *A* and *B* are arbitrary, we have shown that the change of energy between two states of a system is independent of the process, i.e., the method by which the change of state is

carried out. Therefore, this change must depend only on the states of the system and must be a change in a property. If we choose one state as an arbitrary datum for energy, then the energy relative to this state depends only on the state of the system. Thus, the energy of a system in state 1 relative to a reference state 0 is

$$E_1 = E_0 + Q_{0-1} - W_{0-1} \tag{2.18}$$

where the values of the heat transfer and work transfer interactions can be determined from the path (line) integrals

$$Q_{0-1} = \int_{\text{state 0}}^{\text{state 1}} \delta Q \tag{2.19}$$

and

$$W_{0-1} = \int_{\text{state 0}}^{\text{state 1}} \delta W \tag{2.20}$$

where the integrals are evaluated for *any* single process with a defined path between state 0 and state 1. (It must be the same process and path for *both* Q and W.) Since δQ and δW are not integrable functions themselves, it is necessary to use the path specification to express these interactions in terms of the values of the properties along the path in order to carry out the integrations contained in equations (2.19) and (2.20). For convenience, it is customary to assign the energy of the reference state the value zero; thus $E_0 = 0$.

Note that the individual energy transfers, the integral of δQ and the integral of δW, are individually related to specific changes in the stored energy of the system only in especially simple cases. In more complex cases, the integrals will each depend upon the process used to change the system from state 0 to state 1 so that only their combination is related to changes in stored energy through equation (2.3). For example, a coupled system could have the same change of state as the result of a heat transfer process without work transfer or as the result of a work transfer without a heat transfer.

Example 2E.1: Consider a thermodynamic system whose state can be specified by two independent properties. The states of such a system can be represented conveniently in graphical form as shown in Figure 2E.1.

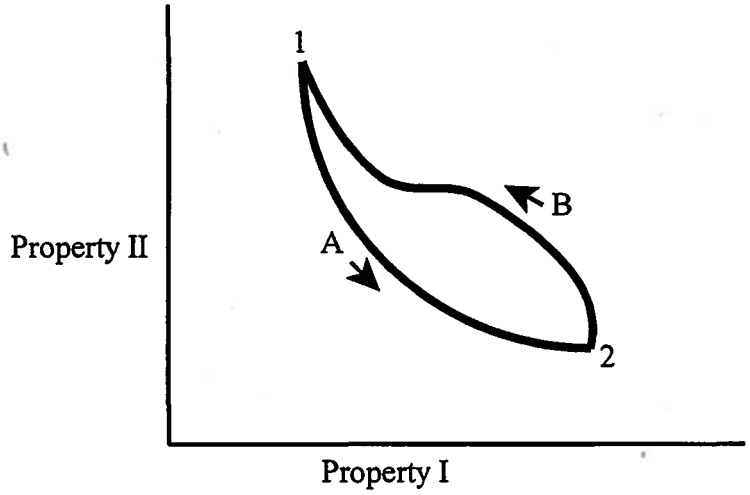

Figure 2E.1 States of a System with Two Independent Properties

The states 1 and 2 are states specified by the values of the properties (I_1,II_1) and (I_2,II_2), respectively. Consider a process A by which the state of the system changes from state 1 to 2 and experiences work transfer $(W_{1\text{-}2})_A = -23$ kJ and a heat transfer $(Q_{1\text{-}2})_A = 11$ kJ. The energy in state 1 referenced to some datum state is $E_1 = 32$ kJ. If the state of the system is subsequently restored to state 1 by means of a process B in which there was a work transfer $(W_{2\text{-}1})_B = -46$ kJ, calculate the heat transfer $(Q_{2\text{-}1})_B$.

Solution: From the first law it follows that for process B

$$(Q_{2-1})_B = E_1 - E_2 + (W_{2-1})_B$$

where E_2 must be determined from the application of the first law to process A. Thus,

$$E_2 = E_1 + (Q_{1-2})_A - (W_{1-2})_A$$

or

$$E_2 = 32 \text{ kJ} + 11 \text{ kJ} + 23 \text{ kJ} = 66 \text{ kJ}$$

Then

$$(Q_{2-1})_B = 32 \text{ kJ} - 66 \text{ kJ} - 46 \text{ kJ} = -80 \text{ kJ}$$

2.6 Work Transfer

To apply the first law of thermodynamics to physical situations, it is now necessary for us to elucidate the details associated with the evaluation of the heat transfer, work transfer, and change in stored energy for engineering systems. The change in stored energy can be expressed in a straightforward fashion by means of the constitutive relations which we will take up later, but the interactions, particularly the heat transfer, are somewhat more complicated to deal with. Fortunately, in the case of the work transfer, we have our experience from our study of the mechanics of particles and rigid bodies to draw from. In order for a work transfer interaction to occur, there are two requirements that must be met: (1) the environment must exert a concentrated boundary force on the system and (2) there must be a displacement of the system boundary in response to this applied force. We define the resulting work transfer in the following manner:

> The infinitesimal work transfer δW *from* a system due to a concentrated tension boundary force $\vec{F}$ *exerted on the system* by its environment is given by the negative scalar product of the force vector $\vec{F}$ and the infinitesimal outward displacement vector $d\vec{r}$ of *the boundary mass points* at the instantaneous point of application of the boundary force. Thus

$$-\delta W = \vec{F} \cdot d\vec{r} \tag{2.21}$$

The negative sign appearing in equation (2.21) is simply a matter of thermodynamic convention introduced in the early development of the subject. Also in equation (2.21) we have used the symbol δ rather than d to distinguish between an infinitesimally small interaction and the infinitesimally small change of state arising from the interaction. The integration of equation (2.21) for a finite displacement of the boundary of the system is relatively straightforward when the force always acts through the same boundary point. In this case the resulting work transfer

$W_{1\text{-}2}$ from the system is simply the integral of equation (2.21),

$$-W_{1-2} = \int_{\vec{r}_1}^{\vec{r}_2} \vec{F} \cdot d\vec{r} \tag{2.22}$$

where $\vec{r}$ in this case is simply the displacement of the one boundary point through which the force $\vec{F}$ is continuously applied. The work transfer depends upon the details of how the force $\vec{F}$ varies as the boundary is displaced. Thus, the work transfer cannot be determined from the initial and final states of the system except in the special case of a pure conservative mechanical system.

In the more complex case in which the concentrated force $\vec{F}$ moves from point to point along the boundary while at the same time the boundary is moving, the integration of equation (2.21) requires special care. In this case, the displacement of the point of application of force $\vec{F}$ is *not* the same as the instantaneous displacement of the system boundary where $\vec{F}$ is applied. The displacement $d\vec{r}$ is the displacement of the mass point of the boundary during the time that the force $\vec{F}$ is applied to that point. Thus, in a finite process the displacement vector $\vec{r}$ is not related to the displacement of a single point on the boundary of the system. The classic example of a process of this type is the force applied to a system boundary through a rolling contact point.

2.7 The Role of Models in the Analysis of Thermodynamic Systems

The first and second laws of thermodynamics govern the behavior of every system regardless of the specifics of the physical situation. By applying these laws, we are able to predict the behavior of a system when it is subjected to a set of known physical conditions. In addition, we can also use these laws to design systems that will produce desired outcomes. However, the information that we obtain from these applications is only as good as the information that we provide in the analysis. In particular, these laws are mathematical expressions whose application to a given physical situation requires that the physical situation itself be represented by similar mathematical expressions that idealize the physical situation to a greater or lesser degree depending upon the information we seek. These idealizations of the physical situation constitute the models that we referred to in Chapter 1, and the formulation of the appropriate model for a given situation is a skill that the engineer develops with practice. A certain amount of trial and error is necessary before one becomes a successful practitioner of the art of modeling. In this treatment, we shall provide the experience necessary to become proficient at modeling thermodynamic systems.

The models themselves are expressed in terms of a collection of constitutive relations that relate the properties and physical parameters necessary to describe the physical situation at the level of complexity required by the information we seek. Typically, the more detailed the information we seek, the more complex the model necessary. The complexity of the model necessary in a particular instance is not always obvious at the outset of the modeling process, but the best model will be the simplest one that provides the desired information. Over the years, engineering practice has developed a "catalog" of models that have proven useful at one time or another. It could be said that on some level engineering practice is simply a matter of choosing the right model from the "catalog." Once the model has been chosen, the analysis of the situation is reduced to relatively straightforward mathematical manipulation of the laws of

thermodynamics and the constitutive relations of the model. The whole "catalog" is too vast to describe here, but we will present a subset that should prove valuable for the design and analysis of most thermal-fluid systems. We begin our discussion of thermodynamic models with a presentation of the set of simplest models that find widespread usage in thermal-fluids engineering. Although extremely simple in their makeup, they are useful to model many physical situations.

2.8 Pure Conservative Mechanical Systems: Simple Models for Uncoupled Mechanical Energy Storage Modes

Pure conservative mechanical systems are examples of a set of models of real systems for which the thermodynamic behavior is especially simple for several reasons:

(1) These systems can experience but a single interaction, work transfer, which makes them uncoupled in the thermodynamic sense.

(2) These systems are *adiabatic* at all times, i.e., they cannot experience heat transfer.

(3) These systems have a single energy storage mode peculiar to the particular system.

(4) The behavior of these systems can be predicted by the first law of thermodynamics alone. The second law of thermodynamics is not necessary to predict or analyze their behavior.

As a consequence of these special characteristics, pure conservative mechanical system behavior is particularly simple:

(1) The stored energy of the system can be changed only by work transfer. Thus, it follows that the work transfer itself is a property of these systems **(but only for these systems)**. Hence,

$$\oint(\delta W)_{\text{pure conservative system}} = 0 \tag{2.23}$$

This is, in fact, the reason these systems are called pure conservative mechanical systems.

(2) These systems have a single independent property, the value of which is sufficient to specify the state of the system. Thus, their energy constitutive relations simply relate the one stored energy mode to this independent property.

(3) These systems have no entropy. (This will become apparent in Chapter 3.) Hence, they have no entropy constitutive relation.

(4) Since they have no entropy, these systems are capable of reversible processes only. (This, too, will become apparent in Chapter 3.)

In spite of these very special characteristics, there are many examples of systems of this type, and they are very useful in thermal-fluids engineering for modeling the uncoupled energy storage modes described in equation (2.2). We describe below several of these energy storage modes which will prove useful in our subsequent study and analysis of the behavior of thermal-fluids systems. Note that we identify the models in terms of *physical characteristics* which are actually *properties* of the system that do not change for the physical situations for which the models provide useful information.

2.8.1 Kinetic Energy Storage Mode: Pure Translational Mass Model

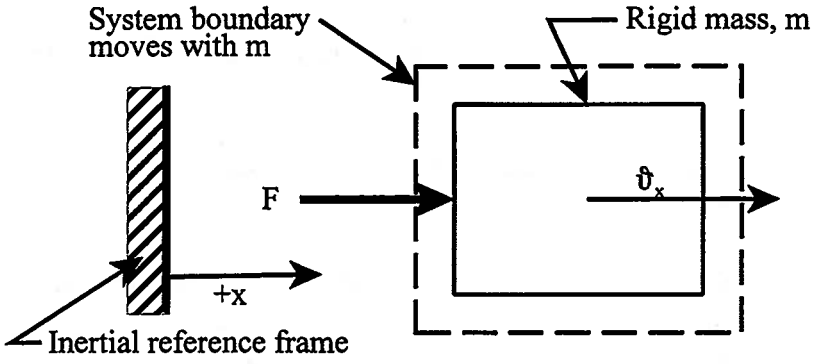

Figure 2.3 Kinetic Energy Storage Mode: Pure Translational Mass Model

Physical characteristic: m = mass of the system

Properties: $\vartheta_x = \dfrac{dx}{dt}$ = velocity of center of mass relative to inertial reference frame

F_x = concentrated boundary force exerted on the system by environment, positive in positive x-direction

Property constitutive relation: $F_x = m\dfrac{d\vartheta_x}{dt}$

Interaction: $-W_{1-2} = \int_{x_1}^{x_2} F_x dx = \int_{x_1}^{x_2} m\vartheta_x d\vartheta_x$

Energy constitutive relation: $(E_2 - E_1)_{kinetic} = \dfrac{1}{2}m\vartheta_{x_2}^{\ 2} - \dfrac{1}{2}m\vartheta_{x_1}^{\ 2}$

Example 2E.2: Compute the work transfer required to increase the translational velocity of a 10 kg mass by 1 m/s when at an initial velocity of 1 m/s. Repeat the calculation for an initial velocity of 10 m/s.

Solution: The system and processes are modeled as a pure translational mass as describe above. Application of the first law gives

$$-W_{1-2} = E_2 - E_1 = \frac{1}{2}m\vartheta_2^{\ 2} - \frac{1}{2}m\vartheta_1^{\ 2}$$

$$-W_{1-2} = \frac{1}{2}(10\text{ kg})(2\text{ m/sec})^2 - \frac{1}{2}(10\text{ kg})(1\text{ m/sec})^2 = 15\text{ J}$$

For an initial velocity of 10 m/s

$$-W_{1-2} = \frac{1}{2}(10\text{ kg})(11\text{ m/sec})^2 - \frac{1}{2}(10\text{ kg})(10\text{ m/sec})^2 = 105\text{ J}$$

The work transfer is from the environment to the system to produce the acceleration.

2.8.2 Elastic Stored Energy Mode: Pure Translational Spring Model

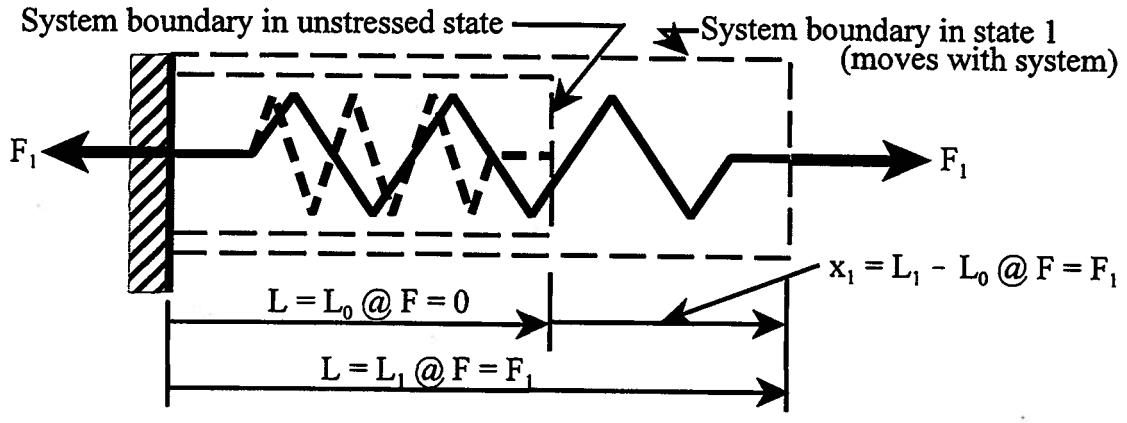

Figure 2.4 Elastic Energy Storage Mode: Pure Translational Spring Model

Physical characteristic: k = spring constant

Properties: x = extension relative to $F = 0$ state, positive for elongation

F = through force on the system boundary, positive for tension

Property constitutive relation: $F = kx$

Interaction: $-W_{1-2} = \int_{x_1}^{x_2} \vec{F} \cdot d\vec{r} = \int_{x_1}^{x_2} F dx$

Energy constitutive relation: $(E_2 - E_1)_{elastic} = \frac{1}{2} k x_2^{\,2} - \frac{1}{2} k x_1^{\,2}$

Example 2E.3: Compute the work transfer and change in energy when the extension of a simple elastic spring is changed from −0.16 m to +0.16 m. The spring constant k is 2000 N/m.

Solution: The system can be modeled as a pure translational spring as described above. The energy change for extension from $x_1 = -0.16$ m to $x_2 = +0.16$ m is

$$E_2 - E_1 = \frac{1}{2} k x_2^{\,2} - \frac{1}{2} k x_1^{\,2}$$

$$E_2 - E_1 = \frac{1}{2}(2000 \text{ N/m})(+0.16 \text{ m})^2 - \frac{1}{2}(2000 \text{ N/m})(-0.16 \text{ m})^2$$

$$E_2 - E_1 = 0$$

The first law gives the work transfer

$$-W_{1-2} = E_2 - E_1 = 0$$

Note that the total work transfer is zero; however, the work transfer from $x_1 = -0.16$ m to $x = 0$ is +25.6 J while the work transfer from $x = 0$ to $x_2 = +0.16$ m is −25.6 J.

2.8.3 Gravitational Stored Energy Mode: Pure Gravitational Spring Model

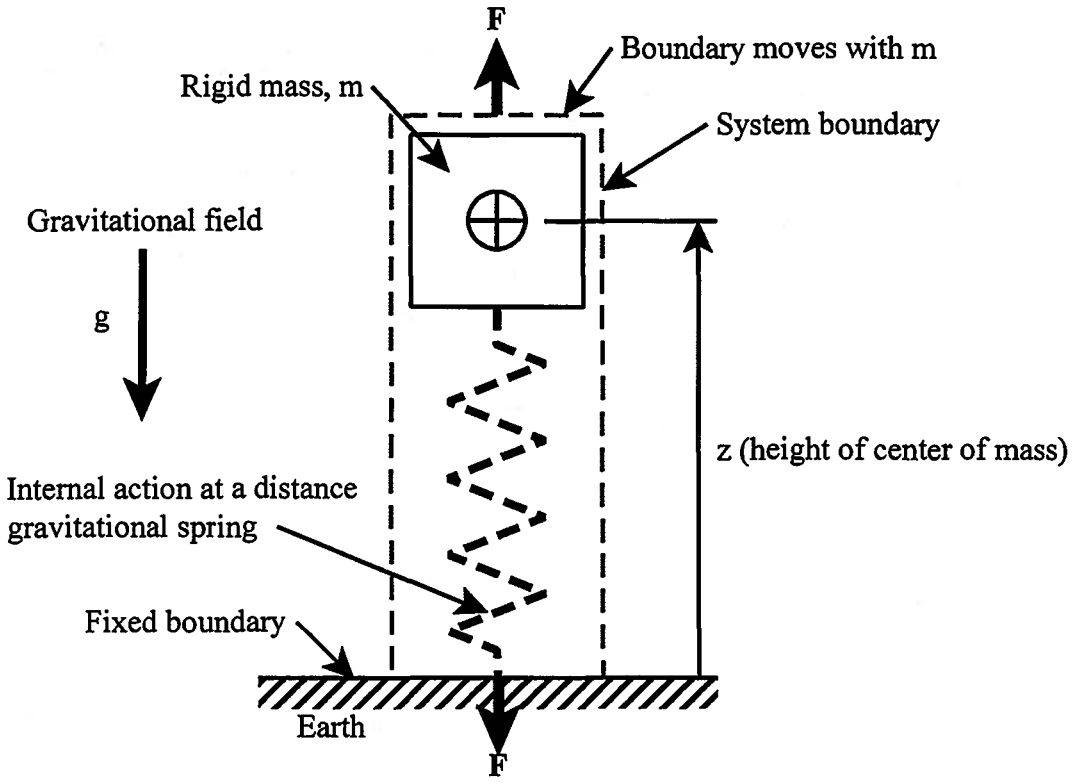

Figure 2.5 Gravitational Energy Storage Mode: Pure Gravitational Spring Model

Physical characteristic:
m = mass
g = acceleration of gravity
$g_{std} = 9.80665$ m/s^2

Properties:
F = through force on the system boundary, positive for tension
z = height of center of mass m, positive upward

Property constitutive relation: $F = mg$

Interaction: $-W_{1-2} = \int_{z_1}^{z_2} \vec{F} \cdot d\vec{r} = \int_{z_1}^{z_2} F dz$

Energy constitutive relation: $(E_2 - E_1)_{gravitational} = mgz_2 - mgz_1$

Example 2E.4: Compute the work transfer required to lift a mass of 100 kg a vertical distance of 1.2 m in a gravitational field of 9.81 m/sec^2.

Solution: The system and the process are defined and modeled as a pure gravitational spring as described above. Application of the first law and substitution of the energy constitutive relation gives

$$-W_{1-2} = E_2 - E_1 = mgz_2 - mgz_1$$

If we take $z_1 = 0$ then $z_2 = 1.2$ m, and the first law becomes

$$-W_{1-2} = (100 \text{ kg})(9.81 \text{ m/sec}^2)(1.2 \text{ m}) - 0$$

$$-W_{1-2} = 1176 \text{ J}$$

The negative sign of the work transfer shows that the work transfer is from the environment to the system.

2.9 The First law of Thermodynamics for an Uncoupled Mechanical System

Consider a system that is uncoupled in the thermodynamic sense so its energy storage modes can be modeled by equation (2.2a). Let the behavior of the system be further restricted in that it can experience work transfer as the only possible form of energy interaction. That is, heat transfer is not a possible energy interaction for this system under any circumstances, so in the absence of any dissipative processes such as those associated with solid or fluid friction, both $Q_{1\text{-}2}$ and $U_{thermal}$ in equation (2.24) become identically zero. Such a system would be known as an uncoupled mechanical system without dissipation, and its energy behavior of the system can be described by combining equations (2.2a) and (2.3) to yield the first law of thermodynamics specific to this type of system.

$$-W_{1\text{-}2} = (E_2 - E_1)_{kinetic} + (E_2 - E_1)_{elastic} + (E_2 - E_1)_{gravitational}$$

$$-W_{1\text{-}2} = \left(\frac{1}{2}m\mathcal{V}_2^{\,2} - \frac{1}{2}m\mathcal{V}_1^{\,2}\right) + \left(\frac{1}{2}kx_2^{\,2} - \frac{1}{2}kx_1^{\,2}\right) + (mgz_2 - mgz_1) \tag{2.24}$$

While at first glance the conditions leading to equation (2.24) might seem highly restrictive, equation (2.24) can be quite useful in engineering practice. There are many circumstances in which it is useful to neglect the effects of friction. For example, equation (2.24) can be useful in estimating the limiting behavior of an uncoupled mechanical system. Such estimates play an important role in system design and are quite common in engineering practice. The following simple examples serve to illustrate this fact.

Example 2E.5: The French high-speed train, TGV-Atlantique, has a normal operating speed of 83.149 m/sec (186 miles/hour). The train consists of two locomotives and ten passenger cars with a total mass of 4.4×10^5 kg (485 tons), and it is propelled by two electric locomotives capable of converting electric power into mechanical power at the rate of 8.8 MW. On a particular section of track, the train enters at a speed of 80 m/sec and an elevation of 0 m and exits at a speed of 40 m/sec and an elevation of 300 m. Estimate the minimum work transfer required to accomplish this change of state and the minimum time required to carry out the process.

Solution: Clearly, the minimum work transfer required will occur in the absence of any dissipative effects such as friction and the drag of the air on the train. If we neglect these, we can model the system (the train) as an uncoupled mechanical system represented by a combination of a pure translational mass and a pure gravitational spring as shown schematically in Figure 2E.5. The work transfer necessary to change the state of the train from ($\mathcal{V}_1$ = 80 m/sec, z_1 = 0 m) to ($\mathcal{V}_2$ = 40 m/sec, z_2 = 300 m) can be determined from the first law for this uncoupled mechanical system. Then

$$-W_{1\text{-}2} = (E_2 - E_1)_{kinetic} + (E_2 - E_1)_{gravitational}$$

$$-W_{1\text{-}2} = \frac{1}{2}m\left(\mathcal{V}_2^{\,2} - \mathcal{V}_1^{\,2}\right) + mg(z_2 - z_1)$$

$$-W_{1\text{-}2} = \frac{1}{2}(4.4 \times 10^5 \text{ kg})\left[(40 \text{ m/sec})^2 - (80 \text{ m/sec})^2\right] + (4.4 \times 10^5 \text{ kg})(9.81 \text{ m/sec}^2)(300 \text{ m} - 0 \text{ m})$$

$$-W_{1\text{-}2} = -1.056 \times 10^9 \text{ J} + 1.2949 \times 10^9 \text{ J}$$

$$W_{1\text{-}2} = -2.3892 \times 10^8 \text{ J}$$

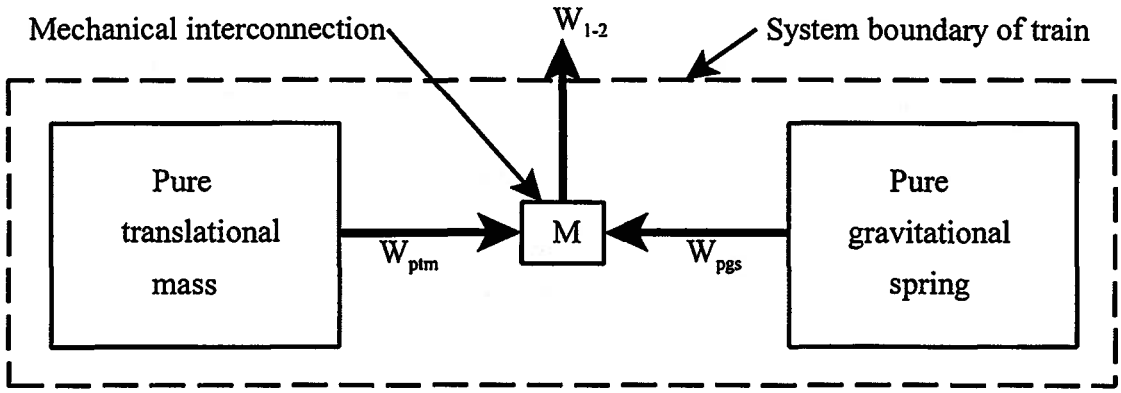

Figure 2E.5 Interaction Diagram for Interaction between Pure translational Mass and a Pure Gravitational Spring

The negative sign of the work transfer indicates that the environment does work on the system in order to change the state of the system (train) as indicated. The energy flow due to work transfer is from the environment into the system in the form of a transfer of electric charge through an electrical potential. If we assume that the work transfer and the power of the locomotives are constant during the time the change of state occurs, the minimum required time is given by

$$\Delta t = \frac{-W_{1\text{-}2}}{-\dot{W}} = \frac{2.3892 \text{ x } 10^8 \text{ J}}{8.8 \text{ x } 10^6 \text{ W}} = 27.15 \text{ sec}$$

Note that even though we can calculate the work transfers W_{ptm} and W_{pgs}, they occur in the model and not in the actual system since the components of the model, the pure translational mass and the pure gravitational spring, represent simultaneously the single lumped mass of the train. It is not possible to find any boundary inside the train across which these two interactions might occur. Note also that interaction W specified in equation (2.24) is the interaction that occurs across the system boundary however that boundary may be defined and not the interaction that might occur internal to the system boundary. The interaction W is the net interaction between the system and the environment and includes the net effect of all internal work transfers.

Clearly, in this example if we had included the both the effects of friction between the wheels of the train and the rails upon which it rides and the friction due to the drag of the air upon the train, the necessary work transfer for the proscribed change of state would have been greater than the estimate given above. In addition, the time required for the change of state would have been greater than that calculated above. We shall take up the effects of friction and drag on the performance of the TGVA in a later example.

Example 2E.6: Consider the game of pinball commonly found in most game rooms on college campuses. (A software simulation of the game can be found in most Microsoft operating systems.) In its typical form, the game consists of a steel ball of mass $M = 67$ gm that is launched up a table inclined at an angle of θ. The table has a length of $L = 1.5$ m and is fitted with a launch track that is curved so that when the ball reaches the apogee of the track it has zero velocity. From this point, the ball starts to roll down the table under the influence of gravity striking various bumpers and flippers in its descent. The launch is effected by having the operator compress a spring that is in contact with the ball in the rest position as shown in Figure 2E6a. The spring is released and the ball begins its movement up the table. In a particular design of this

game, the spring can be modeled as a pure translational spring with a spring constant of $k = 110$ N/m and in the launch position is compressed 6 cm from the free-length (zero stress) position by the operator before being released. Estimate the value of the angle θ.

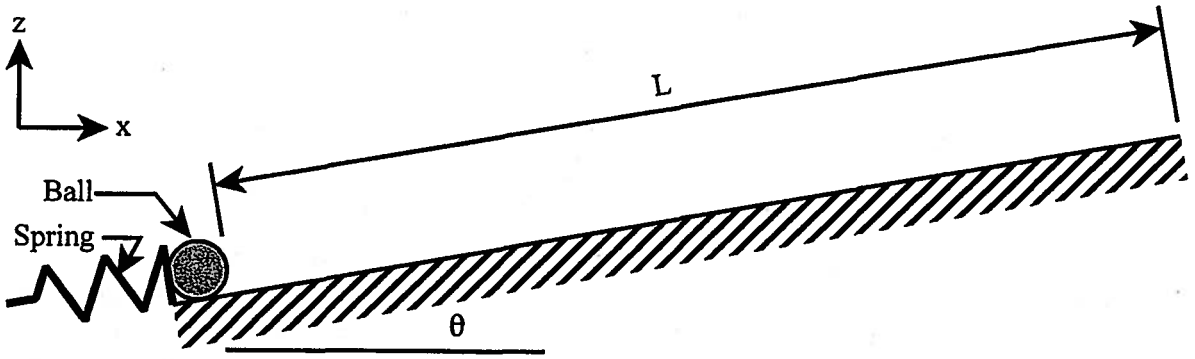

Figure 2E.6a Pinball Game Table

Solution: Consider the system consisting of the spring and the ball. The spring can be modeled as a pure translational spring and the ball can be modeled as a pure gravitational spring and a pur translational mass as shown in Figure 2E.6b. If we neglect the friction between the table and the wall of the launch chute, the analysis will give an estimate of the minimum value of θ. The system of interest is an uncoupled mechanical system whose energy behavior can be

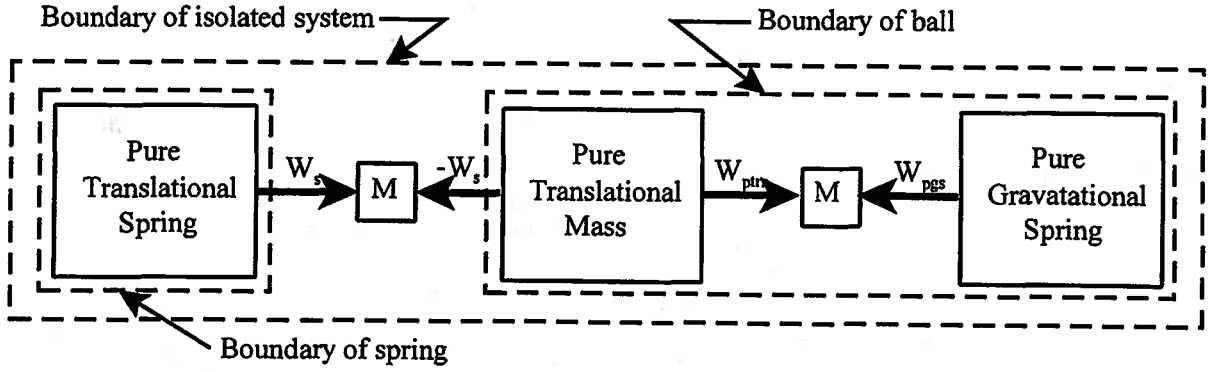

Figure 2E.6b Model of Pinball Game

described by the first law of thermodynamics in the form of equation (2.2a). Thus,

$$-W_{1\text{-}2} = (E_2 - E_1)_{elastic} + (E_2 - E_1)_{gravatational} + (E_2 - E_1)_{kinetic}$$

$$-W_{1\text{-}2} = \frac{1}{2}k\left(x_2^{\,2} - x_1^{\,2}\right) + Mg(z_2 - z_1) + \frac{1}{2}M\left(\mathcal{V}_2^{\,2} - \mathcal{V}_1^{\,2}\right)$$

For the particular case at hand we can define the initial and final states as:

state 1: $x_1 = -0.06$ m, $z_1 = 0$, $\mathcal{V}_1 = 0$ state 2: $x_2 = 0$, $z_2 = L\sin\theta$, $\mathcal{V}_2 = 0$

Note that we have defined the system in such a way that it is an isolated system with $W_{1\text{-}2} = 0$. Then for the states chosen, the first law becomes

$$-W_{1-2} = \frac{1}{2}k\left(x_2^{\,2} - x_1^{\,2}\right) + Mg\left(z_2 - z_1\right) + \frac{1}{2}M\left(\mathcal{G}_2^{\,2} - \mathcal{G}_1^{\,2}\right) = 0$$

$$Mg\left(z_2 - z_1\right) = -\frac{1}{2}k\left(x_2^{\,2} - x_1^{\,2}\right)$$

$$z_2 = L\sin\theta = \frac{kx_1^{\,2}}{2Mg}$$

$$\theta = \arcsin\left(\frac{kx_1^{\,2}}{2LMg}\right) = \arcsin\left(\frac{(110\ \text{N/m})(-0.06\ \text{m})^2}{2(1.5\ \text{m})(0.067\ \text{kg})(9.81\ \text{m/sec}^2)}\right) = 11.58\ ^\circ$$

Note that like the previous example, we cannot identify a physical boundary between the pure gravitational spring and the pure translational mass across which the work transfer shown in the model occurs; that work transfer occurs only in the model and not in the physical system. However, unlike the previous example, there is a physical boundary between the spring and the ball across which the work transfer W_s occurs. In fact, we could have analyzed this situation by defining two separate systems: the ball as one and the spring as the other. The work transfer that occurs between them via the mechanical interconnection is of the same magnitude but opposite sign when viewed from first the spring and then the ball. The first laws for these two systems can be written

$$-\left(W_{1-2}\right)_{spring} = \frac{1}{2}k\left(x_2^{\,2} - x_1^{\,2}\right)$$

$$-\left(W_{1-2}\right)_{ball} = Mg\left(z_2 - z_1\right) + \frac{1}{2}M\left(\mathcal{G}_2^{\,2} - \mathcal{G}_1^{\,2}\right)$$

but since

$$\left(W_{1-2}\right)_{spring} = -\left(W_{1-2}\right)_{ball}$$

we can combine the two first laws to obtain

$$\frac{1}{2}k\left(x_2^{\,2} - x_1^{\,2}\right) + Mg\left(z_2 - z_1\right) + \frac{1}{2}M\left(\mathcal{G}_2^{\,2} - \mathcal{G}_1^{\,2}\right) = 0$$

which is the same result we obtained by defining an isolated system in the first instance.

Note that we have considered only uncoupled mechanical systems in which only the first three terms on the right-hand side of equation (2.2a) are relevant. These are considered the uncoupled modes of mechanical energy storage in that the values of these terms can be changed only by means of a work transfer, and a nonzero value for their sum requires that the term on the left-hand side of the first law for uncoupled mechanical systems, equation (2.24), be nonzero. We have yet to take up the question of the fourth term on the right-hand side of equation (2.2a) which can be changed only by means a heat transfer interaction which is not included in equation (2.24). In order to do this, we need the second law of thermodynamics which is one of the topics addressed in the next chapter of our development. In Chapter 3 we shall also examine the nature of thermodynamic coupling; however, before we do so, we want to examine the concept of coupling in a more general sense. Thermodynamic coupling is just one example, albeit the most important example for thermal-fluids engineering, of the many ways systems can be coupled. To illustrate the coupling concept more fully, we now consider in detail one of these other ways a system can be coupled. We now examine the example of a system that is coupled in the electro-mechanical sense.

2.10 The First Law of Thermodynamics for a Coupled Electro-mechanical System

In the case of the mechanically uncoupled systems shown above, it was obvious from their construction that the systems were uncoupled and therefore possessed separate and distinct energy storage modes associated with each aspect of system behavior. Suppose now, however, we are confronted with a system with unknown internal structure. In order to analyze the behavior of the system, we need to construct a suitable model as we did in the case of the pure mechanical system models previously. To do this, we first need to determine whether the system is coupled or uncoupled. Thus, we require a test for coupling in terms of the external behavior of the system without knowledge of the internal construction.

Suppose, for example, we are presented with an electro-mechanical "black box." We already know that if the internal construction of the box is known, we can ascertain whether the box is electro-mechanically coupled or uncoupled. For instance, if the box is composed of two pure conservative system elements – one a pure translational spring, the other a pure electrical capacitance – the box is uncoupled electro-mechanically. This system, as shown schematically in Figure 2.6, is capable of mechanical work transfer associated with the motion of its boundary

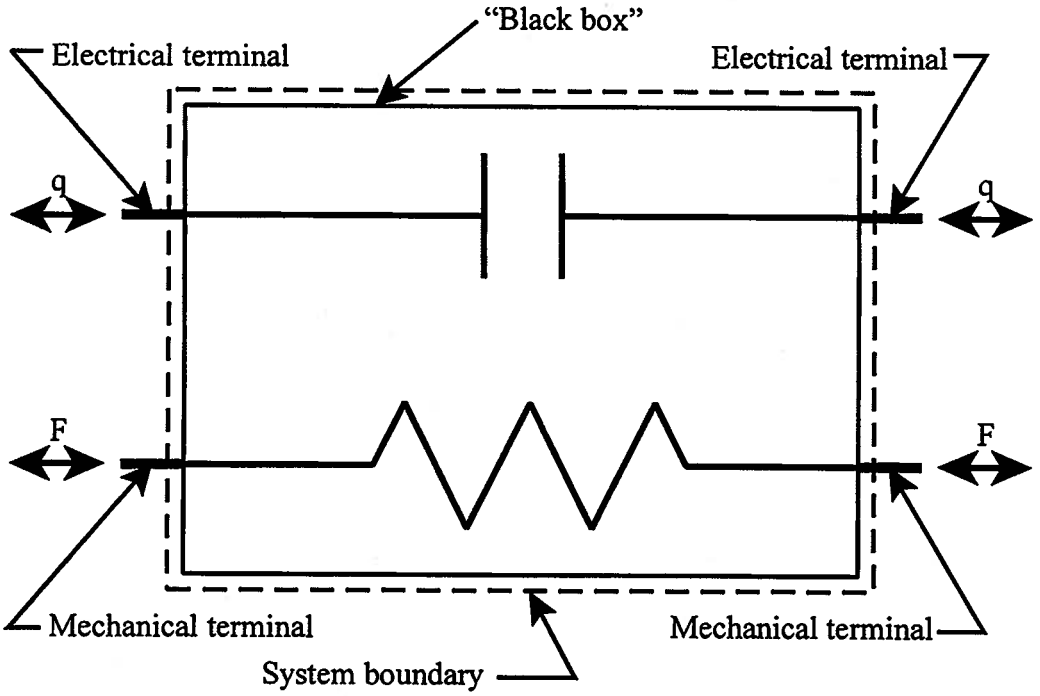

Figure 2.6 An Uncoupled Electro-mechanical System

under the action of a force applied by the environment and an electrical work transfer associated with the transfer of charge from one of its electrical terminals to the other. For this internal construction we know the relevant constitutive relations to be

$$F = kx \quad \text{and} \quad v = \frac{q}{C} \tag{2.25}$$

where k is the spring constant and C is the electrical capacitance. Had we not known the internal construction, the constitutive relations could have been determined by experiment.

From the definition of the work transfer we have

$$-(W_{1-2})_{electrical} = \int_{q_1}^{q_2} v\,dq \quad \text{and} \quad -(W_{1-2})_{mechanical} = \int_{x_1}^{x_2} F\,dx \tag{2.26}$$

and from the first law we have

$$(E_2 - E_1)_{uncoupled} = (E_2 - E_1)_{mechanical} + (E_2 - E_1)_{electrical} = \int_{x_1}^{x_2} F\,dx + \int_{q_1}^{q_2} v\,dq \tag{2.27}$$

For this uncoupled electro-mechanical system, it is obvious that the mechanical work transfer affects only the mechanical properties F and x and not the electrical properties. Furthermore, the effect of the mechanical work transfer is manifest as a change in the stored mechanical energy $(E_2 - E_1)_{mechanical}$. In a similar fashion, electrical work transfer affects only the electrical properties v and q and not the mechanical properties. In addition, the effect of the electrical work transfer is manifest as a change in the stored electrical energy $(E_2 - E_1)_{electrical}$. Because of the "pure conservative" nature of the components of this uncoupled system, there is no dissipation (mechanical friction in the case of the spring and electrical resistance in the case of the capacitance). Then the permissible paths of the processes that this system can experience are as shown in Figure 2.7.

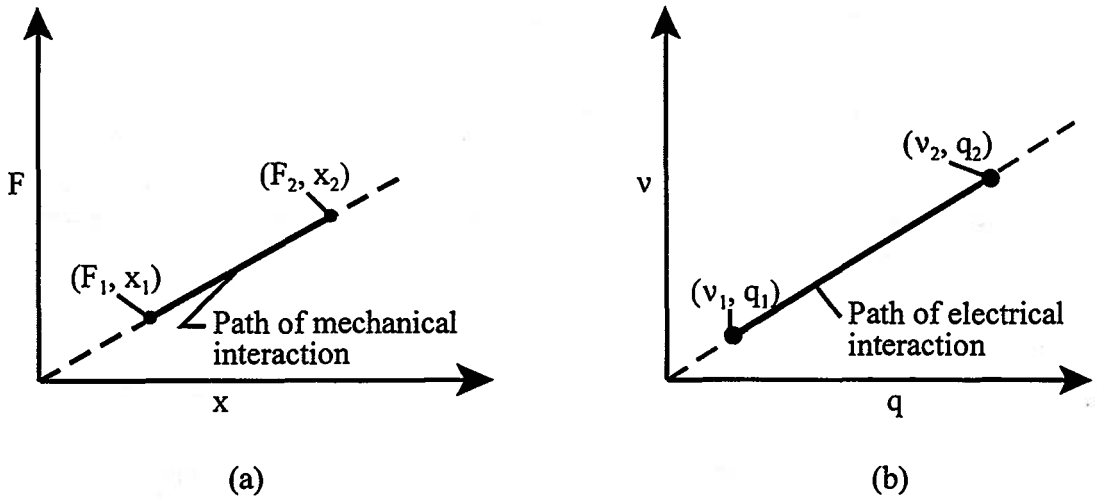

Figure 2.7 Paths of Mechanical and Electrical Interactions in an Uncoupled Electro-mechanical System

It follows that all paths of all processes executed by this system must be somewhere along the lines shown on the F-x plane and the v-q plane of Figure 2.7. Then for any cycle executed by this system, not only do we have

$$-\oint \delta W_{net} = -\oint \delta W_{mechanical} - \oint \delta W_{electrical} = \oint dE_{uncoupled} = \oint d\left(E_{mechanical} + E_{electrical}\right) = 0 \tag{2.28}$$

but also

$$-\oint \delta W_{mechanical} = \oint dE_{mechanical} = 0 \tag{2.29}$$

and

$$-\oint \delta W_{electrical} = \oint dE_{electrical} = 0 \tag{2.30}$$

as well.

It is apparent from equations (2.29) and (2.30) that during the cycle the system

experiences no net mechanical interaction and no net electrical interaction. In this sense, the system can be regarded as electro-mechanically uncoupled. In fact, we can use equations (2.29) and (2.30) to formulate a generalized test for an uncoupled system, viz.

> For a given system, the properties associated with two different energy transfer interactions are uncoupled if for *all* cycles executed by the system, in the absence of *any dissipative effects*, the net interaction for *each* mode of energy transfer is individually zero. Thus,
>
> $$\oint \delta(\text{interaction}) = 0 \qquad (2.31)$$

Each group of properties can then be used to characterize a separate, independent aspect of system behavior. As a consequence of equation (2.31), it is possible to define only a single stored energy form associated with a single given interaction, and this single stored energy form can be altered only by the one particular type of non-dissipative interaction. All other types of non-dissipative interactions will not affect it.

Thus, for a system of unknown internal construction which is capable of two distinctly different energy interactions, we can determine whether the properties necessary to describe each of these two interactions are coupled in any way by simply applying the above test. If the properties in question pass the above test, they are uncoupled, and it is then possible, as far as these two interactions are concerned, to construct a system model composed solely of "pure conservative" system elements. It follows, then, that the system will have separate constitutive relations for each aspect of system behavior. Typically, these models are quite simple from a thermodynamic point of view, and because of their simplicity, they tend to be of limited utility in thermal-fluids systems devoted to energy conversion.

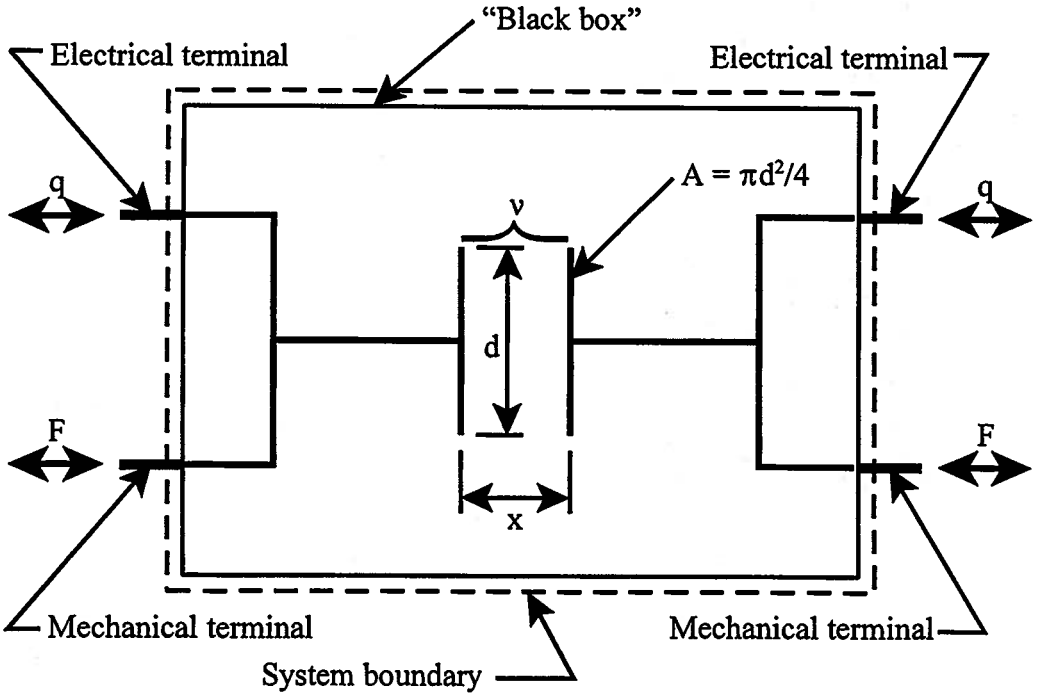

Figure 2.8 A Coupled Electro-mechanical System

Of greater interest are those systems that exhibit coupling of some sort. For example, suppose that the internal construction of our "black box" consists of a parallel plate capacitor in which two plates of area A are separated by a mechanically variable vacuum gap of thickness x as shown in Figure 2.8. Such a system is capable of experiencing a work transfer by means of a displacement of its mechanical terminals or by means of a transfer of electrical charge from one electrical terminal to the other. However, this situation is quite different from the one depicted in Figure 2.6. Specifically, if the electric potential difference between the plates is v and the charge on the capacitor is q, the constitutive relations for the system can be determined by experiment to be

$$v = \frac{qx}{\varepsilon_0 A} \quad \text{and} \quad F = \frac{vq}{2x} = \frac{q^2}{2\varepsilon_0 A} \tag{2.32}$$

where ε_0 is the permitivity of free space and F is the external force required to hold one plate in a static position. Then for an infinitesimal change of state of this system, the first law becomes

$$\begin{aligned} -\delta W_{net} &= -\delta W_{mechanical} - \delta W_{electrical} = dE_{coupled} \\ dE_{coupled} &= F dx + v dq \end{aligned} \tag{2.33}$$

and for a finite change of state from state 1 to state 2, we have

$$\left(E_2 - E_1\right)_{coupled} = \int_{x_1}^{x_2} F dx + \int_{q_1}^{q_2} v dq \tag{2.34}$$

which appears similar to equation (2.27), but is quite different since the constitutive relations of equations (2.32) each contain both mechanical and electrical properties.

In order to integrate the right-hand side of equation (2.34), we need to establish a path since these integrals are line integrals. In particular, we would like to apply the test for coupling of equation (2.31), so we need to find just one cycle of the system for which equation (2.31) is not satisfied. Consider the cycle *ABCD* shown in Figure 2.9. The coupled nature of the constitutive relations (2.32) causes the path of integration of equation (2.34) to enclose an area whereas in the uncoupled case, the paths are simply lines with no enclosed area (cf. Figure 2.7).

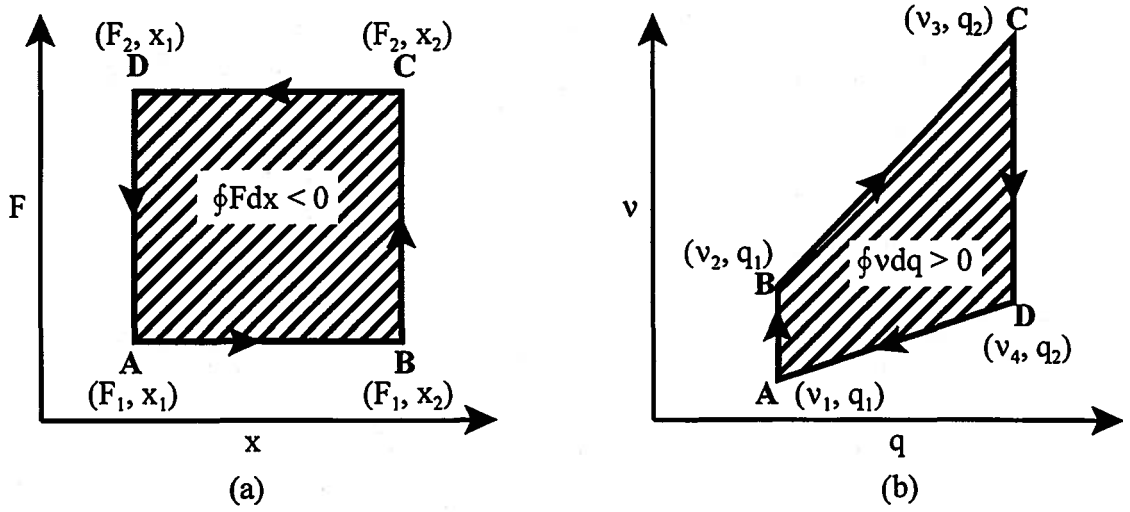

Figure 2.9 Cycle of an Electro-mechanically Coupled System

Physically, the cycle *ABCD* would be carried out in the following steps:

Path $A \rightarrow B$: Charge q_1 fixed and force F_1 fixed as plate spacing increases from x_1 to x_2 by means of a mechanical interaction

Path $B \rightarrow C$: Plate spacing x_2 fixed as charge increases from q_1 to q_2 by means of an electrical interaction

Path $C \rightarrow D$: Charge q_2 fixed and force F_2 fixed as plate spacing decreases from x_2 to x_1 by means of a mechanical interaction

Path $D \rightarrow A$: Plate spacing x_1 fixed as charge increases from q_2 to q_1 by means of an electrical interaction

If we apply the first law to each process of the cycle in turn, we obtain the following results:

$$\begin{aligned}
(E_B - E_A)_{coupled} &= \int_{x_1}^{x_2} F dx + \int_{q_1}^{q_2} v dq = F_1 (x_2 - x_1) \\
(E_C - E_B)_{coupled} &= \int_{x_1}^{x_2} F dx + \int_{q_1}^{q_2} v dq = \frac{x_2}{\varepsilon_0 A}\left(\frac{q_2^2}{2} - \frac{q_1^2}{2}\right) \\
(E_2 - E_1)_{coupled} &= \int_{x_1}^{x_2} F dx + \int_{q_1}^{q_2} v dq = F_2 (x_1 - x_2) \\
(E_2 - E_1)_{coupled} &= \int_{x_1}^{x_2} F dx + \int_{q_1}^{q_2} v dq = \frac{x_1}{\varepsilon_0 A}\left(\frac{q_1^2}{2} - \frac{q_2^2}{2}\right)
\end{aligned} \tag{2.35}$$

and

$$\begin{aligned}
-\oint \delta W_{mechanical} &= F_1 (x_2 - x_1) + F_2 (x_1 - x_2) < 0 \\
-\oint \delta W_{electrical} &= \frac{x_2}{\varepsilon_0 A}\left(\frac{q_2^2}{2} - \frac{q_1^2}{2}\right) + \frac{x_1}{\varepsilon_0 A}\left(\frac{q_1^2}{2} - \frac{q_2^2}{2}\right) > 0 \\
-\oint \delta W_{net} &= -\oint \delta W_{mechanical} - \oint \delta W_{electrical} = 0
\end{aligned} \tag{2.36}$$

Thus, during this cycle, energy enters the system by means of an electrical work transfer and leaves by means of a mechanical work transfer. For this cycle which has no dissipative processes, the net work transfer and the energy change are zero and the first law is satisfied. The net mechanical interaction of equations (2.36) is represented by the negative area enclosed by the path *ABCD* on Figure 2.9, and the net electrical interaction of equations (2.36) is represented by the positive area enclosed by the path *ABCD* on Figure 2.9. The magnitudes of these areas are such that the net interaction for the cycle as represented by their algebraic sum is zero.

We have shown, then, that there exists at least one cycle for which the net mechanical interaction is nonzero and the net electrical interaction is nonzero. That is,

$$\oint \delta W_{mechanical} \neq 0 \quad \text{and} \quad \oint \delta W_{electrical} \neq 0 \tag{2.37}$$

but the first law for this system without dissipation requires that

$$\oint \delta W_{net} = 0 = \oint \delta W_{mechanical} + \oint \delta W_{electrical}$$

or

$$\oint \delta W_{electrical} = -\oint \delta W_{mechanical} \tag{2.38}$$

Equations (2.38) show that the properties associated with the two types of interactions are

interrelated, that is, coupled to one another. Clearly, since we knew the specific constitutive relations at the outset, we knew that the properties were coupled and that there was no separate mechanical constitutive relation and no separate electrical constitutive relation. On the basis of the information gained from this example, we can formulate the following general test for coupled properties:

> For a given system, the properties associated with two different energy transfer interactions are coupled if for at least one cycle executed by the system, in the *absence of any dissipative effects*, the net interaction for each mode of energy transfer is individually nonzero. Thus
>
> $$\oint \delta(\text{interaction}) \neq 0 \tag{2.39}$$
>
> However, to satisfy the first law of thermodynamics, the net energy interaction for *all* modes of energy transfer taken together must be zero for *any* cycle.

As a consequence of equation (2.39), the coupled system does not have a separate aspect of behavior associated a given interaction. The system simply possesses a coupled state that cannot be traced to a particular interaction. Any one of the coupled interactions is capable of changing all of the properties (in the present case, mechanical or electrical) of the system. In particular, the stored coupled energy is a property and is fixed by the specification of the values for a set of independent properties of the system. For example, in the case of the electro-mechanically coupled system, the change in energy for a change of state from a state 1 with the values of the independent properties (x_1, q_1) to a state 2 with the values of the independent properties (x_2, q_2) can be determined by the integration along a general path in the manner of equation (2.35), viz.

$$\left[E_2(x_2,q_2) - E_1(x_1,q_1)\right]_{coupled} = \frac{1}{2\varepsilon_0 A}\left(x_2 q_2^{\,2} - x_1 q_1^{\,2}\right) \tag{2.40}$$

Clearly the energy is electro-mechanical in nature and not the sum of a separate mechanical energy and a separate electrical energy.

An additional consequence of the coupling is that the system model cannot be constructed of pure system models that each represent some aspect of system behavior. The system model must now have constitutive relations that include all the coupled properties. Of course while some of the properties necessary to specify the state of the system may be coupled, there may be still others that are uncoupled. In such cases, the complete system model will include both coupled and uncoupled components with pure system models used to model the uncoupled aspects of system behavior.

While we have now developed formal tests for coupling in thermal-fluid systems, the full significance of the coupling remains to be shown. Coupling can exist between many different aspects of system behavior, but it is the coupling between the thermal and mechanical aspects of system behavior that interests us most. As we shall see, it is this form of coupling that allows us to covert the energy stored in the fossil fuels that nature has provided into mechanical energy that can be used to meet the needs of society.

Our work thus far has been focused on the work transfer interaction, but the thermodynamic coupling that is of such paramount importance in the energy conversion process is based upon the heat transfer interaction. In Chapter 3, we shall take up the heat transfer

interaction as it applies to the changes that it can produce within the system boundary. Our study of this topic will enable us to formulate the second law of thermodynamics. It will also reveal some of the important differences between the two energy interactions, work transfer and heat transfer. We shall then develop a simple model appropriate for the uncoupled thermal energy storage mode as well as a form of the first law of thermodynamics appropriate for a generalized uncoupled system without dissipation. We shall also develop another simple model that provides a connection between thermal and mechanical system behavior when dissipation is present. We shall also introduce a new property, entropy, that will help us to track the effects of heat transfer on system behavior.

APPENDIX

FOSSIL FUELS AS ENERGY RESOURCES

Virtually all of the goods and services that we desire in modern society require energy for their production, transportation, or consumption. Nature has given us the necessary energy stored in the hydrocarbon bonds of fossil fuels (coal, oil, and natural gas). This chemical binding energy can usually be released by oxidizing the hydrogen and carbon atoms that make up the fossil fuel thereby taking them from their metastable equilibrium state in the fossil fuel to their stable equilibrium state in the products of the oxidation reaction. The energy released in this manner usually appears in the form of a heat transfer. It is the task of the thermal-fluids engineer to convert the energy released in this manner into a form that is most useful to accomplish the objective at hand.

One way to accomplish this is through the use of a system that operates in cycles. For such a system, the first law of thermodynamics states that the *net* energy transferred to the cyclic system in the form of a heat transfer from the environment, of which the oxidation reaction is but one part, can be converted into a work transfer, but the second law of thermodynamics states that of the energy transferred *into* the system in the form of a heat transfer from the oxidation reaction, only a small portion of it can be converted into a work transfer. This is a consequence of the fact that the entropy that accompanies the energy in a heat transfer must ultimately be returned to the environment in the form of another heat transfer interaction. Since no entropy can be transferred with the work transfer, this means that a significant portion of the incoming energy (in the form of a heat transfer) must be returned to the environment (also in the form of a heat transfer) along with the entropy. Thus, the second law of thermodynamics requires that *net* energy transfer into the cyclic system via heat transfer be significantly less than the *total* amount entering. It follows, then, that if the energy entering the cyclic system originated as a heat transfer from the oxidation of a fossil fuel, only a small portion, typically on the order of 30 percent, of this energy can be converted to a work transfer. The ratio of the energy leaving the cyclic system in the form of a work transfer to the energy entering the cyclic system in the form of a heat transfer is known as the energy conversion efficiency of the cyclic system. One of the major challenges facing the thermal-fluids engineer, is the maximization of this energy conversion efficiency. Thermal-fluids engineers are continually searching for new methods of carrying out the energy conversion process that will produce the largest possible work transfer from a given heat transfer. Recent advances in energy conversion technology have increased energy conversion efficiency to levels as high as 60 percent for economically practical systems.

To put this in perspective, it is worth examining the demand for fossil fuels on the national level in the United States. Because the magnitude of energy demand on this level is so large, energy is usually expressed in terms of "quads" where one "quad" is one quadrillion or 10^{15} Btu. Note that this is not a recognized unit for energy in the SI unit system. The conversion factors for various unit systems are:

$$
\begin{aligned}
1 \text{ quad} &= 10^{15} \text{ Btu} = 1.055 \times 10^{18} \text{ Joules} \\
&= 172 \times 10^{6} \text{ barrels of fuel oil} \\
&= 44.34 \times 10^{6} \text{ tons of coal} \\
&= 10^{12} \text{ cubic feet of natural gas} \\
&= 2.93 \times 10^{11} \text{ kilowatt-hours electric power}
\end{aligned}
$$

For an energy conversion efficiency of 30 percent, the energy transferred from the fuel as 1 quad of heat transfer produces 0.3 quad of net electrical power. Thus, from the point of view of power generation, 1 quad of fuel is equivalent to 0.849×10^{11} kilowatt-hours net electrical power. In the United States in recent years, the U.S. Energy Information Administration estimates that annual fuel demand has been about 75 quads from the following sources:

Coal	16.25 quads
Fuel oil	
Domestic	14.6 quads
Imported	16.4 quads
Natural gas	18.75 quads
Nuclear	6 quads
Renewable	3 quads

Distribution of fuel demand by use is estimated at:

Power generation	20 quads
Space heating	11 quads
Transportation	16 quads
Industrial, other than power	25 quads
Other	4 quads

Of the several fuel types, natural gas is a favorite since it is easily transported by pipeline, produces minimal pollutants upon oxidation, and requires simple hardware for utilization. For these reasons and the fact that the price of natural gas is regulated federally, it is considered to be relatively cheap fuel. Except for untapped reserves known to exist (1) near the coast of the Gulf of Mexico in very deep geopressured/geothermal aquifers and (2) in difficult-to-separate Appalachian shale formations, U.S. natural gas supplies have been predicted to last 10-20 years; however, such predictions are not very reliable because of the variable effects of economic and regulatory factors on consumption, production, and exploration. For example, it was estimated in 1948 that natural gas reserves would last approximately 35 more years.

On the other hand, the technically and economically recoverable reserves of coal in the U.S. are estimated to be 4.727×10^{11} tons. Unfortunately, coal is a "dirty" fuel because it contains a large number of impurities such as sulfur, nitrogen, and ash that produce pollutants upon oxidation. However, methane, one of the major components of natural gas, can be produced from coal by distillation. Coal can then be used to replace natural gas supplies as natural gas reserves are exhausted.

Problems

2.1 (a) Estimate the energy stored in a nine volt battery used in transistor radios, smoke detectors for the home, etc.

(b) Estimate the energy stored in a car battery.

(c) Estimate the energy stored in a cord of hardwood firewood.

(d) Estimate the energy stored in a gallon of gasoline.

2.2 A world-class sprinter runs the 200 meter dash in 19.32 sec. If the mass of the sprinter is 100 kg and if his acceleration is constant throughout the race, calculate his kinetic energy at the end of the dash. Calculate the average power (in horsepower, where 1 HP = 745.7 W) he expends during the race. If the typical efficiency of human effort for an athlete in good condition is about 20%, estimate the amount of energy consumed from the sprinter's reserves during the race. If the energy content of a chocolate bar is 200 calories (Food manufacturers specify the energy content of their products in "big" calories which are actually kilocalories.), how many chocolate bars would be required to supply the necessary energy for the race?

2.3 A very fast top-fuel dragster can complete the quarter-mile in 4.5 sec. If a typical dragster has a mass of 1000 kg and if the acceleration is constant throughout the quarter-mile, calculate the speed (in miles per hour) at the end of the quarter-mile. Also, calculate the average horsepower developed by the engine (1 HP = 745.7 W). If the energy conversion efficiency of the engine is 25%, calculate the amount of fuel consumed by the dragster. The fuel used in these vehicles is nitromethane, CH_3NO_2, which has an energy content (usually referred to as its heating value) of 11.629 MJ/kg. If the heating value of gasoline (approximately C_8H_{18}) is 44 MJ/kg, why don't these dragsters use gasoline instead of a fuel with such a low heating value?

2.4 A fully loaded commercial airliner has a mass of 3×10^5 kg. It begins its flight from rest at sea level and accelerates to a cruise speed of 268 m/sec at an altitude of 11 km.

(a) If the fuel used by the engines has an energy content (usually referred to as its heating value) of 42.5 MJ/kg, estimate the minimum amount of fuel required to reach cruise speed and altitude assuming that all the energy contained in the fuel can be used for propulsion and that the mass of the aircraft remains constant throughout the acceleration to cruise speed.

(b) Considering that the propulsion engines are heat engines whose energy conversion efficiency (conversion of energy in the form of heat transfer from the fuel to propulsive work transfer to the aircraft) is limited by the second law of thermodynamics, revise your estimate reported in part (a) above.

(c) What happened to the energy that represents the difference between your two estimates?

2.5 Roger Clemens, an extraordinary major league baseball pitcher formerly of the Boston Red Sox, can throw a baseball (mass = 255.4 gm) at a consistent speed of 90 miles/hour (measured at home plate) throughout a game.

(a) In a recent game Clemens required 115 pitches to complete the game. Estimate the amount of energy he expended during the game just throwing the ball. Note that the energy

conversion efficiency of a human engaged in this type of activity is about 15%.

(b) The energy content of a chocolate candy bar is approximately 200 calories. (Food manufacturers specify the energy content of their products in "big" calories which are actually kilocalories.) Estimate the number of chocolate candy bars Clemens would have to consume in this game in order to maintain his mass.

2.6 Consider the fossil fuel data presented in the Appendix of Chapter 2. If the fuel demand for natural gas and coal in the U.S. were to remain constant and were to be met only from coal reserves in the future, estimate the "life" of U.S. coal reserves.

2.7 A rigid mass M hangs from a steel cable, stretching the cable a length x_1 beyond its free length $x_0 = 0$. The mass is raised just enough to relieve the tension in the cable and is then dropped.

(a) Describe a model that would enable you to determine the maximum force on the cable after the mass is dropped.

(b) What is the maximum force on the cable?

(c) What are the limitations of your model?

2.8 As shown in Figure 2P.8, a child's toy consists of a small car ($m_{car} = 0.5$ kg) that travels on a track after being released from rest from the position A ($v_A = 0$, $z_A = 1$ m). The car travels down the incline and enters the loop-the-loop section of track at location B ($v_B = ?$, $z_B = 0$ m). If the car has sufficient speed at location B, the car travels around the loop and exits again at location B traveling in its original direction. As the designer of this toy, it is necessary for you to specify the maximum diameter of the loop-the-loop section. To do this, you assume that there is no friction between the car and the track and you model the situation appropriately.

(a) For the car as a system, calculate the work transfer for the process that takes the car from position A to position B.

(b) What is the velocity of the car at position B?

(c) What is the maximum possible value of the diameter D for the car to stay on the track at position C?

(d) What is the velocity of the car at position C?

(e) After exiting the loop at position B, what is the maximum altitude that the car can attain?

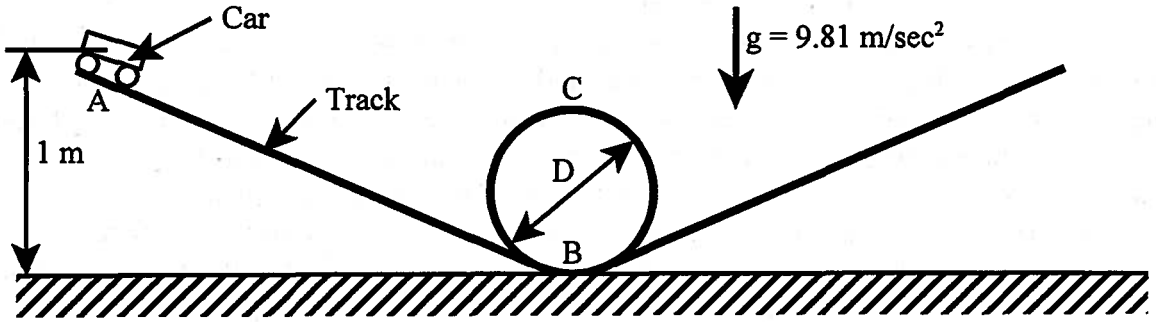

Figure 2P.8

2.9 As shown in Figure 2P.9, a sphere of mass m_{sphere} = 10 kg is suspended from a massless rod attached to a frictionless pivot bearing. The support rod has a length L = 10 m measured from the center of the sphere to the center of the pivot bearing. In the initial state of the sphere, it is held motionless by a support string in a position such that the support rod is horizontal. There is a pure translational spring of spring constant k located with its axis horizontal at a position 10 m below the center of the pivot bearing. In its initial state, the spring is at its free length. The support string is cut and the sphere is allowed to descend. The free end of the spring is located so that the spring and the sphere make contact when the support rod is vertical.

(a) Describe in words the history of the motion of the spring and the sphere after the support string is cut.

(b) For the sphere as a system, determine the work transfer for the process by which the spring moves from its initial state to the state where it just begins to make contact with the spring.

(c) Determine the value of the spring constant k such that the maximum deflection of the spring is 1 cm. Assume that the radius of the sphere is much larger than 1 cm.

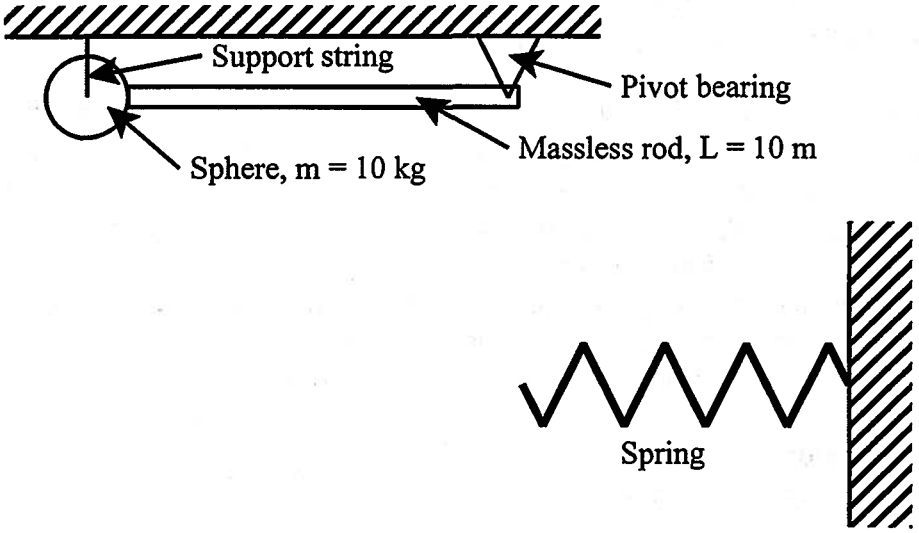

Figure 2P.9

2.10 In its simplest form, a steam power plant, which uses water as the working fluid, consists of four major components: (1) a steam generator which converts the water to steam at the same pressure, (2) a positive shaft work machine (usually a turbine) which extracts the work from the steam as the steam decreases in pressure, (3) a condenser which converts the steam back into water at the same pressure as the discharge from the positive shaft work machine, and (4) a pump that increases the pressure of the water back to the level maintained in the steam generator. Thus, the water experiences a cyclic change of state as it circulates through the plant.

In a particular design, each kilogram of water, as it circulates through the plant, experiences a positive heat transfer of 1200 kJ from the oxidation of a fossil fuel in the steam generator during each cycle. In addition, the net positive work transfer experienced by each kilogram of water during a cycle is 400 kJ. What is the heat transfer between the water and the coolant used in the condenser as the water passes through each cycle?

2.11 The state of a given closed system can be changed from state 1 to state 2 by two processes A and B. For process A the heat transfer for the system is $(Q_{1\text{-}2})_A = +15$ kJ and the work transfer is $(W_{1\text{-}2})_A = +4$ kJ. For process B the work transfer is $(W_{1\text{-}2})_B = -19$ kJ.

(a) For process B, what is the heat transfer $(Q_{1\text{-}2})_B$?

(b) In yet another process C for this same system, the state is changed from state 1 to state 2 with no heat transfer $(Q_{1\text{-}2})_C = 0$. What work transfer $(W_{1\text{-}2})_C$ would be required?

(c) What must be the relation between the work transfer and the heat transfer for any process that changes the state of the same system from state 1 to state 2?

2.12 As shown in the state diagram of Figure 2P.12, a closed system with two independent properties undergoes a process that changes its state from state *a* to state *b* along path *a-c-b*. During this process, the heat transfer is $Q_{a\text{-}c\text{-}b} = 30$ kJ and the work transfer is $W_{a\text{-}c\text{-}b} = 25$ kJ.

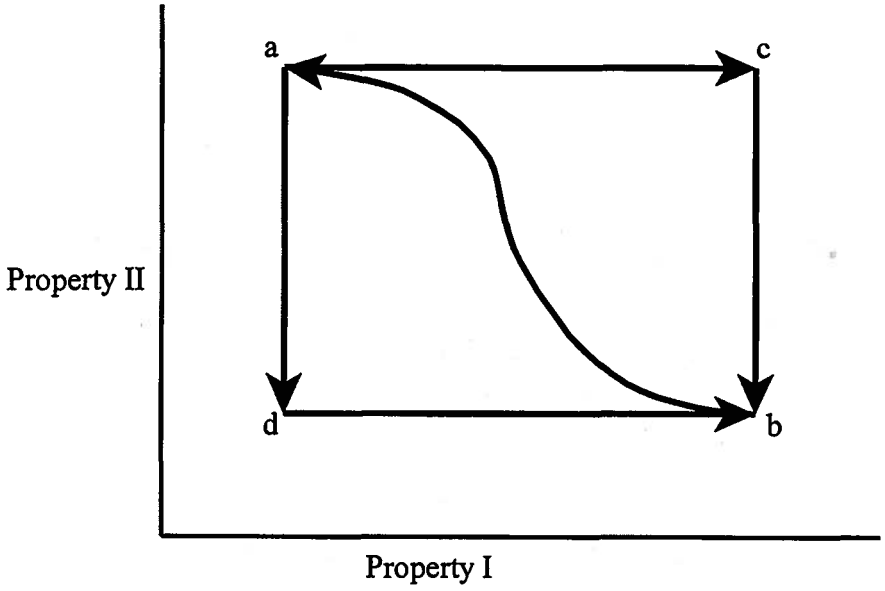

Figure 2P.12

(a) If the system follows the path *a-d-b* while experiencing a work transfer of $W_{a\text{-}d\text{-}b} = 7.6$ kJ, determine the heat transfer $Q_{a\text{-}d\text{-}b}$ for the same path.

(b) If the system now returns directly from state *b* to state *a* over the path shown while experiencing a work transfer of $W_{b\text{-}a} = -18.5$ kJ, what is the heat transfer $Q_{b\text{-}a}$ for the process along the path *b-a*?

(c) Determine the heat transfer for the paths *a-c* and *c-b* if the energy of the system at state *a* is $E_a = 7.7$ kJ, the energy of the system at state *c* is $E_c = 46.0$ kJ, and processes *a-d* and *c-b* are zero work transfer processes.

2.13 The *conservative* (no dissipation) mechanical system shown in Figure 2P.13 has two means for work transfer interactions. One means is by translation, x, of the shaft while under tension, F. The other means is by a torque, τ, along the shaft rotating at an angular velocity, ω. The state of the system is completely specified when x and ω are specified. The constitutive relations for the

system are:

$$\tau = A\frac{d}{dt}\left[(B-x)^2\,\omega\right] \qquad 0<x<B$$

$$F = A(B-x)\omega^2 \qquad 0<x<B$$

The work transfer along the rotating shaft in terms of τ and ω is given by

$$-\delta W_{rotating} = \tau d\theta = \tau\frac{d\theta}{dt}dt = \tau\omega dt$$

$$-\delta W_{rotating} = A\omega d\left[(B-x)^2\,\omega\right]$$

The work transfer along the translating shaft is

$$-\delta W_{translational} = Fdx$$

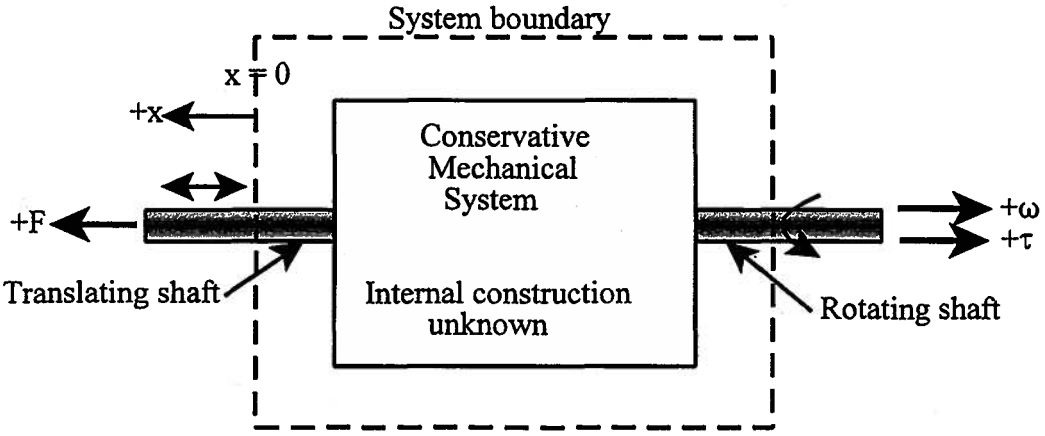

Figure 2P.13

(a) With the aid of the proper test, determine whether the two means of work transfer for this system are coupled.

(b) Determine the energy of this system as a function of x and ω. The energy of the system is zero in the state for which $x = 0$ and $\omega = 0$.

(c) Determine the two work transfers and the energy change for the system when the system changes from x_1 to x_2 at constant ω ($\omega \neq 0$ and $x_2 > x_1$).

2.14 The solenoid shown in Figure 2P.14 has the following characteristics:

The inductance of the coil depends upon the position of the plunger and is given by

$$L = \frac{5.2 \text{ x } 10^{-2} \text{ m henry}}{x + 10^{-4} \text{ m}}$$

where x is the displacement of the plunger in mm from the full "in" position ($x = 0$). The external tensile force to hold the plunger at a position x depends upon the current in the coil and is given by

$$F = \left(2.6 \text{ x } 10^{-2}\,\frac{\text{Nm}^2}{\text{amp}^2}\right)\frac{i^2}{\left(x + 10^{-4} \text{ m}\right)^2}$$

These two relations are valid for $0 < x \leq 10$ mm and $F \leq 650$ N. Both electrical and mechanical dissipation are negligible in the model. Note:

$$\lambda = Li \quad \text{and} \quad v = \frac{d\lambda}{dt} = \frac{d}{dt}(Li)$$

where v is the voltage at the electrical terminals.

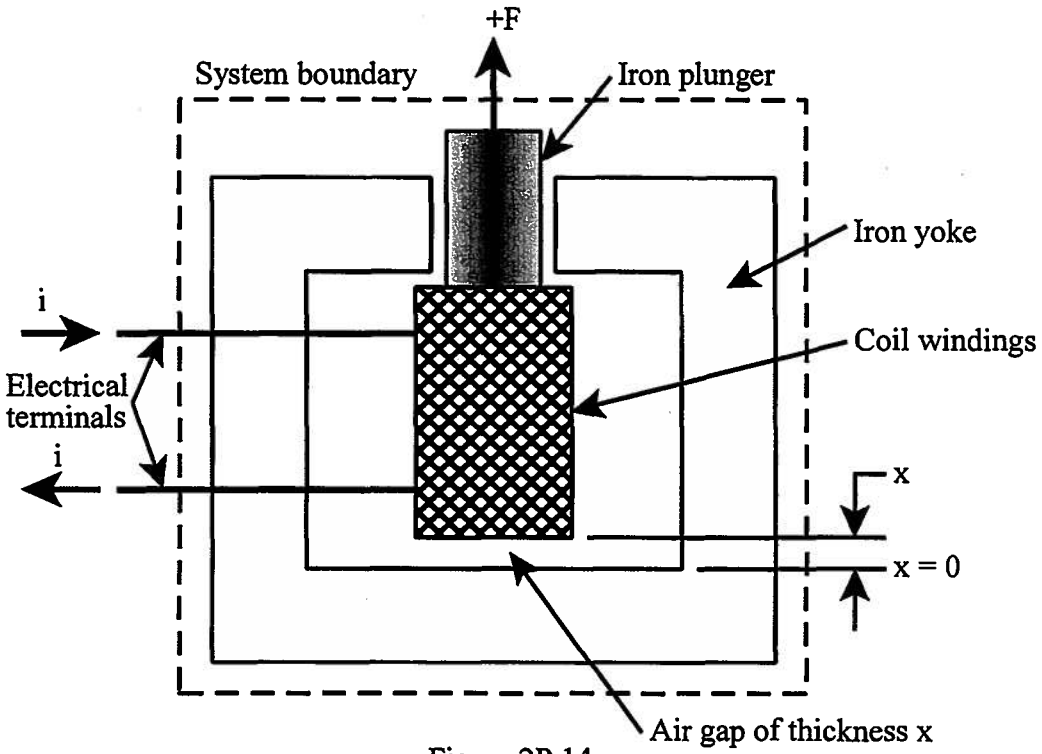

Figure 2P.14

(a) Apply the appropriate test to decide whether this solenoid should be modeled as coupled or uncoupled.

(b) How must the current i change with the position x so that no electrical work transfer occurs when the plunger moves? Determine the mechanical work transfer (in Joules) when the solenoid in the state $x_1 = 10$ mm and $i_1 = 1$ amp is changed to the state $x_2 = 0$ by means of an interaction involving no electrical work transfer.

(c) Determine the energy of the system, relative to the zero energy state, as a function of i and x and again as a function of F and x. The state of zero energy is one for which $i_0 = 1$amp and $x_0 = 0$.

(d) Construct a cycle for the model of the solenoid for which:

$$\oint \delta W_{mechanical} < 0 \quad \text{and} \quad \oint \delta W_{electrical} > 0$$

(e) Could this solenoid be used as an electric motor?

CHAPTER 3

Equilibrium and the Second Law of Thermodynamics

3.1 Run Down to Equilibrium

From our study of the dynamic behavior of rigid bodies, it is well known that if left to themselves, i.e., isolated from their environment, all mechanical systems in motion will eventually run down to a state of static equilibrium. They achieve this a state of rest through the action of mechanical friction during which the system minimizes, in a manner consistent with the isolation of the system, whatever mechanical energy it may have had associated with its motion. From the first law of thermodynamics, equation (2.1), we know that the total stored energy of the system will remain unchanged by this process since the system is isolated. Then in accordance with equation (2.2), it must be the case that the energy has simply changed from one storage mode to another. In fact, as we will soon see when we examine the models for these various energy storage modes, the energy was converted from stored mechanical energy to stored thermal energy. This leads to the familiar concept of the generation of thermal energy by mechanical dissipation. In the early days of the study of thermodynamics, this was thought of as the mechanical equivalent heat. One of the central features of this notion of the run down to equilibrium is the fact that the process always goes in the same direction with the stored mechanical energy mode decreasing while the stored thermal energy mode is increasing.

This concept of the run down to equilibrium is not limited to mechanical systems running down under the action of friction. It is, in fact the general concept that underlies the whole science of thermodynamics. For example, consider two thermodynamic systems A and B in an initial state such that they have initial temperatures different one from the other, $(T_A)_1 < (T_B)_1$. The two systems are brought into communication with each other in a manner similar to that depicted in Figure (2.1) with the exception that there is no mechanical interconnection, only a thermal interconnection. If the two systems are taken together to form a composite system isolated from the environment, they will run down to an equilibrium state characterized by a single temperature uniform throughout the composite system, $(T_A)_2 = (T_B)_2$. According to the first law of thermodynamics, equation (2.1), the total stored energy of the composite system remains constant. In keeping with equation (2.7a), the heat transfer experienced by subsystem A with the lower initial temperature will be positive, $(Q^{AB})_{1\text{-}2} > 0$, while the heat transfer experienced by subsystem B with the higher initial temperature will be negative, $(Q^{BA})_{1\text{-}2} < 0$, such that $(Q^{AB})_{1\text{-}2} = -(Q^{BA})_{1\text{-}2}$. As was the case with the mechanical systems, the process of the thermal run down to equilibrium always proceeds in the same direction, namely toward a state of uniform temperature. Again, the process cannot be reversed without breaking the conditions of isolation. In this sense, the process of run down to equilibrium is said to be *irreversible*.

3.2 The Second Law of Thermodynamics

Because of the universal nature of this phenomenon of the run down to equilibrium, it can be generalized in a manner that permits it to be applied to all systems regardless of their nature. This generalization is known as the second law of thermodynamics, and it generalizes the

concept of run down to equilibrium in much the same manner that the first law of thermodynamics generalizes the concept of energy. The quantity that measures the extent of the run down to equilibrium is called the *entropy*. During the course of the irreversible run down process, entropy is generated. In fact, as we shall see later, entropy is generated in *any* irreversible process. Conversely, a process is irreversible because it generates entropy. This concept of entropy generation is an extension of the earlier concept of the generation of thermal energy in processes involving mechanical dissipation, and it is one of the many interpretations of the entropy.

Like the first law of thermodynamics, the second law of thermodynamics can be stated in many different ways, and each way can be useful in a particular set of circumstances. However, all of these forms are equivalent and universal in their applicability. Also like the first law, the second law is phenomenological in that it is based upon our physical experience.

3.3 Entropy as a Property and the Second Law of Thermodynamics

As we shall soon prove, the entropy, represented by the symbol S, is a property of a system. Like the energy, it is an extensive property that can be stored within the system boundary, and also like the energy, it can be transferred across the system boundary by means of an interaction. Like any other property, the value of the entropy in a given state is fixed by the properties that define the state of the system. Just as the first law of thermodynamics expresses the conservation of the stored energy for an isolated system, the second law of thermodynamics expresses the conservation of the entropy for an isolated system. There is, however, one important exception. The entropy of an isolated system is conserved only for processes that are reversible. As we have already seen, an irreversible process in an isolated system generates entropy. Thus, the second law of thermodynamics for an isolated system can be written

$$(S_2 - S_1)_{isolated} \geq 0 \tag{3.1}$$

or if the generated entropy, S_{gen}, is explicitly identified

$$(S_2 - S_1)_{isolated} = S_{gen} \tag{3.2}$$

where $S_{gen} > 0$ for irreversible processes and $S_{gen} = 0$ for reversible processes.

Entropy is transferred into or out of a system by means of a heat transfer only. The fact that heat transfer involves the transfer of energy and entropy is the feature that distinguishes this interaction from work transfer which involves the transfer of energy only. For two systems A and B interacting in the manner of Figure 2.1, we can define the entropy transfer associated with the heat transfer Q^{AB} for system A as

$$\left(S_{transfer}\right)^{AB} = \int_{state\ 1_A}^{state\ 2_A} \frac{\delta Q^{AB}}{T_A} \tag{3.3}$$

where T_A is the temperature at that point on the boundary of system A where Q^{AB} crosses and states 1_A and 2_A are the initial state and final states, respectively, of system A for the heat transfer interaction. The integral of equation (3.3) is evaluated along the path of the interaction, i.e., along the sequence of states that the system passes through. Similarly, we can write for system B

$$\left(S_{transfer}\right)^{BA} = \int_{state\ 1_B}^{state\ 2_B} \frac{\delta Q^{BA}}{T_B} \tag{3.4}$$

Since the point on the boundary where the heat transfer and, hence, the entropy transfer, occurs is common to the two systems A and B, it must be the case that $T_A = T_B$. (Note that since the temperatures of the two systems may not be uniform, this is not the same as saying that the temperatures of the two systems are the same. The fact that $T_A = T_B$ means only that their temperatures are equal at the point of contact where the entropy transfer occurs across their boundaries.) Also, we have from equation (2.7a) that $Q^{AB} = -Q^{BA}$. Then it follows that like the heat transfers, the entropy transfers between two interacting systems are equal in magnitude and opposite in sign. Thus,

$$\left(S_{transfer}\right)^{AB} = -\left(S_{transfer}\right)^{BA} \tag{3.5}$$

If the process that resulted in the entropy transfer between the two systems was reversible, there was no entropy generated during the interaction. Then it follows from equation (3.1) that

$$\left(S_2 - S_1\right)_{A\ reversible} = -\left(S_2 - S_1\right)_{B\ reversible} \tag{3.6}$$

Since the two systems A and B are the only ones exchanging entropy, from equation (3.5) it follows that for each system

$$\left(S_2 - S_1\right)_{reversible} = \left(S_{transfer}\right)_{reversible} \tag{3.7}$$

or

$$\left(S_2 - S_1\right)_{reversible} = \left[\int_{state\ 1}^{state\ 2} \frac{\delta Q}{T}\right]_{reversible} \tag{3.8}$$

Thus, for the reversible process, the change in stored entropy is equal to the entropy transferred across the system boundary with the heat transfer, and entropy is conserved. When two systems interact in a reversible manner, the increase in stored entropy of one system is balanced by a decrease in the stored entropy of the other system in precisely the same amount. The total stored entropy of the composite system remains unchanged by the reversible interaction. We conclude that the only way that a system can change entropy in a reversible manner is by reversible entropy transfer and, hence, heat transfer, across the system boundary.

For a process to be reversible and, hence, generate no entropy, it is necessary that the system be in continuous equilibrium. This means that there is no ambiguity about the temperature that appears in the integral for the entropy transfer. The temperature is uniform throughout the system, including the boundary where the heat transfer occurred. Note also that there cannot be friction of any kind present during the change of state. Furthermore, since equation (3.8) places no restriction on the process by which the system changed state, except the very important one that it must be reversible, it must be true that the entropy transfer must be the same for *any* reversible process connecting the same two end states. We can now use this result to prove that the entropy is indeed a property.

3.4 The Second Law of Thermodynamics for a System Executing a Cycle

It is now worthwhile for us to consider an alternative statement of the second law of thermodynamics, a statement that will enable us to prove mathematically that the entropy is indeed a property. Consider a system that executes a reversible cycle. Because the cycle is reversible, there is no generation of entropy. Then as a result of the reversible cycle, the system must be in the same condition at the end of the cycle as it was in the beginning of the cycle. Furthermore, since no entropy was generated during the reversible cycle, the amount of entropy in the system must be the same before and after the cycle. Therefore, there can be no net entropy transfer across the boundary for this reversible cycle. Then we can state the second law of thermodynamics in the following way:

> The net entropy transfer between a system and the environment is zero for a *reversible* cycle executed by the system. That is,
>
> $$\left[\oint \frac{\delta Q}{T}\right]_{reversible} = 0 \qquad (3.9)$$

We may now use equation (3.9) to show that the entropy change $S_2 - S_1$ is a change in a property of the system. Consider the situation depicted in Figure 3.1.

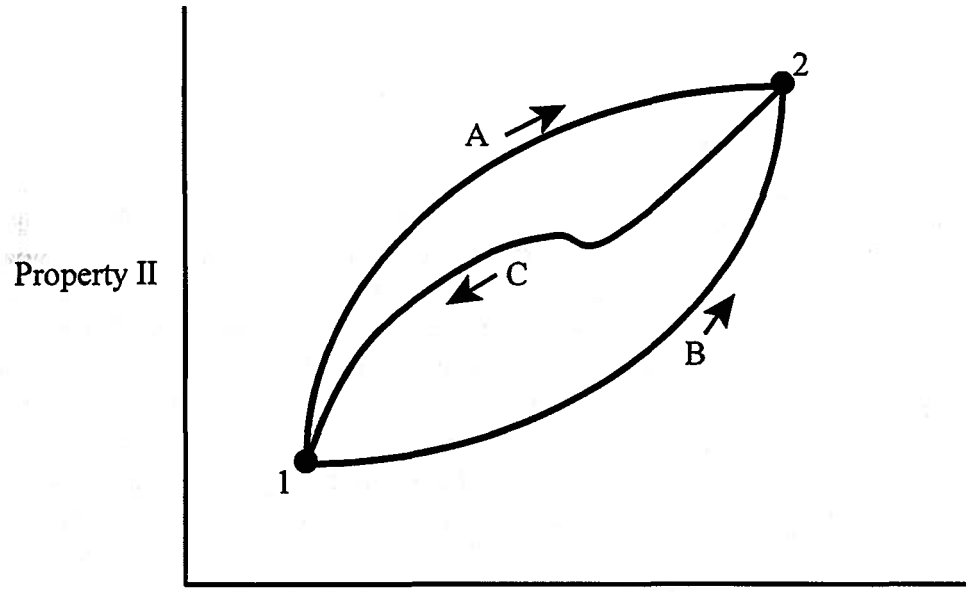

Figure 3.1 Change of State in System with Two Independent Properties

The system is one for which two independent properties are adequate to specify the state. Thus, each point in the plane of Figure 3.1 represents a state of the system. (Note: our proof is not restricted to systems of this type. We have used this example simply because it is easier to present in graphical form.) The state of the system is changed from state 1 to state 2 by two different reversible processes, A and B involving entropy transfer with the environment. From equation (3.8) we have

$$\left[\int_{\text{state 1}}^{\text{state 2}} \frac{\delta Q}{T}\right]_{\text{reversible A}} = (S_2 - S_1)_{\text{reversible A}} \tag{3.10}$$

and

$$\left[\int_{\text{state 1}}^{\text{state 2}} \frac{\delta Q}{T}\right]_{\text{reversible B}} = (S_2 - S_1)_{\text{reversible B}} \tag{3.11}$$

Now we can find some other process to return the system from state 2 to state 1, say reversible process C such that

$$\left[\int_{\text{state 2}}^{\text{state 1}} \frac{\delta Q}{T}\right]_{\text{reversible C}} = (S_2 - S_1)_{\text{reversible C}} \tag{3.12}$$

If we apply the second law of thermodynamics to one reversible cycle consisting of process A and process C and to a second reversible cycle consisting of process B and process C, we have from equation (3.9)

$$\left[\int_{\text{state 1}}^{\text{state 2}} \frac{\delta Q}{T}\right]_{\text{reversible A}} + \left[\int_{\text{state 2}}^{\text{state 1}} \frac{\delta Q}{T}\right]_{\text{reversible C}} = 0 \tag{3.13}$$

and

$$\left[\int_{\text{state 1}}^{\text{state 2}} \frac{\delta Q}{T}\right]_{\text{reversible B}} + \left[\int_{\text{state 2}}^{\text{state 1}} \frac{\delta Q}{T}\right]_{\text{reversible C}} = 0 \tag{3.14}$$

Thus, from equations (3.13) and (3.14) it follows that the entropy transfer for any two reversible processes between state 1 and state 2 must have the same value, or

$$\left[\int_{\text{state 1}}^{\text{state 2}} \frac{\delta Q}{T}\right]_{\text{reversible A}} = \left[\int_{\text{state 1}}^{\text{state 2}} \frac{\delta Q}{T}\right]_{\text{reversible B}} \tag{3.15}$$

Thus, when we substitute the definition of the entropy change, equation (3.8), we show that

$$(S_2 - S_1)_{\text{reversible A}} = (S_2 - S_1)_{\text{reversible B}} \tag{3.16}$$

Since processes A and B are arbitrary reversible processes, we have shown that the change of entropy between two states of a system is independent of the process by which the process is carried out provided that the process is reversible. Once we have established the value of the entropy for every state in this manner, we have established the entropy as a property for each state. It then follows that the entropy will always have the same value in any given state regardless of the nature of the process, reversible or irreversible, by which that state was attained. However, the relationship between the entropy transfer and the entropy change for a process is dependent upon the nature of the process. In the case of an irreversible process, we have already seen that the entropy change is comprised of two components: (1) the entropy transfer and (2) the entropy generated by the irreversibility. Thus

$$(S_2 - S_1)_{\text{irreversible process}} = S_{\text{transfer}} + S_{\text{gen}} \tag{3.17}$$

or

$$(S_2 - S_1)_{irreversible\ process} = \left[\int_{state\ 1}^{state\ 2} \frac{\delta Q}{T}\right]_{irreversible\ process} + S_{gen} \tag{3.18}$$

Since $S_{gen} > 0$ for an irreversible process, it follows that for a given set of end states 1 and 2,

$$\left[\int_{state\ 1}^{state\ 2} \frac{\delta Q}{T}\right]_{irreversible} < \left[\int_{state\ 1}^{state\ 2} \frac{\delta Q}{T}\right]_{reversible} \tag{3.19}$$

The inequality of equation (3.19) is to be interpreted in the true algebraic sense. That is, if the heat transfer is negative, the entropy transfer in the irreversible case will be more negative than the reversible case for a given set of end states. Of course, this means that the magnitude of the entropy transfer in the irreversible case is greater than the magnitude of the entropy transfer in the reversible case. The physical interpretation of this is that in order to decrease the stored entropy of a system, there must be a negative entropy transfer. If the process by which this occurs is irreversible, for a given change of state the entropy transfer must carry away not only the entropy associated with the change of state, but also the entropy generated by the irreversibilities of the process.

We can now write the second law in the general form

$$(S_2 - S_1) = \int_{state\ 1}^{state\ 2} \frac{\delta Q}{T} + S_{gen} \tag{3.20}$$

where $S_{gen} > 0$ for irreversible processes and $S_{gen} = 0$ for reversible processes.

3.5 Temperature and Heat Transfer

In our discussion of the second law of thermodynamics thus far, we have presumed a certain level of familiarity with the concepts of temperature and heat transfer from the reader's prior experience with physical systems. Now that we have developed the second law of thermodynamics, we can refine these primitive notions, at least at an introductory level, with the promise to present more rigorous definitions as our experience in this area expands with further study.

To aid us in this process, we now introduce the simplest model that illustrates these concepts as well as all of the other thermal aspects that we have just introduced, namely entropy transfer, entropy generation, and entropy storage. In addition, this model provides us with the means to describe the uncoupled thermal energy storage mode that we introduced in Chapter 2. It is important to recognize that the stored thermal energy and the stored entropy of this model are functions of a single independent property, temperature, which *in this model* can be changed only by means of a heat transfer interaction. In spite of its simplicity, this model is also extremely useful on a practical level for modeling the thermal behavior of solids and liquids that do not change volume significantly as the result of heat transfer interactions or changes in temperature.

3.5.1 Thermal Energy Storage Mode: Pure Thermal System Model

The central features of this model are:

Physical characteristics:	m = mass
	C = heat capacity
	$c = C/m$ = specific heat
Properties:	T = temperature
	U = stored thermal energy
	S = stored entropy
Interaction:	$Q_{1\text{-}2}$ = heat transfer
Energy constitutive relation:	$U_2 - U_1 = C(T_2 - T_1) = mc(T_2 - T_1)$
Entropy constitutive relation:	$S_2 - S_1 = mc \ln\left(\frac{T_2}{T_1}\right)$

At this stage of our development of the subject, we have not yet developed the formalism necessary to express the heat transfer $Q_{1\text{-}2}$ in terms of an interaction integral as we did with the work transfer. Thus, we cannot use the first law of thermodynamics to derive an expression for changes in stored thermal energy. At this point we must content ourselves with using the energy constitutive relation that expresses the stored thermal energy in terms of the temperature to describe the behavior of the pure thermal system. (Note that we have introduced the symbol U to denote the stored energy forms that can be influenced by heat transfer. As will become apparent later, in the coupled case U can be increased *or* decreased by work transfer as well as heat transfer in the absence of dissipation.)

For the pure thermal system model, we have introduced some additional physical parameters that require further elaboration. We define the *heat capacity, C,* of a pure thermal system to be the change in stored thermal energy per unit change in temperature. Thus,

$$C = \frac{dU}{dT} \tag{3.21}$$

The heat capacity per unit mass of the system is known as the *specific heat capacity, c,* where

$$c = \frac{C}{m} = \frac{1}{m}\frac{dU}{dT} = \frac{du}{dT} \tag{3.22}$$

and u is the stored thermal energy per unit mass. In general, the specific heat and the heat capacity are functions of the temperature, but in many cases, these parameters can be regarded as constants independent of temperature. Indeed, the rationale for the pure thermal system model can be found in the data obtained from measurements of the specific heat of various materials. The measurements are carried out under conditions in which the pressure imposed on the material is maintained constant at atmospheric pressure while the temperature is changed by means of a heat transfer interaction.

These measurements reveal that for materials like metals, the specific heat is nearly constant over a very wide range of temperature. Examples of such data are shown in Figure 3.2 for the metals copper, aluminum, and 304 stainless steel over the temperature range of 200 - 1400 K. For each particular metal, the data are normalized with respect to the value of the specific heat of the metal measured at the temperature 373.15 K (100 C). By presenting the data in this dimensionless form, we are able to combine data for several different metals on a single graph. Note that the vertical axis in Figure 3.2 is the *logarithm* of the specific heat normalized

with respect to its value at 373.15 K. The logarithmic form rather than the linear form has the tendency to compress the data somewhat; however, because the range of temperatures is so large, we are justified in saying that the specific heat is nearly constant and that the pure thermal system model provides an adequate representation of the physical situation, particularly for small variations in temperature.

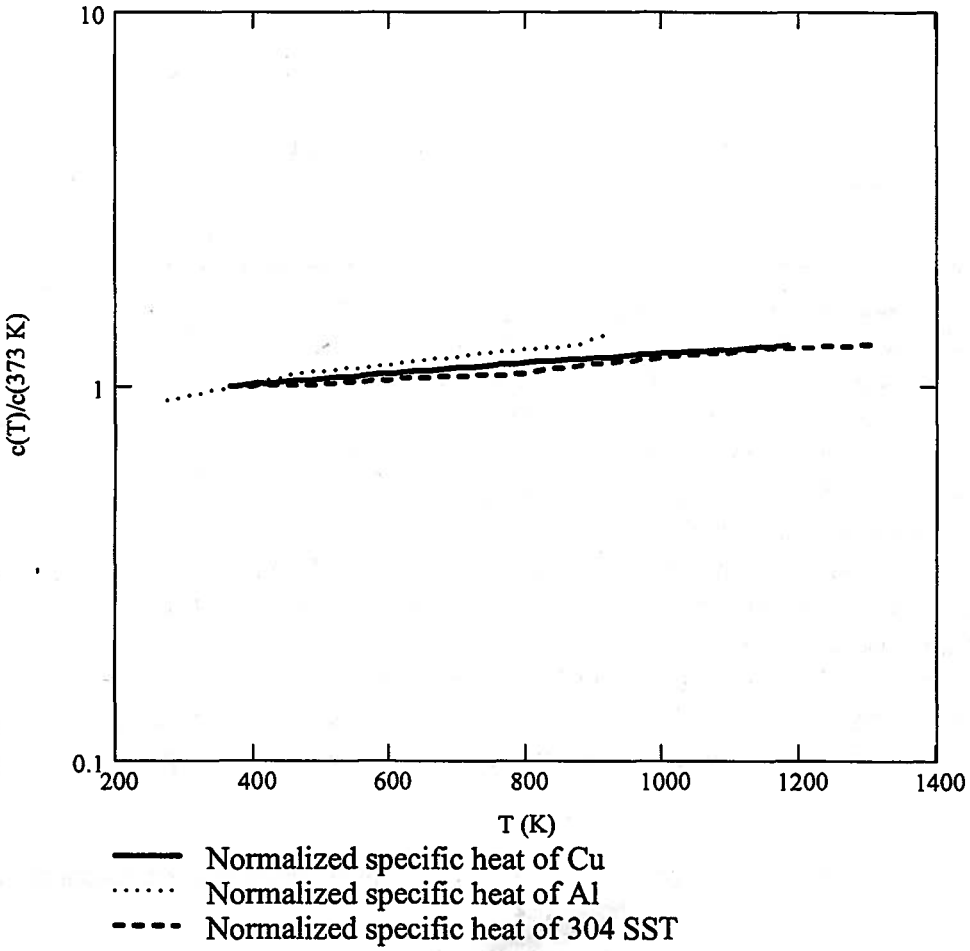

Figure 3.2 The Temperature Dependence of the Specific Heat for Selected Metals

The behavior of the specific heat demonstrated in Figure 3.2 is not unique to metals. As shown in Figure 3.3, non-metallic solids show a similar behavior with just a slightly stronger temperature dependence than metals. However, the temperature dependence is still weak enough that the pure thermal system model provides an adequate representation of their thermal behavior, particularly over narrow temperature ranges.

In a similar fashion, the thermal behavior of many liquids can also be described in terms of the pure thermal system model. In the case of liquids, however, the temperature ranges of interest are much smaller since the liquids will undergo changes of phase (from liquid to vapor and from liquid to solid) at both the upper and lower limits of temperature. Over this relatively narrow temperature range, the specific heat is constant to within a few percent for most liquids. Figure 3.4 presents the specific heat data for water at atmospheric pressure over the temperature

range 0 C to 100 C. It appears, then, that the pure thermal system model provides an adequate representation of the thermal behavior of liquids as well as solids.

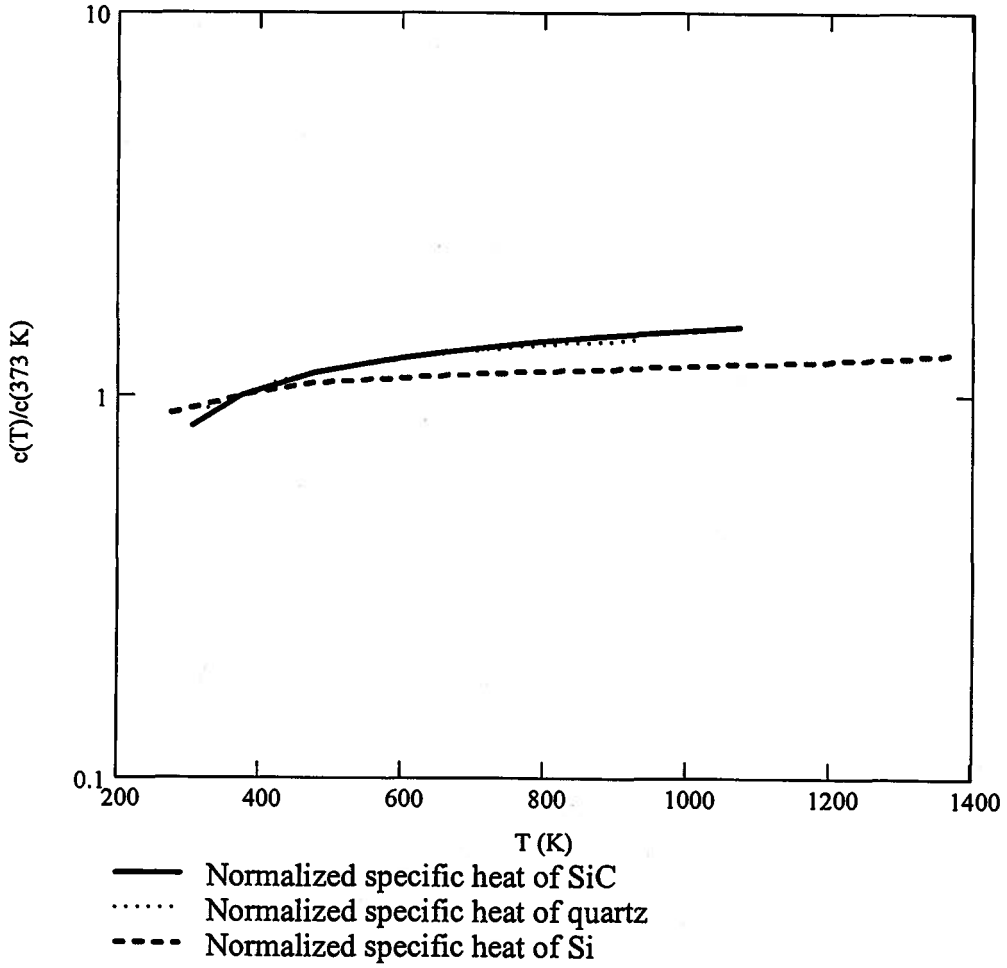

Figure 3.3 The Temperature Dependence of the Specific of Selected Non-metallic Solids

In these cases for which the specific heat is constant, the energy constitutive relation takes the form given above, namely

$$U_2 - U_1 = m(u_2 - u_1) = mc(T_2 - T_1) = C(T_2 - T_1) \tag{3.23}$$

The entropy constitutive relation for the pure thermal system model can be derived from equation (3.8) by considering a reversible process between two states specified by the temperatures T_1 and T_2. Since the process is reversible, all the states along the path from state 1 to state 2 are equilibrium states with uniform temperature throughout the pure thermal system. For an infinitesimal change of state along this path, the first law for the process is given by

$$\delta Q_{reversible} = dU = mcdT \tag{3.24}$$

where we have substituted equation (3.22). Then equation (3.8) becomes

$$(S_2 - S_1)_{reversible} = \left[\int_{T_1}^{T_2} \frac{\delta Q}{T}\right]_{reversible} = \left[\int_{T_1}^{T_2} \frac{mcdT}{T}\right]_{reversible} = mc\ln\left(\frac{T_2}{T_1}\right) \qquad (3.25)$$

where the reversible nature of the path ensures that the pure thermal system passes through states with identifiable temperature so that the integral in equation (3.25) can be carried out. Since the

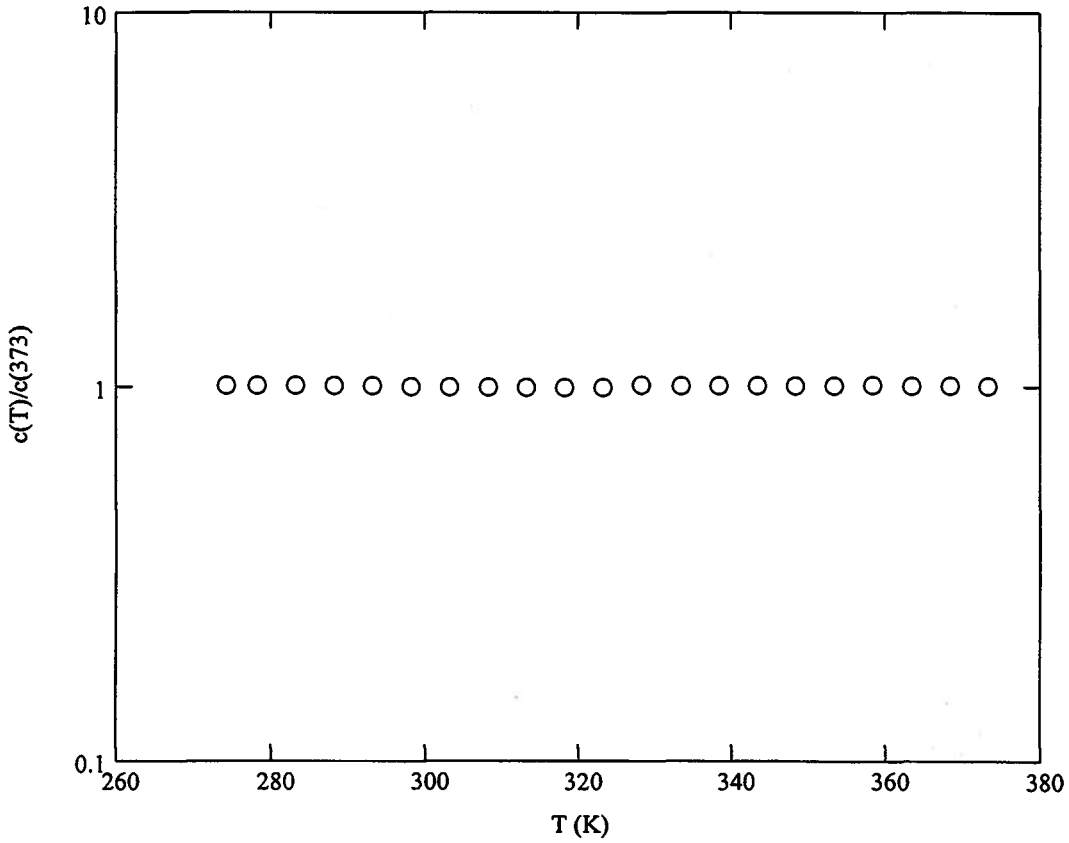

Figure 3.4 The Temperature Dependence of the Specific Heat of Liquid H_2O at Atmospheric Pressure

Table 3.1
Specific Heat of Selected Materials at 100 C and Atmospheric Pressure

Material	**Specific Heat (J/kg K)**
Aluminum (pure)	916.95
Copper (electrolytic tough pitch)	361.76
304 Stainless Steel	377.35
Silicon	770.41
Silicon Carbide	820.65
Quartz	830.28
H_2O (liquid)	4215.67

end states are specified, the value for the change of entropy calculated in equation (3.25) can be assigned to those two states for all time. Then the entropy constitutive relation for the pure thermal system, that is, the change in entropy between states 1 and 2 becomes

$$S_2 - S_1 = mc \ln\left(\frac{T_2}{T_1}\right) \tag{3.26}$$

regardless of the path that connects states 1 and 2.

This result might at first glance seem contradictory since we used a reversible process and path to determine it, and we now claim that this value is valid for the change in entropy between these two states 1 and 2 regardless of the process used to get the system from state 1 to state 2. The point is that the entropy is a state function so that the entropy has a unique value in each and every state of the system. For a reversible process between states 1 and 2, the value of the entropy change calculated from equation (3.26) will be equal to the entropy transferred across the system boundary during the process. However, in the case of an irreversible process between these same two states 1 and 2, the value of the entropy change calculated from equation (3.26) will exceed the value of the entropy transferred across the system boundary by the amount of the entropy generated during the irreversible process. From this simple model it should be apparent that the entropy is a state function with a unique value in every state regardless of the process by which the system attained that state, but the entropy transfer and the entropy generated depend upon the process and cannot be related to the end states of the process. (Note that in the special case of the reversible process, we have not yet specified the manner in which reversibility can be realized in a practical sense, but we will take up this question in detail in Chapter 4.)

There is a special case of the pure thermal system known as a *heat reservoir* that is very useful in thermal-fluids engineering. It is a model for systems of mass so large that the heat capacity approaches infinity. This means that the system can experience heat transfer interactions of any magnitude with negligible change in temperature. The heat reservoir model is the limiting case of the pure thermal system model in which any amount of energy (and entropy) can be exchanged with the environment while the temperature of the heat reservoir remains fixed in time and uniform in space. This further implies that there is no entropy generation during the heat transfer interaction. Note that even though the temperature of the heat reservoir does not change, its state does change in accordance with the amount of energy and entropy transfer associated with the interaction.

In formulating the pure thermal system element model we have in effect the first limited definition of heat transfer[1]:

> *Heat transfer* is the energy transfer interaction that occurs between pure thermal systems.

Although the concept of temperature is familiar from the sense of touch, we can now give a

---

[1] A more rigorous definition of heat transfer will be given in Chapter 4.

simple definition of temperature[2]:

> *Temperature* is the property of a system which indicates the potential for heat transfer with other systems.

We may also define the inequality of temperature:

> Two systems (or a system and its environment) in communication are *unequal in temperature* when they experience a heat transfer interaction at a finite rate.

We may define equality of temperature and thermal equilibrium:

> Two systems (or a system and its environment) in communication are *equal in temperature* when they reach a state of mutual *thermal equilibrium* for which all heat transfer interactions cease.

The utility of the temperature as a unique measure of the potential of a system for heat transfer is guaranteed by the generalization called the *zeroth law of thermodynamics* which can be stated as follows:

> If two systems are each equal in temperature to a third system, then the temperatures of the two systems themselves are equal.

The sign convention for heat transfer and the sign convention for temperature change are such that:

> For a heat transfer in the absence of work transfer, the heat transfer is positive for the low temperature system which increases in energy and negative for the high temperature system which decreases in energy. For the system with the positive heat transfer, the temperature change is positive or in the limiting case zero.

In the considerably more complex situations which we shall consider in subsequent chapters, it is usually more convenient to identify heat transfer interactions by means of the property temperature.

> An interaction between two closed systems is a heat transfer if the interaction is solely the result of the temperature difference between the two systems.

The terms *adiabatic* and *diathermal* are used to model the heat transfer characteristics of the boundary of a system. The property known as the thermal conductivity is used as an indication of the heat transfer characteristics of a material. A material with a high value for the thermal

---

[2] A more formal definition of temperature will be given after we have introduced more complex models for thermodynamic systems.

conductivity will allow a larger heat transfer rate as the result of a given temperature difference than a material with a low value for the thermal conductivity. When the material in the vicinity of a system boundary has a low value for the thermal conductivity, the boundary itself is often modeled as a complete barrier to heat transfer despite the temperature difference across the boundary. The boundary is then said to be *adiabatic.* Processes within systems surrounded by adiabatic boundaries are termed *adiabatic processes.* A system must be surrounded by an adiabatic boundary to be *thermally isolated* from the environment. In short, the term adiabatic implies: modeled as zero heat transfer. Very few real boundaries or processes are absolutely free from heat transfer, but the adiabatic model is used when the heat transfer is insignificant compared to the other aspects of the situation.

When the boundary of a system is within an environment which has a high value for the thermal conductivity, the boundary frequently may be modeled as a perfect conductor such that large heat transfer rates can occur with a vanishingly small temperature difference. The boundary of the system is then said to be a *diathermal boundary.* The temperature difference across a diathermal boundary is always zero or of infinitesimal magnitude.

Having defined equality of temperature and a method for ordering temperatures from low to high, we can now discuss temperature scales, temperature measurement, and thermometers. One of the serious difficulties in developing thermodynamics is that the definition of the fundamental thermodynamic temperature scale depends upon the second law of thermodynamics; however, the second law of thermodynamics demands the concept of temperature for its development.

We will use the thermodynamic Kelvin scale of temperature throughout this development. When we consider systems executing cycles while in communication with more than one heat reservoir, we will be able to show the special significance of a thermodynamic temperature scale. The traditional practical centigrade and Fahrenheit temperature scales are linearly related to the Kelvin scale within a negligible margin of error. The modern Celsius scale is defined in terms of the thermodynamic Kelvin scale. The relations between the temperature scales are

$$C = K - 273.15 \tag{3.27}$$

$$F = \frac{9}{5}K - 459.67 \tag{3.28}$$

A *thermometer* is a system which samples and measures the potential of systems for heat transfer. In order to effect the sampling and measurement, the thermometer should be capable of convenient thermal communication with other systems *without experiencing any work transfer.* When a thermometer is placed in thermal communication with a system for temperature measurement, a heat transfer occurs until the thermometer and the system are in thermal equilibrium and temperature equality has been established. If the heat transfer does take place in the absence of work transfer, a change of state of the thermometer occurs which is manifested in a change of an observable (mechanical or electrical) property of the thermometer. When thermal equilibrium prevails, the observable property will remain constant. The magnitude of the heat transfer necessary to achieve thermal equilibrium between the thermometer and the system must be such that it produces an undetectable change of state in the system but a significant change of state in the thermometer. These requirements are usually satisfied by careful thermometer design. A typical example of such a design is the mercury-in-glass thermometer in which the change of

state of the thermometer is revealed by a change in the volume occupied by the mercury. In this case, the observable property is the height of the mercury in the glass capillary tube.

The historic Fahrenheit and centigrade temperature scales were established and defined by bringing the mercury-in-glass thermometer into thermal equilibrium with water at its atmospheric pressure boiling point. The height of the mercury column in the constant bore capillary tube was arbitrarily assigned the value 100 C or 212 F. (Any other numbers would have been just as suitable.) The thermometer was then brought into thermal equilibrium with water at its atmospheric pressure freezing point, and the height of the mercury arbitrarily assigned the value 0 C or 32 F. The change of state of the thermometer was assumed to be linear. Hence, the distance on the capillary tube between these two points was divided into 100 equal parts or "degrees" to define the centigrade scale and 180 equal parts to define the Fahrenheit scale. The scales were then linearly extrapolated above and below the fixed points by using the same distance for each degree change in temperature.

In SI units, the heat capacity and the entropy are expressed in the same units, J/K, and the specific heat capacity and the specific entropy are also expressed in the same units, J/kg K. Two useful conversion factors are:

$$1 \text{ Btu/R} = 1.899101 \times 10^3 \text{ J/K}$$

$$1 \text{ Btu/lbm R} = 4.1868 \times 10^3 \text{ J/kg K}$$

3.5.2 Heat Transfer, Entropy Transfer, and Entropy Generation in the Pure Thermal System Model

As we have just shown, the essence of the of the pure thermal system model is its ability to experience heat transfer. The unique characteristic of heat transfer is that it involves the transfer of both energy and entropy. It follows, then, that the pure thermal system can experience entropy transfer as well as heat transfer. In fact, as we have seen from the second law, this is one of the two ways that the stored entropy of a system can be changed. The other way, of course, is by entropy generation by irreversible processes internal to the system boundary. In section 3.1, we alluded to the connection between the process of run down to equilibrium by thermal means and the generation of entropy. We now use this connection in the context of the pure thermal system model to develop further the concepts inherent in the second law, namely, the relationship between heat transfer, entropy transfer, and entropy generation. Although we shall employ the pure thermal system model to demonstrate these concepts, the applicability of our observations will not be limited to this model.

For this purpose, let us now consider two pure thermal systems, A and B, characterized by their masses, m_A and m_B, and their specific heats, c_A and c_B. Let these systems have initial temperatures $(T_A)_1$ and $(T_B)_1$, respectively, with $(T_A)_1 < (T_B)_1$. As shown in Figure 3.5, we now provide a thermal interconnection between these two systems in the form of a thermal conductor that functions in a manner analogous to an electrical conductor interposed between two electrical systems. That is, for a given difference in the electrical potential of the electrical systems, the electrical conductance, i.e., the ability of the electrical conductor to transport energy by the transfer of electrons from system A to system B varies directly as the cross-sectional area of the conductor and inversely as the length of the conductor with a characteristic of the material of the conductor, the electrical conductivity, as the constant of proportionality. Similarly for the thermal

conductor, the thermal conductance varies directly as the cross-sectional area of the conductor and inversely as the length of the conductor with the thermal conductivity as the constant of proportionality.

Although not central to the following discussion, suppose that we choose a conductor of long length and small cross-sectional area and fabricated from a material of low thermal conductivity. Then the thermal conductance of this conductor will be small, or conversely, its thermal resistance will be high. When this conductor is placed between systems A and B, the end of the thermal conductor in contact with system A will assume the temperature of the surface of system A, and the end in contact with system B will assume the temperature of system B. if the

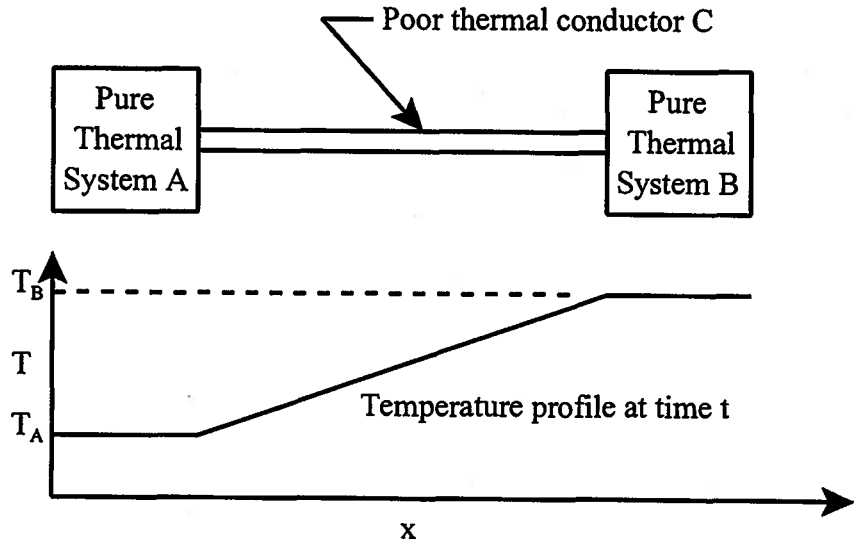

Figure 3.5 Heat Transfer Interaction Between Two Pure Thermal Systems Via a Poor Thermal Conductor

lateral surface of the conductor is adiabatic, there will develop in the conductor a linear temperature gradient from end A to end B. If the thermal resistance of the conductor is sufficiently high, there will be no temperature gradients in either system A or system B. The only temperature gradient that appears in this physical situation will be in the thermal conductor itself. That is, as energy flows from system B to system A, the temperatures of the respective systems will vary with time but be uniform in space as the run down to equilibrium proceeds toward the state of uniform temperature throughout systems A and B together.

The rate at which energy flows from system B to system A is limited by the value of the thermal conductance, K, of the thermal conductor, viz.

$$\dot{Q}^{AB} = K(T_B - T_A) = -\dot{Q}^{BA} \tag{3.29}$$

From equation (3.29) it is evident that the run down to equilibrium proceeds at a decreasing rate as the temperatures of the two systems approach each other. However, the final equilibrium temperature itself is determined not by the rate at which the run down to equilibrium proceeds but by the first law of thermodynamics. If the thermal conductor is of negligible mass compared to the systems A and B, we can construct an isolated system consisting of system A and system B

together. Then the first law gives

$$(U_2 - U_1)_{isolated} = (U_2 - U_1)_A + (U_2 - U_1)_B = 0 \tag{3.30}$$

If we substitute the energy constitutive relations for the two systems A and B and solve for the final equilibrium temperature T_2, we get

$$T_2 = \frac{m_A c_A (T_A)_1 + m_B c_B (T_B)_1}{m_A c_A + m_B c_B} \tag{3.31}$$

Once the final equilibrium temperature has been established by the first law, we can use the second law to examine the nature of the reversibility of the process.

For the isolated system, the second law is given by

$$(S_2 - S_1)_{isolated} = (S_2 - S_1)_A + (S_2 - S_1)_B = S_{gen} \tag{3.32}$$

where $S_{gen} > 0$ if the run down to equilibrium is irreversible and $S_{gen} = 0$ if it is reversible. We can calculate the entropy changes of the individual systems A and B from their entropy constitutive relations. Thus,

$$m_A c_A \ln\left(\frac{T_2}{(T_A)_1}\right) + m_B c_B \ln\left(\frac{T_2}{(T_B)_1}\right) = S_{gen} \tag{3.33}$$

It can be shown that the left-hand side of equation (3.33) becomes

$$m_A c_A \ln\left(\frac{T_2}{(T_A)_1}\right) + m_B c_B \ln\left(\frac{T_2}{(T_B)_1}\right) \to C^2 \frac{\left[(T_B)_1 - (T_A)_1\right]}{(T_A)_1} \tag{3.34}$$

where C is a constant so that S_{gen} is indeed positive and goes to zero only in the limit as the difference in the initial temperatures of the systems A and B goes to zero, i.e., as

$$(T_B)_1 - (T_A)_1 \to 0 \tag{3.35}$$

Then for an isolated system consisting of two pure thermal systems with different initial temperatures, the run down to equilibrium generates entropy and is irreversible. The irreversibility implies that the process proceeds in one direction only such that the higher temperature system continually decreases in temperature and the lower temperature system continually increases in temperature until the final equilibrium temperature is reached.

In the situation described above the entropy is generated in the thermal conductor that allows the two pure thermal systems A and B to communicate via a heat transfer interaction. The end of the conductor in contact with system B is at the temperature of system B and the end in contact with system A is at the temperature of system A. Then for the conductor as a system, the rate of entropy flow at each end is given by

$$\begin{aligned} \left(\dot{S}_{transfer}\right)_{end\ B} &= \frac{-\dot{Q}^{BC}}{T_B} > 0 \\ \left(\dot{S}_{transfer}\right)_{end\ A} &= \frac{\dot{Q}^{BC}}{T_A} < 0 \end{aligned} \tag{3.36}$$

where $\dot{Q}^{BC} < 0$ since the energy flows from system B to system A because of the temperature difference between the two systems. Notice that since $T_B > T_A$ for all states except the final equilibrium state, the rate of entropy transfer out of the thermal conductor at end A is greater in magnitude than the rate of entropy transfer into the conductor at end B. Thus entropy was

generated as the energy associated with the heat transfer flowed down the temperature gradient in the conductor. This phenomenon will be examined in greater detail in Chapter 6. However, this observation is a general one, viz,

Heat transfer down a finite temperature gradient generates entropy and is, therefore, an irreversible process.

The use of the thermal conductor in this situation is an artifice that reveals the relationship between entropy transfer and entropy generation. It is not a necessary component for run down to equilibrium between two pure thermal systems initially at different temperatures. The two systems can simply be brought into direct contact thermal contact at a mutual interface. For that situation the temperatures at the common boundary are of course equal with entropy transfers for the two systems A and B equal in magnitude but opposite in sign. As we shall see in Chapter 6, a temperature gradient develops within each of the pure thermal systems A and B so that the entropy generation associated with the run down to equilibrium occurs in these internal temperature gradients.

Example 3E.1: A pure thermal system with a heat capacity of 500 J/K is at an initial temperature of 400 K. It is brought into thermal communication with a heat reservoir whose temperature is 300 K, and the pure thermal system and the heat reservoir are allowed to experience a heat transfer interaction. Find the final equilibrium temperature of the heat reservoir and the pure thermal system. Calculate the heat transfer experienced by the pure thermal system and the entropy generated in the process. For the heat reservoir, calculate the change in stored thermal energy and the change in stored entropy.

Solution: This is a classical example of a run down to equilibrium by heat transfer. The models employed in the analysis are precisely the models described in Section 3.5. Since the heat reservoir can experience heat transfer of any magnitude without changing temperature, the final equilibrium temperature must be the temperature of the heat reservoir, $T_2 = 300$ K.

Form an isolated system consisting of the pure thermal system (PTS) and the heat reservoir (HR) together. For this system there are no interactions with the environment. Thus, from the first law, there is no change in the stored thermal energy of the composite system, viz.

$$(E_2 - E_1)_{isolated} = (U_2 - U_1)_{PTS} + (U_2 - U_1)_{HR} = 0$$

and with the aid of the energy constitutive relation for the pure thermal system model

$$(U_2 - U_1)_{HR} = -(U_2 - U_1)_{PTS} = -C(T_2 - T_1)_{PTS} = -(500 \text{ J/K})(300 \text{ K} - 400 \text{ K}) = 5 \text{ x } 10^4 \text{ J}$$

Thus the stored thermal energy of the heat reservoir has increased even though its temperature remains fixed. From the first law for the pure thermal system

$$(Q_{1\text{-}2})_{PTS} = (U_2 - U_1)_{PTS} = -5 \text{ x } 10^4 \text{ J}$$

Thus the heat transfer was from the pure thermal system to the heat reservoir, i.e., from the high temperature system to the low temperature system. From the second law for the heat reservoir,

$$(S_2 - S_1)_{HR} = \int_{\text{state 1}}^{\text{state 2}} \left(\frac{\delta Q}{T}\right)_{HR} = \frac{1}{T_{HR}} \int_{\text{state 1}}^{\text{state 2}} \delta Q = \frac{(Q_{1\text{-}2})_{HR}}{T_{HR}} = \frac{(U_2 - U_1)_{HR}}{T_{HR}} = 166.67 \text{ J/K}$$

Pure thermal System to Heat Reservoir

where the temperature of the heat reservoir appears outside the integral because it is constant. From the entropy constitutive relation for the pure thermal system

$$(S_2 - S_1)_{PTS} = C\ln\left(\frac{T_2}{T_1}\right) = (500\ \text{J/K})\ln\left(\frac{300\ \text{K}}{400\ \text{K}}\right) = -143.84\ \text{J/K}$$

The second law for the isolated system then becomes

$$(S_2 - S_1)_{isolated} = (S_2 - S_1)_{HR} + (S_2 - S_1)_{PTS} = 166.67\ \text{J/K} - 143.84\ \text{J/K}$$
$$(S_2 - S_1)_{isolated} = 22.83\ \text{J/K} = S_{gen}$$

The positive value for the entropy generation confirms that the run down to equilibrium is indeed irreversible.

3.5.3 Entropy Generation by Mechanical Dissipation: Pure Dissipative System Model

Although we have expanded our "catalog" of system models to the point where we can now manage both mechanical and thermal interactions on an elementary level, our "catalog" remains incomplete. With the models we have discussed thus far, we are unable to explain the run down to equilibrium of a mechanical system that we discussed briefly in Section 3.1. This is a common physical occurrence that underlies the second law of thermodynamics. It is rooted in the way the stored energy of a thermal system can be increased by means of a work transfer. It is a phenomenon we have all experienced at an early age, for example, when we dragged an object across a floor and observed that the point of contact between the object and the floor became hot, i.e., increased in temperature. This phenomenon is a simple example of mechanical friction that perplexed early thermodynamicists for many years. For the early workers in the field, the difficulty lay in the fact that a mechanical interaction resulted in a change in a thermal aspect of the system when they had always thought of thermal and mechanical behavior as separate aspects of system behavior. Today we now know that the dissipation of mechanical energy associated with this type of friction and other similar phenomena can be easily described by means of a unique system model known as the pure dissipative system model.

Consider the mechanical system consisting of the spring and mass shown in Figure 3.6. The composite system is initially at rest with the mass at some equilibrium position $x_1 = 0$. If the mass is now displaced to some new location x_2 by means of an external work transfer, the stored mechanical energy of the system is changed. The mass is now released from this position (external force removed) and the system is allowed to oscillate.

One of the simplest models that we can use to represent this physical situation would consist of a pure translational mass and a pure translational spring in a vacuum. For this model the initial work transfer to the composite system would be stored within the spring subsystem as elastic energy. When the mass is released from position x_2, there is a work transfer from the spring subsystem to the mass subsystem. By means of this work transfer, the stored kinetic energy of the mass will increase at the expense of the stored elastic energy of the spring. Thus, the work transfer for the spring is positive while that for the mass is negative. The work transfer for the composite system is, of course, zero. When the mass reaches the position x_1 again, the

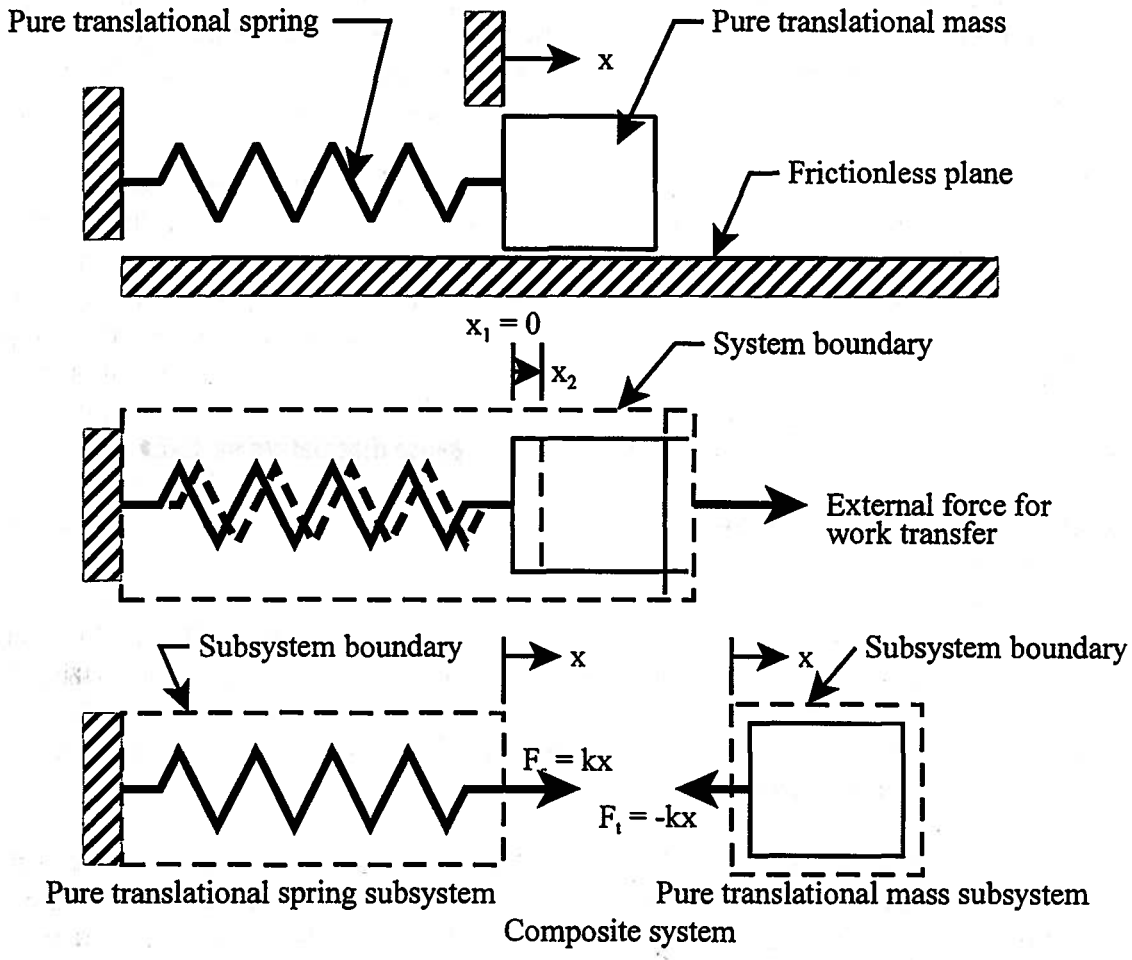

Figure 3.6 Mechanical System

stored elastic energy of the spring has been reduced to its original zero value; however, the kinetic energy of the mass has increased by an amount equal to the change in the stored elastic energy of the spring. At this position, the mass begins to experience a positive work transfer while the spring experiences a negative work transfer. This process continues indefinitely with the work transfer between the two constituent subsystems reversing sign at the limits of travel of the mass and at the position x_1. The nature of the oscillation is such that the total stored mechanical energy of the composite system is a constant; it does not change with time. Further, this mechanical energy stored within the composite system is equal to the energy transferred by means of the original work transfer to the composite system.

If we were to compare the performance of this model with the performance of a real physical system, we would find that there is a disparity. The total stored mechanical energy of the physical system is not constant; it decreases with the passage of time. For a given spring and mass, at a given time, the magnitude of the disparity will depend rather strongly upon the circumstances, ranging from quite small to quite large. In all cases, the disparity increases in magnitude with time. Finally, the real physical system exhibits a behavior very different from the model described above. After some period of time, the physical system ceases to oscillate and

attains a state of internal equilibrium. In the physical situation just described, the final state of mechanical equilibrium is very nearly identical to the initial state of mechanical equilibrium. As a consequence, the system cannot be returned to its original state by a process that will recover the original work transfer. A system which behaves in this manner is said to be non-conservative since the energy associated with the original work transfer is not conserved.

It is then apparent that the system model described previously is not an adequate representation of the real physical system, especially after a long time has passed. In fact, closer inspection of the situation reveals that any model composed of pure conservative system components is insufficient to describe the behavior of the real physical system. (This is not to imply, however, that there are not those special situations for which the model composed of pure conservative systems is sufficient.) Accordingly, we would like to incorporate into our system model a component which will permit us to represent the non-conservative nature of physical systems. The system model with this capability is called a pure dissipative system.

In order to be able to describe the nature of pure dissipative systems, it is worth considering some examples of dissipative phenomena in real physical systems that can be modeled as uncoupled.

(1) In a simple Newtonian fluid the rate of dissipation of mechanical energy is proportional to the square of the rate of deformation within the fluid. The fluid property viscosity is the constant of proportionality in the constitutive relation characterizing the dissipation, and in this manner the viscosity serves as a measure of the dissipative nature of the fluid. With all other things equal, the fluid with the larger value for the viscosity will have the greater dissipation.

(2) The dissipation associated with the sliding of the surface of one rigid solid over the surface of a second rigid solid is known as friction. One example is called Coulomb friction. The friction coefficient (analogous to the fluid property viscosity) is the proportionality factor between the dissipative response (the friction force) and the system input (the load force normal to the interface between the surfaces). However, unlike viscosity, the coefficient of friction is a property of the two solid surfaces involved and not just the solids themselves. Thus, the friction coefficient describes the dissipative nature of the interface. Dissipation of this type is important in the selection of construction material for bearings or brakes.

(3) Perhaps more closely related to the viscous dissipation of a fluid is the bulk dissipation of a solid. Normally, this type of dissipation in solid systems is quite small and is usually neglected. However, there are those instances in which such a dissipation is significant. For example, the selection of the material of construction of a bell or the frame of a machine tool must consider dissipation of this type. Unfortunately, this form of dissipation in solid systems is more complex than in the case of a fluid. Other complexities arise in the deformation of a solid material beyond its elastic limit and into its plastic range where it acquires a permanent deformation after the loading forces are relaxed. Also in this category is the deformation of a viscoelastic material. This can be seen in some commercial plastics that initially assume a deformed state but gradually return to the original state when the load is removed.

From the foregoing examples, it is apparent that there exist in nearly all mechanical systems dissipative effects which, for convenience, we group under the general heading "friction". Dissipative phenomena are not restricted to purely mechanical systems alone, however. Other types of systems also exhibit dissipative phenomena, but whether these dissipative effects are of any consequence in a given physical situation depends upon the prevailing circumstances. In formulating system models for those cases with significant dissipation, we would like, if possible, to lump all the dissipative effects into a single component, thereby greatly simplifying the analysis of system behavior. The pure system model with the desired behavior is a *pure dissipative system model.*

The unique nature of the pure dissipative system model lies in the fact that it cannot store energy or entropy in any form. According to the first law of thermodynamics, this means that it cannot have any net energy interaction. Then whatever energy is transferred into the system via a work transfer must be transferred out as a heat transfer. (Note that it is a peculiar characteristic of this model that both the work transfer and the heat transfer must always be negative and equal in magnitude.) Since the heat transfer interaction transports both energy and entropy, according to the second law of thermodynamics the entropy transfer must be negative (out of the system) and equal in magnitude to the entropy generated in the dissipative process. Because of this relationship between entropy generation and entropy transfer, it is necessary to know the details of the heat transfer process in order to determine the behavior of this model. For this reason, this model is rarely used alone. It is usually combined with a pure thermal system model or some other system model capable of heat transfer interactions. This point is illustrated in Section 3.7. The central features of this model are:

Physical characteristics:	Depends upon mechanism of dissipation
Properties:	Depends on configuration
Interactions:	$-W_{1-2} = \int \vec{F} \cdot d\vec{r}$
	$Q_{1-2} = W_{1-2}$
Energy constitutive relation:	None (It cannot store energy.)
Entropy constitutive relation:	None (It cannot store entropy.)

Two classic examples of pure dissipative system models are: (1) the pure translational damper of system dynamics and (2) the pure electrical resistor of electrical circuit theory.

Example 3E.2: Compute the work transfer and heat transfer for a dashpot damper that is extended at a constant rate of 1.2 m/s for 0.1 seconds. The damping coefficient b is 17 Ns/m.

Solution: The damper can be modeled as a linear pure translational damper with the physical characteristic of $b = 17$ Ns/m; the properties F, the through force on the system boundary, and $\hat{v}$, the rate of extension of the boundary; and the property constitutive relation $F = b\hat{v}$. Since $\hat{v} = dx/dt$, the work transfer is given by

$$-W_{1-2} = \int_{t_1}^{t_2} F dx = \int_{t_1}^{t_2} b\vartheta dx = \int_{t_1}^{t_2} b\vartheta^2 dt = b\vartheta^2(t_2 - t_1)$$

$$-W_{1-2} = (17 \text{ N sec / m})(1.2 \text{ m / s})^2(0.1 \text{ sec} - 0 \text{ sec}) = 2.45 \text{ J}$$

Since the pure dissipative system model has no stored energy mode, the first law requires

$$Q_{1-2} = W_{1-2} = -2.45 \text{ J}$$

Until the system experiencing the thermal interaction with the pure dissipative system model is identified, we cannot calculate the entropy transfer or the entropy generated for this model.

3.6 The Early History of Thermodynamics

It is worth noting at this point that some of the terminology of thermodynamics currently in use appears contradictory and illogical in light of the accepted definitions. This terminology is a product of the evolutionary development of thermodynamics and has remained in use for historical reasons. Although the origin of thermodynamics can be traced to the discovery of fire, it was not until the eighteenth century that the basic concepts of thermodynamics were formalized. These developments paralleled similar developments in the science of mechanics which were progressing rapidly from the early works of Newton. Like modern thermodynamics, the non-relativistic mechanics of today appears in much the same form as it did in the eighteenth century.

During this period of rapid advancement in science, the phenomena associated with temperature and heat transfer were receiving considerable attention from Gabriel D. Fahrenheit, Anders Celsius and others who together formulated what was then known as the caloric theory. In keeping with the conservation principles which were being concurrently developed in mechanics, heat or caloric was regarded as a quantity which was conserved and flowed from one system to another. In this form, the simple concepts of the caloric theory were adequate to describe the behavior of systems that could be modeled as pure thermal systems and the interactions that occurred between systems of this type. However, despite considerable effort and ingenuity, these simple concepts were just not adequate to model more complex physical situations.

In spite of the deficiencies of the caloric theory, much of its terminology remains in use in thermodynamics today. For example, the terms "specific heat" and "heat capacity" originated from the concepts of stored heat and are now actually misnomers for the energy derivatives with respect to temperature, equations (3.21) and (3.22). The term "latent heat" (to be defined later) is another example of a term still in use today. This term was originally devised for the more complex process associated with heat transfer to a boiling liquid. The adjective "latent" was used for this particular type of heat transfer since it did not produce the increase in temperature normally associated with heat transfer to a liquid.

Since the caloric theory preceded the formulation of the first law of thermodynamics, it was not recognized that in a coupled thermodynamic system the heat transfer and work transfer are related. Thus, a separate system of units was used for each of these interactions. The heat transfer units were originally defined in terms of the heat transfer required to produce a given change of state of a given mass of water. The calorie was defined as the heat transfer necessary to change the temperature or one gram of water at atmospheric pressure from 15 C to 16 C. The

British thermal unit (Btu) was defined as the heat transfer required to change the temperature of one pound of water at atmospheric pressure from 59.5 F to 60.5 F.

During the first half of the nineteenth century, the first law of thermodynamics was formulated to relate properly the mechanical and thermal behavior of systems. One of the early workers in this regard was Count Rumford (Benjamin Thomson) who, after making some observations of the heat transfer process resulting from the boring of cannon barrels, tried to relate work transfer and heat transfer in the context of the caloric theory. For a number of years this interrelation remained the subject of considerable controversy and confusion. The matter remained unsettled until the careful measurements by James Prescott Joule during the period 1840-1848 established a firm experimental foundation for the first law of thermodynamics and set the stage for the formulation of the second law.

These experiments consisted of a brake or paddlewheel surrounded by a bath of water that was thermally isolated from the environment. The experiment can be modeled as an uncoupled thermodynamic system consisting of two subsystems, a pure dissipative subsystem in thermal communication with a pure thermal subsystem. Joule carefully measured the work transfer to the dissipative subsystem and the resulting change of state manifested by a temperature change in the pure thermal subsystem. *In the model*, there is a negative work transfer for the pure dissipative subsystem with a concomitant negative heat transfer of equal magnitude since the pure dissipative subsystem cannot store energy. Since the dissipative subsystem can interact thermally only with the thermal subsystem, this thermal interaction results in a positive heat transfer for the pure thermal subsystem which produces the aforementioned temperature increase. In a subsequent experiment, Joule measured the heat transfer necessary to produce the same temperature change in the thermal subsystem in the absence of work transfer to the dissipative subsystem. Joule's results showed that this heat transfer was always proportional to the work transfer but not equal to it because he measured the two interactions in independent units. The constant of proportionality measured by Joule is referred to as the "mechanical equivalent of heat" and is given the symbol J. In reality, the constant is merely the factor for converting from one set of energy units to another. Thus, the numerical value of J is different for each combination of work transfer and heat transfer units. On this basis it is possible to formulate the modern definition of the calorie as

$$1 \text{ calorie} = 4.1868 \text{ Joules}$$

This modern definition was formulated so that the old definition from caloric theory is still true.

The real significance of Joule's measurements was that the measurements led to the eventual conclusion that both work transfer and heat transfer are energy interactions and that either can change the energy of the system. Thus, work transfer and heat transfer interactions *do not* involve two separate quantities that are individually conserved. Despite Joule's proof that the two energy interactions are equivalent in their measurement, subsequent study has shown that these two interactions are clearly not equivalent in every way since work transfer involves the transfer of energy only, but heat transfer involves the transfer of both energy and entropy. As will be shown later through the second law of thermodynamics, this difference sets specific numerical limits on the interchangeability of heat and work transfer.

3.7 Uncoupled Thermodynamic Systems

With the system models that we now have at our disposal, we are in a position to analyze the simplest class of thermodynamic systems, namely uncoupled thermodynamic systems. These systems are thermodynamic in the sense that they can experience both work transfer and heat transfer interactions, but they are uncoupled because the thermal and mechanical aspects are independent in the absence of dissipation. If dissipation occurs, the situation is slightly more complicated because it provides a means for connecting (but not coupling) the thermal and mechanical behavior. However, with or without dissipation, this class of systems is uncoupled because it is impossible to decrease their thermal stored energy by means of a positive adiabatic work transfer. In spite of this limitation, this class of systems finds widespread application in engineering practice, and we shall present a number of examples illustrating this behavior.

3.7.1 Uncoupled Thermodynamic Systems without Mechanical Dissipation

As an introduction to the modeling of the multidimensional behavior of uncoupled thermodynamic systems, we consider first systems without mechanical dissipation. These uncoupled systems can be modeled as an assembly of pure conservative system models and pure thermal system models as shown in Figure 3.7. Since the conservative system components

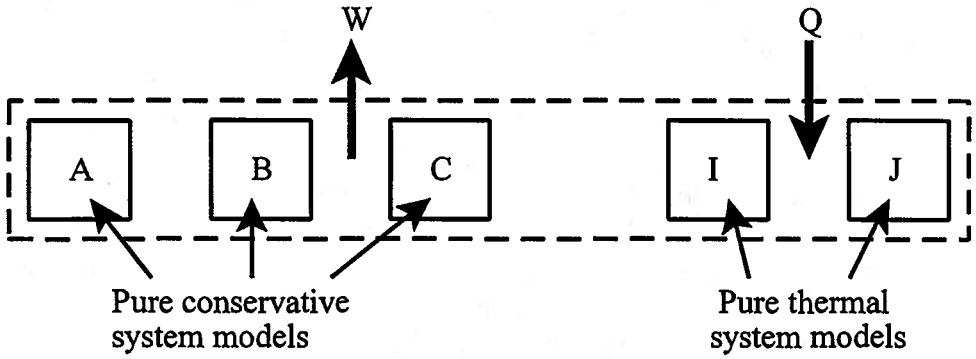

(a) Total system model

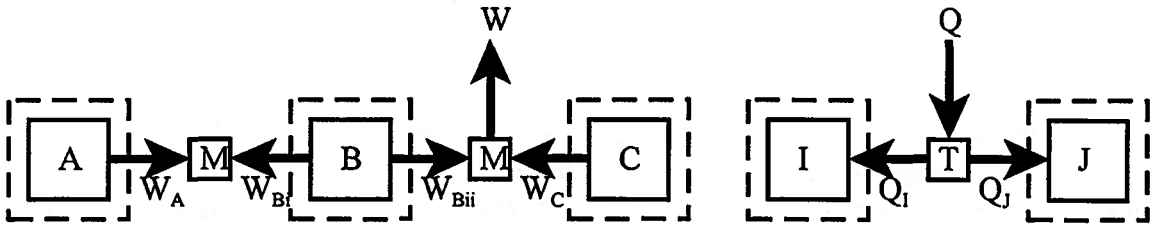

(b) Subsystems and interconnections

Figure 3.7 Model for Uncoupled Thermodynamic System without Dissipation

interact only by work transfer and the thermal system components only by heat transfer, the thermal components cannot interact with or influence the mechanical components and vice versa. Thus, the pure thermal system models describe the *thermal aspects* of the physical situation, and they are completely divorced from the *mechanical aspects* of the physical situation which are described by the pure conservative system models. Systems that can be modeled in this manner

are called *uncoupled systems* because of this separation of thermal and mechanical behavior.

The first law of thermodynamics for an uncoupled system is the sum of the first law expressions for each of the system components included in the model. When these expressions are added, all internal interactions between subsystem models cancel. Then the net external energy interactions equal the sum of the energy changes for all subsystems included in the model. The internal interactions cancel because each appears twice; once with a positive sign and once with a negative sign. The relation between the thermodynamic system and the component subsystems is illustrated in Figure 3.7. Figure 3.7 (a) shows the total system model with external interactions Q and W. Figure 3.7 (b) shows the pure system models as interacting subsystems. The *thermal and mechanical interconnections* are used to interrelate the interactions at the contiguous boundaries of the subsystems. The net interaction at every interconnection must be zero.

We can now develop the first law of thermodynamics for the uncoupled system by summing the first law for each pure system element which is a subsystem. For the three pure conservative system models *A, B,* and *C,* respectively

$$-W_A = (E_2 - E_1)_A \tag{3.37}$$

$$-(W_{Bi} + W_{Bii}) = (E_2 - E_1)_B \tag{3.38}$$

$$-W_C = (E_2 - E_1) \tag{3.39}$$

For the two pure thermal system models

$$Q_I = (U_2 - U_1)_I \tag{3.40}$$

$$Q_J = (U_2 - U_1)_J \tag{3.41}$$

The three interconnection equations are

$$-W_A - W_{Bi} = 0 \tag{3.42}$$

$$-W_{Bii} - W_C + W = 0 \tag{3.43}$$

$$-Q_I - Q_J + Q = 0 \tag{3.44}$$

When we sum equations (3.37, 3.38, 3.39, 3.40, and 3.43), we obtain

$$-W = (E_2 - E_1)_A + (E_2 - E_1)_B + (E_2 - E_1)_C \tag{3.45}$$

and from summing equations (3.40, 3.41, and 3.45), we obtain

$$Q = (U_2 - U_1)_I + (U_2 - U_1)_J \tag{3.46}$$

Note that the internal interactions W_A, W_{Bi}, W_{Bit}, W_C, Q_I, and Q_J each appear once in a subsystem first law and once in an interconnection equation with the opposite sign. Thus, all internal interactions add to zero in the sum for the first law for the total system.

For an uncoupled thermodynamic system without dissipation, the first law of thermodynamics is in two independent and uncoupled parts. The conservative, work transfer related part, is

$$-W_{1\text{-}2} = \sum_i (E_2 - E_1)_i \tag{3.47}$$

where the energy change summation is for all conservative subsystem models. The heat transfer related part is

$$Q_{1\text{-}2} = \sum_i (U_2 - U_1)_i \tag{3.48}$$

where the summation is for all thermal subsystem models. It is this separation of the first law

with separate forms of stored energy that characterizes the system with uncoupled properties. The use of the uncoupled system model without dissipation is illustrated in the following example.

Example 3E.3: A lead sphere with a mass of 0.1 kg free falls a distance of 30 m in a vacuum tank while experiencing heat transfer with the cooler tank walls, Figure 3E.3. The initial velocity is zero, and the initial temperature is 400 C. The final temperature is 200 C. The specific heat of lead is 133 J/kg C. The acceleration of gravity is 9.80 m/s^2.

Determine the final velocity of the lead shot and the values of the heat transfer and work transfers involved in the process.

Solution:

Step 1: Select the system: The system is the lead shot in the gravitational field. The system boundary is defined in Figure 3E.3 (a). The boundary is moving, but the boundary force is zero; thus, the work transfer W is zero. The heat transfer across the boundary by thermal radiation is Q.

Step 2: Model behavior: The lead shot is modeled as an assembly of a pure translational mass, a pure gravitational spring, and a pure thermal system shown in Figure 3E.3 (b).

Step 3: Model the processes: The interaction between the pure translational mass and the pure gravitational spring is an internal interaction within the system. The system has no external work transfer. The external heat transfer for the system is Q from the environment to the system. The mechanical processes are without any dissipation. From the constitutive relations for the pure system elements we have

$$(E_2 - E_1)_{kinetic} = \tfrac{1}{2} m \vartheta_2^{\,2} - \tfrac{1}{2} m \vartheta_1^{\,2}$$

$$(E_2 - E_1)_{gravitational} = mgz_2 - mgz_1$$

$$(U_2 - U_1)_{thermal} = mc(T_2 - T_1)$$

Step 4: Apply the laws of thermodynamics: For an uncoupled system without dissipation, the first law is

$$-W_{1-2} = (E_2 - E_1)_{kinetic} + (E_2 - E_1)_{gravitational}$$

$$Q_{1-2} = (U_2 - U_1)_{thermal}$$

Since W_{1-2} is zero, it follows that

$$(E_2 - E_1)_{kinetic} = -(E_2 - E_1)_{gravitational}$$

$$\tfrac{1}{2} m \vartheta_2^{\,2} - 0 = -(0 - mgz_1)$$

$$\vartheta_2 = \sqrt{2gz_1} = \sqrt{2(9.8\ \text{m/s}^2)(30\ \text{m})} = 24.2\ \text{m/s}$$

Note that the scalar first law does not establish the direction of the velocity.

$$Q_{1-2} = mc(T_2 - T_1)$$

$$Q_{1-2} = (0.1\ \text{kg})(133\ \text{J/kg C})(200\ \text{C} - 400\ \text{C}) = -2660\ \text{J}$$

The negative sign indicates the heat transfer is from the system to the environment.

For the system defined in Figure 3E.3 (a) and modeled in Figure 3E.3 (b), the work transfer is zero so the total mechanical energy of the system remains constant. The gravitational energy is

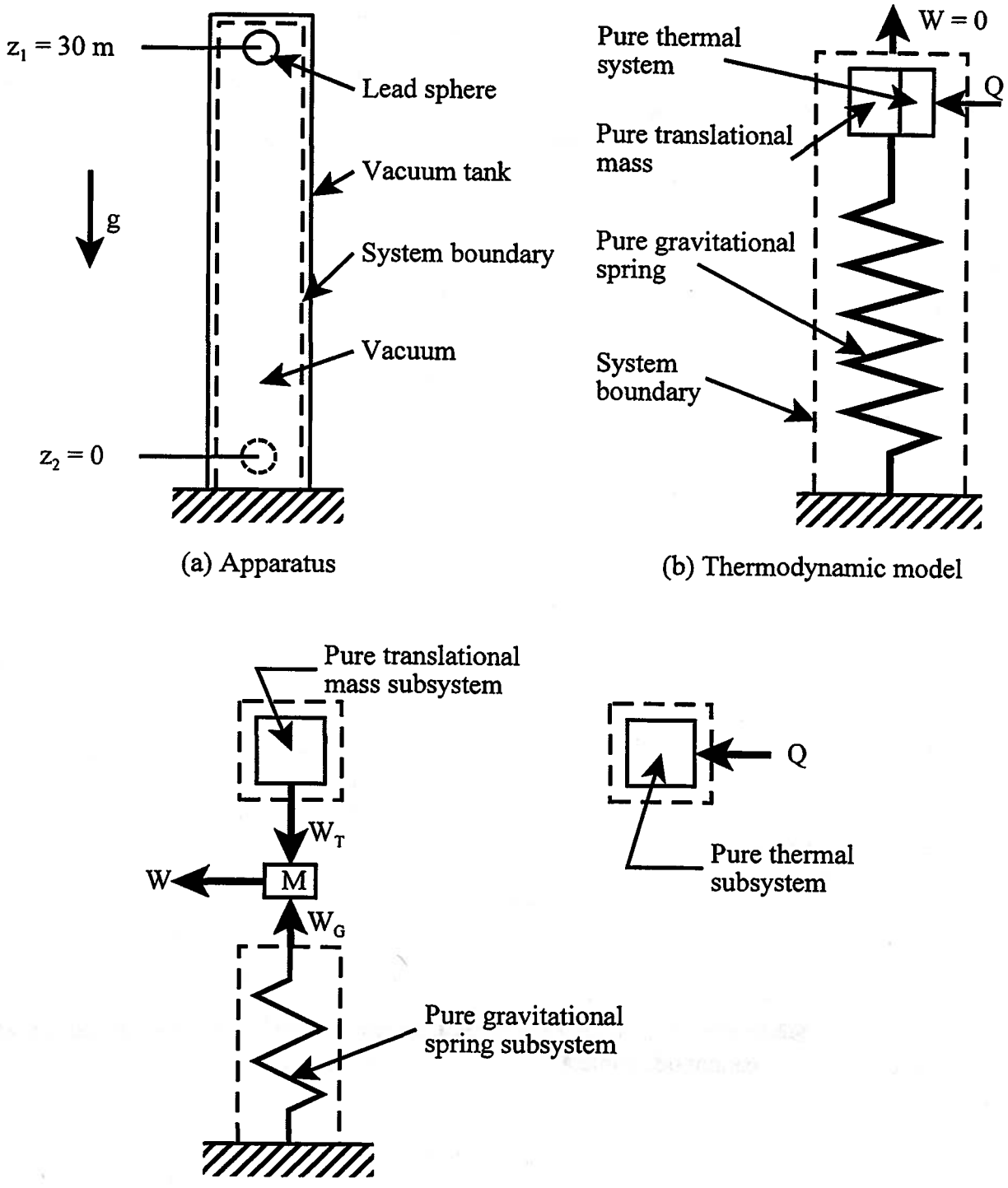

(a) Apparatus

(b) Thermodynamic model

(c) Component subsystems and internal interactions

Figure 3E.3 Uncoupled Thermodynamic System without Dissipation

converted to kinetic energy by internal interactions. The negative heat transfer decreases the stored thermal energy of the system.

Additional understanding of this problem is obtained by determining the internal interactions between the component subsystems. The subsystems and interconnections are shown in Figure 3E.3 (c). When the first law is applied to the subsystems, we have for the pure thermal system

$$Q_{1-2} = (U_2 - U_1)_{thermal} = -2660 \text{ J}$$

For the pure translational mass

$$-W_T = (E_2 - E_1)_{kinetic} = \tfrac{1}{2} m \mathcal{G}_2^{\,2} - 0$$
$$-W_T = \tfrac{1}{2}(0.1 \text{ kg})(24.25 \text{ m/s})^2 = 29.4 \text{ J}$$

For the pure gravitational spring

$$-W_G = (E_2 - E_1)_{gravitational} = 0 - mgz_1$$
$$-W_G = -(0.1 \text{ kg})(9.80 \text{ m/s}^2)(30 \text{ m}) = -29.4 \text{ J}$$

Thus, the work transfer for the gravitational spring subsystem transfer is negative and is into the translational mass subsystem. However, we must remember that we can identify this work transfer across the boundary between subsystems only in our model Figure 3E .3 (b) and (c). In the real physical system Figure 3E.3 (a) there is no geometric boundary between the gravitational and inertial effects.

3.7.2 Uncoupled Thermodynamic System with Mechanical Dissipation

A physical situation similar to that used by Joule in his experiments can also be used to show the connection between mechanical dissipation and entropy generation. The uncoupled thermodynamic system with dissipation has the outward appearance of thermodynamic coupling, but once the internal behavior is known, this turns out not to be the case. This apparent connection between the thermal and mechanical aspects in the presence of dissipation is uni-directional. The thermal stored energy of the system can be increased by means of a negative work transfer interaction through the mechanism of dissipation, but it cannot be decreased by a positive work transfer. That is, thermal processes cannot influence the mechanical aspects of system behavior. Dissipation only allows mechanical processes to influence the thermal aspects. Therefore, the system cannot be coupled. Consider the physical situation shown schematically in Figure 3.8.

This uncoupled thermodynamic system with dissipation is modeled as an assembly of subsystems with pure conservative mechanical systems representing the mechanical aspects, pure thermal systems representing the thermal aspects, and pure dissipative systems representing the dissipative aspects. The first law of thermodynamics for the uncoupled system with dissipation is the sum of the first law expressions for each subsystem. As before, all internal interactions between subsystems are eliminated in the addition. Figure 3.8 shows the relation between the total system and the subsystems composed of the pure system models.

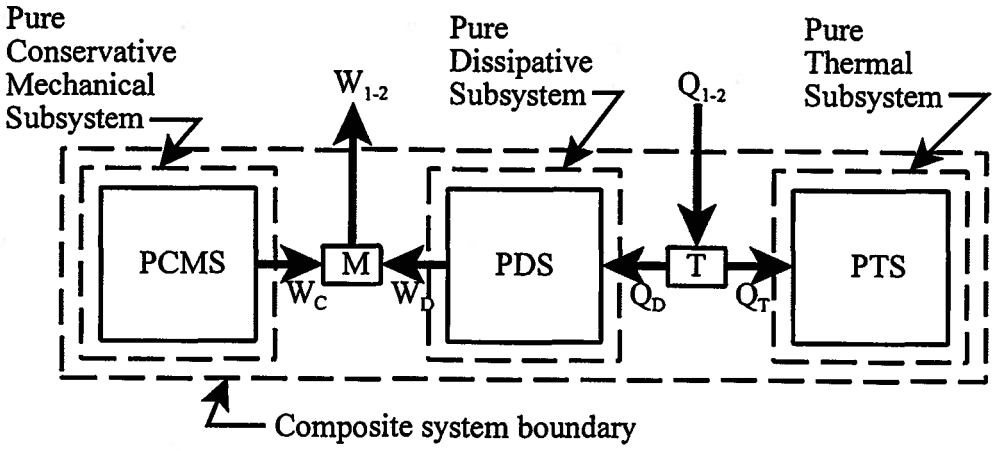

Figure 3.8 Model of Uncoupled Thermodynamic System with Dissipation

The first law expressions for the subsystems are

$$-W_C = (E_2 - E_1)_C \tag{3.49}$$

$$Q_D - W_D = 0 \tag{3.50}$$

$$Q_T = (U_2 - U_1)_T \tag{3.51}$$

The interconnection equations are

$$-W_C - W_D + W_{1-2} = 0 \tag{3.52}$$

$$-Q_T - Q_D + Q_{1-2} = 0 \tag{3.53}$$

By direct summation of equations (3.49-3.53), the first law for the system is

$$Q_{1-2} - W_{1-2} = (E_2 - E_1)_C + (U_2 - U_1)_T \tag{3.54}$$

When an uncoupled system undergoes a process involving dissipation, the first law does not separate into two independent equations because the dissipation provides an internal interaction between the mechanical and thermal aspects of the system. If we combine equations (3.49) and (3.52), we have

$$-(W_{1-2} - W_D) = (E_2 - E_1)_C \tag{3.55}$$

and if we combine equations (3.51) and (3.53), we have

$$Q_{1-2} - Q_D = (U_2 - U_1)_T \tag{3.56}$$

But we know that Q_D and W_D are negative so we can conclude

$$(E_2 - E_1)_C < -W_{1-2} \tag{3.57}$$

$$(U_2 - U_1)_T > Q_{1-2} \tag{3.58}$$

When dissipation occurs during a process in an uncoupled system, the increase in stored mechanical energy is less than the mechanical work transfer into the system. Further, the increase in stored thermal energy is greater than the heat transfer into the system, as expressed by equations (3.57) and (3.58). In effect the dissipation "creates" the thermal energy at the expense of the "loss" of an equal amount of mechanical energy as required by the first law, equation (3.54).

In order to see the relationship between the dissipation of mechanical energy and the

generation of entropy, it is necessary to consider the case in which no entropy is transferred into the pure thermal subsystem by heat transfer. Then $Q_{1\text{-}2} = 0$ and the stored thermal energy increases only by means of the mechanical dissipation W_D. The first law of thermodynamics for the system shown in Figure 3.5 then becomes

$$-W_{1\text{-}2} = (E_2 - E_1)_C + (U_2 - U_1)_T \tag{3.59}$$

From equations (3.55) and (3.56) and the fact that $W_D = Q_D$, it is clear that

$$-W_D = (U_2 - U_1)_T = C(T_2 - T_1)_T \tag{3.60}$$

Thus since $W_D < 0$, the stored thermal energy and, hence, the temperature of the pure thermal system model increases as a result of the dissipation. Since the entropy of the pure thermal system is a function of its temperature, it follows from the entropy constitutive relation for the pure thermal system that the entropy of the pure thermal system also has increased as a result of the dissipation.

$$(S_2 - S_1)_T = C\ln\left(\frac{T_2}{T_1}\right) \tag{3.61}$$

The second law of thermodynamics for the uncoupled system with dissipation becomes

$$S_2 - S_1 = (S_2 - S_1)_T = S_{transfer} + S_{gen} \tag{3.62}$$

Since we are considering the case for which there is no external heat transfer, there is no entropy transfer and equation (3.62) reduces to

$$S_{gen} = (S_2 - S_1)_T = C\ln\left(\frac{T_2}{T_1}\right) > 0 \tag{3.63}$$

Thus, the entropy generated is a direct consequence of the mechanical dissipation. The use of the uncoupled system model with dissipation is illustrated in the following example.

Example 3E.4: A spring is connected within an oil filled piston-cylinder apparatus as shown in Figure 3E.4. The spring is slowly extended by pulling on the string. The string is cut and the spring returns to the unextended length. Determine the final temperature and the entropy generated during the run down to equilibrium.

The initial conditions, state 1, are: the spring is at zero force, and the oil, spring, and piston are at 20 C. During the stretching process, the spring extends 0.1 m to state 2. After the string is cut the spring returns to the unextended length, state 3. The spring constant is 1000 N/m. The combined heat capacity of the spring, oil and piston is 4000 J/C.

Solution:

Step 1: Select system: The system for analysis is the collection of components within the boundary drawn at the cylinder wall.

Step 2: Model the behavior: The system is modeled as a pure translational spring, a pure translational damper, and a pure thermal system representing the thermal aspects of the spring, the oil, and the piston. The cylinder wall is modeled as adiabatic.

Step 3: Model the process: The process 1-2 is modeled as a conservative process since the extension is assumed slow enough so that the damping force may be taken as zero. This process has no heat transfer since the system is surrounded by an adiabatic wall. The process 2-3 is modeled as a zero work transfer process with dissipation. The work transfer is zero since the motion at the system boundary is zero. This process is also adiabatic.

Step 4: Apply the laws of thermodynamics: The first law of thermodynamics for the system defined in Figure 3E.4 (b) is

$$Q - W = (E_f - E_i)_E + (U_2 - U_1)_T$$

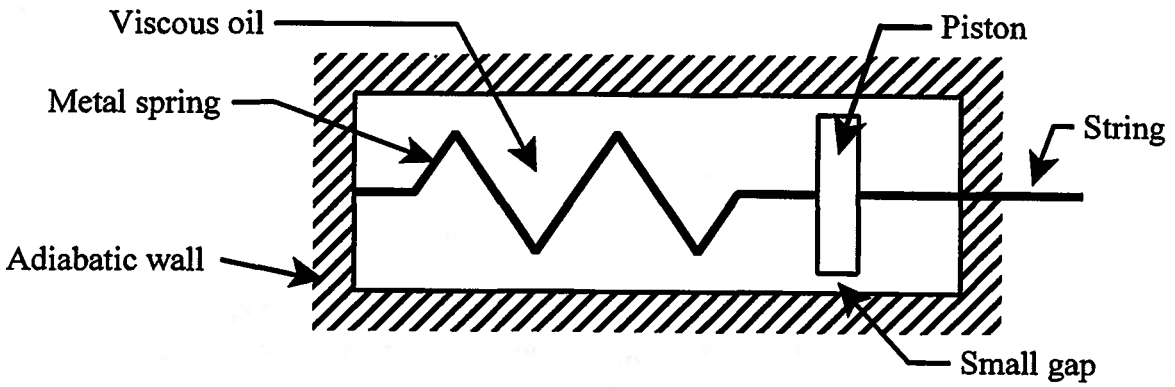

(a) Apparatus

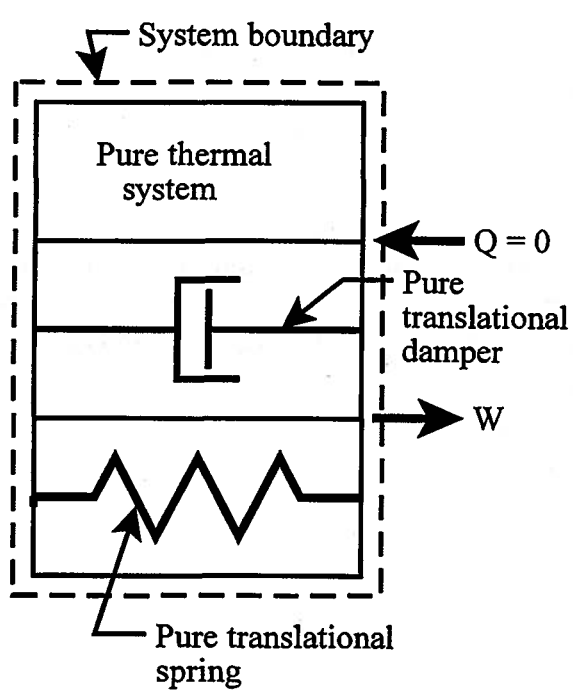

(b) Thermodynamic model

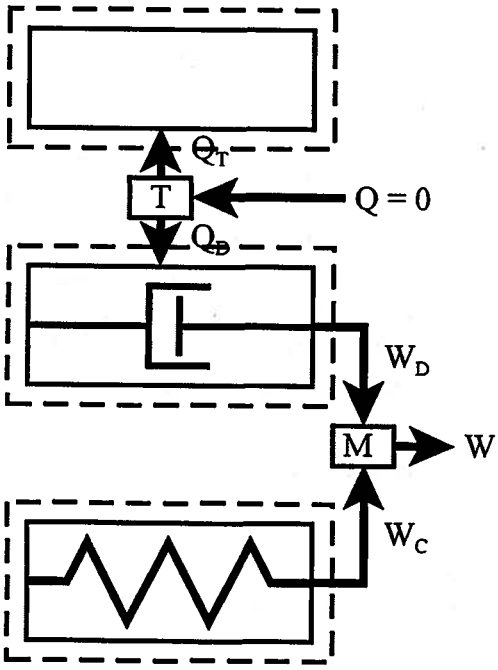

(c) Subsystem models

Figure 3E.4 Uncoupled Thermodynamic System with Mechanical Dissipation

where the energy change is the sum of the energy changes for each uncoupled system included in the model. For the conservative process 1-2 the first law separates.

$$Q_{1-2} = (U_2 - U_1)_T = 0 = C(T_2 - T_1)$$

$$-W_{1-2} = (E_2 - E_1)_E = \tfrac{1}{2}kx_2^2 - \tfrac{1}{2}kx_1^2$$

$$-W_{1-2} = \tfrac{1}{2}(1000\ \text{N/m})(0.1\ \text{m})^2 - 0 = 5\ \text{J}$$

For the dissipative process 2-3 the first law becomes

$$Q_{2-3} - W_{2-3} = (E_3 - E_2)_E + (U_3 - U_2)_T = 0$$

Since $Q_{2\text{-}3} = W_{2\text{-}3} = 0$,

$$C(T_3 - T_2) = -\tfrac{1}{2}kx_3^{\,2} + \tfrac{1}{2}kx_2^{\,2}$$

but $x_3 = x_1 = 0$, and $T_2 = T_1$. Thus

$$T_3 - T_1 = \frac{k}{2C}x_2^{\,2}$$

$$T_3 = 20 + \frac{1000\ \text{N/m}}{2(4000\ \text{J/C})} = 20.00125\ \text{C}$$

It is important to note that, for the system defined by the boundary shown in Figure 3E.4 (b), the temperature rise is the result of internal dissipation and not the result of a heat transfer.

For the entropy generated by this dissipative process, we can apply the second law of thermodynamics to the model shown in Figure 3E.4(b). Then since no entropy is generated in conservative processes, the only entropy generated occurs during process 2-3.

$$S_3 - S_2 = S_{transfer} + S_{gen}$$

But since the system is adiabatic, it follows that $S_{transfer} = 0$. Then substituting the entropy constitutive relation for the pure thermal system, we get

$$S_{gen} = S_3 - S_2 = C\ln\left(\frac{T_3}{T_2}\right) = (4000\ \text{J/C})\ln\left(\frac{293.15125\ \text{C}}{293.15}\right) = 0.0171\ \text{J/K}$$

This entropy is generated through the action of viscous dissipation in the oil.

This physical situation can also be analyzed by considering the individual subsystems shown in Figure 3E.4 (c). The analysis here is more involved; however, it provides additional information about the internal interactions involved in each process. For the conservative process 1-2 we have assumed the damping force is zero so

$$(W_D)_{1\text{-}2} = (Q_D)_{1\text{-}2} = 0$$

The heat transfer interconnection equation requires

$$-Q_T - Q_D + Q = 0$$

$$(Q_T)_{1\text{-}2} = Q_{1\text{-}2} - (Q_D)_{1\text{-}2} = 0 - 0 = 0$$

The first law for the thermal subsystem is

$$0 = (U_2 - U_1)_T = C(T_2 - T_1)$$

$$T_2 = T_1$$

The first law for the spring subsystem is

$$-(W_C)_{1\text{-}2} = \tfrac{1}{2}kx_2^{\,2} - \tfrac{1}{2}kx_1^{\,2} = 5\ \text{J} - 0 = 5\ \text{J}$$

The mechanical interconnection equation requires

$$W_D + W_C - W = 0$$

$$-W_{1\text{-}2} = -(W_C)_{1\text{-}2} - (W_D)_{1\text{-}2} = 5\ \text{J} - 0 = 5\ \text{J}$$

For the dissipative process 2-3, the first law for the spring requires

$$-(W_C)_{2\text{-}3} = \tfrac{1}{2}kx_3^{\,2} - \tfrac{1}{2}kx_2^{\,2} = 0 - 5\ \text{J} = -5\ \text{J}$$

Since $W_{2\text{-}3} = 0$, the mechanical interconnection equation requires

$$(W_D)_{2\text{-}3} = -(W_C)_{2\text{-}3} = -5\ \text{J}$$

The first law for the damper requires

$$-(W_D)_{2\text{-}3} = -(Q_D)_{2\text{-}3} = 5\ \text{J}$$

Since $Q_{2\text{-}3} = 0$, the thermal interconnection equation requires

$$(Q_T)_{2\text{-}3} = -(Q_D)_{2\text{-}3} = 5\,\text{J}$$

The first law for the thermal subsystem is

$$(Q_T)_{2\text{-}3} = (U_3 - U_2)_T = C(T_3 - T_2)$$

But $T_2 = T_1$, thus

$$T_3 = T_1 + \frac{(Q_T)_{2\text{-}3}}{C} = 20\,\text{C} + \frac{5\,\text{J}}{4000\,\text{J/C}} = 20.00125\,\text{C}$$

For the entropy generation, we cannot examine any one subsystem alone but have to consider the combination of the damper and the thermal subsystems because of the interrelationship between entropy generation and entropy transfer. From the second law for this combination of subsystems, we have

$$S_{gen} = S_3 - S_2 - S_{transfer} = C\ln\left(\frac{T_3}{T_2}\right) - 0 = (4000\,\text{J/C})\ln\left(\frac{293.15125\,\text{C}}{293.15\,\text{C}}\right) - 0 = 0.0171\,\text{J/K}$$

where we have used the fact that $S_{transfer} = 0$ since the system is adiabatic.

Example 3E.5: A resistive heating element is used to heat an oil bath contained within an imperfectly insulated container, Figure 3E.5 (a). The element is supplied with 16 amperes

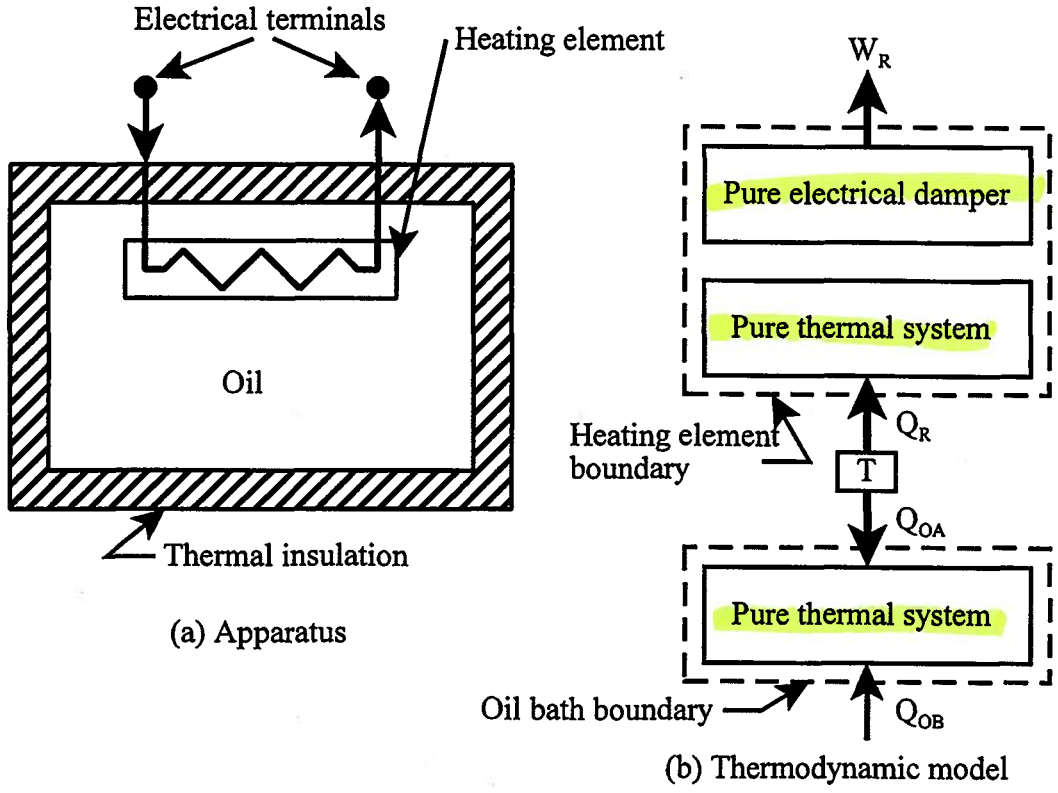

Figure 3E.5 Uncoupled Thermodynamic System with Electrical Dissipation

of current at a potential of 220 volts for 60 seconds. The mass of the heating element is 0.5 kg and the mass of the oil is 2 kg. The specific heat of the heating element is 700 J/kg C and of the

oil is 2100 J/kg C. The initial temperature of the oil and heating element is 17 C and the final equilibrium temperature is 21.12 C. What is the heat transfer to the oil from the heating element? What is the heat transfer to the insulation around the oil container?

Solution:

Step 1: Select systems: Two systems are defined as shown in Figure 3E.5 (b). System *R* is the heating element and system *0* is the oil bath, with the boundaries as shown. System *R* has electrical work transfer W_R at the terminals and heat transfer Q_R from the oil bath. System *0* has heat transfer Q_{OA} from the heater and Q_{OB} from the insulation.

Step 2: Model behavior: System *R* is modeled as a pure electrical damper and a pure thermal system. System *0* is modeled as a pure thermal system.

Step 3: Model processes: The process in system *R* is dissipative with a negative work transfer, an increase in stored thermal energy *U*, and a negative heat transfer. The process in system *0* is thermal with two heat transfers and a change in thermal energy *U*. The pure electrical damper model (more commonly known as the resistor) for system *R* is the electrical analog of the pure translational damper described previously. The boundary force (the voltage) is determined by the rate at which charge crosses the boundary (current). The general constitutive relation gives the potential difference v (voltage) as a function of the current i. For the linear resistor

$$v = iR$$

where the constant of proportionality *R* is the electrical resistance. For the work transfer interaction, we have

$$-W_{1-2} = \int_{q_1}^{q_2} v\,dq = \int_{q_1}^{q_2} iR\,dq$$

But $dq = idt$. Then for system *R*

$$-W_R = \int_{t_1}^{t_2} i^2 R dt = \int_{t_1}^{t_2} vi\,dt$$

$$-W_R = (220\text{ V})(16\text{ A})(60\text{ sec}) = 211.2\text{ kWsec} = 211.2\text{ kJ}$$

where the constitutive relation for the damper (resistor) has been used to eliminate *R*. For the thermal system component of system *R*

$$(U_2 - U_1)_R = (mc)_R (T_2 - T_1)_R$$

For system *0*

$$(U_2 - U_1)_O = (mc)_O (T_2 - T_1)_O$$

Step 4: Apply the laws of thermodynamics: For system *R* the first law gives

$$Q_R - W_R = (U_2 - U_1)_R = (mc)_R (T_2 - T_1)_R$$

$$Q_R = W_R + (mc)_R (T_2 - T_1)_R$$

$$Q_R = -21.12\text{ kJ} + (0.5\text{ kg})(0.7\text{ kJ / kg C})(21.12\text{ C} - 17\text{ C})$$

$$Q_R = -19.64\text{ kJ}$$

For system *0* the first law gives

$$Q_{OA} + Q_{OB} = (U_2 - U_1)_O = (mc)_O (T_2 - T_1)$$

The thermal interconnection equation is

$$Q_R + Q_{OA} = 0$$

$$Q_R + Q_{OA} = 0$$

Thus

$$Q_{OB} = (mc)_O(T_2 - T_1) + Q_R$$
$$Q_{OB} = (2\text{ kg})(2.1\text{ kJ / kg C})(21.12\text{ C} - 17\text{ C}) + (-19.64\text{ J})$$
$$Q_{OB} = -1.96\text{ kJ}$$

The heat transfer from the heater to the oil is $Q_{OA} = -Q_R = 19.64$ kJ . The heat transfer to the insulation is $-Q_{OB} = 1.96$ kJ. This process is clearly a dissipative process, but in order to determine the entropy generated in the process, we would need to know the properties of the insulation and whether there was any entropy transfer to the environment surrounding the apparatus.

3.8 Thermal Dissipation

In the previous section we saw how the process of mechanical dissipation in the uncoupled thermodynamic system led to the generation of entropy. We also saw how the run down to equilibrium of a mechanical system generates entropy through the dissipation of mechanical energy. We have also seen how entropy can be generated by the process of a thermal run down to equilibrium. By analogy with the run down to equilibrium of mechanical systems, this run down to equilibrium of thermal systems leads to "thermal dissipation." While we are not yet in a position to show the details of this mechanism of "thermal dissipation", we can certainly examine the underlying physics of the concept in the context of the second law of thermodynamics.

In the course of a thermal run down to equilibrium, the two interacting systems exchange energy and entropy via the heat transfer interaction by which they are strive to reach a state of mutual equilibrium characterized by a common uniform temperature. During this equilibration process, the assembly of these two systems forms an isolated system. According to the first law of thermodynamics for this isolated system, equation (2.1), there is no net change of energy of the assembly even though the energies of the individual component subsystems A and B do change. As we showed in section 3.5.2, entropy is generated in this thermal run down to equilibrium in order for both the first and second laws of thermodynamics to be satisfied simultaneously.

Suppose that we take a different approach to the equilibration process. In this new approach, we interpose between systems A and B a third system C that operates in *reversible* cycles while in thermal communication with A and B as shown schematically in Figure 3.9. This is permissible as long as system C executes an integral number of cycles and therefore experiences no net change of state, i.e., no net change of energy or entropy, as the two systems A and B equilibrate. When the energy and entropy exchanges between systems A and B via the cyclic system C are complete, systems A and B have each experienced a net change of state but system C has not because of its cyclic nature. Because system C operates in reversible cycles, it generates no entropy, and as we showed in section 3.4, equation (3.9), it experiences no net entropy transfer. This means that whatever entropy transfer occurs between systems A and C during the equilibration process, a similar entropy transfer of equal magnitude but opposite sign

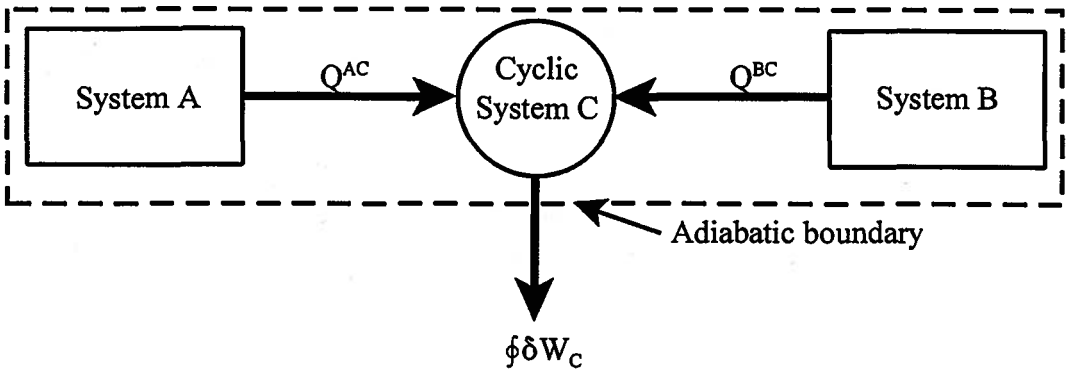

Figure 3.9 Thermal Equilibration between Two Systems Via a Cyclic System

occurs between system B and C. Then the function of system C is simply to facilitate the transfer of entropy between systems A and B in a reversible manner. It follows, then, that the equilibration process between systems A and B is reversible in this new configuration.

In order to satisfy the second law for the adiabatic system consisting of A + B + C, it must be the case that for the process of thermal equilibration to be reversible

$$(S_2 - S_1)_{A+B+C} = (S_2 - S_1)_A + (S_2 - S_1)_B + \oint dS_C = 0$$

Since the entropy is a property,

$$\oint dS_C = 0$$

because there can be no net change in any property for any cycle of any system by definition. It follows, then, that

$$(S_2 - S_1)_A = -(S_2 - S_1)_B \tag{3.64}$$

Thus, one system decreases in entropy while the other increases in entropy by an equal amount during this reversible process. According to the first law for the adiabatic system A+B+C,

$$-(W_{1-2})_{A+B+C} = (U_2 - U_1)_{A+B+C} = (U_2 - U_1)_A + (U_2 - U_1)_B + \oint dU_C \tag{3.65}$$

Since the stored energy is also a property,

$$\oint dU_C = 0$$

and it follows that

$$-(W_{1-2})_{A+B+C} = (U_2 - U_1)_A + (U_2 - U_1)_B = \oint \delta W_C \tag{3.66}$$

Thus the net decrease in energy that occurs during the equilibration process between systems A and B via system C results in a work transfer from the adiabatic composite system.

From the perspective of system C, the heat transfer between the system with the higher temperature and system C will be positive and the heat transfer between the system with the lower temperature and system C will be negative. In order for the two entropy transfers associated with these two heat transfer interactions to be equal in magnitude and opposite in sign, it must be the case that the one that occurs at the higher temperature must be greater in

magnitude. Thus the magnitude of the positive heat transfer (viewed from system C) must be greater than the magnitude of the negative heat transfer, and the *net* heat transfer for system C must be positive. Then since system C operates in an integral number of cycles, it follows from the first law for system C that the net work transfer for system C is equal to its net heat transfer.

$$\oint \delta Q_C - \oint \delta W_C = \oint dU_C = 0 \tag{3.67}$$

and

$$\oint \delta W_C = \oint \delta Q_C > 0 \tag{3.68}$$

Thus, when two systems come to a state of mutual thermal equilibrium in a reversible manner via a third cyclic system, there is no net change in entropy of the two systems but there is a net decrease in energy of the two systems and a net positive work transfer to the environment. This is in distinct contrast to the case of the run down to equilibrium via simple heat transfer which is irreversible and results in no work transfer. It is this work transfer that could have been realized had the equilibration process been carried out reversibly that is the origin of the "dissipation" during the simple run down to equilibrium. This is what we mean by the term "thermal dissipation" in reference to irreversible heat transfer processes occurring between two systems with different initial temperatures.

It is important to note that the final mutual equilibrium state for systems A and B will be different depending upon whether this state is achieved reversibly or irreversibly. In the reversible equilibration process, the two systems A and B experience a net reduction in their total energy due to the work transfer from the cyclic system C to the environment. Thus, in the reversible case, the final uniform equilibrium temperature of the two systems is typically lower than it would have been after a simple run down to equilibrium.

Example 3E.6: Two pure thermal systems A and B are each in initial states characterized by the temperatures $T_{1A} = 500$ K and $T_{1B} = 250$ K, respectively. The heat capacities of the two systems are $C_A = 100$ J/K and $C_B = 200$ J/K, respectively. (a) Determine the final equilibrium temperature $(T_2)_{irrev}$ of the two systems for a simple run down to equilibrium. (b) Determine the final equilibrium temperature $(T_2)_{rev}$ of the two systems for a reversible equilibration process. (c) Determine the "thermal dissipation" of the simple run down to equilibrium.

Solution: (a) For the simple run down to equilibrium, the first law for the isolated composite system A+B is given by

$$(U_2 - U_1)_{A+B} = C_A(T_2 - T_{1A}) + C_B(T_2 - T_{1B}) = 0$$

Then substituting the energy constitutive relation for the pure thermal system model, we have

$$C_A(T_{1A} - T_2) = C_B(T_2 - T_{1B})$$

$$(100 \text{ J/K})(500 \text{ K} - T_2) = (200 \text{ J/K})(T_2 - 250 \text{ K})$$

$$T_2(200 \text{ J/K} + 100 \text{ J/K}) = 50 \text{ kJ} + 50 \text{ kJ} = 100 \text{ kJ}$$

$$(T_2)_{irrev} = \frac{100 \text{ kJ}}{300 \text{ J/K}} = 333.33 \text{ K}$$

(b) For the reversible equilibration process, we have a situation similar to that depicted in Figure 3.6. Then if we apply the second law to the reversible composite system inside the adiabatic boundary, we have

$$(S_2 - S_1)_{A+B+C} = (S_2 - S_1)_A + (S_2 - S_1)_B + \oint dS_C = 0$$

Then because the entropy is a property

$$\oint dS_C = 0$$

Substituting the entropy constitutive relation for the pure thermal system model, we have

$$C_A \ln\left(\frac{T_{1A}}{T_2}\right) = C_B \ln\left(\frac{T_2}{T_{1B}}\right)$$

$$T_2^{C_A+C_B} = T_{1A}^{C_A} \cdot T_{1B}^{C_B}$$

$$T_2^3 = (500\text{ K})(250\text{ K})^2$$

$$(T_2)_{rev} = 314.98\text{ K}$$

(c) If we apply the first law to the reversible case, we have

$$-(W_{1-2})_{A+B+C} = (U_2 - U_1)_A + (U_2 - U_1)_B + \oint dU_C$$

If we substitute the energy constitutive relation for the pure thermal system and equation (3.66), we get

$$(W_{1-2})_{A+B+C} = (100\text{ J/K})(500\text{ K} - 314.98\text{ K}) + (200\text{ J/K})(250\text{ K} - 314.98\text{ K})$$

$$(W_{1-2})_{A+B+C} = 5.506\text{ kJ}$$

This is the 'thermal dissipation" associated with the irreversible heat transfer process of the simple run down to equilibrium. It is the energy that was "dissipated" during the irreversible process in the sense that this much energy could have been realized in the form of a work transfer had the equilibration process been reversible.

This can be seen more clearly by connecting the cyclic system to a pure dissipative system in thermal communication with the composite system A+B as shown in Figure 3E.6.

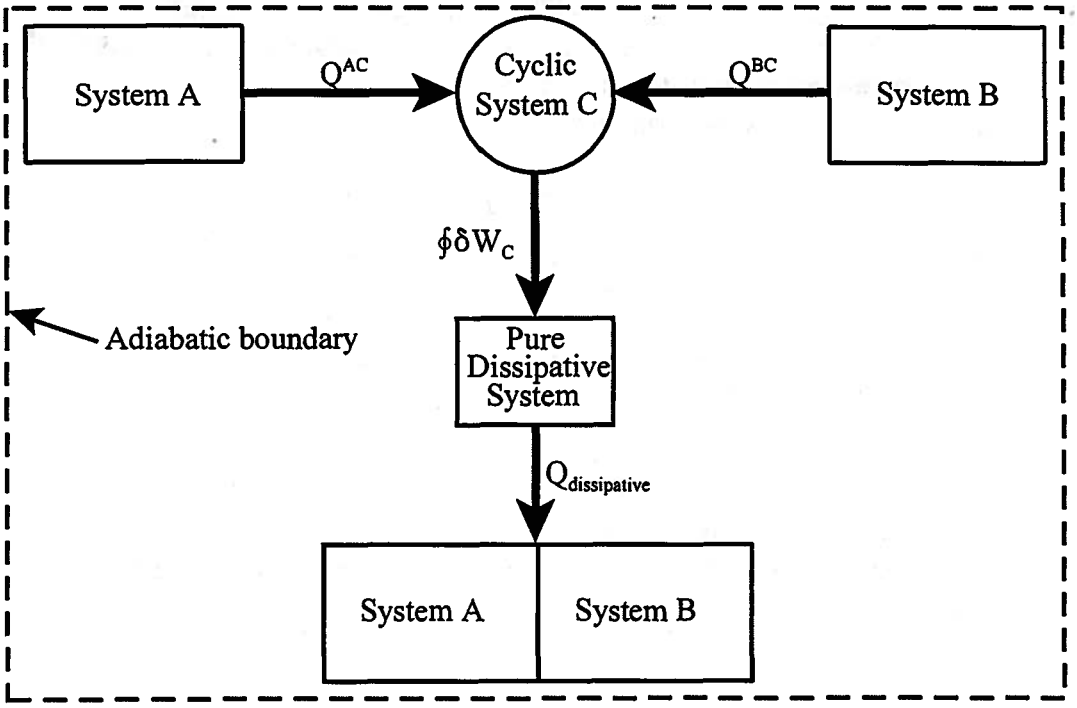

Figure 3E.6 Irreversible Thermal Equilibration between Two Systems

Then this composite system experiences heat transfer in the amount of 5.506 kJ which will change the temperature of the composite system from 314.98 K to some new value T_3 which can be determined by applying the first law to the composite system. Thus

$$(C_A + C_B)\left[T_3 - (T_2)_{rev}\right] = 5.506 \text{ kJ}$$

$$T_3 = (T_2)_{rev} + \frac{5.506 \text{ kJ}}{C_A + C_B} = 314.98 \text{ K} + \frac{5.506 \text{ kJ}}{(100 \text{ J/K} + 200 \text{ J/K})}$$

$$T_3 = 333.33 \text{ K}$$

which is precisely the final equilibrium temperature that results from the irreversible run down to equilibrium.

Problems

3.1 As part of a heat treating operation, a steel part with a mass of 100 kg is to be quenched from a temperature of 1000 C to a temperature of 50 C by plunging the part into a water bath enclosed in an adiabatic chamber. The initial temperature of the water bath is 20 C. The water bath and the steel part can be modeled as pure thermal systems with c_{water} = 4. 187 kJ/kg K and c_{steel} = 0.473 kJ/kg K.

(a) Describe a model suitable to determine the amount of water necessary to perform this part of the heat treating process. State all the assumptions associated with this model.

(b) What is the necessary amount of water?

(c) Calculate the heat transfer for the system consisting of the steel part and the water?

(d) Calculate the heat transfer for the steel part.

(e) Calculate the heat transfer for the water.

(f) Calculate the entropy change for the system consisting of the steel part and the water.

(g) Calculate the entropy change for the steel part.

(h) Calculate the entropy change for the water.

(i) Calculate the entropy transfer for the system consisting of the steel part and the water.

(j) Calculate the entropy generated for the system consisting of the steel part and the water.

(k) Was this part of the heat treating operation reversible or irreversible?

3.2 As an alternative to the heat treating operation of Problem 1 above, the steel part is to be cooled to the same final temperature, 50 C, by means of a process that uses a device that operates in cycles and transfers energy and entropy from the steel part to the same water bath as Problem 3.1 above except that the process is now conducted in a reversible manner as shown in Figure 3P.2.

(a) Describe a model suitable to determine the amount of water necessary to perform this part of the heat treating process. State all the assumptions associated with this model.

(b) What is the necessary amount of water?

(c) Calculate the heat transfer for the system consisting of the steel part and the water?

(d) Calculate the heat transfer for the steel part.

(e) Calculate the heat transfer for the water.

(f) Calculate the entropy change for the system consisting of the steel part and the water.

(g) Calculate the entropy change for the steel part.

(h) Calculate the entropy change for the water.

(i) Calculate the entropy transfer for the system consisting of the steel part and the water.

(j) Calculate the entropy generated for the system consisting of the steel part and the water.

(k) Was this part of the heat treating operation reversible or irreversible?

(l) Why are the answers to Problem 2 different from those of Problem 1?

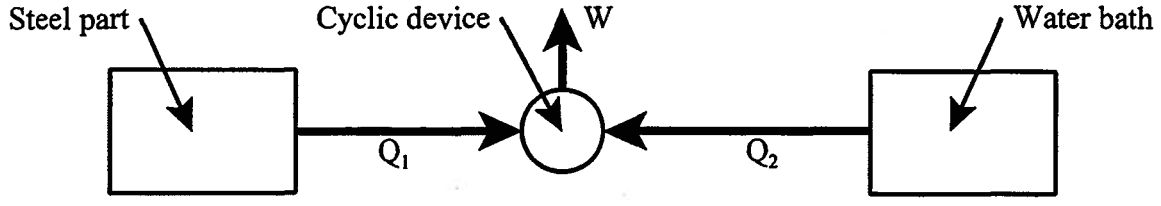

Figure 3P.2

3.3 Figure 3P.3 shows a particular design of an electron beam welder which is a device that employs a beam of high energy electrons (20 kV) in a high vacuum chamber to melt a very localized spot on a metal target. In welding, the parts to be joined are electrically grounded and used as the target while the beam traverses the seam to be welded. In a certain application, two parts are to be welded in a manner such that the temperature of a particular area, remote from the weld itself, must not exceed 205 C. As the design engineer, it is necessary for you to determine, in a very simple way, a safe limit for the welding time for each value of the current setting of the welder.

The data for the welding machine are:

acceleration voltage 20 kV

beam current 0 to 300 mA.

The data for the parts are:

$m_{parts} = 0.5$ kg

$c_{parts} = 875$ J/kg K

$(T_{parts})_{initial,\ maximum} = 33$ C

(a) For a system consisting of the parts to be welded, formulate in thermodynamic terms a model that will enable you to determine the necessary design information.

(b) Using this model, plot welding time as a function of beam current.

(c) For the system defined in part (a) above, calculate values for the work transfer, heat transfer, changes in energy and entropy, and entropy transfer for the maximum value of beam current.

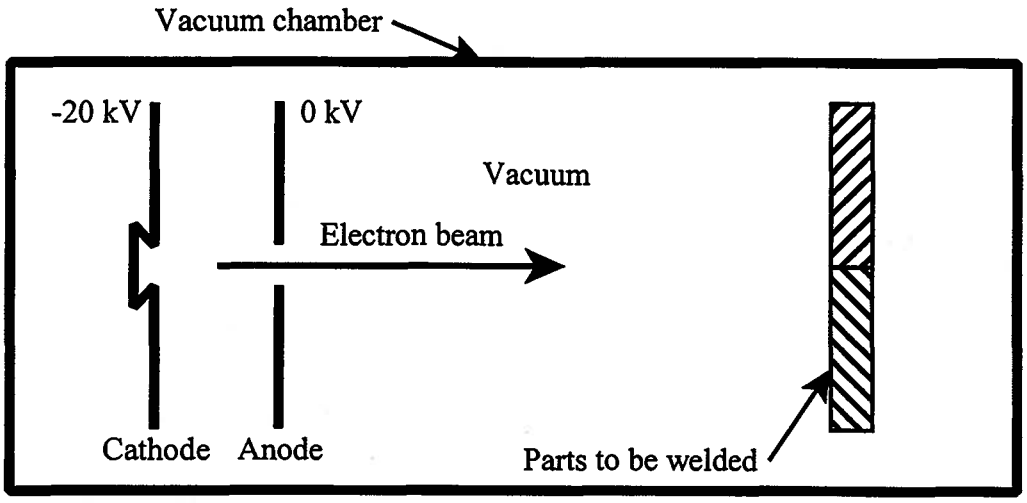

Figure 3P.3

3.4 A system consists of an elastic coil spring. When the spring is compressed 20 mm from the unstressed (zero force) state, the work transfer for the system is -20 Joules. Is it possible for the spring system to return to its original unstressed state with neither a heat transfer nor a work transfer? Present your answer in the form of a model with all interactions and energy changes clearly specified.

3.5 A freight handling system consists of the equipment shown in Figure 3P.5. Boxes of freight move down the frictionless roller conveyor from the second floor to the first floor of a building where they are readied for shipment. The boxes are brought to a stop by sliding them across the horizontal loading platform. The coefficient of sliding friction between the platform and the boxes is $f_s = 0.5$.

(a) Define the system and an appropriate model to determine the minimum length of the platform necessary to stop the boxes.

(b) What is the required length? Does this length depend upon the mass of the box?

(c) For a system consisting of the box, the conveyor, the platform, and the surrounding air, determine the work transfer, heat transfer, and the change in energy for the process by which the box slides down the conveyor and comes to equilibrium.

(d) For this system, is there any entropy transfer? Any change in entropy? Any entropy generated?

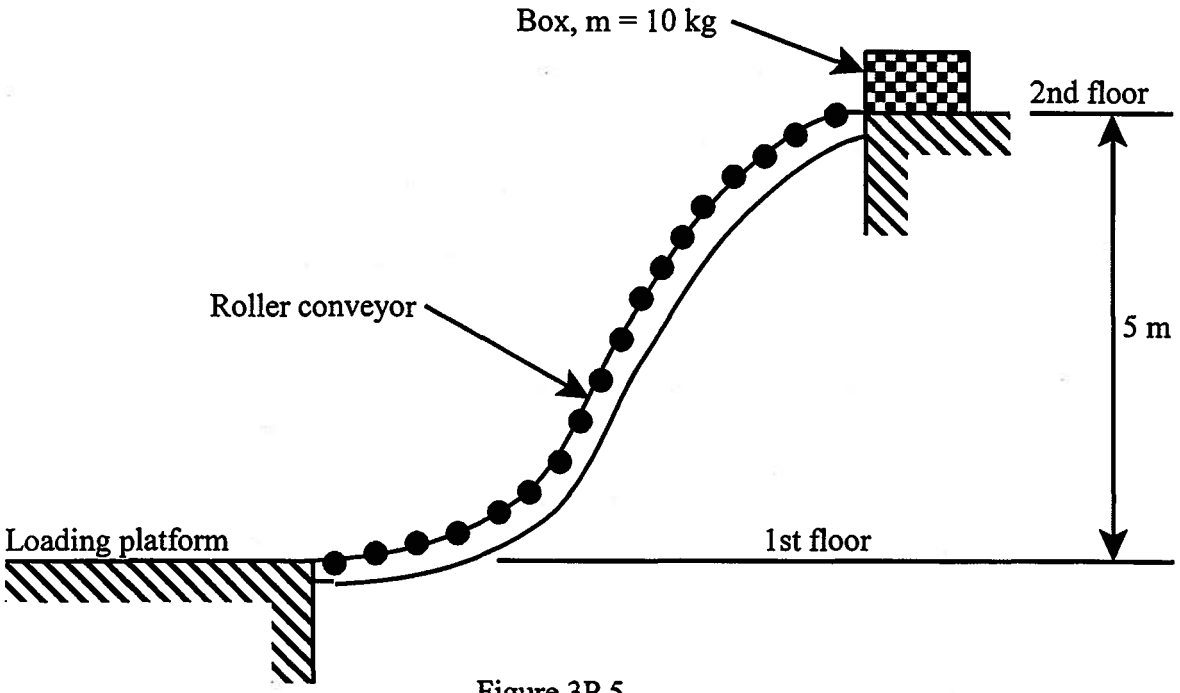

Figure 3P.5

3.6 A dynamometer is a device used to measure the power output (the rate of positive work transfer) of a heat engine or a prime mover. One type of dynamometer is an absorption dynamometer in which all of the power produced by the machine is dissipated. There are techniques available for measuring the rate at which the energy is dissipated so that it is possible to measure power in this manner. One technique for making such a measurement is shown in Figure 3P.6. The beam of the dynamometer is supported on the knife edge *0*, and with the engine running, mass W is added to the beam and the brake band is tightened. The position L of the mass is adjusted until the engine just begins to stall with the beam in mechanical equilibrium in the horizontal position. With the mass W removed and the brake band free of the flywheel, the arm is in mechanical equilibrium with the beam horizontal. On a particular test $W = 25$ kg, $L = 0.6$ m, and $N = 1640$ revolutions per minute.

(a) Formulate a thermodynamic model that would enable you to determine the output of the engine.

(b) Use this model to determine the power output at this speed for the engine being tested.

(c) If the test is conducted in the ambient atmosphere of a typical laboratory, determine the work transfers, heat transfers, and changes in stored energy for the dynamometer and the environment as a composite system. Note that the engine is not part of this system.

(d) An alternate dynamometer design would be to couple a direct current electrical generator to the engine being tested. The electrical output from the generator is then passed through a bank of resistors. Describe the nature, i.e., positive, negative, or zero, of the work transfers, heat transfers, and changes in stored energy for the system consisting of:

(i) the generator, resistors, and environment

(ii) the generator and resistors

(iii) the resistors

(iv) the resistors and the environment

(v) the environment

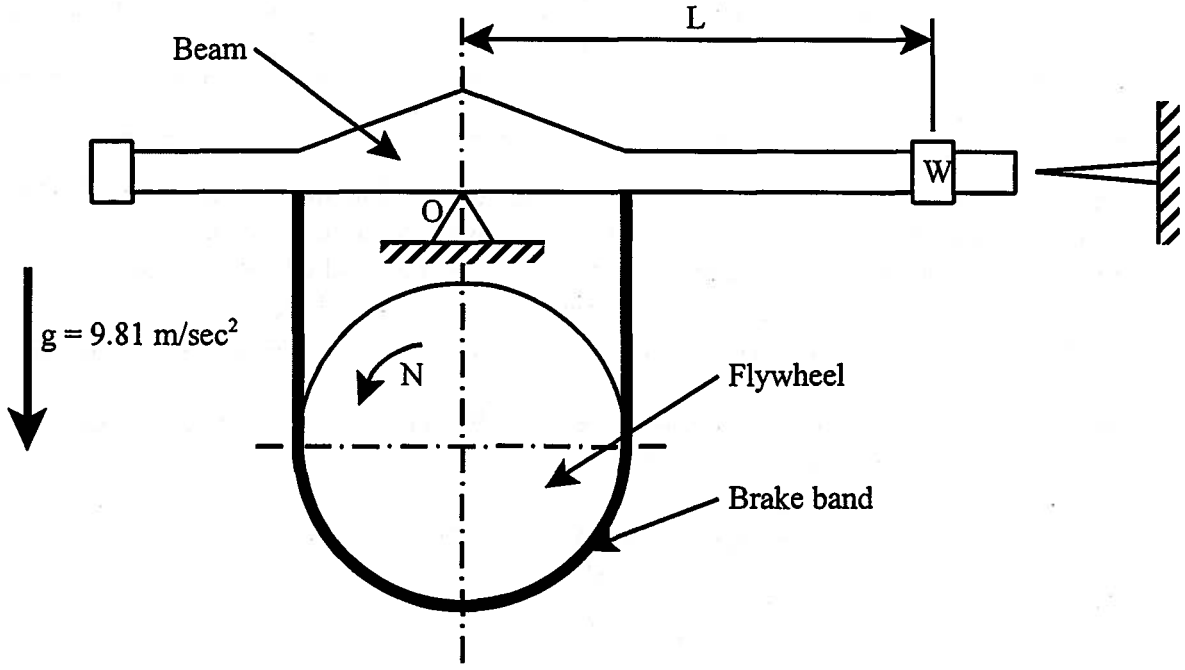

Figure 3P.6

3.7 A system consists of an externally insulated vessel filled with water. Immersed in the water is a paddle wheel which is driven by an electric motor via a shaft that passes through the top of the vessel. The electric motor delivers a constant 200 watts of mechanical power to the shaft. When the vessel contains 5 kg of water, it is found that if the motor operates for a time period of 1130 seconds, the temperature of the complete system consisting of water, paddle wheel, shaft, and vessel, will eventually increase uniformly by 6 C. If the mass of the water in the vessel is increased to 10 kg, it is found that 1758 seconds are required to change the uniform temperature of the system 6 C with the same power input rate of 200 watts.

(a) Describe a model that will enable you to determine the heat capacity of the vessel, shaft, and paddle wheel combined and the specific heat of the water.

(b) What is the heat capacity (in J/K) of the vessel and paddle wheel combined?

(c) What is the specific heat of the water in J/kg K?

(d) Make a table similar to Table 3P.7 specifying whether the heat transfer, work transfer, change in stored energy, change in stored entropy, entropy transfer, and entropy generated is positive, negative, or zero for a given change of temperature of the following systems: the shaft and paddle wheel; the vessel; and the water. Do the same for the composite system consisting of shaft and paddle wheel, vessel, and water.

Table 3P.7

SYSTEM	$Q_{1\text{-}2}$	$W_{1\text{-}2}$	$E_2 - E_1$	$S_2 - S_1$	$S_{transfer}$	S_{gen}
shaft and paddlewheel						
vessel						
water						
composite system						

3.8 A string-mass system is assembled as shown in Figure 3P.8. The pulley and string may be assumed to be massless. The support string restrains the assembly in the position shown. When the support string is cut, the rider of mass m_r and the mass m_2 descend while the mass m_1 rises. The mass m_2 will pass through the hole in the bracket but the rider will not.

(a) Determine the maximum distance s which the mass m_2 descends from the starting position.

(b) Describe the behavior of the rider in terms of its various stored energy modes.

(c) Is there a work transfer involved? If so, where?

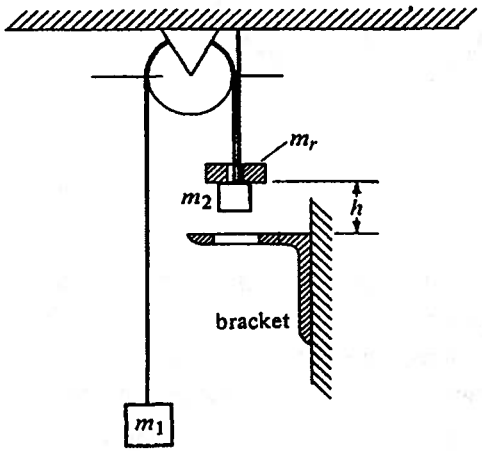

Figure 3P.8

3.9 A self-contained electric hoist consists of an electric motor, a winch with a cable, and a brake. The cable is attached to a fixed support in the roof above as in Figure 3P.9. The electric motor lifts the hoist and load. The brake is used to control the rate of descent of the hoist with the motor off.

(a) Construct a model suitable for a simple description of the energy changes and energy transfer associated with lifting a load with this hoist and returning the empty hoist back to the lower level.

(b) Use the model to describe the energy transfers and energy changes during this operation.

(c) How would the model and the energy transfer and changes be modified if the electric motor were powered by batteries carried on the hoist?

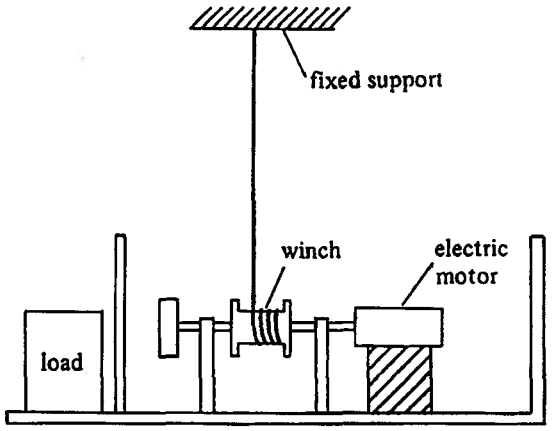

Figure 3P.9

3.10 A block of silver with a mass of 10 kg is at an initial temperature of 600 K. This block is brought into thermal contact with a 10 kg block of fused silica glass whose initial temperature is 200 K. The two blocks interact only with each other, i.e., they are isolated from the rest of the world, and are allowed to run down to equilibrium.

(a) Find the final equilibrium temperature of the two blocks.

(b) Complete a table similar to Table 3P.10 where state 1 is the initial state and state 2 is the final state.

For silver: k = 420 W/m K, ρ = 10,500 kg/m^3, c = 235 J/kg K
For glass: k = 1.38 W/m K, ρ = 2220 kg/m^3, c = 745 J/kg K

Table 3P.10

SYSTEM	$Q_{1\text{-}2}$	$W_{1\text{-}2}$	$U_2 - U_1$	$S_2 - S_1$	$S_{transfer}$	S_{gen}
Ag block						
glass block						
Ag + glass						

3.11 Two identical loaves of freshly-baked bread A and B are removed from the oven to cool. The uniform internal temperature of the bread in the initial state is 180 C. One loaf is allowed to cool by placing it in a large room filled with air at a temperature of 21 C. The other loaf is placed in a refrigerated box maintained at 4 C by a reversible refrigerator and allowed to cool to a uniform temperature of 21 C before being removed from the box and placed in the room at 21 C. The refrigerator executes an integral number of cycles. The final uniform temperature of the bread is the same in both cases, 21 C, and the bread can be modeled as a pure thermal system with a heat capacity of 1 kJ/C. The room air can be modeled as a heat reservoir at 21 C and the inside of the refrigerator can be modeled as a heat reservoir at 4 C. The two cooling schemes are shown schematically in Figure 3P.11.

(a) Calculate the change in entropy of each of the two loaves of bread. Do the two loaves experience the same change of state?

(b) If the cooling process in each case results in the temperature of the bread remaining spatially uniform at all times but changing with time (not a good model), what does this imply about the rate of heat transfer between the environment and the bread relative to the rate of heat transfer within the bread itself?

(c) What is the entropy transfer for the room air in each case? Explain why these results are different or are the same.

(d) Calculate S_{gen} for the two cooling protocols. Explain why these results are different or are the same.

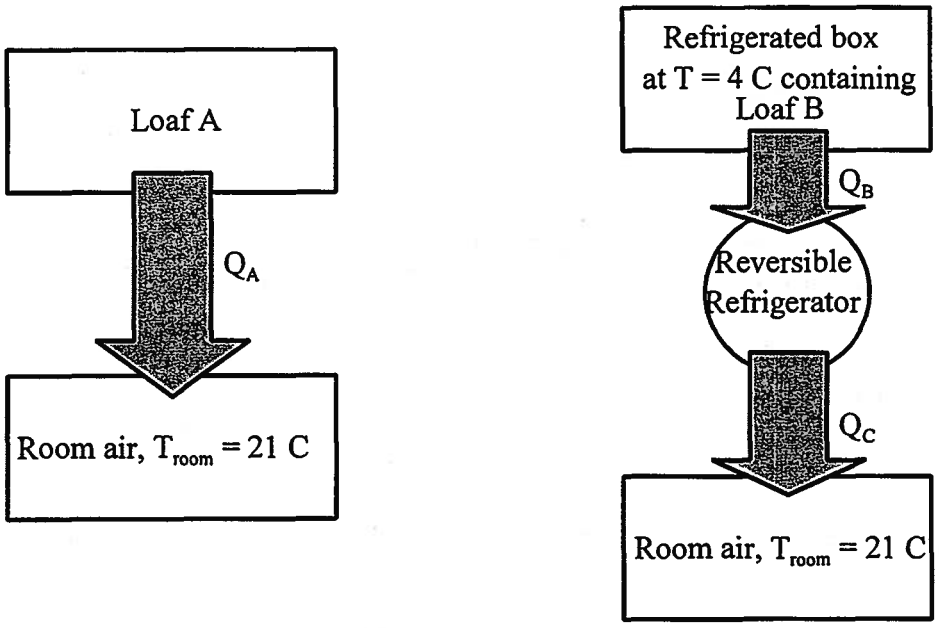

Figure 3P.11

3.12 An insulated copper container with a mass of $m_{container}$ = 5 kg contains water, m_{water} = 40 kg. The water is stirred by a paddle wheel connected to an electric motor by means of a shaft as shown in Figure 3P.12. The mass of the paddle wheel and the mass of the shaft are negligible. By virtue of this stirring action, the uniform temperature of the system consisting of the vessel and the water rises at a rate of 0.05 K/s.

(a) Formulate a model that will enable you to describe this situation in thermodynamic terms.

(b) Make a table showing the rates of heat transfer, work transfer, the rate of change of stored energy, the rate of change of stored entropy, and the rate of entropy generation of the system consisting of:

(i) The water.

(ii) The container.

(iii) The water and the container.

(iv) The water, the container, and the motor.

Note: The specific heat of copper is $c_{Cu} = 385$ J/kg K while that of water is $c_{water} = 4187$ kJ/kg K.

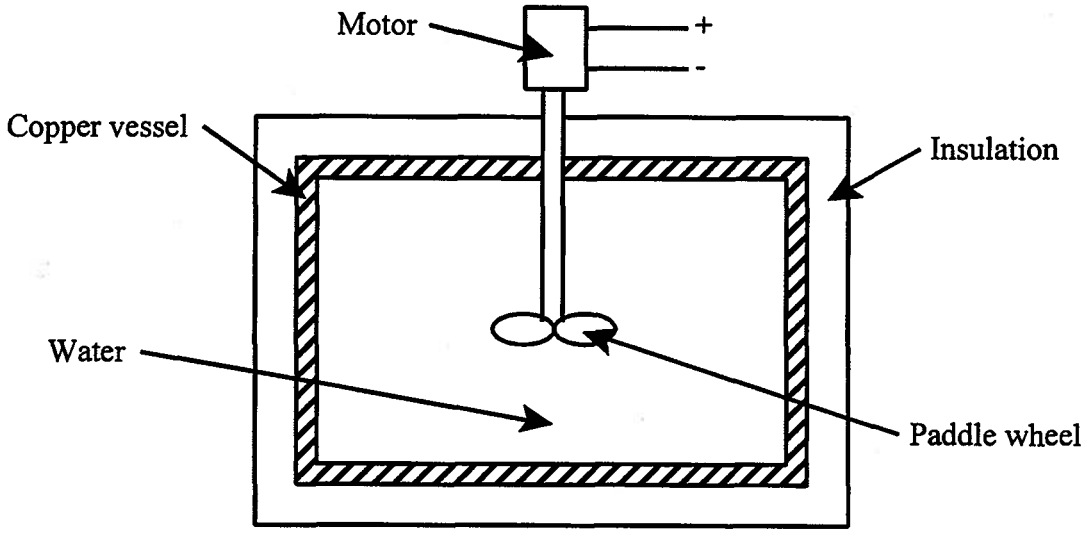

Figure 3P.12

CHAPTER 4

Simple Models for Thermal-Fluid Systems

4.1 The Prominence of Fluid Systems

In order to decide which models are going to be most useful in our study of thermal-fluid systems, it is worthwhile to examine the makeup of these systems. While we shall have much to say about this later, matter exists in three forms or *phases* as they are known in the lexicon of thermal-fluids engineering: solid, liquid, and gas. From a thermodynamic point of view, the degree of thermodynamic coupling that these phases exhibit determines the complexity of the models necessary to describe their behavior. The more strongly coupled the phase of the material that makes up the system, the more complex the model. While we have not yet developed the formalism that will enable us to describe thermodynamic coupling in a rigorous sense, we can appeal to common experience. Basically, thermodynamic coupling is a measure of our ability to change the entropy of a material by a displacement of its boundaries without changing its temperature. Perhaps a more obvious manifestation of thermodynamic coupling is the relative ease with which we can decrease the temperature of a material by displacing its boundaries adiabatically.

Our common physical experience shows that of the three forms of matter, gases are by far the most strongly coupled from a thermodynamic point of view, followed by liquids and solids in that order. This is, in fact, the order of interest that these materials hold for us from a thermodynamic point of view. On the simplest level, thermal-fluid systems encountered in engineering practice are basically fluids (either liquids or gases) contained in a solid envelope. The heat transfer and work transfer interactions occur across the envelope, which if properly designed, facilitates them if they are desirable or inhibits them if they are undesirable. In addition, in well-designed thermal-fluid systems the changes of state that either produce or result from these interactions occur in the fluids and not in the solid envelope since it is so weakly coupled thermodynamically. For these reasons, solids have the simplest thermal-fluid models, followed by liquids and finally gases with the most complex models of all. At this stage of our development, there are two fluid models, namely the *incompressible fluid model* and the *ideal gas model*, that will prove useful both for expanding our understanding of thermal-fluid systems and for modeling these systems. But before studying these models in any detail, it is appropriate to explore the differences between solids and fluids.

4.2 Solids vs. Fluids: Mechanical Equilibrium

As we mentioned previously, the class of materials known as fluids exists in both the liquid and gas forms, or phases. From basic physics, we know that what appears to be a continuous distribution of material is, in fact, a collection of discrete molecules in constant motion. These molecules are all exerting on one another a force that arises from the electron configuration of the individual atoms that make up these molecules. The nature of this force is attractive when the molecules are far apart and repulsive when the molecules are closer together. In the case of the gas phase, the molecules are so widely spaced that they move almost independently of one another. As a result, most of the time they lie outside the range of these molecular forces. However, in the natural course of their motion, the molecules do come close

enough to one another on occasion that they experience the attractive forces. Due to this force of attraction, they are drawn even closer together until the forces eventually become repulsive and drive the molecules away from one another. This close encounter is called a "collision" even though the molecules do not actually collide in the sense of a collision between billiard balls. They have, however, come close enough to one another to exchange energy and momentum. At the molecular level, it is these pseudo-collisions that are responsible for the transport of energy, which is manifested in the macroscopic property *thermal conductivity*, and momentum, which manifests itself in the macroscopic property *viscosity*.

In the liquid phase, the molecules are packed much more closely together, and they lack the kinetic energy of motion necessary to escape the attractive forces. As a result, liquid molecules behave in a much more cooperative fashion as though they were a collection of particles loosely bound together. One manifestation of this collective behavior is the influence of gravity. Compared to gases, the influence of gravity in liquids is large. For example, when a liquid is introduced into a vessel under the influence of gravity, the liquid forms a free surface that together with the walls and bottom of the vessel contain the liquid. Thus, the liquid itself may not occupy the entire volume of the container. For gases, on the other hand, the influence of gravity is small and the gas is free to expand and fill the entire volume of the container with no free surface. There are many other features that distinguish liquids from gases, and we shall consider more of these in detail when we present a more rigorous macroscopic description of these two phases in our study of the *pure substance model* later in this development.

At this point, we are more interested in the distinction between fluids and solids. The difference between these two classes of materials can be readily described in terms of the ability of the material to sustain a shear force applied to its boundary. (Recall that a shear force is a force applied to a surface of a body such that the force lies in the plane of the surface to which it is being applied.) A solid can sustain a shear while remaining at rest, but in contrast, a shear force applied to a liquid necessarily produces a motion of the liquid in the direction of the shear force as each layer of the fluid slides over its neighboring layers. For fluid systems in a state of thermodynamic equilibrium, there are no shear forces and the normal forces exerted on the system boundary by the environment are distributed over the system boundary and are transmitted throughout the system.

In a fluid, then, the boundary force is expressed in terms of the *pressure* where the pressure is the boundary force per unit area of the boundary acting in a direction normal, i.e., perpendicular, to the boundary. In general, the pressure is different over different regions of the system boundary, and it is necessary for us to think in terms of the pressure varying from point to point over the boundary. Mathematically, the pressure at a point in the fluid is defined as the force per unit area for a small area enclosing the point. Specifically, if ΔA is a small area enclosing the point, and ΔA_c is the smallest area over which we can consider the fluid as a *continuum* (i.e., as matter distributed in space in a continuous manner rather than as discrete molecules), we define the pressure P at a point as

$$P = -\lim_{\Delta A \to \Delta A_c} \frac{\Delta F_n}{\Delta A} = -\frac{d\vec{F}_n}{d\vec{A}} = -\frac{d\vec{F}_n}{\vec{n}dA} \tag{4.1}$$

where ΔF_n is the component of the boundary force on ΔA normal to ΔA and is taken to be positive when the fluid is in tension and $\vec{n}$ is the outward normal to the area dA. Then

$$d\vec{F}_n = -P\vec{n}dA \tag{4.2}$$

Consider the situation shown in Figure 4.1 in which we have a solid and a fluid loaded in

simple compression. The solid is simply a cylindrical block of solid material placed between the

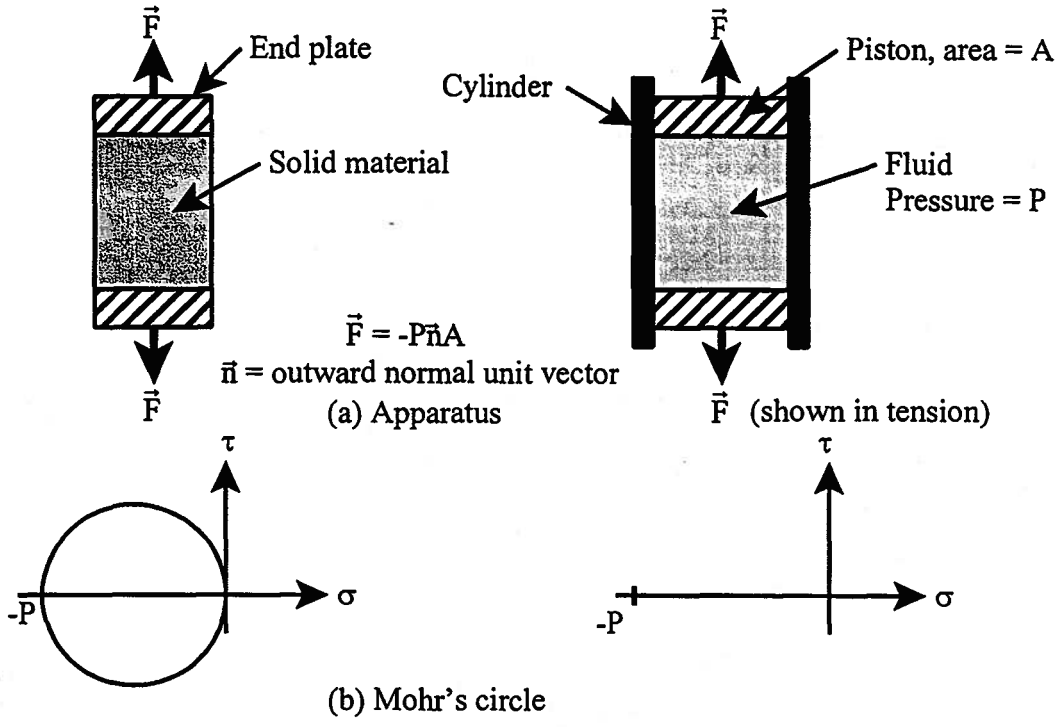

Figure 4.1 State of Stress in Solid and Fluid Loaded in Simple Compression

plates used to impose the load. The fluid, on the other hand must be confined in a cylinder fitted with a piston. If we plot Mohr's circle to determine the state of stress on any plane located at an arbitrary point in the material, we note that in the equilibrium state, the stress in the fluid is independent of the direction of orientation of the plane, but in the solid, the state of stress depends markedly upon the orientation of the plane of interest. In the solid there are shear stresses on all planes except the plane normal to the direction of application of the load, but in the fluid there are no shear stresses whatsoever. The state of stress in the fluid is said to be *hydrostatic*. We conclude that for a fluid in a state of mechanical equilibrium, the force at the boundary is normal to the boundary and the pressure in the fluid describes completely the boundary forces. If the fluid is not in a state of mechanical equilibrium but is instead subject to a rate of shear, the boundary force has components in the plane of the boundary and a stress tensor is required to describe the boundary force. (Later in this development we shall describe a relatively simple model for this sort of dynamic behavior known as the Newtonian fluid, but at present we are concerned with the static situation.)

> In the equilibrium state, the fluid pressure at a point is the same regardless of the orientation of the boundary that includes that point. That is, when mechanical equilibrium prevails in the fluid, the force due to pressure at a point (as contrasted with body forces due to fields such as the gravitational field of the earth, for example) is the same in all directions.

4.3 Measurement of Pressure in Fluids

In thermodynamics the pressure is measured relative to the zero force condition or complete vacuum. This pressure is often termed absolute pressure to distinguish it from a pressure difference which is measured by common pressure gages. The absolute pressure of the atmosphere is termed atmospheric pressure. For example, a gas contained in a flexible, unstressed, partially collapsed bag would be at atmospheric pressure with the pressure forces of the gas inside the bag exactly balanced by the pressure of the atmosphere. A fluid system at equilibrium at a pressure different from the pressure of its environment must be confined within a mechanical structure (a tank) which can provide the forces arising from the pressure difference. For example, consider the system consisting of the gas sealed in a cylinder by a leak-free frictionless piston as in Figure 4.2. At equilibrium, the force exerted on the piston face by the gas pressure balances the gravitational force on the piston and the weight plus the atmospheric pressure force on the top of the piston. If the pressure on the top of the piston is changed, the piston will move until the gas pressure inside the cylinder adjusts to a new equilibrium value. The pressure above the piston could be changed by placing the apparatus inside a tank and evacuating or pressurizing the tank.

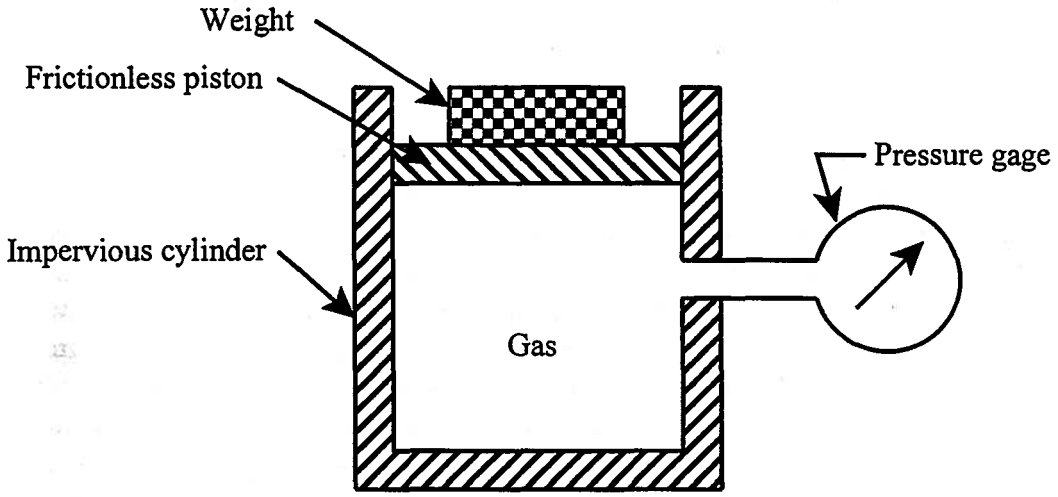

Figure 4.2 Piston-cylinder Apparatus

Since most common pressure gages such as the one shown in Figure 4.2 measure differential pressure relative to atmospheric pressure, the term gage pressure is widely used. Thus, the absolute pressure is the sum of the gage pressure measured with the standard pressure gage and the atmospheric pressure. Common vacuum gages measure pressures less than atmospheric pressure relative to atmospheric pressure. Hence, an increasing vacuum reading is actually a decreasing absolute pressure. In Figure 4.3 the relations between pressure measurements are shown.

Most instruments used in measuring pressure or pressure difference operate by measuring the pressure force on a sensing element. In the most common instruments, the pressure force is balanced by gravity or by the stress in an elastic element. In a manometer, the weight of a column of liquid balances the difference in pressure forces. In a dead weight pressure balance, the calibrated weights on a piston of known area balance the difference in pressure. In a bourdon

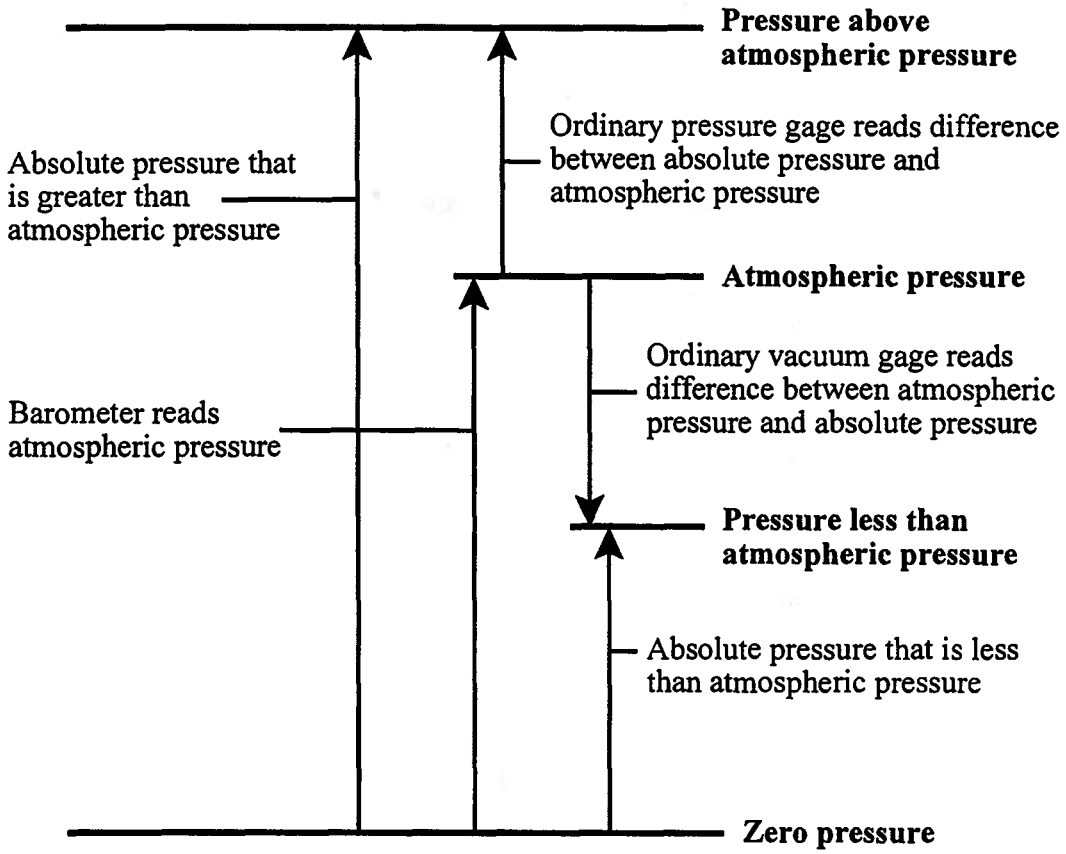

Figure 4.3 Terms Used to Describe Pressure Measurements

tube pressure gage (the common dial type gage), the pressure difference is balanced by the elastic stresses in a curved tube of oval cross section. A rack and pinion movement transforms the small deflection of the bourdon tube into indicating needle rotation. In the diaphragm pressure gage, the pressure difference is balanced by the stresses in an elastic diaphragm. The deflection of the diaphragm is indicated mechanically or electrically. Some pressure gages, called pressure transducers, use piezoelectric crystals that produce a voltage proportional to the pressure.

Any differential pressure gage becomes an absolute pressure gage when one of the pressures applied to the instrument is a complete vacuum, that is, zero pressure. An absolute pressure gage for measuring the absolute pressure of the atmosphere is called a barometer. It is formed by filling with mercury (or some other dense liquid) a tube closed at one end and open at the other as shown in Figure 4.4. This tube is then inverted, and the open end is immersed in a tank of mercury. As the mercury in the tube tries to flow out into the pool of mercury, the pressure in the space between the surface of the mercury in the tube and the end of the tube is essentially zero. That is, a vacuum forms in this volume trapped between the mercury and the end of the tube. This causes some mercury to evaporate from the surface of the mercury in the tube, and the trapped volume becomes filled with mercury vapor. Thus the pressure in the trapped volume becomes the pressure of the mercury vapor. Since the value of the vapor pressure of mercury at 20 C is only 0.16 N/m^2 which is indeed negligible compared to the value of P_{atm} = 1.0135 x 10^5 N/m^2, the pressure P_0 is often regarded as zero to a first approximation. Since the boundary force on a fluid in static equilibrium is distributed uniformly throughout the fluid, the

pressure on the plane coincident with the free surface of the fluid is P_{atm} everywhere. Then a force balance on the column of mercury bounded by this plane at the open end of the tube and the free surface at the closed end requires

$$P_{atm}A = \rho_0 ghA + P_0 A \tag{4.3}$$

where ρ_0 is the density of mercury. If P_0 is zero, equation (4.1) reduces to[1]

$$P_{atm} = P_0 + \rho_0 gh = \rho_0 gh \tag{4.4}$$

Thus, the column height, h, is proportional to the atmospheric pressure, P_{atm}. Mercury is used as the fluid in barometers because its high density and incompressible nature result in a reasonable column height. In addition, the vapor pressure of mercury at typical environmental temperatures is quite low and produces a value of P_0 that can be neglected in all but the most precise work.

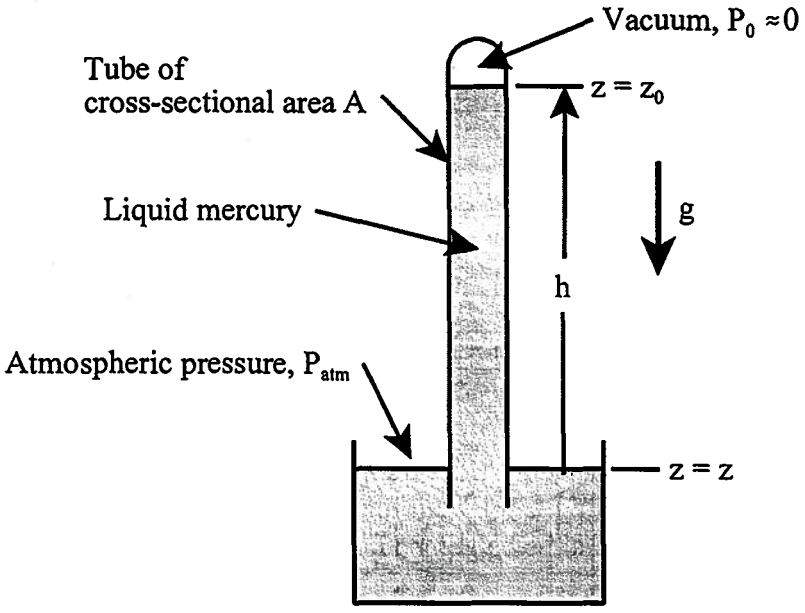

Figure 4.4 Mercury Barometer

The unit of pressure in International System of Units, abbreviated SI from the French "Le Système International d'Unités", is the pascal, Pa, where:

$$1\ \text{Pa} = 1\ \text{N/m}^2$$
$$1\ \text{kPa} = 10^3\ \text{N/m}^2$$
$$1\ \text{MPa} = 10^6\ \text{N/m}^2$$
$$1\ \text{mPa} = 10^{-3}\ \text{N/m}^2$$
$$1\ \mu\text{Pa} = 10^{-6}\ \text{N/m}^2$$

In engineering practice, a variety of pressure units have been widely used with many of the units related directly to a specific instrument for measuring pressure. In the now defunct British system of units, the common pressure units are pounds force per square inch, lbf/in^2;

---

[1] This result will be developed in greater detail in section 4.4.

pounds force per square foot, lbf/ft^2; and inches of mercury column, in Hg (for standard density mercury in standard gravity). Before SI units were adopted, the metric units for pressure were kilogram force per square centimeter (kgf/cm^2), bar, and millimeters of mercury column (mm Hg or Torr). The pressure unit "standard atmosphere" was used in both the British and the metric system. Table 4.1 gives equivalents of various pressure units.

TABLE 4.1
Equivalents of Pressure Units

$1\ \text{Pa} = 1\ \text{N/m}^2$

$1\ \text{lbf/in}^2 = 144\ \text{lbf/ft}^2 = 6.895 \times 10^3\ \text{N/m}^2$

$1\ \text{psia} = 1\ \text{lbf/in}^2$ absolute pressure

$1\ \text{psig} = 1\ \text{lbf/in}^2$ gage pressure

$1\ \text{in Hg (32 F)} = 0.491\ \text{lbf/in}^2 = 3.386 \times 10^3\ \text{N/m}^2$

$1\ \text{mm Hg (0 C)} = 1\ \text{Torr} = 10^3\ \text{micron Hg} = 1.333 \times 10^2\ \text{N/m}^2$

$1\ \text{std atm} = 14.696\ \text{lbf/in}^2 = 29.921\ \text{in Hg (32 F)}$

$1\ \text{std atm} = 760.0\ \text{mm Hg (0 C)} = 1.0133 \times 10^5\ \text{N/m}^2$

$1\ \text{bar} = 10^5\ \text{N/m}^2$

$1\ \text{kgf/cm}^2 = 9.807 \times 10^4\ \text{N/m}^2$

Example 4E.1: On March 23, 1995, a tornado was reported in Walnut Grove, California. The atmospheric pressure at the earth's surface was recorded as 850 mb, i.e. 850×10^{-3} bars.

(a) Compute the value of this pressure in Pascals.

(b) What would have been the height of a mercury filled barometer at this pressure at a location where $g = 9.80\ \text{m/s}^2$? (The density of mercury is $\rho_{Hg} = 13{,}560\ \text{kg/m}^3$.)

(c) A building with a flat roof 10 m x 10 m is filled with air at a pressure of $P_{inside} = 1.01325 \times 10^5\ \text{N/m}^2$ as the tornado passes over. There is insufficient time to ventilate the building as the tornado approaches. Compute the net force exerted on the roof as the tornado passes overhead.

Solution: Since $1\ \text{bar} = 10^5\ \text{N/m}^2 = 10^5\ \text{Pa}$, $850 \times 10^{-3}\ \text{bar} = (10^5\ \text{Pa/bar})(850 \times 10^{-3}\ \text{bar}) = 8.50 \times 10^4\ \text{Pa}$. If we assume that the pressure inside the barometer is zero, then equation (4.2) gives

$$h = \frac{P_{atm}}{\rho g}$$

$$h = \frac{8.50 \times 10^4\ \text{N/m}^2}{(1.356 \times 10^4\ \text{kg/m}^3)(9.80\ \text{m/s}^2)} = 0.639\ \text{m} = 639\ \text{mm}$$

If we take the z-direction to be aligned with the gravity field of the earth with the positive direction upward, the air inside the building exerts a force in this direction equal to

$$F_{+z} = P_{inside} A$$

$$F_{+z} = (1.01325 \times 10^5\ \text{N/m}^2)(10\ \text{m})(10\ \text{m}) = 1.01325 \times 10^7\ \text{N}$$

In the negative z-direction, we have the atmosphere exerting a force in the amount of

$$F_{-z} = -P_{atm}A$$

$$F_{-z} = -(8.50 \text{ x } 10^4 \text{ N/m}^2)(10 \text{ m})(10 \text{ m}) = -8.50 \text{ x } 10^6 \text{ N}$$

Then the net force trying to lift the roof off of the building is

$$F_{net} = F_{+z} + F_{-z}$$

$$F_{net} = 10.1325 \text{ x } 10^6 \text{ N} - 8.50 \text{ x } 10^6 \text{ N} = 1.6325 \text{ x } 10^6 \text{ N}$$

This is a rather substantial force and could, depending upon the method of construction, tear the roof off the building. However, most building damage during tornadoes is a consequence of impact from flying debris.

4.4 Fluid Models

In formulating models for fluid systems there are a number of choices to be made. The issue of coupling is one of the more important ones because of the strong influence it has on possible system behavior. As we have already mentioned, thermodynamic coupling is strongly linked to the compressibility of the fluid. Thus, we need to have models capable of representing both
compressible and incompressible behavior. The viscosity of the fluid is also important because of its connection with potential mechanically dissipative phenomena in the fluid. Two models have been formulated for addressing the issues mentioned above: (1) the incompressible fluid and (2) the ideal gas. Both of these find widespread use in engineering design and analysis.

4.4.1 The Inviscid Incompressible Fluid Model

The central features of the model are:

Physical Characteristics:

- m = mass
- ρ = density = mass/unit volume
- v = specific volume = $1/\rho$ = volume/unit mass
- c = specific heat
- μ = viscosity = 0
- k = thermal conductivity

Properties:

- P = pressure
- T = temperature
- V = volume
- U = stored thermal energy
- S = stored entropy

Interactions:

- $W_{1\text{-}2}$ = work transfer
- $Q_{1\text{-}2}$ = heat transfer

Property Constitutive Relation: $\rho = constant$ or $v = constant$

Energy Constitutive Relations:

$$(E_2 - E_1)_{kinetic} = \tfrac{1}{2} m \vartheta_2^{\,2} - \tfrac{1}{2} m \vartheta_1^{\,2}$$

$$(E_2 - E_1)_{gravitational} = mg(z_2 - z_1)$$

$$(U_2 - U_1)_{thermal} = mc(T_2 - T_1)$$

Entropy Constitutive Relation:

$$S_2 - S_1 = mc \ln\left(\frac{T_2}{T_1}\right)$$

The inviscid incompressible fluid model is widely used to describe the thermodynamic and dynamic behavior of liquids for which viscous effects are negligible. However, there are circumstances for which it also can be successfully used to describe the dynamic, but not the thermodynamic, behavior of gases in which viscous effects are negligible. We shall explore cases of both situations extensively. This model is uncoupled so it possesses the various uncoupled energy storage modes described in Chapter 2. The uncoupled behavior also manifests itself in the fact that the temperature of the fluid can be changed only by heat transfer. In this regard, its thermal behavior is identical to that of the pure thermal system.

4.4.2 The Viscous Incompressible Fluid Model

While similar in many respects to the simpler model of the inviscid incompressible fluid, the viscous incompressible fluid differs in one significant way. It has a non-zero viscosity which significantly changes the dynamic behavior of the fluid during flow. Furthermore, during flow, the temperature of the viscous incompressible fluid can be increased by the internal dissipation of kinetic energy through the action of viscosity. While this may appear to be an example of coupled behavior, it is not coupled in the true thermodynamic sense since the temperature of this fluid cannot be decreased by a positive adiabatic work transfer. Thus, with the exception of a non-zero value for the viscosity, this model is virtually identical to the previous one:

Physical Characteristics:

m = mass
ρ = density = mass/unit volume
v = specific volume = $1/\rho$ = volume/unit mass
c = specific heat
μ = viscosity $\neq 0$
k = thermal conductivity

Properties:

P = pressure
T = temperature
V = volume
U = stored thermal energy
S = stored entropy

Interactions:

$W_{1\text{-}2}$ = work transfer
$Q_{1\text{-}2}$ = heat transfer

Property Constitutive Relation:

$\rho = constant$ or $v = constant$

Energy Constitutive Relations:

$$(E_2 - E_1)_{kinetic} = \tfrac{1}{2} m \mathcal{G}_2^{\,2} - \tfrac{1}{2} m \mathcal{G}_1^{\,2}$$

$$(E_2 - E_1)_{gravitational} = mg(z_2 - z_1)$$

$$(U_2 - U_1)_{thermal} = mc(T_2 - T_1)$$

Entropy Constitutive Relation:

$$S_2 - S_1 = mc \ln\left(\frac{T_2}{T_1}\right)$$

4.4.3 The Ideal Gas Model

When the density of the fluid is low and the temperature and pressure are moderate and compressibility effects are significant, the ideal gas model is often an adequate representation of fluid behavior. This model is an exact description of the behavior of real gases in the limit as the density of the gas approaches zero. On a microscopic scale, this model implies that there are no interactions amongst the molecules that make up the gas, i.e., that the gas molecules do not collide with one another.

The error involved in the use of this model depends heavily upon the gas being modeled. For example, for a simple gas like helium, the ideal gas model is accurate over several orders of magnitude of pressure and temperature, but for a more complex gas like carbon dioxide, this model is limited to a rather narrow range of temperatures and pressures. While simple mathematically, this model is very significant from a thermal-fluids point of view since it is the simplest fluid model that is thermodynamically coupled. For this reason, we will make extensive use of this model to illustrate many of the features of the laws of thermodynamics, fluid mechanics, and heat transfer. The central features of the ideal gas model are:

Physical characteristics:

m = mass

$\overline{R}$ = universal gas constant
= 8.3134 kJ/(kg-mole) K

c_v = specific heat at constant volume (assumed constant)

M = molecular weight

$R = \dfrac{\overline{R}}{M}$ = gas constant

Properties:

P = pressure

V = volume

T = temperature

U = stored internal energy

S = stored entropy

Property constitutive relation: $PV = mRT$

Interactions:

$W_{1\text{-}2}$ = work transfer

$Q_{1\text{-}2}$ = heat transfer

Energy constitutive relation: $U_2 - U_1 = mc_v(T_2 - T_1)$

Entropy constitutive relation: $S_2 - S_1 = mc_v \ln\left(\dfrac{T_2}{T_1}\right) + mR \ln\left(\dfrac{V_2}{V_1}\right)$

The ideal gas model has an energy constitutive relation that expresses the coupled internal energy in terms of the temperature only. This unique relationship has the appearance of being an uncoupled stored thermal energy mode, but this is not the case. It is truly a coupled energy mode as can be seen by solving the property constitutive relation for the temperature and substituting the result in the energy constitutive relation, we obtain

$$U_2 - U_1 = mc_v\left(\frac{P_2V_2}{mR} - \frac{P_1V_1}{mR}\right) = \frac{c_v}{R}(P_2V_2 - P_1V_1) \tag{4.5}$$

where the internal energy is now expressed in terms of the mechanical properties P and V and thus U appears to be a stored mechanical energy. It follows, then, that the stored internal energy cannot be separated into thermal and mechanical components. There is just the one stored energy form that is coupled and it is known as the internal energy. As other evidence of thermodynamic coupling, we note from the property constitutive relation that the temperature influences the mechanical aspects. If we increase the temperature of the ideal gas model while holding the volume constant, we observe that the pressure increases. Similarly, if we increase the temperature while holding the pressure constant, we observe that the volume increases.

The most explicit expression of thermodynamic coupling in the ideal gas model is that the

entropy can be expressed in terms of both mechanical and thermal properties. By substituting the property constitutive relation in the entropy constitutive relation given above, we may obtain two other equivalent forms for the entropy constitutive relation. It is left as an exercise to show that

$$S_2 - S_1 = m(c_v + R)\ln\left(\frac{T_2}{T_1}\right) - mR\ln\left(\frac{P_2}{P_1}\right) \tag{4.6}$$

and

$$S_2 - S_1 = mc_v \ln\left(\frac{P_2}{P_1}\right) + m(c_v + R)\ln\left(\frac{V_2}{V_1}\right) \tag{4.7}$$

Thus the stored entropy of the ideal gas model can be changed by changing either one or both of the thermal and mechanical properties. However, entropy can be transferred across the boundary of a closed system only by means of a heat transfer interaction.

Note that both stored energy and stored entropy are defined by the first and second laws of thermodynamics in terms of interactions that transfer energy and entropy. Thus the absolute values for the stored energy and entropy cannot be defined. However, we can define their values with respect to an arbitrary reference state as we did in equation (2.18) for the energy. Since all thermodynamic calculations involve only the differences in energy and entropy, these arbitrary constants always subtract out of the calculations.

Although not immediately obvious, the ideal gas model possesses the interesting feature that it can be used to define a temperature scale known as the ideal gas temperature scale. The ratio of any two temperatures T_1 and T_2 on this temperature scale is defined as

$$\frac{P_2V_2}{P_1V_1} = \frac{T_2}{T_1} \tag{4.8}$$

Here, P_2V_2 is the pressure-volume product when the ideal gas is at equilibrium at the temperature T_2 and P_1V_1 is the pressure-volume product when the same ideal gas system is at the equilibrium temperature T_1. In order to establish numerical values on the ideal gas temperature scale, an arbitrary value must be assigned to one temperature. By convention, this temperature is selected as the freezing point of pure water at the pressure 611.3 N/m^2. This is the triple point for water, a unique state in which all three phases of water (solid, liquid, and gas) can coexist in equilibrium. The Kelvin temperature is an ideal gas temperature scale for which the assigned value is 273.16 K for the triple point of water. The number 273.16 K was selected for the Kelvin scale so that this temperature scale would match the old centigrade or Celsius practical temperature scales. The latter temperature scales set the freezing point of water at one atmosphere pressure at 0 C and the boiling point of water at the same pressure as 100 C. This makes a temperature change of 1 K on the Kelvin scale the same as a change of 1 C on the old centigrade or the Celsius scale. On the older practical temperature scales, the triple point of water is 0.01 C. Thus, the Kelvin ideal gas temperature is related to the Celsius temperature by the familiar relation:

$$T(\mathrm{K}) = t(\mathrm{C}) + 273.15 \tag{4.9}$$

A part of the generality of the ideal gas temperature scale results from the fact that equation (4.8) is true for any ideal gas system regardless of the size of the system or the chemical composition of the gas. This generality may be illustrated by considering two ideal gas systems which are initially in mutual thermal equilibrium. If these two systems are isolated and each cooled to the state at which the pressure-volume product for each system is one-half the initial value of each system, then equation (4.8) shows that each will be at a temperature exactly one-half of the initial temperature. Thus, the systems are in mutual equilibrium and if placed in thermal communication, no heat transfer would occur.

In order to be able to use the ideal gas model for real gases under the appropriate conditions, it is necessary to have engineering values for the various physical characteristics. The values for some gases encountered in engineering practice are given in Table 4.2.

TABLE 4.2
Physical Characteristics for the Ideal Gas Model of Some Common Gases

Ideal gas model	*Composition*	*Molecular Wt.*	*R, kJ/kg K*	c_v, *kJ/kg K*
Carbon Dioxide	CO_2	44.01	0.189	0.662
Oxygen	O_2	32.00	0.260	0.657
Air		28.97	0.287	0.716
Nitrogen	N_2	28.01	0.297	0.741
Helium	He	4.00	2.078	3.153
Hydrogen	H_2	2.02	4.116	10.216

Example 4E.2: Consider a room 3 m x 4 m x 3 m filled with air. If the pressure of the air in the room is 1.013 x 10^5 Pa and the air temperature is 300 K, calculate the mass of the air in the room assuming that the ideal gas model is valid.

Solution: From the property constitutive relation for the ideal gas,

$$m = \frac{PV}{RT}$$

where from Table 4.2, R = 0.287 kJ/kg K. Then

$$m = \frac{(1.013 \times 10^5 \text{ N/m}^2)(3 \text{ m})(3 \text{ m})(4 \text{ m})}{(287 \text{ J/kg K})(300 \text{ K})} = 42.36 \text{ kg}$$

Example 4E.3: Helium is contained in a piston-cylinder apparatus fitted with a spring as shown in Figure 4E.3. The spring has a spring constant of $k = 10^5$ N/m and maintains the gas in mechanical equilibrium. The gas experiences a heat transfer interaction at a rate which is slow relative to the rate at which equilibrium can be established throughout the gas. Thus the pressure and temperature are uniform throughout the gas at all times even though they are both changing with time throughout the process. The piston is frictionless and the spring can be modeled as a pure translational spring. Calculate the work transfer experienced by the gas as the pressure increases from P_1 = 1.013 x 10^5 Pa to P_2 = 3.039 x 10^5 Pa. What is the temperature of the helium in state 2 if T_1 = 300 K and V_1 = 0.1 m^3? Calculate the heat transfer experienced by the helium.

Solution:

Step 1: Select system: The system for analysis is the helium.

Step 2: Model the behavior: The helium is modeled as an ideal gas; the spring is modeled as a pure translational spring; the piston is modeled as frictionless; the cylinder wall is modeled as thermally conducting.

Step 3: Model the process: The process in the helium is modeled as a series of equilibrium states for which the pressure and temperature are uniform throughout the gas but changing with time. The process in the spring is modeled as conservative.

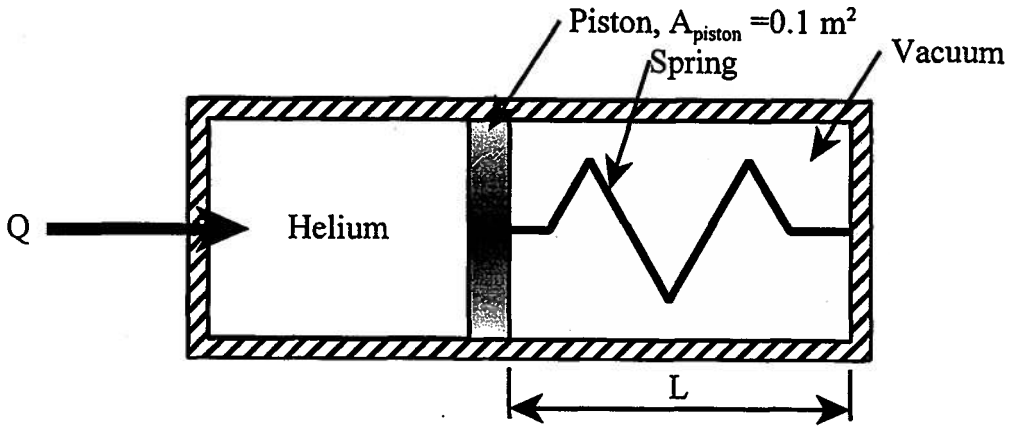

(a) Piston-cylinder Apparatus

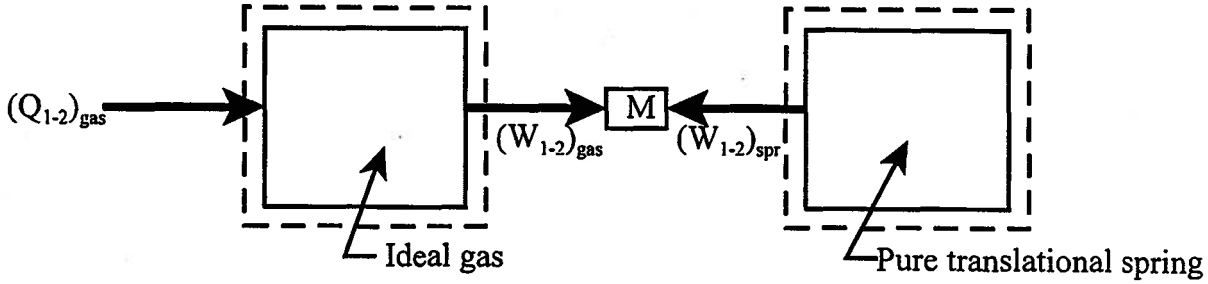

(b) System Model

Figure 4E.3 Piston-cylinder Apparatus Filled with Gas Experiencing Heat Transfer

Step 4: Apply the laws of thermodynamics: The first law of thermodynamics for the spring system shown in Figure 4E.3 is

$$(E_2 - E_1)_{elastic} = -(W_{1-2})_{spring}$$

Substituting the energy constitutive relation for the spring, we get

$$-(W_{1-2})_{spring} = \tfrac{1}{2}kx_2^{\,2} - \tfrac{1}{2}kx_1^{\,2}$$

where x is the length of the spring, L, measured relative to its length in the unstressed condition, L_0. Then

$$x_1 = L_1 - L_0 \quad \text{and} \quad x_2 = L_2 - L_0$$

For the mechanical interconnection we have

$$(W_{1-2})_{gas} = -(W_{1-2})_{spring}$$

Then

$$(W_{1-2})_{gas} = \tfrac{1}{2}kx_2^{\,2} - \tfrac{1}{2}kx_1^{\,2}$$

The mechanical equilibrium of the piston requires that there be no net boundary force on the piston. Then for the piston

$$\sum F_x = F_{gas} + F_{spring} = 0$$

$$PA_{piston} - kx = 0$$

$\frac{1}{2}k(x_2^2 - x_1^2)$

It follows then that

$$x_1 = \frac{P_1 A_{piston}}{k} \text{ and } x_2 = \frac{P_2 A_{piston}}{k}$$

Then the work transfer experienced by the gas is

$$(W_{1-2})_{gas} = \frac{A_{piston}^2}{2k}(P_2^2 - P_1^2)$$

$$(W_{1-2})_{gas} = \frac{(0.1\ \text{m}^2)^2}{2(10^5\ \text{N/m})}\left[(3.039 \times 10^5\ \text{N/m}^2)^2 - (1.013 \times 10^5\ \text{N/m}^2)^2\right]$$

$$(W_{1-2})_{gas} = 4.105\ \text{kJ}$$

From the property constitutive relation for the ideal gas model, it follows that

$$\frac{P_1 V_1}{T_1} = \frac{P_2 V_2}{T_2}$$

or

$$T_2 = T_1\left(\frac{P_2 V_2}{P_1 V_1}\right)$$

But

$$V_2 = V_1 + \Delta V = V_1 + A_{piston}(L_2 - L_1) = V_1 + A_{piston}\left[(L_2 - L_0) - (L_1 - L_0)\right] = V_1 + A_{piston}(x_2 - x_1)$$

$$V_2 = 0.1\ \text{m}^3 + (0.1\ \text{m}^2)\left(\frac{(3.039 \times 10^5\ \text{N/m}^2)(0.1\ \text{m}^2)}{(10^5\ \text{N/m})} - \frac{(1.013 \times 10^5\ \text{N/m}^2)(0.1\ \text{m}^2)}{(10^5\ \text{N/m})}\right)$$

$$V_2 = 0.1203\ \text{m}^3$$

Then

$$T_2 = (300\ \text{K})\left(\frac{(3.039 \times 10^5\ \text{N/m}^2)(0.1203\ \text{m}^3)}{(1.013 \times 10^5\ \text{N/m}^2)(0.1\ \text{m}^3)}\right)$$

$$T_2 = 1082\ \text{K}$$

From the energy constitutive relation and the property constitutive relation for the ideal gas model, we have

$$U_2 - U_1 = mc_v(T_2 - T_1) = c_v \frac{P_1 V_1}{R T_1}(T_2 - T_1)$$

$$U_2 - U_1 = (3153\ \text{J/kg K})\frac{(1.013 \times 10^5\ \text{N/m}^2)(0.1\ \text{m}^3)}{(2078\ \text{J/kg K})(300\ \text{K})}(1082\ \text{K} - 300\ \text{K})$$

$$U_2 - U_1 = 40.065\ \text{kJ}$$

Then from the first law of thermodynamics for the gas

$$(Q_{1-2})_{gas} = U_2 - U_1 + (W_{1-2})_{gas} = 40.065\ \text{kJ} + 4.105\text{kJ} = 44.171\ \text{kJ}$$

4.5 Pressure Distribution in a Static Fluid

Now that we have established the various models that can be used to describe the dynamic and thermodynamic behavior of fluids under the conditions found in typical engineering situations, we need to examine the details of this behavior. In keeping with our general approach

of proceeding from the simple to the complex, we begin our examination with the simplest case, namely the static situation. We have already seen that in the case of static equilibrium, there are no shear forces in the fluid and a force applied at the boundary of a fluid is distributed uniformly throughout the fluid. However, suppose that in addition to this boundary force there is also a body force exerted by some magnetic, electric, or gravitational force field. How do the conditions of equilibrium determine the manner in which the fluid responds to these applied forces? For the purposes of this analysis, let us assume that the pressure is distributed throughout the fluid in an arbitrary fashion such that at any location in space specified by the coordinates (x, y, z), the pressure has the value P where

$$P = P(x, y, z)$$

Consider the fluid element shown in Figure 4.5.

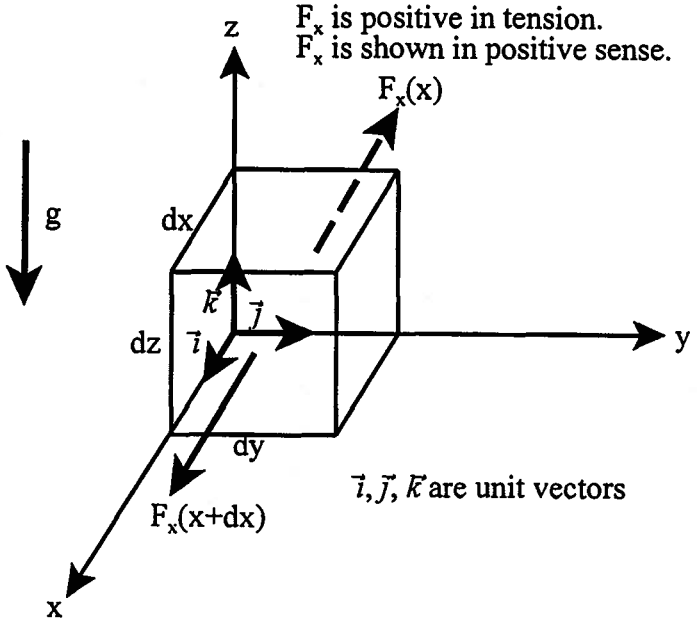

Figure 4.5 x-component of Surface Force Imposed on Fluid Element

The faces of the element are subjected to surface forces due to the action of the pressure distribution in the fluid. Consider first the x-direction. The sum of the forces in the x-direction is

$$\sum F_x = F_x(x+dx) - F_x(x) = dF_x \tag{4.10}$$

where

$$F_x(x) = -PdA = -Pdydz \tag{4.11a}$$

and

$$F_x(x+dx) = -(P + \frac{\partial P}{\partial x}dx)dydz \tag{4.11b}$$

Then

$$dF_x = -\frac{\partial P}{\partial x}dxdydz \tag{4.12}$$

Similarly, for the y- and z-directions, we have

$$dF_y = -\frac{\partial P}{\partial y}dxdydz \tag{4.13}$$

$$dF_z = -\frac{\partial P}{\partial z} dxdydz \tag{4.14}$$

Then the net surface force vector, $d\vec{F}_{surface}$, is

$$d\vec{F}_{surface} = \vec{i}\, dF_x + \vec{j} dF_y + \vec{k} dF_z = \left(-\vec{i}\,\frac{\partial P}{\partial x} - \vec{j}\,\frac{\partial P}{\partial y} - \vec{k}\,\frac{\partial P}{\partial z} \right) dxdydz \tag{4.15}$$

The term in parentheses is just the gradient in the pressure. Then equation (4.15) can be written

$$\text{grad } P = \nabla P = -\frac{d\vec{F}_{surface}}{dxdydz} \tag{4.16}$$

The body force acting on the fluid element shown in Figure 4.5 due to the gravitational field of the earth, $d\vec{F}_{body}$, is determined from the pure gravitational spring model. Then

$$d\vec{F}_{body} = \rho \vec{g}\, dxdydz = \rho g \vec{k} dxdydz \tag{4.17}$$

Then applying Newton's second law of motion to the fluid element, we find that the net force acting on the fluid element is just equal to the product of the mass of the element and its acceleration $\vec{a}$, viz.

$$d\vec{F}_{net} = d\vec{F}_{surface} + d\vec{F}_{body} = \vec{a}\, dm = \rho \vec{a}\, dxdydz$$

Then the equation governing the pressure distribution in the fluid becomes

$$-\nabla P + \rho \vec{g} = \rho \vec{a}$$

Since we are considering the static situation for which there are no accelerations and no shear forces, the pressure distribution in the fluid is governed by the relation

$$-\nabla P + \rho \vec{g} = 0 \tag{4.18}$$

For the case in which the z-direction is aligned with the acceleration of gravity,

$$g_x = 0$$

$$g_y = 0$$

$$g_z = -g$$

and equation (4.18) can be written in rectangular coordinates.

$$\frac{\partial P}{\partial x} = 0$$

$$\frac{\partial P}{\partial y} = 0 \tag{4.19}$$

$$\frac{\partial P}{\partial z} = -\rho g$$

For the case at hand, namely one in which we have a fluid in static equilibrium in which gravity is the only body force and it is aligned with the z-direction, we see that the pressure varies only in the z-direction so that all horizontal planes in the fluid have the same pressure acting on them. Then equations (4.19) can be simplified to a single ordinary derivative, viz.

$$\frac{dP}{dz} = -\rho g \tag{4.20}$$

Therefore, we can draw the following conclusions about a fluid in static equilibrium in the gravitational field of the earth:

1. There is no shear stress in a fluid in static equilibrium.
2. The normal stress (pressure) in the fluid varies only with distance measured in a direction parallel to the gravity vector (typically the vertical direction).
3. The pressure is the same at all points on a given horizontal plane in the fluid.
4. The pressure is independent of the shape of the container.
5. The pressure increases with depth in the fluid.

Example 4E.4: To provide an appropriate level of passenger comfort, the passenger cabin on a commercial aircraft is pressurized by mechanical means so that the interior pressure is equivalent to the atmospheric pressure that one would find at an altitude of 1524 m (5000 ft). The pressure at zero altitude is 1.013×10^5 N/m^2. The temperature is maintained constant at 20 C by the cabin air-conditioning system. Estimate the pressure at the operating condition of the cabin interior if the atmosphere can be modeled as an ideal gas with R = 287 J/kg K.

Solution: The atmosphere is a fluid for which the altitude behavior of the pressure can be described by equation (4.20), i.e.,

$$\frac{dP}{dz} = -\rho g$$

But from the property constitutive relation for the ideal gas model

$$\rho = \frac{m}{V} = \frac{P}{RT}$$

Then it follows that

$$\frac{dP}{dz} = -\frac{P}{RT} g$$

or upon separating variables

$$\frac{dP}{P} = -\frac{g}{RT} dz$$

Then integrating this expression, we get

$$\ln \frac{P}{P_0} = -\frac{g}{RT}(z - z_0)$$

or

$$P = P_0 e^{-\frac{g}{RT}(z - z_0)}$$

If we take z_0 =0 and substitute the appropriate properties and constants, we get

$$P = (1.013 \times 10^5 \text{ N/m}^2) e^{-\frac{(9.80 \text{ m/s}^2)(1524 \text{ m})}{(287 \text{ J/kg K})(293 \text{ K})}}$$

$$P = 8.482 \times 10^4 \text{ N/m}^2$$

Although the temperature of the air is maintained constant in this example by mechanical means, this is not the case in the atmosphere itself. At this altitude in the atmosphere, the pressure and temperature would be very different from the result shown here (cf. Problem 4.8).

4.6 Measurement of Pressure by Means of Fluid Level: Barometers and Manometers

Now that we have established the dependence of pressure in a static fluid on the depth in a fluid, we can use this dependence to measure pressure in a fluid. Recall the barometer depicted in Figure 4.4. From equation (4.20) and the fact that pressure on a horizontal plane in a fluid in

static equilibrium is everywhere the same, we have for the barometer

$$\frac{dP}{dz} = -\rho g$$

But if the fluid can be modeled as an incompressible fluid, $\rho = \rho_0 =$ constant. Then

$$\int_{P_0}^{P} dP = -\int_{z_0}^{z} \rho_0 g \, dz \tag{4.21}$$

where P is the pressure exerted on the free surface of the pool of mercury by the environment and P_0 is the pressure exerted on the surface of the mercury inside the tube by the mercury vapor that fills the volume trapped between this surface and the closed end of the tube. In addition, z is the height of the surface of the mercury where the pressure is P and z_0 is the height of the surface of the mercury where the pressure is P_0. Then integration of equation (4.21) gives

$$P - P_0 = -\rho_0 g(z - z_0) = \rho_0 g(z_0 - z) \tag{4.22}$$

If we measure z relative to the free surface of the pool of mercury, it follows that $z_0 = h$ and $z = 0$. Then

$$z_0 - z = h \tag{4.23}$$

and

$$P = P_0 + \rho_0 g h \tag{4.24}$$

which is identical to equation (4.4). Equation (4.24) is the fundamental equation describing the use of a fluid filled column to measure the pressure in the same or other fluid. Equation (4.24) applies to both barometers and manometers. A barometer differs from a manometer in that the barometer is used to measure absolute pressure in a fluid. In the case of the barometer, the vapor pressure of the mercury is so small ($P_0 = 0.16$ N/m^2 at 20 C) that P_0 is often neglected in comparison with the pressure being measured, the pressure of the environment (for example, $P_{atm} = 1.0135 \times 10^5$ N/m^2). A manometer, on the other hand, measures relative pressure in which P_0 cannot, in general, be neglected. In a typical application of a manometer, this pressure measurement is relative to the pressure of the atmosphere so that in these cases $P_0 = P_{atm}$.

As an example of the operation of a manometer and the application of equation (4.24), consider the situation shown in Figure 4.6. Two empty cylindrical tanks erected side by side are connected by means of a manometer containing a liquid (such as mercury) of high density ρ_M. With both tanks evacuated, the level of this fluid in the manometer lies in the plane $z = 0$. Tank A is filled with a liquid of density ρ_A to a level h_A above the manometer connection. Tank B is filled with a different liquid of density ρ_B to a level h_B above its manometer connection. The volume above the liquid in each tank is pressurized by means of an ideal gas. These two volumes are interconnected via another manometer filled with a liquid of high density ρ_m. The pressure in gas A is increased to the value P_{0A} and the pressure in gas B is increased to the value P_{0B}. In response to these applied pressures, the liquid level in the upper manometer deflects so that the difference in height of the two legs is L. Similarly, the liquid level in the lower manometer deflects so that the difference in height of the two legs is H.

We can now determine the various pressures by application of equation (4.24). In doing so, we make use of the observations of section 4.2, namely that the influence of gravity on the behavior of gases is negligible compared to that of liquids. In particular, we assume that the hydrostatic pressure in gases can be neglected. As justification for this assumption, we point out that the densities of gases in situations for which manometers are employed for pressure measurement are on the order of 1 kg/m^3 while those of liquids used in manometers are on the order of 1000 kg/m^3 (H_2O) to 13,560 kg/m^3 (Hg). Thus, the pressure throughout gases in most engineering situations can be regarded as uniform and independent of the vertical dimension of the container.

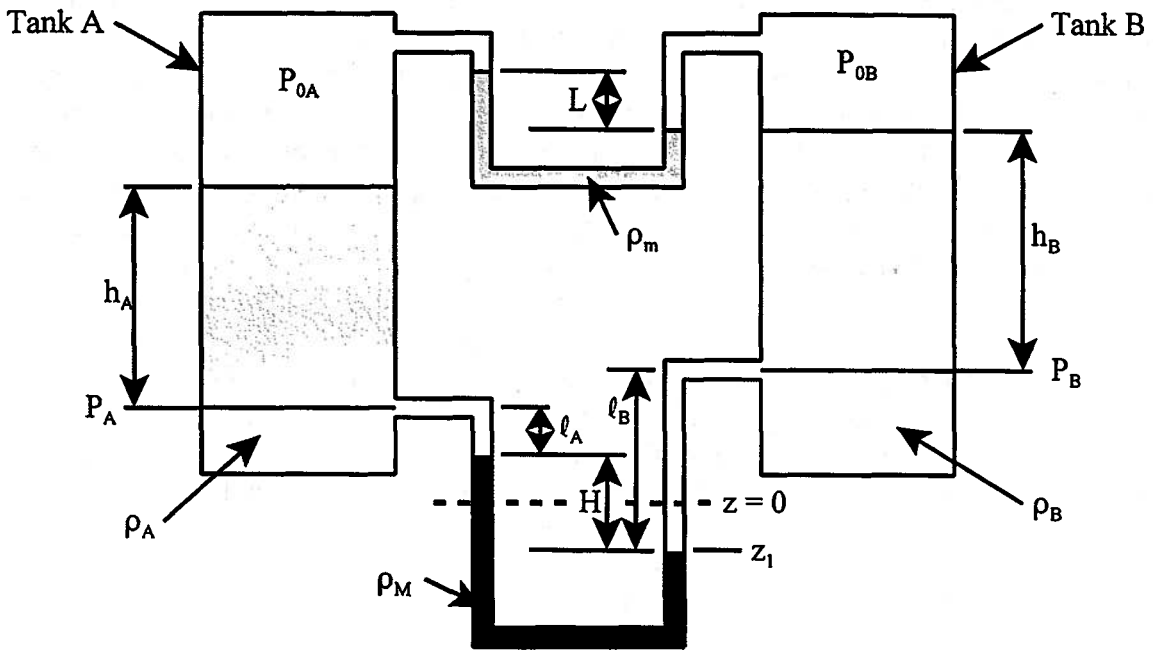

Figure 4.6 Pressure Measurement by Liquid Filled Manometers

Then in Figure 4.6 the pressures at the two points where the lower manometer attaches to the two tanks are given by

$$P_A = P_{0A} + \rho_A g h_A \quad \text{and} \quad P_B = P_{0B} + \rho_B g h_B \tag{4.25}$$

and the difference in pressure is given by

$$P_B - P_A = (P_{0B} - P_{0A}) + \rho_B g h_B - \rho_A g h_A \tag{4.26}$$

Although not true in general, in many cases we can neglect the densities of the gases in the two tanks compared to the density of the liquid in the upper manometer. Then we can write

$$P_{0B} - P_{0A} = \rho_m g L \tag{4.27}$$

so that the pressure difference between A and B becomes

$$P_B - P_A = \rho_m g L + \rho_B g h_B - \rho_A g h_A \tag{4.28}$$

Alternatively, since the pressure is everywhere the same on the plane z_1, we can write

$$P_A + \rho_A g \ell_A + \rho_M g H = P_B + \rho_B g \ell_B \tag{4.29}$$

where the expression on the left-hand side of equation (4.29) is the pressure on that portion of the z_1-plane coincident with the left-hand leg of the manometer, and the expression on the right-hand side of equation (4.29) is the pressure on that portion of the z_1-plane coincident with the right-hand leg of the manometer. Then the pressure difference between A and B can also be written

$$P_B - P_A = \rho_A g \ell_A + \rho_M g H - \rho_B g \ell_B \tag{4.30}$$

Another way in which the manometer can be used to measure the pressure difference in this situation is to determine the location of the zero plane in the lower manometer before the liquids are admitted to the two tanks. This is known as "zeroing the manometer". Then if ℓ_{0A} and ℓ_{0B} denote the locations of the zero level of the liquid in the manometer relative to the point of attachment of the manometer to the tanks, the pressure difference can also be written

$$P_B - P_A = \rho_B g(\ell_{0B} + \frac{H}{2}) - \rho_A g(\ell_{0A} - \frac{H}{2}) - \rho_M g H \tag{4.31}$$

In all of these applications of the manometer for measuring pressure, keep in mind that the value of the pressure will be the same at any two points in the same horizontal plane in a continuous volume of a given liquid. The fundamental parameter in manometer design is the choice of fluid which allows the engineer to select a fluid of a density sufficient to produce readily measurable deflections of the fluid level for a given pressure to be measured. In some applications for which the pressure differential is small, the leg of the manometer in which the liquid level is being measured is inclined so that length measurements are made along the hypotenuse which amplifies the reading and improves the precision of the measurement.

Example 4E.5: A cylindrical tank which is open to the atmosphere is filled with water to a depth of 2.5 m as shown in Figure 4E.5. A U-tube manometer is connected to the tank at a point 0.7 m above the tank bottom. The manometer is filled with an immiscible liquid with a density twice that of the water ($\rho_{water} = 10^3$ kg/m^3). Prior to filling the tank, the manometer is "zeroed" with the liquid level 0.2 m below the point of attachment to the tank. Determine the difference in the heights of the manometer liquid in the two legs of the manometer.

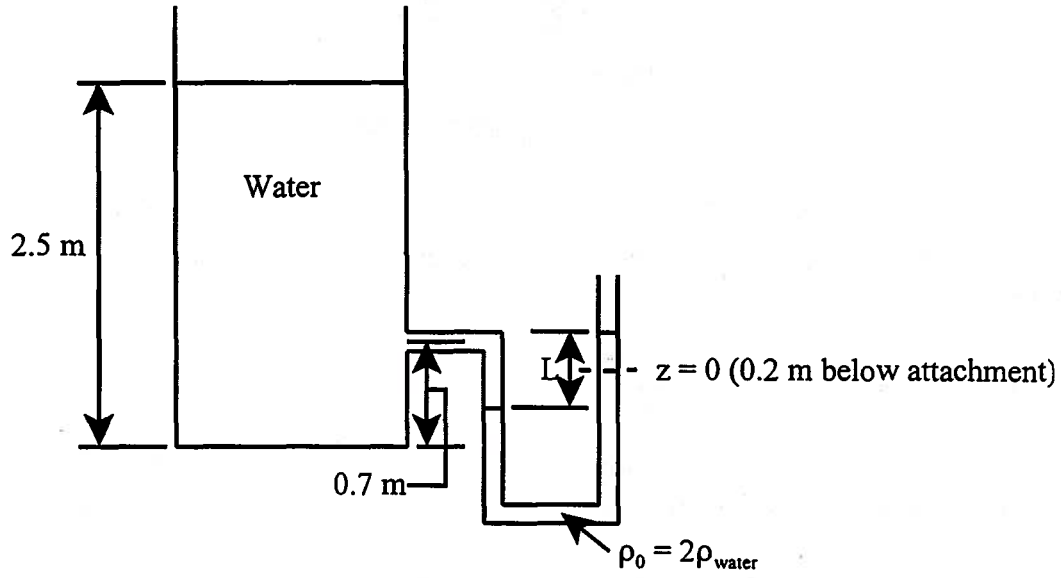

Figure 4E.5 Water Tank with Manometer

Solution: The pressure, P_a, of the water at the point of attachment of the manometer is given by equation (4.24), viz.

$$P_a = P_{atm} + \rho_{water} g h = P_{atm} + (10^3 \text{ kg/m}^3)(9.80 \text{ m/s}^2)(2.5 \text{ m} - 0.7 \text{ m})$$

$$P_a = P_{atm} + 1.764 \text{ x } 10^4 \text{ N/m}^2$$

The pressure, P_i, at the plane containing the interface of the water and the manometer liquid is given by

$$P_i = P_a + \rho_{water} g(0.2 \text{ m} + \frac{L}{2}) = P_{atm} + \rho_0 g L$$

Solving this expression for L, we get

$$\rho_0 g L = 2\rho_{water} g L = \rho_{water} g(0.2 + \frac{L}{2}) + 1.764 \text{ x } 10^4 \text{ N/m}^2$$

$$L = \left[0.2 \text{ m} + \frac{1.764 \text{ x } 10^4 \text{ N/m}^2}{(10^3 \text{ kg/m}^3)(9.80 \text{ m/s}^2)}\right] \frac{1}{1.5 \text{ m}}$$

$$L = 1.333 \text{ m}$$

4.7 Hydrostatic Forces on Stationary Submerged Surfaces

In engineering practice there are many circumstances in which surfaces are exposed to the action of the fluid pressure forces determined in the preceding section. For example, these forces must be considered when designing a dam or a tank to store a large quantity of water. Also, it is these forces that enable ships and boats of all manner of design to float and remain upright in a wide variety of conditions at sea. Evaluation of these forces in these and many other applications requires the specification of the magnitude and direction of the force as well as the line of action of the resultant force.

4.7.1 Hydrostatic Force on a Plane Submerged Surface

Figure 4.7 shows a plane surface immersed in a fluid at an angle of θ to the free surface of the fluid. Ambient pressure P_0 acts everywhere on the free surface. The density of the fluid is ρ. The xyz coordinate system is configured so that the xy plane is coincident with the plane surface and the z axis is normal to the plane surface.

Since there are no shear stresses in a fluid in static equilibrium, the pressure forces act normal to the surface. The pressure force acting on an element of the upper surface, dA, is given by

$$d\vec{F} = -P\vec{n}dA \tag{4.32}$$

where the negative sign appears because the force acts in a direction opposite to the outward normal, $\vec{n}$, that defines the direction associated with the element of area dA. It follows then that the resultant force on the surface is given by the integral of equation (4.32) over the area A.

$$\vec{F}_R = \int_A -P\vec{n}dA \tag{4.33}$$

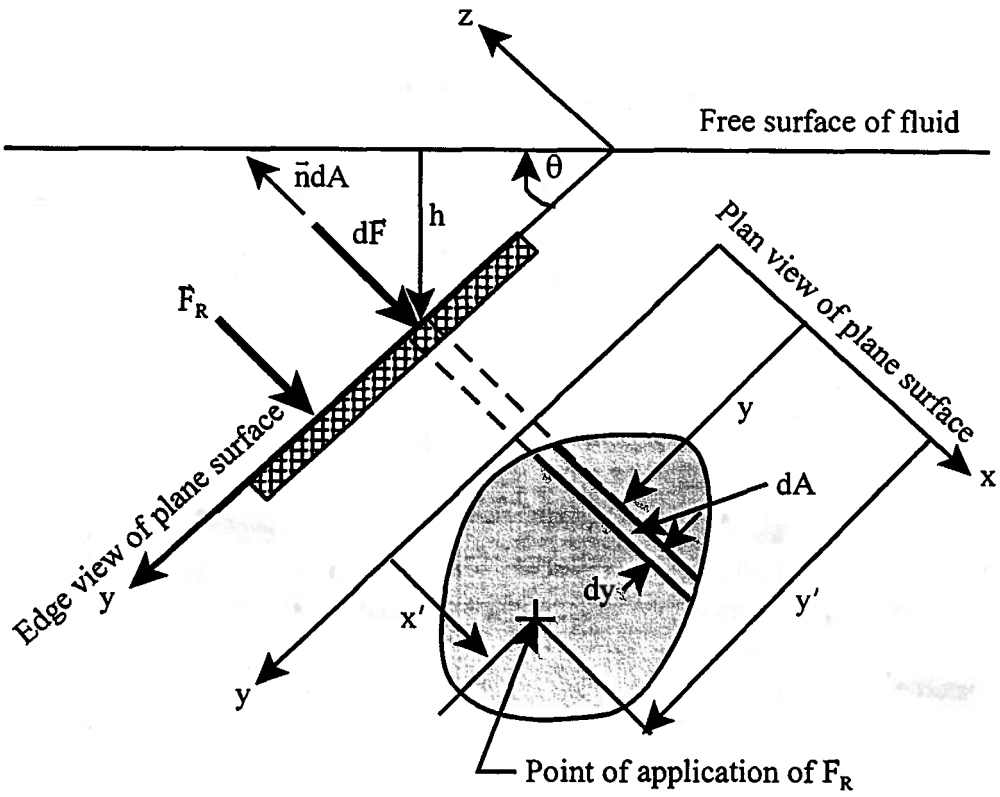

Figure 4.7 Plane Submerged Surface

In order to evaluate equation (4.33), we need to know the relationship between P and dA. From equation (4.20)

$$\frac{dP}{dh} = \rho g \tag{4.34}$$

where h is measured positive downward from the free surface of the fluid. If the pressure at the free surface of the fluid is P_0, we can integrate equation (4.34) to get P as a function of h, viz.,

$$\int_{P_0}^{P} dP = \int_{0}^{h} \rho g dh \tag{4.35}$$

Then

$$P = P_0 + \rho g h \tag{4.36}$$

and the magnitude of the force F_R becomes

$$F_R = P_0 A + \rho g \int_A h dA \tag{4.37}$$

But $h = y \sin\theta$. Then

$$F_R = P_0 A + \sin\theta \int_A y dA \tag{4.38}$$

To calculate the point of application of the resultant force, we simply make use of the fact that the moment of the resultant force about any axis must be the same as the moment of the distributed force about the same axis. Then if (x', y') denote the coordinates of the point of application of the resultant force as shown in Figure 4.7, it must be the case that

$$x' F_R = \int_A x P dA \tag{4.39}$$

and

$$y' F_R = \int_A y P dA \tag{4.40}$$

The line of action of the resultant force passes through the point (x', y') and is normal to the submerged surface in the direction opposite to the outward normal to the surface.

Notice that if y_{CG} denotes the y-position of the *centroid* (also known as the *center of gravity*) of the submerged plane surface measured in the plane of the surface, it follows that

$$y_{CG} = \frac{1}{A} \int y dA \tag{4.41}$$

and equation (4.38) becomes

$$F_R = P_0 A + (\rho g \sin\theta) y_{CG} A = P_0 A + (y_{CG} \sin\theta) \rho g A \tag{4.42}$$

But $y_{CG} \sin\theta = h_{CG}$. Then

$$F_R = P_0 A + \rho g h_{CG} A = (P_0 + \rho g h_{CG}) A = P_{CG} A \tag{4.43}$$

Thus, under conditions of hydrostatic equilibrium, the force acting on a plane submerged surface is equal to the product of the hydrostatic pressure at the centroid of the surface and the area of the surface. The force acts through the *center of pressure* whose coordinates are given by equations (4.39) and (4.40). Note that the locations of the centroid and the center of pressure are not coincident. The locations of the centroids of some common geometric shapes are given in Table 4.3.

TABLE 4.3
Centroids of Common Shapes

Triangular Area:

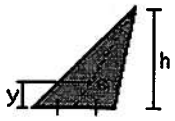

Height, y, of centroid from base: $\frac{h}{3}$

The centroid is located on the median of the triangle at a height *y* above the base.

Quarter Circle Area:

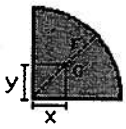

Horizontal component,*x*, of centroid: $\frac{4 \cdot r}{3 \cdot \pi}$

Vertical component,*y*, of centroid: $\frac{4 \cdot r}{3 \cdot \pi}$

Semicircular Area:

Distance, *y*, of centroid from center: $\frac{4 \cdot r}{3 \cdot \pi}$

Semiparabolic Area:

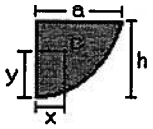

Horizontal component,*x*, of centroid: $\frac{3 \cdot a}{8}$

Vertical component,*y*, of centroid: $\frac{3 \cdot h}{5}$

Example 4E.6: A penstock is a tunnel of circular cross-section cut into the rock surrounding dams used in the generation of electricity by hydroelectric means. The purpose of the penstocks is to feed the water from the reservoir behind the dam into the water turbines that drive the generators that "generate" the electricity, i.e. convert mechanical work transfer into electrical work transfer. The Hoover Dam on the Arizona-Nevada border is an example of such a

dam. This dam is capable of "generating" 2,080 megawatts of electricity by converting the gravitational potential energy of the water trapped behind it into kinetic energy of water streams acting on the turbines of 17 turbine-generator units located at the base of the dam. The penstocks of Hoover Dam are 4 m in diameter with a vertical height of 180 m. Since not all of the turbine-generator units are in use all the time, the idle units can be shut down by closing a valve in the penstock. For the purposes of this example, we can represent the valve as a circular disk placed over the end of the penstock. As shown in Figure 4E.6, the disk is hinged at one end and held closed by a force, F_C, normal to it at the other end. Neglecting the weight of the disk, determine the magnitude of the force F_C.

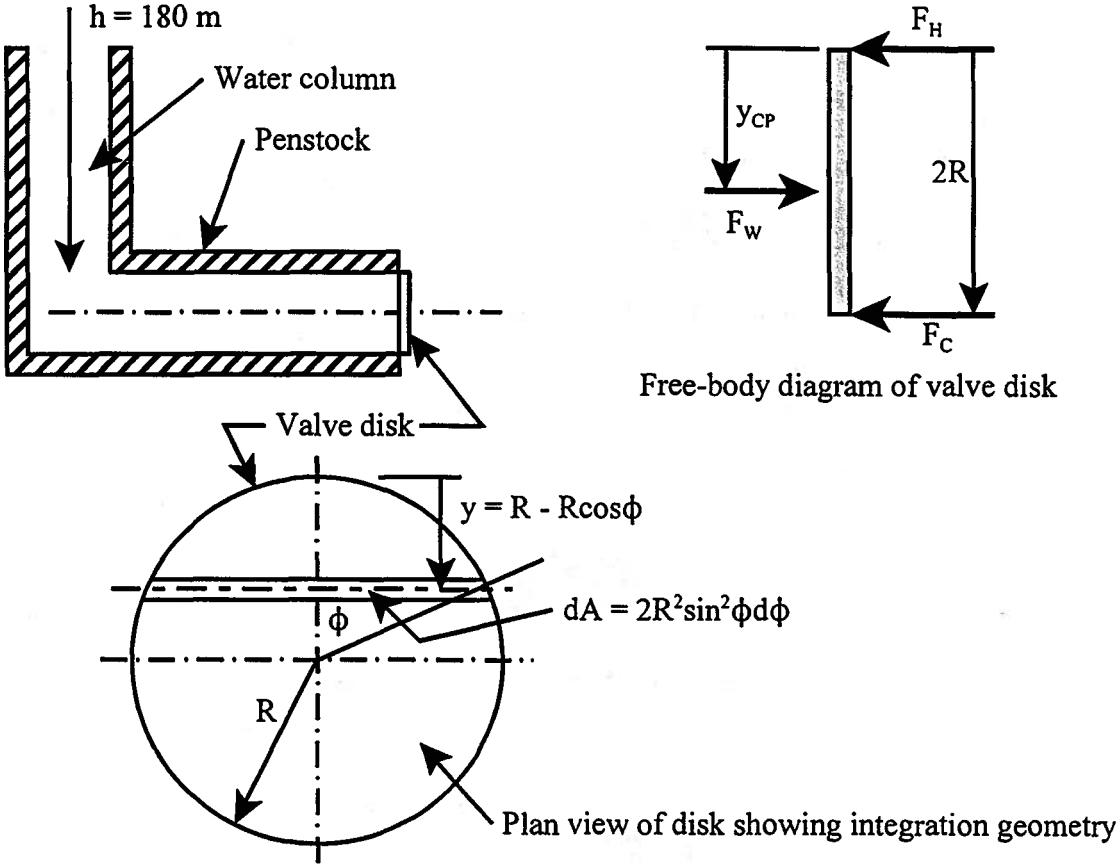

Figure 4E.6 Penstock and Valve Disk

Solution: When the valve is closed, mechanical equilibrium of the valve disk requires that there be three forces acting on the disk: a force F_W due to the pressure of the water acting on the disk; a force F_C holding the disk in the closed position; and a force F_H which is the reaction force at the hinge. All of these forces act normal to the disk. Then from the free-body diagram, it is evident that equilibrium requires

$$\sum M_{hinge} = F_C(2R) - F_W y_{CP} = 0$$

where we have neglected the weight of the disk. If h_0 denotes the height of the water column at the hinge, the height of the water column, h, at any location y on the disk is

$$h = h_0 + y\sin\theta$$

where in the present case $\theta = 90°$. Applying equation (4.38), we can determine the location of the center of pressure. Substituting the appropriate values for the various constants, we get y_{CP} =

2.0055 m. The fact that y_{CP} lies below the location of the centroid is typical. The fact that it lies only a small distance below in this case is a consequence of the fact that most of the area on which the hydrostatic pressure acts lies at locations with values of y close to the location of the centroid (in this case the center of the disk). The force F_C is then given by

$$F_C = \frac{F_W y_{CP}}{2R} = \frac{\rho g(h_0 + R\sin\theta)\pi R^2 y_{CP}}{2R}$$

$$F_C = \frac{(10^3 \text{ kg/m}^3)(9.81 \text{ m/sec}^2)(180 \text{ m} + 2 \text{ m})\pi(2 \text{ m})^2(2.0055 \text{ m})}{2(2 \text{ m})} = 1.1249 \text{ x } 10^7 \text{ N}$$

4.7.2 Hydrostatic Force on a Curved Submerged Surface

Hydrostatic forces on curved submerged surfaces can best be determined by evaluating their components and making use of the results of the previous section. Consider the curved surface that bounds a fluid as shown in Figure 4.8. The fluid element which is of unit length normal to the plane of the figure is bounded on the right-hand side by a curved surface that exerts a force F_H in the negative x-direction and on the bottom by a flat surface that exerts a force F_V in the negative z-direction. The upper free surface of the fluid element is exposed to the atmosphere. The atmosphere also acts on the right-hand boundary and contributes a force $P_{atm}h$ in the negative x-direction. The fluid element is bounded in the left-hand side by additional fluid with properties identical to those of the fluid element.

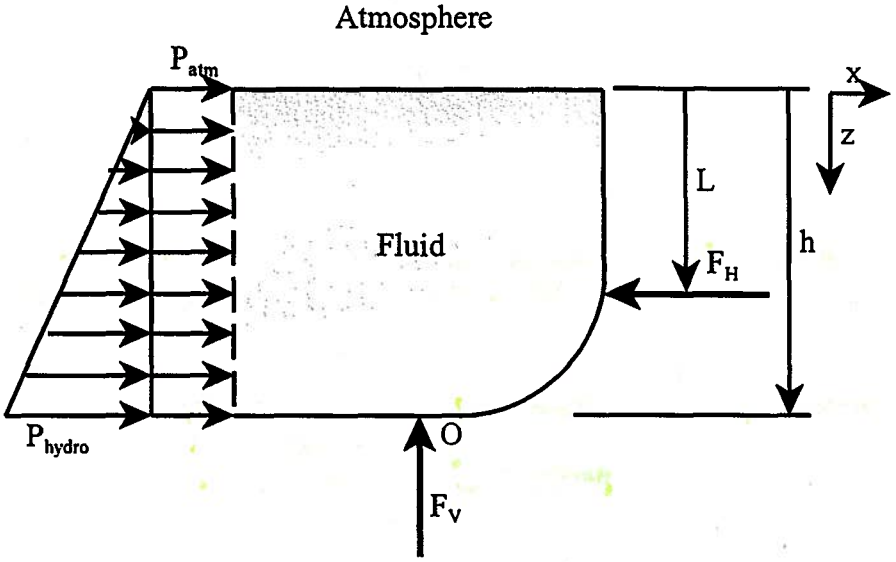

Figure 4.8 Forces on a Body of Fluid with Curved Boundaries

The force acting on the left-hand side of the fluid element has two contributions both of which act in the positive x-direction: one due to the atmospheric pressure acting uniformly over the left-hand face; the other due to the hydrostatic pressure of the adjacent fluid acting over the same surface.

For a fluid element of unit length normal to the plane of the page, mechanical equilibrium requires that there be no net force acting in the x-direction. Thus

$$\sum F_x = \int_0^h P_{atm}\,dz + \int_0^h P_{hydro}\,dz - F_H - P_{atm}h = 0$$

$$F_H = P_{atm}h + \int_0^h \rho g z\,dz - P_{atm}h = \rho g \frac{h^2}{2} \tag{4.44}$$

where we have made use of equation (4.20). Notice that the average value for the hydrostatic pressure is

$$\left(P_{hydro}\right)_{ave} = \rho g \frac{h}{2} \tag{4.45}$$

Then the externally applied force can be written

$$F_H = \left(P_{hydro}\right)_{ave} A \tag{4.46}$$

To determine the point of application of this force necessary to keep the element in equilibrium, we make use of the fact that in the equilibrium state the net moment about the point O (the point of application of the vertical force) is zero. Then if moments in the clockwise direction are considered positive

$$\sum M_O = P_{atm} h\left(\frac{h}{2}\right) + \int_0^h P_{hydro}(h-z)dz - F_H(h-L) - P_{atm} h\left(\frac{h}{2}\right) = 0 \tag{4.47}$$

Substituting the expression for the hydrostatic pressure as a function of z and carrying out the integration, we obtain

$$\int_0^h \rho g z h dz - \int_0^h \rho g z^2 dz = F_H(h-L) \tag{4.48}$$

Substituting equation (4.44) into equation (4.48) and integrating, we get

$$\rho g \frac{h^2}{2}(h-L) = -\rho g \frac{h^3}{6} = \rho g \frac{h^2}{2}\left(\frac{h}{3}\right)$$
$$h - L = \frac{h}{3} \tag{4.49}$$

and

$$L = \frac{2}{3} h \tag{4.50}$$

Notice that the magnitude of the externally applied horizontal force is equal to the product of the average hydrostatic pressure and the area of the curved surface projected on the vertical plane. This is a general result that applies to any curved surface regardless of its shape. Note also that the point of application of the horizontal force (z-coordinate of the center of pressure) is two-thirds of the distance between the free surface and the bottom edge of the curved surface and is measured downwards from the free surface. This is a general result, also, and derives from the fact that the hydrostatic pressure distribution appears "triangular" in shape since it increases linearly with depth (See Figure 4.8.). Since the centroid of a triangle is two-thirds of the distance from its apex to its base as measured from the apex, it follows that the point of application of the average hydrostatic pressure can be thought of occurring at this point.

For the vertical component of the externally applied force, consideration of mechanical equilibrium in the vertical direction requires that this boundary force be equal in magnitude and opposite in direction to the body force due to the action of gravity of the fluid mass that lies above the curved surface. Note that this fluid mass includes the mass of the column of air that lies above the free surface as well as the liquid immediately adjacent to the curved surface. Alternatively, the body force associated with the column of air could be replaced by the boundary force that acts at the interface between the liquid and the atmosphere and is equal to the product of the atmospheric pressure and the cross-sectional area of the column of air measured normal to the vertical axis.

We could also determine the vertical component of force acting on the curved surface bounding the fluid by integrating the vertical component of the pressure distribution, $P = P(z)$,

due to the combined action of the hydrostatic pressure of the fluid on this surface and the pressure of the atmosphere acting on the free surface of the liquid. This, of course, requires knowledge of the area of the bounding surface as a function of the vertical coordinate z, viz. $A = A(z)$. If θ is the included angle between the normal to the surface and the x-axis, the two-dimensional integral over the area becomes a one-dimensional integral in z.

$$F_V = \int_A P(z)dA_z \tag{4.51}$$

where dA_z is the element of area normal to the z-direction and $dA_z = R\sin\theta d\theta$.

Example 4E.7: Large quantities of liquids, such as petroleum products, are usually stored in large containers called tanks. At a manufacturing site such as a refinery, there may be many such tanks concentrated in a relatively small area known as a tank farm. In the event of a mechanical failure of a tank that results in a leak of the liquid from the tank, it is necessary to provide some means of containing the liquid so that the spill can be cleaned up before there is significant damage to the environment. The simplest form of containment is a berm, or wall, placed around the tank that serves as a dam to create a temporary reservoir of the spilled liquid.

A typical berm design consists of a vertical wall that is curved or slanted at the base so that the force due to the liquid acting on the wall has a downward component as well as a horizontal component. The horizontal component produces a moment that acts to overturn the wall while the downward component produces a moment that acts in the opposite direction and tends to keep the wall seated on its base.

Consider the example shown in Figure E4.7. The wall is 4m high and 0.3 m thick with a curved lower surface of radius 1 m and is designed to contain a liquid of density $\rho = 800$ kg/m^3.

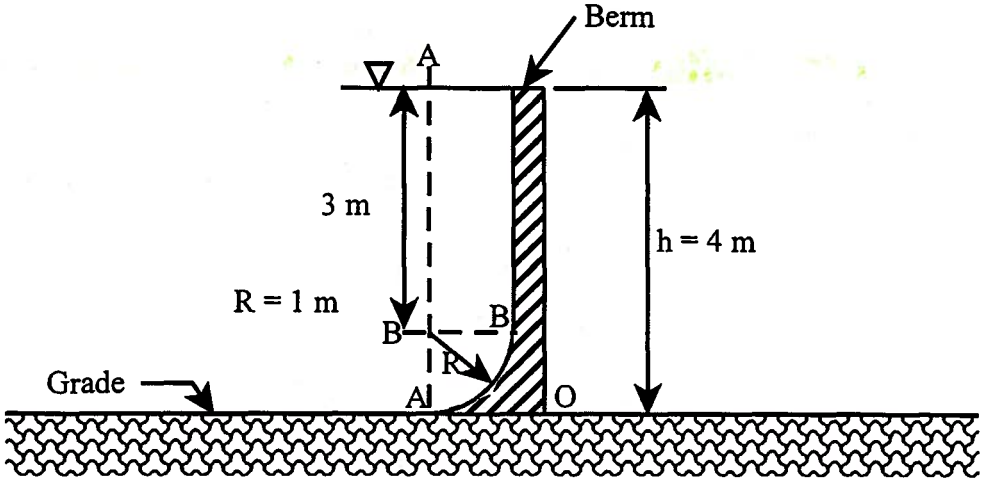

Figure 4E.7 Berm for Petroleum Storage Tank

The berm is exposed to the spilled liquid on its left-hand face. The pressure of the atmosphere is $P_{atm} = 1.0135 \times 10^5$ N/m^2 and the acceleration of gravity is 9.81 m/sec^2.

For a unit length of wall, the horizontal force acting on the wall due to the hydrostatic pressure of the liquid that would fill the reservoir in the event of a leak is F_H where

$$F_H = \int_0^A PdA = \int_0^h (\rho g z)(dz) = \rho g\left(\frac{z^2}{2}\right)_0^h = \rho g\left(\frac{h^2}{2}\right)$$

$$F_H = (800 \text{ kg/m}^3)(9.81 \text{ m/sec}^2)\left[\frac{(4 \text{ m})^2}{2}\right] = 6.28 \times 10^4 \text{ N}$$

and acts in the positive x-direction. Note that atmospheric pressure acts on both sides of the wall so that F_H is the *net* horizontal force (per unit length of wall) acting on the wall. The moment due to this force about the point O is

$$(M_O)_{CW} = F_H \cdot \frac{h}{3} = (6.28 \text{ x } 10^4 \text{ N})\left(\frac{4 \text{ m}}{3}\right) = 8.37 \text{ x } 10^4 \text{ N-m}$$

and acts in the clockwise direction. There are three contributions to the vertical force F_V acting on the curved surface of the wall. One of these, F_{V1}, is due to the pressure of the atmosphere acting on the area of the curved surface projected on the horizontal plane. The second contribution, F_{V2}, is due to body force acting on the rectangular mass of liquid bounded by the vertical plane of the wall, the vertical imaginary plane *A-A*, the horizontal imaginary plane *B-B*, and the unit dimension L normal to the plane of Figure E4.7. The third contribution, F_{V3}, is due to the body force acting on the mass of liquid contained in the quarter cylinder bounded by the curved surface, the vertical imaginary plane *A-A*, the horizontal imaginary plane *B-B*, and the unit dimension L normal to the plane of Figure E4.7. Thus,

$$F_{V1} = P_{atm} \cdot R \cdot L = (1.0135 \text{ x } 10^5 \text{ N/m}^2)(1 \text{ m})(1 \text{ m}) = 1.0135 \text{ x } 10^5 \text{ N}$$

$$F_{V2} = \rho V_2 g = (800 \text{ kg/m}^3)(3 \text{ m})(1 \text{ m})(1 \text{ m})(9.81 \text{ m/sec}^2) = 2.35 \text{ x } 10^4 \text{ N}$$

$$F_{V3} = \rho V_3 g = \rho \frac{\pi R^2}{4} L g = (800 \text{ kg/m}^3)\left(\frac{\pi (1 \text{ m})^2}{4}\right)(1 \text{ m})(9.81 \text{ m/sec}^2)$$

$$F_{V3} = 6.16 \text{ x } 10^3 \text{ N}$$

$$F_V = F_{V1} + F_{V2} + F_{V3} = 1.31 \text{ x } 10^5 \text{ N}$$

Each of these contributions produces a moment in the counterclockwise direction. The moment arm in each case is determined by the location of the centroid of the respective volume. The determination of the moment arms for the first two contributions is straightforward because of their simple shapes. The moment arm is 0.5 m from the inside surface of the wall plus the thickness of the wall, 0.3 m. The location of the centroid for the third contribution is given by the data of Table 4.3. Thus,

$$(M_O)_{V1} = F_{V1} r_{V1} = (1.0135 \text{ x } 10^5 \text{ N})(0.8 \text{ m}) = 8.11 \text{ x } 10^4 \text{ N-m}$$

$$(M_O)_{V2} = F_{V2} r_{V2} = (2.35 \text{ x } 10^4 \text{ N})(0.8 \text{ m}) = 1.88 \text{ x } 10^4 \text{ N-m}$$

$$(M_O)_{V3} = F_{V3} r_{V3} = (6.16 \text{ x } 10^4 \text{ N})\left[1 \text{ m} - \frac{4(1 \text{ m})}{3\pi} + 0.3 \text{ m}\right] = 5.39 \text{ x } 10^4 \text{ N-m}$$

then the net moment in the counter-clockwise direction is the sum of these last three contributions. Thus,

$$(M_O)_{CCW} = 8.11 \text{ x } 10^4 \text{ N-m} + 1.88 \text{ x } 10^4 \text{ N-m} + 5.39 \text{ x } 10^4 \text{ N-m}$$

$$(M_O)_{CCW} = 1.54 \text{ x } 10^5 \text{ N-m}$$

and the net moment acting on the wall is then

$$(M_O)_{net} = (M_O)_{CCW} - (M_O)_{CW} = 1.54 \text{ x } 10^5 \text{ N-m} - 8.37 \text{ x } 10^4 \text{ N-m}$$

$$(M_O)_{net} = 7.01 \text{ x } 10^4 \text{ N-m}$$

Thus there is a net moment acting on the wall in a counterclockwise direction to maintain it in the upright position. This is the reason berms and dams each have a "foot" at the base of the structure located on the fluid side of the object.

As noted above, the vertical component of the force acting on the curved surface could be

determined by integrating the vertical component of the pressure distribution over the curved surface. The pressure on this surface is given by three contributions: (1) the atmospheric pressure acting on the free surface, (2) the pressure on the horizontal plane *B-B* where the curved surface is just tangent to the vertical portion of the wall, and (3) the hydrostatic pressure of the fluid contained between the horizontal plane *B-B* and the curved surface. Thus,

$$P(z) = P_{atm} + \rho g(h - R) + \rho g R \sin\theta$$

and integrating the vertical component of this pressure over the surface (for unit length of wall) we obtain

$$F_V = \int_0^{\frac{\pi}{2}} P_{atm} R \sin\theta \, d\theta + \int_0^{\frac{\pi}{2}} \rho g h R \sin\theta \, d\theta + \int_0^{\frac{\pi}{2}} \rho g R^2 \sin^2\theta \, d\theta$$

$$F_V = P_{atm} R + \rho g h R + \frac{\pi}{4} \rho g R^2$$

$$F_V = (1.0135 \text{ x } 10^5 \text{ N/m}^2)(1 \text{ m})^2 + (800 \text{ kg/m}^3)(9.81 \text{ m/sec}^2)\left[(3 \text{ m})(1 \text{ m}) + \frac{\pi}{4}(1 \text{ m})^2\right]$$

$$F_V = 1.0135 \text{ x } 10^5 \text{ N} + 2.35 \text{ x } 10^4 \text{ N} + 6.16 \text{ x } 10^4 \text{ N} = 1.31 \text{ x } 10^5 \text{ N}$$

which is the same result as before.

4.7.3 Forces on Submerged Objects of Uniform Density: Buoyancy

It is a common childhood experience that when an object such as a stone is dropped into a container filled with a fluid like water, its volume becomes completely submerged in the fluid, and the stone sinks to the bottom of the container. However, when an object like a block of wood is dropped into the same container, it floats on the surface with only a portion of its volume submerged in the fluid. This phenomenon is a consequence of the well-known principle originally attributed to the ancient Greek scholar Archimedes. The results of the preceding section can be used to elucidate the details of this principle.

As shown in two dimensions in Figure 4.9, when an object is completely submerged in a fluid, there is a net boundary force, known as the buoyancy force, that acts in the upwards direction. This buoyancy force is due to the fact that the upper and lower surfaces of the object are at different levels in the fluid, and, hence, are exposed to different hydrostatic pressures over

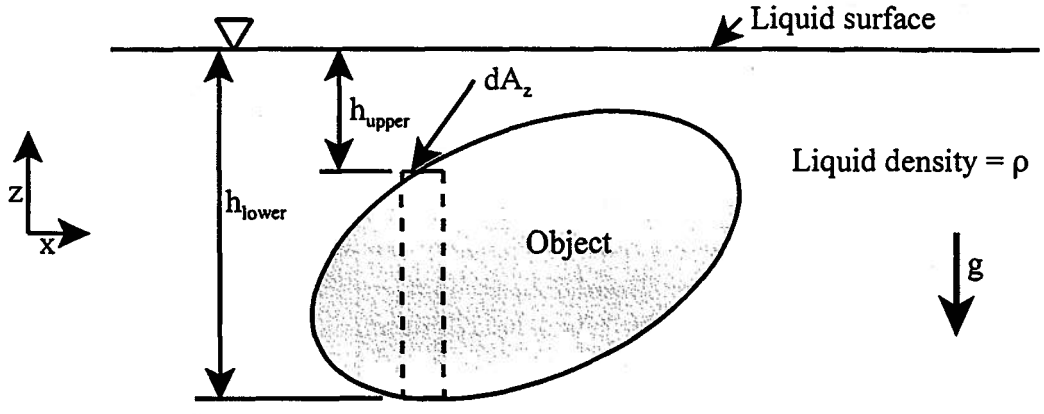

Figure 4.9 Object Submerged in a Liquid of Density ρ

the respective surfaces. If we integrate the pressure distribution over the lower surface, we obtain an upward force that exceeds the downward force obtained by integrating the pressure distribution over the upper surface. This buoyancy force, F_B, is given by

$$F_B = \int_A \rho g\left(h_{lower} - h_{upper}\right) dA_z = \rho g \int_A \left(h_{lower} - h_{upper}\right) dA_z = \rho g V_o \tag{4.52}$$

where V_o is the volume of the object. Thus, the buoyancy force is simply equal to the body force acting on *the volume of fluid displaced by the object*. Since the buoyancy force is due to the action of gravity, its line of action is aligned with the action of gravity in the vertical direction. Furthermore, since there is no net moment on this volume of displaced fluid, the line of action of the buoyancy force must pass through the centroid of the *displaced fluid*, not the centroid of the object. This apparent point of application of the buoyancy force is known as the *center of buoyancy*. This collection of facts about the buoyancy and its direction of action is known as the Archimedes Principle. Whether the object sinks or floats depends upon the magnitude of this buoyancy force in relation to the body force on the object due to the action of gravity.

The net force acting on the submerged object is given by the summation of the buoyancy force F_B and the force due to gravity acting on the object itself, F_G, viz.

$$\left(F_{net}\right)_z = \sum F_z = F_B - F_G = (\rho - \rho_o) g V_o \tag{4.53}$$

where we have assumed that the density of the object, ρ_o, is uniform throughout the volume, V_o, of the object. Thus if the uniform density of the object is greater than the density of the fluid that it displaces, the net force will act in the negative z-direction and the object will sink. If the net force is zero, the object will be in mechanical equilibrium regardless of its position in the fluid and will have neither the tendency to rise or to sink. This state is known as neutral buoyancy and is the state that submarines use to maintain their positions at any specific depth.

4.7.4 Forces on Floating Objects of Uniform Density: Stability

If the uniform density of the object is less than the density of the fluid, the net force will be positive and the object will rise to the surface with a portion of its volume now extending above the free surface of the fluid. In this case the volume of fluid displaced, V_{fluid}, will be less than the volume of the object. The net force acting on the object of uniform density will now be zero in this condition and equation (4.53) becomes

$$\left(F_{net}\right)_z = \sum F_z = F_B - F_G = \rho_{fluid} g V_{fluid} - \rho_o g V_o = \rho_{fluid} g V_{fluid} - W_o \tag{4.54}$$

and

$$\therefore V_{fluid} = \frac{W_o}{\rho_{fluid} g} \tag{4.55}$$

where W_o is the weight of the now floating object. Note that the results of equation (4.53) can be easily extended to objects of non-uniform density by replacing the product $\rho_o V_o$ with an appropriate integral of the density over the volume of the object which when multiplied by g becomes the weight (the gravity force) of the object, W_o, used in equation (4.54). Of course, the buoyancy force and the gravity force act in opposite directions.

The point of application of this gravity body force is the centroid of the object itself, known as the *center of gravity,* which is coincident with the *center of buoyancy* only in the unique case for an object of uniform density for which the density of the fluid and the density of the object are identical. In all other cases, these two apparent points of application are different (even in the case of a neutrally buoyant submerged object for which the buoyancy force just

equals the gravity force). However, as shown in Figure 4.10a, when the floating object is in a state of stable static equilibrium, the center of buoyancy lies on a vertical line above the center of gravity so that the buoyancy force and the gravity force are collinear.

In practice, however, the situation is far from static. Due to the action of waves on the surface of the fluid, the floating body is subject to small lateral forces or perturbations that may be periodic or random in nature. The result of these perturbations is a rotation of the floating body about an axis that lies in the plane of the fluid surface. This rotation upsets the alignment of the buoyancy force and the gravity force and produces a couple as the lines of action of the two forces, F_B and F_G, shift from collinear to parallel. (See Figure 4.10b.) As long as this couple acts to counter the original perturbation, the situation is a stable one and the floating object will right itself. However, if the perturbation causes the center of buoyancy to shift so that the resulting couple now acts in the same direction as the original perturbation as in Figure 4.10c, the situation becomes unstable and the floating object will "turn turtle" and invert itself. [Dr. Alfred Keil, a renown naval architect who is the former Dean of Engineering at MIT and the former Director of the David Taylor Model Basin where the U. S. Navy tests its ship designs, once remarked: "Naval architecture (the science of ship design) is really quite simple and can be reduced to two very fundamental principles. The vessel must be designed so that: (1) it floats and (2) it floats in the upright position." Obviously, Dr. Keil's remark was made with tongue in cheek, but his point is well taken. Before naval architects can deal with any of the many other issues that are of concern to them in ship design, they must first have a vessel that floats in the stable, upright position.]

Naval architects describe these stable and unstable situations of floating symmetric bodies in terms of a characteristic of the vessel design known as the *metacenter*. As shown in Figure 4.10, the metacenter is that point at which the line of action of the buoyancy force intersects the vertical axis of the center of gravity (in this case the axis of symmetry) of the floating object. As long as the metacenter lies above the center of gravity, G, the couple $F_G d$

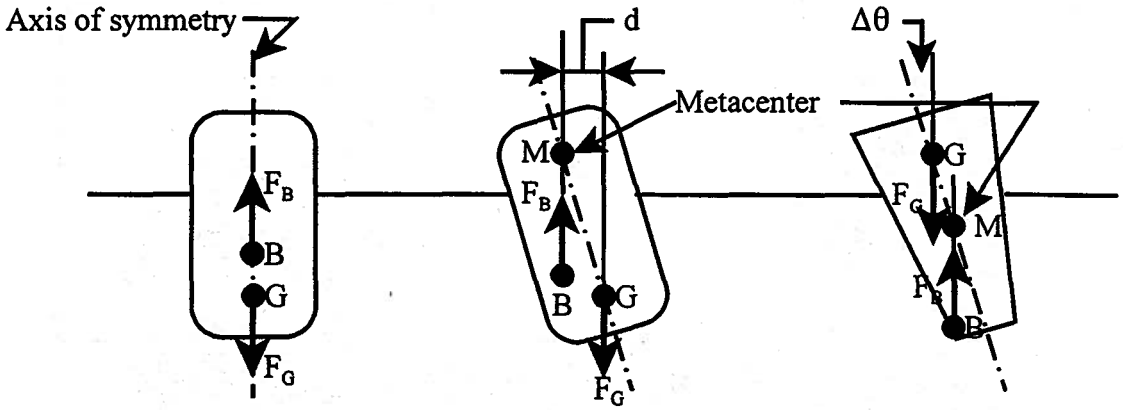

(a) Unperturbed Situation (b) Stable object (c) Unstable object

Figure 4.10 Floating Object in Unperturbed and Perturbed States

(where d is the distance between the lines of action of the two forces) acts to restore the vessel to the unperturbed position and the situation is stable with respect to small angular perturbations of the vertical axis of the center of gravity. However, if the metacenter lies below the center of gravity, the couple $F_G d$ acts to increase further the rotation of the vessel and the vessel will overturn. Note that as the vessel rotates about an axis in the plane of the surface of the fluid, the location of the center of buoyancy shifts about. The difficulty, then, in performing such a stability analysis on a real ship, boat, or other floating structure is finding the location of the center of buoyancy as the floating object moves about. Also note that if the center of buoyancy B lies

above the center of gravity G, the floating object is always stable.

In the case of sailing vessels such as racing yachts, one of the consequences of the action of the wind on the sails which are located at relatively large distances above the waterline of the vessel is to cause the vessel to experience large angular displacements about the roll axis. To insure that the vessel will remain stable and right itself from these large perturbations, it is common practice for yacht designers to place a large mass (ballast) as far below the waterline as practical. This places the center of gravity as low as possible.

Example 4E.8: Glaciers form from fallen snow by a complex series of thermodynamic processes that involve melting, refreezing, refreezing after pressure melting (known as regelation), and compaction. As a consequence of these processes, the density of the snowpack increases from about that of freshly fallen snow ($\rho = 500$ kg/m^3) to approximately 840 kg/m^3. At this point the air trapped between ice crystals is sealed off as bubbles by the refreezing of melted snow and any further increases in density occur by compression of the trapped air bubbles. The maximum density of the ice in the glacier rarely exceeds 900 kg/m^3. Thus the density of glacial ice is slightly less than that of pure ice ($\rho_{ice} = 917$ kg/m^3 at 0 C and 1 atm pressure) but significantly less than that of pure water ($\rho_{water} = 1000$ kg/m^3 at 0 C and 1 atm) and seawater ($\rho_{sw} = 1025$ kg/m^3 at 0 C and 1 atm).

Driven by gravity, these glaciers, particularly those in Greenland, move at speeds of up to 24 m/day. For the glaciers with a small frontal area, the speed of movement is faster than the rate of melting. Upon reaching the edge of the landmass, these small, "fast" glaciers then produce overhanging ledges that eventually break off by a process known as "calving" and fall into the sea as icebergs.

Consider the case of a cubical iceberg of length L on each side. If $\rho_{sw} = 1025$ kg/m^3 and $\rho_{iceberg} = 900$ kg/m^3, determine the dimension h and show that this iceberg is stable for the position shown in Figure 4E.8a.

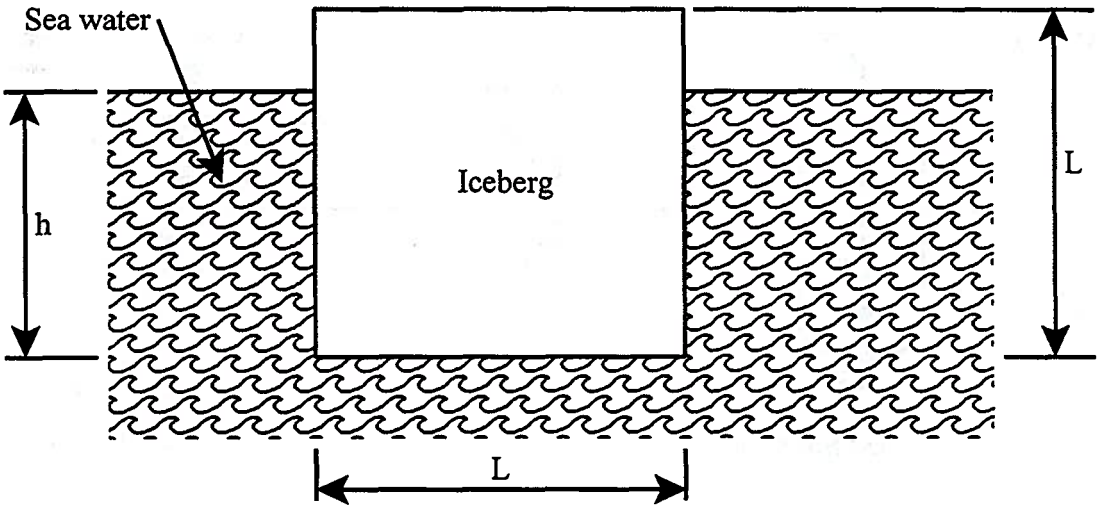

Figure 4E.8a

Solution: The gravity force is given by

$$F_G = \rho_{iceberg} g V_{iceberg} = \rho_{iceberg} g L^3$$

and the buoyancy force is

$$F_B = \rho_{sw} g V_{sw} = \rho_{sw} g h L^2$$

where V_{sw} is the volume of seawater displaced by the floating iceberg. Since the two forces F_B and F_G are equal in magnitude and opposite in sign for a floating object, we can equate them and solve for h. Then

$$h = \frac{\rho_{iceberg} L}{\rho_{sw}} = \frac{(900 \text{ kg/m}^3)L}{1025 \text{ kg/m}^3} = 0.87805L$$

Thus an iceberg floats with about 88 percent or 7/8 of its volume under water. (This is the origin of the expression "just the tip of the iceberg" in reference to a subject that is more involved than might appear on the surface.)

In order to determine whether this is a stable floating position, it is necessary to examine the behavior of the cube when displaced from the vertical position by small angles of rotation θ as shown in Figure 4E.8b. We can do this by calculating the restoring moment due to the couple $F_G d$ as indicated above, or we can determine the position of the metacenter M as shown in Figure 4.10 above. If the distance between M and B is greater than the distance between G and B, the object is floating in a stable position. If the distance MB is less than GB, the object is floating in an unstable position. The new position B' of the center of buoyancy is determined by finding the centroid of the submerged volume $aObBcd$. From the definition of the centroid, the x-coordinate of the location of the centroid, $\bar{x}_{BB'}$, is given by

$$\bar{x}_{BB'} V_{aObBcd} = \int_{V_{AOBcd}} x dV + \int_{V_{OBb}} x dV - \int_{V_{OAa}} x dV = 0 + \int_{V_{OBb}} xLdA - \int_{V_{OAa}} xLdA$$

$$\bar{x}_{BB'} V_{aObBcd} = 0 + \int_{V_{OBb}} xL(x \tan\theta dx) - \int_{V_{OAa}} xL(x \tan\theta dx) = \tan\theta \int_{waterline} x^2 dA_{waterline}$$

$$\bar{x}_{BB'} V_{aObBcd} = I_O \tan\theta$$

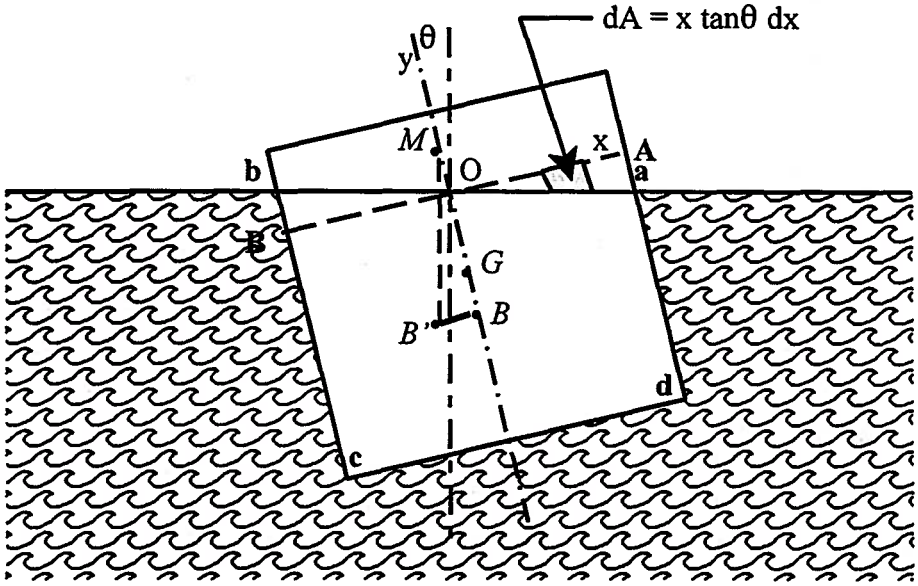

Figure 4E.8b

where the first integral on the right-hand side vanishes because of the symmetry of volume $Abcd$ and I_O is the moment of inertia of the area of the waterline about the axis of rotation O. Notice that in the limit of small angles of rotation θ, this moment of inertia becomes the moment of

inertia of the area of the original waterline. Note also that

$$MB = \frac{\bar{x}_{BB'}}{\tan\theta} = \frac{I_O}{V_{aObBcd}} = \frac{I_O}{V_{submerged}} = MG + GB \tag{4.56}$$

Then

$$MG = \frac{I_O}{V_{submerged}} - GB \tag{4.57}$$

Equation (4.57) is a general result that can be applied to any shape body provided the area at the waterline is well defined. The stability criterion is then

$$MG > 0 \tag{4.58}$$

which is just the condition that the metacenter lie above the center of gravity of the floating object.

For the case of the cubical iceberg, the location of the center of gravity is a distance $L/2$ measured from the bottom of the iceberg. The location of the center of buoyancy is a distance $h/2$ also measured from the bottom of the iceberg, but since $h = 0.87805\,L$, we have

$$GB = \frac{L}{2} - \frac{h}{2} = \frac{L}{2}(1 - 0.87805) = 0.061L$$

and

$$\frac{I_O}{V_{submerged}} = \left(\frac{L^4}{12}\right)\left(\frac{1}{L^2 h}\right) = \left(\frac{L^4}{12}\right)\left(\frac{1}{0.87805L^3}\right) = 0.0949L$$

Then the location of the metacenter becomes

$$MG = 0.0949L - 0.061L = 0.034L$$

Since $MG > 0$, this position of the floating iceberg is stable.

4.8 Pressure Distribution in a Fluid in Rigid-Body Motion

In sections 4.4 through 4.6, we concerned ourselves with forces generated in fluids at rest. We now direct our attention to an extension of this situation in which the fluid is moving as a rigid body. As we shall soon see, this situation is of some limited practical importance for fluids confined within the walls of a container provided there is no relative motion between the fluid and the container walls. (The situation in which there is relative motion between the fluid and the container walls is of much greater importance since it gives rise to a work transfer interaction. This situation will be the focus of our attention in Chapter 5.) There are two cases worthy of study: (1) a fluid under constant linear acceleration and (2) a fluid in rigid body rotation.

4.8.1 Fluid Under Constant Linear Acceleration

In section 4.4 we developed an expression, equation (4.18), for the pressure distribution in a fluid that was at rest. Consider the fluid element of Figure 4.5 except that now the fluid is under constant linear acceleration $\vec{a}$. Then from Newton's second law of motion,

$$d\vec{F}_{net} = d\vec{F}_{surface} + d\vec{F}_{body} = \vec{a}\,dm \tag{4.59}$$

Substituting equations (4.15), (4.16), and (4.17) into equation (4.59), we obtain

$$\begin{aligned} &(-\vec{i}\frac{\partial P}{\partial x} - \vec{j}\frac{\partial P}{\partial y} - \vec{k}\frac{\partial P}{\partial z})dxdydz + \rho\vec{g}dxdydz = \rho\vec{a}dxdydz \\ &-\nabla P + \rho(\vec{g} - \vec{a}) = 0 \end{aligned} \tag{4.60}$$

Then in the x, y, and z directions, respectively, we have

$$\frac{\partial P}{\partial x} = \rho(g_x - a_x)$$
$$\frac{\partial P}{\partial y} = \rho(g_y - a_y) \qquad (4.61)$$
$$\frac{\partial P}{\partial z} = \rho(g_z - a_z)$$

Consider the case of rectangular tank of liquid under constant linear acceleration as shown in Figure 4.10. The tank is aligned so that the z-axis is vertical and the acceleration has components a_x and a_z in the x- and z-directions, respectively. Also, the acceleration of gravity is in the negative z-direction. If we consider a fluid particle at the free surface of the liquid, the net acceleration experienced by the particle is the vector sum of a and g (noting, of course, that g is

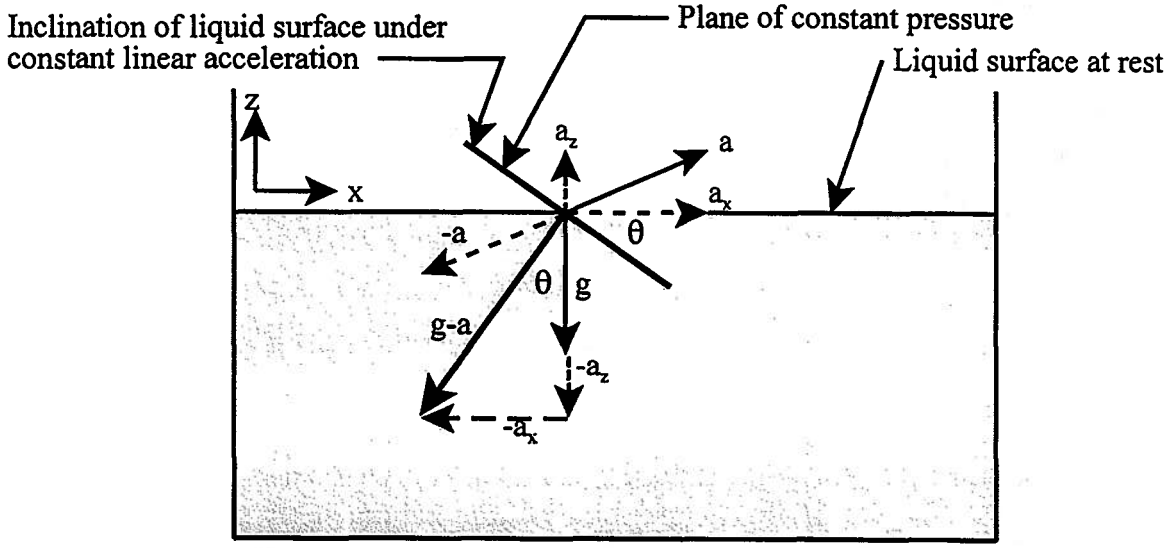

Figure 4.11 Tank of Liquid Under Constant Linear Acceleration

in the negative z-direction. This net acceleration is inclined at an angle θ with respect to the vertical direction where

$$\theta = \tan^{-1}\frac{-a_x}{g_z - a_z} = \tan^{-1}\frac{-a_x}{-g - a_z} = \tan^{-1}\frac{a_x}{g + a_z} \qquad (4.62)$$

From equation (4.60), it is apparent that the planes of constant pressure, defined by $\nabla P = 0$, lie perpendicular to the net acceleration vector and are thus inclined at an angle θ to the original position of the free surface. Since the free surface is itself a plane of constant pressure, it, too, must be inclined at this same angle. Notice that these results are independent of the shape of the container as long as the liquid volume is continuous.

Example 4E.9: In a soda fountain, a stein of root beer is slid along a counter top from one patron to another at constant linear acceleration. The dimensions of the stein are $D = 7.5$ cm and $L = 15$ cm tall. If the level of the free surface of the root beer before the stein is set in motion is 10 cm from the bottom of the stein, what is the maximum permissible acceleration without spilling the root beer. Calculate the maximum gage pressure due to the liquid in the stein.

Solution: As shown in Figure 4E.9, the maximum allowed height of the liquid is 15 cm.

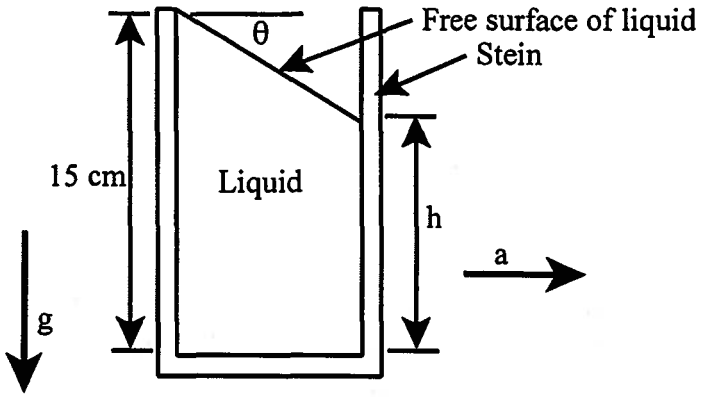

Figure 4E.9

The volume of liquid in the stein at the outset is

$$V = \frac{\pi D^2}{4} L = \frac{\pi (0.075 \text{ m})^2}{4} (0.1 \text{ m}) = 4.418 \text{ x } 10^{-4} \text{ m}^3$$

The volume of liquid under acceleration remains the same, but the dimensions of the volume have changed due to the displacement of the free surface. Then

$$V = \frac{\pi D^2}{4} h + \frac{\pi D^2}{4(2)} (15 - h) = \frac{\pi (0.075 \text{ m})^2}{4} h + \frac{\pi (0.075 \text{ m})^2}{4(2)} (0.15 \text{ m} - h) = 4.418 \text{ x } 10^{-4} \text{ m}^3$$

Solving for h gives $h = 5$ cm. Then

$$\theta = \tan^{-1}\left(\frac{10}{7.5}\right) = 53.13°$$

Since the acceleration due to the motion of the stein is entirely in the x-direction,

$$a_x = g \tan\theta = (9.81 \text{ m/sec}^2) \tan 53.13° = (9.81 \text{ m/sec}^2)(1.33) = 13.08 \text{ m/sec}^2$$

This is a pretty "healthy" acceleration, and the catcher should exercise some caution when stopping the stein in order to receive the maximum amount of the beverage in drinkable form. The maximum gage pressure in the stein can be found in the corner of the stein where the height of the liquid is 0.15 m. The pressure is given by

$$P - P_{atm} = \rho g H = (10^3 \text{ kg/m}^3)(9.81 \text{ m/sec}^2)(0.15 \text{ m}) = 1.4715 \text{ x } 10^3 \text{ N/m}^2$$

Notice that in determining this result, we used the vertical height of the liquid and the vertical component of the acceleration. As an alternate method of calculation, we could have used the total acceleration and the height of the liquid column above the corner but measured normal to the free surface of the liquid since the planes of constant pressure are parallel to the free surface under acceleration. From Figure 4.11, the total acceleration is given by

$$a_{total} = \frac{g}{\cos\theta} = \frac{9.81 \text{ m/sec}^2}{\cos 53.13°} = 16.35 \text{ m/sec}^2$$

The normal distance to the free surface is

$$H_{normal} = (0.15 \text{ m}) \cos 53.13° = 0.090 \text{ m}$$

Then the gage pressure in the corner is

$$P - P_{atm} = \rho a_{total} H_{normal} = (10^3 \text{ kg/m}^3)(16.35 \text{ m/sec}^2)(0.090 \text{ m}) = 1.4715 \text{ x } 10^3 \text{ N/m}^2$$

which is precisely the same result as before.

4.8.2 Fluid in Rigid-Body Rotation at Constant Angular Velocity

Consider the case of a cylindrical container of radius R filled with a liquid to a height h_0. The container is set into motion at a constant angular velocity ω as shown in Figure 4.12.

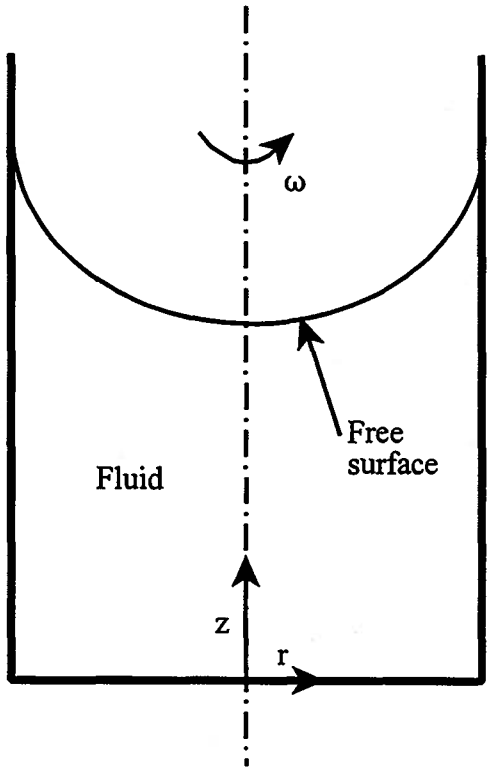

Figure 4.12 Cylindrical Container of Fluid in Rotation About Its Centerline

Through the action of viscosity, the fluid adjacent to the vertical wall and the horizontal bottom is set into motion. This fluid drags along with it adjacent layers of fluid. With the passage of time, the amount of fluid involved in this rotational motion gradually increases until eventually all of the fluid is in rotation with the container and the fluid and container rotate with a uniform angular velocity ω as though they were a single solid body.

Because of the cylindrical geometry of this situation, it is most easily studied in cylindrical coordinates (r, θ, and z) representing the radial, tangential, and axial directions, respectively. In the steady state, the tangential velocity ϑ_θ of a fluid particle at location r is given by $\vartheta_\theta = r\omega$ while the velocities in the radial and axial directions are zero. The acceleration in the tangential and axial directions are also zero, but the acceleration in the radial direction is a_r where $a_r = -r\omega^2$. For this situation, equation (4.60) still holds, but in cylindrical coordinates, the gradient operator becomes

$$\nabla = \vec{i}_r \frac{\partial}{\partial r} + \vec{i}_\theta \frac{1}{r}\frac{\partial}{\partial \theta} + \vec{i}_z \frac{\partial}{\partial z} \tag{4.63}$$

where $\vec{i}_r$, $\vec{i}_\theta$, $\vec{i}_z$ are the unit vectors in the r, θ, and z directions, respectively. Since $g_r = g_\theta = 0$ and $g_z = -g$, equation (4.60) becomes

$$-\left(\vec{i}_r\frac{\partial P}{\partial r}+\vec{i}_\theta\frac{1}{r}\frac{\partial P}{\partial \theta}+\vec{i}_z\frac{\partial P}{\partial z}\right)-\vec{i}_z\rho g=\vec{i}_r\rho\omega^2 r \tag{4.64}$$

Then the component equations become

$$\begin{aligned}\frac{\partial P}{\partial r}&=\rho\omega^2 r\\ \frac{\partial P}{\partial \theta}&=0\\ \frac{\partial P}{\partial z}&=-\rho g\end{aligned} \tag{4.65}$$

From equations (4.65), it follows that $P = P(r, z)$ and the variation of P is

$$\begin{aligned}dP&=\frac{\partial P}{\partial r}dr+\frac{\partial P}{\partial z}dz\\ dP&=\rho\omega^2 r\,dr-\rho g dz\end{aligned} \tag{4.66}$$

Equation (4.66) can now be integrated to find the relationship in the pressure between any two arbitrary points (r, z) and (r_1, z_1). Then

$$\int_{P_1}^{P}dP=\int_{r_1}^{r}\rho\omega^2 r\,dr-\int_{z_1}^{z}\rho g dz$$

$$P-P_1=\frac{\rho\omega^2}{2}\left(r^2-r_1^2\right)-\rho g\left(z-z_1\right) \tag{4.67}$$

If we take the point at the free surface on the centerline of rotation as the reference point, where

$$\begin{aligned}P_1&=P_{atm}\\ r_1&=0\\ z_1&=h_1\end{aligned} \tag{4.68}$$

Then equation (4.67) becomes

$$P-P_{atm}=\frac{\rho\omega^2 r^2}{2}-\rho g(z-h_1) \tag{4.69}$$

We note that the pressure everywhere on the free surface is P_{atm}. Then the left-hand side of equation (4.69) becomes zero and the right-hand side reduces to an expression describing the free surface itself.

$$z=h_1+\frac{r^2\omega^2}{2g} \tag{4.70}$$

Thus, under rigid-body rotation, the free surface of the liquid assumes the shape of a paraboloid of revolution with the vertex on the free surface at the center of rotation.

To determine the height of the liquid at the vertex, we make use of the fact that the volume of the liquid is unchanged by the rotation. The original volume of the liquid is given by

$$V=\pi R^2 h_0 \tag{4.71}$$

For the fluid in rigid body rotation, the volume is given by

$$V=\int_0^R\int_0^z 2\pi r dr dz=\int_0^R 2\pi r z dr=\int_0^R 2\pi r\left(h_1+\frac{r^2\omega^2}{2g}\right)dr$$

$$V = \pi\left(h_1 R^2 + \frac{R^4\omega^2}{4g}\right) \tag{4.72}$$

Combining equations (4.71) and (4.72), we can determine h_1.

$$h_1 = h_0 - \frac{R^2\omega^2}{4g} \tag{4.73}$$

Substituting equation (4.73) into (4.70), we get the equation of the free surface.

$$z = h_0 - \frac{R^2\omega^2}{2g}\left(\frac{1}{2} - \frac{r^2}{R^2}\right) \tag{4.74}$$

Example 4E.10: Consider a cylindrical container of liquid in rigid-body rotation. Initially the container is filled with liquid to a level h_0 measured from the bottom of the container. Determine the angular velocity ω_{max} for which the bottom of the container is just exposed as the free surface is depressed under constant angular rotation. How high must the sides of the container be in order for all of the liquid to remain in the container at this angular velocity?

Solution: From equation (4.73) it is apparent that h_1 will be zero if the following condition is met:

$$h_0 = \frac{R^2\omega^2}{4g}$$

$$\omega_{max} = \frac{2\sqrt{gh_0}}{R}$$

Substituting this result into equation (4.74), we find

$$z_{max} = h_0 - \frac{4gh_0}{R^2}\frac{R^2}{2g}\left(\frac{1}{2} - \frac{R^2}{R^2}\right) = h_0 - 2h_0\left(-\frac{1}{2}\right)$$

$$z_{max} = 2h_0$$

Thus, in order for all the liquid to remain in the container at maximum angular velocity, the container can be no more than half full.

Problems

4.1 As shown in Figure 4P.1, one kg of helium gas is constrained in a piston-cylinder apparatus between two frictionless, massless pistons with identical areas, $A_P = 0.5$ m^2. One piston is connected to a mechanical matching element (MME) that maintains the gas in mechanical equilibrium for all positions of the piston and the other is connected to a pure translational spring. The gas is in thermal communication with a pure thermal system, $C = 4000$ J/K, through the cylinder wall. In state 1, the temperature of the gas is $T_1 = 300$ K and the volume is $V_1 = 1$ m^3. The mechanical matching element SLOWLY displaces piston A to the right until the volume of the gas is reduced to 0.333 m^3 in state 2. Throughout this process, the gas and the pure thermal system remain in thermal equilibrium. The helium can be modeled as an ideal gas.

(a) What is the temperature of the gas in state 2? Does your answer depend upon the spring constant? ($k = 5.7 \times 10^6$ N/m)

(b) How many meters is the spring compressed from its zero force position (free length) in state 1? How many meters is it compressed from its zero force position in state 2?

(c) What is the work transfer experienced by the mechanical matching element during the process 1→2?

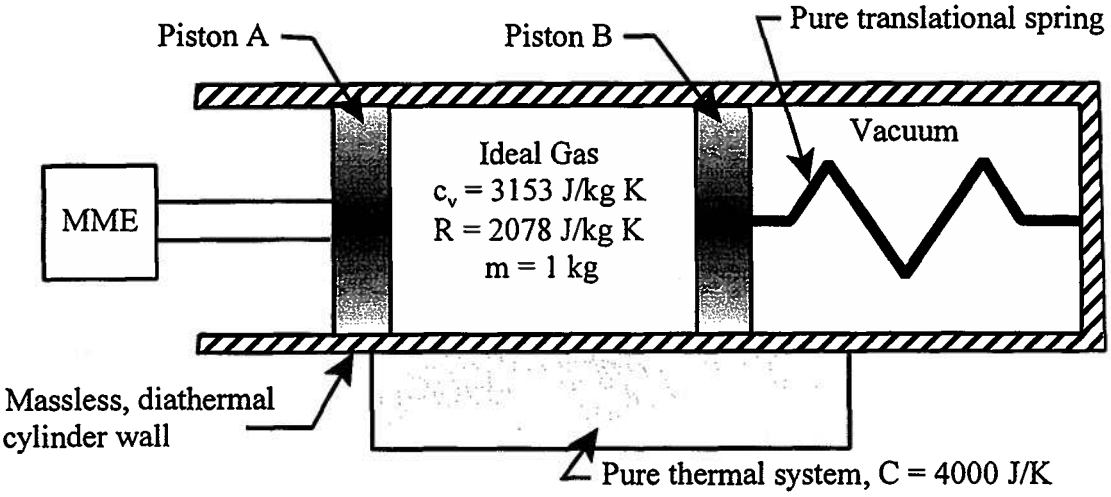

For the gas: state 1: $T_1 = 300$ K, $V_1 = 1$ m^3
state 2: $T_2 = ?$, $V_2 = 0.333$ m^3

Figure 4P.1

4.2 The typical student shower is approximately 20 minutes in duration. Assume that the shower head in the typical dorm bathroom delivers hot water at the Department of Energy approved rate of 2 gal/min. Assume that the water enters the hot water heater at the temperature of 20 C and that the typical hot water heater delivers water at a temperature of 60 C. Assume that the water temperature for a typical shower is 43 C.

(a) Model the water as an incompressible fluid and estimate the amount of energy required to heat the hot water.

(b) Estimate the amount of natural gas required for this heating process if the heating value of natural gas is 37.2 MJ/m^3.

(c) Estimate the amount of entropy generated in the mixing of the hot and cold water streams in order to produce the shower water.

4.3 A balloon (modeled as a massless hollow sphere) with a volume of 1 m^3 contains helium at a pressure of 1.2 x 10^5 N/m^2 and a temperature of 300 K. The conditions of the atmosphere are: $P_{atm} = 10^5$ N/m^2, $T_{atm} = 300$ K. A tank of mass 10 kg contains 1 m^3 of water ($\rho_w = 10^3$ kg/m^3). The tank containing the water rests on a scale that is being used to determine the weight of the tank and its contents. Calculate the reading on the scale in Newtons for each of the three following conditions:

(a) The balloon is attached to the tank by means of a string and floats freely in the atmosphere.

(b) The balloon is attached to the tank by means of a string tied to the bottom of the tank and is completely submerged in the water.

(c) The balloon is held completely submerged under the surface of the water by means of a force mechanism attached to the ceiling above the scale.

4.4 A pump slowly introduces mercury into the bottom of the closed cylindrical tank ($D = 30$ cm) shown in Figure 4P.4. In the initial state shown, the absolute pressure of the air is $(P_{air})_1 = 80$ x 10^3 N/m^2. The mercury is introduced **slowly** enough so that the air is compressed isothermally with no entropy generation until the pump stops when the air pressure reaches $(P_{air})_2 = 1.20$ x 10^5 N/m^2. All fluids remain at the temperature of the atmosphere $T_{atm} = 20$ C. The volume of all tubing can be considered negligible compared to the volume of the tank.

The air can be modeled as an ideal gas with $R = 287$ J/kg K and $c_v = 716$ J/kg K. The mercury and the water can be modeled as incompressible fluids with $\rho_{Hg} = 13609$ kg/m^3 and $\rho_{water} = 998.21$ kg/m^3.

(a) Determine the value of h (in cm) if the atmospheric pressure is $P_{atm} = 10^5$ N/m^2.

(b) For the air as a system, determine the change in stored internal energy, $U_2 - U_1$, and the change in stored entropy, $S_2 - S_1$.

(c) For the air as a system, determine the work transfer, $W_{1\text{-}2}$, and the heat transfer, $Q_{1\text{-}2}$.

(d) For the air as a system, determine the entropy transfer, $S_{transfer}$.

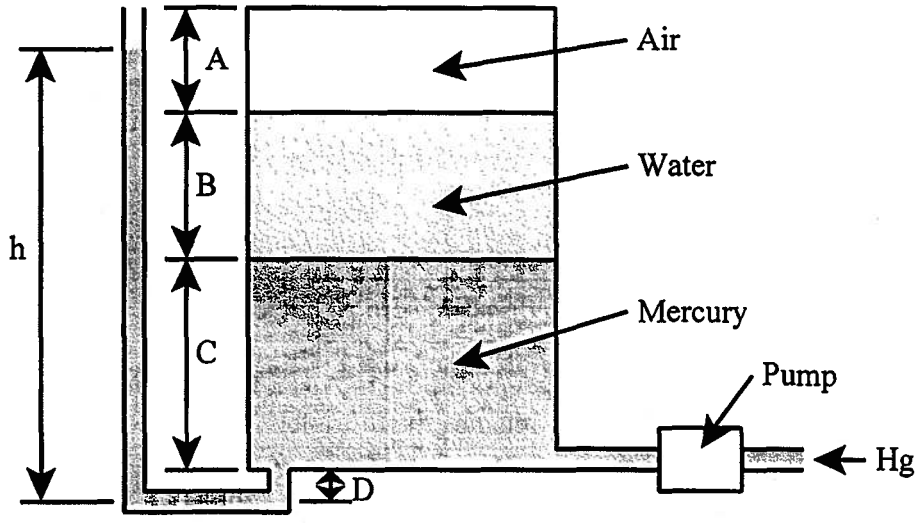

A = 8 cm B = 9 cm C = 10 cm D = 2 cm

Figure 4P.4

4.5 As shown in Figure 4P.5, the piston of a piston-cylinder apparatus contains air and is fitted with a set of weights such that a pressure of $P_{air} = 1 \times 10^5$ N/m^2 is required to maintain the piston in mechanical equilibrium. In the initial state ($P_1 = 2 \times 10^5$ N/m^2, $T_1 = 300$ K, and $V_1 = 1$ m^3), the air, which can be modeled as an ideal gas, is in thermal equilibrium with a heat reservoir at $T_{HR} =$ 300 K. The piston is held in mechanical equilibrium by means of a pin. The pin is removed, and the air, the piston, and the heat reservoir seek a new equilibrium state.

(a) For the air as a system, calculate the following: V_2, T_2, P_2, $U_2 - U_1$, $Q_{1\text{-}2}$, $W_{1\text{-}2}$, $S_2 - S_1$, $S_{transfer}$, and S_{gen}.

(b) Was the process experienced by the air reversible? Why or why not?

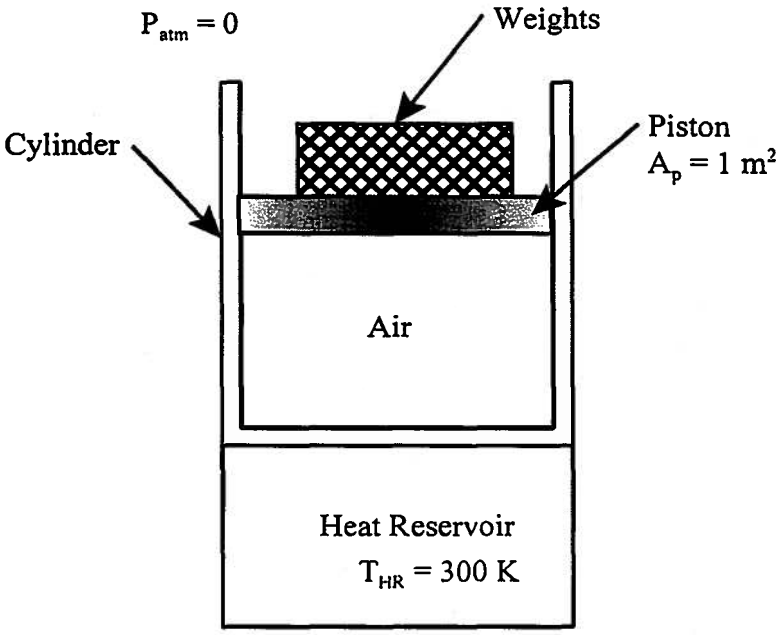

Figure 4P.5

4.6 As shown in Figure 4P.6, a piston-cylinder apparatus is divided into two separate compartments of equal volume, $V = 1$ m^3, by means of a thin rigid membrane. One compartment contains air, $P_1 = 10^5$ N/m^2 and $T_1 = 300$ K, while the other is evacuated. The adiabatic piston is loaded with a mass such that a pressure of 10^5 N/m^2 is required to support it in mechanical equilibrium. In the initial state, a pin holds the piston in a fixed position.

(a) The membrane ruptures and the air expands to fill the entire volume of the cylinder. The air is allowed to come to equilibrium in state 2. Model the air as an ideal gas and calculate P_2 and T_2.

(b) The pin is now removed and the piston is free to move. After some time the air and the piston reach a new equilibrium state 3. Calculate V_3 and T_3.

(c) For the air as a system, calculate the interactions for the various changes of state.

(d) For the air as a system, calculate the entropy transfer for the two processes, 1 → 2 and 2 → 3. Calculate the change of entropy of the air for these two processes. From these data, what conclusions can be drawn regarding their reversibility?

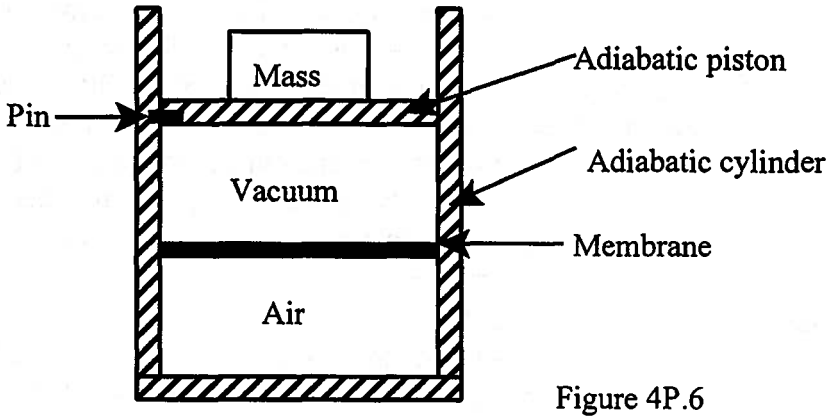

Figure 4P.6

4.7 As shown in the Figure 4P.7, a glass tube is formed in the shape of the letter U. One end of the tube is sealed and contains air. The other end is open to the atmosphere and is filled with mercury. The cross-sectional area of the tube is 1 cm^2. The air trapped in the sealed end is in thermal communication with the environment at a temperature of T_{atm}. The tube is placed outdoors on a hot summer day and allowed to reach the equilibrium state shown in the sketch. The tube is then brought indoors and allowed to reach a new equilibrium state with the air inside the room at $T_{atm} = 300$ K, $P_{atm} = 10^5$ N/m^2. The air can be modeled as an ideal gas.

(a) For the new equilibrium state, calculate the difference in height of the mercury in the two legs of the tube. The density of mercury is $\rho_{Hg} = 13.6 \times 10^3$ kg/m^3.

(b) Calculate the change in entropy of the air for this change of state.

(c) The run down to equilibrium process ultimately results in a heat transfer to the air inside the room which does not change temperature because it is so large compared to the U-tube. Use this information to calculate the entropy generated during the equilibration process.

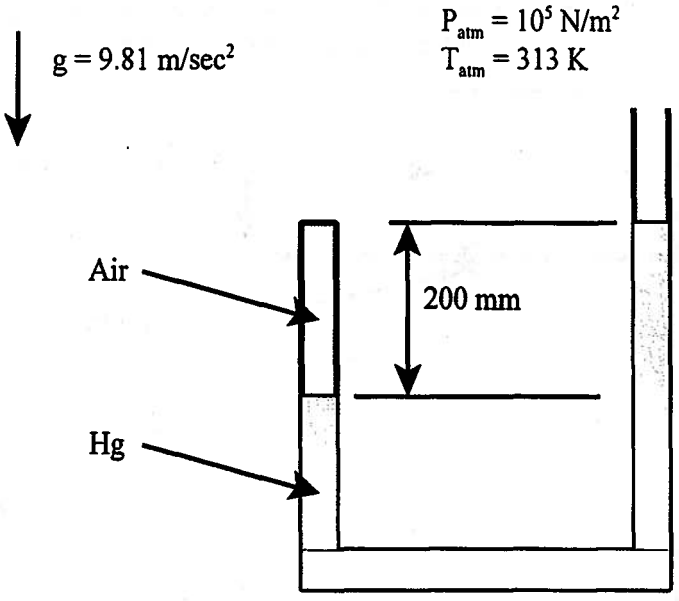

Figure 4P.7

4.8 Thermodynamically, the atmosphere is a complex system. There exists a model of the atmosphere called the U.S. Standard Atmosphere that was developed for the purpose of evaluating the necessary thermodynamic information for the design of satellites, spacecraft, and aircraft. In this model the conditions at sea level are $P_0 = 1.0133 \times 10^5$ N/m^2 and $T_0 = 15$ C. The lowest layer of this atmosphere is called the troposphere and ranges from sea level to an altitude of 11 km, the altitude at which commercial aircraft fly. In the troposphere, the thermodynamic temperature is found to vary linearly with the altitude according to the relation

$$T = T_0 - Bz$$

where z is the altitude and B is the lapse rate, $B = 0.00650$ K/m.

(a) Derive an expression for the pressure of the atmosphere as a function altitude.

(b) Calculate the temperature and pressure of the atmosphere at an altitude of 11 km

(c) A simpler model of the atmosphere assumes that the atmosphere is *isothermal*, that is has a fixed uniform temperature. Derive an expression for the pressure as a function of altitude for this model. How do the two models compare?

4.9 Two identical adiabatic vessels are located one above the other with the upper one 10 m above the lower one. The upper vessel contains 1 m^3 of mercury at a temperature of 300 K and is fitted with a plug in its bottom. At some instant of time the plug is removed and the upper vessel empties into the lower one. After some period of time, the mercury comes to equilibrium. No mercury is spilled in the process which takes place in a vacuum.

(a) Describe a thermodynamic model that will allow you to determine the new equilibrium state for the mercury.

(b) Specify the new equilibrium state for the mercury.

(c) Calculate the work transfer $W_{1\text{-}2}$ and heat transfer $Q_{1\text{-}2}$ for the mercury.

(d) Calculate the change in entropy $S_2 - S_1$ for the mercury.

(e) Calculate the entropy transfer $S_{transfer}$ for the mercury.

(f) Show by proper thermodynamic arguments whether the process of draining the mercury from the upper vessel into the lower vessel was reversible or irreversible.

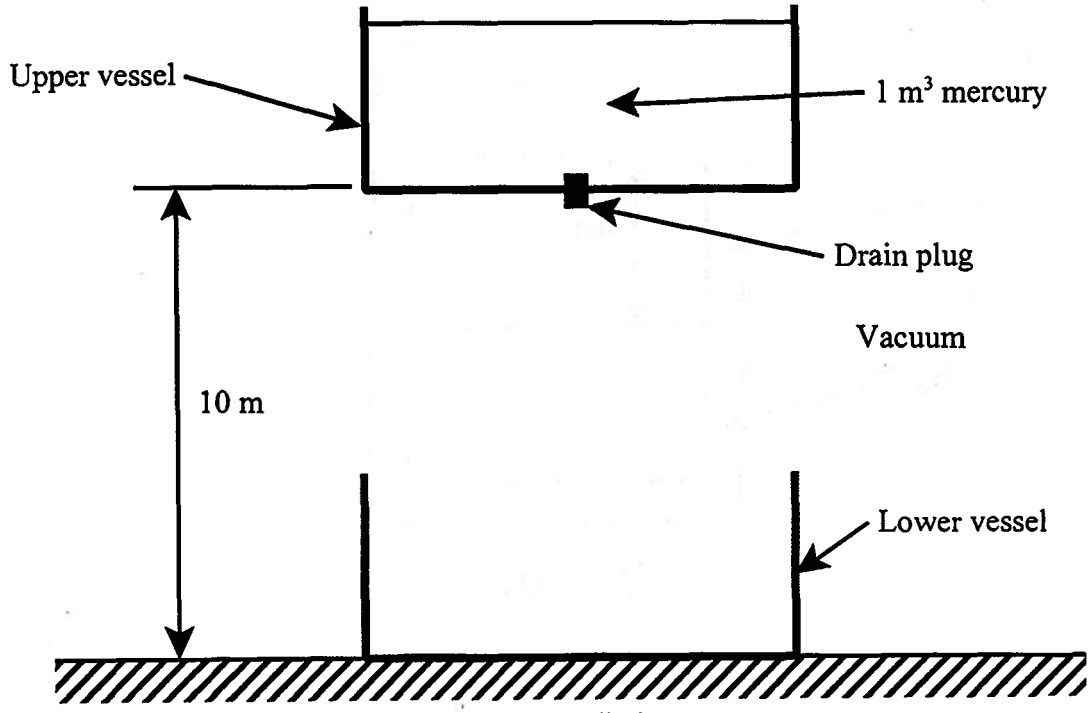

Figure 4P.9

4.10 As shown in Figure 4P.10, a manometer tube is closed at one end and contains mercury. Air is trapped between the closed end and the mercury. The air can be modeled as an ideal gas in thermal equilibrium with the environment at a temperature of 300 K. The manometer tube is of circular cross-section with an area of 1 cm^2. An additional amount ($\Delta V = 6$ cm^3) of liquid mercury is **slowly** added to the open end of the manometer, and the manometer seeks a new equilibrium position with the gas.

(a) Specify L_2 and h_2.

(b) Specify the new equilibrium state of the gas in terms of P_2 and T_2.

(c) Calculate the change in energy $U_2 - U_1$ of the gas.

(d) Calculate the change in entropy $S_2 - S_1$ of the gas.

(e) Calculate the entropy transfer $S_{transfer}$ for the gas.

(f) Show by proper thermodynamic arguments whether the process of adding the mercury was reversible or irreversible.

For mercury: $\rho = 13530$ kg/m^3

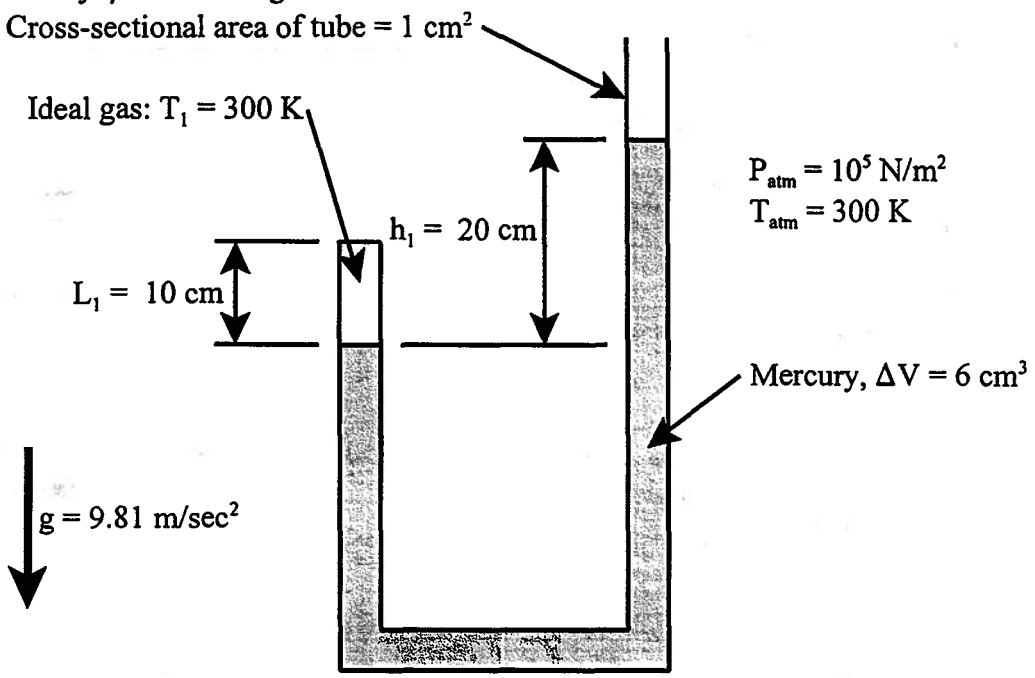

Figure 4P.10

4.11 Consider the high-speed French *Train à Grande Vitesse-Atlantique* (TGV-Atlantique) that operates between Paris and Lyon (*cf.* Example 2E.5). In a high-speed trial of its capability on May 18, 1990, the train was reduced to three cars and two locomotives for a total mass of 2.36 x 10^5 kg (260 tons). The total power capability of the locomotives was upgraded to 11.936 MW (16,000 HP). On a horizontal stretch of track, this train reached a speed of 143.19 m/sec (320.3 mi/hr).

(a) Estimate the force due to air drag and rolling friction acting on this train during the run.

(b) If this force scales with the square of the speed, estimate the power required to operate this train at the normal operating speed of 83.149 m/sec. How does this result compare with the data presented in Example 2E.5 in which the train had four cars and a mass of 4.4 x 10^5 kg? Why are the two power requirements different?

4.12 Consider the iceberg of Example 4E.8. Suppose that instead of a cubical shape, the iceberg formed is a rectangular parallelepiped of height L in the vertical direction, length L normal to the plane of Figure 4P.12, and width W as shown. If the density of seawater is $\rho_{sw} = 1025$ kg/m^3 and the density of the iceberg is $\rho_{iceberg} = 900$ kg/m^3, determine the ratio W/L for which the iceberg becomes unstable and "turns turtle".

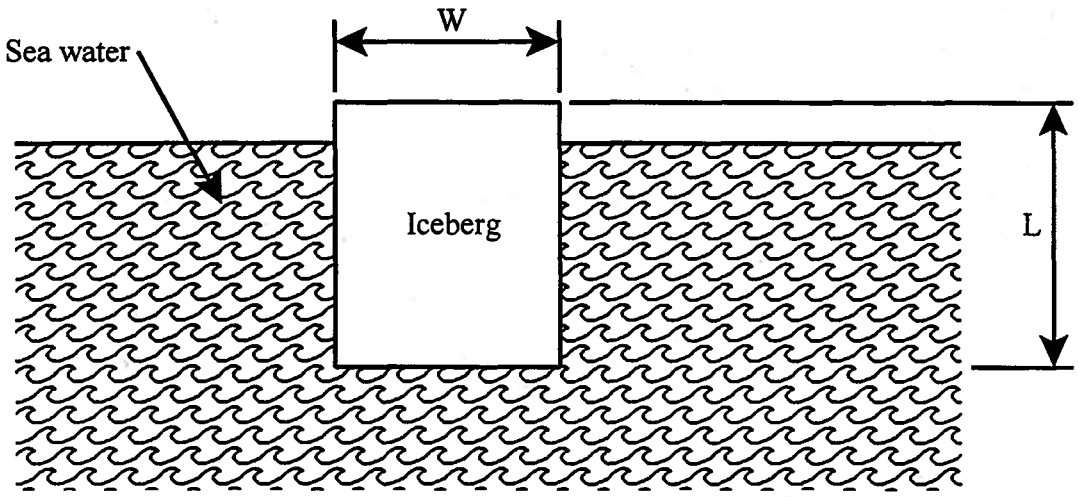

Figure 4P.12

4.13 A spar buoy is a rod-like shape that is used as a marker in a body of water. As shown in Figure 4P.13a, the buoy is weighted to float with its axis vertical and a portion of the rod extending above the free surface of the water. In a particular design, the rod has a diameter of $D = 5$ cm and a length of $L = 3.5$ m. The rod is constructed of wood with a density of $\rho_{wood} = 500$ kg/m^3. A spherical weight of concrete, $\rho_{concrete} = 2306$ kg/m^3, is attached to the end of the rod so that the rod floats with a length of $\ell = 0.5$ m extending above the free surface of the water. The density of the water in which the rod floats is $\rho_{water} = 1000$ kg/m^3.

(a) Determine the mass of concrete necessary for the buoy to float in the attitude shown in Figure 4P.13a.

(b) As a result of a storm, the buoy has drifted and has run aground in the attitude shown in Figure 4P.13b. Determine the angle θ if weighted end of the buoy is at a depth of $d = 2.5$ m there are no moments exerted on the concrete weight.

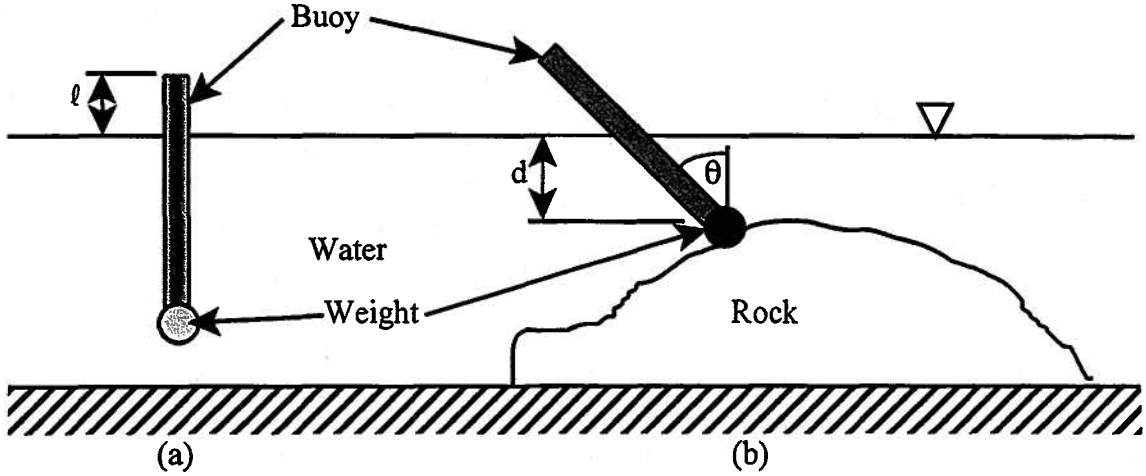

Figure 4P.13

4.14 A solid right circular cone has of height $H = 1$ m and a base of radius of $R = 0.5$ m. The cone, which is constructed of a material with a density of $\rho_{cone} = 900$ kg/m^2 floats in water with a density of $\rho_{water} = 10^3$ kg/m^3.

(a) What is the height h of the cone that is exposed above the waterline?

(b) Does the cone float with the base up or the point up?

4.15 A piston-cylinder apparatus is filled with helium at an initial temperature of $T_1 = 40$ C. As shown in Figure 4P.15, the piston is loaded with weights such that a helium pressure of $P = 5 \times 10^5$ N/m^2 is required to support the weights. The initial volume of the helium is $V_1 = 10$ m^3. The helium is cooled to a temperature of $T_2 = 30$ C by means of a system that operates in an integral number of reversible cycles. The cyclic system uses the atmosphere at a temperature of 35 C as a heat reservoir.

(a) Calculate the heat transfer from the helium to the cyclic system.

(b) Calculate the work transfer experienced by the cyclic system in order to provide the heat transfer of part (a) above.

(c) Calculate the work transfer experienced by the helium inside the cylinder during the cooling process.

(d) Calculate the heat transfer experienced by the atmosphere as a result of the cooling process in the helium.

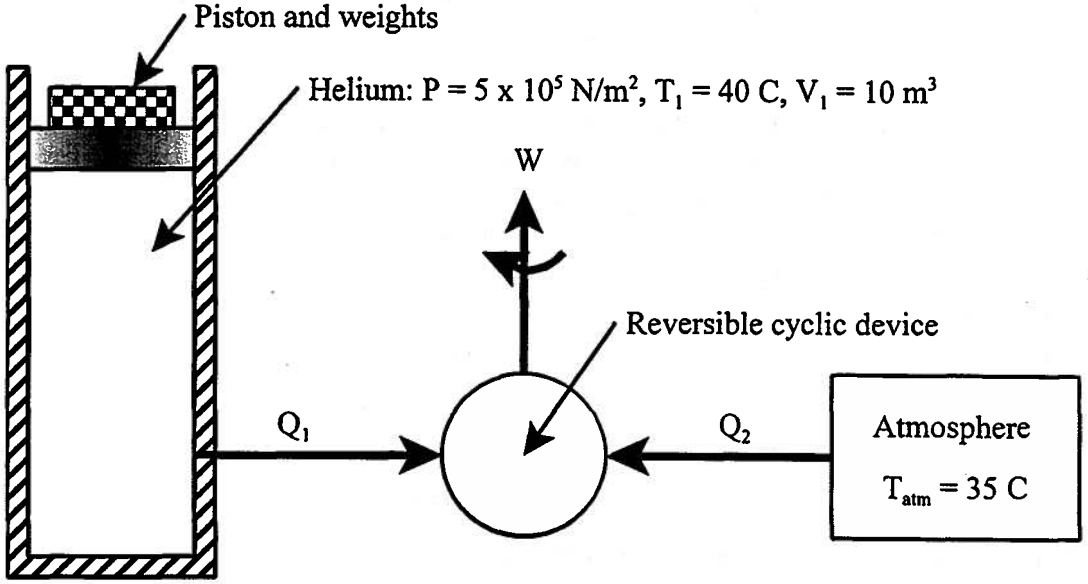

Figure 4P.15

4.16 A group of engineering students has designed a vehicle powered by a new type of engine. As a test of the engine, the students wish to measure the acceleration of the vehicle under various operating conditions. One of the students has constructed an accelerometer from a U-tube manometer as shown in Figure 4P.16. The U-tube is to be filled with mercury and attached to the vehicle.

(a) Show that under constant linear acceleration to the right with $D << L$, the acceleration is proportional to the height h of the mercury above the 0-level. How does the height h depend upon the density of the fluid used?

(b) If $L = 15$ cm, what is the maximum acceleration that can be measured with this device?

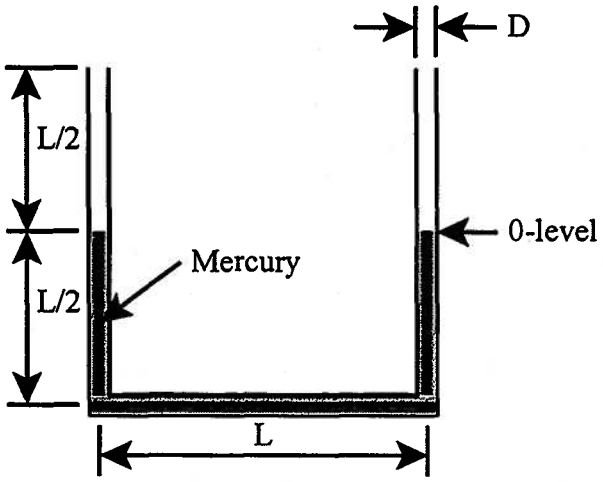

Figure 4P.16

4.17 A manometer identical to that shown in Figure 4P.16 now has the left leg sealed off. Trapped in the volume between the mercury and the sealed end is air at a pressure of $P_1 = 10^5$ N/m^2 and a temperature of $T_1 = 300$ K. The manometer is now set into constant angular rotation with the right leg serving as the axis of rotation. What is the angular velocity necessary so that the trapped air is compressed to half its original volume, $V_2 = 0.5V_1$, when it has reached thermal equilibrium with the environment at $T_{env} = 300$ K?

4.18 As shown in Figure 4P.18, a tank is mounted on wheels and filled with water. The tank is vented to the atmosphere as shown. A balloon filled with helium at a pressure of $P_{He} = 1.3 \times 10^5$ N/m^2 is attached to the bottom of the tank by a string. The diameter of the balloon is $d = 10$ cm. The tank now accelerates to the right with a constant acceleration of $a = 5$ m/sec^2. The density of the water is $\rho_{water} = 1000$ kg/m^3.

(a) Determine the angle of inclination of the balloon.

(b) Does the balloon lean to the left or to the right?

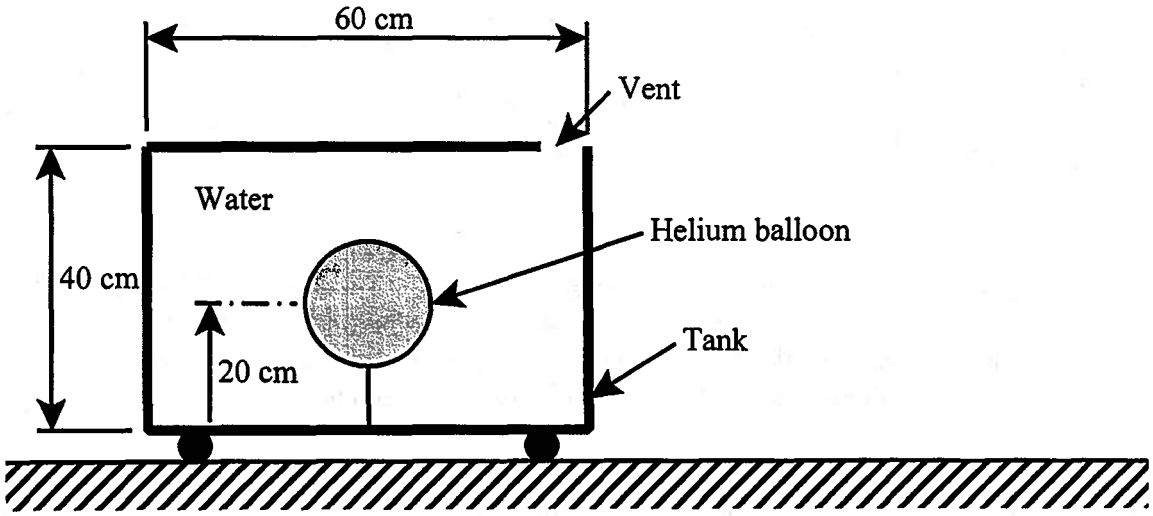

Figure 4P.18

CHAPTER 5

Work Transfer Interactions in Thermal-Fluid Systems

5.1 Forces on Moving Boundaries of Fluid Systems

In applying the first law of thermodynamics to real engineering systems, we have seen that there are two issues that need to be addressed. First, we must have a means to calculate the energy change for the system under study, and second, we must have a means to calculate the energy interactions that caused this change in energy. In the first instance, the models that we have developed for solid and fluid systems commonly encountered in engineering practice serve this end. As shown in Figure 5.1, we have now developed a rather extensive collection of system models. Although many of these models are rather simple in form, they are, nonetheless, valuable in the appropriate circumstances. Once the initial and final equilibrium states of a given process are known, the particular energy constitutive relation for the model at hand can be used to calculate the energy change.

In the second instance, we have formulated an operational definition for the work transfer interaction [cf. equation (2.2)], and for the moment, we have left an operational definition for the heat transfer interaction for future discussion. To apply equation (2.2) for the work transfer, we must determine the force exerted on the boundary of the system of interest. For the models of pure conservative mechanical systems discussed in Chapter 2, the determination of this force is straightforward and is dictated by the force acting at the system boundary which is instantaneously transmitted throughout the entire mass of the model due to both its one-dimensional nature and its rigid (or elastic) character. Thus the boundary force is often referred to as the "through force." The mass of the system and the force on the boundary are then directly interrelated through the property constitutive relations or the laws of motion. However, for the fluid system models introduced in Chapter 4, the situation is not so simple.

Fluids, both liquid and gas, are highly deformable and in some cases even compressible. Their boundaries tend to conform to the shape of the container they occupy, and as a consequence, the movement of a portion of the boundary does not immediately cause all of the mass elements of the fluid to move in response to the applied force. Instead, this motion of the boundary initiates a wave that delineates the volume of the fluid that is moving in response to the boundary motion. This wave then propagates throughout the fluid and becomes the mechanism by which the fluid system adjusts to the new boundary configuration induced by the work transfer. This wave causes the pressure in the fluid to change as the wave is reflected from the other boundaries of the fluid system. Until the wave reaches the undisturbed regions of the fluid, that quiescent fluid has no knowledge of the fact that the boundary of the fluid has been displaced. While the waves are propagating, the pressure in the fluid is not uniform, and it is not possible to identify a single, spatially uniform, equilibrium value for the pressure.

As a consequence, it is not possible in general to relate the boundary force responsible for the work transfer interaction to the pressure of the fluid through consideration of the free-body diagram of the moving boundary. Ideally, this force could be determined from the pressure exerted on the system boundary by the fluid inside the system boundary, but complex wave motion in the fluid due to the movement of the boundary itself may preclude this possibility.

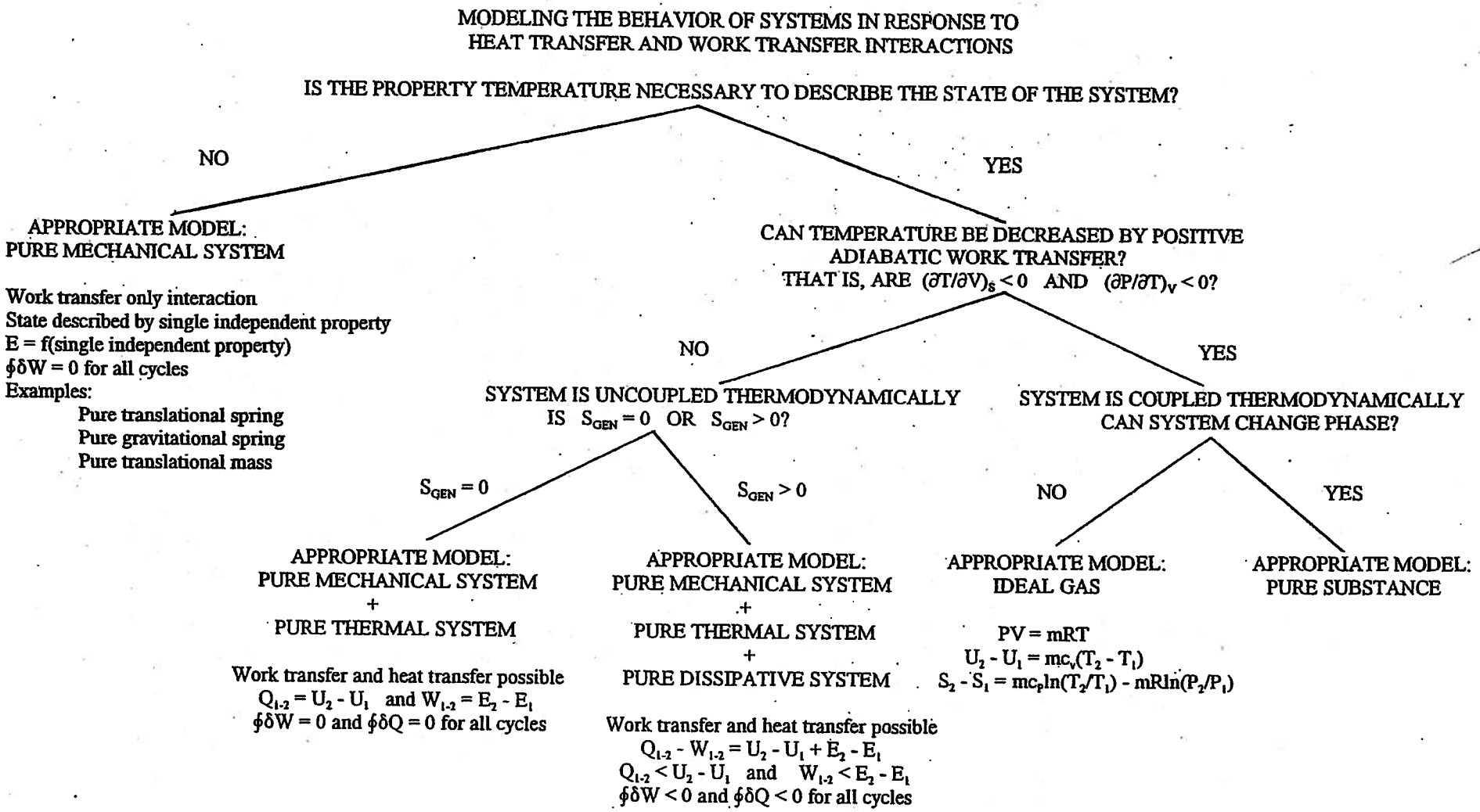

Figure 5.1 Models of Thermodynamic Systems

5.2 Moving Boundaries in a Channel of Liquid

The preceding discussion can best be illustrated by the following example. Figure 5.2 is a schematic representation of an open channel of liquid of width b normal to the plane of the paper. The channel extends a distance L to the right and is bounded on the left by a moveable wall. The wall is acted upon by a mechanism that applies precisely the right amount of force to move the wall to the right at a constant velocity $\Delta\vartheta$. As the wall moves, the fluid immediately in front of it is accelerated to the right. This moving fluid, in turn, pushes the fluid immediately in front of it and so on up the length of the channel until eventually the fluid at the far wall is displaced.

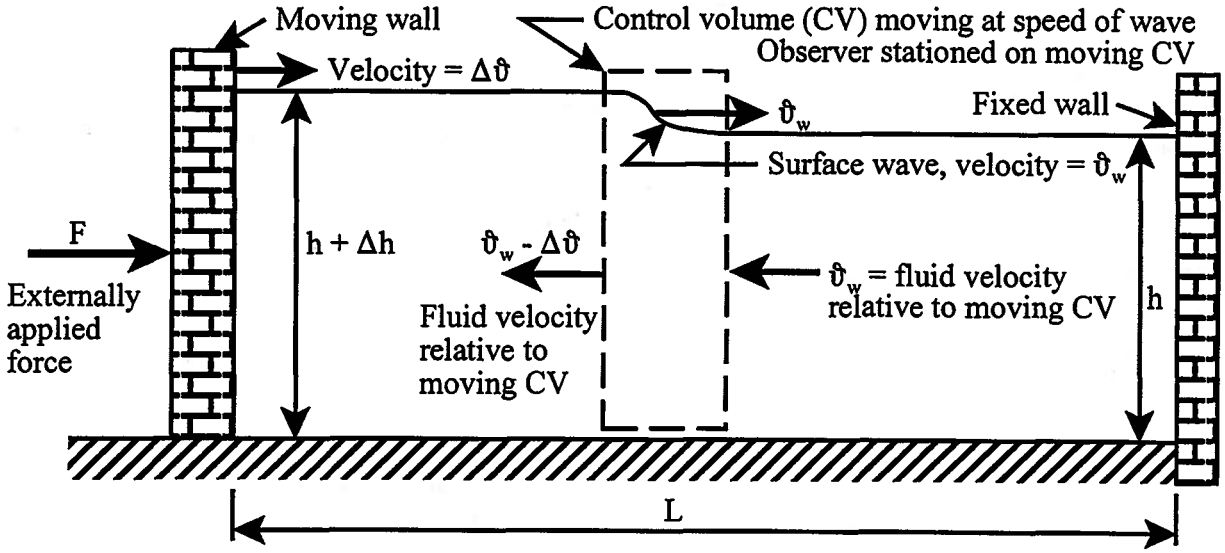

Figure 5.2 Open Channel of Liquid Bounded by Moving Wall on One End

This situation is analogous to the case of a long line of people oriented front to back in much the same manner as an orderly queue outside a theater. At some point in time, the last person in the line, in anticipation of the opening of the doors of the theater, decides to move forward by pushing the person in front of him who in turn pushes the person in front of her. While this is going on in the rear of the line, the person at the front of the line is completely unaware that there is any disturbance. In time, the disturbance propagates to the front of the line and the first person in line is pushed forward. The propagating disturbance is called a wave. Notice that the wave propagates at some velocity known as the wave velocity which is different from the velocity of movement of the people in the line.

In the open channel of liquid, the wave ahead of the moving wall propagates at the velocity ϑ_w and is manifested as an increase in the depth of the liquid immediately in front of the moving wall. As shown in Figure 5.2, this new depth of the liquid is $h + \Delta h$. In order to determine the velocity of propagation of the wave, we must examine the dynamics of the process. To this end, we make use of an analytical tool known as a *control volume*. In this case, the control volume consists of a rigid volume that surrounds the wave and moves with it at the velocity of the wave as shown in Figure 5.2. Our point of observation of the wave is on this moving control volume, so the wave looks the same to us at all times. This is similar to the vantage point of a surfer riding a wave on a surfboard. Thus, the fluid ahead of the wave appears to be approaching the control volume at the velocity of the wave, ϑ_w, while the fluid behind the

wave appears to be leaving the control volume at the velocity $\vartheta_w - \Delta\vartheta$.

We describe the behavior of the fluid entering and leaving in terms of two fundamental equations based on fundamental physical principles: the *Continuity Equation* and the *Momentum Equation*. The Continuity Equation is based on the principle of *Conservation of Mass* that states that matter can be neither created nor destroyed inside the control volume. Then rate of change of mass inside the control volume must be zero. Since the rate of change of mass inside the control volume is also equal to the difference between the rate at which mass enters the control volume and the rate at which mass leaves the control volume, we have

$$\frac{dm_{CV}}{dt} = \dot{m}_{in} - \dot{m}_{out} = 0 \tag{5.1}$$

But in general

$$\dot{m} = \rho A \vartheta \tag{5.2}$$

where ρ is the density of the fluid and A is the cross-sectional area of the flow path normal to the velocity vector. Then for the moving control volume,

$$\rho(bh)\vartheta_w - \rho[b(h+\Delta h)](\vartheta_w - \Delta\vartheta) = 0 \tag{5.3}$$

Combining terms, we get

$$\vartheta_w h - \vartheta_w h - \vartheta_w \Delta h + h\Delta\vartheta + \Delta\vartheta\Delta h = 0$$

and neglecting terms of second order such as $\Delta\vartheta\Delta h$, we get

$$\frac{\Delta\vartheta}{\vartheta_w} = \frac{\Delta h}{h} \tag{5.4}$$

The Momentum Equation is based on *Newton's Second Law of Motion* as it applies to the control volume. According to Newton's Second Law of Motion, the net force on the control volume is equal to the time rate of change of the momentum. Then

$$\sum \vec{F} = \frac{d}{dt}(m\vec{\vartheta})$$

but for the control volume, there are two contributions to the rate of change of momentum: one due to the difference between the momentum fluxes into and out of the control volume; the other due to the rate at which the momentum changes within the control volume itself. That is,

$$\begin{Bmatrix}\text{net force}\\ \text{on CV}\end{Bmatrix} = \begin{Bmatrix}\text{net flux of}\\ \text{momentum}\\ \text{out of CV}\end{Bmatrix} + \begin{Bmatrix}\text{rate of change}\\ \text{of momentum}\\ \text{stored in CV}\end{Bmatrix} \tag{5.5}$$

For the steadily moving control volume in Figure 5.2, the last term on the right of equation (5.5) vanishes because the flow is steady. Then if F_f is the force on the face of the control volume facing in the direction of travel of the wave and F_b is the force on the face of the control volume facing toward the moving wall, equation (5.5) becomes

$$F_b - F_f = \dot{m}\vartheta_{out} - \dot{m}\vartheta_{in} \tag{5.6}$$

But from Figure 5.2

$$-F_f = (P_{ave}A)_{front} = \left(\rho g\frac{h}{2}\right)(bh) = \left(\rho gb\frac{h^2}{2}\right)$$

$$-F_b = (P_{ave}A)_{back} = \left(\rho g\frac{h+\Delta h}{2}\right)\left[b(h+\Delta h)\right] = \left[\rho gb\frac{(h+\Delta h)^2}{2}\right] \tag{5.7}$$

$$\dot{m} = \rho A\vartheta = \rho(bh)\vartheta_w$$

Then upon substitution of equations (5.7), equation (5.6) becomes

$$\left(\rho g b\frac{h^2}{2}\right)-\left[\rho g b\frac{(h+\Delta h)^2}{2}\right]=\rho(bh)\vartheta_w[(\vartheta_w-\Delta\vartheta)-\vartheta_w]$$

or

$$g\left[\frac{h^2}{2}-\frac{h^2}{2}-h\Delta h-\frac{(\Delta h)^2}{2}\right]=-h\vartheta_w\Delta\vartheta=-\vartheta_w{}^2\Delta h \tag{5.8}$$

If we neglect terms of second order such as $(\Delta h)^2$, equation (5.8) becomes

$$\vartheta_w{}^2=gh$$

or

$$\vartheta_w=\sqrt{gh} \tag{5.9}$$

Thus the velocity of the wave varies as the square root of the depth of the channel in the undisturbed region. The amplitude of the disturbance can be determined by substituting equation (5.4) into equation (5.9). Then

$$\Delta h=\Delta\vartheta\sqrt{\frac{h}{g}} \tag{5.10}$$

Thus the greater the piston velocity, the larger is the amplitude of the disturbance. Also, the greater the depth in the undisturbed region, the larger is the amplitude of the disturbance.

Both of these results are intuitively obvious since the faster the piston moves, the more fluid it displaces in a given time interval. Since the disturbance wave always travels at the same speed regardless of piston velocity [cf. equation (5.9)], the wave will always travel the same distance in a given time interval. Thus for higher piston speeds, the lineal distance between the piston face and the wave front is reduced. Thus to accommodate the increased fluid volume, it is necessary to increase the cross-sectional area, and, hence, the depth of fluid, by increasing the amplitude of the disturbance. Similarly, for greater undisturbed fluid depths, a given piston travel displaces a greater fluid volume than in shallower depths. This increased displacement can be accommodated only by greater amplitude disturbances.

In the physical situation depicted in Figure 5.2, the force on the moving wall is given by

$$-F=P_{ave}A=\left(\frac{\rho g(h+\Delta h)}{2}\right)[b(h+\Delta h)]=\rho g b\frac{(h+\Delta h)^2}{2}=\rho g b\left(\frac{h^2+2h\Delta h+(\Delta h)^2}{2}\right)$$

If we once again neglect terms of second order, such as $(\Delta h)^2$, we have

$$-F=\rho g b\frac{h^2}{2}\left(1+2\frac{\Delta h}{h}\right)=\rho g b\frac{h^2}{2}\left(1+2\frac{\Delta\vartheta}{\vartheta_w}\right)$$

where we have made use of equation (5.4). Then the force on the wall becomes

$$-F=\rho g b\frac{h^2}{2}+\rho g b h^2\frac{\Delta\vartheta}{\vartheta_w} \tag{5.11}$$

In equation (5.11), the first term on the right-hand side represents the *quasi-static* force acting on the moving wall, i.e. the force that the fluid would exert on the wall if the wall were stationary, and the second term on the right-hand side represents the relative dynamic force necessary to accelerate the fluid contained between the moving wall and the wave front.

The fluid adjusts its pressure, i.e. its depth, by means of this wave which propagates ahead of the moving wall into the undisturbed fluid. The wave is then reflected from the far wall

before the moving wall can catch up to it. This reflected wave further increases the depth of the fluid by another amount Δh as it propagates back toward the moving wall. The time of travel, Δt, of the initial wave toward the stationary wall which is a distance L away is given by

$$\Delta t = \frac{L}{\vartheta_w}$$

During this time interval, the moving wall travels a distance ΔL where

$$\Delta L = \Delta\vartheta\Delta t = L\frac{\Delta\vartheta}{\vartheta_w} \tag{5.12}$$

During the time interval required for the wave to travel the length of the channel and be reflected back from the far wall to reach the moving wall once again, the moving wall will have traveled a distance $2\Delta L$ and the depth of the channel will have increased by an amount $2\Delta h$. The fluid volume added by this increased depth is ΔV where

$$\Delta V = 2(\Delta h)L$$

The fluid volume displaced by the movement of the wall is ΔV_D where

$$\Delta V_D = 2(\Delta L)h$$

It should be the case that $\Delta V = \Delta V_D$. Then

$$2(\Delta h)L = 2(\Delta L)h$$

or

$$\frac{\Delta h}{h} = \frac{\Delta L}{L} \tag{5.13}$$

From equation (5.4), the continuity equation, we have

$$\frac{\Delta h}{h} = \frac{\Delta\vartheta}{\vartheta_w} \tag{5.14}$$

But from equation (5.12) we have

$$\frac{\Delta L}{L} = \frac{\Delta\vartheta}{\vartheta_w} \tag{5.15}$$

Combining equations (5.14) and (5.15), we obtain confirmation of equation (5.13). Thus the relative strength of the disturbance, i.e. the wave, depends upon the displacement of the moveable wall relative to the length of the channel. The rate at which the depth of the channel is increasing as a result of this wave is

$$\frac{\Delta h}{\Delta t} = \frac{h\left(\frac{\Delta\vartheta}{\vartheta_w}\right)}{\frac{L}{\vartheta_w}} = h\frac{\Delta\vartheta}{L} \tag{5.16}$$

In the quasi-static limit, the rate at which the depth of the channel changes must be negligible in order for us to use the undisturbed depth to calculate the pressure on the wall. From equation (5.16), it follows that the velocity of the moving wall must also be vanishingly small in this limit.

The purpose of examining the dynamics of wave propagation in the fluid filled channel was to establish the conditions under which we could calculate the work transfer at the moving boundary by means of the quasi-static model. From the results of equations (5.11) and (5.16), we have seen that the quasi-static model is appropriate when the speed of the moving wall is "slow" relative to the wave speed in the fluid. Just how "slow" is slow enough depends upon the error that we are willing to accept in using this model. There is no universal answer that says the speed

of the moving boundary must be a certain percentage of the wave speed. Like most modeling decisions, it is a question of the quality of the information required for the situation at hand. In some cases a value of 50 percent may be sufficient whereas in another situation the appropriate value might be 1 percent. In any case, if the quasi-static model is appropriate, the work transfer in this open channel situation due to the displacement of the fluid in contact with the moving wall is given by equation (2.22)

$$(W_{1-2})_{\substack{quasi-\\static}} = -\int_{x_1}^{x_2} \vec{F} \cdot d\vec{x}$$

However, in the quasi-static model, the force exerted on the boundary by the environment is related to the pressure of the fluid inside the system boundary. Then from equilibrium considerations for the moving wall

$$F = -P_{ave} A$$

and

$$(W_{1-2})_{\substack{quasi-\\static}} = \int_0^{\Delta L} P_{ave} A dx = \int_0^{\Delta L} \rho g \frac{h}{2} (hb) dx = \rho g b \frac{h^2}{2} \Delta L \qquad (5.18)$$

The sign of the work transfer is determined by the sign of ΔL. A displacement that shortens the length of the channel would be negative.

Example 5E.1: A tank that is open to the atmosphere is initially filled with water to a depth $h_1 = 0.5$m with a length $L_1 = 2$ m as shown in Figure 5E.1. The end walls have a breadth $b = 1$ m measured normal to the plane of Figure 5E.1 and atmospheric pressure acts on all surfaces not exposed to water. The left-hand wall of the tank can be moved horizontally to the right. This wall is moved quasi-statically until the length of the channel is decreased to $L_2 = 1$m.

(a) Determine the net force on the left-hand wall as a function of the wall displacement x.

(b) Determine the work transfer, $(W_{1-2})_{wall}$, from the wall to the water.

(c) Determine the change of stored gravitational potential energy of the water $(E_2 - E_1)_{\substack{grav\\water}}$ and relate it to $(W_{1-2})_{wall}$.

(d) Estimate the speed at which the left-hand wall can be moved such that the quasi-static model for the work transfer will predict the value of $(W_{1-2})_{wall}$ within one percent of its true value.

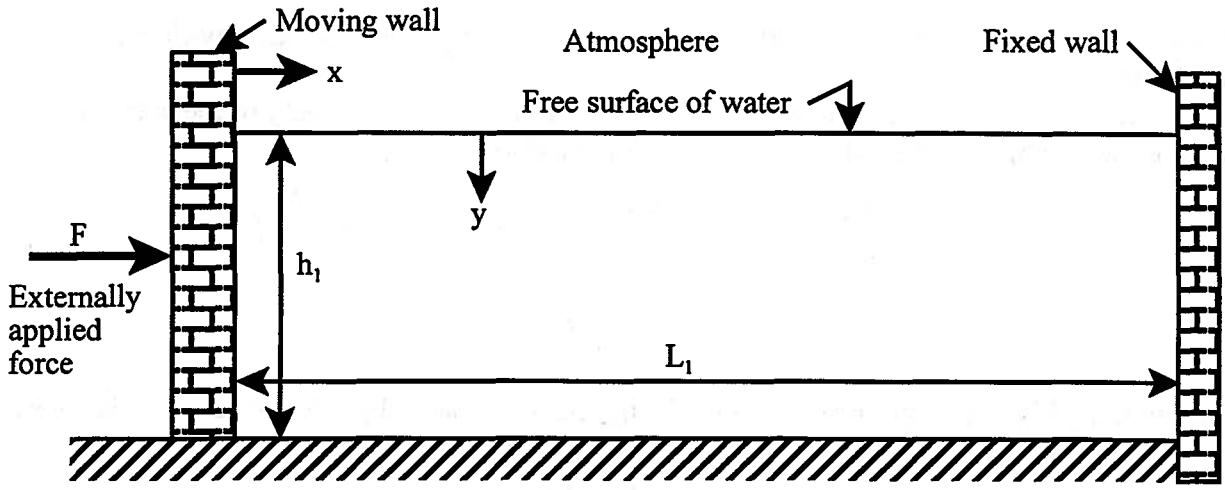

Figure 5E.1 Open Tank of Water Bounded by Moving Wall on One End

Solution: (a) The moveable wall has a force exerted on it that is due to the action of the

atmosphere and the water. Then for the positive x-direction shown, the net force acting on a differential area dA at a depth y is given by

$$dF_{net} = \sum dF_x = P_{atm}dA - (P_{atm} + \rho gy)dA$$

$$dF_{net} = -\rho gydA = -\rho gybdy$$

Then the net force acting over the entire wetted surface of the wall is

$$F_{net} = -\int_0^{-h} \rho gbydy = -\frac{\rho gbh^2}{2}$$

where the negative sign indicates that the force acts in the negative x-direction. In order to express this net force in terms of the displacement x, we can relate the value of h at any time to the value of x by making use of the fact that: (1) the mass of the water trapped between the two walls is constant and (2) the water can be modeled as an incompressible fluid. Then

$$m_{water} = \rho h_1 L_1 b = \rho hLb$$

$$h = \frac{h_1 L_1}{L} = \frac{h_1 L_1}{L_1 - x}$$

Then

$$F_{net} = -\frac{\rho gb}{2}\frac{h_1^2 L_1^2}{(L_1 - x)^2}$$

(b) We note that the wall is displaced from $x_1 = 0$ to $x_2 = L_1 - L_2$. From equation (2.22), we have

$$(W_{1-2})_{wall} = -\int_{x_1}^{x_2} Fdx = -\int_0^{(L_1 - L_2)} \left[-\frac{\rho gb}{2}\frac{h_1^2 L_1^2}{(L_1 - x)^2}\right] dx$$

$$(W_{1-2})_{wall} = \frac{\rho gbh_1^2}{2}\frac{L_1(L_1 - L_2)}{L_2}$$

$$(W_{1-2})_{wall} = \frac{(10^3 \text{ kg/m}^3)(9.81 \text{ m/sec}^2)(1 \text{ m})(0.5 \text{ m})^2}{2}\frac{(2 \text{ m})(2 \text{ m} - 1 \text{ m})}{1 \text{ m}} = 2.4525 \text{ x } 10^3 \text{ J}$$

Note that since the value for the work transfer for the wall is positive, the energy flow is *from* the wall *into* the water.

(c) Consider now the change in stored gravitational potential energy of the water. For this purpose we can model the water as a pure gravitational spring. Then

$$(E_2 - E_1)_{grav\ water} = m_{water}(z_{CM_2} - z_{CM_1}) = \rho gbh_1\left(\frac{h_2}{2} - \frac{h_1}{2}\right)$$

but

$$h_2 = h_1\frac{L_1}{L_2}$$

Substituting this result into the expression for the change of stored gravitational potential energy of the water, we get

$$(E_2 - E_1)_{grav\ water} = \frac{\rho gbh_1^2}{2}\frac{L_1(L_1 - L_2)}{L_2} = (W_{1-2})_{wall}$$

Thus the work transfer from the wall to the water is precisely equal to the increase in stored

gravitational potential energy of the water as would be expected by applying the first law of thermodynamics to the water. It should be noted that there are two other work transfer interactions experienced by the water but these are equal in magnitude and opposite in sign so they "cancel" each other out as far as their effect on the state of the water. One of these interactions is the negative work transfer from the atmosphere to the water at the water-wall interface; the other is the positive work transfer from the water to the wall at the free surface of the water.

(d) To determine the maximum velocity of the wall that would allow us to use the quasi-static model for the work transfer interaction, we note in equation (5.11) that the contribution of the dynamic force acting on the wall is given by the second term on the right-hand side of that expression. The relative importance of the dynamic force will occur when the water is shallowest since the wave speed will be smallest for that condition. Since a one percent error in the work transfer implies a one percent error in the force for a given displacement of the wall, it follows that if the speed of the wall is $\Delta \vartheta$, the maximum wall speed is given by

$$\frac{2\Delta\vartheta}{\vartheta_w} = \frac{2\Delta\vartheta}{\sqrt{gh}} < 0.01$$

$$\Delta\vartheta < \frac{0.01\sqrt{(9.81\ \text{m/sec}^2)(0.5\ \text{m})}}{2} = 0.011\ \text{m/sec}$$

Thus for this particular physical situation, the quasi-static model provides an accurate description of the work transfer for any wall speed less than 0.011 m/sec. Clearly, in general, the validity of the quasi-static model depends upon the size of the system to which it is being applied.

5.3 Moving Boundaries in a Volume of Gas

Because gases are more strongly coupled thermodynamically than liquids, the behavior of a moving boundary in a gas is more significant from a thermodynamic point of view than that of a liquid. In fact, the performance of many engineering systems depends upon the forces acting on moving boundaries in gases -- systems such as gas compressors, the powerplants of all types of vehicles, and aircraft propellers to name a few. The classical embodiment of the moving boundary in a gas is the familiar piston-cylinder apparatus.

Typically, the basic design of these systems consists of a piston fitted inside a cylinder of circular cross-section. The cylinder is closed at the end remote from the piston. By sound engineering design, the interface between the piston and the cylinder can be made leak free and nearly frictionless. As the piston moves, the pressure of the gas is exerted on the face of the piston, and work transfer occurs. When the piston moves into the cylinder to decrease the volume of the gas, the result is a negative work transfer for the gas. On the other hand, when the piston moves out of the cylinder to increase the volume of the gas, the result is a positive work transfer for the gas. In either case, the gas always contracts or expands to keep the cylinder filled with gas at all times. The gas is made aware of the motion of the piston by means of pressure waves analogous to the liquid surface waves described in the section 5.2. These local changes in pressure propagate from the moving piston through the cylinder at a high rate of speed.

In the case of a contracting gas volume, the pressure waves are compressive in nature with elevations in pressure across the waves. That is, the gas in front of the wave is undisturbed, but the gas behind the wave is elevated in pressure and in motion due to the motion of the piston. In the case of an expanding gas volume, the pressure waves are expansive in nature with a

decrease in pressure across the wave. In these rarefaction waves, the gas ahead of the wave is undisturbed, but the gas behind the wave is moving toward the piston at a pressure that is less than the pressure in the undisturbed gas. The gas pressure throughout the cylinder adjusts to accommodate the new volume by means of these high-speed pressure waves as they are reflected back and forth alternately, first by the stationary end of the cylinder and then by the moving piston face. If the piston moves "slowly enough", the adjustment in gas pressure via the pressure waves appears to be infinitely fast, relatively speaking, and on a time scale characteristic of the motion of the piston, the gas appears at all times to have a pressure that is uniform in space but varying in time.

In order to be able to judge whether the piston is moving slowly enough, we need to know the speed of propagation of the pressure waves. To this end, consider the piston-cylinder arrangement shown in Figure 5.3. A long cylinder is fitted with a frictionless piston of

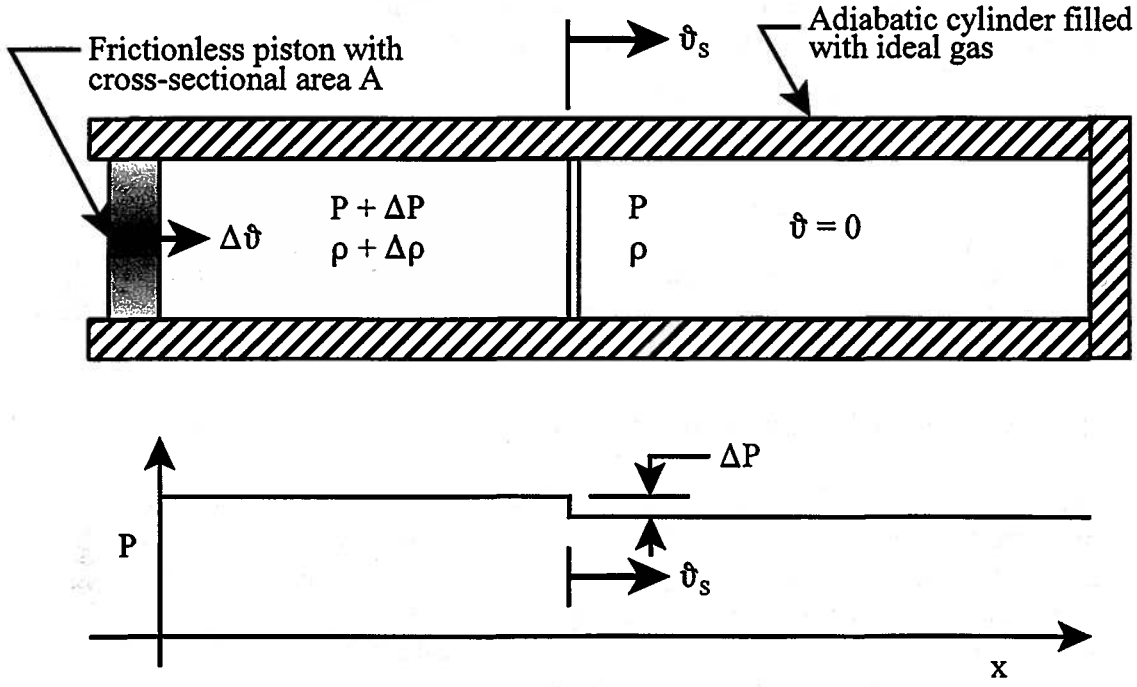

Figure 5.3 Propagation of a Compression Wave in a Gas due to a Moving Boundary

cross-sectional area A and filled with a fluid that can be modeled as an ideal gas. As the piston moves slowly to the right at a constant speed $\Delta\hat{v}$, it causes an infinitesimal disturbance in the form of a compression wave to propagate to the right at a speed of $\hat{v}_s$ where $\hat{v}_s >> \Delta\hat{v}$. The fluid in front of the wave is undisturbed with a pressure of P, a density ρ, and a speed $\hat{v} = 0$. The fluid contained in the volume bounded by the wave front on the right and the piston on the left moves with the speed $\Delta\hat{v}$ and has a pressure of $P + \Delta P$ and a density of $\rho + \Delta\rho$. Measurement of this phenomenon in the laboratory has shown that the speed of the wave is constant as long as the piston moves with a constant speed. We note then that the volume contained between the wave front and the piston face will increase with time because the wave moves with a speed that is so much greater than the speed of the piston. This condition means that the mass contained in this "disturbed" volume will also increase with time.

We now adopt the approach that we used in section 5.2. We place our point of observation on the wave itself and "ride the wave". Once again, we find that from this vantage point the situation looks the same at all times. It appears that the fluid in front of the wave approaches the wave with the speed ϑ_S and fixed thermodynamic state (P,ρ) while the fluid behind the wave is leaving with the constant speed $\vartheta_S - \Delta\vartheta$ and fixed thermodynamic state $(P + \Delta P, \rho + \Delta\rho)$. We now identify a small *control volume* shown in Figure 5.4 that contains the

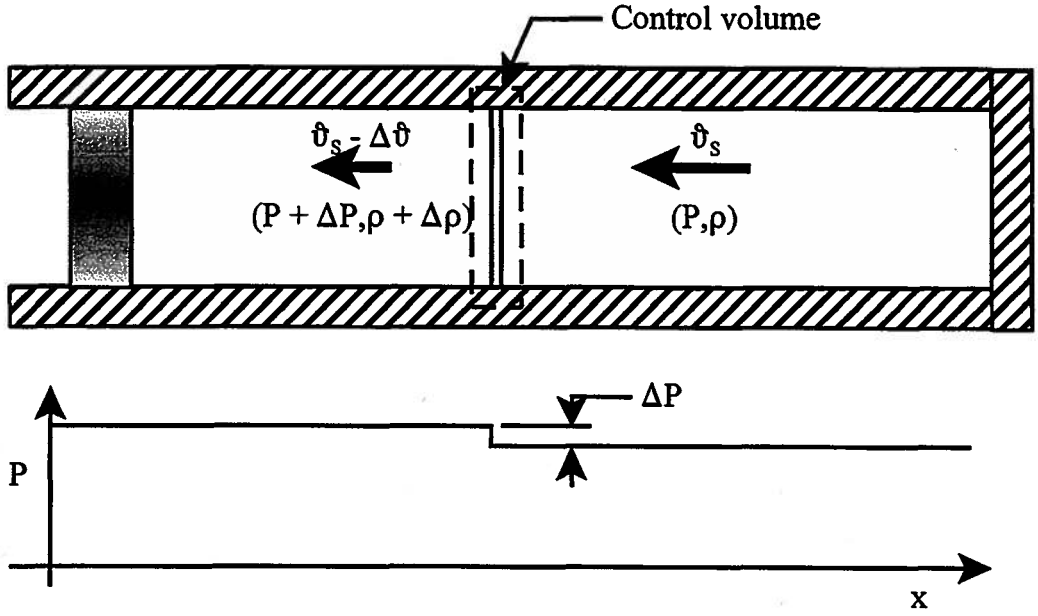

Figure 5.4 Control Volume for Compression Wave Propagating in a Gas

wave and moves at the constant speed ϑ_S. By the principle of the *Conservation of Mass*, equation (5.1), the amount of mass contained within this volume does not change with time even though there is a different identity of the mass particles inside the control volume at each instant of time. To the observer stationed on the moving control volume, it appears at any instant of time that mass enters the control volume from the front at the rate $\rho\vartheta_S A$ (cf. Equation 5.2) and that mass leaves the control volume from the back at the rate $\rho(\vartheta_S - \Delta\vartheta)A$. Then from equation (5.1) it follows that

$$\rho\vartheta_S A - (\rho + \Delta\rho)(\vartheta_S - \Delta\vartheta)A = 0$$

Combing terms and dividing by A, we get

$$\rho\vartheta_s - \rho\vartheta_s + \rho\Delta\vartheta - \Delta\rho\vartheta_s + \Delta\rho\Delta\vartheta = 0$$

or

$$\frac{\Delta\rho}{\rho} = \frac{\Delta\vartheta}{\vartheta_s} \tag{5.19}$$

where we have neglected terms of second order. Thus the relative strength of the disturbance is determined by the speed of the piston relative to the speed of the wave in the undisturbed gas. We now establish the relationship between the forces on the control volume and the momentum flux by applying the momentum equation, equations (5.5) and (5.6). Since

$$-F_f = PA$$

$$-F_b = (P + \Delta P)A$$

equation (5.6) becomes

$$PA-(P+\Delta P)A=\rho A\vartheta_s(\vartheta_{out}-\vartheta_{in})$$

Combining terms, dividing by A, substituting equation (5.19), and neglecting terms of second order, we get

$$\Delta P=\rho\vartheta_S\Delta\vartheta \tag{5.20}$$

If we now substitute equation (5.19), equation (5.20) becomes

$$\vartheta_s^{\,2}=\frac{\Delta P}{\Delta\rho} \tag{5.21}$$

Since we are interested in the limiting case in which this disturbance is infinitesimal in magnitude and does not generate any entropy, it follows that

$$\lim_{\Delta S\to 0}\left(\frac{\Delta P}{\Delta\rho}\right)=\left(\frac{\partial P}{\partial\rho}\right)_S$$

Then, the speed of propagation of the disturbance can be related to a partial derivative of the constitutive relation for the gas.

$$\vartheta_S^{\,2}=\left(\frac{\partial P}{\partial\rho}\right)_S \tag{5.22}$$

Experiment has shown that ϑ_s is the speed of sound for frequencies in the audible range. If we can model the gas as an ideal gas, we can use the entropy constitutive relation to compute the value of the derivative in equation (5.22), viz.

$$S_2-S_1=mc_v\ln\left(\frac{P_2}{P_1}\right)+m(c_v+R)\ln\left(\frac{\rho_1}{\rho_2}\right)=0 \tag{5.23}$$

If we let $\gamma=(c_v+R)/c_v$, equation (5.23) can be rewritten in the form

$$P=C\rho^{\gamma} \tag{5.24}$$

where C is a constant. The speed of sound then becomes

$$\vartheta_S^{\,2}=\left(\frac{\partial P}{\partial\rho}\right)_S=C\gamma\rho^{\gamma-1}=\frac{C\gamma\rho^{\gamma}}{\rho}=\frac{\gamma P}{\rho} \tag{5.25}$$

but from the property constitutive relation $P=\rho RT$, we have

$$\vartheta_S^{\,2}=\gamma RT \tag{5.26}$$

Thus for a given gas, the values of γ and R are fixed and the speed of sound increases with temperature. For monatomic gases like helium, the value of γ is very nearly 1.67 whereas for diatomic gases like nitrogen and oxygen, the value of γ is very nearly exactly 1.4. As the complexity of the molecule increases, triatomic, etc., the value of γ tends toward unity as a limit. For a given value of γ, the speed of sound increases as the molecular weight decreases. Some typical values of the speed of sound are given for various ideal gas models in Table 5.1. Note the large difference in the values for air and helium. This accounts in large part for the "Donald Duck"-like sound that results when talking with one's lungs full of helium.

The force exerted on the piston by the gas then becomes

$$-F=(P+\Delta P)A=PA+\rho\vartheta_s\Delta\vartheta A=PA+\rho\vartheta_s^{\,2}\frac{\Delta\vartheta}{\vartheta_s}A=PA+\rho\gamma RT\frac{\Delta\vartheta}{\vartheta_s}A \tag{5.27}$$

where we have substituted equations (5.19), (5.20), and (5.26). If we now substitute the property

constitutive relation, equation (5.27) becomes

$$-F = PA + \gamma PA\frac{\Delta\vartheta}{\vartheta_s} = PA\left(1+\gamma\frac{\Delta\vartheta}{\vartheta_s}\right) \tag{5.28}$$

TABLE 5.1
Speed of Sound from the Ideal gas Model for Some Common Gases

Ideal Gas Model	*Molecular Wt.*	*R, kJ/kg K*	*c_v, kJ/kg K*	*γ*	*ϑ_s @ T = 300 K, m/s* *ϑ_s @ T = 1000 K, m/s*
Air	28.97	0.287	0.716	1.4008	347.29 634.06
Helium	4.00	2.078	3.153	1.6591	1016.98 1856.77
Hydrogen	2.02	4.116	10.216	1.4029	1316.17 2402.98

In equation (5.28), the first term on the right-hand side represents the *quasi-static* force acting on the piston, i.e. the force that the gas would exert on the piston if the piston were stationary, and the second term on the right-hand side represents the relative dynamic force necessary to accelerate the gas contained between the piston face and the wave front. Clearly, if the quasi-static model is to have any validity for the movement of the boundary of the gas, i.e., for the second term on the right-hand side of equation (5.28), the piston speed must be slow relative to the wave speed. The error associated with this model is a function of the relative speed of the piston and the characteristics of the gas embodied in the parameter γ.

Note that since any piston speed at all will make the term in question greater than zero, it becomes a matter of what degree of error we are willing to accept in using the quasi-static model. Like most modeling decisions, it is a question of the quality of the information required for the situation at hand. In some cases a value of 50 percent may be sufficient whereas in another situation the appropriate value might be 1 percent. In any case, if the quasi-static model is appropriate, the force exerted on the piston by the environment will be identical in magnitude and opposite in sign to the force exerted on the piston by the gas since in the quasi-static model, there is no acceleration of the gas or the piston. Then work transfer for the gas due to the moving piston is given by

$$(W_{1-2})_{\substack{quasi-\\static}} = \int_{state1}^{state2} PA\,dx = \int_1^2 P\,dV \tag{5.29}$$

Note that because of the coupling in the gas, we cannot give a general result for the integration of equation (5.29). We need to know the path of the process, i.e., the way in which P varies as V changes due to the quasi-static displacement of the piston.

For processes for which the quasi-static model is not valid, the gas still achieves equilibrium by the propagation of pressure waves after the piston comes to rest at a new value of volume. Throughout their motion, the waves are being damped by the action of the viscosity and the thermal conductivity of the gas. It is through this process of damped pressure wave action that the gas eventually achieves a state of mechanical equilibrium with the piston. The final

equilibrium state is one that has values of pressure and temperature that are consistent with the property constitutive relation for the final volume.

Clearly, the damping process is irreversible in nature and does generate entropy. The magnitude of the entropy generation depends upon the amplitude of the waves which ultimately can be traced to the speed of the piston relative to the speed of propagation of the waves. The faster the piston moves, the greater the entropy generation. The slower the piston moves, the smaller the entropy generation.

Example 5E.2: In the design of automotive engines, thermal-fluid engineers study the details of the thermodynamic processes taking place inside the engine during a typical operating cycle. These engineers make extensive use of thermal-fluids models to analyze and design the various aspects of engine operation. One of the most common engine cycles used in automotive power plants is the four-stroke design comprised of an intake stroke, a compression stroke, a power stroke, and an exhaust stroke. The simplest model for this series of thermodynamic processes experienced by the working fluid is known as the *Otto cycle* named after Nikolas August Otto (1832-1891), a merchant from Cologne who first introduced a four-stroke engine design at the Paris Exposition of 1878. Of particular interest to automotive engineers, are the work transfer processes that occur during the Otto cycle.

A particular engine design under study is a V-8 configuration utilizing eight piston-cylinder combinations, each with a piston diameter of 101 mm and a stroke of 91 mm. Estimate the error associated with using the quasi-static model to describe the compression stroke of this engine at an operating speed of 3,000 rpm.

Solution: The error in question is contained in the second term on the right-hand side of equation (5.28). This error will depend upon the piston speed and the speed of sound in the gas that comprises the working fluid. During the compression stroke, this gas consists of fuel vapor and air that will serve as the oxidizer of the fuel. Since a typical fuel:air ratio (by mass) in an engine is on the order of 0.068, we will model the gas as air only for the purposes of this estimate. Let us assume that the air can be modeled as an ideal gas and that the temperature of the air is on the order of 300 K. Then from Table 5.1, the speed of sound in the air at 300 K is 347.29 m/sec. Since the piston completes two strokes (once down and once up) during each revolution of the engine, the piston speed is given by

$$\Delta\mathcal{S} = \frac{2(91\text{ mm})(3{,}000\text{ rev/min})}{(1{,}000\text{ mm/m})(60\text{ sec/min})} = 9.1\text{ m/sec}$$

Then the error, e, is given by

$$e = \gamma\frac{\Delta\mathcal{S}}{\mathcal{S}_s} = 1.4008\frac{9.1\text{ m/sec}}{347.29\text{ m/sec}} = 0.0367 = 3.67\%$$

This result is an upper bound on the error since the fluid temperature will increase during the compression process which in turn will increase the speed of sound and decrease the error. This small error reveals that the quasi-static model is a reasonable model for the compression process; however, deciding that the quasi-static model is appropriate is only the first step in the modeling process. There remains an even more difficult step in developing an appropriate model for the heat transfer processes that are taking place simultaneously with the work transfer processes. In the next section of this chapter, we will begin looking at ways of treating these other aspects of thermal-fluid behavior.

5.4 The Quasi-static Process: A Model

In sections 5.2 and 5.3 we studied in a quantitative manner the response of a fluid system to the motion of its boundary. We saw how the system adjusts to the changing volume associated with the movement of the boundary. We saw how this changing volume leads to changes in the pressure of the system as well. We saw how the system seeks a state of internal mechanical equilibrium by adjusting its pressure through fluid dynamic processes internal to the system. We also saw that if the motion of the boundary was slow enough, we could determine the work transfer in terms of the equilibrium thermodynamic properties of the system. The generalization of these observations is the *quasi-static model* for a process in a thermal-fluid system.

> A *quasi-static process* is a model for a dynamic process in which the state of the system is changing at a rate which is slow compared to the rate at which the system approaches the equilibrium state by means of energy transfer and entropy transfer processes *internal* to the system boundary. Internally, the system appears to be in equilibrium at all times throughout the process even though its state is changing with time. The equilibrium properties thus provide a complete description of the state of the system at all times throughout the process.

The implications of this model are substantial. In particular, the model implies that there are no gradients in any of the thermodynamic properties during the process since the system adjusts instantly to the newly imposed volume caused by the motion of the boundary. This implication is somewhat restrictive since many work transfer processes in thermal-fluid systems proceed at rates which result in gradients in temperature and/or pressure. Nevertheless, the model is extremely useful in the design and analysis of thermal-fluid systems as long as the user is aware of its limitations. Since these limitations are rooted in the rate processes by which the system seeks the equilibrium state, we shall devote considerable attention to these processes in this treatment.

5.5 Reversible Processes

There is a special subset of the class of quasi-static processes that we have just studied, namely *reversible processes*. Reversible processes are the idealized limit of real processes. As a class, reversible processes possess unique characteristics:

1. By definition, a reversible process generates no entropy.
2. A reversible process is a sequence of equilibrium states.
3. A reversible process can proceed in the reverse direction just as readily as in the forward direction.
4. A reversible process takes an infinitely long time to be carried out.

Reversible processes are most easily visualized in terms of an isolated system that is in *neutral equilibrium* with respect to one independent property.

5.5.1 Neutral equilibrium in mechanical systems

A mechanical system is in neutral equilibrium when it is in equilibrium for every value of the neutral property. For example, a perfectly spherical ball on a perfectly horizontal plane is in neutral equilibrium with respect to its position on the plane. Regardless of its x- and y-coordinates on the plane, the ball is always in equilibrium. Therefore, as the ball is moved along the plane, it passes through a continuum of neutral equilibrium states. A further example is shown in Figure 5.5. The two identical masses suspended in a gravity field are in neutral

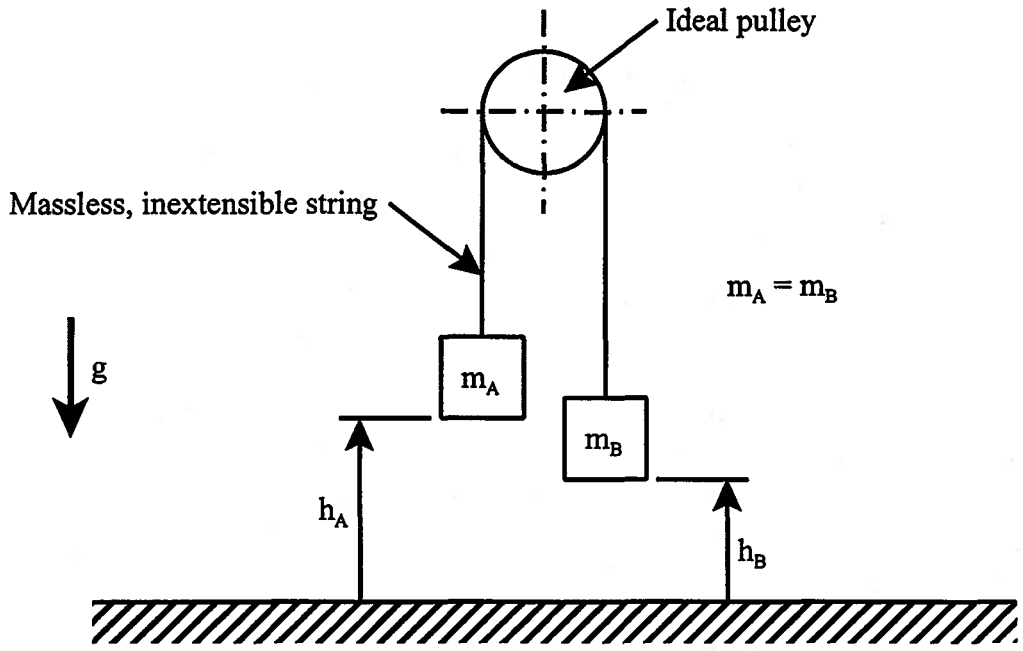

Figure 5.5 Neutral Equilibrium in a Mechanical System

equilibrium with respect to height when suspended by a massless, inextensible string over an ideal pulley. For each of the masses, the force in the string exactly balances the body force due to the gravity field regardless of the position of the height of the masses. No external work transfer is required to change the heights even though the two masses interact with a significant work transfer. This is an isolated system in neutral equilibrium.

Mechanical systems can be constructed so that they are always in neutral equilibrium by including mechanical matching elements in the assembly. A *mechanical matching element* is a mechanical system that maintains another mechanical system in static equilibrium through the application of precisely the correct force, regardless of position. The combined system is then in neutral equilibrium with respect to the position variable. For example, in the system shown in Figure 5.6, the cable is a mechanical matching element for the pure translational spring.
The mechanical matching element (MME) is a perfectly flexible cable with a mass per unit length of m_c/L. On the right-hand side of the pulley, the cable is longer by an amount $2x$. This results in a force of $F_R = 2x(m_c/L)g$. The force required to stretch the spring is $F_S = kx$ where x is measured relative to the unstretched position of the spring. The force on the left-hand side of the pulley is $F_L = F_S$. Then in neutral equilibrium, the sum of the moments about the axis of the pulley O is zero, and if we take the clockwise moments to be positive, we have

$$\sum M_O = 0$$

$$F_R R - F_L R = 0$$

and

$$F_L = F_R$$

and

$$kx = 2x\left(\frac{m_c}{L}\right)g$$

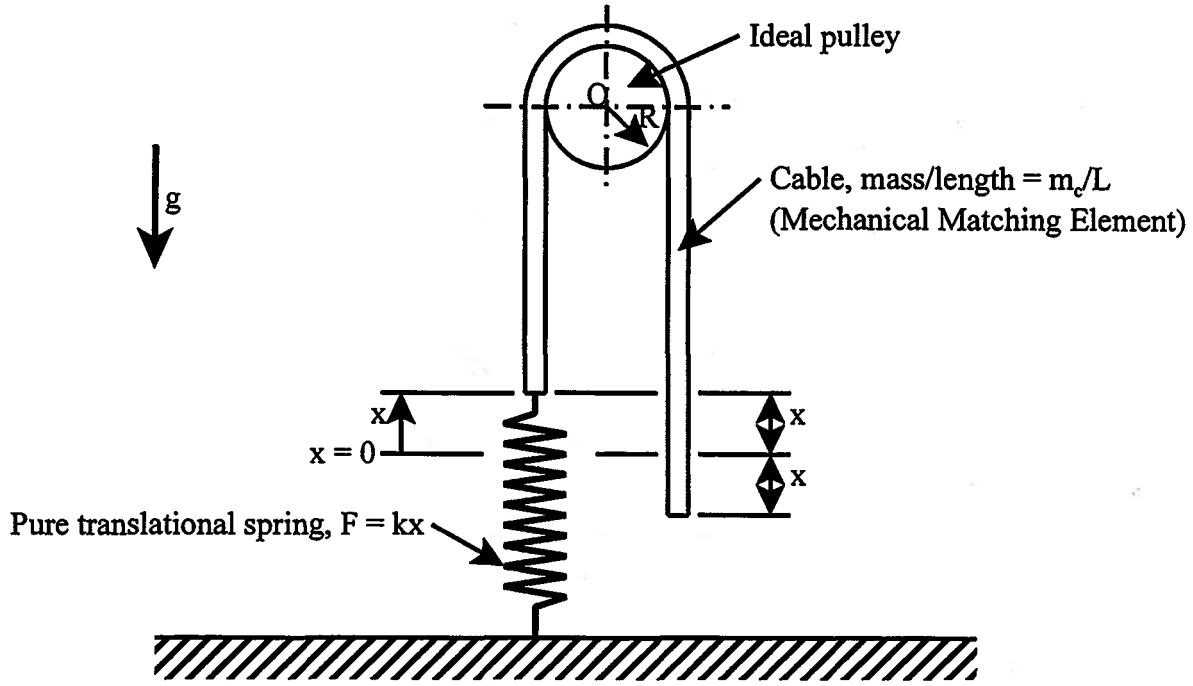

Figure 5.6 Mechanical System with Mechanical Matching Element

Then the required characteristic for the cable is

$$\left(\frac{m_c}{L}\right)=\frac{k}{2g} \tag{5.30}$$

For a cable with this characteristic, the spring will always be in equilibrium regardless of the value of x. Then the cable and the spring form an isolated system in neutral equilibrium. The interaction diagram is shown in Figure 5.7. The mechanical matching element matches the force of the rest of the system for all displacements at its mechanical interaction boundary.

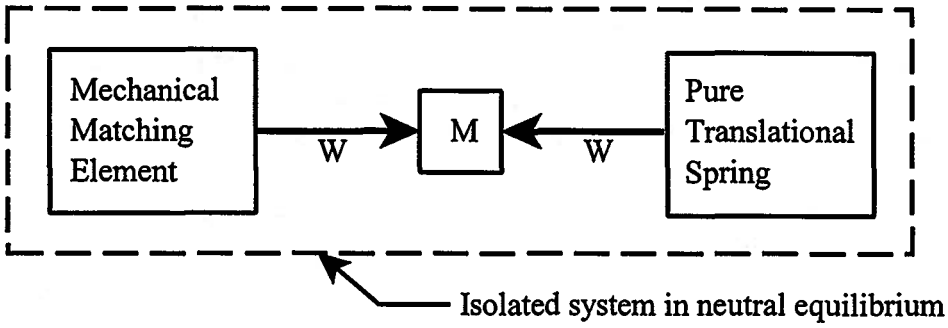

Figure 5.7 Interaction Diagram for Isolated System in Neutral Equilirium

5.5.2 Neutral equilibrium in an ideal gas

The concept of neutral equilibrium can be extended to a more complex system that includes an ideal gas and a mechanical matching element. In this case, because the gas is coupled, there is the potential for simultaneous work transfer and heat transfer interactions, and these heat transfer interactions can influence the mechanical aspects of the behavior of the gas. Thus, the specification of the conditions for neutral equilibrium require not only the specification

of the conditions for mechanical equilibrium, but also the further specification of the conditions associated with the heat transfer interactions. In this more complex case, the mechanical and thermal aspects of system behavior can no longer be treated independently as they were in the previous examples. This concept can be best illustrated through a series of examples.

5.5.2.1 Reversible isothermal process in an ideal gas: As the first example, consider the case in which the gas is in thermal communication with a heat reservoir as shown in the interaction diagram of Figure 5.8.

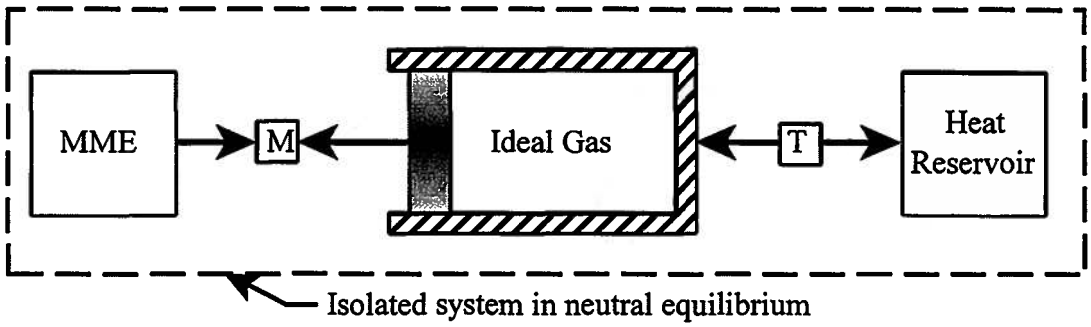

Figure 5.8 Ideal Gas, Heat Reservoir, and Mechanical Matching Element in Neutral Equilibrium

For all positions of the piston and corresponding volumes of the gas, the mechanical matching element applies a force to the piston, via the mechanical interconnection, that precisely matches the opposing force due to the pressure of the gas acting on the piston . Because the gas is coupled, the pressure of the gas at any volume is determined by its temperature. Thus the piston is in neutral equilibrium with respect to the volume of the gas and its corresponding temperature. The thermal interconnection provides the means for temperature of the gas to be identical to that of the heat reservoir for all volumes of the gas and therefore the same for all volumes.

As an example of the way in which such a process might be carried out, consider the apparatus shown in Figure 5.9 as one possible physical embodiment of the mechanical matching element of Figure 5.8. The gas in Figure 5.9 is in thermal communication with a heat reservoir whose temperature is T. If the cam is properly designed, the entire apparatus consisting of gas, piston, cylinder, and heat reservoir can remain in neutral equilibrium regardless of the value of X. That is, the gas exerts a pressure on the face of the piston which is exactly counteracted by a force due to the action of gravity on the mass, m_{wt}. Under these circumstances, there will be no net moment acting on the gear-cam subassembly. From the condition for rotational equilibrium about the point O, it follows that

$$r_1 F_{piston} = m_{wt} g r_2$$

but for the rack and gear combination,

$$r_1 \Theta = X$$

Thus,

$$F_{piston} = \frac{m_{wt} g r_2 \Theta}{X} \tag{5.31}$$

The force resulting from the gas pressure acting on the piston face is

$$F_{piston} = P_{gas} A_p$$

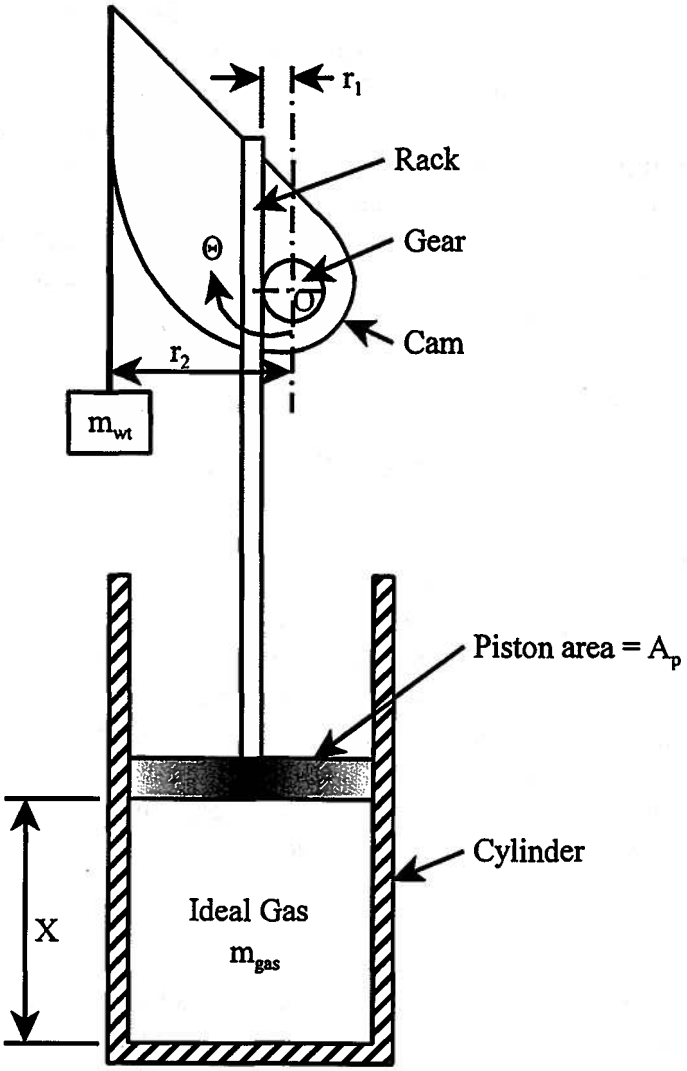

Figure 5.9 Ideal Gas with Mechanical Matching Element

For an ideal gas, the property constitutive relation gives

$$P_{gas} = \frac{m_{gas}RT}{V_{gas}} = \frac{m_{gas}RT}{XA_p}$$

Thus,

$$F_{piston} = \frac{m_{gas}RT}{X} \tag{5.32}$$

Combining equations (5.31) and (5.32), we get the relation defining the cam geometry that will insure that the piston, cylinder, gas, and heat reservoir will be in neutral equilibrium.

$$r_2\Theta = \frac{m_{gas}RT}{m_{wt}g} \tag{5.33}$$

With the cam design specified in equation (5.33), the piston is always in mechanical equilibrium regardless of its position because the externally applied force always matches the force exerted by the gas, hence the name *mechanical matching element*. The operation of the

mechanism involves increasing the mass m_{wt} by a small amount δm_{wt}. When this additional mass is first added, the mechanical equilibrium of the piston is upset. The force exerted by the cam mechanism on the piston will be greater than the force on the of the gas on the piston face. As a result, the piston will move down in an attempt to re-establish mechanical equilibrium. By means of this downward motion of the piston, there is a work transfer from the mass m_{wt} into the gas. This negative work transfer for the gas will increase the energy and the temperature of the gas until the rate of heat transfer from the gas to the reservoir is equal to the rate of work transfer. Thus, the piston will continue to move down as long as the additional mass δm_{wt} is in place. The magnitude of the temperature increase can be determined from equation (5.33) to be

$$r_2\Theta = \frac{m_{gas}R(T+\delta T)}{(m_{wt}+\delta m_{wt})g}$$

$$\delta T = \frac{r_2\Theta(m_{wt}+\delta m_{wt})g}{m_{gas}R} - T$$

The rate at which the process proceeds is controlled by the heat transfer rate from the gas at the temperature $T + \delta T$ to the reservoir at the temperature T. The process will stop and equilibrium will be re-established at any state, i.e., volume, when the mass δm_{wt} is removed from m_{wt}.

As the size of the incremental mass δm_{wt} is decreased, the magnitude of the temperature increment δT decreases and the temperature of the gas approaches the temperature of the reservoir. The process then proceeds at a slower rate. In the limit of an infinitesimal change in the mass, dm_{wt}, the process is quasi-static and the temperature of the gas becomes the temperature of the heat reservoir while the pressure of the gas becomes the equilibrium pressure. The work transfer for the ideal gas as a system is given by equation (5.29)

$$W_{1-2} = \int_{V_1}^{V_2} P dV \tag{5.34}$$

for this quasi-static process. The pressure in equation (5.34) is the equilibrium pressure given by the property constitutive relation for the gas. The temperature is the equilibrium temperature, i.e., the temperature of the heat reservoir. The work transfer for a quasi-static process in an ideal gas whose temperature is maintained constant throughout the process is thus

$$W_{1-2} = \int_{V_1}^{V_2} \frac{mRT}{V} dV = mRT \int_{V_1}^{V_2} \frac{dV}{V} = mRT \ln\left(\frac{V_2}{V_1}\right) \tag{5.35}$$

where the path of integration of the line integral representing the work transfer is one for which the temperature is constant.

Since the temperature of the gas is the same throughout the process, it follows that $T_2 = T_1$ and, hence, by the energy constitutive relation for the ideal gas $U_2 = U_1$. The first law of thermodynamics then gives the required heat transfer

$$Q_{1-2} = W_{1-2} + (U_2 - U_1) = W_{1-2} = mRT \ln\left(\frac{V_2}{V_1}\right) \tag{5.36}$$

With the system in equilibrium at state 2, the mass m_{wt} is decreased by an infinitesimal amount dm_{wt}. The system will then execute a quasi-static expansion which can be stopped at equilibrium state 1 by returning m_{wt} to its original value. Thus, the system completes a cycle. The work transfer for this second process will be

$$W_{2-1} = \int_{V_1}^{V_2} mRT \frac{dV}{V} = mRT \ln\left(\frac{V_1}{V_2}\right)$$

by the same arguments as for the process from state 1 to state 2. The net work transfer for the cycle is then

$$\oint \delta W = W_{1-2-1} = W_{1-2} + W_{2-1} = mRT\left[\ln\left(\frac{V_2}{V_1}\right) + \ln\left(\frac{V_1}{V_2}\right)\right] = 0$$

Similarly, the net heat transfer for the cycle is

$$\oint \delta Q = Q_{1-2-1} = Q_{1-2} + Q_{2-1} = W_{1-2} + W_{2-1} = \oint \delta W = 0$$

Since the temperature of the gas is constant and identical to the temperature of the heat reservoir throughout the cycle, it follows that the net entropy transfer for the cycle must also be zero since the net heat transfer for the cycle is zero. Then from the second law

$$\oint \frac{\delta Q}{T} = \frac{1}{T}\oint \delta Q = \oint dS + \oint \delta S_{gen} = 0$$

but by definition, it is true that for any property, including the entropy, there can be no net change in the property for any cycle. Then

$$\oint dS = 0$$

Then

$$\oint \delta S_{gen} = 0$$

and the cycle must be reversible since no entropy was generated. Since a reversible cycle can be made up of only reversible processes (any single irreversible process in the cycle would generate entropy and require the net entropy transfer for the cycle to be negative which would mean that the cycle would be irreversible), it follows that both processes that made up the cycle in question must be reversible. Hence, we have found a means (in principle, at least) to execute a reversible, isothermal process in an ideal gas. The heat transfer and work transfer interactions for this reversible process are given by equations (5.35) and (5.36).

In the reversible isothermal compression of an ideal gas, energy is transferred into the gas by a negative work transfer and energy and entropy are transferred out to the heat reservoir by means of a negative heat transfer. The stored energy of the gas remains unchanged; however, the gas does change state since the pressure increases, the volume decreases, and the entropy decreases. In contrast to a similar process in a pure dissipative system which is experiencing a negative work transfer and a negative heat transfer, this process is reversible and the work transfer is recovered when the system is returned to its original state. The interrelation between the work transfer and the heat transfer in the present case is the result of the coupled constitutive relation of the gas rather than the result of a dissipation. Had the ideal gas behaved as an uncoupled mechanical system, the increased force on the piston confining the gas would have had to have been the result of an increase of the energy of the system. Clearly, this is not the case with this thermodynamically coupled system.

For the outward motion of the piston in which the gas experiences a positive work transfer, thermal energy and entropy stored in the heat reservoir are transferred into the gas by means of a positive heat transfer for the gas. None of this energy is stored in the gas since the temperature of the gas does not change. The energy that is transferred into the gas as a heat transfer is transferred out to the mechanical matching element as a work transfer. The net result is

that some of the thermal energy that was stored in the heat reservoir is now stored in the mechanical matching element as mechanical energy. Thus, the entropy and the volume of the gas have increased while the gas pressure has decreased. In effect, the gas has acted as a transducer converting thermal energy into mechanical energy by means of its coupled behavior.

The appearance of the outward motion of the piston from an entropy perspective is significantly different from the energy perspective. Associated with the heat transfer from the heat reservoir to the gas is an entropy transfer that increases the stored entropy within the gas. This can be seen from the entropy constitutive relation for the gas, section 4.3.3, since the volume changes while the temperature remains constant. No entropy is transferred to the mechanical matching element since it is a pure mechanical system which has no entropy. The net result of this reversible isothermal expansion is that the entropy transferred along with the energy during the heat transfer interaction with the heat reservoir remains within the gas while the energy does not. This is shown schematically in Figure 5.10.

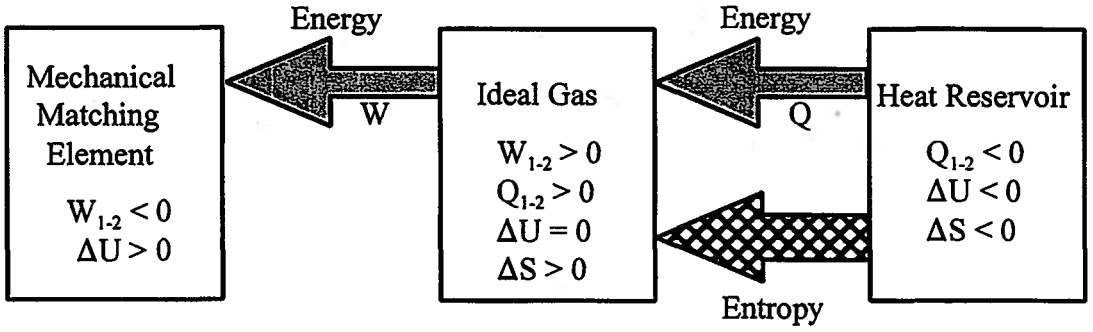

Figure 5.10 Energy and Entropy Flows for an Isothermal Expansion Process in an Ideal Gas

The relation between the pressure and the volume in the gas is shown in Figure 5.11. The hyperbola (solid line) represents the path of the process. Since the composite system of gas, piston, and mechanical matching element is in neutral equilibrium, the piston can move in either direction along this path without any external driving force. If the piston moves out, thereby

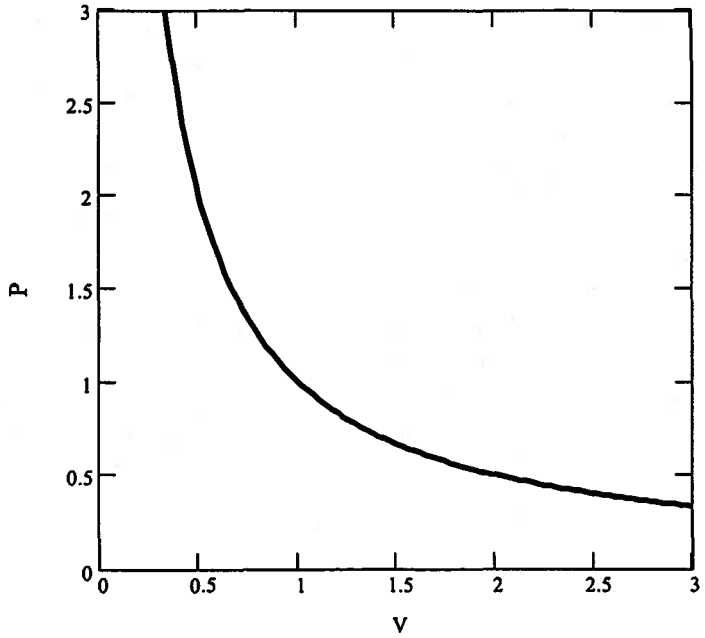

Figure 5.11 Path of a Reversible Isothermal Process in an Ideal Gas with mRT = 1

producing an increase in volume, and then moves back to its original position by decreasing volume, the initial state in the isolated system is recovered in every respect. Such processes that follow the neutral equilibrium path are defined as *reversible processes*. The inward and outward motion of the piston forms a cycle with no net entropy transfer and because it is a cycle, no net entropy change. Therefore, there is no entropy generation, and by the second law of thermodynamics, such a cycle is reversible and is composed only of reversible processes.

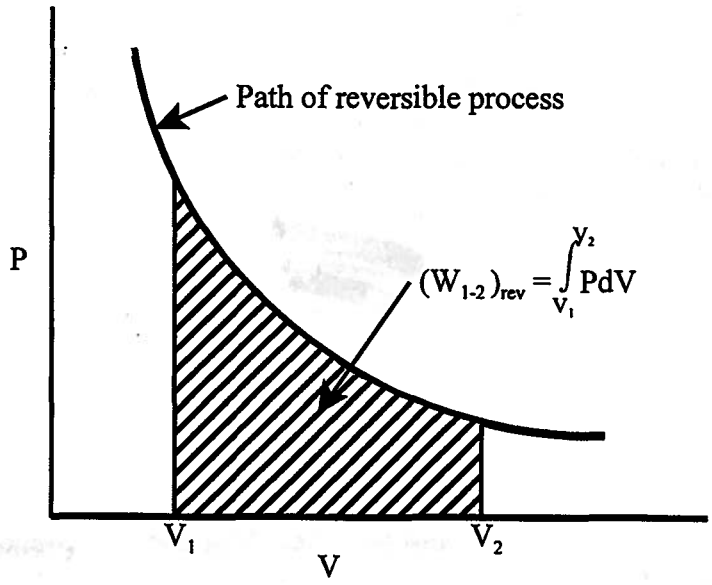

Figure 5.12 Graphical Representation of Reversible Work Transfer

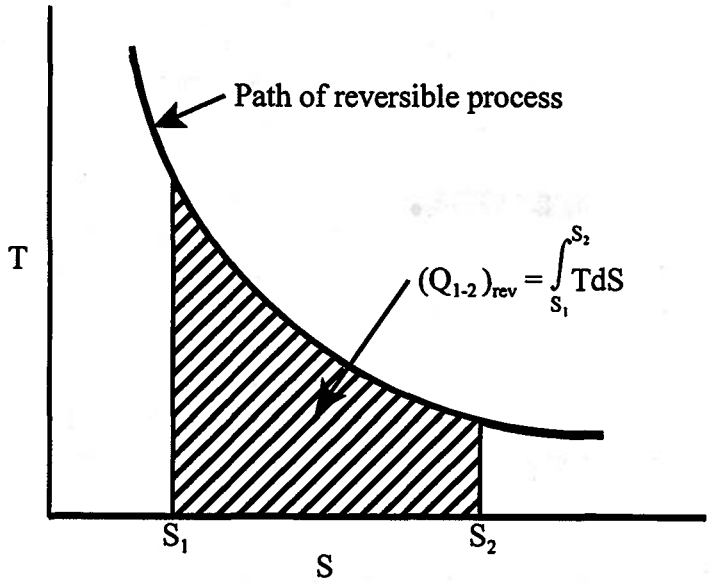

Figure 5.13 Graphical Representation of Reversible Heat Transfer

Since a reversible process is a sequence of equilibrium states, every state that the system passes through, hence its path, can be described in terms of equilibrium properties. This means

that the path of a reversible process can be represented graphically by a path on a plane with equilibrium properties as the ordinate and the abscissa, such as the *P-V* plane or the *T-S* plane. Recall that every point on such a plane represents a unique equilibrium state. Thus reversible processes, such as the reversible isothermal process described above, would appear as a continuous line (cf. Figure 5.11). As shown in Figures 5.12 and 5.13, the *P-V* plane and the *T-S* plane are particularly useful in this regard. The reversible work transfer, $(W_{1\text{-}2})_{rev}$, can be represented graphically by an area on the *P-V* plane between the path of the process and the abscissa.

$$(W_{1-2})_{rev} = \int_{V_1}^{V_2} P dV$$

Since the pressure is always positive, the area, and, hence, the work transfer is positive for increasing volume, $dV > 0$, and negative for decreasing volume, $dV < 0$.

Since all of the states the reversible process passes through are reversible, we can write the second law in differential form.

$$dS = \frac{\delta Q}{T}$$

where the entropy generation term vanishes since the process is reversible. Then we can solve for the heat transfer

$$\delta Q = T dS$$

$$(Q_{1-2})_{rev} = \int_1^2 T dS$$

where we have integrated along the path of the process for which we know the functional relationship between *T* and *S*. Thus, the reversible heat transfer can be represented graphically by an area on the *T-S* plane. Since the thermodynamic temperature is always positive, the heat transfer is positive for increasing entropy, $dS > 0$, and negative for decreasing entropy, $dS < 0$.

Example 5E.3: The objective here is to compare two processes in which the end states are identical but the paths are very different. In particular, we wish to compare: (1) a quasi-static process in an ideal gas connecting two states with identical temperatures with (2) a non-quasi-static process connecting the same two states. From this comparison, we should be able to draw some conclusions that are generally applicable to the differences between quasi-static and non-quasi-static processes.

A. Consider first the quasi-static process. As shown in the Figure 5E.3a, a piston-cylinder apparatus is connected to a mechanical matching element that operates so that the piston is always in a state of mechanical equilibrium regardless of its position. The cylinder is filled with air that can be modeled as an ideal gas. In the initial state, $P_1 = 2 \times 10^5$ N/m^2, $T_1 = 300$ K, and $V_1 = 1$ m^3. The air is in thermal communication with a heat reservoir with $T_{HR} = 300$ K. Through the action of the mechanical matching element, the piston is withdrawn at a rate which is slow relative to the rate at which thermal equilibrium is established between the air and the heat reservoir. Thus, the expansion process can be modeled as a series of states all with the same temperature, 300 K. The expansion process continues until the pressure of the gas is reduced to $P_2 = 1 \times 10^5$ N/m^2.

(a) For the air as a system, calculate the following: V_2, T_2, $Q_{1\text{-}2}$, $W_{1\text{-}2}$, $U_2 - U_1$, $S_2 - S_1$, $S_{transfer}$, and S_{gen}.

B. Now consider the non-quasi-static process. As shown in Figure 5E.3b, the piston of the piston-cylinder apparatus is now fitted with a set of weights such that a gas pressure of 1×10^5 N/m^2 is required to maintain the piston in mechanical equilibrium. In the initial state, the air,

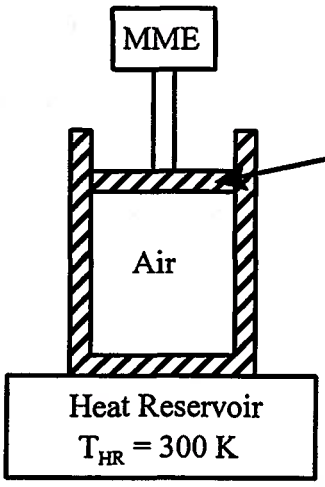

Figure 5E.3a

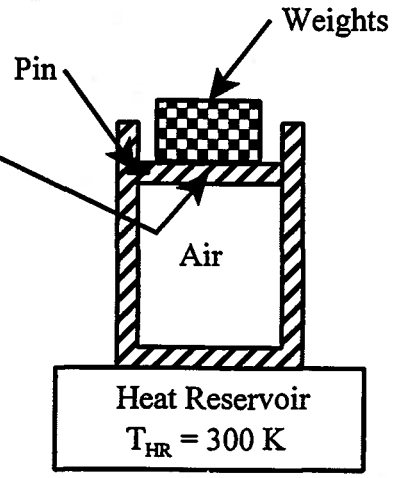

Figure 5E.3b

which can be modeled as an ideal gas, has the following properties: $P_1 = 2 \times 10^5$ N/m^2, $T_1 = 300$ K, and $V_1 = 1$ m^3. In the initial position, the piston is held in mechanical equilibrium by means of a pin since the gas pressure is greater than the pressure required to support the piston. The gas is initially in thermal equilibrium with a heat reservoir at $T_{HR} = 300$ K. The pin is removed and the gas seeks a new equilibrium state.

(b) For the gas as a system, calculate the following: P_2, V_2, T_2, $Q_{1\text{-}2}$, $W_{1\text{-}2}$, $U_2 - U_1$, $S_2 - S_1$, $S_{transfer}$, and S_{gen}.

(c) What conclusions can be drawn about the differences between these two processes?

Solution: (a) The process A is quasi-static because the mechanical matching element insures that the piston is always in a state of mechanical equilibrium regardless of its position. That is, taken together, the gas, the piston and the mechanical matching element are in a state of neutral equilibrium. Furthermore, since the gas is always in thermal equilibrium with the heat reservoir, the gas temperature is always 300 K. Then it follows that $T_2 = 300$ K and

$$V_2 = V_1\left(\frac{P_1}{P_2}\right)\left(\frac{T_2}{T_1}\right) = (1\text{ m}^3)\left(\frac{2 \times 10^5\text{ N/m}^2}{1 \times 10^5\text{ N/m}^2}\right)\left(\frac{300\text{ K}}{300\text{ K}}\right) = 2\text{ m}^3$$

Since the process is quasi-static and isothermal, the work transfer is given by equation (5.35).

$$W_{1\text{-}2} = mRT_1 \ln\left(\frac{V_2}{V_1}\right) = P_1V_1 \ln\left(\frac{V_2}{V_1}\right) = (2 \times 10^5\text{ N/m}^2)(1\text{ m}^3)\ln\left(\frac{2\text{ m}^3}{1\text{ m}^3}\right) = 1.386 \times 10^5\text{ J}$$

Applying the first law to the gas and substituting the energy constitutive relation, we obtain

$$Q_{1\text{-}2} - W_{1\text{-}2} = U_2 - U_1 = mc_v(T_2 - T_1) = mc_v(T_1 - T_1) = 0$$

$$Q_{1\text{-}2} = W_{1\text{-}2} = 1.386 \times 10^5\text{ J}$$

Since the gas did not change energy, the energy associated with the work transfer from the gas to the piston and thence to the mechanical matching element came from the heat reservoir in the form of a heat transfer. Thus, the gas is coupled in the thermodynamic sense since it is able to convert a heat transfer into a work transfer. From the entropy constitutive relation, we have

$$S_2 - S_1 = mc_P \ln\left(\frac{T_2}{T_1}\right) - mR\ln\left(\frac{P_2}{P_1}\right) = mc_P \ln\left(\frac{T_1}{T_1}\right) - \frac{P_1V_1}{T_1}\ln\left(\frac{P_2}{P_1}\right)$$

$$S_2 - S_1 = 0 - \frac{(2 \text{ x } 10^5 \text{ N/m}^2)(1 \text{ m}^3)}{300 \text{ K}} \ln\left(\frac{1 \text{ x } 10^5 \text{ N/m}^2}{2 \text{ x } 10^5 \text{ N/m}^2}\right) = 462.098 \text{ J/K}$$

Since the heat transfer interaction occurs between the gas and the heat reservoir, the entropy transfer is given by

$$S_{transfer} = \frac{Q_{1-2}}{T_{HR}} = \frac{1.386 \text{ x } 10^5 \text{ J}}{300 \text{ K}} = 462.098 \text{ J/K}$$

Applying the second law to the gas and solving for the entropy generation, we get

$$S_{gen} = (S_2 - S_1) - S_{transfer} = 462.098 \text{ J/K} - 462.098 \text{ J/K} = 0$$

Since no entropy is generated and since the temperature of the gas remains constant throughout the process, this quasi-static process is a reversible isothermal process.

(b) The non-quasi-static nature of process *B* derives from the fact that once the pin is pulled, the net force acting on the piston is not zero since the gas pressure is actually twice the pressure required to maintain the piston in mechanical equilibrium. Then the piston accelerates upward and generates a rarefaction wave that propagates through the gas and is reflected off the bottom of the cylinder. The process of wave generation and reflection continues until finally the gas attains mechanical equilibrium with the piston at a pressure of $P_2 = 1 \text{ x } 10^5 \text{ N/m}^2$. The final equilibrium temperature is determined by the equilibrium between the heat reservoir and the gas, viz., $T_2 = 300$ K. Then the final equilibrium volume is determined by the property relation for the gas, viz., $V_2 = 2 \text{ m}^3$.

Since the process is not quasi-static, the work transfer cannot be determined from the integral of PdV since there is no unique, uniform value of P at each value of V due to the wave action. The work transfer must be determined from the behavior of the system that the gas is interacting with, viz., the piston. Then if we model the piston as a pure gravitational spring and apply the first law to the piston, we have

$$-(W_{1-2})_{piston} = E_2 - E_1 = m_{piston} g(z_2 - z_1)$$

where z is measured from the bottom of the cylinder. Note that when the piston is in mechanical equilibrium with the gas, the body force due to gravity acting on the piston is equal in magnitude and opposite in sign to the boundary force exerted by the gas. Hence,

$$m_{piston} g = P_{piston} A_{piston}$$

where P_{piston} is the gas pressure required to support the piston in equilibrium. Then since the work transfer experienced by the piston is exactly equal in magnitude but opposite in sign to the work transfer experienced by the gas, we have

$$(W_{1-2})_{gas} = -(W_{1-2})_{piston} = P_{piston} A_{piston}(z_2 - z_1) = P_{piston}(V_2 - V_1)_{gas}$$

where we have made use of the fact that the volume of the cylinder is given by $V = A_{piston} z$. In this last expression it would appear that the work transfer for the gas is equal to the integral of PdV where P is a constant P_{piston}. However, this is not the case since the pressure of the gas is equal to P_{piston} only in the final equilibrium state. There is no equilibrium gas pressure that we can define or measure during the non-quasi-static process. Then

$$(W_{1-2})_{piston} = (1 \text{ x } 10^5 \text{ N/m}^2)(2 \text{ m} - 1 \text{ m}) = 1 \text{ x } 10^5 \text{ J}$$

Since there is no net change in the temperature of the gas during this process, the first law for the gas gives

$$Q_{1-2} - W_{1-2} = U_2 - U_1 = mc_v(T_2 - T_1) = mc_v(T_1 - T_1) = 0$$

$$Q_{1-2} = W_{1-2} = 1 \text{ x } 10^5 \text{ J}$$

Since the change of state for process *A* is identical to that for process *B*, it follows that each of the properties changes by the same amount in the two processes. Then for process *B*

$$(S_2 - S_1)_{process\ B} = (S_2 - S_1)_{process\ A} = 462.098\ \text{J/K}$$

The same cannot be said for the entropy transfer since it depends upon the heat transfer interaction which is clearly not the same for the two processes. Then

$$S_{transfer} = \frac{Q_{1-2}}{T_{HR}} = \frac{1 \times 10^5\ \text{J}}{300\ \text{K}} = 333.333\ \text{J/K}$$

Applying the second law we can determine the entropy generated.

$$S_{gen} = (S_2 - S_1) - S_{transfer} = 462.098\ \text{J/K} - 333.333\ \text{J/K} = 128.765\ \text{J/K}$$

Since entropy is generated in the non-quasi-static process, it is irreversible.

(c) We note that for the two processes, the change of state is identical. This means that the change in each of the properties *P*, *T*, *V*, *U*, and *S* will be the same for the two processes. However, the non-quasi-static process generated entropy because of the complex wave action and the ensuing damping process, and as a result, the positive work transfer was less for the non-quasi-static process for the same change of state. This is a general result, namely that the generation of entropy will always "dissipate" some of the positive work transfer if, in fact, any positive work transfer could be produced. We also conclude that knowing the end states of a process is not sufficient to determine the interactions that could result. Even though the initial and final states of process *B* were at the same temperature, the process itself was not an isothermal process. In fact, for much of the process, we could not even define a temperature of the gas. It follows that we must know the path of the process as well as the end states. In the quasi-static case, the system proceeded through a series of well-defined equilibrium states, but in the non-quasi-static process, the system proceeded through some equilibrium states and some non-equilibrium states with the result that the work transfer was reduced.

5.5.2.2 Reversible adiabatic process in an ideal gas: As yet another example of a reversible process in an ideal gas, consider the motion of the piston in the classical piston-cylinder apparatus as shown in Figure 5.9. In Section 5.3, we showed that the motion of the boundary of a gas produces a temporary non-uniform distribution of pressure in the gas. The process by which the gas equalizes the pressure throughout its volume occurs by means of pressure waves which propagate throughout the volume at the speed of sound. For a volume of reasonable dimensions (on the order of meters), this process occurs in milliseconds. While we have yet to examine the physical processes associated with heat transfer interactions, we will soon see that these processes occur in a time frame that can be measured in seconds, minutes, or even longer. Thus, the time required for pressure equalization in a gas is extremely short, much shorter, in fact, than the time required for temperature equalization. This is typical of thermal-fluids systems encountered in engineering practice; in general, not all of the events of interest occur on the same time scale.

For the case at hand, the time scale of the physical process of moving the boundary may be long enough to permit pressure equalization but too short to permit temperature equalization. Then, a reasonably rapid change of the volume of a gas confined within a cylinder as in Figure 5.9 may be modeled as occurring without thermal communication between the gas and the cylinder walls. Although the gas can never be completely thermally isolated from the walls of its container, it is often reasonable to model this situation as adiabatic, i.e., one in which no heat

transfer is possible with the walls. Some thermodynamicists formulate this model by assuming that the confining walls are incapable of heat transfer, that is, zero thermal conductivity, but a more realistic approach would be to assume that the gas itself is incapable of heat transfer. The thermal conductivities of metals range from 20 to 400 W/m K, while the thermal conductivities of gases range from 0.02 to 0.3 W/m K. Thus in the typical physical situation, a steep temperature gradient occurs in the gas very close to the wall with the bulk of the gas at a more uniform temperature.

A word of caution is appropriate here. There is a tendency for the student unfamiliar with the adiabatic process model to apply the model in situations where it is an inadequate representation of the process. In particular, one should avoid using this model for processes in very small systems which have a very high surface area to volume ratio. In those cases, it is possible for heat transfer to dominate most other processes with the result that the isothermal model might be more appropriate. At the other extreme are systems that are so large that the pressure waves by which the system seeks internal mechanical equilibrium would require a sizable amount of time to propagate throughout the system. In such cases, the pressure would not be uniform on the time scale of the change of state; thus, the necessary conditions for the quasi-static model described in Section 5.3 would not be satisfied.

For our present purposes, however, let us assume that the quasi-static conditions are satisfied and that the ideal gas is not in thermal communication with the confining walls. In this case, work transfer is the only interaction with the environment and the interaction diagram would appear as shown in Figure 5.14.

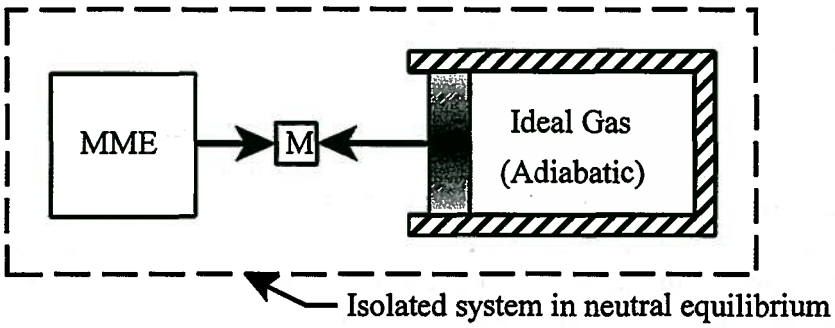

Figure 5.14 Ideal Gas and Mechanical Matching Element in Neutral Equilibrium

Through the use of a mechanical matching element similar to the mechanism shown in Figure 5.9, the force-displacement characteristics of the piston can be matched to the pressure-volume characteristics of the confined gas which cannot experience heat transfer with the confining walls. The necessary conditions for neutral equilibrium, which will establish the path of the reversible process, are determined by the first law of thermodynamics and the property constitutive relation of the gas. Since the gas is in continuous equilibrium with the mechanical matching element, the work transfer for each infinitesimal change of state is given by

$$\delta W = PdV \tag{5.37}$$

where P and V are the equilibrium properties of the gas in each of the states of neutral equilibrium. The first law for the gas combined with the energy constitutive relation for the gas gives

$$\delta Q - \delta W = dU = mc_v dT \tag{5.38}$$

where c_v is the specific heat at constant volume and T is the equilibrium temperature of the gas in any of the states of neutral equilibrium. Since there is no heat transfer interaction for the gas because of the adiabatic condition, equations (5.37) and (5.38) can be combined to give

$$-PdV = mc_v dT \tag{5.39}$$

Substituting the property constitutive relation into equation (5.39), we obtain

$$-\frac{dV}{V} = \frac{c_v}{R}\frac{dT}{T} \tag{5.40}$$

If we take the natural logarithm of the property constitutive relation, we get

$$\ln P + \ln V = \ln(mR) + \ln T \tag{5.41}$$

The differential of equation (5.41) is

$$\frac{dP}{P} + \frac{dV}{V} = \frac{dT}{T} \tag{5.42}$$

Substituting equation (5.42) into equation (5.40) and separating variables, we obtain

$$-\left(\frac{R+c_v}{c_v}\right)\frac{dV}{V} = \frac{dP}{P} = -\gamma\frac{dV}{V} \tag{5.43}$$

where we have introduced the notation

$$\gamma = \frac{R+c_v}{c_v} \tag{5.44}$$

Then equation (5.43) can be integrated to give

$$-\gamma \ln V = \ln P + \ln C$$

where C is the constant of integration. When the logarithmic terms are combined

$$\ln\left(PV^{\gamma}C\right) = 0$$

$$PV^{\gamma}C = 1$$

or

$$PV^{\gamma} = \text{constant} \tag{5.45}$$

Equation (5.45) defines the path of the reversible adiabatic process for the ideal gas with constant R and c_v. If the pressure and volume are known in one state (state 1), equation (5.45) can be written

$$PV^{\gamma} = P_1V_1^{\gamma} \tag{5.46}$$

Using the property constitutive relation, we can express the path, equation (5.46), in terms of P and T or T and V. Thus,

$$\frac{T}{T_1} = \left(\frac{P}{P_1}\right)^{\frac{\gamma-1}{\gamma}}$$

$$\frac{T}{T_1} = \left(\frac{V}{V_1}\right)^{1-\gamma} \tag{5.47}$$

For the reversible, adiabatic path in the ideal gas, equations (5.46) or (5.47), it is left as an exercise to show that the isolated system consisting of the adiabatic gas and the mechanical matching element shown in Figure 5.9 can be made neutrally stable by using a cam for which

$$r_2\Theta = \frac{P_1V_1^{\gamma}}{m_{wt}g}V^{1-\gamma} \tag{5.48}$$

where P_1 is the pressure for which the volume is $A_p X_1$. The nature of the neutral equilibrium can be determined by a stepwise analysis similar to Section 5.5.2.1.

If the mass m_{wl} on the mechanism is increased by δm_{wp} the piston will move down, and the gas will be compressed quasi-statically until the imbalance force due to δm_{wl} is reduced by removing the excess mass δm_{wf}. The gas will then follow equation (5.46) to the state (P_2, V_2) with the corresponding T_2 given by the property constitutive relation. If the mass is now decreased by δm_{wp} the system piston will move up and the gas will expand quasi-statically following equation (5.46). When the gas has returned to the state (P_1, V_1), the temperature must be T_1 in order to satisfy the equation of state. It follows that the entropy has returned to its original value, and since there was no entropy transfer because there was no heat transfer, the quasi-static adiabatic process is a reversible adiabatic process.

Recall that for an adiabatic process, the first law gives the work transfer for the gas. Then

$$-(W_{1-2})_{adiabatic} = mc_v(T_2 - T_1)$$

$$-(W_{1-2})_{adiabatic} = mc_v T_1\left(\frac{T_2}{T_1} - 1\right) \tag{5.49}$$

where we have made use of the fact that there is no heat transfer for the adiabatic process. Notice that equation (5.49) applies to any adiabatic process, reversible or irreversible. For the reversible adiabatic case that uses the cam of equation (5.48), we can use the path described in equation (5.47). Then the reversible adiabatic work transfer becomes

$$-(W_{1-2})_{\substack{reversible\\adiabatic}} = mc_v T_1\left[\left(\frac{P_2}{P_1}\right)^{\frac{\gamma-1}{\gamma}} - 1\right]$$

$$-(W_{1-2})_{\substack{reversible\\adiabatic}} = mc_v T_1\left[\left(\frac{V_2}{V_1}\right)^{1-\gamma} - 1\right] \tag{5.50}$$

where

$$mc_v T_1 = \frac{c_v}{R} P_1 V_1 \tag{5.51}$$

The reversible adiabatic process in the ideal gas is similar to a pure mechanical process in that a work transfer into the system increases both the energy of the system and the force (due to gas pressure) at the system boundary. As a result of the coupling, the increase in the energy of the system from the work transfer caused an increase in temperature even though there was no heat transfer.

Example 5E.4: Consider the engine of example 5E.2. In this engine, the compression ratio, r_c, is $r_c = V_1/V_2 = 9$ and the initial temperature of the air is $T_1 = 300$ K. Estimate the temperature, T_2, of the air at the end of the compression process and the work transfer, $W_{1\text{-}2}$, required to compress the air prior to combustion.

Solution: Since the piston speed is 9.1 m/sec, the compression process proceeds so rapidly there is insufficient time for the gas to attain thermal equilibrium with the walls of the cylinder as the gas is being compressed. Hence the process can be modeled as adiabatic. We have already established that the piston speed is so small relative to the speed of sound that the process can be modeled as quasi-static. Hence, it is reasonable to assume further that it is also reversible. For a reversible adiabatic process in an ideal gas, the path is one for which PV^γ = constant and the relationship between T, V, and P is given by equation (5.47). Then

$$T_2 = T_1\left(\frac{V_2}{V_1}\right)^{1-\gamma} = T_1\left(\frac{V_1}{V_2}\right)^{\gamma-1} = (300\text{ K})(9)^{1.4008-1} = 723.7\text{ K}$$

Thus it is clear that our previous estimate of the speed of sound in the air was a conservative one. The work transfer is given by equation (5.50). Thus

$$-(W_{1-2})_{\substack{reversible\\adiabatic}} = mc_vT_1\left[\left(\frac{V_1}{V_2}\right)^{\gamma-1}-1\right] = \frac{c_v}{R}P_1V_1\left[\left(\frac{V_1}{V_2}\right)^{\gamma-1}-1\right] = \frac{c_vP_1\pi D^2L}{4R}\left[\left(\frac{V_1}{V_2}\right)^{\gamma-1}-1\right]$$

$$(W_{1-2})_{\substack{reversible\\adiabatic}} = -\frac{716\text{ J/kg K}}{287\text{ J/kg K}}(1\text{ x }10^5\text{ N/m}^2)\frac{\pi(0.091\text{ m})^2}{4}(0.101\text{ m})\left(9^{1.4008}-1\right)$$

$$(W_{1-2})_{\substack{reversible\\adiabatic}} = -231.474\text{ J}$$

5.5.2.3 Reversible isochoric heat transfer to an ideal gas at constant volume: When an ideal gas experiences an energy change as a result of a heat transfer interaction without a simultaneous work transfer (no change in volume), the temperature of the gas must change as a consequence of the first law and the energy constitutive relation. For this heat transfer interaction to be reversible, it must occur with a system whose temperature matches that of the gas exactly throughout the interaction. Ideally, this other system should be a thermal matching element analogous to the mechanical matching element that we have described above. That is, the gas must be in thermal communication with a system that is in continuous neutral equilibrium with the gas. Clearly, it must be the case that the only heat transfer interaction that this thermal matching element can experience must be with the gas.

Unfortunately, because of the unique pressure-volume-temperature characteristics of the ideal gas, there is no single system that can meet the necessary requirements reversibly. However, these requirements can be met reversibly by combining another ideal gas with a mechanical matching element as shown in the interaction diagram of Figure 5.15.

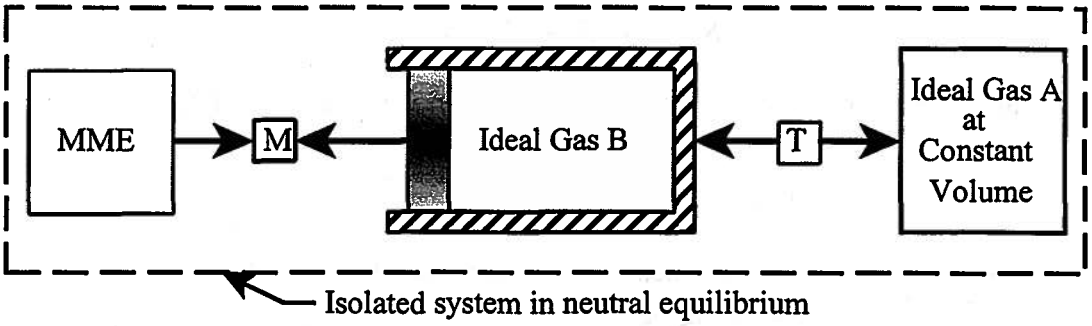

Figure 5.15 Ideal Gas at Constant Volume, Ideal Gas in a Piston-Cylinder, and a Mechanical Matching Element in Neutral Equilibrium

The isolated system in neutral equilibrium shown in Figure 5.15 is arranged so that gas A has a reversible heat transfer while its volume remains constant. When the piston confining gas B moves down, mechanical energy leaves the mechanical matching element and is transferred by means of a work transfer interaction to gas B. The resulting increase in energy in gas B causes its temperature to increase. This temperature increase causes energy to be transferred by means of a heat transfer interaction to gas A to maintain thermal equilibrium between gas B and gas A. For continuous equilibrium, i.e., a reversible process, the interaction must be slow enough so that all

temperature gradients approach zero. Thus, no entropy will be generated in gas A.

Since the sequence of states in gas A is a sequence of equilibrium states, we can write the first law for an infinitesimal change of state in gas A as

$$\delta Q = dU = mc_v dT \tag{5.52}$$

where we have made use of the fact that there is no work transfer for a gas undergoing a reversible change of state at constant volume. For a finite change of state, we have

$$(Q_{1-2})_{\substack{reversible \\ const.vol.}} = mc_v(T_2 - T_1) \tag{5.53}$$

If we rearrange equation (5.53), we find that the physical significance of the name for c_v, i.e., specific heat at constant volume, becomes apparent.

$$c_v = \frac{(Q_{1-2})_{\substack{reversible \\ const.vol.}}}{m(T_2 - T_1)} \tag{5.54}$$

Thus c_v is the reversible heat transfer per unit mass per unit temperature change for an ideal gas at constant volume. In any other circumstance it does not have this significance, but it does retain the name. In any other circumstance, c_v should be simply regarded as another gas constant that provides the constant of proportionality between the internal energy of the ideal gas and its temperature.

For the reversible heat transfer process at constant volume, we can compute the entropy transfer between gas A and gas B. Then, from the second law for this reversible process with no entropy generation

$$\delta S_{transfer} = \frac{\delta Q}{T} = dS \tag{5.55}$$

Substituting equation (5.52) into equation (5.55), we get

$$\delta S_{transfer} = dS = \frac{mc_v dT}{T} \tag{5.56}$$

which for a finite change of state can be integrated to give

$$S_{transfer} = (S_2 - S_1)_{gasA} = mc_v \ln\frac{T_2}{T_1} \tag{5.57}$$

Notice that this result could have been obtained from the entropy constitutive relation for the ideal gas

$$(S_2 - S_1)_{gasA} = mc_v \ln\frac{T_2}{T_1} + mR\ln\frac{V_2}{V_1} = mc_v \ln\frac{T_2}{T_1} \tag{5.58}$$

since $V_1 = V_2$. Note that for the isolated system, the second law requires

$$(S_2 - S_1)_{isolated} = (S_2 - S_1)_{gasA} + (S_2 - S_1)_{gasB} = 0 \tag{5.59}$$

Then

$$(S_2 - S_1)_{gasB} = -(S_2 - S_1)_{gasA} = -m_A(c_v)_A \ln\frac{T_2}{T_1} \tag{5.60}$$

If desired, we could derive the pressure-volume characteristics, i.e., the path of the process, in gas B by applying the first law in differential form to gas B and integrating it.

Example 5E.5: For ideal gas B in Figure 5.15, determine the relationship between the pressure and the volume in gas B that establishes the force-displacement relation that must be met by the mechanical matching element in order for the piston bounding gas B to be in mechanical equilibrium in all positions.

Solution: For gas B as a system, the first law for an infinitesimal change of state can be written

$$\delta Q - \delta W = dU = m_B c_{v_B} dT_B$$

Since the process in gas B is reversible, we can write $\delta W = PdV$. Then

$$\delta Q - PdV = m_B c_{v_B} dT_B$$

For the thermal interconnection between gas A and gas B,

$$\delta Q^{BA} = -\delta Q^{AB} = -m_A c_{v_A} dT_A$$

Substituting this result into the first law and rearranging terms, we get

$$-PdV = \left(m_A c_{v_A} + m_B c_{v_B}\right) dT_B$$

We can eliminate dT_B from the first law by forming the differential of the property constitutive relation, $PV = mRT$,

$$dT_B = \frac{1}{m_B R_B}(VdP + PdV)$$

Substituting this result into the first law and separating variables, we get

$$\frac{dP}{P} = -\frac{dV}{V}\left(\frac{1+N}{N}\right)$$

where

$$N = \frac{m_A c_{v_A} + m_B c_{v_B}}{m_B R_B}$$

Integrating the differential equation, we get the path in gas B.

$$PV^{\beta} = \text{ constant}$$

$$\beta = \frac{1+N}{N} = \frac{m_A c_{v_A} + m_B c_{v_B} + m_B R_B}{m_A c_{v_A} + m_B c_{v_B}}$$

This relationship determines the force-displacement behavior of the mechanical matching element (MME).

5.5.2.4 Reversible constant pressure process in an ideal gas: For an ideal gas in neutral equilibrium at constant pressure, any heat transfer will also result in a work transfer and vice versa. As shown in Figure 5.16, the isolated system in neutral equilibrium is arranged to maintain gas A at constant pressure. When the piston confining gas B moves inward, mechanical energy

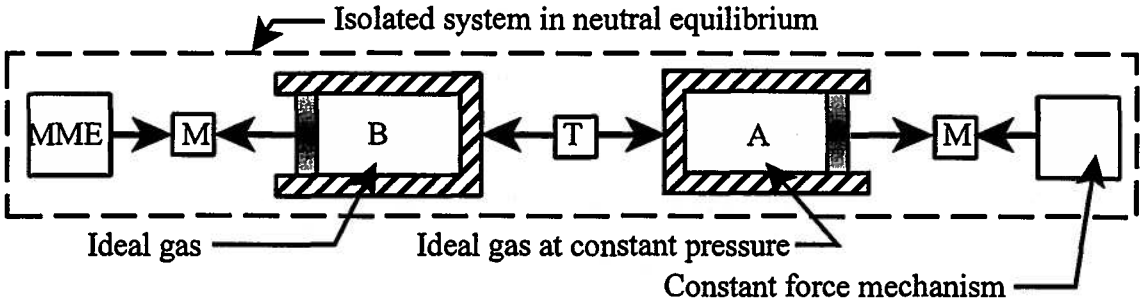

Figure 5.16 Ideal Gas at Constant Pressure in Neutral Equilibrium

leaves the mechanical matching element and is transferred to gas B by means of a work transfer interaction. This work transfer increases the energy of gas B which manifests itself as an increase

in the temperature of gas B. The temperature increase causes a heat transfer interaction to occur between gas B and gas A. This heat transfer to gas A increases both the energy and the temperature of gas A. As a result of the temperature increase, gas A expands against the constant force mechanism. Thus the work transfer associated with the motion of the piston of gas A increases the energy of the constant force mechanism. The result is that the energy from the mechanical matching element goes to increase the temperature and energy of gases A and B and to increase the energy of the constant force mechanism.

Since gas A goes through a series of equilibrium states, the first law for an infinitesimal change of state becomes

$$\delta Q - \delta W = dU = mc_v dT \tag{5.61}$$

but for continuous equilibrium in gas A,

$$\delta W = PdV \tag{5.62}$$

Since the pressure in gas A is constant, the property constitutive relation yields

$$dV = \frac{mR}{P} dT \tag{5.63}$$

Combining equations (5.62) and (5.63), we get

$$\delta W = mRdT \tag{5.64}$$

Substituting equation (5.64) into equation (5.62), we get

$$\delta Q = m(c_v + R)dT = mc_P dT \tag{5.65}$$

where we have introduced c_P, the specific heat at constant pressure (a misnomer since the work transfer is included) and for the ideal gas model, $c_P = c_v + R$. For a finite change of state for gas A at constant pressure in the isolated system in neutral equilibrium, the first law becomes

$$(Q_{1-2})_{\substack{reversible \\ const.press.}} = mc_P(T_2 - T_1) = \frac{c_P}{R} P(V_2 - V_1) \tag{5.66}$$

and the work transfer becomes

$$(W_{1-2})_{\substack{reversible \\ const.press.}} = P(V_2 - V_1) = mR(T_2 - T_1) \tag{5.67}$$

Since this process is reversible, it does not generate any entropy. Then the entropy transfer becomes

$$\delta S_{transfer} = \frac{\delta Q}{T} = dS \tag{5.68}$$

Then substituting equation (5.65) into equation (5.68), we get

$$\delta S_{transfer} = dS = \frac{mc_P dT}{T} \tag{5.69}$$

and for a finite change of state, we can integrate equation (5.69). Then

$$S_{transfer} = S_2 - S_1 = mc_P \ln \frac{T_2}{T_1} \tag{5.70}$$

Equation (5.70) could also be obtained from the entropy constitutive relation

$$S_2 - S_1 = mc_P \ln \frac{T_2}{T_1} - mR \ln \frac{P_2}{P_1} = mc_P \ln \frac{T_2}{T_1} \tag{5.71}$$

since $P_2 = P_1$.

Example 5E.6: In many homes in the Eastern United States, heating is provided by hot water which circulates through pipes which are exposed on their outer surfaces to the

atmospheric air in the various rooms of the house. Because of the temperature difference between the water and the room air, a heat transfer interaction occurs that warms the air in the room. In older heating system designs, the driving force for the circulation of the hot water was provided by the difference in buoyancy between the hotter water which had not yet experienced the heat transfer interaction with the room air and the cooler water which had already experienced this interaction. The hotter water would rise because it was less dense (more buoyant) and the colder water would fall because it was more dense (less buoyant). By arranging supply and return piping appropriately, the hot water could be circulated throughout the house. This configuration, which was known as "natural convection hot water heating", has largely been replaced by "forced convection hot water heating" in which the driving force for circulating the hot water is provided by a pump.

One of the problems that plagues natural convection heating systems is an air lock. Water in a typical home plumbing system has a measurable amount of air dissolved in it. As the air is heated in the "boiler", the water comes out of solution and forms air bubbles in the piping. If these air bubbles get into the wrong place in the piping system, the buoyancy force is not sufficient to move the water and the air bubble along in the pipe. The result is an air lock which effectively shuts down the heating system. In practice, piping system design must provide a means of removing this air lock if the heating system is to be function properly.

Figure 5E.6 shows a pipe with a cross-sectional area of $A_{pipe} = 2$ cm^2 containing an air bubble with a volume of $V_1 = 2$ cm^3 at a temperature of $T_1 = 90$ C . The pipe is open to the atmosphere, $P_{atm} = 10^5$ N/m^2, a 3 m long column of water, $\rho_{water} = 10^3$ kg/m^3, trapped above the air bubble. The air in the bubble experiences a quasi-static heat transfer that reduces the temperature of the bubble to $T_2 = 50$ C. Calculate the new volume V_2 of the bubble, the heat transfer, $Q_{1\text{-}2}$, necessary to effect this change of state, and the work transfer, $W_{1\text{-}2}$, experienced by the air during this change of state.

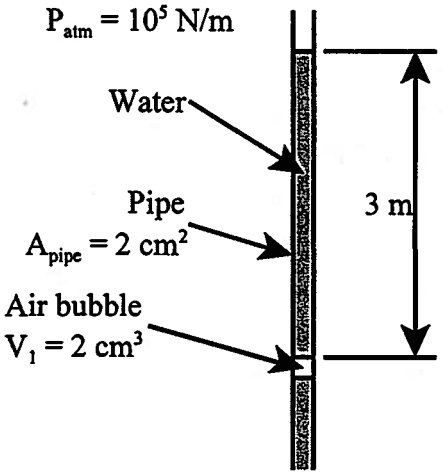

Figure 5E.6

Solution: If we model the air as an ideal gas, the volume after the heat transfer process can be determined from the property constitutive relation. Since the pressure is constant, we have

$$V_2 = V_1 \frac{T_2}{T_1} = (2 \text{ x } 10^{-6} \text{ m}^3)\left(\frac{323.15 \text{ K}}{363.15 \text{ K}}\right) = 1.78 \text{ x } 10^{-6} \text{ m}^3$$

Since the column of water above the air bubble imposes a constant pressure on the bubble as it

experiences quasi-static heat transfer with the surroundings, we can model the process experienced by the air as a quasi-static, constant pressure process. Then the heat transfer can be determined from equations (5.65) and (5.66).

$$(Q_{1-2})_{\substack{reversible\\const.press.}} = mc_P(T_2 - T_1) = m(c_v + R)(T_2 - T_1) = \frac{P_1V_1}{RT_1}(c_v + R)(T_2 - T_1)$$

$$(Q_{1-2})_{\substack{reversible\\const.press.}} = \frac{(P_{atm} + \rho gh)V_1}{RT_1}(c_v + R)(T_2 - T_1)$$

$$(Q_{1-2})_{\substack{reversible\\const.press.}} = \frac{[10^5\ \text{N/m}^2 + (10^3\ \text{kg/m}^3)(9.81\ \text{m/sec}^2)(3\ \text{m})](2 \times 10^{-6})}{(287\ \text{J/kg K})(363.15\ \text{K})} \cdot (716\ \text{J/kg K} + 287\ \text{J/kg K})(323.15\ \text{K} - 363.15\ \text{K})$$

$$(Q_{1-2})_{\substack{reversible\\const.press.}} = -0.09965\ \text{J}$$

where the negative sign indicates that the heat transfer is from the air bubble into the environment. The work transfer is given by equation (5.67).

$$(W_{1-2})_{\substack{reversible\\const.press.}} = P(V_2 - V_1)$$

$$(W_{1-2})_{\substack{reversible\\const.press.}} = [10^5\ \text{N/m}^2 + (10^3\ \text{kg/m}^3)(9.81\ \text{m/sec}^2)(3\ \text{m})](1.78\ \text{m}^3 - 2\ \text{m}^3)$$

$$(W_{1-2})_{\substack{reversible\\const.press.}} = -0.0285\ \text{J}$$

where the negative sign indicates that the work transfer is into the air bubble from the water.

5.5.2.5 Polytropic process in an ideal gas: We have just examined the thermodynamic details of four different quasi-static processes in an ideal gas. We note that each of these processes follows a sequence of equilibrium states that can be easily depicted on the *P-V* plane. The general form is

$$PV^n = \text{constant} \tag{5.72}$$

where the value of the constant depends upon the property that is unchanged by the energy interactions that occur during the process. Specifically,

constant pressure process: $n = 0$

constant temperature process: $n = 1$

constant entropy process: $n = c_P / c_v$, $1.67 > n > 1$

constant volume process: $n = \infty$

As an example of the differences amongst these various paths, consider Figure 5.17. All processes start out in the same initial state, and with the exception of the constant volume process, end up at the same final volume $V_2 = 4V_1$. Note the differences in slopes of the various paths. For the constant entropy process, the value of the exponent n is largest for monatomic gases and decreases to a limiting value of unity as the molecular structure of the gas becomes more complex. That is, for a diatomic gas, the value of n is smaller than for a monatomic gas but larger than for a triatomic gas and so on. Thus the path of the constant entropy process approaches that of the constant temperature process as the gas molecule becomes more complex. For these more complex molecules, thermodynamic coupling is weaker than in the simpler molecules for which the only means of energy storage in the coupled form, i.e., internal energy, is in the kinetic energy of the individual molecules that make up the gas. For the more complex gas molecules, energy also can be stored as internal energy in the various rotational and vibrational modes of the molecule.

For the quasi-static, polytropic process in the ideal gas model, the work transfer for an infinitesimal change of state is given by

$$(\delta W)_{\substack{quasi\\static}} = PdV$$

and since $PV^n = P_1V_1^n = P_2V_2^n$, the work transfer for a quasi-static, finite change of state becomes

$$(W_{1-2})_{\substack{quasi\\static}} = \int_{V_1}^{V_2} PdV = \frac{1}{1-n}(P_2V_2 - P_1V_1) \tag{5.73}$$

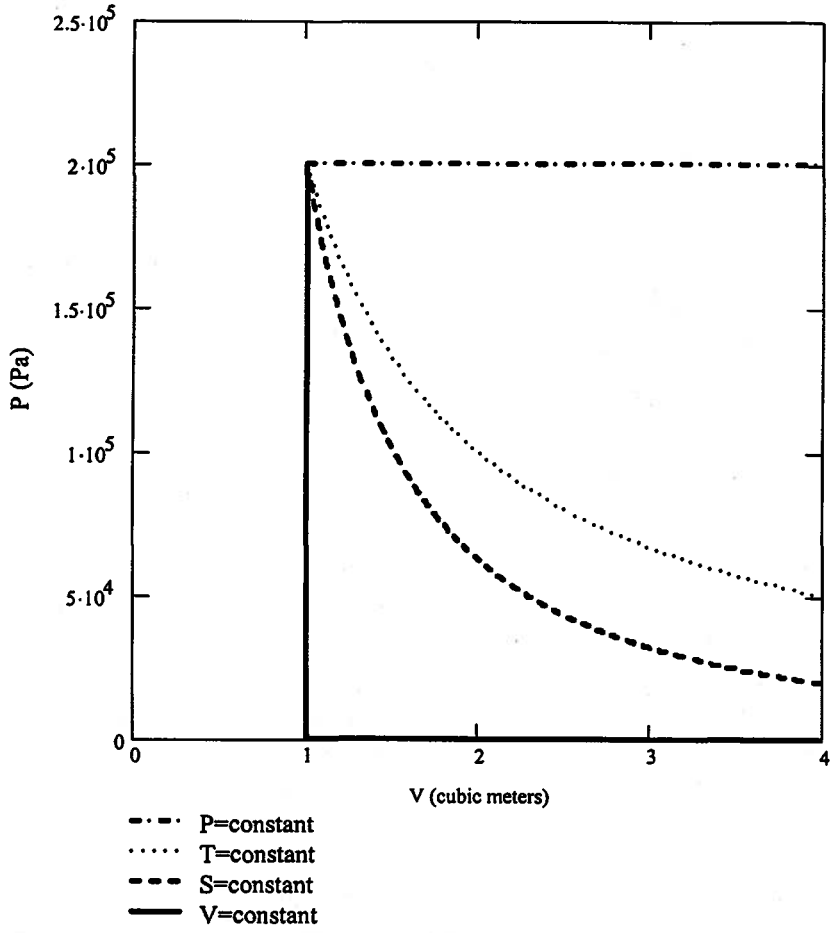

Figure 5.17 Paths of Quasi-static Thermodynamic Processes in an Ideal Gas

In the case of $n = 1$, equation (5.73) becomes indeterminate and by applying L'Hospital's Rule reduces to

$$(W_{1-2})_{\substack{quasi-static\\isothermal}} = mRT\ln\left(\frac{V_2}{V_1}\right)$$

which is identical to equation (5.35). For the corresponding heat transfer for the quasi-static process, equation (5.73) or (5.35) can be substituted into the first law.

5.6 Quasi-static, Irreversible Heat Transfer to an Ideal Gas at Constant Volume

We now take up the case of a process that is quasi-static but irreversible. Consider an ideal gas that has experienced a reversible adiabatic expansion from some initial state V_0 to some other

state 1 with a larger volume V_1. It is evident from equation (5.47) that in state 1, the gas temperature T_1 will be lower than the temperature of the gas in the initial state ($T_1 < T_0$). If we now place the gas in thermal communication with a heat reservoir at the original temperature T_0, the gas will experience a heat transfer and change temperature to state 2 where T_2 is the original temperature, T_0. Suppose that we require the gas to experience this heat transfer while its volume remains constant. That is, let the gas return to T_0 from T_1 by a process for which the work transfer is zero. Furthermore, let this heat transfer process occur at such a rate that the rate at which energy enters the system from the heat reservoir is much slower than the rate at which the energy redistributes itself inside the system. Then the process will be quasi-static within the system boundary, and the state of the system can be described by the equilibrium properties at all times. That is, the temperature of the gas will be spatially uniform at all times but will be changing with time as the energy interaction is occurring. Physically, this means that the principal resistance to heat transfer (a concept to be discussed in detail in Chapter 6) lies outside the system boundary.

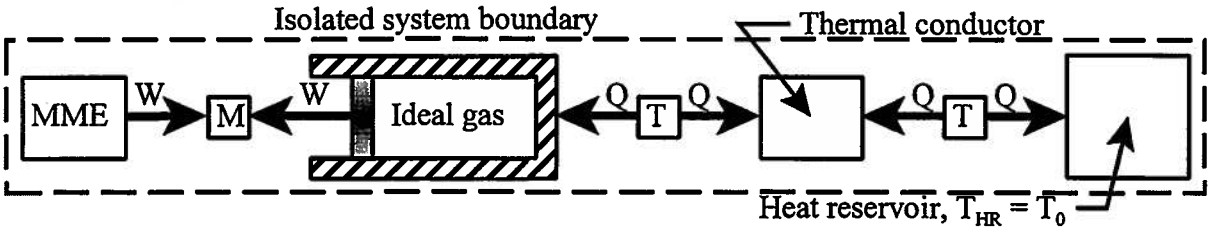

Figure 5.18 Heat Transfer to an Ideal Gas at Constant Volume

In a practical sense, this situation could be realized by placing an intermediate system of low thermal conductance (high thermal resistance) between the ideal gas and the heat reservoir. The interaction diagram for this configuration is shown in Figure 5.18. The mechanical matching element is used to change the temperature of the ideal gas from T_0 to T_1 by means of a reversible adiabatic process that displaces the piston and produces a volume change from V_0 to V_1. The piston is then locked in position and the mechanical interconnection between the mechanical matching element and the gas is switched off. The gas is then placed in thermal communication with the heat reservoir via the thermal conductor. The temperature of the gas then changes from T_1 back to T_0 by means of a simple heat transfer process in which the temperature at each end of the thermal conductor is identical to the temperature of the system in contact with it by virtue of the high thermal resistance of the thermal conductor. As we will see in Chapter 6, this means that there is a gradient in temperature within the thermal conductor.

For the process from state 1 to state 2 in which the volume of the gas is constant, the first law for the gas gives

$$(Q_{1-2})_{gas} = U_2 - U_1 = mc_v(T_2 - T_1) = mc_v(T_0 - T_1)$$

The first law for the heat reservoir becomes

$$(Q_{1-2})_{HR} = -(Q_{1-2})_{gas} = mc_v(T_1 - T_0)$$

Since $V_1 = V_2$ and $T_2 = T_0$, the entropy constitutive relation for the gas becomes

$$(S_2 - S_1)_{gas} = mc_v \ln\left(\frac{T_2}{T_1}\right) + mR\ln\left(\frac{V_2}{V_1}\right) = mc_v \ln\left(\frac{T_0}{T_1}\right)$$

Applying the second law to the heat reservoir, we get

$$(S_2 - S_1)_{HR} = (S_{tramsfer})_{HR} = \frac{(Q_{1-2})_{HR}}{T_{HR}} = \frac{mc_v(T_1 - T_0)}{T_0}$$

Applying the second law to the isolated system, we get

$$(S_2 - S_1)_{isolated} = (S_2 - S_1)_{gas} + (S_2 - S_1)_{HR} = mc_v \ln\left(\frac{T_0}{T_1}\right) + \frac{mc_v(T_1 - T_0)}{T_0} = S_{GEN} \qquad (5.74)$$

Let us define a new parameter S_{GEN}^* such that

$$S_{GEN}^* = \frac{S_{GEN}}{mc_v} = \ln\left(\frac{T_0}{T_1}\right) + \frac{T_1 - T_0}{T_0} = \frac{T_1 - T_0}{T_0} - \ln\left(\frac{T_1}{T_0}\right) \qquad (5.75)$$

If we let $\Delta T = T_1 - T_0$, equation (5.75) can be written

$$S_{GEN}^* = \frac{\Delta T}{T_0} - \ln\left(1 + \frac{\Delta T}{T_0}\right) \geq 0 \qquad (5.76)$$

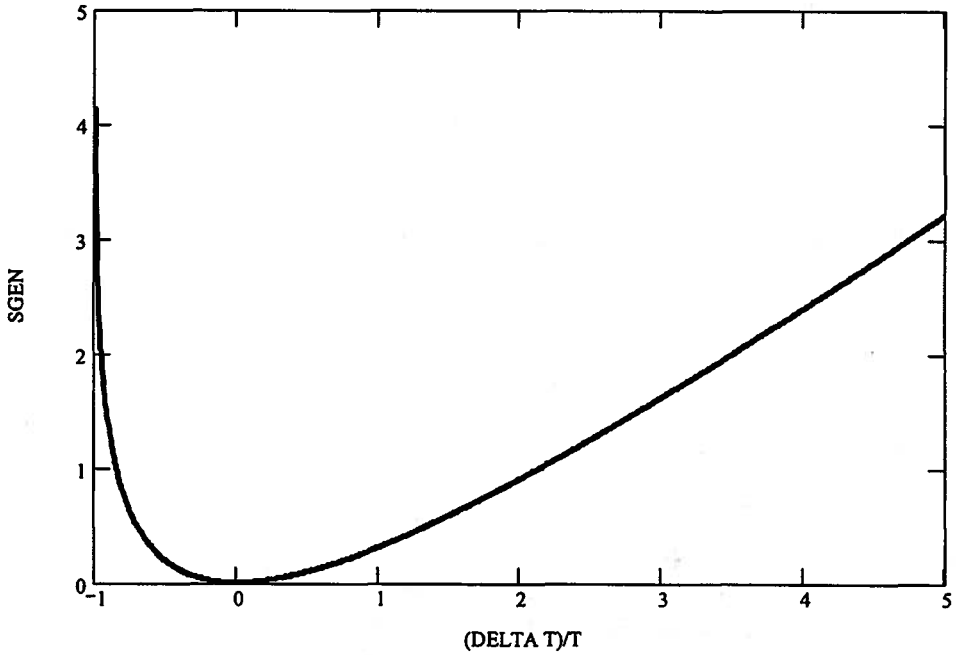

Figure 5.19 Entropy Generation by Simple Heat Transfer

If we plot the left-hand side of equation (5.76) versus $\Delta T/T_0$ as in Figure 5.19, we see that the change in entropy of the isolated system shown in equation (5.74) is indeed always positive and approaches zero only in the limit as ΔT approaches zero. Thus the quasi-static constant volume heat transfer process in the ideal gas is irreversible. The irreversibility lies in the heat transfer process in the thermal conductor as entropy is generated by the energy flowing down the temperature gradient. We shall examine this phenomenon in detail in Chapter 6.

There are two generalizations that follow from the analysis of this simple situation:

1. *All reversible processes are quasi-static, but not all quasi-static processes are reversible. Reversible processes are a subset of quasi-static processes.*

2. *Simple heat transfer through a finite temperature difference is irreversible.*

Note that the gas started out at the same temperature as the heat reservoir, and the mechanical matching element was used to change the temperature of the gas reversibly and adiabatically from this value to a lower value so that there then existed a temperature difference that would permit simple heat transfer between the gas and the heat reservoir. Thus, in state 1 the gas has the same entropy but a different temperature from state 0. In state 2, the gas has the same temperature as state 0 and the same volume as state 1.

5.7 Limitations Imposed by the Second Law of Thermodynamics on the Heat Transfer During a Change of State

In sections 5.5 and 5.6 we examined work transfer processes in a thermodynamically coupled thermal-fluid system, the ideal gas model. The coupled thermodynamic system possesses the unique ability to increase its stored energy by means of a positive heat transfer and then to decrease the stored energy by the same amount by means of a positive work transfer. However, in the general case, the positive work transfer that can occur during a change of state in a coupled system is limited by the second law of thermodynamics because the second law imposes limits on the heat transfer.

Equation (3.20) constitutes a valid statement of the second law of thermodynamics for a change of state. In effect, this equation establishes an upper limit on the entropy transfer for a given change of state. Further, with the addition of certain restrictions, this equation can be used to establish a limit on the heat transfer that a system can experience during a given change of state. For example, for an infinitesimal change of state by a reversible process which by definition generates no entropy, equation (3.20) can be written in the differential form

$$(\delta Q)_{reversible} = TdS \tag{5.77}$$

Integrating equation (5.77) for a reversible change of state from state 1 to state 2, we obtain the total heat transfer for that change of state.

$$(Q_{1-2})_{reversible} = \int_1^2 TdS \tag{5.78}$$

Clearly in carrying out the integration of equation (5.78) we must first establish the path connecting states 1 and 2. Graphically the integral in equation (5.78) is represented by the area between the path of the process and the abscissa on the temperature-entropy plane as is shown for path A in Figure 5.20. Since this area represents the heat transfer in a reversible process, the temperature-entropy diagram is useful for graphically illustrating the reversible processes. If some other reversible process proceeds from state 1 to state 2 along path B in Figure 5.19, then the area between this path and the abscissa, and the heat transfer $(Q_{1\text{-}2})_{rev\,B}$ will be larger for this new reversible process along path B than for the first reversible process along path A (shaded area in Figure 5.20). The sign convention for this graphical representation is such that the area, and hence the reversible heat transfer, is positive if the area lies to the right as we proceed from the initial state to the final state along the path of the process. When the area lies to the left as we proceed, its sign is negative.

In the case of an irreversible process between two end states, the second law of thermodynamics does not determine the heat transfer itself but rather the upper limit for the heat transfer. In fact this upper limit can be established only when the path of the irreversible process is known. Specifically, for an infinitesimal change of state by an irreversible process, equation (3.20) can be written in differential form

$$(\delta Q)_{irreversible} < TdS \tag{5.79}$$

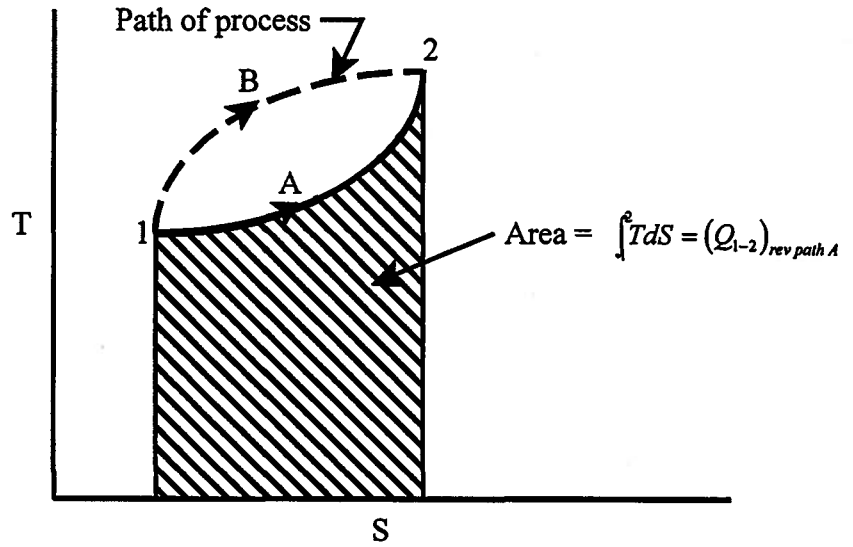

Figure 5.20 Graphical Representation of the Heat Transfer for a Reversible Process

If the path of the irreversible process by which the system changes state is known, equation (5.79) can be integrated.

$$(Q_{1-2})_{irreversible} < \int_1^2 TdS \tag{5.80}$$

Equation (5.80) can be used only for irreversible processes that proceed through states with identifiable temperature and entropy. Also, it follows from equation (5.80) that the heat transfer for an irreversible process cannot be represented graphically by the area between the path of the process and the abscissa on a temperature-entropy diagram. For a reversible process connecting the same two end states along the same path as the irreversible process of equation (5.80), we can combine equations (5.78) and (5.80). Thus,

$$(Q_{1-2})_{irreversible} < (Q_{1-2})_{reversible} \tag{5.81}$$

Equation (5.81) can be used only to compare the heat transfer for reversible and irreversible processes along the same path.

There are many interesting and physically important applications of equations (5.78) and (5.80), but several merit special attention. For example, consider the case of a system experiencing an isothermal change of state. The path for such a process, be it reversible or irreversible, is one of constant temperature. Then, the integrals in equations (5.78) and (5.80) become especially simple and the heat transfer must be of such a magnitude that

$$(Q_{1-2})_{isothermal} \leq T(S_2 - S_1) \tag{5.82}$$

where equality holds only in the case of a reversible isothermal process.

As another, somewhat different example of the limitations imposed by the second law of thermodynamics on heat transfer, consider the case of a system that experiences heat transfer with a single heat reservoir. If we establish an isolated system by setting a boundary that includes both the system and the heat reservoir, we can apply the second law of thermodynamics in the form of equation (3.1). Then

$$(S_2 - S_1)_{isolated} \geq 0 \tag{5.83}$$

Since the entropy is an extensive property, we can write

$$(S_2 - S_1)_{isolated} = (S_2 - S_1)_{system} + (S_2 - S_1)_{HR} \tag{5.84}$$

Then combining equations (5.83) and (5.84), we get

$$(S_2 - S_1)_{system} \geq -(S_2 - S_1)_{HR} \tag{5.85}$$

For the heat reservoir, the second law becomes

$$(S_2 - S_1)_{HR} = \frac{(Q_{1-2})_{HR}}{T_{HR}} \tag{5.86}$$

Since the isolated system is adiabatic, we have

$$(Q_{1-2})_{isolated} = (Q_{1-2})_{system} + (Q_{1-2})_{HR} \tag{5.87}$$

Then

$$(Q_{1-2})_{system} = -(Q_{1-2})_{HR} \tag{5.88}$$

and equation (5.86) becomes

$$(S_2 - S_1)_{system} \geq \frac{(Q_{1-2})_{system}}{T_{HR}} \tag{5.89}$$

Then the second law limit on the heat transfer for this system in communication with a heat reservoir becomes

$$(Q_{1-2})_{system} \leq T_{HR}(S_2 - S_1)_{system} \tag{5.90}$$

where equality holds only in the case of a reversible process.

5.8 Limitations Imposed by the Second Law of Thermodynamics on the Work Transfer During a Change of State

The limit that the second law of thermodynamics places on the heat transfer during a given process may be combined with the first law of thermodynamics to establish a limit for the work transfer during a given process. As with the heat transfer, the upper limit on the work transfer between two states is not established until the path followed during the change of state is established or other equivalent restrictions are imposed.

Consider first the case of a reversible process. From the first law of thermodynamics, equation (2.3), we have

$$(W_{1-2})_{rev} = (Q_{1-2})_{rev} - (U_2 - U_1) \tag{5.91}$$

Substituting equation (5.78) into equation (5.91), we obtain

$$(W_{1-2})_{rev} = \int_1^2 TdS - (U_2 - U_1) \tag{5.92}$$

Thus once the path of a reversible process between two given states is specified, equation (5.78) establishes the heat transfer and the first law of thermodynamics establishes the work transfer. In other words, the specification of the path of a process and the fact that it is reversible are sufficient to completely establish all thermodynamic information about the process, interactions included.

In the case of an irreversible process, however, a great deal more information is necessary. From the first law of thermodynamics, equation (2.3), we have

$$(W_{1-2})_{irrev} = (Q_{1-2})_{irrev} - (U_2 - U_1) \tag{5.93}$$

Substituting equation (5.80) into equation (5.93), we obtain

$$(W_{1-2})_{irrev} < \int_1^2 TdS - (U_2 - U_1) \tag{5.94}$$

Thus in the case of an irreversible process, specification of the path connecting two given end states is not sufficient to establish the interactions with the environment. Some other means must be used to determine the heat transfer and the work transfer. Given only the path and the end states, the first and second laws of thermodynamics only establish the upper limits for these interactions in the case of an irreversible process.

The limits on the work transfer can also be established for the special cases considered in section 5.7. For the isothermal process, the heat transfer is given by equation (5.82) which can also be written in the form

$$(Q_{1-2})_{isothermal} \le (TS)_2 - (TS)_1 \tag{5.95}$$

since the temperature is constant. The first law of thermodynamics, equation (2.3), can be written in the form

$$(W_{1-2})_{isothermal} = (Q_{1-2})_{isothermal} - (U_2 - U_1) \tag{5.96}$$

Combining equations (5.95) and (5.96), we obtain

$$(W_{1-2})_{isothermal} \le -\left[(U - TS)_2 - (U - TS)_1\right] \tag{5.97}$$

The combination of properties U - TS is itself a property called the *Helmholtz free energy* of the system and is denoted by the symbol F. Then equation (5.97) can be written

$$(W_{1-2})_{isothermal} \le -(F_2 - F_1) \tag{5.98}$$

The physical interpretation of equation (5.98) is that in a reversible isothermal process, the work transfer from the system will be given by the decrease in the property F. For this restricted class of processes (isothermal) the decrease in F is the amount of energy which is "free" to be extracted as a work transfer. In any real (irreversible) isothermal process, the work transfer from the system will be less than this limiting reversible work transfer.

Equation (5.98) is most useful for systems which are considerably more complex than the systems which we have considered. It is especially useful for systems with coupling between the thermal, mechanical, electrical, and chemical properties as occurs, for example, in an electrolytic cell. In this case the work transfer in equation (5.98) includes electrical work transfer as well as mechanical work transfer.

An even more restricted class of processes than those just considered is the isothermal process at constant pressure. Obviously this class of processes can occur only in complex systems in which more properties than just the pressure and temperature are required to fix the state of the system. An electrolytic cell would be such a system. For this class of processes, equation (5.98) must apply; however, the uniformity of pressure allows us to evaluate separately that part of the work transfer that results from the motion of the boundary against the constant pressure. The work transfer is then

$$(W_{1-2})_{isothermal} = (W_{1-2})_{\substack{isothermal \\ non\ PdV}} + P(V_2 - V_1) \tag{5.99}$$

When we combine equations (5.98) and (5.99), we get

$$(W_{1-2})_{\substack{isothermal \\ non-PdV}} \le -\left[(U + PV - TS)_2 - (U + PV - TS)_1\right] \tag{5.100}$$

The combination of properties ($U + PV$ - TS) is itself a property, called the *Gibbs free energy,* of the system and is denoted by the symbol G. Then equation (5.100) can be written

$$(W_{1-2})_{\substack{isothermal \\ non\ PdV}} \le -(G_2 - G_1) \tag{5.101}$$

The physical interpretation of equation (5.101) is that in a reversible isothermal process which is also a constant pressure process, the work transfer not associated with the boundary displacement will be given by the decrease in the property G. For example, in an electrolytic cell operating at constant T and P, the amount of energy which is "free" to produce an electrical work transfer will be given by the decrease in the Gibbs free energy for the process. In the real (irreversible) case, the electrical work transfer will be less than this reversible work transfer.

Consider once again the case of a system that can experience heat transfer with a single heat reservoir. This situation is physically important because quite often engineering systems are in thermal communication with only the atmosphere which is often modeled as a heat reservoir. in equation (5.90) we have already established the limit on the heat transfer for this case. Substituting this result into the first law of thermodynamics, equation (2.3), we obtain

$$W_{1\text{-}2} \leq -\left[(U - T_{HR}S)_2 - (U - T_{HR}S)_1\right] \tag{5.102}$$

Here T_{HR} is the thermodynamic temperature of the heat reservoir and $W_{1\text{-}2}$ is the total work transfer from the system as it changes from state 1 to state 2 by any process involving a heat transfer with a reservoir at T_{HR}. Obviously, when the system is continuously in thermal equilibrium with the heat reservoir, equations (5.102) and (5.97) are identical since the temperatures of the system and the reservoir are identical.

If in addition to being in thermal communication with the heat reservoir, the system is immersed in an atmosphere at a uniform pressure P_{atm}, then part of the work transfer $W_{1\text{-}2}$ in equation (5.102) will be associated with the motion of the boundary of the system against the pressure of the atmosphere. Since the work transfer to the atmosphere cannot usually be used to any advantage, we may think of the total work transfer as the sum of a useful work transfer and the work transfer associated with the displacement of the atmosphere. Thus,

$$W_{1\text{-}2} = (W_{1\text{-}2})_{useful} + P_{atm}(V_2 - V_1) \tag{5.103}$$

Combining equations (5.102) and (5.103), we obtain

$$(W_{1\text{-}2})_{useful} \leq -\left[(U + P_{atm}V - T_{atm}S)_2 - (U + P_{atm}V - T_{atm}S)_1\right] \tag{5.104}$$

Since the atmosphere will usually also serve as the heat reservoir, atmospheric temperature has replaced the temperature of the heat reservoir. The combination of properties $(U + P_{atm}V - T_{atm}S)$ is itself a property of the system-atmosphere combination which we denote by the symbol Φ. Then equation (5.104) can be written

$$(W_{1\text{-}2})_{useful} \leq -(\Phi_2 - \Phi_1) \tag{5.105}$$

For the system-atmosphere combination, equation (5.105) establishes the limit on the useful work transfer for a given change of state as determined by the change in the property Φ. There is, however, a limit on the values assumed by the property Φ. For some particular state, necessarily one in which the pressure of the system is P_{atm} and the temperature of the system is T_{atm}, the property Φ assumes its minimum value Φ_{min}. Then, the change of state determined by $\Phi - \Phi_{min}$ represents the absolute maximum for the useful work transfer available from a given state of the system-atmosphere combination. Accordingly, Keenan[1] has defined a new property, called the *availability* and denoted by the symbol Λ, which represents the maximum useful work transfer available from a given state of a system-atmosphere combination. Thus,

---

[1] Keenan, J. H., *Thermodynamics*, John Wiley & Sons, New York, 1941, Chapter 17.

$$\Lambda = \Phi - \Phi_{min} \tag{5.106}$$

where for any given system-atmosphere combination Φ differs from Λ by a constant. Equation (5.106) can then be combined with equation (5.105) so that the useful work transfer for a particular change of state of the system-atmosphere is given by

$$(W_{1-2})_{useful} \leq -(\Lambda_2 - \Lambda_1) \tag{5.107}$$

The physical interpretation of equation (5.107) is that the useful work transfer from a reversible process in a system-atmosphere combination is given by the decrease in the availability of the system-atmosphere combination. An irreversible process between the same two end states for the system, but a different end state for the atmosphere, would have a smaller useful work transfer. Since the system-atmosphere combination constitutes an isolated system, the reversible process results in no generation of entropy; however, the irreversible process generates entropy. It is convenient, then, to think of the reduction in work transfer for the irreversible process as a "dissipation" of potentially useful work transfer due to entropy generation. The analogy with mechanical dissipation stemming from the generation of entropy in a mechanically dissipative process is obvious. If the output from the system-atmosphere were a pure conservative mechanical system as shown schematically in Figure 5.21, the increase in its energy from the work transfer interaction would be less in the irreversible case than in the reversible case by virtue of this "dissipation."

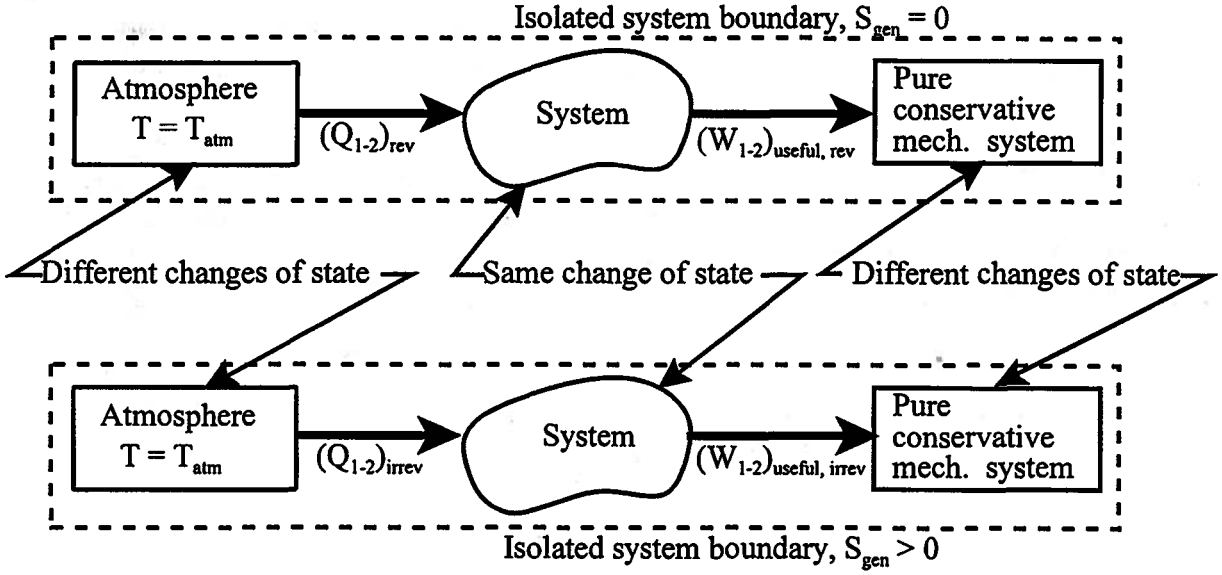

Figure 5.21 Reversible and Irreversible processes in a System-Atmosphere Composite

The difference between the reversible and irreversible useful work transfer for a given change of state is termed the *irreversibility, I,* of the irreversible process experienced by the system-atmosphere combination. Thus

$$I = (W_{1-2})_{useful, rev} - (W_{1-2})_{useful, irrev} \tag{5.108}$$

Regardless of the nature of the reversibility of the process, the first law for the system-atmosphere composite requires

$$-(W_{1-2})_{useful} = (U_2 - U_1)_{system} + (U_2 - U_1)_{atm} \tag{5.109}$$

but the system has the same change of state in the two cases. Then

$$I = (W_{1-2})_{useful, rev} - (W_{1-2})_{useful, irrev} = (U_2 - U_1)_{atm, irrev} - (U_2 - U_1)_{atm, rev} \tag{5.110}$$

For the constant temperature atmosphere, the second law requires

$$(U_2 - U_1)_{atm} = T_{atm}(S_2 - S_1)_{atm} \tag{5.111}$$

Then

$$I = T_{atm}\left[(S_2 - S_1)_{atm,\ irrev} - (S_2 - S_1)_{atm,\ rev}\right] \tag{5.112}$$

The second law for the isolated system in the reversible case requires

$$(S_2 - S_1)_{isolated} = (S_2 - S_1)_{system} + (S_2 - S_1)_{atm\ rev} = 0 \tag{5.113}$$

and the second law for the isolated system in the irreversible case gives

$$(S_2 - S_1)_{isolated\ irrev} = (S_2 - S_1)_{system} + (S_2 - S_1)_{atm\ irrev} = S_{gen} \tag{5.114}$$

Combining equations (5.113) and (5.114), we get

$$S_{gen} = (S_2 - S_1)_{atm\ irrev} - (S_2 - S_1)_{atm\ rev} \tag{5.115}$$

Then

$$I = (W_{1-2})_{useful,\ rev} - (W_{1-2})_{useful,\ irrev} = T_{atm}S_{gen} \tag{5.116}$$

For the same change of state in the system, all entropy generated by the irreversible processes in the system must be transferred to the atmosphere since the atmosphere is the only system that can experience an entropy transfer as a result of all irreversibilities. If we divide the system into subsystems and apply equation (3.20) to each subsystem, we can find the origin of the generated entropy and thus localize the loss of useful work with minimum calculation effort. The use of equation (5.104) or equation (5.108) to localize the irreversibility requires additional calculations.

Example 5E.7: In a particular automotive engine design, the cylinder contains gas at a pressure of 5 x 10^5 N/m^2 and a temperature of 1600 K at the end of the power stroke just prior to the opening of the exhaust valve. If the atmosphere is at a pressure of 10^5 N/m^2 and a temperature of 300 K, calculate the maximum useful work transfer that could be extracted from each kg of this "waste" gas. Assume that the gas can be modeled as an ideal gas with R = 0.287 kJ/kg K and c_v = 0.716 kJ/kg K.

Solution: We need to determine the maximum useful work that can be extracted from this gas as it attains thermal and mechanical equilibrium with the atmosphere. Thus, for the gas P_1 = 5 x 10^5 N/m^2 and T_1= 1600K; P_2 = 10^5 N/m^2 and T_2= 300 K. From the second law of thermodynamics,

$$Q_{1-2} \le T_{atm}(S_2 - S_1)$$

where from the entropy constitutive relation

$$S_2 - S_1 = m(R + c_v)\ln\left(\frac{T_2}{T_1}\right) - mR\ln\left(\frac{P_2}{P_1}\right)$$

$$S_2 - S_1 = (1\text{ kg})(287\text{ J/kg K} + 716\text{ J/kg K})\ln\left(\frac{300\text{ K}}{1600\text{ K}}\right) - (1\text{ kg})(287\text{ J/kg K})\ln\left(\frac{10^5\text{ N/m}^2}{5\text{ x }10^5\text{ N/m}^2}\right)$$

$$S_2 - S_1 = -1.2171\text{ x }10^3\text{ J/K}$$

Then

$$Q_{1-2} \le (300\text{ K})(-1.2171\text{ x }10^3\text{ J/K})$$

$$Q_{1-2} \le -3.6513\text{ x }10^5\text{ J}$$

The total work transfer for the gas is the sum of the useful work transfer and the work transfer to the atmosphere. Then

$$W_{1-2} = (W_{1-2})_{useful} + P_{atm}(V_2 - V_1)$$

where from the property constitutive relation

$$V_1 = \frac{mRT_1}{P_1} = \frac{(1\text{ kg})(287\text{ J/kg K})(1600\text{ K})}{5\text{ x }10^5\text{ N/m}^2} = 9.184\text{ x }10^{-4}\text{ m}^3$$

$$V_2 = \frac{mRT_2}{P_2} = \frac{(1\text{ kg})(287\text{ J/kg K})(300\text{ K})}{10^5\text{ N/m}^2} = 8.610\text{ x }10^{-4}\text{ m}^3$$

Then

$$W_{1-2} = (W_{1-2})_{useful} + (10^5\text{ N/m}^2)\left(8.610\text{ x }10^{-4}\text{ m}^3 - 9.184\text{ x }10^{-4}\text{ m}^3\right)$$

$$W_{1-2} = (W_{1-2})_{useful} - 5.74\text{ J}$$

Then from the first law of thermodynamics

$$W_{1-2} = Q_{1-2} - (U_2 - U_1) = Q_{1-2} - mc_v(T_2 - T_1)$$

or

$$(W_{1-2})_{useful} \le (5.74\text{ J}) - (3.65\text{ x }10^5\text{ J}) - (1\text{ kg})(716\text{ J/kg K})(300\text{ K} - 1600\text{ K})$$

$$(W_{1-2})_{useful} \le 5.6568\text{ x }10^5\text{ J}$$

Thus the maximum useful work transfer is 5.6568×10^5 J. This typical result for automotive engines reveals that a considerable amount of potential work transfer is being lost in the conventional exhaust process. For this reason, thermal-fluids engineers in the automotive industry have devoted much attention to turbo charging in recent years.

5.9 Entropy as a Measure of Dissipation

As we have seen in the foregoing discussions, the property entropy plays a pivotal role in determining the magnitudes of the heat transfer and work transfer that result when a system interacts with its environment. By generalizing our observations of the role of entropy during interactions between a system and its environment, we can formulate a macroscopic, physical interpretation of the property entropy. In general, when thermodynamic systems experience irreversible processes, their performance is degraded relative to the performance that they could have achieved had the processes been reversible. In effect, the system has "dissipated" some of its potential, and as shown in Example 5E.3, the entropy that is generated in these irreversible processes provides a quantitative measure of this "dissipation" of performance. We now elaborate on this concept by considering a more general example.

A piston-cylinder apparatus shown schematically in Figure 5.22 contains a gas that can be modeled as an ideal gas in the initial state T_1, P_1, and V_1. The gas is to experience an adiabatic expansion to some new volume V_2 with the objective of producing a positive work transfer. In order to understand the possible impact of any irreversibilities that might occur during the expansion, let us examine the behavior of the entropy of the gas under these conditions. The first law of thermodynamics gives

$$Q_{1-2} - W_{1-2} = U_2 - U_1 \tag{5.117}$$

Since the process is adiabatic, there is no heat transfer. Since the gas is ideal, we can substitute the energy constitutive relation for the energy change, and the first law reduces to

$$W_{1-2} = mc_v(T_1 - T_2) \tag{5.118}$$

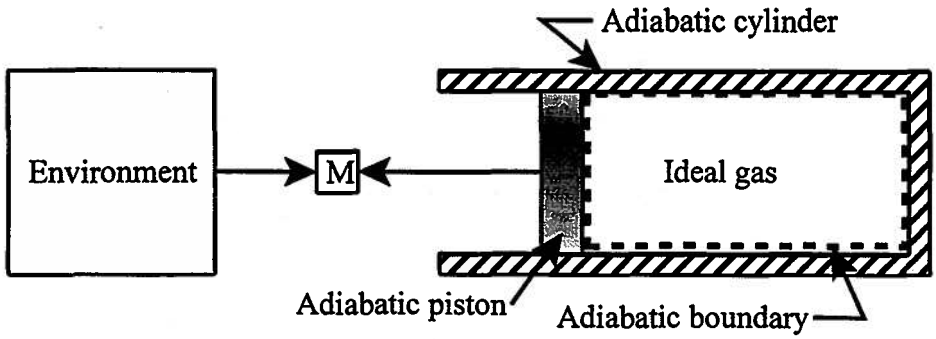

Figure 5.22 Adiabatic Expansion of an Ideal Gas

This result shows clearly that since T_1 is fixed and since the temperature of the gas will decrease as we expand the gas and take energy out of it as it does work against the environment, the maximum work transfer for these conditions will occur for the minimum value of T_2. We now show with the aid of the second law of thermodynamics that the lower bound on T_2 occurs for a reversible process. The general form of the second law for a closed system is

$$S_2 - S_1 = \int_{state\,1}^{state\,2} \frac{\delta Q}{T} + S_{gen} \tag{5.119}$$

where the term on the left-hand side of equation (5.119) is the change of entropy of everything inside the system boundary and is calculated from the entropy constitutive relation for the system. The first term on the right-hand side of equation (5.119) is the entropy transfer across the system boundary associated with the heat transfer interaction. The second term on the right-hand side of equation (5.119) is the entropy generated inside the system boundary as a consequence of irreversible processes and is always positive or in the reversible limit equal to zero.

For the case at hand, the adiabatic boundary means that there is no heat transfer, and, hence, no entropy transfer across the system boundary. Thus the first term on the right-hand side of equation (5.119) vanishes. Then the only way that this adiabatic system can experience a change in entropy is by virtue of any irreversibilities that may occur during the process. (In fact this observation is true for *any* adiabatic process of *any* system.) Let us consider first the case of a reversible process for which $S_{gen} = 0$. Then according to equation (5.119) the entropy of the system is constant, but the entropy constitutive relation gives

$$S_2 - S_1 = mc_v \ln\left(\frac{T_2}{T_1}\right) + mR \ln\left(\frac{V_2}{V_1}\right) \tag{5.120}$$

Then since equation (5.119) reduces to $S_2 - S_1 = 0$, the entropy constitutive relation, equation (5.120), can be solved for the final temperature, $T_2 = (T_2)_{REV}$. Then

$$(T_2)_{REV} = T_1\left(\frac{V_1}{V_2}\right)^{\frac{R}{c_v}} \tag{5.121}$$

Then from equation (5.118), the work transfer for this reversible adiabatic expansion of an ideal gas becomes

$$(W_{1-2})_{\substack{REV \\ Q=0}} = mc_v\left[T_1 - (T_2)_{REV}\right] \tag{5.122}$$

with the final temperature given by equation (5.121).

To show that the reversible case gives the lower bound on T_2 which in turn will give the maximum value for W_{1-2} for a given value of V_2, consider the irreversible case for which $S_{gen} > 0$. Then for this adiabatic process, the second law, equation (5.119) reduces to

$$S_2 - S_1 = mc_v \ln\left(\frac{T_2}{T_1}\right) + mR \ln\left(\frac{V_2}{V_1}\right) = S_{gen} \tag{5.123}$$

where the final temperature now becomes $T_2 = (T_2)_{IRREV}$. From equation (5.121) we have a relation between the volume and the temperature in the reversible case, viz.

$$\frac{V_2}{V_1} = \left(\frac{T_1}{(T_2)_{REV}}\right)^{\frac{c_v}{R}} \tag{5.124}$$

Substituting equation (5.124) into equation (5.123) and solving for the final temperature in the irreversible case, we get

$$(T_2)_{IRREV} = (T_2)_{REV}\, e^{\left(\frac{S_{gen}}{mc_v}\right)} \tag{5.125}$$

Then the work transfer for the irreversible adiabatic expansion of an ideal gas becomes

$$(W_{1-2})_{\substack{IRREV \\ Q=0}} = mc_v\left[T_1 - (T_2)_{IRREV}\right] \tag{5.126}$$

where the final temperature is given by equation (5.125).

We can now determine the difference between two adiabatic expansions of an ideal gas that are identical except for the very important fact that one expansion is reversible while the other is reversible. Then combining equations (5.122) and (5.126), we get

$$(W_{1-2})_{\substack{REV \\ Q=0}} - (W_{1-2})_{\substack{IRREV \\ Q=0}} = mc_v\left[(T_2)_{\substack{IRREV \\ Q=0}} - (T_2)_{\substack{REV \\ Q=0}}\right] \tag{5.127}$$

Substituting equation (5.125) for the final temperature in the irreversible case, we get

$$(W_{1-2})_{\substack{REV \\ Q=0}} - (W_{1-2})_{\substack{IRREV \\ Q=0}} = mc_v(T_2)_{REV}\left[e^{\left(\frac{S_{gen}}{mc_v}\right)} - 1\right] > 0 \tag{5.128}$$

Thus, since $S_{gen} > 0$ and $mc_v > 0$, $(T_2)_{IRREV} > (T_2)_{REV}$ and the work transfer in the irreversible case is *always* less than the work the work transfer in the reversible case.

Since this reduction in the work transfer due to irreversibilities for the adiabatic processes is such a strong function of the entropy that is generated, it is often convenient to think of this situation in the sense that some of the work that could have been obtained by a reversible expansion was "dissipated" by the irreversibilities present in the irreversible expansion. This result can be generalized to any expansion process in any coupled thermodynamic system as follows:

> Due to the entropy generated in an irreversible process, the work transfer realized in an irreversible expansion will always be less than the work transfer that would have resulted if the expansion had been carried out in a reversible manner. In effect, some of the potential positive work transfer is "dissipated" internally to generate the entropy associated with the irreversibilities.

We shall show in Chapter 7 that this interpretation of the entropy is also valid for the case in which the system is experiencing a sequence of processes that form a cycle.

PROBLEMS

5.1 A channel with a width of 1 m normal to the page is closed at one end with a rigid sloping wall with slope as shown in Figure 5P.1. At the other end, the channel is bounded by a vertical wall that is free to move. This wall moves at a vanishingly slow rate (quasi-statically) so that the length of the channel is reduced from 11 m to 6 m.

(a) Determine the net force on the wall in the x-direction as a function of the wall position x measured relative to its initial position.

(b) Determine the work transfer from the mechanical matching element to the water by integrating the definition of the work transfer

$$W_{mme} = -\int_{x_1}^{x_2} F(x)dx$$

(c) How does this work transfer manifest itself in the water?

(d) Estimate the speed at which the wall can move and still have the quasi-static model be within one percent of the actual performance of the model. That is, calculate the speed that would be slow enough to justify using the quasi-static model.

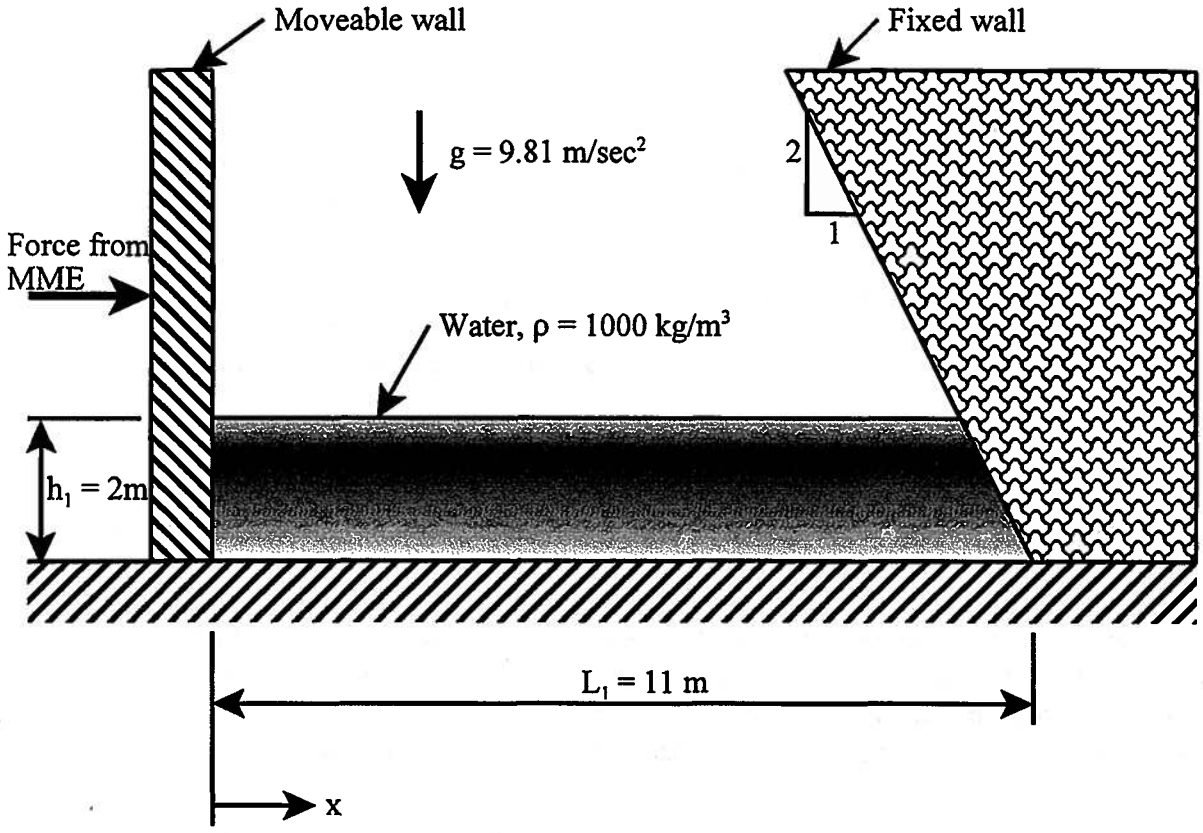

Figure 5P.1

5.2 As shown in Figure 5P.2, a vertical cylinder closed at the top end is connected to a mechanical matching element whose function is to provide precisely the correct force to maintain the cylinder in a state of mechanical equilibrium. This mechanical matching element is used to lower the cylinder to the surface of a very large body of water. When the lower end of the cylinder is in contact with the surface of the water, atmospheric air is trapped inside the cylinder. The pressure of the air inside the cylinder is increased by lowering the cylinder further while the trapped air is

in thermal and mechanical equilibrium with the air and water in the environment. The walls of the cylinder have negligible mass and thickness. The air can be modeled as an ideal gas with R = 287 J/kg K and c_v = 716 J/kg K. **(Note: L = 10 m and A = 0.1 m²)**

(a) Derive an expression for the height *h* in terms of the following: the pressure *P* of the air in the cylinder, the density of water ρ, gravity *g*, the length *L*, and the atmospheric pressure P_{atm}.

(b) Use this expression to calculate the value of *P* when $h = 0$.

(c) For the trapped air as a system, calculate the work transfer for the process from $P_1 = P_{atm}$ to $P_2 = P(h = 0)$.

(d) On a set of coordinates with *P* as the vertical axis and *V*, the volume of the air inside the cylinder at any instant of time as the horizontal axis, show the path of the process experienced by the trapped air. Pay careful attention to the shape of the path. Show states 1 and 2 on the path.

(e) Calculate the heat transfer experienced by the trapped air for this process.

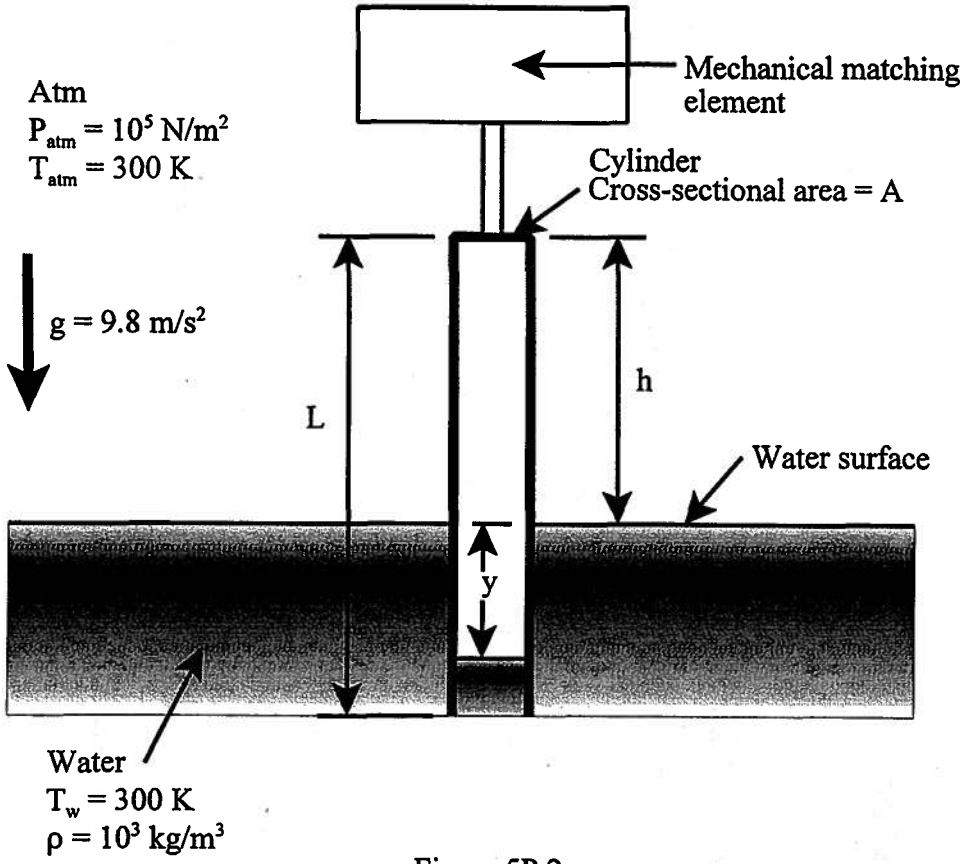

Figure 5P.2

5.3 As a design engineer for the U.S. Navy, you have been asked to design a cannon to be mounted on board a large ship. The cannon is to have a maximum range of 20 km with a projectile mass of 10^3 kg. The length of the barrel of the cannon is 20 m with a bore of 0.5 m. The projectile is propelled by the combustion of gun powder in a volume of the barrel behind the projectile. For the purposes of this analysis, assume that the combustion is instantaneous and produces a high pressure gas that forces the projectile out of the barrel as the gas expands. In designing the barrel for adequate strength, we need to know the maximum pressure of this gas necessary to achieve the projectile performance objectives. Model the propellant gas as an ideal gas with the characteristics of air. Assume that the gas expands to atmospheric pressure by the time the projectile leaves the barrel. If the volume of the gases behind the projectile at the end of

combustion is cylindrical with D = 0.5 m and L_0 = 1 m, use an appropriate model for the expansion of the propellant gas to estimate its maximum pressure.

5.4 The objective here is to examine the difference between a quasi-static process connecting two states and a non-quasi-static process connecting the same two states.

A. Consider first the quasi-static process. As shown in the Figure 5P.4a, a piston-cylinder apparatus is connected to a mechanical matching element that operates so that the piston is always in a state of mechanical equilibrium regardless of its position. The cylinder is filled with air that can be modeled as an ideal gas. In the initial state, $P_1 = 2 \times 10^5$ N/m^2, $T_1 = 300$ K, and $V_1 = 1$ m^3. The air is in thermal communication with a heat reservoir with $T_{HR} = 300$ K. Through the action of the mechanical matching element, the piston is withdrawn at a rate which is slow relative to the rate at which thermal equilibrium is established between the air and the heat reservoir. Thus, the expansion process can be modeled as a series of states all with the same temperature, 300 K. The expansion process continues until the pressure of the gas is reduced to $P_2 = 1 \times 10^5$ N/m^2.

(a) For the air as a system, calculate the following: V_2, T_2, $Q_{1\text{-}2}$, $W_{1\text{-}2}$, $S_2 - S_1$, $S_{transfer}$, and S_{gen}.

B. Consider the non-quasi-static process. As shown in Figure 5P.4b, the piston of the piston-cylinder apparatus is now fitted with a set of weights such that a gas pressure of 1×10^5 N/m^2 is required to maintain the piston in mechanical equilibrium. In the initial state, the air, which can be modeled as an ideal gas, has the following properties: $P_1 = 2 \times 10^5$ N/m^2, $T_1 = 300$ K, and $V_1 = 1$ m^3. In the initial position, the piston is held in mechanical equilibrium by means of a pin. The gas is initially in thermal equilibrium with a heat reservoir at $T_{HR} = 300$ K. The pin is removed and the gas seeks a new equilibrium state.

(b) For the gas as a system, calculate the following: V_2, T_2, $Q_{1\text{-}2}$, $W_{1\text{-}2}$, $S_2 - S_1$, $S_{transfer}$, and S_{gen}.

(c)Why do these two processes yield different results?

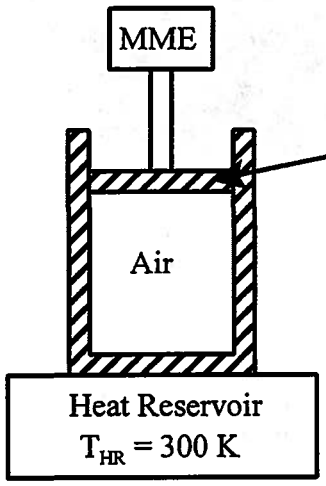

Figure 5P.4a

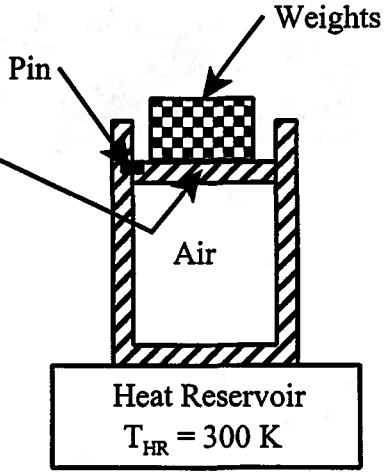

Figure 5P.4b

5.5 As shown in Figure 5P.5, 10 grams of air (modeled as an ideal gas) are confined in a piston-cylinder apparatus in which the cylinder is fabricated from a material whose thermal conductivity is infinite but whose outside surfaces are adiabatic. The piston is fabricated from a material whose thermal conductivity is zero. The cylinder can be modeled thermally as a pure thermal system with C = 10^3 J/kg K. Inserted in the gas through the cylinder wall is a paddle wheel which is

attached to a shaft. The shaft and the paddle wheel are fabricated from a material whose thermal conductivity is also zero. In the initial equilibrium state, the air, the piston-cylinder apparatus, and the paddle wheel are in a state of mechanical and thermal equilibrium at a pressure of $P_1 = 10^5$ N/m^2 and a temperature of $T_1 = 300$ K. The shaft is set rotating for a brief period of time and then stopped. After the system has reached a new equilibrium state, it is found that the piston is displaced upward a distance such that the volume has increased by 10 percent.

(a) What is the temperature and the volume of the air in the new equilibrium state?
(b) Calculate the work transfer interaction between the air and the paddle wheel.
(c) Calculate the heat transfer experienced by the air.
(d) Calculate the changes in entropy for the air and for the piston-cylinder apparatus.
(e) What is the entropy transfer for the air and for the cylinder?
(f) Is the work transfer process between the paddle wheel and the air reversible? Why?
(g) Is the work transfer process between the paddle wheel and the air quasi-static? Why?
(h) Is the work transfer process between the piston-weights and the air reversible? Why?
(i) Is the work transfer process between the piston-weights and the air quasi-static? Why?
(j) Is the heat transfer process between the air and the cylinder reversible? Why?

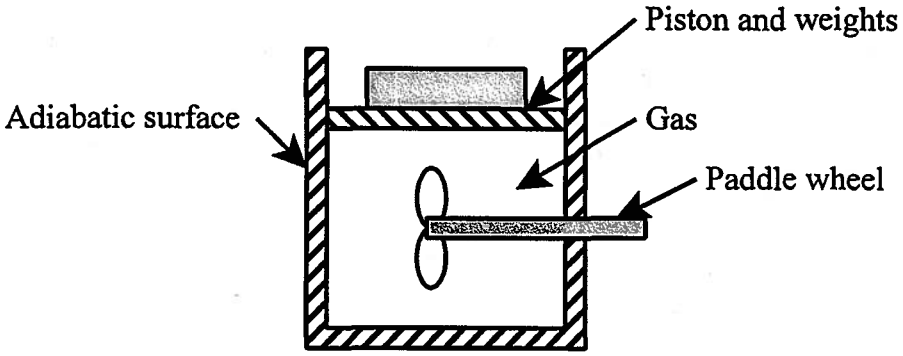

Figure 5P.5

5.6 As shown in Figure 5P.6, a piston-cylinder apparatus A is fitted with a piston that is in contact with a chain suspended from a fixed support. The pressure of the air confined in the apparatus is determined by the mass of the piston, the length of chain (mass/length = 10 kg/m) lying on top of the piston, and the area of the piston ($A_p = 0.05$ m^2). For example, if the piston moves up 1 m, the mass of chain lying on top of the piston increases by 10 kg and the pressure on the air increases by 1960 N/m^2. The air is in thermal communication with air contained in a similar piston-cylinder apparatus B that is connected to a mechanical matching element. As the mechanical matching element displaces piston B, gas A and gas B experience changes of state such that they are always in thermal equilibrium with each other. The only heat transfer experienced by the gases A and B is via the perfect thermal connection between them. Both pistons A and B are always in mechanical equilibrium regardless of their positions. The initial state of gas A is: $P_{1A} = 10^3$ N/m^2, $T_{1A} = 300$ K, $V_{1A} = 0.1$ m^3. Piston B is now displaced inward, and in response, piston A moves upward a distance of 0.5 m. The air can be modeled as an ideal gas.

(a) For gas A as a system, calculate the following: P_{2A}, T_{2A}, V_{2A}, $S_{2A} - S_{1A}$, $S_{transfer}$, S_{gen}.
(b) For gas A as a system, calculate: $W_{1\text{-}2}$ and $Q_{1\text{-}2}$.
(c) Was the process experienced by gas A reversible? Why?

5.7 One kg of air is confined within an adiabatic piston-cylinder apparatus as shown in Figure 5P.7. The volume contained within the cylinder between the two piston faces is divided into two compartments by a partition with a small hole. The initial state of the air, which can be modeled

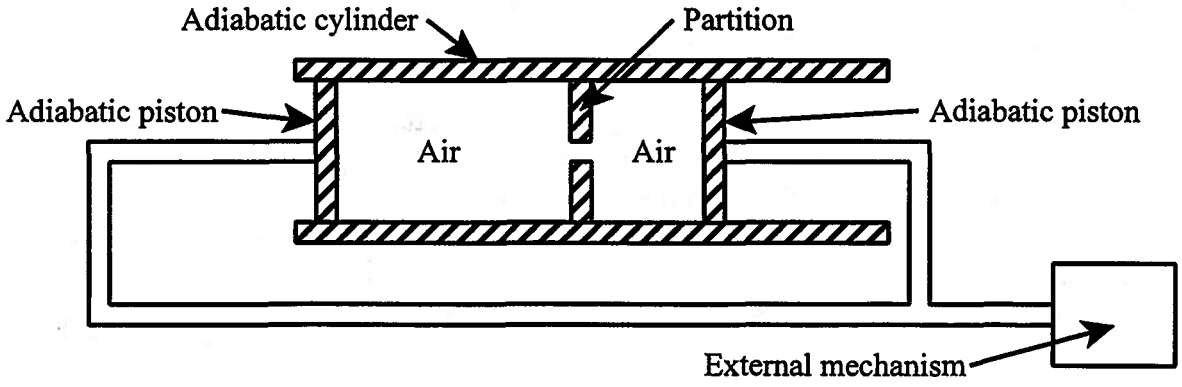

Figure 5P.7

as an ideal gas, is $P_1 = 1.4 \times 10^6$ N/m^2 and $T_1 = 350$ K. The two moveable pistons are clamped together so that when they move, the distance between the faces remains constant. An external mechanism is now connected to the pistons and moves the pistons through some distance. Observation of the mechanism reveals that a work transfer of $W_{1\text{-}2} = -33.9$ kJ was experienced by the air. After the pistons came to rest, the system returns to equilibrium.

(a) Determine the final state of the gas, P_2 and T_2.

(b) Was the work transfer process quasi-static? Why?

(c) Was the work transfer process reversible? Why?

5.8 One kg of air which can be modeled as an ideal gas is confined in a piston-cylinder apparatus by means of a frictionless piston as shown in Figure 5P.8. The gas is compressed quasi-statically so that thermal equilibrium is maintained between the gas and the piston-cylinder apparatus. The piston-cylinder apparatus is externally isolated so that there is no heat transfer between the piston-cylinder apparatus and the environment. The piston-cylinder apparatus has a mass of 2.5 kg and can be modeled as a pure thermal system with a specific heat of 1 kJ/kg K.

(a) If the initial state of the gas is an equilibrium state, determine the differential relationship between the pressure and volume of the gas for a quasi-static compression or expansion.

(b) Determine the integral form of the differential relation of part (a) above. That is, find $P = P(V)$.

(c) If the initial state of the gas is $P_1 = 1.8 \times 10^6$ N/m^2 and $T_1 = 300$ K, determine the final temperature of the complete system (consisting of gas and piston-cylinder apparatus) for a compression process by which the volume is reduced to one-half its original value, $V_2 = 0.5V_1$.

(d) What is the work transfer experienced by the gas for this process?

(e) What is the heat transfer experienced by the piston-cylinder apparatus for this process?

(f) What is the change in internal energy of the gas?

(g) Show that the process is reversible.

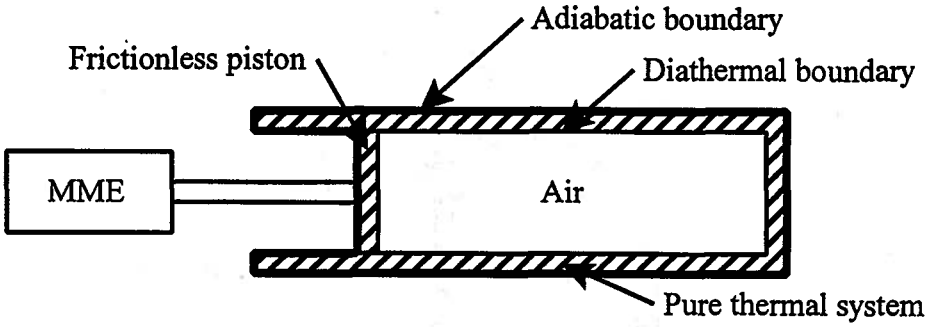

Figure 5P.8

5.9 A rigid, adiabatic, chamber is divided by a movable, adiabatic piston into two compartments of equal volumes as shown in Figure 5P.9. The piston, which moves without friction, is initially held in place with a pin. One compartment is filled with air at $P_1 = 6 \times 10^5$ N/m^2 and $T_1 = 25$ C while the other compartment is evacuated. Assume that the piston can be modeled as a solid body of zero mass. Also, assume that the air can be modeled as an ideal gas.

(a) Determine the final temperature T_2 of the air after the pin is removed and the system comes to equilibrium.

(b) What is the final pressure P_2 for this process?

(c) What is the work transfer $W_{1\text{-}2}$ for the air?

(d) Was the process experienced by the air quasi-static? Why?

(e) Prove by thermodynamic arguments whether the process experienced by the air was reversible or irreversible.

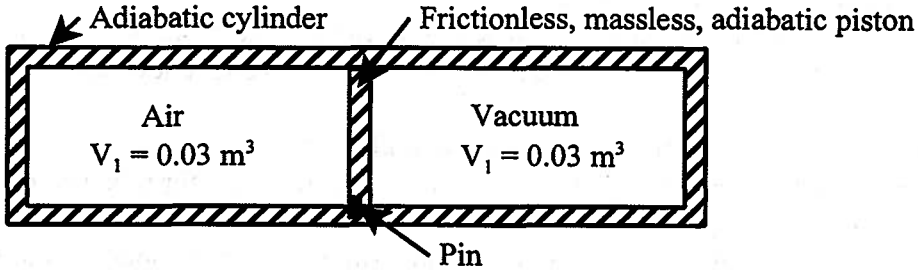

Figure 5P.9

5.10 A heavy piston encloses air within an adiabatic, vertical cylinder as shown in Figure 5P.10. The adiabatic piston, $m_{piston} = 10$ kg and $A_{piston} = 10$ cm^2, moves in the cylinder without leakage or friction. The initial equilibrium state of the air is $P_1 = 1.4 \times 10^5$ N/m^2, $T_1 = 300$ K and $V_1 = 100$ cm^3. Initially the piston must he held in place with a pin. The pin is removed and the piston moves until finally a new mutual equilibrium is established between the air and the piston. The air can be modeled as an ideal gas. For a system consisting of the air only:

(a) Determine the final pressure and temperature of the gas.

(b) Determine the heat transfer, $Q_{1\text{-}2}$, the work transfer, $W_{1\text{-}2}$, and the change in the internal energy, $U_2 - U_1$, for the process by which the air seeks a new equilibrium state.

(c) Can the process executed by the air be modeled as quasi-static? Why?

(d) Is the process executed by the air reversible or irreversible? Prove your answer.

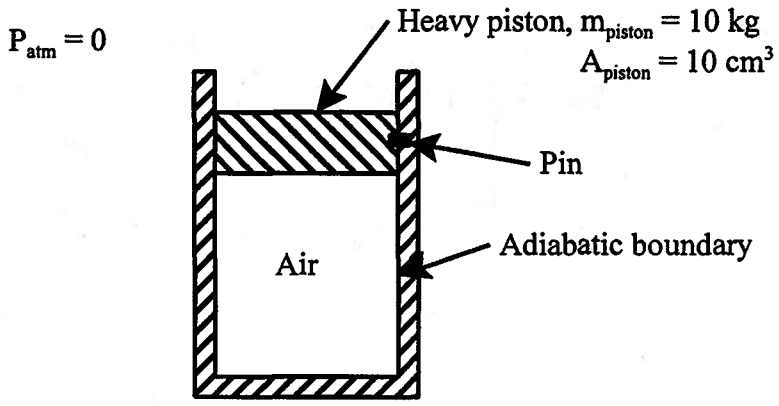

Figure 5P.10

5.11 As shown in Figure 5P.11, air is contained in a piston-cylinder apparatus which is also fitted with a damper. The following models can be used:

Air:	Ideal gas; $P_1 = 5 \times 10^4$ N/m^2, $T_1 = 350$ K
Damper:	Pure translational damper
Piston:	Rigid, frictionless piston with mass of 100 kg and a cross-sectional area of 0.01 m^2 and an initial height h_1 of 0.1 m
Cylinder:	Rigid
Gas-cylinder boundary:	Adiabatic
Gas-piston boundary:	Adiabatic
Gas-damper boundary:	Diathermal

The piston is initially held in mechanical equilibrium at the position $h_1 = 0.1$ m, by means of a pin. At some instant, the pin is removed and the piston comes to a new equilibrium position h_2.

(a) Determine the value of h_2 for this new equilibrium position.

(b) Determine the pressure, P_2, and temperature, T_2, of the air for this new equilibrium position of the piston.

(c) Was the process $h_1 \rightarrow h_2$ reversible or irreversible? Use the proper thermodynamic arguments to substantiate your answer.

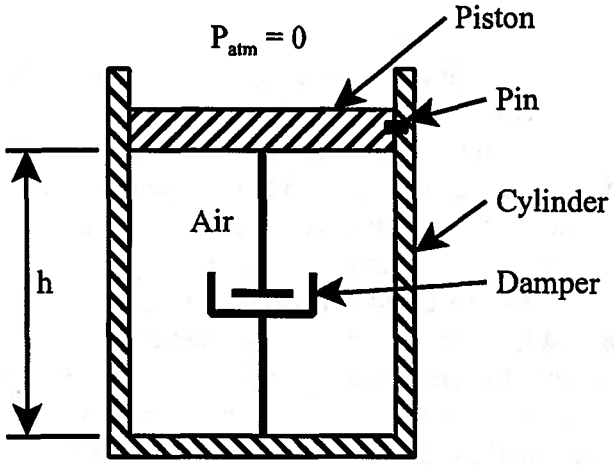

Figure 5P.11

5.12 An adiabatic tank *A* is connected to an adiabatic cylinder *B* through a valve and insulated line as shown in Figure 5P.12. The cylinder *B* is closed by a movable, frictionless, adiabatic piston of cross-sectional area 0.01 m^2. The mass of the piston is such that a pressure of 1.4×10^5 N/m^2 is

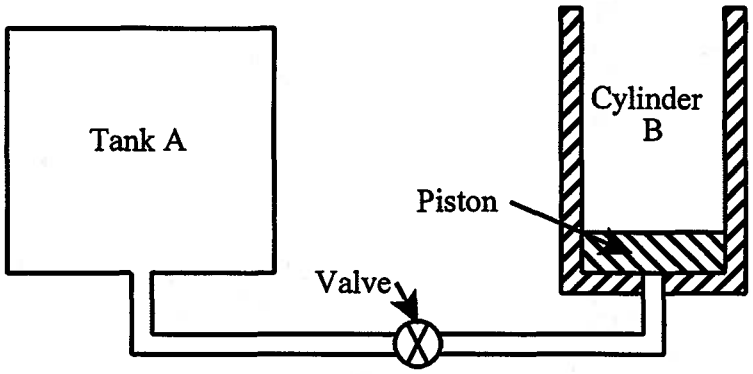

Figure 5P.12

required to support it alone. Atmospheric pressure is $P_{atm} = 10^5$ N/m^2. Initially tank *A* contains 1 kg of air at $P_{1A} = 1.4 \times 10^6$ and $T_{1A} = 40$ C. Assume the air can be modeled as an ideal gas. and that cylinder *B* is initially empty. The volume in the connecting tube is negligible. The valve in the tube is opened thereby allowing air to flow from *A* to B.

(a) Determine the final height of the piston B.

(b) Assuming all the gas is at the same final temperature determine the final temperature of the gas.

(c) Determine the work transfer to the piston.

(d) Determine by proper test whether the process of allowing the air to flow from the tank and into the cylinder is reversible or irreversible.

5.13 A rigid, insulated tank with a volume of 2 m^3 is initially evacuated and isolated from the environment by means of a valve. At some instant, the valve is opened and the tank fills with air from the atmosphere. When mechanical equilibrium is established between the contents of the tank and the environment, the valve is closed. (Note that since the rate at which mechanical equilibrium is established is orders of magnitude faster than the rate at which thermal equilibrium is established, the contents of the tank are not in thermal equilibrium with the environment when the valve is closed.) Atmospheric pressure is 10^5 N/m^2 and atmospheric temperature is 20 C. If the air can be modeled as an ideal gas, determine the final pressure and temperature of the air in the tank when the tank is full.

HINT: Approach this problem by considering a system consisting of the atmospheric air which will finally fill the tank. Since no mass crosses the system boundary, such a system can be regarded as a closed system. Carefully examine the system boundary for work transfer during the process of filling the tank.

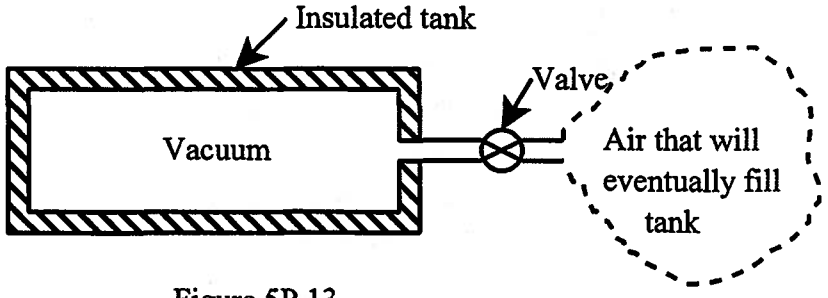

Figure 5P.13

5.14 Two vertical, well-insulated cylinders, *A* and *B*, closed on top by pistons, are connected through a tube with a valve as shown in Figure 5P.14. The pistons are loaded with weights such

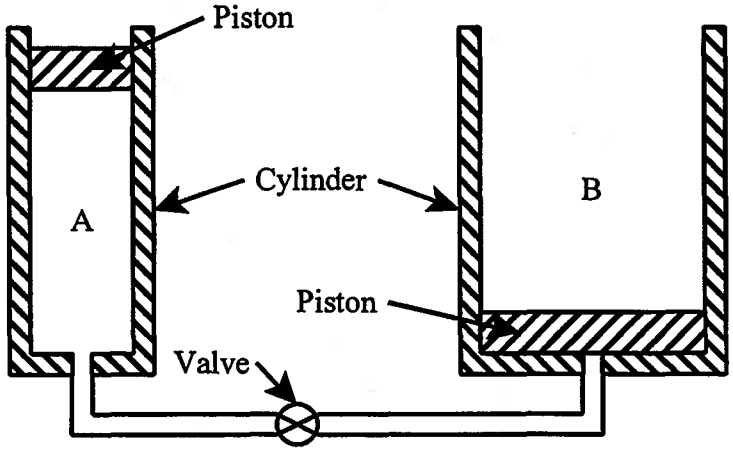

Figure 5P.14

that gas pressures of 1.4×10^6 N/m^2 and 1.4×10^5 N/m^2, respectively, are necessary to support the pistons. The cross-sectional areas of the pistons are 0.025 m^2 and 0.25 m^2, respectively. Initially cylinder *A* contains 0.4 kg of air, which can be modeled as an ideal gas, while cylinder *B* is empty. The initial temperature of the gas in cylinder *A* is 300 K.

The valve in the tube connecting the two cylinders is opened thereby allowing air to flow from *A* to *B*. The air attains mechanical equilibrium with the pistons before it reaches thermal equilibrium with the environment. This state of mechanical equilibrium is the final state of interest. The volume of the connecting tube is negligible.

(a) Determine the final height of the piston and weights in cylinder *B*.

(b) Determine the final temperature of the air in cylinder *B*.

(c) Determine the work transfer experienced by the air.

(d) Show by the proper thermodynamic arguments that the process is irreversible. What part of the process generates the entropy?

5.15 Consider a closed system of an ideal gas with constant specific heat c_v and gas constant *R*. Let the gas be in an initial state with a pressure P_1 and a volume V_1. Let the gas expand adiabatically to a new volume V_2. If the expansion is reversible, the final pressure and temperature after the expansion can be determined from the relation $P_1 V_1^{\gamma} = P_2 V_2^{\gamma}$. Let the values of the pressure and temperature so determined be P_{2r} and T_{2r}, respectively. If the expansion had been irreversible, the final pressure and temperature would have assumed the values P_{2i} and T_{2i}, respectively. Clearly, these values depend upon the work transfer out of the system during the expansion.

(a) Show that it is always true that $P_{2r} \neq P_{2i}$ and $T_{2r} \neq T_{2i}$.

(b) Decide by proper thermodynamic arguments whether

$$P_{2i} < P_{2r},\ P_{2i} > P_{2r},\ \text{or}\ \left[P_{2i} < P_{2r}\ \text{and}\ P_{2i} > P_{2r}\right]$$

(c) Decide by proper thermodynamic arguments whether

$$T_{2i} < T_{2r},\ T_{2i} > T_{2r},\ \text{or}\ \left[T_{2i} < T_{2r}\ \text{and}\ T_{2i} > T_{2r}\right]$$

(d) Show from the results to (a) through (c) above whether

$$(W_{1-2})_{rev} > (W_{1-2})_{irrev}\ \text{or}\ (W_{1-2})_{rev} < (W_{1-2})_{irrev}$$

5.16 As shown in Figure 5P.16, 5 gm of air is contained in a piston-cylinder apparatus. The cylinder is well-insulated and the piston is attached to a spring with a spring constant of $k = 2000$

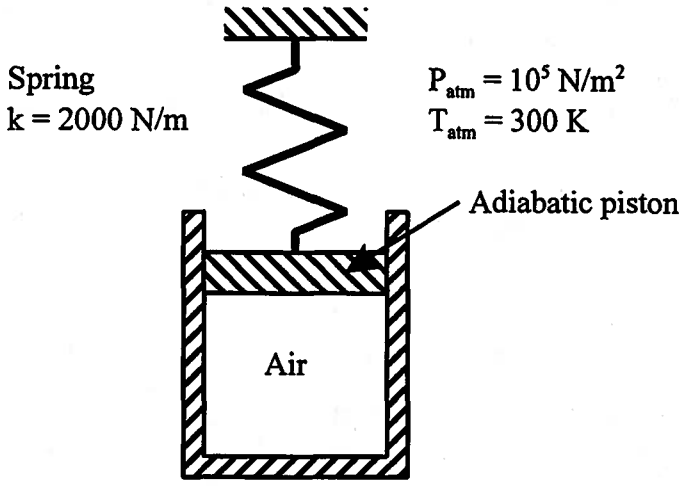

Figure 5P.16

N/m and a free length of 10 cm. Initially the piston is held in place by a pin with the air in an unknown initial state. For this initial condition, the length of the spring is $L_1 = 8$ cm. The pin is removed and the system comes to a new equilibrium state for which the spring has a new length of $L_2 = 5$ cm and the air is at a pressure of $P_2 = 1.1 \times 10^5$ N/m^2 and a volume of $V_2 = 4 \times 10^{-3}$ m^3. The piston has negligible mass and an area of 0.01 m^2. The atmosphere acting on the piston has a pressure of $P_{atm} = 10^5$ N/m^2 and a temperature of $T_{atm} = 300$ K. The air can be modeled as an ideal gas.

(a) Determine the initial state of the air, namely P_1, T_1, and V_1.

(b) How much entropy is generated in this process by which the air attains the final equilibrium state from the initial state? What is the source of the entropy generation?

5.17 As shown in Figure 5P.17, two adiabatic cylinders, each with a cross-sectional area of $A_c = 0.01$ m^2 and each containing helium gas, are allowed to communicate thermally via a copper thermal conductor connected between them. The heat capacity of this conductor is $C = 1000$ J/K. Cylinder A is fitted with a massless, adiabatic, frictionless piston supporting a mass of $M = 100$ kg. Cylinder B is fitted with two adiabatic, frictionless pistons, I and II, of negligible mass with the helium gas contained between them. Piston I is attached to a mechanical matching element (MME). The volume trapped between piston II and the end of the cylinder contains liquid mercury, $\rho_{Hg} = 13530$ kg/m^3. A small diameter tube of negligible volume connects the liquid mercury space to the back of the piston in cylinder A. As the pressure on the liquid mercury increases, the mercury flows out of the tube onto the piston and mass M in cylinder A, thereby increasing the total mass on the piston.

In the initial state, all materials are at the temperature of $T_1 = 300$ K. The mercury just fills the connecting tube to a height $h_{A1} = 10$ m. The initial height of the mercury in cylinder B is $h_{B1} = 0.5$ m. The initial volume of helium in cylinder A is $V_{A1} = 2$ m^3. The initial volume of helium in cylinder B is $V_{B1} = 1$ m^3.

(a) What are the pressures of the helium in cylinders A and B in the initial state, P_{A1} and P_{B1}?

(b) What are the masses of the helium in cylinders A and B, m_A and m_B?

The MME now displaces piston I very slowly until the pressure of the helium is 5 percent higher than it was in the initial state, i.e., $P_{B2} = 1.05P_{B1}$. The temperature of the helium in cylinders A and B, as well as that of the copper thermal conductor is uniform, but not constant, throughout this process. The pressure of the helium in each cylinder is spatially uniform throughout the process.

(c) What is the value of h_{B2}?

(d) What is the uniform temperature of the thermal conductor in the final state, T_2?

The helium can be modeled as an ideal gas with $R = 2078$ J/kg K and $c_v = 3153$ J/kg K. The acceleration of gravity is $g = 9.81$ m/sec^2.

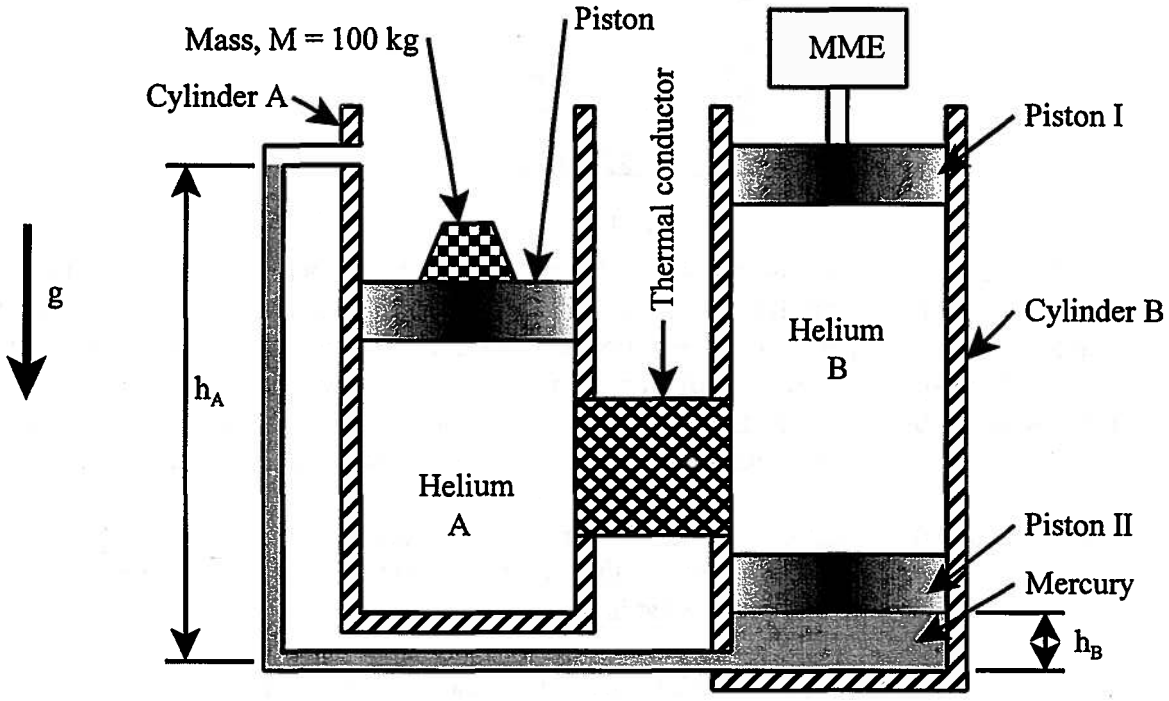

Figure 5P.17

CHAPTER 6

Heat Transfer Interactions in Thermal-Fluid Systems: An Introduction

6.1 Introduction

We now turn our attention to the development of the means to characterize the heat transfer interactions in thermal-fluid systems. Because the underlying physical phenomena are so complex, the heat transfer interactions are much more difficult to characterize than the work transfer interactions. In fact the complexity of heat transfer interactions is so great that we often have to rely upon empirical approaches guided by rather sophisticated analyses to reveal the underlying physical phenomena. For this reason we structure our study of heat transfer interactions so that we first consider the simpler aspects of the subject and then progress through the other aspects of the subject in order of increasing complexity. We begin our study with a brief introduction of the three modes of heat transfer: conduction, convection, and radiation. This is followed by a study of the concept of thermal resistance, a simple but powerful means of evaluating heat transfer interactions in a broad spectrum of physically important situations. Unfortunately, the thermal resistance concept sometimes oversimplifies the nature of the heat transfer interactions, and we are forced to resort to more elaborate approaches. These approaches will be developed in the context of the specific heat transfer modes which we shall study in the following order: conduction, convection, and radiation. We have specifically chosen this order because we need to develop first the relevant theories of thermodynamics and fluid mechanics that support these modes.

6.2 Modes of Heat transfer

As we have shown in Chapters 2 and 3, an interaction between two closed systems is a *heat transfer* if the interaction is solely the result of the temperature difference between the two systems. We have observed that in the course of this heat transfer interaction, both energy and entropy are transferred between the two interacting systems. For the purposes of analyzing the behavior of systems involved in heat transfer interactions, it is convenient to categorize the mode of energy transfer according to the mechanism by which energy and entropy is transported between the two interacting systems. Depending upon the physical mechanism that dominates the interaction, three distinct modes of heat transfer are recognized for this purpose: conduction, convection, and radiation. This is not to say that in every case there is a dominant mode of heat transfer. On the contrary, in general all three modes may be of equal importance in a given situation, but we can identify certain situations in which a single mode is dominant. For these cases, we can develop a method of analysis that will enable us to predict the response of a system to a temperature difference via that mode of heat transfer.

6.2.1 Conduction

The three phases of matter - gases, liquids, and solids - transfer energy by conduction in slightly different ways. In gases, energy is transferred from one location to another by virtue of the collisions between the gas molecules. Consider the following situation: two surfaces extending to infinity in all directions are separated from one another by a distance L and this intervening space is filled with a gas at some pressure P. One surface is at the higher temperature T_{hot} while the other surface is at the lower temperature T_{cold}. A gas molecule collides

with the high temperature surface and acquires some energy consistent with the principles of the conservation of energy and the conservation of momentum. The molecule carries this energy with it as it moves away from the surface. As we noted in Section 4.2, by virtue of the random motion of the gas molecules, the molecules eventually come under the influence of the long-range forces of attraction (known as van der Waals forces) that act between them. As two gas molecules are pulled together, they eventually come close enough that these intermolecular forces become repulsive in nature and their trajectories are deflected and a "collision" is said to occur even though the molecules never actually touch. During the collision, some energy is exchanged between the two molecules. This energy exchange process continues to occur as the original molecule collides with others and as other molecules that it has collided with collide with still others. Through this process of successive collisions, some energy from the high temperature surface eventually reaches the low temperature surface.

From a phenomenological point of view, this energy transfer process in the gas manifests itself as a temperature gradient in the gas with energy and entropy flowing down this gradient from the high temperature surface to the low temperature surface by the process known as heat conduction. The famous French mathematician and physicist Fourier (Jean Baptiste Fourier, 1768-1820) was the first to describe this phenomenon in quantitative terms. He proposed a phenomenological law that now bears his name, the Fourier Conduction Law, that states that the heat transfer rate, i.e. the energy flowing per unit time, $\dot{Q}$, is directly proportional to this temperature gradient and the cross-sectional area of the gas through which the energy is flowing, viz.

$$\dot{Q} = -kA\left(\frac{dT}{dx}\right) \tag{6.1}$$

where (dT/dx) is the temperature gradient and k is the constant of proportionality known as the thermal conductivity, a physical characteristic of the gas. The minus sign is necessary in order to make the value of the heat transfer positive for a negative temperature gradient.

For the case of a conduction path of constant cross-sectional area A and length L, fabricated from a material of fixed thermal conductivity k, we can integrate the Fourier Conduction Law from $x = 0$ where $T = T_1$ to $x = L$ where $T = T_2$, viz.,

$$\dot{Q}\int_0^L dx = -kA\int_{T_1}^{T_2} dT$$

or

Conduction!

$$\dot{Q} = \left(\frac{kA}{L}\right)(T_1 - T_2) \tag{6.2}$$

In the case of liquids, the mechanism of conduction is quite similar to that in gases except that the molecules are much closer together and the forces of attraction are much stronger. The net result is precisely the same as that for gases with the heat transfer rate given by the Fourier Conduction Law except that the values for the thermal conductivity of liquids are significantly larger than the values for gases.

For solids, the final result is that the heat transfer rate is once again given by the Fourier Conduction Law except that the values of the thermal conductivity for solids are typically much higher than the values for liquids. In the case of solids, however, the fundamental mechanism of conduction is somewhat different. Solids are more complex than gases or liquids because their molecules are arranged in a more orderly fashion called a lattice. The atoms are locked in the lattice by their van der Waals forces. The atoms in the lattice vibrate with a frequency proportional to the local temperature. Since the temperature varies along the lattice, this local vibration of these tightly coupled atoms is distributed in frequency with the higher frequency

modes excited in the regions of higher temperature. In some solids, such as metals, the electrons in the outer shells of the atoms are so loosely bound to their parent atoms that they can freely associate themselves with neighboring atoms. In effect, they become free to roam through the lattice, associating themselves first with one atom then another. As they move about through the lattice, the electrons transport energy in much the same manner as the molecules of a gas as they collide with the atoms of the lattice and other free electrons. In other solids such as insulators, there are no free electrons and the energy that enters the solid by conduction is taken up by increasing the amplitude of the lattice vibrations. This localized change in amplitude induces a change in the amplitude of neighboring atoms, and the energy of conduction propagates through the insulator as a lattice wave. Some representative values of thermal conductivity for typical engineering materials are given in Table 6.1.

Table 6.1
Thermal Conductivity of Sample Materials

Material	Thermal Conductivity, k (W/m K)
Copper	386
Aluminum	204
Brass (70% Cu, 30% Zn)	111
Mild steel	64
Stainless steel, 18-8	15
Mercury	8.4
Concrete	1.4
Pyrex glass	1.09
Water	0.611
Neoprene rubber	0.19
Engine oil, SAE 50	0.145
White pine, perpendicular to grain	0.10
Polyvinyl chloride (PVC)	0.092
Freon 12	0.071
Cork	0.043
Fiberglass (medium density)	0.038
Polystyrene	0.028
Air	0.027

From Mills, A.F., *Heat and Mass Transfer*, Richard D. Irwin, Inc., 1995, p. 10.

6.2.2 Convection

The transport of energy by convection is essentially a two-step process involving a moving fluid, either a liquid or a gas, in contact with a solid at some interface between them. In the first step, energy is exchanged between a particle of the fluid and the solid by the mechanism of conduction described above. The fluid particle then moves to another location either by virtue of the change in density of the fluid that results from the conduction process itself or by a work transfer involving some sort of shaft-work device such as a pump, a compressor, a blower, or a fan. As a consequence of the bulk motion of the fluid, the fluid particle comes into contact with additional fluid at some other location where energy exchange occurs once again. The difference between these two energy exchanges is that this second exchange of energy occurs between two quantities of fluid rather than between a quantity of fluid and the surface of a solid. Thus, for convection to occur, there must be a solid in contact with a fluid and the fluid must be in motion.

In the case of convection, the heat transfer rate can be calculated from Newton's Law of Cooling in which the rate of heat transfer is assumed to be proportional to the difference between the temperature of the surface and the temperature of the fluid (the "driving force" for heat transfer) and the area of the surface. Thus,

Convection! $\longrightarrow \dot{Q} = h_c A_s (T_s - T_\infty)$ (6.3)

where the heat transfer coefficient for convection, h_c, is a quantity that depends upon the nature of the flow field and the various temperatures of the participating media. The temperature T_s is the temperature of the solid surface and the temperature T_∞ is the temperature of the fluid at some specific location usually far removed from the surface.

Newton's Law of Cooling is not really a phenomenological law in the same sense as the first law of thermodynamics but rather is a definition of the convective heat transfer coefficient, h_c. It is deceptively simple in that the heat transfer coefficient depends upon whether the motion of the fluid is due to changes of density of the fluid derived from the heat transfer process itself (called *natural convection*) or due to the work transfer in some sort of shaft work machine (a process called *forced convection*). Furthermore, whether the convection process is natural or forced, the resulting heat transfer is highly dependent upon the nature of the fluid motion, i.e. whether the motion is *laminar* characterized by the smooth motion of one layer of fluid over another dominated by the viscosity of the fluid, or is *turbulent* characterized by the random motion of small parcels of fluid called eddies dominated by the inertia of the fluid itself. Some ranges of values for the convection heat transfer coefficient are presented in Table 6.2.

6.2.3 Radiation

The term "radiation" implies energy transfer by virtue of some sort of wave phenomenon. This energy can be due to a pressure wave such as in sound radiation from a loudspeaker, or it can be due to an electromagnetic wave such as in radio transmission. Thermal or heat radiation is virtually the same as radio transmission since the two depend upon the propagation of an electromagnetic wave. In fact, all forms of energy transmission by electromagnetic waves are identical in behavior since they can be described by the well-known Maxwell's Equations. The only difference among them is the wavelength or frequency of the radiation. In heat radiation, we are concerned primarily with wavelengths ranging from 0.1 to 100 μm (1 μm = 10^{-6} m). This range lies largely in the infrared region of the electromagnetic spectrum.

In heat radiation we are usually concerned with the energy transfer between two surfaces separated by either a vacuum or some medium transparent to the wavelengths of interest. This points to one of the significant differences between radiation and the other two modes of heat

Table 6.2
Typical Values of the Convective Heat Transfer Coefficient, h_c

Convection Configuration	Convection Heat Transfer Coefficient, h_c ($W/m^2 K$)
Natural convection, air	3 - 25
Natural convection, water	15 - 100
Forced convection, air	10 - 200
Forced convection, water	50 - 10,000
Forced convection, liquid sodium	10,000 - 100,000
Condensing steam	5,000 - 50,000
Boiling water	3,000 - 100,000

From Mills, A.F., *Heat and Mass Transfer*, Richard D. Irwin, Inc., 1995, p. 22.

transfer. Conduction and convection require the presence of a material medium for the transport of the energy from one system to another while radiation can occur between systems that have no connecting medium, i.e. are separated by a vacuum.

The energy that emanates from a surface during radiation heat transfer has its origins in the atoms or electrons that make up the surface. These microscopic particles are in motion and associated with that motion is energy. As the energy of motion changes through collisions or some other kinetic process, energy is given off in the form of electromagnetic waves. These waves carry energy through space by virtue of the oscillations of the electromagnetic field that permeates all space. These packets of energy can also be modeled as particles called *photons*. In order to characterize in analytical form the complex physical processes that produce the radiation emanating from a surface, we make use of a model known as the *blackbody*. This model will enable us to predict the behavior of radiating systems in thermodynamic terms.

For a given surface temperature, it can be shown from thermodynamic arguments that the blackbody emits the maximum amount of energy possible. It also absorbs all radiant energy incident upon it. In this sense, it is both the ideal emitter and the ideal absorber. In the late nineteenth century, Stefan and Boltzmann showed independently that the energy emitted per unit time per unit area into the half space bounding a blackbody surface at temperature T is given by

$$\frac{\dot{Q}}{A} = \sigma T^4 \tag{6.4}$$

where σ is the Stefan-Boltzmann radiation constant and $\sigma = 5.67 \times 10^{-8}$ W/m^2 K^4. This heat flux is commonly known as the blackbody emissive power. For the case of two blackbody surfaces, 1 and 2, exchanging energy by thermal radiation, the net heat flux between them is given by

$$\frac{\dot{Q}}{A} = \sigma T_1^4 - \sigma T_2^4 \tag{6.5}$$

Real surfaces emit only a fraction of the energy that blackbody surfaces do at the same temperature. To account for this, we make use of the concept of the emissivity, ϵ, which in effect is the emission efficiency of the surface measured against the blackbody standard. In general, the emissivity is a function of the temperature of the surface, the wavelength of the radiation, and the angle of the propagation vector of the emitted photon. In the simplest model of

a real emitting surface, the emissivity is assumed to be independent of these influences and is called a gray body with the value of ϵ fixed ($\epsilon < 1$). Real surfaces also absorb only a fraction of the energy that blackbody surfaces do, and to account for this, we make use of the concept of the absorptivity, α, which is an absorption efficiency measured against the blackbody standard. For the gray surface model, the value of α is fixed ($\alpha < 1$). In the context of the gray surface model, the values of α and ϵ are set for any given surface. Some approximate values for representative engineering surfaces are shown in Table 6.3. It can be shown from thermodynamic arguments that the emissivity and absorptivity of a gray surface are equal, i.e. $\epsilon = \alpha$. This is not true in general, however.

For a physical situation involving the transfer of energy by radiation between two gray surfaces, 1 and 2, the rate of heat transfer will depend upon the two temperatures T_1 and T_2 as well as the values of the emissivities ϵ_1 and ϵ_2 and the geometry of the two surfaces and their orientation to one another. All of these influences are incorporated into a single factor called the transfer factor, F_{12}. Thus for the rate at which energy that leaves surface 1 and is intercepted by surface 2, we have

$$\dot{Q}_{12} = A_1 F_{12}(\sigma T_1^4 - \sigma T_2^4) \tag{6.6}$$

where a great deal of information is contained in the transfer factor F_{12}. We are not yet in a position to calculate this quantity, but for the simple, yet common, situation of a small gray body in a large environment, i.e. area A_1 is small compared to area A_2, $F_{12} \approx \epsilon_1$ and the rate of energy transfer becomes

$$\dot{Q}_{12} = \varepsilon_1 A_1(\sigma T_1^4 - \sigma T_2^4) \tag{6.7}$$

Table 6.3
Total Hemispherical Emissivities of Sample Engineering Surfaces

Surface	Total Hemispherical Emissivity, ϵ
Aluminum alloy, unoxidized	0.035
Black anodized aluminum	0.80
Chromium plating	0.16
Stainless steel, type 312, lightly oxidized	0.30
Inconel X, oxidized	0.72
Black enamel paint	0.78
White acrylic paint	0.90
Asphalt	0.88
Concrete	0.90
Soil	0.94
Pyrex glass	0.80

From Mills, A.F., *Heat and Mass Transfer*, Richard D. Irwin, Inc., 1995, p.15.

Although this result is a gross simplification of a complex situation, it is often useful in

engineering practice.

With some rearrangement, equation (6.7) can be cast in a form similar to Newton's Law of Cooling, viz.,

$$\dot{Q}_{12} = \varepsilon_1 A_1 \sigma (T_1^2 + T_2^2)(T_1 + T_2)(T_1 - T_2) \tag{6.8}$$

where if $T_1 \approx T_2$, we can set $(T_1^2 + T_2^2)(T_1 + T_2) \approx 4T_m^3$ with $T_m = (T_1 + T_2)/2$. Then

$$\dot{Q} = \varepsilon_1 A_1 \sigma (4T_m^3)(T_1 - T_2) \tag{6.9}$$

and

Radiation! →

$$\dot{Q}_{12} \approx A_1 h_r (T_1 - T_2) \tag{6.10}$$

where $h_r = 4\epsilon_1 \sigma T_m^3$ and is called the radiation heat transfer coefficient. It is left as an exercise to show that the error associated with this approximation depends upon the temperatures T_1 and T_2.

6.3 Thermal Resistance

Upon inspection of the Fourier Conduction Law, Newton's Law of Cooling, and equation (6.10), we note that they all have a similar form, namely that they are an expression for a rate of energy transfer, $\dot{Q}$, equal to the product of a potential difference, $(T_1 - T_2)$, and a constant of proportionality, hA. This form bears a strong resemblance to Ohm's Law

$$I = \frac{\phi_1 - \phi_2}{\Re} \tag{6.11}$$

where the rate of charge transfer (current), I, is equal to the ratio of the electrostatic potential difference (voltage), $(\phi_1 - \phi_2)$, and a constant of proportionality, $\Re$, the resistance. Thus, by analogy we can write the expressions for the heat transfer rate in the steady state as

$$\dot{Q} = \frac{(T_1 - T_2)}{R_{th}} \tag{6.12}$$

where R_{th} is the thermal resistance. Thus, for steady state conduction heat transfer normal to a plane slab of thickness L, we have

$$R_{cond} = \frac{L}{kA} \tag{6.13}$$

and for convection heat transfer we have

$$R_{conv} = \frac{1}{h_c A} \tag{6.14}$$

and for radiation heat transfer

$$R_{rad} = \frac{1}{h_r A} \tag{6.15}$$

These resistances can be manipulated in precisely the same fashion as the electrical resistance. We can assemble series and parallel thermal resistance circuits to describe complex heat transfer configurations in the steady state, i.e. in situations for which the temperatures and rates of heat transfer do not change with time, involving multiple modes of heat transfer either in series or in parallel, or both. For example, consider the configuration shown in Figure 6.1. This situation is representative of a typical composite wall design frequently used in building construction. The wall is comprised of slabs of solid material placed face to face with convection

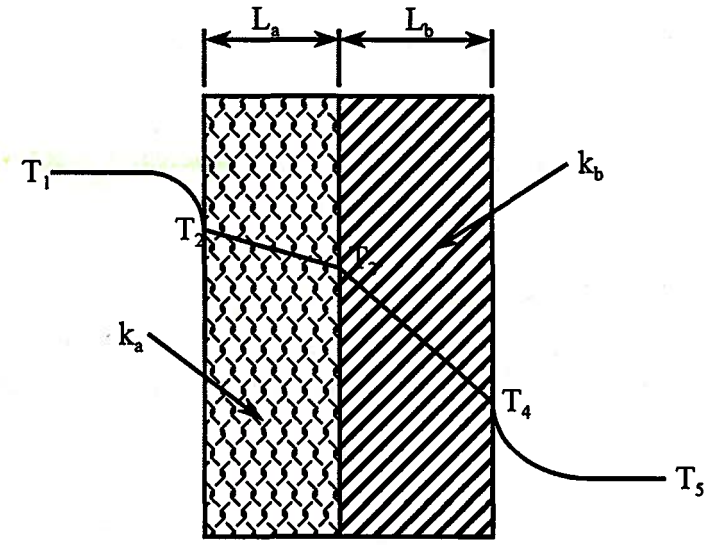

Figure 6.1 Section through Composite Wall

on one side, conduction through the composite solid, and convection and radiation on the other side. A fluid (air) at temperature T_1 is on one side of the wall with a fluid (air) at a temperature T_5 on the other side. Steady-state heat transfer through this composite wall can be analyzed easily with the aid of the thermal resistance concept and the associated thermal circuit shown in Figure 6.2.

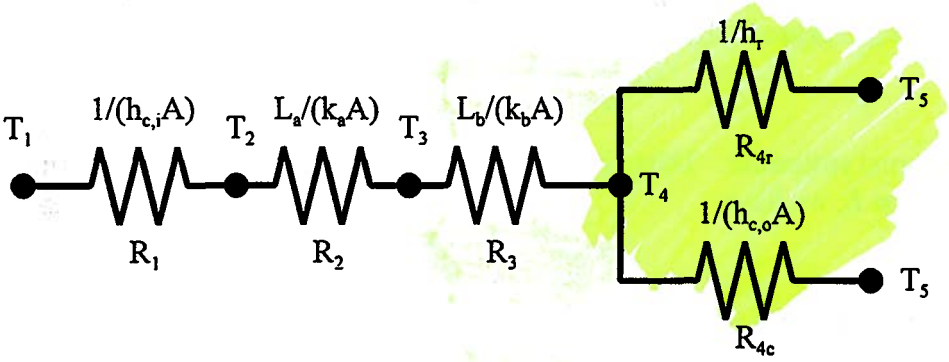

Figure 6.2 Equivalent Thermal Resistance Circuit

The temperature profile through the wall is shown in Figure 6.1 and is the result of energy flowing through the series of resistances R_1, R_2, R_3, and R_4 where

$$R_1 = \frac{1}{h_{c,i}A} \tag{6.16}$$

$$R_2 = \frac{L_a}{k_a A} \tag{6.20}$$

$$R_3 = \frac{L_b}{k_b A} \tag{6.21}$$

$$R_4 = \frac{R_{conv,o} R_{rad}}{R_{conv,o} + R_{rad}} = \frac{1}{h_{c,o} A + h_r A} \tag{6.22}$$

and we have assumed that the temperature of the surroundings for thermal radiation is the same as the temperature for convection. Thus

$$\dot{Q} = \frac{(T_1 - T_5)}{\sum_{i=1}^{4} R_i} \tag{6.23}$$

Example 6E.1: As shown in Figure 6E.1, a surface-mounted transistor is mounted on a printed circuit board (PCB) which is maintained at 35 C. The transistor which is 8 mm wide by 4 mm long is exposed to an air flow with a temperature of 25 C and a convection heat transfer coefficient of 50 W/m^2 K. The stagnant air gap (k_a = 0.0263 W/m K) between the transistor case and the PCB is 0.2 mm with the transistor supported on three current leads each having a cross-section of 1 mm by 0.25 mm and a length of 4 mm. The leads (k_l = 25 W/m K) are attached and thermally grounded to the transistor case on one end while the other end is thermally grounded and attached to the PCB. Model the transistor case as isothermal and assume that thermal radiation from the case is negligible. Estimate the temperature of the transistor case when the power dissipation in the transistor is 150 mW.

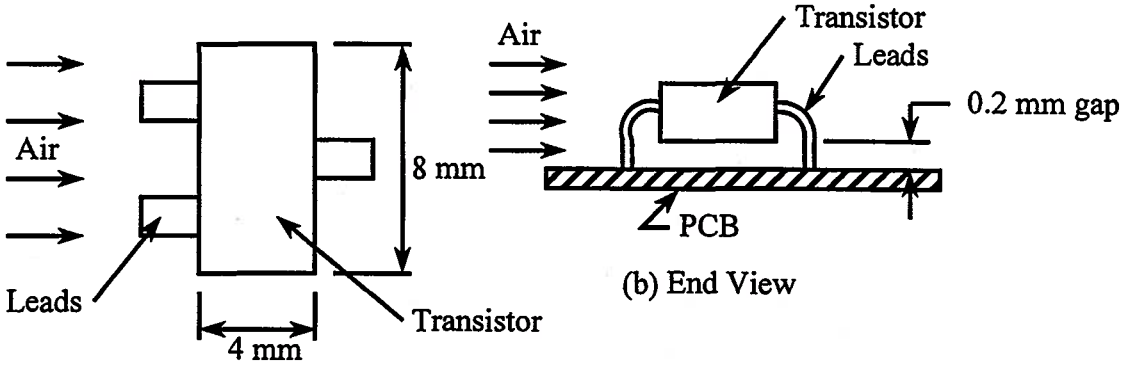

Figure 6E.1 Surface-mounted Transistor

Solution: This heat transfer configuration can be readily analyzed with the aid of the thermal resistance concept. To do this, it is first necessary to establish the various paths for heat transfer interactions between the transistor case and its environment. There are several:
(1) There is a conduction path from the case to the PCB via the three current leads. For each lead, this path has a thermal resistance given by

$$R_{lead} = \frac{L_{lead}}{k_{lead} A_{lead}} = \frac{4 \times 10^{-3} \text{ m}}{(25 \text{ W / m K})(10^{-3} \text{ m})(0.25 \times 10^{-3})} = 640 \text{ K / W}$$

Since there are three leads in parallel, the net resistance due to conduction through the leads is

$$R_{leads} = \frac{R_{lead}}{3} = 213.33 \text{ K / W}$$

(2) There is another conduction path via the stagnant air gap underneath the transistor. The resistance of this path is given by

$$R_{gap} = \frac{L_{gap}}{k_{air} A_{gap}} = \frac{0.2 \text{ x } 10^{-3} \text{ m}}{(2.63 \text{ x } 10^{-2} \text{ W / m K})(4 \text{ x } 10^{-3} \text{ m})(8 \text{ x } 10^{-3} \text{ m})} = 237.64 \text{ K / W}$$

(3) There is a convection path from the transistor case to the air flowing over the case. The resistance of this path is given by

$$R_{conv} = \frac{1}{h_c A_{top}} = \frac{1}{(50 \text{ W / m}^2 \text{ K})(4 \text{ x } 10^{-3} \text{ m})(8 \text{ x } 10^{-3} \text{ m})} = 625 \text{ K / W}$$

In drawing the thermal circuit for this configuration, we note that the three thermal resistances have a common terminal, namely the temperature of the case, but the two conduction resistances have their other terminal in common, namely the temperature of the PCB, while the convection resistance has its other terminal at the temperature of the air. Thus, the circuit would appear as follows:

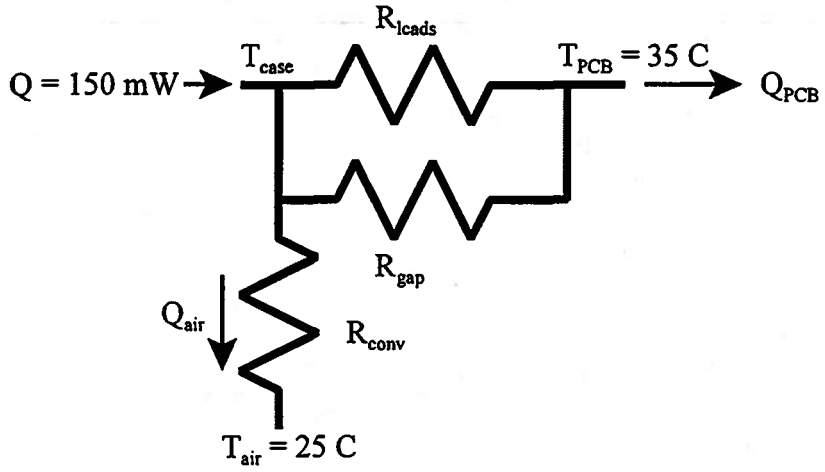

Since R_{leads} and R_{gap} are in parallel, the equivalent resistance is R_e which is given by

$$R_e = \frac{R_{leads} R_{gap}}{R_{leads} + R_{gap}} = \frac{(213.33 \text{ K / W})(237.64 \text{ K / W})}{(213.33 \text{ K / W}) + (237.64 \text{ K / W})} = 112.41 \text{ K / W}$$

Then

$$\dot{Q}_{total} = \dot{Q}_{air} + \dot{Q}_{PCB}$$

$$\dot{Q}_{total} = \frac{T_{case} - T_{air}}{R_{air}} + \frac{T_{case} - T_{PCB}}{R_e}$$

$$150 \text{ x } 10^{-3} \text{ W} = \frac{T_{case} - 25 \text{ C}}{625 \text{ K/W}} + \frac{T_{case} - 35 \text{ C}}{112.41 \text{ K/W}}$$

$$T_{case} = 47.8 \text{ C}$$

6.4 Conduction in Cylindrical Geometries

Many engineering systems employ cylindrical geometries such as tubes, pipes, and rods as part of their construction. In many of these situations, the heat transfer in these systems occurs in the radial direction. For example, a pipe is used to transport steam from a central location to local heat exchangers (such as the radiators in the classrooms on a university campus). The pipe must be insulated in order to minimize the heat transfer interaction radially outward between the

flowing steam and the air surrounding the pipe over the path of transport. If this were not done, the resulting heat transfer would cause the fluid would be too low in temperature by the time it reached the local heat exchanger thereby rendering it useless as a heat transfer medium. In order to design the appropriate insulation to minimize this radial heat transfer, we need to analyze heat transfer in a cylindrical geometry. In doing so, we must account for the fact that the area for energy flow increases with the radius.

Consider the case of a thick-walled cylinder as shown in cross-section in Figure 6.3. For

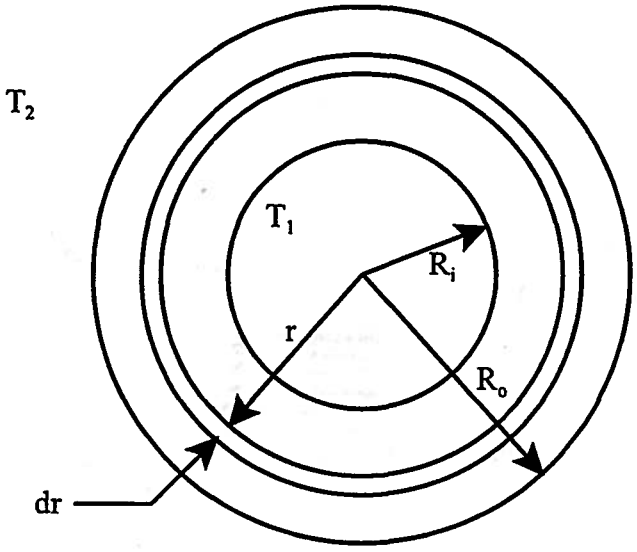

Figure 6.3 Radial Heat Transfer in a Cylinder

heat transfer in the radial direction, the same amount of energy passes through the cylindrical surface at $r + dr$ as passes through the cylindrical surface at r; thus, the rate of energy flow is independent of r. Then

$$\dot{Q} = \text{constant} \tag{6.24}$$

but from Fourier's Law of Conduction

$$\frac{\dot{Q}}{A} = -k\left(\frac{dT}{dr}\right) \tag{6.25}$$

But the surface area of a cylinder of length L is given by

$$A = 2\pi rL \tag{6.26}$$

where L is the length of the cylinder measured normal to the cross-section of Figure 6.3. Then

$$\dot{Q} = -2\pi rLk\left(\frac{dT}{dr}\right) \tag{6.27}$$

If k is independent of temperature, we can divide both sides of this equation by $2\pi kL$. Then

$$\frac{\dot{Q}}{2\pi kL} = -r\left(\frac{dT}{dr}\right) = \text{constant} = C_1 \tag{6.28}$$

We can write this expression in the form

$$\left(\frac{dT}{dr}\right) = -\frac{C_1}{r} \tag{6.29}$$

which can be integrated to give

$$T = -C_1 \ln r + C_2 \tag{6.30}$$

with boundary conditions $T(R_i) = T_1$ and $T(R_o) = T_2$. Then

$$\begin{aligned} T_1 &= -C_1 \ln R_i + C_2 \\ T_2 &= -C_1 \ln R_o + C_2 \end{aligned} \tag{6.31}$$

Solving equations (6.31) for C_1, we get

$$C_1 = \frac{T_1 - T_2}{\ln \frac{R_o}{R_i}} \tag{6.32}$$

Substituting this result into equation (6.28), we get

$$\dot{Q} = \frac{2\pi kL(T_1 - T_2)}{\ln \frac{R_o}{R_i}} \tag{6.33}$$

Then by virtue of our analogy with Ohm's Law, we can write the thermal resistance for conduction in the radial direction as

$$R_{th} = \frac{\ln \frac{R_o}{R_i}}{2\pi kL} \tag{6.34}$$

As an example of the application of this concept, consider the situation shown in Figure 6.4: an insulated pipe carrying a high temperature fluid like superheated steam with convection on the inside and convection and radiation on the outside.

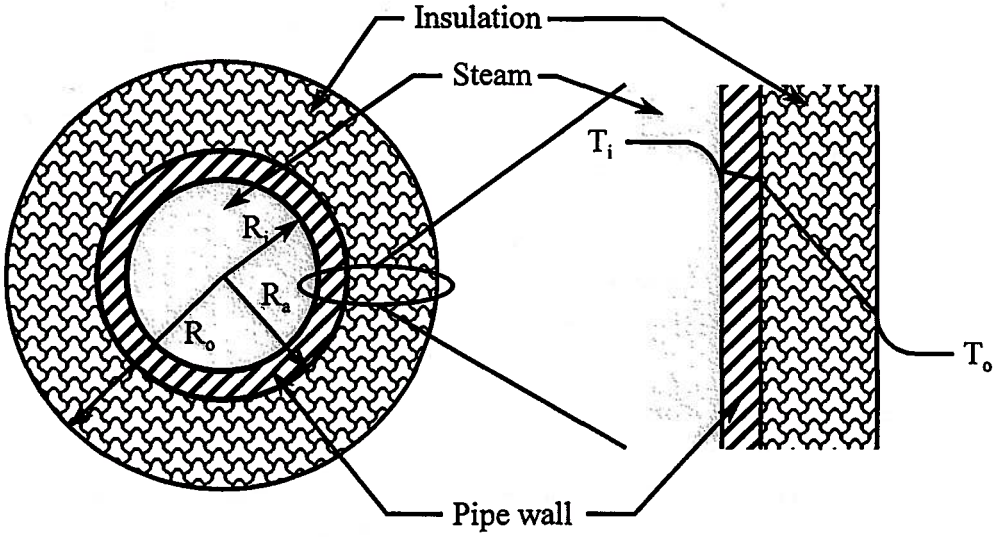

(a) crossectional view (b) temperature distribution

Figure 6.4 Insulated Steam Pipe

The thermal circuit of this composite cylinder is identical to the one shown in Figure 6.2 for a composite plane wall except that now the resistances are given by

$$R_1 = \frac{1}{h_{c,i} 2\pi R_i L} \tag{6.35}$$

$$R_2 = \frac{\ln \frac{R_a}{R_i}}{2\pi k_a L} \tag{6.36}$$

$$R_3 = \frac{\ln \frac{R_o}{R_a}}{2\pi k_b L} \tag{6.37}$$

$$R_4 = \frac{1}{(h_{c,o} + h_r) 2\pi R_o L} \tag{6.38}$$

Using this approach, we can formulate a Newton's Law of Cooling for this composite cylindrical geometry, viz.

$$\dot{Q} = \overline{U} A (T_1 - T_2) = \frac{(T_1 - T_2)}{\sum_{i=1}^{4} R_i} \tag{6.39}$$

where we have introduced the concept of the *overall heat transfer coefficient,* $\overline{U}$, and the *overall thermal conductance,* $\overline{U}A$, (which is defined as the reciprocal of the net thermal resistance for the heat transfer geometry at hand) becomes for this case in which all the thermal resistances shown in Figure 6.2 are in series

$$\frac{1}{\overline{U}A} = \sum_{i=1}^{4} R_i = \frac{1}{h_{c,i} 2\pi R_i L} + \frac{\ln \frac{R_a}{R_i}}{2\pi k_a L} + \frac{\ln \frac{R_o}{R_a}}{2\pi k_b L} + \frac{1}{(h_{c,o} + h_r) 2\pi R_o L} \tag{6.40}$$

Notice that in the rate equation, equation (6.39), since we always include the area in the form of the product $\overline{U}A$, it makes no difference which area is used, the outside area of the insulation or the inside area of the pipe. However, when the individual terms are separated out, the value of the factor $\overline{U}$ itself does depend upon the area chosen. When manufacturers cite data for the overall heat transfer coefficients for their heat transfer products, they include the specification for the area to be used in calculating the overall thermal conductance.

Example 6E.2: An example of radial heat transfer in cylindrical geometries that has great practical significance concerns the current carrying capabilities of electrical conductors such as those used in the electrical wiring of a home. The conductor, typically made of copper or aluminum, must be electrically insulated from its environment for safety reasons including prevention of injury from electrical shock and prevention of fire due to electrical breakdown of combustible building materials. However, the electrical insulation also acts as thermal insulation which can limit its ability to carry electrical current. The conductor has a finite electrical resistance, albeit a small one. This means that some of the electrical energy carried by the current will be dissipated in the conductor. Ultimately, this dissipated energy has to be conducted to the outer surface of the electrical insulation where it can be transferred to the environment by convection. For a given convective heat transfer coefficient between the outer surface of the insulation and the surrounding air, the magnitude of the dissipated energy that can be transferred in this fashion depends upon the outside diameter of the insulation. This, in turn, limits the amount of current that can be carried since the dissipated energy depends upon the square of the

current.

Consider the case of a 10 gage (American Wire Gage) copper conductor with a diameter of 2.588 x 10^{-3} m and a length of 1 m covered with Teflon© insulation (k_{teflon} = 0.45 W/m K). The heat transfer coefficient for convection at the outer surface is h_o = 16 W/m^2 K. The surroundings and ambient air are at a temperature of 295 K. The temperature of the conductor is 40 C (313). Plot the heat transfer through the insulation as a function of the outside radius of the insulation.

Solution: Since there are only two thermal resistances in the heat transfer path, resistance due to conduction through the insulation and resistance to convection off the outer surface, and since the temperatures of the environment and the conductor are known, we can write

$$\dot{Q} = \frac{(T_i - T_\infty)}{\sum_j R_j} = \frac{(T_i - T_\infty)}{R_{cond} + R_{conv}}$$

where if r_o is the outside radius of the insulation and r_i is the inside radius

$$R_{cond} = \frac{\ln \frac{r_o}{r_i}}{2\pi k L}$$

and

$$R_{conv} = \frac{1}{h_o 2\pi r_o L}$$

Then

$$\dot{Q} = \frac{(313\text{ K} - 295\text{ K})(2\pi)(1\text{ m})}{\frac{\ln\left(\frac{r_o}{1.294 \text{ x } 10^{-3}\text{ m}}\right)}{(0.45\text{ W/m K})} + \frac{1}{(16\text{ W/m K})r_o}}$$

This result can be plotted as shown below.

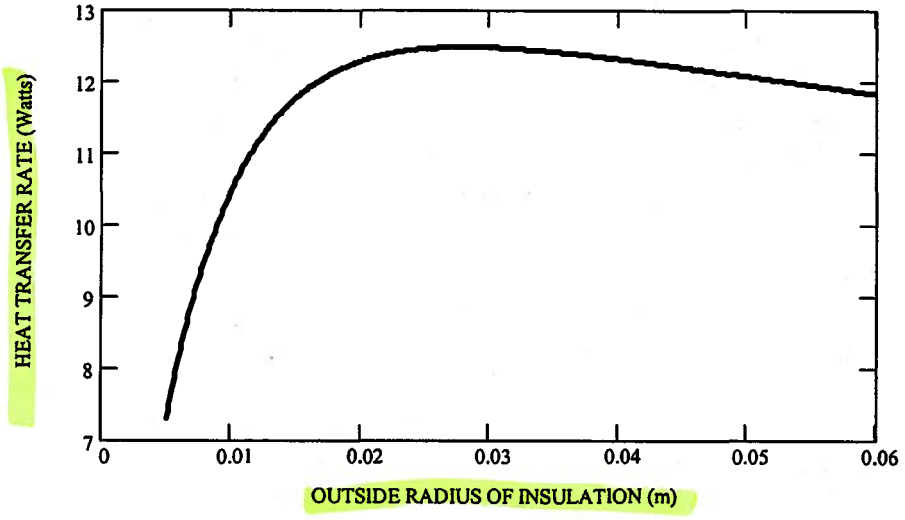

Notice that the heat transfer rate exhibits a maximum as the outside radius of the insulation is increased. The radius of the insulation at which this maximum occurs is known as the critical radius, r_c. The physical explanation behind this behavior of the heat transfer rate is that at small values of the outside radius, convection and radiation heat transfer from the outer surface dominate the heat transfer process. Thus, as the radius increases from small values, the heat

transfer rate increases rapidly because the surface area increases so rapidly. All the while, however, the thermal resistance is increasing because the path length for conduction is also increasing. In the neighborhood of r_c, the thermal resistance for conduction is comparable to the thermal resistance for convection and radiation combined. As the radius increases beyond the critical value, the thermal resistance for conduction dominates, and the heat transfer rate decreases slowly.

The value of the critical radius can be determined by differentiating the function for the heat transfer rate with respect to the outside radius and setting the result equal to zero. The value of the radius that satisfies this expression is known as the critical radius, r_c, where $r_c = k/h_o$. For the situation given above, $r_c = 2.8125 \times 10^{-2}$ m. This is an absurdly large value that has no practical significance for copper conductors for which electrical dissipation is low. The concept of critical radius for thermal insulation on steam pipes and refrigeration tubing is important, however. It is worth noting, however, that for commercially available 10 gage (AWG) copper wire for use in residential applications, $r_o = 2.121 \times 10^{-3}$ m. Then the above values for T_i, T_∞, h_o, and k_{teflon} give

$$\dot{Q} = 3.7 \text{ Watts}$$

The value of the electrical resistance of 1 m of copper wire of this diameter is $R_{electrical} = 3.2766 \times 10^{-3}$ ohms. Then

$$I = \sqrt{\frac{\dot{Q}}{R_{electrical}}} = \sqrt{\frac{3.7 \text{ Watts}}{3.2766 \times 10^{-3} \text{ ohms}}} = 33.604 \text{ Amps}$$

This is precisely the value of rated current at 40 C for this conductor.

6.5 Conduction Heat Transfer and Entropy Generation in the Uncoupled Thermal-Fluid System

Consider the case of a thermal-fluid system whose stored energy modes can be modeled entirely by uncoupled energy storage modes such as the pure thermal energy storage mode, chemical energy storage mode, elastic stored energy mode, electrical energy storage mode, etc. with dissipation. In the discussion that follows, we are interested in three phenomena: (1) the way in which energy is dissipated in the various non-thermal modes and appears in the thermal mode as manifested by a change in the temperature of that mode; (2) the way in which the energy and entropy transfer manifest themselves as a change in temperature within this system; and (3) the way in which entropy is generated as a consequence of conduction heat transfer. For these purposes, let us model the thermal energy storage mode as a pure thermal system such that it is this model element that experiences the heat transfer and entropy transfer experienced by the mass as a whole.

6.5.1 Conduction Heat Transfer in the Uncoupled Thermal-Fluid System

Let us consider within an uncoupled thermal-fluid system, a rectangular differential volume, *dxdydz*, as shown in Figure 6.5. Let the mass within this volume experience conduction heat transfer and entropy transfer in all three coordinate directions, x, y, and z, simultaneously. At some instant of time, t, let the temperature distribution in the pure thermal system element be $T(x, y, z)$ such that the property temperature has meaning at every value of x, y, and z within the system. (This condition is usually referred to as "local thermodynamic equilibrium" since the property temperature has meaning only in the equilibrium state, but the state under consideration is clearly not a true equilibrium state since the temperature is not uniform throughout the mass of

the system.) Let $\dot{q}(x)$ be the rate of energy transfer per unit cross-sectional area by conduction heat transfer at the location x (also known as the heat flux), and let $\dot{j}(x)$ be the concomitant rate of entropy transfer per unit cross-sectional area (also known as the entropy flux) for the x-direction where

$$\dot{j}(x) = \frac{\dot{J}(x)}{A} = \frac{\dot{Q}(x)/A}{T(x)} = \frac{\dot{q}(x)}{T(x)} \tag{6.41}$$

and $T(x)$ is the temperature at the location x.

Heat fluxes and entropy fluxes in other coordinate directions are similar to one shown.

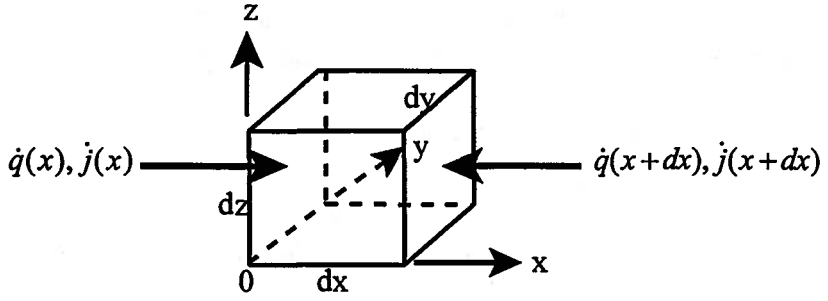

Figure 6.5 x-component of Heat Flux and Entropy Flux in Elemental Volume

If $\dot{q}_{gen}$ is the rate at which energy is "dissipated" irreversibly per unit mass by all energy storage modes other than the thermal energy storage mode and u is the thermal energy per unit mass stored in the volume element of the pure thermal system, the first law for the volume element becomes

$$\begin{aligned}&\left[\dot{q}(x) - \dot{q}(x+dx)\right]dydz + \left[\dot{q}(y) - \dot{q}(y+dy)\right]dxdz + \left[\dot{q}(z) - \dot{q}(z+dz)\right]dxdy = \\ &= \rho\frac{\partial u}{\partial t}dxdydz + \rho\dot{q}_{gen}dxdydz\end{aligned} \tag{6.42}$$

If we expand each of the heat flux terms for the various directions in a Taylor series, we get

$$\begin{aligned}\dot{q}(x+dx) &= \dot{q}(x) + \frac{\partial\dot{q}(x)}{\partial x}dx \\ \dot{q}(y+dy) &= \dot{q}(y) + \frac{\partial\dot{q}(y)}{\partial y}dy \\ \dot{q}(z+dz) &= \dot{q}(z) + \frac{\partial\dot{q}(z)}{\partial z}dz\end{aligned} \tag{6.43}$$

Substituting equation (6.43) into equation (6.42) and dividing through by *dxdydz*, we get

$$\rho\frac{\partial u}{\partial t} = -\left(\frac{\partial\dot{q}(x)}{\partial x} + \frac{\partial\dot{q}(y)}{\partial y} + \frac{\partial\dot{q}(z)}{\partial z}\right) + \rho\dot{q}_{gen} \tag{6.44}$$

but the Fourier Conduction law gives

$$\dot{q}(x) = -k\frac{\partial T}{\partial x}$$
$$\dot{q}(y) = -k\frac{\partial T}{\partial y} \qquad (6.45)$$
$$\dot{q}(z) = -k\frac{\partial T}{\partial z}$$

and the energy constitutive relation for the pure thermal system model gives

$$u - u_0 = c\left(T - T_0\right) \qquad (6.46)$$

Substituting equations (6.45) and (6.46) into equation (6.44)and dividing through by the product ρc, we obtain

$$\frac{\partial T}{\partial t} = \frac{1}{\rho c}\left[\frac{\partial}{\partial x}\left(k\frac{\partial T}{\partial x}\right) + \frac{\partial}{\partial y}\left(k\frac{\partial T}{\partial y}\right) + \frac{\partial}{\partial z}\left(k\frac{\partial T}{\partial z}\right)\right] + \frac{\dot{q}_{gen}}{c} \qquad (6.47)$$

If the thermal conductivity is isotropic, i.e., the same value regardless of direction, equation (6.47) can be written

$$\frac{\partial T}{\partial t} = \frac{k}{\rho c}\left(\frac{\partial^2 T}{\partial x^2} + \frac{\partial^2 T}{\partial y^2} + \frac{\partial^2 T}{\partial z^2}\right) + \frac{\dot{q}_{gen}}{c} \qquad (6.48)$$

Notice that the term $k/\rho c$ is a characteristic of the material and for this reason is given a special name, the ***thermal diffusivity***, and symbol, α.

$$\alpha = \frac{k}{\rho c} \qquad (6.49)$$

The thermal diffusivity has the dimensions m^2/sec in the S.I. unit system and physically represents the ratio of the rate at which energy is conducted through unit area of a material in response to a unit temperature difference placed across the material to the change in stored thermal energy that would result from unit change in the temperature of a pure thermal system fabricated from that material. For example, consider two geometrically identical pure thermal systems, one fabricated from a material with a large value of the thermal diffusivity, α_{large}, while the other is fabricated from a material with a small value of the thermal diffusivity, α_{small}. A unit of energy introduced into the system with α_{large} will diffuse throughout the system by thermal conduction faster and produce a larger temperature change in unit time than the system with α_{small}. For a given geometry, thermal systems fabricated from materials with α_{large} will run down to equilibrium more quickly than similar systems fabricated from materials with α_{small}.

Equation (6.47) is a second order partial differential equation known as the ***heat diffusion equation.*** Unlike Fourier's Conduction Law which is a vector equation, it is a scalar equation. Equation (6.47) provides the basis for the study of conduction heat transfer in pure thermal systems, and its solution will provide the temperature distribution in the system as a function of time, $T(x, y, z, t)$. Although equation (6.47) is expressed in Cartesian coordinates, it is often more appropriate to use this expression in cylindrical coordinates or spherical coordinates as dictated by the physical situation.

In cylindrical coordinates:

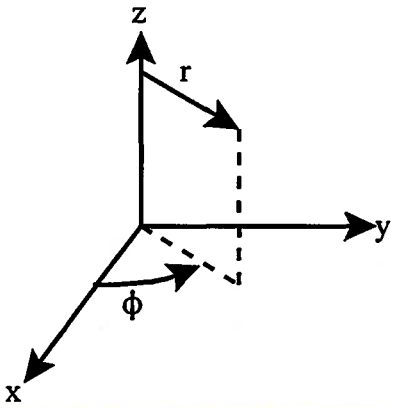

$$\rho c\frac{\partial T}{\partial t}=\frac{1}{r}\frac{\partial}{\partial r}\left(kr\frac{\partial T}{\partial r}\right)+\frac{1}{r^2}\frac{\partial}{\partial \phi}\left(k\frac{\partial T}{\partial \phi}\right)+\frac{\partial}{\partial z}\left(k\frac{\partial T}{\partial z}\right)+\rho\dot{q}_{gen} \tag{6.50}$$

In spherical coordinates:

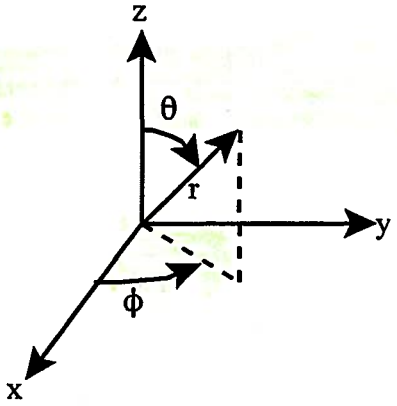

$$\rho c\frac{\partial T}{\partial t}=\frac{1}{r^2}\frac{\partial}{\partial r}\left(kr^2\frac{\partial T}{\partial r}\right)+\frac{1}{r^2\sin^2\theta}\frac{\partial}{\partial \phi}\left(k\frac{\partial T}{\partial \phi}\right)+\frac{1}{r^2\sin\theta}\frac{\partial}{\partial \theta}\left(k\sin\theta\frac{\partial T}{\partial \theta}\right)+\rho\dot{q}_{gen} \tag{6.51}$$

Notice that the heat diffusion equation can be written in the vector form

$$\rho c\frac{\partial T}{\partial t}=\nabla\left(k\nabla T\right)+\rho\dot{q}_{gen} \tag{6.52}$$

where the vector operator ∇ has the form appropriate for the coordinate system employed.

We now have the means to determine the response of the pure thermal system model to irreversible processes that redistribute the stored energy within the boundary of an uncoupled thermal-fluid system. As the heat diffusion equation shows, the response of the system will depend upon the ability of the system to conduct and store energy within the system boundary.

Example 6E.3: Consider the case of a rod fabricated from an electrically resistive material. The length of the rod is L, the thermal conductivity of the rod material is k, the density of the rod material is ρ, and the specific heat of the rod material is c. The rod is clamped in supports at $x = 0$ and $x = L$ such that the temperature of the rod at these two points is T_0. An electrical current I passes steadily through the rod and irreversibly dissipates energy in the amount of $\dot{q}_{gen}$ per unit mass of the rod. The lateral (curved) surface of the rod is adiabatic.

We wish to determine the temperature distribution in the rod in the steady state so that we can be sure that the rod will not melt as a result of the dissipation of electrical energy in the rod (also known as "Joule heating"). We also wish to determine the amount of cooling that must be

provided at the ends of the rod in order to fix the temperature at the ends of the rod at T_0.

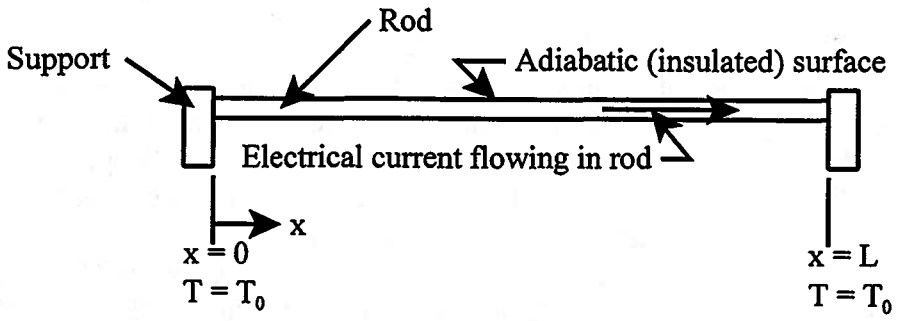

Figure 6E.3a Electrical Resistor Carrying Electrical Current

Solution: This physical situation is clearly one dimensional and steady and can be described by the steady, one-dimensional form of equation (6.48). Then

$$\frac{k}{\rho c}\frac{d^2T}{dx^2} = -\frac{\dot{q}_{gen}}{c}$$

If we integrate this expression, we get

$$\frac{dT}{dx} = -\frac{\rho\dot{q}_{gen}}{k}x + C_1$$

where C_1 is a constant of integration to be determined from the boundary conditions. Integrating a second time, we get

$$T = -\frac{\rho\dot{q}_{gen}}{2k}x^2 + C_1x + C_2$$

Since $T = T_0$ at $x = 0$, it follows that $C_2 = T_0$. At $x = L$, we have $T = T_0$ so

$$T_0 = -\frac{\rho\dot{q}_{gen}}{2k}L^2 + C_1L + T_0$$

$$\therefore C_1 = \frac{\rho\dot{q}_{gen}L}{2k}$$

After rearranging some terms, the temperature distribution becomes

$$T - T_0 = \frac{\rho\dot{q}_{gen}L^2}{2k}\left[\left(\frac{x}{L}\right) - \left(\frac{x}{L}\right)^2\right]$$

Thus, the temperature distribution is parabolic in shape. The maximum temperature will occur where the temperature distribution has zero slope, i.e., the temperature gradient vanishes. Then

$$\frac{dT}{dx} = \frac{\rho\dot{q}_{gen}}{k}\left(\frac{L}{2} - x\right) = 0$$

Then $T = T_{max}$ at $x = L/2$, and

$$T_{\max} = T_0 + \frac{\rho\dot{q}_{gen}L^2}{8k}$$

A plot of the temperature distribution for the case of $\frac{\rho\dot{q}_{gen}L^2}{2k} = 4$ is shown in Figure 6E.3b.

The rate at which energy flows into the supports from the rod is given by the Fourier Conduction

Law applied to the rod at the point of attachment. Thus, at $x = 0$

$$\dot{Q} = -kA_c\left(\frac{dT}{dx}\right)_{x=0} = -kA_c\left(\frac{\rho\dot{q}_{gen}L}{2k}\right) = -\frac{\rho\dot{q}_{gen}A_cL}{2}$$

The negative sign indicates that the heat transfer is out of the end of the rod. By symmetry there is an equal rate of energy flow out of the rod at $x = L$. Note that because the lateral surface of the rod is adiabatic, half the energy dissipated electrically flows down the temperature gradient and out each end of the rod. In practice, it would be necessary to provide this much cooling at each support in order to maintain the temperature of the end of the rod fixed. Usually this cooling would be provided by some sort of convection heat transfer configuration. Note that the midpoint of the rod behaves as though it were adiabatic since the temperature gradient vanishes at that point.

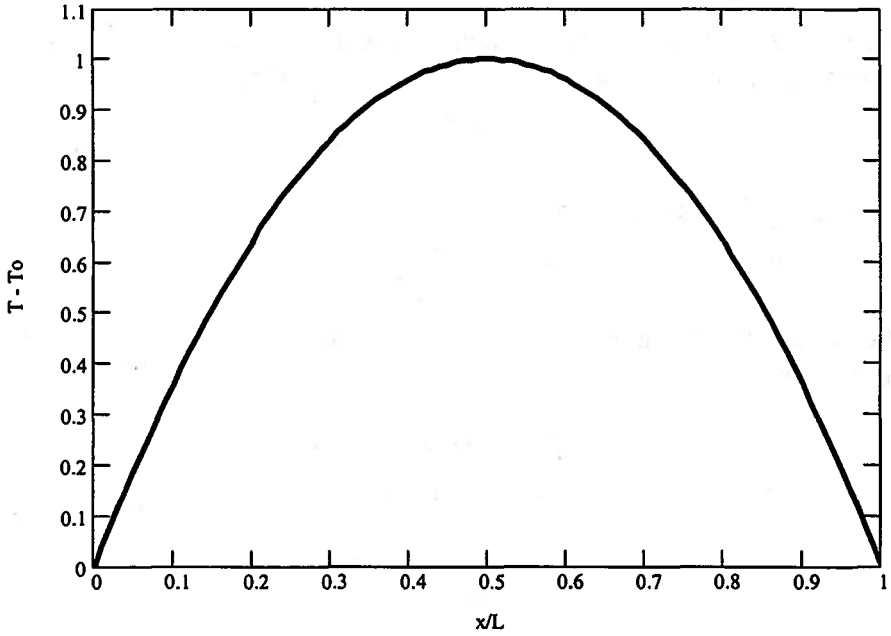

Figure 6E.3b Temperature Distribution in an Electrically Conducting Rod with Fixed End Temperatures and Adiabatic Outer Surface

6.5.2 Entropy Generation by Conduction Heat Transfer in an Uncoupled Thermal-Fluid System

We now turn our attention to the entropy generated by conduction heat transfer in the uncoupled thermal-fluid system. For the differential volume of Figure 6.5, the second law can be written as a rate equation, viz.

$$\frac{\partial S}{\partial t} = \sum_i \dot{J}_i + \dot{S}_{gen} \tag{6.53}$$

where the term on the left-hand side represents the time rate of change of the entropy stored within the volume by all processes; the first term on the right-hand side represents the rate at which entropy is transferred across the system boundary via the heat transfer interaction; and the second term on the right-hand side represents the rate at which entropy is generated within the system boundary by means of irreversible processes.

The instantaneous rate of change of the entropy stored within the volume is given by

$$\frac{\partial S}{\partial t} = \rho\frac{\partial s}{\partial t}dxdydz \tag{6.54}$$

where s is the stored entropy per unit mass. The rate of entropy generation within the system boundary by irreversible processes is given by

$$\dot{S}_{gen} = \rho \dot{s}_{gen} dxdydz \tag{6.55}$$

where $\dot{s}_{gen}$ is the rate of entropy generation per unit mass. Then with the aid of equations (6.54) and (6.55), equation (6.53) becomes

$$\begin{aligned} \rho \frac{\partial s}{\partial t} dxdydz = &\left(\frac{\dot{J}(x)}{A_c} - \frac{\dot{J}(x+dx)}{A_c} \right) dydz + \left(\frac{\dot{J}(y)}{A_c} - \frac{\dot{J}(y+dy)}{A_c} \right) dxdz + \\ &+ \left(\frac{\dot{J}(z)}{A_c} - \frac{\dot{J}(z+dz)}{A_c} \right) dxdy + \rho \dot{s}_{gen} dxdydz \end{aligned} \tag{6.56}$$

The entropy flow can be expanded in a Taylor series as

$$\begin{aligned} \dot{J}(x+dx) &= \dot{J}(x) + \frac{\partial \dot{J}(x)}{\partial x} dx \\ \dot{J}(y+dy) &= \dot{J}(y) + \frac{\partial \dot{J}(y)}{\partial y} dy \\ \dot{J}(z+dz) &= \dot{J}(z) + \frac{\partial \dot{J}(z)}{\partial z} dz \end{aligned} \tag{6.57}$$

where we have retained only terms of first order. Then the second law becomes

$$\rho \frac{\partial s}{\partial t} dxdydz = -\left[\left(\frac{1}{A_c} \frac{\partial \dot{J}(x)}{\partial x} \right) + \left(\frac{1}{A_c} \frac{\partial \dot{J}(y)}{\partial y} \right) + \left(\frac{1}{A_c} \frac{\partial \dot{J}(z)}{\partial z} \right) \right] dxdydz + \rho \dot{s}_{gen} dxdydz \tag{6.58}$$

Dividing equation (6.58) through by $\rho dxdydz$, we get

$$\frac{\partial s}{\partial t} = -\frac{1}{\rho} \left[\left(\frac{1}{A_c} \frac{\partial \dot{J}(x)}{\partial x} \right) + \left(\frac{1}{A_c} \frac{\partial \dot{J}(y)}{\partial y} \right) + \left(\frac{1}{A_c} \frac{\partial \dot{J}(z)}{\partial z} \right) \right] + \dot{s}_{gen} \tag{6.59}$$

but for the gradient of the entropy flux, we have

$$\begin{aligned} \frac{\partial \dot{J}(x)/A_c}{\partial x} &= \frac{\partial}{\partial x} \left(\frac{\dot{q}(x)}{T} \right) = \frac{1}{T} \left(\frac{\partial \dot{q}(x)}{\partial x} \right) - \frac{\dot{q}(x)}{T^2} \left(\frac{\partial T}{\partial x} \right) \\ \frac{\partial \dot{J}(y)/A_c}{\partial y} &= \frac{\partial}{\partial y} \left(\frac{\dot{q}(y)}{T} \right) = \frac{1}{T} \left(\frac{\partial \dot{q}(y)}{\partial y} \right) - \frac{\dot{q}(y)}{T^2} \left(\frac{\partial T}{\partial y} \right) \\ \frac{\partial \dot{J}(z)/A_c}{\partial z} &= \frac{\partial}{\partial z} \left(\frac{\dot{q}(z)}{T} \right) = \frac{1}{T} \left(\frac{\partial \dot{q}(z)}{\partial z} \right) - \frac{\dot{q}(z)}{T^2} \left(\frac{\partial T}{\partial z} \right) \end{aligned} \tag{6.60}$$

From the Fourier Conduction Law we have

$$\begin{aligned} \dot{q}(x) &= -k \frac{\partial T}{\partial x} \\ \dot{q}(y) &= -k \frac{\partial T}{\partial y} \\ \dot{q}(z) &= -k \frac{\partial T}{\partial z} \end{aligned} \tag{6.61}$$

Then equations (6.60) become

$$\frac{\partial \dot{J}(x)/A_c}{\partial x} = -\frac{1}{T}\left[\frac{\partial}{\partial x}\left(k\frac{\partial T}{\partial x}\right)\right] + \frac{k}{T^2}\left(\frac{\partial T}{\partial x}\right)^2$$
$$\frac{\partial \dot{J}(y)/A_c}{\partial y} = -\frac{1}{T}\left[\frac{\partial}{\partial y}\left(k\frac{\partial T}{\partial y}\right)\right] + \frac{k}{T^2}\left(\frac{\partial T}{\partial y}\right)^2 \qquad (6.62)$$
$$\frac{\partial \dot{J}(z)/A_c}{\partial z} = -\frac{1}{T}\left[\frac{\partial}{\partial z}\left(k\frac{\partial T}{\partial z}\right)\right] + \frac{k}{T^2}\left(\frac{\partial T}{\partial z}\right)^2$$

Then equation (6.59) becomes

$$\frac{\partial s}{\partial t} = \frac{1}{\rho T}\left[\frac{\partial}{\partial x}\left(k\frac{\partial T}{\partial x}\right)\right] - \frac{k}{\rho T^2}\left(\frac{\partial T}{\partial x}\right)^2 + \frac{1}{\rho T}\left[\frac{\partial}{\partial y}\left(k\frac{\partial T}{\partial y}\right)\right] - \frac{k}{\rho T^2}\left(\frac{\partial T}{\partial y}\right)^2 + \frac{1}{\rho T}\left[\frac{\partial}{\partial z}\left(k\frac{\partial T}{\partial z}\right)\right] - \frac{k}{\rho T^2}\left(\frac{\partial T}{\partial z}\right)^2 + \dot{s}_{gen} \qquad (6.63)$$

If we now solve equation (6.63) for the entropy generation per unit mass, we obtain

$$\dot{s}_{gen} = \frac{\partial s}{\partial t} - \frac{1}{\rho T}\left[\frac{\partial}{\partial x}\left(k\frac{\partial T}{\partial x}\right)\right] + \frac{k}{\rho T^2}\left(\frac{\partial T}{\partial x}\right)^2 - \frac{1}{\rho T}\left[\frac{\partial}{\partial y}\left(k\frac{\partial T}{\partial y}\right)\right] + \frac{k}{\rho T^2}\left(\frac{\partial T}{\partial y}\right)^2 - \frac{1}{\rho T}\left[\frac{\partial}{\partial z}\left(k\frac{\partial T}{\partial z}\right)\right] + \frac{k}{\rho T^2}\left(\frac{\partial T}{\partial z}\right)^2 \qquad (6.64)$$

This is the *entropy generation equation* that enables us to determine the entropy generated by heat transfer by conduction through a temperature gradient. We can simplify equation (6.64) by noting that the entropy per unit mass can be determined from the entropy constitutive relation for the pure thermal system model. Then since

$$ds = \frac{c\,dT}{T} \qquad (6.65)$$

and

$$\frac{\partial s}{\partial t} = \frac{c}{T}\left(\frac{\partial T}{\partial t}\right) \qquad (6.66)$$

and

$$\dot{s}_{gen} = \frac{c}{T}\left(\frac{\partial T}{\partial t}\right) - \frac{1}{\rho T}\left[\frac{\partial}{\partial x}\left(k\frac{\partial T}{\partial x}\right)\right] + \frac{k}{\rho T^2}\left(\frac{\partial T}{\partial x}\right)^2 - \frac{1}{\rho T}\left[\frac{\partial}{\partial y}\left(k\frac{\partial T}{\partial y}\right)\right] + \frac{k}{\rho T^2}\left(\frac{\partial T}{\partial y}\right)^2 - \frac{1}{\rho T}\left[\frac{\partial}{\partial z}\left(k\frac{\partial T}{\partial z}\right)\right] + \frac{k}{\rho T^2}\left(\frac{\partial T}{\partial z}\right)^2 \qquad (6.67)$$

Substituting the first law in the form of equation (6.47) into equation (6.67), we obtain the final expression for the rate of entropy generation per unit mass by heat conduction and irreversible processes within the system boundary.

$$\dot{s}_{gen} = \frac{k}{\rho T^2}\left[\left(\frac{\partial T}{\partial x}\right)^2 + \left(\frac{\partial T}{\partial y}\right)^2 + \left(\frac{\partial T}{\partial x}\right)^2\right] + \frac{\dot{q}_{gen}}{T} \qquad (6.68)$$

Thus as the first term on the right-hand side of equation (6.68) shows, the entropy generation by conduction heat transfer alone is proportional to the square of the temperature gradient.

Example 6E.4: Consider the physical situation shown in Figure 6E.4 in which two heat reservoirs at different temperatures T_1 and T_2 ($T_1 > T_2$) are connected by a slender rod of length L

and cross-sectional area A_c, density ρ, and thermal conductivity k. In the steady state, energy and entropy flows by conduction heat transfer from one heat reservoir to the other through the rod.

Determine the rate of entropy generation in the rod.

Solution: As shown in Example 6E.3, for this steady, one-dimensional situation, the heat diffusion equation becomes

$$\frac{d^2T}{dx^2} = 0$$

Integrating this expression twice and applying the boundary conditions $T = T_1$ at $x = 0$ and $T = T_2$ at $x = L$, we get

$$T(x) = T_1 - \left(\frac{x}{L}\right)(T_1 - T_2)$$

Then

$$\frac{dT}{dx} = \frac{T_2 - T_1}{L} = \text{constant}$$

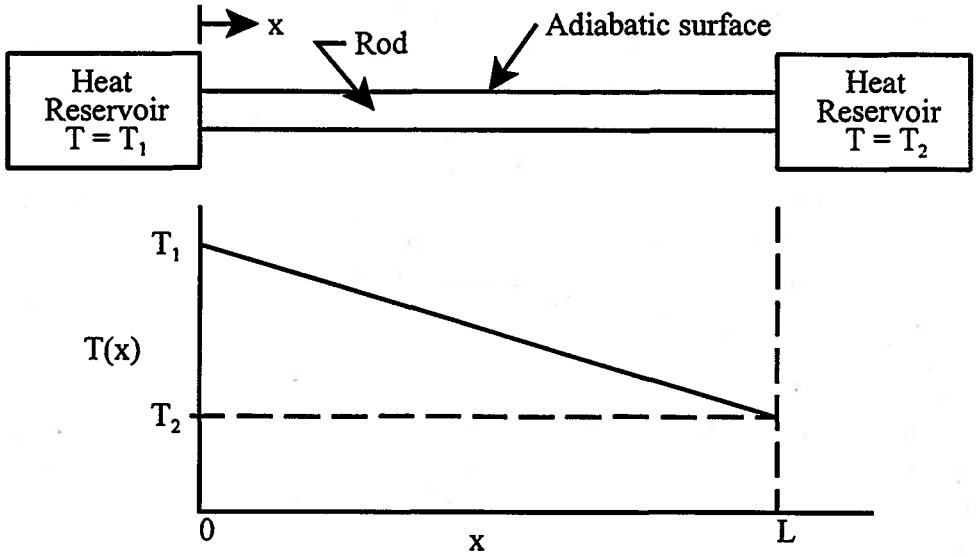

Figure 6E.4 Simple Conduction Heat Transfer Between Two Heat Reservoirs

Since the only irreversible process in the rod is the heat transfer process, the last term on the right hand side of equation (6.68) vanishes. Then

$$\dot{S}_{gen} = \int_{x=0}^{x=L} \dot{s}_{gen}\rho dxdydz = \int_{x=0}^{x=L} \frac{k}{\rho T^2}\left(\frac{\partial T}{\partial x}\right)^2 \rho dxdydz = k\left(\frac{T_2 - T_1}{L}\right)^2 \int_{x=0}^{x=L} \frac{A_c dx}{T^2}$$

$$\dot{S}_{gen} = kA_c\left(\frac{T_2 - T_1}{L}\right)^2 \int_{x=0}^{x=L} \frac{1}{T^2}\frac{dx}{dT}dT = kA_c\left(\frac{T_2 - T_1}{L}\right)^2 \int_{T_1}^{T_2} \left(\frac{L}{T_2 - T_1}\right)\frac{dT}{T^2}$$

which reduces to

$$\dot{S}_{gen} = \dot{Q}\left(\frac{1}{T_2} - \frac{1}{T_1}\right)$$

Physically this result shows that in the steady state the entropy generated within the rod is equal to the net entropy transfer out the ends of the rod.

6.6 Steady-state Heat Transfer from Extended Surfaces: Fins

As a natural consequence of the irreversible nature of their operation, many engineering systems dissipate energy at a fixed rate. Some well-known examples include the disk brake assembly in an automobile or the central processing unit in a personal computer. In each case, it is necessary to provide some sort of cooling to the system in order to maintain the temperature of the system at some steady value. That is, the system must get rid of the dissipated energy by some heat transfer mechanism or face the consequences of a steadily increasing operating temperature that will lead to a catastrophic failure such as a meltdown. Typically, the operating temperature is above the ambient temperature so this is readily accomplished by placing the surface of the system in contact with a fluid, frequently the ambient atmosphere, and transferring the dissipated energy from the surface to the fluid via the convection heat transfer mechanism described in Section 6.2.2.

Unfortunately, in many circumstances, the magnitude of the prevailing heat transfer coefficient is such that the surface area of the system available for heat transfer is insufficient to transfer the energy necessary to maintain the operating temperature at a safe steady level. The thermal design engineer is then faced with making one of two choices: either to modify the flow characteristics of the fluid in order to increase the heat transfer coefficient or to increase the surface area for heat transfer. The latter approach is often the more reasonable choice of the two. The surface area is usually increased by fabricating a set of fin-like structures that are either firmly attached to the surface of the system or are an integral part of the surface itself. Typically, the shape of these fins is such that their transverse dimensions are small compared to their axial dimension. Thus, we are able to model these fins as slender rods known as "pin fins."

6.6.1 Heat Transfer from Pin Fins

Consider the pin fin shown schematically in Figure 6.5. The fin consists of a right circular cylinder of perimeter P with its axis aligned along the x-axis. The base of the fin is attached to the surface being cooled with its circumferential area exposed to a fluid with a convective heat transfer coefficient of h_c. Consider an element of this cylinder bounded by the planes at location x and at location $x + dx$.

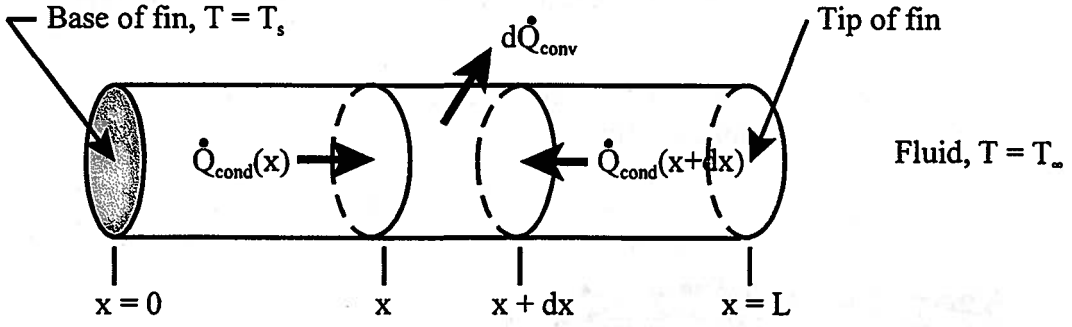

Figure 6.6 Pin Fin of Circular Geometry

If we apply the first law of thermodynamics to the element shown, we obtain for the steady-state with no work transfer,

$$\dot{Q}_{cond}(x) - \dot{Q}_{cond}(x+dx) - d\dot{Q}_{conv} = 0 \tag{6.69}$$

Physically, equation (6.69) says that the energy conducted into the element at the left face is just equal to the sum of the energy conducted out at the right face plus the energy convected off the circumferential surface. Expanding the conduction terms in a Taylor series, we get

$$\dot{Q}_{cond}(x+dx) = \dot{Q}_{cond}(x) + \frac{d\dot{Q}_{cond}(x)}{dx} \tag{6.70}$$

Substituting equation (6.70) and Newton's Law of Cooling into equation (6.69), we get

$$-\frac{d\dot{Q}_{cond}(x)}{dx}dx - h_c dA_s(T - T_\infty) = 0 \tag{6.71}$$

where T is the temperature of the element and dA_s is its surface area. Since

$$dA_s = Pdx \tag{6.72}$$

we can rewrite equation (6.71) with the aid of the Fourier Conduction Law. Then

$$-\frac{d}{dx}\left(-kA_c\frac{dT}{dx}\right)dx - h_c P(T - T_\infty)dx = 0 \tag{6.73}$$

$$kA_c\frac{d^2T}{dx^2}dx - h_c P(T - T_\infty)dx = 0 \tag{6.74}$$

where we have taken the thermal conductivity k to be a constant independent of temperature. Then

$$\frac{d^2T}{dx^2} - \frac{h_c P}{kA_c}(T - T_\infty) = 0 \tag{6.75}$$

Since T_∞ is constant, we can write

$$\frac{d^2}{dx^2}(T) = \frac{d^2}{dx^2}(T - T_\infty) \tag{6.76}$$

Then the first law of thermodynamics for the fin becomes

$$\frac{d^2(T - T_\infty)}{dx^2} - \frac{h_c P}{kA_c}(T - T_\infty) = 0 \tag{6.77}$$

Equation (6.77) is often referred to as the "fin equation" since it describes the transfer of energy in the fin in the steady-state. To solve this linear, second-order differential equation to obtain the steady-state temperature distribution in the fin, we define the fin parameter m which has the dimensions of (1/length) as

$$m^2 = \frac{h_c P}{kA_c} \tag{6.78}$$

Then the fin equation becomes

$$\frac{d^2(T - T_\infty)}{dx^2} - m^2(T - T_\infty) = 0 \tag{6.79}$$

Assume the solution of equation (6.79) is of the form

$$T - T_\infty = ce^{ax} \tag{6.80}$$

Substituting equation (6.80) into equation (6.79), we get

$$\frac{d^2(T - T_\infty)}{dx^2} = a^2 ce^{ax} = a^2(T - T_\infty) = m^2(T - T_\infty) \tag{6.81}$$

Then

$$a = \pm\sqrt{m^2} = \pm m \tag{6.82}$$

Then the solution takes the form

$$T - T_\infty = c_1 e^{mx} + c_2 e^{-mx} \tag{6.83}$$

Since there are two constants of integration appearing in equation (6.83), we need to have two boundary conditions to determine them. For the first boundary condition, we have that at the base of the fin, $x = 0$, the temperature of the fin must be identical to the temperature of the surface, T_s. Then

$$T_s - T_\infty = c_1 + c_2 \tag{6.84}$$

For the second boundary condition, we need to know the condition at the tip of the fin, $x = L$. There are three possibilities of practical interest:

(1) The fin is modeled as infinitely long so that the fin temperature approaches the temperature of the fluid in the limit as the length of the fin becomes infinite. That is,

$$T \to T_\infty \text{ as } x \to \infty \tag{6.85}$$

(2) The tip of the fin is insulated so that there is no heat transfer from the end of the fin. This condition is a reasonable one in many cases since the cross-sectional area of the fin is so small in comparison with the total surface area that any heat transfer from it is negligible in comparison with the heat transfer from the circumferential surface of the fin. Then for this case

$$\left(\frac{dT}{dx}\right)_{x=L} = 0 \tag{6.86}$$

(3) The tip of the fin experiences convective heat transfer with a heat transfer coefficient of h_L so that the boundary condition becomes

$$-kA_c\left(\frac{dT}{dx}\right)_{x=L} = h_L A_c[T(x=L) - T_\infty] \tag{6.87}$$

For the practical reasons cited above and the fact that the resulting solution is mathematically simpler to use than the result we shall obtain for case 3, we shall develop the solution for case 2 in detail. If we apply equation (6.86) to equation (6.83), we obtain for the derivative

$$\frac{d(T - T_\infty)}{dx} = mc_1 e^{mx} - mc_2 e^{-mx} \tag{6.88}$$

which at $x = L$ becomes

$$mc_1 e^{mL} - mc_2 e^{-mL} = 0 \tag{6.89}$$

Then

$$c_2 = c_1 e^{2mL} \tag{6.90}$$

Substituting this result into equation (6.84), we obtain

$$T_s - T_\infty = c_1 + c_1 e^{2mL} \tag{6.91}$$

Then the constants of integration become

$$c_1 = \frac{(T_s - T_\infty)}{1 + e^{2mL}}$$
$$c_2 = \frac{(T_s - T_\infty)}{1 + e^{-2mL}} \tag{6.92}$$

Then we can write the solution for the temperature distribution in the fin as

$$\frac{T - T_\infty}{T_s - T_\infty} = \frac{e^{mx}}{1 + e^{2mL}} + \frac{e^{-mx}}{1 + e^{-2mL}} = \frac{e^{-m(L-x)} + e^{m(L-x)}}{e^{mL} + e^{-mL}} \tag{6.93}$$

But the definition of the hyperbolic cosine gives

$$\cosh u = \frac{e^{u} + e^{-u}}{2} \tag{6.94}$$

Then the temperature distribution can be written

Adiabatic tip

$$\frac{T - T_\infty}{T_s - T_\infty} = \frac{\cosh m(L-x)}{\cosh mL} = \frac{\cosh mL\left(1 - \frac{x}{L}\right)}{\cosh mL} \tag{6.95}$$

Note that as $L \to \infty$, equation (6.95) reduces to

$$\frac{T - T_\infty}{T_s - T_\infty} = e^{-mx} \tag{6.96}$$

which is the solution for the infinitely long fin, case 1.

For case 3, the fin with convective heat transfer from the tip, it can be shown by methods similar to those above that the temperature distribution is given by

$$\frac{T - T_\infty}{T_s - T_\infty} = \frac{\cosh m(L-x) + \frac{h_L}{mk}\sinh m(L-x)}{\cosh mL + \frac{h_L}{mk}\sinh mL} \tag{6.97}$$

To see the influence of the various parameters, we can plot the dimensionless temperature of equation (6.95) as shown in Figure 6.7.

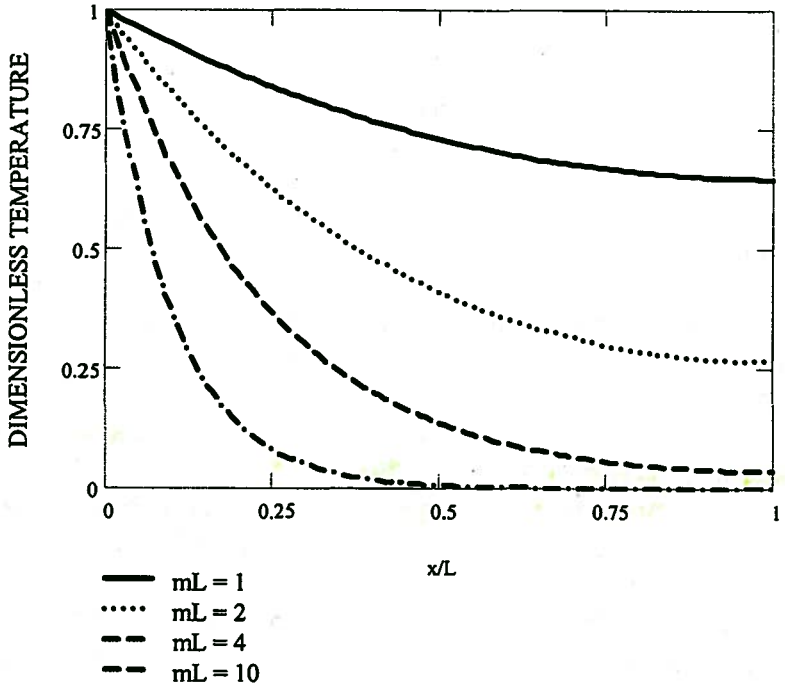

Figure 6.7 Dimensionless Temperature Distribution in a Fin Insulated at the Tip

As an illustration of the information contained in Figure 6.7, consider two fins A and B of identical geometry with identical environmental conditions. Let the only difference between the two fins be their thermal conductivities. Fin A has a geometry and a thermal conductivity that results in a value of the fin parameter mL such that $(mL)_A = 1$. The thermal conductivity of fin B is 25 percent of that of fin A. Thus, $k_A = 4k_B$. Then it follows that $(mL)_B = 2$. From Figure 6.7, it

follows that the dimensionless temperatures for these two fins at the midpoints of their lengths are 0.736 and 0.419 for A and B, respectively. Then

$$\frac{(T_{L/2}-T_\infty)_A}{(T_{L/2}-T_\infty)_B}=1.757$$

Thus, as we would expect, the higher the value of the thermal conductivity, the more nearly isothermal is the fin and the further out the influence of the surface temperature propagates.

To evaluate the total heat transfer from the fin, we recognize that the energy that enters the base of the fin ultimately is carried away by convection to the fluid. Then for the fin insulated at the tip

$$\dot{Q}=-kA_c\left(\frac{dT}{dx}\right)_{x=0} \tag{6.98}$$

where

$$\left(\frac{dT}{dx}\right)_{x=0}=\frac{-m\sinh mL}{\cosh mL}=-m\tanh mL \tag{6.99}$$

Thus

$$\dot{Q}=\sqrt{h_cPkA_c}(T_s-T_\infty)\tanh mL \tag{6.100}$$

Note that this same result can be obtained by integrating Newton's Law of Cooling over the entire surface area of the fin since all of this energy is ultimately transferred to the fluid by convection.

$$\dot{Q}=\int_0^L h_cP(T-T_\infty)dx=\sqrt{h_cPkA_c}(T_s-T_\infty)\tanh mL \tag{6.101}$$

For the two fins A and B described above, it follows that

$$\frac{\dot{Q}_A}{\dot{Q}_B}=\frac{2\tanh 1}{\tanh 2}=1.58$$

Thus, the heat transfer from the fin made from the higher thermal conductivity material is significantly greater; however, the relationship is not linear.

6.6.2 Fin Efficiency

In the design of fin systems to achieve a particular result, there are many parameters that need to be considered. There is the material of construction, the cross-sectional area, the perimeter, the length, the mass of material and even the heat transfer coefficient. A convenient way of evaluating the various fin designs is a parameter known as the fin efficiency. Although the fin efficiency, η_f, varies between the values of 0 and 1, unlike many other efficiencies defined in thermodynamics, a value close to 1 does not necessarily imply optimum design. Rather the fin efficiency simply serves as a measure of the ability of the fin to transfer energy per unit area of exposed surface. The fin efficiency is defined as the actual heat transfer rate of the fin relative to the maximum heat transfer rate for the given geometry, a rate which would result if the entire fin were at the same temperature as its base. Thus a value of fin efficiency close to unity simply means that the fin is nearly isothermal. Then

$$\eta_f=\frac{\dot{Q}}{h_cPL(T_s-T_\infty)} \tag{6.102}$$

For the case of a fin insulated at the tip, this expression reduces to

$$\eta_f=\frac{\tanh mL}{mL} \tag{6.103}$$

which is also approximately true for the case with convection from the tip (case 3) provided that

$(h_c t/k) < 0.0625$. The fin efficiency is plotted in Figure 6.8.

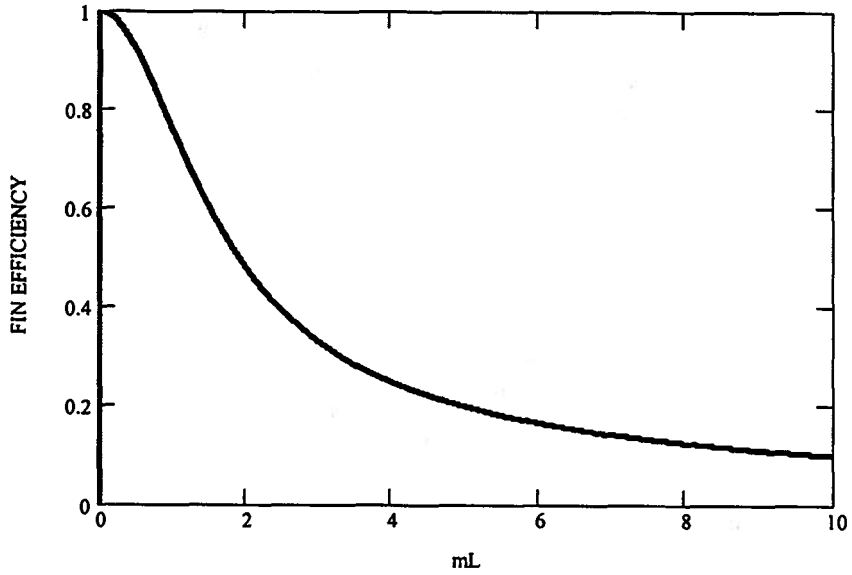

Figure 6.8 Fin Efficiency for a Fin Insulated at the Tip

Note that when $mL > 4$, $\eta_f \sim 1/mL$. A small value of mL corresponds to a short, thick fin of high thermal conductivity, whereas large values of mL correspond to long, thin fins of low thermal conductivity. When the value of mL is small, T does not fall much below T_s, and the fin is an efficient heat transfer mechanism. In effect, the fins have truly increased the surface area of the system whose temperature we are trying to control. It should be understood, however, that a fin design with a fin efficiency of nearly unity is not optimal from the point of view of energy transferred per unit mass or per unit cost. As the fin efficiency approaches unity, the entropy generation in the solid decreases; however, the entropy generation in the fluid increases.

Example 6E.5: An array of eight aluminum alloy fins ($k = 175$ W/m K), each 3 mm wide, 0.4 mm thick, and 40 mm long, is used to cool an electronic component. When the base of the fins is at 340 K and the ambient air is at 300 K, estimate the dissipated power that the fins can transfer in the form of a heat transfer with a combined convection and radiation heat transfer coefficient of $h = 8$ W/m^2 K.

Solution: First determine the fin geometry. The cross-sectional area of one fin is given by

$$A_c = (3 \times 10^{-3} \text{ m})(4 \times 10^{-4}) = 1.2 \times 10^{-6} \text{ m}^2$$

The perimeter of one fin is

$$P = 2(3 \times 10^{-3} \text{ m} + 4 \times 10^{-4} \text{ m}) = 6.8 \times 10^{-3} \text{ m}$$

Then the fin parameter is

$$m^2 = \frac{h_c P}{k A_c} = \frac{(8 \text{ W/m}^2 \text{ K})(6.8 \times 10^{-3} \text{ m})}{(175 \text{ W/m K})(1.2 \times 10^{-6} \text{ m}^2)} = 259 \text{ m}^{-2}$$

$$m = 16.1 \text{ m}^{-1}$$

$$mL = (16.1 \text{ m}^{-1})(0.04 \text{ m}) = 0.644$$

The maximum possible heat transfer from one fin is

Heat transfer for fin

$$\dot{Q} = h_c PL(T_s - T_\infty) = (8\ \text{W/m}^2\ \text{K})(6.8 \times 10^{-3}\ \text{m})(0.04\ \text{m})(340\ \text{K} - 300\ \text{K})$$

$$\dot{Q} = 8.70 \times 10^{-2}\ \text{W}$$

η Q = actual heat transfer.

The fin efficiency is

$$\eta_f = \frac{\tanh mL}{mL} = \frac{\tanh(0.644)}{0.644} = 0.881$$

For the array of 8 fins, the heat transfer rate is given by

$$\dot{Q} = 8(8.70 \times 10^{-2}\ \text{W})(0.881) = 0.613\ \text{W}$$

which is the maximum allowable power dissipation in the component. The temperature at the end of the fins is

$$\frac{T_L - T_\infty}{T_s - T_\infty} = \frac{\cosh m(L-x)}{\cosh mL} = \frac{\cosh(0)}{\cosh(0.644)} = 0.823$$

$$T_L = 300\ \text{K} + (340\ \text{K} - 300\ \text{K})(0.823) = 332.93\ \text{K}$$

6.6.3 Finned Surfaces

Typically the fin is part of an array similar to that of Example 6E.5 above. The fin is integrally cast with, or bonded at its base to, a larger (parent) surface that is usually the containment envelope of a thermal-fluid system. The portion of the parent surface that is not covered by fins also participates in the heat transfer interaction between the fluid medium of the environment and the thermal-fluid system. Then the total surface area involved, A_{total}, consists of the area of all the fins plus the exposed area of the parent surface, A_P. If there are N identical fins each of surface area A_{fin}, the total heat transfer surface area becomes

$$A_{total} = NA_{fin} + A_P \tag{6.104}$$

The maximum possible heat transfer rate for this configuration would occur if the total surface area were at the temperature of the parent surface, T_s. Then if there is a uniform heat transfer coefficient over the total surface area, the maximum heat transfer rate would be

$$\dot{Q}_{\max} = h_c A_{total}(T_s - T_\infty) \tag{6.105}$$

However, the actual heat transfer rate, $\dot{Q}_{total}$, is less than this because the efficiency of the individual fins is less than unity. Then combining equations (6.102), (6.104), and (6.105), we get

$$\dot{Q}_{total} = N\eta_f h_c A_{fin}(T_s - T_\infty) + h_c A_P(T_s - T_\infty) \tag{6.106}$$

Solving equation (6.104) for A_P and substituting the result into equation (6.106), we get

$$\dot{Q}_{total} = \left[N\eta_f A_{fin} + \left(A_{total} - NA_{fin}\right)\right] h_c (T_s - T_\infty) = \left[1 - \frac{NA_{fin}}{A_{total}}\left(1 - \eta_f\right)\right] h_c A_{total}(T_s - T_\infty) \tag{6.107}$$

If we rewrite equation (6.107) in the form

$$\dot{Q}_{total} = \eta_{surf}\dot{Q}_{\max} \tag{6.108}$$

where we have now defined the heat transfer efficiency of the surface, η_{surf}, to be

$$\eta_{surf} = 1 - \frac{NA_{fin}}{A_{total}}\left(1 - \eta_f\right) \tag{6.109}$$

The efficiency of the surface depends entirely upon the geometry of the surface and the fin efficiency. It can be calculated from the configuration and the heat transfer coefficient for the surface and then substituted into equation (6.109) to determine the heat transfer from the total surface area.

Example 6E.6: The Intel Pentium© III Xeon Processor runs at 550 MHz and dissipates 50 W of power. The design of the envelope of the processor provides a "thermal plate" that is used to achieve the proper thermal control of the device. We wish to design an array of circular pin fins that mounts on this "thermal plate" and is fitted with a small fan that provides sufficient air flow to achieve the thermal design operating point. The maximum allowable temperature of the plate is 68 C with an air temperature of 45 C. The dimensions of the plate itself are 12.3 cm by 15.2 cm. A proposed design consists of an array of 15 x 19 = 285 aluminum (k_{Al} = 168 W/m K) pin fins each with the dimensions D = 4 mm and L = 21 mm. The airflow provided by the fan results in a convection heat transfer coefficient of h_c = 25 W/m^2 K. Is this design adequate to handle the load of 50 W?

Solution: We first need to calculate the fin parameter, m. The cross-sectional area of a fin is

$$A_c = \frac{\pi D^2}{4} = \frac{\pi(0.004\text{ m})^2}{4} = 1.257 \text{ x } 10^{-5}\text{ m}^2$$

Then

$$m = \sqrt{\frac{h_c P}{k A_c}} = \sqrt{\frac{(25\text{ W/m}^2\text{ K})(\pi)(0.004\text{ m})}{(168\text{ W/m K})(1.257 \text{ x } 10^{-5}\text{ m}^2)}} = 12.199\text{ m}^{-1}$$

Then the fin efficiency is

$$\eta_f = \frac{\tanh mL}{mL} = \frac{\tanh\left[(12.199\text{ m}^{-1})(0.021\text{ m})\right]}{(12.199\text{ m}^{-1})(0.021\text{ m})} = 0.979$$

The surface area of a fin is

$$A_f = \pi DL = \pi(0.004\text{ m})(0.021\text{ m}) = 2.639 \text{ x } 10^{-4}\text{ m}^2$$

and the exposed area of the parent surface is

$$A_p = (0.123\text{ m})(0.152\text{ m}) - 285(1.257 \text{ x } 10^{-5}\text{ m}^2) = 0.01515\text{ m}^2$$

Then the total heat transfer area is

$$A_{total} = NA_f + A_p = 285(2.639 \text{ x } 10^{-4}\text{ m}^2) + 0.01515\text{ m}^2 = 0.09036\text{ m}^2$$

The overall heat transfer efficiency of this surface is

$$\eta_{surf} = 1 - \left(\frac{NA_f}{A_{total}}\right)(1-\eta_f) = 1 - \left(\frac{285(2.639 \text{ x } 10^{-4}\text{ m}^2)}{0.09036\text{ m}^2}\right)(1-0.979) = 0.982$$

The maximum possible heat transfer from this array is

$$\dot{Q}_{max} = h_c A_{total}(T_s - T_\infty) = (25\text{ W/m}^2\text{ K})(0.09036\text{ m}^2)(68\text{ C} - 45\text{ C}) = 51.959\text{ W}$$

Then the actual heat transfer from the array is

$$\dot{Q}_{total} = \eta_{surf}\dot{Q}_{max} = 0.982(51.959\text{ W}) = 51.037\text{ W}$$

Thus, for the operating conditions specifed, the proposed array is adequate to achieve the design operating conditions for the Intel Pentium© III Xeon processor.

6.7 Transient Heat Transfer Interactions Between a Solid and a Fluid Environment

We have just seen how the steady-state operating temperature of a solid can be maintained by means of a heat transfer interaction between a solid and a fluid environment with

the aid of fins which increase the active heat transfer area of the solid. There is yet another broad class of physical situations involving the interaction between a solid and a fluid environment for which the time history of the heat transfer interaction, rather than the steady-state behavior, is important. Such might be the case, for example, during a heat treating operation in which a solid body at high temperature is immersed in a fluid, either a liquid or a gas, at low temperature in order to achieve some particular metallurgical state of the solid. Similarly, in the event of a fire in building, the materials of construction are suddenly exposed to gases at extremely high temperatures that can lead to the spread or the extinguishment of the fire under depending upon the conditions that prevail. In cases of this type, the focus of our attention is on the thermal history of the solid, i.e. the spatial distribution of temperature within the solid as a function of time, rather than the steady-state heat transfer interaction.

6.7.1 The Biot Number

In general, the thermal history of the solid is governed by the rate at which energy can be distributed within the solid relative to the rate at which energy can be transported from the fluid to the solid through the interface between them. The dominant heat transfer mode inside the solid is conduction whereas the dominant heat transfer mode in the fluid is convection. These rates are governed by the thermal resistances associated with the particular modes of heat transfer. Their relative magnitudes can be expressed by the dimensionless group of the physical characteristics that describe these modes. This group, known as the *Biot number* and denoted by the symbol *Bi*, is defined as the ratio of the internal resistance to conduction heat transfer to the external resistance to convection heat transfer. If L_c is some characteristic length of the solid defined as the ratio of the volume of the solid, V, divided by the surface area of the solid, A_s, ($L_c = V/A_s$) we can write the Biot number in the form

$$Bi = \frac{\text{internal conduction resistance}}{\text{external convection resistance}} = \frac{L/k_{solid}A_c}{1/h_c A_s} \approx \frac{h_c L_c}{k_{solid}} \qquad (6.110)$$

Depending upon the magnitude of the Biot number, the heat transfer interaction between a solid and a fluid can be grouped into one of three general categories:

Category 1: The principal resistance to heat transfer lies within the fluid. (Bi ≪ 1)

This category, which represents one extreme of the physical situation of interest, can be the result of either one of two conditions. On the one hand, the mechanism of energy transport within the fluid may be so slow that as each unit of energy passes through the interface between the solid and the fluid, it is redistributed over all the mass elements of the solid before the next unit of energy can pass through the interface. On the other hand, the mechanism of energy transport within the solid may be so fast that any amount of energy that passes through the interface is immediately redistributed over the mass elements of the solid before the next unit of energy can pass through the interface. In both cases, the result is the same: the temperature of the solid can be modeled as being uniform at all times. That is, the temperature of the solid changes with time, but during any time interval, all the mass elements of the solid change temperature by the same amount. All the temperature gradients associated with the heat transfer interaction lie within the fluid. Thus, in the context of this model, the heat transfer interaction is reversible within the solid but irreversible within the fluid. This model is usually called the *lumped thermal capacitance model.*

Category 2. The principle resistance to heat transfer lies within the solid. (Bi → ∞)

This category, which lies at the other extreme, can also be the result of either one of two

conditions. On the one hand, the mechanism of energy transport within the fluid is so fast that energy is transported through the interface faster than it can be redistributed within the solid. On the other hand, the energy transport within the solid is so slow that energy is transported through the interface faster than it can be redistributed within the solid. The net result in these two cases is the same: the temperature of the surface of the solid immediately assumes the temperature of the fluid and all temperature gradients lie within the solid. The temperature of the fluid is modeled as being uniform at all times. (In the typical situation in practice, the volume of the fluid is so large that the temperature of the fluid is modeled as uniform in space and constant in time.) Thus, in the context of this model, the heat transfer interaction is reversible within the fluid but irreversible within the solid, and the fluid behaves as a heat reservoir.

Category 3. The resistance to heat transfer in the fluid is comparable to the resistance to heat transfer in the solid. (Bi ~ 1)

In this category, the rate at which energy is transported within the fluid is of the same order of magnitude as the rate at which energy is transported within the solid. As a consequence, thermal gradients exist in both the fluid and the solid, and the heat transfer interaction is irreversible in both the fluid and the solid.

As an illustration of the significance of this grouping, let us consider an example of each. Consider a slab of solid material whose properties (except temperature, T) have known fixed values. The slab has an initial temperature T_i and is plunged into a bath that has a lower temperature T_∞. With the origin of the geometry placed at the midplane of the slab, the dimensions of the slab extend to infinity in the y- and z-directions and to L in the positive x-direction and $-L$ in the negative x-direction. Since $V = 2zyL$ and $A_s = 2zy$, the characteristic length, V/A_s, becomes L, the half-thickness of the slab. Thus, the Biot number is $Bi = h_c L_c / k_{solid}$. Let us now examine the three possibilities in detail.

6.7.2 The Lumped Thermal Capacitance Model (Bi << 1)

For the solid as a system, the first law of thermodynamics can be written in rate form as

$$\dot{Q} - \dot{W} = \frac{dU}{dt} \tag{6.111}$$

We have already stated (and will soon show in detail) that the heat transfer interaction is reversible from the point of view of the solid when $Bi << 1$. Thus, there is a unique, spatially uniform temperature, T, inside the solid at all times even though it is changing with time. We can, therefore, model the solid as a pure thermal system, known in this case as a *lumped thermal capacitance* for reasons that will soon become apparent. Since the solid is passing through a series of equilibrium states during the interaction, we can write the energy constitutive relation in differential form, viz.

$$dU = mcdT = \rho cVdT \tag{6.112}$$

where ρ is the density of the solid material and c is its specific heat. Since there is no work transfer, we can write the first law of thermodynamics in the form

$$\boxed{\dot{Q} = \rho cV \frac{dT}{dt}} \tag{6.113}$$

where for cooling of the solid, the heat transfer rate is negative and

$$\frac{dT}{dt} < 0 \tag{6.114}$$

From Newton's Law of Cooling we have

$$\dot{Q} = -h_c A_s (T - T_\infty) \tag{6.115}$$

where the minus sign on the right-hand side of equation (6.115) makes the heat transfer rate negative for $T > T_\infty$ as it must be since the heat transfer is from the system. Then combining equations (6.113) and (6.115), we have for the first law of thermodynamics of the solid

$$\rho c V \frac{dT}{dt} = -h_c A_s (T - T_\infty) \tag{6.116}$$

with the initial condition that $T = T_i$ at $t = 0$. If we change variables so that $\theta = T - T_\infty$ equation (6.116) can be written

$$\frac{d\theta}{dt} = -\frac{h_c A_s}{\rho c V}\theta \tag{6.117}$$

If we separate variables, equation (6.117) becomes

$$\frac{d\theta}{\theta} = -\frac{h_c A_s}{\rho c V} dt \tag{6.118}$$

If we now integrate equation (6.118), we get

$$\int_{\theta_i}^{\theta} \frac{d\theta}{\theta} = -\frac{h_c A_s}{\rho c V} \int_0^t dt \tag{6.119}$$

or

$$\ln\left(\frac{\theta}{\theta_i}\right) = -\frac{h_c A_s}{\rho c V} t \tag{6.120}$$

where we have made use of the initial condition. If we exponentiate both sides of equation (6.120), we get

$$\frac{\theta}{\theta_i} = e^{-\frac{h_c A_s}{\rho c V} t} \qquad \frac{T - T_\infty}{T_i - T_\infty} = e^{-t/\tau} \tag{6.121}$$

Note that the coefficient of t in the exponent of equation (6.121) has the dimensions of (time)$^{-1}$ thereby making the exponent itself dimensionless "time". Then we can write

$$\tau = \frac{\rho c V}{h_c A_s} = \left(\frac{1}{h_c A_s}\right)(\rho c V) = R_{th} C_{th} \tag{6.122}$$

where τ is the time constant of this interaction and R_{th} and C_{th} are the appropriate thermal resistance and capacitance, respectively, for this situation. Thus during the heat transfer interaction, the solid behaves as a lumped thermal capacitance C_{th} "discharging" through the thermal resistance R_{th}, thereby extending the electrical analog concept for heat transfer. The equivalent electrical circuit is shown in Figure 6.9.

The response of the lumped thermal capacitance to immersion in the fluid medium can be shown graphically in dimensionless form by plotting equation (6.121) as in Figure 6.10. Note that the time required for the solid to reach true thermal equilibrium with the fluid is infinite for this model; however, the difference between the temperature of the solid and the temperature of the fluid decreases to less than one percent of the initial temperature difference by the time 4.6 time constants have passed.

Since the exponent in equation (6.122) is dimensionless, we can use it to define a new dimensionless parameter. Thus

$$\frac{h_c A_s t}{\rho c V} = \frac{h_c t}{\rho c L_c} = \left(\frac{h_c L_c}{k_{solid}}\right)\left(\frac{k_{solid}}{\rho c}\right)\left(\frac{t}{L_c^2}\right) = \left(\frac{h_c L_c}{k_{solid}}\right)\left(\frac{\alpha t}{L_c^2}\right) = Bi \bullet Fo \tag{6.123}$$

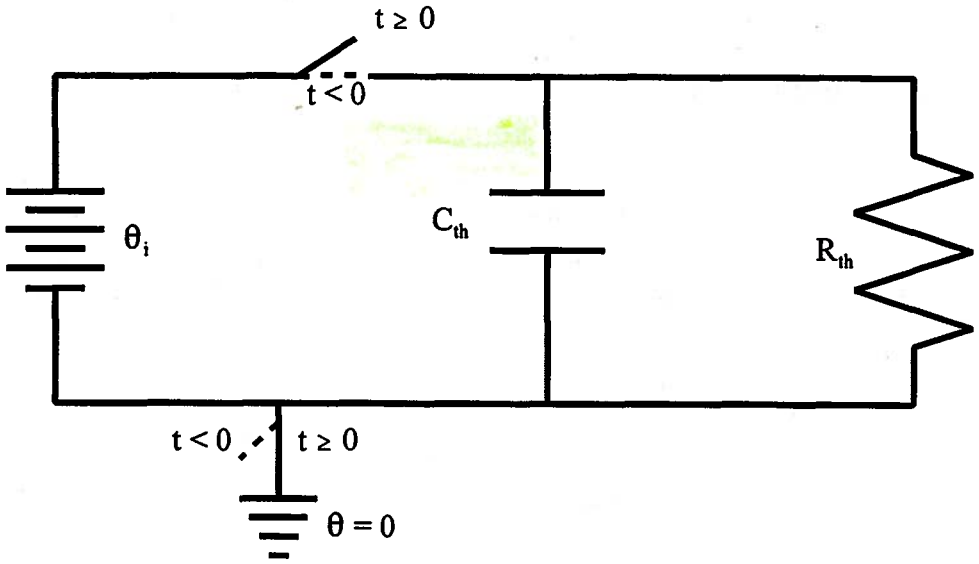

Figure 6.9 Equivalent Thermal Circuit for Lumped Thermal Capacitance

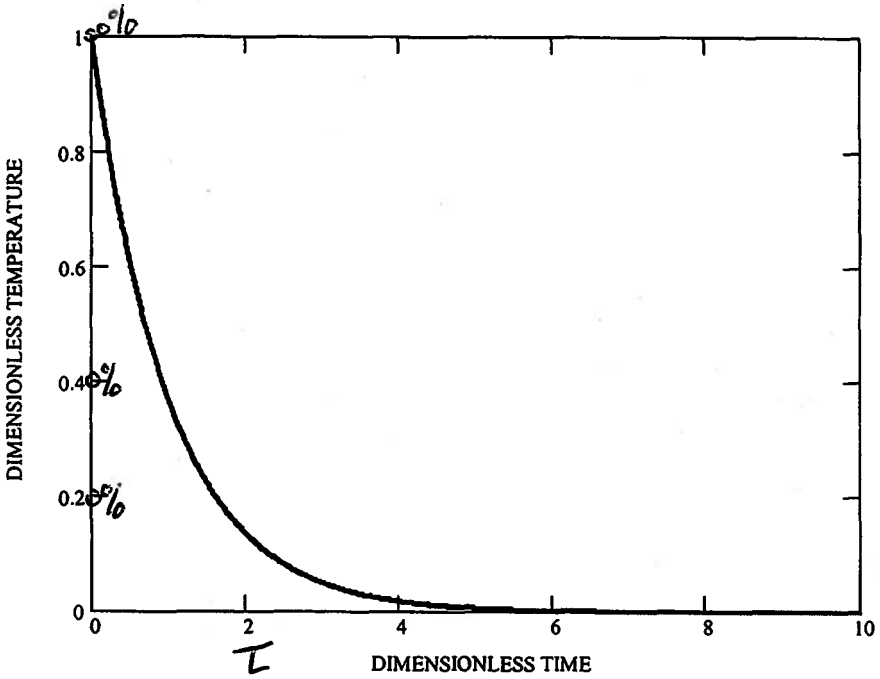

Figure 6.10 Dimensionless Response of the Lumped Thermal Capacitance Model

where we have made use of the definition of the thermal diffusivity, α, and we have introduced the *Fourier number*, *Fo*, where

$$Fo = \frac{\alpha t}{L_c^2} = \frac{t}{t_c} \qquad \alpha = \frac{K}{\rho c} \qquad (6.124)$$

where t_c is the characteristic time ($t_c = L_c^2/\alpha$) that represents the time required for a thermal

disturbance to diffuse a distance L_c. Recall that the characteristic length, L_c, for a slab of thickness $2L$ is L. Then in dimensionless form, the time history of the temperature in a solid with an initial value of T_i immersed in an infinite fluid with a temperature T_∞ is

$$\frac{\theta}{\theta_i} = \frac{T - T_\infty}{T_i - T_\infty} = e^{-Bi \cdot Fo} \tag{6.125}$$

Equation (6.125) is plotted in Figure 6.11 for various values of the Biot number. Notice that for a given solid, the poorer the convection heat transfer between the solid and the fluid, i.e., the smaller the value of the Biot number, the longer is the time required for the solid to reach a given internal temperature.

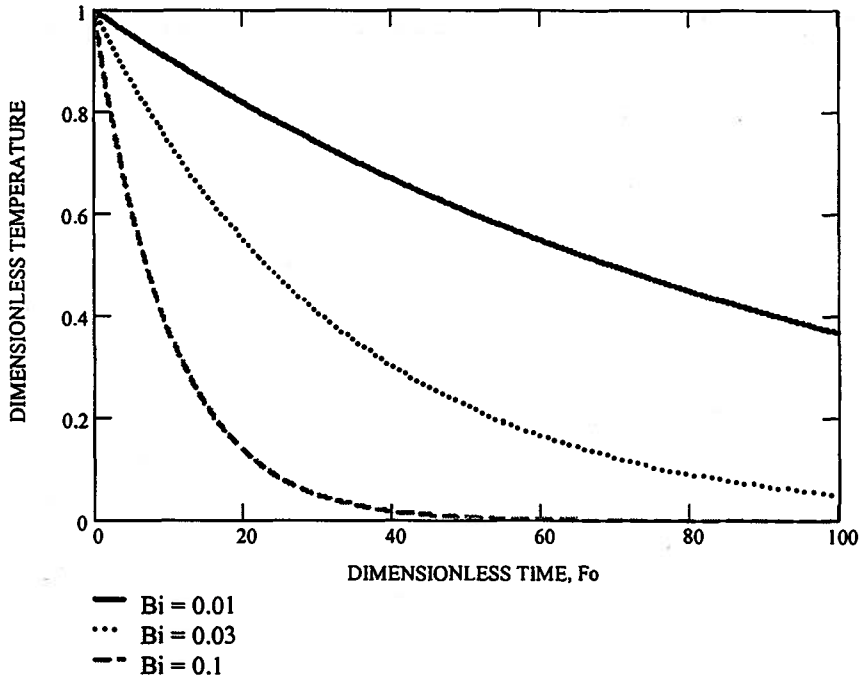

Figure 6.11 Lumped Thermal Capacitance Model in Terms of Biot and Fourier Numbers

It will be shown in Section 6.6.4 that the lumped thermal capacitance model is valid only for $Bi < 0.1$. We now examine the nature of the irreversibility in this heat transfer interaction. For the solid as a system, we can calculate the entropy generation from the second law of thermodynamics, viz.

$$(S_{gen})_{solid} = (S_2 - S_1)_{solid} - (S_{transfer})_{solid} \tag{6.126}$$

The entropy transfer from the fluid to the solid is given by

$$(S_{transfer})_{solid} = \int_0^{t_{final}} \frac{\dot{Q}}{T} dt = -\int_0^{t_{final}} \frac{h_c A_s (T - T_\infty)}{T} dt \tag{6.127}$$

where we have substituted the rate equation for the heat transfer rate, equation (6.115). Using the chain rule for derivatives, we can rewrite equation (6.127) in the form

$$(S_{transfer})_{solid} = -\int_0^{t_{final}} \frac{h_c A_s (T - T_\infty)}{T} \frac{dt}{dT} dT \tag{6.128}$$

Substituting equations (6.116) and (6.122) into equation (6.128), we get for the entropy transfer from the fluid to the solid

$$(S_{transfer})_{solid} = \int_{T_i}^{T_f} \frac{h_c A_s (T - T_\infty)}{T} \frac{\tau}{(T - T_\infty)} dT = h_c A_s \tau \int_{T_i}^{T_f} \frac{dT}{T} = (\rho c V)_{solid} \ln\left(\frac{T_f}{T_i}\right) \quad (6.129)$$

The change in entropy is given by the entropy constitutive relation for the pure thermal system model, viz.

$$(S_2 - S_1)_{solid} = (mc)_{solid} \ln\left(\frac{T_2}{T_1}\right)_{solid} = (\rho V c)_{solid} \ln\left(\frac{T_f}{T_i}\right)_{solid} \quad (6.130)$$

Substituting equations (6.129) and (6.130) into equation (6.126), we get

$$(S_{gen})_{solid} = (\rho c V)_{solid} \ln\left(\frac{T_f}{T_i}\right)_{solid} - (\rho c V)_{solid} \ln\left(\frac{T_f}{T_i}\right)_{solid} = 0 \quad (6.131)$$

Thus, since no entropy is generated internally in the solid, the heat transfer interaction in the solid is reversible. For the fluid as a system, we can apply the second law of thermodynamics in a form similar to equation (6.126) to determine the entropy generated in the fluid as a result of this interaction. It is first necessary to determine the change of state in the fluid. If the final temperature, T_{final}, is truly the run-down- to-equilibrium temperature for the heat transfer interaction between a fluid system of large size and a solid system of relatively small size, then the temperature of the fluid does not change and $T_{final} = T_\infty$. Under these circumstances, the initial and final temperatures of the fluid system are well defined. In fact, they are equal to the uniform temperature T_∞. Although the temperature of the fluid does not change as a result of the heat transfer interaction, the state of the fluid does change since both the energy and the entropy do change. We can model the fluid as an incompressible fluid, but there are no simple constitutive relations that we can use to calculate the changes in these two properties since the fluid behaves as though it were a system of infinite size. We must rely, then, on the first and second laws of thermodynamics to do this. If we consider the composite system consisting of the solid and the fluid taken together, this system is isolated. Thus the first law of thermodynamics shows that

$$(U_f - U_i)_{fluid} = -(U_f - U_i)_{solid} = -[\rho c V (T_f - T_i)]_{solid} = -[\rho c V (T_\infty - T_i)]_{solid} \quad (6.132)$$

To determine the change in entropy of the fluid, we need to find a reversible process that will produce this same energy change with no generation of entropy. Then according to the second law of thermodynamics, the change in entropy will be equal to the entropy transfer for this reversible process.

$$(S_2 - S_1)_{fluid} = \int_{state1}^{state2} \left(\frac{\delta Q}{T}\right)_{\substack{fluid \\ reversible}} \quad (6.133)$$

Note that since the temperature of the fluid does not change, the temperature at the boundary where the reversible heat transfer of equation (6.133) occurs is equal to the temperature of the fluid. Since this temperature is constant, it can be taken outside the integral. Then equation (6.133) becomes

$$(S_2 - S_1)_{fluid} = \frac{1}{T_\infty} \int_{state1}^{state2} (\delta Q)_{\substack{fluid \\ reversible}} = \frac{(Q_{i-f})_{\substack{fluid \\ reversible}}}{T_\infty} \quad (6.134)$$

Since the fluid system experiences no work transfer, the first law of thermodynamics for the fluid becomes

$$(Q_{i-f})_{fluid} = (U_f - U_i)_{fluid} = [\rho c V (T_i - T_\infty)]_{solid} \quad (6.135)$$

Then the change in the stored entropy of the fluid is simply

$$(S_2 - S_1)_{fluid} = \frac{[\rho cV(T_i - T_\infty)]_{solid}}{T_\infty} \tag{6.136}$$

Since the solid and the fluid together form an isolated system, the entropy transfer for the fluid is just the negative of the entropy transfer for the solid, viz.

$$(S_{transfer})_{fluid} = -(S_{transfer})_{solid} = -(\rho cV)_{solid} \ln\left(\frac{T_\infty}{T_i}\right) \tag{6.137}$$

Then the entropy generation in the fluid is given by

$$(S_{gen})_{fluid} = \frac{(\rho cV)_{solid}(T_i - T_\infty)}{T_\infty} - (\rho cV)_{solid} \ln\left(\frac{T_i}{T_\infty}\right) \tag{6.138}$$

If we write $T_i - T_\infty = \Delta T$, we can show that $(S_{gen})_{fluid} > 0$.

$$(S_{gen})_{fluid} = (\rho cV)_{solid}\left[\frac{\Delta T}{T_\infty} - \ln\left(1 + \frac{\Delta T}{T_\infty}\right)\right] \tag{6.139}$$

Since $(\rho cV)_{solid}$ is always positive, we need to show that the term in square brackets is always positive. Since $0 < T_i < \infty$,

$$-1 < \frac{\Delta T}{T_\infty} < \infty$$

Then a plot of the term in square brackets as shown in Figure 6.12 proves that $(S_{gen})_{fluid} > 0$. Thus the heat transfer interaction in the fluid is always irreversible except in the limit as the temperature of the fluid and the solid become identical. It follows, then, that the fluid cannot be modeled as a heat reservoir since the heat reservoir model can experience only reversible processes.

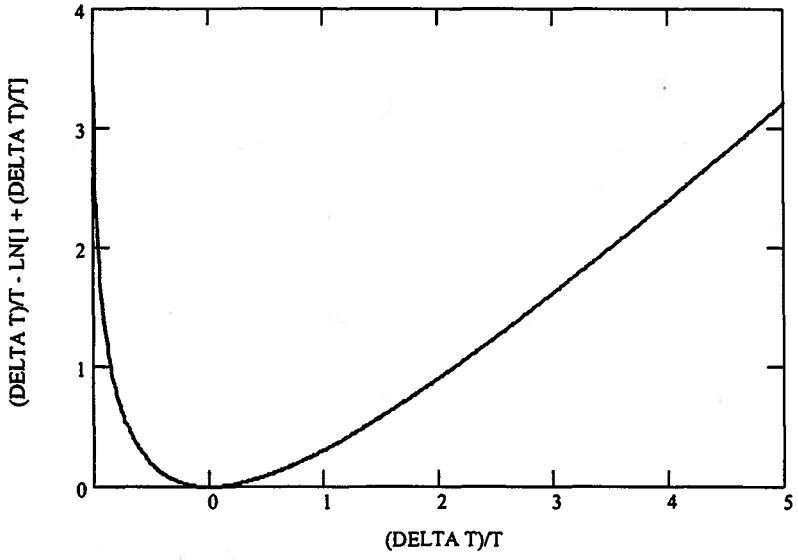

Figure 6.12 Entropy Generation in a Fluid Due to Heat Transfer with a Solid

If we expand the logarithmic term appearing in equation (6.139),we get

$$\ln\left(1+\frac{\Delta T}{T_\infty}\right)=\frac{\Delta T}{T_\infty}-\frac{1}{2}\left(\frac{\Delta T}{T_\infty}\right)^2+\ldots \tag{6.140}$$

Substitution of equation (6.140) into equation (6.139) gives

$$(S_{gen})_{fluid}=\frac{(\rho cV)_{solid}}{2}\left(\frac{\Delta T}{T_\infty}\right)^2 \tag{6.141}$$

Since $(S_{gen})_{fluid}$ approaches zero faster than ΔT as ΔT approaches zero, the entropy generation becomes zero in the limit of zero temperature difference and the heat transfer interaction becomes reversible.

Example 6E.7: Aluminum structural shapes such as I-beams and angles are formed by "hot rolling" the material while it is at elevated temperature, usually in the range of 300 C to 400 C. During a particular hot rolling process, aluminum shapes with a characteristic dimension of 1 cm (The material is actually 2 cm thick.), exit from the mill at a temperature of T_i = 400 C. The post-forming heat treatment process, which is not rate sensitive, requires cooling to a temperature of 40 C. The cooling process is to be carried out by natural convection in air at a temperature of T_∞ = 30 C with a heat transfer coefficient of h_c = 10 W/m^2 K. Estimate the time required for the cooling process and compare it with the required time for a process using water with a heat transfer coefficient of h_c = 100 W/m^2 K.

The properties of the aluminum are: ρ = 2770 kg/m^3, c = 875 J/kg K, k = 174 W/m K.

Solution: We first need to determine the Biot number to determine which rate process represents the rate-limiting process. For the first method of cooling, the Biot number is

$$Bi=\frac{h_c L_c}{k_s}=\frac{(10\text{ W/m}^2\text{ K})(0.01\text{ m})}{174\text{ W/m K}}=5.75\text{ x }10^{-4}$$

Since $Bi < 0.1$, the rate limiting process is the rate of heat transfer by convection off the surface of the aluminum, and we can model the aluminum as a lumped thermal capacitance. Then the time constant for the first cooling method is

$$\tau_1=\frac{\rho cV}{h_c A_s}=\frac{(2770\text{ kg/m}^3)(875\text{ J/kg K})}{(10\text{ W/m}^2\text{ K})(0.01\text{ m})}=2423.8\text{ sec}$$

According to equation (6.121), the time required to cool to 40 C by the first method is given by

$$t=-\tau_1\ln\left(\frac{40\text{ C}-30\text{ C}}{400\text{ C}-30\text{ C}}\right)=-(2423.8\text{ sec})\ln(0.02703)=8752.1\text{ sec}=2.43\text{ hr}$$

Since the second method results in a heat transfer coefficient that is ten times higher, the Biot number for the second method is Bi = 5.75 x 10^{-3}, and the lumped thermal capacitance model remains valid. The time constant for the second method is only one tenth that of the first method. Then, the time required to cool would be only one-tenth as long or 0.243 hr if the water temperature is the same as the air temperature. Thus, the throughput of the forming process could be increased significantly by using water cooling.

6.7.3 Heat Reservoir Model (Bi → ∞)

We now consider the case for which the value of the Biot number lies at the other extreme, namely very large values approaching infinity in the limit. As we might expect, the temperature gradients in this case will lie in the solid and not the fluid. Thus, the fluid will experience a reversible heat transfer interaction while the solid will experience an irreversible interaction. Then in the limit of infinitely large Biot number, the fluid will behave as a true heat

reservoir. We thus have a means to quantitate the conditions under which the heat reservoir model is valid. Returning to our physical situation described at the outset of Section 6.6, we note that the temperature of the slab is now spatially non-uniform and changing with time. Thus, in order for us to quantitate the time history of this temperature distribution, it is necessary for us to solve the one-dimensional heat conduction equation. From equation (6.48), we have

$$\frac{\partial^2 T}{\partial x^2} = \frac{1}{\alpha}\frac{\partial T}{\partial t} \tag{6.142}$$

with one initial condition and two boundary conditions. For the initial condition, we have that the initial uniform temperature of the slab is T_i, i.e.

$$T(x,0) = T_i \tag{6.143}$$

For one of the boundary conditions we note that the temperature distribution in the slab will be symmetric about its midplane. Thus the temperature gradient will vanish in the center of the slab for all times, i.e.

$$\left(\frac{\partial T}{\partial x}\right)_{x=0} = 0 \tag{6.144}$$

For the second boundary condition, we have the condition that the energy conducted to the surface of the slab from within must be carried away by convection from its outer surface, i.e. the rate of energy flow to the surface determined by the Fourier Conduction Law in the solid must be exactly the same as that due to convection determined from Newton's Law of Cooling in the fluid. Thus, for unit cross-sectional for energy flow

$$-k\left(\frac{\partial T}{\partial x}\right)_{x=L} = h_c[T(L,t) - T_\infty] \tag{6.145}$$

As we saw in the previous section, it is usually worthwhile to analyze the siuation in non-dimensional form so that the result can be applied to any similar situation simplt by scaling the results according to the appropriate parameters. Then we can non-dimensionalize this analysis through the use of the following variables:

$$\begin{aligned} \theta &= T - T_\infty \\ \theta_i &= T_i - T_\infty \\ \theta^* &= \frac{\theta}{\theta_i} \\ x^* &= \frac{x}{L} \\ t^* &= \frac{\alpha t}{L_c^{\,2}} = Fo \end{aligned} \tag{6.146}$$

It follows, then, that the conduction equation and its initial and boundary conditions can be written

$$\begin{aligned} &\frac{\partial^2 \theta^*}{\partial x^{*2}} = \frac{\partial \theta^*}{\partial Fo} \\ &\theta^*(x^*,0) = 1 \\ &\left(\frac{\partial \theta^*}{\partial x^*}\right)_{x^*=0} = 0 \\ &\left(\frac{\partial \theta^*}{\partial x^*}\right)_{x^*=1} = -Bi\,\theta^*(1,t^*) \end{aligned} \tag{6.147}$$

For the case in which the Biot number is infinitely large, the surface temperature of the solid becomes identical to the temperature of the fluid immediately upon immersion. Then equations (6.147) take a slightly different form.

$$\frac{\partial^2\theta^*}{\partial x^{*2}} = \frac{\partial\theta^*}{\partial Fo}$$
$$\left(\frac{\partial\theta^*}{\partial x^*}\right)_{x^*=0} = 0 \qquad (6.148)$$
$$\theta^*(1,t^*) = 0$$

In order to determine the solution for θ^* that satisfies the requiste conditions, we make use of a mathematical method known as the separation of variables in which the solution is formulated as the product of two functions, one a function of x^* only, the other a function of Fo only. Then the solution for θ^* becomes

$$\theta^*(Fo,x^*) = G(Fo)\cdot H(x^*) \qquad (6.149)$$

If we now substitute this solution into the conduction equation, we get

$$H\frac{dG}{dFo} = G\frac{d^2H}{dx^*} \qquad (6.150)$$

Equation (6.150) can be rearranged as

$$\frac{1}{G}\frac{dG}{dFo} = \frac{1}{H}\frac{d^2H}{dx^{*2}} \qquad (6.151)$$

which now separates the variables with Fo appearing on the left and x^* appearing on the right of equation (6.151). The only way that the left-hand side can equal the right-hand side is for each side to be equal to a constant. For reasons that will become apparent shortly, this constant must be a negative number, say $-\lambda^2$. Then

$$\frac{dG}{dFo} + \lambda^2 G = 0$$
$$\frac{d^2H}{dx^{*2}} + \lambda^2 H = 0 \qquad (6.152)$$

which have the solutions

$$G = C_1 e^{-\lambda^2 Fo}$$
$$H = C_2\cos\lambda x^* + C_3\sin\lambda x^* \qquad (6.153)$$

Then

$$\theta^*(Fo,x^*) = e^{-\lambda^2 Fo}(A\cos\lambda x^* + B\sin\lambda x^*) \qquad (6.154)$$

where $A = C_1C_2$ and $B = C_1C_3$. Applying the boundary conditions, we get

$$\left(\frac{\partial\theta^*}{\partial x^*}\right)_{x^*=0} = e^{-\lambda^2 Fo}(-A\lambda\sin\lambda x^* + B\lambda\cos\lambda x^*)_{x^*=0} = 0 \qquad (6.155)$$

which requires that $B = 0$, and

$$(\theta^*)_{x^*=1} = (Ae^{-\lambda^2 Fo}\cos\lambda x^*)_{x^*=1} = 0 \qquad (6.156)$$

which in turn requires that $\cos\lambda x^* = 0$ or

$$\lambda_n = (n+\tfrac{1}{2})\pi \qquad n = 0,1,2,3,\ldots \qquad (6.157)$$

The λ_n are the eigenvalues for this solution, and the eigenfunction corresponding to the nth eigenvalue is

$$\theta_n^*(Fo,x^*) = A_n e^{-(n+\frac{1}{2})^2\pi^2 Fo}\cos(n+\tfrac{1}{2})\pi x^* \tag{6.158}$$

Then the general solution is the sum of the series of solutions

$$\theta^*(Fo,x^*) = \sum_{n=0}^{\infty} A_n e^{-(n+\frac{1}{2})^2\pi^2 Fo}\cos(n+\tfrac{1}{2})\pi x^* \tag{6.159}$$

The constants are determined from the initial condition

$$(\theta^*)_{Fo=0} = \sum_{n=0}^{\infty} A_n \cos(n+\tfrac{1}{2})\pi x^* = 1 \tag{6.160}$$

This is a Fourier series expansion of the number 1. In general, in the initial state there may be a temperature distribution in the solid before immersion in the fluid. Then

$$(\theta^*)_{Fo=0} = f(x^*) \tag{6.161}$$

and the Fourier expansion of this initial temperature distribution is

$$f(x^*) = \sum_{n=0}^{\infty} A_n \cos(n+\tfrac{1}{2})\pi x^* \tag{6.162}$$

where the coefficients are given by

$$A_n = 2\int_0^1 f(x^*)\cos(n+\tfrac{1}{2})\pi x^* dx^* \tag{6.163}$$

For a uniform initial temperature, $f(x^*) = 1$ and

$$A_n = \frac{2}{(n+\frac{1}{2})\pi}[\sin(n+\tfrac{1}{2})\pi x^*]_0^1 = \frac{2(-1)^n}{(n+\frac{1}{2})\pi} \tag{6.164}$$

Then

$$\theta^*(Fo,x^*) = \sum_{n=0}^{\infty} \frac{2(-1)^n}{(n+\frac{1}{2})\pi} e^{-(n+\frac{1}{2})^2\pi^2 Fo}\cos(n+\tfrac{1}{2})\pi x^* \tag{6.165}$$

Then in terms of the original parameters the temperature distribution becomes

$$\frac{T-T_\infty}{T_i-T_\infty} = \sum_{n=0}^{\infty} \frac{2(-1)^n}{(n+\frac{1}{2})\pi} e^{-(n+\frac{1}{2})^2\pi^2 Fo}\cos(n+\tfrac{1}{2})\pi\frac{x}{L} \tag{6.166}$$

This dimensionless temperature distribution is shown in Figure 6.13 for various values of the Fourier number, i.e. for different times. In Figure 6.13, increasing values of the Fourier number represent later times. Notice that for the early times, the temperature at the midplane of the slab is unaffected by the cooling at the surface, but with the passage of time the influence of the surface diffuses into the slab and the temperature at the midplane begins to drop. Notice also that the surface temperature immediately takes on the temperature of the fluid as we required in the boundary conditions because of the infinite value of the Biot number. If the Biot number is finite, the surface temperature is a function of time and the solution of the conduction equation is more complicated. This situation is considered in Section 6.6.4.

For the rate of heat transfer out of the slab, the Fourier Conduction Law gives

$$\frac{\dot{Q}}{A_c} = -k_{solid}\left(\frac{\partial T}{\partial x}\right)_{x=0} \tag{6.167}$$

Substituting equation (6.166) into equation (6.167) gives

$$\frac{\dot{Q}}{A_c} = -k_{solid}(T_i-T_\infty)\sum_{n=0}^{\infty} \frac{2(-1)^n}{(n+\frac{1}{2})\pi} e^{-(n+\frac{1}{2})^2\pi^2 Fo}\frac{\partial}{\partial x}[\cos(n+\tfrac{1}{2})\pi\frac{x}{L}]_{x=L} \tag{6.168}$$

or

$$\frac{\dot{Q}}{A_c} = \frac{2k_{solid}(T_i - T_\infty)}{L} \sum_{n=0}^{\infty} \frac{2(-1)^n}{(n+\frac{1}{2})\pi} e^{-(n+\frac{1}{2})^2 \pi^2 Fo} \tag{6.169}$$

The series appearing in equation (6.169) converges very rapidly except for small values of the Fourier number. For $Fo \geq 0.2$, i.e. long times, we need only the first term in the series. Then

$$\frac{\dot{Q}}{A_c} = \frac{2k_{solid}(T_i - T_\infty)}{L} e^{-(\frac{\pi}{2})^2 Fo} \tag{6.170}$$

and the temperature gradient in the slab at the interface between the solid and the fluid is linear with a value that decays exponentially with time. For short times, more terms than just the first are required; however, in the limit of very short times, i.e. $Fo \leq 0.05$, it can be shown that the series reduces to

$$\lim_{Fo \to 0} \frac{\dot{Q}}{A_c} = \frac{k_{solid}(T_i - T_\infty)}{\sqrt{\pi \alpha t}} \tag{6.171}$$

Note from Figure 6.13 that the temperature in the center of the slab remains unchanged for short times, i.e. small values of the Fourier number, and that the time dependent effects are confined to the vicinity of the interface between the solid and the fluid. As equation (6.137) shows, the thickness of the slab is of no consequence since L does not appear in the result for the

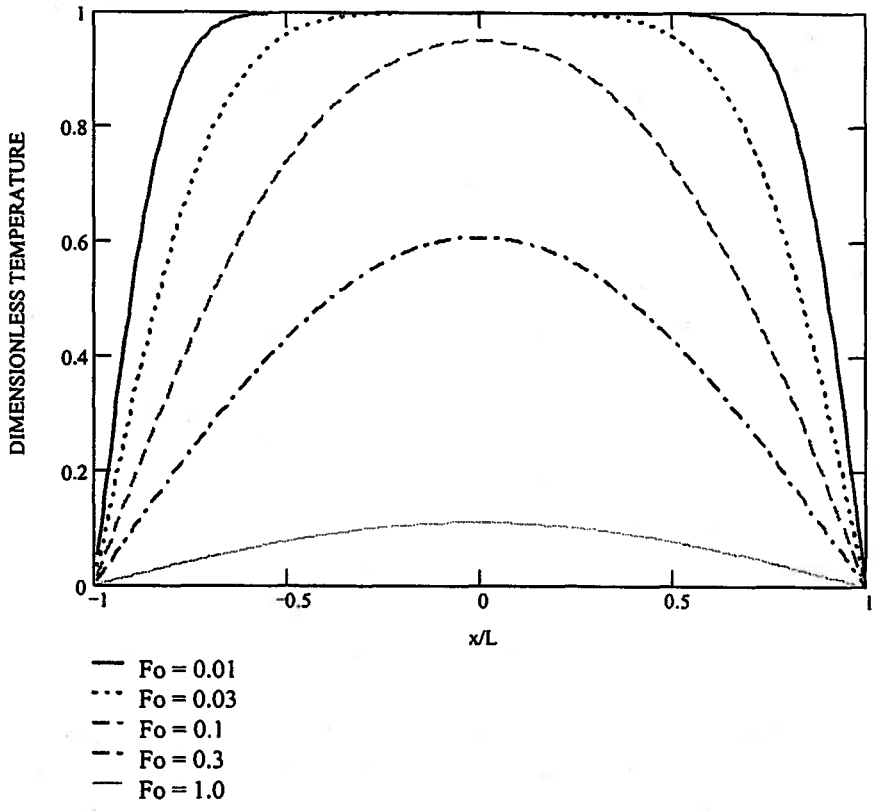

Figure 6.13 Temperature Distribution in a Slab Cooled by Convection with Bi → ∞

heat flux as $Fo \to 0$. In effect, as far as the center of the slab is concerned, the slab appears to be infinitely thick and the center is unaffected by the heat transfer interaction at the boundary. This result gives rise to the concept of the semi-infinite solid model which we will consider in detail Section 6.7.

In considering the nature of the reversibility of this heat transfer interaction, the analysis is nearly identical to the previous case except that now we note that in the limit as $Bi \to \infty$, the

only temperature gradients present lie in the solid and not the fluid. Under these conditions, the temperature of the fluid remains both spatially uniform and constant in time throughout the interaction; consequently, the interaction is reversible in the fluid but irreversible in the solid. In fact, in the limit as $Bi \to \infty$, the thermodynamic behavior of the fluid is unique in that it can experience only reversible heat transfer interactions while maintaining constant temperature. As we saw in Chapter 3, a system that meets these criteria is known as the *heat reservoir model.* No real system truly fulfills all the requirements of the model, but for many systems the departures from the model are so small that we are justified in using it.

It is interesting to note that the case for $Bi << 1$ that we considered previously bears some similarity to the present model in that the final equilibrium temperature of the fluid may be identical to its initial temperature; however, in that case the rate limiting heat transfer process for the interaction was in the fluid and not in the solid. Therefore, the temperature gradient and, hence, the irreversibility associated with the interaction resided in the fluid. For this reason, the fluid involved in an interaction with $Bi << 1$ can never be modeled as a heat reservoir even though it may meet some of the requirements for that model. The one crucial requirement of reversible heat transfer interactions in the fluid is lacking.

6.7.4 Bi ~ 1:

Now we consider the case in which the internal resistance to conduction is of the same order of magnitude as the external resistance to convection, i.e. Bi ~ 1. As before the conduction equation yields solutions of the form

$$\theta^*(Fo,x^*) = e^{-\lambda^2 Fo}(A\cos\lambda x^* + B\sin\lambda x^*) \tag{6.172}$$

From the first boundary condition,

$$\left(\frac{\partial\theta^*}{\partial x^*}\right)_{x^*=0} = 0 \tag{6.173}$$

we conclude that $B = 0$ and that

$$\theta^*(Fo,x^*) = Ae^{-\lambda^2 Fo}\cos\lambda x^* \tag{6.174}$$

From the second boundary condition,

$$\left(\frac{\partial\theta^*}{\partial x^*}\right)_{x^*=1} = -Bi\theta^*(1,t) \tag{6.175}$$

Substitution of the general solution yields

$$Ae^{-\lambda^2 Fo}\lambda\sin\lambda = BiAe^{-\lambda^2 Fo}\cos\lambda \tag{6.176}$$

or

$$\cot\lambda = \frac{\lambda}{Bi} \tag{6.177}$$

which is a transcendental equation with an infinite number of roots or eigenvalues. To each of the roots corresponds a solution with an eigenfunction $\cos\lambda_n x^*$ and an arbitrary constant A_n. Then the general solution is their sum

$$\theta^*(Fo,x^*) = \sum_{n=1}^{\infty} A_n e^{-\lambda_n^2 Fo}\cos\lambda_n x^* \tag{6.178}$$

where the constants are determined from the initial condition

$$\theta^*(0,x^*) = \sum_{n=1}^{\infty} A_n\cos\lambda_n x^* = 1 \tag{6.179}$$

As before

$$A_n = 2\int_0^1 f(x^*)\cos\lambda_n x^* dx^* \tag{6.180}$$

and

$$A_n = \frac{2\sin\lambda_n}{\lambda_n + \sin\lambda_n\cos\lambda_n} = \frac{4\sin\lambda_n}{2\lambda_n + \sin 2\lambda_n} \tag{6.181}$$

Then the dimensionless temperature distribution for the slab for the general case where $Bi \sim 1$ becomes

$$\frac{T - T_\infty}{T_i - T_\infty} = \sum_{n=1}^{\infty} e^{-\lambda_n^2 Fo} \frac{2\sin\lambda_n}{\lambda_n + \sin\lambda_n\cos\lambda_n}\cos\lambda_n\frac{x}{L} \tag{6.182}$$

where λ_n are the roots of equation (6.143) which can be rewritten in the form

$$\lambda_n \tan\lambda_n = Bi \tag{6.183}$$

Table A.1 in Appendix A gives the first four roots of equation (6.183) for various values of the Biot number. Figure 6.14 shows the temperature distribution of equation (6.182) for $Bi = 1.0$. The temperature gradient at the surface of the slab ($x/L = 1$ and $x/L = -1$) is given by the boundary condition of equation (6.175), which for a given value of the Fourier number, results in a steeper temperature gradient at the surface for larger values of the Biot number. This behavior of the temperature distribution is anticipated from our solution for the limiting case of $Bi \to \infty$. From Figure 6.14, note also that for a given value of the Biot number, the temperature gradient at the surface of the slab decreases with the passage of time, i.e., as the Fourier number increases. This implies that the rate of heat transfer slows as the run down to equilibrium proceeds and is consistent with the fact that the equilibrium state for this model is realized only in the limit of infinite time.

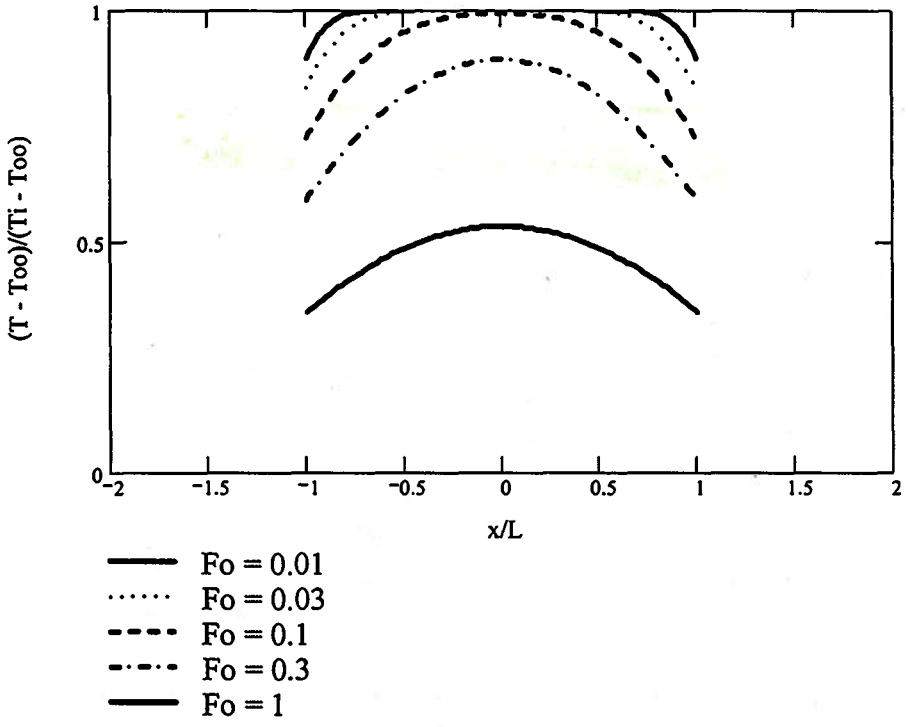

Figure 6.14 Temperature Distribution in a Slab for $Bi = 1$

Since the final equilibrium state takes infinitely long to attain, it is often useful to know how far the slab has progressed toward this state at any given instant of time. Since the final equilibrium

state is known from the application of the first law to the slab, we can calculate the energy change for the run down to equilibrium. We can then use the temperature distribution of equation (6.182) to determine the fraction of the total energy change U_2 - U_1 achieved over a time interval $\Delta t = t - t_0$ where the time t_0 marks the time of the beginning of the run down to equilibrium.

For a slab of thickness $2L$, consider a volume measuring a unit area on the surface of the slab and $2L$ thick. For this system, the first law becomes

$$\dot{Q} = 2\rho cL\frac{\partial T}{\partial t} \tag{6.184}$$

If we integrate equation (6.184) over the time interval of interest, we get

$$Q_{i-a} = \int_{t_0}^{t} \dot{Q}dt = 2\rho cL\int_{T_i}^{T_a}\frac{\partial T}{\partial t}dt = 2\rho cL\left(\overline{T}_a - T_i\right) \tag{6.185}$$

where state a is the state at time t and state i is the initial state at time t_0. Note that at time t the system is not in an equilibrium state since the temperature is not uniform. Then the quantity $\overline{T}_a$ represents the mass-averaged temperature of the system in state a which becomes the volume-averaged temperature because the density is constant. If Φ represents the progress toward the final equilibrium state for which $T_f = T_\infty$, then

$$\Phi = \frac{(U_a - U_i)}{(U_f - U_i)} = \frac{Q_{i-a}}{Q_{i-f}} = \frac{2\rho cL\left(\overline{T}_a - T_i\right)}{2\rho cL\left(T_f - T_i\right)} = 1 - \frac{\left(\overline{T}_a - T_i\right)}{\left(T_i - T_\infty\right)} \tag{6.186}$$

where

$$\frac{\overline{T}_a - T_\infty}{T_i - T_\infty} = \frac{1}{2L}\int_{-L}^{L}\sum_{n=1}^{\infty} e^{-\lambda_n^2 Fo}\frac{2\sin\lambda_n}{\lambda_n + \sin\lambda_n\cos\lambda_n}\cos\left(\lambda_n\frac{x}{L}\right)dx$$
$$\frac{\overline{T}_a - T_\infty}{T_i - T_\infty} = \sum_{n=1}^{\infty} e^{-\lambda_n^2 Fo}\frac{2\sin\lambda_n}{\lambda_n + \sin\lambda_n\cos\lambda_n}\frac{\sin\lambda_n}{\lambda_n} \tag{6.187}$$

Thus,

$$\Phi = 1 - \sum_{n=1}^{\infty} e^{-\lambda_n^2 Fo}\frac{2\sin\lambda_n}{\lambda_n + \sin\lambda_n\cos\lambda_n}\frac{\sin\lambda_n}{\lambda_n} \tag{6.188}$$

In Figure 6.15, we have plotted the response of the slab to convective cooling for various conditions. Figure 6.15 can be used to estimate the time required for the run down to equilibrium for one-dimensional pure thermal systems. For a slab of a given geometry and material, Figure 6.15 shows clearly the effect of the rate process of heat transfer on the surface of the slab. Under these circumstances, an increase in the Biot number reflects an increase in the convective heat transfer coefficient on the surface. Thus, large values of the Biot number result in more rapid run down to equilibrium as large values of h_c result in high rates of heat transfer for a given temperature difference. Of course, the larger the Biot number, the larger the internal thermal resistance due to conduction in the slab relative to the external thermal resistance associated with the convection off the surface. Larger values of the Biot number increase the irreversibility in the slab. As the Biot number decreases, the irreversibility shifts from the slab into the fluid. For $Bi <$ 0.1, the heat transfer process in the slab can be modeled as reversible with all irreversibility concentrated in the fluid. For transient cooling of a slab, Figure 6.16 shows the difference between the simple lumped thermal capacitance model and the complete model that led to equation (6.188). Notice that for $Bi \le 0.1$ the lumped thermal capacitance model is an adequate model for the transient response of the slab during the run down to equilibrium, but at larger values of the Biot number, this simple model greatly over-estimates the response with the error increasing with Biot number. Although we have considered only the one-dimensional case of a

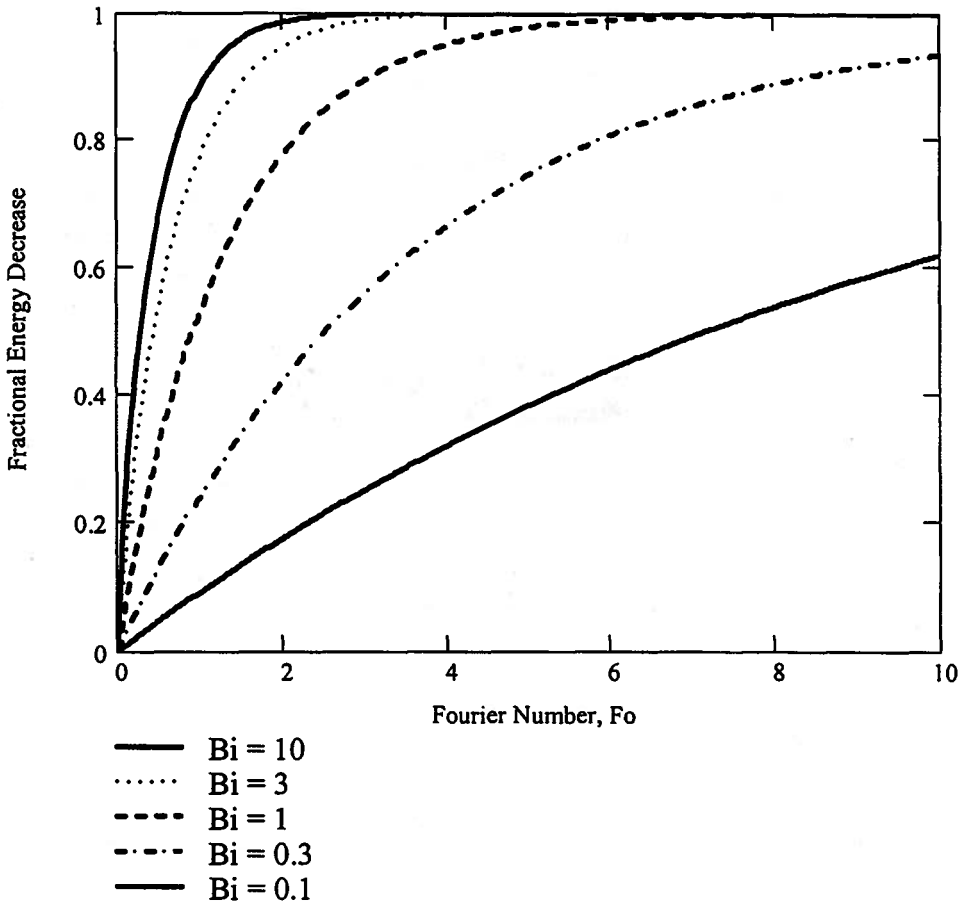

Figure 6.15 Response of a Slab to the Process of Run Down to Equilibrium

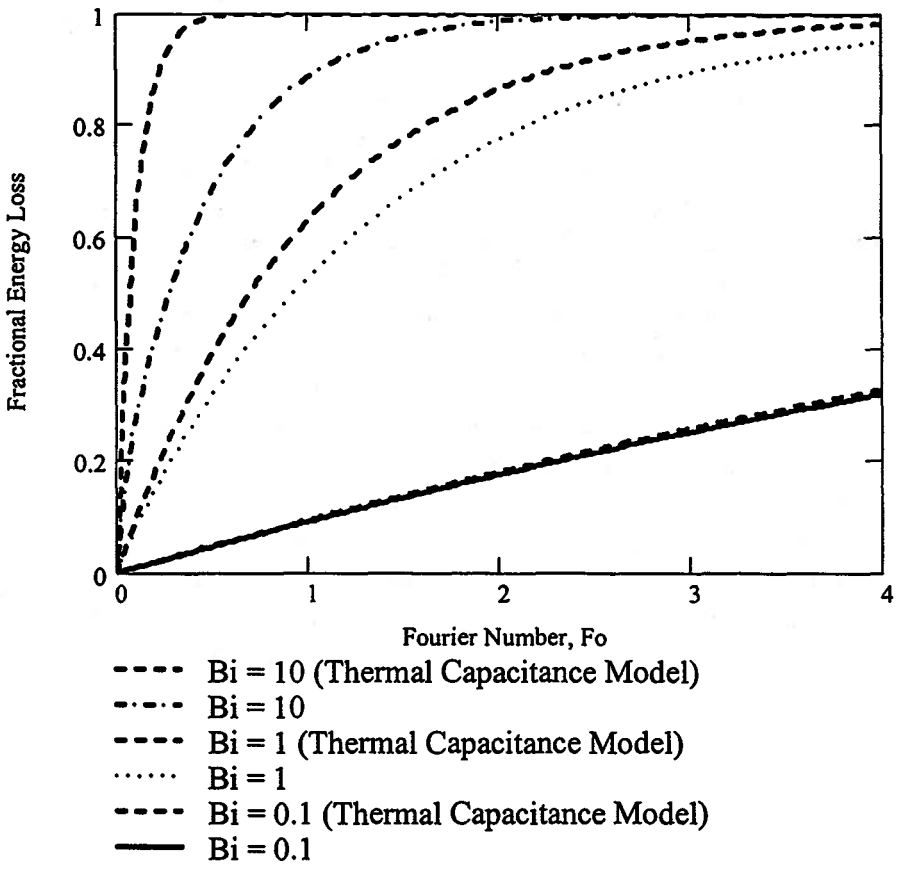

Figure 6.16 Comparison of the Pure Thermal Capacitance Model with the Complete Model

slab of thickness $2L$, the approach embodied in equations (6.182) and (6.188) is a general one and can be extended rather easily to other geometries such as a cylinder or sphere as has been done by Mills[1].

In engineering practice, we are often interested only in the time history of the highest temperature of the system. For the slab, this is the temperature at the midplane, $x = 0$. For this case, Mills shows that the series solution of equation (6.182) converges so rapidly at long times ($Fo > 0.2$) that only the first term need be evaluated. Then for the midplane temperature, equation(6.182) becomes

$$\left[\frac{T_{x=0} - T_\infty}{T_i - T_\infty}\right]_{Fo>0.2} = Ae^{-\lambda_1^2 Fo} \tag{6.189}$$

where $\lambda_1 = f_1(Bi)$ and $A = f_2(Bi)$. In retaining only the first term of the series solution, it can be shown that the temperature distribution in the slab can be expressed in terms of the temperature at the midplane. When this temperature distribution is substituted into equation (6.186), there results a new form for equation (6.188) in terms of the midplane temperature. Then we can write the one-term approximation for equation (6.188) as

$$\Phi_{Fo>0.2} = 1 - B\frac{T_{x=0} - T_\infty}{T_i - T_\infty} \tag{6.190}$$

where $B = f_3(Bi)$. Values of λ_1^2, A, and B for various values of Bi are given in Table A.2 of Appendix A.

In determining the transient response of a one-dimensional thermal-fluid system to convection heat transfer from its surface, we use the simplest model consistent with the desired accuracy of the result. Thus, if $Bi \le 0.1$, we would use the lumped thermal capacitance model. Otherwise, the more complete model of equation (6.188) should be employed. If we are interested only in long time behavior of the slab, $Fo > 0.2$, the simplified solutions of equations (6.189) and (6.190) can be used. If $Bi > 0.1$ and we are interested in short-term response, Figure 6.13 suggests another possibility known as the semi-infinite solid model which we shall describe in the following section.

Example 6E.8: Efforts to conserve energy take many forms such as the storage of "thermal energy". By promoting heat transfer between a fluid (usually a high temperature gas) and a solid, the "thermal energy" stored in the fluid may be stored in the solid for use at a later time. This technique is often used to store the "waste energy" in the exhaust stream from an internal combustion engine or from an industrial furnace. In the case at hand, a high temperature gas stream flows from a solar collector during the daylight hours. The energy in this stream is to be stored in bricks for use in heating the interior space of a building during the night when the sun does not shine. The hot gas (air) flows in passages created by a series of parallel brick walls separated by some appropriate distance. Through the mechanism of convective heat transfer, energy and entropy flows from the gas into the bricks thereby increasing their temperature. During the nighttime, the gas flow is shut off and cold air from the living space is circulated over the bricks, warming the air and subsequently heating the living space.

In a particular design, the hot gas at a temperature of 400 C flows through passages in the brick structure. The gas is in thermal communication with both sides of the typical brick wall which is 10 cm thick. The properties of the brick are: ρ 2645 kg/m^3, c = 960 J/kg K, k = 1.0 W/m

---

[1] Mills, A. F., *Heat Transfer*, Richard D. Irwin, Inc., Boston, MA, 1992, pp. 171-172.

K. The convective heat transfer coefficient for the flowing gas is 100 W/m^2 K and the initial temperature of the wall is 20 C. How much time is required for the wall to attain 90 percent of the total possible energy storage if the gas can be considered to have a fixed temperature? What is the temperature at the midplane of the wall at this time?

Solution: The characteristic length is half the wall thickness since the wall is experiencing heat transfer on both sides. The Biot number for this situation is

$$Bi = \frac{h_c L_c}{k} = \frac{(100 \text{ W/m}^2 \text{ K})(0.05 \text{ m})}{1 \text{ W/m K}} = 5.0$$

Since $Bi \sim 1$, it will be necessary for us to use the series solution for the temperature distribution. Since we are interested in the behavior at long times of exposure, it is likely that the Fourier number is going to be large enough to use the single term approximation to the series. Let us assume this to be the case and then check this assumption later. Then from Appendix A.2, $\lambda = 1.3138$, $A = 1.2402$, and $B = 0.7362$. Then for the temperature at the midplane of the wall, equation (6.190) gives

$$T_{x=0} = T_\infty + \frac{(T_i - T_\infty)(1-\Phi)}{B} = 400 \text{ C} + \frac{(20 \text{ C} - 400 \text{ C})((1-0.9)}{0.7362} = 348.38 \text{ C}$$

The Fourier number, Fo, when this temperature is reached is given by equation (6.189), viz.

$$Fo = \frac{\ln A - \ln\left(\frac{T_{x=0} - T_\infty}{T_i - T_\infty}\right)}{\lambda^2} = \frac{\ln 1.2402 - \ln\left(\frac{348.38 \text{ C} - 400 \text{ C}}{20 \text{ C} - 400 \text{ C}}\right)}{1.3138^2} = 1.281$$

Clearly $Fo > 0.2$ so we are justified in using the single term approximation. The thermal diffusivity of the brick is

$$\alpha = \frac{k}{\rho c} = \frac{1 \text{ W/m K}}{(2645 \text{ kg/m}^3)(960 \text{ J/kg K})} = 3.938 \text{ x } 10^{-7} \text{ m}^2/\text{sec}$$

Then the time required to reach the desired energy storage level is given by

$$t = \frac{Fo L_c^2}{\alpha} = \frac{1.281(0.05 \text{ m})^2}{3.938 \text{ x } 10^{-7} \text{ m}^2/\text{sec}} = 8133 \text{ sec} = 2.259 \text{ hr}$$

6.8 Semi-Infinite Solid Model

As shown in Figures 6.13 and 6.14, the slab takes a while before the midplane ($x = 0$) knows that a heat transfer interaction has taken place at the surface. Obviously this response is a function of the Biot number, but typically if $Fo < 0.05$ and $Bi > 0.1$, the slab appears infinitely thick as far as the midplane is concerned. Since this situation is common in engineering practice, there is a specific model, known as the *semi-infinite solid*, that has been developed to describe it. The temperature distribution that results from a heat transfer interaction at the surface of the semi-infinite solid has been obtained as a closed form solution of the heat diffusion equation for a variety of boundary conditions at the surface.

These solutions have considerable utility in engineering practice for describing heat treatment processes in metals for which we are concerned with producing surfaces of particular hardness for use in cutting tools such as saw blades, chisels, and drills and in machine elements such as bearings, fasteners, and gears. Typically, the desired surface condition can be realized by increasing the temperature of the part to a uniform high value dictated by the metallurgy and then

cooling the part rapidly at the surface so that the layer of material near the surface undergoes a rapid change of phase that often leaves the surface material in a local state of metastable equilibrium of characteristically high hardness. The heat transfer interactions necessary to achieve the desired result can be designed with the aid of the semi-infinite solid model.

There are many other applications of this model as well, and we shall enumerate them as we develop the details of the model. Regardless of the application, the essence of the model is the one-dimensional form of the heat diffusion equation

$$\frac{\partial T}{\partial t} = \alpha \frac{\partial^2 T}{\partial x^2} \tag{6.191}$$

with boundaryconditions and an initial condition appropriate to the application at hand. We now consider several cases that are useful in the practice of thermal-fluids engineering.

Case I, Constant Surface Temperature: This is the situation in which the surface temperature of the semi-infinite solid is instantaneously set equal to some fixed value, T_s, by plunging the slab into a fluid at temperature T_s for which the convection heat transfer coefficient is effectively infinite. As we shall see subsequently, one way this situation can be realized in practice by immersing a high temperature solid into a liquid whose boiling point (saturation temperature) is less than the initial temperature of the solid with the resulting heat transfer coefficient $h_c \sim 10^5$ W/m^2 K. Clearly, for this case, $Bi \to \infty$ which we have already considered in detail, but we now analyze the situation in the context of the semi-infinite solid model. The initial condition is

$$T = T_i \quad @ \quad t = 0 \tag{6.192a}$$

and the boundary conditions are

$$\begin{aligned} T &= T_s \quad @ \quad x = 0 \\ T &\to T_i \quad @ \quad x \to \infty \end{aligned} \tag{6.192b}$$

Graphically, this situation would appear as shown in Figure 6.17.

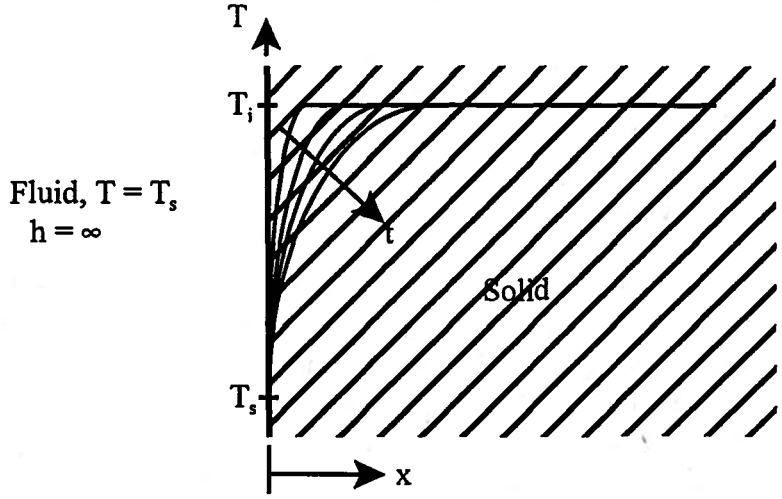

Figure 6.17 Temperature History of a Semi-Infinite Solid with a Sudden Change in Surface Temperature

To solve equation (6.191) for this case, we first partially non-dimensionalize it by defining a dimensionless temperature θ where

$$\theta = \frac{T - T_i}{T_s - T_i} \tag{6.193}$$

Then equation (6.191) becomes

$$\frac{\partial\theta}{\partial t}=\alpha\frac{\partial^2\theta}{\partial x^2} \tag{6.194}$$

and equations (6.192) become

$$\begin{aligned}\theta&=0 \quad @ \quad t=0\\ \theta&=1 \quad @ \quad x=0\\ \theta&\to 0 \quad @ \quad x\to\infty\end{aligned} \tag{6.195}$$

Through the methods of dimensional analysis, we can define a single dimensionless similarity variable η that will enable us to fully non-dimensionalize equation (6.194) while at the same time convert this partial differential equation into an ordinary differential equation. Let η be defined as

$$\eta=\frac{x}{\sqrt{4\alpha t}} \tag{6.196}$$

Substituting equation (6.196) into (6.194), we obtain

$$\begin{aligned}-\frac{x}{2t\sqrt{4\alpha t}}\frac{d\theta}{d\eta}&=\frac{\alpha}{4\alpha t}\frac{d^2\theta}{d\eta^2}\\ -2\eta\frac{d\theta}{d\eta}&=\frac{d^2\theta}{d\eta^2}\end{aligned} \tag{6.197}$$

with boundary conditions

$$\begin{aligned}\theta&=1 \quad @ \quad \eta=0\\ \theta&=0 \quad @ \quad \eta\to\infty\end{aligned} \tag{6.198}$$

If we let $d\theta/d\eta=\zeta$, equation (6.197) becomes

$$-2\eta\zeta=\frac{d\zeta}{d\eta} \tag{6.199}$$

If we separate variables in equation (6.199), we get

$$\frac{d\zeta}{\zeta}=-2\eta d\eta=d\left(\eta^2\right) \tag{6.200}$$

Integrating equation (6.200), we get

$$\zeta=\frac{d\theta}{d\eta}=C_1e^{-\eta^2} \tag{6.201}$$

Integrating equation (6.201), we get

$$\theta=C_1\int_0^{\eta}e^{-u^2}du+C_2 \tag{6.202}$$

From the first of the boundary conditions (6.198), we get $C_2 = 1$. From the second of boundary conditions (6.198), we get

$$C_1\int_0^{\infty}e^{-u^2}du+1=0 \tag{6.203}$$

The definite integral appearing in equation (6.203) has the value

$$\int_0^{\infty}e^{-u^2}du=\frac{\sqrt{\pi}}{2} \tag{6.204}$$

Then combining equations (6.203) and (6.204), we get

$$C_1=-\frac{2}{\sqrt{\pi}} \tag{6.205}$$

Combining equations (6.202) and (6.205), we get

$$\theta = \frac{T - T_i}{T_s - T_i} = 1 - \frac{2}{\sqrt{\pi}} \int_0^{\eta} e^{-u^2} du = 1 - \text{erf}\,\eta = \text{erfc}\,\eta = \text{erfc}\,\frac{x}{\sqrt{4\alpha t}} \tag{6.206}$$

where we have introduced two new functions called the *error function,* written erf η, and the *complementary error function*, written erfc η, where

$$\text{erf}\,\eta = \frac{2}{\sqrt{\pi}} \int_0^{\eta} e^{-u^2} du$$
$$\text{erfc}\,\eta = 1 - \text{erf}\,\eta \tag{6.207}$$

The complementary error function is tabulated in Appendix B and plotted in Figure 6.18.

The heat flux at the surface of the semi-infinite solid can be found by applying the Fourier Conduction law to the temperature profile given in equation (6.206). Thus

$$\dot{q}_s = -k\left(\frac{\partial T}{\partial x}\right)_{x=0} = -k(T_s - T_i)\frac{\partial}{\partial x}\left[1 - \frac{2}{\sqrt{\pi}} \int_0^{\eta} e^{-u^2} du\right]_{x=0}$$
$$\dot{q}_s = -k(T_s - T_i)\left[-\frac{2}{\sqrt{\pi}} e^{-\eta^2} \frac{1}{\sqrt{4\alpha t}}\right]_{x=0} = \frac{k(T_s - T_i)}{\sqrt{\pi \alpha t}} \tag{6.208}$$

Equation (6.208) is identical to the result obtained for the slab with $Bi \to \infty$, equation (6.171).

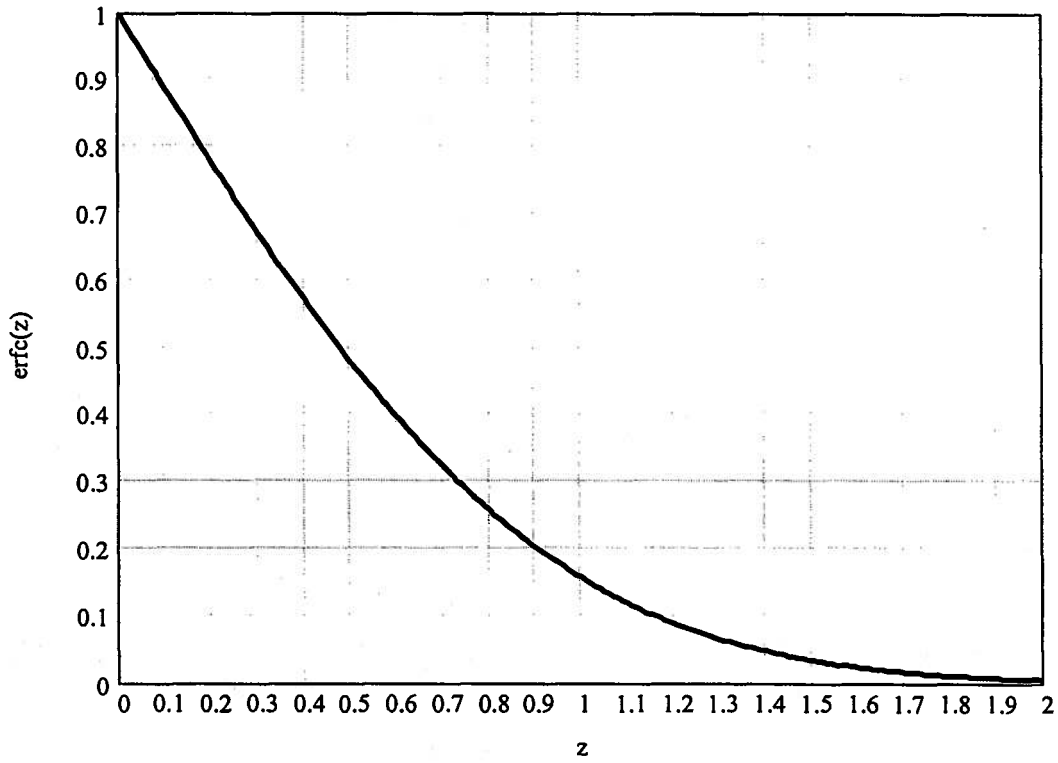

Figure 6.18 The Complementary Error Function

Case II, Constant Heat Flux at the Surface: Suppose the surface is suddenly exposed to a constant heat flux $\dot{q}_s^{\circ}$ at time $t = 0$ as might be the case for laser irradiation of the surface. The temperature history of the solid would appear as shown in Figure 6.19. The solution of the heat diffusion equation by the method shown above is

$$T - T_i = \frac{\dot{q}_s}{k}\left[\sqrt{\frac{4\alpha t}{\pi}} e^{-\frac{x^2}{4\alpha t}} - x\,\text{erfc}\left(\frac{x}{\sqrt{4\alpha t}}\right)\right] \tag{6.209}$$

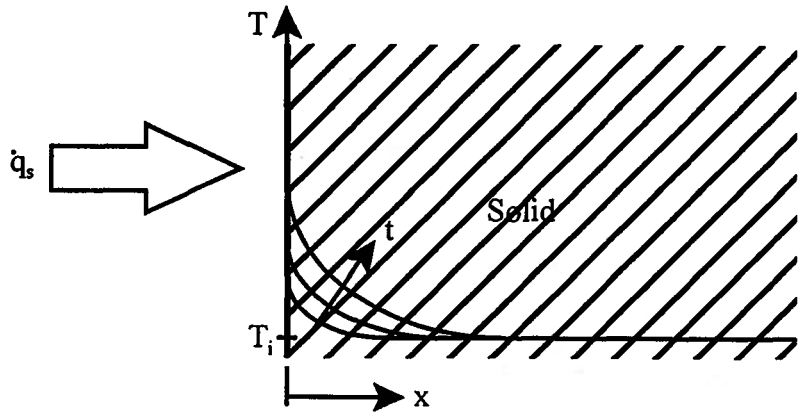

Figure 6.19 Temperature History of Semi-Infinite Solid with Constant Heat Flux at Surface

Case III, Convective Heat Transfer at the Surface: Suppose that the surface of the semi-infinite solid is suddenly exposed to a fluid at a temperature of T_∞ at time $t = 0$ and the convective heat transfer coefficient is h_c. Then the time history of the temperature in the solid would appear as shown in Figure 6.20.

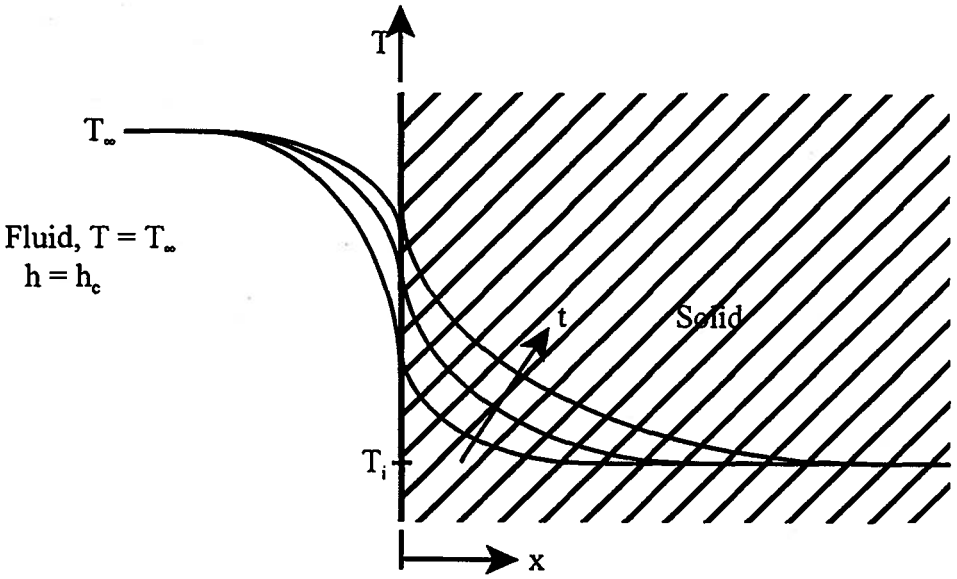

Figure 6.20 Temperature History of a Semi-Infinite Solid Suddenly Immersed in a Fluid

The solution of the heat diffusion equation by the method described above is

$$\frac{T-T_i}{T_\infty-T_i}=\operatorname{erfc}\frac{x}{\sqrt{4\alpha t}}-e^{\left[\frac{h_c x}{k}+\left(\frac{h_c}{k}\right)^2 \alpha t\right]}\operatorname{erfc}\left[\frac{x}{\sqrt{4\alpha t}}+\frac{h_c}{k}\sqrt{\alpha t}\right] \tag{6.210}$$

It is worth noting that equation (6.210) contains the solution to both cases I and III. In the limit as $h_c \to \infty$, equation (6.210) reduces to equation (6.206). If we set

$$z=\frac{x}{\sqrt{4\alpha t}} \qquad \text{and} \qquad a=\frac{h_c\sqrt{\alpha t}}{k} \tag{6.211}$$

equation (6.210) can be written

$$\frac{T-T_i}{T_s-T_i}=\theta=\operatorname{erfc} z-e^{2az+a^2}\operatorname{erfc}(z+a) \tag{6.212}$$

Equation (6.212) is plotted in Figure 6.21. For large values of a ($a = 10$), equation (6.212) reduces to equation (6.206).

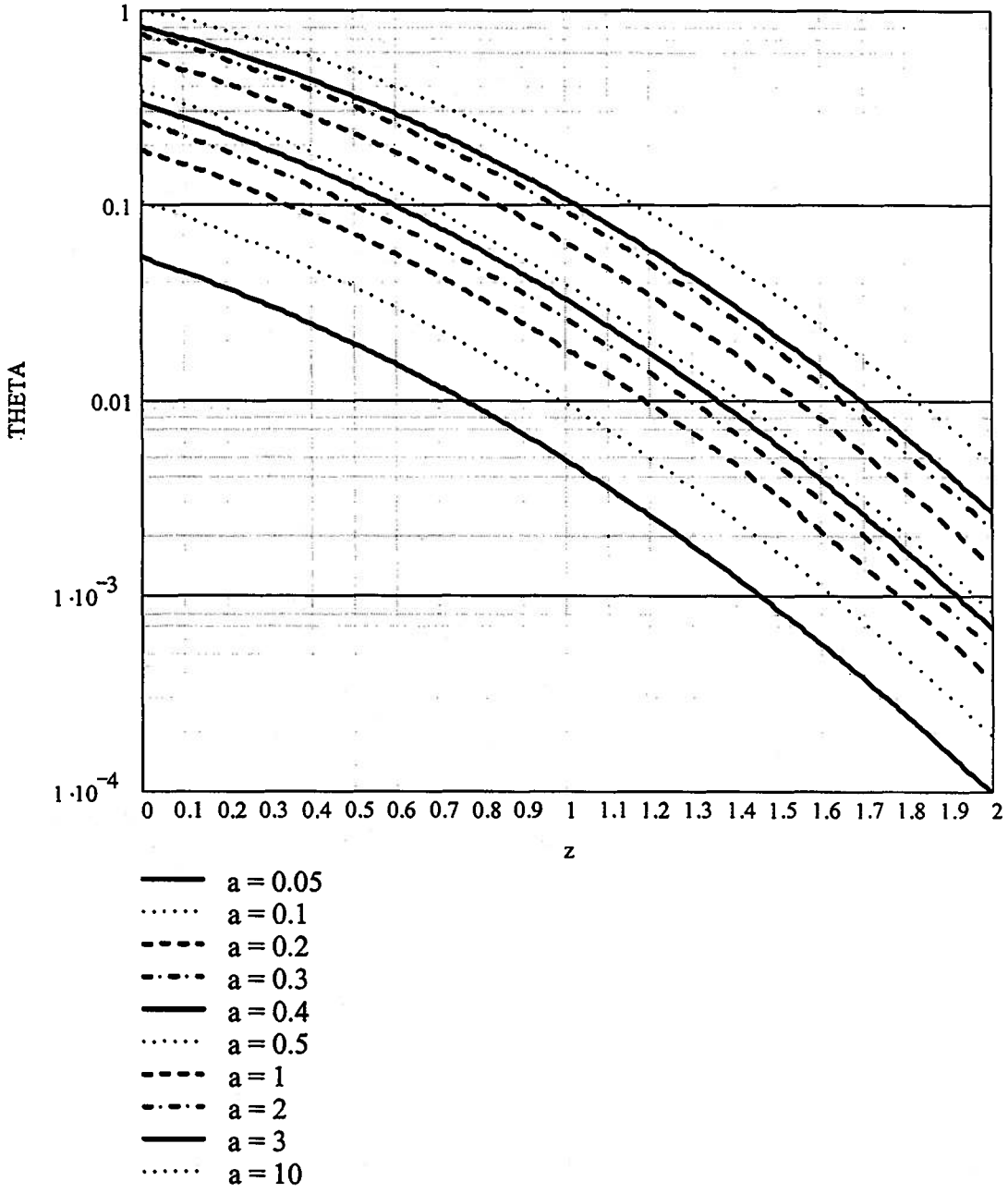

Figure 6.21 Temperature History of a Semi-Infinite Solid Suddenly Immersed in a Fluid

There are two other cases of heat transfer interactions in the semi-infinite solid that are of practical interest.

Case IV, Surface Energy Pulse: If energy is suddenly deposited on the surface in the amount of E per unit area at time $t = 0$ as might be the case of a pulsed laser and none of this energy is lost from the surface, the resulting temperature history is given by

$$T - T_i = \frac{E}{\rho c\sqrt{\pi\alpha t}} e^{-\frac{x^2}{4\alpha t}} \tag{6.213}$$

This result is shown schematically in Figure 6.22.

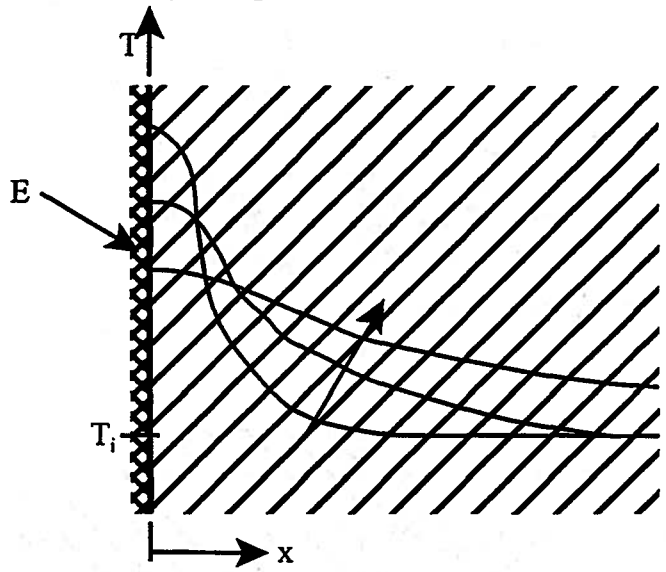

Figure 6.22 Temperature History of a Semi-Infinite Solid with Energy Pulse E per unit area in Surface

Case V, Periodic Variation of Surface Temperature: There are numerous situations in which the temperature of the surface of a semi-infinite solid varies periodically. Seasonal and diurnal variations of the temperature of the surface of the earth are classical examples. In these case we wish to determine the time-wise variation of the temperature at some location within the earth. The surface temperature can be characterized as

$$T_s - T_i = \left(T_s^* - T_i\right)\sin\omega t \tag{6.214}$$

where T_s is the instantaneous value of the surface temperature, T_s^* is the maximum value of the temperature of the surface, and T_i is the mean value of the temperature variation. The value of the temperature at any location x within the semi-infinite solid at any instant of time is given by

$$\frac{T - T_i}{T_s^* - T_i} = e^{-x\sqrt{\omega/2\alpha}} \sin\left[\omega t - x\sqrt{\frac{\omega}{2\alpha}}\right] \tag{6.215}$$

Thus, the temperature at any location varies exponentially with distance from the surface and sinusoidally with time but with a phase shift from the surface temperature variation.

6.8.1 Two Semi-Infinite Solids in Simple Thermal Communication

Anyone who has walked on the bathroom floor in bare feet has experienced the phenomenon in which the floor itself "feels" cold but a mat or carpet which is at the same temperature as the floor "feels" considerably warmer. This is a classical example of the semi-infinite solid model in which the surfaces of two semi-infinite solids (feet and floor) at different initial temperatures are brought into contact. The temperature of the interface between the two solids comes to a new value T_s that is between the initial temperatures of the two solids and remains constant as long as the semi-infinite solid model is valid. For long times, this model is invalid and ultimately the two solids run down to a common equilibrium temperature that is different from T_s.

The value of T_s can be determined by recognizing that when the two solids are brought

into thermal communication, they form an isolated system. The ensuing heat transfer interaction is internal to the isolated system so that the heat flux for one solid is the negative of the heat flux of the other solid. Then for two solids A and B,

$$\dot{q}_A = -\dot{q}_B \tag{6.216}$$

where the heat flux is given by equation (6.208)

$$\frac{k_A\left(T_s - T_{A,i}\right)}{\sqrt{\pi\alpha_A t}} = \frac{-k_B\left(T_s - T_{B,i}\right)}{\sqrt{\pi\alpha_B t}} \tag{6.217}$$

Solving equation (6.217) for T_s, we get

$$T_s = \frac{T_{A,i}\sqrt{(k\rho c)_A} + T_{B,i}\sqrt{(k\rho c)_B}}{\sqrt{(k\rho c)_A} + \sqrt{(k\rho c)_B}} \tag{6.218}$$

Schematically, the situation appears as in Figure 6.23.

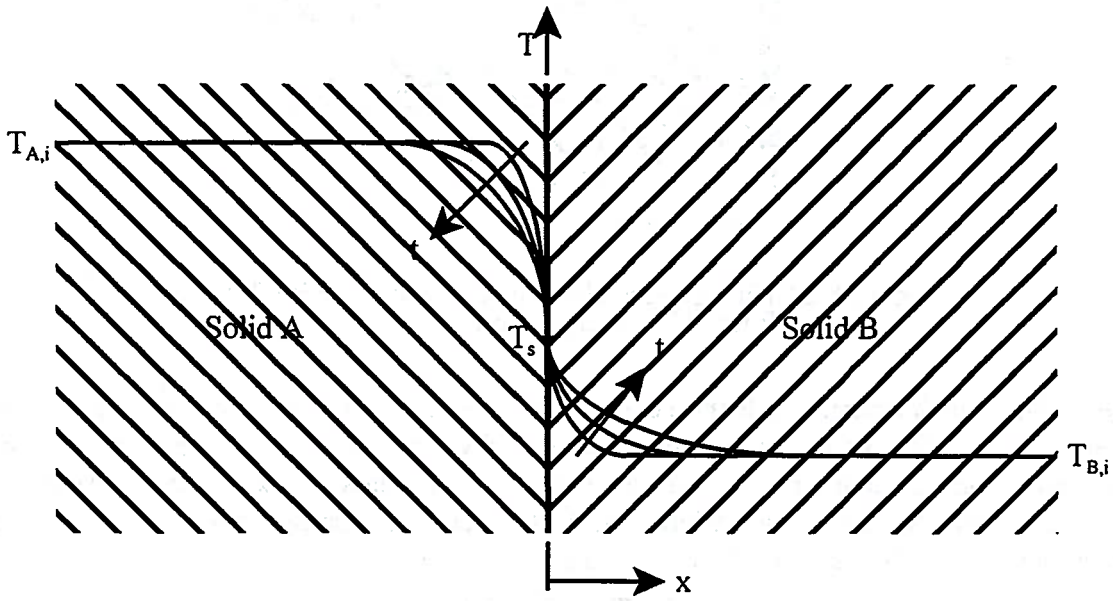

Figure 6.23 Two Semi-Infinite Solids in Simple Thermal Communication

Example 6E.9: The heat treatment of 4340 steel to form martensite requires that the steel be cooled from 650 C to 150 C at a rate of at least 8.3 C/sec. In a particular heat treatment process a steel part at an initial temperature of $T_i = 650$ C is plunged into a liquid that results in a heat transfer coefficient so large that it can be modeled as infinite. This liquid causes the surface temperature of the part to become $T_s = 90$ C instantaneously. To what depth will the martensite phase penetrate the surface of the part in this heat treatment process?

Solution: The time required to cool the steel is t where

$$t = \frac{650\text{ C} - 150\text{ C}}{8.3\text{ C/sec}} = 60.24\text{ sec}$$

The dimensionless temperature is

$$\frac{T - T_i}{T_s - T_i} = \frac{150\text{ C} - 650\text{ C}}{90\text{ C} - 650\text{ C}} = 0.89286 = \text{erfc}\,\eta$$

Then from Appendix B, $\eta = 0.09524$ and

$$x = \eta\sqrt{4\alpha t} = 0.09524\sqrt{4(11.9 \text{ x } 10^{-6}\text{ m}^2/\text{sec})(60.24\text{ sec})} = 5.1 \text{ x } 10^{-3}\text{ m} = 5.1\text{ mm}$$

Table A.1
The First Four Roots of the Transcendental Equation $\lambda_n \tan \lambda_n = Bi$

$Bi = \frac{h_c L}{k_s}$	λ_1	λ_2	λ_3	λ_4
0	0	3.1416	6.2832	9.4248
0.001	0.0316	3.1419	6.2833	9.4249
0.01	0.0998	3.1448	6.2848	9.4258
0.02	0.1410	3.1479	6.2864	9.4269
0.04	0.1987	3.1543	6.2895	9.4290
0.06	0.2425	3.1606	6.2927	9.4311
0.08	0.2791	3.1668	6.2959	9.4333
0.1	0.3111	3.1731	6.2991	9.4354
0.2	0.4328	3.2039	6.3148	9.4459
0.4	0.5932	3.2636	6.3461	9.4670
0.6	0.7051	3.3204	6.3770	9.4879
0.8	0.7910	3.3744	6.4074	9.5087
1.0	0.8603	3.4256	6.4373	9.5293
2.0	1.0769	3.6436	6.5783	9.6296
3.0	1.1925	3.8088	6.7040	9.7240
4.0	1.2646	3.9352	6.8140	9.8119
5.0	1.3138	4.0336	6.9096	9.8928
6.0	1.3496	4.1116	6.9924	9.9667
7.0	1.3766	4.1746	7.0640	10.0339
8.0	1.3978	4.2264	7.1263	10.0949
9.0	1.4149	4.2694	7.1806	10.1502
10.0	1.4289	4.3058	7.2281	10.2003
20.0	1.4961	4.4915	7.4954	10.5117
40.0	1.5325	4.5979	7.6647	10.7334
60.0	1.5451	4.6353	7.7259	10.8172
80.0	1.5514	4.6543	7.7573	10.8606
100.0	1.5552	4.6658	7.7764	10.8871
∞	1.5708	4.7124	7.8540	10.9956

Table A.2
Coefficients in the One-term Approximation for Convection Cooling of a Slab

Bi	λ_1^2	A	B
0.1	0.09678	1.016	0.9839
0.2	0.1873	1.031	0.9691
0.4	0.3519	1.058	0.9424
0.6	0.4972	1.081	0.9192
0.8	0.6257	1.102	0.8989
1	0.7401	1.119	0.8811
2	1.160	1.180	0.8176
4	1.600	1.229	0.7540
6	1.821	1.248	0.7229
8	1.954	1.257	0.7047
10	2.042	1.262	0.6928
20	2.238	1.270	0.6665
30	2.311	1.272	0.6570
40	2.321	1.272	0.6521
50	2.371	1.273	0.6490
100	2.419	1.273	0.6429
∞	2.467	1.273	0.6366

Appendix B
The Complementary Error Function

η	erfc η	η	erfc η	η	erfc η
0.00	1.0000	0.76	0.2825	1.52	0.03159
0.02	0.9774	0.78	0.2700	1.54	0.02941
0.04	0.9549	0.80	0.2579	1.56	0.02737
0.06	0.9324	0.82	0.2462	1.58	0.02545
0.08	0.9099	0.84	0.2349	1.60	0.02365
0.10	0.8875	0.86	0.2239	1.62	0.02196
0.12	0.8652	0.88	0.2133	1.64	0.02038
0.14	0.8431	0.90	0.2031	1.66	0.01890
0.16	0.8210	0.92	0.1932	1.68	0.01751
0.18	0.7991	0.94	0.1837	1.70	0.01621
0.20	0.7773	0.96	0.1746	1.72	0.01500
0.22	0.7557	0.98	0.1658	1.74	0.01387
0.24	0.7343	1.00	0.1573	1.76	0.01281
0.26	0.7131	1.02	0.1492	1.78	0.01183
0.28	0.6921	1.04	0.1414	1.80	0.01091
0.30	0.6714	1.06	0.1339	1.82	0.01006
0.32	0.6509	1.08	0.1267	1.84	0.009264
0.34	0.6306	1.10	0.1198	1.86	0.008528
0.36	0.6107	1.12	0.1132	1.88	0.007844
0.38	0.5910	1.14	0.1069	1.90	0.007210
0.40	0.5716	1.16	0.1009	1.92	0.006622
0.42	0.5525	1.18	0.09516	1.94	0.006077
0.44	0.5338	1.20	0.08969	1.96	0.005574
0.46	0.5153	1.22	0.08447	1.98	0.005108
0.48	0.4973	1.24	0.07949	2.00	0.004678
0.50	0.4795	1.26	0.07476	2.10	0.002979
0.52	0.4621	1.28	0.07027	2.20	0.001863
0.54	0.4451	1.30	0.06599	2.30	0.001143
0.56	0.4284	1.32	0.06193	2.40	0.000689
0.58	0.4121	1.34	0.05809	2.50	0.000407
0.60	0.3961	1.36	0.05444	2.60	0.000236
0.62	0.3806	1.38	0.05098	2.70	0.000134
0.64	0.3654	1.40	0.04771	2.80	0.000075
0.66	0.3506	1.42	0.04462	2.90	0.000041
0.68	0.3362	1.44	0.04170	3.00	0.000022
0.70	0.3222	1.46	0.03895	3.20	0.000006
0.72	0.3086	1.48	0.03635	3.40	0.000002
0.74	0.2953	1.50	0.03389	3.60	0.000000

PROBLEMS

6.1 Small spheres of lead, known as "shot", are used in the manufacture of shotgun shells and other items that require small diameter lead spheres. The lead shot are manufactured by cooling molten lead droplets in air. The requisite heat transfer process is provided by allowing the droplets to fall through ambient air in a tower designed specifically for this purpose. The lead is cooled by forced convection over the surface of the sphere (heat transfer coefficient h_c) and the small solid spheres are collected at the bottom of the tower.

(a) Formulate a model comprised of pure system elements that can be used to describe the behavior of the sphere as it is released with initial velocity of zero and initial temperature T_1 from the top of the tower and falls through the air a distance h. In your model, include the drag exerted by the air on the sphere. Show all the interactions experienced by the sphere during its motion from $\vartheta = \vartheta_1 = 0$ m/sec at $z_1 = 0$ m to $\vartheta = \vartheta_2$ m/sec at $z_2 = -h$ m. From the First Law of Thermodynamics, derive one or more expressions involving the parameters h, h_c, T_1, ϑ_1, and z_1 that would allow you to calculate the velocity ϑ_2 and temperature T_2. Is your model coupled or uncoupled? Why?

(b) In a particular design, 3 mm diameter solid lead spheres with an initial temperature of 601 K are cooled by forced convection during free fall in ambient air with a temperature of 300 K. The convection heat transfer coefficient is $h_c = 240$ W/m^2 K. The properties of lead are $\rho = 11340$ kg/m^3, $c = 129$ J/kg K, and $k = 34$ W/m K. What is the Biot number for this situation? Formulate an appropriate model to describe the temperature at the center of the sphere as the sphere cools. Determine the height of the tower necessary to reduce the temperature of the center of the lead sphere to 180 C. Assume that the sphere is released with an initial velocity of zero and is allowed to fall freely through the air in the tower with $g = 9.8$ m/sec^2. For the purposes of this calculation, assume that the drag of the air on the sphere can be neglected.

(c) Calculate the entropy transfer for the lead for this cooling process.

(d) Calculate the entropy change of the air for this process.

(e) Calculate the entropy transfer for the air for this process.

(f) Calculate the entropy generated in this cooling process, and comment on the reversibility of this process and identify the source of the irreversibility if there is one.

6.2 In the manufacture of steel sheet, steel 1 cm thick exits from the rolling mill at a temperature of 600 C and is quenched in a very large bath of oil whose temperature is constant at 30 C.

(a) If the heat transfer coefficient between the oil and the steel is $h_c = 400$ W/m^2 K, calculate the time required to cool the steel sheet to 100 C.

(b) If a typical steel sheet is 1.25 m wide by 2.5 m long, calculate the change in entropy of the steel for the process by which it reaches thermal equilibrium with the oil bath from its initial temperature of 600 C.

(c) Calculate the entropy transfer for the steel for this process.

(d) Calculate the entropy change of the oil bath for this process.

(e) Calculate the entropy transfer for the oil bath for this process.

(f) Calculate the entropy generated in this run down to equilibrium, and comment on the reversibility of this process and identify the source of the irreversibility if there is one.

For the steel: $k_{st} = 50$ W/m K, $\rho_{st} = 7800$ kg/m^3, $c_{st} = 450$ J/kg K
For the oil: $k_{oil} = 0.1445$ W/m K, $\rho_{oil} = 883$ kg/m^3, $c_{oil} = 1900$ J/kg K

6.3 The air in an empty warehouse is to be maintained at an average bulk temperature of 20 C by means of an electric heater. The warehouse can be modeled as a simple box with inside dimensions 20 m wide by 40 m long by 10 m high. Assume that the surface area of the walls is the same inside the building as outside. The walls and flat roof of the warehouse have a composite structure as shown in Figure 6P.3. The inside layer is plaster board 10 mm thick (k_{pb} = 0.17 W/m K); the middle layer is a glass fiber blanket 100 mm thick (k_f = 0.038 W/m K); and the outside layer is plywood 20 mm thick (k_{pw} = 0.117 W/m K). The convective heat transfer coefficient between the air and the inside surface of the walls is h_i = 3 W/m^2 K. On a cold winter day the temperature of the air outside is T_o = -15 C and has a convective heat transfer coefficient of h_o = 60 W/m^2 K at the outer surface of the warehouse. Radiation from the outside surface of the walls to the environment can be neglected.

(a) Draw the equivalent thermal circuit for the walls and ceiling.

(b) Determine the temperature of the walls at the inside surface and the outside surface and sketch the temperature distribution through the walls.

(c) Determine the heat transfer rate at the inside surface of the walls.

(d) Calculate the electric power required to maintain the average temperature inside the warehouse at T_i = 20 C.

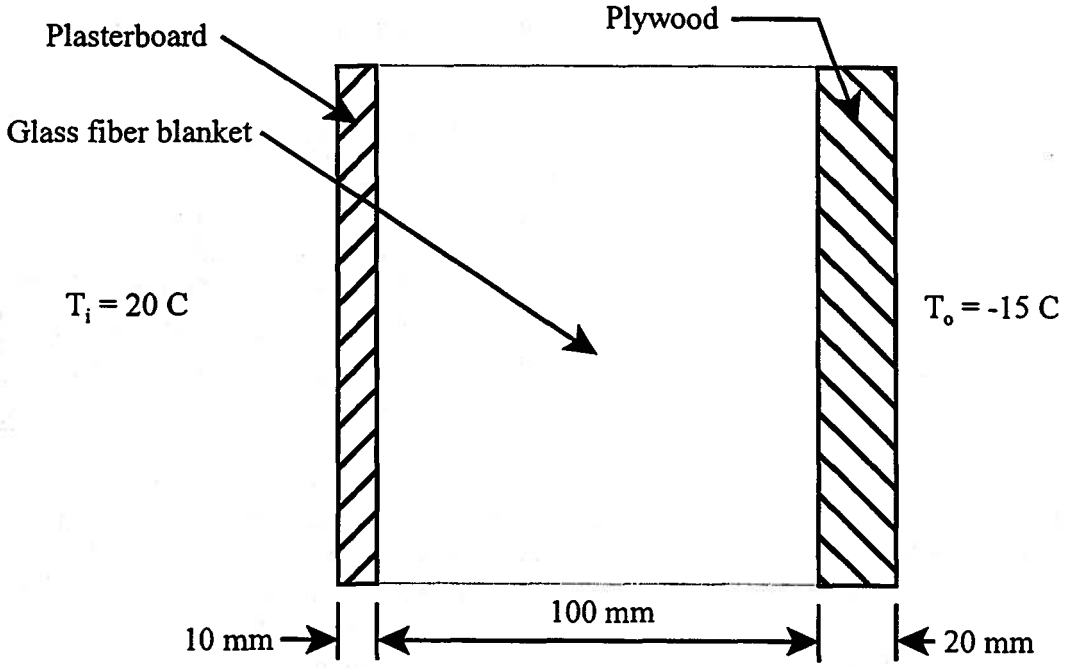

Figure 6P.3

6.4 In the plumbing industry, a common method of joining copper tubing is through the use of fittings that have internal diameters slightly larger than the copper tubes that are being joined. The tubes are assembled into the fitting and the whole assembly is heated by a fossil fuel flame to the melting point of an alloy that is used to bond the joint together. The molten liquid alloy, known as solder, is drawn into the joint by capillary action and the heat source is removed. The joint is allowed to cool by natural convection with the air, and the water-tight bond is formed as the solder forms a complex alloy system with the copper tubing. For the preservation of the health of the people who might drink water from these pipes, Federal law now requires these solders to be lead free. Antimony-tin alloys are now commonly used for these purposes.

Estimate the shortest possible length of solder (D = 1.5 mm) that could be used

comfortably by the plumber if the melting point of the solder is 240 C and its thermal conductivity is 65 W/m K. At a temperature of 50 C, most materials are too hot to hold for any extended time. The heat transfer coefficient for combined convection and radiation from the solder surface to the air is $h = 6$ W/m^2 K. The temperature of the atmosphere is $T_{atm} = 300$ K.

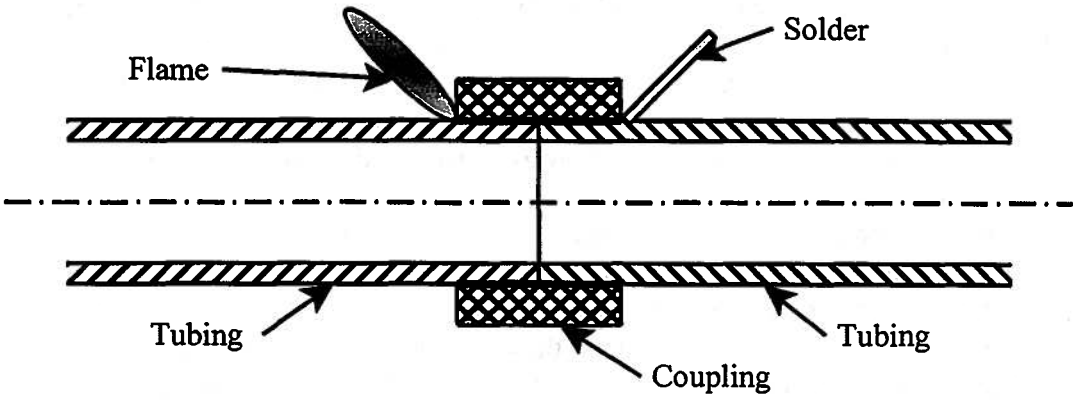

Figure 6P.4 Cross-section of Copper Tubes Joined by Soldering

6.5 One of the difficulties in measuring the temperatures of gas streams subject to rapid temperature fluctuations is that the response time of the thermocouple used for this purpose is too long to provide an accurate temperature measurement. In a particular application, the thermocouple junction can be modeled as a sphere. The convection heat transfer coefficient between the junction and the gas stream is known to be 400 W/m^2 K, and the junction thermophysical properties are $k = 20$ W/m K, $c = 400$ J/kg K and $\rho = 8500$ kg /m^3. Calculate the junction diameter required for the thermocouple to have a time constant of 0.5 sec. If the junction is at an initial temperature of 25 C and is placed in a gas stream at a temperature of 200 C, how long will it take for the junction to reach a temperature of 199 C?

6.6 As shown in Figure 6P.6, a solid cylindrical probe (diameter = 12.5 mm) is used to measure fluid temperature with a temperature sensor embedded in its tip. The probe is inserted through the wall of a duct into a water stream that has a uniform temperature of 80 C. The overall length of the probe is 200 mm and 85 mm of this length are exposed to the water stream while the remaining length is exposed to the ambient air whose temperature is 20 C. The convection heat transfer coefficient between the surface of the probe and the water, h_i, is $h_i = 1100$ W/m^2 K while that between the probe surface and the air, h_o, is $h_o = 10$ W/m^2 K. The thermal conductivity of the probe material is $k_{probe} = 177$ W/m K. The probe is thermally isolated from the duct wall, but there is a water-tight seal to prevent water from leaking out of the duct.

(a) Using the equations that describe heat transfer from extended surfaces, describe a one-dimensional heat transfer model that will enable you to determine the temperature at the tip of that portion of the probe immersed in the water while the other portion of the probe is exposed to the air. State all assumptions in your model. (No differential equations, please!)

(b) For a geometry in which the origin of the x-axis is in the middle of the duct wall, sketch the temperature distribution $T = T(x)$ in the probe. Pay careful attention to the slope, dT/dx, at each end of the probe and at the origin and the values of T at these locations.

(c) Estimate the error in the measured temperature $\Delta T_{error} = T_{tip} - T_{water}$ for this probe configuration. Does the error increase or decrease as the immersion length increases? Why?

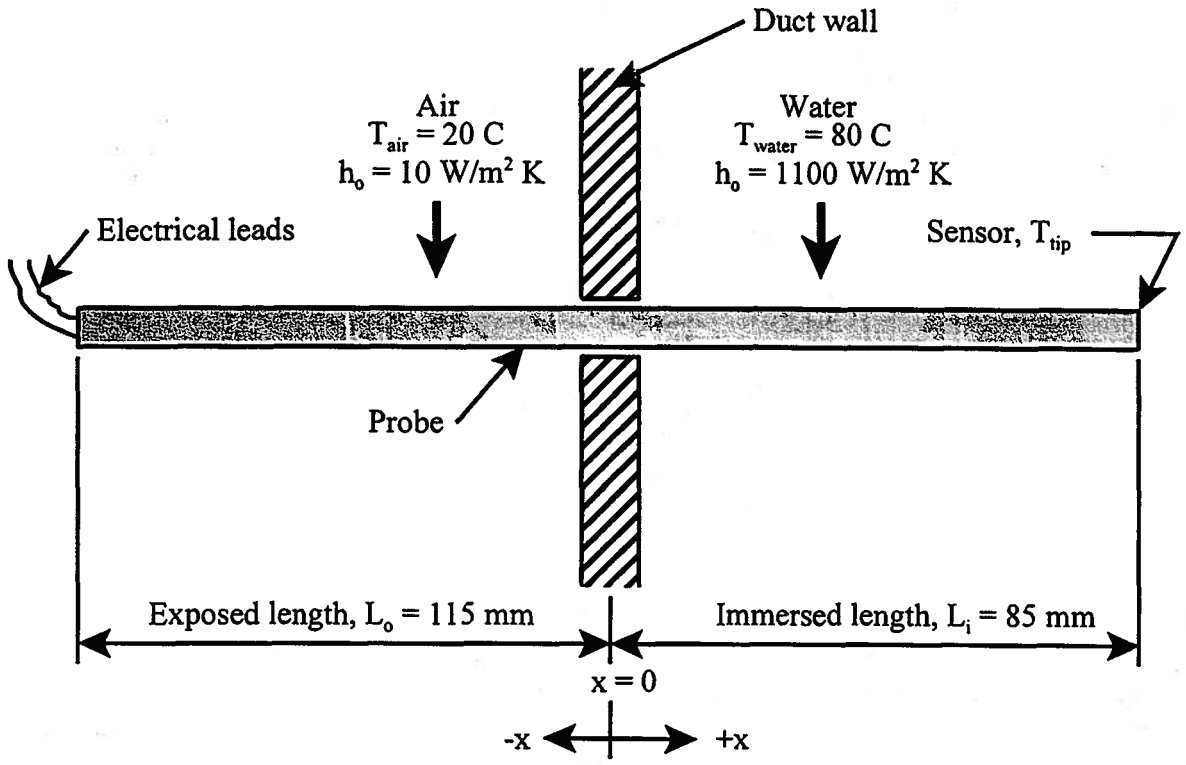

Figure 6P.6

6.7 Soft drinks are packaged in aluminum cans that can be modeled as cylinders 6.5 cm in diameter and 12 cm long. A firm markets a foam rubber sleeve called a "Koolie" that fits tightly over the outside of the can for the purpose of increasing the "holding time" of the can. The sleeve is 9 cm long with a wall thickness of 1.2 cm. The wall thickness of the aluminum can is 0.1 mm. A full soft drink can is removed from an ice chest at a time when the contents of the can are at a uniform temperature of 0 C. The sleeve is immediately placed on the can and the wise student immediately drinks enough of the soft drink to bring the level of the beverage down to the top of the sleeve. The contents of the can are then allowed to run down to equilibrium with the environment, T_{env} = 30 C. The convection heat transfer coefficient between the air and the outer surface of the "Koolie" is h_c = 5 W/m² K. Neglect radiation heat transfer. Neglect the heat transfer through the top and bottom of the can. Model the soft drink as water. Assume that conduction is the only mode of heat transfer in the fluid inside the can.

(a) Show that for the can and its contents $Bi_{effective} < 0.1$.

(b) Assume that the student does not drink any more of the soft drink and use the appropriate model to estimate the amount of time necessary for the contents of the can to reach a temperature of 25 C on a day when T_{env} = 30 C.

(c) On a set of axes with T(C) as the ordinate and t(sec) as the abscissa, sketch (not plot) the temperature-time history of the contents of the can. On this same set of axes, show the temperature of the outside surface of the "Koolie" as a function of time.

In parts (d) through (f) below, assume that the "Koolie" functions solely as a thermal resistance with no mass.

(d) Calculate the entropy change of the soft drink for the process by which its temperature changes from T_i = 0 C to T_f = 30 C.

(e) Calculate the entropy transfer across the interface between the outside surface of the

"Koolie" and the atmospheric air.

(f) Calculate the entropy change of the atmospheric air.

For water: $k_w = 0.556$ W/m K, $\rho_w = 1000$ kg/m^3, $c_w = 4217$ J/kg K
For air: $k = 0.0249$ W/m K, $\rho = 1.311$ kg/m^3, $c_p = 1009$ J/kg K
For foam rubber: $k_{fr} = 0.030$ W/m K, $\rho_{fr} = 70$ kg/m^3

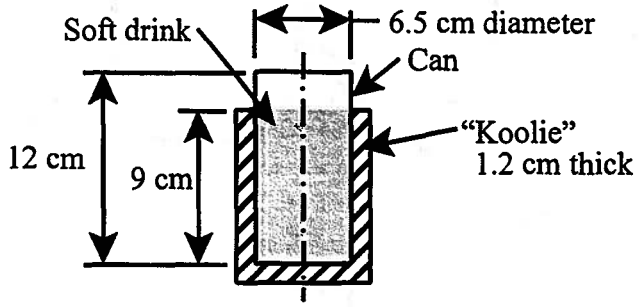

Figure 6P.7

6.8 A high temperature furnace is constructed with water cooled outer walls to protect the workers in the area. As shown in cross-section in Figure 6P.8, the walls are of composite structure with a water cooled brass plate on the outside and a layer of insulation on the inside. The brass plate is 2 mm thick with copper tubing 3 mm in diameter soldered to its surface at intervals of 10 cm. Cooling water passes through the tubes at a rate sufficient to maintain them at a temperature of 315 K. The insulation inside the furnace is 1.5 cm thick and is exposed to air at 600 K.

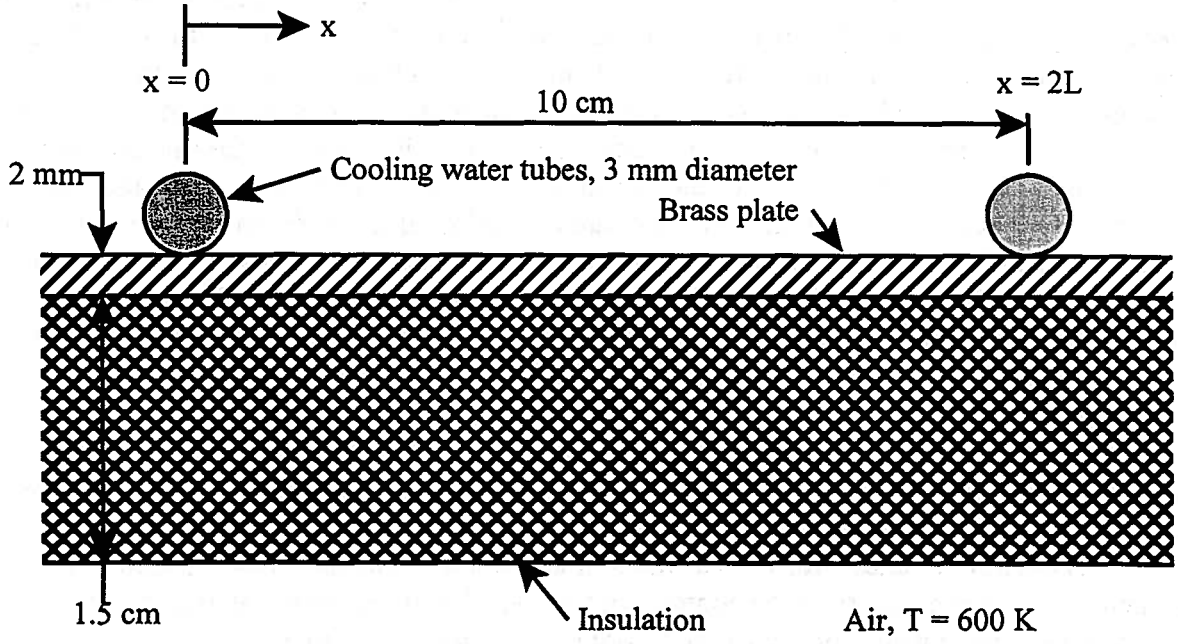

Figure 6P.8

The heat transfer from the brass plate to the air in the room where the furnace is located is negligible compared to the heat transfer between the brass plate and the insulation. The thermal resistance to convection and radiation heat transfer between the air in the furnace and the insulation is negligible. The heat transfer from the air in the furnace to the surrounding walls

passes through the insulation and is intercepted by the brass plate where it is conducted along the plate into the water in the tubes. For all planes normal to the plane of the plate, the temperature in the brass plate can be modeled as uniform. The temperature of the brass does vary in the x-direction.
For brass: $k_{brass} = 111$ W/m K For the insulation: $k_{ins} = 0.16$ W/m K

(a) Sketch (not plot) the steady-state temperature distribution $T = T(x)$ in the brass plate between the cooling tubes. Pay close attention to the slope dT/dx of the resulting curve.

(b) Where is the point of highest temperature in the brass? What is the heat transfer per unit cross-sectional area in the x-direction at this point?

(c) Using an appropriate model for this heat transfer configuration, estimate the steady-state temperature at this point.

6.9 A plane wall of a furnace is fabricated from plane carbon steel($k_{steel} = 60$ W/m K, $\rho_{steel} = 7850$ kg/m^3, and $c_{steel} = 430$ J/kg K) and is of thickness $L = 10$ mm. To protect this steel surface from the corrosive effects of the furnace combustion gases, one surface of the wall is coated with a thin ceramic film which for a unit surface area has a thermal resistance of $R_{ceramic} = 0.01$ m^2 K/W. The opposite surface of the steel is well insulated from the surroundings.

When the furnace is first started up, the wall is at a uniform initial temperature of 300 K. The combustion gases enter the furnace at a temperature of $T_\infty = 1300$ K and immediately establish a convection heat transfer coefficient of 25 W/m^2 K at the ceramic film surface. The film has negligible thermal capacitance.

(a) How long will it take for the inner surface of the steel to reach a temperature of 1200 K?

(b) What is the temperature, T_s, of the exposed ceramic film at this time?

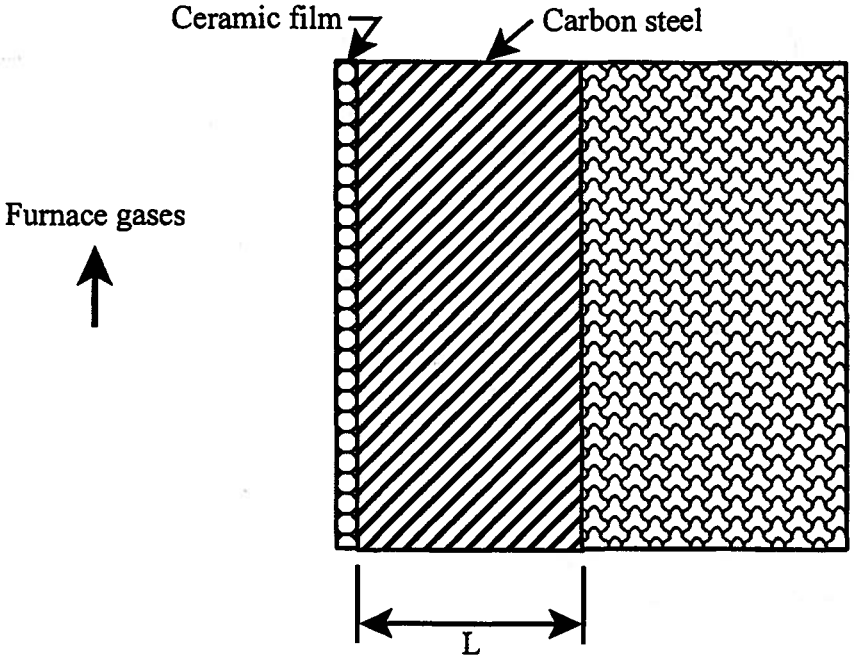

Figure 6P.9

6.10 Consider an air cooled pin fin for which the heat transfer rate is given by

$$\dot{Q} = hA_{surface}\eta_f(T_b - T_\infty)$$

where h is the heat transfer coefficient between the surface of the fin and the ambient air at the

temperature T_∞. The temperature at the base of the fin where it is attached to the parent surface is T_b and the efficiency of a fin of length L is η_f where

$$\eta_f = \frac{\tanh(mL)}{mL}$$

where m is the fin parameter

$$m = \sqrt{\frac{hP}{kA_c}}$$

where P is the perimeter of the fin, A_c is the cross-sectional area of the fin for conduction heat transfer, and k is the thermal conductivity of the fin material.

(a) Show that m can be written

$$m = \sqrt{\frac{R_{axial}}{R_{surface}L^2}}$$

where R_{axial} is the thermal resistance to conduction heat transfer along the axis of the fin and $R_{surface}$ is the thermal resistance to convection and radiation heat transfer between the surface of the fin and the ambient air.

(b) It has been proposed to modify a simple plate fin by adding secondary fins perpendicular to the original primary fin. The dimensions of the primary fin are: Length, $L = 60$ mm; thickness, $t = 0.5$ mm; width normal to the plane of Figure 6P.10, $w = 65.8$ mm. The base temperature is $T_b = 50$ C and the ambient temperature is $T_\infty = 35$ C. The dimensions of the secondary fins are: Length, $L_s = 2$ mm; thickness, $t = 0.5$ mm; width, $w = 65.8$ mm. On each side of the primary fin there are 13 secondary fins arranged along the length of the primary fin with a separation of 4.5 mm between fin centerlines. If the parent surface is considered a plate with the fins attached normal to this surface, the side view would appear as shown with air flow and width w normal to the plane of the page.

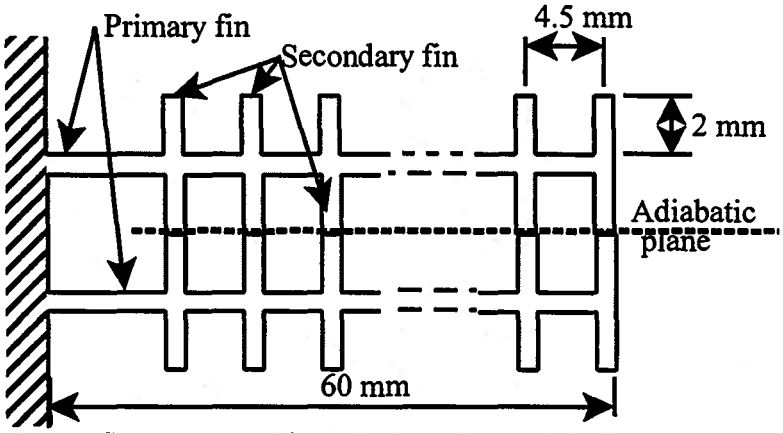

2 primary fins shown with secondary fins attached (not to scale)
Figure 6P.10

(i) Show that the fin efficiency of a secondary fin is essentially one.

(ii) Use the result of (a) above to determine the fin efficiency of a primary fin with the secondary fins attached.

(iii) Calculate the heat transfer rate for a single primary fin with attached secondary fins.

6.11 Carbon steel shafts 0.1 m in diameter are heat treated in a gas-fired furnace in which the products of combustion gases are at a temperature of $T_\infty = 1200$ K and provide a convection heat transfer coefficient of $h_c = 100$ W/m^2 K.

The properties of steel are: $\rho_{steel} = 7832$ kg/m^3, $c_{steel} = 434$ J/kg K, $k_{steel} = 64$ W/m K

(a) Calculate the Biot number for this configuration.

(b) If the shafts enter the furnace at a temperature of $T_i = 300$ K, how long must they remain in the furnace for the centerline temperature to reach 800 K?

6.12 As shown in the sketch below, a stainless steel rod ($k_{stainless\ steel} = 13$ W/m K) of length $L = 60$ cm and diameter $D = 3$ cm is welded to a furnace wall and passes through 20 cm of insulation before emerging into the surrounding air. The temperature of the furnace wall is $T_{wall} = 300$ C and the temperature of the air is $T_{air} = 20$ C. The heat transfer coefficient between the rod, which is assumed to be insulated on the tip, and the air is known to be $h_c = 13$ W/m^2 K.

(a) Sketch the temperature of the rod as a function of x where $x = 0$ at the furnace wall and $x = L$ at the tip of the rod.

(b) Calculate the temperature of the rod 20 cm from the furnace wall.

(c) Calculate the temperature of the tip of the rod.

(d) What is the heat transfer from the rod to the surrounding air?

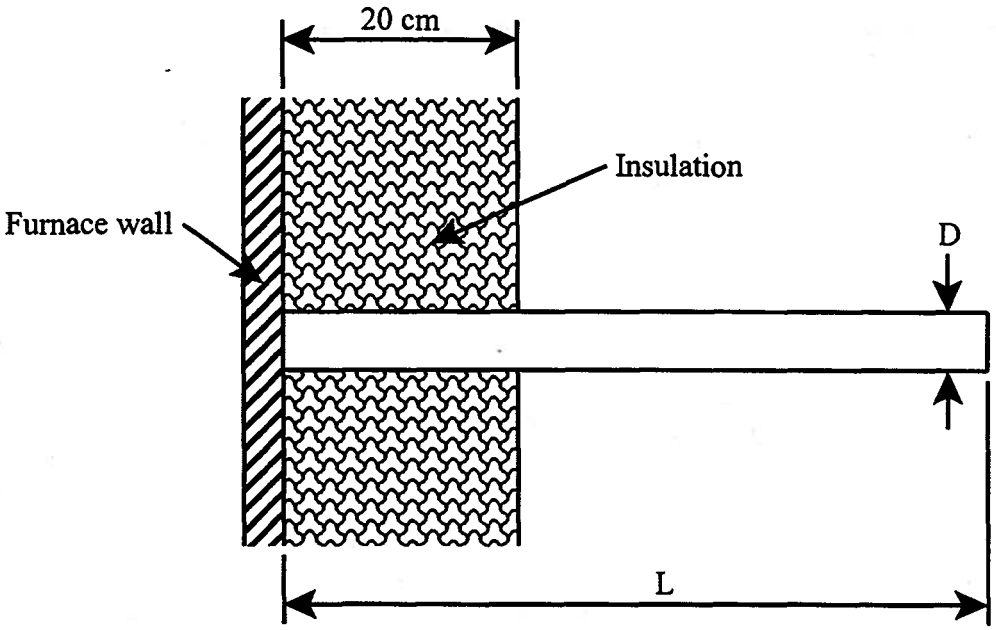

Figure 6P.12

6.13 An apparatus to measure the heat capacity of a small test sample is shown in Figure 6P.13b. A heater and a thermometer are mounted permanently on a sapphire disk of radius 2 mm and thickness 250 μm. The sapphire disk is suspended in a high vacuum by six very fine (50 μm diameter) steel wires attached to the disk at one end and to a large copper ring (not shown) at the other end. The copper ring is maintained at a constant temperature of 300 K. Radiation heat transfer is negligible in this apparatus.

In using the apparatus, the heater is pulsed on and immediately shut off. During a time interval during and just after the "heat" pulse, the temperature of the platform is recorded as a function of time. From these data, the heat capacity of the test sample is inferred. If the mass of the sample is also known, the specific heat capacity of the sample can be determined.

A typical temperature versus time plot when there is no test sample in the apparatus is shown in Figure 6P.13a. Table 6P.13 gives numerical values for the temperature and time of points 1 and 2 in the graph. Similarly, Table 1 also gives the values for points 1 and 2 for the following cases: (1) a sample of brass of mass 20.0 mg and (2) a sample of unknown material of mass 25.1 mg.

NOTE: 1 μm = 10^{-6} m and 1 mg = 10^{-3} gm = 10^{-6} kg

(a) By focusing on the sapphire disk, argue that the temperature throughout the heater, the sample, the sapphire and the thermometer can be modeled as uniform as the system cools back down after the heat pulse. Because the disk and the sample are cooled by a process other than convection, the Biot number itself is not appropriate. Instead, develop and use a dimensionless ratio similar to the Biot number that provides the same sort of information. For the purpose of estimating the value of this ratio, assume that length of each of the supporting wires is on the order of one centimeter. (This is not the actual length of the wires.) Be quantitative.

(b) From the data given in Table 1 and an appropriate model, determine the **actual** total thermal resistance of the steel wires.

(c) From the data given in Table 1 and an appropriate model, determine the heat capacity of the apparatus without a sample.

(d) From the data given in Table 1 and an appropriate model, determine the **specific** heat capacity (J/kg K) of the unknown sample.

(e) If 10 mW of power is applied to the heater in a steady manner instead of a pulsed manner, estimate the new temperature reading of the thermometer.

NOTE: 1 mW = 10^{-3} W

Properties: Steel: $k_{steel} = 60$ W/m K

Brass: $k_{brass} = 111$W/m K, $c_{brass} = 380$ J/kg K, $\rho_{brass} = 8530$ kg/m^3

Sapphire: $k_s = 46$ W/m K, $c_s = 765$ J/kg K, $\rho_s = 3970$ kg/m^3

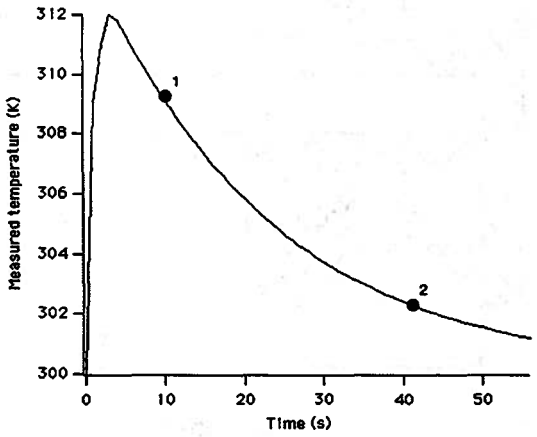

Figure 1 Temperature history of the disk with no sample in place

Table 1

	t_1(sec)	T_1(K)	t_2(sec)	T_2(K)
No sample	10	309.10	42	302.21
Brass sample	10	309.65	42	306.37
Unknown sample	10	309.72	42	305.67

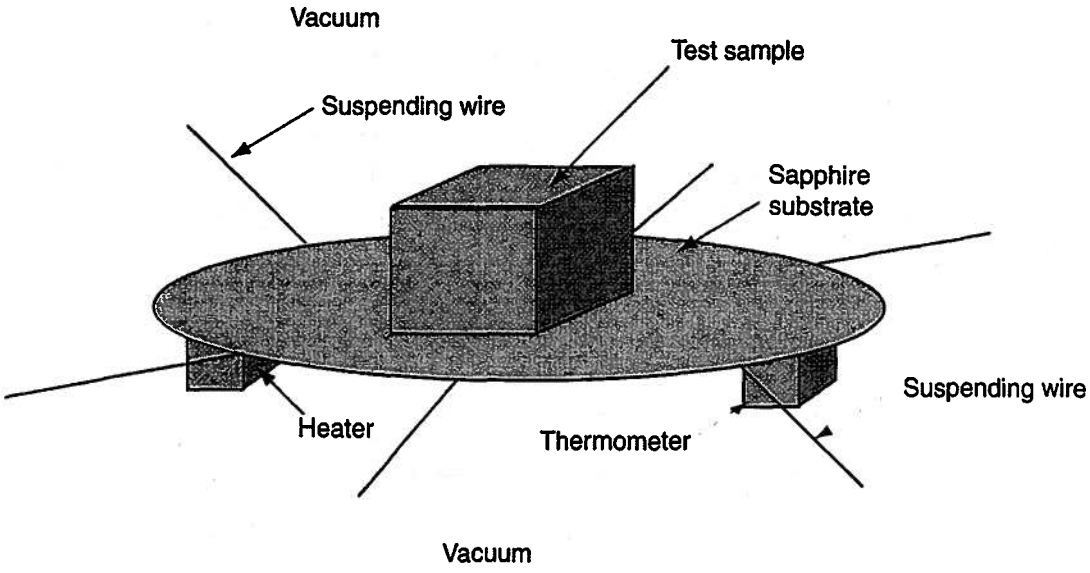

Figure 6P.13b

6.14 As shown in Figure 6P.14, a brass cylinder of diameter $D = 2$ cm and length $L = 10$ cm is suspended in a vacuum chamber on a Kevlar cord of diameter $d = 3$ mm and length $l = 5$ cm. Initially, the temperature of the brass cylinder is $T_i = 90$ K. The walls of the chamber are maintained at a constant temperature of $T_w = 77$ K.

(a) Assuming that the only heat transfer path for the cylinder is through the Kevlar cord, develop a ratio similar to the Biot number for the brass cylinder and show that its value is *much* smaller than 0.1 for this system.

(b) If the brass cylinder and the walls of the vacuum chamber can be modeled as black bodies ($\varepsilon = 1$), estimate the radiation heat transfer coefficient per unit area of the brass cylinder, h_{rad}, when $T_{cylinder} = 90$ K and $T_w = 77$ K.

(c) Show that the effective Biot number for radiation heat transfer is *much* smaller than 0.1.

(d) Use an appropriate model to estimate the amount of time necessary for the brass cylinder to reach the temperature $T_{cylinder} = 80$ K when the vacuum chamber wall is at the constant temperature $T_w = 77$ K.

Properties:

Brass: $k_{brass} = 111$ W/m K, $c_{brass} = 380$ J/kg K, $\rho_{brass} = 8530$ kg/m^3

Kevlar: $k_{kevlar} = 0.2$ W/m K

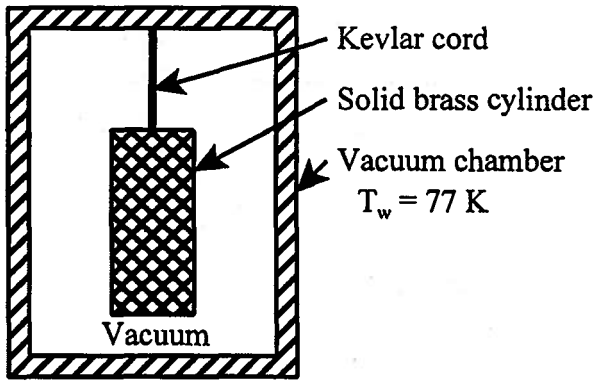

Figure 6P.14

6.15 Cooling devices used for thermal control of central processing units (CPUs) in personal computers are manufactured by many different companies. The specification of one design for the Intel Pentium-III®, the M1 manufactured by PC Power Cooling specifies a thermal resistance between the case of the CPU and the ambient air (T_{air} = 35 C) of 0.75 C/W. The M1 cooler is fitted with a fan that circulates 12 CFM (ft^3/min) of ambient air. The following table describes the array of aluminum (k_{Al} = 174 W/m K) fins mounted on the M1 cooler:

Length of Fin (mm)	Width of Fin (mm)	Thickness of Fin (mm)	Number of Fins
9.5	6.35	1.0	30
9.5	8.0	1.0	20
14.3	6.35	1.0	21
14.3	8.0	1.0	14
14.3	6.35	2.0	6
14.3	8.0	2.0	4

For a CPU operating at 1 GHz, Intel specifies power dissipation of 33 W with a maximum case temperature of 75 C.

(a) Calculate the average convective heat transfer coefficient, h_c (W/m^2 K), for the M1 cooler if we can neglect any heat transfer from the parent surface on which the fins are mounted and the fins can be modeled as having adiabatic tips. (There are two ways of obtaining this information. Do they give the same result?)

(b) Calculate the fin efficiency of each class of fin assuming that the adiabatic tip model holds.

6.16 In heating systems for homes, a common heat exchanger design is a copper tube fitted with aluminum fins (k_{Al} = 174 W/m K) that is built into the baseboard of the room in which temperature control is desired. As shown in Figure 6P.16a, hot water, T_{water} = 95 C, is circulated through the copper tube and room air, T_{air} = 21 C, is circulated over the aluminum fins by natural convection. The mass flow rate of the hot water is so large that its temperature does not change. Thus the temperature of the surface of the copper tube can be modeled as constant at T_{wall} = 95 C. Figure 6P.16 also shows that the thickness of the fin material is 0.28 mm and the dimensions of a typical fin is 70 mm wide by 63.5 mm high. The aluminum fins are swaged onto a copper tube 22.23 mm diameter. The density of fins is 180 fins/lineal meter of copper tube.

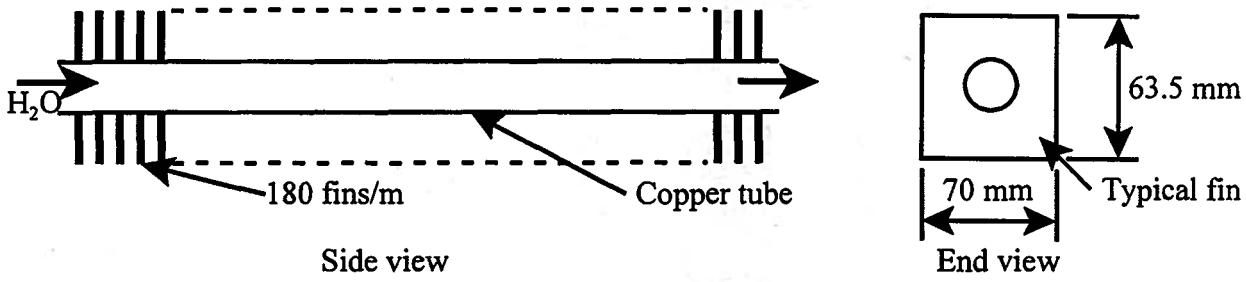

Figure 6P.16a

A small room of dimensions 2 m wide by 3 m long with a ceiling height of 2.75 m has one of the narrow walls and the ceiling exposed to the outside environment. All other walls and the floor are interior partitions and can be modeled as adiabatic. The one exterior wall and the ceiling are of composite construction as shown in cross-section below. The inside layer is plaster board 10 mm thick (k_{pb} = 0.17 W/m K); the middle layer is a glass fiber blanket 100 mm thick (k_f = 0.038 W/m K); and the outside layer is plywood 20 mm thick (k_{pw} = 0.117 W/m K). The heat transfer coefficient for natural convection over the fins is h_f = 5 W/m^2 K; the heat transfer coefficient for natural convection over the interior walls is h_i = 3 W/m^2 K; and the heat transfer coefficient for forced convection over the exterior walls is h_o = 60 W/m^2 K. Thermal radiation can be neglected.

(a) Estimate the heat transfer rate per meter of finned tubing.

(b) For a day in which the environmental temperature is T_{env} = -15 C, estimate the length of finned copper tubing that would be required to maintain the interior temperature at 21 C.

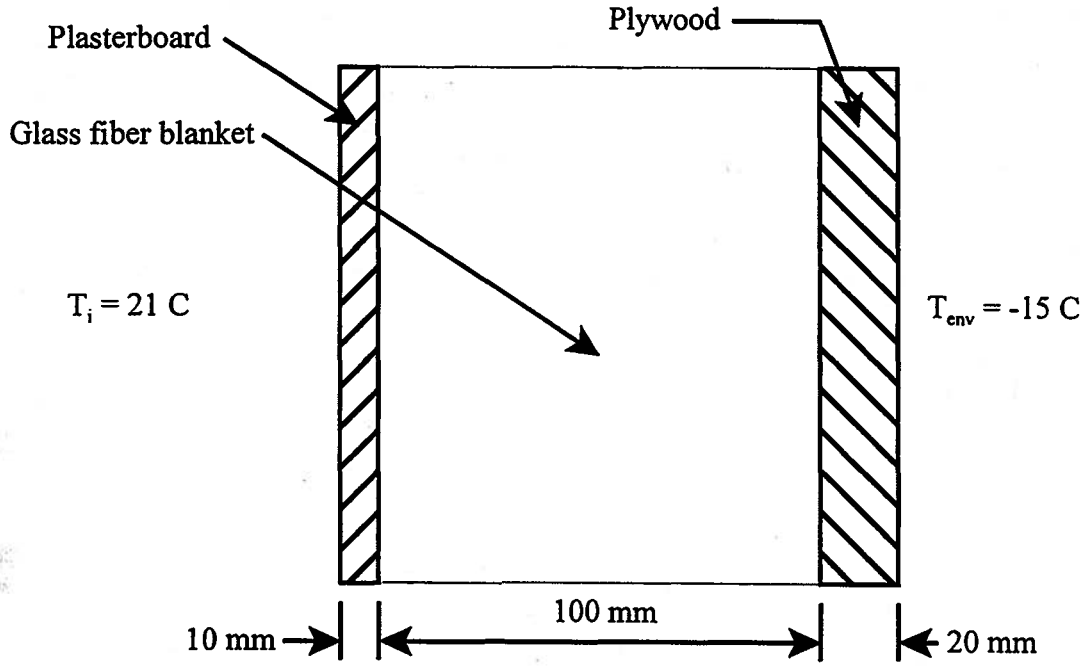

Cross-section of Walls and Ceiling

Figure 6P.16b

6.17 In our discussion of work transfer in systems in Chapter 5, we saw that in order for a work transfer to be considered quasi-static, the velocity of the boundary in motion that was causing the work transfer had to be much slower than the speed of the wave produced by the boundary motion. In the case of heat transfer, there is a change in surface temperature caused by a heat transfer interaction at the surface. The fundamental mechanism by which this change in boundary conditions propagates throughout a system is significantly different from the case associated with boundary motion. In the thermal case, the change propagates by the mechanism of diffusion rather than by wave motion.

We can use the semi-infinite solid model to estimate the conditions under which a system can be regarded as thermally quasi-static. Consider the case of a system experiencing an instantaneous change of surface temperature as a result of a heat transfer interaction at its surface. Let us define the "penetration depth" of this temperature change to be that location, δ, at which

the change in local temperature is one percent of the change in the boundary temperature resulting from the heat transfer interaction.

(a) Use the results of the analysis of the semi-infinite solid model given in equation (6.206) to estimate this depth. That is, find $\delta = \delta(\alpha,t)$.

(b) For a gaseous system (air at 300 K and 1 atm) with a characteristic length of 10 cm, use this expression to find a characteristic time t when $k_{air} = 0.0267$ W/m K, $\rho_{air} = 1.177$ kg/m^3, and $c_P = 1005$ J/kg K. Compare this time with the characteristic time for copper system with the same characteristic length with $k_{Cu} = 401$ W/m K, $\rho_{Cu} = 8933$ kg/m^3, and $c = 385$ J/kg K. How does this time compare with the characteristic time for wave propagation in the same media? What conclusions can you draw for the comparison of the time associated with the attainment of thermal equilibrium and the time associated with the attainment of mechanical equilibrium?

6.18 We wish to examine the steady-state operation of an ice rink to be used in international competition so that we might design this rink. The rules for international hockey require that the rink must be 61 m long by 26 m wide (area = 1586 m^2). Testing has shown that the ideal ice surface temperature for skating should be $T_{ice} = -5$ C. The temperature of the air immediately above the ice surface is to be maintained at a constant temperature of $T_{air} = 3.5$ C.

As shown in Figure 6P.18a, the ice is 2 cm thick and is formed on a concrete slab 12 cm thick. The midplane of this concrete slab is also the midplane of an array of pipes carrying a heat transfer fluid consisting of 50% ethylene glycol (antifreeze) and 50% water. This configuration enables us to model the midplane of the pipes as an isothermal surface 6 cm below the bottom of the ice slab.

(a) To calculate the heat transfer load due to convection at the ice surface, the ASHRAE (American Society of Heating, Refrigeration, and Air-conditioning Engineers) recommends a convective heat transfer coefficient between the ambient air and the ice surface of $h_c = 6.37$ W/m^2 K. Calculate the convective heat transfer load, $\dot{Q}_c$, on the ice surface in watts.

(b) For the heat load due to thermal radiation from the ceiling of the rink to the ice surface, the ceiling of the arena can be modeled as a blackbody at a temperature of $T_c = 288$ K with dimensions 76 m long by 41 m wide (area = 3116 m^2). Recall that the view factor gives the fraction of energy that is emitted by one surface and intercepted by another surface. For this configuration, the view factor for energy emitted by the ceiling and intercepted by the ice surface is 0.34. The ice can be modeled as a blackbody at the temperature of $T_i = 268$ K. Recall that the reciprocity theorem for view factors gives $A_{ceiling}F_{ceiling\text{-}ice} = A_{ice}F_{ice\text{-}ceiling}$. Calculate the radiation heat transfer load, $\dot{Q}_r$, in watts on the ice surface.

(c) If these convective and radiative heat transfer loads represent the principal heat transfer loads on the ice surface, calculate the total heat transfer load on the ethylene glycol, $\dot{Q}_{tot}$.

(d) Estimate the temperature at the midplane of the concrete slab.

(e) Estimate the power required to operate the refrigeration plant necessary to maintain the ice surface. Assume that the refrigeration load is removed at the temperature of the midplane of the concrete and rejected to the environment at $T_{env} = 25$ C. See Figure 6P.18b.

For ice: $k_{ice} = 2.22$ W/m K, $\rho_{ice} = 910$ kg/m^3, $c_{ice} = 1930$ J/kg K
For concrete: $k_{conc} = 1.4$ W/m K, $\rho_{conc} = 2100$ kg/m^3, $c_{conc} = 880$ J/kg K
For air: $k_{air} = 0.0258$ W/m K, $\rho_{air} = 1.2425$ kg/m^3, $c_{P,air} = 1007$ J/kg K,
The Stefan-Boltzmann radiation constant is: $\sigma = 5.67 \times 10^{-8}$ W/m^2 K^4

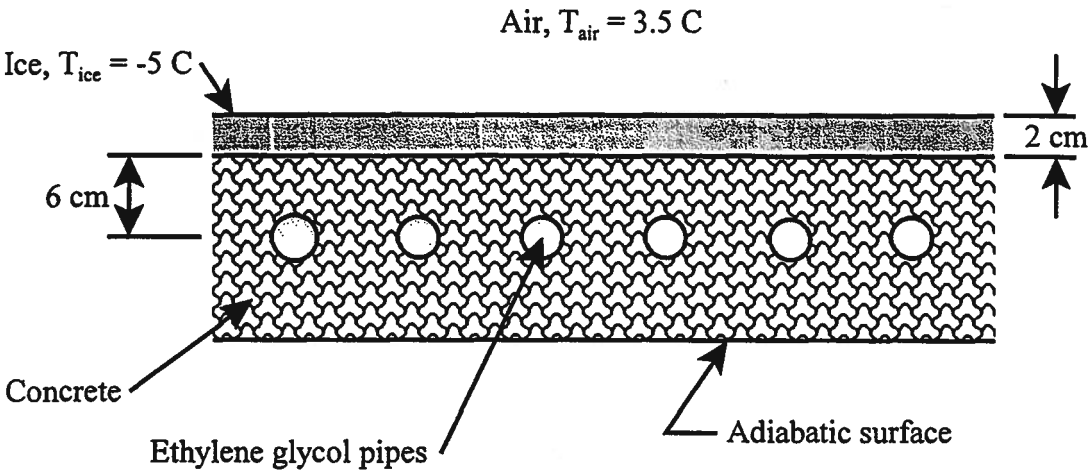

Figure 6P.18a

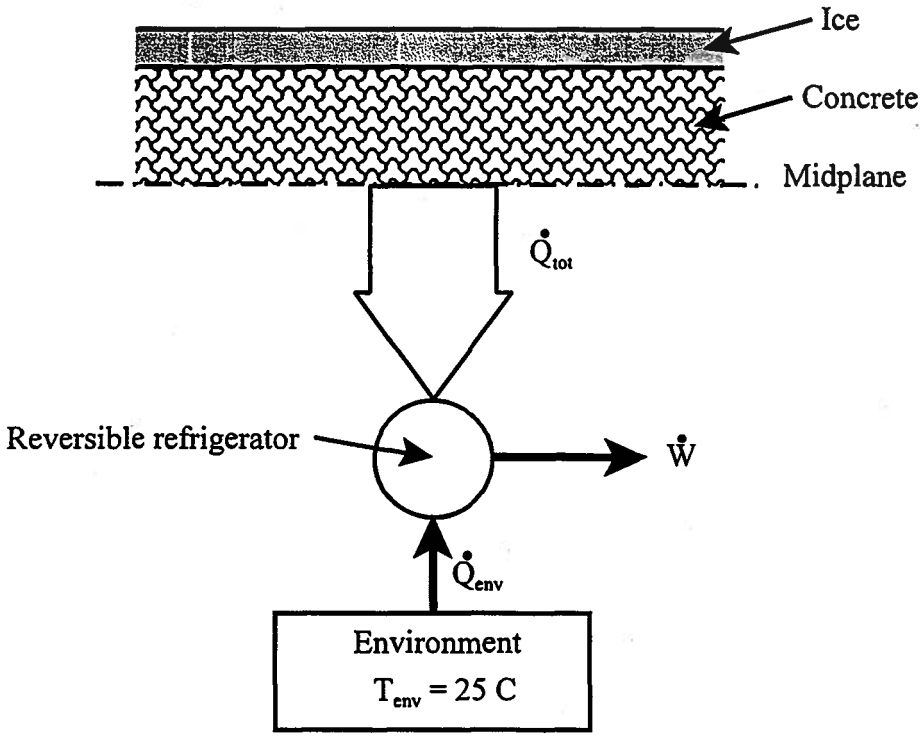

Figure 6P.18b

CHAPTER 7

Energy Conversion: Heat Transfer to Work Transfer

7.1 Introduction

Unlike other members of the animal kingdom, humans choose to live in environments that are not "natural habitats." At the very least, humans need to be able to provide themselves with heat and light as well as the many manufactured articles that they cannot live without. All of this takes energy. Fortunately, Nature has provided humankind with abundant stores of energy in the form of fossil fuels such as coal, oil, and natural gas to meet this need. Unfortunately, this stored energy is not available as work transfer that would enable humans to satisfy their energy needs in the most direct manner possible. The energy stored in the chemical bonds of the fossil fuels can be made available for useful purposes only in the form of a heat transfer. It then becomes the job of the thermal-fluids engineer to devise the means for converting the heat transfer into work transfer. This process is widely known as "energy conversion" which is an important sector of the world economy subject not only to the laws of thermodynamics, but also to the laws of diverse political entities as well. In this chapter, we shall develop strategies for achieving the desired energy conversion and determine the limits set on this energy conversion process by the laws of thermodynamics.

As we have already seen in Chapters 5 and 6, it is a straightforward matter to convert a work transfer to a heat transfer through simple dissipation. In a dissipative process, the energy associated with the work transfer can be converted entirely to heat transfer and the entropy associated with the resulting heat transfer can be generated as required by the second law of thermodynamics. For the reverse conversion, heat transfer to work transfer, the process is not so simple since the heat transfer interaction carries both energy and entropy whereas the work transfer carries only energy. Thus, during the conversion process, it is necessary for us to do something with the entropy since it cannot go into the work transfer. In this type of energy conversion process, we need to concern ourselves with the manner in which both the energy and the entropy are affected. In fact, as we shall soon see, the second law of thermodynamics dictates that the entropy dominates the process and prevents us from converting all the energy available from the heat transfer into work transfer.

One of the simplest models that we can formulate to describe this energy conversion process represents the source of energy as a high temperature heat reservoir. The second law of thermodynamics then requires that there must be at least a minimum of one other heat reservoir at a lower temperature to provide a place to put the entropy associated with the heat transfer. This low temperature heat reservoir also functions as the energy sink where the "unconverted" energy of the high temperature heat transfer can be "dumped." In effect, the energy conversion process is a multiple step process that involves drawing energy and entropy from the high temperature heat reservoir via a heat transfer interaction, converting a portion of the energy into a work transfer interaction with the environment, and finally rejecting the "unconverted" heat transfer energy and all of the entropy (*both* that transferred from the high temperature heat reservoir and any entropy generated in the conversion process) to the energy sink. This process requires the use of a fluid, known as the *working fluid*, that is coupled in the thermodynamic sense. The coupled working fluid thus moves between the two heat reservoirs carrying the necessary energy and entropy.

Since we would like to have the work transfer available on a continual basis without

having to continually replace the working fluid, thermal-fluids engineers have developed "cycles" in which the working fluid shuttles back and forth between the heat reservoirs without experiencing a net change of state. In this manner, the working fluid undergoes a series of thermodynamic processes that form the cycle when strung together. These processes involve heat transfer and work transfer interactions with the heat reservoirs and the environment such that the net heat transfer and net work transfer are both positive in sign and direction when viewed from the working fluid. This, then, constitutes the energy conversion process of heat transfer to work transfer. The system that performs the energy conversion is known as a heat engine. Our objective here is to determine the principles that govern the conceptual design of these heat engines that are the foundation of the energy conversion or "power" industry.

Note that in a conceptual sense these cycles can be run in the opposite direction (including those cycles which are not reversible in the thermodynamic sense) and produce a positive heat transfer from the low temperature heat reservoir and a negative heat transfer with the high temperature heat reservoir. As will become apparent shortly, the second law of thermodynamics requires that the net heat transfer for such a cycle must be negative. Then the first law of thermodynamics for the cycle requires that the net work transfer for the cycle must also be negative if only two heat reservoirs are involved. These kinds of cycles are called heat pumps or refrigeration cycles and are the foundation of the refrigeration and air conditioning industries.

7.2 The Carnot Cycle: A Reversible Cycle of a Coupled Fluid in Thermal Communication with Two Heat Reservoirs

In 1824, the French military engineer Sadi Carnot proposed a reversible cycle for the conversion of heat transfer to work transfer. This cycle is often used as the "gold standard" against which the performances of other cycles are measured, but for reasons that will become apparent later, this cycle is not used at all in practical systems. This cycle which bears Carnot's name operates between two heat reservoirs and consists of a total of four processes: two reversible isothermal processes that occur while the working fluid, which must be coupled in the thermodynamic sense in order for the cycle to work, is in thermal communication with the two heat reservoirs (one at a time) and two reversible adiabatic processes that occur while the working fluid is isolated from them. In spite of the practical limitations of the Carnot cycle, we can gain much insight into the workings of energy conversion cycles in general by examining the way in which this cycle operates.

Consider the operation of a Carnot cycle in which the working fluid is an ideal gas, the only coupled fluid model available to us at this time. In effect, the ideal gas shuttles back and forth between the two heat reservoirs carrying energy and entropy while experiencing work transfer interactions with the environment and heat transfer interactions with the two heat reservoirs. The operation of the cycle can be viewed either in terms of the energy being transported by the ideal gas or in terms of the entropy being transported, but the entropy point of view provides much greater insight.

Figure 7.1 shows an ideal gas, two heat reservoirs and the mechanical matching elements required to transport entropy reversibly between the heat reservoirs with a Carnot cycle. The interactions shown in Figure 7.1 are for all of the four processes. For any given process the mechanical and thermal interconnections are switched "on" or "off" as given by Table 7.1. The four processes A, B, C, and D that make up the cycle can be represented in terms of temperature

and entropy coordinates for the gas as shown in Figure 7.2. The basic parameters of the cycle are

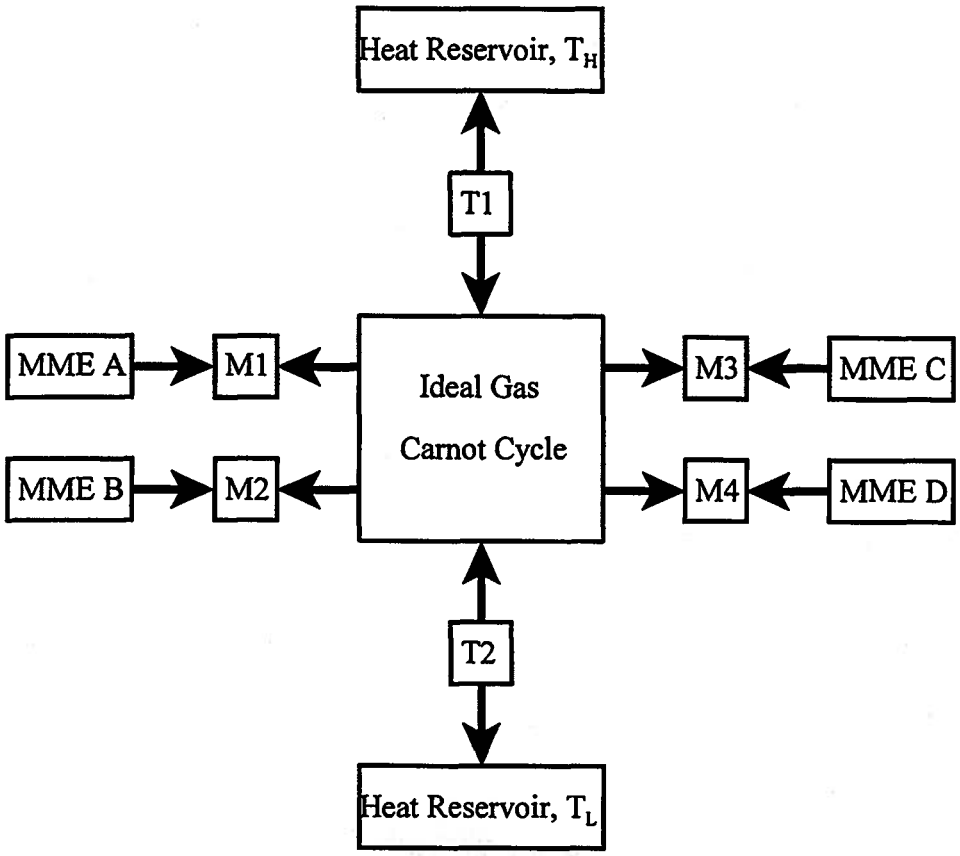

Figure 7.1 Ideal Gas, Heat Reservoirs, and Mechanical Matching Elements Necessary for Executing the Carnot Cycle in an Ideal Gas

Table 7.1 Settings for Interconnections for the Carnot Cycle

Interconnection	Process A	Process B	Process C	Process D
T1	**ON**	OFF	OFF	OFF
T2	OFF	OFF	**ON**	OFF
M1	**ON**	OFF	OFF	OFF
M2	OFF	**ON**	OFF	OFF
M3	OFF	OFF	**ON**	OFF
M4	OFF	OFF	OFF	**ON**

set by the temperatures of the two heat reservoirs T_H and T_L and the entropy transfers for processes A and C. For the isothermal process, Process A, the heat transfer for the gas is given by the first law.

$$Q_A - W_A = U_2 - U_1 \tag{7.1}$$

Since Process A is reversible and isothermal, we can determine the work transfer from

$$W_A = \int_{V_1}^{V_2} P dV = mRT_H \int_{V_1}^{V_2} \frac{dV}{V} = mRT_H \ln \frac{V_2}{V_1} \tag{7.2}$$

where we have substituted the property constitutive relation for the pressure of the ideal gas. Then since the energy constitutive relation for the ideal gas experiencing this isothermal process is

$$U_2 - U_1 = mc_v (T_2 - T_1) = 0 \tag{7.3}$$

the first law for the gas becomes

$$Q_A = W_A = mRT_H \ln \frac{V_2}{V_1} \tag{7.4}$$

The second law applied to the ideal gas gives

$$S_2 - S_1 = \int_1^2 \frac{\delta Q}{T} + S_{gen} \tag{7.5}$$

where $S_{gen} = 0$ since Process A is reversible and

$$S_2 - S_1 = \frac{1}{T_H} \int_1^2 \delta Q = \frac{Q_A}{T_H} \tag{7.6}$$

since Process A is also isothermal. Then combining equations (7.4) and (7.6), we obtain

$$S_2 - S_1 = mR \ln \frac{V_2}{V_1} \tag{7.7}$$

Thus, the magnitude of the expansion from V_1 to V_2 determines the amount of entropy transferred from the high temperature reservoir.

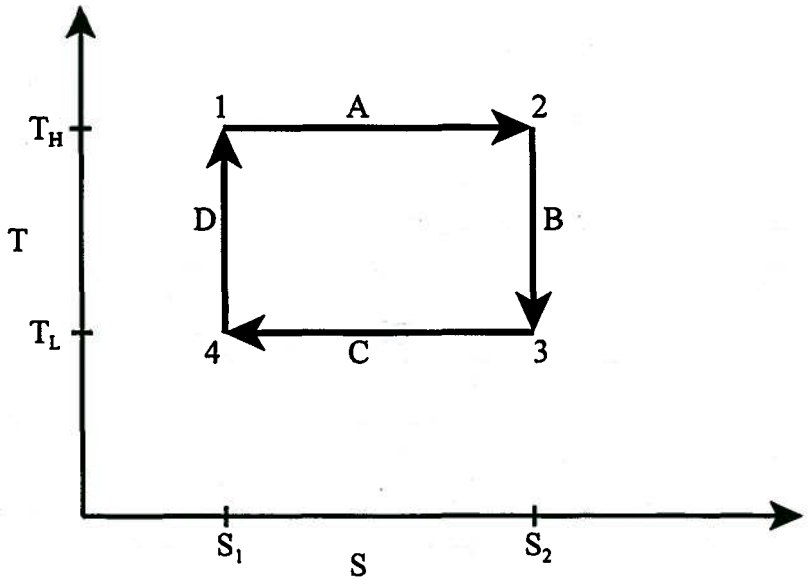

Figure 7.2 Temperature-Entropy Representation of the Carnot Cycle

For Process C, the entropy change S_4 - S_3 is the negative of that for Process A as Figure 7.2 clearly shows. By a line of reasoning similar to that resulting in equation (7.7), we have

$$S_4 - S_3 = mR \ln \frac{V_4}{V_3} = -(S_2 - S_1) \tag{7.8}$$

Then

$$mR \ln \frac{V_4}{V_3} = -mR \ln \frac{V_2}{V_1} \tag{7.9}$$

and

$$\frac{V_3}{V_4} = \frac{V_2}{V_1} \tag{7.10}$$

It follows, then, that the volume ratio for the isothermal expansion process while the ideal gas is in thermal communication with the high temperature heat reservoir is the reciprocal of the volume ratio for the isothermal compression process while the ideal gas is in thermal communication with the low temperature heat reservoir. Then the entropy transfers between the ideal gas and the heat reservoirs are determined by the magnitudes of the volume ratios which are, in fact, identical. Thus the two entropy transfers of the Carnot cycle are also identical, viz.,

$$\frac{Q_A}{T_H} = mR \ln \frac{V_2}{V_1} = -mR \ln \frac{V_4}{V_3} = -\frac{Q_C}{T_L} \tag{7.11}$$

Then from equation (7.10), we have

$$\frac{V_3}{V_2} = \frac{V_4}{V_1} \tag{7.12}$$

Thus, the volume ratios of the two adiabatic processes are also the reciprocals of one another.

The volume ratio V_3/V_2 can be determined from the reversible adiabatic expansion process, Process B. From the second law, we find that the entropy of the ideal gas remains unchanged during Process B.

$$S_3 - S_2 = \int_2^3 \frac{\delta Q}{T} + S_{gen} = 0 \tag{7.13}$$

The entropy constitutive relation then gives

$$S_3 - S_2 = mR \ln \frac{V_3}{V_2} + mc_v \ln \frac{T_3}{T_2} = 0 \tag{7.14}$$

and

$$\frac{V_3}{V_2} = \left(\frac{T_2}{T_3}\right)^{\frac{c_v}{R}} = \left(\frac{T_H}{T_L}\right)^{\frac{c_v}{R}} \tag{7.15}$$

Thus, the volume ratios of the adiabatic processes are determined by the ratio of the thermodynamic temperatures of the heat reservoirs. Furthermore, the "size" of the Carnot cycle itself is determined by the temperatures of the heat reservoirs and the entropy transfers between the working fluid and the heat reservoirs.

From an operational point of view, the Carnot cycle consists of: (1) transferring entropy from the high temperature heat reservoir at T_H into the ideal gas; then (2) reducing the temperature of the ideal gas to the temperature T_L of the low temperature heat reservoir by transferring energy out of the gas in the form of a work transfer; then (3) transferring entropy out of the gas and into the low temperature heat reservoir at T_L; and finally (4) increasing the temperature of the ideal gas back up to T_H by drawing energy from the environment in the form of a work transfer. The reversible isothermal processes are used to transfer entropy to and from

the gas, and the reversible adiabatic processes are used to change the temperature of the gas from that of one heat reservoir to that of the other. Note that from equation (7.11), the net entropy transfer for the Carnot cycle is zero.

$$\frac{Q_A}{T_H}+\frac{Q_C}{T_L}=0 \tag{7.16}$$

As we shall show in Section 7.3, this is true of *all* reversible cycles in thermal communication with two heat reservoirs.

The purpose of constructing a cycle such as the Carnot cycle is to be able to convert a positive heat transfer into a net positive work transfer. There are two ways in which we can determine the net positive work transfer. In the first of these, we recognize that the net energy change for the cycle must be zero since the energy is a property, and by definition, there can be no net change in any property for a cycle. Then from the first law we have

$$\oint \delta Q - \oint \delta W = \oint dU = 0 \tag{7.17}$$

and

$$\begin{aligned} \oint \delta W &= \oint \delta Q = Q_A + Q_B + Q_C + Q_D \\ \oint \delta W &= T_H (S_2 - S_1) + 0 + T_L (S_4 - S_3) + 0 \\ \oint \delta W &= T_H (S_2 - S_1) - T_L (S_2 - S_1) \\ \oint \delta W &= (T_H - T_L)(S_2 - S_1) \end{aligned} \tag{7.18}$$

The net result of the entropy transfer between the two reservoirs is a decrease in the thermal energy stored in the heat reservoirs and a net increase in the mechanical energy stored in the mechanical matching elements. This gain in mechanical energy is the result of the net work transfer from the ideal gas during the cycle. Notice that the net work transfer is equal to the entropy transferred from the high temperature heat reservoir times the temperature difference between the two heat reservoirs, and this result is independent of the particular characteristics of the working fluid. The only requirement is that the working fluid must be coupled in the thermodynamic sense.

Alternatively, we could evaluate the net work transfer for the cycle from the evaluation of the work transfer for each of the component processes of the cycle. Thus

$$\oint \delta W = W_A + W_B + W_C + W_D \tag{7.19}$$

Substituting equation (7.2) and (7.11) into equation (7.19) and recognizing that the interactions with the heat reservoirs do not involve any work transfer, we obtain

$$\begin{aligned} \oint \delta W &= 0 + mRT_H \ln\frac{V_2}{V_1} + 0 + mRT_L \ln\frac{V_4}{V_3} \\ \oint \delta W &= (T_H - T_L) mR \ln\frac{V_2}{V_1} \end{aligned} \tag{7.20}$$

Substituting equation (7.7) into equation (7.20), we obtain the same result as equation (7.18) which was derived from the second law.

$$\oint \delta W = (T_H - T_L)(S_2 - S_1) \tag{7.21}$$

Note that since $T_H > T_L$ and $S_2 > S_1$, the net work transfer for the Carnot cycle is positive. Since the net entropy transfer for the Carnot cycle is zero as shown in equation (7.11), we have

$$\oint \delta S_{transfer} = \oint \frac{\delta Q}{T} = \frac{Q_H}{T_H} + \frac{Q_L}{T_L} = 0 \tag{7.22}$$

Note also that upon substituting equation (7.6) into equation (7.21), we obtain the somewhat surprising result that only a fraction of the energy associated with the positive heat transfer Q_H from the high temperature heat reservoir can be converted into a positive work transfer.

$$\oint \delta W = (T_H - T_L)\frac{Q_H}{T_H} = Q_H\left(1 - \frac{T_L}{T_H}\right) \tag{7.23}$$

This is an important result which we shall consider in detail in Section 7.5.

Example 7E.1: A Carnot cycle of an ideal gas is in thermal communication with two heat reservoirs at temperatures $T_H = 1000$ K and $T_L = 300$ K, respectively. The rate of heat transfer with the high temperature heat reservoir is $\dot{Q}_H = 100$ MW.

(a) Determine the rate of heat transfer with the low temperature heat reservoir.

(b) Determine the rate of work transfer between the ideal gas Carnot cycle and the environment.

Solution: (a) In engineering practice, it is commonly the case that the interactions experienced by energy conversion devices operating in a cyclic manner are expressed on a rate basis as in the present example. That is, the heat transfer from the high temperature heat reservoir is given in terms of Watts rather than Joules. With the understanding that the cyclic device completes an integral number of cycles, the equations derived from the first and second laws of thermodynamics that describe the performance of these cycles remain valid. Then from equation (7.22) we have

$$\dot{Q}_L = -\dot{Q}_H \frac{T_L}{T_H}$$

$$\dot{Q}_L = -(100\text{ MW})\frac{300\text{ K}}{1000\text{ K}} = -30\text{ MW}$$

where the heat transfer to the low temperature heat reservoir is negative meaning that the energy flows from the ideal gas cycle to the heat reservoir.

(b) From equation (7.23) we have

$$\oint \delta W = Q_H\left(1 - \frac{T_L}{T_H}\right)$$

$$\oint \delta W = (100\text{ MW})\left(1 - \frac{300\text{ K}}{1000\text{ K}}\right) = 70\text{ MW}$$

Notice that only 70 percent of the energy transferred from the source (high temperature heat reservoir) can be converted to a work transfer even for this reversible cycle. This is a consequence of the entropy transfer between the heat reservoirs via the Carnot cycle and not a consequence of any "losses" that might occur during the interactions. This latter possibility will be taken up later.

7.3 A General Reversible Cycle of a Coupled Fluid in Thermal Communication with Two or More Heat Reservoirs

We shall now show that the second law of thermodynamics requires that equation (7.22) must apply to *any* reversible cycle of *any* system experiencing heat transfer with only two heat reservoirs regardless of the constitutive relations for the working fluid and the specific nature of the reversible processes that form the reversible cycle. To this end, consider a general reversible

cycle which transfers energy and entropy via heat transfer interactions with two heat reservoirs during its general reversible cycle as shown schematically in Figure 7.3. The number and nature of the mechanical matching elements necessary to maintain neutral equilibrium in the working fluid during the work transfer interactions will depend upon the types of processes that constitute the cycle under study and the constitutive relations of the working fluid.

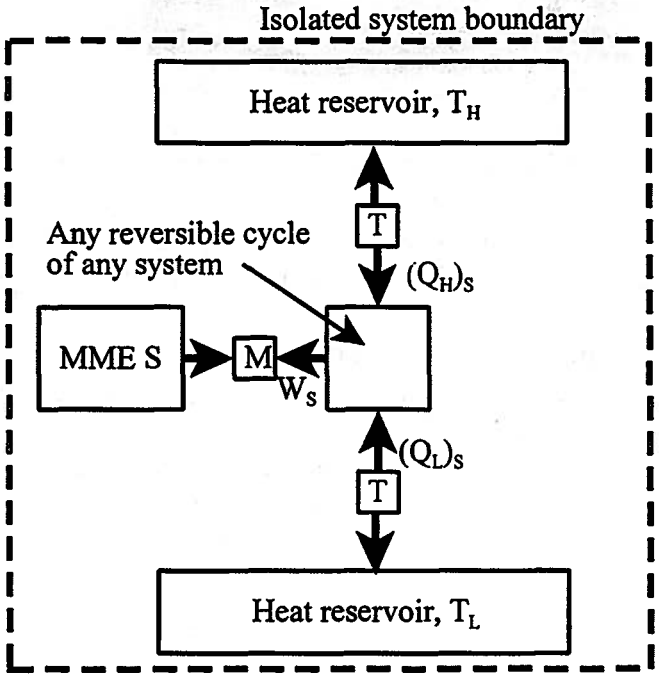

Figure 7.3 Any Reversible Cycle of Any System Interacting with Two Heat Reservoirs

The second law applied to the reversible cycle of interest takes the form

$$\oint dS = \oint \delta S_{transfer} + \oint \delta S_{gen} = 0 \tag{7.24}$$

since the entropy of the working fluid of the cycle is a property. However, since the cycle is also reversible, there is no entropy generated and equation (7.24) reduces to

$$\oint dS = \oint \delta S_{transfer} = 0 \tag{7.25}$$

The entropy transfers with the two heat reservoirs are simply Q_H/T_H and Q_L/T_L, respectively. Then equation (7.25) becomes

$$\oint \delta S_{transfer} = \frac{Q_H}{T_H} + \frac{Q_L}{T_L} = 0 \tag{7.26}$$

which is identical to equation (7.22). In fact, it is a simple matter to increase the number of heat reservoirs in thermal communication with the general reversible cycle to any arbitrary number n with a concomitant change in the number and kind of mechanical matching elements. Then for this case the expression equivalent to equation (7.26) is

$$\oint \delta S_{transfer} = \sum_{i=1}^{n} \frac{Q_i}{T_i} = 0 \tag{7.27}$$

where Q_i/T_i is the entropy transfer between the working fluid of the cycle and the heat reservoir whose temperature is T_i.

Thus, we are led to the important conclusion that for any reversible cycle of any system in thermal communication with any number of heat reservoirs, there is no net entropy transfer. It is

equally important to note that equation (7.27) applies to cycles that run in the forward direction as heat engines or in the reverse direction as heat pumps. It makes no difference whether the net heat transfer and, hence, the net work transfer for the reversible cycle is positive (heat engine) or negative (heat pump). The only requirement for equation (7.27) to hold is that the cycle must be reversible.

The result shown in equation (7.27) can be extended to even more general situations where the n different heat reservoirs can be replaced with systems in neutral equilibrium that have a temperature that varies as the entropy is transferred in or out. For example, the heat reservoirs could be replaced by pure thermal systems with constant (and finite) specific heats. For these systems, the temperature changes as energy and entropy is transferred across the system boundary via heat transfer. In this case, the entropy transfer for the cycle during the interaction with system i must be viewed as the collective effect of a series of infinitesimal interactions each of which transfers entropy in the amount of

$$\left(\delta S_{transfer}\right)_i = \frac{\delta Q_i}{T_i} \tag{7.28}$$

Then the net entropy transfer with system i becomes

$$\left(S_{transfer}\right)_i = \int_i \frac{\delta Q_i}{T_i} \tag{7.29}$$

Then for a reversible cycle of the heat engine or heat pump, the second law gives

$$\oint dS = \sum_{i=1}^{n}\left(S_{transfer}\right)_i = \sum_{i=1}^{n}\int_i \frac{\delta Q_i}{T_i} = 0 \tag{7.29}$$

Example 7E.2: A pure thermal system A with a heat capacity $m_A c_A$ is at a temperature T_1. A second pure thermal system B with a heat capacity $m_B c_B$ is also at T_1.

(a) Devise an ideal gas cycle that will increase the temperature of A to T_{2A} in a reversible manner in one cycle. The necessary entropy is to be drawn in a reversible manner from B thereby decreasing the temperature of B to an unknown value T_{2B}.

(b) What is the temperature T_{2B}?

(c) What is the net work transfer for the cycle?

Solution: (a) The assembly of hardware shown schematically in Figure 7E.1 will accomplish the desired result. We assume that the temperature of the ideal gas is at T_1 at state 1 for the gas. With the thermal interconnection TA switched on and the thermal interconnection TB switched off, the appropriate mechanical matching element compresses the gas increasing the temperature of pure thermal system A and the gas simultaneously. The necessary entropy to be transferred to pure thermal system A comes from the stored entropy in the gas since there is no entropy transfer between the gas and the matching mechanical elements. When the temperature of pure thermal system A reaches T_{2A}, the gas is in state 2 as shown in Figure 7E.2b. The thermal interconnection TA is switched off and the gas then expands reversibly and adiabatically (constant S) while transferring energy to the next matching mechanical element. When the temperature of the gas decreases to T_1, the gas is in state 3 and the process is stopped. The thermal interconnection TB is turned on and the gas and pure thermal system B are held in neutral

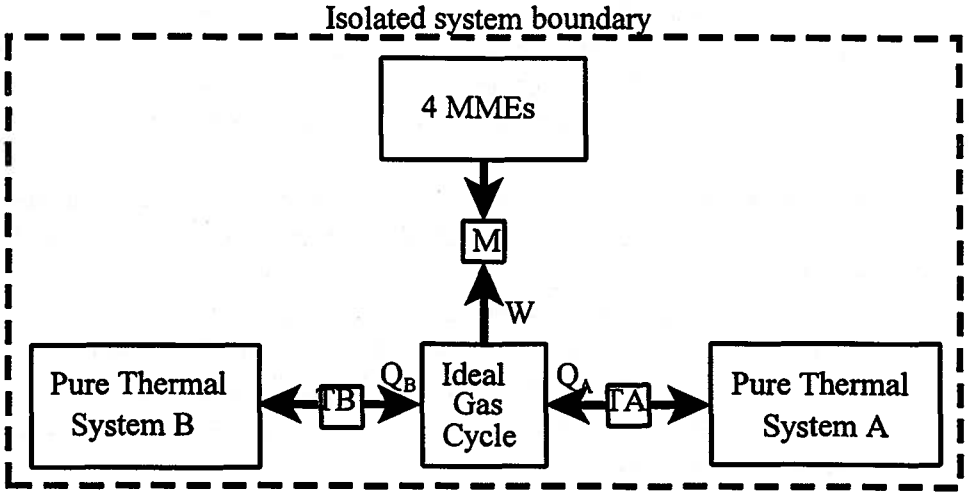

Figure 7E.2a Reversible Heat Transfer Between Two Pure Thermal Systems

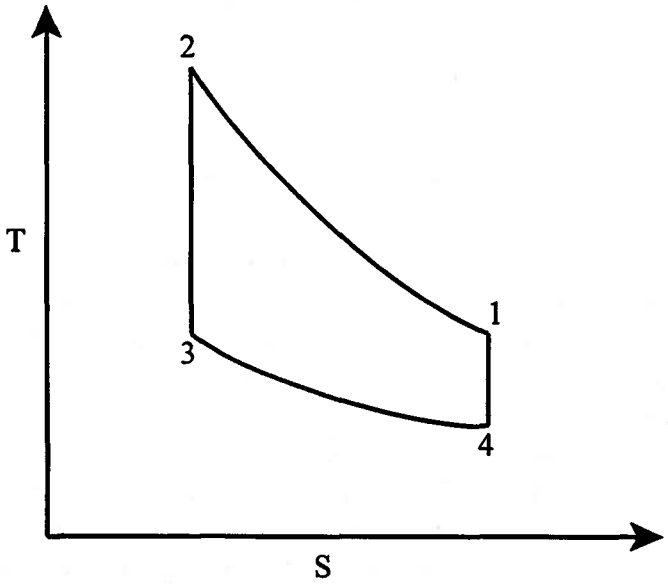

Figure 7E.2b Reversible Ideal Gas Cycle

equilibrium with the third matching element. The gas now expands, decreasing the temperature of pure thermal system B and the gas simultaneously. During this process, entropy is transferred from pure thermal system B to the gas until the entropy of the gas returns to the original value, S_1. The gas is now in state 4 with $T = T_{2B}$ and $S = S_1$. The thermal interconnection TB is switched off and the gas is then compressed reversibly and adiabatically (constant S) back to state 1 where $T = T_1$.

(b) To find T_{2B} we apply the second law to the isolated system shown in Figure 7E.2a. Since all processes in the isolated system during the cycle are reversible, the total stored entropy is constant. Also, the change in entropy of the ideal gas for the complete cycle is zero since stored entropy is a property. Thus, there is no net entropy change for the composite subsystem

consisting of the pure thermal system A plus the pure thermal system B. Then

$$\left(S_{final}-S_{initial}\right)_A+\left(S_{final}-S_{initial}\right)_B=0$$

Substituting the entropy constitutive relation, we get

$$m_A c_A \ln\frac{T_{2A}}{T_1}+m_B c_B \ln\frac{T_{2B}}{T_1}=0$$

$$T_{2B}=T_1\left(\frac{T_{2A}}{T_1}\right)^{-\frac{m_A c_A}{m_B c_B}}$$

(c) To evaluate the work transfer for the ideal gas cycle, apply the first law to the isolated system. The first law for the isolated system requires that the sum of the energy changes for all the subsystems total zero. The change in the stored energy of the gas for a complete cycle is zero since the energy is a property. Thus, the first law for the isolated system gives

$$\oint dU_{gas}+m_A c_A\left(T_{2A}-T_1\right)+m_B c_B\left(T_{2B}-T_1\right)+\sum_{i=1}^{4}\left(E_{final}-E_{initial}\right)_{MME_i}=0$$

Since only the ideal gas interacts with the mechanical matching elements, the net work transfer for the gas during the cycle is equal to the sum of the energy changes of the mechanical matching elements. Then

$$\oint \delta W=\sum_{i=1}^{4}\left(E_{final}-E_{initial}\right)_{MME_i}=-m_A c_A\left(T_{2A}-T_1\right)-m_B c_B\left(T_{2B}-T_1\right)$$

Example 7E.3: A heat engine provides a simple model of a power plant. The magnitude of the heat transfer interaction with the energy sink is an issue of particular concern in the energy conversion industry. Since the environment is usually used as the energy sink, there can be adverse ecological consequences on a local scale from excessive heat transfer with the environment. This is particularly true if a river or estuary is used as the energy sink. The entire ecological balance of the body of water can be upset by the low temperature heat transfer from the power plant. Plankton or algae growth are most easily affected as the local temperature changes in response to the heat transfer process. There then results concomitant changes in other aquatic life forms. Because of their low operating temperatures, nuclear energy sources are particularly troublesome in this regard. Compare the magnitudes of the thermal pollution produced by an oil fired power plant and a nuclear plant given that both plants produce 10^3 MW of power and both plants use the environment at a temperature of T_L = 300 K as an energy sink. The equivalent temperature of the oil fired energy source is $(T_H)_{oil}$ = 800 K while the temperature of the nuclear energy source is $(T_H)_{nuclear}$ = 550 K.

Solution: For the sake of comparison, we will assume that the two operating cycles of these power plants are reversible. From the second law of thermodynamics for a reversible system in communication with two heat reservoirs, equation (7.26), we have

$$\frac{Q_H}{T_H}+\frac{Q_L}{T_L}=0$$

From the first law for the cycle we have

$$\oint \delta W=\oint \delta Q$$

$$W=Q_H+Q_L$$

Combining the first and second law expressions, we get

$$\frac{W-Q_L}{T_H}+\frac{Q_L}{T_L}=0$$

Solving for the low temperature heat transfer, we get

$$-(Q_L)_{oil}=\left[\frac{T_L}{(T_H)_{oil}-T_L}\right]W$$

$$-(Q_L)_{nuclear}=\left[\frac{T_L}{(T_H)_{nuclear}-T_L}\right]W$$

Then

$$-(Q_L)_{oil}=\left[\frac{300\text{ K}}{800\text{ K}-300\text{ K}}\right](10^3\text{ K})=600\text{ MW}$$

$$-(Q_L)_{nuclear}=\left[\frac{300\text{ K}}{550\text{ K}-300\text{ K}}\right](10^3\text{ K})=1200\text{ MW}$$

Thus, the thermal pollution emanating from the nuclear plant is double that of the oil fired plant. Bear in mind that this is only an estimate since we assumed reversible operation for both plants, and this surely will not be the case for the actual plants. However, this estimate does provide us with a good idea of the nature of the problem of thermal pollution from various plant designs.

7.4 Heat Engine Efficiency and Heat Pump Coefficient of Performance

In engineering practice, the thermal-fluids engineer is always concerned with the economics of the systems that he/she designs. This includes both the capital cost of the design, i.e., the cost to manufacture the system, and the operating cost of the design, i.e., the cost to operate the system on an annual basis. In order to be able to compare competing designs in a manner that reflects these economic concerns, thermal-fluids engineers have developed a collection of performance parameters that facilitate such comparisons for heat engines that are used in the energy conversion industry (power industry) and for heat pumps and refrigerators used in the environmental control industry (air conditioning and refrigeration industry). As we might expect the irreversibilities present in any design will influence both capital costs and operating costs, and we will give special attention to these in subsequent material in this treatment. However, quite apart from any issues regarding the manner in which irreversiblities may affect the performance of systems that operate in a cyclic manner, the performance of these devices is limited even for reversible operation by the entropy transfer through the device. The performance parameters that will prove most useful should reflect this physical limitation as well as lend themselves to showing the effects of irreversibilities on system performance while at the same time providing information about the economic aspects of the design.

For simple comparisons of energy conversion systems operating between an energy source that can be modeled in simplest terms as a high temperature heat reservoir and an energy sink that can be modeled as a low temperature heat reservoir, the performance parameter that has proven most useful over the years is the heat engine efficiency. This parameter, η, is also known by other names such as the energy conversion efficiency and the thermal efficiency. It is defined as the ratio of the desired output of the heat engine (that which can be sold on the energy market) to the input to the cycle necessary to make the cycle work (that which must be purchased on the fuel market). The net work transfer per cycle reflects the output of the heat engine, and the high

temperature heat transfer per cycle reflects the "expensive"input. Thus,

$$\eta = \frac{\text{net work transfer /cycle}}{\text{high temperature heat transfer/cycle}} = \frac{\oint \delta W}{Q_H} \tag{7.30}$$

For a reversible heat engine, we can substitute equation (7.23) for the net work transfer per cycle. Then equation (7.30) becomes

$$\eta_{reversible} = \frac{Q_H\left(1-\frac{T_L}{T_H}\right)}{Q_H} = 1-\frac{T_L}{T_H} \tag{7.31}$$

Since the Carnot cycle is the most widely known (but not the only example) of the reversible heat engines, equation (7.31) is often written

$$\eta_{Carnot} = 1-\frac{T_L}{T_H} \tag{7.32}$$

Typically, efficiencies of the type defined in equation (7.30) have values in the range from 0 to 1; however, the value of the reversible heat engine efficiency can approach unity only if $T_H >> T_L$. For practical heat engine designs, the atmosphere or a large body of water such as the ocean or a river usually serves as the energy sink with T_L ~ 300 K. The energy source is typically the oxidation reaction of a fossil fuel with an effective temperature T_H ~ 1000 K to 1200 K. Thus, practical values for the temperature ratio T_L/T_H appearing in equation (7.31) are on the order of 0.3 to 0.25 with values of the heat engine efficiency limited to the range of 70 % to 75% under the best of circumstances. Throughout the 20th century, practical limits imposed by heat engine design resulted in $\eta < 40\%$; however, as shown in Chapter 15, at the turn of the 21st century, advances in metallurgy and manufacturing technology have facilitated creative practical heat engine designs with η ~ 60% .

In the case of the heat pump or refrigerator, the efficiency defined in equation (7.30) is not appropriate since these cycles run in the reverse direction. For these applications the desired effect is the heat transfer from the low temperature heat reservoir (the refrigeration load) or, in the case of the heat pump, the heat transfer to the high temperature heat reservoir with the "expensive" input in both cases being the net work transfer required to operate the cycle (usually electricity drawn from the electrical power grid). For refrigeration applications, thermal-fluids engineers have defined the coefficient of performance, COP, as the relevant performance parameter. Thus,

$$COP = \frac{\text{refrigeration effect/cycle}}{-\text{net work transfer/cycle}} = \frac{Q_L}{-\oint \delta W} \tag{7.33}$$

where the negative sign has been introduced into the denominator of the definition in order to make the values of the resulting parameter positive since the net work transfer for the cycle will be negative. From the first law for the refrigeration cycle

$$-\oint \delta W = -\oint \delta Q = -Q_H - Q_L \tag{7.34}$$

Combining equations (7.33) and (7.34), we get

$$COP = \frac{Q_L}{-Q_H - Q_L} = \frac{1}{-\frac{Q_H}{Q_L} - 1} \tag{7.35}$$

For the reversible refrigerator operating between two heat reservoirs, we can solve equation

(7.26) for the ratio of the heat transfers for the two heat reservoirs. Then

$$-\left(\frac{Q_H}{Q_L}\right)_{reversible} = \frac{T_H}{T_L} \tag{7.36}$$

and equation (7.35) applied to the reversible refrigerator becomes

$$COP_{reversible} = \frac{1}{\frac{T_H}{T_L} - 1} \tag{7.37}$$

Note that unlike the values of the heat engine efficiency which have 1 as an upper bound, the values of the coefficient of performance do not have an upper bound. As the temperature of the refrigeration load approaches that of the energy sink $T_L \to T_H$, $COP_{reversible} \to \infty$. This observation implies that no work transfer is required pump entropy at constant temperature. On the other hand, as the temperature of the refrigeration load approaches zero thermodynamic temperature, as it can in certain cryogenic applications, the coefficient of performance approaches zero (As $T_L \to 0$, $COP_{reversible} \to 0$.) This observation implies that an infinite work transfer is necessary to pump entropy at zero thermodynamic temperature. For typical household refrigerators, $T_L \sim$ 250 K and $T_H \sim$ 350 K. Then the value of the coefficient of performance of a reversible household refrigerator is $COP_{reversible} \sim 2.5$. Practical refrigerator designs such as those described in Chapter 15 have values of $COP \sim 2$. Air conditioning units which typically operate over a much narrower range of temperatures ($T_L \sim$ 280 K and $T_H \sim$ 350 K) have values of $COP_{reversible} \sim$ 4 with practical values of $COP \sim 3$.

For heat pumps, which are finding increasing use for domestic heating in certain parts of the U.S., particularly in the South and Southwest, the appropriate performance parameter is also known as the coefficient of performance, COP_{HP}, but is defined differently from equation (7.33). Thus,

$$COP_{HP} = \frac{\text{heating effect/cycle}}{\text{net work transfer/cycle}} = \frac{Q_H}{\oint \delta W} = \frac{Q_H}{Q_H + Q_L} \tag{7.38}$$

Substituting equation (7.26) into equation (7.38), we obtain for the reversible heat pump

$$(COP_{HP})_{reversible} = \frac{1}{1 - \frac{T_L}{T_H}} \tag{7.39}$$

Depending upon the application, heat pump designs vary widely in detail. Although they are basically refrigerators being used for heating or cooling a living space, they use different parts of the environment for the low temperature heat reservoir. Some designs use atmospheric air while some others use ground water such as a lake or a well. More recently, a design known as a geothermal heat pump uses the earth itself as the low temperature heat reservoir. Performance varies considerably depending upon the design, but the geothermal design which is now strongly recommended by the U.S. Department of Energy has values of $COP_{HP} \sim 15$ when used for cooling a space and $COP \sim 3.5$ when used for heating a space.

Example 7E.4: The California Energy Commission operates an Appliance Certification Program that maintains a database on the performance of a wide variety of appliances. These databases are available to the public so that they might make "energy intelligent" decisions in the purchase of appliances. A particular heat pump product of the "water source" design has the following performance characteristics with the water source at the temperature 70 F (294.6 K):

$$\dot{Q}_H = -10^5 \text{ Btu/hr}$$

$$COP = 4.5$$

(a) Estimate the work transfer rate necessary to operate this heat pump.

(b) Estimate the value of *COP* if the "water source" is at the temperature 50 F (284.4 K).

(c) Estimate the work transfer rate necessary to operate the heat pump with this new "water source" temperature and the same high temperature heat transfer rate.

Solution: (a) Since 1 Btu/hr = 0.2929 Watts,

$$\dot{Q}_H = \left(-10^5 \text{ Btu/hr}\right)\left(0.2929 \text{ W/Btu/hr}\right) = -29.29 \text{ kW}$$

From the definition of the *COP*

$$\oint \delta W = \frac{\dot{Q}_H}{COP} = \frac{-29.29 \text{ kW}}{4.5} = -6.51 \text{ kW}$$

where the negative sign indicates the work transfer is into the heat pump cycle. The test data supplied by the California Energy Commission reports $W = -6511$ W.

(b) The *COP* should scale in a manner similar to the $COP_{reversible}$ if the source temperature is changed. Then

$$(COP)_{new} = (COP)_{old}\left(\frac{T_H}{T_H - (T_L)_{new}}\right)\left(\frac{T_H - (T_L)_{old}}{T_H}\right)$$

The equivalent temperature of the high temperature heat reservoir can be estimated for the purposes of this analysis by assuming that the heat pump operates in a reversible manner. Then from equation (7.39)

$$T_H = \frac{T_L (COP)_{reversible}}{(COP)_{reversible} - 1} = \frac{(294.6 \text{ K})4.5}{4.5 - 1} = 378.77 \text{ K}$$

Then

$$(COP)_{new} = 4.5\frac{378.77 \text{ K} - 294.6 \text{ K}}{378.77 \text{ K} - 284.4 \text{ K}} = 4.0$$

(c) Using this new value for the *COP*, we obtain

$$\oint \delta W = \frac{\dot{Q}_H}{(COP)_{new}} = \frac{-29.29 \text{ kW}}{4.0} = -7.32 \text{ kW}$$

In practice, the scaling of the *COP* would not be quite so simple because of a variety of changes in the details of the heat pump cycle dictated by the use of a lower temperature source, but the method shown above does provide a "quick" estimate of what we would expect to find with a more detailed analysis using the methods to be presented in Chapter 15.

7.5 Entropy as a Measure of the "Quality" of Heat Transfer

As we have already seen, the property entropy has many macroscopic physical interpretations that help us understand the behavior of thermal-fluid systems. Each of these interpretations is valid in general, but, typically, each one adds insight in some specific aspect of thermal-fluid system behavior. In Chapter 5, for example, we saw that we could view the entropy as a measure of dissipation. In the present context, we have seen how the entropy provides an explanation of the way in which a reversible heat engine cycle such as the Carnot cycle operates.

In effect, the reversible heat engine cycle is nothing more than an "entropy pump" that transfers entropy from a high temperature heat reservoir to a low temperature heat reservoir. In the process of this entropy transfer, a net positive work transfer results, hence the name "heat engine cycle." Upon closer examination, we find that for a given magnitude of heat transfer from the high temperature heat reservoir, the more entropy that is transported along with it, the less value that heat transfer has for energy conversion. The temperature of the heat reservoir is just as important as the energy of the heat transfer. In short, in comparing two heat transfer interactions for utilization in heat engines, it is necessary to know both the energy transfer and the associated entropy transfer. Two heat transfer interactions that transfer the same amount of energy are not necessarily equal unless their entropy transfers are equal as well.

To illustrate this fact, let us consider two reversible heat engines operating between two heat reservoirs. The first heat engine experiences a heat transfer Q_H with one heat reservoir at the temperature $(T_H)_1$ and another heat transfer $(Q_L)_1$ with a second heat reservoir at the temperature T_L. The second heat engine also experiences heat transfer Q_H with one heat reservoir at the temperature $(T_H)_2$ where $(T_H)_1 > (T_H)_2$ and another heat transfer $(Q_L)_2$ with a second heat reservoir at the temperature T_L.

For the first heat engine, the first law gives

$$\oint \delta W = \oint \delta Q \tag{7.40}$$

or

$$W_1 = Q_H + (Q_L)_1 \tag{7.41}$$

and the second law gives

$$\oint dS = \oint \delta S_{gen} + \oint \frac{\delta Q}{T} = 0 \tag{7.42}$$

since the entropy is a property. Since the heat engine is reversible, $\oint \delta S_{gen} = 0$. Then,

$$\frac{Q_H}{(T_H)_1} + \frac{(Q_L)_1}{T_L} \tag{7.43}$$

For the second reversible heat engine, we get similar results from the application of the first and second laws, viz.

$$W_2 = Q_H + (Q_L)_2 \tag{7.44}$$

and

$$\frac{Q_H}{(T_H)_2} + \frac{(Q_L)_2}{T_L} = 0 \tag{7.45}$$

Subtracting equation (7.44) from equation (7.41), we get

$$W_1 - W_2 = (Q_L)_1 - (Q_L)_2 \tag{7.46}$$

Equations (7.43) and (7.45) can be solved simultaneously for the expression on the right-hand-side of equation (7.46), viz.

$$(Q_L)_1 - (Q_L)_2 = \frac{Q_H T_L}{(T_H)_1} - \frac{Q_H T_L}{(T_H)_2} \tag{7.47}$$

Then the difference in net work transfer from these two reversible heat engines becomes

$$W_1 - W_2 = Q_H T_L \left[\frac{(T_H)_1 - (T_H)_2}{(T_H)_1 (T_H)_2} \right] \tag{7.48}$$

Since $(T_H)_1 > (T_H)_2$ and $Q_H > 0$, it follows that $W_1 > W_2$.

This important result is due to the fact that reversible heat engines "pump" entropy from a high temperature reservoir to a low temperature reservoir. Since the entropy transferred from the high temperature heat reservoir was less for the first heat engine than for the second heat engine even though the energy transfer was the same in both cases, the entropy transferred to the low

temperature heat reservoir was also less for the first engine than for the second. Since the temperature of the low temperature heat reservoir was the same in both cases, the heat transfer with the low temperature heat reservoir was less for the first heat engine than for the second. Then the first law requires that the net heat transfer, and hence the net work transfer, for the first engine must be greater than for the second. Thus we are led to the following interpretation for the entropy:

> The energy transferred in the form of a heat transfer from a higher temperature source has a higher "quality" (greater value for energy conversion purposes) than the energy transferred as a heat transfer from a lower temperature source because it carries less entropy.

Thus, we can say that the entropy is a measure of the quality of heat transfer. This result is depicted graphically in Figure 7.4.

Notice in Figure 7.4 that for the two heat engines, the flows of energy from the high temperature heat reservoirs are the same, but the entropy flows are not. For the heat engine using the high temperature heat reservoir with the lower temperature, $(T_H)_2$, the entropy flow is greater. Then to transfer this greater entropy to the low temperature heat reservoir, which is identical in the two cases, more energy is required. Thus there is less energy available to flow to the environment in the form of a work transfer.

7.5 The Effect of Irreversibilty on the Performance of Heat Engines and Heat Pumps

In all of the cases discussed in this chapter thus far, the systems operated in such a way that all processes involved were reversible. However, in engineering practice, nearly all systems generate entropy by virtue of their irreversible nature. For the case of an irreversible system operating in a cycle while in thermal communication with two heat reservoirs, the second law shows that the entropy generated will cause the net work transfer for the cycle to be less than the net work transfer for a reversible cycle interacting with the same heat reservoirs.

For any cycle of a system interacting with two heat reservoirs, the second law takes the form

$$\oint dS = \oint \delta S_{transfer} + \oint \delta S_{gen} = \frac{Q_H}{T_H} + \frac{Q_L}{T_L} + \oint \delta S_{gen} \tag{7.49}$$

Then if the heat transfer with the high temperature reservoir is fixed, we can solve equation (7.49) for the heat transfer with the low temperature heat reservoir in the irreversible case. Thus,

$$(Q_L)_{irreversible} = -Q_H \frac{T_L}{T_H} - T_L \oint \delta S_{gen} \tag{7.50}$$

Since the heat transfer with the low temperature heat reservoir is negative for the heat engine, equation (7.50) shows that the magnitude of this heat transfer will increase in the irreversible case due to the entropy generated in the cycle. From the first law, we have for the net work transfer for the irreversible cycle

$$\oint \delta W = \oint \delta Q = Q_H + Q_L \tag{7.51}$$

Substituting equation (7.50) into equation (7.51), we get

$$\oint (\delta W)_{irreversible} = Q_H \left(1 - \frac{T_L}{T_H}\right) - T_L \oint \delta S_{gen} \tag{7.52}$$

According to equation (7.23), the first term on the right-hand side of equation (7.52) is the work transfer for a reversible cycle operating between the same two heat reservoirs. Then equation

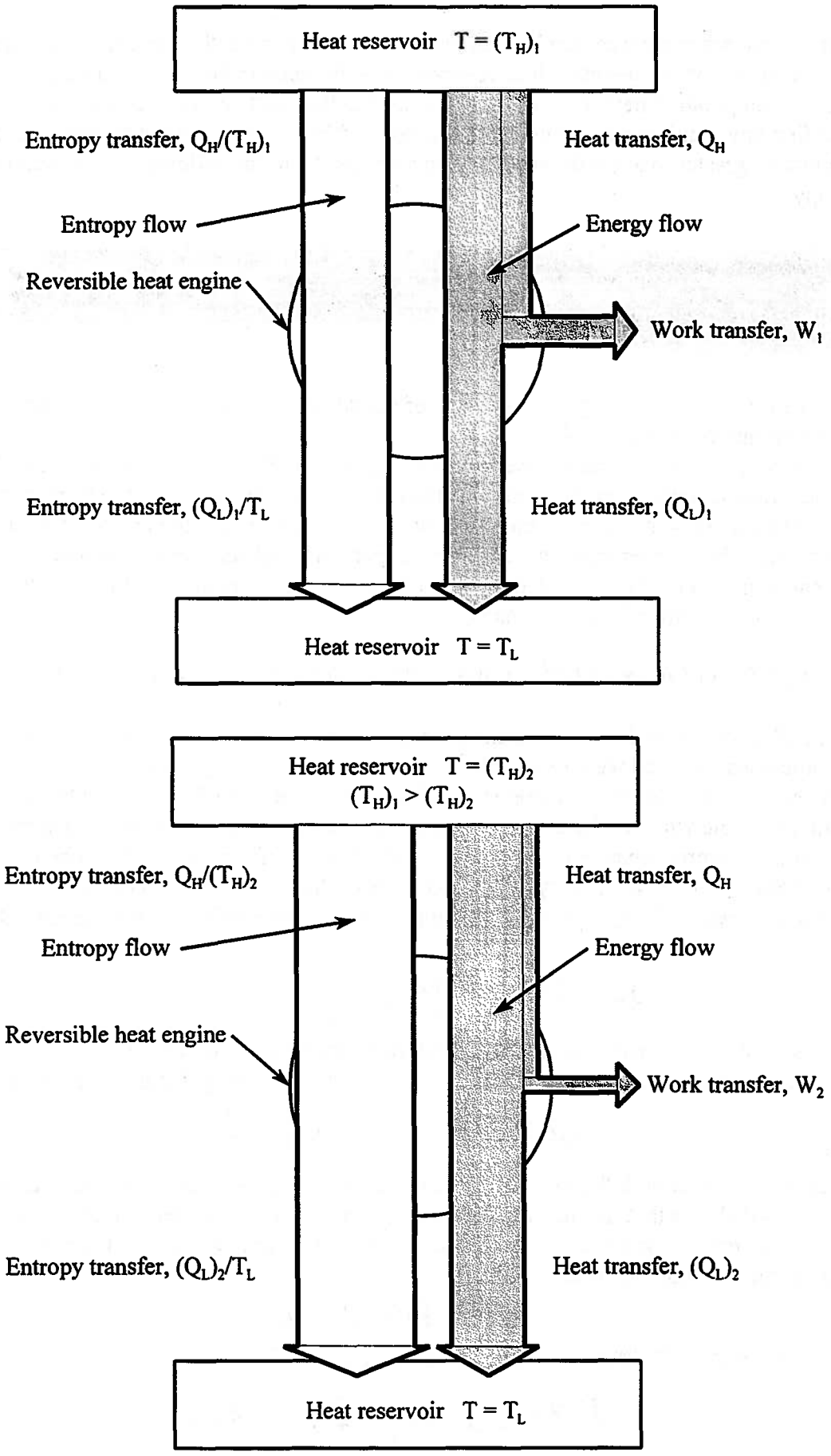

Figure 7.4 Energy and Entropy Flows for Reversible Heat Engines with Different High Temperature Heat Reservoirs

(7.52) becomes

$$\oint(\delta W)_{reversible} - \oint(\delta W)_{irreversible} = T_L \oint \delta S_{gen} \tag{7.53}$$

Since $T_L > 0$ and $S_{gen} > 0$, the effect of the irreversibilities in the cycle is to reduce the work transfer. Equation (7.53) shows clearly the influence of the entropy generation on the degradation of performance as a result of irreversibilities. One convenient way to think of this result is that some of the positive work transfer of the irreversible heat engine was internally "dissipated" to generate the entropy associated with the irreversibilities. This result is shown graphically in Figure 7.5.

Notice in Figure 7.5 that the entropy flow from the high temperature heat reservoir into the cycle is the same for both the reversible and the irreversible cycles. However, the entropy flow out of the irreversible is greater than that for the reversible cycle since some entropy was generated inside the irreversible cycle. Since entropy is a property, there can be no net change in the entropy of the cycle. Then the entropy flow out of the irreversible cycle must be the sum of the entropy flow in and the entropy generated. This increased flow of entropy requires an increased flow of energy to the low temperature heat reservoir which is identical in both the reversible and irreversible cycles. As a result, there is less energy that can flow from the cycle to the environment in the form of a work transfer in the irreversible cycle.

If we divide equation (7.52) through by the high temperature heat transfer, we have

$$\eta_{irreversible} = \frac{\oint(\delta W)_{irreversible}}{Q_H} = \left(1 - \frac{T_L}{T_H}\right) - \frac{T_L}{Q_H}\oint \delta S_{gen} \tag{7.54}$$

However, the first term on the right-hand side of equation (7.54) is the energy conversion efficiency for a reversible cycle. Then

$$\eta_{irreversible} = \eta_{reversible} - \frac{T_L}{Q_H}\oint \delta S_{gen} \tag{7.55}$$

Since $T_L > 0$, $Q_H > 0$, and $S_{gen} > 0$, it follows that another effect of the irreversibilities in the heat engine cycle is to reduce the energy conversion efficiency below that of the reversible cycle by an amount proportional to the entropy generated. The greater the amount of entropy generated, the greater will be the reduction. These irreversibilities are primarily due to heat transfer down a temperature gradient and viscous dissipation at various locations in the cycle.

In the case of the refrigeration cycle, the irreversibilities have a similar effect on the cycle. From the second law, equation (7.49), we have

$$(Q_H)_{irreversible} = -Q_L \frac{T_H}{T_L} - T_H \oint \delta S_{gen} \tag{7.56}$$

The first law for the refrigeration cycle is

$$\oint \delta W = \oint \delta Q = Q_H + Q_L \tag{7.57}$$

Substituting equation (7.56) into equation (7.57), we get

$$\oint(\delta W)_{irreversible} = Q_L\left(1 - \frac{T_H}{T_L}\right) - T_H \oint \delta S_{gen} \tag{7.58}$$

The first term on the right-hand side of equation (7.58) is the work transfer for a reversible refrigeration cycle. Then equation (7.58) can be written

$$\oint(\delta W)_{irreversible} = \oint(\delta W)_{reversible} - T_H \oint \delta S_{gen} < 0 \tag{7.59}$$

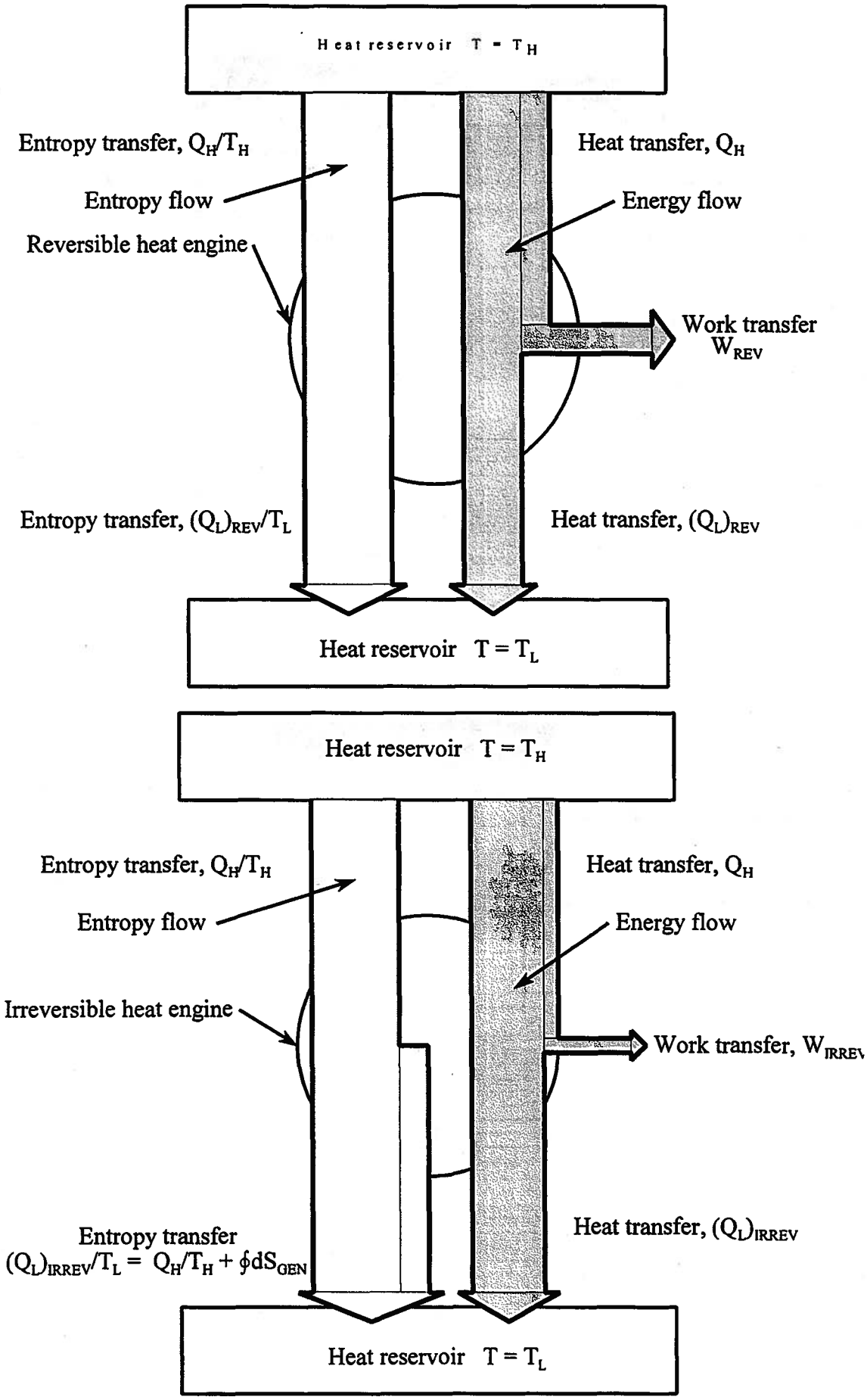

Figure 7.5 Effect of Entropy Generation on Energy and Entropy Flows in a Heat Engine

Since $\oint(\delta W)_{reversible} < 0$, $T_H > 0$, and $S_{gen} > 0$, it follows that

$$\left|\oint(\delta W)_{irreversible}\right| > \left|\oint(\delta W)_{reversible}\right| \tag{7.60}$$

Thus the effect of the irreversibilities in the refrigeration cycle is to increase the work transfer required to operate the cycle. The more entropy that is generated in the cycle, the greater the magnitude of the work transfer required to operate the cycle. Similarly, dividing equation (7.56) through by Q_L, we get

$$\frac{(Q_H)_{irreversible}}{Q_L} = -\frac{T_H}{T_L} - \frac{T_H}{Q_L}\oint \delta S_{gen} \tag{7.61}$$

Substituting equation (7.61) into equation (7.35), we obtain

$$(COP)_{irreversible} = \frac{1}{\frac{T_H}{T_L} - 1 + \frac{T_H}{Q_L}\oint \delta S_{gen}} \tag{7.62}$$

Since $T_H > 0$, $Q_L > 0$, and $S_{gen} > 0$, it follows that

$$(COP)_{irreversible} < (COP)_{reversible} \tag{7.63}$$

Thus, another effect of the irreversibilities in the refrigeration cycle is to reduce the *COP* of the cycle.

Example 7E.5: A new power plant design known as a combined cycle design utilizes a combination of two cycles, a Rankine cycle and a Brayton cycle, to convert a high temperature heat transfer into a work transfer. This design provides the highest energy conversion efficiency available at the time of this writing. A plant currently under construction claims an energy conversion efficiency of $\eta = 0.60$ with a high temperature heat reservoir with an effective temperature of $T_H = 1703$ K. The plant is to produce a net work transfer of 500 MW with a low temperature heat reservoir with $T_L = 300$ K. Determine the rate of entropy generation from this plant.

Solution: The high temperature heat transfer for the plant is given by the definition of the energy conversion efficiency.

$$\dot{Q}_H = \frac{\oint(\delta W)_{irreversible}}{\eta} = \frac{500 \text{ MW}}{0.60} = 833.33 \text{ MW}$$

If the cycle had been reversible, the power output from the cycle would have been

$$\oint(\delta W)_{reversible} = \dot{Q}_H\left(1 - \frac{T_L}{T_H}\right) = (833.33 \text{ MW})\left(1 - \frac{300 \text{ K}}{1703 \text{ K}}\right) = 686.53 \text{ MW}$$

The rate of entropy generation can be determined from equation (7.53). Thus

$$\dot{S}_{gen} = \frac{\oint(\delta W)_{reversible} - \oint(\delta W)_{irreversible}}{T_H} = \frac{686.53 \text{ MW} - 500 \text{ MW}}{1703} = 1.0953 \text{ x } 10^5 \text{ W/K}$$

This is a sizable amount of entropy generation and is probably rooted in the heat transfer processes between the working fluid in the Brayton cycle and the energy source. In Chapter 15 we will explore this in some depth.

7.6 The Stirling Cycle: A Heat Engine Cycle Using a Coupled Fluid in Thermal Communication with Two Heat Reservoirs

Thus far, the focus of this chapter has been the conversion of energy from thermal sources into net positive work transfer via cyclic devices that we called heat engines. We also saw that it was possible conceptually to run these heat engines in reverse to produce a refrigeration effect. Most of our discussion has been rather abstract, discussing the performance of these devices in terms of entropy and energy transfers in closed cycles. The only specific cycle that we discussed at any length was the Carnot cycle, and we showed that to be an impractical cycle in Appendix 7A . In this section, we attempt to synthesize the abstract concepts we have introduced heretofore and apply them to a "real world" practical example, the Stirling cycle. Our choice of the Stirling cycle as an example is based on two considerations. First, the Stirling cycle is easily modeled using the methodology already developed. There are other cycles that are perhaps technologically more important, such as the Rankine cycle and the vapor compression refrigeration cycle, but they require developments that we have not yet introduced. The second reason is that the Stirling cycle is used in practical systems, and we shall discuss a few of these at the end of this section.

Historically, the Stirling engine predates the Carnot heat engine concept, but the science of thermodynamics was not sufficiently mature at the time to interpret the performance of the device properly nor to appreciate fully its implications for heat engine design. The engine that now bears his name was invented in 1816 by Robert Stirling (1790 – 1878), a Scottish minister whose grandfather, Michael, was a pioneer in the development of the threshing machine. However, it was not until 1850 that the simple and elegant dynamics of the engine were first explained by the inventor of the Rankine cycle, Professor William John McQuorn Rankine (1820 – 1872) of the University of Glasgow.

Our approach here is to consider an ideal Stirling cycle from the perspective of the thermodynamic models we have developed earlier. Our analysis will support the previous, very general discussion the entropy and energy flow through a reversible cyclic device. We shall follow this with a more realistic, but still highly idealized, irreversible Stirling cycle model. We shall then turn to still more realistic embodiments of the Stirling cycle using dual pistons or a piston-displacer arrangement. Finally, we shall take up several examples of practical Stirling machines.

7.6.1 Basic Concepts of the Stirling Engine Cycle

The Stirling engine uses a working fluid that can be modeled as an ideal gas. Like the Carnot cycle heat engine, the Stirling cycle heat engine experiences a net positive work transfer by interacting with two heat reservoirs in a cycle comprised of four separate processes. As shown in the *T-V* and *P-V* diagrams of Figure 7.6, the Stirling cycle engine consists of an isothermal expansion of the gas at the temperature T_H while in thermal communication with the high temperature heat reservoir (process 1 to 2); an isochoric (constant volume) heat transfer process to reduce the temperature of the gas to the low temperature T_L (process 2 to 3); an isothermal compression at the temperature T_L while in thermal communication with the low temperature heat reservoir (process 3 to 4); and an isochoric heat transfer process to increase the temperature of the gas back to its original high temperature T_H (process 4 to 1).

Conceptually, the Stirling cycle is very similar to the Carnot cycle shown in Figure 7.1 except that the locations of the mechanical matching elements are somewhat more complex in that the thermal matching element also includes a mechanical matching element. In the present case, it is a bit clearer if we construct a gedanken experiment that will demonstrate the Stirling

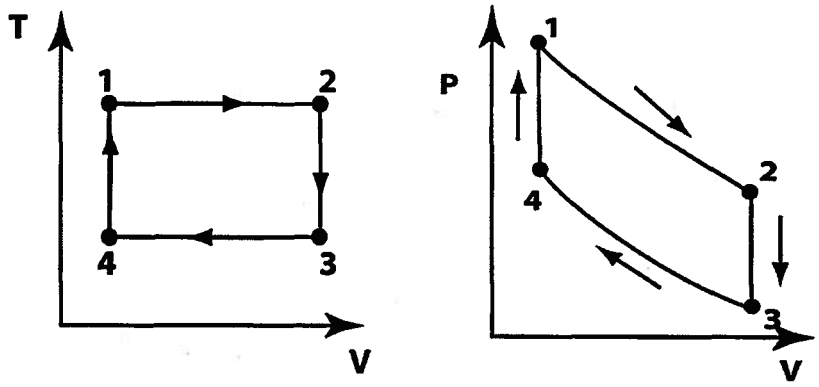

Figure 7.6 Thermodynamic States for the Stirling Cycle Heat Engine

cycle using the elements shown in Figure 7.7. The thermal energy that will be converted to a useful work transfer is drawn, along with its associated entropy, from a high temperature reservoir at temperature T_H, and the same amount of entropy is rejected to a low temperature reservoir at temperature T_L. The ideal gas that will experience the Stirling cycle is contained in the piston/cylinder apparatus labeled "power producing element" (PPE) to distinguish it from the mechanical matching element contained in the thermal matching element. It is the PPE that will produce net positive power after the cycle has been fully executed. The other piston/cylinder apparatus labeled "thermal matching element" (TME) is used to change the temperature of the ideal gas in the power producing element from T_H to T_L and back again. We will assume for the sake of simplicity that the walls of both piston/cylinders have zero heat capacity. We will also assume that the gas in the thermal matching element and the power producing element are initially at the temperature of the high temperature reservoir, T_H.

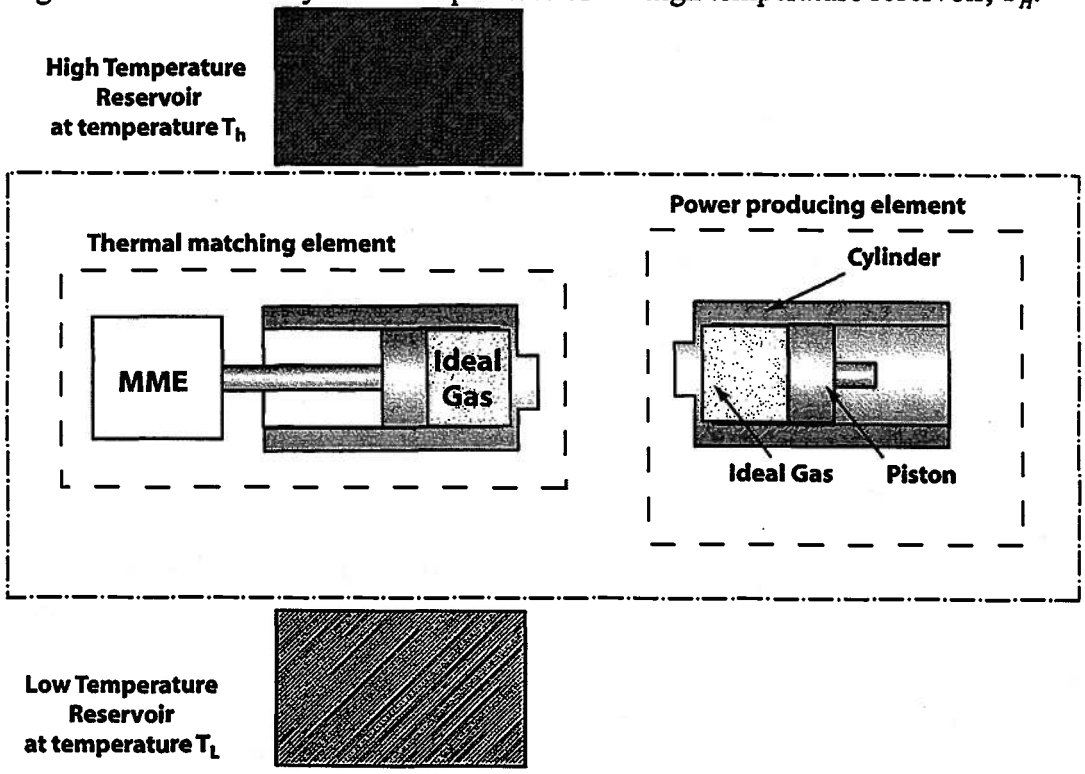

Figure 7.7 Basic Elements of the Stirling Cycle

(The energy source for the cycle is the high temperature heat reservoir. The work output of the cycle comes from the piston cylinder labeled as the "power producing element" (PPE). The thermal matching element (TME) is used to change the temperature of the ideal gas in the PPE from T_H to T_L and back again.)

The Stirling cycle is executed by the gas in the PPE using the procedure depicted in Figure 7.8. In state 1 the ideal gas in the PPE is at temperature $T_1 = T_H$ and has volume V_1. The

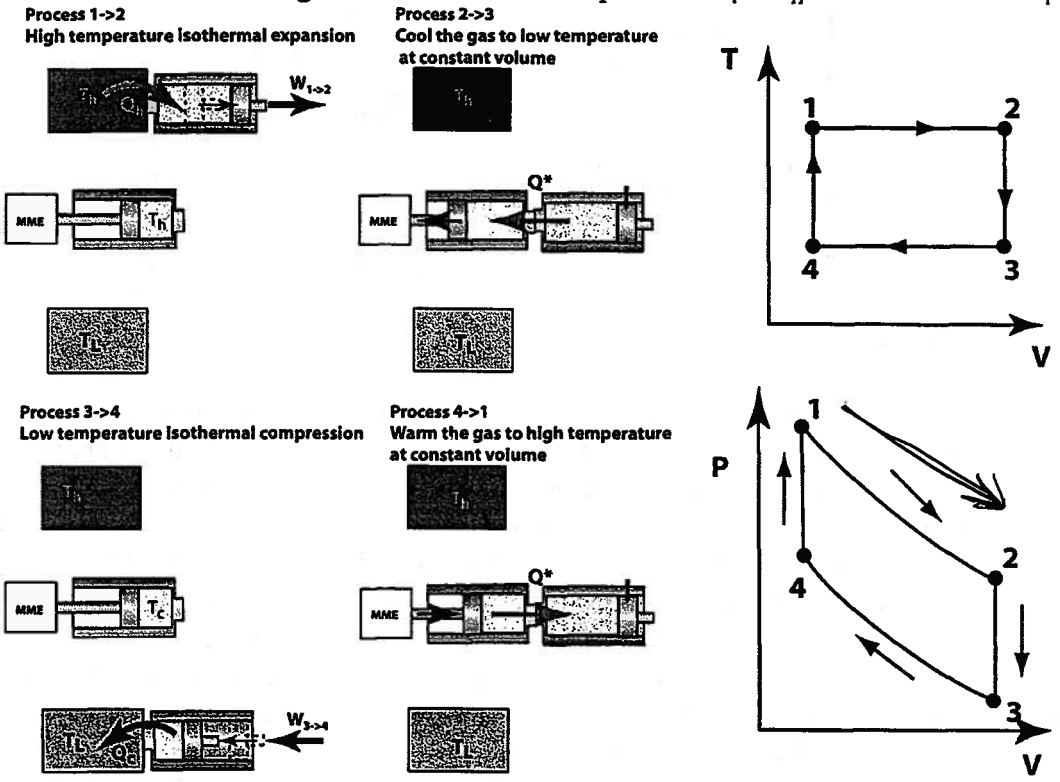

Figure 7.8 The Four Component Processes of the Stirling Cycle

PPE is brought into thermal contact with the high temperature reservoir. The gas is then slowly expanded so that it remains in thermal equilibrium with the high temperature reservoir throughout the process until the volume of the gas is V_2 with $T_2 = T_H$ (state 2). This means that the process from state 1 to state 2 is reversible. In this reversible isothermal expansion process, the gas in the PPE experiences a positive work transfer, $W_{1\text{-}2} > 0$, with the environment. The PPE is then thermally disconnected from the high temperature reservoir and its piston is locked in place. The gas in the PPE is now brought into thermal contact with the TME. Since the gases in these devices are both at temperature T_H, there is no heat transfer upon contact between the two systems. The mechanical matching element in the TME now slowly begins to expand the gas in the TME while maintaining thermal equilibrium with the gas in the PPE. Since the gases in the TME and the PPE are in thermal equilibrium throughout the process, the gas in the PPE experiences a reversible negative heat transfer, $Q_{2\text{-}3} < 0$, at constant volume$V_2 = V_3$. The expansion process of the gas in the TME, which is reversible by virtue of the continuous thermal equilibrium between the two gas systems, continues until the mutual equilibrium temperature of the gases in the TME and the PPE reaches the temperature of the low temperature heat reservoir T_L. The gas in the PPE is now in state 3 with $T_3 = T_L$. The PPE is now thermally isolated from the TME and put in thermal contact with the low temperature heat reservoir. The gas in the PPE is now slowly compressed so that it remains in thermal equilibrium with the low temperature heat reservoir throughout the process until the volume of the gas is restored to volume $V_4 = V_1$ (state 4). In this process from state 3 to state 4, which is also reversible, the gas in the PPE

experiences a negative work transfer with the environment, $W_{3\text{-}4} < 0$. With the piston of the PPE once again locked in place, the gas in the PPE is now returned back to state 1, $V_4 = V_1$, by bringing it into thermal communication with the gas in the TME and allowing the MME to slowly, and reversibly, recompress the gas in the TME until the temperature of both gases returns to T_H. The gas in the PPE has now experienced a reversible positive heat transfer, $Q_{3\text{-}4} > 0$, at constant volume$V_4 = V_1$.

In the process 1 → 2, the gas within the PPE experienced a positive work transfer with the environment by virtue of the displacement of the piston and a simultaneous negative heat transfer with the high temperature reservoir. The work transfer for the gas in this process is easily calculated,

$$W_{1\text{-}2} = \int_1^2 P\,dV = m_{PPE}RT_H \int_1^2 \frac{dV}{V} = m_{PPE}RT_H \ln\left(\frac{V_2}{V_1}\right) \tag{7.64}$$

where m_{PPE} is the mass of the gas in the PPE. Since the temperatures of the end states of process 1 → 2 are the same, the constitutive relation for the internal energy of the ideal gas shows that the internal energy of the gas is constant during this isothermal process. Then the first law for the gas as a system requires that the heat transfer to the gas is the same as the work transfer from the gas or

$$\begin{aligned} U_2 - U_1 &= Q_{1\text{-}2} - W_{1\text{-}2} \\ m_{PPE}c_v(T_2 - T_1) = 0 &= Q_{1\text{-}2} - W_{1\text{-}2} \\ Q_{1\text{-}2} = W_{1\text{-}2} &= m_{PPE}RT_H \ln\left(\frac{V_2}{V_1}\right) \end{aligned} \tag{7.65}$$

Similar arguments apply to the other isothermal compression process from state 3 to 4. Realizing that $V_1 = V_4$ and $V_2 = V_3$, we find that the heat and work transfers for process 3 to 4 are

$$Q_{3\text{-}4} = W_{3\text{-}4} = \int_3^4 P\,dV = m_{PPE}RT_L \int_3^4 dv = m_{PPE}RT_L \ln\left(\frac{V_4}{V_3}\right) = -m_{PPE}RT_c \ln\left(\frac{V_2}{V_1}\right) \tag{7.66}$$

The heat transfer for process 2 to 3, $Q_{2\text{-}3}$, can be calculated by noting that the gas in the PPE is held at constant volume. Under these conditions, $dV = 0$ so there is no work transfer for the reversible process 2 → 3 and the first law reduces to

$$Q_{2\text{-}3} = U_3 - U_2 = m_{PPE}c_v(T_3 - T_2) = -m_{PPE}c_v(T_H - T_L) \tag{7.67}$$

Similarly, from the first law the, heat transfer for the other constant volume process 4 → 1 is

$$Q_{4\text{-}1} = U_1 - U_4 = m_{PPE}c_v(T_1 - T_4) = m_{PPE}c_v(T_H - T_L) \tag{7.68}$$

The processes associated with the thermal matching element are presumed to be reversible by definition. The MME maintains mechanical equilibrium throughout the processes in the cycle and the heat transfers into and out of the TME are assumed to be slow enough so that no substantial temperature gradients appear within the gases or across the heat transfer surfaces of the TME. The change in the internal energy of the TME after the cycle has been executed can be calculated using the system boundary shown as a dotted line around the TME in Figure 7.7. The first law applied to that system is

$$\Delta U_{TME} = \sum Q - \sum W = Q_{2\text{-}3} + Q_{4\text{-}1} - 0 = m_{PPE}c_v(T_H - T_L) - m_{PPE}c_v(T_H - T_L) = 0 \tag{7.69}$$

Thus the internal energy of the TME is unaltered by the cycle. The entropy change of the TME after the cycle can be calculated using the second law and realizing that all the internal processes in the TME are reversible with no entropy generation. Then

$$\Delta S_{TME} = \oint \frac{\delta Q}{T} + S_{gen} = -\int_2^3 \frac{m_{PPE} c_v}{T} dT - \int_4^1 \frac{m_{PPE} c_v}{T} dT + 0 = \int_{T_L}^{T_H} \frac{m_{PPE} c_v}{T} dT - \int_{T_L}^{T_H} \frac{m_{PPE} c_v}{T} dT = 0 \quad (7.70)$$

Hence, there is no entropy change in the TME. Since the two thermodynamic properties (U and S) are unchanged over a cycle, we conclude then that the TME is in the same thermodynamic state at the end of the cycle as it was at the beginning of the cycle. The same conclusion holds for the PPE, since two thermodynamic properties (T and V) are unchanged over a cycle. We conclude that the thermodynamic state of the ideal gas in the PPE is the same at the end of the cycle as it was at the beginning of the cycle as it must be for any cycle.

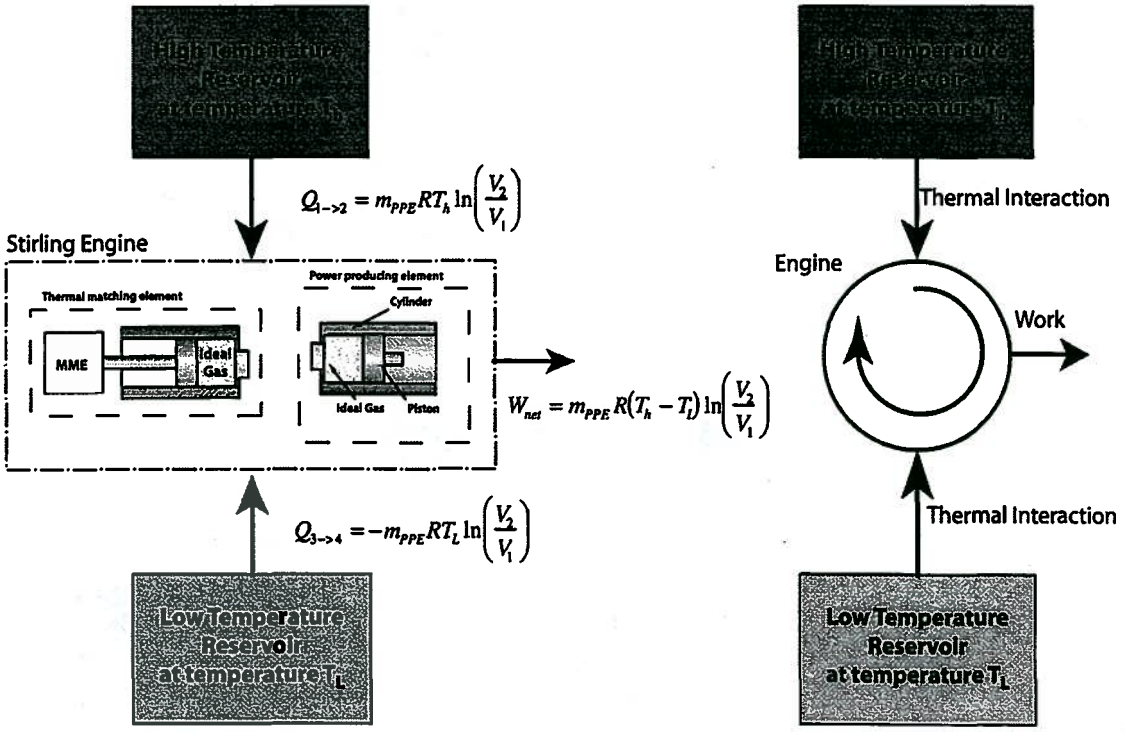

Figure 7.9 The Reversible Stirling Engine Apparatus and Its Symbolic Representation

As shown in Figure 7.9, we can identify the combined system of the TME and the PPE as an example of the generic engine described in Chapter 7. From the perspective of the Stirling engine, the net effect after one cycle is a positive heat transfer from the high temperature heat reservoir of magnitude

$$Q_H = m_{PPE} R T_H \ln\left(\frac{V_2}{V_1}\right) \quad (7.71)$$

and a negative heat transfer to the low temperature heat reservoir of

$$Q_L = -m_{PPE} R T_L \ln\left(\frac{V_2}{V_1}\right) \quad (7.72)$$

where the negative sign indicates the that the heat transfer is from the Stirling engine to the low temperature reservoir. According to equations (7.65) and (7.66), the net work transfer for the Stirling engine for the cycle is

$$\oint \delta W = W_{net} = W_{1-2} + W_{3-4} = m_{PPE} R (T_H - T_L) \ln\left(\frac{V_2}{V_1}\right) \tag{7.73}$$

For the Stirling engine as a system, the entropy transfer for the high temperature heat transfer interaction is

$$S_{trans,H} = \frac{Q_{1-2}}{T_H} = m_{PPE} R \ln\left(\frac{V_2}{V_1}\right) \tag{7.74}$$

and the entropy transfer for the low temperature heat transfer interaction is

$$S_{trans,L} = \frac{Q_{3-4}}{T_L} = -m_{PPE} R \ln\left(\frac{V_2}{V_1}\right) \tag{7.75}$$

From the second law for the cycle, we have that since the entropy is a property

$$\oint dS = \oint dS_{transfer} + \oint \delta S_{gen} = 0$$

$$\oint \delta S_{gen} = \oint dS_{transfer} = S_{trans,H} + S_{trans,L} = m_{PPE} R \ln\left(\frac{V_2}{V_1}\right) - m_{PPE} R \ln\left(\frac{V_2}{V_1}\right) \tag{7.76}$$

$$\oint \delta S_{gen} = 0$$

Thus the cycle is indeed reversible.

The energy conversion efficiency of the cycle is

$$\eta \equiv \frac{\oint \delta W}{Q_H} = \frac{m_{PPE} R (T_H - T_L) \ln\left(\frac{V_2}{V_1}\right)}{m_{PPE} R T_L \ln\left(\frac{V_2}{V_1}\right)} = \frac{(T_H - T_L)}{T_H} = 1 - \frac{T_L}{T_H} \tag{7.77}$$

This is precisely the same value as the Carnot efficiency given in equation (7.32). This is to be expected since the Stirling cycle is another example of a reversible cycle in thermal communication with two heat reservoirs.

As equation (7.76) shows, there is no entropy generated by the highly idealized Stirling cycle discussed here. We have already shown that the gases inside this control volume are in the same state at the beginning and end of the cycle, and the entropy transferred into the Stirling engine is the same as that transferred out. A pictorial representation of the energy and entropy flows associated with the Stirling cycle is shown in Figure 7.10. As shown in Section 7.5, the entropy transferred into the cycle from the high temperature reservoir flows directly through the cycle and out to the low temperature reservoir. The Stirling engine absorbs thermal energy (and entropy) from the high temperature heat reservoir, converts part of the energy to useful work, and discharges the remaining energy to the low temperature reservoir as thermal energy. In the case of reversible operation, all of the entropy absorbed from the high temperature heat reservoir is discharged to the low temperature heat reservoir.

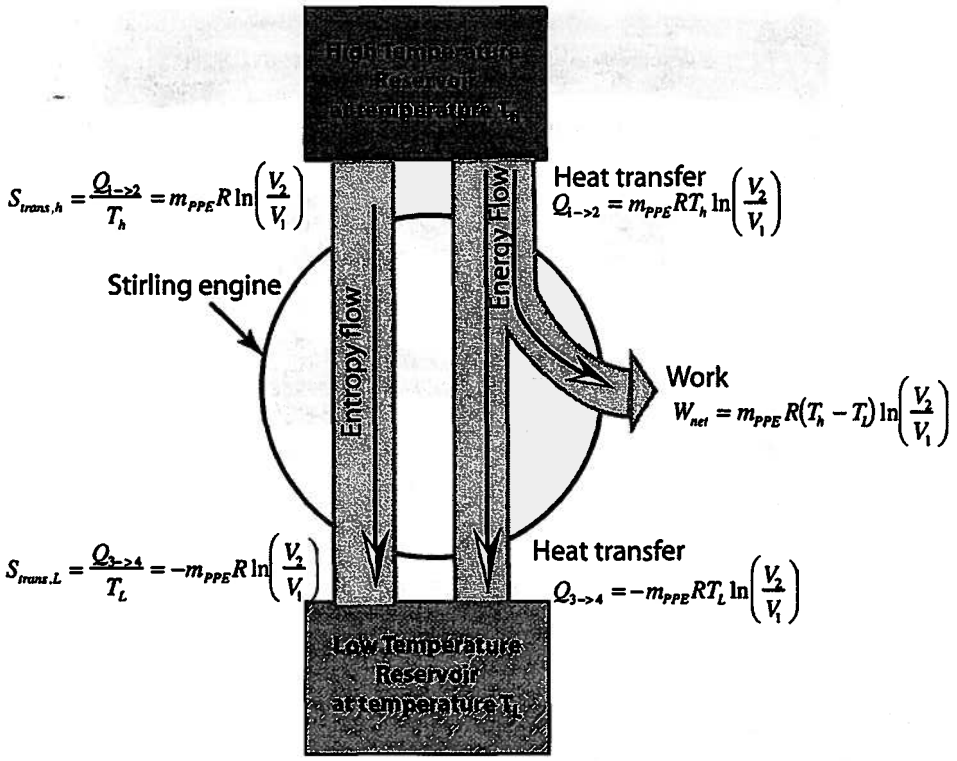

Figure 7.10 Energy and Entropy Flows for the Reversible Stirling Engine

Another model for the Stirling engine is shown in Figure 7.11. Here the thermal matching element is comprised of individual heat reservoirs whose temperatures span the range from T_H to T_L. If we assume that the temperatures of the reservoirs are uniformly spaced from T_L to T_H, the temperature difference between each of the reservoirs, ΔT, is related to the number of thermal matching element reservoirs, n, by the relation

$$\Delta T = \frac{T_H - T_L}{n+1} \tag{7.78}$$

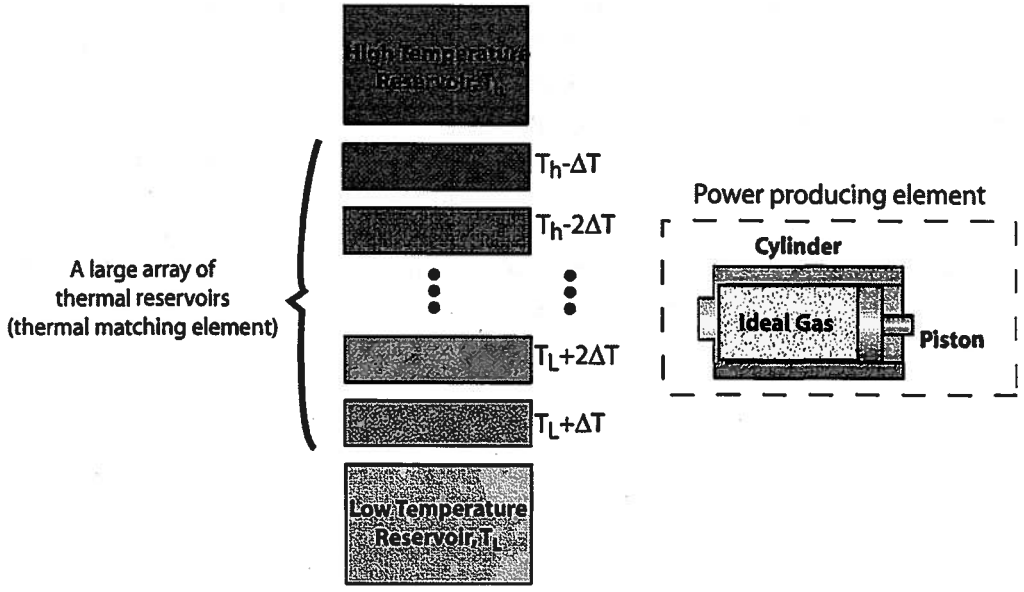

Figure 7.11 Basic Elements for a Stirling Engine Design

As before, the cycle begins by expanding the gas in the piston cylinder while the gas is in contact with the high temperature reservoir, process 1 → 2 in Figure 7.7. The gas is in good thermal contact with the high temperature reservoir and the expansion process is slow enough so that no temperature gradients appear within the gas or between the gas and the high temperature reservoir. Consequently, there is one (and only one) temperature in the gas so that the temperature of the gas versus the volume of the gas can be plotted on the *T-V* plot as shown in Figure 7.12 (process 1 → 2). The corresponding *P-V* plot is also shown in Figure 7.12. Following the end of the expansion process (state 2), the gas is cooled at constant volume to the temperature of the low temperature heat reservoir (state 3) by successively bringing the gas into thermal contact with a series of heat reservoirs. The pressure of the gas in state 3 is lower than the pressure in state 2. The gas is now isothermally compressed back to its original volume while in constant thermal equilibrium with the low temperature heat reservoir (state 4). Finally, the piston/cylinder apparatus is warmed back up at constant volume by successively bringing the gas into thermal communication with the same series of thermal reservoirs, but in the reverse order to that in process 2 → 3. The gas is now back in its original state and the process can be repeated.

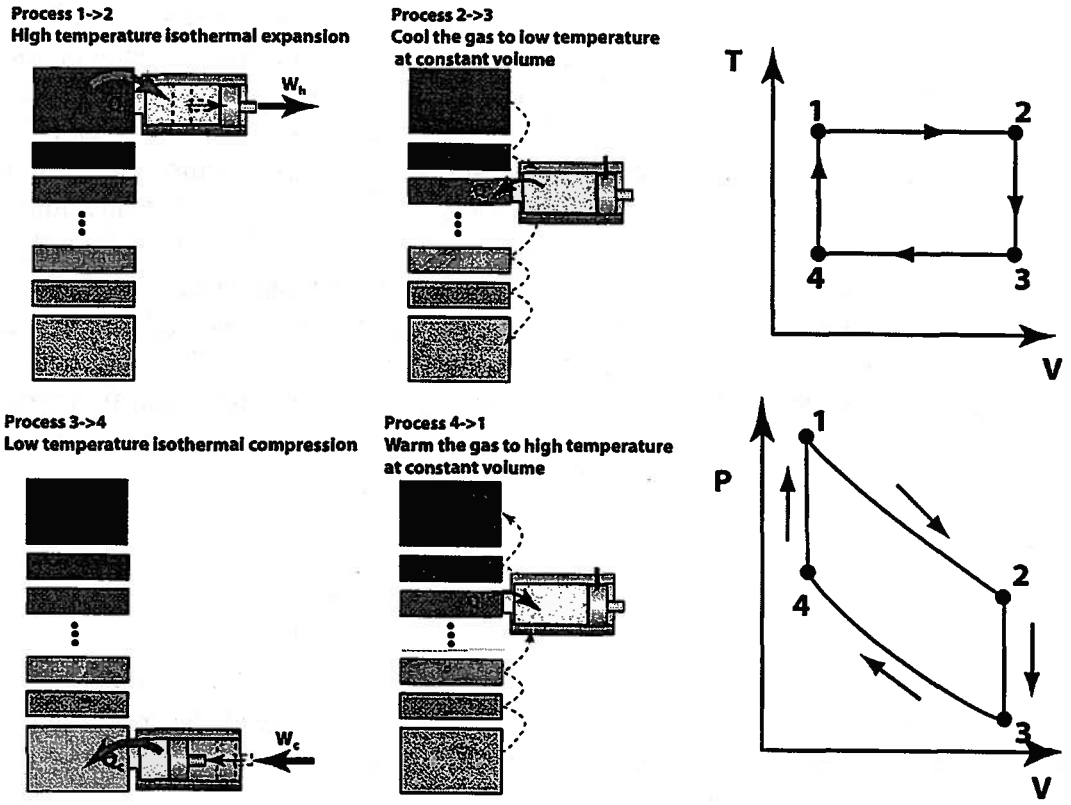

Figure 7.12 The Four Processes that Comprise the Stirling Engine Cycle

The expansion and compression processes have already been discussed at length. The work transfers experienced by the PPE as given by equations (7.64) and (7.66) are identical to the earlier model of the Stirling cycle. Consequently the net work transfer for this cycle is the same as the previous model given by equation (7.73). However, since the constant volume cooling and heating processes are a bit different from before, we need to insure that the

thermodynamic states of the TME heat reservoirs are unchanged after the cycle has been fully executed. To gain some insight into this aspect of the cycle, let us consider one of the TME heat reservoirs at a temperature T_i that has a value between T_H and T_L. In one cycle there are two thermal interactions with this heat reservoir. One of these interactions cools the PPE from $T_i + \Delta T$ to T_i and the other warms the PPE from $T_i - \Delta T$ to T_i. The corresponding heat transfers during these interactions are easily calculated. The heat transfer from the TME heat reservoir for the PPE cooling process is

$$Q_I = -\int_{T_i+\Delta T}^{T_i} m_{PPE} c_v dT = m_{PPE} c_v \Delta T \tag{7.79}$$

Similarly, the heat transfer into the TME heat reservoir for the PPE warming process is

$$Q_{II} = -\int_{T_i-\Delta T}^{T_i} m_{PPE} c_v dT = -m_{PPE} c_v \Delta T \tag{7.80}$$

The heat transfer interactions of the high and low temperature heat reservoirs are different from the previous model. The heat transfers during the expansion and compression processes are the same as before, but there is an additional heat transfer process due the slight temperature mismatch when the PPE is first brought into contact with each of the heat reservoirs. Let us consider the process when the PPE is first brought into contact with the low temperature reservoir. The temperature of the gas in the PPE is hotter than the low temperature reservoir ($T_L + \Delta T$ versus T_L) so that there is a heat transfer in the amount of $m_{PPE} c_v \Delta T$ from the PPE to the low temperature reservoir before the compression process begins. Similarly, when the PPE is first brought into contact with the high temperature reservoir, the temperature of the PPE is lower than the temperature of the high temperature reservoir ($T_H - \Delta T$ versus T_H). Consequently, there is a heat transfer of $m_{PPE} c_v \Delta T$ from the high temperature reservoir to the PPE before the expansion process begins. The total heat transfer from the high temperature reservoir to the PPE is the sum of the heat transfer required to bring the PPE to thermal equilibrium plus the subsequent heat transfer associated with the thermal expansion process,

$$Q_H = m_{PPE} c_v \Delta T + m_{PPE} R T_H \ln\left(\frac{V_2}{V_1}\right) \tag{7.81}$$

Similarly, for the low temperature heat reservoir, we have

$$Q_L = -\left[m_{PPE} c_v \Delta T + m_{PPE} R T_L \ln\left(\frac{V_2}{V_1}\right)\right] \tag{7.82}$$

For each cycle, the heat transfers to and from the high temperature and low temperature heat reservoirs are larger than before while the net work transfer for the cycle has remained the same. The efficiency of this engine is lower than the reversible Stirling we discussed earlier. From equations (7.63), (7.78), and (7.81), the efficiency for this cycle is

$$\eta \equiv \frac{W}{Q_H} = \frac{m_{PPE} R (T_H - T_L) \ln\left(\frac{V_2}{V_1}\right)}{m_{PPE} R T_H \ln\left(\frac{V_2}{V_1}\right) + m_{PPE} c_v \Delta T} = \left(1 - \frac{T_L}{T_H}\right)\left[1 + \frac{c_v \Delta T}{(n+1) R T_H \ln\left(\frac{V_2}{V_1}\right)}\right]^{-1}$$

$$\eta = \left(1 - \frac{T_L}{T_H}\right)\left[1 + \left(1 - \frac{T_L}{T_H}\right)\frac{c_v}{(n+1)R\ln\left(\frac{V_2}{V_1}\right)}\right]^{-1} \tag{7.83}$$

The lower efficiency for this configuration is due to the irreversibilities associated with heat transfer across a finite temperature difference. Note that when ΔT approaches zero (or the number of TME reservoirs, n, approaches infinity) the efficiency approaches that of the reversible engine, namely $\eta_{rev} = (1 - T_L/T_H)$.

7.6.2 The Irreversible Stirling Cycle Engine

Suppose now that the cycle is irreversible due to some irreversible process internal to the cycle. Let us determine the amount of entropy generated by the irreversibility whatever it might be. If we define a system boundary that encloses both the PPE and the TME heat reservoirs, there are only two heat transfers, one from the high temperature reservoir and the other with the low temperature reservoir. The entropy transfers from the high temperature heat reservoir can be calculated if we recognize that the temperature of the system boundary in contact with the reservoir is at T_H where the heat transfer occurs. The total entropy transfer from the high temperature heat reservoir is

$$S_{H,trans} = \frac{Q_H}{T_H} = \frac{m_{PPE}RT_H\ln\left(\frac{V_2}{V_1}\right) + m_{PPE}c_v\Delta T}{T_H} \tag{7.84}$$

Similarly, the entropy transfer associated with the low temperature heat reservoir is

$$S_{L,trans} = \frac{Q_L}{T_L} = -\frac{m_{PPE}RT_L\ln\left(\frac{V_2}{V_1}\right) + m_{PPE}c_v\Delta T}{T_L} \tag{7.85}$$

Note that the entropy flow into the machine is smaller than the entropy flow out of this machine ($|S_{L,trans}| > |S_{H,trans}|$). The entropies of the components within the control volume are the same at the end of the cycle as they were at the beginning of the cycle. (All components within the control volume have been returned to the original thermodynamic state by the end of the cycle.) The entropy generation within the control volume can be calculated using the second law,

$$S_{gen} = S_{final} - S_{initial} - \sum S_{trans} = 0 - S_{H,trans} - S_{L,trans} = m_{PPE}c_v\Delta T\left(\frac{1}{T_L} - \frac{1}{T_H}\right) \tag{7.86}$$

Consistent with our findings with the efficiency, the entropy generation goes to zero as ΔT approaches zero. Since T_L is smaller than T_H and all the other quantities on the extreme right hand side of equation (7.86) are positive, the entropy generation is also positive, as expected. These entropy and energy flows for this cycle are presented graphically in Figure 7.13.

7.6.3 Practical Stirling Cycle Engine Designs

Now that we have established that the Stirling cycle can produce a positive net work transfer when operated between two heat reservoirs, it now remains for us to design a practical Stirling engine since neither of the previously discussed machines is practical. A version of a more practical Stirling engine utilizing a double piston configuration is shown in Figure 7.14. Here there are two piston/cylinders connected by an array of small diameter tubes. The left-hand

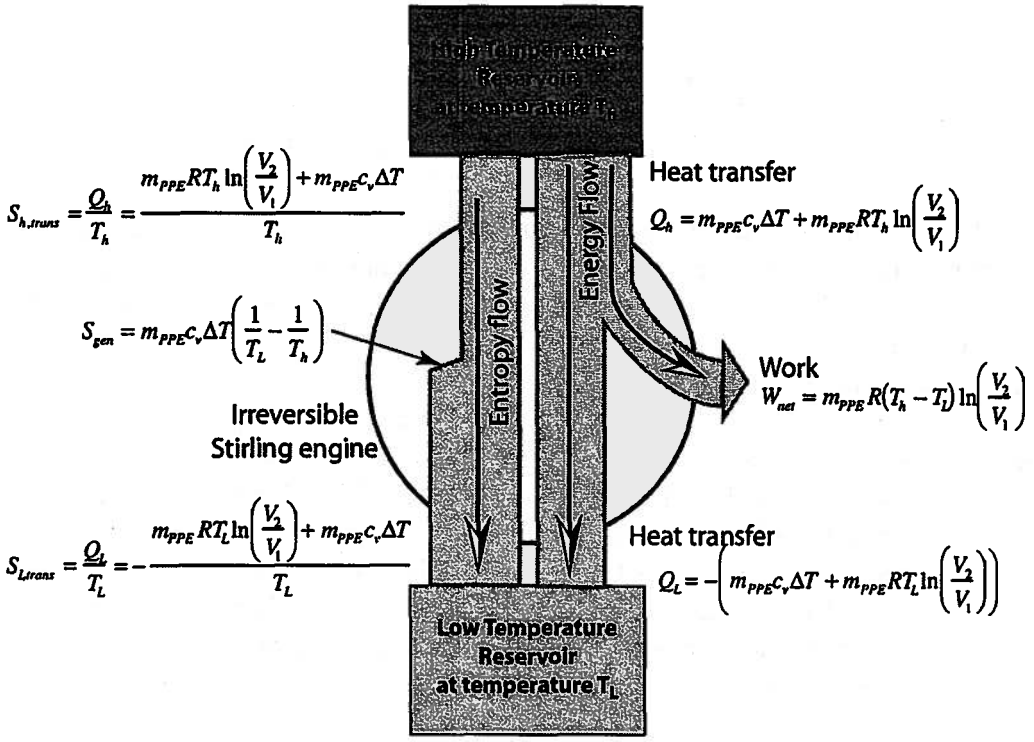

Figure 7.13 Energy and Entropy Flows for the Irreversible Stirling Engine

cylinder is always in thermal contact with the high temperature heat reservoir and the right-hand cylinder is always in thermal contact with the low temperature heat reservoir. The small diameter
tubes are in thermal contact with a large array of thermal capacitances at temperatures that are evenly distributed from T_H to T_L, the temperatures of the two heat reservoirs. This structure is referred to as the *regenerator*. We will assume that the thermal conduction along the length of the tubes is negligible and that the thermal contact between a fluid particle in one of the tubes and the local thermal capacitance is excellent. Let us also assume that the internal volume of the regenerator (the volume in the tubes) is negligible compared to the volume in the piston/cylinders.

The operation of the double piston Stirling engine starts with all the working fluid in the high temperature piston/cylinder. Recall that the regenerator volume is negligible. Then the gas is expanded isothermally while experiencing a positive heat transfer interaction Q_H with the high temperature heat reservoir (process 1 → 2). The work transfer associated with the expansion of the gas is absorbed and stored in a flywheel (not shown). In process 2 → 3, the high and low temperature pistons are now displaced in tandem so that the total internal volume in the Stirling engine remains constant while the gas flows from the high temperature piston through the regenerator to the low temperature piston. If the displacement is slow enough, the pressure of the gas in the low temperature piston is the same as that in the high temperature piston. Since the volumes swept by the high temperature and low temperature pistons are the same, the work transfer for the high temperature piston is equal in magnitude and opposite in sign to the work transfer experienced by the low temperature piston. (The magnitudes of the integrals of PdV are identical for the two pistons.) The net effect is that the gas experiences no net work transfer during the process 2 → 3. As the gas particles travel through the passages of the regenerator, they

see progressively cooler walls and, consequently, transfer energy and entropy to the walls. This process is reversible in the limit of an infinity of large thermal capacitances and good thermal contact between the gas particles and the walls. Ideally the gas emerges from the regenerator into the low temperature cylinder at the temperature of the low temperature heat reservoir, T_L. In state 3 the gas is entirely contained in the low temperature cylinder. Process 3 → 4 is an isothermal compression process in the low temperature cylinder. The gas in this cylinder experiences a negative heat transfer $-Q_L$ with the low temperature heat reservoir. Process 4 → 1 is another tandem piston displacement of the gas through the regenerator. The process is done at constant total internal volume. For the same reasons outlined earlier for process 2 → 3, there is no net work transfer in this process. The heat transfer from the solid surfaces in the regenerator to the gas warms the gas back up to temperature T_H and restores the regenerator to the same thermodynamic state it had prior to executing the cycle. The system is now ready to repeat the cycle.

It is worth noting that in this design of a practical Stirling engine, the regenerator is a thermal matching element. It is usually not constructed by running tubes through thermal capacitances as shown above, but rather the fluid is passed through an array of packed screens or metal shot inside a containing tube. In the case of the screens, the fluid passes through the holes and the thermal capacitance is provided by the material of the screen wire mesh. In the metal shot case, the flow is through the interstices between the balls of shot and the thermal capacitance is provided by the balls themselves.

We have shifted from using heat reservoirs in the previous analysis of the TME to a thermal capacitance in the regenerator. Heat reservoirs are idealizations of a thermal capacitance. (Recall that a heat reservoir is a pure thermal system with an infinitely large heat capacity.) In the practical world, the thermal capacitance need not be infinite but it does need to be "big enough". Practically speaking this is just a matter of making sure there are enough screens or balls of shot in the regenerator.

The expansion and compression processes in the actual Stirling engine are generally adiabatic. This is a consequence of the rather large dimensions inside the piston/cylinder and the rather short times taken for the compression and expansion processes in a practical machine. The heat transfers to and from the hot and cold heat reservoirs are achieved when the fluid is driven though a heat exchanger mounted on either side of the regenerator. These heat exchangers are present in Figure 7.14 since the regenerator tubes pass through the hot and cold heat reservoirs prior to entering the pistons.

There are still other Stirling engine configurations that use a displacer and a piston. An example of this piston-displacer type Stirling engine is the Stirling engine built as part of subject 2.670, Mechanical Engineering Tools, a required course in the Mechanical Engineering curriculum at MIT. A photograph of a typical machine built by a student is shown in Figure 7.15. A schematic diagram of the internal workings of this engine is shown in Figure 7.16. The steps of the Stirling cycle using this embodiment are shown in Figure 7.17.

The displacer differs from a piston in that it is not a sealed device and cannot support a pressure gradient across it. Hence, a displacer does not do work on the gas. However, the displacer does support a very large temperature gradient across it. Ideally, the temperature varies linearly from T_H on one end to T_L on the other. The narrow gap between the displacer and the steel shell acts as the regenerator passage. The regenerator heat capacity is provided by the materials in the steel shell and the displacer. The quantitative aspects of the heat transfer and work transfer will be ignored here. We have already discussed them at length in the very simple

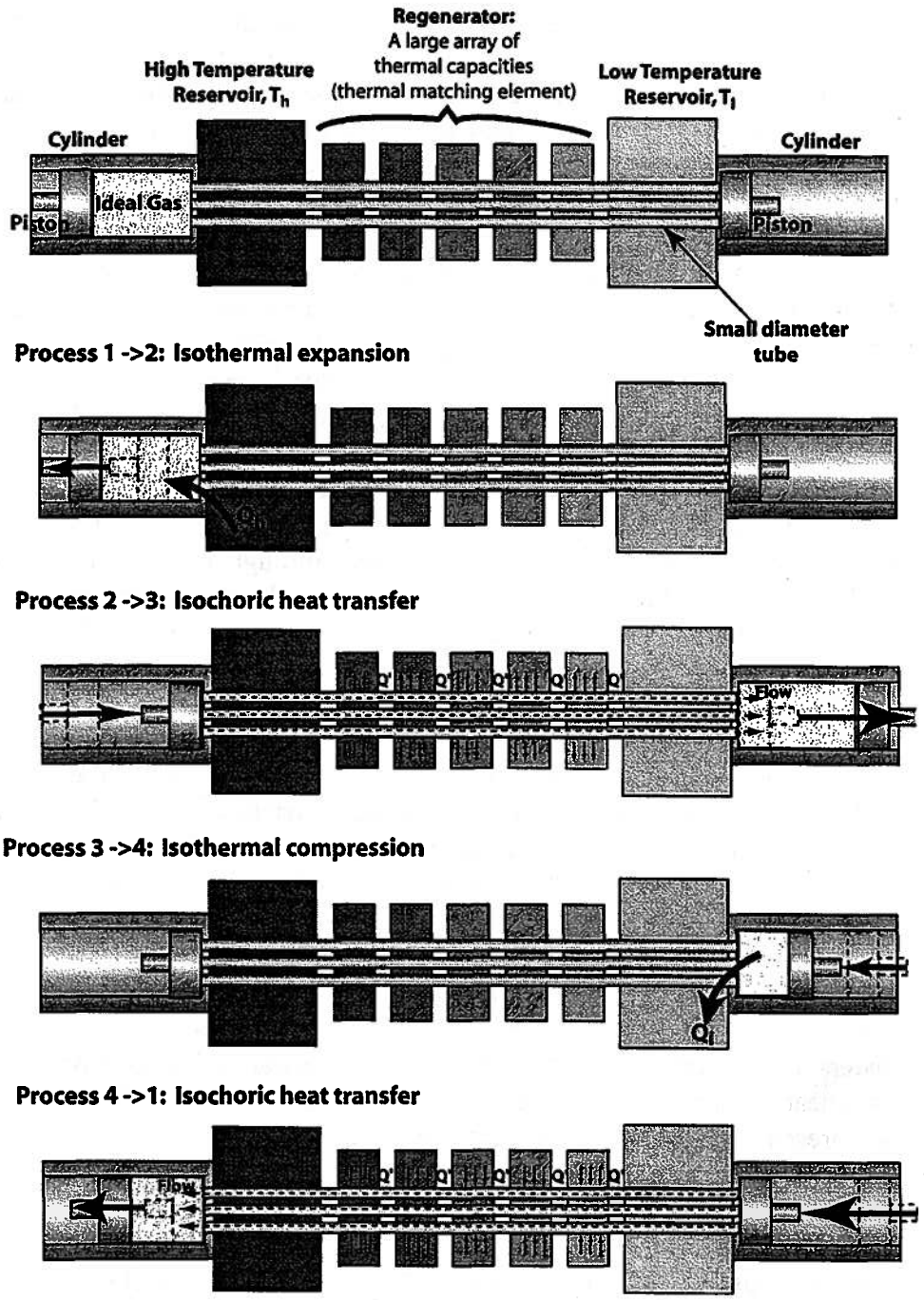

Figure 7.14 A Stirling Cycle Engine in the Double Piston Configuration

models discussed at the beginning of this section and have established the overall behavior of the cycle. State 1 for the displacer piston Stirling engine is shown at the top of Figure 7.17. The displacer is positioned entirely to the right and the gas is at high temperature. In process 1 → 2, the power piston is moved to expand the gases in the Stirling engine, with a positive work transfer for the gas and a negative work transfer for the environment. Some of the gas in the high temperature space of the engine will flow into the displacer gap and allow the remaining gas in the high temperature space to expand. As the gas expands, ideally isothermally, energy

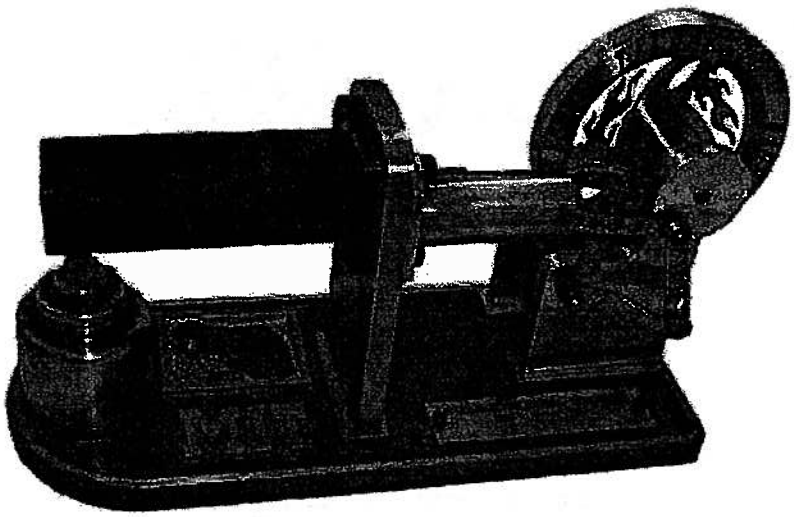

Figure 7.15 A Stirling Engine Built by an MIT Student in Subject 2.670

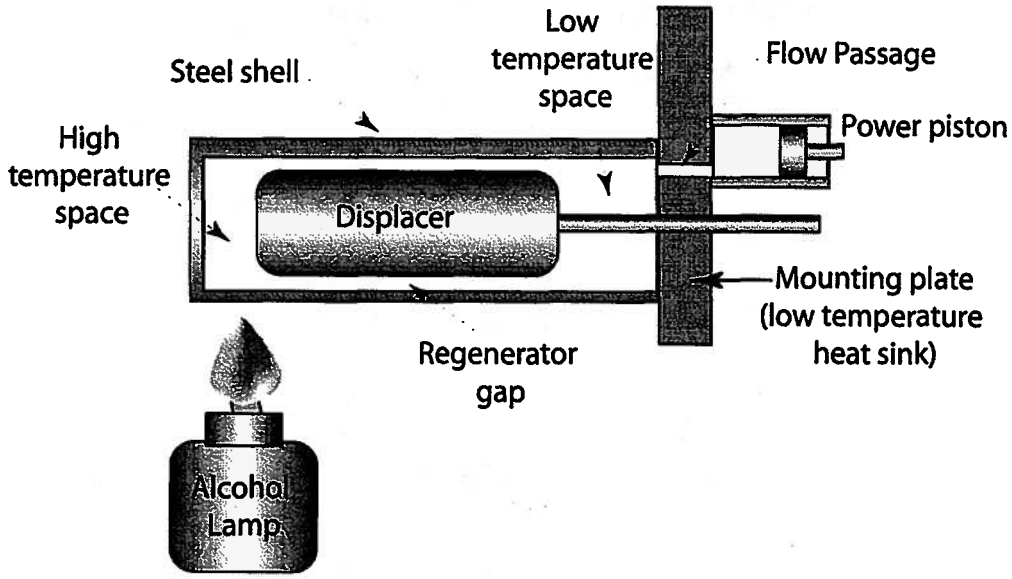

Figure 7.16 Schematic Diagram of the Workings of the Stirling Engine of Figure 7.15

and entropy is absorbed from the high temperature heat reservoir (the alcohol flame). Process 2 → 3 is a displacement. The displacer is moved from right to left while the power piston is held motionless. The hot gas is forced to flow through the displacer gap where it is cooled to T_L by transferring energy and entropy to the displacer and the surrounding steel shell. Presumably, the gas emerges from the gap at the temperature of the low temperature space, T_L. In process 3 → 4, the power piston is moved to compress the gas inside the engine. Since the average temperature of the gas is now low (and the gas pressure is consequently low) the work transfer necessary to compress the gas is smaller in magnitude than the work transfer from the gas in the high temperature expansion process. Finally, process 4 → 1 is another displacement where the gas is reheated in the displacer gap to the original temperature T_H.

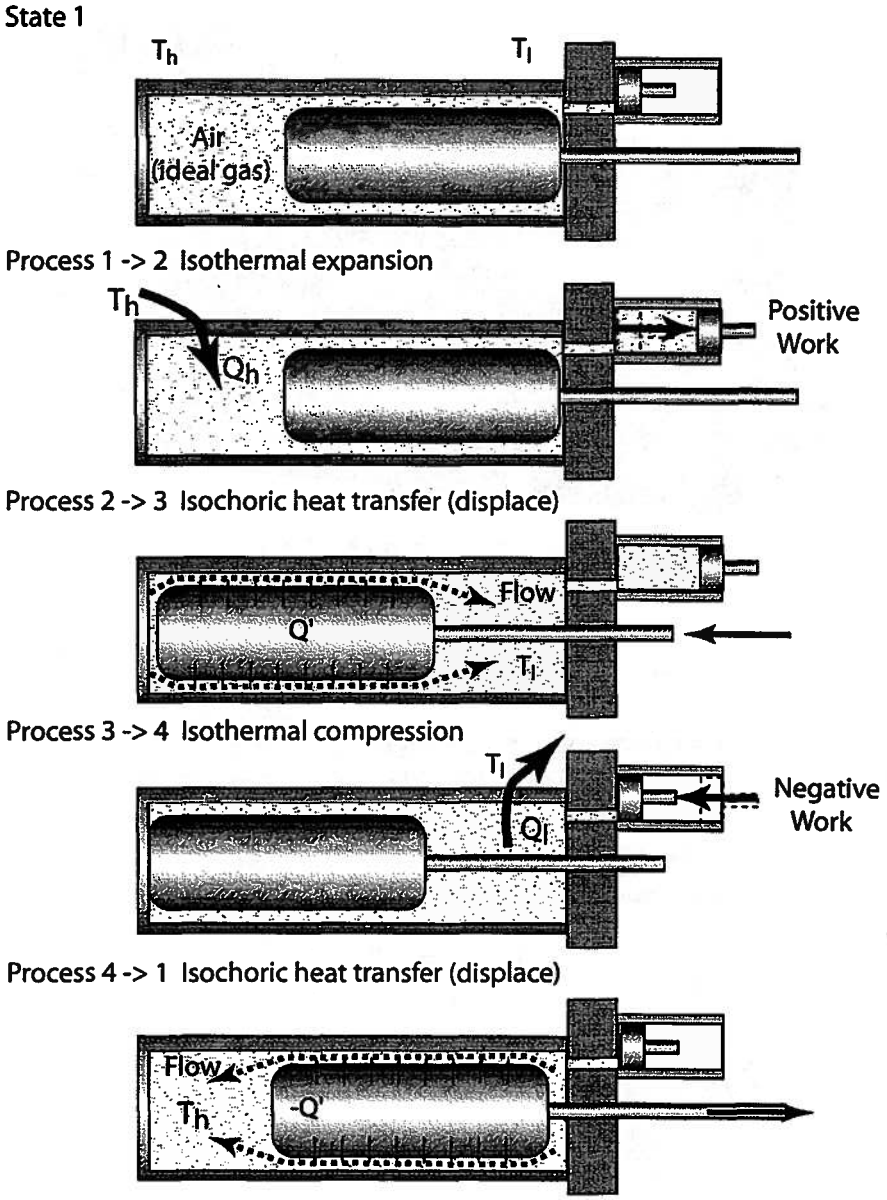

Figure 7.17 Operation of the Stirling Cycle Engine of Figure 7.15

We have emphasized the Stirling engine in this discussion, but the Stirling cycle can also be used to make a refrigerator. All the concepts discussed earlier can be easily adapted to a refrigeration cycle. The engine in Figure 7.14 operates as a refrigerator if the "high temperature heat reservoir" is held at low temperature and the "low temperature heat reservoir" is held at high temperature. The execution of the cycle as shown (with the temperatures reversed) results in a heat transfer from a low temperature region and a heat transfer into the high temperature region. This is a refrigerator. It is left as an exercise to show that net work transfer for this refrigeration cycle is negative.

7.6.4 Historical and Current Examples of Stirling Cycle Machines

We have already mentioned briefly the history of the early development of the Stirling Engine. Many variations of this engine type (hot air engines) were built in the 19th century.

Around 1850, John Ericsson powered a 2200 ton vessel with a hot air engine that delivered 224 kW at 9 revolutions per minute. The four pistons of the engine were each 4.5 meters in diameter and had a stroke of 1.83 m.

In the early 20th century, the Herreshoff Manufacturing Company, builders of several successful America's Cup defenders, installed Stirling engines in their boats. By World War I, however, it became clear that the internal combustion engine was a better and cheaper alternative than either the hot air engine or the steam engine for most applications.

In the 1930's, the Philips Electric Company in the Netherlands began a Stirling engine development program that resulted in Stirling engine driven 1 kW generators and a 149 kW four piston Stirling engine in 1948. This work sparked interest in the United States that resulted in work being done for automotive applications by Ford and General Motors from the 1950's until as late as the 1980's.

More recent developments include an announcement by British Gas (in 2003) that they have developed and plan to market a combined heat and power system for the home. The unit uses a Stirling engine to drive a small generator to provide electric power to the home. The gases that have passed through the Stirling hot heat exchanger are then used to heat water for domestic use and to provide hot water for heating the home.

Stirling cycle machines also have been developed for use as coolers for refrigeration and cryogenic applications. Figure 7.18 is a photograph of the Twinbird Stirling refrigeration unit. This unit can provide 40 W of cooling at temperatures of –23.3 C when the waste heat is exhausted at 35 C. The unit consumes about 33 W under these conditions. This particular unit is sized for a small refrigerator application. A cooler like this could, for example, be used to actively cool an ice chest using solar panels to provide power to the Stirling cooler. This unit should be commercially available in 2004.

Figure 7.18 Twinbird Stirling Refrigeration Unit

Figure 7.19 is an example of a Stirling cryocooler that is being used to cool superconducting filters in cell phone base stations. The superconducting filters perform better than conventional room temperature electronic filters allowing more calls to be handled by the cell phone base station. These superconducting filters must be cooled to temperatures around 70K for proper operation. The STI cryocooler shown in Figure 7.20 provides 5.75 W of cooling power at 80 K with 100 W of input power when the waste heat is rejected at 35 C.

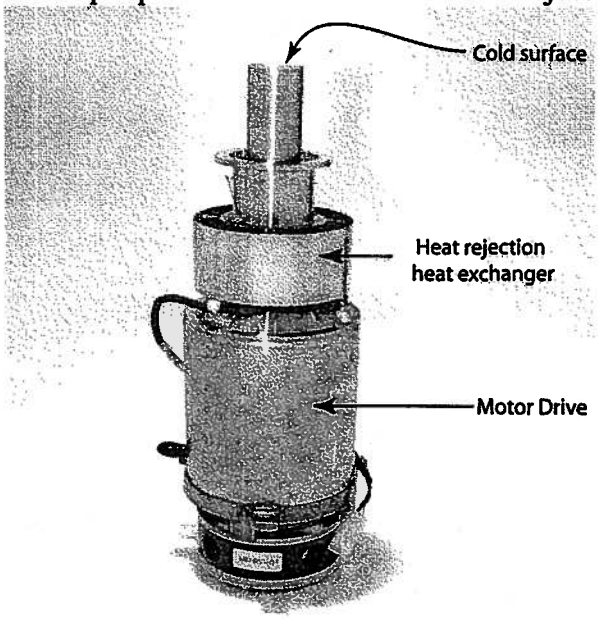

Figure 7.19 The STI Cryocooler

Figures 7.20 and 7.21 show examples of coolers that were developed (and used) for NASA and ESA space applications. Many of the radiation detectors used in space telescopes must be operated at cryogenic temperatures for optimum performance. The Stirling cryocooler can be designed with desirable low-temperature performance and a low overall mass, traits that are important to a space-qualified cooler. The Ball Aerospace Stirling Cryocooler shown in Figure 7.20 is a three-stage Stirling cryocooler in contrast to the single stage machines discussed above. These three-stage machines are capable of achieving temperatures below 25 K. At 35 K the cooler can deliver a cooling power of 0.4 W while consuming 81 W of electric power and rejecting heat at 25 C. The Sunpower M77 cryocooler, shown in Figure 7.21, is currently flying on the HESSI satellite. (HESSI carries an imaging spectrometer for observing hard x-rays and gamma rays emitted from solar flares.) The M77 can provide 4 W of cooling at 77 K with an input power of 100 W. We leave it as an exercise to compare the efficiency of these machines to the ideal Carnot *COP* expected for the ideal Stirling cooler.

As a final practical example of Stirling cycle engines, consider the system that has been developed by Kockum for submarines. A schematic diagram of the operating principle of the Kockum's air independent propulsion (AIP) system is shown schematically in Figure 7.22. Diesel fuel and pure oxygen are burned at high pressure to fire the Stirling engine. The high pressure exhaust gases are then dissolved into seawater and discharged to the sea.

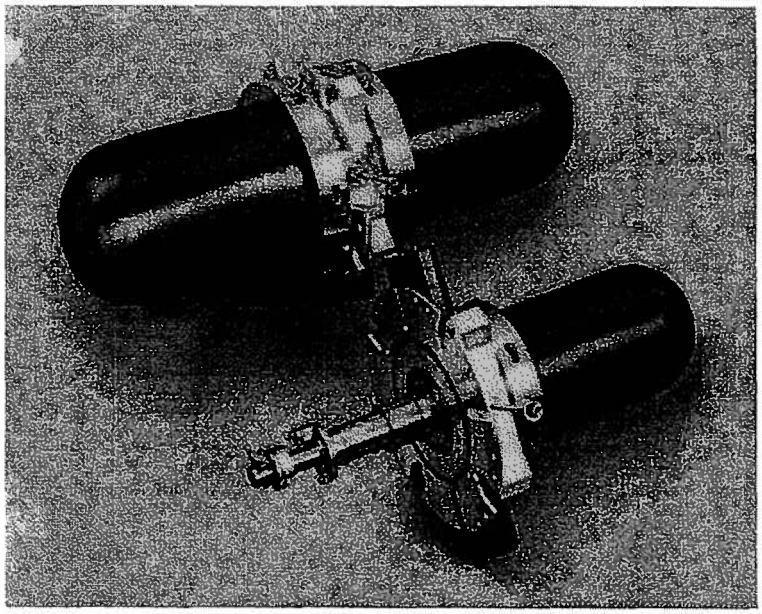

Figure 7.20 Three-stage Cryocooler for Space Application (Ball Aerospace SB335)

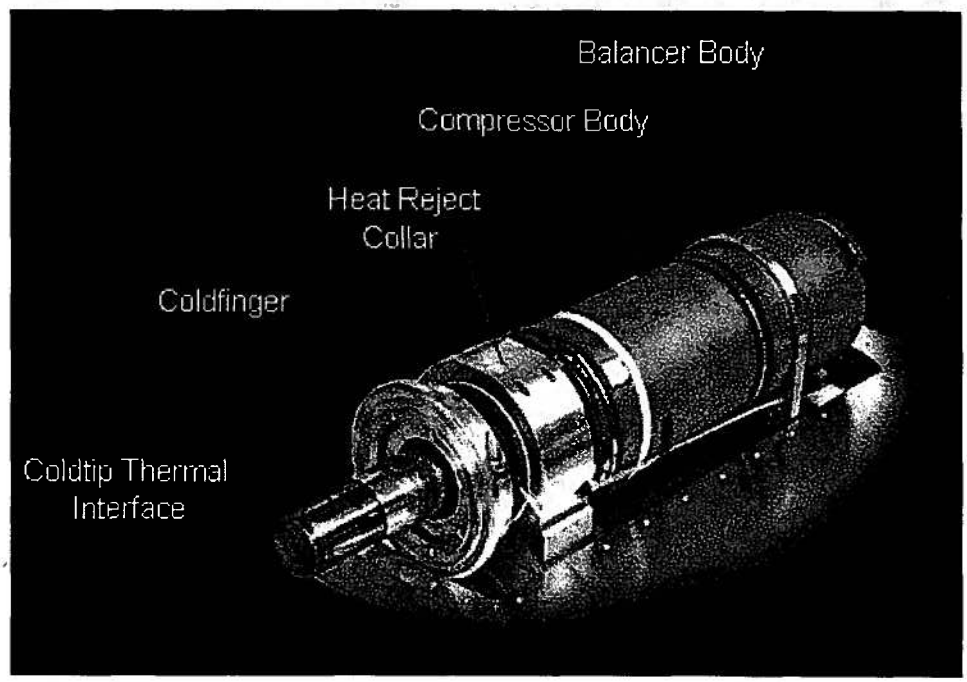

Figure 7.21 The Sunpower M77 Cryocooler

The electric power generated by the Stirling engine driven generator can be stored in a battery bank or can be directly fed to the main motor to propel the submarine. The oxygen is stored in liquid form in a cryogenic tank. The time the submarine can remain submerged is generally limited by the supply of liquid oxygen stored on board the vessel. This AIP system extends the submergence time from a few days for a conventional diesel-electric submarine to weeks. Figure 7.23 shows the Swedish submarine HMS Nacken which was retrofitted with a Stirling-

based AIP system. The performance of the Nacken with the Stirling AIP units has led to the use of the AIP unit in the Swedish Gotland Class and the Australian Collins Class submarines.

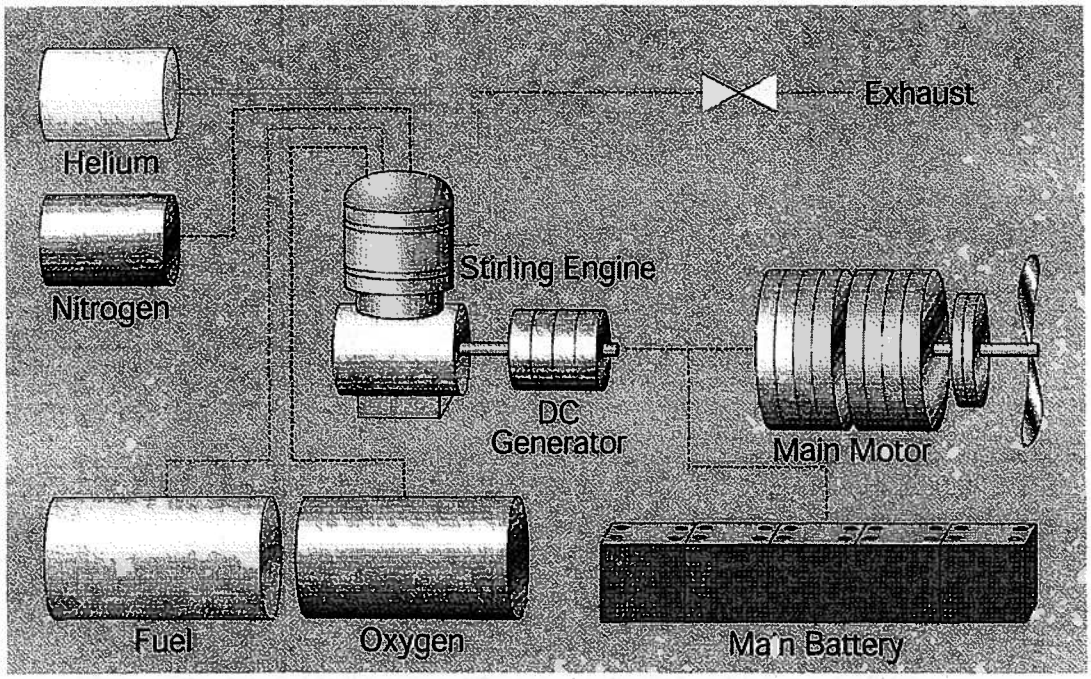

Figure 7.22 The Kockum AIP System for Submarines

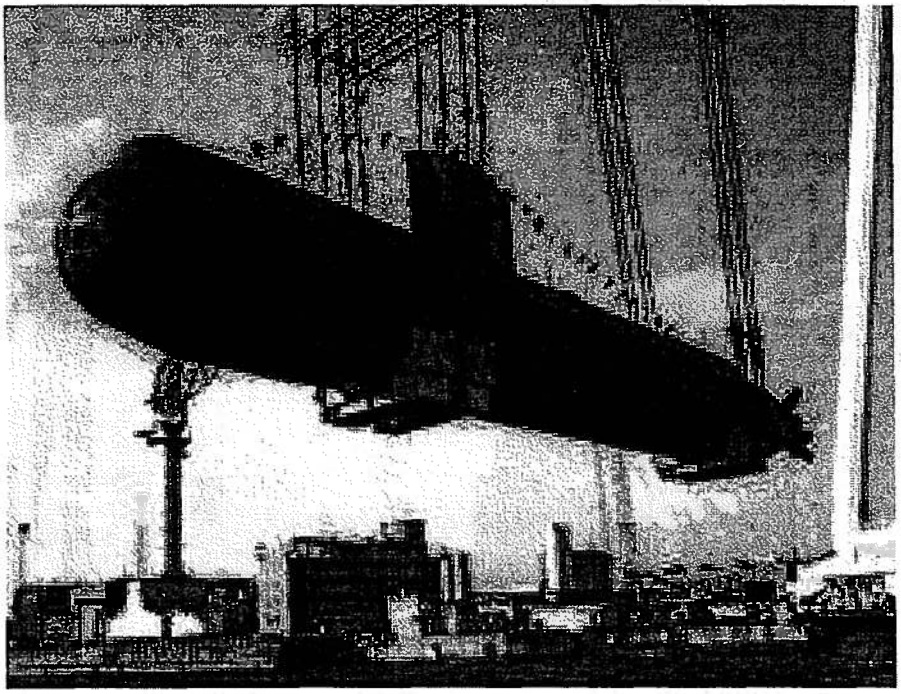

Figure 7.23 The HMS Nacken Equipped with a Stirling Cycle Based AIP

7.7 Thermodynamic Temperature Scale

Finally, we close our discussion of energy conversion with an important observation. Equation (7.22) is a general relation between the heat transfers for a reversible cycle and the temperature at which the heat transfers take place. This equation may be used as the least restrictive method of defining temperature ratios. Equation (7.22) can be written as

$$\frac{T_H}{T_L} = -\frac{Q_H}{Q_L} \tag{7.87}$$

Thus, the ratio of the temperatures of the two heat reservoirs may be defined in terms of the ratio of the heat transfers for any reversible cycle of any system in thermal communication with these heat reservoirs. Any temperature scale which is defined in terms of these heat transfers is termed a thermodynamic temperature scale, and as equation (7.87) shows, its definition is independent of the constitutive relation of the system. Useful thermodynamic temperature scales are established by assigning an arbitrary value to a readily reproducible thermodynamic state of some working fluid. All other temperatures on that thermodynamic temperature scale are then determined relative to this reference state by equation (7.64). The reproducible state used as the reference state is frequently the triple point of water (the state in which all three phases of water, solid, liquid, and vapor, can co-exist in thermodynamic equilibrium). The thermodynamic Kelvin scale of temperature assigns the value 273.16 K to this state. The thermodynamic Rankine scale of temperature assigns the value 491.69 R to this state. The Kelvin and Rankine thermodynamic temperature scales are identical with the ideal gas temperature scales because of the special nature of the constitutive relation of the ideal gas.

Appendix 7A

The Impracticality of a Carnot Cycle Using an Ideal Gas as the Working Fluid

Since the Carnot cycle is usually introduced as the "ideal" reversible cycle, it is quite natural to think of the Carnot cycle as the cycle with the highest energy conversion efficiency. This is a common misunderstanding. Any reversible cycle in thermal communication with only two heat reservoirs will have the same energy conversion efficiency as the Carnot cycle. Two examples of other cycles with the same efficiency as the Carnot cycle are the Stirling cycle and the Ericson cycle. (It is left as a Problem exercise to show that this is indeed the case.) Another common misunderstanding with respect to the Carnot cycle is that the reason that the Carnot cycle is not the basis of the design for large energy conversion plants is that the cycle must be reversible to operate and reversible processes cannot be realized in thermal-fluids engineering practice. This is not quite the case. There are many processes in thermal-fluids engineering practice that are very nearly reversible and are used as part of practical cycles. These processes could be used as part of the construction of a Carnot cycle, but the Carnot cycle is not practical for other reasons that we shall now show.

Consider the Carnot cycle using the ideal gas helium, $R = 2078$ J/kg K and $c_v = 3117$ J/kg K, as shown on the *T-S* diagram of Figure 7A.1.

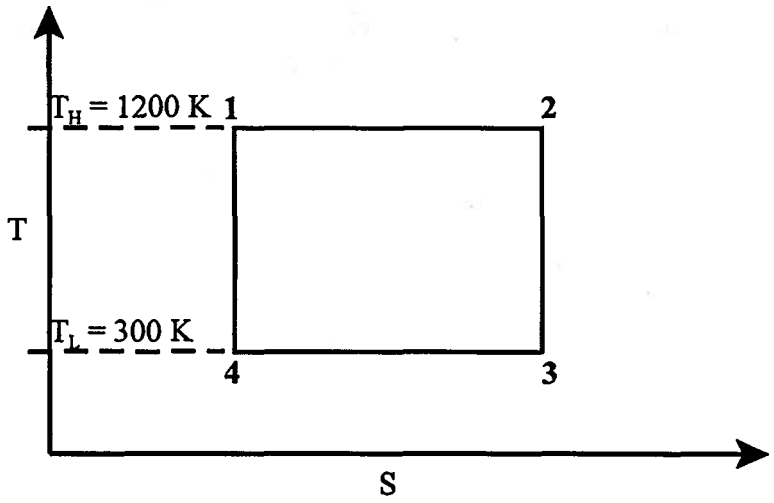

Figure 7A.1 Carnot Cycle Using Helium

The Carnot cycle executes a reversible isothermal process, 1 → 2, while the gas is in thermal communication with a high-temperature heat reservoir at the temperature of $T_H = 1200$ K. The gas temperature is then changed from that of the high-temperature heat reservoir to that of the low-temperature heat reservoir by means of a reversible, adiabatic expansion of the gas, 2 → 3. The gas then executes a reversible isothermal process, 3 → 4, while in thermal communication with a low-temperature heat reservoir at the temperature of $T_L = 300$ K. Finally, the cycle is completed by changing the gas temperature from that of the low-temperature heat reservoir to that of the high-temperature heat reservoir by means of a reversible, adiabatic compression of the gas, 4 → 1.

On the *P-v* plane, the cycle would appear as shown in Figure 7A.2 where we have arbitrarily taken the value of the initial specific volume of the gas, $v = V/m$, to be $v_1 = 1$ m^3/kg.

We have also taken the specific volume in state 2 to be $v_2 = 2.5902$ m^3/kg for reasons that will become apparent shortly. Then for a plot with a linear pressure scale, we have Figure 7A.2.

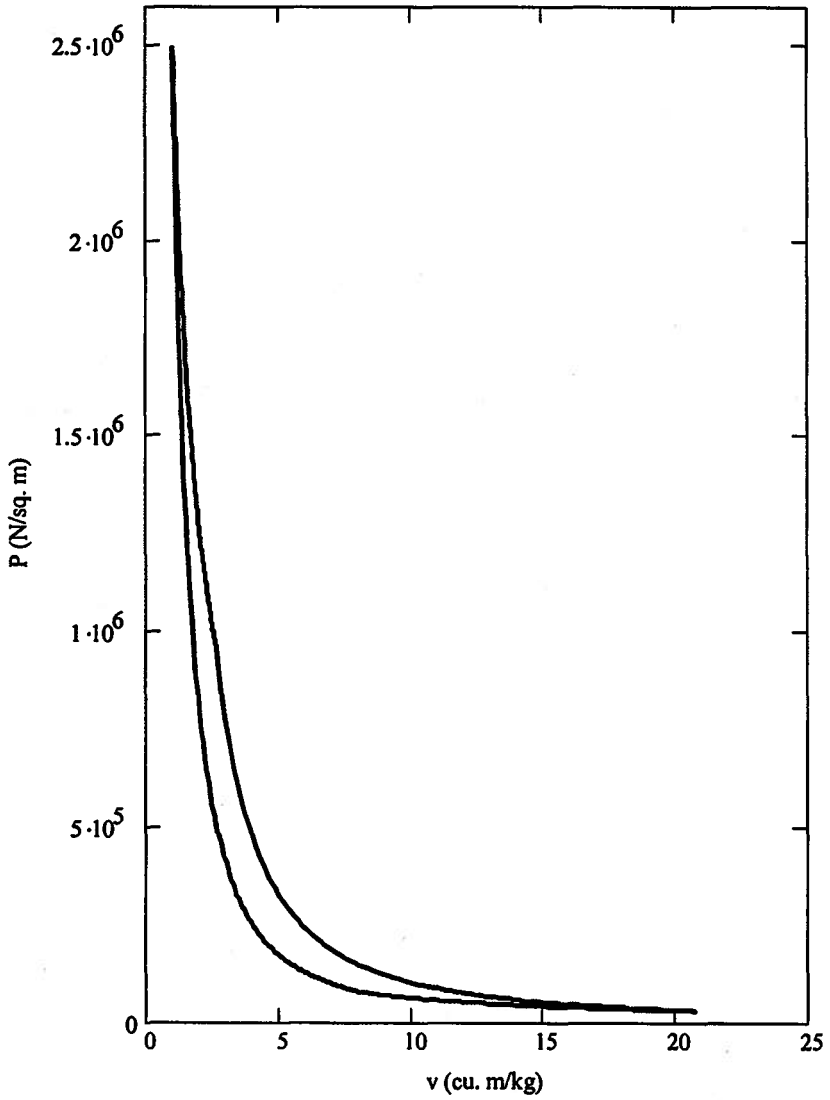

Figure 7A.2 Carnot Cycle for Helium with $T_H = 1200$ K and $T_L = 300$ K

Since the processes involved are reversible, the work transfer for the various processes can be represented by the area between the path of the process and the abscissa. Upon inspecting Figure 7A.2, we are immediately struck by the fact that the sum of the work transfers for the negative work transfer processes, 3 → 4 and 4 → 1, is very nearly equal in magnitude to the sum of the work transfers for the positive work transfer processes. Thus net positive work transfer for the cycle as represented by the area enclosed by the cycle on the *P-v* plane as we traverse the path of the cycle in the clockwise direction is relatively small despite the high pressures involved. As we shall soon see, this is one of the reasons that the Carnot cycle is not suitable for practical energy conversion systems. The Carnot cycle can be seen a bit more clearly if we use a logarithmic scale for the pressure as in Figure 7A.3. Because of the logarithmic pressure scale, care must be

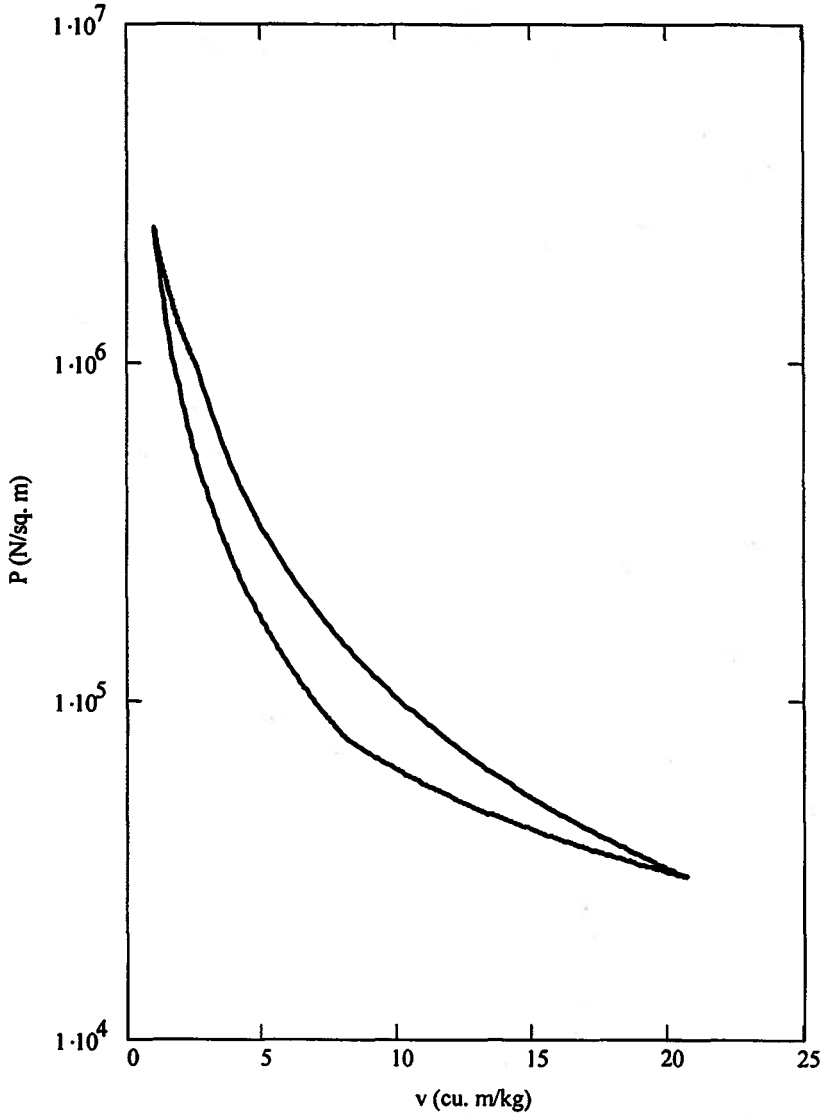

Figure 7A.3 Carnot Cycle for Helium with $T_H = 1200$ K and $T_L = 300$ K

exercised in the interpretation of the areas on this plot. The work transfer for the various processes can no longer be represented by the area between the path of the process and the abscissa.

There are two measures by which we can quantitate the effect of the large negative work transfer on Carnot cycle design. The first of these is the *mean effective pressure*, $P_{mean\ effective}$, which quantitates the effectiveness of the cycle in utilizing the available size of the device. The mean effective pressure provides a relative measure of the size and weight of different engines and is defined as

$$P_{mean\ effective} = \frac{\text{Net work per cycle}}{\text{Volume displaced per cycle}} \tag{7A.1}$$

As equation (7A.1) shows, the larger the mean effective pressure, the smaller the engine necessary to meet a given work requirement. The net work transfer for the cycle can be determined by applying the first law to each of the processes that make up the cycle and then

summing all the results. Thus, from equation (7.2) and the following equations, we have

$$\begin{aligned} W_{1-2} &= mRT_H \ln\frac{V_2}{V_1} \\ W_{2-3} &= mc_v(T_2 - T_3) = mc_v(T_H - T_L) \\ W_{3-4} &= mRT_L \ln\frac{V_4}{V_3} \\ W_{4-1} &= mc_v(T_4 - T_1) = mc_v(T_L - T_H) \end{aligned} \tag{7A.2}$$

But from equation (7.12),

$$\frac{V_2}{V_1} = \frac{V_3}{V_4} \tag{7A.3}$$

Then the net work transfer is given by

$$\oint \delta W = W_{1-2} + W_{2-3} + W_{3-4} + W_{4-1}$$

$$\oint \delta W = mRT_H \ln\frac{V_2}{V_1} + mc_v(T_H - T_L) - mRT_L \ln\frac{V_2}{V_1} - mc_v(T_H - T_L) \tag{7A.4}$$

$$\oint \delta W = mR(T_H - T_L)\ln\frac{V_2}{V_1}$$

The mean effective pressure is given by

$$P_{mean\ effective} = \frac{\oint \delta W}{V_3 - V_1} = \frac{mR(T_H - T_L)\ln\frac{V_2}{V_1}}{V_3 - V_1} \tag{7A.5}$$

We can non-dimensionalize the mean effective pressure by dividing by the peak pressure in the cycle. This will make it easier to apply to Carnot cycles in general. Then

$$\frac{P_{mean\ effective}}{P_1} = \frac{\oint \delta W}{P_1(V_3 - V_1)} = \frac{mR(T_H - T_L)\ln\frac{V_2}{V_1}}{P_1(V_3 - V_1)} \tag{7A.6}$$

But for the adiabatic process 2 → 3, the path is given by

$$P_2 V_2^{\gamma} = P_3 V_3^{\gamma} \tag{7A.7}$$

Then

$$\frac{V_3}{V_2} = \left(\frac{P_2}{P_3}\right)^{1/\gamma} = \left(\frac{T_2}{T_3}\right)^{1/\gamma-1} = \left(\frac{T_H}{T_L}\right)^{1/\gamma-1} \tag{7A.8}$$

Then

$$P_1(V_3 - V_1) = P_1 V_1\left[\left(\frac{V_3}{V_2}\right)\left(\frac{V_2}{V_1}\right) - 1\right] = P_1 V_1\left[\left(\frac{T_H}{T_L}\right)^{1/\gamma-1}\left(\frac{V_2}{V_1}\right) - 1\right] \tag{7A.9}$$

Combining equations (7A.6) and (7A.9), we get

$$\frac{P_{mean\ effective}}{P_1} = \frac{\oint \delta W}{P_1(V_3 - V_1)} = \frac{mR(T_H - T_L)\ln\frac{V_2}{V_1}}{P_1(V_3 - V_1)} = \frac{mR(T_H - T_L)\ln\frac{V_2}{V_1}}{P_1V_1\left[\left(\frac{T_H}{T_L}\right)^{1/\gamma-1}\left(\frac{V_2}{V_1}\right)-1\right]}$$

$$\frac{P_{mean\ effective}}{P_1} = \frac{mR(T_H - T_L)\ln\frac{V_2}{V_1}}{mRT_H\left[\left(\frac{T_H}{T_L}\right)^{1/\gamma-1}\left(\frac{V_2}{V_1}\right)-1\right]} \tag{7A.10}$$

$$\frac{P_{mean\ effective}}{P_1} = \frac{\left(1-\frac{T_L}{T_H}\right)\ln\frac{V_2}{V_1}}{\left[\left(\frac{T_H}{T_L}\right)^{1/\gamma-1}\left(\frac{V_2}{V_1}\right)-1\right]} = \frac{\eta\ln\frac{V_2}{V_1}}{\left[\left(\frac{T_H}{T_L}\right)^{1/\gamma-1}\left(\frac{V_2}{V_1}\right)-1\right]}$$

where we have made use of equation (7.32). Because of the small magnitude of this ratio, it is more convenient to plot equation (7A.10) multiplied by a factor of 20. This result is shown in Figure 7A.4.

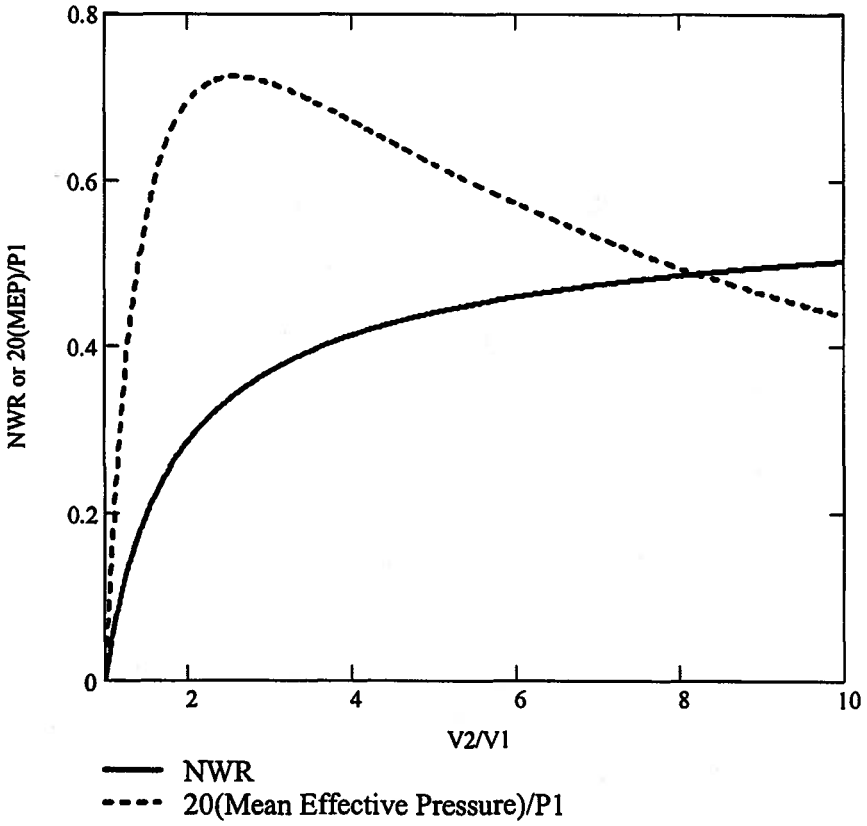

Figure 7A.4 Carnot Cycle Performance

Notice that the mean effective pressure exhibits a maximum value that can be determined by differentiating equation (7A.10) with respect to the volume ratio V_2/V_1 and setting the result equal to zero. Then the locus of the maximum is the root of the equation

$$\frac{\left(\frac{T_H}{T_L}\right)^{1/\gamma-1}\left(\frac{V_2}{V_1}\right)\ln\left(\frac{V_2}{V_1}\right)}{1-\left(\frac{T_H}{T_L}\right)^{1/\gamma-1}\left(\frac{V_2}{V_1}\right)}=1 \qquad (7A.11)$$

$$\left(\frac{V_2}{V_1}\right)=2.5902$$

The value of the mean effective pressure at this value for the volume ratio is

$$P_{mean\ effective}=0.0362P_1 \qquad (7A.12)$$

This extremely small value of the mean effective pressure implies that it is necessary to have a very large engine in order to realize a net work transfer per cycle of any reasonable magnitude. For example, most engines run at a speed of 3600 rpm. Then in order to obtain a power output of 10^8 Watts with the engine of this example, the engine size would have to be

$$\dot{W}_{net}=NP_{mean\ effective}(V_3-V_1)=N(0.0362P_1)(V_3-V_1)$$

$$\dot{W}_{net}=(120\pi\ \text{rad/sec})(0.0362)(2.4936\ \text{x}\ 10^6)(V_3-V_1)=10^8\ \text{W}$$

$$(V_3-V_1)=2.94\ \text{m}^3\approx 3{,}000\ \text{L}$$

Given the typical power per unit volume of moderate performance automobile engines, an automobile engine of relatively conservative design could produce this much power with a displacement of 447 L. Thus, the Carnot design requires a disproportionately large engine. Moreover, given the requirement for reversible heat transfer during the isothermal processes, it is unlikely that the engine could be run at 3600 rpm. We shall return to this point below.

The second measure of Carnot cycle performance that is relevant is the *Net Work Ratio*, *NWR*, which is defined as

$$NWR=\frac{\text{net work transfer per cycle}}{\text{gross work transfer per cycle}} \qquad (7A.13)$$

The Net Work ratio is sigificant because it is a measure of the sensitivity of the cycle to irreversibilities in the processes that make up the cycle. The smaller the value of *NWR*, the more sensitive the cycle is to irreversibilities. Then, making use of equations (7A.2), we have

$$NWR=\frac{mR(T_H-T_L)\ln\frac{V_2}{V_1}}{mRT_H\ln\frac{V_2}{V_1}+mc_v(T_H-T_L)}=\frac{\left(1-\frac{T_L}{T_H}\right)}{1+\frac{c_v}{R}\frac{1}{\ln\frac{V_2}{V_1}}\left(1-\frac{T_L}{T_H}\right)} \qquad (7A.14)$$

$$NWR=\frac{\eta}{1+\eta\left(\frac{1}{\gamma-1}\right)\frac{1}{\ln\frac{V_2}{V_1}}}$$

where we have again used equation (7.32). Equation (7A.14) is plotted as a function of the volume ratio V_2/V_1 in Figure 7A.4. At the volume ratio of $V_2/V_1 = 2.5902$ for which the mean effective pressure is maximum, the value of the Net Work Ratio is only 0.3437 which is less than half the limiting value for *NWR*, η, which in this case is 0.750. Thus, in the design of the engine, some compromise must be reached between the size of the engine and the effect of the irreversibilities which will most certainly be present in the operation of the cycle.

We can take the analysis of the Carnot cycle even further by recognizing that if the various processes that make up the Carnot cycle are to be carried out in a closed system such as a piston-cylinder apparatus (a reciprocating engine), the gas must be in thermal equilibrium with the metal parts during both the isothermal processes and the adiabatic processes. This presents the most serious practical limitation of the closed system design of the Carnot cycle. Since the gas must experience positive heat transfer when its temperature is high and negative heat transfer when its temperature is low, the cylinder walls must experience the same temperature changes as the gas during the adiabatic processes in order for the walls and the gas to be in thermal equilibrium at the start of the isothermal processes. For this to happen, the cylinder walls and the gas must be in thermal equilibrium throughout the adiabatic processes. Thus, it is not the gas that is adiabatic, but rather the combination of the gas and the cylinder walls. As we shall see, the magnitudes of the energy transfers required to change the temperature of the cylinder walls during the adiabatic processes are considerably larger than those required to change the temperature of the gas during these processes. This is problematic since the metal walls are uncoupled in the thermodynamic sense which means that the bulk of the energy transfer simply re-circulates in the metal parts and can never be converted to a positive work transfer.

To quantitate this phenomenon, let us examine the adiabatic processes in detail. Let m_s be the mass of the structural parts in a typical cylinder and m_g be the mass of the gas in the cylinder. Since the gas and the cylinder walls must be in thermal equilibrium during the adiabatic processes, the first law for an infinitesimal change of state of the system consisting of the gas and the cylinder walls is

$$\delta Q - \delta W = dU = dU_{gas} + dU_s = m_g c_v dT + m_s c dT = \left(m_g c_v + m_s c\right) dT \tag{7A.15}$$

Since the process is adiabatic and reversible, $\delta Q = 0$ and $\delta W = PdV$. Then

$$-PdV = \left(m_g c_v + m_s c\right) dT \tag{7A.16}$$

Differentiating the ideal gas property constitutive relation $PV = mRT$ logarithmically, we get

$$\begin{aligned} \frac{dT}{T} &= \frac{dP}{P} + \frac{dV}{V} \\ dT &= \frac{T}{P} dP + \frac{T}{V} dV = \frac{1}{mR}\left(VdP + PdV\right) \end{aligned} \tag{7A.17}$$

Substituting equation (7A.17) into equation (7A.16) and separating variables, we get

$$\begin{aligned} -PdV &= \frac{m_g c_v + m_s c}{m_g R}\left(VdP + PdV\right) \\ -\frac{dV}{V}\left[1 + \frac{m_g R}{m_g c_v + m_s c}\right] &= \frac{dP}{P} \end{aligned} \tag{7A.18}$$

If we let

$$n = 1 + \frac{m_g R}{m_g c_v + m_s c} \tag{7A.19}$$

equation (7A.18) becomes

$$-n\frac{dV}{V}=\frac{dP}{P} \tag{7A.20}$$

Equation (7A.20) can be integrated to give the P-V relation for the system consisting of the gas plus the cylinder walls, viz.

$$\begin{aligned} -n\ln V+\ln C&=\ln P\\ PV^n&=C \end{aligned} \tag{7A.21}$$

A simple first order estimate of the exponent n can be obtained by neglecting the contribution of the cylinder head and considering the cylinder wall as the only contribution to the structure of the cylinder. The mass of the structure is then limited by the maximum stress σ that the cylinder wall can withstand. The hoop stress in a cylinder of wall thickness t and diameter D is given by

$$\sigma=P\frac{D}{2t} \tag{7A.22}$$

If L is the length of the stroke of the piston, the volume of structural materials V_s is given approximately by

$$V_s=\pi DtL=\frac{\pi D^2LP}{2\sigma} \tag{7A.23}$$

Thus, the mass of the structure is

$$m_s=\frac{\pi D^2LP\rho_s}{2\sigma} \tag{7A.24}$$

where ρ_s is the density of the material of the cylinder wall. The mass of the gas in the cylinder is from the ideal gas property constitutive relation

$$m_g=\frac{PV}{RT}=\frac{\pi D^2}{4}L\frac{P}{RT} \tag{7A.25}$$

Then dividing equation (7A.24) by equation (7A.25), we get

$$\frac{m_s}{m_g}=\frac{2\rho_sRT}{\sigma} \tag{7A.26}$$

The limiting value for this ratio will occur at the highest temperature at which the allowable stress is lowest. As a typical value for this ratio consider a steel cylinder for the helium gas Carnot engine under discussion. Then

$$\begin{aligned} \rho_s&=7817\ \text{kg/m}^3\\ \sigma&=137\ \text{x}\ 10^6\ \text{N/m}^2\\ c&=472\ \text{J/kg K} \end{aligned} \tag{7A.27}$$

Then at the temperature $T_H=1200$ K, equation (7A.26) gives

$$\frac{m_s}{m_g}=\frac{2\left(7817\ \text{kg/m}^3\right)\left(2078\ \text{J/kg K}\right)\left(1200\ \text{K}\right)}{137\ \text{x}\ 10^6\ \text{N/m}^2}=284.56 \tag{7A.28}$$

Then the exponent n becomes

$$n=1+\frac{2078\ \text{J/kg K}}{3117\ \text{J/kg K}+284.56\left(472\ \text{J/kg K}\right)}=1.0151 \tag{7A.29}$$

Thus, n is very nearly unity. As n approaches unity, the system approaches uncoupled behavior

and as we shall now show, the values of NWR and $P_{mean\ effective}/P_1$ both approach zero. For a volume ratio $V_2/V_1 = 2.5902$, with this value of $n = 1.0151$ in place of γ, the volume ratio required to produce the temperature ratio $T_H/T_L = 4$ is from equation (7A.8) $V_3/V_2 = 6.572 \times 10^{39}$, and from equation (7A.10), the ratio $P_{mean\ effective}/P_1$ is reduced to 4.183×10^{-41}. Again, using n in place of γ in equation (7A.14), the value of NWR becomes 0.0141. These values show that thermally cycling the mechanical structure of the Carnot engine cylinder causes the closed system Carnot engine to be completely impractical. Even though the engine theoretically still has the reversible efficiency in this model, the very small value of NWR indicates that any departure from reversible operation will drastically reduce the energy conversion efficiency.

Thus the two performance parameters $P_{mean\ effective}$ and NWR show that the energy conversion efficiency is not the only parameter to be considered when designing an energy conversion system. Furthermore, these two parameters also show that the Carnot cycle is not the energy conversion cycle of choice. The low value of the mean effective pressure requires an engine of enormous size for a given power output in spite of its high energy conversion efficiency, and the low value of the Net Work Ratio renders the Carnot cycle highly sensitive to the effects of irreversibilities. Thermally cycling the walls of the engine further exacerbates the problem.

All of these considerations did not take into account the rate processes involved. Consider the engine size estimated following equation (7A.12). The diameter of the single cylinder is on the order of $D \sim 1$ m. Then from equation (7A.22), for a peak pressure on the order of $P \sim 2.5 \times 10^6$ N/m^2, the thickness is on the order of $t \sim 0.01$ m. At the temperature of 1200 K, the thermal conductivity for steel is on the order of $k_s \sim 25$ W/m K and the specific heat is on the order of $c \sim 1000$ J/kg K. During the isothermal processes, the gas and the walls have to be in thermal equilibrium. This means that the Biot number for the heat transfer processes must be $Bi < 0.1$ for the cylinder walls to be uniform in temperature. Then

$$h_c \approx \frac{(Bi)k_s}{t} = \frac{0.1(25\ \text{W/m K})}{0.01\ \text{m}} = 250\ \text{W/m}^2\ \text{K} \qquad (7A.30)$$

From equation (6.210), the time constant τ for the heat transfer process in the cylinder wall is

$$\tau = \left(\frac{k_s}{h_c}\right)^2 \frac{1}{\alpha} = \left(\frac{25\ \text{W/m K}}{250\ \text{W/m}^2\ \text{K}}\right)^2 \frac{(7817\ \text{kg/m}^3)(1000\ \text{J/kg K})}{25\ \text{W/m K}} = 3125\ \text{sec} \qquad (7A.31)$$

If the frequency of the piston motion is on the order of the reciprocal of the time constant, it is apparent that the engine speed must be absurdly low and the size of the engine must then be absurdly large in order to produce any reasonable amount of power. Thus, the Carnot cycle with a reciprocating engine and an ideal gas as the working fluid is not practical from the point of view of the rate processes involved as well.

Problems

7.1 A home freezer operates with an electric motor rated at 250 watts. During a hot summer day (T_{atm} = 33 C) it is observed that the motor is on half the time while the freezer executes an integral number of cycles.

(a) Estimate the heat transfer into the freezer per hour, if its interior temperature is maintained at $T_0 = -17$ C.

(b) What is the heat transfer from the freezer to the atmosphere during the hour?

7.2 In order to provide power to an undersea community, it has been proposed to build a heat engine operating in a cycle that uses the warm surface water of the Gulf Stream as the high temperature heat reservoir, and the cold deep water as the low temperature heat reservoir. If the surface water is at 30 C and the deep water is at 4 C, determine the heat transfer rate (kW) from the high temperature heat reservoir necessary to provide 1 megawatt (10^6 Watts) of power with a reversible engine.

7.3 A closed thermodynamic system employs the cycle shown in Figure 7P.3.

(a) What is the net quasi-static work transfer for this cycle? If the system traverses the cycle in the counterclockwise sense, is the work transfer positive or negative? If the system traverses the cycle in the clockwise sense, is the work transfer positive or negative?

(b) If the system performs as a heat engine and the heat transfer to the low temperature heat reservoir is 50 MJ, determine the thermal efficiency of the cycle.

(c)If the system performs as a refrigerator and the heat transfer to the high temperature heat reservoir is 50 MJ, determine the coefficient of performance of the system (*COP*).

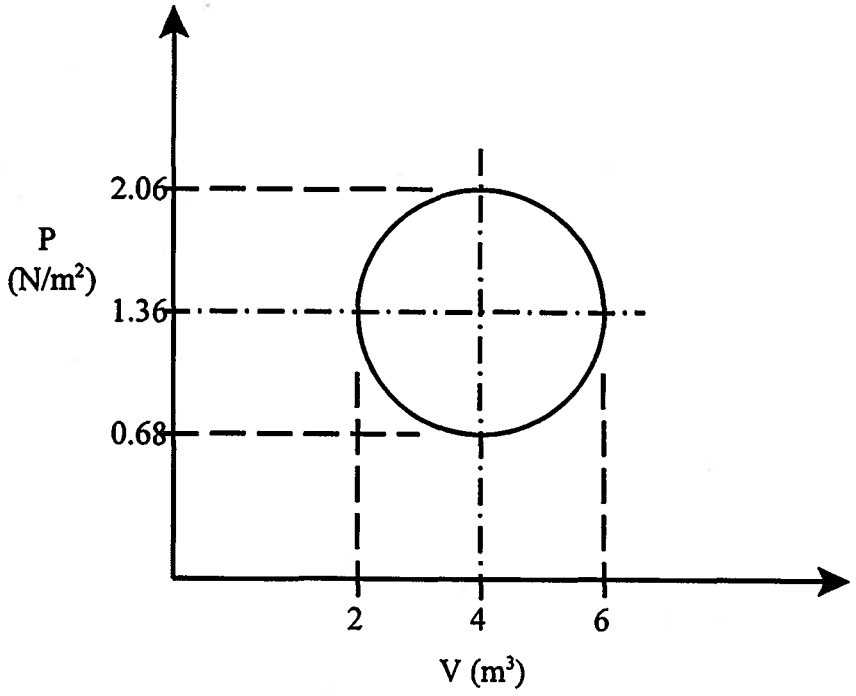

Figure 7P.3

7.4 For an NHL hockey rink, the heat transfer from the air above the ice to the ice surface is at a rate of 400 kW. The ice surface temperature is maintained by a refrigerator that uses the air outside the building as the high temperature heat reservoir and the lowest layer of ice as the low temperature heat reservoir.

(a) When the lowest layer of ice is at a temperature of −9 C and air outside the building is at a temperature of 15 C, estimate the minimum cost of maintaining the ice at this fixed temperature for 24 hours. For this level of power consumption, electric power costs $0.06/kWh.

(b) Would you expect the operating costs of the refrigerator to increase or decrease as the temperature of the outside environment decreases? Assume everything else remains unchanged.

(c)In actual practice, a substantial temperature gradient in the ice is required in order to establish heat transfer from the ice surface to the lowest layer where the cooling pipes of the refrigeration system are located. For the conditions described above, the ice surface temperature is − 3 C while the temperature of the lowest layer is −9 C. Show from considerations of the COP that it would be substantially cheaper to operate the refrigerator if the refrigeration load were removed at the actual ice surface temperature rather than the temperature of the lowest layer.

7.5 During winter, the interior of a building is to be maintained at a temperature T_i. Because the exterior walls of the building are imperfectly insulated, the interior of the building experiences a negative heat transfer at a rate Q when the temperature of the atmosphere is T_{atm}, $T_{atm} < T_i$.

(a) What is the electric power required to maintain an interior temperature T_i if the power is dissipated in electric resistors inside the building?

(b) What would be the minimum electric power required if a heat pump were employed?

7.6 Recently ecologists have expressed considerable concern over the thermal pollution produced by electrical power plants. However, there is another source of thermal pollution. In the summer, the increase in electrical power consumption is considerable. The bulk of this increase is used to operate air conditioning systems. For example, in New York City, statistics compiled by the Consolidated Edison Co. show that the daily increase in electrical power consumption during the summer months is 2×10^9 Watts. Let us assume that all of this increase is used to operate air conditioning systems. Let us also assume that we can model these air conditioning systems as refrigerators that operate in cycles while maintaining the temperature of the air conditioned spaces at a steady temperature of 21 C. Model the environment (atmosphere) as a heat reservoir at 33 C.

(a)Estimate the rate of thermal pollution (Watts) of the environment (atmosphere) due to these air conditioning systems.

(b) Does this estimate represent a lower bound or upper bound on the rate of thermal pollution? Explain your answer.

7.7 Currently the Stirling engine is receiving considerable attention in the engineering literature. The ideal Stirling engine employs a closed ideal gas system. The cycle of the working fluid consists of two reversible isothermal processes (state 1 to state 2 and state 3 to state 4) and two reversible constant volume processes, (state 2 to state 3 and state 4 to state 1). The heat transfer for the isothermal process 1-2 is from the heat reservoir at T_H and the heat transfer for the isothermal process 3-4 is to the heat reservoir at T_L. The gas is cooled at constant volume (process 2-3) by a reversible heat transfer to the elements of the thermal regenerator. The thermal

regenerator stores this energy and returns it to the gas when the gas is heated at constant volume (process 4-1). The thermal regenerator consists of a series of elements each at an infinitesimally different temperature so that the element of the regenerator in contact with the gas is always at the temperature of the gas.

(a) Show that for a perfect regenerator, i.e. a regenerator with no net change of energy, the specific heat of the ideal gas at constant volume must be independent of pressure. (That is, the ideal cycle requires an ideal gas.)

(b) Show that the energy conversion efficiency (thermal efficiency or heat engine efficiency) is identical to that of a Carnot cycle.

7.8 The Servel gas refrigerator may be considered a cyclic device. It produces a refrigeration effect with no net work transfer. The design is widely used for refrigeration where there is no ready access to the electrical power grid as in remote cabins in the woods. The device experiences positive heat transfers Q_H at a high temperature T_H and Q_L at a low temperature T_L and a heat transfer Q_I with the environment at T_I. The system has no work transfer in or out. The performance of this machine may be given by the ratio (Q_L/Q_H), the refrigeration effect divided by the positive heat transfer at the high temperature.

(a)Determine the limits imposed on this ratio by the second law of thermodynamics.

(b)Find the numerical value of this limit for $T_H = 450$ K, $T_L = 270$ K and $T_I = 290$ K.

7.9 A Carnot heat engine is used as a source of mechanical power for a Carnot refrigerator. The heat engine experiences a positive heat transfer Q_{HE} with a heat reservoir at the temperature T_{HE} and a heat transfer QLE with a heat reservoir at a temperature T_{LE}. On the other hand, the refrigerator experiences a positive heat transfer Q_{LR} with an isothermal refrigeration load at a temperature T_{LR} and a heat transfer Q_{HR} with a heat reservoir at a temperature T_{HR}.

(a) Formulate an expression for the ratio Q_{LR}/Q_{HE} in terms of the various temperatures of the heat reservoirs.

(b) On the basis of this expression, what statements can you make regarding the possible range of values for this ratio of heat transfers?

(c) Show that if $T_{LE} = T_{LR}$, this system becomes identical to the reversible Servel refrigerator. (See problem 7.8.)

7.10 A heat engine is in thermal communication with two heat reservoirs HR_1 and HR_2. The temperatures of these heat reservoirs are 600 K and 300 K, respectively. The thermal communication between the two heat reservoirs and the engine is not perfect in the sense that a finite temperature difference is required to establish heat transfer between each of the heat reservoirs and the heat engine. For heat reservoir HR_1. the temperature difference is 50 K and for heat reservoir HR_2. the temperature difference is 25 K.

(a) If the heat engine experiences a positive heat transfer of 1000 kJ/cycle with the heat reservoir HR_1, estimate the reduction in the work transfer/cycle associated with the imperfect thermal communication.

(b) As an engineer, it is your job to improve the performance of this heat engine. One of the obvious ways to accomplish this feat is to improve the thermal communication between the heat reservoirs and the heat engine. Which of the two heat interactions would yield the greater return for a given reduction in temperature difference? Explain your answer.

7.11 Consider a reversible heat engine which executes an integral number of cycles while having heat transfer interactions with three heat reservoirs, HR_1, HR_2, and HR_3 at 400K, 300 K, and 200 K, respectively, as shown in Figure 7P.11. For one cycle, the engine experiences a positive heat transfer of 1600 J with HR_1 and a positive work transfer of 250 J with the environment.

(a) Find the heat transfer for the other heat reservoirs.

(b) Evaluate the entropy transfer for each reservoir and for the engine.

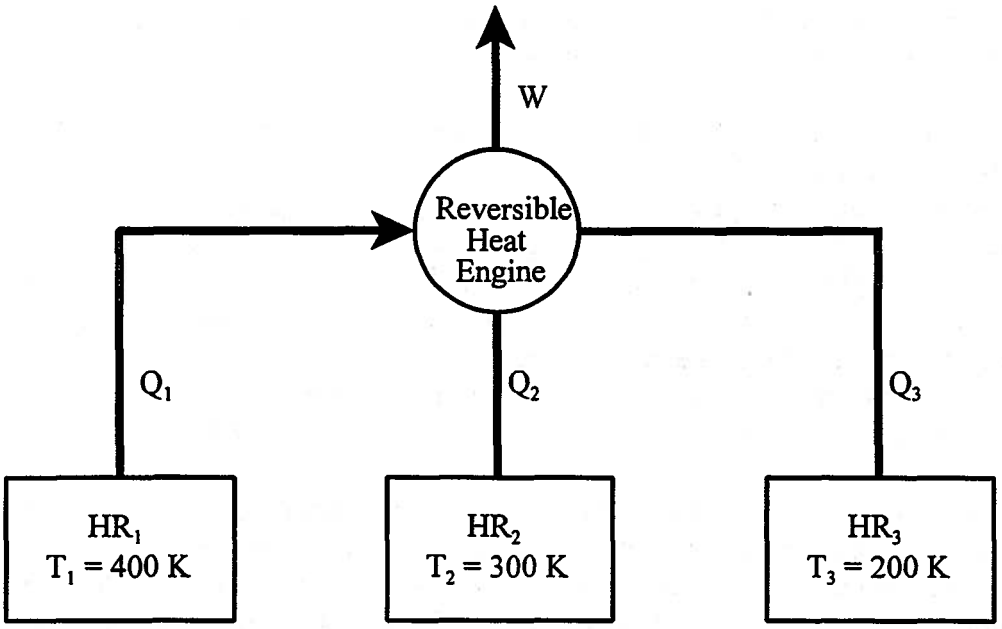

Figure 7P.11

7.12 A convenient and very effective means of heat transfer from a space vehicle or satellite is by thermal radiation to the depths of space which is used as a heat reservoir with an extremely low temperature, namely, 0 K. For this situation the rate at which a body radiates to this heat reservoir is proportional to the surface area of the radiator and the fourth power of its thermodynamic temperature. However, in order to minimize the weight of a space vehicle or satellite, it is necessary to minimize the area of the radiator since its weight is directly proportional to its surface area. Suppose that a space vehicle or satellite contains a reversible heat engine that experiences a positive heat transfer Q_H (not fixed) from an energy source modeled as a heat reservoir whose temperature is fixed at T_H. This engine delivers a fixed work transfer W and ultimately uses the depths of space as an energy sink also modeled as a heat reservoir. Show that the least radiator weight for this system is obtained when the temperature of the radiator, T_R, is such that $T_R = 0.75T_H$.

7.13 As shown in Figure 7P.13, a piston-cylinder apparatus is fitted with a frictionless piston and contains 4 kg of an ideal gas, $R = 287$ J/kg K, $c_v = 716$ J/kg K, in an initial state $P_1 = 4 \times 10^5$ N/m^2 and $T_1 = 400$ K. The gas is to be cooled to $T_2 = 200$ K by means of a reversible heat transfer interaction with a reversible cyclic device that is also in thermal communication with a heat reservoir at $T_{HR} = 300$ K.

(a) For the ideal gas as a system, calculate the following: $U_2 - U_1$, $S_2 - S_1$, $S_{transfer}$, $Q_{1\text{-}2}$, $W_{1\text{-}2}$

(b) For the cyclic device as a system, calculate: Q_1, Q_2, W
(c) For the heat reservoir as a system, calculate: $U_2 - U_1$, $S_2 - S_1$, $S_{transfer}$, $Q_{1\text{-}2}$

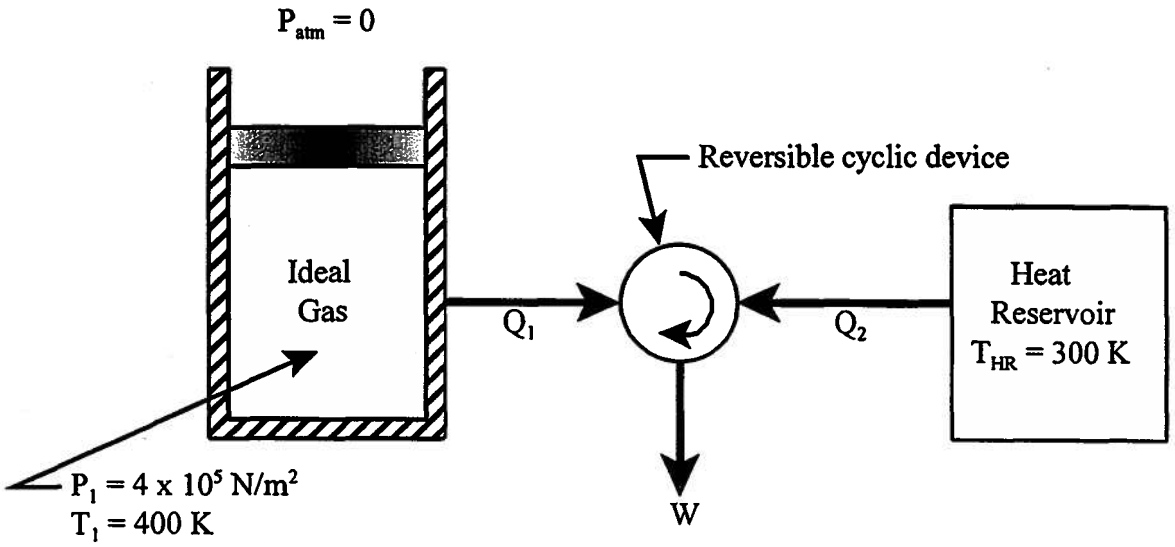

Figure 7P.13

7.14 Two blocks of copper, $c = 385$ J/kg K and $k = 401$ W/m K, are in thermal equilibrium at a temperature of $T_1 = 300$ K. The mass of block A is $m_A = 100$ kg and the mass of block B is $m_B = 50$ kg. A reversible cyclic device is placed in thermal contact with the two blocks via thermal interconnections that can be switched on and off at will. The cyclic device experiences a work transfer interaction of $W_{cycle} = -1.3234$ MJ with the environment.

(a) Determine the final equilibrium temperatures of the two blocks, T_{2A} and T_{2B}.

(b) If the two blocks are now brought into simple thermal communication and allowed to run down to equilibrium with no work transfer involved, what is the new equilibrium temperature, T_3?

(c) If the blocks were made of a material with the same value for the specific heat but a thermal conductivity of $k = 1$ W/m K, how would the answer to part (a) be affected?

7.15 (a) Show that if a reversible cyclic device is allowed to communicate with three or more heat reservoirs, the net work transfer for the cyclic device can be zero. What is the net heat transfer for the cyclic device under these circumstances?

(b) A solar powered air conditioning system operates with a refrigeration load of 300 kW at an effective temperature of 10 C. If the environment is at a temperature of 310 K and the effective solar collector temperature is 400 K, estimate the minimum area of solar collector necessary. The solar insolation is 750 W/m^2.

7.16 Three blocks of copper, A, B, and C, have initial temperatures $T_{1A} = 700$ K, $T_{1B} = 400$ K, and $T_{1C} = 100$ K, respectively. The heat capacities of the three blocks are $C_A = 2$ kJ/K, $C_B = 1$ kJ/K, and $C_C = 1$ kJ/K, respectively. A reversible cyclic device is available to interact with these blocks in a reversible manner. In one complete cycle of this device, the temperatures of the three blocks are equilibrated to a single value T_2 with no net work transfer with the environment. What is the maximum value that T_2 can have?

CHAPTER 8

Open Thermal-Fluid Systems

8.1 Introduction

Thus far in our discussion of the behavior of thermal-fluid systems, we have focused our attention on *closed systems* that constitute a single piece of matter known as a *control mass*. We have determined the behavior of the control mass by following the time-history of its progress through processes by which its state was changed through interactions that involved the transfer of energy and entropy between the control mass and the environment. This approach, known as the Lagrangian approach, is widely used in the study of mechanical systems where the identity of the object of interest is known and the analysis is performed upon that specific object.

There is, however, another class of thermal-fluid systems, known as *open systems*, that do not contain a fixed quantity of matter of known identity. For this class of systems we adopt an alternative point of view, known as the Eulerian approach. In this approach, we do not study the time-history of an object of specific identity, but rather we study what happens to a large collection of objects as they move through a specific location in space. We adopt this point of view every time we sit on the bank of a river or a creek and watch the water flow past obstacles in the stream. We look at specific features in the flow that are seemingly stable in front of us. For example, a small wave that remains in front of a rock as the flow strikes it maybe of interest to us. We are not really aware of the details of the motion of a specific water particle, but, rather, we are aware of the array of velocities in the water as it flows around the rock. Under these circumstances, it makes sense to describe the motion of the water around the rock in terms of a velocity field in which we specify the velocity vector $\vec{v}$ of the water at a particular point (x, y, z) at a specific time t, i.e., $\vec{v} = \vec{v}(x, y, z, t)$. In the Eulerian view, we are not interested in the detailed behavior of specific fluid particles of known identities, but rather in the behavior of the fluid particle that occupies point (x, y, z) at time t.

In our discussion of the flow in the stream, we can mentally jump between these two points of view by looking at the features of the flow at a specific position or by watching the motion of a leaf as it travels on the surface of the water. The Eulerian approach is of greatest utility when a large array of objects is under consideration (in the stream, the objects are the water particles) but is rather cumbersome for a single particle. Similarly, the Lagrangian approach is cumbersome for many particles but is quite efficient for single particle dynamics.

In our studies of the mechanical behavior of solid bodies and in our studies of the thermal-fluid systems up to this point, we have developed an understanding of the physical laws that govern the behavior of these systems from the Lagrangian point of view. These laws have included the conservation of mass, the first and second laws of thermodynamics, Newton's second law of motion (the linear momentum equation) and the angular momentum equation. At this point in our study of the behavior of thermal-fluid systems, we develop an integral formulation of these physical laws from the Eulerian point of view.

8.2 Control Volumes and the Conservation of Mass

In the Lagrangian point of view, the object of interest is a control mass whereas in the Eulerian approach the object of interest is the *control volume*. Each of the physical laws

(conservation of mass, first and second laws of thermodynamics, Newton's second law of motion, and conservation of angular momentum) will assume a form that relates the parameters that describe the flow of matter through the control volume and the properties that describe the state of matter in the flow to a time derivative of a property of the system. For example, Newton's second law of motion relates a force acting on the control volume to the time derivative of the momentum in the control volume and the change of momentum of the fluid as it flows through the control volume. Since we already know how to express each of these laws using the control mass approach, we would like to transfer this knowledge to the control volume.

Control volumes are arbitrary constructs. In general, the control volume can move, change shape and size, but in many cases the control volume has fixed shape and size and is fixed in space. The major difference between a control volume and a control mass is that mass is allowed to pass through the surface of the control volume, the *control surface*, whereas the control mass contains a fixed amount of mass. The fact that this mass passing through the control surface contains energy, entropy, and momentum stored within it means that we now need to consider a new set of possible interactions between the system and the environment. The task confronting us, then, is to develop a means of analyzing the behavior of these open systems.

In the analysis of the behavior of a given open thermal-fluid system using the control volume approach, the choice of control volume is somewhat arbitrary since there are usually several different control volumes to choose from, but the analysis can be made significantly easier by choosing the "right" control volume. The choice of "the right" control volume is not always obvious, but the ability to choose the "right" control volume comes as a matter of experience.

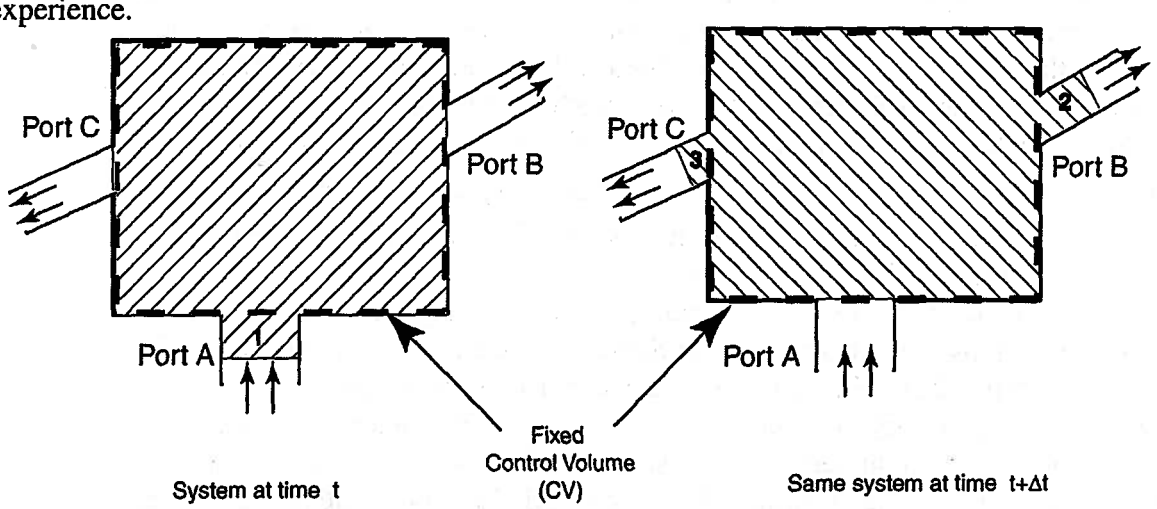

Figure 8.1 Two images of a control mass flowing through a control volume at time t and at time $t+\Delta t$. The control mass is crosshatched and the control volume is the heavy dashed line.

We shall begin our study of the behavior of open thermal-fluid systems with the formulation of the conservation of mass. Figure 8.1 depicts in schematic fashion a control volume representation of a physical open thermal-fluid system. There are three ports A, B, and C in which port A has an inflow and ports B and C have outflows. On the left in Figure 8.1, we have "painted" a control mass with crosshatching. A fixed control volume is also shown by the heavy dotted line. The same situation is shown an instant Δt later in the figure on the right in Figure 8.1. During the time interval Δt, the control mass has moved. Mass 1, which is the part of

the control mass outside the control volume at time t, has moved into the control volume by the time $t+\Delta t$. Masses 2 and 3, initially inside the control volume, have moved outside the control volume at time $t+\Delta t$.

The mass in the control volume at time t is related to the mass in the control mass by

$$M_{CV}(t) = M_{CM}(t) - m_1 \tag{8.1}$$

Similarly for the time $t+\Delta t$

$$M_{CV}(t+\Delta t) = M_{CM}(t+\Delta t) - m_2 - m_3 \tag{8.2}$$

The time rate of change of the mass in the control volume is then defined as

$$\frac{dM_{CV}}{dt} \equiv \lim_{\Delta t \to 0} \frac{M_{CV}(t+\Delta t) - M_{CV}(t)}{\Delta t} \tag{8.3}$$

Substituting equations 8.1 and 8.2 into 8.3, we obtain

$$\begin{aligned} \frac{dM_{CV}}{dt} = \lim_{\Delta t \to 0} \frac{M_{CM}(t+\Delta t) - M_{CM}(t)}{\Delta t} + \lim_{\Delta t \to 0} \frac{m_1(t+\Delta t) - m_1(t)}{\Delta t} \\ - \lim_{\Delta t \to 0} \frac{m_2(t+\Delta t) - m_2(t)}{\Delta t} - \lim_{\Delta t \to 0} \frac{m_3(t+\Delta t) - m_3(t)}{\Delta t} \end{aligned} \tag{8.4}$$

The first term on the right hand side of equation (8.4) is the time derivative of the mass of the control mass. The second term on the right is the mass flow rate into the control volume through port A. The third and fourth terms are the mass flow rates out of the control volume at ports B and C. We can rewrite equation (8.4) as

$$\frac{dM_{CM}}{dt} = \frac{dM_{CV}}{dt} - \sum_{in} \dot{m}_{in} + \sum_{out} \dot{m}_{out} \tag{8.5}$$

Equation (8.5) is a transformation equation that enables us to shift our point of view from the control mass to the control volume. In the present case, it relates the time derivative of the mass for the control mass system to that for the control volume system. The first summation is over all the inflowing ports (port A in Figure 8.1) while the second summation is over the outflowing ports (ports B and C in Figure 8.1).

The expression of the conservation of mass for a control mass is given by

$$\frac{dM_{CM}}{dt} = 0 \tag{8.6}$$

which is an acknowledgment that the mass of a control mass does not vary with time. Substituting the equation (8.6) into the transformation equation (8.5), we obtain the expression for the conservation of mass for the control volume.

$$\frac{dM_{CV}}{dt} = \sum_{in} \dot{m}_{in} - \sum_{out} \dot{m}_{out} \tag{8.7}$$

The time rate of change of the mass in the control volume is equal to the rate at which mass flows into the volume minus the rate at which mass flows out of the control volume. This result may seem intuitively obvious but the method used to determine this equation is very powerful and can be used to develop the control volume forms of the other fundamental equations (first and second laws of thermodynamics, Newton's second law of motion, etc.).

Before we extend the analysis to the other physical laws, it is useful to cast the transformation equation, equation (8.5), in terms of the fluid velocities and the density of the fluid. This is very straightforward for the term on the left-hand side of equation (8.5), which is the rate of change of the mass in the control volume. Since the total mass in the control volume is just the integral of the density of the fluid, ρ, over the control volume, we have

$$M_{CV} = \int_{CV} \rho dV \tag{8.8}$$

where dV is the differential volume.

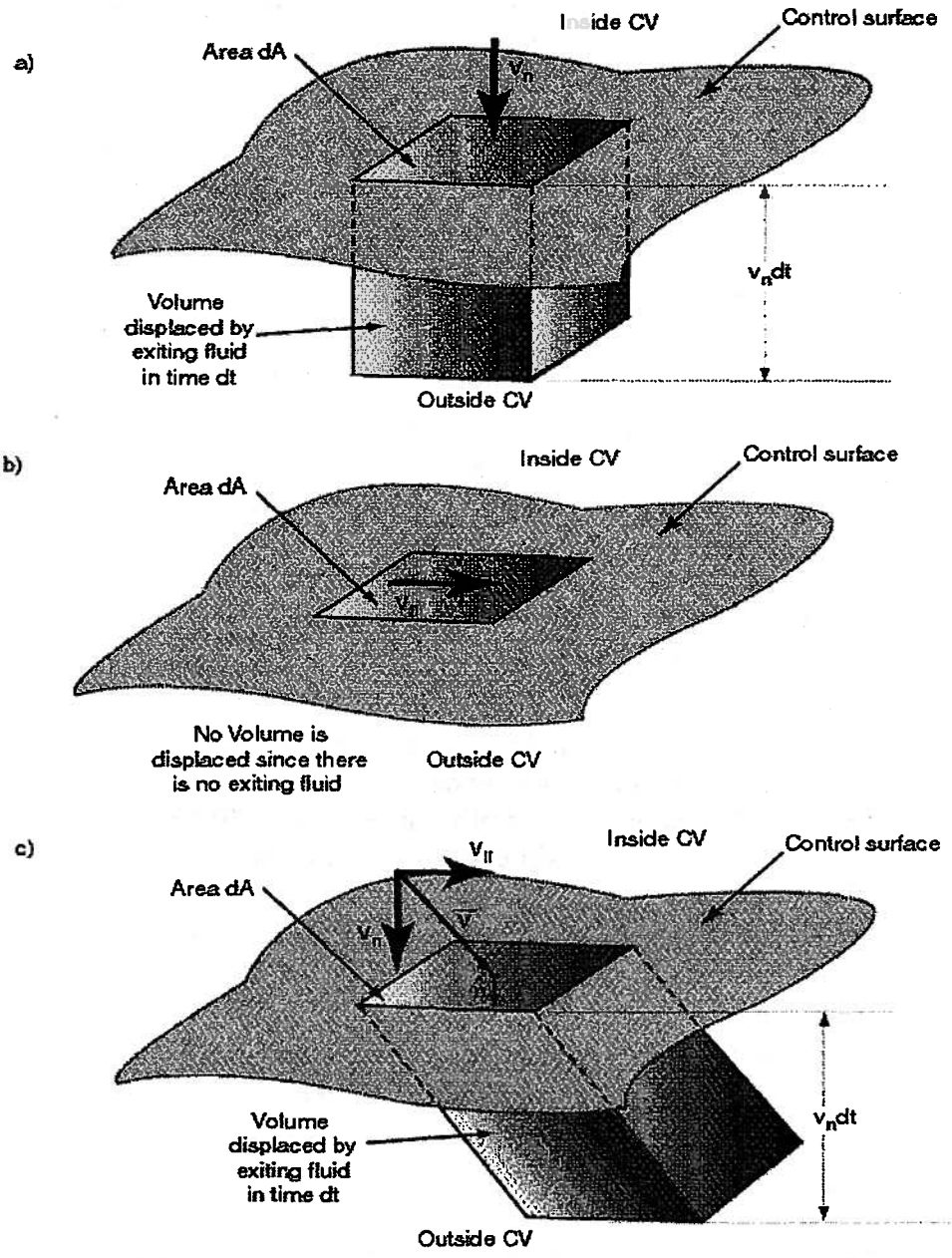

Figure 8.2 Schematic diagram of the flow through a differential area dA

The mass flow rate into and out of the control volume is a little more difficult to express in terms of the fluid density and velocity. Figure 8.2 depicts a portion of the control surface that bounds the control volume. Consider the mass flow in time dt through a differential area dA of the control surface. We presume that the variations in the velocity fields and the curvature of the control surface are negligible on the time and spatial scales of the figure.

Figure 8.2(a) shows the case for which the velocity of the fluid is normal to the control surface. In time dt, the fluid passing through the element of surface area dA travels a distance

$\vartheta_n dt$. The fluid that has passed through the surface must then occupy the volume $dV = \vartheta_n dA dt$. The mass of fluid of density ρ that occupies this volume is then

$$\rho dV = \rho \vartheta_n dt dA = d\dot{m} dt$$

where $d\dot{m}$ is the flow rate of fluid out of the control volume through dA and is given by

$$d\dot{m} = \rho \vartheta_n dA \tag{8.9}$$

Note that ϑ_n is measured in the coordinate system attached to the control volume and, hence, is the velocity normal to the control surface seen by an observer moving with the control volume.

Figure 8.2(b) considers the case where the fluid has a velocity that is parallel to the control surface. In this case no fluid passes through the surface element dA and the mass flow rate across the control surface is zero. Perhaps this conclusion is made easier by considering a person in a room standing before an open window in a rainstorm in which the rain is falling vertically. From the perspective of this person, the observer, the plane of the open window is parallel to the velocity of the raindrops and hence no raindrops enter the room.

Figure 8.2(c) considers the case when there is both a parallel and normal component to the velocity at the position of the surface element. The addition of the parallel component to the normal velocity field serves only to skew the original volume shown in Figure 8.2(a) but does not change its volume. We conclude that the mass flow rate out of the control volume through the surface dA is

$$d\dot{m} = \rho \vartheta_n dA = \rho \left(\vec{\vartheta}_r \cdot \vec{n} \right) dA \tag{8.10}$$

where $\vec{n}$ is the outwardly directed normal to the surface dA. The subscript r on the velocity vector in equation (8.10) is a reminder that the velocity is measured relative to the control surface since the point of observation is fixed to the control volume. We discuss this point further in Example 8.1.

At a given instant of time, the total mass flow rate out of the control volume is just the integral of all the individual values of $d\dot{m}$ over the entire control surface or

$$\dot{m} = \int_{CS} \rho \left(\vec{\vartheta}_r \cdot \vec{n} \right) dA \tag{8.11}$$

Note that this integral is positive when performed over a region of fluid flowing out of the control volume and negative when applied to a region where the fluid is flowing into the control volume. To see this we note that the integral is just a sum of differential elements. The density ρ is always positive and the surface area dA is always positive. The scalar product $\vec{\vartheta}_r \cdot \vec{n}$ is the product of the magnitudes (Recall that magnitudes are always positive.) of the relative velocity vector and the outward unit normal vector multiplied by the cosine of the angle between these vectors. It is the cosine of the angle between the vectors, then, that determines the sign of the mass flow integral. If the integral is performed over a port where the velocity is directed out of the control volume, the angle in question is between 0 and $\pi/2$ and the sign of the cosine is positive. Thus, the integral is also positive. Similarly, if the integral is performed over a surface where the flow is into the control volume, the angle between the velocity vector and the outward normal unit vector is between $\pi/2$ and π, and the sign of the cosine is negative. Thus, in this case the integral is also negative. Finally, if the integral is performed over a surface that has no flow, such as the case when the control surface is coincident with a solid wall, the integral is zero. We see, then, that the integral in equation (8.11) accounts for mass flows both into and out of the control volume. Then the transformation equation, equation (8.5), can be cast as

$$\frac{dM_{CM}}{dt} = \frac{d}{dt}\int_{CV} \rho\, dV + \int_{CS} \rho \left(\vec{\vartheta}_r \cdot \vec{n}\right) dA \tag{8.12}$$

Once again, the time rate of change of the control mass appears on the left-hand side of equation (8.12). The first term on the right-hand side is the time rate of change of the mass in the control volume, and the second term on the right-hand side is the mass flow rate out of the control volume (remember, a negative value indicates a net mass flow rate into the control volume). Since by definition the mass of the control mass is constant, the conservation of mass in the control volume formulation reduces to

$$0 = \frac{d}{dt}\int_{CV} \rho\, dV + \int_{CS} \rho \left(\vec{\vartheta}_r \cdot \vec{n}\right) dA \tag{8.13}$$

In words, equation (8.13) says: "The rate at which the mass accumulates inside the control volume must equal the rate at which the mass 'leaks out' of the control volume."

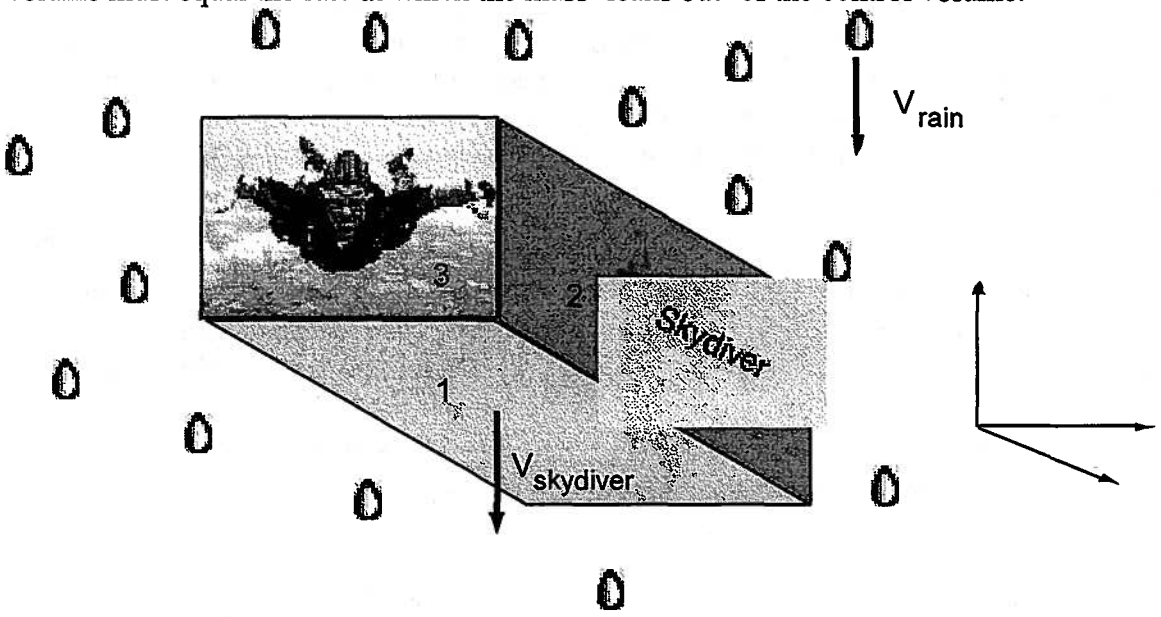

Figure 8E.1 A schematic diagram of a skydiver in a rainstorm

Example 8E.1: A skydiver jumps into a rainstorm and reaches a terminal velocity of 44 m/s as she descends through the rain. As she falls, she presents a cross sectional of 0.25 m^2 normal to the direction of descent. (This is the area of surface 1 in Figure 8E.1 above.) The mass of water in the air per cubic meter is 1 kg.

a) What is the mass of water that strikes the skydiver in a second and in what direction if the terminal velocity of the rain is 44 m/s?

b) What is the mass of water that strikes the skydiver in a second and in what direction if the terminal velocity of the rain is 30 m/s?

c) What is the mass of water that strikes the skydiver in a second and in what direction if the terminal velocity of the rain is 50 m/s?

Solution: a) In case a, the skydiver and the rain are falling with the same velocity. From the perspective of the skydiver the raindrops are stationary and, hence, we would expect that the skydiver does not get wet. The rate of water mass that strikes the skydiver is zero.

Figure 8.3 depicts the skydiver as she falls in the rainstorm. We have depicted her as a box to keep the geometry simple. The relative velocity between the control volume moving with the

skydiver and the raindrops is $\vec{v}_r = 44$ m/sec - 44 m/sec = 0. The conservation of mass equation (8.13) becomes

$$\frac{d}{dt}\int_{CV}\rho\,dV = -\int_{CS}\rho\left(\vec{\vartheta}_r\cdot\vec{n}\right)dA = -\int_{CS}\rho\ (0)\,dA = 0$$

The volume integral is the rate of accumulation of mass in the control volume, the quantity asked for in the problem. The surface integral is zero since there is no net transfer of mass across the surface of the control volume ($\vec{v}_r = 0$). We see from this example that the velocity of the fluid relative to the control volume is the appropriate velocity for determining the volume flux in the surface integral.

(b) In part (b), the skydiver is traveling faster than the rain. This means that the skydiver will catch up to the rain as she falls. The conservation of mass, equation 8.12, requires

$$\frac{d}{dt}\int_{CV}\rho\,dV = -\int_{CS}\rho\left(\vec{\vartheta}_r\cdot\vec{n}\right)dA = -\int_{1}\rho\left(\vec{\vartheta}_r\cdot\vec{n}\right)dA - 2\int_{2}\rho\left(\vec{\vartheta}_r\cdot\vec{n}\right)dA - 2\int_{3}\rho\left(\vec{\vartheta}_r\cdot\vec{n}\right)dA - \int_{top}\rho\left(\vec{\vartheta}_r\cdot\vec{n}\right)dA$$

We have divided up the surface integral into integrals over surfaces 1, 2, 3 and the top surface. The factors of two in front of the integrals for surfaces 2 and 3 account for the fact that there are two of each. The first integral is over surface 1. The density of the water in the air, ρ, is 1kg/m^3. The velocity of the water relative to the skydiver is

$$\vec{\vartheta}_r = \vec{\vartheta}_{rain} - \vec{\vartheta}_{skydiver} = -30\,\vec{k} - (-44\,\vec{k}) = 14\,\vec{k}\ \text{m/sec}$$

where $\vec{k}$ is the unit vector in the upward direction. The outwardly directed normal for the integral over surface 1 is in the negative z-direction or $-\vec{k}$. The integral over surface 1 becomes

$$\int_{1}\rho\left(\vec{\vartheta}_r\cdot\vec{n}\right)dA = \int_{1}(1)\,(14\vec{k})\cdot(-\vec{k})\,dA = -14\int_{1}dA = -(14\ \text{m/sec})(1\ \text{kg/m}^3)(0.25\ \text{m}^2) = -3.5\ \text{kg/sec}$$

This integral tells us that 3.5 kg of water *enters* (hence the negative sign) the control volume through surface 1 in one second. In the integral for surface 2, ρ and $\vec{v}_r$ are the same as for surface 1 and the outwardly directed normal is $\vec{k}$. The surface integral for surface 2 is

$$\int_{2}\rho\left(\vec{\vartheta}_r\cdot\vec{n}\right)dA = \int_{2}(1\ \text{kg/m}^3)\,(14\ \text{m/sec}\,\vec{k})\cdot(\vec{i})\,dA = -(14\ \text{m/sec})\int_{2}\vec{k}\cdot\vec{i}\,dA = -(14\ \text{m/sec})\int_{2}(0)\,dA$$

$$\int_{2}\rho\left(\vec{\vartheta}_r\cdot\vec{n}\right)dA = 0\ \text{kg/sec}$$

Thus, there is no mass flow across surface 2. The integral over surface 3 is evaluated in a similar fashion. The density and relative velocity are unchanged, but the outwardly directed normal is now $-\vec{j}$ and the integral over surface 3 becomes

$$\int_{3}\rho\left(\vec{\vartheta}_r\cdot\vec{n}\right)dA = \int_{3}(1\ \text{kg/m}^3)\,(14\ \text{m/sec}\,\vec{k})\cdot(-\vec{j})\,dA = -(14\ \text{m/sec})\int_{3}\vec{k}\cdot\vec{j}\,dA = -(14\ \text{m/sec})\int_{3}(0)\,dA$$

$$\int_{3}\rho\left(\vec{\vartheta}_r\cdot\vec{n}\right)dA = 0\ \text{kg/sec}$$

Finally, we have the integral over the top surface of the skydiver. We presume that the water striking the skydiver is absorbed by her clothes and that none 'leaks" past the skydiver. In this case the density of the water immediately behind the skydiver is zero. The surface integral for the top surface becomes

$$\int_{top}\rho\left(\vec{\vartheta}_r\cdot\vec{n}\right)dA = \int_{top}(0)\,(14\ \text{m/sec})\left(\vec{k}\cdot\vec{k}\right)dA = (14\ \text{m/sec})\int_{top}(0)\,dA = 0$$

The total water that strikes and is absorbed by her clothes is

$$\frac{d}{dt}\int_{CV}\rho\,dV=-\int_{1}\rho\left(\vec{\vartheta}_r\cdot\vec{n}\right)dA\;-2\int_{2}\rho\left(\vec{\vartheta}_r\cdot\vec{n}\right)dA\;-2\int_{3}\rho\left(\vec{\vartheta}_r\cdot\vec{n}\right)dA-\int_{top}\rho\left(\vec{\vartheta}_r\cdot\vec{n}\right)dA$$

$$\frac{d}{dt}\int_{CV}\rho\,dV=-(-3.5\text{ kg/sec})-2(0)-2(0)-0=3.5\text{ kg/sec}$$

Since all of the water enters through surface 1, we would expect her downward facing surface would be thoroughly wet.

c)We approach this part in exactly the same way as part b. The relative velocities of the rain to the skydiver (the control volume) is

$$\vec{\vartheta}_r=\vec{\vartheta}_{rain}-\vec{\vartheta}_{skydiver}=-(50\text{ m/sec})\vec{k}-(-44\text{ m/sec})\vec{k}=-(6\text{ m/sec})\vec{k}$$

Notice that the relative velocity is in the downward direction. This means that from the perspective of the control volume (the skydiver) the rain is falling in the downward direction. This also means that the water will be entering the control volume through its top surface rather than the bottom surface as in part (b) above. The conservation of mass, equation (8.13), requires

$$\frac{d}{dt}\int_{CV}\rho\,dV=-\int_{CS}\rho\left(\vec{\vartheta}_r\cdot\vec{n}\right)dA=-\int_{1}\rho\left(\vec{\vartheta}_r\cdot\vec{n}\right)dA-2\int_{2}\rho\left(\vec{\vartheta}_r\cdot\vec{n}\right)dA-2\int_{3}\rho\left(\vec{\vartheta}_r\cdot\vec{n}\right)dA-\int_{top}\rho\left(\vec{\vartheta}_r\cdot\vec{n}\right)dA$$

In this case the water is falling faster than the skydiver and the skydiver "shades" surface 1 from the water flow so that the density of water at surface 1 is zero. The integral over surface 1 becomes

$$\int_{1}\rho\left(\vec{\vartheta}_r\cdot\vec{n}\right)dA=\int_{1}(0)\,(-6\text{ m/sec})\left(\vec{k}\cdot-\vec{k}\right)dA=(6\text{ m/sec})\int_{1}(0)\,dA=0\text{ kg/sec}$$

As already shown in part (b), the integrals over surfaces 2 and 3 are zero because their surface normals are orthogonal to the relative velocity. The integral over the top surface is non-zero,

$$\int_{top}\rho\left(\vec{\vartheta}_r\cdot\vec{n}\right)dA=\int_{top}(1\text{ kg/m}^3)\,(-6\text{ m/sec})\left(\vec{k}\cdot\vec{k}\right)dA=-(6\text{ m/sec})\int_{top}dA=-(6\text{ m/sec})(0.25\text{ m}^2)$$

$$\int_{top}\rho\left(\vec{\vartheta}_r\cdot\vec{n}\right)dA=-1.5\text{ kg/sec}$$

The total mass flow rate into the control volume is then

$$\frac{d}{dt}\int_{CV}\rho\,dV=-\int_{1}\rho\left(\vec{\vartheta}_r\cdot\vec{n}\right)dA-2\int_{2}\rho\left(\vec{\vartheta}_r\cdot\vec{n}\right)dA-2\int_{3}\rho\left(\vec{\vartheta}_r\cdot\vec{n}\right)dA-\int_{top}\rho\left(\vec{\vartheta}_r\cdot\vec{n}\right)dA$$

$$\frac{d}{dt}\int_{CV}\rho\,dV=-(0)-2(0)-2(0)-(-1.5\text{ kg/sec})=1.5\text{ kg/sec}$$

In one second, the skydiver's clothes would absorb 1.5 kg of water. Since it is the top surface integral that is negative, the upward surface of the skydiver gets wet.

It should be noted that the terminal velocities assumed for the raindrops in this example are much higher than would ordinarily be observed.

Example 8E.2: As shown in Figure 8E.2, a viscous incompressible fluid enters a circular pipe with a uniform velocity of 1 m/s. By virtue of the action of viscosity in the fluid, the fluid exits the pipe with a parabolic velocity distribution of the form

$$\vec{\vartheta}_{exit} = \vartheta_{max}\left(1-\left(\frac{r}{r_{pipe}}\right)^2\right)\vec{k}$$

where r is the radial coordinate in the pipe and r_{pipe} is the inner radius of the pipe. What is ϑ_{max}, the velocity of the fluid at $r = 0$ at the exit of the pipe?

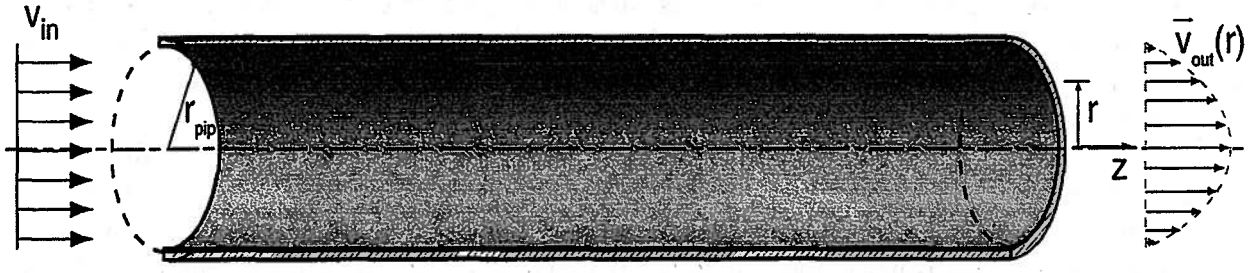

Figure 8E.2 Flow of a Viscous Fluid in a Circular Pipe with Uniform Velocity at Entrance

Solution: We use the conservation of mass equation (also known as the continuity equation) to relate the outgoing flow velocities to the incoming velocities. The first step in the analysis is to choose a control volume. We choose the right circular cylinder defined by the inside of the pipe as the control volume. Since the fluid is incompressible, the density of the fluid is constant. Then, the volume integral in the continuity equation, equation (8.13), simplifies to

$$\frac{d}{dt}\int_{CV}\rho\, dV = \rho\frac{d}{dt}\int_{CV} dV = \rho\left[\frac{d}{dt}\left(V_{pipe}\right)\right] = \rho[0] = 0$$

The time derivative is zero because we recognize that we have chosen a control volume whose volume does not change with time, namely the volume of the pipe.

The surface integral in the continuity equation naturally divides into three separate surface integrals: (1) over the inlet area to the pipe, (2) over the inner surface area of the pipe, and (3) one over the exit area of the pipe. More explicitly, the continuity equation requires

$$0 = \int_{CS}\rho\left(\vec{\vartheta}_r\cdot\vec{n}\right)dA = \int_{inlet}\rho\left(\vec{\vartheta}_r\cdot\vec{n}\right)dA + \int_{\substack{pipe\\surface}}\rho\left(\vec{\vartheta}_r\cdot\vec{n}\right)dA + \int_{outlet}\rho\left(\vec{\vartheta}_r\cdot\vec{n}\right)dA$$

The surface integral over the inlet to the pipe is

$$\int_{inlet}\rho\left(\vec{\vartheta}_r\cdot\vec{n}\right)dA = \rho\int_{inlet}\vartheta_{in}\left(\vec{k}\cdot-\vec{k}\right)dA = -\rho\vartheta_{in}\int_{inlet}dA = -\rho\vartheta_{in}A_{pipe}$$

where A_{pipe} is the cross sectional area of the pipe.

Since there is no flow through the surfaces of the pipe, the velocity component normal to the surface of the pipe must be zero. Then the scalar product of the fluid velocity at the surface of the pipe with the normal to that surface must be zero; hence, the surface integral over the pipe surface area must also be zero.

Finally, there is the surface integral over the exit of the pipe.

$$\int_{outlet}\rho\left(\vec{\vartheta}_r\cdot\vec{n}\right)dA = \int_0^{r_{pipe}}\rho\left\{\vartheta_{max}\left(1-\left(\frac{r}{r_{pipe}}\right)^2\right)\vec{k}\right\}\cdot\vec{k}\;(2\pi r)\,dr = 2\pi\rho\vartheta_{max}\int_0^{r_{pipe}}\left(1-\left(\frac{r}{r_{pipe}}\right)^2\right)r\,dr$$

$$\int_{outlet}\rho\left(\vec{\vartheta}_r\cdot\vec{n}\right)dA = \frac{1}{2}\rho\vartheta_{max}\pi r_{pipe}^2 = \frac{1}{2}\rho\vartheta_{max}A_{pipe}$$

Substituting all these results into the continuity equation, we get

$$0 = \frac{1}{2}\rho \vartheta_{max} A_{pipe} - \rho \vartheta_{in} A_{pipe}$$

$$\vartheta_{max} = 2\vartheta_{in} = 2 \text{ m/sec}$$

Thus, the maximum velocity in the parabolic velocity distribution for viscous flow in a pipe is just twice the average velocity of the flow. As we shall see later in our discussion of viscous flows, this parabolic velocity distribution results only under certain flow conditions. Once these conditions are no longer valid, the parabolic velocity distribution gives way to a more complex velocity distribution.

Example 8E.3: As shown in Figure 8E.3, a large rectangular tank is filled with water with density ρ_{water} = 1000 kg/m^3. The inlet mass flow rate is $\dot{m}_1$ = 1 kg/sec. At some instant, the mass flow rate in drain 2 is $\dot{m}_2$ = 0.45 kg/sec and in drain 3 is $\dot{m}_3$ =0.5 kg/sec. At this same instant, the depth of the water in the tank is H = 0.5 meters. If the length of the tank is L = 10 m and the width is W = 2 m, at what rate does the water surface rise in the tank?

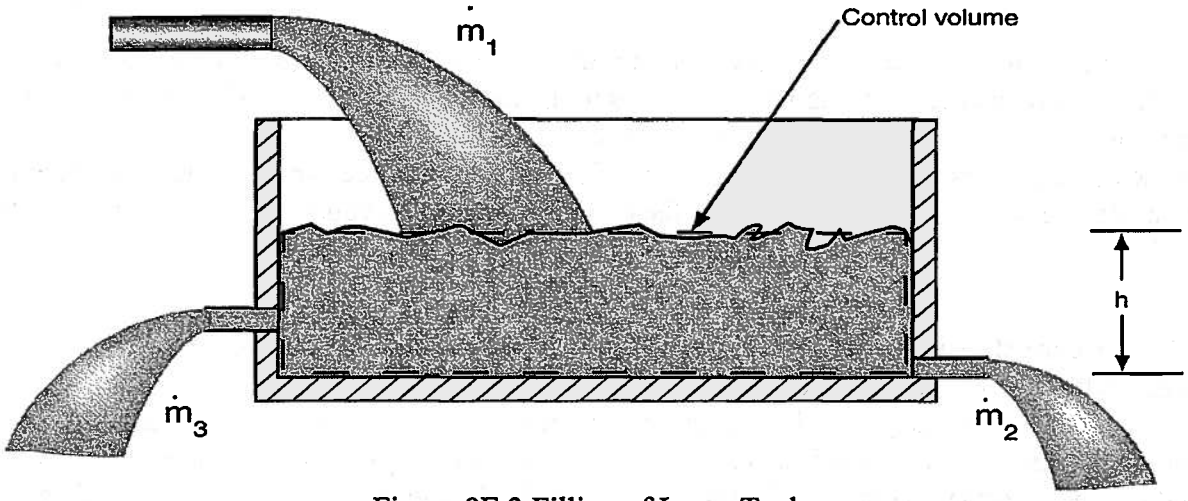

Figure 8E.3 Filling of Large Tank

Solution: The continuity equation can be applied using the control volume shown in Figure 8E.3. The upper surface of the control volume moves with and corresponds to the top surface of the water in the tank. Once again, the continuity equation is given by

$$0 = \frac{d}{dt}\int_{CV} \rho \, dV + \int_{CS} \rho \left(\vec{\vartheta}_r \cdot \vec{n}\right) dA$$

The surface integral can be broken up into five terms corresponding to different parts of the control surface,

$$\int_{CS} \rho \left(\vec{\vartheta}_r \cdot \vec{n}\right) dA =$$

$$\int_1 \rho \left(\vec{\vartheta}_r \cdot \vec{n}\right) dA + \int_2 \rho \left(\vec{\vartheta}_r \cdot \vec{n}\right) dA + \int_3 \rho \left(\vec{\vartheta}_r \cdot \vec{n}\right) dA + \int_{\substack{tank \\ surface}} \rho \left(\vec{\vartheta}_r \cdot \vec{n}\right) dA + \int_{\substack{free \\ surface}} \rho \left(\vec{\vartheta}_r \cdot \vec{n}\right) dA$$

The first integral 0n the right-hand side is over the area where the water flow 1 enters the control volume. Since the scalar product between the fluid velocity and the outward normal is negative, the value of this integral is -$\dot{m}_1$. The second and third integrals are over ports 2 and 3 and have values of $\dot{m}_2$ and $\dot{m}_3$, respectively. The fourth integral is over the surfaces of the tank. Since the

tank surfaces are non-porous, the velocity of the water normal to the walls must be zero. The fourth surface integral must then be zero. The final surface integral is over the free surface of the water. Since the control volume moves with the water on the free surface, the relative velocity between the water and the control surface is zero; hence, the scalar product between the surface normal and the relative velocity is zero. Consequently, the final surface integral is zero. Thus,

$$\int_{CS} \rho \left(\vec{\vartheta}_r \cdot \vec{n}\right) dA = -\dot{m}_1 + \dot{m}_2 + \dot{m}_3 + 0 + 0 = -\dot{m}_1 + \dot{m}_2 + \dot{m}_3$$

If we model the water as incompressible, the volume integral becomes

$$\frac{d}{dt}\int_{CV} \rho\, dV = \rho \frac{d}{dt}\int_{CV} dV = \rho \frac{d}{dt} LWH = \rho LW \frac{dH}{dt}$$

The quantity we seek is *dH/dt*. Substituting the last two results into the continuity equation and collecting terms results in

$$\frac{dH}{dt} = \frac{\dot{m}_1 - \dot{m}_2 - \dot{m}_3}{\rho LW} = \frac{(1 \text{ kg/sec}) - (0.45 \text{ kg/sec}) - (0.5 \text{ kg/sec})}{(1000 \text{ kg/m}^3)(10 \text{ m})(2 \text{ m})} = 2.50 \text{ x } 10^{-6} \text{ m/sec}$$

At this rate, it would take 400 sec to increase the depth of the tank one millimeter.

8.3 Reynolds Transport Theorem

In section 8.2, in the context of performing an accounting of the mass of fluid in a control volume, we developed a transformation equation, equation (8.5), that enabled us to take our knowledge of the time dependent behavior of the mass of a control mass and apply it to a control volume. In effect, it enabled us to shift from the Lagrangian approach which is convenient for determining the behavior of systems of fixed identity to the Eulerian approach which is convenient for determining the time course of events that transpire in a region of space. We now generalize this transformation equation so that it might be applied to any extensive property (*cf.* Section 1.6.4) of a control mass. This generalization is known as the *Reynolds Transport Theorem* and is named for a British mechanical engineer, Osborne Reynolds (1842 - 1912), who made many important contributions to our fundamental knowledge of the behavior of fluid systems. The work of Reynolds greatly accelerated the development of thermal-fluid systems components for energy conversion in the early years of the 20th century, and we shall have extensive recourse to his work in subsequent developments of the behavior of thermal-fluids systems.

Although we have already developed the transformation equation for mass, the Reynolds Transport Theorem is a general expression from which we can formulate the particular forms of the transformation equation for the extensive properties energy, entropy, linear momentum, and angular momentum. Because it is general in nature, it must also apply to mass. Suppose we let B represent any of these extensive properties and b represent the associated mass specific quantity where $b = B/M$. For example, in the case for which mass is the extensive property, B becomes M and the mass specific quantity becomes $b = M/M = 1$. Similarly, in the case of linear momentum, B is $M\vec{v}$ and $b = M\vec{v}/M = \vec{v}$. To establish the form of the Reynolds Transport Theorem, we simply repeat the procedure of Section 8.2 for this general extensive property B.

Figure 8.1a shows the fluid flow through a control volume at time t. Because B is extensive, the total value of B is just the sum of all the values of B for the contributing parts. Then

$$B_{CV}(t) = B_{CM}(t) - B_1 \tag{8.14}$$

Similarly for time $t + \Delta t$ [*cf.* Figure 8.1 (b)], we have

$$B_{CV}(t+\Delta t) = B_{CM}(t+\Delta t) - B_2 - B_3 \tag{8.15}$$

The time rate of change of the property B in the control volume is defined as

$$\frac{dB_{CV}}{dt} \equiv \lim_{\Delta t \to 0} \frac{B_{CV}(t+\Delta t) - B_{CV}(t)}{\Delta t} \tag{8.16}$$

Combining equations (8.14), (8.15), and (8.16), we get

$$\frac{dB_{CV}}{dt} = \lim_{\Delta t \to 0} \frac{B_{CM}(t+\Delta t) - B_{CM}(t)}{\Delta t} + \lim_{\Delta t \to 0} \frac{B_1(t+\Delta t) - B_1(t)}{\Delta t} - \lim_{\Delta t \to 0} \frac{B_2(t+\Delta t) - B_2(t)}{\Delta t} - \lim_{\Delta t \to 0} \frac{B_3(t+\Delta t) - B_3(t)}{\Delta t}$$

which becomes in the limit

$$\frac{dB_{CM}}{dt} = \frac{dB_{CV}}{dt} - \sum_{in} \dot{B} + \sum_{out} \dot{B} \tag{8.17}$$

where $\dot{B}$ is the flow rate of B that flows into or out of the control volume.

We now would like to cast equation (8.17) into a more general form in the same way we cast equation (8.5) into the more general form equation(8.11). The first term on the right-hand-side of equation (8.17) is the time derivative of B in the control volume. Since B is extensive, the total B is the sum of all the values of dB associated with each of the differential volumes in the control volume. Thus

$$B_{CV} = \int_{CV} \rho b \, dV \tag{8.18}$$

The terms associated with the mass flow into and out of the control volume can be handled in the same way as before. The mass that flows through the control surface in time dt through surface dA is, as before,

$$d\dot{m}dt = \rho \vartheta_n dA dt = \rho \left(\vec{\vartheta}_r \cdot \vec{n} \right) dA dt$$

The flow of B associated with this mass flow is just b times this quantity

$$d\dot{B}dt = b \, d\dot{m}dt = \rho b \left(\vec{\vartheta}_r \cdot \vec{n} \right) dA dt$$

Then the flow rate of B is given by

$$d\dot{B} = b d\dot{m} = \rho b \left(\vec{\vartheta}_r \cdot \vec{n} \right) dA \tag{8.19}$$

The net flow of B out of the control volume is calculated by integrating over the entire surface of the control volume. Since the integral naturally assigns a positive sign for outflows and a negative sign for inflows, we find

$$\sum_{out} \dot{B} - \sum_{in} \dot{B} = \int_{CS} \rho b \left(\vec{\vartheta}_r \cdot \vec{n} \right) dA \tag{8.20}$$

Combining equations (8.17), (8.18), and (8.20), we get

$$\frac{dB_{CM}}{dt} = \frac{d}{dt} \int_{CV} \rho b \, dV + \int_{CS} \rho b \left(\vec{\vartheta}_r \cdot \vec{n} \right) dA \tag{8.21}$$

This is the *Reynolds Transport Theorem* that provides an expression for the transformation of a time derivative of an extensive property in a control mass system to a set of expressions in a control volume approach. We can now use this expression to transform the physical laws that we know for a control mass into the equivalent form for a control volume. The first term on the

right-hand-side of equation (8.21) is the time rate of change of the property B in the control volume. The second term accounts for the variation in the property B due to the flow of B across the control surface that encloses the control volume.

If we have indeed formulated the Reynolds Transport Theorem properly, we should be able to generate the conservation of mass equation that we derived earlier. In this case, as we stated previously, $B = M$ and $b = M/M = 1$. Substituting these quantities into the Reynolds Transport Theorem, equation (8.21), and recognizing dM_{CM}/dt has the value of zero for the control mass system, we find

$$\frac{dM_{CM}}{dt} = \frac{d}{dt}\int_{CV} \rho\, dV + \int_{CS} \rho\left(\vec{\vartheta}_r \cdot \vec{n}\right) dA = 0 \tag{8.22}$$

which is the expression we derived earlier for the conservation of mass from the control volume viewpoint, equation (8.12).

8.4 The First Law of Thermodynamics for the Control Volume

The first law of thermodynamics is a phenomenological statement of the effect that energy interactions between a system and its environment have on the system itself. For the case of a control mass experiencing an energy interaction that results in a finite change of state of the mass, we have already expressed the first law in the form [*cf.* equation (2.3)]

$$Q - W = \left(E_2 - E_1\right) \tag{8.23}$$

If we are interested in the rate at which the state is changing as a consequence of the energy interactions, we can write equation (8.24) in the form

$$\dot{Q} - \dot{W} = \frac{dE_{CM}}{dt} \tag{8.24}$$

which applies at any instant of time.

If we now allow mass to cross the system boundary, the system becomes an open system, and the mass crossing the system boundary carries energy. This gives rise to a whole host of energy interactions that were not possible for the control mass. To account for these energy interactions, we make use of the control volume approach. The transformation from control mass to control volume is accomplished with the aid of the Reynolds Transport Theorem in the form of equation (8.21). Since the first law of thermodynamics is concerned with energy, $B = E$ and $b = E/M = e$. Then the right-hand-side of equation (8.24) can be expressed in the form

$$\frac{dE_{CM}}{dt} = \frac{d}{dt}\int_{CV} \rho e\, dV + \int_{CS} \rho e\left(\vec{\vartheta}_r \cdot \vec{n}\right) dA \tag{8.25}$$

Combining equations (8.24) and (8.25), we get

$$\dot{Q} - \dot{W} = \frac{d}{dt}\int_{CV} \rho e\, dV + \int_{CS} \rho e\left(\vec{\vartheta}_r \cdot \vec{n}\right) dA \tag{8.26}$$

Equation (8.26) is the simplest form of the first law of thermodynamics as it applies to a control volume. The first term on the right side of equation (8.26) is the rate at which energy accumulates within the control volume as a result of heat transfer and work transfer energy interactions across the control surface [the left-hand-side of equation (8.26)] and the net energy flowing out of the control volume with the mass crossing the control surface [the second term on the right-hand-side of equation (8.26)].

As we discussed in Chapter 2, Section 2.3, there are several energy storage modes that are important in a thermal-fluid system of unit mass. In addition to the kinetic energy storage mode, $\mathcal{V}^2/2$, and the gravitational potential energy storage mode, gz, there is the thermal energy storage mode for an incompressible fluid model and the internal energy storage mode for the ideal gas model, both of which can be represented by the symbol u. Then

$$e = u + \frac{\mathcal{V}^2}{2} + gz \tag{8.27}$$

Then equation (8.26) can be written

$$\frac{d}{dt}\int_{CV} \rho\left(u + \frac{\mathcal{V}^2}{2} + gz\right)dV = \dot{Q} - \dot{W} - \int_{CS} \rho\left(u + \frac{\mathcal{V}^2}{2} + gz\right)\left(\vec{\mathcal{V}}_r \cdot \vec{n}\right)dA \tag{8.28}$$

As we stated above, the flow of energy associated with the mass flow into and out of the control volume leads to additional energy interactions that were not present in the case of the control mass. These interactions manifest themselves most readily in the form of work transfers. Therefore, it is necessary to expand the work transfer term appearing in equation (8.28) to account for these interactions. As mass moves across the control surface, it is acted upon by normal stresses (pressure) and shear stresses (either due to shear in a solid or due to viscous shear in a fluid) present at the control surface. Since the mass at the boundary where these forces act is in motion, we have the essential elements of a work transfer, namely, a force acting on a boundary and a displacement of that boundary in response to the force. We can then separate the rate of work transfer into three identifiable components: (1) $\dot{W}_p$ due to pressure acting on the mass in motion at the ports of entry and exit; (2) $\dot{W}_{shaft}$ due to shear stresses acting on solid elements in motion at the control surface (usually a shaft that pierces the control surface and is used to drive, or be driven by, some sort of shaft-work machine inside the control volume); and (3) $\dot{W}_{\substack{fluid\\shear}}$ due to shear stresses arising from the action of viscosity in the fluid. Then

$$\dot{W} = \dot{W}_p + \dot{W}_{shaft} + \dot{W}_{\substack{fluid\\shear}} \tag{8.29}$$

The first term on the right-hand-side of equation (8.29) is known as the *rate of flow work transfer* and originates with the work transfer experienced by the fluid as it enters or leaves the control volume as shown in Figure 8.3. From the point of view of the fluid in the control mass and the control volume, the situations depicted in Figures 8.1 and 8.3 are entirely equivalent. In Figure 8.3 the fluid ahead of and behind the control mass has been replaced by imaginary pistons. The rate of work transfer term in equation (8.26) is the rate of work transfer experienced by the control mass. Since the fluid at each of the ports exerts a pressure locally on its respective piston that is different from zero, this fluid will experience a work transfer associated with the displacement of its respective piston as the piston moves in response to the applied pressure during the process that takes place in the control mass during the time interval from t to $t + \Delta t$. For example, the magnitude of the flow work transfer for the piston in port B during the time interval Δt is

$$W_B = -F_B dx_B = P_B A_B dx_B = P_B dV_B = P_B \frac{dM_B}{\rho_B} = (Pv)_B dM_B \tag{8.30}$$

where the subscript B refers to port B and v is the specific volume, $v = 1/\rho$. Then, in the limit as $\Delta t \to 0$, the instantaneous rate of flow work transfer at port B becomes

$$\dot{W}_B = (Pv)_B \frac{dM_B}{dt} = \dot{m}_B (Pv)_B \tag{8.31}$$

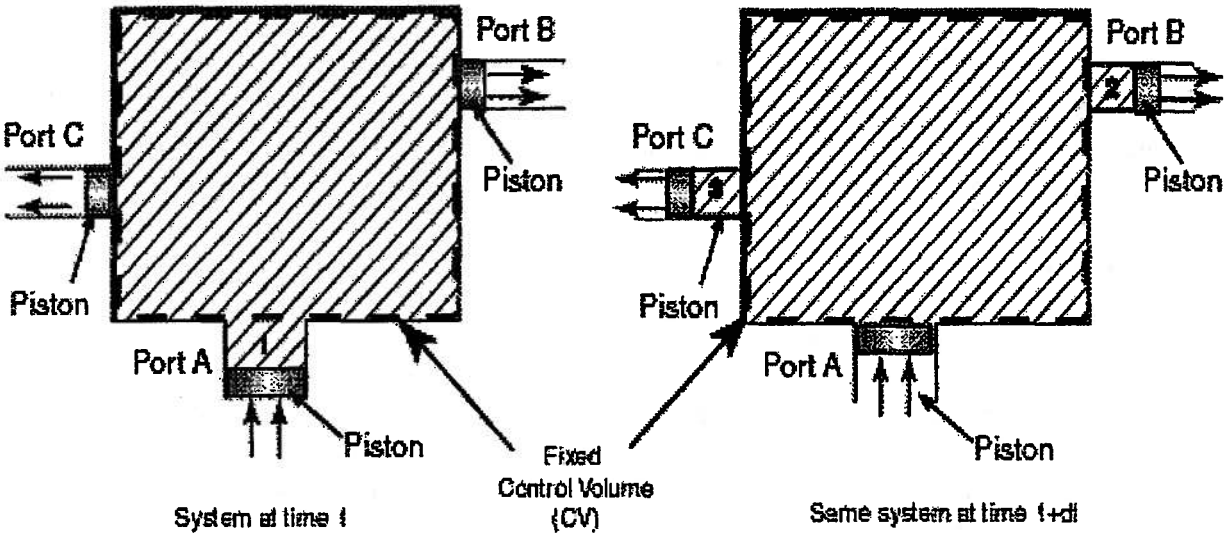

Figure 8.3 Mass Flow in the Control Volume

Thus, the local rate of flow work transfer due to the flow of a fluid across a control surface is equal to the product of the local mass flow rate, the local pressure and the local specific volume of the fluid. Using the equivalent expressions for the rates of flow work transfer for the other ports, we can find the instantaneous net rate of flow work transfer for the control mass to be

$$\dot{W}_P = \dot{m}_B P_B v_B + \dot{m}_C P_C v_C - \dot{m}_A P_A v_A = \sum_{out} (\dot{m} P v)_{out} - \sum_{in} (\dot{m} P v)_{in} \tag{8.32}$$

where we have extended the result to a general control volume with a finite number of mass flow ports with the summation in each case over all exit ports and entry ports, respectively.

In the limit of an infinite number of ports, each of infinitesimal cross-sectional area dA_i, the summation in equation (8.32) becomes an integral over the control surface. Thus,

$$\dot{W}_P = \int_{CS} \rho (Pv) \left(\vec{\vartheta}_r \cdot \vec{n} \right) dA \tag{8.33}$$

Note that for regions of mass inflow, the integral is negative because the scalar product of the velocity and the outwardly directed normal is negative.

The second term on the right-hand-side of equation (8.29) applies to those regions where the control surface is pierced by a shaft that is used to drive, or be driven by, some sort of shaft-work machine inside the control volume. A torque on the shaft produces a shear stress on any plane normal to the axis of rotation of the shaft, and since this plane is in motion in the direction in which these stresses act, a shaft work transfer results. The rate of shaft work transfer is then the product of the shear stresses integrated over the plane, i.e., the torque, and the velocity of rotation in the plane.

The third term on the right-hand-side of equation (8.29) is due to the action of viscosity in the fluid. For fluid in the vicinity of a solid wall, the viscosity produces a velocity gradient in the fluid. For the Newtonian fluid model (to be discussed subsequently), the product of the local velocity gradient in the fluid and the viscosity determines the local shear stress acting on the fluid particles in the plane where the velocity gradient was evaluated. If the fluid particles are in motion, we have all the essential ingredients for a work transfer. A force acting on a boundary, and a displacement of that boundary in response to the force. However, according to the Newtonian fluid model, the fluid right at a solid boundary has the same velocity as the boundary

(This is known as the no-slip boundary condition.). Then, if we locate the control surface coincident with a solid surface that is stationary, there is no work transfer since there is no displacement of the boundary even though there is a force acting on that boundary. Under these conditions, the third term on the right-hand-side of equation (8.29) vanishes. Note, however, that this term does not vanish if the control surface is located on a plane where the fluid is in motion.

Then combining equations (8.28), (8.29), and (8.33), we get a new form for the first law of thermodynamics for a control volume, namely,

$$\frac{d}{dt}\int_{CV}\rho\left(u+\frac{\vartheta^2}{2}+gz\right)dV=\dot{Q}-\dot{W}_{shaft}-\int_{CS}\rho\left(u+Pv+\frac{\vartheta^2}{2}+gz\right)\left(\vec{\vartheta}_r\cdot\vec{n}\right)dA \tag{8.34}$$

The quantity on the left-hand-side of equation (8.34) is the instantaneous time rate of change of the energy inside the control volume (dE_{CV}/dt). According to the first law, this rate of change of energy within the control volume is equal to the net rate of heat transfer into the control volume less the rate at which shaft work transfer crosses the control surface less the rate at which energy is convected out of the control volume by the mass flow across the control surface. The convection term now has an additional contribution due to the flow work experienced by the fluid particles as they enter and exit the control volume.

The combination of properties $u + Pv$ appearing in equation (8.34) is itself a property that appears frequently in the analysis of thermal-fluid systems and is known as the specific enthalpy, h. The enthalpy, H, of a given mass of fluid is defined as

$$H=U+PV \tag{8.35}$$

where U is the internal energy of that mass of fluid, P is the pressure in the fluid and V is the volume of that mass of fluid. Then with the aid of equation (8.35), equation (8.34) becomes

$$\frac{d}{dt}\int_{CV}\rho\left(u+\frac{v^2}{2}+gz\right)dV=\dot{Q}-\dot{W}_{shaft}-\int_{CS}\rho\left(h+\frac{v^2}{2}+gz\right)\left(\vec{\vartheta}_r\cdot\vec{n}\right)dA \tag{8.36}$$

or for the case of a finite number of ports on the control surface we can write the same equation in the form of the mass flows through ports and the total energy in the control volume, E_{CV},

$$\frac{dE_{CV}}{dt}=\dot{Q}-\dot{W}_{shaft}+\sum_{in}\dot{m}_{in}\left(h+\frac{\vartheta^2}{2}+gz\right)_{in}-\sum_{out}\dot{m}_{out}\left(h+\frac{\vartheta^2}{2}+gz\right)_{out} \tag{8.37}$$

Equations (8.36) and (8.37) are the forms of the first law that we shall use most frequently in the analysis of thermal-fluids systems.

Example 8E.4: A pump is used to pump water out of a well and into a storage tank as shown in the Figure 8E.4. The pressure in the storage tank is maintained at a constant absolute pressure of $5\text{x}10^5$ Pa using a flexible membrane (sometimes referred to as a bladder) and a large volume of air as shown. The pump is placed 100 m below the surface of the earth. Assume that the temperature of the water entering the pump is the same as the temperature of the water entering the storage tank. Assume that all heat transfers are negligible.

a) How much electrical power is required to pump water into the storage tank at a volumetric rate of 7 liters/min if the water surface is 50 m below the surface of the earth?

b) How much electrical power is required if the water surface is at the surface of the earth itself?

Solution: (a) The first step in analyzing a thermal-fluid system such as this in all these problems is to choose a control volume. We have chosen the control volume shown as a dashed line in Figure 8E.4. We will assume that the vertical dimensions of all the objects, except for the

depth of the well and the water level in the well are unimportant. (The typical vertical dimension in the tank and of the pump is 1 meter, which is small compared to the depth of the well.) We will also assume that the pump is in steady operation and that the water level in the well remains constant in time.

We can apply the continuity equation to the control volume

$$0 = \frac{d}{dt}\int_{CV} \rho\, dV + \int_{CS} \rho\left(\vec{\vartheta}_r \cdot \vec{n}\right) dA = \frac{d}{dt}\int_{CV} \rho\, dV - \dot{m}_{well} + \dot{m}_{tank}$$

where $\dot{m}_{well}$ is the mass flow rate of water into the pump and $\dot{m}_{tank}$ is the mass flow rate into the tank. The volume integral can be separated into the sum of integrals over areas where the density does not change or

$$\frac{d}{dt}\int_{CV} \rho\, dV = \frac{d}{dt}\int_{water} \rho_w\, dV + \frac{d}{dt}\int_{plastic} \rho_p\, dV + \frac{d}{dt}\int_{air} \rho_{air}\, dV + \frac{d}{dt}\int_{metal} \rho_m\, dV$$

These four integrals are integrals over the volumes in the control volume that contain water ($\rho = \rho_w$), plastic ($\rho = \rho_p$), air ($\rho = \rho_{air}$) and metal ($\rho = \rho_m$). Because the densities appearing in each of

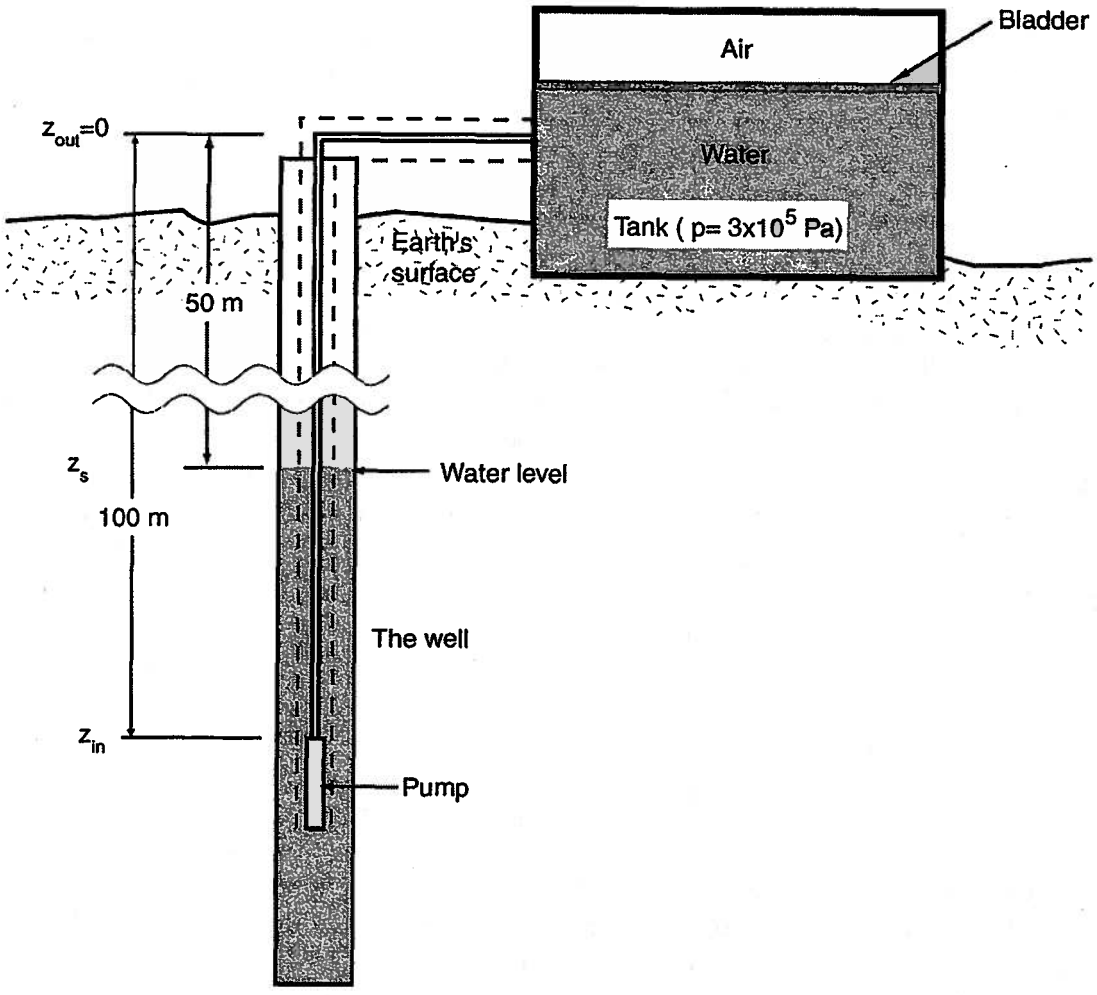

Figure 8E.4 Artesian Well

the integrals are now constant, we can take the density outside of each integral and perform the integration. The volume integral then becomes

$$\frac{d}{dt}\int_{CV}\rho_w\,dV=\frac{d}{dt}\left[\rho_w V_w+\rho_p V_p+\rho_{air}V_{air}+\rho_m V_m\right]=0$$

where V_w, V_p, V_{air}, and V_m are the volumes of the water, plastic, air and metal inside the control volume, respectively. Since the densities and the volumes of all these quantities are constant inside the control volume, the time derivative of these quantities is zero. (The pump is in steady operation and the level of water in the well is not changing).

The continuity equation becomes

$$\dot{m}_{well}=\dot{m}_{tank}$$

That is, the mass flow rate into the pump is the same as the mass flow rate into the tank. The mass flow rate can be computed from the volumetric flow rate, $\dot{V}$, given in the problem statement,

$$\dot{m}=\dot{m}_{well}=\dot{m}_{tank}=\rho_w\dot{V}=(1000\text{ kg/m}^3)\frac{(7\text{ x }10^{-3}\text{ m}^3/\text{min})}{60\text{ sec/min}}=0.117\text{ kg/sec}$$

If we assume that the electric motor converts electric power into shaft power with an efficiency of 100%, it is the rate of shaft work transfer that will provide the information we seek. Then, the first law in the form of equation (8.37) can be simplified because there are no heat transfers and there are only two ports where mass flows across the control surface.

$$\frac{dE_{CV}}{dt}=-\dot{W}_{shaft}+\dot{m}\left(h+\frac{\vartheta^2}{2}+gz\right)_{in}-\dot{m}\left(h+\frac{\vartheta^2}{2}+gz\right)_{out}$$

The left-hand-side of the first law is the time derivative of the volume integral of the energy in the control volume. In steady flow, this term vanishes because in steady flow, the system inside the control volume looks exactly the same from one instant in time to another even though different fluid particles occupy different spaces from one instant to the next. However, as a fluid particle moves from one location to another and assumes a new position in the control volume, it assumes all the properties of the fluid particle that previously occupied that position, including the enthalpy, velocity and elevation. Since the total energy in the control volume is just a sum of the energies of the fluid particles, the total internal energy is constant in time for the steady flow case or

$$\frac{dE_{CV}}{dt}\equiv\frac{d}{dt}\int_{CV}\rho\left(u+\frac{v^2}{2}+gz\right)dV=0$$

Then the first law reduces to

$$\dot{W}_{shaft}=\dot{m}\left(h+\frac{\vartheta^2}{2}+gz\right)_{in}-\dot{m}\left(h+\frac{\vartheta^2}{2}+gz\right)_{out}$$

The inflow is at the pump suction port and the outflow is at the inlet port of the tank. From the point of view of good design practice, the fluid velocities at these ports are kept low at these places to avoid unnecessarily high dissipation. We will assume here that the fluid velocities are small enough so that the kinetic energy of the fluid in these locations is negligible. Since the specific enthalpy, h, is the sum of the specific internal energy of the fluid particle and the product of the local pressure and the specific volume, and since the water can be modeled as an incompressible fluid, we can write

$$h=u+Pv=c\left(T-T_0\right)+Pv$$

where we have made use of the energy constitutive relation for the incompressible fluid. The temperature T_0 is an arbitrary reference temperature. Note that for an incompressible fluid the specific volume, v, is a constant. Then for the present case, the first law becomes

$$\dot{W}_{shaft} = \dot{m}c(T_{in} - T_{out}) + \dot{m}v(P_{in} - P_{out}) + \dot{m}g(z_{in} - z_{out})$$

As we shall show in the section 8.5, the first term on the right-hand-side of this expression is associated with dissipation due to viscosity in the fluid. If we assume that the fluid has negligible viscosity, there is no dissipation and this term vanishes. In the present case, we were given information that the fluid temperature is the same at the inlet and the outlet of the control volume. Thus, the first term does indeed vanish in the present case.

The second term on the right-hand-side is the flow work term. It is the rate of work transfer associated with drawing fluid into the pump at pressure P_{in} and forcing the fluid into the tank at pressure P_{out}. The pressure in the tank is known but we need to determine the pressure at the suction port of the pump. Since we have assumed that all the velocities in the well are small, we can use fluid statics to determine the pressure at the suction port of the pump. Since the air immediately above the surface of the water in the well is at atmospheric pressure, P_{atm}, the inlet pressure to the pump is

$$P_{in} = P_{atm} + \rho_w g(z_s - z_{in})$$

where z_{in} = -100 m is the depth of the pump and z_s = -50 m is the depth of the water surface in the well.

The final term on the right-hand-side of the first law is the rate of work transfer necessary to raise the water from the pump to the tank against gravity. Since the specific volume is just the reciprocal of the density, we find the power necessary to drive the pump is

$$\dot{W}_{shaft} = \dot{m}v(P_{atm} + \rho_w g(z_s - z_{in}) - P_{out}) + \dot{m}g(z_{in} - z_{out}) = \dot{m}\left(\frac{P_{atm} - P_{out}}{\rho_w}\right) + \dot{m}g(z_s - z_{out})$$

Notice that the pump depth is immaterial to the power required to pump the fluid; only the level of the water surface is of consequence. The shaft power, i.e., the rate of shaft work transfer, necessary to pump 7 L/sec of water out of a well with a water level 50 m below the surface of the earth is

$$\dot{W}_{shaft} = \dot{m}\left[\left(\frac{P_{atm} - P_{out}}{\rho_w}\right) + g(z_s - z_{out})\right]$$

$$\dot{W}_{shaft} = (0.117 \text{ L/sec})\left[\left(\frac{10^5 \text{ N/m}^2 - 5 \text{ x } 10^5 \text{ N/m}^2}{1000 \text{ kg/m}^3}\right) + (9.81 \text{ m/sec}^2)(-50 \text{ m} - 0 \text{ m})\right] = -104 \text{ W}$$

(b) For the case in which the water surface is a the surface of the earth, we find

$$\dot{W}_{shaft} = \dot{m}\left[\left(\frac{P_{atm} - P_{out}}{\rho_w}\right) + g(z_s - z_{out})\right]$$

$$\dot{W}_{shaft} = (0.117 \text{ L/sec})\left[\left(\frac{10^5 \text{ N/m}^2 - 5 \text{ x } 10^5 \text{ N/m}^2}{1000 \text{ kg/m}^3}\right) + (9.81 \text{ m/sec}^2)(-0 \text{ m} - 0 \text{ m})\right] = -46.8 \text{ W}$$

Since the results for both parts (a) and (b) are negative, the work transfer is into the pump. The large difference between these results shows that a large portion of the work transfer in part (a) is necessary to overcome the gravitational potential energy change of the water.

Example 8E.5: A steady-flow coaxial heat exchanger is shown in Figure 8E.5. This heat exchanger is used to cool a hot oil stream from a large internal combustion engine. The oil

travels through the inner pipe and cooling water travels in the annulus between the outer and inner pipes. If the inlet and outlet temperatures are as shown and the mass flow rate of the oil is 0.2 kg/sec, determine the mass flow rate of the water.

The oil and the water can be modeled as incompressible fluids. The specific heat of the oil is c_{oil} = 2000 J/kg-K and its density is ρ_{oil} = 800 kg/m^3, and the specific heat of the water is c_w = 4300 J/kg-K and its density is ρ_w = 1000 kg/m^3. The pressure difference between the inlet and outlet in each stream can be considered to be zero.

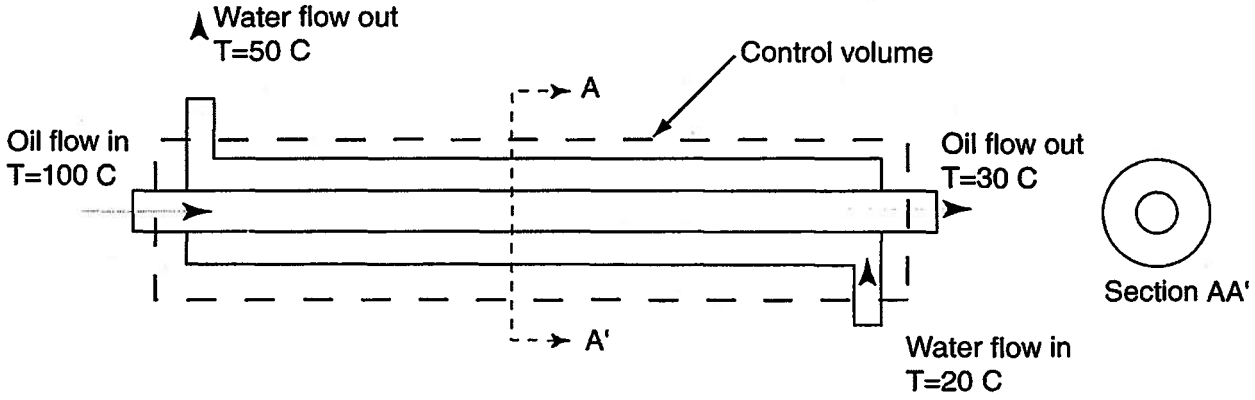

Figure 8E.5 Steady-flow Coaxial Heat Exchanger

Solution: The control volume is shown in Figure 8E.5. Since the heat exchanger is of moderate physical size and since the fluids must be flowing slow enough so that the two fluids can approach thermal equilibrium with one another, we assume that the gravitational effects and the velocities are negligible for this situation. For this control volume the first law becomes

$$\frac{dE_{CV}}{dt} = \dot{Q} - \dot{W}_{shaft} + \dot{m}_{oil}\left(h_{in,oil} - h_{out,oil}\right) + \dot{m}_w\left(h_{in,w} - h_{out,w}\right)$$

We assume that the heat transfer through the control surface is negligible so that $\dot{Q}$ = 0 for this control volume. There are very substantial heat transfers between the fluids within the control volume, but these heat transfers do not appear in the first law because they do not cross the control surface. Since the flow is steady, we conclude that the term dE_{cv}/dt is zero. There are no rotating shafts or electric wires penetrating the control surface so that the rate of shaft work transfer must be zero. Then the first law becomes

$$\dot{m}_w = -\dot{m}_{oil}\frac{h_{in,oil} - h_{out,oil}}{h_{in,w} - h_{out,w}} = -\dot{m}_{oil}\frac{c_{oil}\left(T_{in,oil} - T_{out,oil}\right) + v_{oil}\left(P_{in,oil} - P_{out,oil}\right)}{c_w\left(T_{in,w} - T_{out,w}\right) + v_w\left(P_{in,w} - P_{out,w}\right)}$$

where we have made use of the constitutive relations for the incompressible fluid model.

Since the pressure drops in the flows are negligible, the flow work terms drop out of the equation. Substituting the appropriate values into this expression yields the desired mass flow.

$$\dot{m}_w = -\dot{m}_{oil}\frac{c_{oil}\left(T_{in,oil} - T_{out,oil}\right)}{c_w\left(T_{in,w} - T_{out,w}\right)} = -(0.2\text{ kg/sec})\frac{(2000\text{ J/kg K})(100\text{ C} - 30\text{ C})}{(4300\text{ J/kg K})(20\text{ C} - 50\text{ C})} = 0.217\text{ kg/sec}$$

Example 8.6: A heat exchanger of design similar to the one shown in Figure 8E.5 is used to cool hydrogen gas (instead of oil) using a water stream. The hydrogen gas is at a pressure of $P_{in,H}$ = 6x10^5 N/m^2 at the inlet of the inner tube and at a pressure of $P_{out,H}$ = 5.5x10^5 N/m^2 at the outlet of the inner tube. The mass flow rate of the hydrogen is $\dot{m}_H$ = 0.3 kg/sec. All exit and entry

temperatures are as indicated in Figure 8E.5. There is no significant pressure drop in the water stream. What is the mass flow rate for the water? The specific heat at constant pressure for hydrogen is $(c_P)_H = 14332$ J/kg-K. The specific heat of water is $c_w = 4300$ J/kg-K.

Solution: The control volume is shown in Figure 8E.5. Since the heat exchanger is of moderate physical size and since the fluids must be flowing slow enough so that the two fluids can approach thermal equilibrium with one another, we assume that the gravitational effects and the velocities are negligible for this situation. For this control volume the first law becomes

$$\dot{m}_w = -\dot{m}_H \frac{h_{in,H} - h_{out,H}}{h_{in,w} - h_{out,w}}$$

We now need to determine the enthalpy of hydrogen stream. There is a great simplification that occurs in the enthalpy if the hydrogen is modeled as an ideal gas. The specific enthalpy, by definition, is the specific internal energy plus the product of the pressure and the specific volume, $h = u + Pv$. The specific internal energy is given by the energy constitutive relation for the ideal gas model, namely, $u = c_v T$. The property constitutive relation for the ideal gas model can be substituted for the Pv term. Then the enthalpy for the ideal gas model becomes

$$h \equiv u + Pv = c_v T + RT = (c_v + R)T = c_p T$$

where we have used the specific heat at constant volume introduced in equation (5.65). Unlike the incompressible fluid enthalpy, the ideal gas enthalpy can be expressed exclusively as function of temperature with no knowledge of the pressure or specific volume.

The expressions for the specific enthalpies of the hydrogen and the water can be substituted into our first law expression, resulting in

$$\dot{m}_w = -\dot{m}_H \frac{c_{p,H}\left(T_{in,H} - T_{out,H}\right)}{c_w\left(T_{in,w} - T_{out,w}\right) + v_w\left(P_{in,w} - P_{out,w}\right)}$$

$$\dot{m}_w = -(0.2 \text{ kg/sec})\frac{(14332 \text{ J/kg K})(100 \text{ C} - 30 \text{ C})}{(4300 \text{ J/kg K})(20 \text{ C} - 50 \text{ C}) + (0)} = 1.55 \text{ kg/sec}$$

Note that because of the unique functional dependence of the enthalpy only on temperature for the ideal gas model, it is not necessary to know the pressures in the hydrogen gas stream.

Example 8E.7: High pressure water flows steadily through a straight, horizontal adiabatic pipe. The pressure of the water at the entrance to the pipe is $P_{in} = 10^7$ Pa. Because of an obstruction in the pipe, the pressure of the water at the outlet of the pipe is $P_{out} = 10^5$ Pa. What is the rise in temperature of the water as it passes from the inlet to the outlet of the pipe? The water can be modeled as an incompressible fluid with a specific heat of $c_w = 4300$ J/kg K.

Solution: We choose a control volume that encompasses the pipe. The conservation of mass equation and the steady-state nature of the flow require that the mass flow rates into and out of the pipe be the same. The first law becomes

$$\frac{dE_{CV}}{dt} = \dot{Q} - \dot{W}_{shaft} + \dot{m}_w\left(h_{in,w} - h_{out,w}\right)$$

Since the flow is steady, the term on the left-hand-side is zero. Since the pipe is adiabatic, there is no heat transfer and the first term on the right-hand-side is also zero. Since there are no shafts penetrating the control surface, the rate of shaft work transfer is zero. Then the first law reduces to

$$h_{in,w} = h_{out,w}$$

For the incompressible fluid model for the water, we can write the enthalpy as $h = cT + Pv$. Then in this case the first law becomes

$$c_w T_{in,w} + P_{in,w} v_w = c_w T_{out,w} + P_{out,w} v_w$$

$$c_w (T_{out,w} - T_{in,w}) = v_w (P_{in,w} - P_{out,w})$$

$$(T_{out,w} - T_{in,w}) = \frac{v_w}{c_w}(P_{in,w} - P_{out,w}) = \frac{(P_{in,w} - P_{out,w})}{\rho c_w} = \frac{(10^7 \text{ N/m}^2 - 10^5 \text{ N/m}^2)}{(1000 \text{ kg/m}^3)(4300 \text{ J/kg K})} = 2.30 \text{ K}$$

This is an example of dissipation in a thermal-fluid system. We say the fluid "heats up" even though there is no heat transfer as it flows through the constriction in the pipe. What has actually happened is that the flow work done on the water as it passes from entrance to exit of the pipe has increased the stored thermal energy of the water rather than the kinetic energy of the water (which has remained constant because of the steady-flow conditions in the pipe). In effect, this flow work is "dissipated" in the water increasing its stored thermal energy and, hence, its temperature.

Note also that the inlet pressure is approximately 100 atm and the outlet pressure is approximately 1 atm. Thus, we also see that enormous pressure drops are required to generate any significant temperature changes in liquid water. This is true of any fluid that can be modeled as an incompressible fluid. The pressure drops normally encountered in engineering practice are usually much smaller than this, and the temperature changes that result from the flow work in these fluids are so small that they become insignificant.

Example 8E.8: An insulated tank contains helium gas in an initial state of T_1=300 K and P_1=1.01x10^7 N/m^2. The valve on the tank is opened, and the pressure of the gas in the tank drops as the helium is discharged into the atmosphere. When the pressure inside the tank reaches a final value of 1 atm, i.e., P_2=1.01x10^5 N/m^2, the valve is closed. The helium can be modeled as an ideal gas with a gas constant of R = 2078 J/kg K and a specific heat at constant volume of c_v = 3153 J/kg K and.

(a) What is the temperature of the gas in state 2?

(b) What fraction of the gas remains inside the tank?

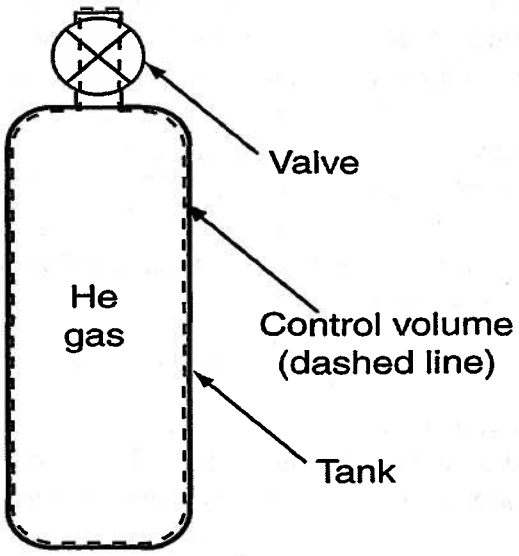

Figure 8E.8 Tank of Helium Discharging to the Atmosphere

Solution: (a) The tank is shown in Figure 8E.8. The control volume, shown by the dashed line, is fixed. For this control volume, there is no inflow and only one outflow of mass. Since the tank is insulated, there is no heat transfer. In point of fact, the process of bleeding down some of the helium in the tank is so fast (since it depends upon mechanical equilibrium, not thermal equilibrium being attained in the gas) there is insufficient time for the gas to experience any significant heat transfer. However, in order for us to establish a final, spatially uniform temperature of the gas inside the tank in the final state, it is necessary for the gas to come to a state of internal thermal equilibrium before there can be any significant heat transfer with the environment. The insulation on the outside of the tank will insure that this is indeed the case. In addition, there is no shaft work transfer since there are no shafts present. Then, the first law becomes

$$\frac{dE_{CV}}{dt} = -\dot{m}_{out} h_{He}$$

where the h_{He} is the enthalpy of the helium exiting the tank which is identical to enthalpy of the helium in the tank at any instant in time. The mass flow rate out of the control volume is $\dot{m}_{out}$. Since we choose to model the helium as an ideal gas, the energy in the control volume is just the internal energy of the gas inside the tank at ant instant. This energy can be expressed in terms of the temperature using the energy constitutive relation for the ideal gas model. Similarly, the enthalpy can be expressed in terms of the temperature using the enthalpy constitutive relation given above.

$$\frac{d\left(mc_v T\right)_{CV}}{dt} = -\dot{m}_{out} c_P T$$

The chain rule can be used to expand the time derivative, viz.

$$\left(\frac{dm_{CV}}{dt}\right) c_v T + m_{CV} c_v \frac{dT}{dt} = -\dot{m}_{out} c_P T$$

The continuity equation can be applied to our control volume so that

$$\frac{dm_{CV}}{dt} = -\dot{m}_{out}$$

Then the first law becomes

$$m_{CV} c_v \frac{dT}{dt} = -\dot{m}_{out} c_P T + \dot{m}_{out} c_v T = -\dot{m}_{out}\left(c_P - c_v\right) T = -\dot{m}_{out} RT = RT \frac{dm_{CV}}{dt}$$

Separating variables, we obtain

$$\frac{c_v}{R}\frac{1}{T}\frac{dT}{dt} = \frac{1}{m_{CV}}\frac{dm_{CV}}{dt}$$

From the property constitutive relation for the ideal gas, we have

$$PV = m_{CV} RT$$

$$\frac{dP}{P} + \frac{dV}{V} = \frac{dm_{CV}}{m_{CV}} + \frac{dT}{T}$$

Since the volume of the tank is constant, we have

$$\frac{1}{m_{CV}}\frac{dm_{CV}}{dt} = \frac{1}{P}\frac{dP}{dt} - \frac{1}{T}\frac{dT}{dt}$$

Substituting this expression into the first law, we get

$$\frac{1}{P}\frac{dP}{dt}=\left(1+\frac{c_v}{R}\right)\frac{1}{T}\frac{dT}{dt}=\frac{c_P}{R}\frac{1}{T}\frac{dT}{dt}$$

Integrating this expression over the time duration of the event, we obtain

$$\int_{P_1}^{P_2}\frac{1}{P}\frac{dP}{dt}dt=\int_{T_1}^{T_2}\frac{c_P}{R}\frac{1}{T}\frac{dT}{dt}dt$$

$$\ln\left(\frac{P_2}{P_1}\right)=\frac{c_P}{R}\ln\left(\frac{T_2}{T_1}\right)$$

Then solving for the temperature when thermal equilibrium is restored inside the tank, we get

$$T_2=T_1\left(\frac{P_2}{P_1}\right)^{\frac{R}{c_P}}$$

Substituting the appropriate values, we get

$$T_2=T_1\left(\frac{P_2}{P_1}\right)^{\frac{R}{c_P}}=(300\text{ K})\left(\frac{1.01\text{ x }10^5\text{ N/m}^2}{1.01\text{ x }10^7\text{ N/m}^2}\right)^{\frac{2078\text{ J/kg K}}{(3153\text{ J/kg K}+2078\text{ J/kg K})}}=48.2\text{ K}$$

(b) To determine the fraction of gas (by mass) remaining inside the tank, we make use of the property constitutive relation for the ideal gas model, namely,

$$\frac{(m_{CV})_2}{(m_{CV})_1}=\frac{P_2}{P_1}\frac{T_1}{T_2}=\frac{(1.01\text{ x }10^5\text{ N/m}^2)}{(1.01\text{ x }10^7\text{ N/m}^2)}\frac{(300\text{ K})}{(48.2\text{ K})}=0.0622$$

8.5 The Second Law of Thermodynamics for the Control Volume

The second law of thermodynamics is an expression of the effect of entropy transfers across a system boundary and entropy generation within a system boundary on the system itself. For a control mass experiencing several heat transfers, each at different locations on its boundary, the second law can be written

$$(S_2-S_1)_{CM}=\sum_i\left(\frac{Q}{T}\right)_i+S_{gen} \tag{8.38}$$

where T_i is the temperature at that point on the boundary where the heat transfer Q_i occurs. The first term on the right-hand-side of equation (8.38) is the net entropy transfer across the system boundary while the second term is the net entropy generated within the boundary. If we are interested in the rate at which the entropy is changing within the boundary of the control mass, we can write equation (8.38) as a rate equation.

$$\frac{dS_{CM}}{dt}=\sum_i\left(\frac{\dot{Q}}{T}\right)_i+\dot{S}_{gen} \tag{8.39}$$

The Reynolds Transport Theorem allows us to transform the left-hand-side of this equation from a control mass viewpoint to that of the control volume. The extensive quantity of interest is the entropy S (corresponding to B in the Reynolds Transport Theorem) and the specific entropy s is the corresponding mass specific quantity (b in the transport theorem). Applying the Reynolds Transport Theorem to equation (8.39) results in

$$\frac{dS_{CM}}{dt} = \frac{d}{dt}\int_{CV} \rho s\, dV + \int_{CS} \rho s\left(\vec{\vartheta}_r \cdot \vec{n}\right) dA = \sum_i \left(\frac{\dot{Q}}{T}\right)_i + \dot{S}_{gen} \tag{8.40}$$

Equation (8.40) can be rearranged to evaluate the time rate of change of the entropy in the control volume, viz.

$$\frac{d}{dt}\int_{CV} \rho s\, dV = \sum_i \left(\frac{\dot{Q}}{T}\right)_i - \int_{CS} \rho s\left(\vec{\vartheta}_r \cdot \vec{n}\right) dA + \dot{S}_{gen} \tag{8.41}$$

This is the second law of thermodynamics for the control volume. The left-hand-side of equation (8.41) is the time rate of change of entropy inside the control volume at some instant of time which also can be written as dS_{CV}/dt. The right-hand-side of equation (8.41) has in addition to the familiar entropy transfer term and the entropy generation term, a term that corresponds to the entropy carried by the mass flowing out of the control volume. We can rewrite this equation in a form that is more appropriate for a control volume with a finite number of inflow ports and outflow ports, viz.

$$\frac{dS_{CV}}{dt} = \sum_i \left(\frac{\dot{Q}}{T}\right)_i + \sum_{in} (\dot{m}s)_{in} - \sum_{out} (\dot{m}s)_{out} + \dot{S}_{gen} \tag{8.42}$$

The two sums "in" and "out" refer to sums over the inflowing ports and outflowing ports, respectively. In each case, the mass flow rate and the specific entropy are evaluated where the mass flows across the control surface. In addition, each of the terms $\dot{m}$ is positive in equation (8.42) since the incoming flows are evaluated in the "in" summation and the outgoing flows are evaluated in the "out" summation.

Example 8E.9: In the interest of improving the fuel efficiency of large truck engines, it has been suggested that a heat engine could be installed on the exhaust system of the truck engine. The design objective would be to use the energy remaining in the products of combustion to provide electrical power for auxiliary systems. The first analysis is always to check if the available energy in the fluid stream is worth the effort of building a device to extract that useful energy. If the mass flow rate of the exhaust gas is $\dot{m} = 0.04$ kg/s, and its pressure and temperature are $P = 10^5$ Pa and $T_{out} = 540$ C, respectively, what is the maximum power that can be generated from the exhaust gases? Assume that the exhaust gas can be modeled as an ideal gas with $c_v = 716$ J/kg K and $R = 287$ J/kg K.

Solution: The system that we are contemplating is shown schematically in Figure 8E.9. Our heat engine will experience a heat transfer from the exhaust gases $\dot{Q}_h$. Although the heat exchanger is depicted as a pipe in Figure 8E.9, in reality, it will be a more complicated structure. The pressure drop across this heat exchanger must be as small as possible because a higher pressure at the exhaust port of the main engine, which is upstream of the system under consideration, will reduce the main engine performance. For the purposes of this estimate, we assume that the pressure drop across the heat exchanger is zero. We estimate that the lowest acceptable temperature at the discharge of the heat exchanger is 40 C to avoid condensation of the H_2O present in the products of combustion. This is essential since condensed water in the exhaust system will enhance the corrosion rates and lead to premature failure of the system. The low temperature reservoir is provided by a heat exchanger that produces at heat transfer between the heat engine and the atmosphere. We will presume in this analysis that the temperature on the heat engine side of this heat exchanger is $T_l = 20$ C.

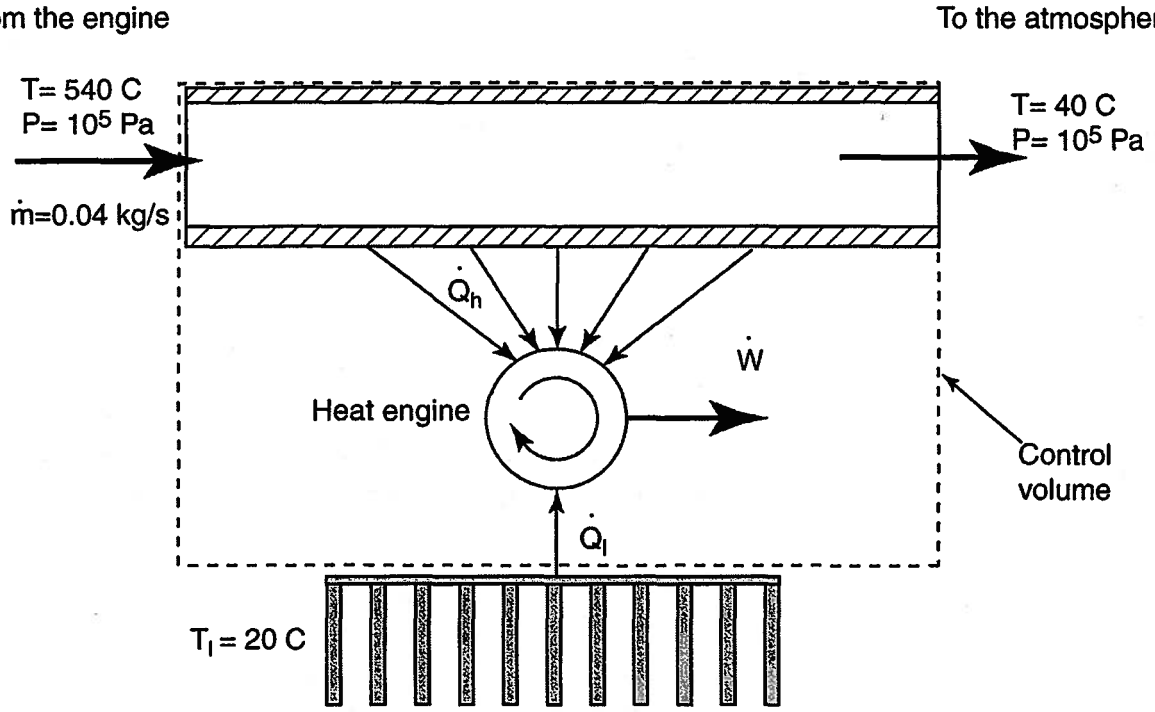

Figure 8E.9 Schematic Diagram of the Exhaust Gas Heat Engine

We choose the control volume shown as a dashed line in Figure 8E.9. There is only one heat transfer and only two mass flows across the boundary. The second law for the control volume becomes

$$\frac{dS_{CV}}{dt} = \frac{\dot{Q}_l}{T_l} + (\dot{m}s)_{in} - (\dot{m}s)_{out} + \dot{S}_{gen}$$

As a design estimate, we wish to determine the maximum possible power output of the heat engine. Although the details of the design of the components of the heat engine and their physical mechanisms are unknown to us at this time, we do know that the best performance of the heat engine would result from reversible operation. For the purposes of this estimate, we assume that the heat engine is reversible with no entropy generation. If we also assume that this system will operate continuously for long periods of time, the heat engine will be operating in steady state. Then we conclude that the time derivative term on the left-hand-side of the second law above must be zero. Finally, applying the continuity equation to the control volume requires that the mass flow rate in must equal the mass flow rate out for steady operation. Incorporating all these observations into the second law we find

$$\dot{Q}_l = \dot{m}T_l(s_{out} - s_{in})$$

Since we are modeling the exhaust gas as an ideal gas, we can use the entropy constitutive relation for the ideal gas to evaluate the specific entropies appearing in the second law. Then

$$\dot{Q}_l = \dot{m}T_l\left[(R + c_v)\ln\left(\frac{T_{out}}{T_{in}}\right) - R\ln\left(\frac{P_{out}}{P_{in}}\right)\right]$$

and

$$\dot{Q}_l = (0.04 \text{ kg/sec})(273 \text{ C} + 20 \text{ C})\bullet$$

$$\bullet\left[(716 \text{ J/kg K} + 287 \text{ J/kg K})\ln\left(\frac{273 \text{ C} + 40 \text{ C}}{273 \text{ C} + 540 \text{ C}}\right) - (287 \text{ J/kg K})\ln(1)\right]$$

$$\dot{Q}_l = -11220 \text{ W}$$

The fact that the heat transfer is negative indicates that the heat transfer is from the engine to the low temperature heat exchanger as we expected. We now know what the "waste heat" is from our heat engine. We can now use this information to determine the work transfer from the heat engine by applying the first law to the control volume. We assume that the velocities and elevations of the incoming and outgoing streams are insignificant. Also, we recognize that the flow is steady so that $dE_{CV}/dt = 0$. Then the first law becomes

$$\dot{W}_{shaft} = \dot{Q}_l + \dot{m}(h_{in} - h_{out})$$

Since we are modeling the exhaust gas as an ideal gas, the enthalpy constitutive relation is

$$h_{in} - h_{out} = (u_{in} - u_{out}) + (P_{in}v_{in} - P_{out}v_{out}) = c_v(T_{in} - T_{out}) + R(T_{in} - T_{out})$$

$$h_{in} - h_{out} = (c_v + R)(T_{in} - T_{out}) = c_P(T_{in} - T_{out})$$

The power is determined by substituting the enthalpy constitutive relation and the heat transfer from the heat engine into the first law. Then

$$\dot{W}_{shaft} = \dot{Q}_l + \dot{m}c_P(T_{in} - T_{out})$$

$$\dot{W}_{shaft} = (-11220 \text{ W}) + (0.04 \text{ kg/sec})(716 \text{ J/kg K} + 287 \text{ J/kg K})(540 \text{ C} - 40 \text{ C}) = 8840 \text{ W}$$

The power is positive, meaning that the heat engine does provide useful output. Note that, as a consequence of the second law, the engine rejects more energy to the low temperature heat exchanger than what it generates as useful power. Nevertheless, this heat engine could provide enough power to drive a refrigeration unit on a trailer.

Example 8E.10: High pressure water flows steadily through a straight, horizontal adiabatic pipe. The pressure of the water at the entrance to the pipe is $P_{in} = 10^7$ Pa. Because of an obstruction in the pipe, the pressure of the water at the outlet of the pipe is $P_{out} = 10^5$ Pa. We have already shown in Example 8E.7 that for this situation the temperature rises 2.30 K as the water flows from the inlet to the outlet of the pipe. If the inlet temperature of the water is 300 K, what is the rate of entropy generation per unit mass flow rate in the pipe? The water can be modeled as an incompressible fluid with a specific heat of $c_w = 4300$ J/kg K.

Solution: The control volume is chosen to encompass all the water inside the pipe. There are no heat transfers and the flow is steady. Continuity requires that the mass flow rates into and out of the pipe are identical. The second law becomes

$$\frac{\dot{S}_{gen}}{\dot{m}} = (s_{out} - s_{in})$$

The entropy constitutive relation for the incompressible fluid model can be substituted into the second law resulting in

$$\frac{\dot{S}_{gen}}{\dot{m}} = c\ln\left(\frac{T_{out}}{T_{in}}\right) = (4300 \text{ J/kg K})\ln\left(\frac{302.3 \text{ K}}{300 \text{ K}}\right) = 32.8 \text{ J/kg K}$$

Note that the entropy generation is positive as required by the second law. Also, notice that if the incompressible fluid (in this case, liquid water) were to decrease in temperature ($T_{out} < T_{in}$) as it flowed past the obstruction, it would constitute a violation of the second law which is an impossibility.

There are situations for which a fluid will decrease in temperature as it passes an obstruction in a pipe, but then its behavior cannot be described in terms of the incompressible fluid model. We will discuss this in greater detail after we have introduced a more complex model to describe the behavior of certain fluids.

Example 8E.11: A Hilsch tube is a rigid wall device which employs a vortex flow to separate a high-pressure stream of gas into two low-pressure streams at different temperatures as shown in Figure 8E.11. The internal interaction which causes the separation is a fluid shear work transfer between the flow in the inner vortex and the outer vortex. In a particular design, the gas is air which can be modeled as an ideal gas with $R = 287$ J/kg K and $c_P = 1003$ J/kg K. The air flows into the inlet port 1 at a rate of $\dot{m}_1 = 0.1$ kg/sec, a pressure of $P_1 = 10^6$ N/m^2, and a temperature of $T_1 = 300$ K. Cold air exits out port 2 at a mass flow rate of $\dot{m}_2 = 0.01$ kg/sec, a pressure of $P_2 = 10^5$ N/m^2, and a temperature of $T_2 = 230$ K. Hot air exits port 3 at a pressure of 10^5 N/m^2. Since the residence time of the fluid inside the Hilsch tube is very small, the walls of the Hilsch tube maybe considered to be adiabatic. The kinetic energies of the gas streams are negligible at the inlets and the outlets and the changes in height are small.

(a) What is the outlet pressure at port 3?

(b) Is the operation reversible?

(c) If the observation is not reversible, what is the value of P_1 for reversible operation, with the same flows, temperatures and outlet pressures as given?

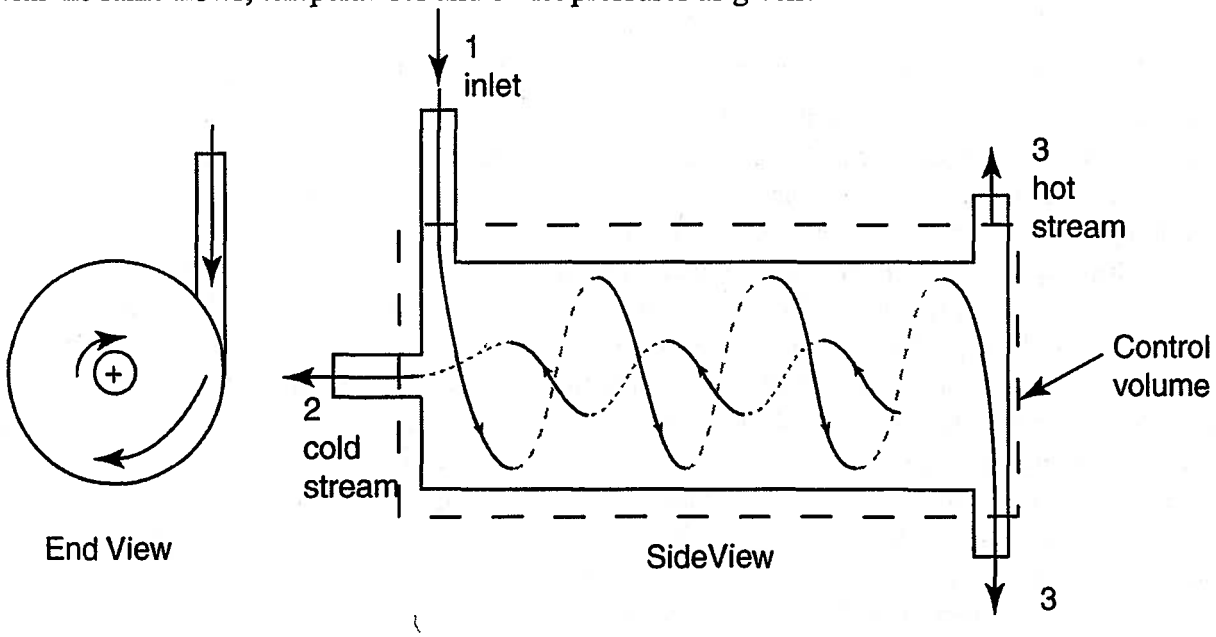

Figure 8E.11 Hilsch Vortex Tube

Solution: We choose the control volume shown in Figure 8E.11. For this control volume, the conservation of mass becomes

$$0 = \dot{m}_1 - \dot{m}_2 - \dot{m}_3$$

$$\dot{m}_3 = \dot{m}_1 - \dot{m}_2 = (0.1 \text{ kg/sec}) - (0.01 \text{ kg/sec}) = 0.09 \text{ kg/sec}$$

Since the air is modeled as an ideal gas, the first law applied to the control volume can be written

$$0 = \dot{m}_1 h_1 - \dot{m}_2 h_2 - \dot{m}_3 h_3 = \dot{m}_1 c_P T_1 - \dot{m}_2 c_P T_2 - \dot{m}_3 c_P T_3$$

Solving for T_3 results in

$$T_3 = \left(\frac{\dot{m}_1}{\dot{m}_3}\right)T_1 - \left(\frac{\dot{m}_2}{\dot{m}_3}\right)T_2 = \left(\frac{0.1 \text{ kg/sec}}{0.09 \text{ kg/sec}}\right)(300 \text{ K}) - \left(\frac{0.01 \text{ kg/sec}}{0.09 \text{ kg/sec}}\right)(230 \text{ K}) = 307.78 \text{ K}$$

(b) Since there are no heat transfers across the boundary of the control volume and the flow is steady, the second law simplifies to

$$0 = \dot{m}_1 s_1 - \dot{m}_2 s_2 - \dot{m}_3 s_3 + \dot{S}_{gen}$$

Combining the second law, the continuity equation, and the entropy constitutive relation for the ideal gas, we obtain

$$\dot{S}_{gen} = \dot{m}_2(s_2 - s_1) + \dot{m}_3(s_3 - s_1) = \dot{m}_2\left[c_P \ln\left(\frac{T_2}{T_1}\right) - R \ln\left(\frac{P_2}{P_1}\right)\right] + \dot{m}_3\left[c_P \ln\left(\frac{T_3}{T_1}\right) - R \ln\left(\frac{P_3}{P_1}\right)\right]$$

$$\dot{S}_{gen} = (0.01 \text{ kg/sec})\left[(1003 \text{ J/kg K}) \ln\left(\frac{230 \text{ K}}{300 \text{ K}}\right) - (287 \text{ J/kg K}) \ln\left(\frac{10^5 \text{ N/m}^2}{10^6 \text{ N/m}^2}\right)\right] +$$

$$+ (0.09 \text{ kg/sec})\left[(1003 \text{ J/kg K}) \ln\left(\frac{307.78 \text{ K}}{300 \text{ K}}\right) - (287 \text{ J/kg K}) \ln\left(\frac{10^5 \text{ N/m}^2}{10^6 \text{ N/m}^2}\right)\right]$$

$$\dot{S}_{gen} = 3.94 \text{ W/K} + 61.8 \text{ W/K} = 65.7 \text{ W/K}$$

Since the rate of entropy generation in the Hilsch tube is non-zero, the process is irreversible.

(c) If the Hilsch tube were reversible, the rate of entropy generation would be zero and the second law would become

$$\dot{m}_1 s_1 = \dot{m}_2 s_2 + \dot{m}_3 s_3$$

This equation says that the entropy convected into the volume is equal to the entropy convected out of the control volume. Once again, using the conservation of mass and the entropy constitutive relations, we get

$$0 = \dot{m}_2\left[c_P \ln\left(\frac{T_2}{T_1}\right) - R \ln\left(\frac{P_2}{P_1}\right)\right] + \dot{m}_3\left[c_P \ln\left(\frac{T_3}{T_1}\right) - R \ln\left(\frac{P_3}{P_1}\right)\right]$$

Since $P_2 = P_3$,

$$\dot{m}_1 R \ln\left(\frac{P_1}{P_2}\right) = \dot{m}_2 c_P \ln\left(\frac{T_1}{T_2}\right) + \dot{m}_3 c_P \ln\left(\frac{T_1}{T_3}\right)$$

$$\ln\left(\frac{P_1}{P_2}\right) = \frac{(0.01 \text{ kg/sec})}{(0.1 \text{ kg/sec})}\frac{(1003 \text{ J/kg K})}{(287 \text{ J/kg K})} \ln\left(\frac{300 \text{ K}}{230 \text{ K}}\right) +$$

$$+ \frac{(0.09 \text{ kg/sec})}{(0.1 \text{ kg/sec})}\frac{(1003 \text{ J/kg K})}{(287 \text{ J/kg K})} \ln\left(\frac{300 \text{ K}}{307.78 \text{ K}}\right) = 0.0124$$

$$P_1 = P_2 e^{0.0124} = 1.0125\, P_2 = 1.0125 \text{ x } 10^5 \text{ N/m}^2$$

8.6 Reversible Flow: The Bernoulli Equation in Steady Flow

Consider a steady flow of an incompressible fluid in some region in space. The velocity vector is constant in time at each and every position within this region. Within this region we can construct curves, called *streamlines*, whose tangents are the local fluid velocities. In steady flow,

these curves correspond to the paths that fluid particles follow. If we collect together the streamlines passing through some area A_1, we form a streamtube which is a cylinder-like volume that follows the streamlines as shown in Figure 8.4.

For our purposes here, we choose a control volume coincident with a streamtube. The fluid enters the streamtube through area A_1 and exits the streamtube through area A_2. There is no flow out of the lateral surface of the streamtube since that surface follows the streamlines. This is a consequence of the fact that the fluid velocity is everywhere tangent to the this surface so the scalar product of the fluid velocity with the outward directed normal to this surface is zero everywhere.

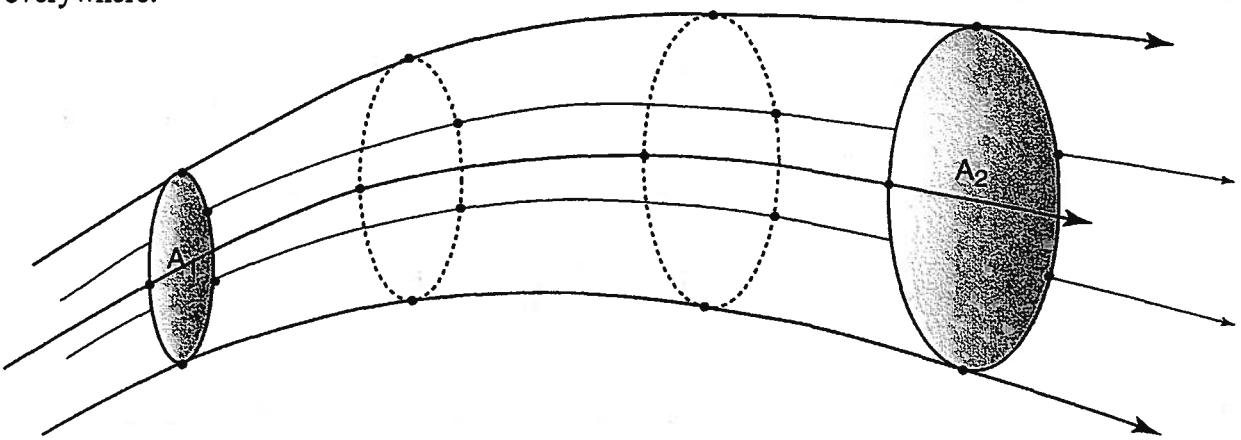

Figure 8.4 Streamtube in Fluid Flow Field

For our purposes here, we will consider the case in which the influence of fluid viscosity is negligible; thus, there is no viscous dissipation in this flow. Also, there is no heat transfer across the control surface so the flow is adiabatic. In addition, we assume that the streamtube we have chosen is small enough in "diameter" so that the flow is "one dimensional" with no variation of fluid properties, namely u, h, s, v, etc. over the entrance cross-sectional area, A_1, and the exit cross-sectional area, A_2. Finally, within the control volume that defines the streamtube, there are no devices requiring shaft work transfer across the control surface.

The continuity equation applied to this streamtube requires

$$\frac{d}{dt}\int_{CV}\rho\,dV+\int_{CS}\rho\left(\vec{\vartheta}_r\cdot\vec{n}\right)dA=0$$

The time derivative of the volume integral is zero because the flow is steady. The surface integral simplifies into two integrals over cross-sectional areas A_1 and A_2. These integrals become the mass flow rates at entrance and at exit from the streamtube. Then

$$\int_{A_1}\rho\left(\vec{\vartheta}_r\cdot\vec{n}\right)dA+\int_{A_2}\rho\left(\vec{\vartheta}_r\cdot\vec{n}\right)dA=-\dot{m}_1+\dot{m}_2=0$$

Thus, $\dot{m}_1=\dot{m}_2=\dot{m}$. Applying the second law to the control volume, we get

$$\frac{dS_{CV}}{dt}=\sum_i\left(\frac{\dot{Q}}{T}\right)_i+\sum_{in}(\dot{m}s)_{in}-\sum_{out}(\dot{m}s)_{out}+\dot{S}_{gen}$$

Since the flow is steady, the left-hand-side of the second law becomes zero. Since the flow is also adiabatic, there is no entropy transfer and the first term on the right-hand-side is also zero. Since

there is no dissipation in the flow, i.e., the flow is reversible, there is no entropy generation. Then the second law reduces to

$$\sum_{in}(\dot{m}s)_{in} - \sum_{out}(\dot{m}s)_{out} = 0$$

$$\dot{m}(s_{in} - s_{out}) = \dot{m}(s_1 - s_2) = 0$$

Since the fluid is incompressible, its density is constant and, hence, its thermal and mechanical aspects are uncoupled. Then its thermal behavior can be described by the pure thermal system model. Then we can use the entropy constitutive relation for the pure thermal system model. Then in the present case, we have

$$\dot{m}c\ln\frac{T_1}{T_2} = 0$$

and it follows that $T_1 = T_2$. The first law is

$$\frac{dE_{CV}}{dt} = \dot{Q} - \dot{W}_{shaft} + \sum_{in}\dot{m}_{in}\left(h + \frac{\vartheta^2}{2} + gz\right)_{in} - \sum_{out}\dot{m}_{out}\left(h + \frac{\vartheta^2}{2} + gz\right)_{out}$$

In the absence of heat transfer and shaft work transfer, the first law becomes for steady flow

$$\left(h + \frac{\vartheta^2}{2} + gz\right)_{A_1} = \left(h + \frac{\vartheta^2}{2} + gz\right)_{A_2}$$

where the values in the parentheses are evaluated on the surfaces indicated by the subscripts. Again, since the fluid is incompressible, we can substitute the corresponding constitutive relation of the pure thermal system model for the enthalpy. Then the first law becomes

$$\left(u + Pv + \frac{\vartheta^2}{2} + gz\right)_{A_1} = \left(u + Pv + \frac{\vartheta^2}{2} + gz\right)_{A_2}$$

$$\left(cT + \frac{P}{\rho} + \frac{\vartheta^2}{2} + gz\right)_{A_1} = \left(cT + \frac{P}{\rho} + \frac{\vartheta^2}{2} + gz\right)_{A_2}$$

Since the temperature of the fluid at surfaces A_1 and A_2 are the same by the second law, we find

$$\left(\frac{P}{\rho} + \frac{\vartheta^2}{2} + gz\right)_{A_1} = \left(\frac{P}{\rho} + \frac{\vartheta^2}{2} + gz\right)_{A_2} \tag{8.43}$$

This is the steady flow *Bernoulli equation* named after Daniel Bernoulli (1700 - 1782) even though he never derived it or used it in his work. However, in his treatise *Hydrodynamica*, Bernoulli showed a relationship between the pressure and the square of the velocity. He also coined the term "hydrodynamics" and became the first to use the calculus in analyzing the dynamic behavior of fluids. This pioneering work set the stage for the work of his contemporary Leonhard Euler (1707 - 1783) and others.

The Bernoulli equation is one of the most used *and most misused* relations in fluid mechanics. If we now shrink the diameter of the streamtube to zero, areas A_1 and A_2 collapse to points on the central streamline. Equation (8.43) then is a relation between any two points on the central streamline. The choice of the positions of the surfaces A_1 and A_2 along the central streamline is entirely arbitrary in our analysis.

The underlying assumptions for the Bernoulli equation include:

(1) *Incompressible flow.* The Bernoulli equation can be applied to liquid and, as we shall show later, low velocity gas flows for which the Mach number (the ratio of the local velocity to

the local speed of sound) is less than 0.3 ($M < 0.3$).

(2) *Steady flow.* We will revisit the Bernoulli equation later to develop a form of the Bernoulli equation that applies to unsteady flow.

(3) *Negligible effects of fluid viscosity.* There is no viscous dissipation in the flow.

(4) *No shaft work transfer.* The Bernoulli relation cannot be applied across a device requiring a shaft work transfer, such as a pump or a turbine. There is, of course, a flow work transfer associated with the movement of the fluid across areas A_1 and A_2.

(5) *No heat transfer.* This constraint can be relaxed in cases where the fluid under consideration is a liquid where the thermal and mechanical energy storage modes are uncoupled. This constraint cannot be relaxed if the fluid is a thermodynamically coupled system such as an ideal gas.

The Bernoulli relation is often misused when it is difficult to identify regions where the viscosity of the fluid exerts negligible influence, i.e., regions where the "no dissipation" assumption is valid. We will show that entropy generation due to motion in a viscous incompressible fluid occurs in locations where the velocity of the fluid changes dramatically in the direction normal to the flow velocity, i.e., there is a significant difference between the velocities on neighboring streamlines. These variations of velocity normal to the direction of flow produce fluid shear in which adjacent layers of fluid move relative to one another in the direction of motion of the fluid overall. In viscous fluids, these regions of high shear are the regions of substantial dissipation, and they occur, in general, in the neighborhood of the solid surfaces that form the physical boundaries of the flow field. As we shall see subsequently, the traditional model for the viscous fluid is the Newtonian fluid model. One of the consequences of this model is that the fluid in contact with a bounding solid surface assumes the velocity of that surface. This is known as the "no-slip" boundary condition. This boundary condition, of necessity, requires that the fluid be in shear with adjacent layers of fluid traveling at different velocities. Thus, we would expect that the Bernoulli equation cannot be applied in the vicinity of a solid wall.

By way of example, let us consider a flow of a viscous fluid past a solid plate as shown in Figure 8.5. A fluid with a uniform velocity distribution approaches the plate with velocity ϑ. As the fluid flows past the plate, the "no-slip" boundary condition dictates that at the surface of the plate, the fluid velocity relative to the plate is zero. A slow moving fluid layer, known as the *boundary layer*, forms over the plate where the fluid velocity makes a transition from the velocity of the solid surface (zero in this case) to the free stream velocity. As we shall show subsequently, the boundary layer on a surface is generally quite thin relative to the dimensions of the surface. Because the velocity changes from zero velocity to the free stream velocity over a thin region, the transverse gradient in the velocity is large. As a result, there is substantial dissipation in the boundary layer, and, consequently, the Bernoulli equation is invalid in the boundary layer. On the other hand, the spatial gradients of the velocity in the free stream region are quite small. Therefore the dissipation in this region is small and the Bernoulli equation is valid.

Figure 8.6 shows an object in a flow field. On the leading surfaces of the object, a thin boundary layer forms. For high enough velocities, there is a point where the boundary layer separates from the object and forms a wake behind the object. The wake is turbulent and consequently, is a region of large shear. The Bernoulli equation does not apply there.

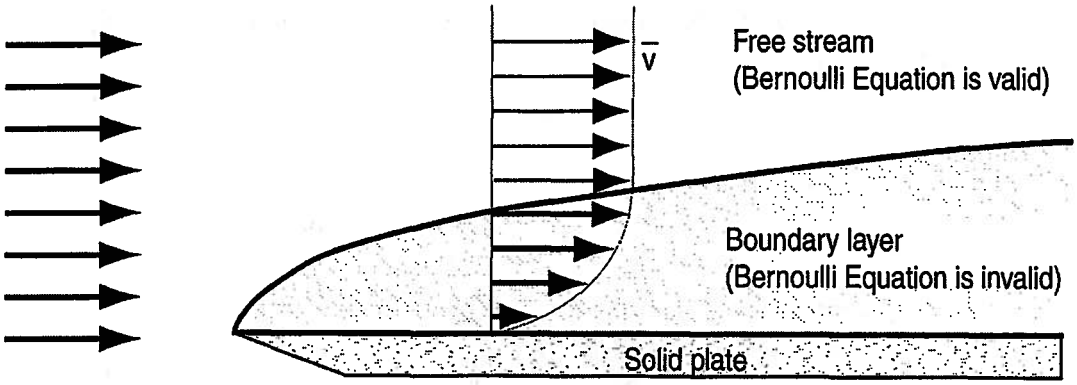

Figure 8.5 Flow of a Viscous Fluid Past a Solid Flat Plate

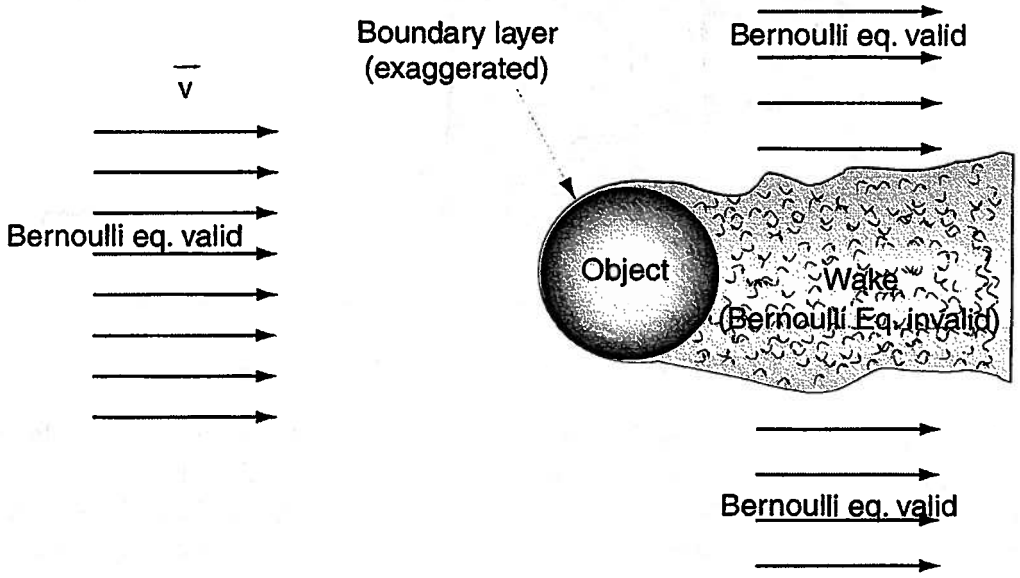

Figure 8.6 Flow of a Viscous Fluid Past a Solid Object

Example 8.12: An open tank of large diameter sits on the floor as shown in Figure 8E.12. Initially, the tank is filled with water to a depth H. The tank has a small hole (compared to the size of the tank) in its side at a height $h = 1$ m above the floor. The water stream emanating normally from the side of the tank strikes the floor at a distance $d = 3$ m from the side of the tank. What is the depth H of the water in the tank?

Solution: The first observation is that the hole in the tank wall is small compared to the overall size of the tank. Hence, we would expect the water level in the tank to fall very slowly. This suggests that the flow in this problem can be modeled as steady flow. We anticipate that the bulk of the flow inside the tank is reversible with regions of high shear confined to the vicinity of the wall of the tank. As shown in Figure 8E.12, we can draw a streamline from point 1 to point 2 and apply the Bernoulli equation to that streamline. Because the size of the tank is much larger than the size of the hole, the velocity of the free surface of the water in the tank is negligible. The pressure at point 2 is P_{atm} and is determined by the atmosphere around the jet as it escapes the tank. The steady flow Bernoulli equation becomes

$$\frac{P_{atm}}{\rho} + gH = \frac{P_{atm}}{\rho} + \frac{\mathcal{V}_2^2}{2} + gh$$

where ϑ_2 is the velocity of the fluid as it exits the hole in the tank. Solving this expression for the velocity out of the tank, we have

$$\vartheta_2 = \sqrt{2g(H-h)}$$

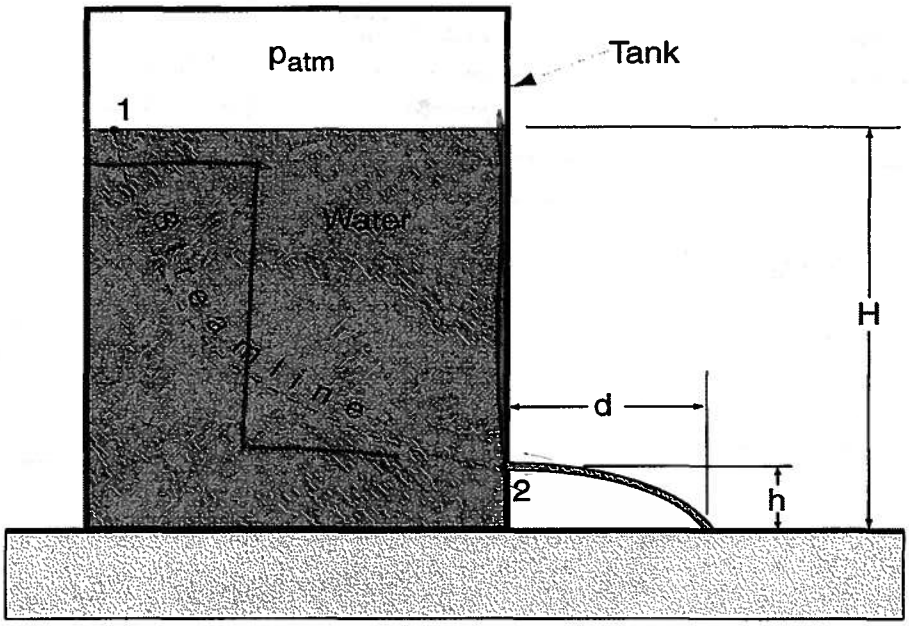

Figure 8E.12 Water Tank with Small Leak

A given fluid particle leaves the tank with this horizontal velocity and travels under the influence of gravity in a ballistic trajectory to the floor. From the point of view of a fluid particle, the effect of gravity can be modeled as a pure gravitational spring and the fluid particle can be modeled as pure translational mass. Then these two models taken together form an isolated system and the first law for that system becomes

$$mg(z_2 - z_1) + \frac{1}{2}m\left(\vartheta_{z2}{}^2 - \vartheta_{z1}{}^2\right) = 0$$

$$g(-h) + \frac{1}{2}\vartheta_{z2}{}^2 = 0$$

$$\vartheta_{z2} = \sqrt{2gh}$$

where we have taken the datum plane for the pure gravitational spring to be the center of the hole and the initial value of the vertical component of velocity of the fluid particle is zero. For constant acceleration, the time required to reach this velocity is given by

$$\frac{d\vartheta_z}{dt} = g$$

$$\int_0^{\vartheta_{z2}} d\vartheta_z = \int_0^t g\,dt$$

$$\vartheta_{z2} = gt$$

Equating the two expressions for the vertical component of velocity of the particle at impact with the floor, we get the time of flight of a fluid particle, viz.

$$t = \sqrt{\frac{2h}{g}}$$

The horizontal distance that a fluid particle travels during this time interval is

$$d = \vartheta_2 t = \vartheta_2 \sqrt{\frac{2h}{g}} = \sqrt{2g(H-h)}\sqrt{\frac{2h}{g}} = 2\sqrt{h(H-h)}$$

This expression can now be solved for the height H of the free surface of the water. Then

$$H = h + \frac{d^2}{4h} = (1\text{ m}) + \frac{(3\text{ m})^2}{4(1\text{ m})} = 3.25\text{ m}$$

Example 8E.13: As shown in Figure 8E.13, air flows steadily at low speed through a horizontal nozzle and discharges to the atmosphere at $P_{atm} = 10^5$ N/m^2. At the nozzle inlet, the area is 0.1 m^2 while at the exit the area is 0.02 m^2. Determine the gage pressure required at the nozzle inlet to produce a discharge speed of 50 m/sec for the following two models:

(a) Model the flow as reversible and incompressible to evaluate the flow conditions.

(b) For the inlet pressure and inlet velocity determined in part (a) above, determine the outlet velocity for a model in which the gas is compressible with an inlet temperature of 300 K.

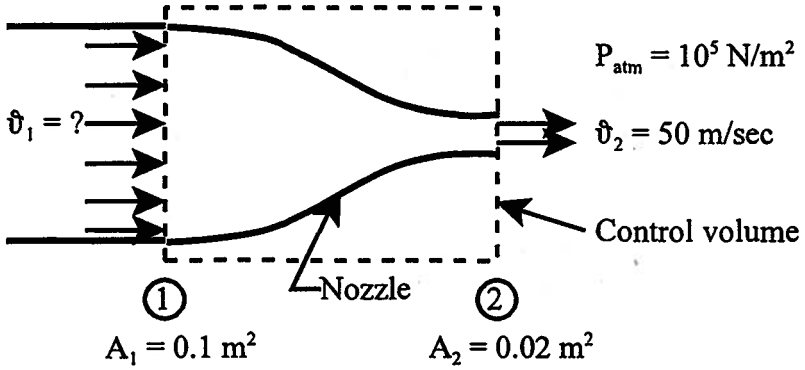

Figure 8E.13 Flow through a Convergent Nozzle

Solution: (a) From the conservation of mass in steady flow

$$\rho_1 A_1 \vartheta_1 = \rho_2 A_2 \vartheta_2$$

Since the fluid is being modeled as incompressible, this reduces to

$$A_1 \vartheta_1 = A_2 \vartheta_2$$

$$\vartheta_1 = \vartheta_2 \frac{A_2}{A_1} = (50\text{ m/sec})\frac{(0.02\text{ m}^2)}{(0.1\text{ m}^2)} = 10\text{ m/sec}$$

Now apply the Bernoulli equation along the streamline that passes along the centerline of the nozzle.

$$P_1 - P_2 = P_1 - P_{atm} = \frac{\rho(\vartheta_2^2 - \vartheta_1^2)}{2} = \frac{P_{atm}(\vartheta_2^2 - \vartheta_1^2)}{2RT}$$

$$P_1 - P_{atm} = \frac{(10^5\text{ N/m}^2)[(50\text{ m/sec})^2 - (10\text{ m/sec})^2]}{2(287\text{ J/kg K})(300\text{ K})}$$

$$P_1 - P_{atm} = 1.394 \times 10^3\text{ N/m}^2$$

Thus the absolute pressure at the inlet to the nozzle is $P_1 = 1.0139 \times 10^5$ N/m^2.

(b) Now suppose that we use the ideal gas model in its complete form. If the expansion through the nozzle is reversible and adiabatic from P_1 to P_{atm}, the second law requires that there is no entropy generation and that $s_1 = s_2$. From the entropy constitutive relation for the ideal gas we have

$$s_2 - s_1 = c_P \ln\frac{T_2}{T_1} - R\ln\frac{P_2}{P_1}$$

Then

$$T_2 = T_1\left(\frac{P_2}{P_1}\right)^{\frac{R}{c_P}} = (300\text{ K})\left(\frac{1\text{ x }10^5\text{ N/m}^2}{1.0139\text{ x }10^5\text{ N/m}^2}\right)^{\frac{287\text{ J/kg K}}{1003\text{ J/kg K}}} = 298.82\text{ K}$$

From the first law for a control volume

$$h_1 + \frac{\mathcal{G}_1^2}{2} = h_2 + \frac{\mathcal{G}_2^2}{2}$$

$$\mathcal{G}_2^2 = \mathcal{G}_1^2 + 2(h_1 - h_2) = \mathcal{G}_1^2 + 2c_P(T_1 - T_2)$$

$$\mathcal{G}_2 = \sqrt{\mathcal{G}_1^2 + 2c_P(T_1 - T_2)} = \sqrt{(10\text{ m/sec})^2 + 2(1003\text{ J/kg K})(300\text{ K} - 298.82\text{ K})}$$

$$\mathcal{G}_2 = 49.723\text{ m/sec}$$

Thus the error associated with using the incompressible fluid model under these circumstances is less than one percent. Note that for a given exit velocity and pressure, we could determine the gage pressure and velocity at inlet to the nozzle for the compressible case by solving the second law, the first law, and the continuity equation simultaneously. The solution is a bit ponderous compared to the solution shown above which provides an estimate of the error inherent in applying the incompressible fluid model to the fluid dynamics of the ideal gas. Note that the Mach number in this case is quite small.

$$\mathcal{G}_{sound} = \sqrt{\gamma RT} = \sqrt{1.4(287\text{ J/kg K})(298.82\text{ K})} = 346.51\text{ m/sec}$$

$$M = \frac{\mathcal{G}_2}{\mathcal{G}_{sound}} = \frac{49.723\text{ m/sec}}{346.51\text{ m/sec}} = 0.143$$

Thus, the value of the Mach number is well below the incompressible limit of 0.3. Note that even though the ideal gas can be modeled as an incompressible fluid for the purposes of determine its dynamic behavior at these low fluid velocities, we cannot use the incompressible fluid model to describe its thermodynamic behavior under any circumstances.

Example 8E.14: The following is an example of an inappropriate application of the Bernoulli equation. A young girl has an aquarium that holds 30 gallons of water. At 8.33 lbm/gal, the weight of the water alone is 250 lbm. Since the girl weighs only 45 lbm herself, this tank is hardly something for her to lift when the water needs changing. To draw the dirty water out of the tank, she uses a siphon with a geometry as shown in Figure 8E.14. Calculate the mass flow rate of water through the siphon tube (I.D. = 8 mm) for the geometry shown. Also calculate the pressure at the point A. Model the water as incompressible with a density $\rho = 1000\text{ kg/m}^3$.

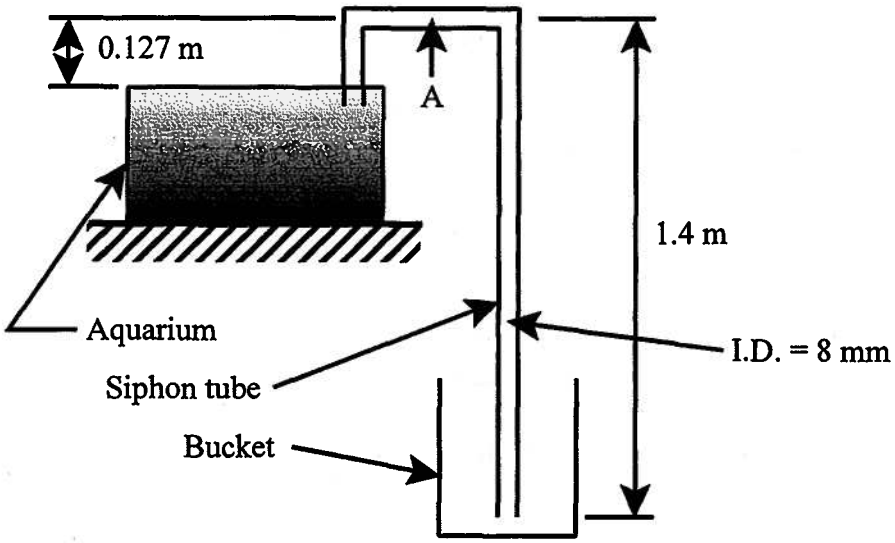

Figure 8E.14

Solution: Let position 1 be the surface of the water in the aquarium and let position 2 be the discharge end of the siphon tube. As in Example 8E.11, the velocity of the free surface is small compared to the velocity in the small diameter tube. Then we can model the flow as steady. If we also model the flow in the tube as having no dissipation (a model that we shall show later to be a poor one), we can apply the Bernoulli equation to the flow between positions 1 and 2, viz.

$$\frac{P_1}{\rho}+\frac{\vartheta_1^2}{2}+gz_1=\frac{P_2}{\rho}+\frac{\vartheta_2^2}{2}+gz_2$$

Since the surface of the aquarium is large relative to the diameter of the tube, $\vartheta_1 \approx 0$. Also, $P_1 = P_2 = P_{atm}$. Then

$$gz_1=\frac{\vartheta_2^2}{2}+gz_2$$

$$\vartheta_2=\sqrt{2g(z_1-z_2)}=\sqrt{2(9.81\ \text{m/sec}^2)(1.40\ \text{m}-0.127\ \text{m}-0)}=5\ \text{m/sec}$$

From the definition of the mass flow rate

$$\dot{m}=\rho A\vartheta=(1000\ \text{kg/m}^3)\frac{\pi(8\ \text{x}\ 10^{-3}\ \text{m})^2}{4}(5\ \text{m/sec})=0.251\ \text{kg/sec}$$

This flow rate is quite a bit faster than the actual flow rate of $\dot{m} = 0.0953$ kg/sec. As will become apparent later, this application of the Bernoulli equation only gives a very rough estimate of the mass flow rate. In applying the Bernoulli equation in this manner, we have violated the assumption that there is no dissipation in the flow. Viscous effects are appreciable here because of the small diameter of the tube.

For the pressure at location A, let us again apply the Bernoulli equation. Then

$$\frac{P_1}{\rho}+\frac{\vartheta_1^2}{2}+gz_1=\frac{P_A}{\rho}+\frac{\vartheta_A^2}{2}+gz_A$$

Since $\vartheta_1 \approx 0$ and since $\vartheta_A = \vartheta_2$ from continuity, the Bernoulli equation reduces to

$$\frac{P_A}{\rho}=\frac{P_1}{\rho}+gz_1-\frac{\vartheta_2^2}{2}-gz_A=\frac{P_1}{\rho}+g(z_1-z_A)-\frac{\vartheta_2^2}{2}$$

$$P_A = P_1 + \rho g(z_1 - z_A) - \rho \frac{\vartheta_2^2}{2}$$

Substituting values for the various parameters, we obtain

$$P_A = (1.013 \times 10^5 \text{ N/m}^2) + (10^3 \text{ kg/m}^3)(9.81 \text{ m/sec}^2)(-0.127 \text{ m})$$
$$-(10^3 \text{ kg/m}^3)\frac{(5 \text{ m/sec})^2}{2}$$
$$P_A = 8.76 \times 10^4 \text{ N/m}^2$$

Thus the pressure in the siphon tube at this location is below atmospheric pressure. This estimate of the pressure is erroneous because in neglecting viscous effects in the flow, we have obtained a flow velocity which is much larger than the actual velocity. Hence, our estimate of the local pressure based on the application of the Bernoulli equation is much lower than the actual value of 9.9991×10^4 N/m^2.

8.7 Reversible Flow: The Bernoulli Equation in Unsteady Flow

In unsteady flow, it is somewhat more convenient to adopt the Lagrangian approach and follow the time history of a fluid particle. For example, consider the differential fluid element in a flow of an incompressible fluid in which the influence of viscosity is negligible. The fluid element is oriented with the streamlines as shown in Figure 8.7. Provided the streamlines are not changing shape with time, the fluid element will travel along the central streamline as time evolves. The distance s along the central streamline is a coordinate for the position of the fluid element and the vector $\vec{s}$ is the local unit vector parallel to the streamline. The other local coordinate is r. The corresponding unit vector is $\vec{r}$ which is normal to the streamline as shown. The third direction is in the q direction, orthogonal to both the r- and the s-directions. In Figure 8.7, the q direction is normal to the plane of the figure. The dimensions of the differential fluid element are $ds \cdot dr \cdot dq$ around the point on the streamline (s, 0, 0). In Figure 8.7, the local curvature of the streamlines is assumed to be in the s, r plane.

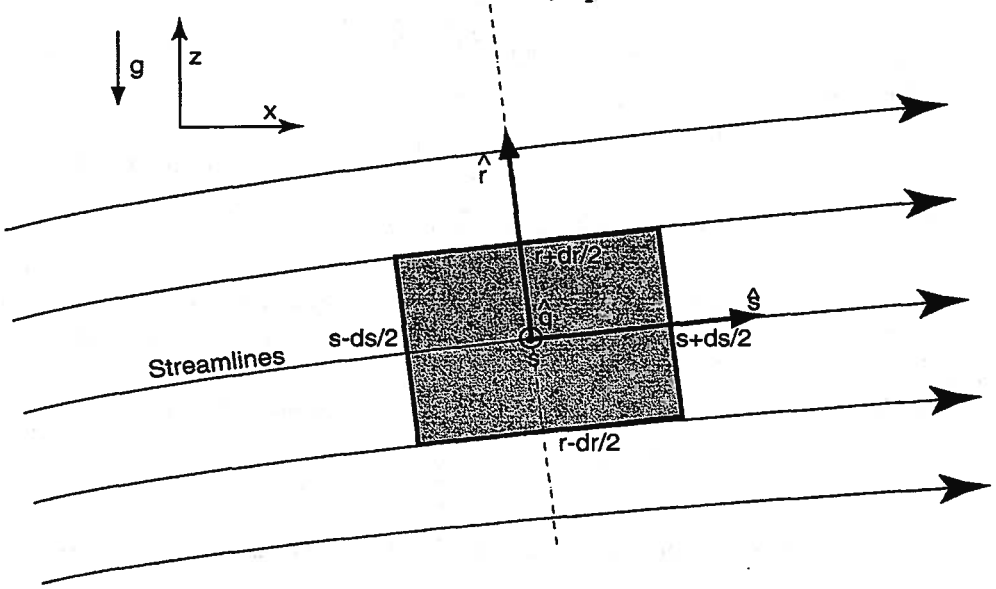

Figure 8.7 A Differential Fluid Particle

According to Newton's second law of motion, the force acting on a particle, F, is equal to the time rate of change of the momentum of that particle, viz.

$$\vec{F} = \frac{d(m\vec{\vartheta})}{dt} = m\vec{a} \tag{8.44}$$

Since the viscosity of the fluid exerts no influence in this case, the forces on the fluid consist of surface forces due to pressure that act normal to the surfaces of the fluid element and body forces due to gravity that act on the body of the fluid element. Viscous shear forces are negligible. The s-component of Newton's second law for the fluid element shown in Figure 8.7 is

$$F_s = P\left(s - \frac{ds}{2}\right)dqdr - P\left(s + \frac{ds}{2}\right)dqdr + \rho dsdrdq\left(\vec{g}\cdot\vec{s}\right) \tag{8.45}$$

The first term and second terms on the right-hand-side of equation (8.45) are the pressure forces on the left face and right faces of the differential element, respectively. The third term on the right-hand-side is the body force due to gravity acting on the fluid element. These three forces accelerate the fluid element along the streamline. The mass of the fluid element is $\rho dsdrdq$. Higher order terms due to the curvature and divergence of the streamlines could be included in equation (8.45), but these terms do not contribute in the differential limit.

The acceleration of the fluid particle is a bit more complicated. In the Eulerian point of view, the velocity is defined as a field of velocities that depend on position and on time. In general, the fluid velocity along the streamline will be different from one point on the streamline to another. In addition, the velocities all along the streamline can vary with time. Because both of these effects can be present, the velocity of the particle is a function of its position on the streamline as well as the time it occupies that position or $\vartheta(s,t)$. The time derivative of the velocity of the particle is the limit of the velocity of the particle evaluated at its new position and new time minus its velocity at the old position evaluated at its old time divided by the elapsed time. Then

$$\frac{d\vartheta}{dt} = \lim_{\Delta t\to 0}\frac{\vartheta\left[s(t+\Delta t),t+\Delta t\right] - \vartheta\left[s(t),t\right]}{\Delta t} \tag{8.46}$$

The first velocity in the numerator of equation (8.46) can be expanded in a double Taylor series about the point s and time t,

$$\vartheta\left[s(t+\Delta t),t+\Delta t\right] = \vartheta(s+\frac{ds}{dt}\Delta t, t+\Delta t) = \vartheta(s,t) + \frac{\partial\vartheta}{\partial s}\frac{ds}{dt}\Delta t + \frac{\partial\vartheta}{\partial t}\Delta t \tag{8.47}$$

Substituting equation (8.47) into equation (8.46), we get

$$a \equiv \frac{d\vartheta}{dt} = \frac{\partial\vartheta}{\partial s}\frac{ds}{dt} + \frac{\partial\vartheta}{\partial t} = \vartheta\frac{\partial\vartheta}{\partial s} + \frac{\partial\vartheta}{\partial t} \tag{8.48}$$

where we have recognized that the derivative ds/dt is the just the velocity of the fluid particle along the streamline. Thus, there are two contributions to the acceleration of a fluid particle: one due to the fact that the fluid particle moves from one location on the streamline where the velocity has one value, to another location on the streamline where the velocity has a different value and the second due to the fact that the fluid velocity at a given point is changing from one instant of time to another by virtue of the unsteady nature of the flow.

Equation (8.48) can be combined with equations (8.44) and (8.45) to obtain

$$P\left(s - \frac{ds}{2}\right)dqdr - P\left(s + \frac{ds}{2}\right)dqdr + \rho dsdrdq\left(\vec{g}\cdot\vec{s}\right) = \rho dsdrdq\left[\vartheta\frac{\partial\vartheta}{\partial s} + \frac{\partial\vartheta}{\partial t}\right] \tag{8.49}$$

Dividing equation (8.49) by the mass of the fluid element $\rho ds dr dq$ and taking the limit as ds approaches zero, we get

$$0 = \frac{\partial \vartheta}{\partial t} + \frac{1}{\rho}\frac{dP}{ds} + \vartheta\frac{\partial \vartheta}{\partial s} - (\vec{g}\cdot\vec{s}) \tag{8.50}$$

Equation (8.50) can be integrated along the streamline to get

$$0 = \int_1^2 \frac{\partial \vartheta}{\partial t} ds + \frac{1}{\rho}\int_1^2 \frac{dP}{ds} ds + \int_1^2 \vartheta\frac{\partial \vartheta}{\partial s} ds - \int_1^2 (\vec{g}\cdot\vec{s}) ds \tag{8.51}$$

In the last integral on the right-hand-side of equation (8.51), the magnitude of g is in the negative z-direction. The integral can be written as

$$-\int_1^2 (\vec{g}\cdot\vec{s}) ds = +g\int_1^2 (\vec{k}\cdot\vec{s}) ds = g\int_1^2 dz = g(z_2 - z_1) \tag{8.52}$$

The scalar product of $\vec{k}$ with $\vec{s}ds$ is just the signed magnitude of ds in the z-direction. The integral of this quantity is just the height difference between the endpoints of the path.

The final result is

$$0 = \int_1^2 \frac{\partial \vartheta}{\partial t} ds + \frac{P_2 - P_1}{\rho} + \frac{\vartheta_2^2 - \vartheta_1^2}{2} + g(z_2 - z_1) \tag{8.53}$$

This is the Bernoulli equation for unsteady flow. If the flow is steady, the partial derivative in time of the fluid velocity is zero and the equation reduces to the steady flow Bernoulli equation, viz.

$$\frac{P_1}{\rho} + \frac{\vartheta_1^2}{2} + gz_1 = \frac{P_2}{\rho} + \frac{\vartheta_2^2}{2} + gz_2 \tag{8.54}$$

Example 8E.15: A constant diameter U-tube, shown in Figure 8E.15, contains a low viscosity, incompressible liquid. Initially one side of the tube is at higher pressure so that there is a height difference h between the two free surfaces of the liquid. The valve is opened to the atmosphere and the pressure on that side of the U-tube immediately falls to atmospheric pressure.

(a) Assuming no dissipation, what is the subsequent motion of the fluid?

(b) What is the period of oscillation?

Solution: The flow is clearly unsteady and can be described by the Bernoulli equation with the streamline shown by the dashed line in Figure 8E.15. The pressures at points 1 and 2 are

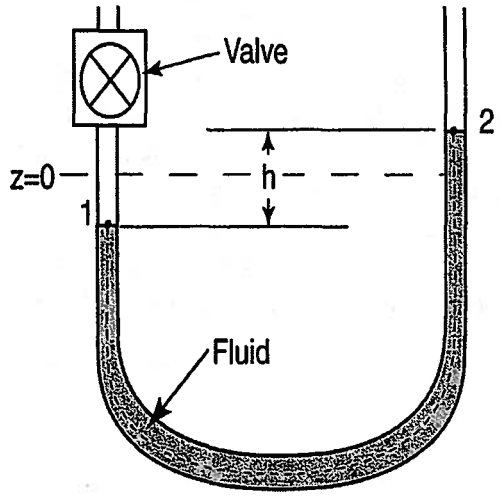

Figure 8E.15 Fluid-filled U-tube

identical and equal to atmospheric after the valve has been opened. The magnitudes of the velocities at points 1 and 2 are equal by continuity. The acceleration of the fluid is constant in the absence of any viscous damping. If the length of this streamline from point 1 to point 2 is L, then the time dependent Bernoulli equation is

$$0=\int_1^2 \frac{\partial \vartheta}{\partial t}ds+\frac{P_2-P_1}{\rho}+\frac{\vartheta_2^2-\vartheta_1^2}{2}+g(z_2-z_1)=L\frac{\partial \vartheta}{\partial t}+g(z_2-z_1)$$

The elevation z_2 is equal and opposite to z_1 because the fluid is incompressible. The velocity ϑ is equal to the time derivative of the position z_2. Then the Bernoulli equation becomes

$$\frac{d^2z_2}{dt^2}+\frac{2g}{L}z_2=0$$

This is the equation for simple harmonic motion. The solution is of the form

$$z_2(t)=\frac{h}{2}\cos\left(\sqrt{\frac{2g}{L}}\,t\right)$$

(b) The solution can be written in the form

$$z_2(t)=\frac{h}{2}\cos(\omega t)$$

where ω is the angular frequency of oscillation and T is the period of oscillation where

$$T=\frac{2\pi}{\omega}=2\pi\sqrt{\frac{L}{2g}}$$

Example 8E.16: A simplified drawing of a shock absorber as might be used on an automobile is shown in Figure 8E.16. This shock absorber consists of an oil filled piston-cylinder apparatus with holes bored in the piston. These holes serve as orifices through which fluid flows during the operation of the shock absorber. By virtue of the viscosity of the fluid, this flow establishes a pressure drop from one side of the orifice, and, hence, the piston, to the other in the direction of flow. This pressure drop ultimately manifests itself as the force that must be applied to the shock absorber during operation. There are N holes of cross sectional area A_d bored through the piston. The area of the piston face is A_p. Under steady conditions and a given force F, at what velocity does the piston move with respect to the cylinder?

Solution: As the piston moves, the oil in chamber A is accelerated, enters the small holes at high velocity, and then exits those holes into chamber B in the form of high velocity jets.

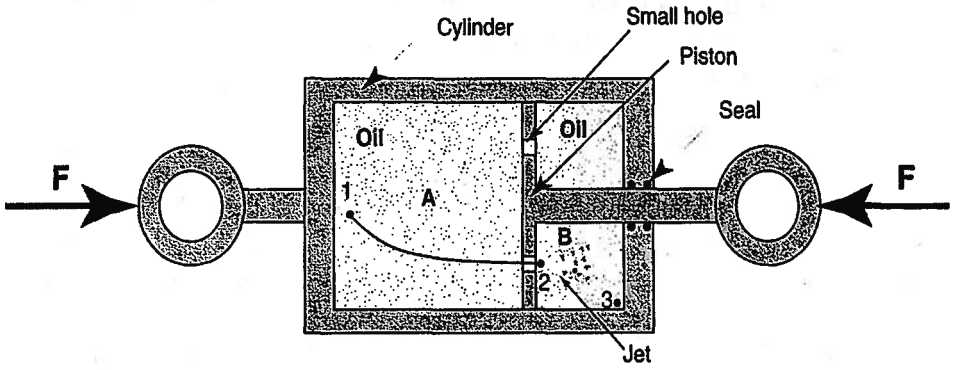

Figure 8E.16 Fluid-filled Shock Absorber

If the holes are short relative to the diameter of the holes, the thickness of the fluid boundary layer in the holes will be a small fraction of the diameter of the hole. (The significance of these constraints will become more apparent when we examine the viscous nature of fluids in detail later.) Outside this boundary layer, the Bernoulli relation can be applied.

The streamline 1-2 connects point 1 in chamber A where the velocity is zero and the pressure is P_A to a point 2 which is in the center of the fluid jet just inside chamber B. The streamlines in the jet around point 2 are all straight and parallel, and as we shall soon see, this means that the pressure at point 2 must be the pressure in chamber B, P_B.

Point 2 has been carefully chosen to ensure that the Bernoulli equation can be applied to the streamline between points 1 and 2. The viscous effects are confined to the boundary layer and the high shear layer at the edge of the fluid jet between the jet and the fluid that is quietly residing in chamber B. Downstream of point 2, this high shear layer ultimately generates turbulence where there is significant dissipation. Because all paths (streamlines) between point 2 and point 3 must pass through the highly turbulent shear region, it is inappropriate to apply the Bernoulli equation between these two points. This is not the case between points 1 and 2. Neglecting gravity, we can write the steady flow Bernoulli equation as

$$P_A - P_B = \frac{\rho \vartheta_2^2}{2}$$

The velocity of the fluid through the holes can be related to the velocity of the piston through the continuity equation,

$$\vartheta_2 = \frac{A_p}{NA_h}\vartheta_p$$

The force F can be calculated by from the pressure distribution on the piston. If we assume that $A_p >> NA_h$, the force is

$$F = A_p(P_A - P_B) = A_p\frac{\rho\vartheta_2^2}{2} = \frac{1}{2}\rho\frac{A_p^{\,3}}{(NA_h)^2}\vartheta_p^{\,2}$$

The force then varies as the velocity squared and is proportional to the area of the piston cubed.

8.8 Effect of Streamline Curvature on Pressure in the Flow Field

In example 8E.16 we alluded to the effect of streamline curvature on pressure in the flow field. We can now determine the nature of that effect by examining the r-component of Newton's second law of motion for the fluid element shown in Figure 8.7. In a manner similar to equation (8.45), the force on the fluid element in the r-direction consists of normal surface forces due to pressure acting on the faces of the element and body forces due to gravity. Then

$$F_r = P\left(r - \frac{dr}{2}\right)dqds - P\left(r + \frac{dr}{2}\right)dqds - \rho dsdrdq\left(\vec{g}\cdot\vec{r}\right) \qquad (8.55)$$

This is the force on the fluid element normal to the direction of travel. This is equal to the product of the mass of the fluid element and its acceleration in the r-direction, $-\vartheta^2/R$, where R is the local radius of curvature of the streamline. Newton's second law of motion becomes

$$-\rho dsdrdq\frac{\vartheta^2}{R} = P\left(r - \frac{dr}{2}\right)dqds - P\left(r + \frac{dr}{2}\right)dqds - \rho dsdrdq\left(\vec{g}\cdot\vec{r}\right) \qquad (8.56)$$

Equation (8.56) can be simplified by dividing through by $\rho ds dr dq$ and taking the limit as dr goes to zero. Then

$$-\rho\frac{\vartheta^2}{R} = -\frac{dP}{dr} - \rho(\vec{g}\cdot\vec{r})$$
$$\frac{dP}{dr} = \rho\frac{\vartheta^2}{R} - \rho(\vec{g}\cdot\vec{r}) \tag{8.57}$$

Thus the radial pressure gradient has two components: one due to the acceleration of the fluid in the radial direction and the other due to the radial component of the acceleration of gravity.

Equation (8.57) can be used to generate a useful boundary condition for the pressure in the center of a jet of fluid discharging from a nozzle into another fluid as shown in Figure 8.8.

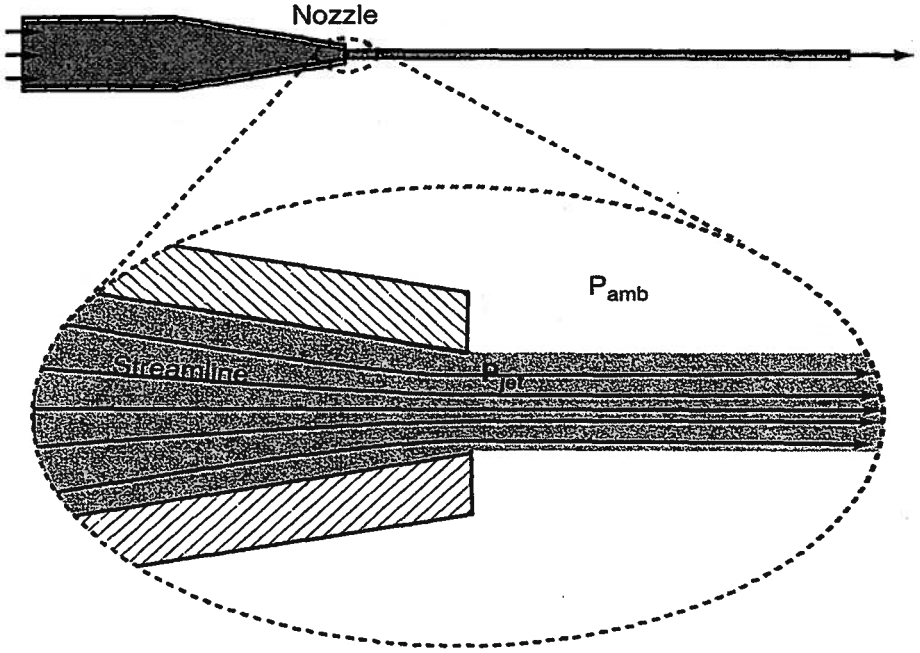

Figure 8.8 Streamlines in a Jet Discharging From a Nozzle

Near the exit of the nozzle, forces due to the shear between the two fluids have not yet established a substantial influence on the flow exiting the nozzle. If the vertical dimensions of the nozzle are small enough, the effect of gravity can also be neglected near the nozzle tip. The streamlines are straight as they leave the nozzle and hence the radius of curvature of the streamlines is infinite there. Equation (8.57) reduces to

$$\frac{dP}{dr} = 0$$

Then near the nozzle tip, the pressure throughout the jet is uniform in the radial direction. If the effect of surface tension at the interface between the two fluids is unimportant and if there are no compressibility effects in the fluid (shock waves), the pressure in the jet must be equal to the ambient pressure in the fluid surrounding the jet or

$$P_{jet} = P_{ambient}$$

8.9 Measurement of Flow Velocity: The Pitot Tube

In 1732, Henri Pitot, an assistant in the chemistry laboratory of the Academy of Sciences in Paris, presented to the Academy a design for an instrument for the measurement of the velocity

of a fluid in a flow field. Pitot's presentation which included data for the distribution of flow velocities as a function of depth in the River Seine was important not only because it introduced a new invention in the field of fluid mechanics, but also because it presented data that changed the prevailing understanding of the flow in rivers.

The use of this device, which bears Pitot's name in recognition of his contribution to modern fluid mechanics, is so widespread in thermal-fluids engineering that its principles of operation merit careful examination. Figure 8.9 shows a typical design for a Pitot tube. The flow is depicted in the reference frame of the Pitot tube itself for which the flow appears steady. The incompressible fluid approaches the Pitot tube from the left of Figure 8.9 at a uniform velocity $\hat{v}$. Figure 8.9 shows the streamlines, the thin boundary layer that forms on the outside surface of the Pitot tube, and the wake behind the device. The Bernoulli equation cannot be used in the boundary layer and wake regions since viscous effects dictate the flow there.

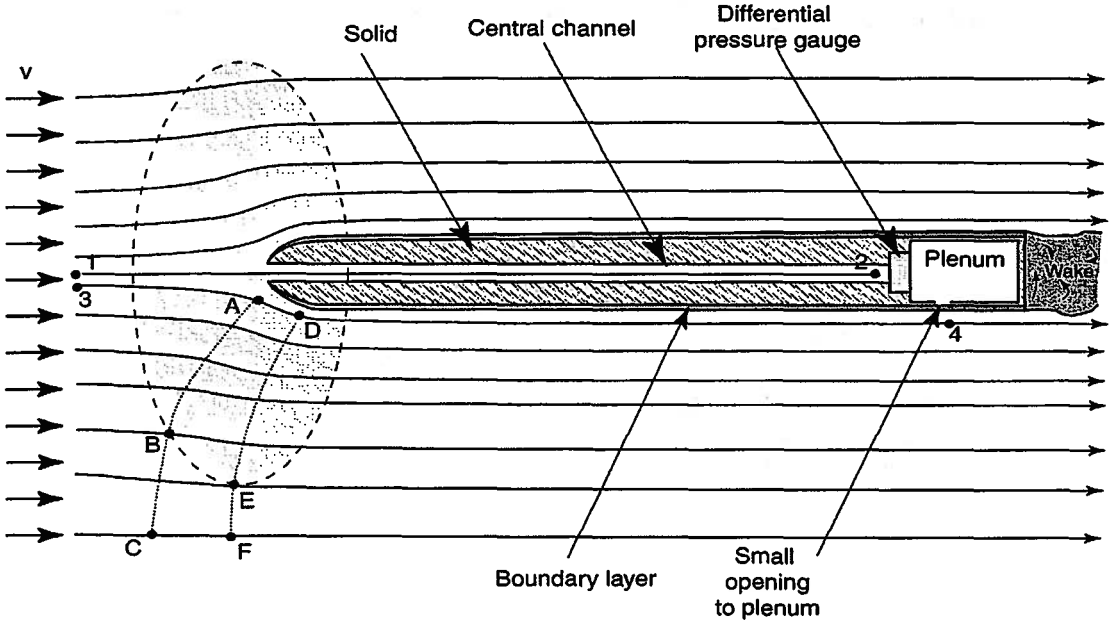

Figure 8.9 A Typical Pitot Tube

The shaded region shows where there is substantial curvature in the streamlines. This is also the region where there is substantial variation in the pressure of the fluid due to the dynamics of the flow. The dashed line between A and B traverses a path of minimum radius of curvature in the streamlines. Because the streamline curvature along this curve is concave downward, the pressure at point A must be larger than that at point B. The radius of curvature of the streamlines along the curve B-C is large, hence there is no substantial gradient in the pressure along this path. Since the pressure far away from the Pitot tube must be the ambient pressure, $P_A > P_B \approx P_C = P_{amb}$.

Similarly, curve D-E traverses a path of minimum radius of curvature, but in this case the curvature is concave upward. The pressure at point D is, therefore, lower than that at point E. The radius of curvature in the streamlines along path E-F is large so that the pressure at E is the same as at F. Thus, $P_D < P_E \approx P_F = P_{amb}$. Equation (8.57) requires that the pressure at point 4 also be ambient pressure since all the streamlines are straight parallel lines there, and the pressure far away from the Pitot tube is ambient pressure.

With the pressure distribution qualitatively determined along the streamline 3-A-D-4, the behavior of the fluid velocity along that streamline can be described using the steady flow Bernoulli equation. At point 3, far ahead of the Pitot tube, the fluid is at uniform velocity ϑ and at pressure P_{amb}. As a fluid particle approaches point A, it encounters an increasing pressure and decelerates as required by the steady Bernoulli equation, equation (8.54). At point A, the fluid particle velocity is a minimum. After the fluid particle passes point A, the particle accelerates in the large negative gradient of pressure between points A and D. At point D the velocity is a maximum along the streamline and the pressure is below ambient. Finally, along path D-4 the pressure returns to ambient. The velocity of the fluid particle at point 4 is the free stream velocity, ϑ, by the steady flow Bernoulli equation.

Consider now the fluid particle that travels along streamline 1-2. At point 1, far ahead of the Pitot tube, the pressure is P_{amb} and the fluid particle travels at a velocity ϑ. Since the central channel of the Pitot tube is sealed, the fluid particle slows to zero velocity as it approaches point 2. The steady flow Bernoulli equation can be applied to this streamline between points 1 and 2, yielding an expression for the pressure at point 2,

$$P_2 - P_{amb} = \rho \frac{\vartheta^2}{2} \tag{8.58}$$

The pressure in the plenum is the same as the pressure at point 4 or P_{amb}. The thin boundary layer that has developed along the upwind surfaces of the Pitot tube will flow over the hole in the side of the tube. This layer is incapable of sustaining a large pressure gradient across it so that the pressure in the plenum must equal the pressure at point 4. (This will be discussed in greater detail when we take up the topic of viscous fluids.) The existence of this highly dissipative boundary layer across the opening to the plenum does not allow the application of the steady flow Bernoulli equation between point 4 and any point within the plenum. Since the pressure sensed by the differential pressure gauge is P_2 - P_4 which is also P_2 - P_{amb}, equation (8.58) can be solved for the velocity of the flow

$$\vartheta = \sqrt{\frac{2(P_2 - P_{amb})}{\rho}} \tag{8.59}$$

A common application of the Pitot tube is for measuring the speed of aircraft flying through still air as shown schematically in Figure 8.10. In this case, the Pitot tube is moving in a

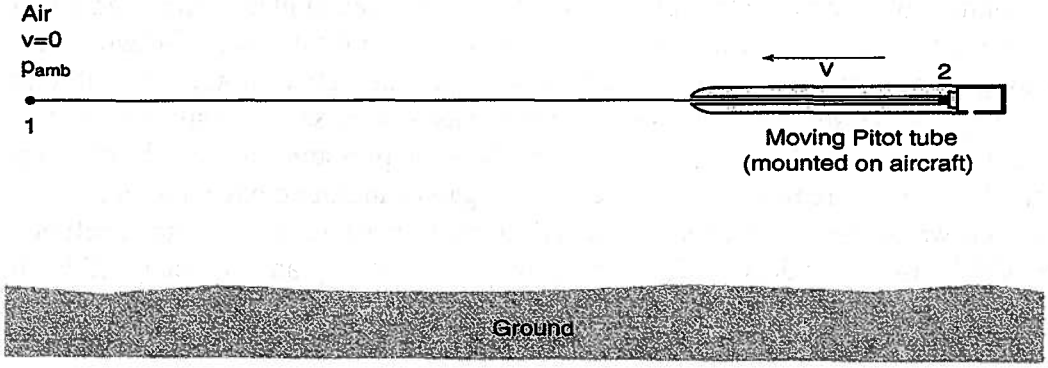

Figure 8.10 Pitot Tube Moving in a Fixed Reference Frame

reference frame attached to the ground. The streamline 1-2 extends from a fixed point well ahead of the Pitot tube where the air velocity is zero to inside the Pitot tube where the velocity of the fluid is the same as the Pitot tube velocity, ϑ. The pressure in the plenum of the Pitot tube is

ambient pressure using the equation (8.57) and the arguments discussed above. The problem as it is now posed is unsteady. The unsteady Bernoulli equation is

$$0 = \int_{s_1}^{s_2} \frac{\partial \vartheta}{\partial t} ds + \frac{P_2 - P_1}{\rho} + \frac{\vartheta_2^2}{2} \tag{8.60}$$

The line integral can be evaluated by using the following identity:

$$\frac{d}{dt}\int_{s_1(t)}^{s_2(t)} \vartheta(s,t) ds = \int_{s_1(t)}^{s_2(t)} \frac{\partial}{\partial t}[\vartheta(s,a)] ds + \left[\vartheta(s,a)\frac{ds_2(t)}{dt}\right]_{x=s_2} - \left[\vartheta(s,a)\frac{ds_1(t)}{dt}\right]_{x=s_1} \tag{8.61}$$

The left-hand-side of equation (8.61) is the time derivative of the line integral of the velocity of the fluid from position s_1 to position s_2. The velocity is zero over most of the length of the integral. There is only a small region near and in the Pitot tube where the velocity is non-zero. The value of this integral over this small region does not depend on time. The time derivative of this integral is therefore zero. The first term on the right-hand-side of equation (8.61) is the desired Bernoulli integral. Since

$$\frac{ds_2}{dt} = -\vartheta_2 \quad \text{and} \quad \vartheta(s_2,t) = -\vartheta_2$$

the second term on the right-hand-side of equation (8.61) is the square of the velocity of the fluid at point 2. The final term on the right-hand-side of equation (8.61) is zero because point 1 is at rest. It follows, then, that the first term on the right-hand-side of equation(8.60) has the value of $-\vartheta_2^2$. Incorporating this into equation (8.60) and solving for the velocity in terms of the pressure difference measured by the pressure gauge, we obtain

$$\vartheta_2 = \sqrt{\frac{2(P_2 - P_{amb})}{\rho}} \tag{8.62}$$

which is the same result as we previously obtained using the steady flow model.

While in principle the Pitot tube seems to be an ideal instrument for measuring local velocity in a flow field, it does suffer from several limitations. Principal among these is the sensitivity of the device to misalignment with the flow. As is evident from Figures 8.9 and 8.10, the principle of operation of the Pitot tube depends upon precise alignment of the central channel of the Pitot tube with the direction of the flow. For even small angles of misalignment (< 10°), also known as yaw angles, the error in the application of the Pitot tube, although small, can be large enough to rule out its use for measurements requiring high accuracy. The Pitot also has limited utility for measurement of flow velocity in gases because of the small pressure differential that develops between the static and dynamic pressures as a result of the low density of the fluid. For measurements of local velocity in gases, another device, the hot wire anemometer, whose operation depends upon heat transfer between the device itself and the flow is more widely used. The details of the operation of the hot wire anemometer will be discussed later when we examine the heat transfer between a flowing fluid and the solid surfaces that bound it. Finally, because of the relatively slow response of fluid-filled tubes to rapid changes in local conditions, the Pitot tube is usually restricted to applications in steady flow.

At this juncture, it is worthwhile to consider another class of flow meters, known as restriction flow meters or obstruction flow meters, whose use in thermal-fluid systems represents another common application of the Bernoulli equation. Unlike the Pitot tube device which is used for measuring local flow velocity in either external or external flows, restriction flow meters are used for measuring volumetric flow rates in internal flows such as those that occur in ducts or pipes.

8.10 Restriction Flow Meters

With few exceptions, restriction flow meters are used to measure volumetric flow rates in internal flows such as water supply systems. The basic idea that underlies the restriction flow meter is that the flow meter causes some reduction in the cross-sectional area of the flow which causes the flow to accelerate locally in order to satisfy the requirements of continuity. As we have seen from the Bernoulli equation, as the flow accelerates along a streamline, the static pressure decreases. We can make use of this behavior of the flow in the neighborhood of the restriction flow meter to measure the flow rate by measuring this change in pressure. Unfortunately, the restriction in the flow also generates entropy in the flow, and, as a result, we cannot apply the Bernoulli equation directly. Thus, for the restriction flow meter, it is not possible to use only the Bernoulli equation combined with the continuity equation to determine the flow rate. More information is required. Over the years, thermal-fluids engineers have developed an empirical means of accounting for the effect of the entropy generation on the flow so that we can apply the Bernoulli equation and the continuity equation indirectly to determine the flow rate.

Consider the restriction flow meter shown schematically in Figure 8.11. In simplest form, the flow meter is a very localized reduction in the cross-sectional area of the conduit carrying the flow. As the fluid tries to get through the reduced area, the streamlines converge, and the flow accelerates. This acceleration leads to a reduction in the local pressure. Consider a fluid particle that originated in the neighborhood of the conduit wall upstream of the flow meter. As this fluid particle passes through the opening of the flow meter, it cannot, due to its inertia, immediately "turn the corner" and return to the neighborhood of the conduit downstream of the flow meter.

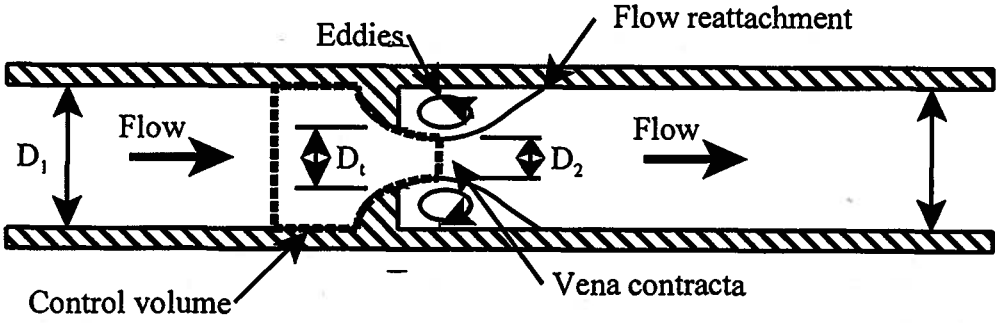

Figure 8.11 Schematic Representation of a Restriction Flow Meter

Instead, it gradually makes its way over to the conduit wall while traveling downstream a distance equivalent to several times the diameter of the conduit. This results in a separation of the flow from the conduit wall immediately behind the flow meter. Some fluid particles do break away from the mainstream of the flow and attempt to fill this void, but these fluid particles become trapped in this void and form eddies as they circulate around and around. It is these eddies that generate entropy as the fluid viscosity tries to damp them out as the fluid layers pass by one another in the eddy. Viscous dissipation in this region is high. In the mainstream of the flow away from the eddies, the flow is relatively well behaved even though the fluid viscosity is making itself felt here as well, albeit less emphatically than in the eddies.

Suppose that the fluid flowing in Figure 8.11 can be modeled as incompressible, and also suppose that for the moment we can neglect the effect of fluid viscosity. Then the flow approaching the control volume in Figure 8.11 has uniform velocity over the area $A_1 = \pi D_1^2/4$.

Similarly, the flow at the exit end of the control volume is uniform over the area $A_2 = \pi D_2^2/4$ where D_2 is not the diameter of the throat of the flow meter, D_t, but rather the diameter of a region of the flow downstream of the opening known as the *vena contracta* where, $D_2 < D_t$ due to the curvature of the streamlines in the neighborhood of the opening. In the vena contracta, the streamlines are straight so that the pressure is uniform across it.

Let us now apply the Bernoulli equation from area A_1 of the control volume to area A_2 of the control volume. Since the conduit is horizontal, we have

$$\frac{P_1}{\rho}+\frac{\vartheta_1^2}{2}=\frac{P_2}{\rho}+\frac{\vartheta_2^2}{2} \tag{8.63}$$

For steady flow, the continuity equation gives

$$\dot{m} = \rho A_1 \vartheta_1 = \rho A_2 \vartheta_2 \tag{8.64}$$

Combining equations (8.63) and (8.64) and solving for the pressure difference between area A_1 and area A_2, we get

$$P_1 - P_2 = \frac{\rho \vartheta_2^2}{2}\left[1-\left(\frac{A_2}{A_1}\right)^2\right] \tag{8.65}$$

However, in the application of these devices, the pressure difference P_1 - P_2 is usually measured directly, and it is the volumetric flow rate (in the case of an incompressible fluid) that we wish to determine. Then solving equation (8.65) for the fluid velocity at area A_2, we get

$$\vartheta_2 = \sqrt{\frac{2(P_1-P_2)}{\rho\left[1-\left(\frac{A_2}{A_1}\right)^2\right]}} \tag{8.66}$$

Then for the volumetric flow rate of an ideal flow meter, we get

$$\dot{V}_{ideal} = A_2 \vartheta_2 = A_2 \sqrt{\frac{2(P_1-P_2)}{\rho\left[1-\left(\frac{A_2}{A_1}\right)^2\right]}} \tag{8.67}$$

As we stated above, for an actual flow meter, the Bernoulli equation does not apply to this flow since the flow is not reversible. Thus, before we can apply equation (8.67) to a particular flow meter design, we need to make some corrections to it. In the first instance, for a particular flow meter of known geometry, we know the area A_t not the area A_2. Thus, in equation (8.67) we would like to replace A_2 with A_t. Secondly, we need to correct for viscous effects. By introducing an experimentally determined discharge coefficient C_d, we can lump together the effects of streamline curvature that produces the vena contracta and fluid viscosity that leads to the viscous dissipation . In addition, it is customary in practice to introduce the parameter β where $\beta = D_t/D_1$. Then for an actual flow meter, equation (8.67) becomes

$$\dot{V}_{actual} = C_d A_t \sqrt{\frac{2(P_1-P_2)}{\rho\left[1-\left(\frac{A_t}{A_1}\right)^2\right]}} = C_d A_t \sqrt{\frac{2(P_1-P_2)}{\rho\left[1-\beta^4\right]}} \tag{8.68}$$

The value for the discharge coefficient C_d will depend upon the flow meter design and the conditions of the flow as characterized by a dimensionless number, the Reynolds number, Re_D, (named after the same Osborne Reynolds who formulated the Reynolds Transport Theorem)

$$Re_D = \frac{\vartheta D \rho}{\mu} \tag{8.69}$$

where μ is the fluid viscosity and all parameters in equation (8.69) are evaluated upstream of the restriction flow meter. (As we shall show in Chapter 9, the Reynolds number plays a vitally important role in describing the nature of a flow field, and little can be said about the nature of a particular flow without recourse to it.)

Since the precise location of the vena contracta along the axis of the conduit is not always known, it is usually not possible to measure the static pressure in that location. Thermal-fluids engineers often resort to measuring P_2 in a location that is more convenient from the point of view of the installation of the restriction flow meter in the flow hardware. As a result, the particular locations for the measurement of the pressures P_1 and P_2 will be dictated by the design of the fluid piping system depending upon the flow meter design, and the effect of the location of the pressure measurement will be reflected in the value of the discharge coefficient.

Restriction flow meters usually are employed in one of three different configurations. In decreasing order of the rate of entropy generation in the flow, they are: (1) the orifice plate, (2) the flow nozzle, and (3) the Venturi meter. The listing also happens to be in increasing order of cost and ease of implementation. Thus in the selection of the particular design employed in a given situation, some trade off needs to be made between cost and acceptable rate of entropy generation.

8.10.1 Orifice Plate Flow Meter

The application of the orifice plate flow meter requires that the orifice plate itself be manufactured to precise specifications as shown in Figure 8.12. Typically the orifice plate is a circular plate that is sandwiched between flanges in a piping system with the locations for measuring local static pressure in the flow (the pressure taps) often incorporated into the mounting arrangement itself. As shown in Figure 8.12, the pressure taps are sometimes located in the pipe rather than in the mounting for the orifice plate. The particular correlation to be used between the measured pressure drop across the orifice plate and the volumetric flow rate depends upon the location of the pressure taps.

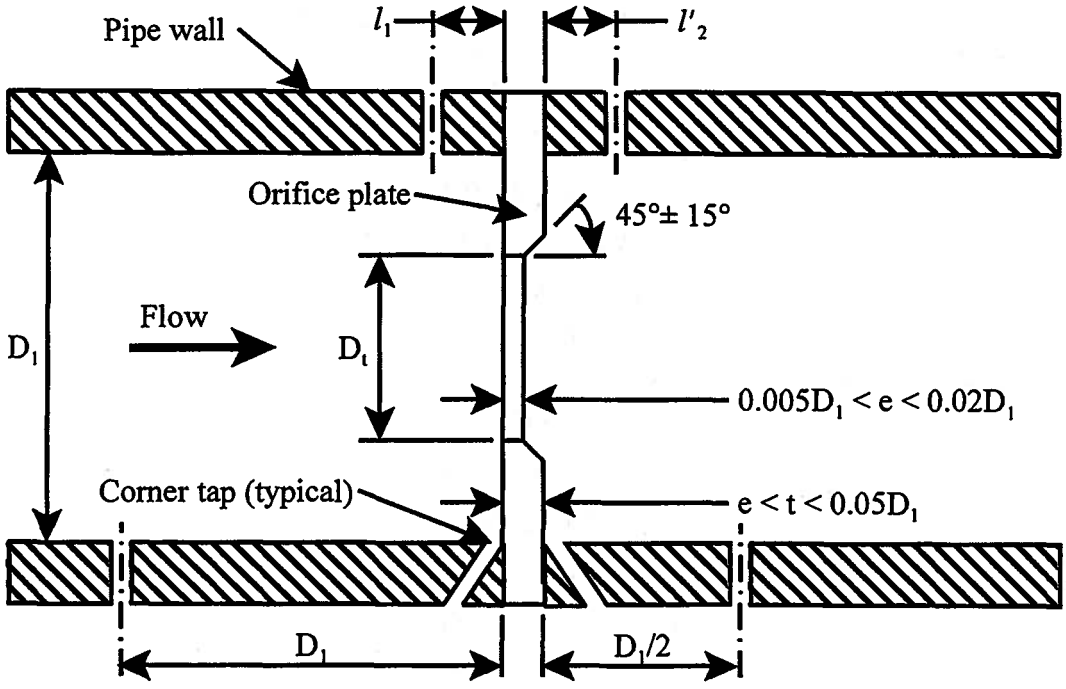

Figure 8.12 Orifice Plate Flow Meter and Pressure Tap Dimensions

As shown in Figure 8.12, there are three different pressure tap configurations: (1) flange taps, (2) corner taps, and (3) taps located at distances D_1 upstream and $D_1/2$ downstream from the orifice plate.

The International Standards Organization (ISO) has correlated the data for the discharge coefficient (ISO 5167-1, Amendment 1, 1998) in the form

$$C_d = 0.5961 + 0.0261\beta^2 - 0.216\beta^8 + 0.000521\left(\frac{10^6\beta}{Re_D}\right)^{0.7} + (0.0188 + 0.0063A)\beta^{3.5}\left(\frac{10^6}{Re_D}\right)^{0.3} + \\ + \left(0.043 + 0.080e^{-10L_1} - 0.123e^{-7L_1}\right)(1 - 0.11A)\frac{\beta^4}{1-\beta^4} - 0.031\left(M_2' - 0.8M_2'^{1.1}\right)\beta^{1.3} \tag{8.70}$$

where $L_1 = l_1/D_1$ and $L_2' = l_2'/D_1$ and

$$A = \left(\frac{19{,}000\beta}{Re_D}\right)^{0.8} \qquad \text{and} \qquad M_2' = \frac{2L_2'}{1-\beta}$$

Note that if $D < 71.12$ mm, the following term should be added to equation (8.70):

$$+0.011(0.75 - \beta)\left(2.8 - \frac{D}{25.4}\right)$$

where D is expressed in millimeters. To utilize equation (8.70), the location of the pressure taps must be known. Then for the various configurations of pressure taps, we have

Flange taps:

$$D_t \geq 12.5 \text{ mm}$$
$$50 \text{ mm} \leq D_1 \leq 1000 \text{ mm}$$
$$0.1 \leq \beta \leq 0.75$$
$$Re_D \geq 4000 \quad \text{and} \quad Re_D \geq 170\beta^2 D_1$$
$$L_1 = L_2' = \frac{25.4}{D_1}$$

where D_1 is expressed in millimeters.

Corner taps:

$$D_t \geq 12.5 \text{ mm}$$
$$50 \text{ mm} \leq D_1 \leq 1000 \text{ mm}$$
$$0.1 \leq \beta \leq 0.75$$
$$Re_D \geq 4000 \text{ for } 0.1 \leq \beta \leq 0.5$$
$$Re_D \geq 16000\beta^2 \text{ for } \beta > 0.5$$
$$L_1 = L_2' = 0$$

Upstream and downstream taps:

$$D_t \geq 12.5 \text{ mm}$$
$$50 \text{ mm} \leq D_1 \leq 1000 \text{ mm}$$
$$0.1 \leq \beta \leq 0.75$$
$$Re_D \geq 4000 \text{ for } 0.1 \leq \beta \leq 0.5$$
$$Re_D \geq 16000\beta^2 \text{ for } \beta > 0.5$$
$$L_1 = 1 \text{ and } L_2' = 0.47$$

8.10.2 Nozzle Flow Meter

The nozzle flow meter exists in two configurations: (1) the ISA 1932 nozzle, which is widely used in Europe but rarely used in the United States, and (2) the ASME long radius nozzle which is more widely used in the United States. As shown in Figure 8.13, the ASME long radius nozzle exists in two configurations: (1) the high ratio ($0.25 \le \beta \le 0.8$) configuration and (2) the low ratio ($0.20 \le \beta \le 0.5$) configuration.

The discharge coefficients C_d are the same for both configurations of the long radius nozzle. For long radius nozzles with

$$50 \text{ mm} \le D_1 \le 630 \text{ mm}$$

$$0.2 \le \beta \le 0.8$$

$$10^4 \le Re_D \le 10^7$$

ISO 5167-1, 1991, gives

$$C_d = 0.9965 - 0.00653\sqrt{\frac{10^6 \beta}{Re_D}} \tag{8.71}$$

where the Reynolds number is evaluated at conditions upstream of the nozzle. Notice that although the discharge coefficient is nearly unity, it still is less than unity because the jet emerging from the nozzle remains detached from the conduit wall a distance equivalent to several conduit diameters downstream from the nozzle exit in a manner similar to the jet emerging from the orifice plate flow meter. Then the flow emerging from the nozzle is similarly separated from the conduit wall, and as we saw previously, this flow configuration generates entropy.

8.10.3 Venturi Tube Flow Meter

As we have just seen, both the orifice plate flow meter and the nozzle flow meter generate entropy by virtue of the detached flow of the emerging jet. By adding a conically diverging conduit section, known as a diffuser, on the downstream side of these flow meters, it is possible to prevent separation of the flow from the conduit wall by allowing a gradual deceleration of the flow as the conduit diameter gradually increases back to the dimension found upstream of the flow meter.

This conduit configuration was studied in detail by the Italian physicist Giovanni Battista Venturi (1746-1822) who found that a conically convergent section of conduit upstream of the throat of the device was necessary if entropy generation was to be minimized. From the point of view of thermal-fluids design, the convergent section is much simpler to deal with since the pressure is decreasing in the direction of flow. This is a stable configuration as the fluid is accelerated in the direction of decreasing pressure. The fluid friction present at the walls of the device is easily overcome by the favorable pressure gradient in the mainstream of the flow. On the other hand, the diverging section is more difficult to deal with since the fluid is being decelerated in the direction of increasing pressure. Because of the additional influence of fluid friction, the fluid in the neighborhood of the wall is decelerated faster than the fluid in the mainstream. As a result, the flow in the neighborhood of the wall can sometimes reverse thereby generating considerable entropy. The net result is a potentially unstable situation that requires careful design. The flow must be decelerated very gradually so as to avoid any possible flow reversal. This means that the diverging section must increase area in the direction of flow much more gradually than the converging section decreased area in the direction of flow. The resulting design is known as a Venturi tube in honor of the individual who first studied these devices.

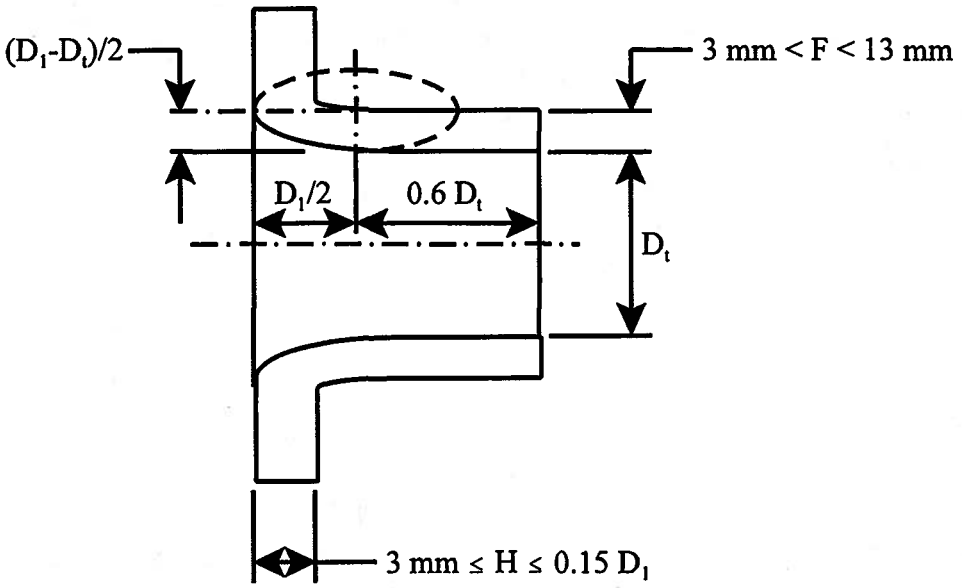

(a) High ratio, long radius ASME nozzle

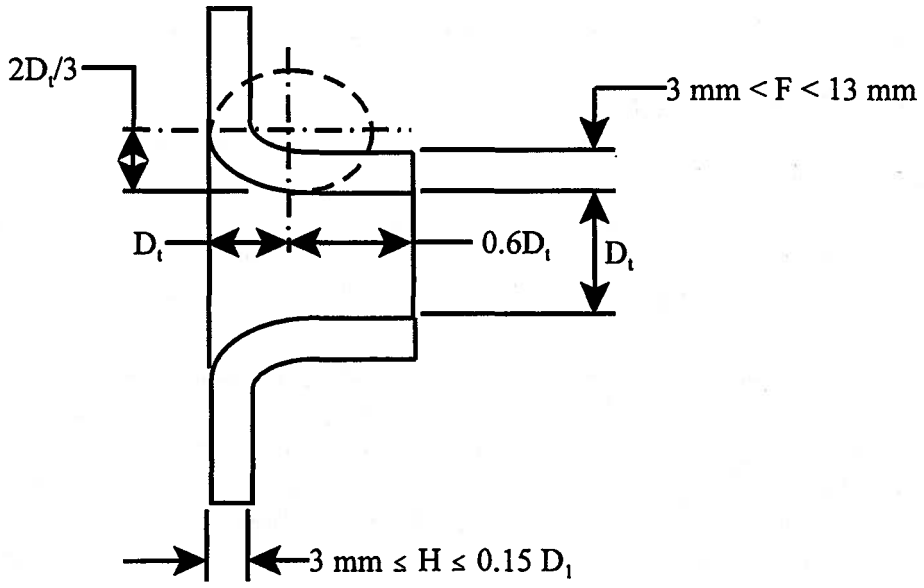

(b) Low ratio, long radius ASME nozzle

Figure 8.13 Long Radius ASME Nozzles (not to scale)

There are two different types of standard Venturi tubes in current use: (1) the classical Venturi tube and (2) the Venturi nozzle. The geometry of the classical Venturi tube is shown in Figure 8.14. The upstream pressure tap in this case is located in the conduit upstream from the beginning of the convergent section a distance equal to one-half the conduit diameter. The other pressure tap is located axially in the middle of the throat.

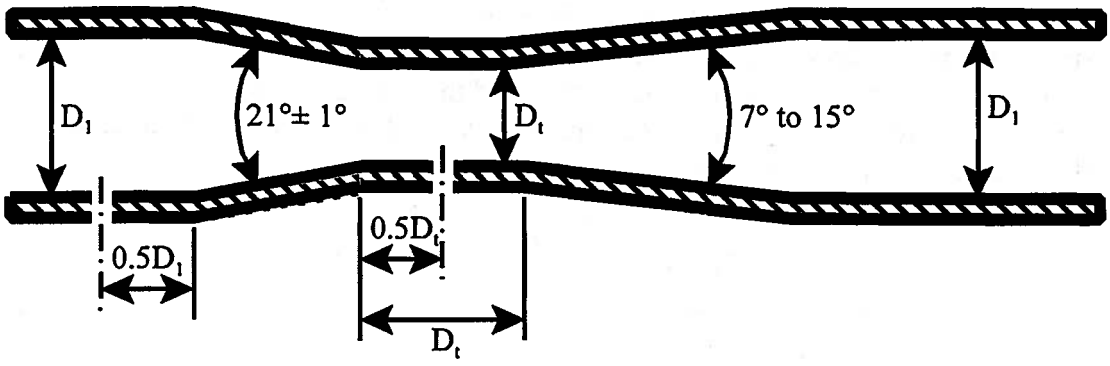

Figure 8.14 Classical Venturi Tube

The performance of the Venturi tube is sensitive to the roughness of the surface of the convergent section which is manufactured in three forms, each of which has its own value for the discharge coefficient. The values reported in ISO 5167-1, 1991, are:

"As cast" convergent section:

$$100 \text{ mm} \le D_1 \le 800 \text{ mm}$$

$$0.3 \le \beta \le 0.75$$

$$2 \times 10^5 \le Re_D \le 2 \times 10^6$$

$$C_d = 0.984$$

Machined convergent section:

$$50 \text{ mm} \le D_1 \le 250 \text{ mm}$$

$$0.4 \le \beta \le 0.75$$

$$2 \times 10^5 \le Re_D \le 1 \times 10^6$$

$$C_d = 0.995$$

Rough-welded sheet-iron convergent section:

$$200 \text{ mm} \le D_1 \le 1200 \text{ mm}$$

$$0.4 \le \beta \le 0.7$$

$$2 \times 10^5 \le Re_D \le 2 \times 10^6$$

$$C_d = 0.985$$

An alternative design of the Venturi tube is to fit a divergent section to the discharge of the ISA 1932 nozzle resulting in a Venturi nozzle (not shown). The upstream pressure tap is a corner tap and the other tap is centrally located (in the axial direction) in the throat. The discharge coefficient for this design reported in ISO 5167-1, 1991, is:

$$65 \text{ mm} \le D_1 \le 500 \text{ mm}$$

$$D_t \ge 50 \text{ mm}$$

$$0.316 \le \beta \le 0.775$$

$$1.5 \times 10^5 \le Re_D \le 2 \times 10^6$$

$$C_d = 0.9858 - 0.196\beta^{4.5}$$

8.10.4 Entropy Generation by Restriction Flow Meters

In order to determine the rate of entropy generation by restriction flow meters, we establish a control volume in Figure 8.11 for which the exit plane is located sufficiently far downstream so that the flow is reattached to the conduit wall. If we denote the state of the fluid at entrance to this control volume by the subscript *in* and the state of the fluid at the exit from this control volume by the subscript *out*, we can apply the second law of thermodynamics for this control volume in the form of equation (8.42), viz.

$$\frac{dS_{CV}}{dt} = \sum_i \left(\frac{\dot{Q}}{T}\right)_i + \sum_{in} (\dot{m}s)_{in} - \sum_{out} (\dot{m}s)_{out} + \dot{S}_{gen} \tag{8.42}$$

For the case in which the flow can be modeled as adiabatic and steady with a single inlet and a single outlet, this expression reduces to

$$\dot{S}_{gen} = \dot{m}(s_{out} - s_{in}) \tag{8.72}$$

If the fluid can be modeled as incompressible, equation (8.72) becomes

$$\dot{S}_{gen} = \dot{m}c \ln \frac{T_{out}}{T_{in}} \tag{8.73}$$

Equation (8.73) can be expressed in dimensionless form as

$$\frac{\dot{S}_{gen}}{\dot{m}c} = \ln \frac{T_{out}}{T_{in}} \tag{8.74}$$

If the flow through the restriction flow meter were reversible and adiabatic, the rate of entropy generation would be zero, and it would follow from equation (8.74) that the inlet and outlet temperatures of the fluid would be identical. However, this is not the case. As described previously, the flow is irreversible. Thus, in order to determine the rate of entropy generation, we first need to determine the increase in temperature of the fluid due to viscous dissipation as it passes through the flow meter. This information can be obtained by applying the first law to the aforementioned control volume. According to equation (8.37)

$$\frac{dE_{CV}}{dt} = \dot{Q} - \dot{W}_{shaft} + \sum_{in} \dot{m}_{in} \left(h + \frac{\vartheta^2}{2} + gz\right)_{in} - \sum_{out} \dot{m}_{out} \left(h + \frac{\vartheta^2}{2} + gz\right)_{out} \tag{8.37}$$

For the control volume of interest, the flow is steady and the kinetic and potential energies are constant with no heat transfer or shaft work transfer. Then equation (8.37) reduces to

$$\begin{aligned} h_{in} &= h_{out} \\ u_{in} + \left(\frac{P}{\rho}\right)_{in} &= u_{out} + \left(\frac{P}{\rho}\right)_{out} \end{aligned} \tag{8.75}$$

Since the fluid can be modeled as incompressible, we can substitute the energy constitutive relation into equation (8.75). Then the temperature of the fluid at outlet becomes

$$T_{out} = T_{in} + \frac{1}{\rho c}(P_{in} - P_{out}) \tag{8.76}$$

Substituting equation (8.76) into equation (8.74), we obtain

$$\frac{\dot{S}_{gen}}{\dot{m}c} = \ln\left[1 + \frac{(P_{in} - P_{out})}{\rho c T_{in}}\right] \tag{8.77}$$

Recall that the pressure difference (P_{in} - P_{out}) appearing in equation (8.77) is the pressure decrease experienced by the flow as a result of having passed through the flow meter after the

flow has been re-established in the conduit rather than the pressure drop (P_1 - P_2) that is measured at the pressure taps utilized for the particular flow geometry of a given flow meter. For the orifice plate flow meter and the nozzle flow meter, these two pressure drops are related by the expression given in ISO 5167-1, 1991, viz.

$$P_{in} - P_{out} = \frac{\sqrt{1-\beta^4} - C_d\beta^2}{\sqrt{1-\beta^4} + C_d\beta^2}(P_1 - P_2) \tag{8.78}$$

For the Venturi tube flow meter, the relation between these two pressure drops is taken from experimental data[1].

To illustrate the relative performance of the various flow meter designs, equations (8.77) and (8.78) have been evaluated for the case of water flowing in a pipe of diameter D_1 =200 mm at a Reynolds number of $Re_D = 10^6$. If $T_{in} = 290$ K, the various properties of the water can be evaluated: $\rho = 999$ kg/m^3, $c = 4186$ J/kg K, and $\mu = 11.00 \times 10^{-4}$ kg/m sec. The results are shown as a function of β in Figure 8.15. Note in general that for a given geometry, the entropy

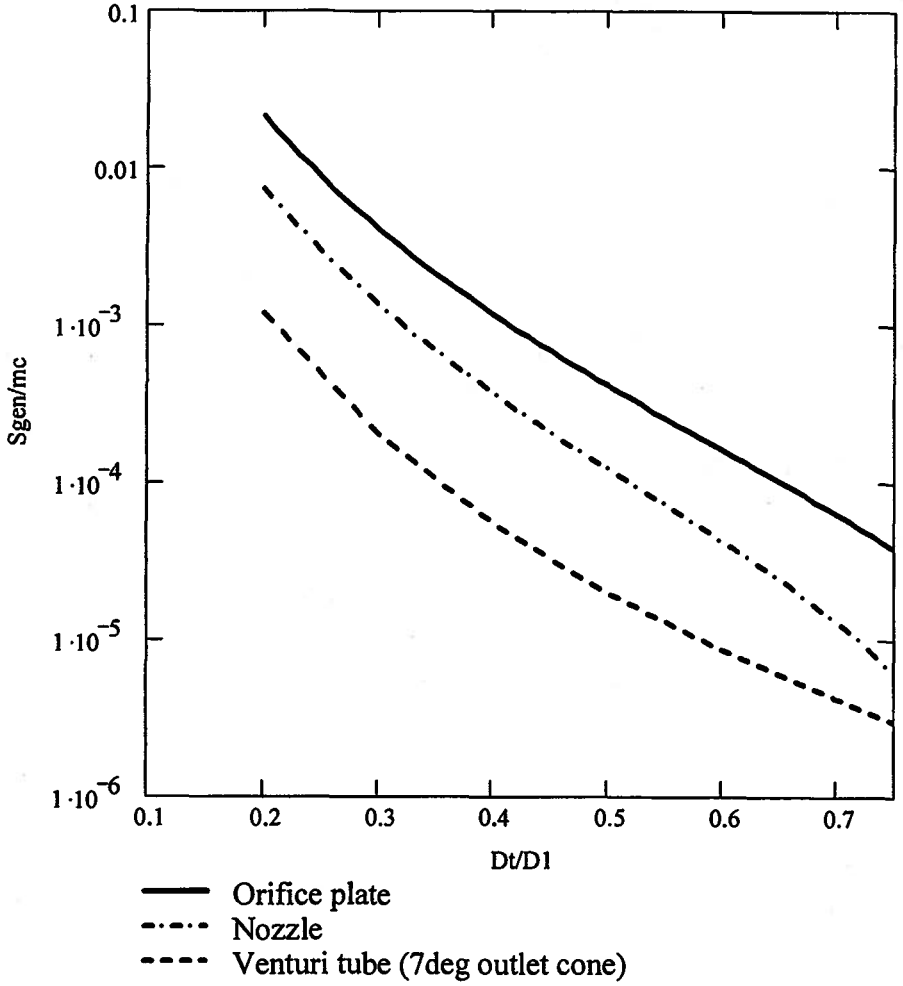

Figure 8.15 Entropy Generation by Restriction Flow Meters

[1] *Fluid Meters: Their Theory and Application*, ed. by H. S. Bean, American Society of Mechanical Engineers, Sixth Edition, 1971, p. 232.

generation in the orifice plate flow meter is greater than that in the nozzle flow meter which, in turn, is greater than that in the Venturi tube flow meter. Also note that as β increases, entropy generation in the nozzle flow meter and the Venturi tube flow meter approach each other. This indicates that the flow at the exit of the nozzle is reattaching to the walls of the conduit in a more nearly reversible fashion as nozzle diameter increases relative to conduit diameter. In effect, as the diameter of the nozzle discharge approaches the diameter of the conduit, the nozzle discharge functions in a manner similar to a diffuser.

8.11 Equation of Linear Momentum for a Control Volume

For a control mass, Newton's second law of motion can be written

$$\vec{F} = M_{cm}\vec{a} = M_{cm}\frac{d\vec{\vartheta}}{dt} = \frac{d}{dt}\left(M_{cm}\vec{\vartheta}\right) = \frac{d}{dt}\left(\vec{P}\right) \tag{8.79}$$

where F is the net force on the control mass and P is the linear momentum of the control mass. We can apply the Reynolds Transport Theorem to Newton's second law by recognizing that the momentum, P, is the extensive property (B) and that the velocity, $\vec{\vartheta}$, is the corresponding specific quantity (b).Then

$$\frac{d}{dt}\left(\vec{P}\right) = \frac{d}{dt}\int_{CV}\rho\vec{\vartheta}dV + \int_{CS}\rho\vec{\vartheta}\left(\vec{\vartheta}_r\cdot\vec{n}\right)dA \tag{8.80}$$

Equations (8.79) and (8.80) can be combined to yield

$$\vec{F} = \frac{d}{dt}\int_{CV}\rho\vec{\vartheta}dV + \int_{CS}\rho\vec{\vartheta}\left(\vec{\vartheta}_r\cdot\vec{n}\right)dA \tag{8.81}$$

Thus, the net force acting on the control volume is equal to the rate of change of momentum of the control volume and its contents plus the net flow of momentum out of the control volume. Note that unlike our previous application of the Reynolds Transport Theorem, we have obtained a vector equation rather than a scalar equation. Thus, in the Cartesian coordinate system, equation (8.81) is actually three equations, one for each of the three coordinate directions x, y, and z. Then for the x-direction, equation (8.81) yields

$$F_x = \frac{d}{dt}\int_{CV}\rho\vartheta_x dV + \int_{CS}\rho\vartheta_x\left(\vec{\vartheta}_r\cdot\vec{n}\right)dA \tag{8.82}$$

where ϑ_x is the x-component of fluid velocity. Note that the vectors appearing in the scalar product retain their vector identity because they are within the vector algebra operation of the scalar product.

The net force acting on the control volume in equation (8.81) is the vector sum of all the forces that are applied to the control volume. These forces can be separated into two classes, surface forces and body forces. Examples of surface forces include shear forces in solids, pressure forces, and viscous forces. The most common example of a body force is the force due to the action of gravity. We can condense these into mathematical form as

$$\frac{d}{dt}\int_{CV}\rho\vec{\vartheta}dV + \int_{CS}\rho\vec{\vartheta}\left(\vec{\vartheta}_r\cdot\vec{n}\right)dA = \int_{CS}(-P\vec{n})\,dA + \int_{CS}(\vec{\tau})\,dA + \int_{CV}\rho\vec{g}\,dV \tag{8.83}$$

The first term on the left-hand-side of equation (8.83) is the rate of change of momentum inside the control volume. The second term on the left-hand-side is the rate at which momentum leaves the control volume. The first term on the right-hand-side of equation (8.83) is the sum of the

forces due to pressure applied to the control surface of the control volume. The second term on the right-hand-side is the sum of all the shear forces acting on the control surface of the control volume. These forces can be due to viscous forces in a fluid or due to shear stresses in solid members that are cut by the control surface. The last term on the right-hand-side of equation (8.83) is the gravitational body force that acts on all the mass inside the control volume at any instant of time.

Since Newton's second law, equation (8.79), is appropriate for inertial, i.e., not accelerating, reference frames, the same restriction must be imposed on the equations derived from that law. Thus the velocities appearing in equation (8.80) must be measured relative to an inertial reference frame. We will relax this restriction subsequently.

Example 8E.17: A fire hose is held by a firefighter in the configuration shown in Figure 8E.17. The diameter at the end of the nozzle is $D_n = 2$ cm. If the mass flow rate through the hose is 500 kg/min, what is the magnitude of the force the firefighter must place on the nozzle to keep it stationary?

Solution: The x-component of force is given by the x-component of the equation of linear momentum. Then

$$\sum F_x = F_{x,firefighter} + \left[\int_{CS} (-P\vec{n})\, dA + \int_{CS} (\vec{\tau})\, dA + \int_{CV} \rho \vec{g}\, dV \right]_x = \frac{d}{dt} \int_{CV} \rho \vartheta_x dV + \int_{CS} \rho \vartheta_x \left(\vec{\vartheta}_r \cdot \vec{n} \right) dA$$

Here we have divided the sum of the forces as the firefighter's applied force to the control volume, the forces due to pressure applied to the control surface, the shear forces across the control surface, and the body force due to gravity. Strictly speaking the firefighter's forces could be accounted for as pressure and shear forces where the control volume cuts the arms of the firefighter. The specifics of the forces in the arms are not of interest to us so that we choose to represent the firefighter as a force vector.

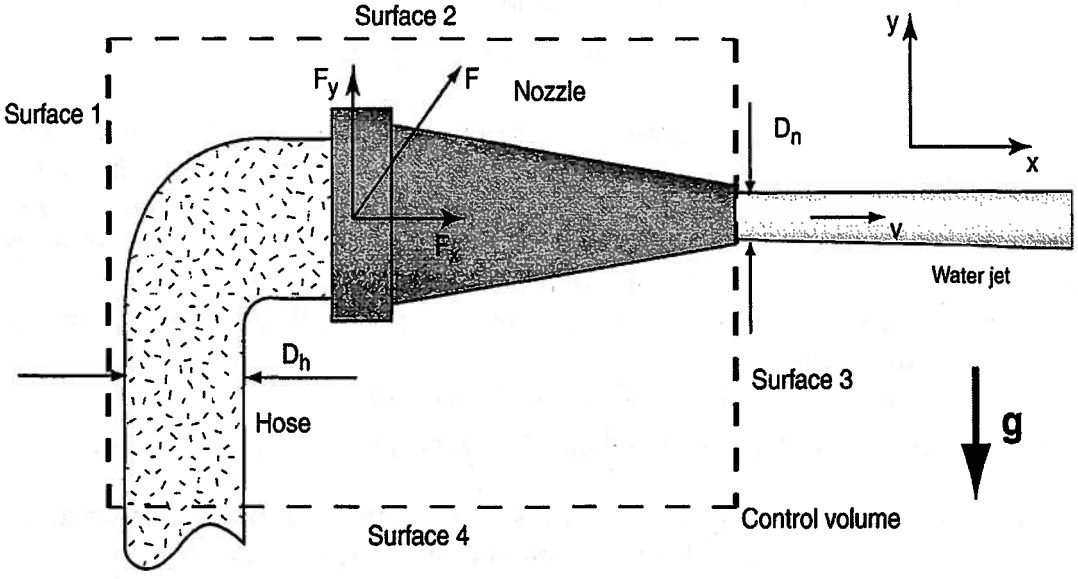

Figure 8E.17 Nozzle on Fire Hose

The pressure integral can be expanded over the four surfaces 1, 2, 3 and 4 as shown in Figure 8E.17.

$$\left[\int_{CS}(-P\vec{n})\,dA\right]_x=\left[\int_1(-P\vec{n})\,dA\right]_x+\left[\int_2(-P\vec{n})\,dA\right]_x+\left[\int_3(-P\vec{n})\,dA\right]_x+\left[\int_4(-P\vec{n})\,dA\right]_x$$

The integrals over surfaces 2 and 4 are in the y-direction only; hence, the x-component of these integrals is zero. The integral over surface 1 is the product of atmospheric pressure P_{atm} and the area of surface 1, A_1. More explicitly,

$$\left[\int_1(-P\vec{n})\,dA\right]_x=\left[-P_{atm}\int_1(-\vec{i})\,dA\right]_x=\left[P_{atm}\left(\int_1 dA\right)\vec{i}\right]_x=P_{atm}A_1$$

where $\vec{i}$ is the unit vector in the x-direction.

In those regions where surface 3 contacts the air, the pressure is clearly P_{atm}. In that region of surface 3 where it encounters the water jet we make use of the results of Section 8.8. The streamlines in the jet are straight and parallel; thus, there can be no pressure gradient across the jet. Then the pressure inside the jet is the same as that outside the jet. Then it must be the case that all of surface 3 is at atmospheric pressure, and the pressure integral for surface 3 becomes

$$\left[\int_3(-P\vec{n})\,dA\right]_x=\left[-P_{atm}\int_3(\vec{i})\,dA\right]_x=\left[-P_{atm}\left(\int_3 dA\right)\vec{i}\right]_x=-P_{atm}A_3=-P_{atm}A_1$$

since $A_3=A_1$. The pressure integrals for surfaces 1 and 3 are equal and opposite. We conclude that the overall contribution of the pressure integral in the mass conservation equation is zero.

The shear stress integral is also zero. We assume that the wall of the hose does not support a net shear stress across surface 4. The fluids, in uniform flow, also do not support a shear stress. (We will discuss the ways in which fluids can support a shear stress later.)

The direction of the gravity integral is in the negative y-direction so that the x-component of this integral is zero.

Then the equation of linear momentum reduces to

$$F_{x,firefighter}=\frac{d}{dt}\int_{CV}\rho\vartheta_x\,dV+\int_{CS}\rho\vartheta_x\,(\vec{\vartheta}_r\cdot\vec{n})dA$$

Let us now consider the first term on the right-hand-side of the momentum equation. It is a time derivative of a volume integral of the x-component of momentum per unit volume of the fluid. Since the flow in the present example is steady, it follows that for a given position, the velocity and the density, and, hence, their product, are not varying with time. The sum (integral) of many time-invariant quantities is itself time-invariant and the time derivative of such a quantity is zero. Since the flow is steady, we conclude that the first term on the right-hand-side of the linear momentum equation must be zero.

We have thus reduced the analysis to solving the surface integral

$$F_{x,firefighter}=\int_{CS}\rho\vartheta_x(\vec{\vartheta}\cdot\vec{n})dA=\int_1\rho\vartheta_x(\vec{\vartheta}\cdot\vec{n})dA+\int_2\rho\vartheta_x(\vec{\vartheta}\cdot\vec{n})dA+\int_3\rho\vartheta_x(\vec{\vartheta}\cdot\vec{n})dA+\int_4\rho\vartheta_x(\vec{\vartheta}\cdot\vec{n})dA$$

The velocity across surfaces 1 and 2 is identically zero so that the integrals over those surfaces are zero. The integral over surface 4 does have a region of flow where there is a non-zero velocity; however, this velocity is entirely in the y-direction. The x-component of the fluid velocity is zero in this region. Then the integral over surface 4 is zero.

The velocity of the jet can be calculated from the mass flow rate, the density of the water and the diameter of the nozzle.

$$\mathcal{9}_{jet} = \frac{\dot{m}}{\rho A_{nozzle}} = \frac{\dot{m}}{\rho \frac{\pi D_n^{\ 2}}{4}} = \frac{(500 \text{ kg/min})/(60 \text{ sec/min})}{(1000 \text{ kg/m}^3)\frac{\pi(0.02 \text{ m}^2)^2}{4}} = 26.5 \text{ m/sec}$$

The integrand over surface 3 is zero everywhere except in the jet where it is a constant value. The integral becomes

$$\int_3 \rho \mathcal{9}_x (\vec{\mathcal{9}}_r \cdot \vec{n}) dA = \int_{jet} \rho \mathcal{9}_{jet} (\mathcal{9}_{jet}) dA = \rho \mathcal{9}_{jet}^2 \int_{jet} dA = \rho \mathcal{9}_{jet}^2 A_{jet} = \rho \mathcal{9}_{jet}^2 \frac{\pi D_n^2}{4}$$

The force in the x-direction imposed by the firefighter is

$$F_{x,firefighter} = \rho \mathcal{9}_{jet}^2 \frac{\pi D_n^2}{4} = (1000 \text{ kg/m}^3)(26.5 \text{ m/sec})^2 \frac{\pi(0.02 \text{ m})^2}{4} = 221 \text{ N}$$

In U.S. units, this is about 50 pounds force.

For pedagogical reasons, we have gone through the evaluation of all the integrals for the linear momentum equation in great detail in this example. With some practice, the student should be able to dispatch most of the non-essential integrals by inspection.

Example 8E.18: In the jet pump shown in Figure 8E.18, a high velocity fluid stream is injected into an insulated pipe where it entrains and pumps a lower velocity water stream down the larger pipe. The pump operates by virtue of the momentum transfer between the smaller, high-velocity stream and the larger, low-velocity stream. The pressure and temperature of the fluid along surfaces 1 and 2 are $P_1 = P_2 = 2\text{x}10^5$ Pa and $T_1 = T_2 = 300$ K, respectively. The respective velocities are $\mathcal{9}_1 = 30$ m/sec and $\mathcal{9}_2 = 0.1$ m/sec. The diameter of the large pipe is $d_2 =$ 5 cm and that of the small pipe is $d_2 = 1$ cm. For the purposes of this analysis, we will assume that the shear stresses on the wall of the pipe are insignificant and that the velocity profiles are as shown in Figure 8E.18.

(a) What is the velocity $\mathcal{9}_3$?
(b) What is the pressure rise in the fluid from surface 1 to 3?
(c) What is the temperature of the fluid on surface 3?
(d) Is the flow reversible? If not, what is the rate of entropy generation in the device?
(e) Can the Bernoulli equation be used between surfaces 1 and 3?

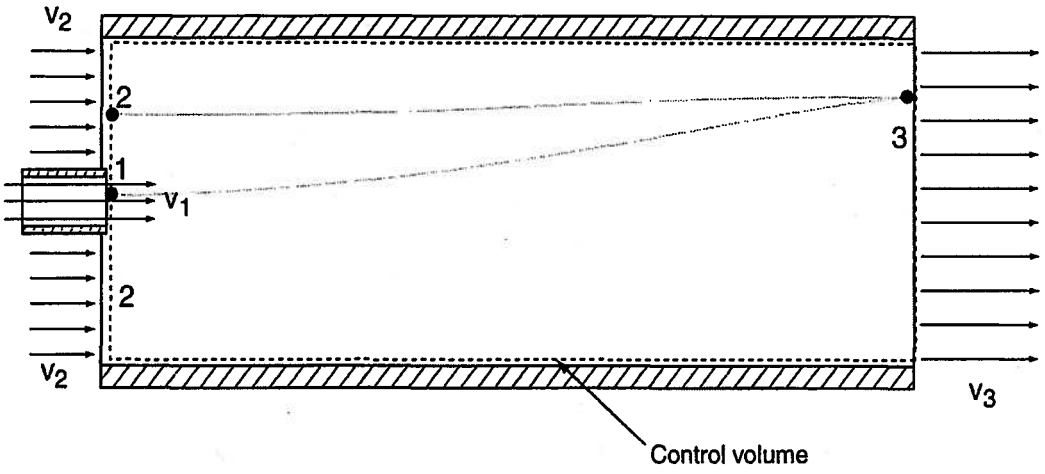

Figure 8E.18 Cross-sectional View of a Jet Pump

Solution: (a) The velocity over surface 3 can be calculated using the continuity equation. Since the flow is steady and we are modeling the water as incompressible, the continuity equation for the control volume shown above becomes

$$0 = -A_1\mathcal{V}_1 - A_2\mathcal{V}_2 + A_3\mathcal{V}_3$$

Then, solving for the velocity at surface 3, we get

$$\mathcal{V}_3 = \frac{A_1\mathcal{V}_1 + A_2\mathcal{V}_2}{A_3} = \frac{d_1^2\mathcal{V}_1 + \left(d_2^2 - d_1^2\right)\mathcal{V}_2}{d_3^2} = \frac{(1\text{ cm})^2(30\text{ m/sec}) + \left[(5\text{ cm})^2 - (1\text{ cm})^2\right](0.1\text{ m/sec})}{(5\text{ cm})^2}$$

$$\mathcal{V}_3 = 1.296\text{ m/sec}$$

(b) The momentum equation can be applied to the control volume. In the model of the flow, we are assuming that the shear stresses on the walls of the pipe are negligible. Also, gravity acts normal to the flow direction. Then the only externally applied forces on the control volume that are of consequence are those due the normal stress, the pressure, acting on each part of the control surface. Furthermore, since we are interested in the steady flow performance of this pump, the linear momentum equation for the horizontal direction becomes

$$\int_{CS}\left(-P\vec{n}\right)dA = \int_{CS}\rho\vec{\mathcal{V}}\left(\vec{\mathcal{V}}_r\cdot\vec{n}\right)dA$$

Integrating these two surface integrals, we obtain the momentum equation in the form

$$P_1\left(A_1 + A_2\right) - P_3A_3 = -\rho\mathcal{V}_1^2A_1 - \rho\mathcal{V}_2^2A_2 + \rho\mathcal{V}_3^2A_3$$

Since $A_1 + A_2 = A_3$, the momentum equation becomes

$$P_3 - P_1 = \rho\frac{\mathcal{V}_1^2A_1 + \mathcal{V}_2^2A_2 - \mathcal{V}_3^2A_3}{A_3}$$

$$P_3 - P_1 = (1000\text{ kg/m}^3)\frac{(30\text{ m/sec})^2(1\text{ cm})^2 + (0.1\text{ m/sec})^2\left[(5\text{ cm})^2 - (1\text{ cm})^2\right] - (1.296\text{ m/sec})^2(5\text{ cm})^2}{(5\text{ cm})^2}$$

$$P_3 - P_1 = 34.33\text{ x }10^3\text{ N/m}^2$$

Notice that because of the momentum transfer between the two incoming streams, the pressure actually increases in the direction of flow.

(c) To determine the temperature at surface 3, we apply the first law to the control volume. Then for adiabatic steady flow with no shaft work transfer, the first law assumes the form

$$0 = \dot{m}_1\left(h_1 + \frac{\mathcal{V}_1^2}{2}\right) + \dot{m}_2\left(h_2 + \frac{\mathcal{V}_2^2}{2}\right) - \dot{m}_3\left(h_2 + \frac{\mathcal{V}_3^2}{2}\right)$$

Substituting the enthalpy constitutive relation for the incompressible fluid model and realizing from continuity that $\dot{m}_3 = \dot{m}_1 + \dot{m}_2$, we obtain

$$0 = \dot{m}_3\left(cT_1 + \frac{P_1}{\rho}\right) - \dot{m}_3\left(cT_3 + \frac{P_3}{\rho}\right) + \dot{m}_1\left(\frac{\mathcal{V}_1^2}{2}\right) + \dot{m}_2\left(\frac{\mathcal{V}_2^2}{2}\right) - \dot{m}_3\left(\frac{\mathcal{V}_3^2}{2}\right)$$

Solving for the temperature change of the fluid as it moves from from surface 1 to surface 3, we obtain

$$T_3 - T_1 = \frac{\left(P_1 - P_3\right)}{\rho c} + \frac{\dot{m}_1}{\dot{m}_3}\left(\frac{\mathcal{V}_1^2}{2c}\right) + \frac{\dot{m}_2}{\dot{m}_3}\left(\frac{\mathcal{V}_2^2}{2c}\right) - \left(\frac{\mathcal{V}_3^2}{2c}\right)$$

The mass flow rates through the various surfaces are given by

$$\dot{m}_1 = \rho A_1 \vartheta_1 = (1000 \text{ kg/m}^3)\frac{\pi(10^{-2} \text{ m})^2}{4}(30 \text{ m/sec}) = 2.356 \text{ kg/sec}$$

$$\dot{m}_2 = \rho A_2 \vartheta_2 = (1000 \text{ kg/m}^3)\frac{\pi(0.05 \text{ m})^2 - \pi(0.01 \text{ m})^2}{4}(0.1 \text{ m/sec}) = 0.1885 \text{ kg/sec}$$

$$\dot{m}_3 = \dot{m}_2 + \dot{m}_1 = 2.544 \text{ kg/sec}$$

Substituting these quantities into expression for the temperature change, we find

$$T_3 - T_1 = \frac{(-34.33 \text{ x } 10^3 \text{ N/m}^2)}{(1000 \text{ kg/m}^3)(4300 \text{ J/kg K})} + \frac{(2.356 \text{ kg/sec})}{(2.544 \text{ kg/sec})}\left(\frac{(30 \text{ m/sec})^2}{2(4300 \text{ J/kg K})}\right) +$$

$$+ \frac{(0.1885 \text{ kg/sec})}{(2.554 \text{ kg/sec})}\left(\frac{(0.1 \text{ m/sec})^2}{2(4300 \text{ J/kg K})}\right) - \left(\frac{(1.296 \text{ m/sec})^2}{2(4300 \text{ J/kg K})}\right) = 0.0887 \text{ K}$$

(c) To examine the reversibility of the flow, we apply the second law. Since the flow is steady and there are no heat transfers across the boundary, the second law becomes

$$0 = \dot{m}_1 s_1 + \dot{m}_2 s_2 - \dot{m}_3 s_3 + \dot{S}_{gen} = \dot{m}_1 (s_1 - s_3) + \dot{m}_2 (s_2 - s_3) + \dot{S}_{gen}$$

where we have made use of the continuity equation. Solving for the rate of entropy generation and using the entropy constitutive relation for the incompressible fluid model, we find

$$\dot{S}_{gen} = \dot{m}_1 (s_3 - s_1) + \dot{m}_2 (s_3 - s_2) = \dot{m}_1 c \ln\left(\frac{T_3}{T_1}\right) + \dot{m}_2 c \ln\left(\frac{T_3}{T_2}\right)$$

$$\dot{S}_{gen} = (2.356 \text{ kg/sec})(4300 \text{ J/kg K}) \ln\left(\frac{300.0887 \text{ K}}{300 \text{ K}}\right) +$$

$$+ (0.1885 \text{ kg/sec})(4300 \text{ J/kg K}) \ln\left(\frac{300.0887 \text{ K}}{300 \text{ K}}\right) = 3.234 \text{ W/K}$$

The entropy generation is non-zero and positive as required by the second law. We conclude, then, that the process of momentum transfer between the two streams is irreversible. Note that the irreversibility does not originate from viscous interactions between the walls and the fluid since we have assumed that shear stresses on the walls of the control volume are negligible, i.e., the walls are modeled as frictionless. Had we assumed that the zero shear stress at the wall was a consequence of inviscid fluid behavior, the velocity profile at the outlet of the pipe would have had the appearance of a slowly moving annulus surrounding a faster moving core since there would be no way to transfer momentum from one stream to another, but we see that this is not the case. The velocity profiles at the beginning and the end of the main pipe are consistent with the assumption of no shear stresses at the walls but a fluid with a finite viscosity. The uniform velocity profile at the outlet of the pipe is established by the viscous and turbulent interactions between the jet and the slowly moving fluid as they enter the large pipe.

There is a finite amount of time required for the uniform velocity profile to be established as a result of this viscous interaction between the two fluid streams. During this time, the fluid travels some distance downstream. This distance necessary for the establishment of the uniform velocity profile is known as the mixing length. It is similar in nature to the entry length required to establish a fully developed velocity profile in a viscous fluid at the entrance of a closed conduit such as a tube or pipe. If the outlet pipe of the jet pump were shorter than the mixing length, the velocity profile at outlet would not be uniform.

Although jet pumps perform in an irreversible manner, they find widespread application in thermal-fluid systems because of their simplicity. Since they have no moving parts that require service and are simple to manufacture, they are inexpensive to buy and to maintain. For this reason, they are often the pump of choice where performance is not the central issue.

(e) We cannot use the Bernoulli equation between any of the ports of this jet pump. All streamlines that we can draw in this system must pass through the dissipative shear zone where the slow and jet flows mix.

Perhaps the absurdity of applying the Bernoulli equation in this case is clearer if we attempt to apply it using the two streamlines shown in Figure 8E.18. On streamline 1-3, the steady flow Bernoulli equation is

$$\left(\frac{P}{\rho}+\frac{\mathcal{V}^2}{2}+gz\right)_1=\left(\frac{P}{\rho}+\frac{\mathcal{V}^2}{2}+gz\right)_3$$

We can solve for the pressure difference between points 1 and 3, and neglecting gravity, we find

$$P_3-P_1=\rho\frac{\mathcal{V}_1^2-\mathcal{V}_3^2}{2}=(1000\ \text{kg/m}^3)\frac{(30\ \text{m/sec})^2-(1.296\ \text{m/sec})^2}{2}=4.49\ \text{x}\ 10^5\ \text{N/m}^2$$

This result is 4.5 atmospheres which is much larger than the correct value of 0.34 atmospheres we calculated earlier. Similarly, we could, with reckless abandon, apply the Bernoulli equation to streamline 2-3 and obtain

$$P_3-P_1=\rho\frac{\mathcal{V}_1^2-\mathcal{V}_3^2}{2}=(1000\ \text{kg/m}^3)\frac{(0.1\ \text{m/sec})^2-(1.296\ \text{m/sec})^2}{2}=-835\ \text{N/m}^2$$

These two results do not even agree with each other.

The Bernoulli equation is a derived relation. We have shown that it is a consequence of the first and second laws for reversible and incompressible flow. (See the full set of restrictions listed above.) We will show shortly that it is also a direct consequence of momentum conservation. If there is a question as to whether the Bernoulli equation is applicable, students should fall back to the more fundamental equations, mass and momentum conservation and the first and second laws of thermodynamics.

Example 8E.19: A jet of water strikes a plate as shown in Figure 8E.19. The stream

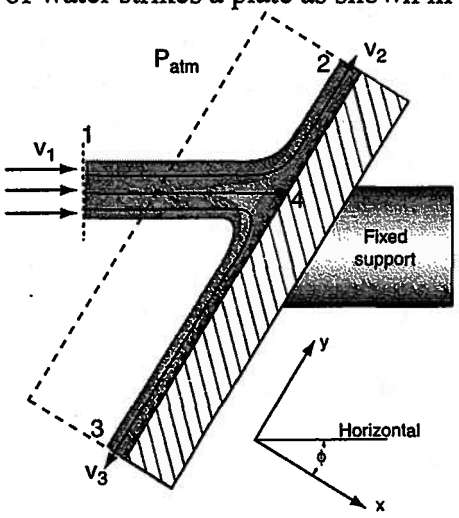

Figure 8E.19 Flow on a Grooved Plate

separates into an upward moving stream along the plate and a downward moving stream along the plate. The streams on the plate are confined by walls (not shown) so that all movement of the streams in positions 2 and 3 are in the y-direction. The velocity and area of the incoming stream is ϑ_1 and A_1.

(a) What is the velocity at position 2 and position 3?

(b) What is the pressure at position 4?

(c) What are the areas at position 2 and position 3?

(d) What is the force in the x-direction on the fixed support due to the fluid flow?

(e) What is the force in the horizontal direction on the fixed support due to the fluid flow?

Solution: (a) We assume that the boundary layers along the plate at position 2 and position 3 are thin when compared to the local thickness of the fluid. The velocities at position 2 and position 3 may then be determined using the Bernoulli equation. The pressures at positions 1, 2 and 3 are atmospheric pressure. This conclusions follows from the same arguments used in the Example 8E.17 above. The streamlines at these positions are parallel; and consequently, the pressure gradient normal to these streamlines is zero. We shall discuss this in more detail shortly. Assuming that gravity effects are small, we obtain the following form for the Bernoulli equation:

$$\frac{P_{atm}}{\rho}+\frac{\vartheta_1^2}{2}=\frac{P_{atm}}{\rho}+\frac{\vartheta_2^2}{2}=\frac{P_{atm}}{\rho}+\frac{\vartheta_3^2}{2}$$

It follows, then, that $\vartheta_1 = \vartheta_2 = \vartheta_3$.

(b) The streamlines diverge around point 4 and are curved. Hence we would expect the pressure at point 4 to be higher than ambient pressure. In addition, we would expect the velocity at point 4 to be zero. This is known as a *stagnation point* in the flow. The Bernoulli equation between points 1 and 4 is then

$$P_4 = P_{atm}+\frac{\rho\vartheta_1^2}{2}$$

(c) The cross sectional areas of the flows at points 2 and 3 can be determined using the y-component of the momentum equation, mass conservation and the dashed control volume shown in Figure 8E.19. The flow is steady so that the time derivative of the volume integral is zero. Consistent with our use of the Bernoulli equation, we will assume that the shear forces (as well as gravity forces) are negligible in our system. The y-component of the momentum equation becomes

$$\left[\int_{CS}(-P\vec{n})\,dA\right]_y=\left[\int_{CS}\rho\vec{\vartheta}\,(\vec{\vartheta}_r\cdot\vec{n})dA\right]_y$$

The integral of the pressure over the control surface can be broken up over the four faces of the control volume. The integral of the pressure over the surface of the plate does not contribute since the normal to the surface is orthogonal to the y-direction. The surface where the flow first enters the control volume (1) does not contribute to the pressure integral for the same reason. Finally, the integrals of the pressure over surfaces 2 and 3 are equal and opposite so that their contributions cancel. We conclude, then, that the y-component of the pressure integral is zero.

The other surface integral can be expanded over the three surfaces that have flow or

$$0=\left[\int_{CS}\rho\vec{\vartheta}\,(\vec{\vartheta}_r\cdot\vec{n})dA\right]_y=\left[\int_1\rho\vec{\vartheta}\,(\vec{\vartheta}_r\cdot\vec{n})dA\right]_y+\left[\int_2\rho\vec{\vartheta}\,(\vec{\vartheta}_r\cdot\vec{n})dA\right]_y+\left[\int_3\rho\vec{\vartheta}\,(\vec{\vartheta}_r\cdot\vec{n})dA\right]_y$$

The integral over surface 1 becomes

$$\left[\int_1\rho\vec{\vartheta}\,(\vec{\vartheta}_r\cdot\vec{n})dA\right]_y=\left[\int_1\rho(\vartheta_1\cos\phi\,\vec{i}+\vartheta_1\sin\phi\,\vec{j})\left[(\vartheta_1\cos\phi\,\vec{i}+\vartheta_1\sin\phi\,\vec{j})\cdot(-\vec{i})\right]dA\right]_y$$

$$=\rho\,\vartheta_1\sin\phi\,(-\vartheta_1\cos\phi)\,A_1^*$$

The area A_1^* is the area of intersection between the incoming water stream and the control surface. Since the stream penetrates the surface at an angle ϕ, A_1^* is larger than the vertical cross sectional area of the stream at position 1, A_1. The two areas are related,

$$A_1^*=\frac{A_1}{\cos\phi}$$

The other integrals can be handled in the same way without the complication of an angled entry into the control volume. The conservation of momentum becomes

$$0=\left[\int_{CS}\rho\vec{\vartheta}\,(\vec{\vartheta}_r\cdot\vec{n})dA\right]_y=-\rho\,\vartheta_1^2\sin\phi\,A_1+\rho\,\vartheta_1^2A_2-\rho\,\vartheta_1^2A_3$$

$$0=A_1\sin\phi-A_2+A_3$$

The conservation of mass can be applied to the control volume yielding

$$0=-\rho\vartheta_1A_1+\rho\vartheta_1A_2+\rho\vartheta_1A_3$$

$$A_1=A_2+A_3$$

Combining this result with the conservation of momentum result, we obtain after some algebraic manipulation

$$A_2=\frac{A_1(1+\sin\phi)}{2}$$

$$A_3=\frac{A_1(1-\sin\phi)}{2}$$

This result agrees with our understanding of the physics of the situation. When $\phi = \pi/2$, the fluid strikes the plate at a glancing angle, and all the flow is through surface 2. When $\phi = 0$, the fluid strikes the plate normally, and in the absence of gravity, we would expect the flow to split equally in the two directions.

(d) The force on the control volume in the x-direction can be determined using the x-component of the momentum equation,

$$\left[\int_{CS}(-P\vec{n})\,dA\right]_x=\left[\int_{CS}\rho\vec{\vartheta}\,(\vec{\vartheta}_r\cdot\vec{n})dA\right]_x$$

The pressure integral does not sum to zero as it did for the y-component. The sum of the forces due to pressure applied to the plate by the liquid is opposite to the force that the support must supply to the plate to keep the plate from moving. We conclude, then, that the integral of the pressure over the surface is the net force applied to the fluid by the plate, F_x.

The convective integral can be split up over the three surfaces with flow. The integrals over surfaces 2 and 3 are zero since neither flow carries any x-momentum. The x-momentum equation reduces to

$$F_x = \left[\int_1 \rho(\vartheta_1 \cos\phi\, \vec{i} + \vartheta_1 \sin\phi\, \vec{j})\left[(\vartheta_1 \cos\phi\, \vec{i} + \vartheta_1 \sin\phi\, \vec{j})\cdot(-\vec{i})\right] dA \right]_x$$

$$F_x = -\rho\, \vartheta_1^2 (\cos\phi)^2 A_1^* = -\rho\, \vartheta_1^2 (\cos\phi) A_1$$

The force required is in the negative x-direction.

(e) The component of the force in the horizontal direction is

$$F_{horizontal} = F_x \cos\phi = -\rho\, \vartheta_1^2 (\cos\phi)^2 A_1$$

Example 8E.20: A hovercraft is a vehicle designed to float on a cushion of air thereby eliminating rolling resistance for land-based vehicles or wake drag for water-based vehicles. The air cushion is usually contained within a fabric skirt that is fashioned around the periphery of the vehicle. Air is drawn in from the atmosphere through a hole in the roof of the vehicle by means of a fan that discharges air under the skirt.

In a particular application of a land-based vehicle shown in Figure 8E.20, the clearance between the bottom of the skirt and the ground is 2.5 cm. The skirt is stretched in a rectangular

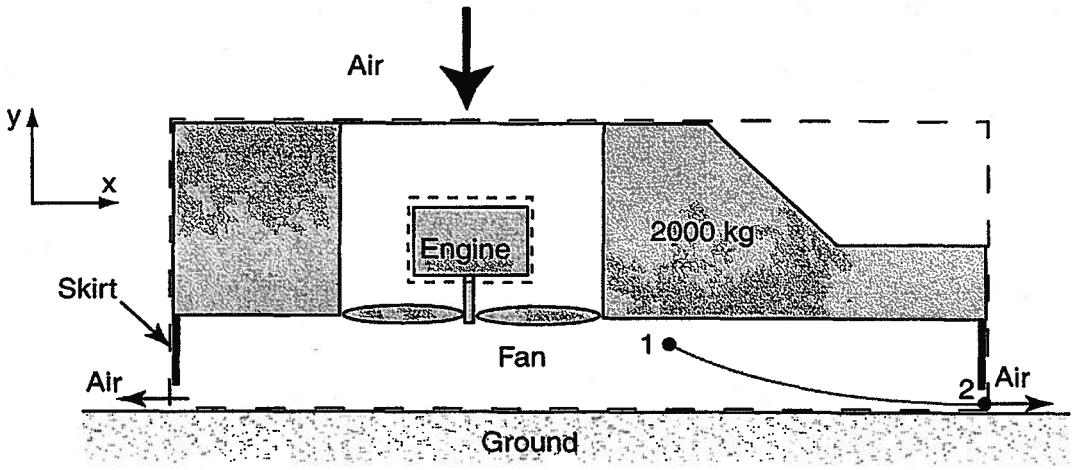

Figure 8E.20 Hovercraft

shape 3m x 9m around the vehicle. The mass of the loaded vehicle, M, is 2000 kg. The air can be modeled as incompressible with a density of 1.2 kg/m^3. The volume of the air cushion is sufficiently large that the velocity of the air in the central portion of the plenum is negligible.

(a) Estimate the volume flow rate necessary to support the vehicle.

(b) Estimate the power required to drive an ideal fan.

Solution: We choose the control surface as shown in Figure 8E.20 by the dashed lines. The momentum equation in the y-direction is

$$\sum F_y = \left[\frac{d}{dt} \int_{CV} \rho \vec{\vartheta}\, dV + \int_{CS} \rho \vec{\vartheta} \left(\vec{\vartheta}_r \cdot \vec{n} \right) dA \right]_y$$

We are interested in steady operation so that the volume integral on the right-hand-side is zero. The only flow that will contribute to the y-component of the surface integral is the flow that enters the top of the hovercraft. (The flows that exit under the skirt of the vehicle do not have a component in the y-direction.) We will assume in this example that the area of the intake port on the top of the hovercraft is large. With this assumption, the velocities and, hence, the surface

integral in the above expression, which depends on $\vec{v}^2$, is negligible. The momentum equation becomes

$$\sum F_y = 0$$

The forces on the control volume include the gravity force and the forces due to the pressure of the gases around the hovercraft. We assume that viscous forces are negligible. If the hovercraft is floating, the pressure inside the plenum under the hovercraft, P_{ins}, will be higher than atmospheric pressure, P_{atm}. The momentum equation becomes

$$0 = \sum F_y = -Mg + P_{ins}A_{ins} - P_{atm}A_{top}$$

$$P_{ins} = P_{atm} + \frac{Mg}{A_{ins}}$$

where A_{ins} is the area under the skirt of the hovercraft and A_{top} is the area of the top surface of the control volume. We have assumed that these areas are the same.

The momentum equation has determined what the pressure must be under the hovercraft for the vehicle to float on a cushion of air. If we model the flow as incompressible and inviscid, the volume flow rate can be determined by the Bernoulli equation. We choose a streamline between points 1 and 2 as shown in Figure 8E.20. We assume that the velocity at point 1 is essentially zero and that there is no substantial height difference between points 1 and 2. The pressure at point 2 is atmospheric pressure. The Bernoulli equation becomes

$$\frac{P_{ins}}{\rho} = \frac{P_{atm}}{\rho} + \frac{\mathcal{G}_2^2}{2}$$

where $\vec{v}_2$ is the velocity at point 2. The velocity of the flow through the gap between the skirt and the ground is

$$\mathcal{G} = \sqrt{\frac{2}{\rho}(P_{ins} - P_{atm})} = \sqrt{\frac{2}{\rho}\left(\frac{Mg}{A_{ins}}\right)} = \sqrt{\frac{2}{(1.2\ \text{kg/m}^3)}\left(\frac{(2000\ \text{kg})(9.806\ \text{m/sec}^2)}{(3\ \text{m})(9\ \text{m})}\right)} = 34.79\ \text{m/sec}$$

The velocity is about 0.1 times the speed of sound in air, justifying the use of the Bernoulli equation. If the velocities were much higher, compressibility effects would be important. Then we could not use Bernoulli equation since it was derived for an incompressible fluid model. The volumetric flow rate of the air is equal to the product of this velocity and the area of the gap between the skirt and the ground or

$$\dot{V} = 2(l+w)h\,\mathcal{G}_2 = 2\,(9\ \text{m} + 3\ \text{m})\left(2.5 \times 10^{-2}\ \text{m}\right)(34.79\ \text{m/sec}) = 20.87\ \text{m}^3/\text{sec}$$

where l and w are the length and width of the vehicle, respectively, and h is the vertical dimension of the gap.

(b) The power required by the vehicle to drive the compressor can be determined using the first law,

$$\frac{dE_{CV}}{dt} = \dot{Q} - \dot{W}_{shaft} + \sum_{in}\dot{m}_{in}\left(h + \frac{\mathcal{G}^2}{2} + gz\right)_{in} - \sum_{out}\dot{m}_{out}\left(h + \frac{\mathcal{G}^2}{2} + gz\right)_{out}$$

In order to make the shaft power non-zero, the control surface is chosen so that the engine is outside the control volume and the shaft between the fan and the engine penetrates the control surface. This is done by defining the control volume as that between the short dash control surface and the long-dash control surface in Figure 8E.20.

Using this new control volume, we find that the term on the left-hand-side of the first law is zero because the flow is steady. We assume that there is no heat transfer across the bounding

surface. The only mass flow into and out of the control volume is the air entering the top of the vehicle and the air exiting under the skirt of the vehicle. By the conservation of mass, these two flows are equal. We assume that gravity effects and the air velocity at the inlet are negligible. The first law becomes

$$\dot{W}_{shaft} = \dot{m}\left(h_{in} - h_{out}\right) + \dot{m}\left(\frac{\mathcal{G}_2^2}{2}\right)$$

Since we are modeling the air as an incompressible fluid, the first law becomes

$$\dot{W}_{shaft} = \dot{m}\left[c(T_2 - T_{in}) + (P_2 - P_{in})v\right] + \dot{m}\left(\frac{\mathcal{G}_2^2}{2}\right)$$

If there are no heat transfers and no entropy generation inside the vehicle (We are making an optimistic estimate.), the second law requires $T_2 = T_{in}$. The pressures P_{in} and P_2 are both atmospheric pressure. We find

$$\dot{W}_{shaft} = \dot{m}\left(\frac{\mathcal{G}_2^2}{2}\right) = \rho A\frac{\mathcal{G}_2^3}{2} = \rho 2(l+w)h\frac{\mathcal{G}_2^3}{2}$$

$$\dot{W}_{shaft} = (1.2\ \text{kg/m}^3)(2)(9\ \text{m} + 3\ \text{m})\left(2.5 \times 10^{-2}\ \text{m}\right)\frac{(34.79\ \text{m/sec})^3}{2} = 15.16 \times 10^3\ \text{W}$$

Example 8E.21: As shown in Figure 8E.21, a snow-plow truck traveling at 14 m/sec clears a swath of snow that is 8 cm deep and one meter wide using a rotary plow. The plow ejects the snow horizontally and perpendicular to the direction of travel at 20 m/sec as viewed from the perspective of the truck driver. The density of the snow is 200 kg/m^3

(a) Calculate the force the plow exerts on the truck using a control volume that moves with the plow.

(b) Calculate the force the plow puts on the truck using a control volume that is fixed to the ground.

Solution: (a) The control volume approach can also be applied to solids as well as liquids. In this case, we choose a control volume around the plow that moves with the plow. This volume is delineated by the short dashed lines in Figure 8E.21.We will assume that

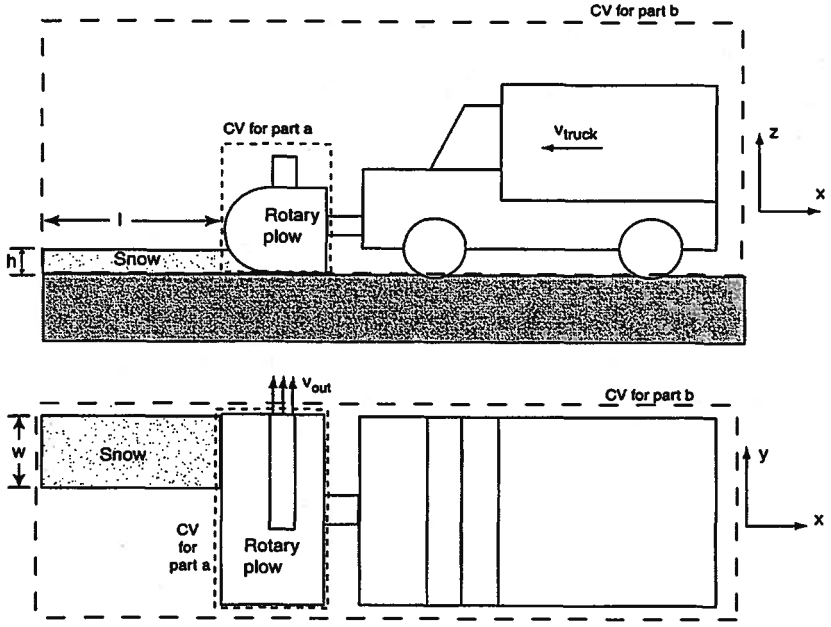

Figure 8E.21 Snow-plow Truck

flow is steady and that the effect of pressure and shear forces is negligible. The x-component of the momentum equation reduces to

$$-F_x = \left[\int_{CS} \rho \vec{\vartheta} \left(\vec{\vartheta}_r \cdot \vec{n} \right) dA \right]_x$$

where F_x is the force the plow exerts on the truck. We can break up the surface integral into two integrals, one over the inlet to the plow and the other over the outlet port of the plow, viz.

$$-F_x = \left[\int_{inlet} \rho \vec{\vartheta} \left(\vec{\vartheta}_r \cdot \vec{n} \right) dA \right]_x + \left[\int_{outlet} \rho \vec{\vartheta} \left(\vec{\vartheta}_r \cdot \vec{n} \right) dA \right]_x$$

We choose our reference frame from which to measure velocities to be that of the driver of the plow. In the first integral, the snow enters the plow with the velocity of the truck, ϑ_{truck}, in the positive x-direction. Since the outwardly directed normal is in the negative x-direction, the first integral becomes

$$\left[\int_{inlet} \rho \vec{\vartheta} \left(\vec{\vartheta}_r \cdot \vec{n} \right) dA \right]_x = \left[\int_{inlet} \rho \vartheta_{truck} \vec{i} \left(\vartheta_{truck} \vec{i} \cdot (-\vec{i}) \right) dA \right]_x = \left[-\rho \vartheta_{truck}^2 \int_{inlet} dA \, \vec{i} \right]_x = -\rho \vartheta_{truck}^2 A_{snow}$$

where A_{snow} is the cross-sectional area of the snow entering the control volume and $\vec{i}$ is the unit vector in the x-direction.

In the second integral, the velocity of the exiting the snow is ϑ_{out} in the y-direction $\vec{j}$. Then second integral becomes

$$\left[\int_{outlet} \rho \vec{\vartheta} \left(\vec{\vartheta}_r \cdot \vec{n} \right) dA \right]_x = \left[\int_{outlet} \rho \vartheta_{out} \vec{j} \left(\vartheta_{out} \vec{j} \cdot \vec{j} \right) dA \right]_x = \left[\rho \vartheta_{out}^2 \int_{inlet} dA \, \vec{j} \right]_x = 0$$

The x-component of the force on the truck is then

$$F_x = \rho \vartheta_{truck}^2 A_{snow} = (200 \text{ kg/m}^3)(14 \text{ m/sec})^2 (1 \text{ m})(0.08 \text{ m}) = 3136 \text{ N}$$

(b) We now choose a control volume that contains both the truck and the plow as shown by the long dashed lines in Figure 8E.21. One end of the control volume is behind the truck while the other end is very far ahead of the truck. For this control volume, there is only one flow that crosses the control surface, namely the discharge of the plow in the positive y-direction. In this case, we measure velocities in the reference frame of the ground. This control volume is not in steady state. Its condition changes with time. The momentum equation is then

$$-F_x = \frac{d}{dt} \left[\int_{CV} \rho \vec{\vartheta} dV \right]_x + \left[\int_{CS} \rho \vec{\vartheta} \left(\vec{\vartheta}_r \cdot \vec{n} \right) dA \right]_x$$

The volume integral can be broken into two parts. The first part is an integral over the quiescent snow lying on the ground. The mass of snow lying on the ground is changing with time; however, the integral of the momentum for the snow on the ground is zero because the velocity is zero. The other part of the volume integral is over the rotary plow itself. The flow appears steady for this volume integral, and the time derivative of this integral must then be zero. We conclude then that the volume integral in the above equation is still zero for this control volume.

The integrand of the surface integral is non-zero only at the outlet port of the plow. In the reference frame fixed to the ground, the velocity of the snow exiting the plow is

$$\vec{\vartheta} = -\vartheta_{truck} \vec{i} + \vartheta_{out} \vec{j}$$

The surface integral becomes

$$\left[\int_{CS}\rho\vec{\vartheta}\left(\vec{\vartheta}_r\cdot\vec{n}\right)dA\right]_x=\left[\int_{CS}\rho\left(-\vartheta_{truck}\vec{i}+\vartheta_{out}\vec{j}\right)\left((-\vartheta_{truck}\vec{i}+\vartheta_{out}\vec{j})\cdot\vec{j}\right)dA\right]_x=\rho\left(-\vartheta_{truck}\right)\vartheta_{out}A_{out}$$

where A_{out} is the cross-sectional area of the snow exiting the outlet port of the plow. Then the force becomes

$$F_x=\rho\left(\vartheta_{truck}\right)\vartheta_{out}A_{out}$$

We have found the desired result, but it is expressed in terms of the unknown velocity of the snow at the outlet port, ϑ_{out}. This unknown can be evaluated by applying the continuity equation.

$$\frac{d}{dt}\int_{CV}\rho dV+\int_{CS}\rho\left(\vec{\vartheta}_r\cdot\vec{n}\right)dA=0$$

The volume integral is the rate of change of mass in the control volume. This is equal to the time derivative of the mass of snow on the ground added to the time derivative of the mass of snow in the rotary plow. The mass of snow on the ground is given by the product of the density of the snow and the volume of the snow still in the control volume. Since the mass of snow in the rotary plow does not change in time, the time derivative of this term is zero. Finally, we recognize that the length, and, hence, the volume, of the snow in the control volume is getting smaller as the truck moves forward. Then

$$\frac{d}{dt}\int_{cv}\rho\,dV=\frac{d}{dt}\int_{\substack{snow\ on\\ ground}}\rho\,dV+\frac{d}{dt}\int_{\substack{snow\ in\\ plow}}\rho\,dV=\frac{d}{dt}(\rho wlh)+0=\rho wh\frac{dl}{dt}=-\rho wh\vartheta_{truck}$$

For the surface integral appearing in the continuity equation, we have

$$\int_{CS}\rho\left(\vec{\vartheta}_r\cdot\vec{n}\right)dA=\int_{CS}\rho\left((-\vartheta_{truck}\vec{i}+\vartheta_{out}\vec{j})\cdot\vec{j}\right)dA=\rho\vartheta_{out}A_{out}$$

Then continuity requires

$$\vartheta_{out}A_{out}=wh\vartheta_{truck}=\vartheta_{truck}A_{snow}$$

where we have made use of the fact that $A_{snow}=wh$. When we substitute this result into the momentum equation, we find

$$F_x=\rho\left(\vartheta_{truck}\right)\vartheta_{out}A_{out}=\rho\vartheta_{truck}^2A_{snow}$$

This result is identical to the result obtained in part (a) above as it should be.

Example 8E.22: Action films with physically oriented protagonists often find a well muscled actor, e.g. "Rambo", holding a large machine gun while "mowing down" his favorite "bad guys". The classic example of this weapon is the Browning M2 50 Caliber Machine Gun which weighs 58 kg and has a bore diameter of 12.7 mm (0.5 inches). The weapon fires at a rate of 550 rounds per minute (9.17 rounds per second). The muzzle velocity is 860 m/sec and the mass of each bullet is 48.5 gm. Neglect any momentum contribution due to the motion of the ammunition belt or the spent shells.

(a) Estimate the average force that the actor must apply to the weapon to counter the recoil in order to hold the weapon while it is being fired.

(b) There is an additional 110 gm of gas exhausted from the weapon behind each bullet. Assume that this gas exits at the velocity of the bullet. Estimate the total average recoil force when the contribution of the gas is included.

(c) Is it likely that the M2 can be fired continuously without a stand or mount?

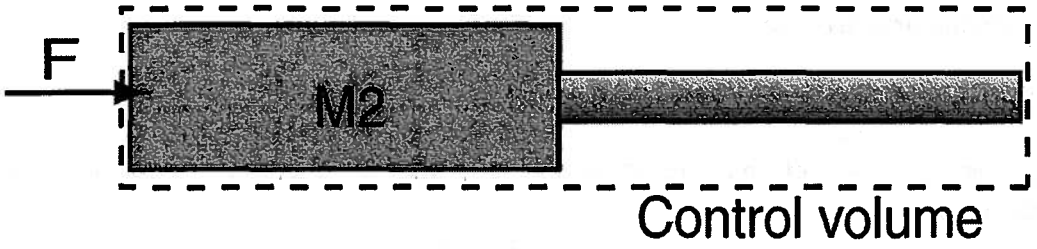

Figure 8E.22 The Browning M2 50 Caliber Machine Gun

Solution: (a) We choose a control volume around the gun as shown in Figure 8E.22. We will assume that there are no net shear forces and no net forces due to pressure. Furthermore, since we are assuming that the actor is applying a force in the x-direction, the horizontal direction, no net gravity forces need be considered. The x-component of the momentum equation is

$$F_x = \frac{d}{dt}\left[\int_{CV} \rho \vec{\vartheta} dV\right]_x + \left[\int_{CS} \rho \vec{\vartheta}\left(\vec{\vartheta}_r \cdot \vec{n}\right) dA\right]_x$$

where F_x is the force in the x-direction that the actor applies to the gun.

Because of the repetitive nature of the firing of the weapon, we would expect an oscillatory recoil force in the gun. However, because the repetition rate is high and the mass of the gun is large, we would expect the oscillations in the force felt by the gunner to be rather small compared to a large average force. In this case, we are interested only in the time-averaged force that the actor must apply to the weapon to keep it from moving. The time average of a quantity B is defined as

$$\bar{B} \equiv \frac{1}{\tau}\int_0^{\tau} B(t)\, dt$$

The physical interpretation of this relation can be seen in Fig. 8E.22b. The quantity B varies in time. The average value of the quantity B, i.e., the average height of the curve, is the area under the curve divided by the width of the curve τ. In other words, the area under curve $B(t)$ is equal to the area under the dotted line.

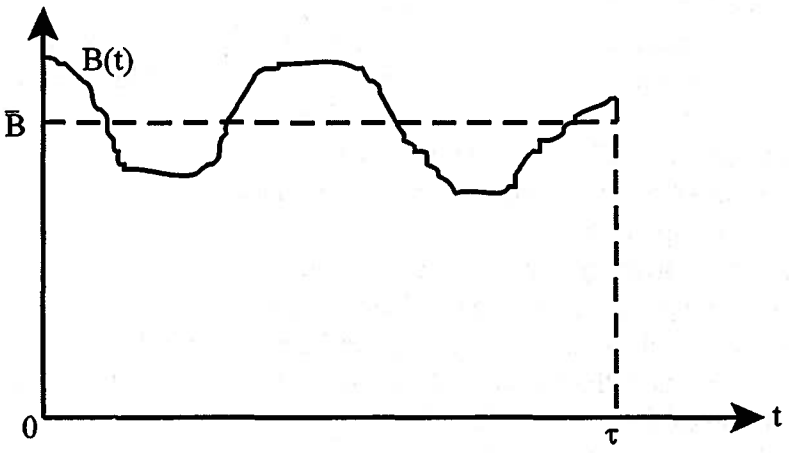

Figure 8E.22b Time Average of Function $B(t)$

The momentum equation can be time averaged by integrating both sides of the equation over time from $t = 0$ to $t = \tau$ and dividing by τ.

$$\overline{F}_x = \frac{1}{\tau}\int_0^\tau dt \frac{d}{dt}\left[\int_{CV} \rho\vec{\vartheta} dV\right]_x + \frac{1}{\tau}\int_0^\tau dt\left[\int_{CS} \rho\vec{\vartheta}\left(\vec{\vartheta}_r \cdot \vec{n}\right) dA\right]_x$$

At first glance this equation might look rather daunting. The first term on the right-hand-side, the control volume integral, can be simplified by performing the time integral,

$$\frac{1}{\tau}\int_0^\tau dt\left[\frac{d}{dt}\int_{CV} \rho u\, dV\right] = \frac{1}{\tau}\left[\int_{CV} \rho u\, dV\right]_{t=0}^{t=\tau}$$

In order to simplify this term further, we need to be more specific about the time τ. We would like to choose a time so as to make the integral above as simple as possible. If we choose a time that is equal to the period of the shots then the control volume integral evaluated at time $t = \tau$ will be identical to the control volume integral evaluated at time $t = 0$. With this choice of τ, the volume integral is zero.

The momentum equation reduces to

$$\overline{F}_x = \frac{1}{\tau}\int_o^\tau dt\left[\int_{CS} \rho u\left(\vec{\vartheta}_r \cdot \vec{n}\right) dA\right]$$

The surface integral is zero everywhere except where the bullets penetrate the control volume. Because the flight of the bullet is normal to and out of the control volume, the scalar product in the integral reduces to u. Then

$$\overline{F}_x = \frac{1}{\tau}\int_0^\tau dt\left[\int_{muzzle} \rho u^2 dA\right]$$

The time dependence of the integrand is sketched in Figure 8E.22c. Each pulse corresponds to the passing of a bullet through the control surface. The parameter t_{shot} is the time it takes the bullet to pass through the control surface. We have chosen time zero to be the instant a bullet begins to pass through the control surface. Note that when time $t = \tau$, the next bullet is beginning to pass through the control surface as required by our earlier assumption. The integrand is everywhere

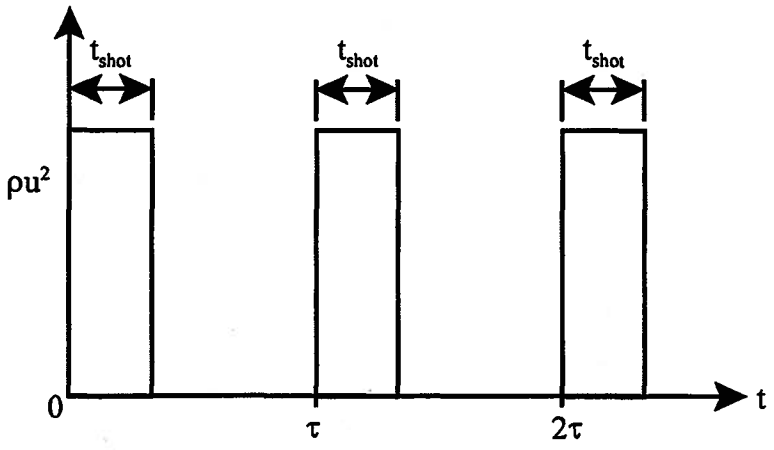

Figure 8E.22c Momentum Flow in the M2 Machine Gun

zero in the interval $[0,\tau]$ except when the bullet passes in the interval $[0,t_{shot}]$ where its value is constant. The integral becomes

$$\overline{F}_x = \frac{t_{shot}}{\tau}\rho u^2 A_b$$

Because ut_{shot} is just the length of the bullet, $\rho A_b(ut_{shot})$, is the same as the mass of the bullet, m_{bullet} (for a bullet that is a right circular cylinder). The number of times the gun fires per second, n, is the reciprocal of the time τ. Our result for the average force required to hold the gun steady is

$$\overline{F}_x = \frac{m_{bullet}u}{\tau} = n\,m_{bullet}\,u = (9.17)(0.0485)(860) = 382.48 \text{ N}$$

(b) A large individual might be able to handle this force, but we have not included the forces due to the gases exiting the gun barrel behind the bullet. There is a 110 gm charge in a 50 caliber shell. If we assume that all of the charge is turned into a gas that follows the bullet out at the muzzle velocity, then using analysis similar to that above, we find

$$\overline{F}_x = n(m_{bullet} + m_{gas})u = (9.17)(0.0485 + .11)(860) = 1250 \text{ N}$$

(c) The gun will generate forces that are far too large for the weapon to be hand-held. A mount of some kind is necessary to operate this weapon.

8.12 Equation of Linear Momentum for a Control Volume with Rectilinear Acceleration

There are many instances in engineering practice in which a vehicle such as a rocket ship, a jet aircraft at take-off, and a jet powered boat derives its acceleration up to its steady operating velocity from the thrust provided by a stream of fluid. The acceleration of the vehicle over this transient period can be derived from the application of the equation of linear momentum applied to a control volume fixed to the accelerating vehicle. However, the equation of linear momentum presented in equation (8.22) or (8.23) does not apply in this case since it was derived for an inertial control volume, i.e., a control volume either fixed in space or moving with constant velocity. For the aforementioned applications, we now consider the case of a control volume accelerating in a rectilinear fashion with respect to an inertial reference frame.

Since Newton's Second Law of Motion for a control mass has been formulated with respect to the inertial reference frame, we need to establish the relationship between $\vec{\vartheta}_{non-inertial}$, the fluid velocity measured relative to the non-inertial reference frame moving with the control volume, and $\vec{\vartheta}_{inertial}$, the fluid velocity measured relative to the inertial reference frame.

$$\vec{\vartheta}_{inertial} = \vec{\vartheta}_{non-inertial} + \vec{\vartheta}_{rf} \tag{8.84}$$

where $\vec{\vartheta}_{rf}$ is the velocity of the non-inertial reference frame itself measured in the inertial reference frame.

Since the motion of the non-inertial reference frame attached to the control volume is pure translation (without rotation) relative to the inertial reference frame, we can take the time derivative of equation (8.84) to get

$$\frac{d\vec{\vartheta}_{inertial}}{dt} = \frac{d\vec{\vartheta}_{non-inertial}}{dt} + \frac{d\vec{\vartheta}_{rf}}{dt} \tag{8.85}$$

or in terms of the various accelerations

$$\vec{a}_{inertial} = \vec{a}_{non-inertial} + \vec{a}_{rf} \tag{8.86}$$

Then if we denote the linear momentum of the control mass by $\vec{P}$, Newton's Second Law of Motion for a control mass becomes

$$\vec{F} = \left(\frac{d\vec{P}}{dt}\right)_{CM} = \int_{CM} \frac{d\vec{\vartheta}_{inertial}}{dt} dM = \int_{CM} \frac{d\vec{\vartheta}_{non-inertial}}{dt} dM + \int_{CM} \frac{d\vec{\vartheta}_{rf}}{dt} dM$$
$$\vec{F} - \int_{CM} \vec{a}_{rf} dM = \int_{CM} \frac{d\vec{\vartheta}_{non-inertial}}{dt} dM = \left(\frac{d\vec{P}_{non-inertial}}{dt}\right)_{CM} \tag{8.87}$$

In applying the Reynolds Transport Theorem to the control volume, we note that

$$B = \vec{P}_{non-inertial} \quad \text{and} \quad b = \vec{\vartheta}_{non-inertial} = \vec{\vartheta}_r$$
$$\left(\frac{d\vec{P}_{non-inertial}}{dt}\right)_{CM} = \frac{d}{dt}\int_{CV} \rho\vec{\vartheta}_r dV + \int_{CS} \rho\vec{\vartheta}_r\left(\vec{\vartheta}_r \cdot \vec{n}\right) dA \tag{8.88}$$

Then if $\vec{F}$ is the force applied by the environment to the control volume accelerating rectilinearly, the equation of linear momentum becomes

$$\vec{F} - \int_{CV} \rho\vec{a}_{rf} dV = \frac{d}{dt}\int_{CV} \rho\vec{\vartheta}_r dV + \int_{CS} \rho\vec{\vartheta}_r\left(\vec{\vartheta}_r \cdot \vec{n}\right) dA \tag{8.89}$$

since the control mass and the control volume coincide when $\Delta t \to 0$. When the control volume is not accelerating relative to the inertial frame of reference, $\vec{a}_{rf} = 0$ and the above expression reduces to equation (8.81).

Example 8E.23: Consider the case of a rocket being propelled in a vertical direction by means of a motor/nozzle combination that discharges hot gases at a constant velocity ϑ_{jet} relative to the rocket. The initial mass of the rocket and its fuel load is M_0, and we can assume that the mass flow rate of the exhaust gases is constant as the propellant is being consumed at a constant rate of $\dot{m}$. Assume that the flow within the rocket is constant, also. Derive an expression for $\vartheta(t)$, the velocity of the rocket as a function of time, with the initial condition that the rocket starts from rest with $\vartheta(0) = 0$. Assume that the drag on the rocket can be neglected for our purposes here.

Solution: As shown in Figure 8E.23, the appropriate control volume is one attached to the rocket and moving with velocity $\vartheta(t)$.

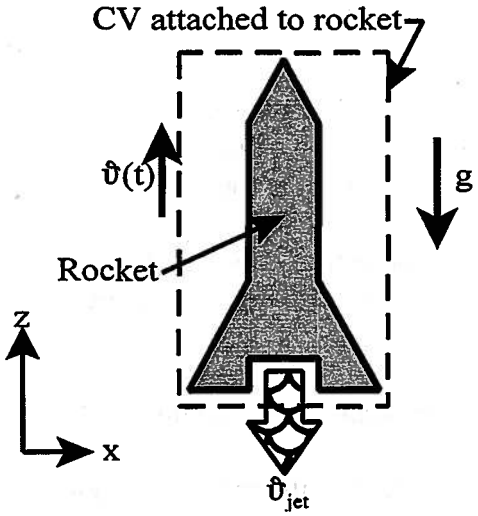

Figure 8E.23 Accelerating Rocket

Clearly this is a non-inertial control volume since the rocket is accelerating from rest. The z-component of the equation of linear momentum is given by

$$\vec{j}\cdot\int_{CV}\rho\vec{g}dV-\vec{j}\cdot\int_{CV}\rho\frac{d\vec{\vartheta}}{dt}dV=\vec{j}\cdot\frac{d}{dt}\int_{CV}-\rho\vartheta_{jet}\vec{j}dV+\vec{j}\cdot\int_{CS}-\rho\vartheta_{jet}\vec{j}\left(-\vartheta_{jet}\vec{j}\cdot\left(-\vec{j}\right)\right)dA$$

where we have made use of the fact that there are no externally applied forces except for the body force due to gravity. Then

$$\int_{CV}\rho gdV-\int_{CV}\rho\frac{d\vartheta}{dt}dV=\frac{d}{dt}\cancel{\int_{CV}\rho\vartheta_{jet}dV}-\int_{A_{jet}}\rho\vartheta_{jet}^{2}dA$$

where we have made use of the fact that the first term on the right-hand side vanishes because the flow of the gas inside the rocket is steady. Then performing the integrals

$$-mg-m\frac{d\vartheta}{dt}=0+\left(-\rho A_{jet}\vartheta_{jet}\right)\left(\vartheta_{jet}\right)=0-\dot{m}\vartheta_{jet}$$

where m is the mass of the rocket at any instant of time and is given by

$$m=M_0-\dot{m}t$$

where M_0 is the initial mass of the rocket. Then rewriting the momentum equation, we have

$$\frac{d\vartheta}{dt}=\frac{\dot{m}\vartheta_{jet}}{m}-g=\frac{\dot{m}\vartheta_{jet}}{M_0-\dot{m}t}-g$$

This expression can be integrated to give

$$\int_0^{\vartheta(t)}d\vartheta=\dot{m}\vartheta_{jet}\int_0^t\frac{dt}{M_0-\dot{m}t}-g\int_0^t dt$$

$$\vartheta(t)=\dot{m}\vartheta_{jet}\int_0^t\frac{dt}{M_0-\dot{m}t}-gt$$

To evaluate the first integral on the right-hand side, make a substitution of variables

$$u=M_0-\dot{m}t$$

$$dt=-\frac{du}{\dot{m}}$$

Then

$$\vartheta(t)=-\vartheta_{jet}\int_{M_0}^{M_0-\dot{m}t}\frac{du}{u}-gt=-\vartheta_{jet}\ln\left(1-\frac{\dot{m}t}{M_0}\right)-gt$$

In practice, it would be necessary to take into account the drag force acting on the rocket. Also, in practice, the jet velocity is made extremely high by appropriate design of the nozzle shape and producing an exhaust stream of very high temperature. The result is that the velocity of the exhaust products are several times the local speed of sound in the exhaust stream. Notice that if the fuel load of the rocket is an appreciable amount of the total mass of the rocket, the velocity of the rocket approaches the velocity of the jet as the "fuel burn" progresses and can actually exceed the jet velocity if the burn continues long enough.

8.13 Equation of Angular Momentum for a Control Volume

Many of the devices designed by thermal-fluid engineers belong to a class of machines known as rotating machines. In these machines, shaft power is either produced or consumed by

the device as a consequence of the change of angular momentum of a fluid as it passes through the device. The analysis of the performance of these machines can be readily accomplished by the use of the control volume approach developed above. Thus, it is worthwhile for us to formulate the equation of angular momentum for an inertial control volume.

Consider first the case of a rigid body. Let there be a moment $\vec{M}$ applied by the environment to the body about its center of mass. The applied moment will produce a rotation about this center, resulting in a change in the angular momentum, H, of the body. According to Newton's second law of motion, we have

$$\vec{M} = \frac{d\vec{H}}{dt} \tag{8.90}$$

where the angular momentum of the body about its center of mass is given by

$$\vec{H} = \sum \left(\vec{r} \times \vec{\vartheta}\right) \delta m \tag{8.91}$$

In this vector relation, $\vec{r}$ is the position vector of the mass element δm with respect to the center of mass and $\vec{v}$ is its velocity. For a rigid body, the combination of equations (8.90) and (8.91) results in another vector equation with component equations similar to

$$M_x = I_x \frac{d\omega_x}{dt} \tag{8.92}$$

where M_x is the component of the applied moment about the x-axis and ω_x is the angular velocity of the body about that axis. For the rigid body, I_x is the moment of inertia about the x-axis, but in the case of a fluid, there is no equivalent of this parameter since the fluid control mass consists of a collection of non-rigid fluid particles each with its own unique velocity. In the fluid, the mass element located at a given position is constantly changing identity so the notion of moment of inertia becomes meaningless.

Then for a control mass of a fluid, we write the instantaneous angular momentum about a point O as

$$\vec{H}_O = \int_{CM} \left(\vec{r} \times \vec{\vartheta}\right) dm \tag{8.93}$$

where $\vec{r}$ is the position vector from O to the elemental mass dm, and $\vec{\vartheta}$ is the instantaneous velocity of that element. Since the fluid particles are in constant motion, we would like to be able to describe the manner in which the angular momentum of the fluid that occupies a particular region of space changes with time. For this purpose, we make use of the Reynolds Transport Theorem. In this case the extensive property B is the angular momentum $\vec{H}$.

$$B = \vec{H} \tag{8.94}$$

and the angular momentum per unit mass about the center of rotation O is then

$$b = \frac{B}{m} = \frac{d\vec{H}_O}{dm} = \vec{r} \times \vec{\vartheta} \tag{8.95}$$

Then from the Reynolds Transport Theorem, we have for the rate of change of the momentum of the control mass

$$\left(\frac{d\vec{H}_O}{dt}\right)_{CM} = \frac{d}{dt}\left[\int_{CV} \left(\vec{r} \times \vec{\vartheta}\right) \rho dV\right] + \int_{CS} \left(\vec{r} \times \vec{\vartheta}\right) \rho \left(\vec{\vartheta}_r \cdot \vec{n}\right) dA \tag{8.96}$$

where the control volume is fixed in space and the velocities appearing in equation (8.96) are measured relative to this fixed control surface. From equation (8.90), we have

$$\left(\frac{d\vec{H}_O}{dt}\right)_{CM} = \sum \vec{M}_O = \sum \left(\vec{r} \times \vec{F}\right)_O \tag{8.97}$$

where F is the force applied by the environment at a position $\vec{r}$ relative to the point O. Then combining equations (8.96) and (8.97), we have

$$\sum \vec{M}_O = \frac{d}{dt}\left[\int_{CV}\left(\vec{r}\times\vec{\vartheta}\right)\rho dV\right] + \int_{CS}\left(\vec{r}\times\vec{\vartheta}\right)\rho\left(\vec{\vartheta}_r\cdot\vec{n}\right)dA \tag{8.98}$$

In the application of equation (8.98), there are three types of moments of interest: (1) moments due to applied surface forces acting on the control mass; (2) moments due to body forces (typically gravity) acting on the control mass; and (3) moments due to torques applied to any shafts that penetrate the control surface. Then

$$\sum \vec{M}_O = \left(\vec{r}\times\vec{F}_{surface}\right) + \int_{CV}\left(\vec{r}\times\vec{g}\right)\rho dV + \vec{T}_{shaft} \tag{8.99}$$

and upon substituting equation (8.98), equation (8.97) becomes the equation of angular momentum for an inertial control volume, viz.

$$\sum\left(\vec{r}\times\vec{F}_{surface}\right) + \int_{CV}\left(\vec{r}\times\vec{g}\right)\rho dV + \vec{T}_{shaft} = \frac{d}{dt}\left[\int_{CV}\left(\vec{r}\times\vec{\vartheta}\right)\rho dV\right] + \int_{CS}\left(\vec{r}\times\vec{\vartheta}\right)\rho\left(\vec{\vartheta}_r\cdot\vec{n}\right)dA \tag{8.100}$$

For the case of a finite number of entry ports and exit ports at which the flow can be modeled as one-dimensional, equation (8.100) becomes

$$\sum\left(\vec{r}\times\vec{F}_{surface}\right) + \int_{CV}\left(\vec{r}\times\vec{g}\right)\rho dV + \vec{T}_{shaft} = \frac{d}{dt}\left[\int_{CV}\left(\vec{r}\times\vec{\vartheta}\right)\rho dV\right] + \sum_{out}\dot{m}_{out}\left(\vec{r}\times\vec{\vartheta}\right)_{out} - \sum_{in}\dot{m}_{in}\left(\vec{r}\times\vec{\vartheta}\right)_{in} \tag{8.101}$$

Example 8E.24: As shown in Figure 8E.24, a fluid that can be modeled as incompressible and inviscid, with density ρ flows from a slot of width b measured normal to the plane of the sketch. The jet, which has a uniform velocity of ϑ_{jet}, strikes an inclined flat plate that is held in

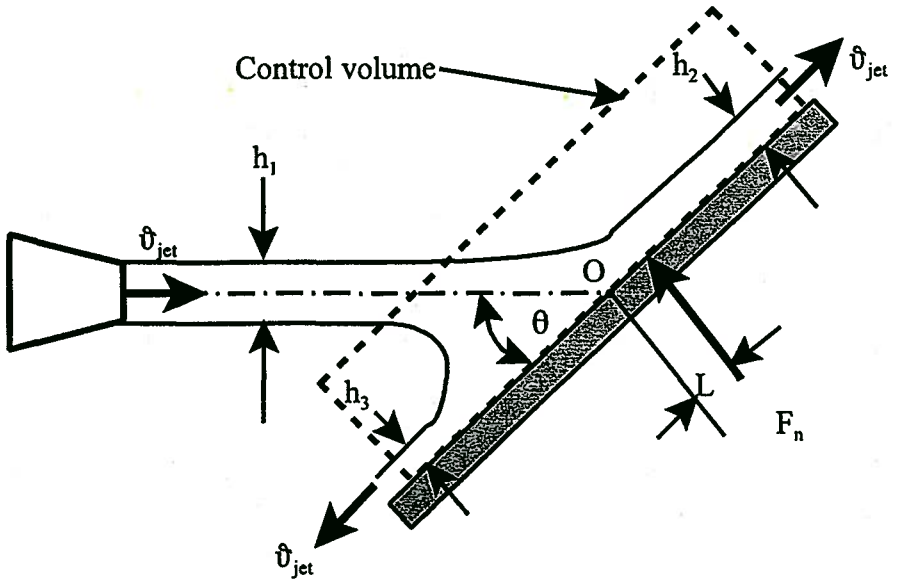

Figure 8E.24 Jet Impinging on an Inclined Flat Plate

position by a force F_n normal to the plate. Upon striking the plate, the jet separates into two individual streams 2 and 3 in which the flow velocity is uniform and equal to the velocity of the original jet ϑ_{jet}. Since the volumetric flow rate is different in each of the streams, the thicknesses of the two streams are unequal with values h_2 and h_3, respectively. Notice that since the fluid is being modeled as inviscid, there is no way for the fluid to exert a shear force on the plate.

(a) Find expressions for h_2 and h_3 as a function of the angle θ and the thickness of the original jet h_1.

(b) By applying the force F_n at the center of pressure, no moments are required to hold the plate in a position of mechanical equilibrium. For a given value of θ, derive an expression describing the location L of the center of pressure with respect to the geometrical center of the plate.

(c) Find an expression for F_n in terms of θ and the parameters used to describe the jet: ρ, ϑ_{jet}, b, and h_1.

Solution: (a) This part of Example 8E.24 is identical to Example 8E.19. Since the flow is inviscid and incompressible with atmospheric pressure acting over locations 1, 2, and 3, the Bernoulli equation is applicable. Thus

$$\frac{P_{atm}}{\rho}+\frac{\vartheta_1^2}{2}=\frac{P_{atm}}{\rho}+\frac{\vartheta_2^2}{2}=\frac{P_{atm}}{\rho}+\frac{\vartheta_3^2}{2}$$

Thus, $\vartheta_1 = \vartheta_2 = \vartheta_3 = \vartheta_{jet}$. There are no forces acting tangential to the plate since the fluid is inviscid. Then the momentum equation tangential to the plate becomes

$$\sum F_t = 0 = \dot{m}_2\vartheta_{jet} + \dot{m}_3\left(-\vartheta_{jet}\right) - \dot{m}_1\vartheta_{jet}\cos\theta$$

$$\rho h_2 b\vartheta_{jet}^{\,2} - \rho h_3 b\vartheta_{jet}^{\,2} - \rho h_1 b\vartheta_{jet}^{\,2}\cos\theta = 0$$

$$h_2 - h_3 - h_1\cos\theta = 0$$

but from continuity

$$\dot{m}_1 = \dot{m}_2 + \dot{m}_3$$

$$\rho h_1 b\vartheta_{jet} = \rho h_2 b\vartheta_{jet} + \rho h_3 b\vartheta_{jet}$$

$$h_1 = h_2 + h_3$$

Then combining the continuity equation and the momentum equation, we get

$$h_2 = \frac{h_1}{2}\left(1+\cos\theta\right)$$

$$h_3 = \frac{h_1}{2}\left(1-\cos\theta\right)$$

(b) To determine the location of the center of pressure, we can apply the angular momentum theorem to the control volume shown. Since the flow is steady and since there are no shaft torques applied and since the body forces are of no consequence here, the angular momentum theorem reduces to

$$\sum\left(\vec{r}\times\vec{F}_{surface}\right) = \sum_{out}\dot{m}_{out}\left(\vec{r}\times\vec{\vartheta}\right)_{out} - \sum_{in}\dot{m}_{in}\left(\vec{r}\times\vec{\vartheta}\right)_{in}$$

If we now apply this result about the location O where the centerline of the jet intersects the front surface of the plate and take moments in the clockwise direction to be positive, we have

$$\sum\left(\vec{r}\times\vec{F}_{surface}\right) = -F_n L = \dot{m}_2\left(\vec{r}_2\times\vec{\vartheta}_2\right) + \dot{m}_3\left(\vec{r}_3\times\vec{\vartheta}_3\right) + 0$$

where the third term on the right-hand side is zero since the centerline of the jet issuing from the nozzle passes through the point O which makes $\vec{r}_1 = 0$. In the one-dimensional bulk flow model, we model the flow as though the entire flow through the centerline of the port. Then the cross product terms become ϑd where d is the distance from the point O to the line of action of the velocity ϑ measured perpendicularly from O. Then

$$-F_n L = \rho \vartheta_{jet} b h_2 \left(\frac{h_2}{2}\vartheta_{jet}\right) + \rho \vartheta_{jet} b h_3 \left(\frac{h_3}{2}\left(-\vartheta_{jet}\right)\right) = \frac{\rho b \vartheta_{jet}^{\,2}}{2}\left(h_2^{\,2} - h_3^{\,3}\right)$$

$$L = -\frac{\rho b \vartheta_{jet}^{\,2}}{2F_n}\left(h_2^{\,2} - h_3^{\,3}\right) = -\frac{\rho b \vartheta_{jet}^{\,2}}{2F_n}\left(h_1^{\,2}\cos\theta\right)$$

where we have substituted the results of part (a) above. We now need to determine the functional form of F_n.

(c) We can determine F_n by applying the equation of linear momentum in the direction normal to the plate. Then

$$\sum F_n = \int_{CS} \rho \vec{\vartheta}\left(\vec{\vartheta}_r \cdot \vec{n}\right) dA$$

$$F_n = \dot{m}_1 \vartheta_{jet} \sin\theta = \rho b h_1 \vartheta_{jet}^{\,2} \sin\theta$$

Now substituting this result into the expression for the location of the center of pressure, we get

$$L = -\frac{h_1 \cot\theta}{2}$$

which indicates that the center of pressure lies below the point O.

Example 8E.25: The small lawn sprinkler shown in Figure 8E.25a rotates at a constant angular speed of 30 rpm. Water enters the sprinkler at a pressure of $P_1 = P_{atm} + 20 \times 10^3$ N/m^2 and a volume flow rate of $\dot{V} = 7.5$ liters per minute. The diameter of each jet is $D_{jet} = 4$ mm.

(a) Calculate the speed of the jet, ϑ_{rel}, relative to each sprinkler nozzle.

(b) Estimate the friction torque, $T_{friction}$, at the sprinkler pivot.

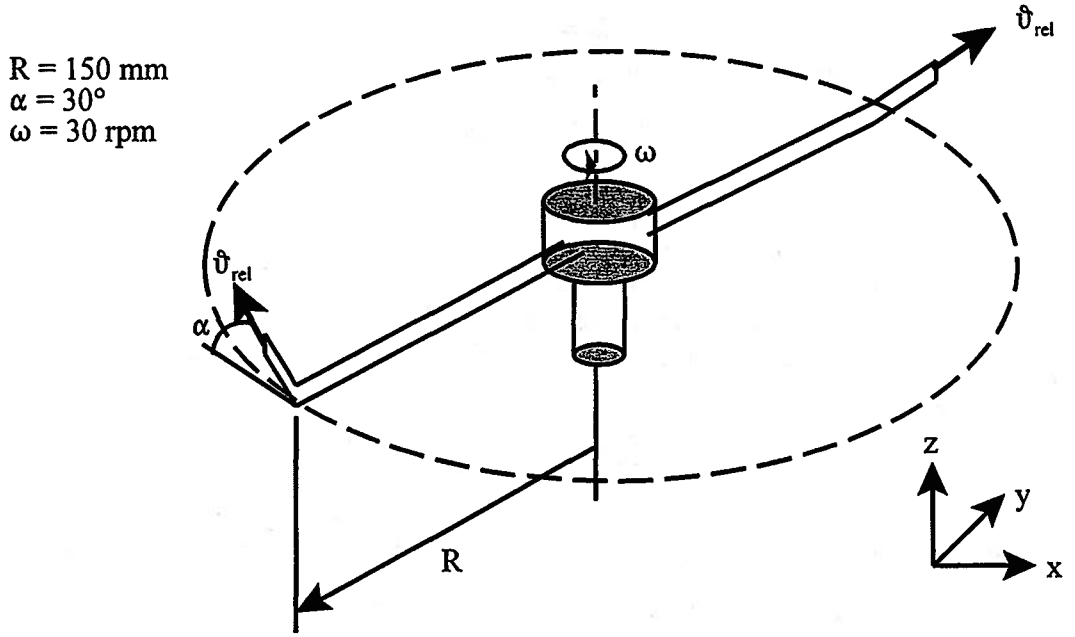

Figure 8E.25a Lawn Sprinkler

Solution: (a) For steady incompressible flow with uniform velocity in the jet, the continuity equation gives

$$\vartheta_{rel} = \frac{\dot{V}}{2A_{jet}} = \frac{\dot{V}}{2}\frac{4}{\pi D_{jet}^{\ 2}} = \frac{7.5\ \text{L/min}}{2(60\ \text{sec/min})}\frac{4(10^{-3}\ \text{m}^3/\text{L})}{\pi(4\ \text{x}\ 10^{-3}\ \text{m})^2}10^6\ \text{mm}^3/\text{m}^3 = 4.97\ \text{m/sec}$$

where the velocity is measured relative to the nozzle. Establish a stationary control volume positioned to encompass the volume swept out by the sprinkler as it rotates. The axis of the control volume is coincident with the axis of rotation of the lawn sprinkler.

(b) To estimate the friction torque at the pivot, we apply equation (8.105), the angular momentum theorem.

$$\sum\left(\vec{r}\times\vec{F}_{surface}\right) + \int_{CV}(\vec{r}\times\vec{g})\rho dV + \vec{T}_{shaft} = \frac{d}{dt}\left[\int_{CV}\left(\vec{r}\times\vec{\vartheta}\right)\rho dV\right] + \int_{CS}\left(\vec{r}\times\vec{\vartheta}\right)\rho\left(\vec{\vartheta}_r\cdot\vec{n}\right)dA$$

We now proceed to compute the individual terms in the angular momentum theorem. Atmospheric pressure acts all over the control surface, and the force due to the water pressure at the inlet acts along the axis of rotation. If follows, then, that

$$\vec{r}\times\vec{F}_s = 0$$

The moments due to the two body forces acting on the water in the two arms of the sprinkler are equal and in opposition to one another. Thus, the torque due to body forces vanishes. Then the only torque acting on the control volume is due to friction at the pivot. Since this torque acts to oppose the motion of the sprinkler, its vector acts in the negative z-direction. Thus

$$\vec{T}_{shaft} = -T_{friction}\vec{k}$$

To evaluate the rate of change of angular momentum in the control volume, we have to form the cross product of the radius vector of each mass element of water and its velocity. If we assume that the mass contained in the tips is negligible compared to the mass in the radial arms, we have for the typical arm as shown below.

Let $\vec{\vartheta}$ be the fluid velocity relative to the fixed coordinates. This velocity has two contributions: the velocity relative to the tube and the tangential velocity associated with the rotation of the arm.

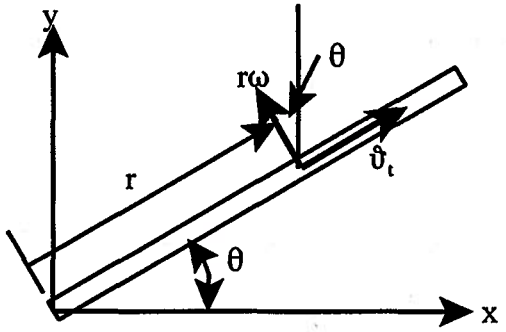

Figure 8E.25b Plan View of Radial Arm of Lawn Sprinkler

From Figure 8E.25b, we have

$$\vec{\vartheta} = (\vartheta_t\cos\theta - r\omega\sin\theta)\vec{i} + (\vartheta_t\sin\theta + r\omega\cos\theta)\vec{j}$$

$$\vec{r} = (r\cos\theta)\vec{i} + (r\sin\theta)\vec{j}$$

Then

$$\vec{r}\times\vec{\vartheta} = (r^2\omega\cos^2\theta + r^2\omega\sin^2\theta)\vec{k} = (r^2\omega)\vec{k}$$

and

$$\int_{arm} \vec{r} \times \vec{\vartheta} \rho dV = \int_0^R (r^2 \omega) \vec{k} \rho A dr = \frac{R^3 \omega}{3} \vec{k} \rho A$$

where A is the cross-sectional area of the tube. It follows, then, that for each tube

$$\frac{d}{dt} \int_{arm} \vec{r} \times \vec{\vartheta} \rho dV = \frac{d}{dt}\left[\frac{R^3 \omega}{3} \vec{k} \rho A \right] = 0$$

We now proceed to evaluate the flow of angular momentum through the control surface. Since we said above that we are going to neglect the mass of fluid in the tips, we can trat this situation as though the jets are located at the end of the arm itself. Then if we let the subscript E denote the end of the arm, the position vector of the location of the jet is

$$\vec{r}_E = (R\cos\theta)\vec{i} + (R\sin\theta)\vec{j}$$

The velocity of the jet has two contributions to it one due to the velocity of the jet relative to the control volume, the other due to the tangential velocity of the tip of the arm. Then

$$\vec{\vartheta}_{jet} = \vec{\vartheta}_{rel} + \vec{\vartheta}_t$$

$$\vec{\vartheta}_{jet} = (\vartheta_{rel}\cos\alpha\sin\theta - \omega R\sin\theta)\vec{i} + (\vartheta_{rel}\cos\alpha\cos\theta + \omega R\cos\theta)\vec{j} + (\vartheta_{rel}\sin\alpha)\vec{k}$$

and for the cross product of the radius vector and the jet velocity we have

$$\vec{r}_E \times \vec{\vartheta}_{jet} = (R\vartheta_{rel}\sin\alpha\sin\theta)\vec{i} - (R\vartheta_{rel}\sin\alpha\cos\theta)\vec{j} - (R[\vartheta_{rel}\cos\alpha - \omega R])\vec{k}$$

Then for one arm

$$\int_{CS} \vec{r} \times \vec{\vartheta}_{jet} \rho \vec{\vartheta} \cdot d\vec{A} = \frac{\rho \dot{V}}{2}\left[(R\vartheta_{rel}\sin\alpha\sin\theta)\vec{i} - (R\vartheta_{rel}\sin\alpha\cos\theta)\vec{j} - (R[\vartheta_{rel}\cos\alpha - \omega R])\vec{k} \right]$$

and for the other arm

$$\int_{CS} \vec{r} \times \vec{\vartheta}_{jet} \rho \vec{\vartheta} \cdot d\vec{A} = \frac{\rho \dot{V}}{2}\left[-(R\vartheta_{rel}\sin\alpha\sin\theta)\vec{i} + (R\vartheta_{rel}\sin\alpha\cos\theta)\vec{j} - (R[\vartheta_{rel}\cos\alpha - \omega R])\vec{k} \right]$$

Then for the entire control surface, we simply sum the last two equations.

$$\int_{CS} \vec{r} \times \vec{\vartheta}_{jet} \rho \vec{\vartheta} \cdot d\vec{A} = -\rho \dot{V} R(\vartheta_{rel}\cos\alpha - \omega R)\vec{k}$$

For the line feeding the sprinkler, the angular momentum is zero since the line is on the axis of rotation. Then combining the various terms

$$-T_{friction}\vec{k} = -\rho \dot{V} R(\vartheta_{rel}\cos\alpha - \omega R)\vec{k}$$

Then

$$T_{friction} = (0.150\text{ m})(10^3\text{ kg/m}^3)\left[\frac{(7.5\text{ L/min})(10^{-3}\text{ m}^3/\text{L})}{60\text{ sec/min}} \right] \bullet$$

$$\bullet \left[(4.97\text{ m/sec})\cos 30^\circ - \frac{(30\text{ rev/min})(2\pi\text{ rad/rev})(0.150\text{ m})}{60\text{ sec/min}} \right]$$

$$T_{friction} = 0.0718\text{ N-m}$$

Notice the interesting result that even in the absence of friction, the angular velocity is limited by the fact that the tangential velocity becomes equal to the jet velocity. Thus, in this case

$$\omega_{max} = \frac{\vartheta_{rel}\cos\alpha}{R} = \frac{(4.97\text{ m/sec})\cos 30^\circ}{0.150\text{ m}} = 28.693\text{ rad/sec} = 274\text{ rpm}$$

8.13.1 The Euler Turbomachine Equation

One of the most common applications of the equation of angular momentum for a control volume is to turbomachines such as pumps and fans that are used to convert a shaft torque into an increase in pressure of a fluid stream by changing its angular momentum as it flows through the device or turbines that are used to convert the angular momentum of a fluid stream into a shaft torque for the purpose of driving some other device. In these cases, the only applied surface forces of consequence are those due to pressure in the entering and exiting fluid streams; however, these forces typically act radially through the center of rotation and, hence, do not contribute any moment to the fluid. The body forces due to gravity do not play any significant role in the operation of these devices and are usually neglected. Then the shaft torque is the only significant moment acting on the control volume. Usually there is one entry port and one exit port. Then equation (8.101) becomes

$$\vec{T}_{shaft} = \dot{m}_{out}\left(\vec{r}\times\vec{\vartheta}\right)_{out} - \dot{m}_{in}\left(\vec{r}\times\vec{\vartheta}\right)_{in} \tag{8.102}$$

If we denote the parameters at the outlet port by the subscript 2 and those at the inlet port by the subscript 1, equation (8.102) becomes for a steady-flow device in which $\dot{m}_{in} = \dot{m}_{out} = \dot{m}$,

$$\vec{T}_{shaft} = \dot{m}\left(\vec{r}_2\times\vec{\vartheta}_2\right) - \dot{m}\left(\vec{r}_1\times\vec{\vartheta}_1\right) \tag{8.103}$$

In vector notation in cylindrical coordinates, we have

$$\begin{aligned}
\vec{r}_1 &= R_1\vec{i}_r + 0\vec{i}_\theta + 0\vec{i}_z \\
\vec{r}_2 &= R_2\vec{i}_r + 0\vec{i}_\theta + 0\vec{i}_z \\
\vec{\vartheta}_1 &= \vartheta_{r1}\vec{i}_r + \vartheta_{t1}\vec{i}_\theta + 0\vec{i}_z \\
\vec{\vartheta}_2 &= \vartheta_{r2}\vec{i}_r + \vartheta_{t2}\vec{i}_\theta + 0\vec{i}_z
\end{aligned} \tag{8.104}$$

Then

$$\left(\vec{r}_1\times\vec{\vartheta}_1\right) = \vec{i}_r\left(0\cdot 0 - 0\cdot\vartheta_{t1}\right) + \vec{i}_\theta\left(0\cdot\vartheta_{r1} - R_1\cdot 0\right) + \vec{i}_z\left(R_1\cdot\vartheta_{t1} - 0\cdot\vartheta_{r1}\right) = R_1\vartheta_{t1}\vec{i}_z \tag{8.105}$$

Similarly

$$\left(\vec{r}_2\times\vec{\vartheta}_2\right) = R_2\vartheta_{t2}\vec{i}_z \tag{8.106}$$

Then equation (8.103) becomes

$$\vec{T}_{shaft} = \dot{m}\left(R_2\vartheta_{t2} - R_1\vartheta_{t1}\right)\vec{i}_z \tag{8.107}$$

This is known as the *Euler turbomachine equation.* Equation (8.107) shows that it is the geometry of the device embodied in the radii at inlet and outlet together with the tangential velocities that determines the shaft torque for the device.

Example 8E.26: As shown in Figure 8E.26, water with a density of $\rho_{water} = 10^3$ kg/m^3 enters a pump axially through a conduit with an inside diameter of $D_i = 2.5$ cm. The flow geometry of the pump is mixed, i.e. the flow enters axially and exits radially with the shape of the impeller vanes arranged purely radially. The volumetric flow rate is $\dot{V} = 0.6$ m^3/sec with an inlet flow velocity that is uniform and axial. The outlet diameter of the impeller is $D_o = 10$ cm, and flow leaves the impeller at a velocity of $\vartheta_{rb2} = 3$ m/sec relative to the radial blades. The impeller rotational speed is $\omega = 3450$ rpm. (AC motors typically run at 1725 or 3450 rpm.)

(a) Determine the impeller exit width, b, and the torque input to the impeller, T_{shaft}.

(b) How much power is required to drive the pump?

(c) Calculate the pressure rise for a reversible adiabatic pump.

Solution: (a) The control volume appears as shown in Figure 8E.26.

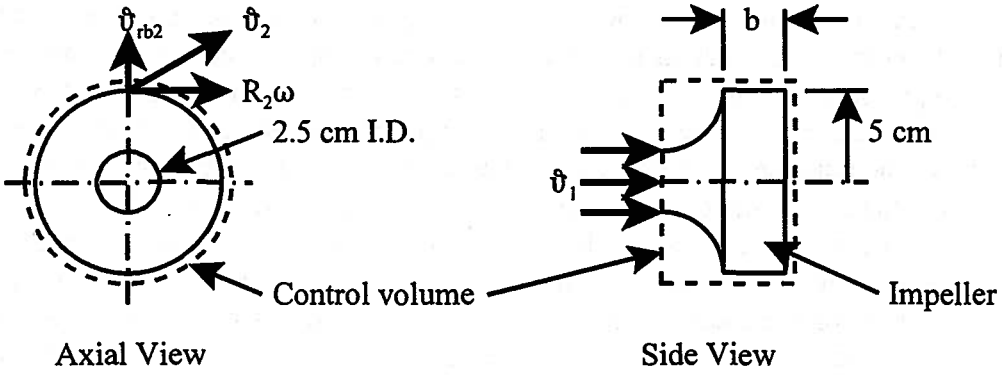

Figure 8E.26 Combined Axial Flow/Radial Flow Pump

The continuity equation becomes

$$\dot{m} = \rho A_1 \vartheta_1 = \rho A_2 \vartheta_2 = \rho \dot{V}$$

$$A_2 = \pi D b_2$$

$$b_2 = \frac{\dot{V}}{\pi D \vartheta_{rb2}} = \frac{(0.6 \text{ m}^3/\text{min})}{(60 \text{ sec/min})\pi(10 \text{ x } 10^{-2} \text{ m})(3 \text{ m/sec})}$$

$$b_2 = 1.061 \text{ x } 10^{-2} \text{ m}$$

The various terms in the equation of angular momentum equation are as follows:

$$\cancel{\vec{r} \times \vec{F}_{surface}} + \cancel{\int (\vec{r} \times \vec{g}) \rho dV} + \vec{T}_{shaft} = \frac{d}{dt}\left[\cancel{\int_{CV} (\vec{r} \times \vec{\vartheta}) \rho dV}\right] + \int_{CS} (\vec{r} \times \vec{\vartheta}) \rho (\vec{\vartheta}_r \cdot \vec{n}) dA$$

where the first term on the left vanishes because the surface forces either have $r = 0$ as at the inlet or are parallel to the radius vector as at the outlet; the second term on the left vanishes because the flow is not driven by gravity; and the first term on the right vanishes because the flow is steady. Then it follows that we just have the vector form of the Euler turbomachine equation, viz.

$$\vec{T}_{shaft} = \int_{CS} (\vec{r} \times \vec{\vartheta}) \rho (\vec{\vartheta} \cdot \vec{n}) dA$$

The integral in this expression has two terms: one for the inlet port and one for the outlet port. Since the inlet port is perpendicular to the axis of rotation and the flow is axial at this location, the inlet port contribution vanishes. Then for the outlet port (location 2) we have

$$\vec{r}_2 = R_2 \vec{i}_r$$

$$\vec{\vartheta}_2 = \vartheta_{rb2} \vec{i}_r + R_2 \omega \vec{i}_\theta$$

$$\vec{r}_2 \times \vec{\vartheta}_2 = R_2 (R_2 \omega) \vec{i}_z = R_2^2 \omega \vec{i}_z$$

Then the expression for the shaft torque becomes

$$T_{shaft} = R_2^2 \omega \rho \vartheta_{rb2} \pi D b_2 = R_2^2 \omega \rho \dot{V}$$

$$T_{shaft} = \frac{(3450 \text{ rev/min})(2\pi \text{ radians/rev})}{60 \text{ sec/min}} (5 \text{ x } 10^{-2} \text{ m})^2 (10^3 \text{ kg/m}^3) \frac{(0.6 \text{ m}^3/\text{min})}{60 \text{ sec/min}}$$

$$T_{shaft} = 9.032 \text{ N m}$$

For the shaft power (thermodynamic sign convention)

$$\dot{W}_{shaft} = -T_{shaft}\omega = -(9.032 \text{ N m})\frac{(3450 \text{ rev/min})(2\pi \text{ radians/rev})}{60 \text{ sec/min}} = -3.263 \text{ kW}$$

$$\dot{W}_{shaft} = -4.37 \text{ HP}$$

(c) For an incompressible fluid flowing steadily through a reversible adiabatic pump, the second law gives

$$\dot{S}_{GEN} = \dot{m}(s_{out} - s_{in}) = \dot{m}c\ln\left(\frac{T_{out}}{T_{in}}\right) = 0$$

$$\therefore T_{out} = T_{in}$$

$$\therefore u_{out} = u_{in}$$

Then the first law becomes

$$-\dot{W}_{shaft} = \dot{m}(h_{out} - h_{in}) = \dot{m}\left((u_{out} - u_{in}) + \frac{P_{out} - P_{in}}{\rho}\right) = \rho\dot{V}\left(\frac{P_{out} - P_{in}}{\rho}\right)$$

$$\therefore P_{out} - P_{in} = \frac{-\dot{W}_{shaft}}{\dot{V}} = \frac{(3.263 \text{ x } 10^3 \text{ W})(60 \text{ sec/min})}{0.6 \text{ m}^3/\text{min}} = 3.263 \text{ x } 10^5 \text{ N/m}^2$$

Notice that if the pump operates in an irreversible manner, the entropy generation term in the second law is non-zero and positive resulting in an increase in temperature of the fluid as it flows through the pump ($T_{out} > T_{in}$). Then the stored thermal energy of the fluid at outlet is greater than the stored thermal energy at inlet ($u_{out} > u_{in}$), and the pressure rise through the pump in the irreversible case is less than the pressure for reversible operation ($P_{out,irrev} < P_{out,rev}$).

8.14 Open Channel Flows

The term "open channel flows" is an all-encompassing term that usually refers to those flow conditions that involve a liquid flowing with a free surface that is exposed to a gas, such as the atmosphere. This is the case, for example, with flow in a river or flow in a drainage ditch or an irrigation canal. Typically the flow patterns in these geometries can be quite complex since the effects of fluid viscosity reveal themselves wherever the flowing fluid comes into contact with the solid surfaces that bound it (the sides and bottom of the channel), but not at the free surface where the fluid is in contact with the gas. Thus that portion of the fluid in contact with the solid surfaces is slowed through the action of viscosity whereas the fluid at the free surface is not. (In reality, there is a slight amount of drag exerted by the gas on the moving free surface of the liquid, but this effect is so small because of the large differences between the viscosity of the gas and that of the liquid, that we are justified in neglecting it.) The net result is that the distribution of velocity in the flowing liquid, i.e., fluid velocity as a function of position in the channel, usually has a complex form that can be determined only by numerical methods (computational fluid dynamics, CFD) or experimental measurements.

Despite the influence of fluid viscosity on the velocity profile in the fluid, there is much that can be learned about the nature of open channel flows by neglecting viscous effects, i.e., by modeling the fluid as inviscid. Through the application of the principles of continuity and linear momentum, as well as the first law of thermodynamics, to a properly formulated control volume, we can actually predict the nature of the flow in open channels under a variety of flow conditions while neglecting the effects of viscosity. In fact, there is even a flow phenomenon that can occur in open channel flows that also requires the application of the second law to the control volume for its proper interpretation. In the present section, we shall do precisely this and discover in the process several open channel flow phenomena that commonly occur in rivers and other open

channels. Throughout this treatment, we shall neglect viscosity and leave its consideration to Chapter 9.

8.14.1 Flow in an Open Channel with a Sloping Bottom

In an open channel flow of a liquid exposed to the atmosphere, the pressure at the free surface is constant and is essentially atmospheric pressure. If the flow is steady, the Bernoulli equation can be applied along the surface. Below the free surface, the pressure is hydrostatic and increases with depth even if the streamlines are parallel. There then results a strong interconnection between the fluid velocity and gravity. This relationship can be seen from the schematic representation of flow in a rectangular open channel of unit width as shown in Figure 8.16.

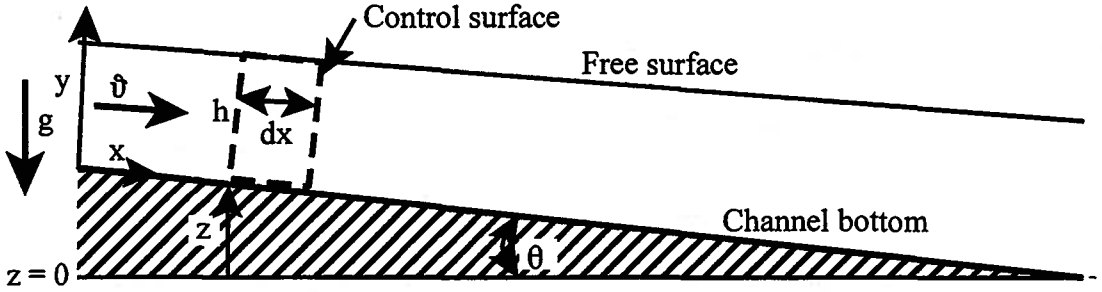

Figure 8.16 Flow in a Rectangular Open Channel of Unit Width

The slope of the channel bottom is given by the angle θ and the depth of the flow measured normal to the channel bottom is given by h. We define a control volume of infinitesimal length dx measured in the direction of flow and extending in the y-direction over the full height of the flow h. In the context of this simple model, we take the fluid velocity to be uniform over the depth of the channel but varying in the direction of flow due to the changing depth. (In reality, this uniform velocity at each position x is some suitable average velocity.) The mass flow rate at any location is $\dot{m}$ and is constant at all values of x.

As shown in Figure 8.17, the forces acting in the x-direction on the control volume consist of (1) a surface force $(F_s)_x$ acting in the positive x-direction due to the hydrostatic pressure acting on the face of the control volume at the location x, (2) a surface force $(F_s)_x + d(F_s)_x$ acting in the negative x-direction due to the hydrostatic pressure acting on the face of the control volume at the location $x + dx$, and (3) the x-component of the body force $(F_b)_x$ due to the action of gravity on the fluid contained in the control volume. There is also a flow of momentum $\dot{m}\vartheta$ into the control volume and a corresponding flow of momentum $\dot{m}\vartheta + d(\dot{m}\vartheta)$ out of the control volume.

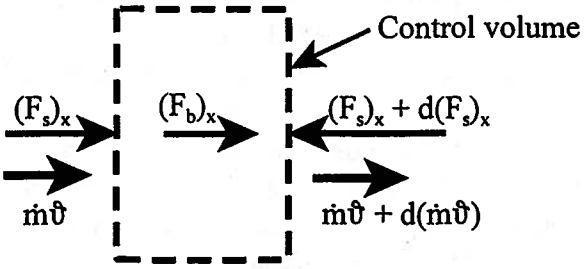

Figure 8.17 x-components of Forces Acting on the Control Volume and Momentum Flows

Then applying the equation of linear momentum for steady flow in the x-direction, we have

$$\begin{aligned}(F_s)_x + (F_b)_x - \left[(F_s)_x + d(F_s)_x\right] &= (\dot{m}\vartheta) + d(\dot{m}\vartheta) - (\dot{m}\vartheta) \\ (F_b)_x - d(F_s)_x &= d(\dot{m}\vartheta)\end{aligned} \tag{8.108}$$

Substituting the appropriate expression for each of the terms in equation (8.108), we get

$$\rho(g\sin\theta)h dx - d\left(\frac{\rho(g\cos\theta)h^2}{2}\right) = d\left(\rho h \vartheta^2\right) \tag{8.109}$$

The continuity equation for this flow geometry is given by

$$\dot{m} = \rho h \vartheta = \text{constant} \tag{8.110}$$

Substituting equation (8.110) into equation (8.109) and recognizing that the fluid density ρ is constant, equation (8.109) can be simplified to

$$h\vartheta d\vartheta + (hdh)(g\cos\theta) - h(g\sin\theta)dx = 0 \tag{8.111}$$

From Figure 8.16, it is evident that

$$\sin\theta\, dx = -dz \tag{8.112}$$

and since the slope of the channel bottom is typically small, it follows that $\cos\theta \approx 1$. Then combining equations (8.111) and (8.112) and using the small slope approximation, we get

$$h\vartheta d\vartheta + ghdh + ghdz = 0 \tag{8.113}$$

From continuity, equation (8.110), we have for the incompressible fluid model used here

$$\frac{dh}{h} + \frac{d\vartheta}{\vartheta} = 0 \tag{8.114}$$

Combining equations (8.113) and (8.114), we get

$$dh\left(1 - \frac{\vartheta^2}{gh}\right) = -dx\left(\frac{dz}{dx}\right) \tag{8.115}$$

In Chapter 5, we showed that the velocity of a small amplitude gravity wave on the surface of an incompressible fluid was $\vartheta_w = \sqrt{g\,h}$. Thus the second term in the parentheses on the left-hand side of equation (8.115) is dimensionless. This combination of terms occurs so frequently in flows involving free surfaces of liquids (fluids that can be modeled as incompressible fluids), it is given a special name, the *Froude number*, in honor of the person who first used it and is denoted by the symbol *Fr*. (See Chapter 10, Section 10.8.) Thus

$$Fr = \frac{\vartheta}{\sqrt{gh}} = \frac{\vartheta}{\vartheta_w} \tag{8.116}$$

Then equation (8.115) becomes

$$\frac{dh}{dx}\left(1 - Fr^2\right) = -\left(\frac{dz}{dx}\right) \tag{8.117}$$

Equation (8.117) actually contains a great deal of information about open channel flows, but before we explore this information, it is worthwhile to examine the implications of equation (8.116) in some detail since it appears in equation (8.117).

The small amplitude gravity surface wave is the means by which disturbances propagate in open channel flows. (By "small" we mean that the amplitude is small compared to the wavelength.) In Chapter 5 we saw that a displacement of the boundary of a shallow (depth of fluid also small compared to the wavelength) open channel produced a disturbance that propagated along the surface of the fluid at the velocity $\vartheta_w = \sqrt{g\,h}$. The same is true for a flowing fluid in an open channel. The small amplitude gravity surface wave is the means by which the fluid upstream of a disturbance such as an obstruction is "informed" of the disturbance downstream. However, for a fluid flowing with a velocity ϑ, it makes a difference whether this velocity is larger or smaller than the wave velocity. If the fluid velocity is smaller than the wave velocity ($Fr < 1$), a fluid particle upstream of an obstruction will be "informed" of the obstruction downstream before it reaches the obstruction; however, if the fluid velocity is greater than the

wave velocity($Fr > 1$), a fluid particle upstream of the obstruction will reach the obstruction before the "information" of the obstruction can reach the particle.

This concept can be best illustrated by the following scenario. Everyone is familiar with the experience of dropping a stone into a stagnant, shallow pond. Ripples (small amplitude gravity waves) are created on the surface of the water by the disturbance and propagate radially outward from the point where the stone entered the water with the ripples evenly spaced. Now imagine a shallow stream in the woods flowing with a velocity ϑ. Imagine an observer positioned on a log bridging the stream. The observer drops a stone into the water. Now, as depicted schematically in Figure 8.18, three different outcomes are possible depending upon whether the flow of the stream is *subcritical* ($Fr < 1$), *critical* ($Fr = 1$), or *supercritical* ($Fr > 1$).

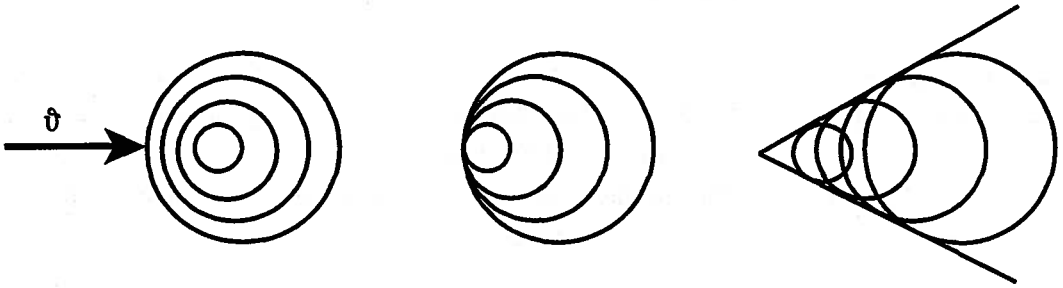

(a) Fr < 1 (b) Fr = 1 (c) Fr > 1

Figure 8.18 Wave Patterns Due to a Point Source

In the case of supercritical flow ($Fr > 1$), Figure 8.18 (c), the ripples form a wedged shape pattern with a characteristic angle θ as shown in Figure 8.19. During a time interval Δt, the center of the disturbance moves a distance $\vartheta \Delta t$ while the wave front moves a distance $\vartheta_w \Delta t$. Then the angle θ, sometimes called the *Froude angle*, is determined from the geometry of the wave pattern as

$$\theta = \arcsin\left(\frac{\vartheta_w \Delta t}{\vartheta \Delta t}\right) = \arcsin\left(\frac{\sqrt{gh}}{\vartheta}\right) = \arcsin\left(\frac{1}{Fr}\right) \tag{8.118}$$

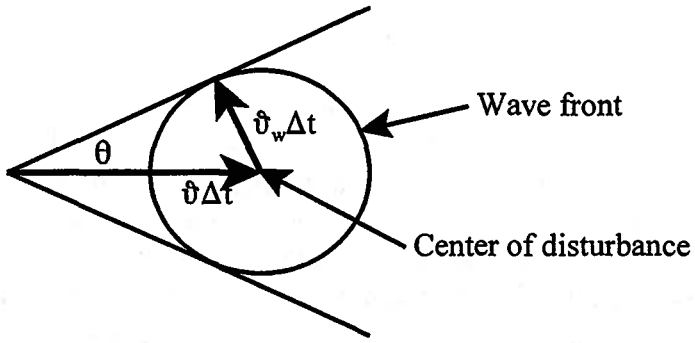

Figure 8.19 Froude Angle in Supercritical Flow

The interpretation of equation (8.117) now becomes obvious. The behavior of the flow is determined by whether the flow is subcritical or supercritical. If the flow is subcritical ($Fr < 1$), the term in parentheses on the left-hand side of equation (8.117) becomes positive and a negative slope of the channel bottom ($dz/dx < 0$) results in an increase in the depth of the flow in the channel. Because of continuity, this means a decrease in the velocity of flow. The physical interpretation is that in subcritical flow, the body force due to gravity that drives the flow is

inadequate to overcome the surface force opposing the motion of the fluid. This results in a loss of momentum which causes the flow to decelerate and, hence, increase in depth. On the other hand, if the flow is supercritical ($Fr > 1$), the term in parentheses on the left-hand side of equation (8.117) becomes negative and a negative slope of the channel bottom ($dz/dx < 0$) results in a decrease in the depth of the flow in the channel. Because of continuity, this means an increase in the velocity of flow. The physical interpretation is that in supercritical flow, the body force due to gravity driving the flow is adequate to overcome the surface force opposing the motion of the fluid. This results in an increase in momentum of the flow which causes the flow to accelerate and, hence, decrease in depth.

A certain amount of caution must be exercised in the application of equation (8.117) since the Froude number does vary in the direction of flow. Thus over finite distances of x, it is necessary to integrate equation (8.117) with the term in parentheses appearing inside the integral. Alternatively, we can apply the Bernoulli equation along the surface from point to point. In the context of the approximation of a gradually sloping channel bottom ($\cos\theta \approx 1$), this becomes

$$\frac{P_{atm}}{\rho}+\frac{\vartheta_1^2}{2}+g(h_1+z_1)=\frac{P_{atm}}{\rho}+\frac{\vartheta_2^2}{2}+g(h_2+z_2) \tag{8.119}$$

which can be simplified to

$$E_1+z_1=E_2+z_2 \tag{8.120}$$

where we have introduced the concept of the specific energy relative to the channel bottom denoted by the symbol E which is given by

$$E\equiv\frac{\vartheta^2}{2g}+h \tag{8.121}$$

Equation (8.121) can be solved simultaneously with the continuity equation.

$$\dot{V}=\vartheta h=\text{constant} \tag{8.122}$$

The solutions are of the form shown in Figure 8.20.

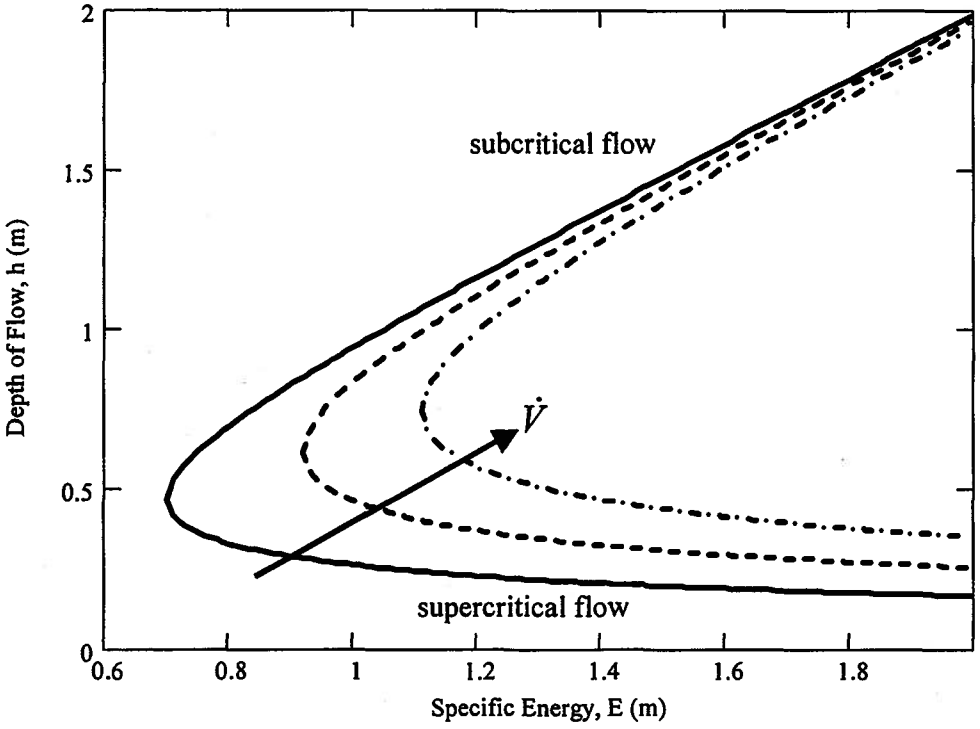

Figure 8.20 Open Flow in a Rectangular Channel

Notice that the combination of the Bernoulli equation and the continuity equation admits two possible solutions that are physically meaningful: one corresponding to subcritical flow, the other corresponding to supercritical flow. Thus for a given volumetric flow rate with a particular value for the specific energy, there are two possible depths of flow: a large one corresponding to subcritical flow with low velocity and small one corresponding to supercritical flow with a high velocity. Notice also that for a given volumetric flow rate, there is a minimum value for the specific energy of the flow. No physically meaningful simultaneous solution of the Bernoulli equation and the continuity equation is possible for flows with specific energy smaller than this minimum value at this flow rate.

Example 8E.27: Consider the case of flow of water in a rectangular channel of width b = 1 m with a slope of $\theta = 2°$. (Note cos $\theta = 0.9999$) The volumetric flow rate is $\dot{V} = 2$ m^3/sec and the depth of flow at a particular location 1 is $h_1 = 1$ m.

(a) Determine the flow velocity at location 1.

(b) Calculate the depth of flow and the local velocity at location 2 where $z_1 - z_2 = 0.5$ m.

(c) Calculate the distance along the channel bottom between locations 1 and 2.

Solution: (a) From continuity,

$$\dot{V} = h_1 \mathcal{V}_1 = 2 \text{ m}^3/\text{sec}$$

$$\mathcal{V}_1 = \frac{\dot{V}}{h_1} = \frac{2 \text{ m}^3/\text{sec}}{1 \text{ m}} = 2 \text{ m/sec}$$

(b) The specific energy of the flow is given by

$$E = \frac{\mathcal{V}^2}{2g} + h$$

and the simultaneous solution of the continuity equation and the expression for the specific energy can be shown graphically as in Figure 8E.27.

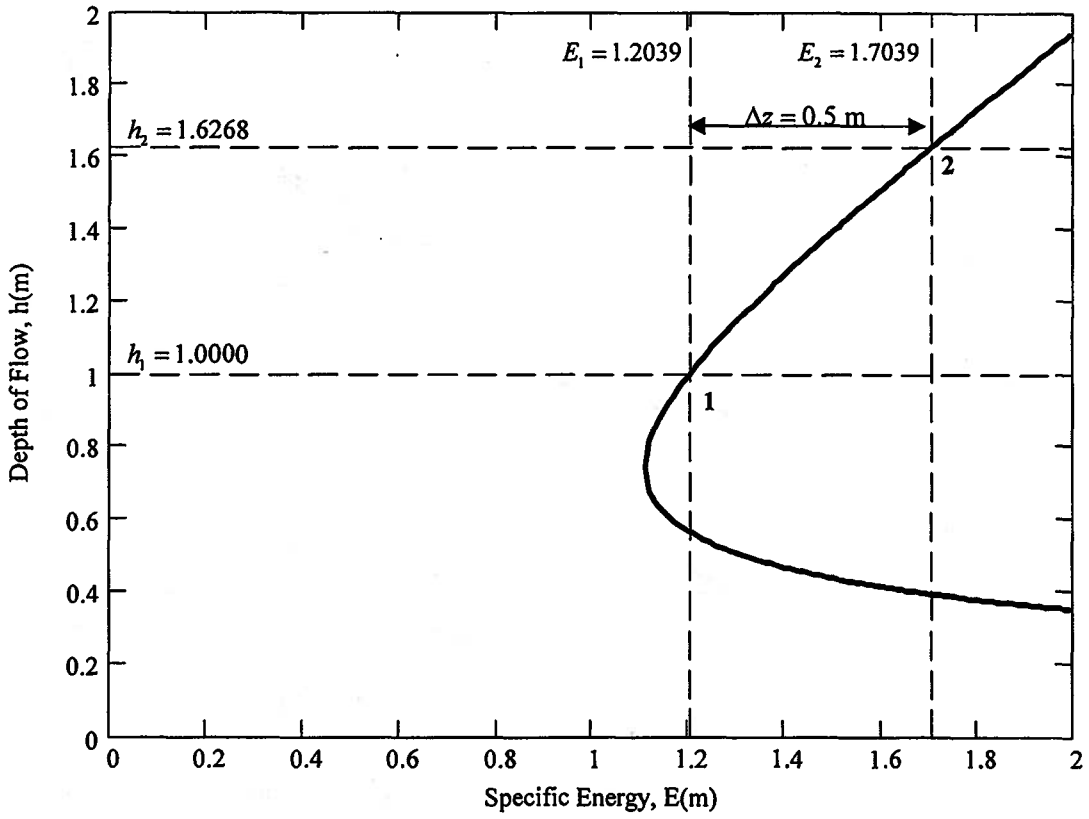

Figure 8E.27 Frictionless Flow in a Rectangular Channel with $\dot{V} = 2$ m^3/sec

The depth of flow and the specific energy at location 1 are indicated on Figure 8E.27. For the geometry under study, it follows from the application of the Bernoulli equation on the surface of the flow

$$\frac{\vartheta_1^2}{2g} + h_1 + z_1 = \frac{\vartheta_2^2}{2g} + h_2 + z_2$$

$$E_1 + z_1 = E_2 + z_2$$

$$E_2 = E_1 + (z_1 - z_2) = E_1 + \Delta z$$

Since

$$E_1 = \frac{\vartheta_1^2}{2g} + h_1 = \frac{(2 \text{ m/sec})^2}{2(9.81 \text{ m/sec})} + 1\text{m} = 1.2039 \text{ m}$$

it follows that

$$E_2 = E_1 + \Delta z = 1.2039 \text{ m} + 0.5 \text{ m} = 1.7039 \text{ m}$$

Entering Figure 8E.27 with this value of E_2 on the abscissa, we get a value of $h_2 = 1.6268$ m. Alternatively, we could combine the continuity equation and the expression for the specific energy to get an expression for h_2, viz.

$$h_2^3 - E_2 h_2^2 + \frac{\dot{V}}{2g} = 0$$

The roots of this equation are: $h_2 = 1.6268$ m (the subcritical depth solution); $h_2 = 0.3946$ m (the supercritical depth solution); and $h_2 = -0.3176$ m (a physically meaningless depth). The velocity at location 2 can now be determined from the continuity equation, viz.

$$\vartheta_2 = \frac{\dot{V}}{h_2} = \frac{2 \text{ m}^3/\text{sec}}{1.6268 \text{ m}} = 1.2294 \text{ m/sec}$$

(c) The distance along the channel bottom between locations 1 and 2 is given by

$$x = \frac{\Delta z}{\sin\theta} = \frac{0.5 \text{ m}}{\sin 2^\circ} = 14.3268 \text{ m}$$

Note that the resulting slope is consistent with our approximation $\cos\theta \approx 1$.

8.14.2 Flow Over a Bump or Depression in the Channel Bottom

Suppose now that the slope of the channel bottom is zero, i.e., the channel bottom is level. Let us now consider the case in which there is a bump in the channel bottom that extends all the way across the width of the channel. That is, the channel bottom has an abrupt, but smooth transition to another level as shown in Figure 8.22.

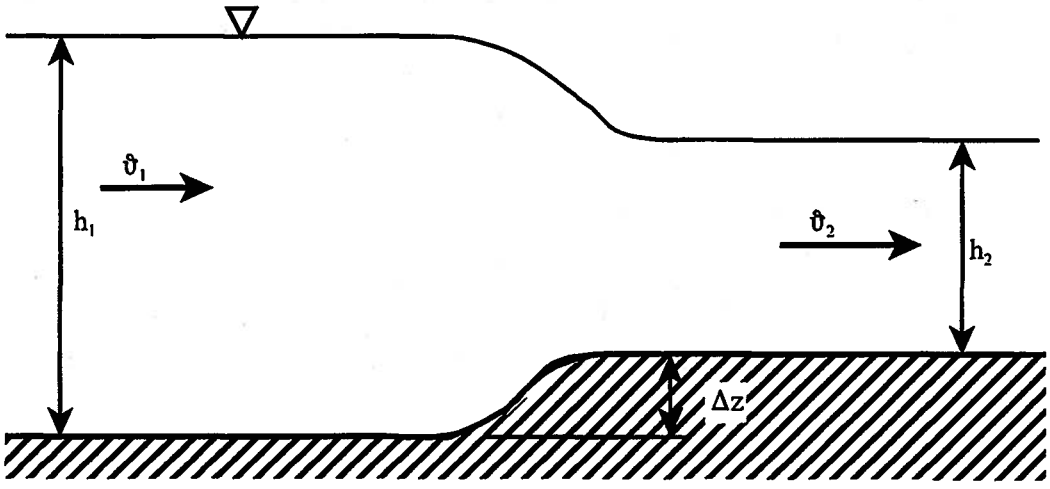

Figure 8.22 Frictionless Open Channel Flow Over a Bump

Such might be the case, for example, in a river or stream where a large flat rock lies on the bottom. Again assuming frictionless flow, equation (8.117) can now be rewritten to reveal the nature of the flow on the raised portion of the channel bottom, viz.

$$dh = -\frac{1}{\left(1 - Fr^2\right)} dz \tag{8.123}$$

From equation (8.123) it appears that the behavior of the frictionless flow is determined by whether the flow is subcritical or supercritical. If the flow is subcritical ($Fr < 1$), the term in parentheses on the right-hand side of equation (8.123) becomes positive and a bump, i.e., an elevation of the channel bottom ($dz > 0$) results in a decrease in the depth of the flow in the channel ($dh < 0$). (Note that because the coefficient of dz is always greater than unity in the case of a subcritical flow, $|dh| > |dz|$.) Because of continuity, this means an increase in the velocity of flow. The physical interpretation is that in subcritical flow, for an appropriately drawn control volume, the surface force opposing the motion of the fluid decreases, and this results in an increase in momentum which causes the flow to accelerate and, hence, decrease in depth because of continuity. On the other hand, if the flow is supercritical ($Fr > 1$), the term in parentheses on the right-hand side of equation (8.123) becomes negative and a bump, i.e., an elevation of the channel bottom ($dz > 0$) results in an increase in the depth of the flow in the channel ($dh > 0$). (Note that in the case of supercritical flow, the relative magnitudes of dh and dz depend upon the magnitude of Fr; however, the signs of the two changes, dh and dz, are always opposite.) In order to satisfy continuity, this means a decrease in the velocity of flow. The physical interpretation is that in supercritical flow, for an appropriately drawn control volume, the surface force opposing the motion of the fluid increases, and this results in a decrease in momentum of the flow which causes the flow to decelerate and, hence, increase in depth in order to satisfy continuity.

Of course, in the case of a depression in the channel bottom, the above arguments are all reversed since now $dz < 0$. In subcritical flow over a depression, the depth of flow increases with a concomitant decrease in velocity. In supercritical flow over a depression, the depth of flow decreases with a concomitant acceleration in the flow.

Example 8E.28: A horizontal open channel flow with an depth of flow of $h_1 = 1.25$ m and a volumetric flow rate of $\dot{V} = 2$ m^3/sec encounters an elevated portion of the channel bottom that is higher than the upstream portion of the channel bottom such that $\Delta z = z_2 - z_1 = 0.2$ m.

(a) Determine the depth of flow and the velocity of flow over the raised portion of the channel bottom.

(b) Determine the maximum elevation Δz_{max} in the channel bottom that the flow can withstand.

(c) Calculate the Froude number for the case in which the elevation is the maximum.

Solution: (a) The velocity at location 1 can be determined from the continuity equation, viz.

$$\mathcal{V}_1 = \frac{\dot{V}}{h_1} = \frac{2 \text{ m}^3/\text{sec}}{1.25 \text{ m}} = 1.60 \text{ m/sec}$$

Then the specific energy at location 1 is

$$E_1 = \frac{\mathcal{V}_1^2}{2g} + h_1 = \frac{(1.60 \text{ m/sec})^2}{2(9.81 \text{ m/sec}^2)} + 1.25 \text{ m} = 1.3805 \text{ m}$$

Applying the Bernoulli equation along the surface of the flow and substituting the appropriate values, we get

$$\frac{\vartheta_1^2}{2g} + h_1 + z_1 = \frac{\vartheta_2^2}{2g} + h_2 + z_2$$

$$E_1 + z_1 = E_2 + z_2$$

$$E_2 = E_1 + (z_1 - z_2) = E_1 - \Delta z$$

$$E_2 = 1.3805 \text{ m} - 0.2 \text{ m} = 1.1805 \text{ m}$$

From Figure 8E.28, this value of the specific energy yields a value of $h_2 = 0.95$ m for the depth of flow for the raised portion of the channel. Alternatively, we can combine the continuity equation and the equation for the specific energy to get a third order equation for h_2, viz.

$$h_2^3 - E_2 h_2^2 + \frac{\dot{V}^2}{2g} = 0$$

The roots of this expression are: $h_2 = 0.9586$ m (the subcritical depth); $h_2 = 0.5852$ m (the supercritical depth); and $h_2 = -0.3634$ m (a physically meaningless result). The velocity for the raised portion of the flow at location 2 can now be determined from the continuity equation, viz.

$$\vartheta_2 = \frac{\dot{V}}{h_2} = \frac{2 \text{ m}^3/\text{sec}}{0.9586 \text{ m}} = 2.0863 \text{ m/sec}$$

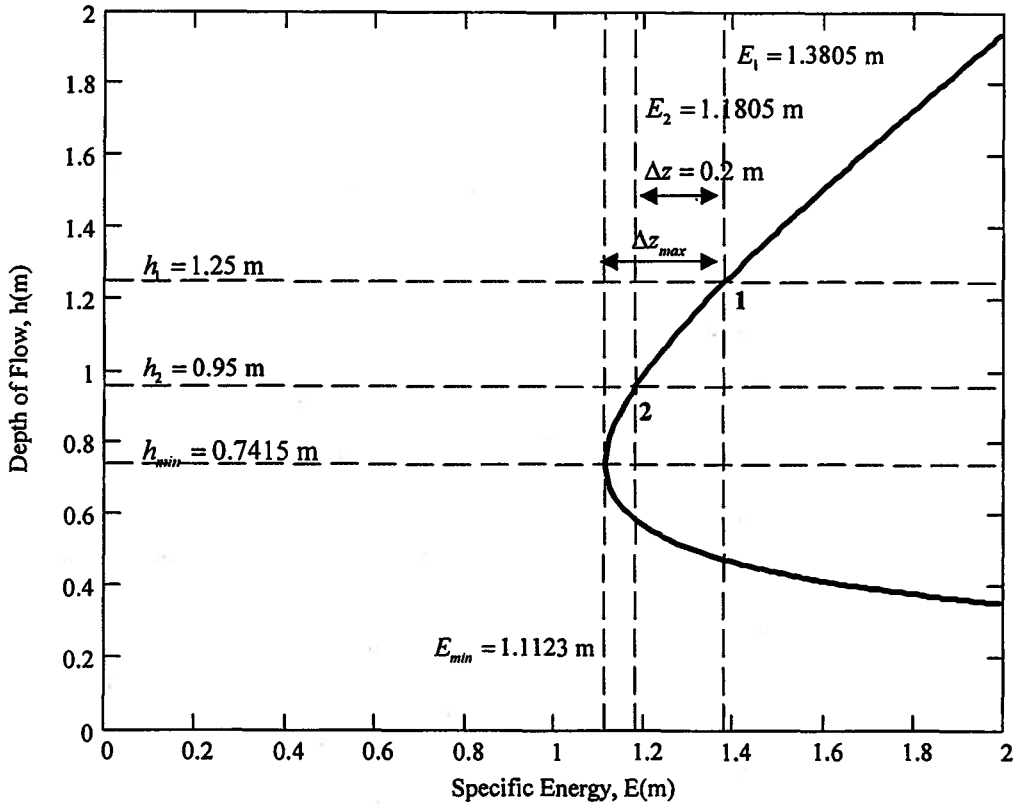

Figure 8E.28 Frictionless Flow in an Open Channel with a Bump, $\dot{V} = 2$ m^3/sec and $\Delta z = 0.20$ m

(b) From Figure 8E.28, it is obvious that the maximum elevation possible for the channel bottom for frictionless flow is the value of z for which the value of the specific energy is minimum. This occurs when the value of the depth of flow is minimum for subcritical flow or maximum for supercritical flow. This is the value of h for which $(dE/dh = 0)_{h = hmin}$. Then since

$$h_2^3 - E_2 h_2^2 + \frac{\dot{V}^2}{2g} = 0$$

Differentiating with respect to E, we get

$$3h^2 \frac{dh}{dE} - E2h\frac{dh}{dE} - 2h\frac{dE}{dE} = 0$$

$$3h^2 - 2Eh - 2h\frac{dE}{dE}\frac{dE}{dh} = 0$$

$$3h - 2E - 2\frac{dE}{dh} = 0$$

Since $(dE/dh = 0)_{h = hmin}$, we have

$$3h_{min} - 2E_{min} = 0$$

$$E_{min} = \frac{3}{2} h_{min}$$

Then from the original equation

$$h_{min}^3 - \frac{3}{2} h_{min}^3 + \frac{\dot{V}^2}{2g} = 0$$

$$h_{min}^3 = \frac{\dot{V}^2}{g}$$

Substituting the appropriate values, we get

$$h_{min} = \frac{\left(2 \text{ m}^3/\text{sec}\right)^2}{\left(9.81 \text{ m/sec}^2\right)\left(1 \text{ m}\right)^2} = 0.7415 \text{ m}$$

This corresponds to a minimum value of E of

$$E_{min} = \frac{3}{2} h_{min} = \frac{3}{2}(0.7415 \text{ m}) = 1.1123 \text{ m}$$

It follows that

$$\Delta z_{max} = E_1 - E_{min} = 1.3805 \text{ m} - 1.1123 \text{ m} = 0.2682 \text{ m}$$

For this elevation of the channel bottom, the depth of flow is $h_{min} = 0.7415$ m and the velocity of a small amplitude gravity surface wave is

$$\vartheta_w = \sqrt{g h_{min}} = \sqrt{\left(9.81 \text{ m/sec}^2\right)\left(0.7415 \text{ m}\right)} = 2.6971 \text{ m/sec}$$

From continuity, the flow velocity is

$$\vartheta = \frac{\dot{V}}{h_{min}} = \frac{2 \text{ m}^3/\text{sec}}{0.7415 \text{ m}} = 2.6971 \text{ m/sec}$$

Then the Froude number on the elevated portion of the channel bottom is

$$Fr = \frac{\vartheta}{\vartheta_w} = \frac{2.6971 \text{ m/sec}}{2.6971 \text{ m/sec}} = 1$$

Thus it follows that the maximum flow velocity that can be attained for the maximum possible elevation of the channel bottom is just the critical velocity. If the elevation of the channel bottom is greater than Δz_{max}, the flow is completely disrupted and must re-establish itself downstream of the transition at the original depth of $h_1$consistent with continuity, which in the present case results in a subcritical velocity.

8.14.3 Hydraulic Jump

As we have just shown, in open channel flows like streams and spillways in flood control systems, the flow of the water can reach supercritical velocities with the velocity of the flow higher than the speed of a small amplitude wave for the given depth of the flow. These supercritical flows can be difficult to sustain since the action of viscosity on the fluid in the neighborhood of the stream bed tends to slow the flow. When this happens, the flow undergoes a spontaneous transition from supercritical flow to subcritical flow via a flow phenomenon known as a hydraulic jump. (The hydraulic jump is the incompressible flow equivalent of a shock wave in compressible flow of gases.) Inside the jump itself, the flow becomes highly turbulent and irreversible and is impossible to characterize in detail. However, the flow upstream and downstream of the jump is well-behaved and it is possible to analyze the conditions that prevail.

Figure 8.23 is a schematic representation of a typical hydraulic jump in a channel of width b. Figure 8.23 also shows a control volume suitable for analysis of the phenomenon.

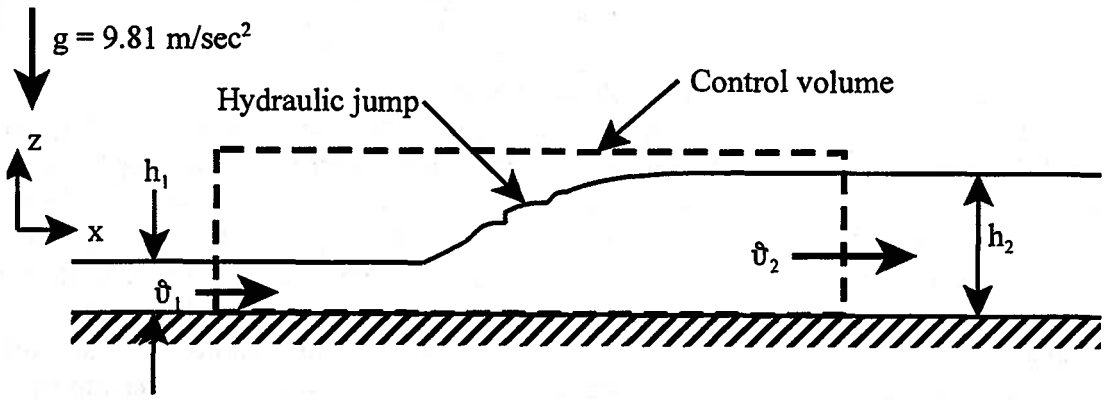

Figure 8.23 Schematic Representation of a Hydraulic Jump

Applying the continuity equation to the control volume of Figure 8.23, we get

$$\rho b h_1 \vartheta_1 = \rho b h_2 \vartheta_2 \tag{8.124}$$

Since the fluid is incompressible, equation (8.118) becomes

$$h_1 \vartheta_1 = h_2 \vartheta_2 \tag{8.125}$$

If there is no externally applied force to the control volume and we neglect the effects of viscosity, the only forces that appear in the equation of linear momentum are the forces due to normal stresses acting on the control surface and the body force due to gravity. Then the equation of linear momentum becomes

$$\cancel{\vec{F}} + \int_{CS}(-P\vec{n})dA + \cancel{\int_{CS}\vec{\tau}dA} + \int_{CV}\rho\vec{g}dV = \frac{d}{dt}\cancel{\int_{CV}\rho\vec{\vartheta}dV} + \int_{CS}\rho\vec{\vartheta}\left(\vec{\vartheta}_r\cdot\vec{n}\right)dA \tag{8.126}$$

However, the body force acts in the z-direction. Then since the control volume has only one port of entry and one exit port and the pressure is hydrostatic, we have for steady flow in the x-direction

$$\vec{i}\cdot\int_{A_1}\left(-P_1\left(-\vec{i}\right)\right)dA + \vec{i}\cdot\int_{A_2}\left(-P_2\vec{i}\right)dA = \vec{i}\cdot\int_{A_1}\rho\vartheta_1\vec{i}\left(\vartheta_1\vec{i}\cdot\left(-\vec{i}\right)\right)dA + \vec{i}\cdot\int_{A_2}\rho\vartheta_2\vec{i}\left(\vartheta_2\vec{i}\cdot\vec{i}\right)dA$$

$$P_1A_1 - P_2A_2 = -\rho\vartheta_1^2A_1 + \rho\vartheta_2^2A_2 \tag{8.127}$$

$$\frac{1}{2}\rho g b h_1^2 - \frac{1}{2}\rho g b h_2^2 = -\rho\vartheta_1^2A_1 + \rho\vartheta_2^2A_2$$

where we have made use of the fact that the pressure is hydrostatic. Combining equations (8.125) and (8.127), we get

$$(h_1 - h_2)\left[h_1 + h_2 - \frac{2\dot{V}^2}{gb^2 h_1 h_2}\right] = 0 \tag{8.128}$$

Equation (8.128) has two possibilities. One is the obvious, but uninteresting solution that the term in parentheses vanishes resulting in $h_1 = h_2$ which corresponds to no disturbance to the flow. The other is the more interesting possibility that the term in square brackets vanishes, viz.

$$h_1 + h_2 - \frac{2\dot{V}^2}{gb^2 h_1 h_2} = 0 \tag{8.129}$$

Then the ratio of the depth of flow upstream to downstream becomes

$$\frac{h_2}{h_1} = \frac{-1 + \sqrt{1 + 8\dfrac{\vartheta_1^2}{gh_1}}}{2} = \frac{1}{2}\left[\sqrt{1 + 8Fr_1^2} - 1\right] \tag{8.130}$$

where we have made use of the definition of the Froude number.

Equation (8.130) allows three possible flow conditions depending upon the magnitude of the Froude number: $Fr_1 > 1$, $Fr_1 < 1$, and $Fr_1 = 1$. Of these three possibilities, only the first, $Fr_1 > 1$, gives rise to the phenomenon known as a *hydraulic jump*. In this case, equation (8.130) predicts the depth of flow downstream of the disturbance will be greater than the depth of flow upstream as depicted in Figure 8.23. If, on the other hand, the upstream flow is subcritical with $Fr_1 < 1$, equation (8.130) predicts that the resulting disturbance will have a downstream flow with a depth less than the upstream flow. As we will show next, this condition violates the second law and, hence, is not physically possible. The case of $Fr_1 = 1$ is uninteresting since equation (8.130) predicts no disturbance with the flow remaining at the same depth.

If we apply the second law to the control volume of Figure 8.23, we obtain the following result since the flow is steady and adiabatic:

$$\frac{dS_{cv}}{dt} = \sum_j \left(\frac{\dot{Q}}{T}\right)_j + \sum_{out} (\dot{m}s)_{out} - \sum_{in} (\dot{m}s)_{in} + \dot{S}_{gen} \tag{8.131}$$

Substituting the continuity equation into equation (8.131), we get

$$\dot{S}_{gen} = \dot{m}(s_2 - s_1) = \dot{m}c \ln\left(\frac{T_2}{T_1}\right) \tag{8.132}$$

Since the rate of entropy generation must always be positive, we conclude that it must be the case that $T_2 > T_1$ otherwise we have a violation of the second law. From the first law for the control volume of Figure 8.23, we have

$$\frac{dE_{cv}}{dt} = \dot{Q} - \dot{W}_{shaft} + \sum_{in}\left[\dot{m}\left(h + \frac{\vartheta^2}{2} + gz\right)\right]_{in} - \sum_{out}\left[\dot{m}\left(h + \frac{\vartheta^2}{2} + gz\right)\right]_{out} \tag{8.133}$$

Then substituting the continuity equation into equation (8.127), we get

$$u_1 + \frac{P_1}{\rho} + \frac{\vartheta_1^2}{2} = u_2 + \frac{P_2}{\rho} + \frac{\vartheta_2^2}{2} \tag{8.134}$$

Substituting the energy constitutive relation into equation (8.134) and rearranging the result, we get

$$c(T_2 - T_1) = \frac{1}{\rho}(P_1 - P_2) + \frac{1}{2}\left(\vartheta_1^2 - \vartheta_2^2\right) \tag{8.135}$$

But

$$P_1 = \frac{1}{2}\rho g h_1 \quad \text{and} \quad P_2 = \frac{1}{2}\rho g h_2$$
$$\mathcal{V}_1^2 = \frac{\dot{V}^2}{(bh_1)^2} \quad \text{and} \quad \mathcal{V}_2^2 = \frac{\dot{V}^2}{(bh_2)^2} \tag{8.136}$$

Combining equations (8.135) and (8.136), we get

$$c(T_2 - T_1) = \frac{g}{2}(h_1 - h_2) + \frac{\dot{V}^2}{2b^2}\left(\frac{h_2^2 - h_1^2}{h_1^2 h_2^2}\right)$$
$$c(T_2 - T_1) = \left(\frac{\dot{V}^2}{2b^2}\frac{h_2^2}{h_1^2 h_2^2} - \frac{gh_2}{2}\right) - \left(\frac{\dot{V}^2}{2b^2}\frac{h_1^2}{h_1^2 h_2^2} - \frac{gh_1}{2}\right) \tag{8.137}$$

Rearranging equation (8.137), we get

$$c(T_2 - T_1) = h_2^2\left(\frac{\dot{V}^2}{2b^2}\frac{1}{h_1^2 h_2^2} - \frac{g}{2h_2}\right) - h_1^2\left(\frac{\dot{V}^2}{2b^2}\frac{1}{h_1^2 h_2^2} - \frac{g}{2h_1}\right) \tag{8.138}$$

By inspection of equation (8.138), we see that if $h_2 > h_1$, the right-hand side of the expression is positive and, hence, $T_2 > T_1$, and the second law is satisfied. However, if $h_2 < h_1$, the right-hand side of the expression is negative and, hence, $T_2 < T_1$, which constitutes a violation of the second law. Thus it follows that the only physically meaningful condition for the appearance of the hydraulic jump is if $Fr_1 > 1$.

While all hydraulic jumps satisfy equation (8.130), they vary somewhat in appearance depending upon the value of the Froude number upstream of the jump. According to Chow (Chow, V. T., *Open Channel Hydraulics*, McGraw-Hill, New York, 1959), a strong jump occurs when $Fr_1 > 9$; a steady jump occurs when $4.5 < Fr_1 < 9$; an oscillating jump occurs when $2.5 < Fr_1 < 4.5$; a weak jump occurs when $1.7 < Fr_1 < 2.5$; and an undular jump occurs when $1 < Fr_1 < 1.7$.

Example 8E.29: For the water channel flow shown in Figure 8E.29a, $h_1 = 1.5$ m, $H = 4$

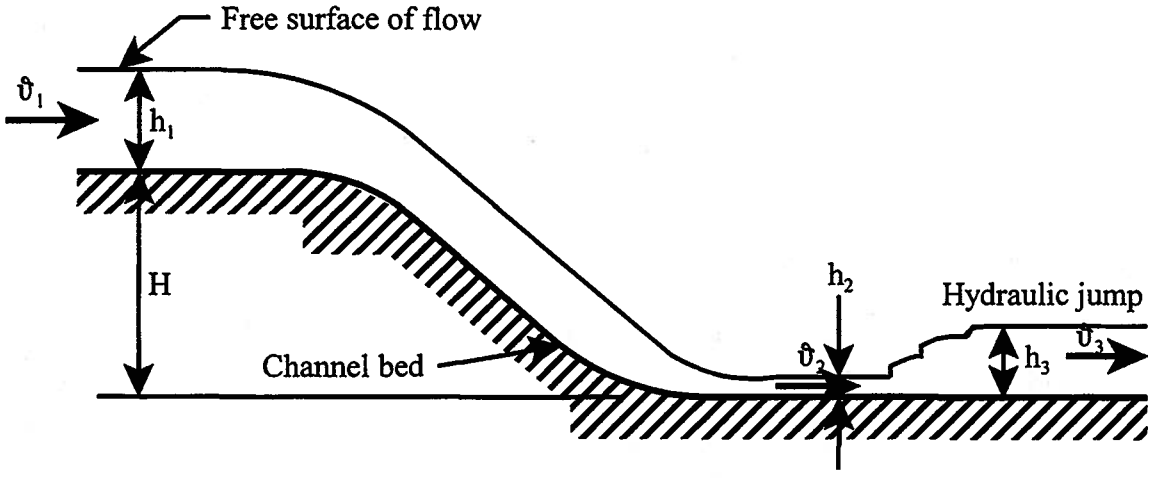

Figure 8E.29a Water Channel Flow

m, and $\mathcal{V}_1 = 3$ m/sec. Neglect the effect of viscosity and assume that the flow is uniform at each of the locations 1, 2, and 3.

(a) Calculate the downstream depth h_2 and show that *two* realistic solutions are possible.

(b) For the two physically meaningful values of h_2, calculate the velocity ϑ_2, the velocity, ϑ_{w2}, of a small disturbance on the surface of the flow, and the Froude number, Fr_2.

(c) Suppose that for the case in which $Fr_2 > 1$ a hydraulic jump occurs downstream of location 2. What would be the depth of flow h_3 and the velocity ϑ_3 downstream of the jump?

Solution: We can use the approach shown in Section 8.14.1 and calculate the specific energy of the flow relative to the channel bottom. Then

$$E_1 = \frac{\vartheta_1^2}{2g} + h_1 = \frac{(3\text{ m})^2}{2(9.81\text{ m})} + 1.5\text{ m} = 1.959\text{ m}$$

Then at location 2, we have

$$E_2 = E_1 + H = 1.959\text{ m} + 4\text{ m} = 5.959\text{m}$$

The solution is shown in graphical form in Figure 8E.29b.

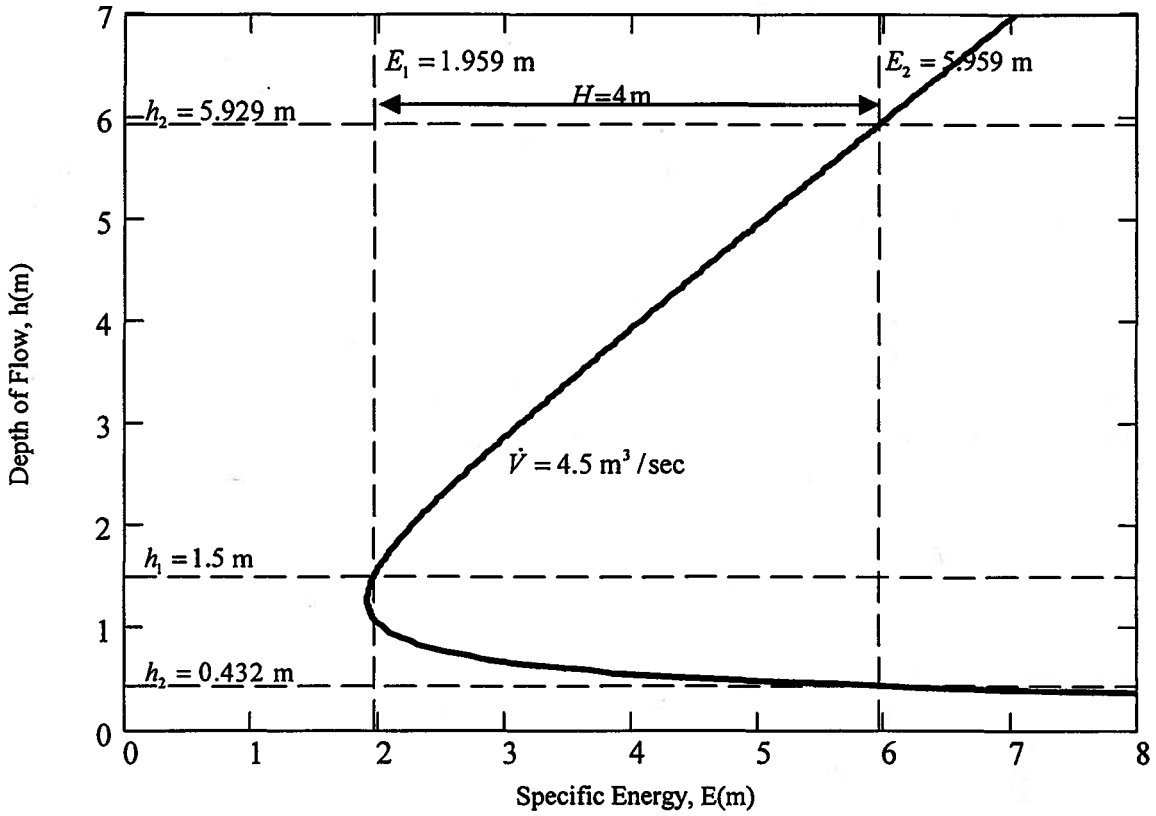

Figure 8E.29b Frictionless Flow in an Open Channel with $\dot{V} = 4.5\text{ m}^3/\text{sec}$

Alternatively, we can combine the Bernoulli equation for a streamline along the surface with the continuity equation to get

$$h_2^3 - \left(\frac{\vartheta_2^2}{2g} + h_2\right)h_2^2 - \frac{\dot{V}^2}{2g} = h_2^3 - E_2 h_2^2 - \frac{\dot{V}^2}{2g} = 0$$

$$h_2^3 - (5.959\text{ m})h_2^2 - \frac{(4.5\text{ m}^3/\text{sec})^2}{2(9.81\text{ m/sec}^2)(1\text{ m})^2} = 0$$

$$h_2^3 - (5.959\text{ m})h_2^2 - 1.032\text{ m}^3 = 0$$

This third-order polynomial has three roots: $h_2 = 5.929$ m (subcritical flow depth); $h_2 = 0.432$ m (supercritical flow depth); and $h_2 = -0.403$ m (physically meaningless).

(b) From continuity

$$\vartheta_{2sub} = \frac{\dot{V}}{h_{2sub}} = \frac{4.5\ \text{m}^3/\text{sec}}{5.929\ \text{m}} = 0.759\ \text{m/sec}$$

$$\vartheta_{2super} = \frac{\dot{V}}{h_{2super}} = \frac{4.5\ \text{m}^3/\text{sec}}{0.432\ \text{m}} = 10.417\ \text{m/sec}$$

Also

$$\vartheta_{wsub} = \sqrt{gh_{2sub}} = \sqrt{\left(9.81\ \text{m/sec}^2\right)\left(5.929\ \text{m}\right)} = 7.626\ \text{m/sec};$$

$$Fr_{2sub} = \frac{\vartheta_{2sub}}{\vartheta_{wsub}} = \frac{0.759\ \text{m/sec}}{7.626\ \text{m/sec}} = 0.100$$

$$\vartheta_{wsuper} = \sqrt{gh_{2super}} = \sqrt{\left(9.81\ \text{m/sec}^2\right)\left(0.432\ \text{m}\right)} = 2.059\ \text{m/sec};$$

$$Fr_{2super} = \frac{\vartheta_{2super}}{\vartheta_{wsuper}} = \frac{10.417\ \text{m/sec}}{2.059\ \text{m/sec}} = 5.060$$

(c) From equation (8.130), the depth of flow downstream of the subsequent hydraulic jump is

$$\frac{h_3}{h_2} = \frac{1}{2}\left[\sqrt{1+8Fr_{2super}{}^2} - 1\right] = \frac{\sqrt{1+8\left(5.060\right)^2} - 1}{2} = 6.673\ \text{m}$$

and from continuity, the velocity downstream of the hydraulic jump is

$$\vartheta_3 = \frac{\dot{V}}{h_3} = \frac{4.5\ \text{m}^3/\text{sec}}{6.673\ \text{m/sec}\left(1\ \text{m}\right)} = 0.674\ \text{m/sec}$$

Since the Froude number of the flow approaching the jump is $4.5 < Fr_{2super} < 9$, the jump is steady.

8.15 Summary of Governing Relations for a Control Volume

A general control volume is shown in Figure 8.24 and the relations that govern its behavior are summarized below:

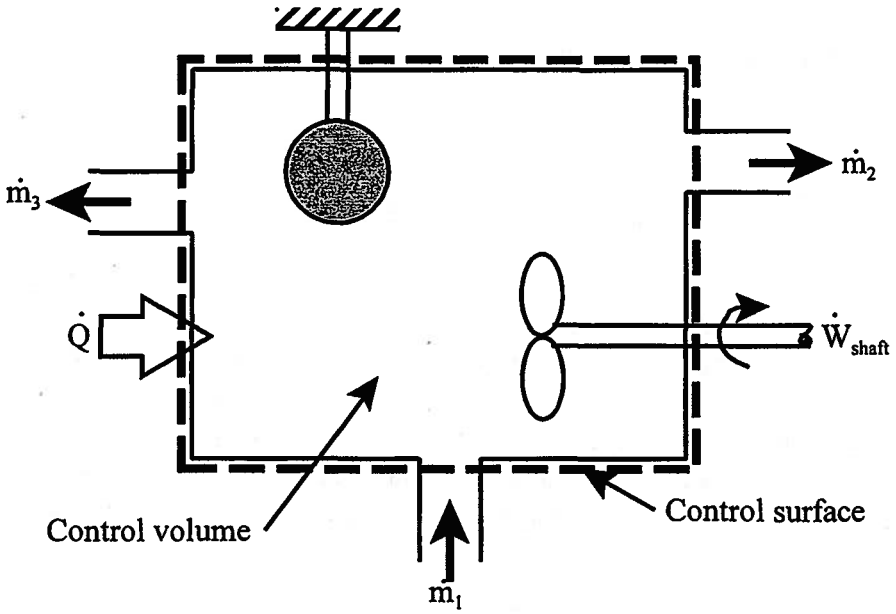

Figure 8.16 General Control Volume

Conservation of Mass (Continuity Equation):

$$\frac{d}{dt}\int_{CV}\rho\,dV=-\int_{CS}\rho\left(\vec{\vartheta}_r\cdot\vec{n}\right)dA \tag{8.13}$$

or for a finite number of entry and exit ports

$$\frac{dM_{CV}}{dt}=\sum_{in}\dot{m}_{in}-\sum_{out}\dot{m}_{out} \tag{8.7}$$

First Law of Thermodynamics:

$$\frac{d}{dt}\int_{CV}\rho\left(u+\frac{v^2}{2}+gz\right)dV=\dot{Q}-\dot{W}_{shaft}-\int_{CS}\rho\left(h+\frac{v^2}{2}+gz\right)\left(\vec{\vartheta}_r\cdot\vec{n}\right)dA \tag{8.36}$$

or for a discrete number of entry and exit ports

$$\frac{dE_{CV}}{dt}=\dot{Q}-\dot{W}_{shaft}+\sum_{in}\dot{m}_{in}\left(h+\frac{\vartheta^2}{2}+gz\right)_{in}-\sum_{out}\dot{m}_{out}\left(h+\frac{\vartheta^2}{2}+gz\right)_{out} \tag{8.37}$$

Second Law of Thermodynamics:

$$\frac{d}{dt}\int_{CV}\rho s\,dV=\sum_i\left(\frac{\dot{Q}}{T}\right)_i-\int_{CS}\rho s\left(\vec{\vartheta}_r\cdot\vec{n}\right)dA+\dot{S}_{gen} \tag{8.41}$$

or for a discrete number of entry and exit ports

$$\frac{dS_{CV}}{dt}=\sum_i\left(\frac{\dot{Q}}{T}\right)_i+\sum_{in}(\dot{m}s)_{in}-\sum_{out}(\dot{m}s)_{out}+\dot{S}_{gen} \tag{8.42}$$

Linear Momentum Equation:

$$\frac{d}{dt}\int_{CV}\rho\vec{\vartheta}dV=\int_{CS}(-P\vec{n})\,dA+\int_{CS}(\vec{\tau})\,dA+\int_{CV}\rho\vec{g}\,dV-\int_{CS}\rho\vec{\vartheta}\left(\vec{\vartheta}_r\cdot\vec{n}\right)dA \tag{8.83}$$

or for a discrete number of entry and exit ports

$$\frac{d}{dt}\int_{CV}\rho\vec{\vartheta}dV=\int_{CS}(-P\vec{n})\,dA+\int_{CS}(\vec{\tau})\,dA+\int_{CV}\rho\vec{g}\,dV-\sum_{out}\left(\dot{m}\vec{\vartheta}\right)_{out}+\sum_{in}\left(\dot{m}\vec{\vartheta}\right)_{in}$$

Angular Momentum Equation:

$$\frac{d}{dt}\left[\int_{CV}\left(\vec{r}\times\vec{\vartheta}\right)\rho dV\right]=\sum\left(\vec{r}\times\vec{F}_{surface}\right)+\int_{CV}\left(\vec{r}\times\vec{g}\right)\rho dV+\vec{T}_{shaft}-\int_{CS}\left(\vec{r}\times\vec{\vartheta}\right)\rho\left(\vec{\vartheta}_r\cdot\vec{n}\right)dA \tag{8.94}$$

or for a discrete number of entry and exit ports

$$\frac{d}{dt}\left[\int_{CV}\left(\vec{r}\times\vec{\vartheta}\right)\rho dV\right]=$$

$$=\sum\left(\vec{r}\times\vec{F}_{surface}\right)+\int_{CV}\left(\vec{r}\times\vec{g}\right)\rho dV+\vec{T}_{shaft}-\sum_{out}\dot{m}_{out}\left(\vec{r}\times\vec{\vartheta}\right)_{out}+\sum_{in}\dot{m}_{in}\left(\vec{r}\times\vec{\vartheta}\right)_{in} \tag{8.95}$$

Note that in the cases for which the flow at a port of entry or exit is modeled as one-dimensional, the properties such as velocity, temperature, energy, enthalpy, and entropy that appear in the above governing relations may , in fact, vary over the port normal to the direction of flow due to the influence of viscosity and thermal conductivity. In these cases, the values used for these properties are taken to be their "mass-averaged" values in the following sense.

Since the fluid velocity is a function of the radial location of the fluid element in the port, the mass flow rate, $\dot{m}$, is given by

$$\dot{m}=\int_0^{R_i}\rho\vartheta 2\pi r dr \tag{8.139}$$

where ρ is the local fluid density ($1/v$), ϑ is the fluid velocity at the radial location r, and R_i is the inside radius of the port. In the context of the one-dimensional flow model, the mass flow rate is given by

$$\dot{m} = (\rho\vartheta)_{ave} A_c \tag{8.140}$$

where the cross-sectional area is $A_c = \pi R_i^2$ and $(\rho\vartheta)_{ave}$ is the average value of the fluid velocity and the density over the cross-section of the port obtained by equating the equations (8.139) and (8.140).

$$(\rho\vartheta)_{ave} = \frac{\int_0^{R_i} \rho\vartheta 2\pi r dr}{\pi R_i^2} \tag{8.141}$$

Note that if the fluid can be modeled as incompressible, we can determine the average value of the fluid velocity, ϑ_{ave}, from equation (8.141).

$$\vartheta_{ave} = \frac{\int_0^{R_i} \rho\vartheta 2\pi r dr}{\rho\pi R_i^2}$$

In a similar manner, we can define other mass-averaged or "bulk" properties appropriate to the one-dimensional "bulk" flow model:

$$h_b = \frac{\int_0^{R_i} \rho\vartheta h 2\pi r dr}{\dot{m}} \tag{8.142}$$

$$T_b = \frac{\int_0^{R_i} \rho\vartheta T 2\pi r dr}{\dot{m}}$$

$$s_{ave} = \frac{\int_0^{R_i} \rho\vartheta s 2\pi r dr}{\dot{m}} \tag{8.143}$$

PROBLEMS

8.1 As shown in Figure 8P.1, rain is falling vertically at a steady mass *flux* of $\dot{m}'' = 6 \times 10^{-3}$ kg/m^2 sec. Each rain drop has a density $\rho_w = 1000$ kg/m^3 and falls at a velocity of $\hat{v} = 30$ m/sec. Model the human body of a person as a rectangular parallelepiped $H = 1.75$ m, $W = 0.75$ m, and $t = 0.25$ m. The person is walking at a speed of $\hat{v}_{walk} = 2$ m/sec.

(a) Estimate the mass density ρ_{rain} (kg water/m^3 air) of raindrops in air.

(b) Estimate the number density n_{drops} (number of raindrops/m^3 air) of raindrops in air.

(c) Estimate the mass of rain that strikes the person on the top plane per unit time (kg water/sec).

(d) Estimate the mass of rain striking the person from the front per unit time (kg water/sec).

(e) Estimate the total rate at which the person gets wet (kg water/sec).

(f) If the person is carrying an umbrella that can be used to cover his/her top or front, how should he/she use it to minimize "wetness" for the walking speed given?

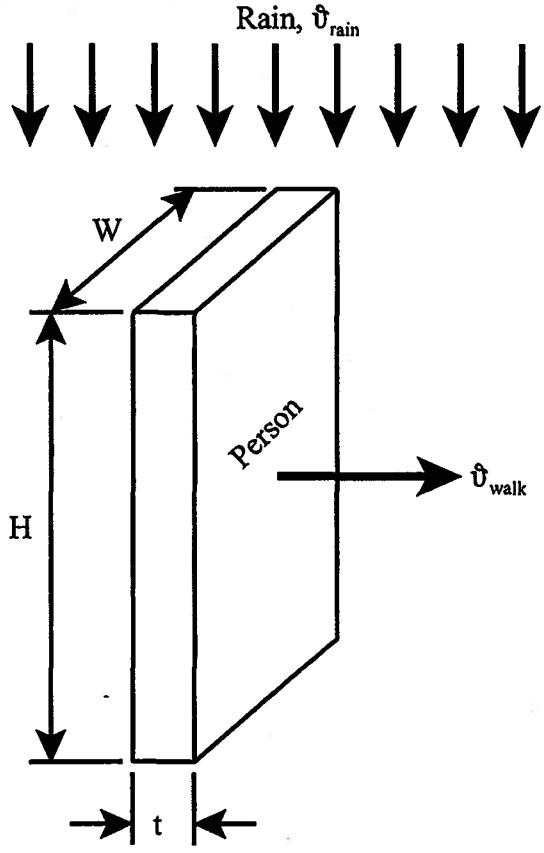

Figure 8P.1

8.2 Some centrifugal pumps are fitted with radial diffusers that are used decelerate the flow being discharged from the rotating impeller. As the flow decelerates, its local static pressure increases thereby increasing the overall pressure ratio of the pump/diffuser combination. In a typical design, the diffuser consists of two parallel plates separated by guide vanes that guide the flow as it is discharged outwards from the rotating impeller as shown in Figure 8P.2. In the ideal steady-flow diffuser, the flow is reversible and adiabatic. For the purposes of this analysis, model the fluid as inviscid and incompressible. At the inlet to the diffuser, $r = R_1$ and the total velocity of the fluid is $\hat{v}_1$ oriented at an angle α_1 to the radial direction.

(a) Obtain an expression for the radial velocity component of the fluid in the diffuser $\hat{v}_r$ at any radius r.

(b) From the equation of angular momentum for a suitable control volume for the diffuser, show that the tangential velocity component of the fluid in the diffuser varies as ($\hat{v}_\theta \cdot r$) = constant.

(c) Use the results of parts (a) and (b) above to estimate the pressure of the fluid at any radial location r.

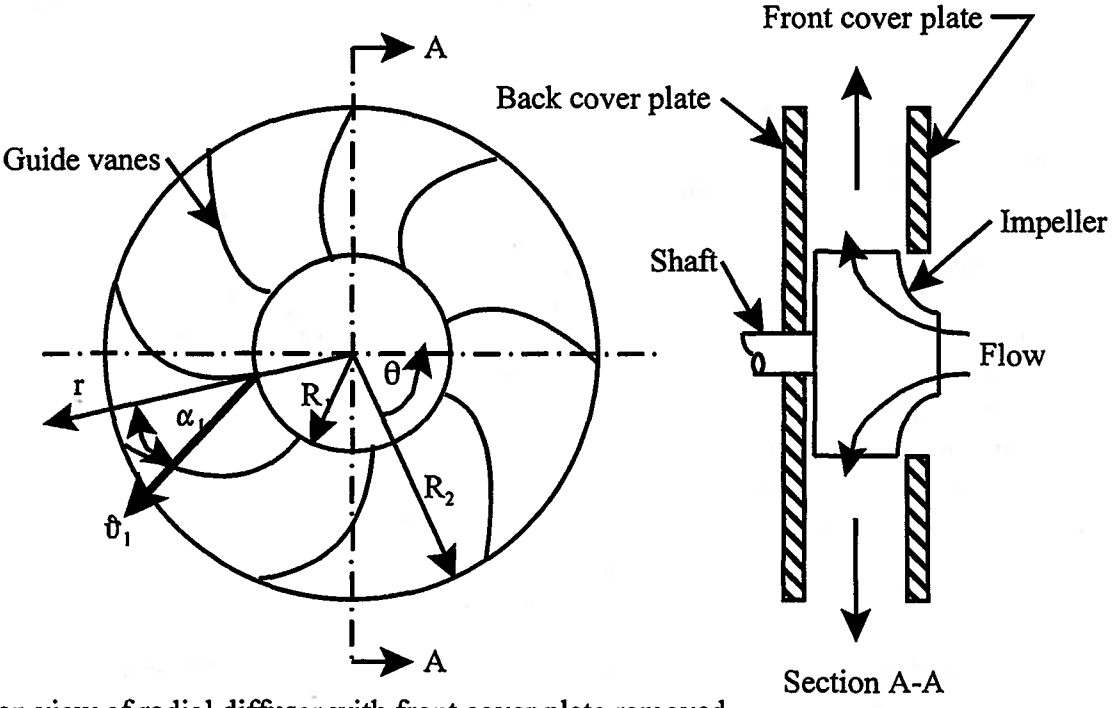

Plan view of radial diffuser with front cover plate removed

Figure 8P.2

8.3 A basic turbojet engine used for aircraft propulsion consists of four components: a compressor to compress the working fluid (air) to high pressure; a combustor to increase the temperature of the working fluid; a turbine to drive the compressor; and a nozzle to provide the thrust that actually propels the aircraft. These engines are tested under steady-flow conditions at sea level in a static test fixture (shown schematically in Figure 8P.3).

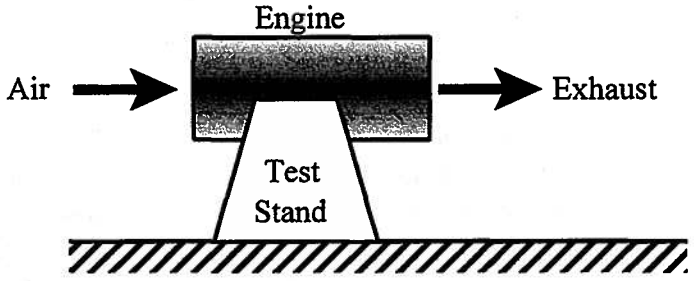

Figure 8P.3

(a) In a static test of a particular engine used in military aircraft, the propulsive gas enters the nozzle section at a pressure of $P_4 = 1.918 \times 10^5$ N/m^2, a temperature of $T_4 = 1117$ K, and zero velocity. The gas expands through the nozzle in a reversible and adiabatic manner to atmospheric

pressure $P_{exit} = P_{atm} = 1.0135 \times 10^5$ N/m^2. The diameter of the nozzle exit is $D_e = 0.506$ m. The working fluid in the engine is air which can be modeled as an ideal gas with $R = 287$ J/kg K and $c_P = 1003$ J/kg K.

Show that the velocity of the gas at the nozzle exit is equal to the local sonic velocity and calculate the force exerted on the engine by the test stand during the test.

(b) In an application of this engine design, an aircraft uses **two** of these engines. The aircraft is flying at a constant speed of 246 m/sec at an altitude of 11 km where the prevailing conditions in the atmosphere are $P_1 = 22.633 \times 10^3$ N/m^2 and $T_1 = 216.65$ K. The inlet diameter of the engine is $D_i = 0.685$ m. The pressure at inlet to the nozzle section is $P_4 = 2.057 \times 10^5$ N/m^2 and the temperature is $T_4 = 1318$ K. The expansion of the gas in the nozzle is still reversible and adiabatic to the prevailing atmospheric pressure, $P_1 = 22.633 \times 10^3$ N/m^2. Note that in this case, the velocity of the gas at exit from the nozzle is not necessarily sonic.

Estimate the drag force acting on the aircraft.

8.4 As shown in Figure 8P.4, air at a pressure of $P_1 = 2 \times 10^5$ N/m^2 and a temperature of $T_1 = 300$ K enters a circular duct of diameter $D = 25$ mm through a well-rounded inlet with uniform speed $\vartheta_1 = 0.870$ m/sec. Due to the action of viscosity, the fluid in the neighborhood of the wall is slowed; however, continuity requires the mass flow rate to be constant. Thus, the fluid near the axis of the duct must speed up to compensate. After a distance on the order of 100 diameters from the entrance, the velocity profile achieves its fully developed configuration and then remains unchanged from then on. For the case at hand, the fully developed velocity profile is attained 2.25 m downstream from the entrance and is given by

$$\frac{\vartheta(r)}{\vartheta_{r=0}} = 1 - \left(\frac{r}{r_{wall}}\right)^2$$

The pressure drop between sections 1 and 2 is $P_1 - P_2 = 1.92$ N/m^2. Find the total force of friction exerted by the tube on the air.

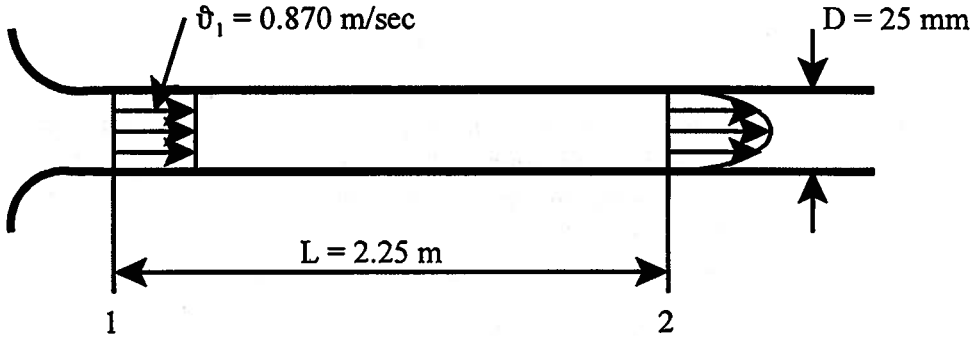

Figure 8P.4

8.5 An internal combustion engine is basically a piston-cylinder apparatus that displaces a fixed amount of air which is drawn into the cylinder each time the piston moves downward during the intake stroke. During the intake stroke, the intake valve opens and allows a fuel-air mixture to pass into the cylinder. The engine produces power by oxidizing fuel in the combustion chamber. The amount of fuel that can be oxidized in this manner is determined the stoichiometry of the fuel. That is, the composition of the fuel (number of carbon atoms, number of hydrogen atoms, etc.) determines how much fuel will react with the air drawn into the engine during the intake stroke of the piston. This process is described in terms of the fuel-air ratio, FA, where

$$FA = \frac{\dot{m}_{fuel}}{\dot{m}_{air}}$$

For example, for gasoline fuel, $FA = 0.0668$.

On many internal combustion engines, a device called a carburetor is used to meter the appropriate amount of fuel and mix it with the incoming air for subsequent oxidation. The carburetor contains a flow passage called a "venturi" that serves two purposes. It meters the amount of air being drawn into the engine and it accelerates the flow locally producing a local region of low pressure that is used to aspirate (siphon) the fuel from a nearby reservoir. The fuel reservoir is itself fitted with a small nozzle called a "metering jet" through which the correct amount of fuel must pass prior to being mixed with the air. Since $\dot{m}_{fuel} << \dot{m}_{air}$, its effect on the mass flow rate at the throat of the venturi can be neglected.

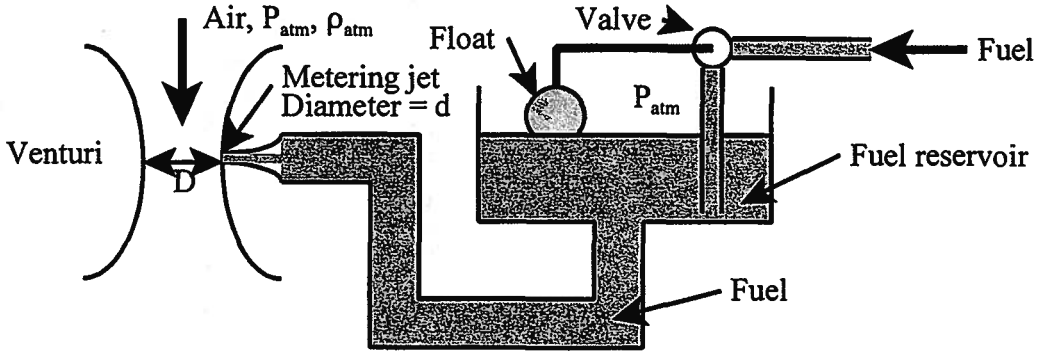

Figure 8P.5

As shown in Figure 8P.5, the venturi has a diameter D and the fuel metering jet has a diameter d. The air is drawn from the atmosphere where the pressure is P_{atm} and the density is ρ_{atm}. The density of the fuel is ρ_{fuel} and the fuel reservoir is vented to the atmosphere so that the pressure of the atmosphere acts on the free surface of the fuel. The metering jet is located at the level of the free surface of the fuel. The fuel level is maintained constant by means of a float operated valve connected to the fuel supply. The air and the fuel can be modeled as incompressible fluids, and the venturi and the fuel metering jet are precision machined so that friction losses in the flow can be ignored.

(a) Derive an expression for the air pressure, P_{min}, at the minimum cross-sectional area of the venturi in terms of P_{atm}, D, ρ_{atm}, and $\dot{m}_{air}$.

(b) Derive an expression for the mass flow rate of the fuel, $\dot{m}_{fuel}$, in terms of P_{atm}, P_{min}, d, and ρ_{fuel}.

(c) Derive an expression for the ratio d/D for a given value of FA.

8.6 As shown in Figure 8P.6, a fireplace with cross-sectional area A_f is fitted with a tall chimney of length L and cross-sectional area A_c, ($A_f = A_c = A$). By virtue of the suction created by the fire and the chimney, cold air of density ρ_c flows into the fireplace at location 1. The pressure of the air entering the fireplace is P_{atm}. The pressure of the air outside the chimney is hydrostatic. Air heated by the fire leaves the fireplace with density ρ_h at location 2. Since the mass flow rate of air required to support the combustion of wood in the fireplace is so much larger than the mass flow rate of wood, the combustion process can be modeled as a simple heat transfer from the environment to the air passing through the fireplace. As a first estimate of the fluid dynamics of this thermal-fluid system, the flow can be modeled as steady, incompressible, and inviscid.

(a) Estimate the pressure of the air at the exit of the chimney, location 3.

(b) Derive an expression for the velocity of the air at the entrance to the chimney, location 2, in terms of the densities ρ_c and ρ_h, the chimney height L, and the acceleration of gravity g.

(c) Based upon the answer to part (b) above, explain why the fireplace does not "draw" well unless the process is started by heating the air at the entrance to the chimney.

(d) Estimate the mass flow rate of air into the chimney.

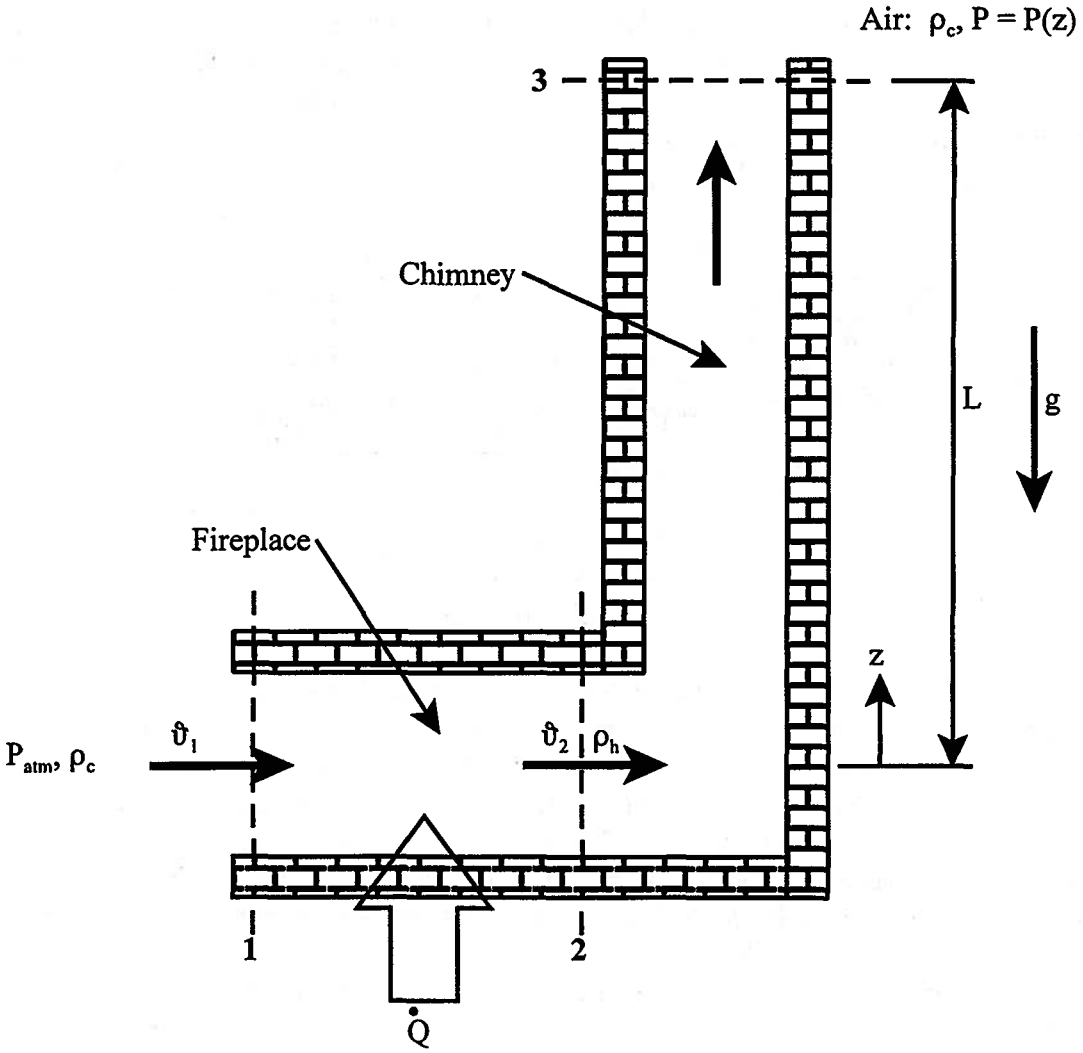

Figure 8P.6

8.7 A rigid, uninsulated vessel with a volume of $V_{vessel} = 2\ m^3$ is fitted with a valve. The valve is initially closed, and in the initial state, the vessel is empty with an initial pressure of 0. The valve is opened and the vessel is allowed to fill with air from the atmosphere. The conditions in the atmosphere are $P_{atm} = 10^5\ N/m^2$ and $T_{atm} = 300\ K$.

Since the characteristic time to establish mechanical equilibrium is so much shorter than the characteristic time required to establish thermal equilibrium, the filling process can be modeled as occurring in two steps. In the first step, the atmospheric air rushes into the vessel in an adiabatic manner until mechanical equilibrium is established between contents of the vessel and the atmosphere. At this time, the pressure of the air inside the vessel is P_{atm} but the temperature is not T_{atm} since the air inside the vessel has not yet reached thermal equilibrium with the walls of the vessel and the outside atmosphere. If the valve remains open at this time, the mass of air inside the vessel will change as the contents of the vessel are allowed to come to

thermal equilibrium with the walls of the vessel and the atmosphere. In this final equilibrium state, the contents of the vessel are at a pressure of P_{atm} and a temperature of T_{atm}.

(a) Estimate the temperature T_1 of the contents of the vessel at the end of the first step of the process when mechanical equilibrium is established but not thermal equilibrium.

(b) Estimate the mass of atmospheric air m_1 inside the vessel at the end of this first step.

(c) Estimate the mass of air m_2 inside the vessel at the end of the second step.

(d) Estimate the heat transfer across the walls of the vessel for the entire process consisting of the two steps.

(e) Estimate the entropy generated in this process of filling the vessel until the final state of thermal and mechanical equilibrium is reached.

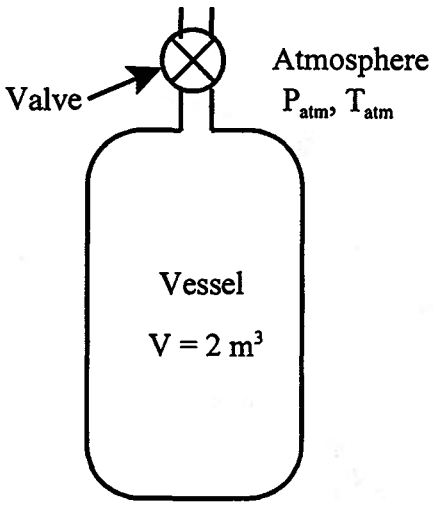

Figure 8P.7

8.8 As shown in the Figure 8P.8, a hopper dumps sand on to a moving belt at the rate of 65/kg/sec. The belt carries the sand a short distance and then drops it off the end of the belt and into a waiting truck. The drive wheels are 80 cm in diameter and rotate clockwise at 150 rev/min. Neglecting friction and air drag, estimate the power required to drive the belt.

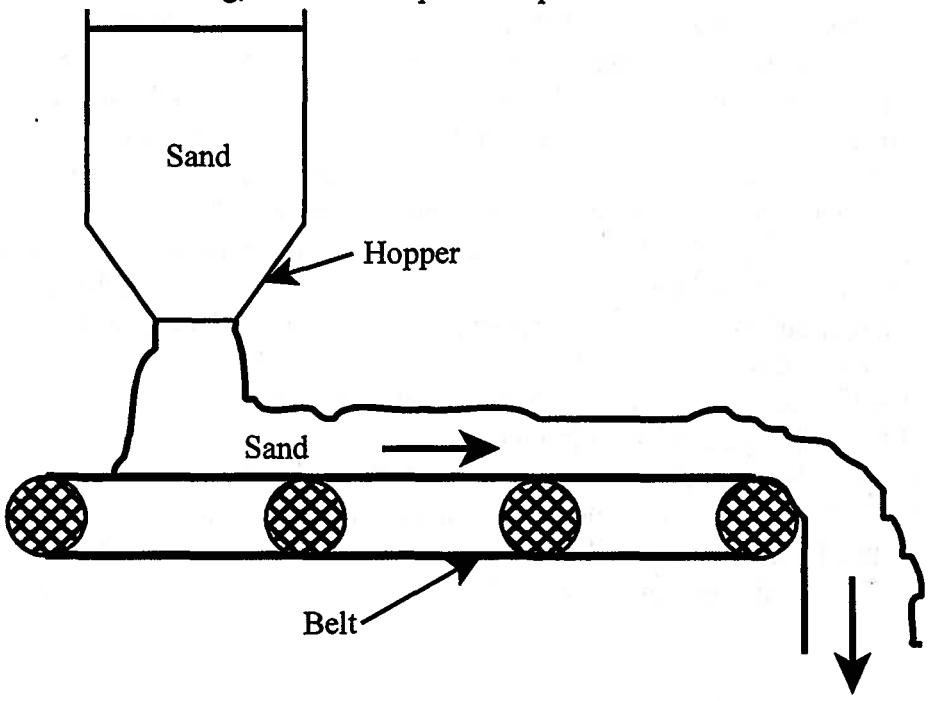

Figure 8P.8

8.9 Figure 8P.9 shows a typical application of a Venturi flow meter with an "as cast" convergent section. The pipe upstream of the Venturi meter has a diameter $D = 0.3$ m. The throat diameter of the meter is $d = 0.12$ m. The pressure drop between the upstream pipe and the throat of the meter is measured with the aid of a mercury-filled manometer. The density of mercury in the manometer is $\rho_{Hg} = 13{,}550$ kg/m^3 and that of the water is $\rho_w = 1000$ kg/m^3.

(a) Determine the mass flow rate (kg/sec) of water in the pipe.

(b) What is the difference in temperature of the water between location 1 and location 3 if $P_1 - P_3 = 0.19(P_1 - P_2)$ due to viscous losses and irreversible under-recovery of pressure in the diffuser section? Note that $c_w = 4181$ J/kg K.

(c) What is the rate of entropy generation in this meter if $T_1 = 293$ K?

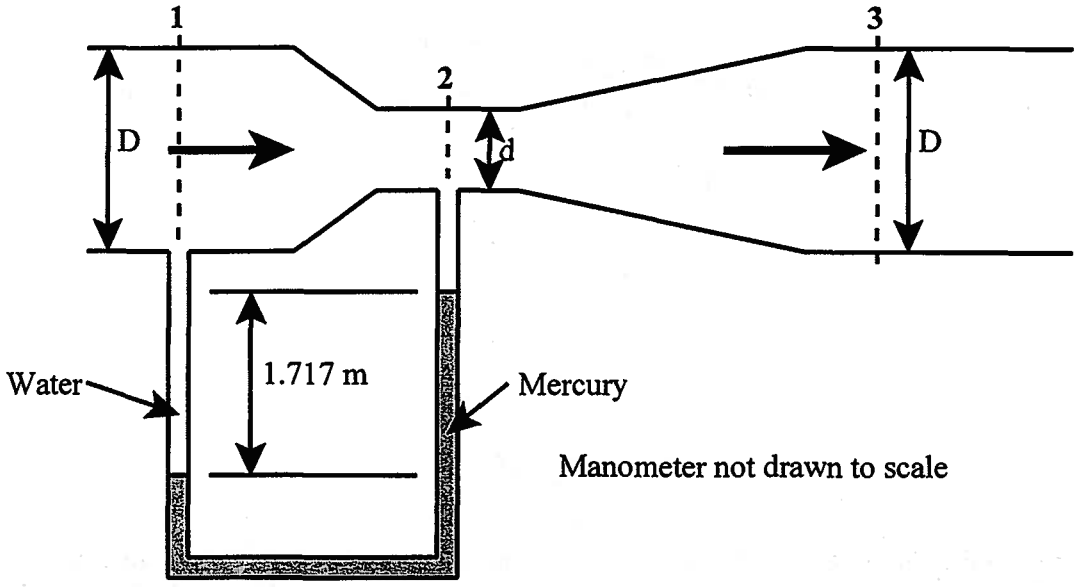

Figure 8P.9

8.10 An attempt is to be made to establish a new world record speed for a boat. The current world record speed is 317.60 mph (141.98 m/sec). The attempt is to set the new record at a speed of 145 m/sec on a day when the ambient air temperature is $T_{atm} = 295$ K. The boat design calls for a hydroplane design to be powered by the thrust from the exhaust nozzle of a jet engine as shown in Figure 8P.6. The nozzle is designed to operate with an inlet temperature of $T_{in} = 591.849$ K and an inlet pressure of $P_{in} = 1.918 \times 10^5$ N/m^2. The velocity of the gas at inlet to the nozzle is essentially zero. The gas expands through the nozzle in a reversible, adiabatic manner with an exit pressure of $P_{exit} = P_{atm} = 1.0135 \times 10^5$ N/m^2. The diameter of the nozzle in the exit plane is $D_e = 0.506$ m. The working fluid can be modeled as an ideal gas with $R = 287$ J/kg K and $c_P = 1003$ J/kg K. As the propulsion engineer, you are required to specify for the hull designer the maximum allowable drag force at this speed.

(a) What is the velocity of the exhaust jet relative to the boat?

(b) What is the speed of sound in the jet?

(c) What is the mass flow rate of air through the engine?

(d) What is the area of the inlet to the engine (not the nozzle)?

(e) With a boat equipped with this engine, what is the maximum allowable drag on the boat at the world record speed of 145 m/sec?

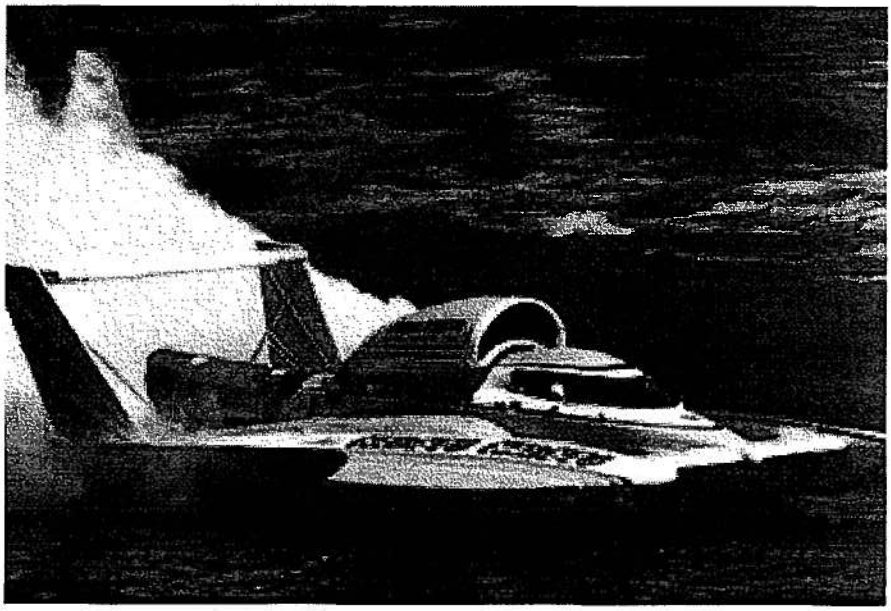

Figure 8P.10

8.11 As shown in Figure 8P.11, a jet ski draws water from the underside of the hull through a 25 cm diameter intake and exhausts water through a 10 cm diameter nozzle in the stern of the jet ski. The volume flow rate of water through the jet ski at full power is 0.088 m^3/s. The density of water is 1000 kg/m^3.

(a) The jet ski is tied to a dock and run at full speed. What is the total tensile force in the tethering line?

(b) The jet ski has a maximum speed of 8 m/s, what is the drag force on the hull at this speed?

(c) If the drag force on the hull could be reduced to zero (an impossibility), what is the maximum speed of the jet ski?

(d) Explain why the force values in parts (a) and (b) are different.

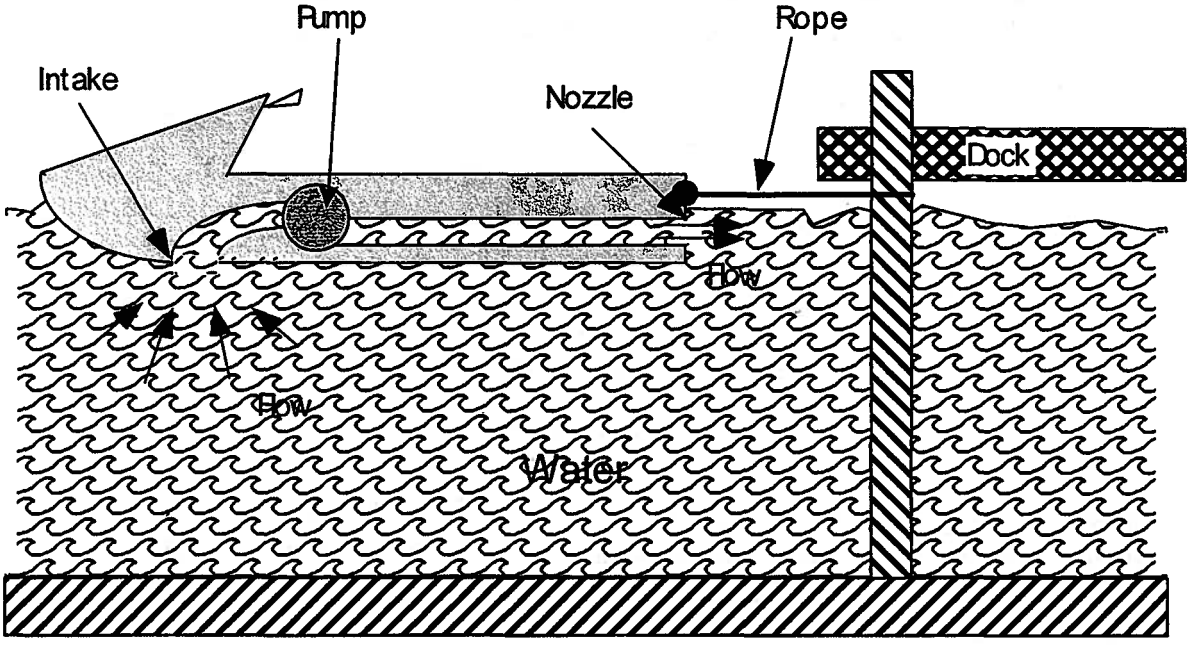

Figure 8P.11

8.12 In a particular application of an orifice plate flow meter with corner pressure taps, water flows at a volumetric flow rate of $\forall = 0.03$ m^3/sec with a density of $\rho = 1000$ kg/m^3 and a viscosity of $\mu = 11 \times 10^{-4}$ kg/m sec. The pipe diameter is $D = 10$ cm and the orifice diameter is $d = 6$ cm.

(a) Estimate the pressure drop $P_{in} - P_{out}$.

(b) Estimate the force on the orifice plate due to the flow assuming that wall friction can be neglected compared with the pressure drop due to the orifice plate.

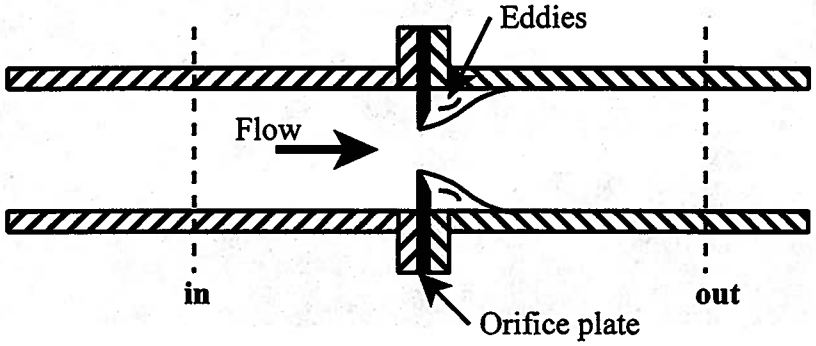

Figure 8P.12

8.13 Air at a pressure of $P_{atm} = 10^5$ N/m^2 and a temperature of $T_{atm} = 300$ K flows along a flat plate whose dimensions are length L and width b. The undisturbed velocity of the air upstream of the leading edge of the plate is $\vartheta_0 = 10$ m/sec. As a result of the action of the viscosity of the air, the air in the neighborhood of the plate is slowed and a boundary layer develops and grows in thickness downstream of the leading edge. At $L = 145$ mm downstream from the leading edge of the plate the boundary layer thickness is $\delta = 2.3$ mm. The velocity profile in the boundary layer at this location is

$$\frac{\vartheta}{\vartheta_0} = \frac{3}{2}\frac{y}{\delta} - \frac{1}{2}\left(\frac{y}{\delta}\right)^2$$

where y is measured normal to the plate. Determine the x-component (horizontal) force per unit of width required to hold the plate stationary if the air can be modeled as incompressible. Note: Only the upper face of the flat plate is exposed to the air flow.

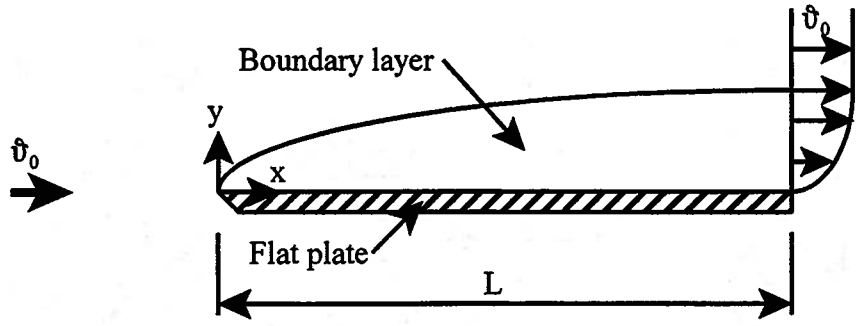

Figure 8P.13

8.14 As shown in Figure 8P.14, a stream of incompressible liquid of density ρ moving at low velocity leaves a nozzle pointed directly upward. Model the flow such that the velocity at any cross-section is uniform and that viscous effects are negligible. The velocity of the jet and the area of the jet at the nozzle exit are ϑ_0 and A_0, respectively.

(a) Derive expressions for the dependence of the jet velocity ϑ and jet area A on the distance z from the nozzle exit.

(b) Estimate the vertical distance required to reduce the jet velocity to zero.

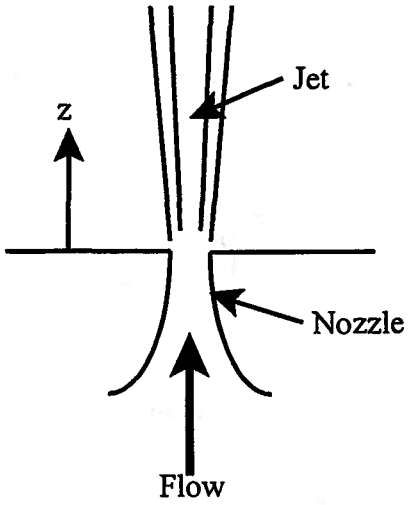

Figure 8P.14

8.15 As shown in Figure 8P.15, water discharges through a well-rounded frictionless orifice under the action of a *constant* head h_1. The jet impinges on a large flat plate that covers the orifice of a second tank in which the water level stands at a height h_2 above the orifice. The areas of the two orifices are identical. Determine the ratio of h_2/h_1 such that the force exerted on the plate by the jet is just sufficient to balance the hydrostatic force on the plate. Assume that the friction force in the vertical direction is sufficient to balance the body force on the plate due to gravity.

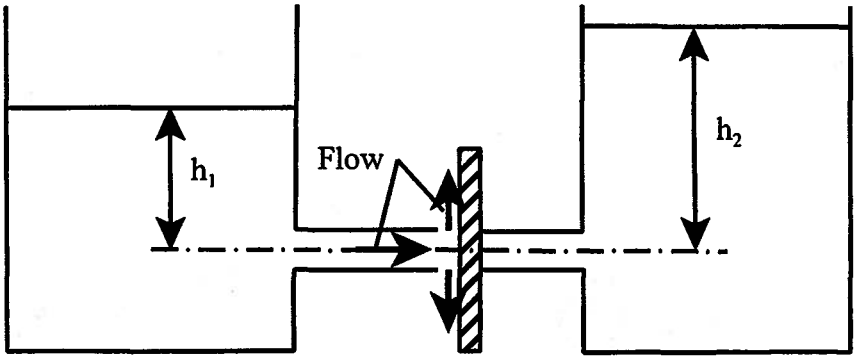

Figure 8P.15

8.16 As shown in Figure 8P.16, two circular disks of radius R are separated by a distance h. The upper disk moves toward the lower disk at constant speed ϑ_0. The space between the two disks is filled with a fluid that can be modeled as inviscid and incompressible fluid with a density ρ that is squeezed out as the disks come together. Assume that at any radial section the velocity is uniform across the gap width h. Note that h is a function of time t. The pressure surrounding the disks is atmospheric. Determine the gage pressure in the fluid at the center of the disks once the advancing fluid front has reached the edge of the disks.

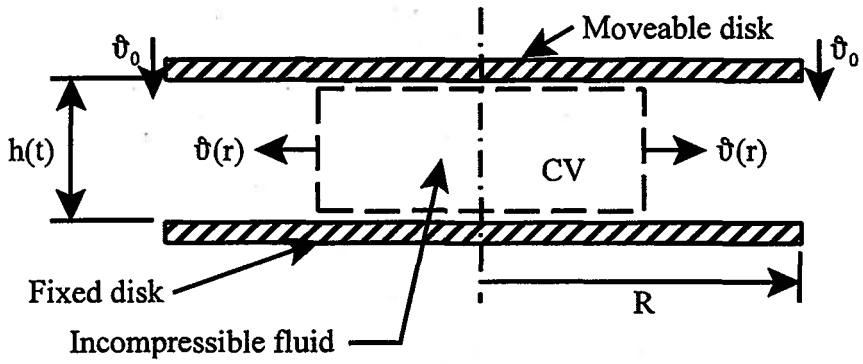

Figure 8P.16

8.17 Figure 8P.17 shows a simplified design of a fuel injector nozzle for an automotive engine. The piston is driven by a solenoid magnet that is switched on for a period of time prescribed by the engine computer. The motion of the piston produces a jet of fuel that is injected into the air stream at atmospheric pressure, $P_{atm} = 10^5$ N/m^2. The gage pressure at location 1 is governed by the delivery pressure of the fuel pump which in this case is 340 x 10^3 N/m^2. The piston diameter is 1 cm and the delivery port has a diameter of 1 mm. In a particular application, at the given engine speed, the fuel requirement is 5.13 x 10^{-5} kg. Assume that the fuel can be modeled as an incompressible liquid with a density of 680 kg/m^3.

(a) Determine the length of time the solenoid must be switched on to meet the fuel requirement.

(b) Determine the force that must be applied by the magnet to the piston for constant velocity fuel delivery.

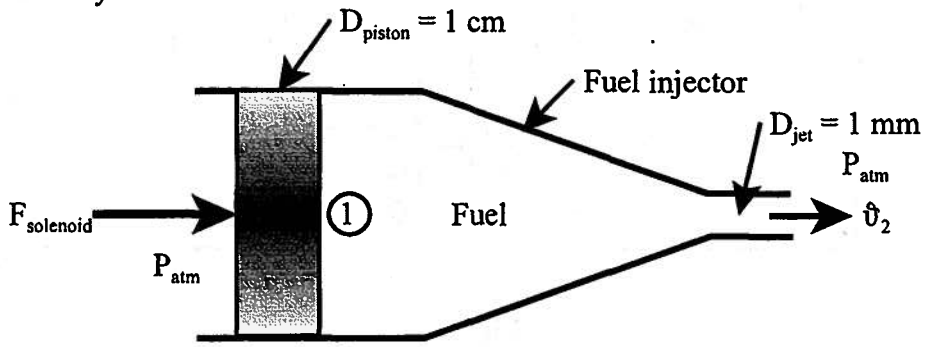

Figure 8P.17

8.18 As shown in Figure 8P.14, air at 300 K is flowing through a duct. The manometer fluid is Meriam red oil ($\rho_{oil} = 0.827\rho_{water}$) and $P_1 = 1.7$ x 10^5 N/m^2. Estimate P_2, $\vec{v}_2$, and $\dot{m}$.

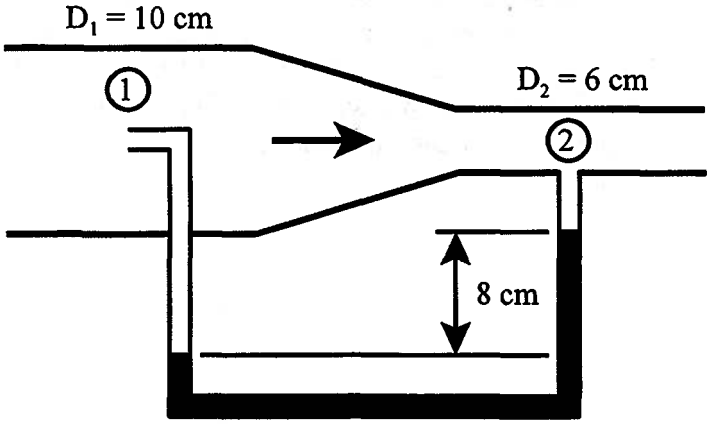

Figure 8P.18

8.19 Figure 8P.19 shows a series of turning vanes struck by a continuous jet of water that leaves a nozzle with a diameter of 50 mm at a velocity of $\vec{v} = 86.6$ m/sec. The vanes move with constant speed $U = 50$ m/sec. All of the mass flow that leaves the jet passes over the vanes. The entry angle of the vanes is $\theta_1 = 30°$ and the exit angle is $\theta_2 = 45°$as shown.

(a) Determine the nozzle angle, α, that will ensure that the jet enters tangent to the leading edge of each vane.

(b) Calculate the force that must be applied to the vanes so that the speed of the vanes remains constant.

(c) The nozzle is supplied from a water reservoir whose free surface is a constant height, h, above the centerline of the nozzle. What is the value of h that will guarantee that the jet velocity will be the value specified above?

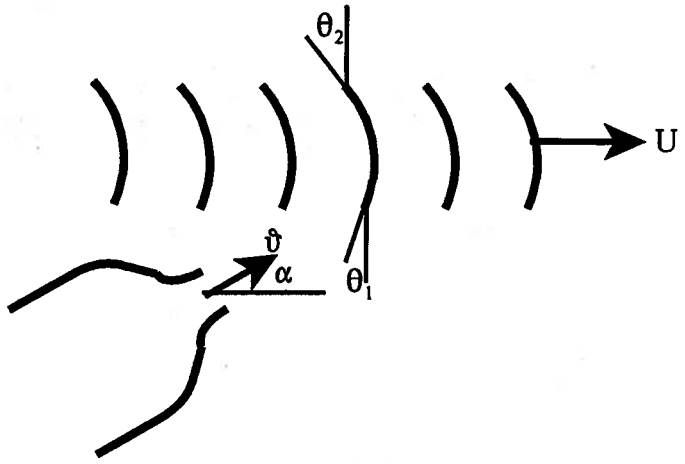

Figure 8P.19

8.20 As shown in Figure 8P.20, a channel contains a stratified, steady flow in which two immiscible, incompressible fluids A and B are flowing from a region of large cross-sectional area, location 1, to a region of reduced cross-sectional area, location 2. The density of stream A is $\rho_A = 2 \times 10^3$ kg/m^3 while that of stream B is $\rho_B = 1 \times 10^3$ kg/m^3. Stream B flows on top of stream A and the velocity of stream A increases from $\vec{v}_{1A} = 1$ m/sec to $\vec{v}_{2A} = 2$ m/sec as it flows from location 1 to location 2. The pressure normal to the direction of flow is uniform at the two locations. Gravitational effects and frictional effects are negligible.

(a) Determine the velocity of stream B at location 2 if its velocity at location 1 is $\vec{v}_{1B} = 1$ m/sec.

(b) Determine the dimension of the channel at location 2 normal to the direction of flow.

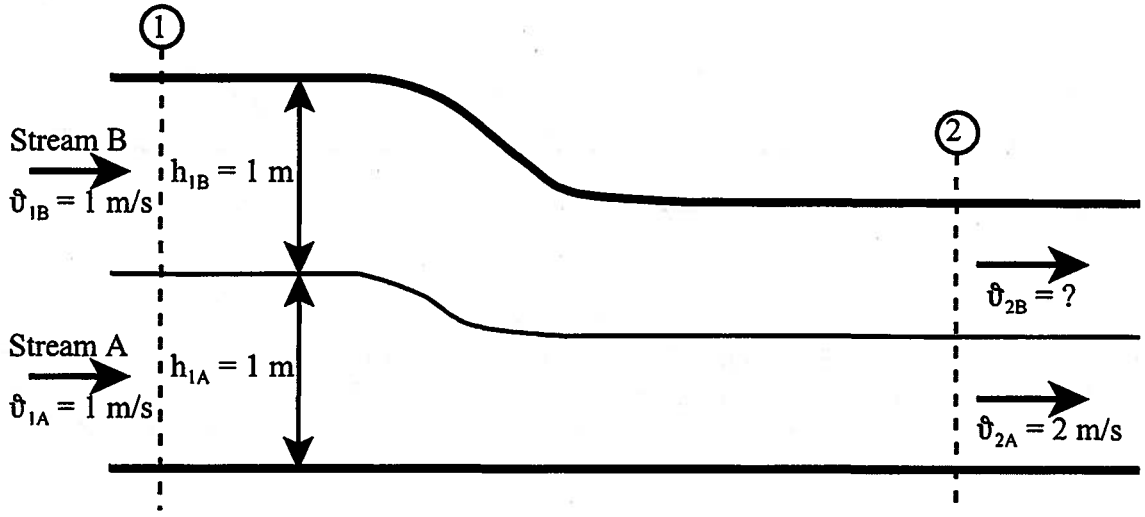

Figure 8P.20

8.21 As shown in Figure 8P.21, a jet of water (A_{jet} = 0.05 m^2) issues from a nozzle with a horizontal velocity of 15 m/sec and strikes a vane mounted on a cart. The vane turns the jet through an angle of θ = 50°. The cart is held stationary by means of a mass attached to one end of a cable whose other end is attached to the cart. The cable passes over a frictionless pulley, and the cart rides on frictionless wheels. Determine the mass, M, necessary to hold the cart in position.

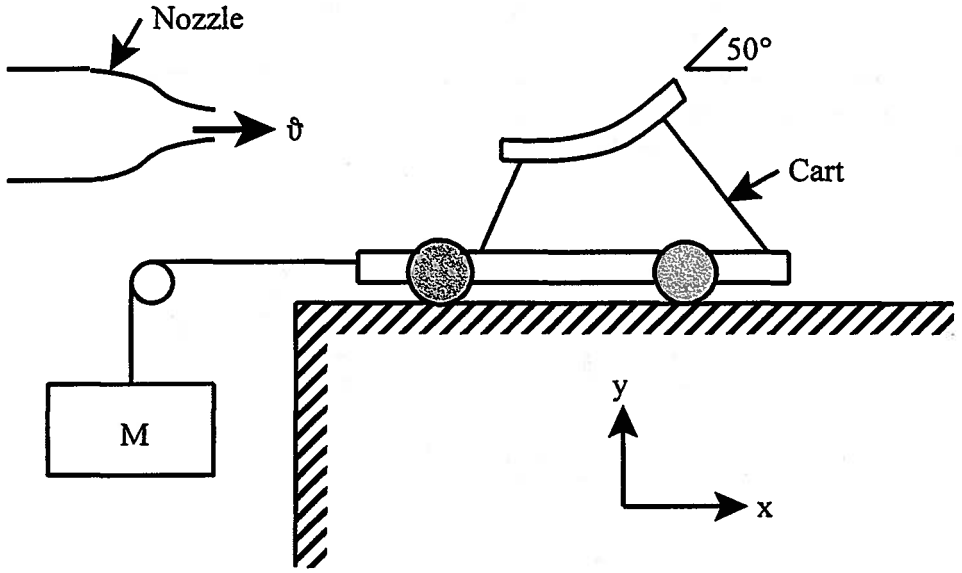

Figure 8P.21

8.22 As shown in Figure 8P.22, a long pipe is connected to a large reservoir initially filled with water to a depth of h = 6 m. The pipe has a diameter of D = 10 cm and a length of L = 10 m and is fitted with a cap at its terminus. The cap is removed and the water in the pipe begins to move. We wish to estimate the time required for the flow velocity to reach its steady value. As a first estimate, neglect the effects of viscosity in the flow.

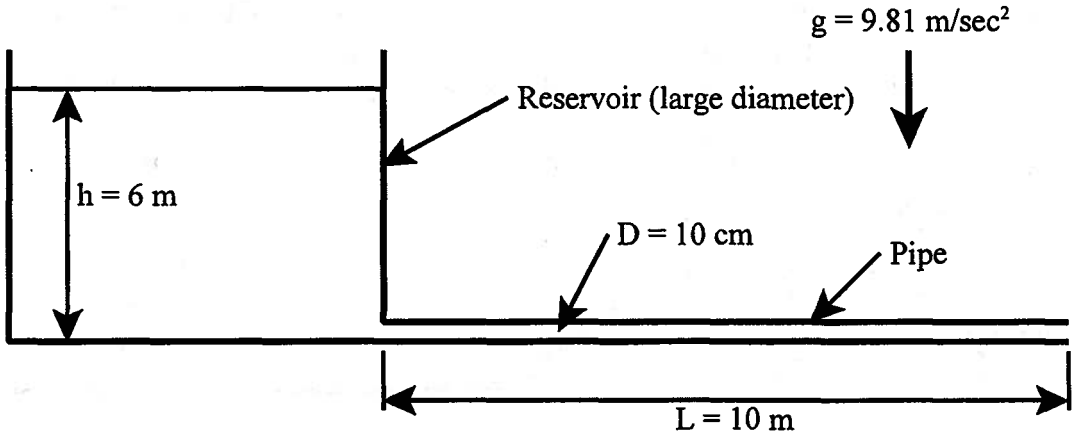

Figure 8P.22

8.23 As shown in Figure 8P.23, a jet of water of density $\rho = 10^3$ kg/m^3 and diameter D = 75 mm is discharged vertically upward from a nozzle. The velocity of the water in the jet, v_0, is uniform across the diameter of the jet as it leaves the nozzle. The jet impinges on the underside of a hori-

zontal disk of mass $M = 30$ kg and supports it in an equilibrium position at a height $h_0 = 3.5$ m above the nozzle exit. The disk is assumed to be stable in the horizontal plane and free to move in the vertical plane.

(a) With the disk in place, what is the volume flow rate of water $\dot{V}$ (m^3/sec) necessary to support the disk at the equilibrium height of h_0?

(b) If the disk is removed, what is the maximum height, h_{max}, that the discharge from the nozzle can reach?

(c) If the disk is dropped onto the jet from a large height $H > h_{max}$, sketch the vertical position $h(t)$ as a function of time t as the disk comes to the final equilibrium position h_0? Explain the shape of this curve in terms of the energy of the disk and the forces that act on it at any position $h(t)$. What determines the length of time required for the disk to reach the final equilibrium state?

(d) If the uniform velocity of the jet is 10 m/sec, what is the maximum mass M_{max} of a disk that the jet can support?

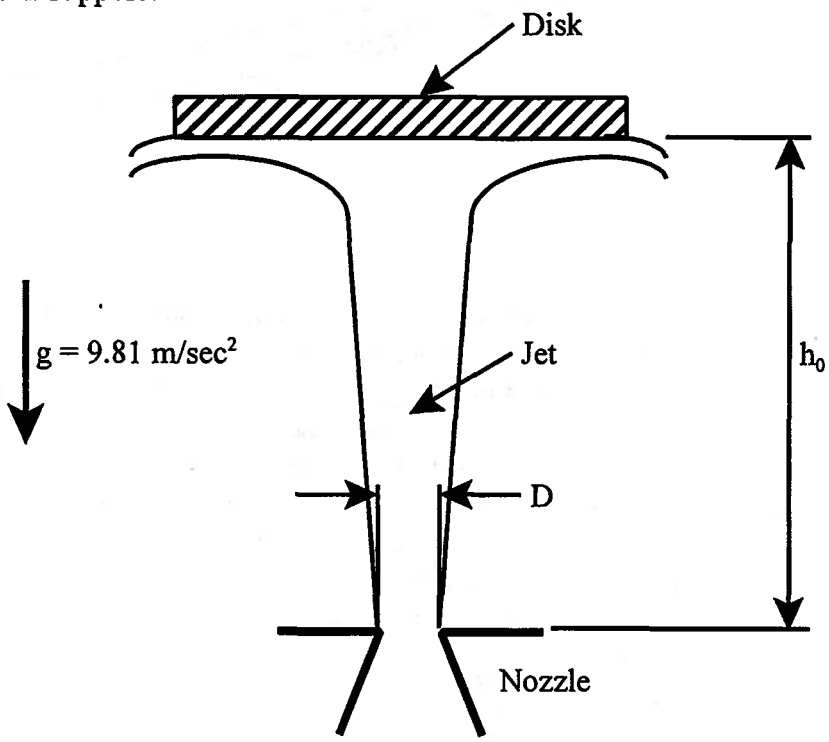

Figure 8P.23

8.24 As shown in Figure 8P.24, a violent rainstorm hits a roof inclined at an angle θ from the horizontal. The rain falls at a mass *flux* of $\dot{m}/A$ where A is measured in the horizontal plane. Each drop falls vertically with the speed $\hat{v}$. A steady-state is established in which the water flows down the inclined roof while the raindrops splatter violently on the top part of the water layer. The objective here is to characterize the water layer.

In the analysis, neglect friction between the water layer and the roof. Also assume that the angle of the free surface of the water layer relative to the roof is very small ($dh/dx << 1$). Note, however, that the roof inclination θ is neither small nor large. Assume further that the raindrops lose their momentum instantaneously upon striking the free surface of the water layer. Finally, it can be assumed that the velocity u of the water in the water layer in the x-direction is independent of y at any location x.

(a) What is the pressure in the water layer just below the free surface?

(b) Calculate the pressure in the water layer at any location x in terms of the local thickness of the water layer $h(x)$ and the location y in the layer.

(c) Consider a control volume in the layer between x and $x + dx$. With the aid of this control volume, derive the differential equation for the water layer thickness $h(x)$.

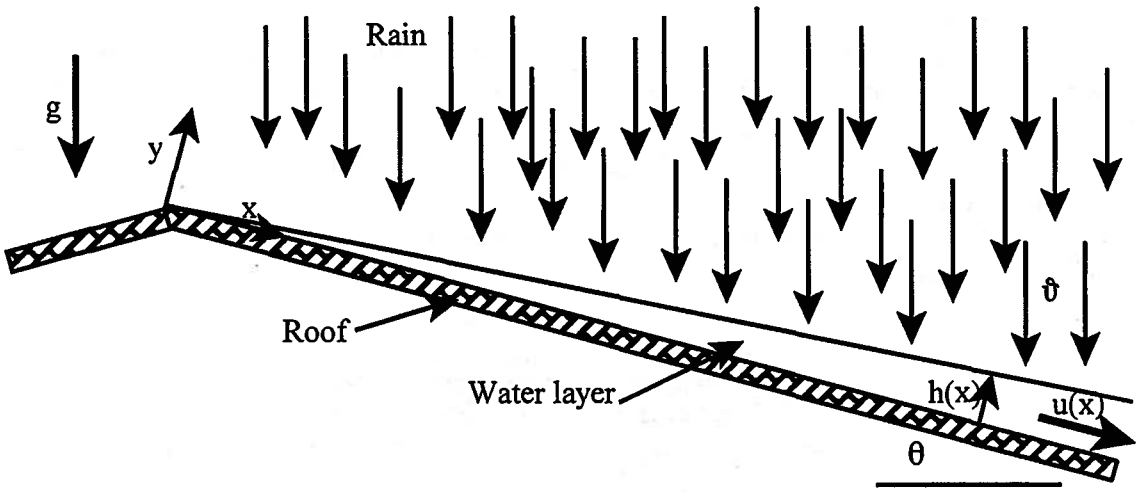

Figure 8P.24

8.26 The Ingersoll Rand Corporation markets a multi-vane air motor, Model No. MOV075AA, that runs on compressed air. At maximum power, the volumetric flow rate of the air is listed at 7.36 m^3/min, measured at standard conditions (P_{std} = 1.0135 x 10^5 N/m^2, T_{std} = 15.89 C). For an air supply at a pressure of P_{in} = 7.22 x 10^5 N/m^2 and a temperature of T_{in} = 289 K, the maximum power of this motor is listed at 7.8 kW with an exhaust pressure of P_{out} = 1.0135 x 10^5 N/m^2.

If we define the efficiency of this motor as the ratio of the actual power developed by the motor to the power that could have been developed by an adiabatic, reversible motor operating with the same inlet and exhaust conditions, what is the efficiency of this motor?
The air can be modeled as an ideal gas with R = 287 J/kg K and c_v = 716 J/kg K.

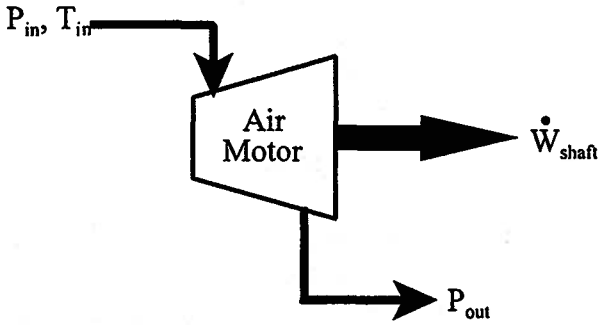

Figure 8P.26

8.25 As shown in Figure 8P.25, a heavy metal barrel of height H and cross-sectional area A_c has been filled with a toxic liquid of density ρ_0 ($\rho_0 < \rho_{water}$) and dropped into a lake of depth D where $D << H$. Unfortunately, due to the corrosive action of the liquid and the water, the barrel has developed leaks at the top and the bottom with areas A_1 and A_2, respectively. This situation can be modeled in a manner that neglects viscosity except for the turbulent flow at the exit of A_1 and the interior region just inside A_2. In addition, the areas of the leaks are small compared to the area of the barrel.

(a) Estimate the velocity at which the toxic liquid leaks out of the barrel relative to the rate of change in the height of the toxic liquid inside the barrel (dh/dt).

(b) Estimate the mass flow rate of the toxic liquid leaking from the barrel, $\dot{m}_{toxic}$.

(c) Estimate the velocity of the water entering the barrel relative to *dh/dt*.

(d) What is the gauge pressure of the water entering the barrel?

(e) What is the gauge pressure of the toxic liquid leaving the barrel?

(f) What is the rate of change of the height of the toxic liquid inside the barrel, *dh/dt*, in terms of g, ρ_0, ρ_{water}, A_c, A_1, A_2, and h?

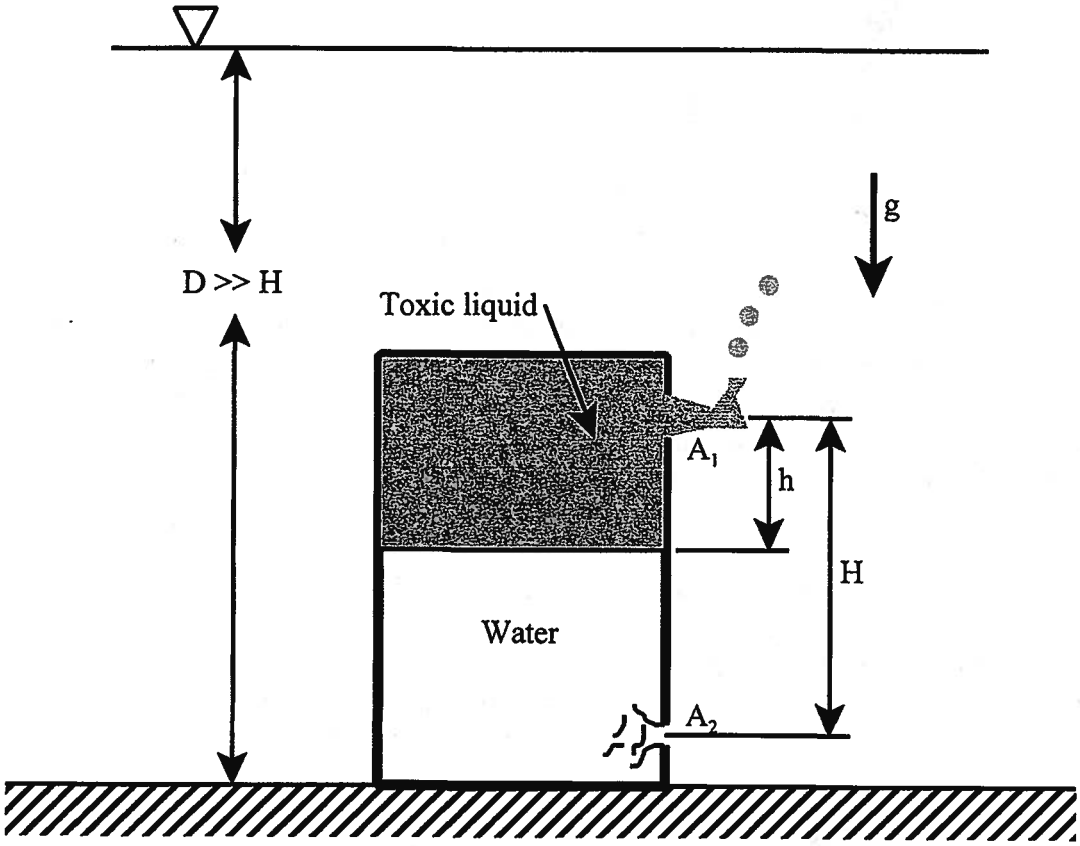

Figure 8P.25

8.27 As shown in Figure 8P.27, a rocket motor used for satellite maneuvering used solid propellant. Since the propellant contains both fuel and oxidizer, it is stored within the motor and consumed as necessary for the maneuvering procedures. The products of combustion of the solid propellant form the working fluid of the nozzle and are used to produce the thrust required for maneuvering. During a maneuver, the pressure inside the motor is $P_0 = 10^6$ N/m^2 and the temperature is $T_0 = 1500$ K until the last of the solid propellant is consumed. The velocity of the propellant gas at entrance to the nozzle is zero at all times. The pressure in the exit plane of the nozzle is $P_e = 10^4$ N/m^2 and the diameter of the nozzle exit is $D_e = 10$ cm. We are attempting to design the propellant containment system and need to know how much propellant must be stored within the motor for a total burn time of 100 sec. Since the fluid residence time within the nozzle is so short that there is insufficient time for any significant heat transfer to occur between the walls of the nozzle and the working fluid, for the purposes of this design, we can model the flow within the nozzle as adiabatic and reversible. The working fluid itself can be modeled as an ideal gas with $R = 189$ J/kg K and $c_v = 662$ J/kg K.

(a) Estimate the mass of propellant M_p that must be stored within the motor so that the pressure P_0 can be sustained for the full 100 sec.

(b) What is the Mach number M_e of the working fluid at exit from the nozzle?

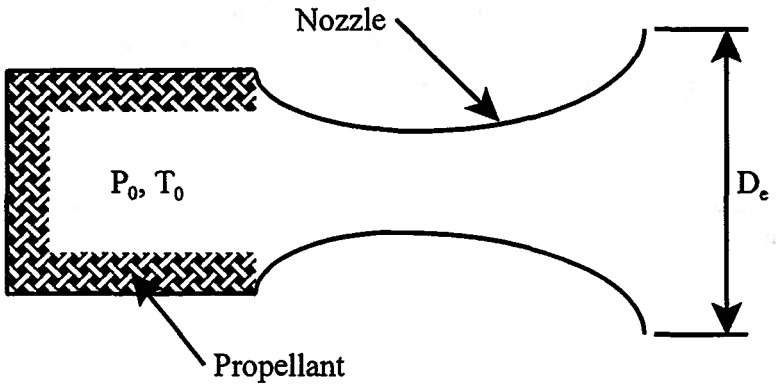

Figure 8P.27

8.28 As shown in Figure 8P.28, a stream of air flowing with uniform velocity ϑ_0 encounters a flat plate aligned normal to the direction of flow and creates a broad, low-velocity wake behind the plate. The velocity profile behind the plate, which has width b in the direction normal to the plane of the Figure 8P.28, can be modeled as having two components: (1) "dead air" with essentially zero velocity in the shadow of the plate and (2) higher velocity air at the periphery with a velocity decaying away from the plate according to the relation

$$\vartheta = \vartheta_0 + \Delta\vartheta e^{-\frac{z}{L}}$$

where $z = 0$ at the edge of the plate and L is the height of the plate.

(a) Find the value of $\Delta\vartheta$ as a function of ϑ_0.

(b) Compute the drag force F_D acting on the plate.

(c) Compute the drag coefficient $C_D = F_D/\rho\vartheta_0^2 Lb$.

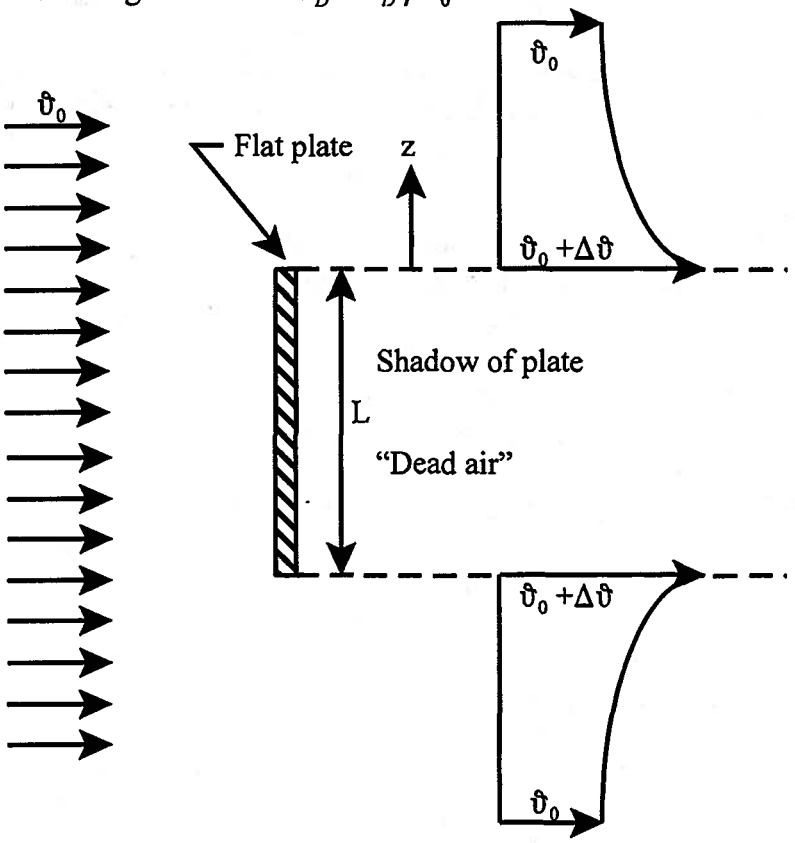

Figure 8P.28

8.29 You are Chief Engineer at *Hot Air Corp.*, and you have recently hired a young engineer, Sandy Beech, from MIT (Matriculating Inept Turkeys, not the real MIT). This ambitious young staff member has just completed tests on one of your new products, an adiabatic air turbine. The tests were conducted in a test stand under conditions of steady flow. Sandy measured the inlet state of the air to be $P_1 = 6 \times 10^5$ N/m^2 and $T_1 = 300$ K. Sandy then measured the mass flow rate through the turbine to be $\dot{m} = 1$ kg/sec. Finally, Sandy measured the outlet state of the air to be $P_2 = 10^5$ N/m^2 and $T_2 = 120$ K.

You know from your own experience with the test stand that the kinetic and gravitational energies of the inlet and outlet streams are negligible.

(a) You analyze Sandy's data to determine the power output of the turbine. What is the result of your analysis?

(b) You are not certain that Sandy knows how to conduct these tests. You apply the ultimate test, the second law, to Sandy's data. Does Sandy have a future at *Hot Air Corp.*?

8.30 A vulture capital firm has hired you as a consultant to evaluate high-tech companies who are seeking funding for their enterprises. They have been approached by group of engineers who claim to have perfected a geothermal energy conversion process that performs in the steady-state according to the data given in Figure 8P.30. What do you advise the vulture capitalists and why?

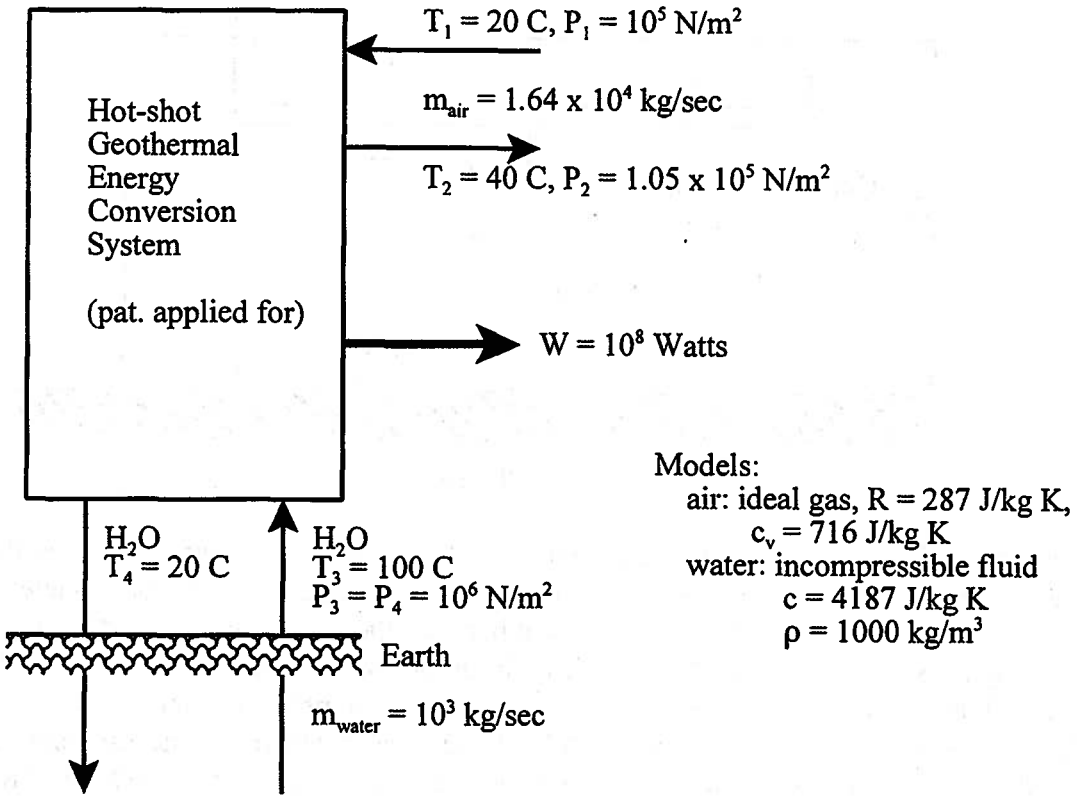

Figure 8P.30

8.31 A student enters a walk-in clothes closet to obtain some clothing and turns on a light inside the closet. After retrieving the clothing, she leaves light on and closes the door. The dimensions of the closet are 2 m x 1 m x 2 m. The bare light bulb is rated at 25 W. There are sufficient air gaps around the closet door to allow the free passage of air with no pressure drop so that the

pressure of the air inside the closet remains constant at atmospheric pressure. The surfaces of the closet can be modeled as a simple thermal resistance with $R_{th} = 0.8$ K/W. The air inside the closet can be modeled as an ideal gas with $c_v = 716$ J/kg K and $R = 287$ J/kg K. The atmospheric pressure is $P_{atm} = 10^5$ N/m^2 and the atmospheric temperature is $T_{atm} = 293$ K. Assume that the temperature of the outside surfaces is T_{atm}.

(a) Derive a differential equation that describes the uniform temperature of the air inside the closet as a function of time.

(b) Use the result of part (a) to estimate the temperature of the air inside the closet at the end of 10 hours. (Note that this will require the solution of a non-linear differential equation.)

(c) Estimate the mass of air inside the closet at the end of 10 hours.

(d) Suppose that the thermal resistance is actually higher than the value specified. Is there a risk of fire under these circumstances?

8.32 As shown in Figure 8P.32, a warehouse is heated by means of a simple heat exchanger consisting of a thin walled copper tube in which high temperature H_2O flows. The H_2O, which flows through the heat exchanger with no change in pressure (10^5 N/m^2), enters at a temperature of $T_{w,in} = 90$ C and exits at a temperature of $T_{w,out} = 40$ C. The water can be modeled as an

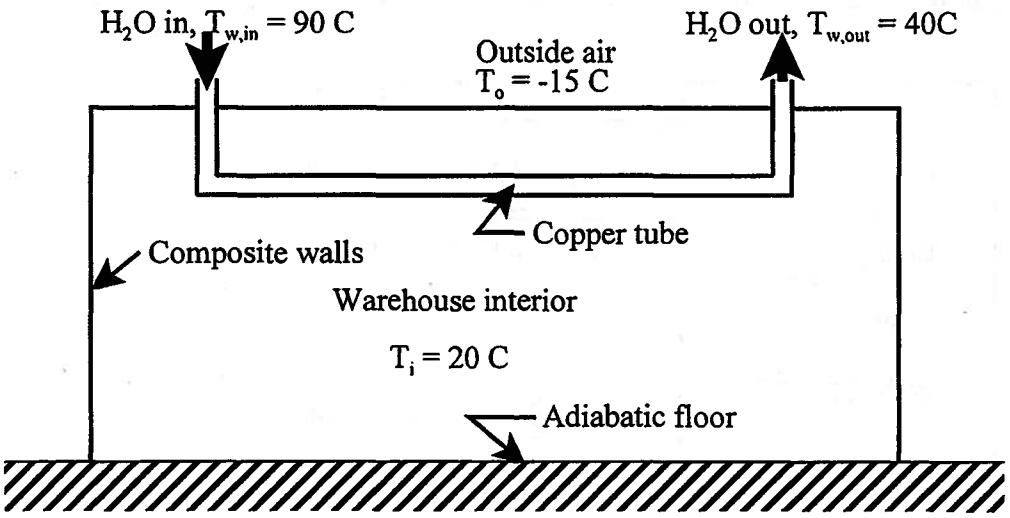

Figure 8P.32a

incompressible fluid with $\rho_w = 1000$ kg/m^3 and $c_w = 4187$ J/kg K. The heat transfer coefficient for the heat transfer process inside the heat exchanger tube is so large that it can be modeled as infinite. The convective heat transfer coefficient between the outside surface of the tube and the surrounding air is $h_c = 7.85$ W/m^2 K. The air in the empty warehouse is to be maintained at an average bulk temperature of $T_i = 20$ C. The convective heat transfer coefficient between the air and the inside surface of the walls is $h_i = 3$ W/m^2 K. On a cold winter day the temperature of the air outside is $T_o = -15$ C and has a convective heat transfer coefficient of $h_o = 60$ W/m^2 K at the outer surface of the warehouse. The warehouse can be modeled as a simple box with inside dimensions 20 m wide by 40 m long by 10 m high. Assume that the surface area of the walls is the same inside the building as outside. The walls and ceiling of the warehouse have a composite structure as shown in Figure 8P.32b. The inside layer is plaster board 10 mm thick ($k_{pb} = 0.17$ W/m K); the middle layer is a glass fiber blanket 100 mm thick ($k_f = 0.038$ W/m K); and the outside layer is plywood 20 mm thick ($k_p = 0.117$ W/m K). As a first estimate of the heat transfer

rate, we are going to neglect thermal radiation.

(a) Draw the equivalent thermal circuit for the heat transfer interaction between the water inside the tube and the air outside the building.

(b) Determine the temperature of the walls at the inside surface and the outside surface and sketch the temperature distribution through the walls. (See sketch below.)

(c) Determine the heat transfer rate at the inside surface of the walls.

(d) Calculate the mass flow rate of the H_2O in kg/sec.

(e) Since the temperature of the length of copper tubing changes as the water flows through it, show that by combining the first law and Newton's Law of Cooling, the appropriate temperature difference to be used in Newton's Law of Cooling is the Log Mean Temperature Difference, ΔT_{LM}, where

$$\Delta T_{LM} = \frac{\left(T_{w,in} - T_i\right) - \left(T_{w,out} - T_i\right)}{\ln\left[\frac{\left(T_{w,in} - T_i\right)}{\left(T_{w,out} - T_i\right)}\right]}$$

(f) Use this Log Mean Temperature Difference to calculate the length of copper tubing required if the outside diameter is 25 mm.

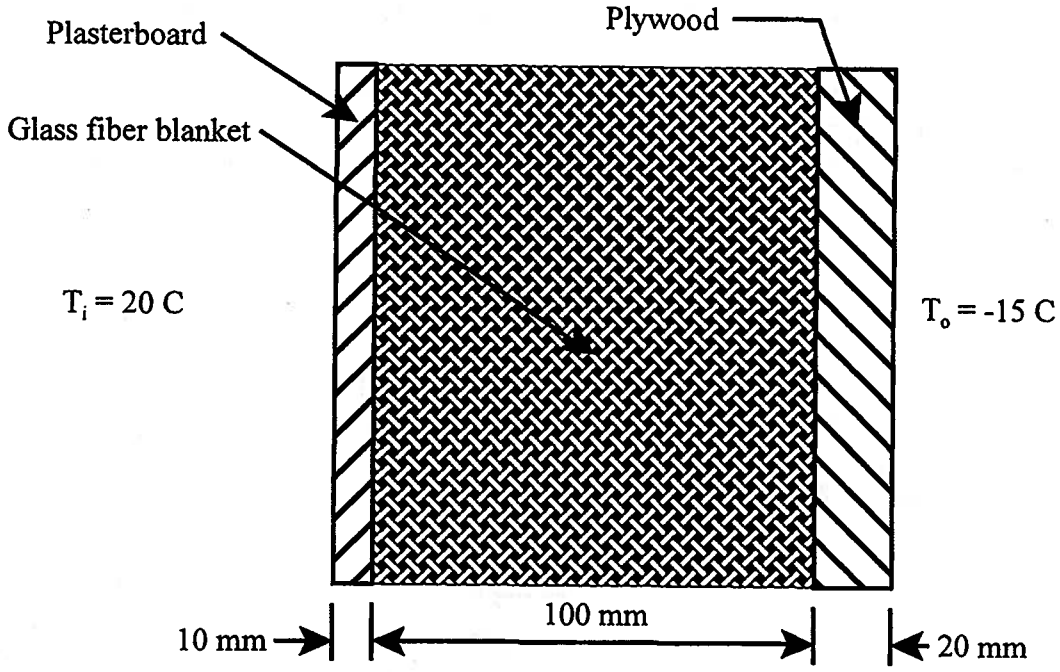

Figure 8P.32b

8.33 As shown in Figure 8P.33, a rigid, insulated tank of volume 2 m^3 is fitted with an electrical resistance heater that dissipates electrical energy at the constant rate of 100 W. In order to maintain the temperature of the air inside the tank at a constant value of 100 C, air is bled from the tank at a variable, but controlled, rate. The air can be modeled as an ideal gas with $R = 287$ J/kg K and $c_v = 716$ J/kg K.

(a) Estimate the instantaneous rate of mass flow from the tank when the pressure inside the tank is $P_2 = 7 \times 10^5$ N/m^2.

(b) What is the mass of air inside the tank in state 2?

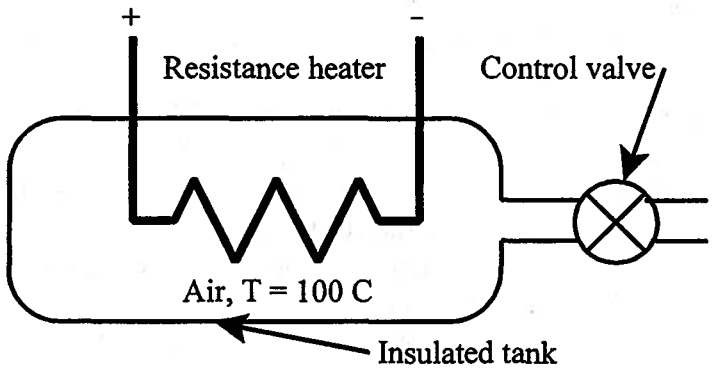

Figure 8P.33

8.34 As shown in Figure 8P.34, a wind of speed $\hat{v}_w = 10$ m/sec blows against the side of a house whose volume is $V = 500$ m^3. On the upwind side of the house, a window of area $A_w = 1$ m^2 is open to the wind. Another window of the same size is also open on the downwind side of the house. The pressure outside the house on the downwind side is the same as that far upwind of the house, P_{atm}. At these low velocities, the air can be modeled as an incompressible fluid with $\rho = 1.2$ kg/m^3.

(a) Estimate the velocity $\hat{v}_h$ of the air blowing through the upwind window.

(b) Estimate the pressure P_h of the air inside the house.

(c) Estimate the time required for the volume flow through the upwind window to equal the volume of the house.

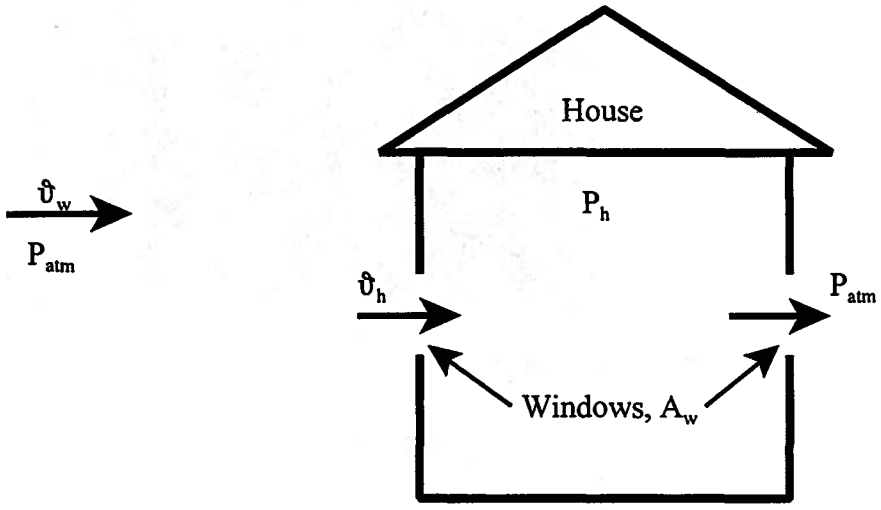

Figure 8P.34

8.35 As the thermal-fluids engineer for an aerospace company, you have been asked to design a shock-absorbing mechanism that can be used to safely land a vehicle on Mars. The vehicle is to experience a strong deceleration prior to the moment of touchdown. Figure 8P.35 shows the proposed design of the device to be attached to the underside of the vehicle.

The device consists of an adiabatic cylinder containing an ideal gas of mass M_g trapped

on top of a layer of incompressible oil and a piston that is fitted to the cylinder with a frictionless seal. The piston is attached to a large disk that acts as a "foot" for the vehicle. The gravitational acceleration on Mars is g and atmospheric pressure at the landing site is P_{atm}. The mass of the vehicle M_v; the mass of the piston-foot assembly is M_p; and the height of the oil layer is L_o. The area of the piston is A. The characteristics of the ideal gas are R and c_v.

At the moment before touchdown, with a very small distance between the foot and the ground, we wish to find the gas pressure or the force acting on the vehicle through the shock absorber. At this moment, the vehicle deceleration is a_z achieved through the use of braking jets fired earlier.

(a) For the moment in question, develop expressions for the gas pressure as a function of the length L_g and the pressure distribution within the oil.

(b) Evaluate the gas pressure in terms of the unknown distance between the piston and the top of the cylinder, L.

(c) Find the total pressure acting on the piston at this same moment.

(d) Develop an expression for the length L in terms of given known quantities in order to use the result in (a) to find the gas pressure P_g.

(e) Soon after touchdown, the braking jets are turned off and the shock absorber takes over. What is the force on the vehicle?

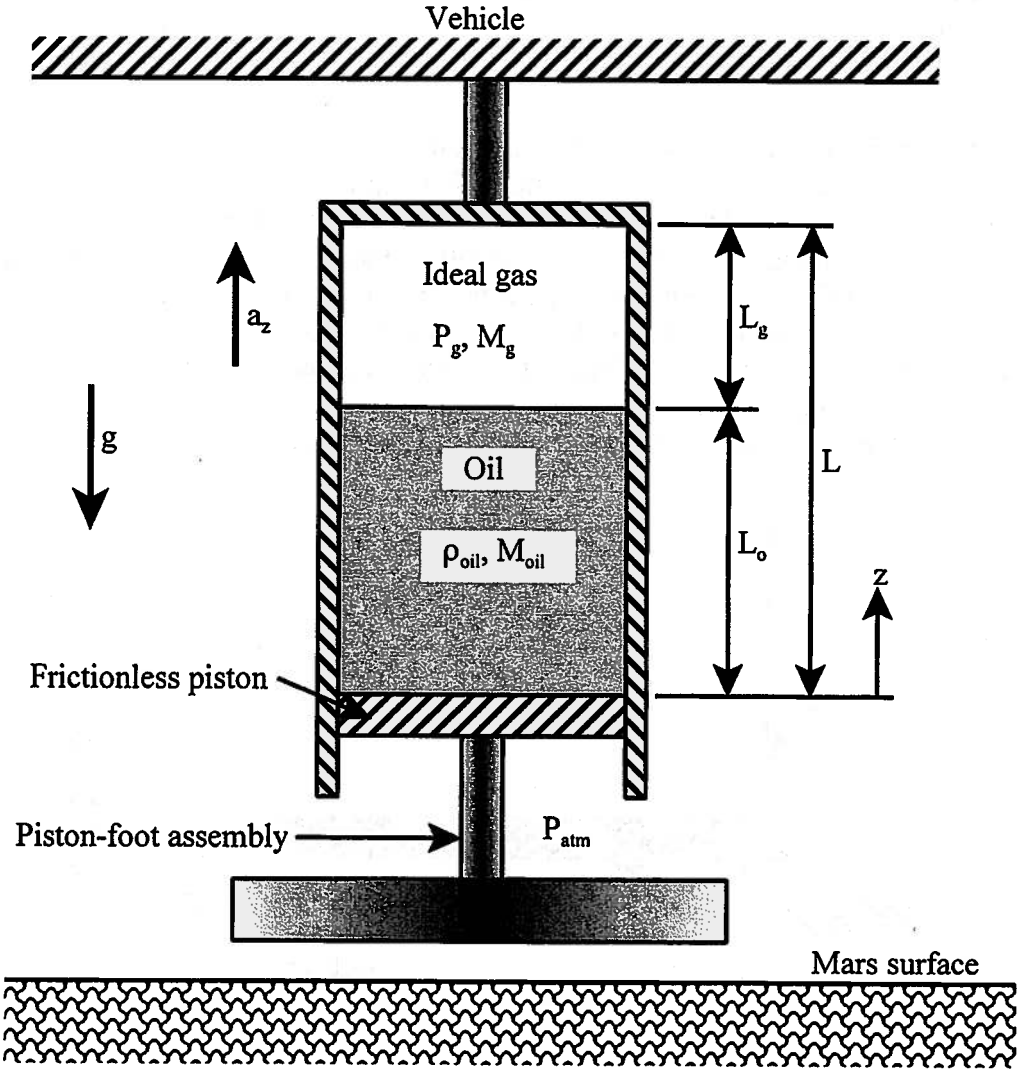

Figure 8P.35

8.36 As shown in Figure 8P.36, water flows over a spillway. The flow is assumed uniform and the pressure is assumed hydrostatic at sections 1 and 2. Model the fluid as inviscid with no losses of any kind.

(a) Calculate the velocity ϑ_2 if the density of water is $\rho = 1000$ kg/m^3 and $g = 9.81$ m/sec^2.

(b) For a unit width of spillway, calculate the force of the water on the spillway.

(c) Calculate the Froude number at location 2. Is the flow at this location subcritical or supercritical?

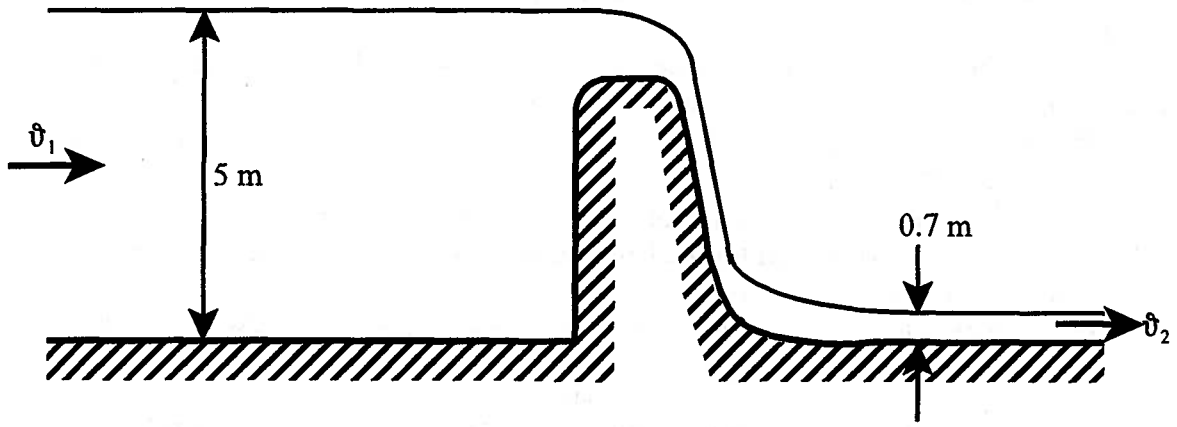

Figure 8P.36

8.37 As shown in Figure 8P.36, a very large tank full of water is mounted on a cart. The tank is fitted with a nozzle with a diameter $D = 25$ mm which allows the water to discharge to the atmosphere, but the cart is tied to a rigid wall with a cable so that it cannot move. The tank is so large that for the time period of interest in this situation, the level of the water can be assumed to be fixed at a height h above the center of the nozzle despite the flow of water from the tank. The water can be modeled as an incompressible fluid with $\rho = 1000$ kg/m^3.

(a) Calculate the average jet velocity, ϑ_{jet}, when the level of the free surface is at a height of $h = 3$ m above the nozzle.

(b) Calculate the tension in the horizontal cable that holds the cart in place when $h = 3$ m.

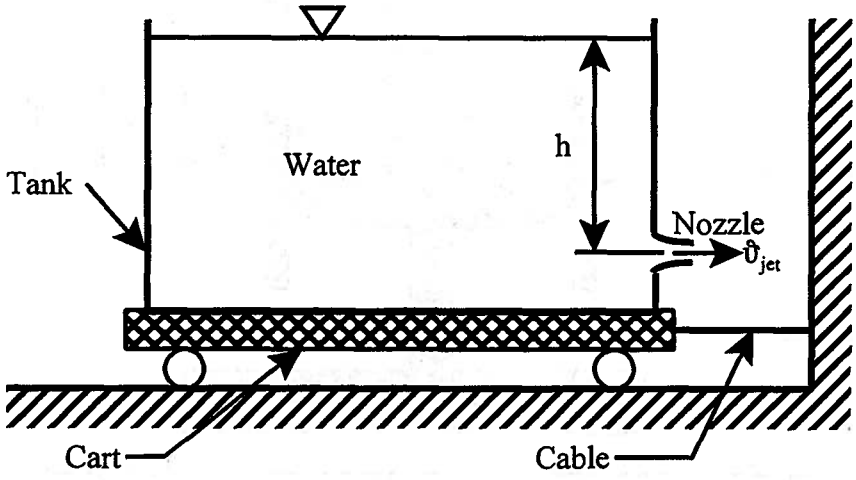

Figure 8P.37

8.38 A sluice gate is a device used to control the flow of water in irrigation and flood control systems. As shown in Figure 8P.38, the gate is a plate with a sharp edge on the bottom. At a location far enough upstream of the gate, the water is essentially quiescent. The gate is raised slightly so that water can flow under it at controlled flow rates into a flume or spillway that is essentially a concrete lined trough. From there, the water can be directed to some specific location. Usually, the water level upstream of the sluice gate is high relative to the water level downstream. In a particular application, the sluice gate is 1 m wide. The level of the water upstream of the gate is $h_1 = 1.5$ m, and downstream of the gate at the location 2 it is $h_2 = 0.0563$ m. The streamlines at location 2 are assumed to be straight and the pressure distributions at both locations are assumed to be hydrostatic. The flow can be modeled as steady.

(a) Estimate the volume flow rate V of the water under the sluice gate.

(b) Estimate the force F acting on the gate itself.

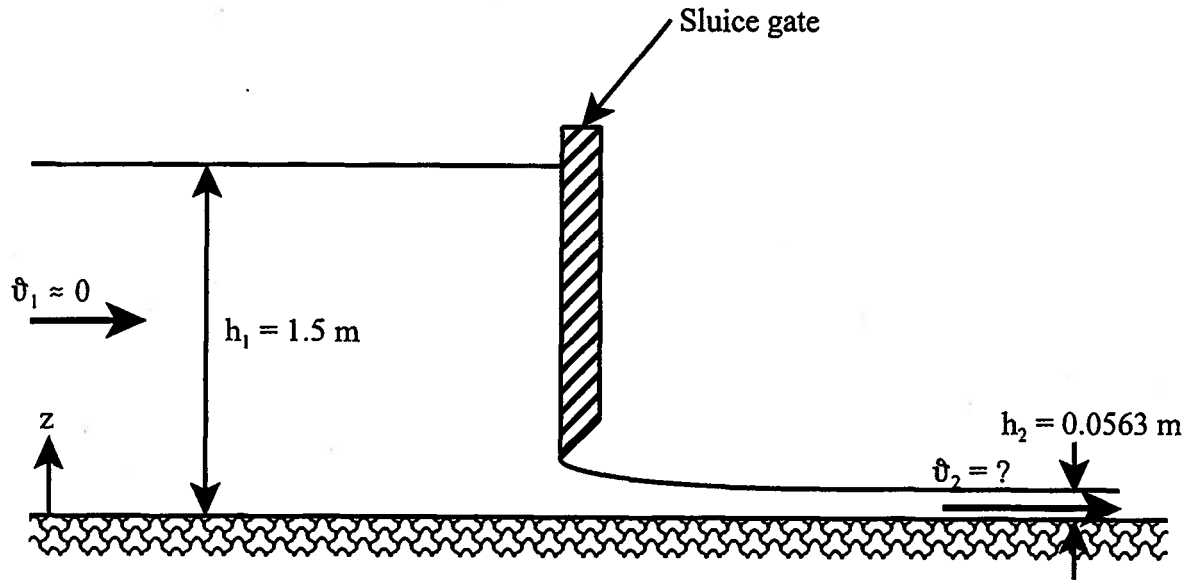

Figure 8P.38

CHAPTER 9

Viscosity and the Transfer of Momentum in a Fluid

9.1 Introduction

In thermal-fluids engineering, it is usually necessary to move the working fluid of the system from one location to another. During this transport process, the fluid frequently comes into contact with the solid surfaces, or more generally the boundaries, that are used to direct its motion. These may include surfaces that enclose the fluid such as the walls of a conduit through which the fluid is flowing or they may be the surfaces over which the fluid flows such as the wings of an aircraft or the body of an automobile. Whenever the fluid comes into contact with these boundaries, interactions occur that involve the transfer of momentum and energy between the fluid and the boundary as a consequence of the transport properties of the fluid, namely the *viscosity* and the *thermal conductivity*. As a result, gradients of fluid velocity and temperature develop in a direction normal to the surface. Knowing these gradients in velocity and temperature, we can determine the properties of the fluid as a function of position relative to the boundary. The larger the values of the viscosity and the thermal conductivity, the stronger the interaction between the fluid and the boundary. This interaction influences the motion of the fluid in a manner such that strongest influence occurs in the immediate neighborhood of the boundary. This influence diminishes rapidly with distance from the boundary so that far from the boundary, the fluid behaves almost as though it had no viscosity or thermal conductivity and its motion can be described with the aid of the Bernoulli equation that we developed in Chapter 8. However, near the boundary, the effect of the transport properties can be of paramount importance in determining the motion of the fluid and, hence, its performance in the thermal-fluid system.

As we have mentioned previously, an incompressible fluid is an uncoupled system so its thermal and mechanical aspects of behavior can be separated. Therefore, for this fluid model, the effects of viscosity and thermal conductivity can be studied separately. In the present chapter, we shall treat the incompressible fluid as a continuum and focus our attention on the fluid viscosity and the process of momentum transfer between the fluid and its boundaries. We shall develop the "tools" necessary to quantitate this interaction in a wide variety of thermal-fluid systems, both those with "internal flows" such as pipes and those with "external flows" such as airplane wings. Furthermore, we shall quantitate the "strength" of the interaction between the fluid and the boundary, and we shall provide some quantitative measure to the distance over which the effect of the viscosity can be felt in the fluid. In Chapter 11, we shall take up the effect of the fluid thermal conductivity and the resulting energy transfer process between the fluid and its boundaries.

Recall that in Chapter 8 we examined the dynamical behavior of a fluid as it flowed through an open system which we modeled as a control volume. Although the control volume approach is general and can be applied to a control volume of any size or shape, we found in Chapter 8 that it is particularly useful when the control surface that defines the control volume is coincident with walls of a physical device such as a thermal-fluid machine. In such cases, we are able to describe the behavior of the device in terms of the thermodynamic states of the fluid as it crosses the control surface. In using the control volume approach in this manner, we model the state of the fluid crossing the control surface as uniform over the areas of the ports where the fluid enters and leaves the control volume. In reality, the values of the properties that define the state of the fluid vary over these areas for the reasons given above. However, if we know the manner in which the properties vary over the area of interest, we can perform a suitable

averaging process over the area to obtain the appropriate average values of the properties to use in the control volume "conservation" equations. As mentioned above, the "tools" that we shall develop in the present chapter will provide the means of describing the dynamical behavior of the fluid under the influence of its viscosity so that we can determine the manner in which the fluid properties vary over the area of any given port of a thermal-fluid machine. To be sure, the results of this study will be applicable to any situation in which we need to describe the dynamical behavior of a fluid at any point in a flow field, but for the present, this will be one of our primary motivations for the study.

9.2 Viscosity

In order to see the influence of viscosity on fluid behavior, we consider a layer of fluid confined between two infinite parallel flat plates separated by a distance H as shown in Figure 9.1. Because the plates are infinite in extent, the effects of the edges of the plates do not need to be considered. Let the upper plate be in motion with the constant velocity ϑ_0 while the lower plate remains at rest. The fluid can be thought of consisting of many thin layers parallel to the plates such that the fluid in contact with the plates adheres to the plates. This is known as the "no slip" boundary condition. As the upper plate moves relative to the lower plate, the fluid at the upper plate moves with the velocity ϑ_0 while the fluid at the lower plate remains stationary. This induces a steady motion in the fluid in the x-direction as the fluid layers slide over one another. Let the velocity of the fluid in the x-direction at any point between the plates be denoted by ϑ_x. As a consequence of the viscosity of the fluid, there is internal friction between adjacent layers. The layer below the top layer will be dragged in the forward direction by the layer above it, but at a velocity somewhat less than the velocity of the layer above. This layer, in turn, will exert a forward drag on the layer beneath it at reduced velocity and so on through the entire fluid layer. As a result of this motion, there is a velocity gradient $d\vartheta_x/dy$ everywhere in the fluid. In the steady state,

$$\frac{d\vartheta_x}{dy} = \frac{\vartheta_0}{H} \tag{9.1}$$

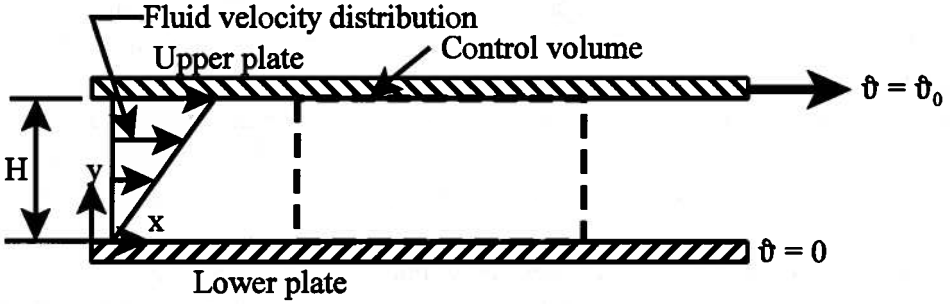

Figure 9.1 Fluid Layer Between Two Flat Plates

This is analogous to the situation in which a deck of playing cards is placed upon a table and a force is exerted on the top card in the plane of this card thereby setting it in motion. The card beneath the top card is dragged along by the friction between the two cards and so on down through the deck until the bottom card is reached which is "stuck" to the table. In the fluid, the frictional forces on the two surfaces of a fluid layer (forward drag on the upper surface and

backward drag on the lower surface) are parallel to the surfaces. Since these forces are in the plane of the surfaces, they tend to shear the layers one over the other. This type of force is known as a shear force, and it gives rise to a type of stress known as a shear stresses which is defined as the shear force divided by the area of the surface over which the force is applied. Since shear stresses, in contrast to the hydrostatic stresses we considered in Chapter 4, are parallel to the surfaces over which they act, we need to specify two directions for a shear stress. By convention, the first of these is the direction normal to the surface over which the force acts and the other is the direction in which it acts. For the case shown in Figure 9.1, the shear stress associated with the relative motion of the two plates is denoted by τ_{yx}.

For the viscous fluids most commonly found in thermal-fluid systems, the shear stress is found to be linearly proportional to the velocity gradient. For this fluid model, known as the Newtonian fluid model, the constant of proportionality is known as the viscosity of the fluid and denoted by the symbol μ. Thus, for the one-dimensional situation shown in Figure 9.1

$$\tau_{yx} = \mu \frac{d\vartheta_x}{dy} \tag{9.2}$$

Physically, this shear stress is the force per unit area that must be applied to the upper plate at all times so that the velocity of the plate can be maintained constant in the presence of the friction in the fluid.

The dissipative nature of the fluid friction manifest in the viscosity of the fluid can be observed by applying the first and second laws of thermodynamics to the control volume fixed in space as shown in Figure 9.1. Let the fluid be modeled as an incompressible fluid. Since the plates are infinite in extent, the fluid has an x-component of velocity only. If the *control volume* (not the plates) has dimensions L in the x-direction, H in the y-direction, and b in the z-direction normal to the plane of the figure, the mass flow rate of the fluid through the control volume in the steady state is given by

$$\dot{m}_{in} = \dot{m}_{out} = \dot{m} = \int_0^H \rho \vartheta_x(y) b dy \tag{9.3}$$

where the fluid velocity $\vartheta_x(y)$ is a function of the distance y measured normal to the plate. By integrating equation (9.1), we can obtain the functional relationship between ϑ_x and y, viz.

$$\vartheta_x = \frac{\vartheta_0}{H} y \tag{9.4}$$

Then equation (9.3) becomes

$$\dot{m} = \int_0^H \rho \frac{\vartheta_0}{H} b y dy = \rho \frac{\vartheta_0 b}{H} \int_0^H y dy = \rho b H \frac{\vartheta_0}{2} = \rho b H \vartheta_{ave} \tag{9.5}$$

Equation (9.5) illustrates the manner in which the average values of the fluid properties can be determined, in this case the average fluid velocity.

Let us examine the fluid control volume of Figure 9.1a in greater detail from the point of view of the forces acting on the fluid control volume in the x-direction. (See Figure 9.1b.)

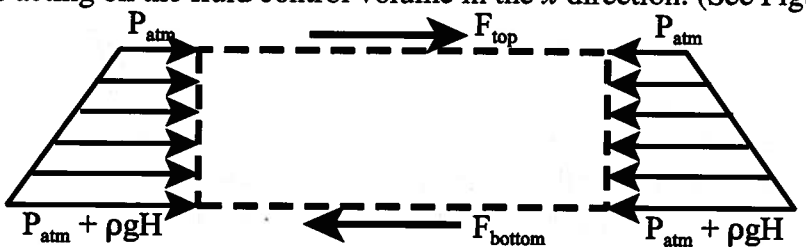

Figure 9.1b Forces on the Control Volume of Figure 9.1a

Since the forces due to normal stresses acting on the ends of the fluid control volume are hydrostatic, the net force acting on the control volume is given by

$$\sum F_x = \left(P_{atm} + \rho g \frac{H}{2}\right) Hb - \left(P_{atm} + \rho g \frac{H}{2}\right) Hb + F_{top} - F_{bottom}$$

$$\sum F_x = \left(P_{atm} + \rho g \frac{H}{2}\right) Hb - \left(P_{atm} + \rho g \frac{H}{2}\right) Hb + \tau_{yx} bL - \tau_{yx} bL = 0$$

where the shear stress acting on the top and bottom surfaces of the fluid control volume are the same since the velocity gradient is constant throughout the fluid layer. (See equation 9.2.) Thus, there is no net force acting on the fluid control volume. This is consistent with the fact that there is no net momentum flow across the control surface for this steady flow situation which can be seen from the equation of linear momentum, viz.

$$\int_{CS} \rho \vec{\vartheta} \left(\vec{\vartheta} \cdot \vec{n}\right) dA = \frac{4}{3} \dot{m} \vartheta_{ave} - \frac{4}{3} \dot{m} \vartheta_{ave} = 0$$

Then for this steady flow situation with no pressure drop in the x-direction, the first law of thermodynamics reduces to

$$\dot{Q} - \dot{W}_{shear} = \dot{m}\left(u_{out} - u_{in}\right) = \dot{m}c\left(T_{out} - T_{in}\right) \tag{9.6}$$

From the definition of the work transfer and the fact that only the boundary mass points on the top of the fluid layer are in motion, the fluid shear power becomes

$$\dot{W}_{shear} = \frac{\delta W_{shear}}{dt} = -\left(F_x\right)_{shear} \frac{dx}{dt} = -F_{top} \frac{dx}{dt} = -\tau_{yx} A \vartheta_0 = -\tau_{yx} bL \vartheta_0 \tag{9.7}$$

Substituting equations (9.1) and (9.2) into equation (9.7), we obtain

$$\dot{W}_{shear} = -\mu \frac{\vartheta_0^{\,2}}{H} bL \tag{9.8}$$

Since the flow is adiabatic, substitution of equation (9.8) into equation (9.6) yields

$$T_{out} = T_{in} + \frac{2\mu \vartheta_0 L}{\rho c H^2} \tag{9.9}$$

Thus as a result of the action of viscosity in the fluid, the temperature of the fluid leaving the control volume is greater than the temperature of the fluid entering the control volume. The rate of entropy generation in the fluid due to viscous dissipation (fluid shear) can be determined by applying the second law of thermodynamics to the control volume. For the adiabatic, steady flow situation shown in Figure 9.1, the second law becomes

$$\dot{S}_{gen} = \dot{m}c\left(s_{out} - s_{in}\right) = \dot{m}c \ln \frac{T_{out}}{T_{in}} \tag{9.10}$$

where we have used the entropy constitutive relation for the incompressible fluid model. Then substituting equation (9.9) into equation (9.10), we obtain

$$\dot{S}_{gen} = \rho \vartheta_0 bc \frac{H}{2} \ln\left(\frac{T_{out}}{T_{in}}\right) = \rho \vartheta_0 bc \frac{H}{2} \ln\left(1 + \frac{2\mu \vartheta_0 L}{\rho c T_{in} H^2}\right) \tag{9.11}$$

From equation (9.11), it is apparent that the more viscous the fluid, i.e., the greater the viscosity of the fluid, the greater the rate of entropy generation. It is also apparent that the smaller the gap between the two plates, the greater the shear and the greater the rate of entropy generation. Note that in the limit of zero viscosity, there is no entropy generation in the control volume due to fluid shear.

For the simple one-dimensional geometry shown in Figure 9.1, we have seen the consequences of fluid shear and the action of viscosity; however, we have not yet seen the relationship between the viscosity and momentum transfer. To do this, we need to examine the fluid on a microscopic scale in which we can identify the individual molecules that make up the fluid. For this purpose, it is most convenient if the fluid is a gas since the kinetic theory of gases molecules is better understood and simpler than that of liquids due primarily to the weak interactions between gas molecules. Suppose the gap between the parallel plates shown in Figure 9.1 is filled with a gas. Consider an imaginary plane located at $y = y_0$ which is being crossed by molecules of gas from above and below. The motion of the molecules in the y- and z-directions is random with zero average velocity, but in the x-direction their average component of velocity is equal to the velocity of bulk motion, $\bar{\vartheta}_x = \vartheta(y)$. Molecules cross the imaginary plane at $y = y_0$ with equal frequency. Each molecule that crosses from above carries with it energy and momentum which are transferred from the layer above to the layer below by the mechanism of molecular collisions. Molecules that cross the plane $y = y_0$ from below transfer energy and momentum from the lower layer to the upper layer. Since there is a velocity gradient in the flowing gas, the molecules, each of mass m, crossing $y = y_0$ from above have a greater average momentum component $m\vartheta_x(y)$ in the x-direction than the molecules below the plane $y = y_0$. Hence, there is a net transfer of momentum from above the plane to below the plane. By Newton's second law of motion, the increase in the x-component of momentum of the lower layer per unit time is equal to the force exerted on it and the decrease in the x-component of momentum of the upper layer is equal to the reaction force. The net effect is the same as if the upper layer exerted a drag force in the x-direction on the lower layer. The net transfer of the x-component of momentum per unit time per unit area of the plane $y = y_0$ is equal to the shear stress τ_{yx} acting on the plane. Thus the viscosity of the gas originates in the net transfer of momentum in the direction of the velocity gradient (but opposite in sense) by molecular collisions.

Using the results of simple kinetic theory of gases, we can develop a quantitative estimate of the viscosity of a gas. Consider again the situation shown schematically in Figure 9.1. Let $m\vartheta_x(y)$ be the x-component of momentum of a gas molecule which varies uniformly in the y-direction due to the velocity gradient in the y-direction associated with the bulk motion of the gas. As we did above, we focus our attention on the imaginary plane $y = y_0$ and determine the net transport of $m\vartheta_x(y)$. The average number of molecules crossing $y = y_0$ per unit area per unit time in either direction is proportional to $n\bar{c}$ where n is the number of molecules per unit volume and $\bar{c}$ is the average velocity of a molecule which is very different from the bulk velocity $\vartheta(y)$. (Typically $\vartheta(y)$ is on the order of 1 m/sec whereas $\bar{c}$ is on the order of 500 m/sec.) When a molecule crosses the $y = y_0$ plane, it carries a value of $m\vartheta_x$ characteristic of that resulting from its last collision. Let $m\vartheta_x(y_0 + \Delta y)$ be the average value of $m\vartheta_x$ transported in the negative y-direction by the molecules crossing $y = y_0$ from above. In the first approximation, Δy represents the average distance a molecule travels since its last collision and is, therefore, equal to the mean free path λ. Then the net amount of $m\vartheta_x$ transported in the negative y-direction is proportional to $n\bar{c}[m\vartheta_x(y_0 + \Delta y) - m\vartheta_x(y_0 - \Delta y)]$. If we perform a Taylor series expansion on the term in square brackets, we get

$$\left[m\vartheta_x(y_0+\Delta y)-m\vartheta_x(y_0-\Delta y)\right]\approx 2\Delta y\frac{d(m\vartheta_x)}{dy}=2\lambda\frac{d(m\vartheta_x)}{dy} \tag{9.12}$$

By our arguments above, the shear stress in the fluid is proportional to the net transport of the x-

component of momentum, viz.

$$\tau_{yx} = 2an\bar{c}\lambda\frac{d(m\vartheta_x)}{dy} = \varphi(n\bar{c}\lambda)\left(\frac{d(m\vartheta_x)}{dy}\right) = \varphi(mn\bar{c}\lambda)\frac{d\vartheta}{dy} \tag{9.13}$$

where a and φ are constants of proportionality. Then combining equations (9.2) and (9.13), we get

$$\mu = \varphi mn\bar{c}\lambda = \varphi\rho\bar{c}\lambda \tag{9.14}$$

where $\rho = mn$ is the density of the gas. By arguments outside the scope of this treatment, J. C. Maxwell showed in 1860 that $\varphi = 1/3$. Thus since the mean free path λ varies inversely with n, the viscosity μ is independent of density or pressure as confirmed by experiment.

If the molecules are modeled as simple billiard balls with no force of attraction between them, the product $n\lambda$ is independent of temperature. Then since the mean speed of the molecules varies as $T^{1/2}$, the viscosity of gases should vary as $T^{1/2}$. Experiment shows that the temperature dependence of the viscosity of gases is actually stronger than this. In 1893, W. Sutherland showed that by accounting for the weak attractive forces of the gas molecules, the viscosity can be related to the temperature by an expression of the form

$$\mu = A\frac{T^{1/2}}{1+\left(\frac{S^*}{T}\right)} \tag{9.15}$$

where A and S^* are constants now known as the Sutherland constants whose values are determined by experiment. Equation (9.15) gives good agreement with the available data. Representative values of the viscosity of gases commonly used in thermal-fluid systems are listed in Table 9.1 along with their Sutherland constants. Note that in the SI unit system, the units of viscosity are (kg/m sec) or (Pa-sec).

Table 9.1 Viscosity of Common Gases at 300 K and 1 atm[a]

Gas	Viscosity, μ (kg/m sec)	A ($K^{-1/2}$)	S^* (K)
Air	18.53×10^{-6}	1.462×10^{-6}	110
Ammonia, NH_3	10.23×10^{-6}	1.418×10^{-6}	420
Carbon dioxide, CO_2	15.02×10^{-6}	1.596×10^{-6}	252
Helium, He	19.94×10^{-6}	1.535×10^{-6}	100
Hydrogen, H_2	8.949×10^{-6}	6.889×10^{-7}	100
Nitrogen, N_2	17.8×10^{-6}	1.408×10^{-6}	111
Oxygen, O_2	20.65×10^{-6}	1.749×10^{-6}	140
Steam, H_2O (at $P = 3.54 \times 10^3$ N/m^2)	9.195×10^{-6}	2.064×10^{-6}	781

a Except for steam, data derived from *Handbook of Heat Transfer*, ed. by W.M. Rohsenow, J.P. Hartnett, and Y.I. Cho, McGraw-Hill, New York, 3d. ed., 1998, Table 2.10, pp. 2.4-2.11. Data for steam from *NIST/ASME Steam Properties*, NIST Standard Reference Database 10, Version 2.11, by A.H. Harvey, A.P. Peskin, and S.A. Klein.

Although we have examined only gases with respect to the transfer of momentum by molecular collisions, the physics are similar for liquids as well. Of course, the quantitative results will be different for the two types of fluids because the molecules of a liquid are more tightly packed into the volume they occupy and , as a result, they interact with one another more strongly than do the molecules of a gas that occupy an equivalent volume. Because of these strong intermolecular forces, the temperature dependence of the viscosity of liquids is quite different from that of gases. As the temperature of a liquid increases, the liquid expands and the intermolecular forces decrease in magnitude. As a result, the viscosity of a liquid decreases as the temperature increases. The viscosities of some representative liquids are given in Table 9.2.

The important point here is that momentum is transferred in a velocity gradient in the fluid by virtue of collisions between the molecules that make up the fluid as these molecules move from one location to another location of different bulk velocity. This transfer of momentum, in turn, leads to entropy generation in the fluid.

Table 9.2 Viscosity of Some Common Liquids at 300 K and 1 atm[a]

Liquid	Viscosity, μ (kg/m sec)
Ethyl alcohol, C_2H_5OH	10.95×10^{-4}
Octane, C_8H_{18}	5.10×10^{-4}
Engine oil, Mobil 1, 10W-30 (at $T = 40$ C)[b]	506.95×10^{-4}
Castor oil	6500×10^{-4}
Water, H_2O[c]	8.538×10^{-4}

a Handbook of Tables for Applied Engineering Science, ed. by R.E. Bolz and G.L. Tuve, 2nd ed., 1973, CRC press, Cleveland, Ohio, Table 1-46, p. 92. *b* Mobil Oil Co. Product Data Sheet. *c NIST/ASME Steam Properties*, NIST Standard Reference Database 10, Version 2.11, by A.H. Harvey, A.P. Peskin, and S.A. Klein.

9.3 The Total Derivative

We now want to examine the way in which the viscosity of the fluid influences the dynamics of fluid behavior, but in order to do this, we need to study the motion of the fluid by looking at the fluid at the most minute level where it still retains its identity as a continuum. That is, we are going to examine an element of fluid that is so small that we can describe flow phenomena on a point by point basis in space, but is still large enough to contain a sufficiently large number of molecules that the thermal-fluid properties can be described by the continuum constitutive relations introduced previously. In formulating this description, we utilize the "conservation" equations that we developed for the control volume in Chapter 8.

We have already seen in Chapter 8 that there are two alternative descriptions of fluid motion: the Lagrangian approach in which we follow the time history of a fluid particle and the Eulerian approach in which we examine the flow at a particular point in space. The two methods are equivalent and lead to the same end result, but each one has its own set of circumstances for which it is the more appropriate method.

In Chapter 8 we saw that in the Lagrangian approach we were concerned with a control

mass, whereas in the Eulerian approach we were concerned with a control volume. The basic physical laws were originally written for a control mass, and we transformed them by means of an important transformation known as the Reynolds Transport Theorem so that they could be applied to a control volume. We now wish to shrink the size of the control volume down to that of a differential element of volume at some point in space as shown in Figure 9.2. The approach

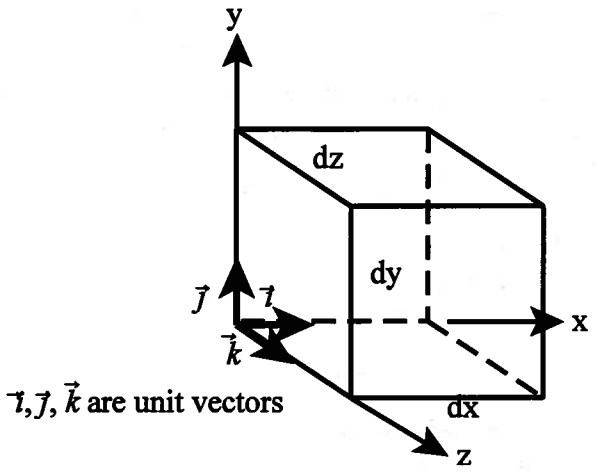

Figure 9.2 Differential Fluid Element

is to follow the time history of a control mass of infinitesimal size, a fluid particle, and to then shrink the time interval of our observation of the history of the particle to zero. In this limit, the fluid particle and the differential volume element become one and the same. The result of this mathematical procedure is the equivalent of the Reynolds Transport Theorem that we used in the case of the finite control volume to transform the time derivative that appears in the Lagrangian approach to the appropriate time derivative for the Eulerian approach. For the differential control volume this transformation is known as the *total derivative* and it provides us with the means to find the proper time rate of change of properties that are specified in terms of both time and the location of the differential control volume in space.

In the Eulerian approach, the properties that describe the flow ρ, T, u, h, s, and $\vec{\vartheta}$ are functions of four independent variables, x, y, z, and t. The values of the properties ρ, T, u, h, s, and $\vec{\vartheta}$ are then specified in terms of the values of the four independent variables, x, y, z, and t. Each property defines a hypersurface in the resulting five-dimensional space. For example,

$$T = T(x, y, z, t) \tag{9.16}$$

defines a hypersurface on which the values of the temperature of the fluid must lie. Similarly, for the velocity vector

$$\vec{\vartheta} = \vartheta_x \vec{i} + \vartheta_y \vec{j} + \vartheta_z \vec{k} \tag{9.17}$$

where

$$\begin{aligned} \vartheta_x &= \vartheta_x(x, y, z, t) \\ \vartheta_y &= \vartheta_y(x, y, z, t) \\ \vartheta_z &= \vartheta_z(x, y, z, t) \end{aligned} \tag{9.18}$$

are the velocity components in the x, y, and z directions.

Consider a fluid particle (which can also be thought of as a control mass denoted by the symbol *CM* as we did in Chapter 8) as it moves a distance Δx, Δy, and Δz in physical space

during the time interval Δt. Let us suppose that we wish to determine the manner in which the fluid temperature changes as the fluid particle moves in space during this time interval. Since the temperature is a function of the four independent variables, x, y, z, and t, it will change by an amount ΔT which will depend upon the amount that each of the independent variables changes. If $\frac{\partial T}{\partial w}$ represents the rate of change of T with respect to the independent variable w, then by the chain rule of differential calculus, the total change in T due to the changes Δw in each of the independent variables is given by

$$\Delta T = \frac{\partial T}{\partial t}\Delta t + \frac{\partial T}{\partial x}\Delta x + \frac{\partial T}{\partial y}\Delta y + \frac{\partial T}{\partial z}\Delta z \tag{9.19}$$

Then if we divide equation (9.19) by Δt, we have

$$\frac{\Delta T}{\Delta t} = \frac{\partial T}{\partial t} + \frac{\partial T}{\partial x}\frac{\Delta x}{\Delta t} + \frac{\partial T}{\partial y}\frac{\Delta y}{\Delta t} + \frac{\partial T}{\partial z}\frac{\Delta z}{\Delta t} \tag{9.20}$$

In the limit as the time interval shrinks to zero ($\Delta t \to 0$), equation (9.20) becomes

$$\left(\frac{dT}{dt}\right)_{CM} = \frac{\partial T}{\partial t} + \left(\frac{dx}{dt}\right)_{CM}\frac{\partial T}{\partial x} + \left(\frac{dy}{dt}\right)_{CM}\frac{\partial T}{\partial y} + \left(\frac{dz}{dt}\right)_{CM}\frac{\partial T}{\partial z} \tag{9.21}$$

where we have used the notation *CM* to identify the derivatives that pertain to the control mass, our fluid particle. Let us now define a new differential operator *D/Dt* such that

$$\frac{D}{Dt} \equiv \left(\frac{d}{dt}\right)_{CM} \tag{9.22}$$

and recognize that the time derivatives of the spatial coordinates traversed by the control mass are simply the instantaneous velocities of the control mass in each of those coordinate directions, viz.

$$\left(\frac{dx}{dt}\right)_{CM} = \vartheta_x, \qquad \left(\frac{dy}{dt}\right)_{CM} = \vartheta_y, \qquad \left(\frac{dz}{dt}\right)_{CM} = \vartheta_z \tag{9.23}$$

Then equation (9.21) becomes

$$\frac{DT}{Dt} = \frac{\partial T}{\partial t} + \vartheta_x\frac{\partial T}{\partial x} + \vartheta_y\frac{\partial T}{\partial y} + \vartheta_z\frac{\partial T}{\partial z} \tag{9.24}$$

where

$$\frac{D}{Dt} = \frac{\partial}{\partial t} + \vartheta_x\frac{\partial}{\partial x} + \vartheta_y\frac{\partial}{\partial y} + \vartheta_z\frac{\partial}{\partial z} \equiv \text{ total derivative} \tag{9.25}$$

Equation (9.24) is also known as the *material derivative* or the *substantial derivative* since it is derived from studying the behavior of a fluid particle. When the total derivative is applied to a property, regardless of whether it is a scalar or a vector, it gives the total time rate of change of that property.

There are two contributions this total time rate of change:

$$\frac{\partial}{\partial t} \tag{9.26}$$

which represents the time rate of change of the property at a given point in space due to the unsteady nature of the flow and is known as the temporal contribution; and

$$\vartheta_x\frac{\partial}{\partial x} + \vartheta_y\frac{\partial}{\partial y} + \vartheta_z\frac{\partial}{\partial z} \tag{9.27}$$

which represents the time rate of change of the property at a given point in space due to the fact

that at a given instant of time, the fluid is at some point in a spatial gradient of that property and is at the same time moving with some velocity in that spatial gradient. This is known as the convective contribution for which the *rate* at which the property changes will depend upon the spatial gradients in the property at the point in question $\left(\frac{\partial}{\partial x}, \frac{\partial}{\partial y}, \text{ and } \frac{\partial}{\partial z}\right)$ *and* the speed at which the fluid is moving at that point ($\hat{v}_x$, $\hat{v}_y$, and $\hat{v}_z$).

To gain some physical sense of the total derivative, consider the following analogy. Imagine yourself riding on a train car or a subway car, and the car is in a tunnel. Suppose that the tunnel is illuminated only by the proverbial light at the end of the tunnel so that the level of illumination in the tunnel will be a function of position in the tunnel as the light entering the tunnel is gradually absorbed by the walls of the tunnel as it travels down the tunnel. That is, there is a spatial gradient in illumination inside the tunnel. The farther into the tunnel the position of observation, the darker it will appear. Now suppose that the car in which you are riding is stopped inside the tunnel and that the intensity of light at the end of the tunnel is modulated in some time-wise fashion such as might occur as a cloud passes over the sun. The time rate of change of light intensity that you would observe by looking out the car window would be that of the rate of change of intensity of the source of illumination. This is equivalent to the first contribution to the total derivative. Now suppose that the light source is fixed in intensity so that there is a fixed spatial gradient in illumination in the tunnel that does not vary with time. Suppose further that the car is now moving in the tunnel. The time rate of change of illumination that you now observe upon looking out the car window will depend upon the spatial gradient in illumination and the speed of the car. This is equivalent to the second contribution to the total derivative.

In a fluid flow field, if the flow is steady, the first contribution to the total derivative vanishes. In a steady, but spatially non-uniform flow field as in a nozzle or diffuser, the fluid velocity can vary in all three directions. As a fluid particle passes through a given point, any one of its properties, such as velocity, changes in response to the spatial variation in the property and the local velocity of the fluid. For example, consider the steady flow of an incompressible fluid in a converging duct as shown in Figure 9.3. As the fluid moves from point A to point B, it speeds up in accordance with the continuity equation. Then even though the flow is steady, the fluid

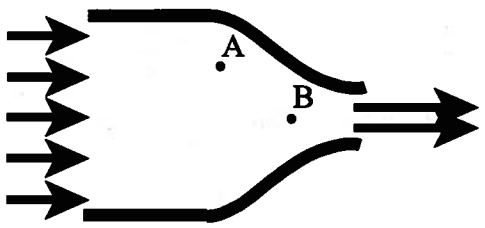

Figure 9.3 Flow in a Converging Duct

accelerates, and this acceleration is described by the convective part of the total derivative.

Thus the total derivative provides information about the rate at which properties of a fluid particle change in the Eulerian approach. In vector notation, it is an operator. Then,

$$\frac{D}{Dt} = \frac{\partial}{\partial t} + \vec{v} \cdot \nabla \tag{9.28}$$

Note that $\vec{v} \cdot \nabla$ is not a scalar product but rather an operator such that

$$\vec{\vartheta}\cdot\nabla=\vartheta_x\frac{\partial}{\partial x}+\vartheta_y\frac{\partial}{\partial y}+\vartheta_z\frac{\partial}{\partial z} \tag{9.29}$$

Note also that since

$$\nabla=\frac{\partial}{\partial x}\vec{i}+\frac{\partial}{\partial y}\vec{j}+\frac{\partial}{\partial z}\vec{k}$$
$$\vec{\vartheta}=\vartheta_x\vec{i}+\vartheta_y\vec{j}+\vartheta_z\vec{k} \tag{9.30}$$

$\nabla\cdot\vec{\vartheta}$, known as the divergence, is an operation but $\vec{\vartheta}\cdot\nabla$ is an operator.

$$\nabla\cdot\vec{\vartheta}=\frac{\partial\vartheta_x}{\partial x}+\frac{\partial\vartheta_y}{\partial y}+\frac{\partial\vartheta_z}{\partial z} \tag{9.31}$$

Thus, the total derivative of a scalar property like the density is

$$\frac{D\rho}{Dt}=\frac{\partial\rho}{\partial t}+\vartheta_x\frac{\partial\rho}{\partial x}+\vartheta_y\frac{\partial\rho}{\partial y}+\vartheta_z\frac{\partial\rho}{\partial z} \tag{9.32}$$

whereas the total derivative in a vector property like the velocity becomes

$$\begin{aligned}\frac{D\vec{\vartheta}}{Dt}=&\left(\frac{\partial\vartheta_x}{\partial t}+\vartheta_x\frac{\partial\vartheta_x}{\partial x}+\vartheta_y\frac{\partial\vartheta_x}{\partial y}+\vartheta_z\frac{\partial\vartheta_x}{\partial z}\right)\vec{i}\\&+\left(\frac{\partial\vartheta_y}{\partial t}+\vartheta_x\frac{\partial\vartheta_y}{\partial x}+\vartheta_y\frac{\partial\vartheta_y}{\partial y}+\vartheta_z\frac{\partial\vartheta_y}{\partial z}\right)\vec{j}\\&+\left(\frac{\partial\vartheta_z}{\partial t}+\vartheta_x\frac{\partial\vartheta_z}{\partial x}+\vartheta_y\frac{\partial\vartheta_z}{\partial y}+\vartheta_z\frac{\partial\vartheta_z}{\partial z}\right)\vec{k}\end{aligned} \tag{9.33}$$

which is the acceleration of the fluid at some point whose Cartesian coordinates are (x, y, z).

We can now use this total derivative to formulate the various "conservation" equations that apply to the differential control volume of Figure 9.2. In formulating these expressions, for the sake of simplicity, we will consider a two-dimensional differential control volume in each case and then extend the results to the three dimensional case.

9.4 Conservation of Mass

In Chapter 8 we showed that the Reynolds Transport Theorem applied to a control mass reduced to

$$\frac{d}{dt}\int_{CV}\rho dV+\int_{CS}\rho\left(\vec{\vartheta}\cdot\vec{n}\right)dA=0 \tag{9.34}$$

but for a rigid control volume fixed in space, equation (9.34) reduces to

$$\int_{CV}\frac{\partial\rho}{\partial t}dV+\int_{CS}\rho\left(\vec{\vartheta}\cdot\vec{n}\right)dA=0 \tag{9.35}$$

Consider the two-dimensional control volume shown in Figure 9.4 with flow through all four of its faces. Because this control volume is of differential size, the first term in equation (9.35) reduces to

$$\int_{CV}\frac{\partial\rho}{\partial t}dV\approx\frac{\partial\rho}{\partial t}dxdy \tag{9.36}$$

and the second term becomes

$$\int_{CS}\rho\left(\vec{\vartheta}\cdot\vec{n}\right)dA=\sum_i\left(\rho_iA_i\vartheta_i\right)_{out}-\sum_i\left(\rho_iA_i\vartheta_i\right)_{in} \tag{9.37}$$

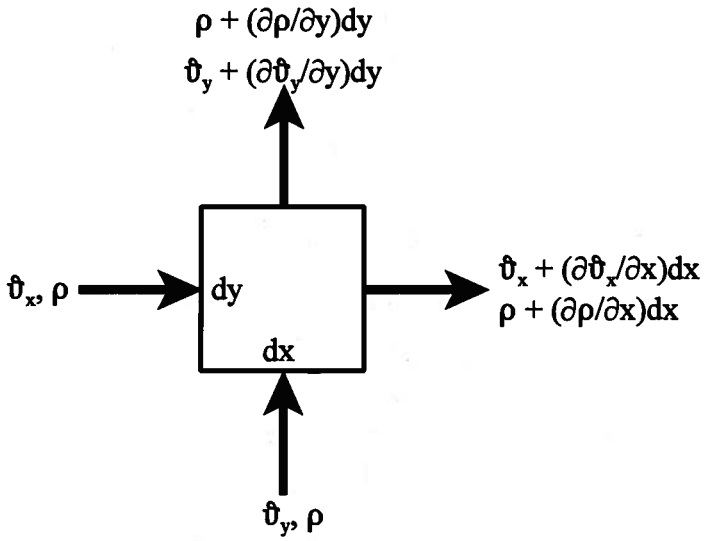

Figure 9.4 Differential Fluid Element Fixed in Space

where

$$\sum_i (\rho_i A_i \vartheta_i)_{out} = \left[\left(\rho + \frac{\partial \rho}{\partial x}dx\right)\left(\vartheta_x + \frac{\partial \vartheta_x}{\partial x}dx\right)\right]dy + \left[\left(\rho + \frac{\partial \rho}{\partial y}dy\right)\left(\vartheta_y + \frac{\partial \vartheta_y}{\partial y}dy\right)\right]dx \quad (9.38)$$

and

$$\sum_i (\rho_i A_i \vartheta_i)_{in} = \rho \vartheta_x dy + \rho \vartheta_y dx \quad (9.39)$$

Carrying out the multiplication in equation (9.38) and neglecting higher order terms, we get

$$\sum_i (\rho_i A_i \vartheta_i)_{out} = \left[\rho \vartheta_x + \rho \frac{\partial \vartheta_x}{\partial x}dx + \vartheta_x \frac{\partial \rho}{\partial x}dx\right]dy + \left[\rho \vartheta_y + \rho \frac{\partial \vartheta_y}{\partial y}dy + \vartheta_y \frac{\partial \rho}{\partial y}dy\right]dx \quad (9.40)$$

Then combining equations (9.37), (9.39), and (9.40), we get

$$\int_{CS} \rho\left(\vec{\vartheta} \cdot \vec{n}\right)dA = \frac{\partial}{\partial x}\left(\rho \vartheta_x\right)dxdy + \frac{\partial}{\partial y}\left(\rho \vartheta_y\right)dxdy \quad (9.41)$$

Substituting equations (9.36) and (9.41) into equation (9.35), we get for the continuity equation

$$\frac{\partial \rho}{\partial t}dxdy + \frac{\partial}{\partial x}\left(\rho \vartheta_x\right)dxdy + \frac{\partial}{\partial y}\left(\rho \vartheta_y\right)dxdy = 0 \quad (9.42)$$

and dividing equation (9.42) through by *dxdy*, we get the two-dimensional continuity equation

$$\frac{\partial \rho}{\partial t} + \frac{\partial}{\partial x}\left(\rho \vartheta_x\right) + \frac{\partial}{\partial y}\left(\rho \vartheta_y\right) = 0 \quad (9.43)$$

but in two dimensions

$$\nabla = \frac{\partial}{\partial x}\vec{i} + \frac{\partial}{\partial y}\vec{j} \quad (9.44)$$

Then the continuity equation in vector notation becomes

$$\frac{\partial \rho}{\partial t} + \nabla \cdot \left(\rho \vec{\vartheta}\right) = 0 \quad (9.45)$$

If we expand equation (9.43), we get

$$\frac{\partial \rho}{\partial t} + \vartheta_x \frac{\partial \rho}{\partial x} + \rho \frac{\partial \vartheta_x}{\partial x} + \vartheta_y \frac{\partial \rho}{\partial y} + \rho \frac{\partial \vartheta_y}{\partial y} = 0$$

$$\left(\frac{\partial \rho}{\partial t}+\vartheta_x\frac{\partial \rho}{\partial x}+\vartheta_y\frac{\partial \rho}{\partial y}\right)+\rho\frac{\partial \vartheta_x}{\partial x}+\rho\frac{\partial \vartheta_y}{\partial y}=0 \tag{9.46}$$

Making use of the definition of the total derivative, we get the vector form of the continuity equation, viz.

$$\frac{D\rho}{Dt}+\rho\nabla\cdot\vec{\vartheta}=0 \tag{9.47}$$

which applies in three dimensions as well.

Note that for an incompressible fluid $D\rho/Dt = 0$ always, so that the continuity equation for this fluid model reduces to $\nabla\cdot\vec{\vartheta}=0$.

9.5 Equation of Linear Momentum for an Inviscid Fluid (Euler Equation)

The differential equation describing the dynamic behavior of a fluid was first derived by Leonhard Euler (1707 - 1783) in 1753 who is the most prolific author of mathematics of all time (886 books and papers). Euler, for whom the Eulerian approach is named, was the first to introduce the concept of the "fluid particle" and, following the example of Daniel Bernoulli with whom he lived from 1730 to 1733, was one of the first mathematicians to use differential and integral calculus to describe fluid behavior. Following Euler's example, we shall first formulate the linear momentum equation for an inviscid fluid model. While this might seem a step backward given the discussion of Section 9.2, the resulting differential equation applies in a fluid flow field remote from the solid surfaces that bound it. In many cases, this is the largest part of the flow. Once we have developed this result, known as the *Euler equation*, we shall use it to determine the effects of the fluid viscosity on the flow.

In formulating the equation of linear momentum, we are concerned with the effects of applied forces acting on the fluid in the flow field. To this end, and keeping with our approach in developing the continuity equation above, we consider the two-dimensional differential control volume shown in Figure 9.5. Two types of forces are of interest here: surface forces and body forces. The only applied surface force that concerns us now is that due to the local pressure acting over each face. The only body force of interest is that due to gravity. If the fluid element is oriented in an arbitrary fashion with respect to gravity, both of these forces contribute to the net force acting along each of the coordinate directions. Then the net force per unit volume F acting

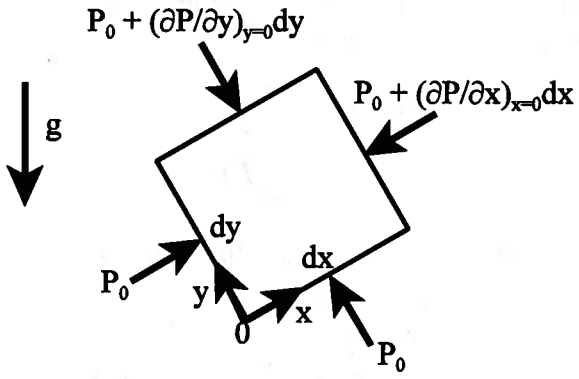

Figure 9.5 Forces Acting on a Differential Fluid Element

on the fluid particle due to surface and body forces is

$$\vec{F}=\vec{F}_{surface}+\vec{F}_{body}=\vec{F}_{\substack{normal\\stresses}}+\vec{F}_{body} \tag{9.48}$$

If we let F_x be the force per unit "volume" *dxdy* due to normal stresses and body forces acting in the *x*-direction

$$F_x dxdy = P_0 dy - \left[P_0 + \left(\frac{\partial P}{\partial x} \right)_{x=0} dx \right] dy + \rho_0 g_x dxdy$$

$$F_x dxdy = -\left(\frac{\partial P}{\partial x} \right)_{x=0} dxdy + \rho_0 g_x dxdy \tag{9.49}$$

Similarly for the *y*-direction, we have

$$F_y dxdy = -\left(\frac{\partial P}{\partial y} \right)_{y=0} dxdy + \rho_0 g_y dxdy \tag{9.50}$$

If we were to extend this analysis to three dimensions in order to include the *z*-direction as well, we would have

$$F_x dxdydz = -\left(\frac{\partial P}{\partial x} \right)_{x=0} dxdydz + \rho_0 g_x dxdydz$$

$$F_y dxdydz = -\left(\frac{\partial P}{\partial y} \right)_{x=0} dxdydz + \rho_0 g_y dxdydz \tag{9.51}$$

$$F_z dxdydz = -\left(\frac{\partial P}{\partial z} \right)_{z=0} dxdydz + \rho_0 g_z dxdydz$$

Then in vector notation (including all three coordinate directions), the net force per unit volume *dxdydz* is

$$\vec{F} = \vec{F}_{\substack{normal \\ stresses}} + \vec{F}_{body} = F_x \vec{i} + F_y \vec{j} + F_z \vec{k}$$

$$\vec{F} = \vec{F}_{\substack{normal \\ stresses}} + \vec{F}_{body} = -\left(\frac{\partial P}{\partial x} \vec{i} + \frac{\partial P}{\partial y} \vec{j} + \frac{\partial P}{\partial z} \vec{k} \right) + \rho g_x \vec{i} + \rho g_y \vec{j} + \rho g_z \vec{k} \tag{9.52}$$

where we have dropped the subscript 0 since the result should apply at any point in the flow field. Making use of the gradient operator of equation (9.30), we have

$$\vec{F} = -\nabla P + \rho \vec{g} \tag{9.53}$$

Having determined the net force acting on the fluid element, we can apply Newton's second law of motion: the applied force is equal to the rate of change of momentum of the fluid particle. Using the acceleration vector defined in equation (9.33), we have

$$\vec{F} dxdydz = \rho \frac{D\vec{\vartheta}}{Dt} dxdydz$$

$$\vec{F} = \rho \frac{D\vec{\vartheta}}{Dt} \tag{9.54}$$

Substituting equation (9.53) into (9.54), we obtain the Euler equation

$$\rho \frac{D\vec{\vartheta}}{Dt} = -\nabla P + \rho \vec{g} \tag{9.55}$$

Equation (9.55) represents the equation of linear momentum in the Eulerian approach. Notice that the terms appearing on the right-hand side of equation (9.55) are the forces per unit volume acting on a fluid particle in the flow field. In particular, notice that the "pressure force" per unit volume is due to the gradient in the pressure, not the pressure itself, acting on the fluid particle.

If we divide equation (9.55) through by the density, we obtain an expression in which all of the terms have the units of acceleration, viz.

$$\frac{D\vec{\vartheta}}{Dt} = -\frac{1}{\rho}\nabla P + \vec{g} \tag{9.56}$$

The left-hand side represents the acceleration of a fluid particle in the Eulerian representation while the first term on the right-hand side represents the acceleration of a fluid particle due to the *gradient* in the pressure and the second term on the right-hand side represents the acceleration of a fluid particle due to the effect of gravity. Equation (9.56) is a vector equation since the acceleration is a vector quantity; therefore, equation (9.56) is really three separate equations, one for each coordinate direction.

$$\begin{aligned}
\frac{\partial \vartheta_x}{\partial t} + \vartheta_x\frac{\partial \vartheta_x}{\partial x} + \vartheta_y\frac{\partial \vartheta_x}{\partial y} + \vartheta_z\frac{\partial \vartheta_x}{\partial z} &= -\frac{1}{\rho}\frac{\partial P}{\partial x} + g_x \\
\frac{\partial \vartheta_y}{\partial t} + \vartheta_x\frac{\partial \vartheta_y}{\partial x} + \vartheta_y\frac{\partial \vartheta_y}{\partial y} + \vartheta_z\frac{\partial \vartheta_y}{\partial z} &= -\frac{1}{\rho}\frac{\partial P}{\partial y} + g_y \\
\frac{\partial \vartheta_z}{\partial t} + \vartheta_x\frac{\partial \vartheta_z}{\partial x} + \vartheta_y\frac{\partial \vartheta_z}{\partial y} + \vartheta_z\frac{\partial \vartheta_z}{\partial z} &= -\frac{1}{\rho}\frac{\partial P}{\partial z} + g_z
\end{aligned} \tag{9.57}$$

(Note that if the y-axis is directed vertically upward, $g_x = 0$, $g_y = -g$, and $g_z = 0$.) Since the Euler equation does not include the viscous forces acting on the fluid element, if we apply it to a real fluid that does have viscous effects, it cannot be applied in the region near the solid surfaces that bound the fluid (known as the boundary layer) where there is fluid shear due to the momentum transfer between the wall and the fluid resulting from the action of the viscosity of the fluid. The Euler equation applies only in that region where viscous effects are negligible far from the boundaries. The Euler equation applies to both compressible and incompressible fluid models.

Example 9E.1: In Section 5.3 of Chapter 5 we considered the case for which a piston traveled at constant velocity in a cylinder containing a compressible fluid that we modeled as an ideal gas. We saw that if the motion of the piston was in a direction to compress the gas, there was a compression wave of small amplitude that propagated through the gas with a speed ϑ_s. The compression of the gas that resulted from the passage of the wave was sufficiently rapid that it could be modeled as adiabatic. Furthermore, if the amplitude of the wave was sufficiently small, the compression process could be modeled as reversible as well. Under these conditions, no entropy is generated by the wave (The eventual damping of the wave is another matter entirely!) and the speed is given by

$$\vartheta_s^2 = \left(\frac{\partial P}{\partial \rho}\right)_s$$

where ϑ_s is the speed of sound and the subscript s on the partial derivative indicates that the derivative should be taken in a plane on which the entropy is constant. We showed in Section 5.3 that for the ideal gas model

$$\vartheta_s = \sqrt{\gamma RT}$$

where $\gamma = c_P/c_v$, the ratio of the two specific heats, and R is the gas constant.

We now consider the case for which the motion of the piston is sinusoidal, i.e., the piston moves back and forth (oscillates) in the cylinder such that its position relative to the midpoint of its travel, x_0, is given by

$$x - x_0 = A\sin\omega t$$

where ω is the frequency of the motion in radians and A is the amplitude of the oscillation. As a result of this motion, the gas in the cylinder is alternately compressed and expanded, and the "disturbance" associated with this alternating compression and expansion propagates into the gas inside the cylinder at a velocity of ϑ_s. This "disturbance" constitutes a longitudinal plane wave, a sound wave, propagating from the piston face into the gas. [Note: There are two types of waves in material media that involve a deformation of the medium: (1) those in which the deformation of the medium takes place in the direction of propagation, and (2) those in which the deformation of the medium is perpendicular to the direction of propagation. The first type of wave is known as a *longitudinal* wave, and the second type is known as a *transverse* wave. In a longitudinal wave, the deformation is a compression or expansion of the medium, but in a transverse wave, the deformation is a shearing deformation of the medium. In a solid, both types of waves may exist, but they travel at different velocities with the velocity of the longitudinal wave always the greater of the two. In an inviscid fluid, shear deformations cannot occur so only longitudinal waves are possible.] The sound wave manifests itself as a local perturbation in the density and the pressure of the gas, as well as a perturbation in the local velocity of the gas.

We now show that by applying the continuity equation and the Euler equation to the gas, we can quantitate the behavior of the density of a one-dimensional traveling sound wave propagating from the piston face.

Solution: For the present purpose, we consider the cylinder to be infinitely long so that we do not have to deal with the events that occur when the wave reaches the far end of the cylinder. For the case of a wave propagating in the x-direction only, we can write the continuity equation in the form [*cf.* equation (9.46)]

$$\frac{\partial \rho}{\partial t} + \vartheta_x \frac{\partial \rho}{\partial x} + \rho \frac{\partial \vartheta_x}{\partial x} = 0$$

and the Euler equation [*cf.* equation(9.57)] becomes

$$\rho\left(\frac{\partial \vartheta_x}{\partial t} + \vartheta_x \frac{\partial \vartheta_x}{\partial x}\right) = -\frac{\partial P}{\partial x}$$

Let us now suppose that as a result of the passage of the compression wave (sound wave), the are slight local perturbations in the pressure, density, and velocity of the gas such that

$$P = P_0 + P^*,\ \rho = \rho_0 + \rho^*,\ \text{and}\ \vartheta_x = \vartheta_0 + \vartheta_x^*$$

where the subscript 0 indicates the rest state (so that $\vartheta_0 = 0$) and the starred quantities represent the perturbations associated with the passage of the sound wave.

If we now substitute these quantities into the one-dimensional forms of the continuity equation and the Euler equation and neglect terms that involve the products of the perturbation quantities, we get

$$\frac{\partial \rho}{\partial t} + \vartheta_x \cancel{\frac{\partial \rho_0}{\partial x}} + \cancel{\vartheta_x \frac{\partial \rho^*}{\partial x}} + \rho_0 \frac{\partial \vartheta_x}{\partial x} + \cancel{\rho^* \frac{\partial \vartheta_x}{\partial x}} = 0$$

$$\frac{\partial \rho}{\partial t} + \rho_0 \frac{\partial \vartheta_x}{\partial x} = 0$$

and

$$\rho_0 \frac{\partial \vartheta_x}{\partial t} + \cancel{\rho^* \frac{\partial \vartheta_x}{\partial t}} + \cancel{\vartheta_x \frac{\partial \vartheta_x}{\partial x}} = 0$$

$$\rho_0 \frac{\partial \vartheta_x}{\partial t} = -\frac{\partial P}{\partial x}$$

But

$$\frac{\partial P}{\partial x}=\left(\frac{\partial P}{\partial \rho}\right)_s\left(\frac{\partial \rho}{\partial x}\right)_s=-\vartheta_s^2\left(\frac{\partial \rho}{\partial x}\right)_s$$

where the subscript s indicates that we are considering reversible, adiabatic (isentropic) compression waves. Then the Euler equation becomes

$$\rho_0\frac{\partial \vartheta_x}{\partial t}=-\vartheta_s^2\left(\frac{\partial \rho}{\partial x}\right)$$

Now combining this last result with the continuity equation, we get → sub in Euler equation

$$\frac{\partial^2\rho}{\partial t^2}=-\rho_0\frac{\partial}{\partial t}\left(\frac{\partial \vartheta_x}{\partial x}\right)=-\rho_0\frac{\partial}{\partial x}\left(\frac{\partial \vartheta_x}{\partial t}\right)=\rho_0\frac{\partial}{\partial x}\left(\frac{1}{\rho_0}\vartheta_s^2\frac{\partial \rho}{\partial x}\right)$$

time derivative of continuity ← → switch derivatives

$$\frac{\partial^2\rho}{\partial t^2}=\vartheta_s^2\frac{\partial^2\rho}{\partial x^2}$$

which is the well-known wave equation. The general solution of this equation is

$$\rho(x,t)=f(x+\vartheta_s t)+g(x-\vartheta_s t)$$

where f and g are arbitrary functions that depend only on the values of $x+\vartheta_s t$ and $x-\vartheta_s t$, respectively. To an observer traveling with velocity $dx/dt=-\vartheta_s$, the value of $x+\vartheta_s t$ would appear constant; thus the first term in the solution represents the motion of a "disturbance" in the negative x-direction. The second term represents another wave moving in the positive x-direction with the velocity $dx/dt=\vartheta_s$. In each case there is no change in the shape and magnitude of the "deformation" as it propagates in its respective direction. Clearly, in the present case we are interested only in the wave propagating in the positive x-direction. Then, guided by the form of the disturbance (the movement of the piston), we can write the solution of the wave equation describing the local density as

$$\rho(x,t)=\rho_0+B\sin\beta(x-\vartheta_s t)$$

where B is the amplitude of the perturbation in the density. At $t=0$, the profile of this wave is $B\sin\beta x$ which is a sine wave of wavelength $\lambda=2\pi/\beta$. Then the wave form becomes

$$\rho(x,t)=\rho_0+B\sin\frac{2\pi}{\lambda}(x-\vartheta_s t)$$

At any fixed value of time, say t_0, the density varies sinusoidally in x with a wavelength of λ. At some time Δt later, the whole sinusoidal curve describing the density is displaced in the positive x-direction by an amount $\Delta x=\vartheta_s\Delta t$. This gives rise to the notion of a "traveling" wave. On the other hand, at any fixed position in the cylinder, the density varies sinusoidally with time. Thus, there are *two* sinusoidal variations in this traveling wave.

9.6 Newtonian Fluid Model

We now wish to take into account the effects of viscosity on the dynamic behavior of a fluid as outlined in Section 9.2. In order to do this, we need to develop a fluid model that accounts for the relationship between viscosity and friction in fluid flow fields. Sir Isaac Newton (1643 - 1727) was one of the first to propose such a relationship in 1687 in his treatise of the "new physics," *Philosophiae Naturalis Principia Mathematica.* In *Principia*, Newton concluded that the shear stress developed by fluid friction is given by the product of the coefficient of viscosity and the velocity gradient as shown in equation (9.2). This expression forms the basis of

a model which has become known as the "Newtonian" fluid model in his honor. The Newtonian fluid model states that the viscous stress in a Newtonian fluid is proportional to the rate of strain. The model developed from this simple statement encompasses a vast array of fluids, such as water, air, and oil plus a host of other fluids that are commonly found in thermal-fluid systems. In fact, the Newtonian fluid model is so all-encompassing that the exceptions to it, such as paint, liquid polymers, and a variety of food stuffs, form the basis of a new branch of thermal-fluids engineering known as non-Newtonian fluid mechanics.

Although the Newtonian fluid model applies to both compressible and incompressible fluids, we shall consider here only the incompressible case. While at first glance this may seem overly restrictive, it turns out (as we shall soon show) that the incompressible model applies even to the flow of fluids like gases that we normally think of as being compressible *provided the flow velocities are less than 30 percent of the speed of sound.* The incompressible Newtonian fluid model presents the stress/rate-of-strain relationship in terms of a set of constitutive relations between the shear stresses and the corresponding rates-of-strain in the fluid, viz.

$$\tau_{xx} = 2\mu\frac{\partial \vartheta_x}{\partial x}, \qquad \tau_{yy} = 2\mu\frac{\partial \vartheta_y}{\partial y}, \qquad \tau_{zz} = 2\mu\frac{\partial \vartheta_z}{\partial z}$$

$$\tau_{xy} = \tau_{yx} = \mu\left(\frac{\partial \vartheta_x}{\partial y} + \frac{\partial \vartheta_y}{\partial x}\right)$$

$$\tau_{xz} = \tau_{zx} = \mu\left(\frac{\partial \vartheta_z}{\partial x} + \frac{\partial \vartheta_x}{\partial z}\right) \tag{9.58}$$

$$\tau_{yz} = \tau_{zy} = \mu\left(\frac{\partial \vartheta_y}{\partial z} + \frac{\partial \vartheta_z}{\partial y}\right)$$

where μ is the now familiar coefficient of viscosity. Notice that we have introduced the normal stresses τ_{ii} which are due to extensional rates-of-strain. Since the viscosity is *isotropic* (equal in all directions) in the Newtonian fluid model, these normal stresses are directly proportional to the extensional rates-of-strain with the same constant of proportionality as the shear stresses are proportional to the shear strain rates.

9.7 Navier-Stokes Equation

In order to take into account the effect of viscosity on fluid motion, we need to develop the equation of linear momentum for a viscous fluid. To do this, we need to formulate an expression for the viscous surface forces in terms of the viscous stresses introduced above. Again, in the interests of simplicity, we resort to the two-dimensional differential fluid element shown in Figure 9.6.

If $F_{x,viscous}$ represents the viscous surface force per unit "volume" (the two-dimensional "volume" *dxdy*) acting in the *x*-direction, we have for the *x*-component of the viscous surface force

$$F_{x,viscous}dxdy = -\tau_{xx}dy + \left(\tau_{xx}dy + \frac{\partial \tau_{xx}}{\partial x}dxdy\right) - \tau_{yx}dx + \left(\tau_{yx}dx + \frac{\partial \tau_{yx}}{\partial y}dydx\right)$$

$$F_{x,viscous}dxdy = \frac{\partial \tau_{xx}}{\partial x}dxdy + \frac{\partial \tau_{yx}}{\partial y}dxdy$$

$$F_{x,viscous} = \frac{\partial \tau_{xx}}{\partial x} + \frac{\partial \tau_{yx}}{\partial y} \tag{9.59}$$

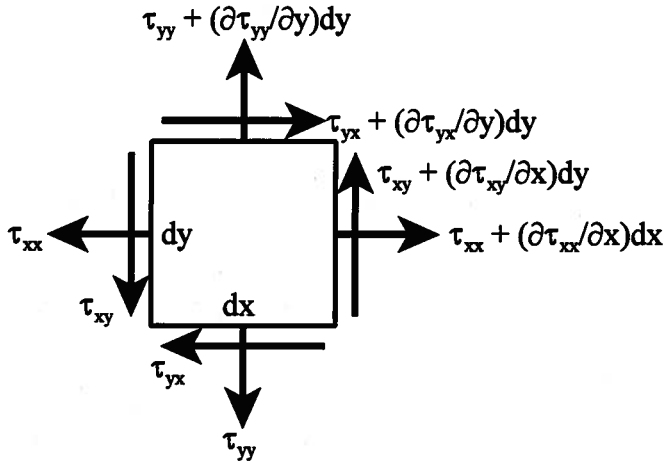

Figure 9.6 Viscous Stresses on a Two-Dimensional Differential Fluid Element

If we extend the result of equation (9.59) to three dimensions, the *x*-component of the viscous surface force per unit volume (*dxdydz*) becomes

$$F_{x,viscous} = \frac{\partial \tau_{xx}}{\partial x} + \frac{\partial \tau_{yx}}{\partial y} + \frac{\partial \tau_{zx}}{\partial z} \tag{9.60}$$

Similarly for the *y*- and *z*-components, we have

$$\begin{aligned} F_{y,viscous} &= \frac{\partial \tau_{xy}}{\partial x} + \frac{\partial \tau_{yy}}{\partial y} + \frac{\partial \tau_{zy}}{\partial z} \\ F_{z,viscous} &= \frac{\partial \tau_{xz}}{\partial x} + \frac{\partial \tau_{yz}}{\partial y} + \frac{\partial \tau_{zz}}{\partial z} \end{aligned} \tag{9.61}$$

If we substitute the stress/rate-of-strain constitutive relations given in equation (9.58) into equations (9.60) and (9.61) and make use of the continuity equation, we obtain for the three components of the viscous surface force per unit volume

$$\begin{aligned} F_{x,viscous} &= \mu\left(\frac{\partial^2 \vartheta_x}{\partial x^2} + \frac{\partial^2 \vartheta_x}{\partial y^2} + \frac{\partial^2 \vartheta_x}{\partial z^2}\right) \\ F_{y,viscous} &= \mu\left(\frac{\partial^2 \vartheta_y}{\partial x^2} + \frac{\partial^2 \vartheta_y}{\partial y^2} + \frac{\partial^2 \vartheta_y}{\partial z^2}\right) \\ F_{z,viscous} &= \mu\left(\frac{\partial^2 \vartheta_z}{\partial x^2} + \frac{\partial^2 \vartheta_z}{\partial y^2} + \frac{\partial^2 \vartheta_z}{\partial z^2}\right) \end{aligned} \tag{9.62}$$

Since the Laplacian operator ∇^2 in Cartesian coordinates is given by $\nabla^2 = \left(\frac{\partial^2}{\partial x^2} + \frac{\partial^2}{\partial y^2} + \frac{\partial^2}{\partial z^2}\right)$, the Laplacian operating on the velocity vector gives

$$\nabla^2 \vec{\vartheta} = \left(\frac{\partial^2 \vartheta_x}{\partial x^2} + \frac{\partial^2 \vartheta_x}{\partial y^2} + \frac{\partial^2 \vartheta_x}{\partial z^2}\right)\vec{i} + \left(\frac{\partial^2 \vartheta_y}{\partial x^2} + \frac{\partial^2 \vartheta_y}{\partial y^2} + \frac{\partial^2 \vartheta_y}{\partial z^2}\right)\vec{j} + \left(\frac{\partial^2 \vartheta_z}{\partial x^2} + \frac{\partial^2 \vartheta_z}{\partial y^2} + \frac{\partial^2 \vartheta_z}{\partial z^2}\right)\vec{k} \tag{9.63}$$

Then we can write the viscous surface force per unit volume in vector form as

$$\vec{F}_{viscous} = \mu \nabla^2 \vec{\vartheta} \tag{9.64}$$

Now we can combine equation (9.53) (the "pressure" force and the body force due to gravity)

and equation (9.64) (the viscous force) to obtain the net force per unit volume acting on a fluid particle, viz.

$$\vec{F}_{net} = \vec{F}_{pressure} + \vec{F}_{body} + \vec{F}_{viscous}$$
$$\vec{F}_{net} = -\nabla P + \rho\vec{g} + \mu\nabla^2\vec{\vartheta} \tag{9.65}$$

If we now substitute equation (9.65) into Newton's second law of motion, equation (9.54), we obtain the well-known Navier-Stokes equation. This is the equation of linear momentum for an

$$\rho\frac{D\vec{\vartheta}}{Dt} = -\nabla P + \rho\vec{g} + \mu\nabla^2\vec{\vartheta} \tag{9.66}$$

incompressible viscous fluid.

It is interesting to note that this equation was first formulated in 1822 by a Frenchman, Claude Louis Marie Henri Navier (1785 - 1836) who was a student of Jean Baptiste Joseph Fourier (1768 - 1830) whom we have already identified for his pioneering contributions to the theory of heat transfer by conduction. Although Navier had the correct form of equation (9.66), he did not fully understand the physics of the situation he was trying to model. He did not understand the concept of shear stress in a fluid, but rather he based his work on an attempt to modify the Euler equation to take into account forces between the molecules in the fluid. In Navier's formulation of equation (9.66), the viscosity appeared as a constant coefficient, but he failed to realize its physical significance. It was not until 1843 that another Frenchman, Jean Claude Barre de Saint-Venant (1797 - 1886) recognized that this coefficient was indeed the viscosity of the fluid. Independently, Sir George Gabriel Stokes (1819 - 1903) published a similar derivation of equation (9.66) in 1845. However, this equation was first viewed with some skepticism. When the Navier-Stokes equation became generally known in the mid-nineteenth century, investigators who tried to apply it to their data for flow in a circular pipe found that sometimes it was valid and sometimes it was not. The reason for this apparent dilemma will become apparent in Section 9.8. Nevertheless, equation (9.66) is an extremely important result in thermal-fluids engineering that now bears the names of Navier and Stokes despite the pivotal role played by Saint-Venant.

For the case of rectangular Cartesian coordinates, we can write the Navier-Stokes equation in component form:

$$\left.\begin{aligned}
\rho\left(\frac{\partial\vartheta_x}{\partial t} + \vartheta_x\frac{\partial\vartheta_x}{\partial x} + \vartheta_y\frac{\partial\vartheta_x}{\partial y} + \vartheta_z\frac{\partial\vartheta_x}{\partial z}\right) &= -\frac{\partial P}{\partial x} + \rho g_x + \mu\left(\frac{\partial^2\vartheta_x}{\partial x^2} + \frac{\partial^2\vartheta_x}{\partial y^2} + \frac{\partial^2\vartheta_x}{\partial z^2}\right) \quad (9.67a)\\
\rho\left(\frac{\partial\vartheta_y}{\partial t} + \vartheta_x\frac{\partial\vartheta_y}{\partial x} + \vartheta_y\frac{\partial\vartheta_y}{\partial y} + \vartheta_z\frac{\partial\vartheta_y}{\partial z}\right) &= -\frac{\partial P}{\partial y} + \rho g_y + \mu\left(\frac{\partial^2\vartheta_y}{\partial x^2} + \frac{\partial^2\vartheta_y}{\partial y^2} + \frac{\partial^2\vartheta_y}{\partial z^2}\right) \quad (9.67b)\\
\rho\left(\frac{\partial\vartheta_z}{\partial t} + \vartheta_x\frac{\partial\vartheta_z}{\partial x} + \vartheta_y\frac{\partial\vartheta_z}{\partial y} + \vartheta_z\frac{\partial\vartheta_z}{\partial z}\right) &= -\frac{\partial P}{\partial z} + \rho g_z + \mu\left(\frac{\partial^2\vartheta_z}{\partial x^2} + \frac{\partial^2\vartheta_z}{\partial y^2} + \frac{\partial^2\vartheta_z}{\partial z^2}\right) \quad (9.67c)
\end{aligned}\right\}$$

In equation (9.67), there are four unknowns, P, ϑ_x, ϑ_y, and ϑ_z, and we need four equations by which we can solve for these unknowns. For this purpose, the continuity equation must be included along with equation (9.67). For the incompressible fluid model used in the development of equation (9.67), it follows that

$$\frac{D\rho}{Dt} = 0 \tag{9.68}$$

and the continuity equation, equation (9.47), reduces to

$$\nabla\cdot\vec{\vartheta} = 0 \tag{9.69}$$

In Cartesian coordinates, equation (9.69) becomes

$$\frac{\partial \vartheta_x}{\partial x}+\frac{\partial \vartheta_y}{\partial y}+\frac{\partial \vartheta_z}{\partial z}=0 \tag{9.70}$$

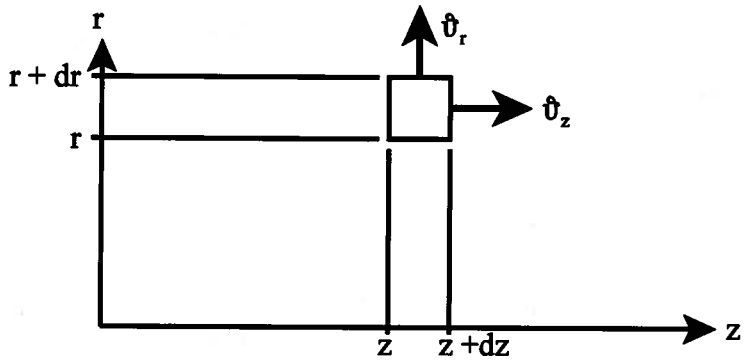

(a) r - z plane

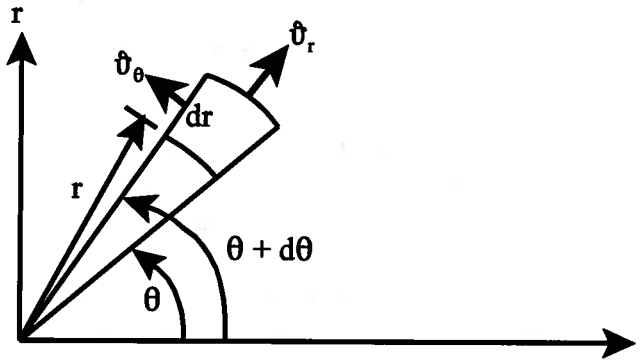

(b) r - θ plane (z-axis normal to plane of figure)

Figure 9.7 Differential Fluid Element in Cylindrical Coordinates

The geometry of many thermal-fluid devices such as pipes, tubes, and cylinders, is cylindrical. The study of the dynamics of fluid flow in these devices is most conveniently accomplished if the Navier-Stokes equation and the continuity equation are posed in cylindrical coordinates r, θ, z, and t. Figure 9.7 shows a differential fluid element in these cylindrical coordinates.

In cylindrical coordinates r, θ, z, and t the continuity equation for the incompressible fluid model is given by

$$\frac{1}{r}\frac{\partial}{\partial r}(r\vartheta_r)+\frac{1}{r}\frac{\partial}{\partial \theta}(\vartheta_\theta)+\frac{\partial}{\partial z}(\vartheta_z)=0 \tag{9.71}$$

The viscous stresses in this coordinate system are given by

$$\tau_{rr}=2\mu\frac{\partial \vartheta_r}{\partial r}, \qquad \tau_{\theta\theta}=2\mu\left(\frac{1}{r}\frac{\partial \vartheta_\theta}{\partial \theta}+\frac{\vartheta_r}{r}\right), \qquad \tau_{zz}=2\mu\frac{\partial \vartheta_z}{\partial z}$$

$$\tau_{r\theta}=\tau_{\theta r}=\mu\left[r\frac{\partial}{\partial r}\left(\frac{\vartheta_\theta}{r}\right)+\frac{1}{r}\frac{\partial \vartheta_r}{\partial \theta}\right], \quad \tau_{\theta z}=\tau_{z\theta}=\mu\left(\frac{\partial \vartheta_\theta}{\partial z}+\frac{1}{r}\frac{\partial \vartheta_z}{\partial \theta}\right), \quad \tau_{zr}=\tau_{rz}=\mu\left(\frac{\partial \vartheta_r}{\partial z}+\frac{\partial \vartheta_z}{\partial r}\right) \tag{9.72}$$

The r-, θ-, and z-components of the Navier-Stokes equation in cylindrical coordinates for the incompressible fluid model with constant viscosity are given by, respectively

$$\rho\left(\frac{\partial \vartheta_r}{\partial t}+\vartheta_r\frac{\partial \vartheta_r}{\partial r}+\frac{\vartheta_\theta}{r}\frac{\partial \vartheta_r}{\partial \theta}-\frac{\vartheta_\theta^{\,2}}{r}+\vartheta_z\frac{\partial \vartheta_r}{\partial z}\right)$$
$$=-\frac{\partial P}{\partial r}+\rho g_r+\mu\left[\frac{\partial}{\partial r}\left(\frac{1}{r}\frac{\partial}{\partial r}(r\vartheta_r)\right)+\frac{1}{r^2}\frac{\partial^2 \vartheta_r}{\partial \theta^2}-\frac{2}{r^2}\frac{\partial \vartheta_\theta}{\partial \theta}+\frac{\partial^2 \vartheta_r}{\partial z^2}\right] \tag{9.73a}$$

$$\rho\left(\frac{\partial \vartheta_\theta}{\partial t}+\vartheta_r\frac{\partial \vartheta_\theta}{\partial r}+\frac{\vartheta_\theta}{r}\frac{\partial \vartheta_\theta}{\partial \theta}-\frac{\vartheta_r\vartheta_\theta}{r}+\vartheta_z\frac{\partial \vartheta_\theta}{\partial z}\right)$$
$$=-\frac{1}{r}\frac{\partial P}{\partial \theta}+\rho g_\theta+\mu\left[\frac{\partial}{\partial r}\left(\frac{1}{r}\frac{\partial}{\partial r}(r\vartheta_\theta)\right)+\frac{1}{r^2}\frac{\partial^2 \vartheta_\theta}{\partial \theta^2}-\frac{2}{r^2}\frac{\partial \vartheta_r}{\partial \theta}+\frac{\partial^2 \vartheta_\theta}{\partial z^2}\right] \tag{9.73b}$$

$$\rho\left(\frac{\partial \vartheta_z}{\partial t}+\vartheta_r\frac{\partial \vartheta_z}{\partial r}+\frac{\vartheta_\theta}{r}\frac{\partial \vartheta_z}{\partial \theta}-\frac{\vartheta_\theta^{\,2}}{r}+\vartheta_z\frac{\partial \vartheta_z}{\partial z}\right)$$
$$=-\frac{\partial P}{\partial z}+\rho g_z+\mu\left[\frac{1}{r}\frac{\partial}{\partial r}\left(r\frac{\partial \vartheta_z}{\partial r}\right)+\frac{1}{r^2}\frac{\partial^2 \vartheta_z}{\partial \theta^2}+\frac{\partial^2 \vartheta_z}{\partial z^2}\right] \tag{9.73c}$$

The Navier-Stokes equation is a non-linear, second-order, partial differential equation as is the Euler equation. Because of the non-linear nature of these equations inherent in the convective term on the left-hand side of equation (9.67) [and equation (9.57) as well] there are no general solutions. However, there are solutions of the Navier-Stokes equation in special cases commonly encountered in thermal-fluids engineering for which the non-linear terms vanish. These are known as fully-developed flows in which the viscous forces dominate and occur at low values of the Reynolds number, and we shall discuss several of the more important cases shortly.

Similarly, for flows in which viscous forces are not important, there are solutions of the Euler equation in special cases known as irrotational flows for which the average angular velocity of every fluid particle is zero. With this information, thermal-fluids engineers can determine the pressure distribution over bodies, such as aerodynamic shapes like aircraft wings and fuselages, immersed in the flow. In fact, this work forms a special subset of thermal-fluids engineering known as aerodynamics. Knowing the pressure distribution on these shapes, the aerodynamicist can then calculate the lift force acting on them. While this work is extremely important (particularly in the aircraft industry), it is outside the scope of the present treatment and we shall not consider it here. Rather, we shall focus our attention on the Navier-Stokes equation which will enable us to determine the drag force acting on these shapes. This information will enable us to design the propulsion plants required to power these vehicles.

The development of powerful, high-speed computers has facilitated the solution of both the Navier-Stokes equation and the Euler equation for more complex cases that are beyond our mathematical capabilities to obtain closed form analytical solutions. This has led to a relatively new subset of thermal-fluids engineering known as computational fluid dynamics. These are the techniques used, for example, to solve the Euler equation for an entire commercial aircraft flying at near sonic speed or to solve the Navier-Stokes equation for the flow field characteristics of a viscous fluid such as water flowing through a complex shape such as the impeller of a pump. Unfortunately, these numerical methods are also outside the scope of the present treatment and will not be considered here.

At this point in our development, what we can do is study those special cases for which

we can develop solutions to the Navier-Stokes equation. However, in order to do this, we need a set of boundary conditions. For the Newtonian fluid model, we have two. At the solid surface bounding the fluid (the wall), we have the no-slip boundary condition in which the fluid "sticks" to the wall so that the velocity of the fluid relative to the wall is zero. In addition, there is no flow through the wall. Then for a stationary wall with a fluid flowing in the x-direction, the boundary conditions become

$$\begin{aligned} \vartheta_x &= 0 \quad \text{(no slip boundary condition)} \\ \vartheta_y &= 0 \quad \text{(no flow through the wall boundary condition)} \end{aligned} \tag{9.74}$$

If the fluid is a liquid that forms a free surface as in the case of an open channel flow, for example, there is an additional boundary condition. Suppose for example that the fluid flowing is water and that it forms a free surface with the atmosphere. From Table 9.1, we note that the viscosity of water is

$$\mu_{water} \sim 10^{-3} \text{ kg/m sec}$$

and that of air is

$$\mu_{air} \sim 1.8 \times 10^{-5} \text{ kg/m sec}$$

Then

$$\frac{\mu_{water}}{\mu_{air}} \sim 50$$

Since the shear stress at the interface between the two fluids is the same, for one-dimensional flow we have

$$(\tau_{air})_{interface} = (\tau_{water})_{interface}$$

or

$$\mu_{air}\left(\frac{d\vartheta_x}{dy}\right)_{air} = \mu_{water}\left(\frac{d\vartheta_x}{dy}\right)_{water}$$

$$\left(\frac{d\vartheta_x}{dy}\right)_{water} = \frac{\mu_{air}}{\mu_{water}}\left(\frac{d\vartheta_x}{dy}\right)_{air} \sim \frac{1}{50}\left(\frac{d\vartheta_x}{dy}\right)_{air}$$

It follows, then, that if we assume the shear stress exerted on the water by the air at the free surface is small, the velocity gradient in the air is also small. Then the velocity gradient in the water is nearly an order of magnitude smaller. Thus we are justified in taking the velocity gradient in the liquid at the free surface to be vanishingly small, i.e., zero. Physically, this is equivalent to saying that the shear stress at the interface is zero. Then despite the fact that the liquid does actually "drag" some of the gas along as it moves, we model the free surface of the liquid as one on which there is no shear stress. The boundary condition at the free surface then becomes

$$\begin{aligned} \tau_{free\ surface} &= 0 \\ \left(\frac{d\vartheta_x}{dy}\right)_{free\ surface} &= 0 \end{aligned} \tag{9.75}$$

9.8 Reynolds Number

As we alluded to in Section 9.8, the solutions that we are about to develop for the Navier-Stokes equation are *mathematically valid* solutions for all values of the parameters involved;

however, experiment shows that these solutions are *physically valid* only for a certain range of these parameters. Outside this range of values, mathematically valid solutions become physically absurd because under certain conditions, the nature of the flow changes dramatically. In the mid-nineteenth century, when the Navier-Stokes equation was applied to flow in a pipe of circular cross-section, this equation predicted a linear relationship between the pressure drop in the flow and the average velocity of the fluid. Experiments showed that sometimes the linear relationship was valid, but at other times the pressure drop depended more nearly upon the square of the velocity as shown schematically (not actual data) in Figure 9.8.

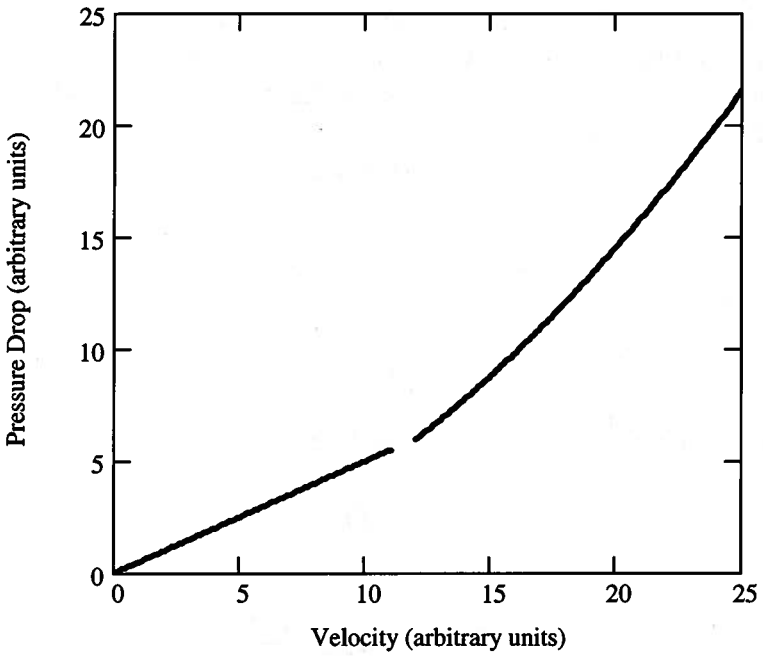

Figure 9.8 Pressure Drop in Pipe Flow (Break in plot indicates change in type of flow.)

It was not until 1883 when Osborne Reynolds (of Reynolds Transport Theorem fame) performed a series of very carefully controlled experiments involving the injection of dye into fluid flowing a circular tube that the underlying physics of this dilemma became apparent. Reynolds found that, indeed, two types of flow do exist: one at relatively low velocities in which the fluid particles slide smoothly past each other in a laminar fashion and produce a linear relationship between pressure drop and average fluid velocity; the other at somewhat higher velocities in which the fluid particles follow a sinuous path that eventually breaks down into a random or turbulent motion and produce a non-linear relationship between pressure drop and average fluid velocity. Reynolds showed that the transition from laminar to turbulent flow depended not just on the velocity, $\hat{v}$, of the fluid but on the parameter $\hat{v}D\rho/\mu$ where D is the diameter of the circular tube. This dimensionless number is now named the Reynolds number in his honor and is usually designated by the symbol *Re*.

The Reynolds number serves to classify many types of flows, not just flow in a circular pipe, provided that the Reynolds number is properly defined in these other geometries. In general, small values of the Reynolds number imply that laminar flow conditions prevail while large values of the Reynolds number imply that turbulent flow prevails. There is usually a critical value of the Reynolds number at which the transition from laminar to turbulent flow occurs. The numerical value of the critical Reynolds number depends upon the flow geometry. For example, for flow in a circular conduit, the transition from laminar to turbulent occurs at a value of

Reynolds number of approximately 2300. In any given case, the value of the critical Reynolds number will vary somewhat since the transition is also influenced by outside disturbances such as background vibrations in the apparatus or the previous history of the turbulence in the fluid. Thus there is actually a range of values over which one might expect the transition to occur. For the purposes of designing thermal-fluid systems, there is a generally accepted value of the critical Reynolds number for each specific geometry.

Although the Reynolds number is a dimensionless number, it does have a "physical nature" to it. For example, the inertia forces associated with a given flow geometry can be determined from Newton's second law of motion, viz.

$$F_{inertia} = ma \tag{9.76}$$

and the mass m can be written

$$m = \rho V \tag{9.77}$$

where the volume, V, has the dimensions of a characteristic length, L, cubed, L^3. Then

$$m \propto L^3 \tag{9.78}$$

The acceleration can be written

$$a = \frac{d\vartheta}{dt} = \vartheta \frac{d\vartheta}{ds} \tag{9.79}$$

Then

$$a \propto \frac{\vartheta^2}{L} \tag{9.80}$$

Then the inertia force can be written

$$F_{inertia} \propto \left(\rho L^3\right)\left(\frac{\vartheta^2}{L}\right) = \rho \vartheta^2 L^2 \tag{9.81}$$

The viscous force can be written

$$F_{viscous} = \tau A = \mu \left(\frac{d\vartheta}{dy}\right) A \tag{9.82}$$

Then

$$F_{viscous} \propto \mu \left(\frac{\vartheta}{L}\right) L^2 = \mu \vartheta L \tag{9.83}$$

Then the ratio of inertia forces to viscous forces in a given flow geometry with a characteristic length L is given by

$$\frac{F_{inertia}}{F_{viscous}} \propto \frac{\rho \vartheta^2 L^2}{\mu \vartheta L} = \frac{\rho \vartheta L}{\mu} = Re \tag{9.84}$$

Since turbulent conditions prevail at large values of Re, it is apparent that turbulent flow is dominated by inertial forces. Since laminar conditions prevail at small values of Re, laminar flow is dominated by viscous forces.

The Reynolds number has utility not only for establishing the transition from laminar to turbulent flow but also for establishing the similarity between flows. This is known as the Principle of Dynamic Similarity and is the basis of all wind tunnel testing of models of aerodynamic shapes. Consider the case of flow of a uniform fluid stream parallel to the x-axis with velocity ϑ_∞ past a fixed obstacle of given shape, an aerodynamic shape for example, and given orientation whose size is specified by a typical length L. Then we introduce non-

dimensional variables according to the following scheme:

$$\vartheta_x^* = \frac{\vartheta_x}{\vartheta_\infty}, \qquad \vartheta_y^* = \frac{\vartheta_y}{\vartheta_\infty}, \qquad \vartheta_z^* = \frac{\vartheta_z}{\vartheta_\infty}, \qquad P^* = \frac{P}{\rho \vartheta_\infty^{\,2}}$$
$$x^* = \frac{x}{L}, \qquad y^* = \frac{y}{L}, \qquad z^* = \frac{z}{L}, \qquad t^* = \frac{\vartheta_\infty t}{L} \tag{9.85}$$

Then in terms of these new dimensionless variables, the continuity equation for the incompressible fluid model, equation (9.70), becomes

$$\frac{\partial \vartheta_x^*}{\partial x^*} + \frac{\partial \vartheta_y^*}{\partial y^*} + \frac{\partial \vartheta_z^*}{\partial z^*} = 0 \tag{9.86}$$

and the Navier-Stokes equation, equation (9.69), becomes

$$\frac{\partial \vartheta_x^*}{\partial t^*} + \vartheta_x^* \frac{\partial \vartheta_x^*}{\partial x^*} + \vartheta_y^* \frac{\partial \vartheta_x^*}{\partial y^*} + \vartheta_z^* \frac{\partial \vartheta_x^*}{\partial z^*} = -\frac{\partial P^*}{\partial x^*} + \frac{\mu}{\vartheta_\infty L \rho}\left(\frac{\partial^2 \vartheta_x^*}{\partial x^{*2}} + \frac{\partial^2 \vartheta_x^*}{\partial y^{*2}} + \frac{\partial^2 \vartheta_x^*}{\partial z^{*2}} \right) \tag{9.87a}$$

$$\frac{\partial \vartheta_y^*}{\partial t^*} + \vartheta_x^* \frac{\partial \vartheta_y^*}{\partial x^*} + \vartheta_y^* \frac{\partial \vartheta_y^*}{\partial y^*} + \vartheta_z^* \frac{\partial \vartheta_y^*}{\partial z^*} = -\frac{\partial P^*}{\partial y^*} + \frac{\mu}{\vartheta_\infty L \rho}\left(\frac{\partial^2 \vartheta_y^*}{\partial x^{*2}} + \frac{\partial^2 \vartheta_y^*}{\partial y^{*2}} + \frac{\partial^2 \vartheta_y^*}{\partial z^{*2}} \right) \tag{9.87b}$$

$$\frac{\partial \vartheta_z^*}{\partial t^*} + \vartheta_x^* \frac{\partial \vartheta_z^*}{\partial x^*} + \vartheta_y^* \frac{\partial \vartheta_z^*}{\partial y^*} + \vartheta_z^* \frac{\partial \vartheta_z^*}{\partial z^*} = -\frac{\partial P^*}{\partial z^*} + \frac{\mu}{\vartheta_\infty L \rho}\left(\frac{\partial^2 \vartheta_z^*}{\partial x^{*2}} + \frac{\partial^2 \vartheta_z^*}{\partial y^{*2}} + \frac{\partial^2 \vartheta_z^*}{\partial z^{*2}} \right) \tag{9.87c}$$

Notice that the coefficient of the viscous force term, the last term on the right-hand side of equation (9.87), is the inverse of the Reynolds number, $1/Re = \mu/\vartheta_\infty L\rho$. The boundary conditions for the Navier-Stokes equation for this flow configuration are:
At infinity:

$$\vartheta_x = U, \qquad \vartheta_y = 0, \qquad \vartheta_z = 0 \tag{9.88}$$

and at the boundary of the solid obstacle:

$$\vartheta_x = \vartheta_y = \vartheta_z = 0 \tag{9.89}$$

Then for the dimensionless Navier-Stokes equation, equation (9.87), the dimensionless boundary conditions equivalent to equations (9.88) and (9.89) are:

$$\vartheta_x^* = 1, \qquad \vartheta_y^* = 0, \qquad \vartheta_z^* = 0$$
$$\vartheta_x^* = \vartheta_y^* = \vartheta_z^* = 0 \tag{9.90}$$

Thus the solution to equation (9.87) subject to the boundary conditions (9.90) determine ϑ_x^*, ϑ_y^*, ϑ_z^*, and P^*. Then for fluids of different densities and viscosities, for streams of different speeds, and obstacles of different sizes, ϑ_x^*, ϑ_y^*, ϑ_z^*, and P^* will be the same so long as the value of Re is the same. The same is true for any stress component divided by $\rho\vartheta_\infty^{\,2}$. Thus the same value of the Reynolds number insures that the flows will be dynamically similar. Thus a model of an aircraft wing could be tested in a water or wind tunnel at the same Reynolds number that corresponds to actual flight conditions on the full size wing, and the dimensionless values of the lift and drag forces measured on the model would be the same as those on the actual wing. We also infer from this solution to the dimensionless Navier-Stokes equation that in an internal flow, such as we might find in a circular pipe, the pressure gradient in the direction of flow is a function of the value of Re only, or

$$\frac{\partial P^*}{\partial x^*} = f\left(Re\right) \tag{9.91}$$

We will make use of this observation later. In fact, in Chapter 10, we will study the process of dimensional analysis in considerable detail since it is a very powerful tool in the analytical and experimental study of thermal-fluid systems. We have included this brief discussion of the Reynolds number at this juncture because it is so intimately connected to the Navier-Stokes equation.

9.9 Laminar Flow

We now examine some classical flow geometries at relatively small values of the Reynolds number (but $Re >> 1$) in which the flow can be classified as laminar. We are motivated by several reasons for doing this: (1) We want to learn how to develop solutions to the Navier-Stokes equation; (2) we want to know what the solutions to the Navier-Stokes equations tell us beyond the obvious velocity distribution in the fluid; (3) we want to try to understand the limitations of the solutions that we do develop, i.e., we want to know what are the other things about the flow that the Navier-Stokes equation cannot tell us; and (4) we want to develop solutions to the Navier-Stokes equation for some common geometries that will be useful to us in the design of thermal-fluid systems.

Example 9E.2: Consider the flow geometry shown in Figure 9E.2 in which a viscous liquid flows steadily down an inclined infinite plane in a uniform film of thickness h. The plane is inclined at an angle θ to the horizontal and the free surface of the liquid is in contact with the atmosphere. The flow is fully developed.

(a) Determine the distribution of pressure, $P(y)$, in the film.

(b) Determine the velocity distribution of the liquid in the film, $\hat{v}_x(y)$.

(c) Determine the shear stress τ_{yx} acting on the surface of the plane.

(d) Determine the volumetric flow rate of liquid in the film, $\dot{V}$.

(e) Determine the average velocity, $\hat{v}_{ave}$, of the liquid in the film.

(f) Determine the steady-state film thickness, h, in terms of the volumetric flow rate, $\dot{V}$, the width of the plate, b, the viscosity of the fluid, μ, and the angle θ.

(g) Determine the rate of entropy generation for a plate of length L.

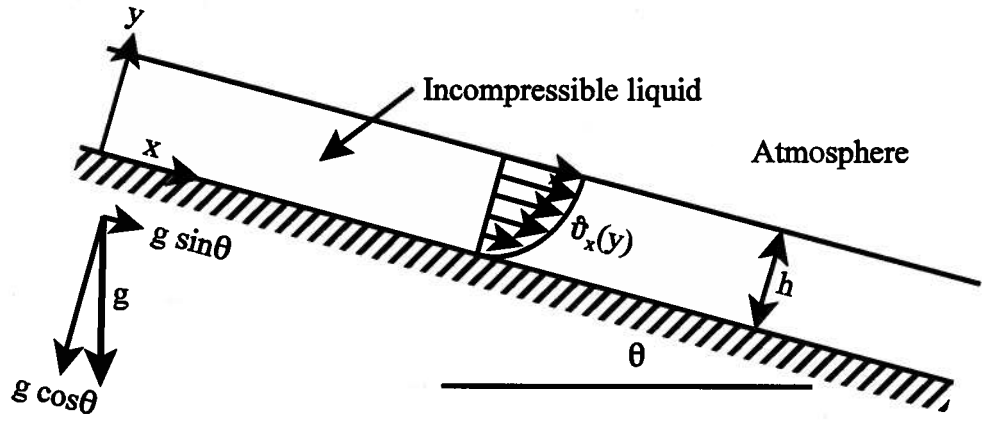

Figure 9E.1 Flow of an Incompressible Fluid Down an Inclined Plane

Solution: (a) The first step in applying the Navier-Stokes equation to a given physical situation is to select the appropriate coordinate system and write down the equation in component form for that geometry. For the case at hand, the rectangular Cartesian coordinate system is the

appropriate coordinate system so we should be working with the Navier-Stokes equation in the form of equation (9.67) and the continuity equation in the form of equation (9.70). For this case the flow is independent of the z-direction, and the flow looks exactly the same at every position along the z-axis. Hence, all derivatives in the z-direction vanish, $\partial/\partial z = 0$. Then since we are working just in x and y coordinate directions, we do not need equation (9.67c) and terms with z-components in them vanish. Since we are looking for the steady flow solution, all the time dependent terms vanish. The fact that the flow is fully developed means that the solution should depend only upon the y-coordinate and not the x-coordinate. That is all properties remain the same regardless the value of x. Then $\partial/\partial x = 0$. In particular,

$$\frac{\partial \vartheta_x}{\partial x} = 0 \quad \text{and} \quad \frac{\partial \vartheta_x}{\partial z} = 0$$

Then

$$\vartheta_x = f(y)$$

and the continuity equation, equation (9.70) reduces to

$$\cancel{\frac{\partial \vartheta_x}{\partial x}} + \frac{\partial \vartheta_y}{\partial y} = 0$$

Then

$$\vartheta_y = f(x, z)$$

but we have already shown that the flow is independent of the x- and z-directions. Then it must be the case that

$$\vartheta_y = \text{constant}$$

From the boundary conditions (9.74), it is apparent that $(\vartheta_y)_{wall} = 0$. Then since $\vartheta_y = \text{constant}$, it must be the case that $\vartheta_y = 0$ everywhere. Then equation (9.67b) becomes

$$\rho\left(\cancel{\frac{\partial \vartheta_y}{\partial t}} + \vartheta_x \cancel{\frac{\partial \vartheta_y}{\partial x}} + \cancel{\vartheta_y} \cancel{\frac{\partial \vartheta_y}{\partial y}} + \cancel{\vartheta_z} \cancel{\frac{\partial \vartheta_y}{\partial z}}\right) = -\frac{\partial P}{\partial y} + \rho g_y + \mu\left(\cancel{\frac{\partial^2 \vartheta_y}{\partial x^2}} + \cancel{\frac{\partial^2 \vartheta_y}{\partial y^2}} + \cancel{\frac{\partial^2 \vartheta_y}{\partial z^2}}\right)$$

or

$$\frac{\partial P}{\partial y} = \rho g_y$$

$$\frac{\partial P}{\partial y} = -\rho g \cos\theta$$

Integrating, we get

$$P = -\rho g y \cos\theta + f(x, z)$$

The boundary condition on the pressure is that $P = P_{atm}$ at $y = h$ and is independent of x and z. Then

$$f(x,z) = P_{atm} + \rho g h \cos\theta$$

and the integral becomes

$$P = P_{atm} + (\rho g \cos\theta)(h - y)$$

Physically, this equation says that the pressure distribution across the thickness of the liquid film is the hydrostatic pressure distribution.

(b) Then it follows that

$$\frac{\partial P}{\partial x} = 0$$

Then equation (9.67a) becomes

$$\rho\left(\cancel{\frac{\partial \vartheta_x}{\partial t}} + \vartheta_x \cancel{\frac{\partial \vartheta_x}{\partial x}} + \cancel{\vartheta_y} \frac{\partial \vartheta_x}{\partial y} + \cancel{\vartheta_z} \cancel{\frac{\partial \vartheta_x}{\partial z}}\right) = -\cancel{\frac{\partial P}{\partial x}} + \rho g_x + \mu\left(\cancel{\frac{\partial^2 \vartheta_x}{\partial x^2}} + \frac{\partial^2 \vartheta_x}{\partial y^2} + \cancel{\frac{\partial^2 \vartheta_x}{\partial z^2}}\right)$$

$$0 = \rho g_x + \mu \frac{\partial^2 \vartheta_x}{\partial y^2}$$

Physically, this equation says that the body force per unit volume due to gravity acting on every fluid particle in the liquid film is exactly balanced by the viscous force which acts on the fluid "stuck" to the plane.

As we have already shown, $\vartheta_x = f(y)$. Then above partial derivative becomes an ordinary derivative. Integrating the x-component of the Navier-Stokes equation, we get

$$\frac{d^2 \vartheta_x}{dy^2} = -\frac{\rho g_x}{\mu} = -\rho g \frac{\sin\theta}{\mu}$$

$$\frac{d \vartheta_x}{dy} = -\rho g \frac{\sin\theta}{\mu} y + C_1$$

$$\vartheta_x = -\rho g \frac{\sin\theta}{\mu} \frac{y^2}{2} + C_1 y + C_2$$

with boundary conditions (9.74) and (9.75)

$$(1) \quad \vartheta_x = 0 \qquad \text{at} \quad y = 0$$

$$(2) \quad \frac{d \vartheta_x}{dy} = 0 \quad \text{at} \quad y = h$$

From the first boundary condition, it follows that $C_2 = 0$. From the second boundary condition, which says that there is no shear stress in the liquid at the liquid-atmosphere interface, we have

$$C_1 = \rho g \frac{\sin\theta}{\mu} h$$

Then the solution of the Navier-Stokes equation for the velocity distribution is

$$\vartheta_x = -\rho g \frac{\sin\theta}{\mu} \frac{y^2}{2} + \rho g \frac{\sin\theta}{\mu} hy$$

$$\vartheta_x = \rho g \frac{\sin\theta}{\mu}\left(hy - \frac{y^2}{2}\right)$$

(c) Then the shear stress acting on any plane in the fluid is given by the first of equations (9.58), viz.

$$\tau_{xy} = \tau_{yx} = \mu\left(\frac{\partial \vartheta_x}{\partial y} + \frac{\partial \vartheta_y}{\partial x}\right)$$

but since we have shown above that $\frac{\partial \vartheta_y}{\partial x} = 0$, the expression for the shear stress becomes

$$\tau_{yx} = \mu \frac{d \vartheta_x}{dy} = (\rho g \sin\theta)(h - y)$$

On the surface of the inclined plate, $y = 0$. Then

$$\left(\tau_{yx}\right)_{\substack{surface \\ of\ plate}} = \rho g h \sin\theta$$

This shear stress is just the x-component of the hydrostatic pressure and acts in the positive x-direction. The force required to hold the plane stationary acts in the negative x-direction and is given by

$$F_{plane} = -\tau_{yx} A = -\rho g h b L \sin\theta$$

where b is the width of the plane normal to the plane of Figure 9E.2 and L is the length of the plane. Notice that the shear force per unit volume of film is exactly equal to the body force acting on that unit volume.

(d) The volumetric flow rate is given by

$$\dot{V} = \int_0^h \vartheta_x b dy = \int_0^h \rho g \frac{\sin\theta}{\mu}\left(hy - \frac{y^2}{2}\right) b dy = \frac{\rho g \sin\theta}{\mu}\frac{bh^3}{3}$$

Clearly, more viscous fluids require thicker films to flow a given volumetric flow rate.

(e) Then the average velocity is given by

$$\vartheta_{ave} = \frac{\dot{V}}{bh} = \frac{\rho g \sin\theta}{\mu}\frac{h^2}{3}$$

(f) The film thickness can be determined from the volumetric flow rate. Thus,

$$h = \left[\frac{3\mu\dot{V}}{\rho g b \sin\theta}\right]^{\frac{1}{3}}$$

Notice that for a film of given thickness, the volumetric flow rate decreases directly as the viscosity of the fluid increases.

(g) The rate of entropy generation is determined from the second law. For an adiabatic, steady-flow film of length L, the second law reduces to

$$\dot{S}_{gen} = \dot{m} c \ln\frac{T_{out}}{T_{in}}$$

where T_{out} is the temperature of the liquid leaving the film and T_{in} is the temperature of the liquid entering the film. These temperatures are determined from the application of the first law to the control volume. Since the pressure over the inlet port is identical to the pressure over the outlet port, the first law for this adiabatic, steady-flow situation reduces to

$$u_{out} - u_{in} = g\left(z_{in} - z_{out}\right) = c\left(T_{out} - T_{in}\right)$$

$$T_{out} = T_{in} + \frac{gL\sin\theta}{c}$$

Since

$$\dot{m} = \rho A \vartheta_{ave} = \rho b h\left(\frac{\rho g \sin\theta}{\mu}\frac{h^2}{3}\right) = \rho\dot{V}$$

the rate of entropy generation for a liquid film of length L, thickness h, and width b is

$$\dot{S}_{gen} = \frac{\rho^2 b h^3 g c \sin\theta}{3\mu}\ln\left(1 + \frac{gL\sin\theta}{cT_{in}}\right) = \rho c\dot{V}\ln\left(1 + \frac{gL\sin\theta}{cT_{in}}\right)$$

Notice that the rate of entropy generation depends only upon the geometry of the film and appears to be independent of the viscosity of the fluid. This is somewhat misleading because in this gravity driven flow, the volumetric flow rate is determined by the viscosity of the fluid and the film thickness.

In developing a solution of the Navier-Stokes equation for this case, the beginning student might be a bit confused about the elimination of certain terms from the component differential equations. In particular, one might reason that we know from our experience in Chapter 8 that a pressure gradient is usually required in the direction of flow of a viscous fluid in order to overcome the effects of viscous dissipation. If that were the case, the x-component of the Navier-Stokes equation would then appear as

$$-\frac{\partial P}{\partial x}+\mu\frac{d^2\vartheta_x}{dy^2}+\rho g_x=0$$

and the y-component would be unchanged from that given above. Then the solution for the velocity distribution would become

$$\vartheta_x=\left(\rho\frac{g\sin\theta}{\mu}-\frac{1}{\mu}\frac{\partial P}{\partial x}\right)\left(hy-\frac{y^2}{2}\right)$$

Since the y-component of the Navier-Stokes equation would be unchanged from that given above, the solution for the pressure distribution given in part (f) above would still be valid. Then the pressure gradient in the direction of flow would be given by

$$\frac{\partial P}{\partial x}=(\rho g\cos\theta)\frac{\partial h}{\partial x}$$

but for the film to be truly fully-developed, the film thickness must be constant in the direction of flow and $\partial h/\partial x = 0$. Then for this case, the pressure gradient in the x-direction must be zero and the x-component of the Navier-Stokes equation is indeed that shown in part (b) above.

Although this solution of the Navier-Stokes equation enables us to characterize this gravity driven, viscosity limited flow completely, there are many things the solution does not tell us. For example, this solution is based upon a simplification of the Navier-Stokes equation that contains only the viscous stresses associated with laminar flow. Therefore, the solution does not tell us when the film will undergo a transition from laminar to turbulent flow which involves the motion of fluid eddies in the flow. As we shall see, the Navier-Stokes equation is capable of describing turbulent flow, but the equation takes on a slightly different form in that case. If the present flow becomes turbulent, the above solution becomes invalid since it assumes that the flow is dominated by viscous forces with no consideration for the inertial forces that are important in turbulent flow. Also, this solution does not tell us the distance the film must travel down the plate before fully-developed flow is established. To determine this length, we would need to solve the Navier-Stokes equation with the non-linear convective terms included. In addition, as anyone who has ever tried to paint a vertical surface has noticed, if too much paint is applied at one time, a film of viscous fluid (albeit a non-Newtonian one), in this case paint, flows down the surface. In a relatively short distance, the advancing front of the paint film breaks up and forms finger-like projections or streaks that painters call "runs". The length of film required for this phenomenon to happen in a Newtonian fluid is not contained in the above solution of the Navier-Stokes equation. It would be necessary for us to do a stability analysis on the advancing film front to determine this distance. The point we are trying to make here is that in any physical situation, the solution of the Navier-Stokes equation can provide us with a lot of information, but that information has its limits in scope and validity. We should not just assume that the solution provides us with a complete picture of the situation.

Example 9E.3: A geometry commonly found in thermal-fluid systems is that of two concentric cylinders, one of which rotates while the other remains stationary: for example, a shaft

rotating in a journal bearing or a fluid viscometer used to measure the viscosity of a fluid. The laminar flow of a liquid in the space between coaxial cylinders is known as *Couette flow* in honor of Maurice Frédéric Alfred Couette, Professor of Physics at the end of the 19th Century at the French provincial university of Angers. Couette published his analysis of this flow geometry and his design of the viscometer in 1890.

There are two possible configurations of this geometry: (1) the inner shaft rotates while the outer cylinder remains stationary; and (2) the outer cylinder rotates while the inner one remains stationary. In either case, the "no-slip" boundary condition causes the fluid "stuck" to the rotating cylinder to be "dragged" along with it while at the same time this boundary condition causes the fluid "stuck" to the stationary cylinder to remain fixed in space. The resulting fluid shear produces a velocity gradient in the fluid and causes the rotating cylinder to exert a torque on the stationary cylinder. In the first configuration, the flow is stable only up to a certain condition whereas in the second configuration, the flow between cylinders has been shown, both theoretically and experimentally, to be inherently stable.

Consider the inherently stable case as shown in Figure 9E.3a. The inner cylinder of radius R_1 is stationary and the outer cylinder of radius R_2 rotates with steady angular velocity ω. The two cylinders are considered long compared to the gap between them which is filled with an incompressible fluid that can be modeled as a Newtonian fluid.

We wish to make the following determinations about the flow field in the gap:

(a) Determine the velocity distribution $v_\theta(r)$ in the fluid in the gap.

(b) Determine the torque exerted on the inner cylinder by fluid shear in the gap between the two cylinders.

(c) For a sufficiently small gap, $R_2 - R_1$, this geometry can be modeled as a simple planar shear flow of the type described in Section 9.2 in which the lower plane is stationary and the upper plane moves with velocity $v_0 = R_2\omega$. If we take as the limiting criterion the requirement that the shear stress on the stationary plane as predicted by the planar model is within one percent of the shear stress predicted by the concentric cylinder model, what are the conditions for which the planar model is a valid representation of the concentric cylinder geometry?

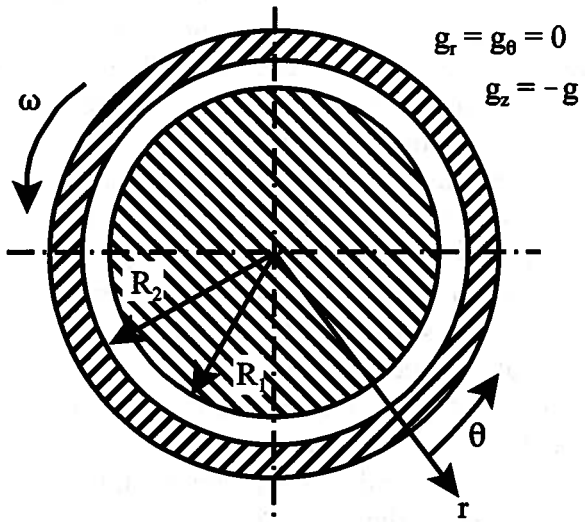

z-axis normal to plane of figure

Figure 9E.3a Rotating Concentric Cylinders

Solution: (a) Since the angular velocity ω is constant, we can model this as a steady flow situation of an incompressible fluid. Then $\partial/\partial t = 0$. For this geometry, there is no flow in the z-direction and there are no variations in any of the flow properties in that direction, i.e., $\partial/\partial z = 0$. The z-component of the Navier-Stokes equation vanishes completely. In addition, the flow is circumferentially symmetric so there is no θ dependence and $\partial/\partial\theta = 0$. Then we are seeking a solution for which v_θ does not depend upon θ. In cylindrical coordinates the continuity equation, equation (9.71), becomes

$$\frac{1}{r}\frac{\partial}{\partial r}(rv_r)+\frac{1}{r}\frac{\partial}{\partial\theta}(v_\theta)+\frac{\partial}{\partial z}(v_z)=0$$

It follows then that

$$rv_r = \text{constant}$$

Since $v_r = 0$ at the solid surface of each cylinder, the continuity equation requires that $v_r = 0$ everywhere. Then the Navier-Stokes equation, equation (9.73a), becomes

$$\rho\left(\frac{\partial v_r}{\partial t}+v_r\frac{\partial v_r}{\partial r}+\frac{v_\theta}{r}\frac{\partial v_r}{\partial\theta}-\frac{v_\theta^2}{r}+v_z\frac{\partial v_r}{\partial z}\right)$$

$$=-\frac{\partial P}{\partial r}+\rho g_r+\mu\left[\frac{\partial}{\partial r}\left(\frac{1}{r}\frac{\partial}{\partial r}(rv_r)\right)+\frac{1}{r^2}\frac{\partial^2 v_r}{\partial\theta^2}-\frac{2}{r^2}\frac{\partial v_\theta}{\partial\theta}+\frac{\partial^2 v_r}{\partial z^2}\right]$$

$$-\rho\frac{v_\theta^2}{r}=-\frac{\partial P}{\partial r}$$

and the Navier-Stokes equation, equation (9.73b), becomes

$$\rho\left(\frac{\partial v_\theta}{\partial t}+v_r\frac{\partial v_\theta}{\partial r}+\frac{v_\theta}{r}\frac{\partial v_\theta}{\partial\theta}-\frac{v_r v_\theta}{r}+v_z\frac{\partial v_\theta}{\partial z}\right)$$

$$=-\frac{1}{r}\frac{\partial P}{\partial\theta}+\rho g_\theta+\mu\left[\frac{\partial}{\partial r}\left(\frac{1}{r}\frac{\partial}{\partial r}(rv_\theta)\right)+\frac{1}{r^2}\frac{\partial^2 v_\theta}{\partial\theta^2}-\frac{2}{r^2}\frac{\partial v_r}{\partial\theta}+\frac{\partial^2 v_\theta}{\partial z^2}\right]$$

or

$$\frac{1}{r}\frac{\partial P}{\partial\theta}=\mu\left[\frac{\partial}{\partial r}\left(\frac{1}{r}\frac{\partial}{\partial r}(rv_\theta)\right)\right]$$

The question is what to do with the pressure term on the left-hand side of this expression. If we are seeking a solution for which v_θ does not depend upon θ, the right-hand side of this expression is then independent of θ. Then the expression is equivalent to

$$\frac{dP}{d\theta} = \text{constant}$$

If we integrate this, we get

$$P = a\theta + b$$

but symmetry requires that $P(\theta = 0) = P(\theta = 2\pi)$ which is impossible for this functional form. Then it follows that P cannot depend upon θ and

$$\frac{\partial P}{\partial\theta}=0$$

Then the θ-component of the Navier-Stokes equation becomes

$$\frac{d}{dr}\left[\frac{1}{r}\frac{d}{dr}(r\vartheta_\theta)\right]=0$$

Integrate once to get

$$\frac{1}{r}\frac{d}{dr}(r\vartheta_\theta)=C_1$$

$$\frac{d}{dr}(r\vartheta_\theta)=C_1 r$$

Integrate a second time to get

$$r\vartheta_\theta=C_1\frac{r^2}{2}+C_2$$

$$\vartheta_\theta=C_1\frac{r}{2}+C_2\frac{1}{r}$$

with boundary conditions

(1) $\vartheta_\theta=\omega R_2$ at $r=R_2$

(2) $\vartheta_\theta=0$ at $r=R_1$

Substituting the two boundary conditions into the expression for ϑ_θ, we get

$$\omega R_2=C_1\frac{R_2}{2}+C_2\frac{1}{R_2}$$

$$0=C_1\frac{R_1}{2}+C_2\frac{1}{R_1}$$

Solving these two equations simultaneously, we get

$$C_1=\frac{2\omega}{1-\left(\frac{R_1}{R_2}\right)^2} \quad \text{and} \quad C_2=\frac{-\omega R_1^{\,2}}{1-\left(\frac{R_1}{R_2}\right)^2}$$

Substituting the expressions for the constants of integration into the expression for ϑ_θ, we get

$$\vartheta_\theta=\frac{\omega r}{1-\left(\frac{R_1}{R_2}\right)^2}-\frac{\omega\frac{R_1^{\,2}}{r}}{1-\left(\frac{R_1}{R_2}\right)^2}=\frac{\omega R_1}{1-\left(\frac{R_1}{R_2}\right)^2}\left[\frac{r}{R_1}-\frac{R_1}{r}\right]$$

(b) To determine the torque exerted on the inner cylinder, we first calculate the shear stress on that cylinder due to the viscous shear in the fluid. From equation (9.72)

$$\tau_{r\theta}=\mu r\frac{d}{dr}\left(\frac{\vartheta_\theta}{r}\right)=\mu r\frac{d}{dr}\left\{\frac{\omega R_1}{1-\left(\frac{R_1}{R_2}\right)^2}\left[\frac{1}{R_1}-\frac{R_1}{r^2}\right]\right\}=\mu\frac{2\omega}{1-\left(\frac{R_1}{R_2}\right)^2}\frac{R_1^{\,2}}{r^2}$$

At $r=R_1$,

$$\tau_{r=R_1}=\mu\frac{2\omega}{1-\left(\frac{R_1}{R_2}\right)^2}$$

If $\mathcal{T}$ is the torque on the inner cylinder, we have for a cylinder of length L

$$\mathcal{T} = \tau_{r=R_1} A = 2\pi R_1 L \mu \frac{2\omega}{1-\left(\frac{R_1}{R_2}\right)^2}$$

where we have neglected any "end effects" due to flow around the end of the cylinder. Thus, we can use this geometry to determine the viscosity of a fluid simply by measuring the geometry of the apparatus, the angular speed of the outer cylinder, and the torque exerted on the inner cylinder. This torque is typically determined by suspending the inner cylinder from a torsional element like a slender rod (or even a wire for low viscosity fluids) and measuring the twist in the element, usually by means of an optical arrangement employing a laser light source and a mirror attached to the torsional element. One simply measures the displacement of the laser light beam as the mirror is rotated by the torque on the inner cylinder and, hence, the torsional element. Knowing the length between the fixed end of the torsional element and the position of the laser light beam, we can determine the angular displacement of the mirror relative to the fixed end of the torsional element. Simple torsion theory then yields the torque on the element and, hence, the cylinder.

(c) Suppose that we now model the flow in the gap as though it were a planar gap; i.e., we neglect the radius of curvature of the cylinders and treat the flow as shown in Figure 9E.2b. This configuration is known as plane Couette flow and commonly occurs in engineering practice. The question is: "Under what conditions is this a good model of circular Couette flow?"

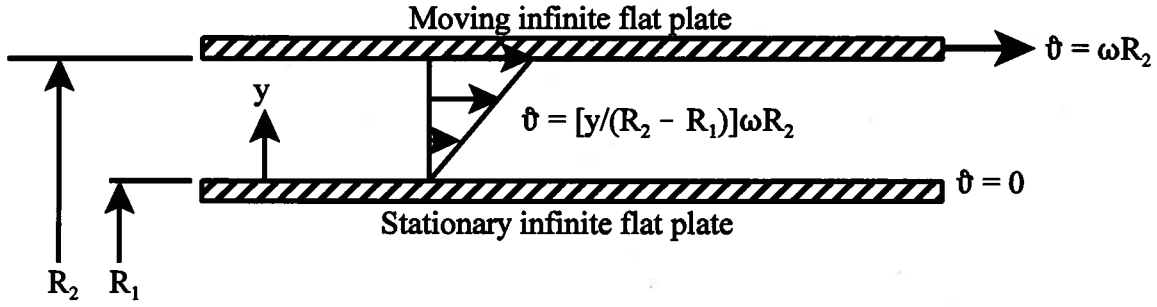

Figure 9E.3b Planar Shear Flow

Consider the shear stress acting on the lower plate.

$$\tau_{planar} = \mu \frac{d\vartheta}{dy} = \mu \frac{\omega R_2}{R_2 - R_1} = \mu \frac{\omega}{1-\frac{R_1}{R_2}}$$

If we had calculated this using the concentric cylinder model, we would have

$$\tau_{r=R_1} = \mu \frac{2\omega}{1-\left(\frac{R_1}{R_2}\right)^2} = \mu \frac{2\omega}{\left(1-\frac{R_1}{R_2}\right)\left(1+\frac{R_1}{R_2}\right)} = \mu \frac{\omega}{\left(1-\frac{R_1}{R_2}\right)} \frac{2}{\left(1+\frac{R_1}{R_2}\right)}$$

Then

$$\frac{\tau_{r=R_1}}{\tau_{planar}} = \frac{2}{\left(1+\frac{R_1}{R_2}\right)}$$

If we require the results of the two models to agree within one percent, we have

$$\frac{\tau_{r=R_1}}{\tau_{planar}} = \frac{2}{\left(1+\frac{R_1}{R_2}\right)} = 1.01$$

$$\frac{R_1}{R_2} = 0.98$$

Then if $R_2 - R_1 < 0.02R_2$, the planar model, which is much simpler to use, will give results with an error of less than one percent.

As we mentioned previously, the configuration that we just considered is inherently stable. However, if we considered the other possible configuration in which the outer cylinder is stationary and the inner cylinder is rotating, it is possible for the flow to become unstable. It is left as an exercise to show that the solution of the Navier-Stokes equation for the velocity distribution for this case is given by

$$v_\theta = \frac{\omega R_1^2}{1-\left(\frac{R_1}{R_2}\right)^2}\left[\frac{1}{r} - \frac{r}{R_2^2}\right]$$

The reason for the instability in this configuration is that the centrifugal force due to the rotation of the inner cylinder tends to drive the fluid toward the outer cylinder. This motion is resisted by a radial viscous force. For certain values of the geometrical and flow parameters, the flow becomes unstable to small disturbances. This instability was studied in great detail in 1923 by Sir Geoffrey I. Taylor (1886 - 1975), famous for his theory of turbulent flow and other fluid flow phenomena. For $R_2 - R_1 << R_1$, Taylor's analysis yielded a well-defined critical value of a dimensionless parameter, now called the "Taylor number" in his honor, at which the base flow becomes unstable to these small disturbances. The Taylor number, Ta, is the ratio of the destabilizing centrifugal force to the stabilizing radial viscous force and is given by

$$Ta = \frac{\rho^2\omega^2 R_1 (R_2 - R_1)^3}{\mu^2}$$

At the value $Ta_{crit} = 1707.8$, the effect of the destabilizing centrifugal force outweighs the effect of the stabilizing radial viscous force and the instability occurs. The resultant toroidal "Taylor vortices", which are rectangular in cross-section and encircle the inner cylinder, are stacked in the axial direction as shown in Figure 9E.3c. Taylor conducted careful experiments that agreed with his theory within a few percent for a wide range of parameters, thus demonstrating that linear stability analyses can make quantitative predictions of patterns. Taylor's work in 1923 was the first to make a direct comparison between a laboratory experiment and a prediction for the formation of a pattern due to an instability.

It is worth noting at this point that because of the assumptions made at the outset of this analysis, we have a sense that the straightforward solution of the Navier-Stokes equation for this configuration is limited in its validity. However, as Taylor showed, if a small disturbance is introduced into this equation and a new solution obtained, a very different and complex character of the flow is revealed. Thus, the Navier-Stokes equation is very powerful in that it is capable of describing the flow of viscous fluids under wide ranging circumstances, but caution must be exercised in interpreting the applicability of the results. In some cases, one has to know in advance what one is looking for from the Navier-Stokes equation.

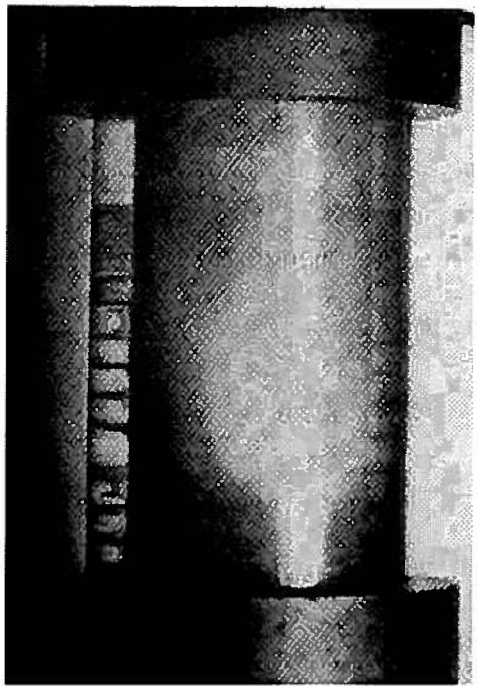

Figure 9E.3c Taylor Vortices Between Rotating Concentric Cylinders
(From *Laminar Boundary Layers*, edited by L. Rosenhead,
Oxford University Press, Oxford, 1963, p. 496f)

Example 9E.4: As shown in Figure 9E.4, a journal bearing for a crankshaft in an automobile engine has a shaft diameter of 75 mm and rides on a film of oil 0.05 mm thick. In a particular application of this bearing, the rotational speed of the crankshaft is 3000 rpm and the bearing is 60 mm long in the plane normal to Figure 9E.4. The viscous dissipation in the oil is accommodated by pumping oil through the gap at a mass flow rate, $\dot{m}_{oil}$, sufficient to produce a temperature increase in the oil of 100 C.

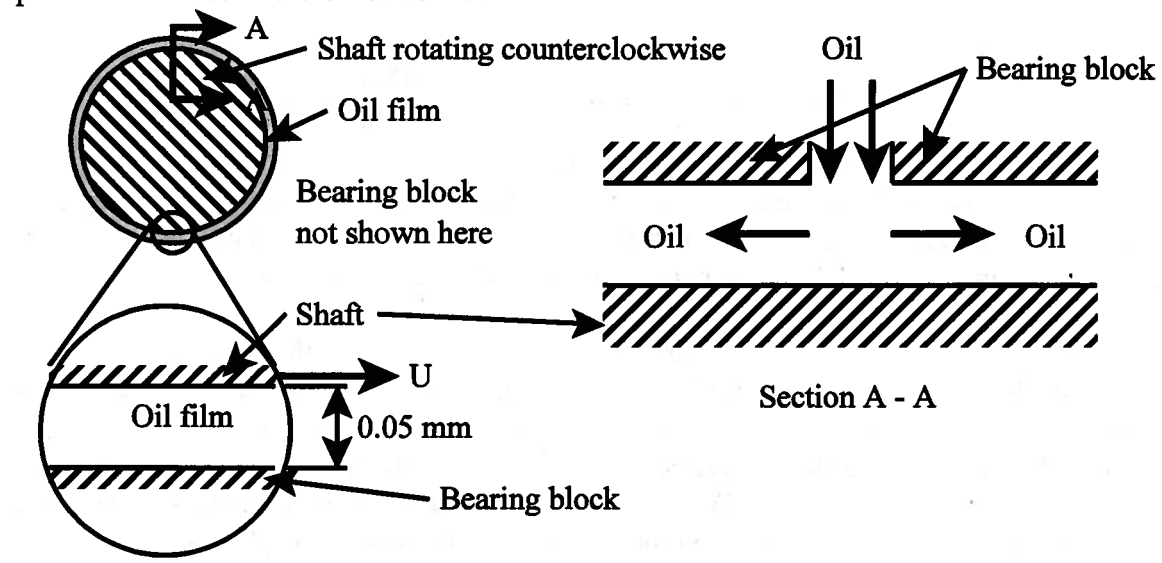

Figure 9E.4 Journal Bearing

The oil properties are as follows: $\rho_{oil} = 854$ kg/m^3, $c_{oil} = 2120$ J/kg K, $\mu_{oil} = 350 \times 10^{-4}$ kg/m sec.

(a) What is the rate of shear work transfer in the bearing?

(b) What is the required mass flow rate of oil through the bearing if the solid surfaces can be modeled as adiabatic?

(c) What is the rate of entropy generation in the oil if the oil enters the bearing at 300 K?

Solution: (a) We saw in Example 9E.3 that if the oil gap is less than 2 percent of the radius of the shaft, we can model the flow in the gap as simple planar shear flow. In the case at hand, 0.02(75 mm) = 1.5 mm. Because the actual oil gap is only 0.05 mm, we can model this bearing as one flat plate moving relative to another. Then

$$\dot{W}_{shear} = -F_{shear}\vartheta_0 = -\tau_{r\theta}A_{surface}\vartheta_0 = -\mu\left(\frac{du}{dy}\right)2\pi RLU = -\mu\left(\frac{R\omega}{a}\right)2\pi RL\vartheta_0$$

$$\vartheta_0 = R\omega = (37.5 \times 10^{-3}\text{ m})\frac{(3000\text{ rev/min})(2\pi\text{ radians/rev})}{(60\text{ sec/min})} = 11.781\text{ m/sec}$$

$$A_{surface} = 2\pi RL = 2\pi(37.5 \times 10^{-3}\text{ m})(60 \times 10^{-3}\text{ m}) = 1.4137 \times 10^{-2}\text{ m}^2$$

$$\dot{W}_{shear} = -(350 \times 10^{-4}\text{ kg/m sec})\left(\frac{11.781\text{ m/sec}}{0.05 \times 10^{-3}\text{ m}}\right)(1.4137 \times 10^{-2}\text{ m}^2)(11.781\text{ m/sec})$$

$$\dot{W}_{shear} = -1.3735 \times 10^3\text{ W}$$

(b) For the adiabatic bearing with negligible kinetic and potential energy in the oil, the steady-flow form of the first law for the bearing reduces to

$$-\dot{W}_{shear} = \dot{m}_{oil}c_{oil}(T_{out} - T_{in})$$

$$\therefore \dot{m}_{oil} = \frac{-\dot{W}_{shear}}{c_{oil}(T_{out} - T_{in})} = \frac{1.3735 \times 10^2\text{ W}}{(2120\text{ J/kg K})(100\text{ C})} = 6.4786 \times 10^{-3}\text{ kg/sec}$$

(c) Since there is no entropy transfer in an adiabatic bearing, the steady-flow form of the second law for the bearing reduces to

$$\dot{S}_{gen} = \dot{m}_{oil}(s_{out} - s_{in}) = \dot{m}_{oil}c_{oil}\ln\left(\frac{T_{out}}{T_{in}}\right)$$

$$\dot{S}_{gen} = (6.4786 \times 10^{-3}\text{ kg/sec})(2120\text{ J/kg K})\ln\left(\frac{400\text{ K}}{300\text{ K}}\right) = 3.951\text{ W/K}$$

This entropy generation is a result of the viscous dissipation in the oil. Ultimately entropy must be transferred at this rate from the oil to the environment in order for the oil situation to be modeled as steady-state. This is the reason that large engines are fitted with oil coolers. Smaller engines rely on simple heat transfer by natural convection from the various external engine surfaces to the environment to cool the oil.

We have just studied two classic examples of flow geometries that illustrate both the power and the limitations of the Navier-Stokes equation in describing the flow of a Newtonian fluid. In both cases we saw that the flow was laminar but could change character as the flow progressed. We also saw that these solutions have practical applications provided we understand the full implications of the solutions. We now wish to extend our study of laminar flows to other special flow geometries that are more commonly found in thermal-fluid systems.

9.9.1 Laminar Internal Flows

The study of laminar flows is naturally divided between "internal flows" and "external flows". Typically, in both of these types of flows, a uniform flow enters a region in which the flow field is bounded in some way by solid boundaries. In the case of internal flows, like the flow of water in a pipe, the solid boundaries completely contain the flow, whereas in external flows, like the flow of air around an aircraft, there are solid objects which are immersed in the flow in some way. In an internal flow, as the uniform flow comes into contact with the solid boundaries, the interaction (momentum transfer) between the fluid and the solid boundaries that define its extent is at first confined to a very small region. But as the flow develops, the effect of the boundaries diffuses into the flow until the influence of the solid boundaries is felt throughout the fluid flow. Thus, in a fully developed internal flow the effect of viscosity extends throughout the flow field. On the other hand, in an external flow, the situation at the outset is similar, but as the flow progresses, the influence of the boundaries is never truly felt throughout the flow field. Rather, the influence of the boundary is confined to a relatively small region known as the *boundary layer*. Inside the boundary layer, viscous effects dominate the behavior of the flow, but outside the boundary layer, the flow is not influenced by the viscosity of the fluid and the fluid can be modeled as though it were inviscid. Because of the simplicity of their solutions of the Navier-Stokes equation, we will first take up the study of laminar internal flows and then follow this with laminar external flows.

9.9.1.1 Laminar Fully-developed Planar Poiseuille Flow The simplest laminar internal flow of a Newtonian fluid is the simple shear flow between infinite parallel flat plates that we discussed in Section 9.2. For that geometry, the flow is actually generated by the viscous drag of the fluid on the moving top plate. The "no-slip" boundary condition of the Newtonian fluid model causes the fluid "stuck" to the top plate to move with the plate. The action of the viscosity of the fluid produces a velocity gradient in the fluid. However, if we now fix the position of both of the plates as shown in Figure 9.9 and we are trying to move a fluid through the space between

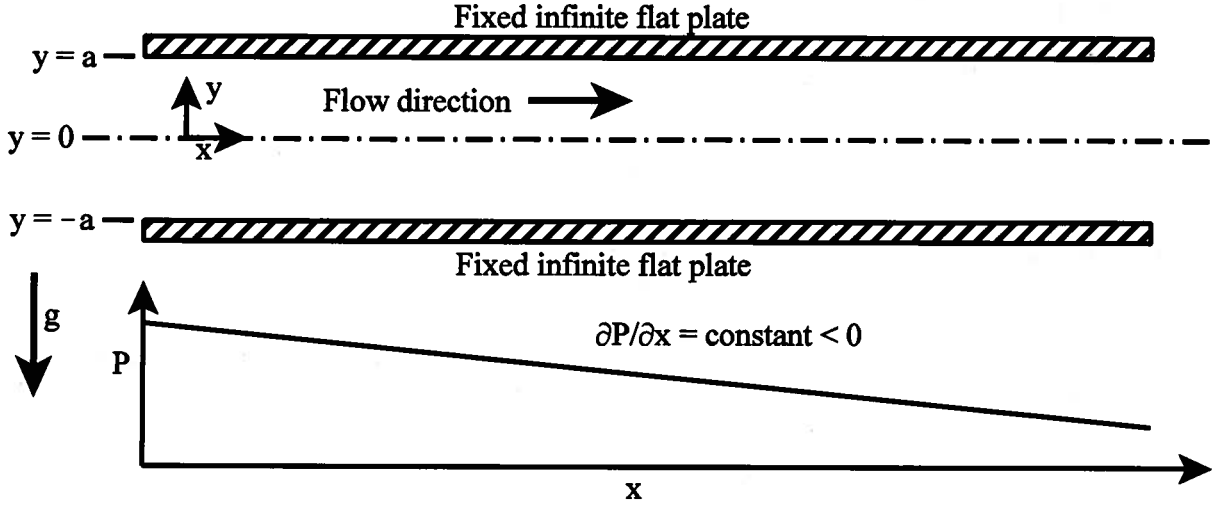

Figure 9.9 Fully-developed Plane Poiseuille Flow Between Fixed Infinite Parallel Flat Plates

them in a steady manner, the action of the viscosity of the fluid requires that we impose (by external means such as a pump) a pressure gradient in the direction of the flow in order to overcome the "viscous drag" of the plates on the fluid. This pressure gradient must be the same

at every position along the x-direction in order to keep the fluid flowing at the same average velocity at each position. This type of flow is known as fully-developed *plane Poiseuille flow* and is just one example of several laminar internal flows driven by a pressure gradient. This class of flows is usually known as "Poiseuille flow" in honor of Jean Marie Louis Poiseuille (1799-1869), a French physician who studied the flow of blood in capillaries. (The unit of viscosity in the cgs system is called the *poise* in his honor.)

Because the flow is fully developed, the flow is steady and the time dependent terms in the Navier-Stokes equation vanish. Also, the flow has the same character at every location along the x-axis, so $\partial/\partial x = 0$. Similarly, the flow is the same in all planes normal to the z-axis, so $\partial/\partial z = 0$. Then from the continuity equation, equation (9.70), we have

$$\cancel{\frac{\partial \vartheta_x}{\partial x}} + \frac{\partial \vartheta_y}{\partial y} + \cancel{\frac{\partial \vartheta_z}{\partial z}} = 0 \tag{9.92}$$

Then ϑ_y = constant. From the boundary condition (9.74), $\vartheta_y(\pm a) = 0$. It follows then that $\vartheta_y = 0$ everywhere. For the x-component of the Navier-Stokes equation we have

$$\rho\left(\cancel{\frac{\partial \vartheta_x}{\partial t}} + \vartheta_x \cancel{\frac{\partial \vartheta_x}{\partial x}} + \cancel{\vartheta_y}\frac{\partial \vartheta_x}{\partial y} + \cancel{\vartheta_z}\cancel{\frac{\partial \vartheta_x}{\partial z}}\right) = -\frac{\partial P}{\partial x} + \cancel{\rho g_x} + \mu\left(\cancel{\frac{\partial^2 \vartheta_x}{\partial x^2}} + \frac{\partial^2 \vartheta_x}{\partial y^2} + \cancel{\frac{\partial^2 \vartheta_x}{\partial z^2}}\right) \tag{9.93}$$

$$-\frac{\partial P}{\partial x} + \mu\frac{\partial^2 \vartheta_x}{\partial y^2} = 0$$

For the y-component of the Navier-Stokes equation we have

$$\rho\left(\cancel{\frac{\partial \vartheta_y}{\partial t}} + \vartheta_x \cancel{\frac{\partial \vartheta_y}{\partial x}} + \cancel{\vartheta_y}\cancel{\frac{\partial \vartheta_y}{\partial y}} + \cancel{\vartheta_z}\cancel{\frac{\partial \vartheta_y}{\partial z}}\right) = -\frac{\partial P}{\partial y} + \rho g_y + \mu\left(\cancel{\frac{\partial^2 \vartheta_y}{\partial x^2}} + \cancel{\frac{\partial^2 \vartheta_y}{\partial y^2}} + \cancel{\frac{\partial^2 \vartheta_y}{\partial z^2}}\right) \tag{9.94}$$

$$-\frac{\partial P}{\partial y} + \rho g_y = 0$$

For the z-component of the Navier-Stokes equation we have

$$\rho\left(\cancel{\frac{\partial \vartheta_z}{\partial t}} + \vartheta_x \cancel{\frac{\partial \vartheta_z}{\partial x}} + \cancel{\vartheta_y}\cancel{\frac{\partial \vartheta_z}{\partial y}} + \cancel{\vartheta_z}\cancel{\frac{\partial \vartheta_z}{\partial z}}\right) = -\frac{\partial P}{\partial z} + \cancel{\rho g_z} + \mu\left(\cancel{\frac{\partial^2 \vartheta_z}{\partial x^2}} + \cancel{\frac{\partial^2 \vartheta_z}{\partial y^2}} + \cancel{\frac{\partial^2 \vartheta_z}{\partial z^2}}\right) \tag{9.95}$$

$$-\frac{\partial P}{\partial z} = 0$$

From the z-component of the Navier-Stokes equation we conclude that the pressure is uniform in the z-direction. From the y-component of the Navier-Stokes equation we conclude that the pressure in the y-direction is hydrostatic. (The dimension in the y-direction is usually small compared to the dimension in the x-direction, so this hydrostatic pressure distribution due to gravity is usually neglected.) From the x-component of the Navier-Stokes equation we have

$$\frac{\partial^2 \vartheta_x}{\partial y^2} = \frac{1}{\mu}\frac{\partial P}{\partial x} = \text{constant} \tag{9.96}$$

Thus the viscous force (per unit volume) is just balanced by the "pressure" force (per unit volume). This is typical of fully-developed internal flows. Integrating equation (9.96) twice, we get

$$\vartheta_x = \frac{1}{\mu}\left[\frac{\partial P}{\partial x}\frac{y^2}{2} + C_1 y + C_2\right] \tag{9.97}$$

For boundary conditions, we have the "no-slip" condition at the surface of the plates. Then

$$\begin{aligned} &(1) \quad \vartheta_x = 0 \quad \text{at} \quad y = a \\ &(2) \quad \vartheta_x = 0 \quad \text{at} \quad y = -a \end{aligned} \tag{9.98}$$

Applying boundary conditions (9.98), we get

$$0 = \frac{1}{\mu}\left[\frac{\partial P}{\partial x}\frac{a^2}{2} + C_1 a + C_2\right] \tag{9.99}$$

and

$$0 = \frac{1}{\mu}\left[\frac{\partial P}{\partial x}\frac{a^2}{2} - C_1 a + C_2\right] \tag{9.100}$$

Solving these two equations simultaneously, we get

$$\begin{aligned} C_2 &= -\frac{\partial P}{\partial x}\frac{a^2}{2} \\ C_1 &= 0 \end{aligned} \tag{9.101}$$

Then the velocity distribution becomes

$$\vartheta_x = \frac{a^2}{2\mu}\left[\frac{\partial P}{\partial x}\left(\frac{y^2}{a^2} - 1\right)\right] \tag{9.102}$$

Thus the velocity distribution is parabolic with the maximum velocity on the centerline of the channel at $y = 0$. Then

$$\vartheta_{max} = -\frac{\partial P}{\partial x}\frac{a^2}{2\mu} \tag{9.103}$$

and equation (9.102) can be written in non-dimensional form and plotted as shown in Figure 9.10

$$\frac{\vartheta_x}{\vartheta_{max}} = 1 - \left(\frac{y}{a}\right)^2 \tag{9.104}$$

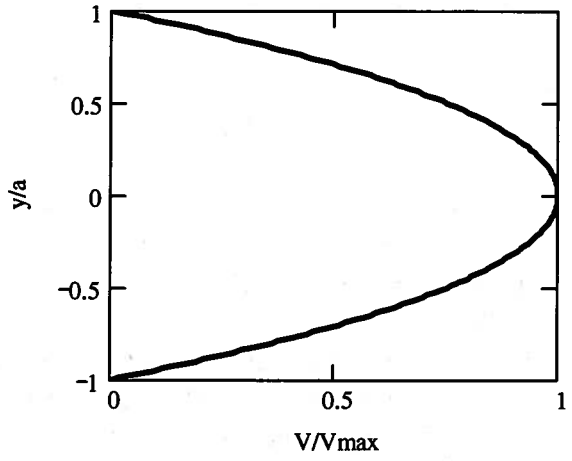

Figure 9.10 Velocity Distribution in Plane Poiseuille Flow Driven by a Pressure gradient

For a channel of width b the volumetric flow rate is given by

$$\dot{V} = \int_0^A \vartheta_x dA = \int_{-a}^{a} \vartheta_x b dy = \frac{\partial P}{\partial x}\frac{a^2 b}{2\mu}\int_{-a}^{a}\left(\frac{y^2}{a^2} - 1\right)dy = -\frac{\partial P}{\partial x}\frac{2a^3 b}{3\mu} \tag{9.105}$$

The average velocity, ϑ_{ave}, is given by

$$\vartheta_{ave} = \frac{\dot{V}}{A} = \left[-\frac{\partial P}{\partial x}\frac{2}{3}\frac{a^3 b}{\mu} \right]\left(\frac{1}{2ab}\right) = -\frac{\partial P}{\partial x}\frac{a^2}{3\mu} = \frac{2}{3}\vartheta_{max} \tag{9.106}$$

For the shear stress in the fluid, we have from equation (9.58)

$$\tau_{yx} = \mu\frac{\partial \vartheta_x}{\partial y} = \frac{\partial P}{\partial x}y \tag{9.107}$$

Thus the shear stress is zero in the center of the gap between the plates and maximum at the surface of the plates.

One of the key issues in the application of the solution that we have just developed is the critical value of the Reynolds number for the transition from laminar to turbulent flow in this configuration. As we have seen in Section 9.8, the definition of the Reynolds number for a particular flow geometry requires the specification of an appropriate characteristic length to describe the geometry. For flow in a circular conduit, the physical diameter of the conduit is the obvious choice for the characteristic length. However, for conduits of non-circular cross-section, the choice may not be so obvious. By convention, the appropriate characteristic length for these geometries is taken to be the *hydraulic diameter* which is defined as

$$D_h = \frac{4A_c}{\wp} \tag{9.108}$$

where A_c is the cross-sectional area of the flow and $\wp$ is the wetted perimeter of the conduit. This definition has been chosen because it yields the physical diameter D of a circular conduit as its hydraulic diameter since $A_c = \pi D^2/4$ and $\wp = \pi D$. For the infinite parallel plate geometry, consider first the case of a duct of rectangular cross-section of height a and width b. Then the hydraulic diameter for that geometry would be

$$D_h = \frac{4(2ab)}{2(2a+b)} = \frac{2(2a)}{\frac{2a}{b}+1} \tag{9.109}$$

Now let $b \to \infty$ since the plates are infinitely wide. Then for the infinite parallel plate geometry

$$D_h = 4a \tag{9.110}$$

and the Reynolds number becomes

$$Re = \frac{4a\rho\vartheta_{ave}}{\mu} \tag{9.111}$$

For this geometry, the lower limit of the critical value of the Reynolds for the transition from laminar to turbulent flow has been determined to be in the range 2200 - 3400 with $Re_{critical} = 2800$ a reasonable value to use for design purposes. For $Re > 2800$, the flow becomes turbulent and equation (9.102) is no longer valid.

9.9.1.2 Laminar flow in the Entry Region for Plane Poiseuille Flow: The flow configuration that we have just studied is known as a fully-developed flow since the effect of the fluid viscosity is felt throughout the flow field and the resulting parabolic velocity distribution has the same appearance (shape) at every value of x. However, this solution to the Navier-Stokes equation for this configuration does not reveal how the flow became fully developed. To see how this happens, we need to examine the *entry region*, the portion of the flow field where this development occurs. The flow field in this entry region can also be described by the Navier-Stokes equation, but now the inertial forces are equally as important as the viscous forces. Since these terms are non-linear, the solution of the Navier-Stokes equation in the entry region is very

complicated mathematically and will not be attempted here; however, there are situations in thermal-fluid systems for which this entry region is important, so it is worth discussing the physics of the situation.

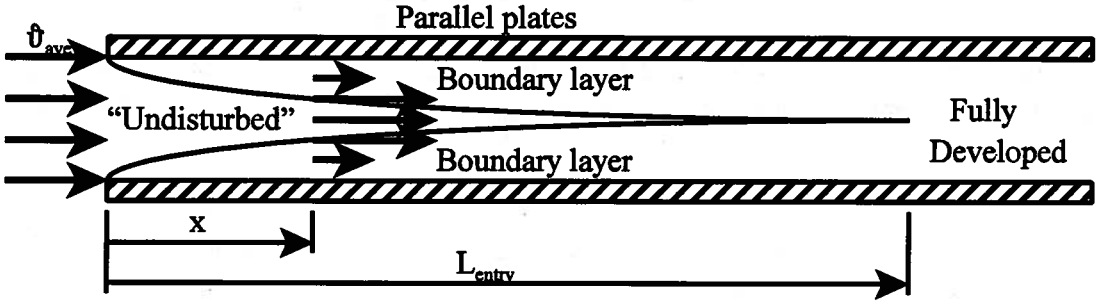

Figure 9.11 Developing Flow in the Entry Region Between Two Parallel Flat Plates

As shown in Figure 9.11, the flow enters the space between plates with a uniform velocity distribution in which the value of $\hat{v}_x = \hat{v}_{ave}$ is the same at every value of y. As the fluid comes into contact with the upper and lower plates, the fluid at the surface of the plates is slowed to zero velocity as a result of the "no-slip" boundary condition of the Newtonian fluid model. Initially, the influence of the solid boundary is confined to a very small region near the surface of the plates, but as the fluid moves downstream, this region of influence, known as the boundary layer, begins to diffuse further out into the flow in a direction normal to the solid boundary (wall). As the flow progresses in the x-direction, the boundary layer grows in thickness. In the boundary layer, the velocity of the fluid varies in a "smooth" way normal to the wall as the fluid layers slide over one another in a laminar fashion. The fluid velocity at the wall is identically zero while the fluid velocity at the outer limit of the boundary layer is equal to the velocity of the fluid in the "undisturbed" flow that has not yet felt the effect of the wall. Then the average fluid velocity in the boundary layer is less than $\hat{v}_{ave}$, and it follows that the average fluid velocity in the "undisturbed" flow must be greater than $\hat{v}_{ave}$ in order to satisfy the continuity equation. Thus in the "undisturbed" region, the fluid is accelerated as the fluid in the boundary layer is decelerated.

Since the fluid in the "undisturbed" region has not yet felt the influence of the wall (hence the modifier "undisturbed" even though the fluid velocity is rapidly changing in this portion of the flow), viscous effects are negligible here and the fluid can be modeled as an inviscid fluid in this region. It follows, then, that the Bernoulli equation is valid in this region. Thus, as the fluid accelerates in the "undisturbed" region, inertial forces are dominant, and the pressure must decrease in accordance with the Bernoulli equation. At small values of x, the "undisturbed" region is by far the largest portion of the flow field. Then the pressure in this region is impressed upon the flow in the boundary layer. As the value of x increases in the entry region, the pressure falls rapidly in a non-linear manner, in fact as the square of the velocity in the "undisturbed" region.

As we move further and further in the x-direction, the boundary layer grows ever larger at the expense of the "undisturbed" region. As the size of the "undisturbed" region shrinks, the flow continues to accelerate until at some value of $x = L_{entry}$, the boundary layers from the top and bottom plates come together, and the local flow velocity in the disappearing "undisturbed" region has reached its maximum value $\hat{v}_{max}$. This is the value of the velocity given in equation (9.103) found on the centerline ($y = 0$) of the fully-developed flow. Thus the flow has become fully-

developed at $x = L_{entry}$. Since the inertial forces are important in the entry region but not in the fully-developed region, we would expect the entry length to depend upon the Reynolds number. Chen[1] has shown that the entry length for plane Poiseuille flow is given by

$$\frac{L_{entry}}{D_h} = 0.011Re + \frac{0.315}{1+0.0175Re} \tag{9.112}$$

As mentioned previously, the flow remains laminar for this configuration for $Re < Re_{critical}$. Then the longest possible entry length would occur at $Re_{critical} = 2800$. Thus from equation (9.112)

$$\left(\frac{L_{entry}}{D_h}\right)_{max} = 30.806 \tag{9.113}$$

an the laminar flow between infinite flat plates spaced a distance $2a$ apart becomes fully developed within $(L_{entry})_{max} = 30.806(D_h) = 30.806(4a) = 123.23a$. Figure 9.12 shows the axial pressure distribution for a sample plane Poiseuille flow of water with $Re = 2800$. The pressure of the water at the inlet to the parallel flat plate geometry is arbitrarily set at $P_{inlet} = 10^6$ N/m^2. The solid line shows the axial pressure distribution assuming fully-developed flow throughout the flow field with no entry region. The dashed line shows the pressure distribution with the effect of the entry region included.

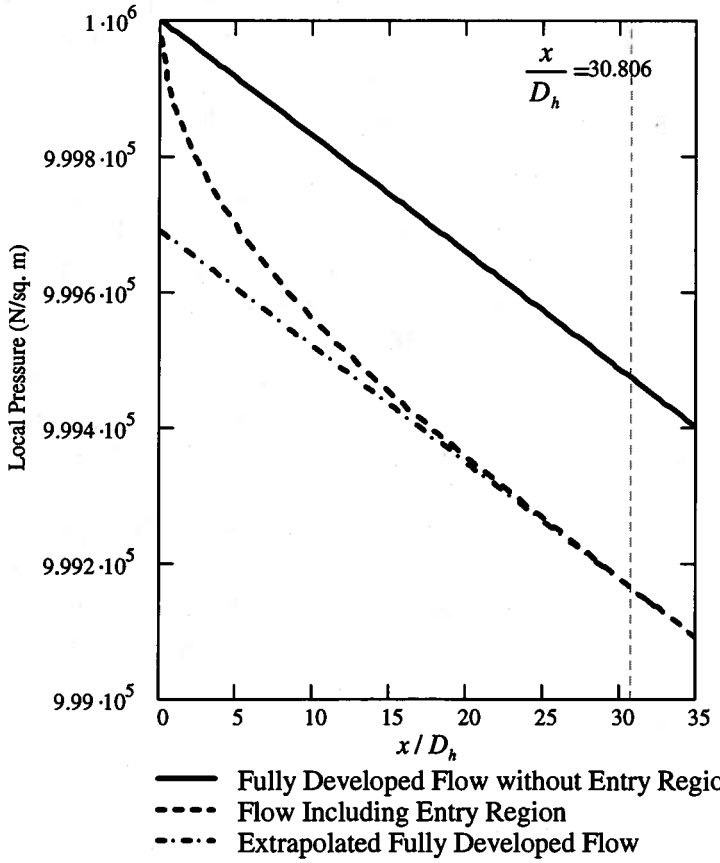

Figure 9.12 Axial Pressure Distribution for Flow of Water Between Infinite Parallel Flat Plates, $Re = 2800$

---

[1] R.Y. Chen, "Flow in the Entrance Region at Low Reynolds Numbers," *J. Fluids Eng.*, (95): 153-158, 1973.

The vertical line indicates the location of the end of the entry region as defined by the full development of the velocity profile ($x/D_h = 30.806$ for $Re = 2800$ for this flow configuration). Notice that the pressure with the entry region included is always lower than the pressure without the entry region taken into account. This additional pressure drop is due to the acceleration of the flow in the "undisturbed" region. Notice also that once the flow becomes fully developed, the pressure gradient is the same in both cases. The difference between the extrapolation of the fully-developed flow and the flow in the entry region shows the rapid decrease in pressure due to the acceleration of the "undisturbed" flow in the entry region.

The effect of the entry region on the drop in pressure that accompanies the flow of a viscous fluid in the space between parallel flat plates can be seen more clearly by making use of the pressure drop correlations of Shah and London[2] derived from solutions of the Navier-Stokes equation for the various flow regimes. These correlations are presented in terms of the following dimensionless parameters:

$$\Delta P^* = \frac{P_{inlet} - P}{\frac{\rho \vartheta_{ave}^{\,2}}{2}} \qquad x^+ = \frac{x}{D_h Re} \tag{9.114}$$

The first of these is the dimensionless pressure drop and the second is the dimensionless length along the axis of the flow channel. According to the work of Shah and London, for laminar flow

$$\left(\Delta P^*\right)_{\substack{fully \\ developed}} = 96x^+$$

$$\left(\Delta P^*\right)_{apparent} = 4x^+ \left[\frac{3.44}{\sqrt{x^+}} + \frac{24 + \frac{0.674}{4x^+} - \frac{3.44}{\sqrt{x^+}}}{1 + 2.9 \text{ x } 10^{-5} \left(x^+\right)^{-2}} \right] \tag{9.115}$$

Equations (9.115) are plotted in Figure 9.13 for a flow with $Re = 2800$. Notice that the pressure drop with the entry region included is always greater than the pressure drop assuming fully-developed flow. The pressure gradient is very steep in early part of the entry region and becomes a constant value in a relatively short distance. Because of this entry effect, modeling the flow as fully-developed throughout thus introduces an error in calculating the pressure drop. This error becomes negligibly small for very long flow channels. Fortunately, most of the situations encountered in thermal-fluids engineering are of this type. Internal flow channels are frequently, but not always, thousands of diameters in length so the error in calculating the pressure drop with the assumption of fully-developed flow is negligible. In the design of a thermal-fluid system, one must always check to see that this assumption is valid.

---

[2] R. K. Shah and A. L. London, *Laminar Flow Forced Convection in Ducts*, Academic Press, new York, 1978, pp. 40-42 and 168.

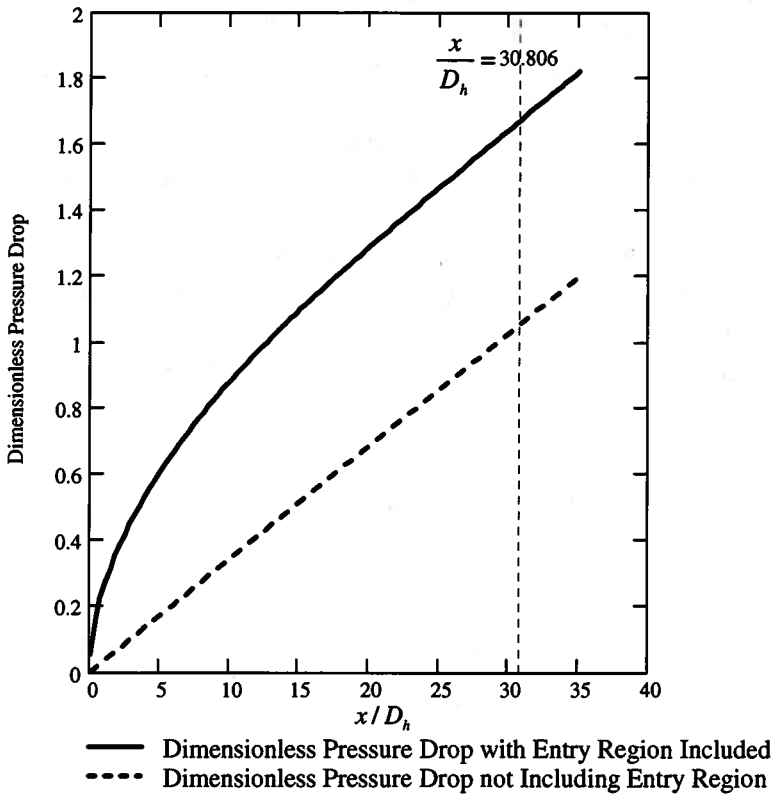

Figure 9.13 Pressure Drop for the Flow of a Viscous Fluid Between Parallel Flat Plates at $Re = 2800$

9.9.1.3 Laminar Couette Flow with a Moving Boundary and a Pressure Gradient: We have already considered the case of a simple shear flow between two parallel flat plates in which one of the plates was moving and the flow was generated by the movement of that plate. We now take up the case in which a pressure gradient is also imposed upon the flow. The flow geometry is shown schematically in Figure 9.14. The upper plate moves with velocity ϑ_0 while

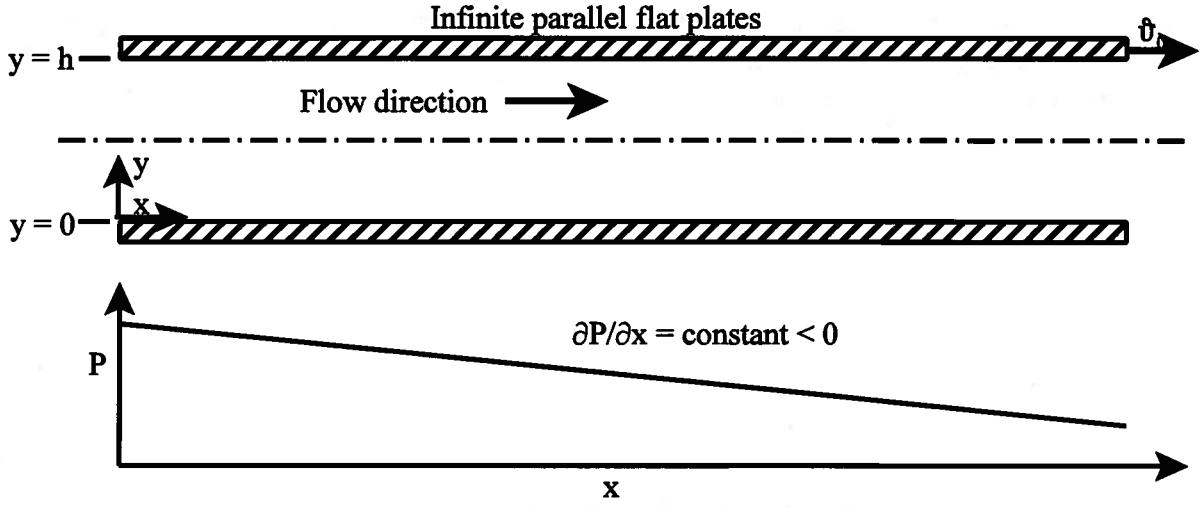

Figure 9.14 Fully-developed Planar Couette Flow with a Moving Boundary

Notice that if the pressure gradient is zero we have the case of the simple shear flow with the linear velocity profile. Thus the general velocity distribution is a simple superposition of a linear

profile typical of the simple shear flow and a parabolic profile typical of flow with a pressure gradient. Superposition of velocity profiles can often be a useful technique for the solution of the Navier-Stokes equation.

Since the velocity profile is a function of y only, the shear stress distribution becomes

$$\tau_{yx} = \mu\frac{\vartheta_0}{h} + h\left(\frac{\partial P}{\partial x}\right)\left[\frac{y}{h} - \frac{1}{2}\right] \tag{9.119}$$

For a channel of width b, the volumetric flow rate becomes

$$\dot{V} = \int_0^h \vartheta_x b dy = \frac{\vartheta_0 hb}{2} - \frac{1}{12\mu}\left(\frac{\partial P}{\partial x}\right)h^3 b \tag{9.120}$$

The average velocity is then given by

$$\vartheta_{ave} = \frac{\dot{V}}{A} = \frac{\vartheta_0}{2} - \frac{1}{12\mu}\left(\frac{\partial P}{\partial x}\right)h^2 \tag{9.121}$$

To determine the maximum velocity in the flow field, we make use of the fact that this occurs where the velocity gradient becomes zero. From equation (9.118) this occurs at

$$y_{\vartheta_{max}} = \frac{h}{2} - \frac{\frac{\vartheta_0}{h}}{\left(\frac{1}{\mu}\right)\left(\frac{\partial P}{\partial x}\right)} \tag{9.122}$$

Thus the location of the point in the flow where the maximum velocity occurs depends upon the magnitude of the pressure gradient as does the value of the maximum velocity itself. Experiment has shown that the laminar flow velocity profile of equation (9.118) is valid up to $Re_{critical} = 1500$ where the Reynolds number is based upon the characteristic length h.

In Figure 9.15 we have plotted in dimensionless form some sample velocity profiles for the three possible cases of the pressure gradient. Notice that if the pressure gradient is negative, meaning that the pressure decreases in the direction of the flow, the flow velocity is always positive. This is known as a favorable pressure gradient and results in flows that are inherently stable. However, if the pressure gradient is positive, meaning that the pressure increases in the direction of flow, it is possible for the velocity profile to have regions where the flow velocity is negative, thereby producing flow reversal. For this reason, this type of pressure gradient is known as an adverse pressure gradient and leads to flows that can become unstable.

As we shall soon see, these cases of flow reversal are extremely important in external flows because they can lead to separation of the flow from the surfaces on which they are occurring. In the case of aerodynamic bodies, this can lead to a significant increase in the drag experienced by the body subjected to the flow. The important point here is that we see that flow reversal can occur when there is an adverse (positive) pressure gradient. Such pressure gradients can occur in external flows when the flow is decelerated as it is on the back side of aerodynamic shapes. This is the reason that aerodynamic shapes such as the bodies of fish are shaped so that the flow on the downstream side of the body is decelerated as slowly as possible. This helps to make the positive pressure gradient as small as possible, thereby minimizing the possibility for flow reversal and eventual separation of the boundary layer from the surface. This separation leads to high aerodynamic drag. In the case of fish, those with poor aerodynamic shapes (high drag) were too slow to escape their faster predators and literally got eaten alive because of poor thermal-fluid design. By the process of natural selection, fish have excellent aerodynamic characteristics.

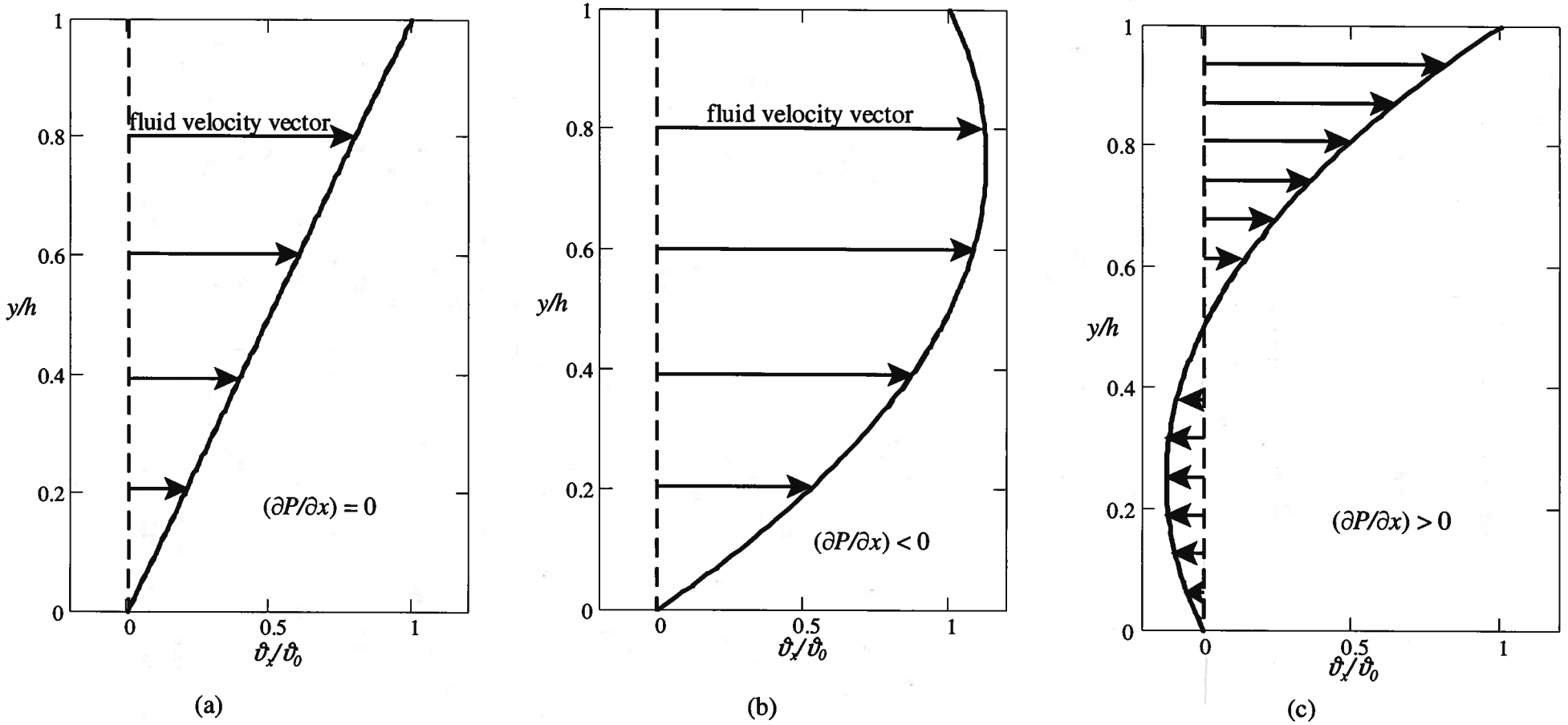

Figure 9.15 The Effect of a Pressure Gradient on Plane Couette Flow

9.9.1.4 Slider Bearings: A common application of the type of flow just considered occurs when the gap h is not a constant but varies slightly along the x-axis. Under these conditions, the pressure gradient is no longer constant. In fact, the pressure varies in the x-direction in such a way that when we integrate this pressure distribution over the upper surface, we find that the flow is capable of supporting a load in the y-direction. The resulting geometry is then a slider bearing capable of supporting enormous loads if properly designed. If we assume that there is no flow in the z-direction and we regard the volumetric flow rate of equation (9.120) as a local value since h is now a function of x, it still must be the case that this flow rate is a constant in the x-direction. Clearly the flow velocity increases as the gap decreases. Then for unit width in the z-direction

$$\frac{d\left(\dot{V}/b\right)}{dx} = \frac{\vartheta_0}{2}\frac{dh}{dx} - \frac{1}{12\mu}\frac{d}{dx}\left(h^3\frac{\partial P}{\partial x}\right) = 0$$

$$\frac{d}{dx}\left(h^3\frac{\partial P}{\partial x}\right) = 6\mu\vartheta_0\frac{dh}{dx} \qquad (9.123)$$

For a channel of variable gap, $h = h(x)$, equation (9.123) determines the approximate pressure distribution provided $dh/dx << 1$. Equation (9.123) is the fundamental equation that describes the performance of simple slider bearings. Notice that due to the presence of the velocity ϑ_0 in equation (9.123), the bearing is hydrodynamic and not hydrostatic. That is, the load carrying capacity (as we shall soon see) is linearly related to the velocity. If $\vartheta_0 = 0$, we have no bearing since that would make the pressure gradient zero. Also note that if ϑ_0 = constant, the pressure distribution depends upon h. We shall now show by way of example that the bearing will respond to an increase in the load by changing the geometry by changing h and/or dh/dx.

Example 9E.4: As shown in Figure 9E.4a, a simple slider bearing has a uniform taper from the inlet, where the gap is H_1, to the exit where the gap is H_2. This gap is filled with oil of viscosity μ and density ρ. The upper surface is stationary and the lower surface moves at a steady velocity ϑ_0. The thickness of the oil film at a location x measured relative to the leading edge of bearing is $h(x)$.

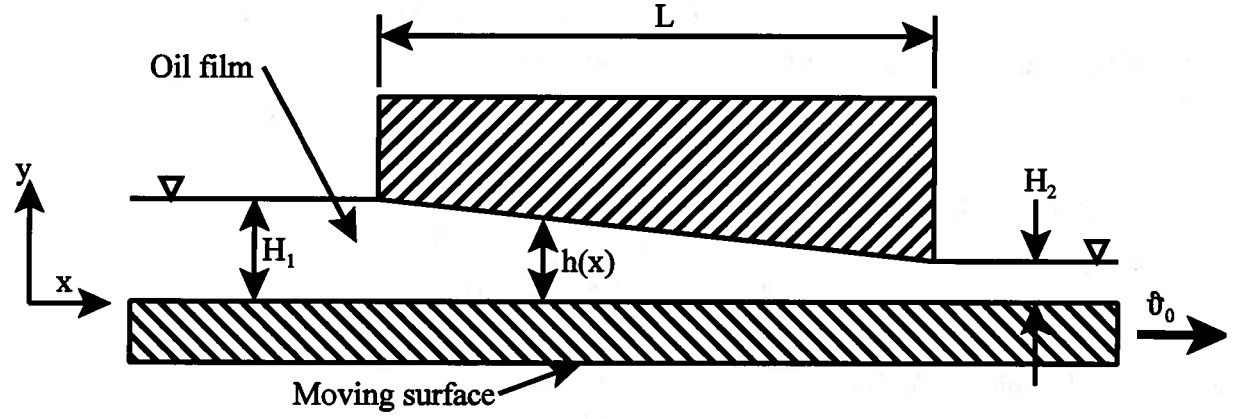

Figure 9E.4a

(a) Show that the pressure gradient along the slider is given by

$$\frac{dP}{dx} = \frac{12\mu\vartheta_0}{h^3}\left(\frac{h}{2} - \frac{H_1H_2}{H_1+H_2}\right)$$

(b) If the pressure at each open end of the bearing is P_{atm}, sketch the pressure profile $P = P(x)$ in the oil film. Find the location the maximum pressure and its value.

(c) If the bearing has dimension b normal to the plane of the sketch, what is the load carrying capacity of the upper block of the bearing?

Solution: (a) The pressure distribution in the bearing is given by equation (9.123). If we integrate this expression with respect to x we obtain

$$\int \frac{d}{dx}\left(h^3 \frac{\partial P}{\partial x}\right) dx = 6\mu \vartheta_0 \int \frac{dh}{dx} dx$$

$$h^3 \frac{\partial P}{\partial x} = 6\mu \vartheta_0 h + C_1$$

$$\frac{dP}{dx} = \frac{6\mu \vartheta_0}{h^2} + \frac{C_1}{h^3}$$

In order to integrate a second time, we note that

$$\frac{dP}{dx} = \frac{dP}{dh}\frac{dh}{dx}$$

but

$$h = H_1 + (H_2 - H_1)\frac{x}{L}$$

Then

$$\frac{dP}{dh} = \left(\frac{L}{H_2 - H_1}\right)\left[\frac{6\mu \vartheta_o}{h^2} + \frac{C_1}{h^3}\right]$$

Integrating this expression, we get

$$P = \frac{-6\mu \vartheta_0 L}{(H_2 - H_1)}\left(\frac{1}{h}\right) - \left(\frac{C_1 L}{H_2 - H_1}\right)\left(\frac{1}{2h^2}\right) + C_2$$

The boundary conditions are

(1) $P = P_{atm}$ at $h = H_1$

(2) $P = P_{atm}$ at $h = H_2$

Then substituting the boundary conditions and solving for C_1, we get

$$C_1 = -12\mu \vartheta_0 \left(\frac{H_1 H_2}{H_1 + H_2}\right)$$

Substituting for C_1 in the expression for dP/dx, we get

$$\frac{dP}{dx} = \frac{12\mu \vartheta_0}{h^3}\left[\frac{h}{2} - \frac{H_1 H_2}{H_1 + H_2}\right]$$

(b) The maximum pressure in the oil film can be determined by setting $dP/dx = 0$ and solving for the value of h. Then

$$\frac{h}{2} - \frac{H_1 H_2}{H_1 + H_2} = 0$$

$$h_{P_{max}} = \frac{2H_1 H_2}{H_1 + H_2}$$

Since

$$h = H_1 + (H_1 - H_2)\frac{x}{L}$$

it follows that the maximum pressure in the gap occurs at

$$x = L\frac{H_1}{H_1 + H_2}$$

From the boundary condition (1), we have upon substitution for C_1 and solving for C_2

$$C_2 = P_{atm} + \frac{6\mu\vartheta_0 L}{H_2^{\,2} - H_1^{\,2}}$$

and

$$P = P_{atm} + \frac{6\mu\vartheta_0 L}{H_2^{\,2} - H_1^{\,2}}\left[1 + \frac{H_1 H_2}{h^2} - \frac{H_2 + H_1}{h}\right]$$

Then the maximum value of the pressure is

$$P_{max} = P_{atm} + \frac{6\mu\vartheta_0 L}{(H_1 + H_2)}\frac{(H_1 - H_2)}{4H_1 H_2}$$

We can rewrite the expression for the pressure in dimensionless form.

$$\frac{P - P_{atm}}{6\mu\vartheta_0 L \Big/ \left(H_1^{\,2} - H_2^{\,2}\right)} = -\left[1 + \frac{H_1 H_2}{h^2} - \frac{H_2 + H_1}{h}\right]$$

and we can combine it with the expression for $h = h(x)$. This yields an expression for the dimensionless pressure as a function of x. The resulting expression can be plotted as shown in Figure 9E.4b for the cases in which $H_1 = 1$ and $H_2 = 0.99$ and $H_1 = 1$ and $H_2 = 0.97$. Notice that as the slope of the slider increases, the maximum pressure increases and the location of the peak pressure shifts downstream.

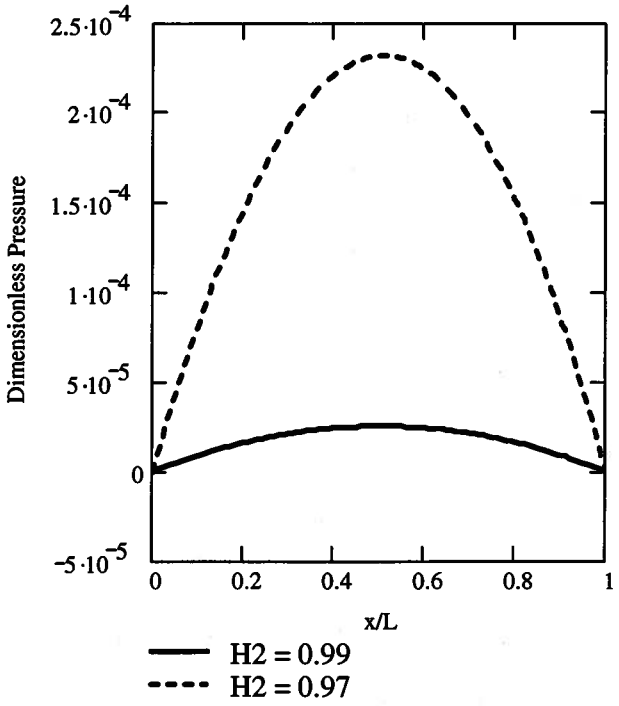

Figure 9E.4b Dimensionless Pressure Distribution Across the Face of a Slider Bearing

(c) The pressure distribution has a parabolic shape that can be integrated to yield the load carrying capability of the bearing.

$$F = \int PdA = \int Pbdx$$

$$\frac{F}{b} = \int_0^L \left(P_{atm} + \frac{6\mu\vartheta_0 L}{H_2^2 - H_1^2} \left[1 + \frac{H_1 H_2}{\left\{ H_1 - (H_2 - H_1)\frac{x}{L} \right\}^2} - \frac{H_1 + H_2}{\left\{ H_1 - (H_2 - H_1)\frac{x}{L} \right\}} \right] \right) dx$$

Figure 9E.4c shows the force per unit width of a slider bearing with the following operating conditions: ϑ_0 = 10 m/sec; μ = 0.50 kg/m sec; L = 1 m; $H_2 = 0.9H_1$. Note the enormous load

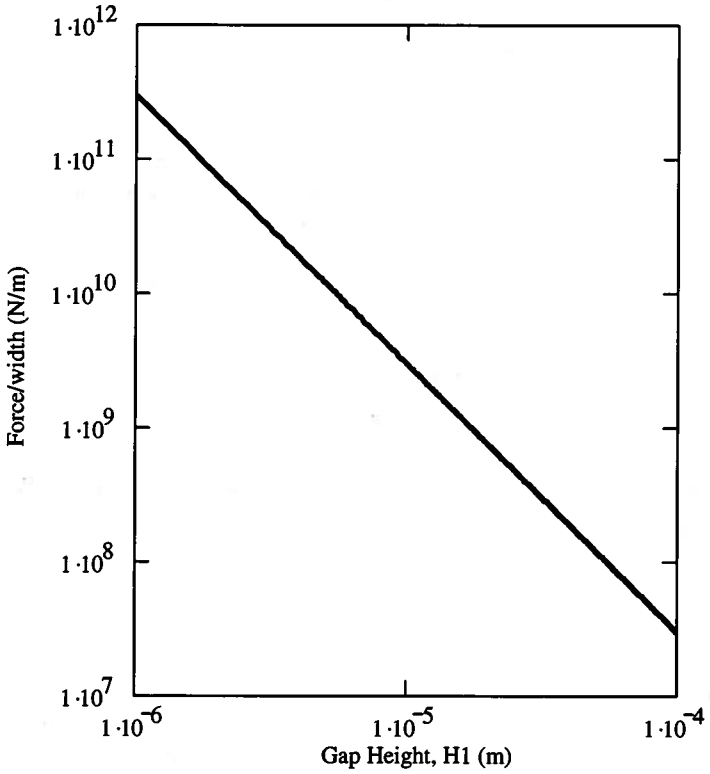

Figure 9E.4c Dependence of Bearing Load Upon Gap Height

carrying capability of the bearing when the oil film is its thinnest. The load carrying capability falls off rapidly as the thickness of the oil film increases. (Note the log-log scale of Figure 9E.4c.) For the thinnest oil films, the machining tolerances of the bearing must be very small in order for the bearing to function as designed. The adjustment of the gap height to a change in load is stable since as load is increased and the gap decreases, the load carrying capability increases. Also note that the larger the angle of inclination of the underside of the bearing, the larger the load. Of course, this increase in the angle has its limits before the assumption of a small angle of inclination is violated and the theory breaks down.

Note also that Boogie boards operate on this principle. In the case of the Boogie board, one has to throw the board to generate a velocity relative to the sheet of water before one jumps on. If there is not sufficient velocity with the proper angle to the water surface, the board sinks when the load is applied. A similar phenomenon applies to the case of a windshield wiper blade sliding over the windshield of an automobile in the rain and to the case of an automobile hydroplaning on a thin film of water on a wet road surface. From Figure 9E.4c, it is not surprising that a 2000 kg automobile can be easily "lifted" (hydroplane) on a thin sheet of water

at turnpike speeds. The faster the speed of the vehicle, the greater the force and the more likely the phenomenon will occur.

9.9.1.5 Fully-developed Laminar Flow in a Circular Conduit: One of the most common geometries for internal flow in thermal-fluid systems is that of a pipe or tube of circular cross-section. For our purposes here, we shall consider the case of steady flow of a fluid in a horizontal pipe with gravity aligned with the vertical, normal to the principal flow direction as shown in Figure 9.16.

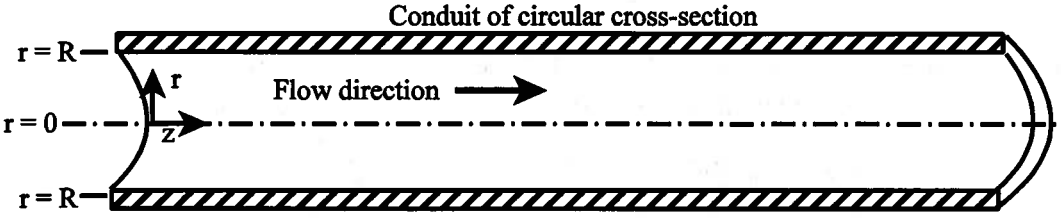

Figure 9.16 Fully-developed Flow in a Circular Conduit

For this geometry, circular coordinates (r, θ, z) are most useful for determining the velocity profile. The z-axis is aligned with the centerline of the pipe and the r-axis is radially outward. We wish to determine the velocity profile for fully-developed steady flow. Under these conditions, there will be no dependence on the z-coordinate so $\partial/\partial z = 0$. In addition, fully-developed flow will be axially symmetric so $\partial/\partial\theta = 0$. Then if there is no swirl, $\vartheta_\theta = 0$, and the continuity equation, equation (9.71), becomes

$$\frac{1}{r}\frac{\partial}{\partial r}(r\vartheta_r)+\frac{1}{r}\frac{\partial}{\partial\theta}(\vartheta_\theta)+\frac{\partial}{\partial z}(\vartheta_z)=0$$
$$\frac{1}{r}\frac{\partial}{\partial r}(r\vartheta_r)=0 \qquad (9.124)$$

Thus, from equation (9.124) it is apparent that $r\vartheta_r$ = constant, but at the wall, $r = R$ and $\vartheta_r = 0$ by the boundary condition, equation (9.74). Then it follows from equation (9.124) that $r\vartheta_r = 0$ and thus $\vartheta_r = 0$ everywhere. Then there is only one velocity component, ϑ_z, and it is a function of r only, $\vartheta_z = \vartheta_z(r)$. Then the r-component of the Navier-Stokes equation, equation (9.73a) becomes

$$\rho\left(\frac{\partial\vartheta_r}{\partial t}+\vartheta_r\frac{\partial\vartheta_r}{\partial r}+\frac{\vartheta_\theta}{r}\frac{\partial\vartheta_r}{\partial\theta}-\frac{\vartheta_\theta^2}{r}+\vartheta_z\frac{\partial\vartheta_r}{\partial z}\right)$$
$$=-\frac{\partial P}{\partial r}+\rho g_r+\mu\left[\frac{\partial}{\partial r}\left(\frac{1}{r}\frac{\partial}{\partial r}(r\vartheta_r)\right)+\frac{1}{r^2}\frac{\partial^2\vartheta_r}{\partial\theta^2}-\frac{2}{r^2}\frac{\partial\vartheta_\theta}{\partial\theta}+\frac{\partial^2\vartheta_r}{\partial z^2}\right] \qquad (9.125a)$$
$$-\frac{\partial P}{\partial r}+\rho g_r=0$$

Thus the pressure is hydrostatic across a plane perpendicular to the z-axis; however, since this dimension is small compared to the axial dimension, the pressure is usually considered uniform over this plane. The θ-component of the Navier-Stokes equation, equation (9.73b) becomes

$$\rho\left(\cancel{\frac{\partial v_\theta}{\partial t}}+\cancel{v_r}\cancel{\frac{\partial v_\theta}{\partial r}}+\cancel{\frac{v_\theta}{r}}\cancel{\frac{\partial v_\theta}{\partial \theta}}-\cancel{\frac{v_r v_\theta}{r}}+v_z\cancel{\frac{\partial v_\theta}{\partial z}}\right)$$

$$=-\frac{1}{r}\frac{\partial P}{\partial \theta}+\cancel{\rho g_\theta}+\mu\left[\frac{\partial}{\partial r}\left(\frac{1}{r}\frac{\partial}{\partial r}\left(r\cancel{v_\theta}\right)\right)+\frac{1}{r^2}\cancel{\frac{\partial^2 v_\theta}{\partial \theta^2}}-\frac{2}{r^2}\cancel{\frac{\partial v_r}{\partial \theta}}+\cancel{\frac{\partial^2 v_\theta}{\partial z^2}}\right] \qquad (9.125b)$$

$$\frac{\partial P}{\partial \theta}=0$$

Thus from equations (9.125a) and (9.125b), it follows that the pressure is a function of z only. The z-component of the Navier-Stokes equation, equation (9.73c) becomes

$$\rho\left(\cancel{\frac{\partial v_z}{\partial t}}+\cancel{v_r}\frac{\partial v_z}{\partial r}+\cancel{\frac{v_\theta}{r}}\cancel{\frac{\partial v_z}{\partial \theta}}-\cancel{\frac{v_\theta^2}{r}}+v_z\cancel{\frac{\partial v_z}{\partial z}}\right)$$

$$=-\frac{\partial P}{\partial z}+\cancel{\rho g_z}+\mu\left[\frac{1}{r}\frac{\partial}{\partial r}\left(r\frac{\partial v_z}{\partial r}\right)+\frac{1}{r^2}\cancel{\frac{\partial^2 v_z}{\partial \theta^2}}+\cancel{\frac{\partial^2 v_z}{\partial z^2}}\right] \qquad (9.125c)$$

$$\mu\frac{1}{r}\frac{\partial}{\partial r}\left(r\frac{\partial v_z}{\partial r}\right)=\frac{\partial P}{\partial z}$$

This is the now familiar result for fully-developed internal flow, namely that the viscous force (per unit volume), the left-hand side of equation (9.125c), is balanced by the net pressure force (per unit volume), the right-hand side of equation (9.125c). Equation (9.125c) also presents the interesting result that the left-hand side is a function of r only and the right-hand side is a function of z only. The only way that this can be true is if equation (9.125c) is equal to a constant. It follows, then, that the pressure gradient in the z-direction is a constant, $(\partial P/\partial z)$ = constant. Then equation (9.125c) can be rearranged and integrated. Thus

$$\mu\frac{\partial}{\partial r}\left(r\frac{\partial v_z}{\partial r}\right)=r\frac{\partial P}{\partial z}$$

$$\mu\int\frac{\partial}{\partial r}\left(r\frac{\partial v_z}{\partial r}\right)dr=\frac{\partial P}{\partial z}\int r dr \qquad (9.126)$$

$$\mu r\frac{\partial v_z}{\partial r}=\frac{\partial P}{\partial z}\frac{r^2}{2}+C_1$$

$$\mu\frac{\partial v_z}{\partial r}=\frac{\partial P}{\partial z}\frac{r}{2}+\frac{C_1}{r}$$

Equation (9.126) can be integrated to yield

$$\mu\int\frac{\partial v_z}{\partial r}dr=\frac{\partial P}{\partial z}\int\frac{r}{2}dr+C_1\int\frac{dr}{r} \qquad (9.127)$$

$$v_z=\frac{r^2}{4\mu}\left(\frac{\partial P}{\partial z}\right)+\frac{C_1}{\mu}\ln r+C_2$$

Since the velocity must be finite at the centerline of the conduit, $r = 0$, it must be true that $C_1 = 0$. Alternatively, we could have noticed in equation (9.126) that if the velocity profile is to be axially symmetric about the centerline of the conduit, $r = 0$, it must be true that $\partial v_z/\partial r = 0$ at the centerline. Then it again follows that $C_1 = 0$. By the "no-slip" boundary condition at the wall of the conduit, $r = R$, the velocity must vanish, $v_z(R) = 0$. Then

$$C_2 = -\frac{R^2}{4\mu}\left(\frac{\partial P}{\partial z}\right) \tag{9.128}$$

Then substituting the boundary conditions into equation (9.127), we get the velocity profile for fully-developed laminar flow in a circular conduit.

$$\vartheta_z = \frac{r^2}{4\mu}\left(\frac{\partial P}{\partial z}\right) - \frac{R^2}{4\mu}\left(\frac{\partial P}{\partial z}\right) = \frac{1}{4\mu}\left(\frac{\partial P}{\partial z}\right)\left(r^2 - R^2\right) = -\frac{R^2}{4\mu}\left(\frac{\partial P}{\partial z}\right)\left[1 - \left(\frac{r}{R}\right)^2\right] \tag{9.129}$$

This velocity profile is a famous result in thermal-fluids engineering and is named Hagen-Poiseuille flow after the two men who first studied it. In Germany in 1839 G. L. Hagen (1797 - 1884) conducted some very meticulous measurements of the flow of water in small-diameter tubes, using the water temperature instead of the viscosity as one of the parameters. A few years later the French physician Jean Louis Poiseuille (1799 - 1869) repeated the experiments independently, using oil and mercury in addition to water. Although neither Poiseuille nor Hagen really understood the mathematics of the phenomenon, they did appreciate the importance of the pressure drop over the length of the tube (pressure gradient) in determining the magnitude of the flow. It was Hagen who generated and correlated the data in the form of "resistance" plots similar to Figure 9.8 that showed the linear dependence of pressure drop upon the average velocity at low velocities. Hagen even anticipated the work of Osborne Reynolds when he noted in 1854 that the flow was not always laminar, "the efflux jet sometimes being clear and sometimes frothy". Similarly, he found that sawdust suspended in the water sometimes moved in straight lines and sometimes very irregularly. In the latter instances he noted that his linear resistance equation no longer applied. Based on this early work and the subsequent work of Reynolds, we now know that the transition from laminar to turbulent flow in a circular conduit occurs for 2300 $\leq Re_{tr} < 10^4$. As a conservative estimate for design purposes, the critical value of the Reynolds number for this flow configuration is generally considered to be $Re_{critical} = 2100$.

The shear stress distribution for Hagen-Poiseuille flow is given by equation (9.72), viz.

$$\tau_{zr} = \tau_{rz} = \mu\left(\cancel{\frac{\partial \vartheta_r}{\partial z}} + \frac{\partial \vartheta_z}{\partial r}\right)$$

$$\tau_{zr} = \tau_{rz} = \frac{r}{2}\left(\frac{\partial P}{\partial z}\right) \tag{9.130}$$

Thus the shear stress is zero at the centerline and maximum at the wall of the conduit.

The volumetric flow rate is given by

$$\dot{V} = \int_0^R \vartheta_z 2\pi r dr = -\int_0^R \frac{R^2}{4\mu}\left(\frac{\partial P}{\partial z}\right)\left[1 - \left(\frac{r}{R}\right)^2\right] 2\pi r dr = -\frac{\pi R^4}{8\mu}\left(\frac{\partial P}{\partial z}\right) \tag{9.131}$$

Notice that since the pressure gradient is negative (meaning that the pressure decreases in the direction of flow, a condition known as a "favorable" pressure gradient), the volumetric flow rate is positive even though there is a negative sign on the right-hand side of equation (9.131).

The average velocity is given by

$$\vartheta_{ave} = \frac{\dot{V}}{A_c} = \frac{\dot{V}}{\pi R^2} = -\frac{R^2}{8\mu}\left(\frac{\partial P}{\partial z}\right) \tag{9.132}$$

Then the velocity profile of equation (9.129) can be written

$$\vartheta_z = 2\vartheta_{ave}\left[1 - \left(\frac{r}{R}\right)^2\right] \tag{9.133}$$

The maximum velocity can be determined by taking the derivative of equation (9.129) and setting it equal to zero and then solving for the appropriate value of r. Then

$$\frac{d\vartheta_z}{dr} = \frac{r}{2\mu}\left(\frac{\partial P}{\partial z}\right) = 0 \qquad (9.134)$$

$$\therefore r = 0$$

Substituting this value of r into equation (9.129), we get

$$\vartheta_{max} = -\frac{R^2}{4\mu}\left(\frac{\partial P}{\partial z}\right) = 2\vartheta_{ave} \qquad (9.135)$$

Then the velocity profile can be written in the form

$$\vartheta_z = \vartheta_{max}\left[1 - \left(\frac{r}{R}\right)^2\right] \qquad (9.136)$$

This velocity profile is plotted in Figure 9.17 which shows the parabolic nature of the distribution. (The physically meaningless negative values of the parameter r/R are used to show the symmetry of the profile about the centerline, $r = 0$, of the conduit.)

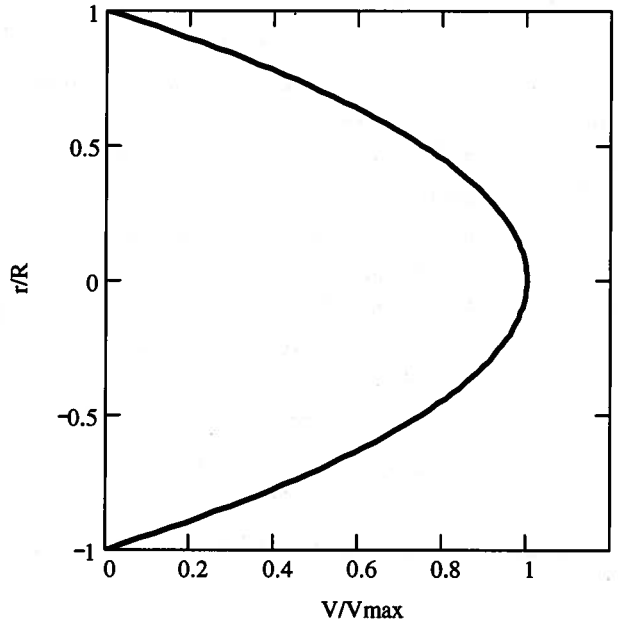

Figure 9.17 Velocity Profile for Fully-developed Laminar Flow in a Circular Conduit

Typically, a thermal-fluid system consists of an assembly of specialized devices of various types, each of which processes the working fluid in some way. These devices are interconnected by circular conduits (pipes) that facilitate the movement of the working fluid from one device to the other. The devices and the pipes are usually, but not always, arranged in a closed circuit so that the working fluid starts out in one location and then passes through all the devices and their interconnecting pipes in succession, and ultimately returns to the starting point. From equation (9.130) it is apparent that in fully developed laminar flow, the amount of incompressible fluid that we can transport, i.e., the volumetric flow rate, through a pipe of fixed dimension is directly proportional to the pressure gradient imposed on the conduit. From the

point of view of a closed circuit of fixed length, this pressure gradient translates into a drop in pressure of the fluid from the beginning of the circuit to its end. Thus, in order for the fluid to flow through the circuit on a continual basis, it is necessary to insert at the start of the circuit a device that increases the pressure of the fluid by the right amount to compensate for the pressure drop around the circuit. The thermal-fluid device that accomplishes this is a pump, but in order to specify the pump required for a given system design, it is necessary to know the magnitude of the pressure drop in the circuit.

To facilitate this design process, thermal-fluids engineers have introduced the concept of a dimensionless parameter known as the friction factor and denoted by the symbol f, that contains the essence of the viscous behavior of a fluid flowing in a conduit. In equation (9.91), we showed that the pressure gradient (expressed in non-dimensional form) in a laminar flow system could be related to the Reynolds number in that system. As we shall now show, for laminar internal flow that relation depends upon the friction factor. Since the pressure gradient appearing in equation (9.131) for the volumetric flow rate for laminar flow in a circular conduit is a constant, it can be integrated for a pipe of length L. Then

$$\begin{aligned}
\frac{dP}{dz} &= -\text{constant} = -a \\
\int_{P_1}^{P_2} dP &= -a\int_0^L dz \\
P_2 - P_1 &= -a(L-0) \\
P_1 - P_2 &= aL \\
a &= \frac{P_1 - P_2}{L} \\
\therefore \frac{dP}{dz} &= -\frac{P_1 - P_2}{L}
\end{aligned} \tag{9.137}$$

Then we can write equation (9.131) in the form

$$\dot{V} = \frac{\pi R^4}{8\mu}\left(\frac{P_1 - P_2}{L}\right) = \frac{\pi R^4}{8\mu}\frac{\Delta P}{L}$$

$$\frac{\Delta P}{L} = \frac{8\mu}{\pi R^4}\dot{V} = \frac{8\mu}{\pi R^4}\vartheta_{ave}A_c = \frac{8\mu}{\pi R^4}\vartheta_{ave}\pi R^2$$

$$\frac{\Delta P}{L} = \frac{32\mu\vartheta_{ave}}{D^2} = \frac{\mu}{\vartheta_{ave}D\rho}\frac{32\rho\vartheta_{ave}^{\,2}}{D}$$

$$\begin{aligned}
\frac{\Delta P}{L} &= \frac{1}{Re}\frac{64}{D}\frac{\rho\vartheta_{ave}^{\,2}}{2} \\
\frac{\Delta P \Big/ \frac{\rho\vartheta_{ave}^{\,2}}{2}}{L/D} &= \frac{64}{Re}
\end{aligned} \tag{9.138}$$

The term on the left-hand side of equation (9.138) is the dimensionless pressure gradient of equation (9.91) and the term on the right-hand side of equation (9.138) is the dimensionless parameter defined as the friction factor. Then

$$\frac{\Delta P / \frac{\rho \vartheta_{ave}^{\,2}}{2}}{L/D} \equiv f \tag{9.139}$$

This formulation can be generalized for all internal flows so that the pressure drop can be written

$$\Delta P = f\left(\frac{L}{D_h}\right)\left(\frac{\rho \vartheta_{ave}^{\,2}}{2}\right) \tag{9.140}$$

where for each particular flow configuration specified by the hydraulic diameter, D_h, the friction factor takes on a unique value. For the case of fully-developed laminar flow in a circular conduit

$$f = \frac{64}{Re} \tag{9.141}$$

For the case of fully-developed laminar flow between infinite parallel flat plates, equation (9.115) gives

$$f = \frac{96}{Re} \tag{9.142}$$

Table 9.3 gives the value of the friction factor for fully-developed laminar flow in conduits of different cross-sections, such as triangles, rectangles, and ellipses. In each case, the value of the friction factor has been obtained by solving the Navier-Stokes equation with the appropriate boundary conditions. (Table 9.3 also contains some additional data that we will make use of in Chapter 11.) In the design of thermal-fluid systems, the pressure drop for fully-developed laminar flow in a conduit of particular cross-section and known length is determined by substituting into equation (9.140) the appropriate values for f and D_h obtained from Table 9.3. The value of the critical Reynolds number for the transition from laminar to turbulent flow in these non-circular cross-sections can be conservatively assumed to be the same as that for the circular cross-section with the appropriate value of D_h used in the Reynolds number.

The friction factor used in equation (9.140) is known as the Darcy friction factor in honor of the French engineer Henry Darcy (1803 - 1858) who was an early pioneer in the field fluid dynamics. Henry Darcy is credited with the invention of the modern style Pitot tube, was the first researcher to suspect the existence of the boundary layer in fluid flow, contributed to the development of the Darcy-Weisbach equation for pipe flow resistance (to be introduced later), made major contributions to open channel flow research, and developed Darcy's Law for laminar flow in homogeneous, porous media. Darcy's Law is a foundation stone for several fields of study including ground-water hydrology, soil physics, and petroleum engineering.

In the thermal-fluids engineering literature there is another friction factor, known as the Fanning friction factor, that is sometimes used, especially in the United Kingdom and Europe. In the United States, the literature devoted to heat transfer phenomena also makes frequent use of the Fanning friction factor. The Fanning friction factor is related to the Darcy friction factor in the following way:

$$f_{Darcy} = 4 f_{Fanning} \tag{9.143}$$

In utilizing tabulated data for the friction factor found in the literature, one must always check to see which friction factor is represented. If the data do not specify, one can always check to see how the friction factor for fully-developed laminar flow in a circular conduit is related to the Reynolds number. If the relationship is that of equation (9.141), the data are for the Darcy friction factor. If the constant of proportionality is 16 and not 64, the data are for the Fanning friction factor.

Table 9.3 Friction Factor and Nusselt Number Data for Laminar Flow in Non-circular Conduits

$$Re = \frac{\vartheta D_h \rho}{\mu} \quad \text{where} \quad D_h = \frac{4A_{cross\text{-}section}}{\wp} = \frac{4A_c}{\wp} \quad \text{and } \wp \text{ is the wetted perimeter}$$

Nu_H is the Nusselt number for constant heat flux and Nu_T is the Nusselt number for constant wall temperature

	Ellipse					Rectangle					Triangle				
b/a	A_c/a^2	$\wp/a$	$f{\cdot}Re$	Nu_H	Nu_T	A_c/a^2	$\wp/a$	$f{\cdot}Re$	Nu_H	Nu_T	A_c/a^2	$\wp/a$	$f{\cdot}Re$	Nu_H	Nu_T
10.00	31.42	4.06	77.26	5.12	3.70	40.00	44.00	84.68	6.78	5.91	10.00	22.10	50.17	2.29	1.34
5.00	15.71	4.20	74.41	4.96	3.77	20.00	24.00	76.28	5.74	4.83	5.00	12.20	51.62	2.51	1.70
2.00	6.28	4.84	67.29	4.56	3.74	8.00	12.00	62.19	4.12	3.39	2.00	6.47	53.28	2.88	2.22
1.00	3.14	6.28	64.00	4.36	3.66	4.00	8.00	56.91	3.61	2.98	1.00	4.83	52.61	3.10	2.46
0.90	2.83	5.97	64.09	4.37	3.66	3.60	7.60	57.04	3.62	2.97	0.90	4.69	52.22	3.12	2.47
0.80	2.51	5.67	64.39	4.39	3.67	3.20	7.20	57.51	3.66	3.01	0.80	4.56	51.84	3.11	2.46
0.70	2.20	5.38	64.98	4.42	3.69	2.80	6.80	58.42	3.75	3.09	0.70	4.44	51.45	3.10	2.45
0.60	1.88	5.11	65.92	4.48	3.72	2.40	6.40	59.92	3.89	3.21	0.60	4.33	51.06	3.06	2.41
0.50	1.57	4.84	67.29	4.56	3.74	2.00	6.00	62.19	4.12	3.39	0.50	4.24	50.49	2.99	2.34
0.40	1.26	4.60	69.18	4.67	3.76	1.60	5.60	65.47	4.47	3.67	0.40	4.15	49.81	2.85	2.18
0.30	0.94	4.39	71.58	4.80	3.78	1.20	5.20	70.05	4.99	4.12	0.30	4.09	49.12	2.71	2.02
0.20	0.63	4.20	74.41	4.96	3.77	0.80	4.80	76.28	5.74	4.83	0.20	4.04	48.63	2.49	1.72
0.10	0.31	4.06	77.26	5.12	3.70	0.40	4.40	84.68	6.78	5.91	0.10	4.01	48.31	2.63	1.37

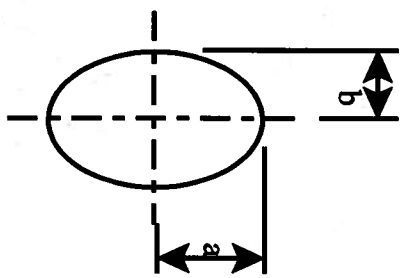

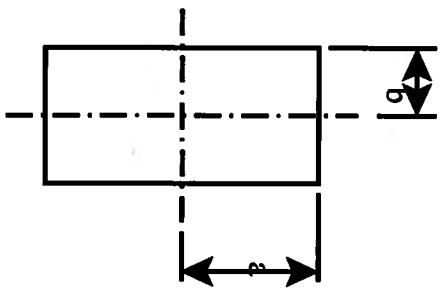

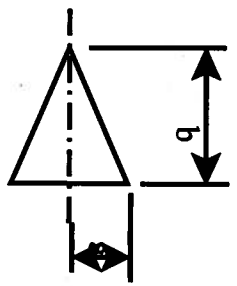

For the fully-developed flow inside the circular conduit, one of the important effects of the fluid friction embodied in the friction factor can be seen from the application of the first law of thermodynamics. For a control volume consisting of a length L of the conduit, there is no heat transfer or shaft work transfer. Furthermore, once the velocity profile becomes fully-developed, the average kinetic energy of the fluid is the same at every location along the axis of the conduit. Then the steady-flow form of the first law becomes

$$h_{out} - h_{in} = 0 \tag{9.144}$$

If we substitute the constitutive relation for the enthalpy for the incompressible fluid model into equation (9.144), we get

$$\begin{aligned} u_{out} - u_{in} &= P_{in}v_{in} - P_{out}v_{out} \\ u_{out} - u_{in} &= v(P_{in} - P_{out}) = \frac{P_{in} - P_{out}}{\rho} = f\left(\frac{L}{D_h}\right)\left(\frac{\vartheta_{ave}^{\,2}}{2}\right) \end{aligned} \tag{9.145}$$

Thus for this adiabatic, incompressible flow, the effect of the fluid friction manifests itself as the flow work transfer in the conduit which, in turn, results in an increase in the stored thermal energy of the fluid. If we substitute the energy constitutive relation for the incompressible fluid model into equation (9.145), we see that the fluid friction produces a temperature increase in the fluid. Thus,

$$\begin{aligned} c(T_{out} - T_{in}) &= f\left(\frac{L}{D_h}\right)\left(\frac{\vartheta_{ave}^{\,2}}{2}\right) \\ T_{out} - T_{in} &= \frac{f}{c}\left(\frac{L}{D_h}\right)\left(\frac{\vartheta_{ave}^{\,2}}{2}\right) \end{aligned} \tag{9.146}$$

If we substitute equation (9.141) into equation (9.146), we see that the temperature increase is directly proportional to the fluid viscosity and the average velocity of the fluid.

$$T_{out} - T_{in} = \frac{64}{Re_{D_h}}\frac{1}{c}\left(\frac{L}{D_h}\right)\left(\frac{\vartheta_{ave}^{\,2}}{2}\right) = \frac{32\mu}{\rho D_h}\frac{\vartheta_{ave}}{c}\left(\frac{L}{D_h}\right) \tag{9.147}$$

From the second law of thermodynamics we can calculate the rate of entropy generation for this flow configuration.

$$\dot{S}_{gen} = \dot{m}(s_{out} - s_{in}) = \dot{m}c\ln\frac{T_{out}}{T_{in}} = \rho c\dot{V}\ln\left(1 + \frac{32\mu L\vartheta_{ave}}{\rho c T_{in} D_h^{\,2}}\right) \tag{9.148}$$

This rate is clearly positive and shows that fluids with higher viscosity generate more entropy for a given flow geometry. Also, the greater the average velocity in a given flow geometry, the greater the rate of entropy generation. Note that this rate of entropy generation is due to the flow work transfer and not the dissipation of kinetic energy in the flow. The kinetic energy of the flow is constant throughout the length of the conduit.

9.9.1.6 Laminar Flow in the Entry Region of a Circular Conduit: The development of fully-developed laminar flow in the circular conduit is analogous to that in the case of infinite parallel flat plates. The only exception is that the entry region in the circular conduit is three-dimensional since the walls wrap around the "undisturbed" region forming a "core" of accelerating flow that can be modeled as inviscid. For uniform velocity at the entrance to the conduit, the boundary layer at the wall starts to grow at the mouth and eventually fills the entire conduit as the flow progresses downstream a distance equal to the entry length, L_{entry}. Within this length, the "undisturbed" flow accelerates until the maximum value of the velocity given by equation

(9.135) is achieved at the centerline. According to Shah and London[3], the entry length data for laminar flow in a circular conduit can be best fit by the relation

$$\left(\frac{L_{entry}}{D_h}\right)_{laminar} = \frac{0.60}{0.035Re+1} + 0.056Re \tag{9.149}$$

Then for flow at the critical value of the Reynolds number, the entry length attains its largest value for laminar flow. Thus, fully-developed flow in a circular conduit occurs within a length of $L \leq 117.61D_h$ depending upon the Reynolds number. The[4] accelerating flow in the "undisturbed" core causes the pressure in the entry region to drop faster than it does in the fully-developed region. Using the dimensionless parameters given in equation (9.114), the dimensionless pressure drop is given by Shah and London[4] as

$$\left(\Delta P^*\right)_{\substack{fully \\ developed}} = 64x^+$$

$$\left(\Delta P^*\right)_{apparent} = 4x^+\left[\frac{3.44}{\sqrt{x^+}} + \frac{16+\frac{1.25}{4x^+}-\frac{3.44}{\sqrt{x^+}}}{1+2.1 \text{ x } 10^{-4}\left(x^+\right)^{-2}}\right] \tag{9.150}$$

Figure 9.18 shows the axial pressure distribution for a sample flow of water in a pipe with $Re = 2100$ according to equation (9.150).

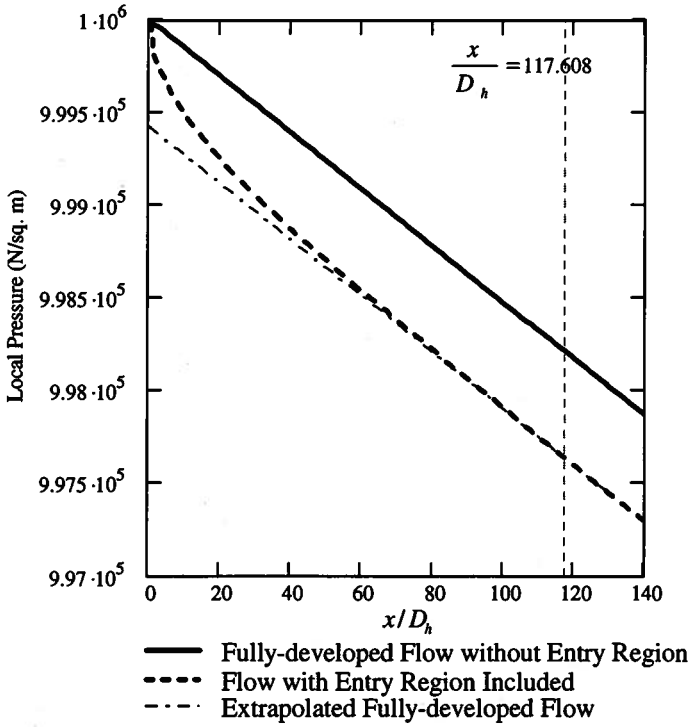

Figure 9.18 Axial Pressure Distribution for Flow of Water in a Pipe, $Re = 2100$

[3] R. K. Shah and A. L. London, *op. cit.*, p. 99.

[4] R. K. Shah and A. L. London, *op. cit.*, p. 98.

The pressure of the water at the inlet to the pipe is $P_{inlet} = 10^6$ N/m^2. The solid line shows the axial pressure distribution assuming fully-developed flow throughout the flow field with no entry region. The dashed line shows the pressure distribution with the effect of the entry region included. This is referred to as the apparent pressure drop. The vertical line indicates the location of the end of the entry region as defined by the full development of the velocity profile (L_{entry} = $117.608D_h$ for $Re = 2100$ for this flow configuration). Notice that the pressure with the entry region included is always lower than the pressure without the entry region taken into account. This is the case even though the pressure gradient is the same in both cases once the flow becomes fully developed. This is a result of the acceleration of the flow in the "undisturbed" region. Also notice that the pressure gradient becomes constant slightly before the velocity profile becomes fully developed with the entry region included. This is a consequence of the fact that the acceleration of the "undisturbed" region must be complete before the velocity profile can be fully established.

The difference between the extrapolation of the fully-developed flow and the flow in the entry region shows the rapid decrease in pressure due primarily to the acceleration of the "undisturbed" flow in the entry region. Comparing Figures 9.12 and 9.18 we see that the effect of the entry region on the local pressure is greater for the case of the flow in a pipe than for flow between infinite parallel flat plates. This is a manifestation of the three-dimensionality of the flow in the pipe. Equations (9.150) are plotted in Figure 9.19 for a flow with $Re = 2100$. The behavior of the data is similar to that for the case shown in Figure 9.13. The major difference is the magnitude of the effect of the entry region in the two cases.

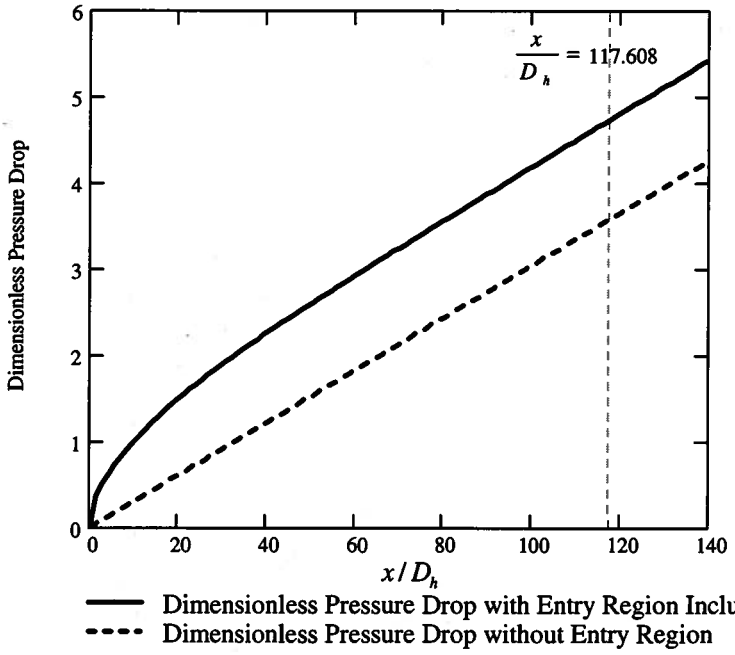

Figure 9.19 Pressure Drop for the Flow of a Viscous Fluid in a Pipe, $Re = 2100$

Example 9E.5: The fuel injection systems on Diesel engines operate at very high pressures since they inject the fuel directly into the cylinder when the pressure of the air inside the piston-cylinder is at or near its highest level before combustion. Typically the fuel pressure in these injection systems is on the order of 1.4×10^7 N/m^2 to 14.0×10^7 N/m^2. The fuel lines used

in these engines are relatively small compared to those in a gasoline engine. In a typical application, the fuel line diameter is on the order of $D = 5$ mm.

(a) If the length of the fuel line is on the order of $L = 1$ m, determine the pressure drop in the line if a typical average flow velocity is $\vartheta_{ave} = 1$ m/sec.

(b) Estimate the mass flow rate of diesel fuel resulting from this pressure drop.

The properties of No. 2 Diesel fuel are: $\rho = 920$ kg/m^3, $\mu = 3.96 \text{ x } 10^{-3}$ kg/m sec

Solution: (a) Typically in solving these types of problems we calculate the Reynolds number first. Then

$$Re = \frac{\rho \vartheta_{ave} D}{\mu} = \frac{(920 \text{ kg/m}^3)(1 \text{ m/sec})(5 \text{ x } 10^{-3} \text{ m})}{3.96 \text{ x } 10^{-3} \text{ kg/m sec}} = 1161.6$$

In this case the flow is clearly laminar. The entry length is

$$\frac{L_{entry}}{D} = \frac{0.60}{0.035Re + 1} + 0.056Re = \frac{0.60(1161.6)}{0.035(1161.6) + 1} + 0.056(1161.6) = 81.782$$

$$L_{entry} = 81.782D = 81.782(5 \text{ x } 10^{-3} \text{ m}) = 0.40891 \text{ m}$$

Thus, approximately 40 percent of the length of the fuel line is entry length; therefore, it will be necessary to account for entry region effects in computing the pressure drop. We then make use of equation (9.145).

$$(\Delta P^*)_{apparent} = 4x^+ \left[\frac{3.44}{\sqrt{x^+}} + \frac{16 + \frac{1.25}{4x^+} - \frac{3.44}{\sqrt{x^+}}}{1 + 2.1 \text{ x } 10^{-4} (x^+)^{-2}} \right]$$

where

$$x^+ = \frac{x}{D_h Re} = \frac{1 \text{ m}}{(0.005 \text{ m})(1161.6)} = 0.17217$$

Then

$$(\Delta P^*)_{apparent} = 4x^+ \left[\frac{3.44}{\sqrt{x^+}} + \frac{16 + \frac{1.25}{4x^+} - \frac{3.44}{\sqrt{x^+}}}{1 + 2.1 \text{ x } 10^{-4} (x^+)^{-2}} \right]$$

$$(\Delta P^*)_{apparent} = 4(0.172) \left[\frac{3.44}{\sqrt{0.172}} + \frac{16 + \frac{1.25}{4(0.172)} - \frac{3.44}{\sqrt{0.172}}}{1 + 2.1 \text{ x } 10^{-4} (0.172)^{-2}} \right] = 12.223$$

$$\Delta P = 12.223 \left(\frac{\rho \vartheta_{ave}^{\ 2}}{2} \right) = 12.223 \left[\frac{(920 \text{ kg/m}^3)(1 \text{ m/sec})^2}{2} \right] = 5.623 \text{ x } 10^3 \text{ N/m}^2$$

If we had assumed fully developed flow, the pressure drop we would have calculated would have been

$$(\Delta P^*)_{\substack{fully \\ developed}} = 64x^+ = 64(0.172) = 11.019$$

$$\Delta P_{\substack{fully \\ developed}} = 11.019 \left(\frac{\rho \vartheta_{ave}^{\ 2}}{2} \right) = 11.019 \left[\frac{(920 \text{ kg/m}^3)(1 \text{ m/sec})^2}{2} \right] = 5.069 \text{ x } 10^3 \text{ N/m}^2$$

Then the percent error in assuming fully-developed flow would have been

$$\text{Error} = \frac{5.623 - 5.069}{5.623}(100\%) = 9.86\%$$

In this case the fully-developed flow solution would have underestimated the pressure drop by nearly 10 percent. As we shall see in Section 9.9.2.1, there is a way of eliminating this error without resorting to the tedium inherent in equation (9.145).

(b) To estimate the mass flow rate we must recognize that the pressure drop including the entry effects is not the appropriate one to determine the volumetric flow rate since a portion of the pressure drop is associated with accelerating the "undisturbed" flow in the entry region and does not contribute to the volumetric flow rate in the sense of equation (9.131). Rather, we simply calculate the mass flow rate from the continuity equation. Then

$$\dot{m} = \rho A_c \vartheta_{ave} = \left(920 \text{ kg/m}^3\right)\left(\frac{\pi(0.005 \text{ m})^2}{4}\right)(1 \text{ m/sec}) = 0.0181 \text{ kg/sec}$$

Had we used equation (9.130), we would have obtained

$$\dot{V} = \frac{\pi R^4}{8\mu}\left(\frac{\partial P}{\partial z}\right) = \frac{\pi(0.005)^4}{128\left(3.96 \text{ x } 10^{-3} \text{ kg/m sec}\right)}\left(\frac{5.623 \text{ x } 10^3 \text{ N/m}^2}{1 \text{ m}}\right) = 2.1782 \text{ x } 10^{-5} \text{ m}^3\text{/sec}$$

$$\dot{m} = \rho\dot{V} = \left(920 \text{ kg/m}^3\right)\left(2.1782 \text{ x } 10^{-5} \text{ m}^3/\text{sec}\right) = 0.0200 \text{ kg/sec}$$

which would have overestimated the mass flow rate by approximately 11 percent. The correct result could have been obtained by applying equation (9.131) over that portion of the flow which was fully-developed (approximately the last 0.6 m).

Example 9E.6: In a classroom demonstration of fully-developed flow in a circular conduit, a student immerses a common drinking straw in a bottle of castor oil and fills the straw with castor oil by sucking on the end of it. By quickly placing her finger over the end of the straw, the student is able to hold the castor oil in the straw. The straw is then raised over the mouth of the bottle with its axis aligned vertically, and the finger is removed to allow the castor oil to drain from the straw back into the bottle. By measuring the amount of time required for the straw to empty, the student can actually determine the viscosity of the castor oil if the flow is indeed fully-developed.

(a) If the dimensions of the straw are $D = 6$ mm and $L = 20$ cm and the properties of castor oil are $\rho = 956.1$ kg/m^3 and $\mu = 0.650$ kg/m sec, how long does it take to empty the straw of castor oil if the flow is fully-developed?

(b) Is the assumption of fully-developed flow justified?

Solution: (a) At first glance this would appear to be an unsteady flow situation since we are measuring the amount of time required to empty a control volume, the straw. However, because of the large viscosity of the castor oil, fully-developed steady laminar flow is established almost immediately upon removing the finger. To see that this is the case, first note that with the finger removed, the pressure acting on the oil trapped in the straw is the same at both ends of the straw, namely atmospheric pressure. Then there is no pressure gradient imposed on the flow. Now assume that the flow is indeed steady and solve the appropriate form of the Navier-Stokes equation, viz.

$$\rho\left(\cancel{\frac{\partial \vartheta_z}{\partial t}}+\cancel{\vartheta_r}\frac{\partial \vartheta_z}{\partial r}+\cancel{\frac{\vartheta_\theta}{r}}\cancel{\frac{\partial \vartheta_z}{\partial \theta}}-\cancel{\frac{\vartheta_\theta^2}{r}}+\vartheta_z\frac{\partial \vartheta_z}{\partial z}\right)$$

$$=-\cancel{\frac{\partial P}{\partial z}}+\rho g_z+\mu\left[\frac{1}{r}\frac{\partial}{\partial r}\left(r\frac{\partial \vartheta_z}{\partial r}\right)+\cancel{\frac{1}{r^2}\frac{\partial^2 \vartheta_z}{\partial \theta^2}}+\cancel{\frac{\partial^2 \vartheta_z}{\partial z^2}}\right]$$

$$-\rho g_z=\mu\left[\frac{1}{r}\frac{\partial}{\partial r}\left(r\frac{\partial \vartheta_z}{\partial r}\right)\right]$$

Since $g_z = -g$, the above equation says that in fully developed flow with straw aligned with the z-axis, the body force (per unit volume) due to gravity is just balanced by the viscous force (per unit volume). Notice that this expression is identical to equation (9.125c) except that the "pressure force" is now replaced by the body force. The process of integration is exactly the same, and we end up with an expression nearly identical to equation (9.129) except that the constant pressure gradient is now replaced by the constant body force per unit volume, namely

$$\vartheta_z=\frac{\rho g R^2}{4\mu}\left[1-\left(\frac{r}{R}\right)^2\right]$$

In a manner similar to equation (9.131), we have for the volumetric flow rate

$$\dot{V}=\frac{\pi R^4 \rho g}{8\mu}$$

Since the volumetric flow rate is constant, the amount of time Δt required to empty the straw is

$$\Delta t=\frac{V}{\dot{V}}=\frac{\pi R^2 L}{\pi R^4 \rho g/8\mu}=\frac{8\mu L}{\rho g R^2}=\frac{8(0.650\ \text{kg/m sec})(0.20\ \text{m})}{(956.1\ \text{kg/m}^3)(9.81\ \text{m/sec})(0.003\ \text{m})^2}=12.32\ \text{sec}$$

Thus the time interval is of such a magnitude that it could be measured easily in the classroom. The question remains, however, as to whether the flow is truly fully-developed.

(b) The average velocity for this flow is given by equation (9.132) with the replacement of the pressure gradient by the body force per unit volume.

$$\vartheta_{ave}=\frac{\rho g R^2}{8\mu}=\frac{(956.1\ \text{kg/m}^3)(9.81\ \text{m/sec}^2)(0.003\ \text{m})^2}{8(0.650\ \text{kg/m sec})}=1.6233\ \text{cm/sec}$$

The Reynolds number for this fully-developed laminar flow is then

$$Re=\frac{\rho \vartheta_{ave} D}{\mu}=\frac{(956.1\ \text{kg/m}^3)(0.016233\ \text{m/sec})(0.003\ \text{m})}{0.650\ \text{kg/m sec}}=0.0716$$

The flow is clearly laminar and the viscous forces dominate. The entry length for this flow is given by equation (9.144). Then

$$\frac{L_{entry}}{D_h}=\frac{0.60}{0.035Re+1}+0.056Re=\frac{0.60}{0.035(0.0716)+1}+0.056(0.0716)=0.603$$

$$L_{entry}=(0.603)(0.006\ \text{m})=3.62\ \text{x}\ 10^{-3}\ \text{m}=3.62\ \text{mm}$$

The entry length is only a small fraction (1.81 percent) of the total length of the straw (3.62 mm vs. 200 mm). The time required for the fluid to travel this distance is about 0.223 sec. Thus the flow does indeed become fully-developed relatively quickly, and this method could then be used to determine the viscosity of a highly viscous fluid like castor oil in the classroom.

Example 9E.7: A computer chip fabricated on a silicon substrate is cooled by passing water through many small square channels machined in parallel in the silicon. The channels are 1 mm on each side and are 20 cm long. The pressure drop for the water flowing in a typical channel is $\Delta P = 1.25 \times 10^3$ N/m^2. Determine the mass flow rate of the cooling water for this flow configuration. The thermal-fluid characteristics of water are: ρ =996 kg/m^3, $\mu = 8.67 \times 10^{-4}$ kg/m sec.

Solution: Normally the starting point in the solution is the calculation of the Reynolds number; however, in this case we are unable to do this because neither the velocity nor the mass flow rate are known. If we can determine the velocity, we can get the mass flow rate. Since L/D_h = 200, let us assume that the flow is fully developed and laminar. Then the pressure drop is given by

$$\Delta P = \rho f \left(\frac{L}{D_h}\right)\left(\frac{\vartheta_{ave}^{\ 2}}{2}\right)$$

For a square channel D_h is the length of one side, and for fully developed laminar flow in a square channel, Table 9.3 gives

$$fRe_{D_h} = 56.91$$

$$f = \frac{56.91}{Re_{D_h}} = \frac{56.91\mu}{\rho \vartheta_{ave} D_h} = \frac{56.91\left(8.67 \times 10^{-4} \text{ kg/m sec}\right)}{\left(996 \text{ kg/m}^3\right)\left(0.001 \text{ m}\right)\vartheta_{ave}}$$

$$f = \frac{4.9539 \times 10^{-2}}{\vartheta_{ave}}$$

Then

$$\Delta P = \rho \left(\frac{0.049539 \text{ m/sec}}{\vartheta_{ave}}\right)\left(\frac{L}{D_h}\right)\left(\frac{\vartheta_{ave}^{\ 2}}{2}\right)$$

$$\therefore \vartheta_{ave} = \frac{2D_h \Delta P}{\rho L (0.049539 \text{ m/sec})} = \frac{2\left(0.001 \text{ m}\right)\left(1.25 \times 10^3 \text{ N/m}^2\right)}{\left(996 \text{ kg/m}^3\right)\left(0.2 \text{ m}\right)\left(0.049539 \text{ m/sec}\right)}$$

$$\vartheta_{ave} = 0.1588 \text{ m/sec}$$

Then the Reynolds number is

$$Re_{D_h} = \frac{\rho \vartheta_{ave} D_h}{\mu} = \frac{\left(996 \text{ kg/m}^3\right)\left(0.1588 \text{ m/sec}\right)\left(0.001 \text{ m}\right)}{8.67 \times 10^{-4} \text{ kg/m sec}} = 181.89$$

The flow is clearly laminar. If we assume that the entry length is on the same order as that for a circular conduit at the same Reynolds number, we have

$$\frac{L_{entry}}{D_h} \approx \frac{0.60}{0.035Re + 1} + 0.056Re = \frac{0.60}{0.035\left(181.89\right) + 1} + 0.056\left(181.89\right) = 10.195$$

Thus the entry length is only 5 percent of the length of the channel, and the assumption of fully developed flow for this case is a reasonable one. Then the mass flow rate of cooling water is

$$\dot{m} = \rho A_c \vartheta_{ave} = \left(996 \text{ kg/m}^3\right)\left(0.001 \text{ m}\right)^2\left(0.1588 \text{ m/sec}\right) = 1.577 \text{ kg/sec}$$

9.9.2 Laminar External Flows

Unlike internal flows, external flows never become fully developed in the sense that the effects of the fluid viscosity are dominant throughout the entire flow geometry as they are in the case of an internal flow, e.g., fully-developed laminar flow in a pipe. In these external flows, the effects of viscosity are confined to small regions near the solid surfaces that bound the flow. These "boundary layers" continue to develop and grow in thickness as the flow proceeds downstream but they never really extend throughout the entire flow field. This means that the nonlinear acceleration terms appearing in the Navier-Stokes equation cannot be neglected as they were for internal flows. Furthermore, within these boundary layers, the fluid velocity changes rapidly in a direction normal to the surface, from zero at the surface to the free-stream value at the outer edge of the boundary layer. This velocity gradient may produce a steep gradient in the shear stress in the fluid. As a result, some of the viscous terms are equally as important as the acceleration terms. Because of the presence of these viscous terms as well as the nonlinear acceleration terms, the solution of the Navier-Stokes equation becomes even more challenging for external flows than it was for internal flows.

The notion that the effects of fluid viscosity can be modeled as being localized to this small region known as the boundary layer was a novel one introduced by Ludwig Prandtl (1875 - 1953) in 1904 and implemented for flow over a flat plate by his student H. Blasius (1883 - 1970) in 1908. For external flows, the introduction of the boundary layer concept represented a major breakthrough that facilitated widespread advances in understanding the effects of fluid viscosity on flow over all sorts of solid bodies.

In the typical external flow situation, a solid body, such as an aircraft or a ship, is moving relative to a fluid which may have a motion of its own. This motion of the fluid in the boundary layers adjacent to the solid surfaces can be described by the Navier-Stokes equation. Outside the boundary layers where the fluid viscosity has no influence on fluid motion, the fluid behaves as though it were inviscid. In this region, the flow can be described by the Euler equation. In the boundary layer, however, the action of fluid viscosity on the solid body results in a velocity gradient in the fluid due to the "no-slip" boundary condition of the Navier-Stokes equation. The net result of this velocity gradient and the action of fluid viscosity leads to a shear stress imposed on the solid surface by the fluid. This shear stress integrated over the surface of the body results in a viscous "drag" force, sometimes called "skin-friction drag," that tends to slow the movement of the body as momentum is transferred from the body to the fluid through this action of viscosity. Initially, the flow in this boundary layer is laminar, but as the boundary layer grows in thickness in the direction of flow, it becomes unstable and the flow undergoes a transition from laminar to turbulent flow. Depending upon the shape of the body, the flow may eventually separate from the body, producing a region of reverse flow or of stagnant fluid. Downstream of this region there is a relatively large "wake" of "disturbed" flow that results in further momentum transfer between the body and the fluid. This produces an additional component of drag known as "profile" drag or "wake" drag. At this point in our development of the subject, we are going to focus on the skin friction drag.

Our approach is to first divide the flow into two regions: (1) the boundary layer flow near the surface of the body where all the viscous effects are confined and (2) the inviscid flow in the free stream outside the boundary layer remote from the surface of the body. We then develop special forms of the components of the Navier-Stokes equation called the boundary layer equations, that apply in the boundary layer. The solution of the boundary layer equations provides us with the velocity profile of the fluid in the boundary layer. From the velocity profile

we can determine the shear stress at the surface of the body, and hence, the skin friction component of the drag on the body. We then determine the shape of the boundary layer so that we can solve the Euler equation for the inviscid flow outside the boundary layer.

In the process of developing the solution for the velocity profile in the boundary layer, we will match the velocity at the outer edge of the boundary layer to the fluid velocity in the mainstream. This is problematic on two counts: (1) we do not really know the location of the outer edge of the boundary layer, and (2) we do not really know the mainstream velocity. In order to resolve this dilemma, we assume that the mainstream velocity is unaffected by the presence of the boundary layer, and we apply this boundary condition by requiring the velocities in the two regions match as the boundary layer thickness becomes infinite. After obtaining the solution for the velocity profile in the boundary layer, we then arbitrarily define the outer limit of the boundary layer as the location at which the fluid velocity in the boundary layer attains 99 percent of the mainstream velocity; however, there is no physical basis for this definition and this choice is arbitrary. We could have just as easily used 95 percent or 90 percent as our definition.

This presents a difficulty when we attempt, after the fact, to determine the effect of the boundary layer on the inviscid flow outside of it by solving the Euler equation in the mainstream. We do not really know the location of the inner boundary of the mainstream. However, closer examination of the physics of the flow in the boundary layer reveals that the retardation of the flow in the boundary layer has the same effect as if we had displaced the streamlines in the mainstream outwardly from the surface of the body by an amount δ^* known as the *displacement thickness* which is related to the boundary layer thickness δ. This displacement, which is a function of x, in turn affects the local velocity and the local pressure in the mainstream since the streamlines are no longer straight but now have some curvature. Thus the inviscid flow in the mainstream "sees" the body *and* the attached boundary layer as a solid streamlined body. Then knowing this displacement thickness, we can determine the flow field around this "streamline body" by solving the Euler equation. We shall demonstrate this approach by considering the example of the flow of a viscous fluid over a flat plate, but first we must develop the boundary layer equations.

9.9.2.1 The Boundary Layer Equations: By its very nature, in its simplest form the boundary layer is a two-dimensional phenomenon. The fluid is flowing in one direction, say the x-direction, and the gradients in velocity and shear stress are occurring in a direction normal to this, say the y-direction. In the laminar boundary layer, the Reynolds number is large but not infinite. Our approach will be to use this fact to simplify the Navier-Stokes equation so that we might develop a solution that describes this two-dimensional situation.

In two-dimensions, the continuity equation and the Navier-Stokes equation in Cartesian coordinates become

$$\frac{\partial \vartheta_x}{\partial x}+\frac{\partial \vartheta_y}{\partial y}=0 \tag{9.151}$$

and

$$\rho\left(\frac{\partial \vartheta_x}{\partial t}+\vartheta_x\frac{\partial \vartheta_x}{\partial x}+\vartheta_y\frac{\partial \vartheta_x}{\partial y}\right)=-\frac{\partial P}{\partial x}+\mu\left(\frac{\partial^2 \vartheta_x}{\partial x^2}+\frac{\partial^2 \vartheta_x}{\partial y^2}\right) \tag{9.152}$$

$$\rho\left(\frac{\partial \vartheta_y}{\partial t}+\vartheta_x\frac{\partial \vartheta_y}{\partial x}+\vartheta_y\frac{\partial \vartheta_y}{\partial y}\right)=-\frac{\partial P}{\partial y}+\mu\left(\frac{\partial^2 \vartheta_y}{\partial x^2}+\frac{\partial^2 \vartheta_y}{\partial y^2}\right) \tag{9.153}$$

respectively, where we have neglected the effect of the gravity body force. (In Chapter 11 we shall see how to deal with this effect.) Let us now non-dimensionalize these three equations in a way that displays the Reynolds number explicitly since the Reynolds number quantitates the relative importance of inertial and viscous effects which are both present in the boundary layer. We can do this by introducing dimensionless parameters in a manner similar to equation (9.85). If L is a characteristic length, ϑ_0 a typical speed, and $Re = \rho L \vartheta_0 / \mu$ the corresponding Reynolds number for the flow as a whole, we can introduce the following set of dimensionless parameters:

$$x^* = \frac{x}{L} \qquad y^* = \frac{y\sqrt{Re}}{L} \qquad t^* = \frac{\vartheta_0 t}{L}$$
$$\vartheta_x^* = \frac{\vartheta_x}{\vartheta_0} \qquad \vartheta_y^* = \frac{\vartheta_y \sqrt{Re}}{\vartheta_0} \qquad P^* = \frac{P}{\rho \vartheta_0^2} \tag{9.154}$$

If we substitute equations (9.154) into equation (9.151), we get the non-dimensional continuity equation, viz.

$$\frac{\partial \vartheta_x^*}{\partial x^*} + \frac{\partial \vartheta_y^*}{\partial y^*} = 0 \tag{9.155}$$

If we substitute equations (9.154) into equations (9.152) and (9.153), we get the component Navier-Stokes equations in non-dimensional form, viz.

$$\frac{\partial \vartheta_x^*}{\partial t^*} + \vartheta_x^* \frac{\partial \vartheta_x^*}{\partial x^*} + \vartheta_y^* \frac{\partial \vartheta_x^*}{\partial y^*} = -\frac{\partial P^*}{\partial x^*} + \frac{1}{Re}\frac{\partial^2 \vartheta_x^*}{\partial x^{*2}} + \frac{\partial^2 \vartheta_x^*}{\partial y^{*2}} \tag{9.156}$$

$$\frac{1}{Re}\left(\frac{\partial \vartheta_y^*}{\partial t^*} + \vartheta_x^* \frac{\partial \vartheta_y^*}{\partial x^*} + \vartheta_y^* \frac{\partial \vartheta_y^*}{\partial y^*}\right) = -\frac{\partial P^*}{\partial y^*} + \frac{1}{Re^2}\frac{\partial^2 \vartheta_y^*}{\partial x^{*2}} + \frac{1}{Re}\frac{\partial^2 \vartheta_y^*}{\partial y^{*2}} \tag{9.157}$$

We now assume that all the derivatives in equations (9.155) through (9.157) are of the same order of magnitude. For the case in which the inertial effects are relatively more important than the viscous effects, the values of Re are large and the limiting forms of equations (9.155) through (9.157) are

$$\frac{\partial \vartheta_x^*}{\partial x^*} + \frac{\partial \vartheta_y^*}{\partial y^*} = 0 \tag{9.153}$$

and

$$\frac{\partial \vartheta_x^*}{\partial t^*} + \vartheta_x^* \frac{\partial \vartheta_x^*}{\partial x^*} + \vartheta_y^* \frac{\partial \vartheta_x^*}{\partial y^*} = -\frac{\partial P^*}{\partial x^*} + \frac{\partial^2 \vartheta_x^*}{\partial y^{*2}} \tag{9.154}$$

$$0 = -\frac{\partial P^*}{\partial y^*}$$

If we now transform these equations back to their dimensional form, we get the boundary layer equations in two dimensions, viz.

$$\frac{\partial \vartheta_x}{\partial x} + \frac{\partial \vartheta_y}{\partial y} = 0 \tag{9.160}$$

$$\rho\left(\frac{\partial \vartheta_x}{\partial t} + \vartheta_x \frac{\partial \vartheta_x}{\partial x} + \vartheta_y \frac{\partial \vartheta_x}{\partial y}\right) = -\frac{\partial P}{\partial x} + \mu \frac{\partial^2 \vartheta_x}{\partial y^2} \tag{9.161}$$

$$0 = -\frac{\partial P}{\partial y} \tag{9.162}$$

Equation (9.162) simply says that the pressure in the boundary layer is uniform at the value in the mainstream flow across each plane x = constant, but not necessarily constant in the direction of flow. It is really equations (9.160) and (9.161) that need to be solved subject to the boundary conditions at the surface $y = 0$

$$\begin{aligned} \vartheta_x &= 0 \quad \text{(no slip boundary condition)} \\ \vartheta_y &= 0 \quad \text{(no flow through the wall boundary condition)} \end{aligned} \tag{9.163}$$

It follows that at the wall, we also have

$$\frac{\partial \vartheta_x}{\partial x} = 0 \qquad \text{and} \qquad \frac{\partial \vartheta_y}{\partial x} = 0 \tag{9.164}$$

At the other extreme, the boundary layer must join the main flow smoothly. The nature of the solutions of the boundary layer equations is such that the mainstream flow is considered to be at infinity. Then

$$\vartheta_x \to \vartheta_0(x) \qquad \text{as} \qquad y \to \infty \tag{9.165}$$

where $\vartheta_0(x)$ is the velocity in the main flow and is in general dependent upon the location x.

The solution of equations (9.160) through (9.162) together with boundary conditions (9.163) through (9.165) provide a description of the flow in a laminar boundary layer. The solutions derived for these equations are not unique in general and may actually provide values of ϑ_y away from the surface that are not physically meaningful. Nevertheless, the solutions of these equations, whose accuracy in many cases varies depending upon the location along the direction of flow, have provided considerable insight into the nature of boundary layer flows. We shall now consider one of these, namely laminar flow over a flat plate, in detail.

9.9.2.2 Laminar Flow Over a Flat Plate: In what has become the classic example of the application of the boundary layer equations, H. Blasius treated the case of steady laminar flow over a flat plate in the absence of a pressure gradient. The fact that the pressure gradient is zero in the boundary layer can be seen by applying the Bernoulli equation in the mainstream flow and invoking equation (9.162). As shown in Figure 9.20, in Blasius's treatment, the flat plate is immersed in a uniform flow of a fluid with constant thermal-fluid properties.

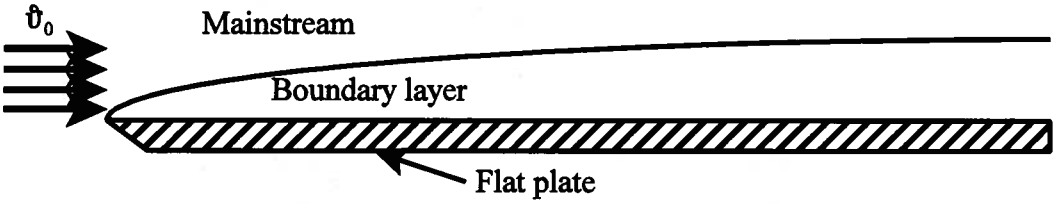

Figure 9.20 Uniform Flow Over a Flat Plate

The uniform velocity is ϑ_0, the density of the fluid is ρ, and the viscosity of the fluid is μ. Under these conditions, the boundary layer equations become

$$\frac{\partial \vartheta_x}{\partial x} + \frac{\partial \vartheta_y}{\partial y} = 0 \tag{9.166}$$

$$\vartheta_x \frac{\partial \vartheta_x}{\partial x} + \vartheta_y \frac{\partial \vartheta_x}{\partial y} = \frac{\mu}{\rho} \frac{\partial^2 \vartheta_x}{\partial y^2} \tag{9.167}$$

In equation (9.167), the term μ/ρ is given a special name, the *kinematic viscosity*. As we shall soon see, this ratio, represented by the symbol ν, plays precisely the same role in momentum transfer that the thermal diffusivity $\alpha = k/\rho c$ plays in heat transfer. Physically, the kinematic viscosity $\nu = \mu/\rho$ is the momentum diffusivity of the fluid and has the units of m^2/sec.

In an attempt to simplify equations (9.166) and (9.167) mathematically, Blasius proposed a coordinate transformation that would reduce these two partial differential equations to a single ordinary differential equation. Prior to Blasius's time, the dynamical behavior of the inviscid model had received extensive study from a mathematical point of view. One of the mathematical techniques used was based upon the premise that there exists a single function, ψ, called the stream function, that satisfies the continuity equation, equation (9.167), exactly if defined properly. If we define the velocity components in the x- and y-directions in the following manner,

$$\vartheta_x \equiv \frac{\partial \psi}{\partial y} \qquad \text{and} \qquad \vartheta_y \equiv -\frac{\partial \psi}{\partial x} \tag{9.168}$$

then it follows that equation (9.167) is satisfied exactly. Blasius adopted this approach and then argued that the velocity profile in the boundary layer should have the same shape at every position x provided it is scaled in some appropriate manner to account for the fact that the boundary layer is growing in thickness as the fluid moves down the plate. That is, the velocity profile is similar at all locations along the plate.

If this is the case, we should be able to express the velocity profile in terms of a dimensionless similarity parameter η that would have the proper scaling built into it. Blasius proposed that the velocity profile in dimensionless form should be a function of this parameter η and that the similarity parameter should be related to the thickness of the boundary layer δ also in dimensionless form. That is,

$$\frac{\vartheta_x}{\vartheta_0} = f'(\eta) \qquad \text{and} \qquad \eta \propto \frac{\delta}{y} \tag{9.169}$$

where f' is the first derivative of a function f. Clearly, from equation (9.169) it follows that the function f is the dimensionless form of the stream function. The reason that the derivative is used instead of the function itself is that the velocity is expressed as a derivative of a stream function in equation (9.168).

Based upon an idea proposed by Stokes in 1851, Blasius argued that the boundary layer thickness should grow like the square root of the position x. Then, in dimensionless form we have

$$\frac{\delta}{x} \propto \frac{1}{\sqrt{Re_x}} \tag{9.170}$$

Then from equation(9.169), the similarity parameter should be of the form

$$\eta = y\sqrt{\frac{\vartheta_0 \rho}{\mu x}} = y\sqrt{\frac{\vartheta_0}{\nu x}} \tag{9.171}$$

Blasius then combined the notion of a stream function as presented in equation (9.168) with his proposed similarity parameter to get the dimensionless stream function, viz.

$$f(\eta) = \frac{\psi}{\sqrt{\nu x \vartheta_0}} \tag{9.172}$$

By formulating the function f in this manner, Blasius was able to get the velocity profile in dimensionless form as he had proposed in equation (9.171), viz.

$$\vartheta_x = \frac{\partial \psi}{\partial y} = \frac{\partial \psi}{\partial \eta}\frac{\partial \eta}{\partial y} = \frac{\partial \psi}{\partial f}\frac{df}{d\eta}\frac{\partial \eta}{\partial y} = \sqrt{\nu x \vartheta_0}\frac{df}{d\eta}\sqrt{\frac{\vartheta_0}{\nu x}} = \vartheta_0 \frac{df}{d\eta}$$
$$\therefore \frac{\vartheta_x}{\vartheta_0} = f'(\eta) \tag{9.173}$$

For the y-component of velocity, we have

$$\vartheta_y = -\frac{\partial \psi}{\partial x} = -\left[\sqrt{\nu x \vartheta_0}\frac{\partial f}{\partial x} + \frac{1}{2}\sqrt{\frac{\nu\vartheta_0}{x}}f\right] = -\left[\sqrt{\nu x\vartheta_0}\frac{df}{d\eta}\left(-\frac{1}{2}\eta\frac{1}{x}\right) + \frac{1}{2}\sqrt{\frac{\nu\vartheta_0}{x}}f\right]$$

$$\vartheta_y = \frac{1}{2}\sqrt{\frac{\nu\vartheta_0}{x}}\left[\eta\frac{df}{d\eta} - f\right] \tag{9.174}$$

$$\therefore \frac{\vartheta_y}{\vartheta_0} = \frac{1}{2}\frac{\left[\eta f'(\eta) - f(\eta)\right]}{\sqrt{Re_x}}$$

From equations (9.173) and (9.174), we can form the partial derivatives appearing in equation (9.167). Then

$$\frac{\partial \vartheta_x}{\partial x} = -\frac{\vartheta_0}{2x}\eta\frac{d^2 f}{d\eta^2} = -\frac{\vartheta_0}{2x}\eta f''$$

$$\frac{\partial \vartheta_x}{\partial y} = \vartheta_0\sqrt{\frac{\vartheta_0}{\nu x}}\frac{d^2 f}{d\eta^2} = \vartheta_0\sqrt{\frac{\vartheta_0}{\nu x}}f'' \tag{9.175}$$

$$\frac{\partial^2 \vartheta_x}{\partial y^2} = \frac{\vartheta_0^2}{\nu x}\frac{d^3 f}{d\eta^3} = \frac{\vartheta_0^2}{\nu x}f'''$$

and equation (9.167) becomes

$$2\frac{d^3 f}{d\eta^3} + f\frac{d^2 f}{d\eta^2} = 2f''' + ff'' = 0 \tag{9.176}$$

with boundary conditions

$$\begin{aligned} &(1) \quad f = 0 \quad \text{at} \quad \eta = 0 \\ &(2) \quad \frac{df}{d\eta} = f' = 0 \quad \text{at} \quad \eta = 0 \\ &(3) \quad \frac{df}{d\eta} = f' \to 1 \quad \text{as} \quad \eta \to \infty \end{aligned} \tag{9.177}$$

Given the nonlinear nature of equation (9.176), Blasius expended considerable effort to devise a method to solve it. His method involved formulating infinite series that were evaluated using a recursive scheme. Today, equation (9.176) can be solved numerically rather easily to yield the results shown in Table 9.4. The resulting velocity profile is plotted in Figure 9.21.

There remains the matter of determining the boundary layer thickness from these results. Establishing the outer limit of the boundary layer is a bit ambiguous since the velocity of the fluid in the boundary layer approaches the mainstream value in asymptotic fashion. By convention, we arbitrarily define the boundary layer thickness to be the value of y for which the velocity attains a value equal to 99 percent of the value in the mainstream. Then from Table 9.4, we have

$$\frac{\vartheta_x}{\vartheta_0} = f' = 0.99 \qquad \text{at} \qquad \eta = 4.9 \tag{9.178}$$

Table 9.4 BLASIUS SOLUTION FOR FLOW OVER FLAT PLATE

η	f	f'	f''
0	0	0	0.33216
0.1	1.66077E-3	0.03322	0.33215
0.2	6.64296E-3	0.06643	0.33208
0.3	0.01495	0.09963	0.33191
0.4	0.02657	0.13280	0.33157
0.5	0.04151	0.16593	0.33101
0.6	0.05975	0.19900	0.33018
0.7	0.08130	0.23196	0.32902
0.8	0.10614	0.26479	0.32748
0.9	0.13425	0.29744	0.32553
1.0	0.16562	0.32988	0.32310
1.1	0.20022	0.36204	0.32016
1.2	0.23802	0.39389	0.31668
1.3	0.27898	0.42536	0.31262
1.4	0.32308	0.45639	0.30795
1.5	0.37025	0.48693	0.30266
1.6	0.42044	0.51690	0.29674
1.7	0.47361	0.54626	0.29019
1.8	0.52967	0.57492	0.28300
1.9	0.58857	0.60284	0.27520
2.0	0.65021	0.62994	0.26681
2.1	0.71453	0.65618	0.25787
2.2	0.78142	0.68150	0.24840
2.3	0.85079	0.70585	0.23847
2.4	0.92255	0.72918	0.22813
2.5	0.99659	0.75146	0.21745
2.6	1.07281	0.77266	0.20649
2.7	1.15109	0.79275	0.19532
2.8	1.23132	0.81172	0.18403
2.9	1.31339	0.82956	0.17269
3.0	1.39719	0.84626	0.16137
3.1	1.48261	0.86183	0.15017
3.2	1.56952	0.87630	0.13913
3.3	1.65783	0.88967	0.12835
3.4	1.74742	0.90198	0.11788
3.5	1.83819	0.91326	0.10777
3.6	1.93004	0.92355	0.09808
3.7	2.02287	0.93289	0.08885
3.8	2.11659	0.94133	0.08012
3.9	2.21111	0.94893	0.07190
4.0	2.30635	0.95573	0.06422
4.1	2.40223	0.96179	0.05709
4.2	2.49868	0.96717	0.05051
4.3	2.59564	0.97191	0.04447
4.4	2.69305	0.97608	0.03896
4.5	2.79084	0.97972	0.03397
4.6	2.88897	0.98289	0.02947
4.7	2.98740	0.98563	0.02545
4.8	3.08609	0.98799	0.02186
4.9	3.18499	0.99002	0.01869
5.0	3.28408	0.99174	0.01590

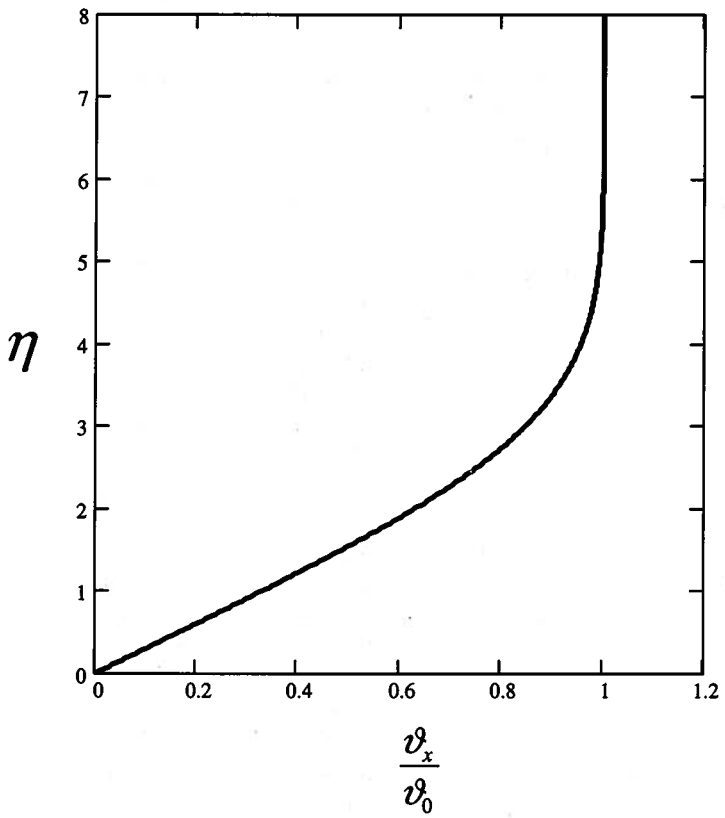

Figure 9.21 Boundary Layer Velocity Profile for a Flat Plate Due to Blasius

Then

$$\eta_{y=\delta} = \delta\sqrt{\frac{\vartheta_0}{\nu x}} = 4.9$$
$$\frac{\delta}{x} = \frac{4.9}{\sqrt{Re_x}} \tag{9.179}$$

where $Re_x = \vartheta_0 x/\nu$ is the local Reynolds number and x is measured from the leading edge of the plate. From equation (9.179) it is apparent that the laminar boundary layer thickness increases as the square root of x.

Our original motivation for studying the laminar boundary layer on a flat plate was to determine the drag force due to skin friction. To this end we compute the shear stress at the wall, τ_w where

$$\tau_w = \mu\left(\frac{\partial \vartheta_x}{\partial y}\right)_{y=0} = \mu\vartheta_0\sqrt{\frac{\vartheta_0}{\nu x}}\left(\frac{d^2 f}{d\eta^2}\right)_{\eta=0} = \mu\vartheta_0\sqrt{\frac{\vartheta_0}{\nu x}}f''_{\eta=0} \tag{9.180}$$

Using the data from Table 9.4, we get

$$\tau_w = 0.332\vartheta_0\sqrt{\frac{\rho\mu^2\vartheta_0}{\mu x}} = \frac{0.332\rho\vartheta_0^2}{\sqrt{Re_x}} \tag{9.181}$$

If we define the friction coefficient, C_f, as

$$C_f \equiv \frac{\tau_w}{\frac{1}{2}\rho\vartheta_0^2} \tag{9.182}$$

the Blasius solution for the flat plate in laminar flow gives

$$C_f = \frac{0.664}{\sqrt{Re_x}} \tag{9.183}$$

For flow on one side of the flat plate, the drag force for a plate of width b and length L is given by

$$F_D = b\int_0^L \tau_w dx = 0.332 b\rho v_0^2 \sqrt{\frac{\mu}{\rho v_0}} \int_0^L \frac{dx}{\sqrt{x}} \tag{9.184}$$

$$F_D = 0.664 b v_0 \sqrt{\rho \mu v_0 L}$$

The drag coefficient, C_D, for one side of the plate is

$$C_D \equiv \frac{F_D}{\frac{1}{2}\rho v_0^2 bL} = \frac{0.664 b v_0 \sqrt{\rho \mu v_0 L}}{\frac{1}{2}\rho v_0^2 bL} = \frac{1.328}{\sqrt{\frac{\rho v_0 L}{\mu}}} = \frac{1.328}{\sqrt{Re_L}} \tag{9.185}$$

All of the results above apply only so long as the flow remains laminar, but unfortunately none of these results tells us when the boundary layer becomes turbulent. For this information, we have to rely upon experimental measurements. These experiments show that there is no specific value of the local Reynolds number, Re_x, at which the transition from laminar to turbulent flow occurs. The data show that the boundary layer on a flat plate in a uniform flow starts out laminar and remains laminar as the flow proceeds down the plate up to a critical value of the local Reynolds number, $Re_{x,critical}$, that depends upon the particular flow situation. In a "very rough" flow $Re_{x,critical}$ can be as small as 8×10^4 whereas in a "very smooth" flow $Re_{x,critical}$ can be as large as 3×10^6. For design purposes, $Re_{x,critical}$ is usually taken to be 5×10^5.

As we shall see, the results above can be applied to many situations in thermal-fluids engineering for which the surfaces can be modeled as flat plates. However, in doing so, we must be mindful of the conditions under which they were formulated. First, in deriving the boundary layer equations, we non-dimensionalized the component Navier-Stokes equations and then neglected certain terms that contained the reciprocal of the Reynolds number. This is valid only insofar as the Reynolds number is large; however, we saw in equations (9.179), (9.181) and (9.183) that the appropriate value of the Reynolds number for these correlations is the *local* Reynolds number for which the appropriate characteristic length is the distance from the leading edge of the plate. Thus, in the neighborhood of the leading edge, this value of the Reynolds number is not large and the Blasius solution is no longer valid in this region because the boundary layer equations on which it is based do not contain the appropriate terms. (This issue has been subsequently addressed in the thermal-fluids engineering literature.) On the other hand, as the flow progresses downstream, the value of x increases, and we can expect the Blasius solution to become more accurate as long as the flow remains laminar.

Second, in postulating a similarity solution, we implicitly assume that the plate extends to infinity in the positive x-direction. If this were not the case and the plate were of finite length L, the trailing edge of the plate would cause a disturbance in the flow that would propagate upstream at the speed of sound by means of pressure waves. The net result would be a change in the velocity profile within the boundary layer that would cause it to be no longer a "similar"one that maintains a fixed shape throughout the length of the plate (assuming that the flow is laminar everywhere). Thus, strictly speaking, the Blasius solution does not apply to a plate of finite length. It is necessary in this case to introduce a set of boundary conditions that apply specifically

to the trailing edge. However, despite this limitation, the Blasius solution in the form of equation (9.184) does provide an estimate of the drag force due to skin friction on one side of the plate. In fact, experimental evidence confirms the validity of equations (9.184) and (9.185) for a plate of length L.

Finally, now that we have obtained a description of the boundary layer, we need to examine our assumption that the uniform flow in the mainstream is not affected by the presence of the boundary layer. This requires a determination of the displacement thickness.

9.9.2.3 The Displacement Thickness: As we have just seen, one of the ways that the boundary layer affects the mainstream flow is the way it affects the continuity of the flow. To see this consider the control volume shown in Figure 9.22. The dimension of the control volume in

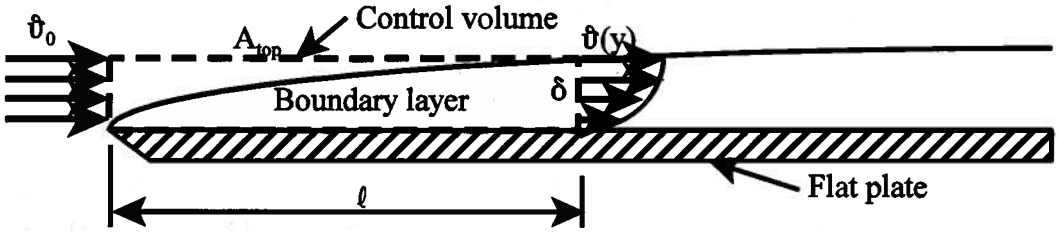

Figure 9.22 Boundary Layer Control Volume

the y-direction is δ and b in the z-direction normal to the plane of Figure 9.22. The fluid velocity entering the control volume is uniform with a value of ϑ_0 and that leaving the control volume is the boundary layer velocity profile shown in Figure 9.21. If we apply continuity in the x-direction we have for the entry and exit planes, respectively

$$\begin{aligned} \dot{m}_{entry} &= \rho b \delta \vartheta_0 \\ \dot{m}_{exit} &= \rho b \int_0^\delta \vartheta_x(y)\, dy \end{aligned} \tag{9.186}$$

Then combining these two expressions we have

$$\dot{m}_{entry} - \dot{m}_{exit} = \rho b \int_0^\delta (\vartheta_0 - \vartheta_x)\, dy > 0 \tag{9.187}$$

since $\vartheta_0 > \vartheta_x$ everywhere in the boundary layer except at the outer edge. Then in order to satisfy continuity, it must be the case that there is some mass flowing through the top area of the control volume, A_{top}. If we had instead selected a streamline as the top boundary of the control volume, there would be no mass flow through this boundary since by definition a streamline is everywhere tangent to the fluid velocity. As shown in Figure 9.23, consider a location L downstream from the leading edge of the plate.

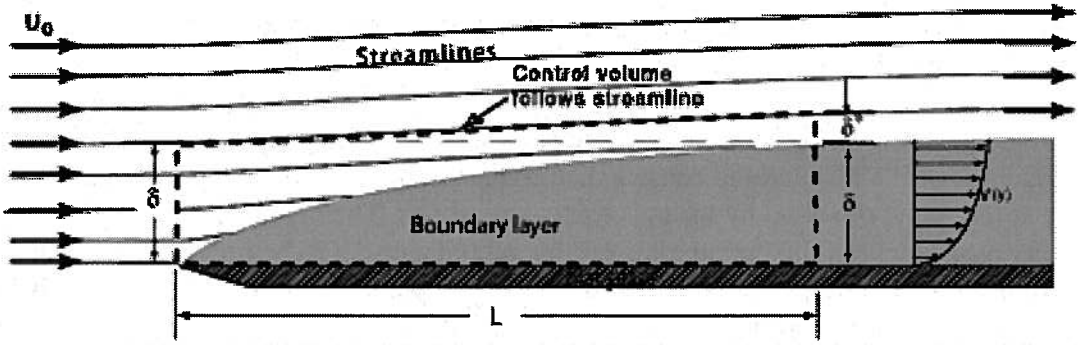

Figure 9.23 Boundary Layer Control Volume

At this location, the boundary layer thickness is δ. At the leading edge, we select a streamline offset from the surface of the plate by a distance δ. At the distance L downstream from the leading edge, this streamline will be displaced from the edge of the boundary layer by an amount δ^*. We now consider the control volume shown in Figure 9.23. Notice that the entry plane extends a considerable distance beyond the boundary layer at the leading edge itself since the Blasius solution is not valid there and hence, we could not define the boundary layer thickness at the leading edge. Then if we apply continuity to this new control volume, we have

$$\begin{aligned} \dot{m}_{in} &= \rho b \delta \vartheta_0 \\ \dot{m}_{out} &= \int_0^{\delta+\delta^*} \vartheta_x(y)\,dy \\ \dot{m}_{in} &= \dot{m}_{out} \end{aligned} \tag{9.188}$$

Evaluating the integrals of equation (9.188), we get

$$\rho b \delta \vartheta_0 = \rho b \int_0^{\delta+\delta^*} \vartheta_x(y)\,dy = \rho b \int_0^{\delta} \vartheta_x(y)\,dy + \rho b \vartheta_0 \int_{\delta}^{\delta+\delta^*} dy$$

$$\rho b \delta \vartheta_0 = \rho b \vartheta_0 \int_0^{\delta} dy = \rho b \int_0^{\delta} \vartheta_x(y)\,dy + \rho b \vartheta_0 \delta^*$$

$$\rho b \vartheta_0 \delta^* = \rho b \vartheta_0 \int_0^{\delta} \left(1 - \frac{\vartheta_x}{\vartheta_0}\right) dy \tag{9.189}$$

$$\delta^* = \int_0^{\delta} \left(1 - \frac{\vartheta_x}{\vartheta_0}\right) dy$$

Physically, the displacement thickness represents the extent of the influence of the viscosity as far as the mass flow rate is concerned. Outside the distance δ^* from the surface of the plate, the flow can be modeled as inviscid as far as mass flow rate is concerned. This distance is a physically meaningful, but not unique, boundary layer thickness. If we substitute the Blasius solution into equation (9.189), we get

$$\delta^* = \int_0^{\infty} \left(1 - \frac{\vartheta_x}{\vartheta_0}\right) dy = \sqrt{\frac{\nu x}{\vartheta_0}} \int_0^{\infty} (1 - f')\,d\eta$$

$$\delta^* = \sqrt{\frac{\nu x}{\vartheta_0}} \lim_{\eta \to \infty} (\eta - f) \tag{9.190}$$

$$\delta^* = 1.719 \sqrt{\frac{\nu x}{\vartheta_0}}$$

where we have extended the upper limit on the integration to infinity since the outer edge of the boundary layer is located there in the Blasius solution. Equation (9.190) can be cast in the same form as equation (9.179) in order to reveal the relative magnitudes of the conventional boundary layer thickness and the displacement thickness.

$$\frac{\delta^*}{x} = \frac{1.719}{\sqrt{Re_x}} \tag{9.191a}$$

Thus the displacement thickness also grows as the square root of x, and for the Blasius solution

$$\delta = 2.85\,\delta^* \tag{9.191b}$$

so that the boundary layer thickness is much greater than the displacement thickness.

Example 9E.8: As shown in Figure 9E.8, air at a temperature of T_{in} = 20 C and a pressure of $P_{in} = 10^5$ N/m^2 enters the space between two infinite parallel plates separated by a distance of $2a$ = 20 cm. The uniform velocity at the entrance to this "parallel plate duct" is ϑ_0 = 0.1 m/sec. A boundary layer grows on each of the two sides of the duct. As the boundary layer grows, the flow in the "undisturbed core" is accelerated. Since the Mach number is so low, the flow can be modeled as incompressible throughout. Then we can use the Blasius solution for flow over a flat plate as a model of the flow in the entry region of the duct by using the displacement thickness δ^* as a measure of the boundary layer thickness in the duct. From this model of the boundary layer thickness, we can determine the behavior of the flow in the undisturbed core and, in turn, make some estimates of the behavior of the flow in the entry region of the parallel plate geometry. Keep in mind that the results that we obtain here are only estimates since the Blasius solution applies only in the case of no pressure gradient in the direction of flow and there is clearly a pressure drop in the entry region of this configuration. We shall also compare these estimates with the accepted models given in Section 9.9.1.1.

For air: $\mu = 1.8 \times 10^{-5}$ kg/m sec, R = 287 J/kg K, c_v = 716 J/kg K

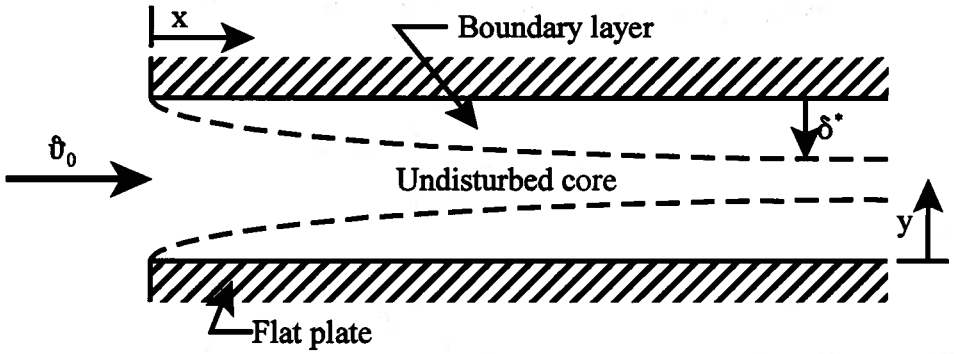

Figure 9E.8

(a) Estimate the average velocity of the flow at a location x = 3 m downstream from the entrance to the duct.

(b) Estimate the average pressure $P_{x=3m}$ in the undisturbed core at this same location.

(c) Use the result of part (b) to compute the apparent friction factor f_{app} for this 3 m length of the duct where

$$\frac{P_{in} - P_{x=3m}}{\frac{1}{2}\rho \vartheta_{ave}^{\ 2}} = f_{app}\frac{4x}{D_h}$$

and D_h is the hydraulic diameter. Recall that for this geometry, $D_h = 4a$ where a is the half distance between the plates. Compare this result with the value calculated from equation (9.115).

(d) Estimate the entry length L_e of this duct, i.e., the length of duct at which the boundary layer just "fills" the duct. Compare this estimate with the value calculated from equation 99.112).

Solution: (a) Since we can model the flow as incompressible and the plates are parallel, the average velocity of this steady flow is constant throughout the length of the duct. Then at a distance of 3 m downstream from the entrance, ϑ_{ave} = 0.1 m/sec. The Reynolds number is

$$Re_{D_h} = \frac{\rho \vartheta_0 D_h}{\mu} = \frac{4(1.189 \text{ kg/m})(0.1 \text{ m/sec})(0.1 \text{ m})}{1.8 \times 10^{-5} \text{ kg/m sec}} = 2643$$

The flow is laminar since $Re_{Dh} < 2800$.

(b) If we take the displacement thickness δ^* as the boundary layer thickness in the entry region, continuity in the entry region gives

$$\rho \vartheta_0 2a = \rho \vartheta_{core} 2\left(a - \delta^*\right)$$

$$\vartheta_{core} = \vartheta_0 \frac{a}{a - \delta^*}$$

but from equation (9.186)

$$\delta^* = \frac{1.719x}{\sqrt{\frac{\rho \vartheta x}{\mu}}} = 1.719x\sqrt{\frac{\mu}{\rho \vartheta x}}$$

The velocity appearing in this expression according is supposed to be the mainstream velocity which according to the Blasius solution is constant. However, in this case the velocity varies because of the acceleration in the "undisturbed" core. Then the displacement thickness can be written

$$\delta^* = 1.719x\sqrt{\frac{\mu}{\rho \vartheta_{core} x}}$$

Then from continuity we have

$$\vartheta_{core} = \vartheta_0 \frac{a}{a - 1.719x\sqrt{\frac{\mu}{\rho \vartheta_{core} x}}} = \vartheta_0 \frac{1}{1 - \frac{1.719}{a}\sqrt{\frac{\mu x}{\rho \vartheta_{core}}}}$$

Solving this expression for ϑ_0, we get

$$\vartheta_{core} - \frac{1.719\sqrt{\vartheta_{core}}}{a}\sqrt{\frac{\mu x}{\rho}} = \vartheta_0$$

If we let $z = \vartheta_{core}^{1/2}$, we can solve this expression by the quadratic formula. Then at $x = 3$m

$$\vartheta_{core} = 0.144 \text{ m/sec}$$

Since the flow in the "undisturbed" core can be modeled as inviscid, we can apply the Bernoulli equation there. Then the pressure drop from the entrance to the location $x = 3$ m is

$$P_{in} - P_{x=3m} = \frac{\rho\left(\vartheta_{core} - \vartheta_0\right)}{2} = \frac{\left(1.189 \text{ kg/m}^3\right)\left[\left(0.144 \text{ m/sec}\right)^2 - \left(0.100 \text{ m/sec}\right)^2\right]}{2}$$

$$P_{in} - P_{x=3m} = 6.375 \text{ x } 10^{-3} \text{ N/m}^2$$

In order to compare this result with equation (9.115) we first calculate the dimensionless coordinate x^+, viz.

$$x^+ = \frac{x}{D_h Re_{D_h}} = \frac{3 \text{ m}}{4(0.1 \text{ m})2643} = 2.838 \text{ x } 10^{-3}$$

Equation (9.115) gives

$$\left(\Delta P^*\right)_{apparent} = 4x^+\left[\frac{3.44}{\sqrt{x^+}} + \frac{24 + \frac{0.674}{4x^+} - \frac{3.44}{\sqrt{x^+}}}{1 + 2.9 \text{ x } 10^{-5}\left(x^+\right)^{-2}}\right]$$

Then

$$\left(\Delta P^*\right)_{apparent} = 4\left(2.838 \text{ x } 10^{-3}\right)\left[\frac{3.44}{\sqrt{\left(2.838 \text{ x } 10^{-3}\right)}} + \frac{24 + \dfrac{0.674}{4\left(2.838 \text{ x } 10^{-3}\right)} - \dfrac{3.44}{\sqrt{\left(2.838 \text{ x } 10^{-3}\right)}}}{1 + 2.9 \text{ x } 10^{-5}\left(2.838 \text{ x } 10^{-3}\right)^{-2}}\right]$$

$$\left(\Delta P^*\right)_{apparent} = 0.779$$

$$\Delta P_{apparent} = \left(\Delta P^*\right)_{apparent}\frac{\rho v_0^{\,2}}{2} = 0.779\frac{\left(1.189 \text{ kg/m}^3\right)\left(0.1 \text{ m/sec}\right)^2}{2} = 4.634 \text{ x } 10^{-3} \text{ N/m}^2$$

Thus the pressure drop calculated using the flat plate model is about 50 percent greater than that determined from a solution of the Navier-Stokes equation. This is due to the fact that the velocity in the "undisturbed" core is constantly changing throughout the entry length and the Blasius solution cannot accommodate either that or the pressure drop itself.

(c) The apparent friction factor is given by

$$f_{app} = \frac{P_{in} - P_{x=3m}}{\dfrac{\rho v_0^{\,2}}{2}}\frac{D_h}{4x} = \frac{\left(6.375 \text{ x } 10^{-3} \text{ N/m}^2\right)}{\dfrac{\left(1.189 \text{ kg/m}^3\right)\left(0.1 \text{ m/sec}\right)^2}{2}}\frac{4(0.1 \text{ m})}{4(3 \text{ m})} = 0.036$$

Similarly,

$$f_{app} = \frac{\left(\Delta P^*\right)_{apparent} D_h}{4x} = \frac{(0.779)(0.4 \text{ m})}{4(3 \text{ m})} = 0.026$$

Obviously since the pressure drop is greater by the flat plate model, the friction factor using that model is greater.

(d) From equation (9.106) it is apparent that when the velocity profile becomes fully-developed the maximum velocity, v_{max}, which is on the centerline of the flow, is $1.5\,v_0$. Then from continuity (part b above) we again have

$$v_{core} - \frac{1.719\sqrt{v_{core}}}{a}\sqrt{\frac{\mu x}{\rho}} = v_0$$

But now $v_{core} = 1.5\,v_0$. Then

$$1.5v_0 - \frac{1.719\sqrt{1.5v_0}}{a}\sqrt{\frac{\mu x}{\rho}} = v_0$$

$$1.5 - \frac{1.719\sqrt{1.5}}{a}\sqrt{\frac{\mu x}{\rho v_0}} = 1$$

Since at the entry length $x = L_{entry}$, we have

$$0.5 = \frac{1.719\sqrt{1.5}}{a}\sqrt{\frac{\mu L_{entry}}{\rho v_0}} = 4\frac{1.719\sqrt{1.5}}{D_h}\sqrt{\frac{\mu L_{entry} D_h}{\rho v_0 D_h}} = 4(1.719)\sqrt{1.5}\sqrt{\frac{L_{entry}}{D_h}}\frac{1}{\sqrt{Re_{D_h}}}$$

$$\frac{L_{entry}}{D_h} = 3.525 \text{ x } 10^{-3}$$

Equation (9.112) gives for large values of the Reynolds number

$$\frac{L_{entry}}{D_h} \approx 11 \text{ x } 10^{-3}$$

Thus the flat plate model underestimates the entry length because it has the displacement boundary layer growing as the square root of x whereas the acceleration in the core of the planar Couette flow makes the boundary layer grow at a much slower rate. Thus it takes a greater distance for the core velocity to accelerate to the value ϑ_{max} than the flat plate model predicts. However, for a simple estimate of the entry length with no other information available, this would not be an unreasonable result.

The purpose of this example is to show that lacking other information, simple models can often give useful, if approximate, information about flow geometries encountered in thermal-fluids engineering practice.

9.9.2.4 Momentum Thickness: Another effect that the boundary layer has upon the flow is to reduce the momentum flow at any given location along the plate compared with the uniform inviscid flow. This momentum deficit is, of course, the origin of the drag force exerted on the plate by the flow. Theodore von Karman (1881 - 1963), another student of Ludwig Prandtl and the founder of the Jet Propulsion Laboratory during World War II, suggested that there exists a *momentum thickness*, θ, due to this momentum deficit that is analogous to the displacement thickness associated with the deficit in the mass flow due to the presence of the boundary layer.

Von Karman defined θ such that the drag force, F_D, is equal to the flow of the deficit of the momentum in the boundary layer and could be calculated according to

$$F_D = \rho b \vartheta_0^2 \theta \tag{9.192}$$

Consider once again the control volume of Figure 9.22 for a flat plate of width b. If we apply the x-component of the equation of linear momentum to this control volume, we have

$$-F_D = \int_{CV} \rho \vartheta_x \left(\vec{\vartheta} \cdot \vec{n}\right) dA = -\rho b \int_0^\delta \vartheta_0^2 dy + \rho b \int_0^\ell \vartheta_0 \vartheta_y dx + \rho b \int_0^\delta \vartheta_x^2 dy \tag{9.193}$$

where F_D is the drag force exerted on the plate by the fluid stream. The three terms on the right-hand side represent the momentum flows through the left, top, and right faces of the control volume, respectively. To eliminate the term for the momentum flow through the top face, we apply the continuity equation to the control volume. Then

$$-\rho b \delta \vartheta_0 + \rho b \int_0^\ell \vartheta_y dx + \rho b \int_0^\delta \vartheta_x dy = 0 \tag{9.194}$$

If we multiply equation (9.194) through by ϑ_0 and subtract the result from equation (9.193), we get

$$\begin{gathered} -F_D = -\rho b \int_0^\delta \vartheta_0^2 dy + \rho b \int_0^\ell \vartheta_0 \vartheta_y dx + \rho b \int_0^\delta \vartheta_x^2 dy + \rho b \delta \vartheta_0^2 - \rho b \vartheta_0 \int_0^\ell \vartheta_y dx - \rho b \vartheta_0 \int_0^\delta \vartheta_x dy \\ -F_D = \rho b \int_0^\delta \vartheta_x^2 dy - \rho b \vartheta_0 \int_0^\delta \vartheta_x dy = \rho b \int_0^\delta \left(\vartheta_x^2 - \vartheta_0 \vartheta_x\right) dy \end{gathered} \tag{9.195}$$

Combining equations (9.192) and (9.195), we get

$$F_D = \rho b \vartheta_0^2 \theta = -\rho b \int_0^\delta \left(\vartheta_x^2 - \vartheta_0 \vartheta_x\right) dy = \rho b \int_0^\delta \vartheta_x \left(\vartheta_0 - \vartheta_x\right) dy \tag{9.196}$$

Then solving for the momentum thickness θ, we get

$$\theta = \int_0^\delta \frac{\vartheta_x}{\vartheta_0}\left(1 - \frac{\vartheta_x}{\vartheta_0}\right) dy \tag{9.197}$$

If we substitute the Blasius solution in equation (9.197), we have

$$\theta = \sqrt{\frac{\nu x}{\vartheta_0}} 2 f'' = 0.664 \sqrt{\frac{\nu x}{\vartheta_0}} \tag{9.198}$$

or in the form of equation (9.191)

$$\frac{\theta}{x} = \frac{0.664}{\sqrt{Re_x}} \tag{9.199}$$

Superimposed on the velocity profile, Figure 9.24 shows the relative magnitudes of the various definitions for boundary layer thickness. Each has its own particular physical significance.

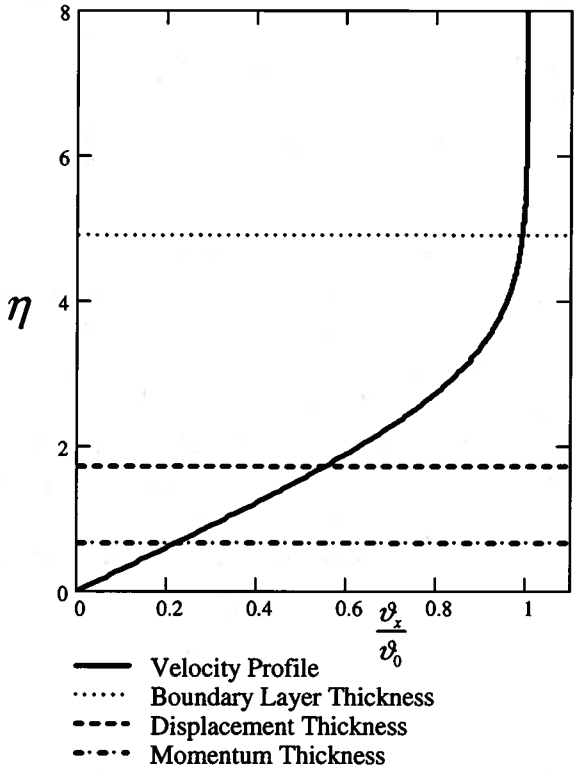

Figure 9.24 Relative Magnitudes of the Boundary Layer, Displacement, and Momentum Thicknesses for Flow Over a Flat Plate

Von Karman also pointed out that the drag force could also be determined from the shear stress on the flat plate. Then

$$F_D = b\int_0^x \tau_w(x)\,dx$$
$$\frac{dF_D}{dx} = b\tau_w \tag{9.200}$$

From equation (9.192) we also have

$$\frac{dF_D}{dx} = \rho b \vartheta_0^2 \frac{d\theta}{dx} \tag{9.201}$$

Combining equations (9.200) and (9.201), we get

$$\tau_w = \rho \vartheta_0^2 \frac{d\theta}{dx} \tag{9.202}$$

Equation (9.202) is known as the momentum integral relation. The local skin friction coefficient, C_f, is defined as

$$C_f \equiv \frac{\tau_w}{\frac{1}{2}\rho \vartheta_0^2} \tag{9.203}$$

For the Blasius solution for laminar flow over a flat plate, we can substitute equations (9.199) and (9.202) into equation (9.203) to get

$$C_f = \frac{0.664}{\sqrt{Re_x}} \tag{9.204}$$

While the displacement thickness, the momentum thickness, and the momentum integral relation seem interesting for the way in which they tie much of the dynamic behavior of the Newtonian fluid model together, they appear at this point to have limited utility since we derived them after we had already developed the Blasius solution for the flat plate. Their value however, lies in the fact that they are integral methods that tend to "average" properties in the boundary layer, and, hence, are less susceptible to the details of the flow. This averaging nature makes them particularly useful for turbulent flows since the solution of the Navier-Stokes equation for turbulent flow is extremely complicated. In the case of turbulent flow, it will be necessary to resort to a semi-empirical determination of the velocity profile in the boundary layer. Then, armed with this velocity profile and the integral methods we have just developed, useful information can be derived for the turbulent flow situation without ever really solving the Navier-Stokes equation. Example 9E.9 illustrates the procedure for a particular laminar velocity profile. As we shall see in Chapter 11, once we can fully describe the momentum transfer process, the description of the energy transfer process follows in a relatively straightforward manner.

Example 9E.9: Because the Blasius solution for the flat plate in laminar flow is numerical and cannot be expressed in closed form, it is a bit unwieldy to employ in practice. For this reason, over the years several different approximations to the Blasius velocity profile have been developed for laminar flow over a flat plate. One such approximation is the parabolic velocity profile originally due to von Karman. For $y \le \delta$, the velocity in the x-direction is given by

$$\frac{\vartheta_x}{\vartheta_0} = 2\left(\frac{y}{\delta}\right) - \left(\frac{y}{\delta}\right)^2$$

and for $y > \delta$

$$\frac{\vartheta_x}{\vartheta_0} = 1$$

The parabolic velocity profile satisfies the boundary conditions

$$(1) \quad \vartheta_x = 0 \quad \text{at} \quad y = 0$$

$$(2) \quad \vartheta_x = \vartheta_0 \quad \text{at} \quad y = \delta$$

As shown in Figure 9E.9, the approximation is quite good through out the thickness of the boundary layer.

(a) For a flat plate of width b, use this parabolic profile to obtain the drag force, F_D, the drag coefficient, C_D, the boundary layer thickness as a function of the position x on the plate, and the skin friction coefficient, C_f.

(b) Estimate the rate of entropy generation in a boundary layer of length ℓ.

(c) Compare the results obtained in part (a) with those obtained from the Blasius solution.

Solution: (a) From equation (9.187), we have

$$F_D = \rho b \vartheta_0^2 \theta$$

Then from equation (9.192) we have

$$\frac{F_D}{\rho b \vartheta_0^2} = \theta = \int_0^\delta \frac{\vartheta_x}{\vartheta_0}\left(1 - \frac{\vartheta_x}{\vartheta_0}\right) dy$$

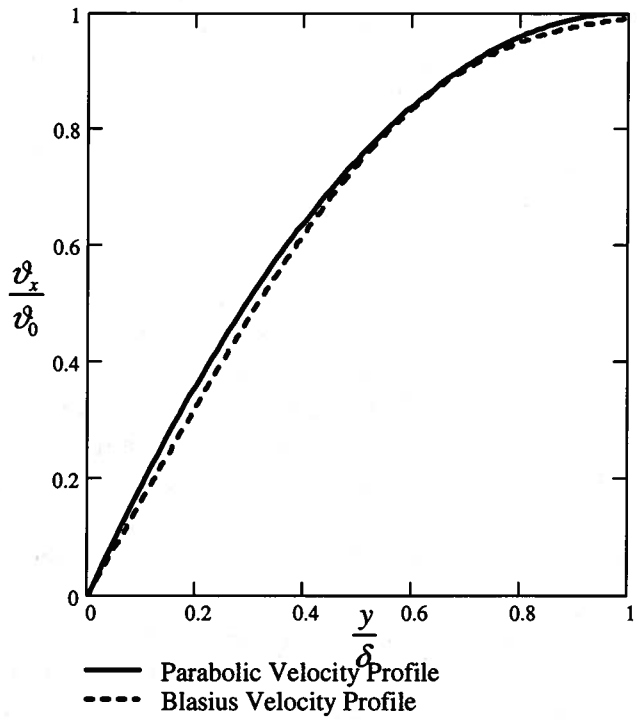

Figure 9E.9 Comparison of the Blasius and Parabolic Velocity Profiles for a Flat Plate

We now substitute the parabolic velocity profile in the integrand. Since the profile is a function of y/δ, let this now become the variable of integration. Then

$$\frac{F_D}{\rho b \vartheta_0^2 \delta} = \frac{\theta}{\delta} = \int_0^1 \frac{\vartheta_x}{\vartheta_0}\left(1-\frac{\vartheta_x}{\vartheta_0}\right) d\left(\frac{y}{\delta}\right)$$

$$\frac{F_D}{\rho b \vartheta_0^2 \delta} = \int_0^1 \left[2\left(\frac{y}{\delta}\right)-\left(\frac{y}{\delta}\right)^2\right]\left[1-2\left(\frac{y}{\delta}\right)+\left(\frac{y}{\delta}\right)^2\right] d\left(\frac{y}{\delta}\right)$$

$$\frac{F_D}{\rho b \vartheta_0^2 \delta} = 2\int_0^1 \left(\frac{y}{\delta}\right) d\left(\frac{y}{\delta}\right) - 5\int_0^1 \left(\frac{y}{\delta}\right)^2 d\left(\frac{y}{\delta}\right) + 4\int_0^1 \left(\frac{y}{\delta}\right)^3 d\left(\frac{y}{\delta}\right) - \int_0^1 \left(\frac{y}{\delta}\right)^4 d\left(\frac{y}{\delta}\right)$$

$$\frac{F_D}{\rho b \vartheta_0^2 \delta} = \frac{2}{15}$$

From the definition of the shear stress in the fluid

$$\tau_w = \mu\left(\frac{\partial \vartheta_x}{\partial y}\right)_{y=0}$$

but if we set $y^* = y/\delta$

$$\frac{\partial \vartheta_x}{\partial y} = \frac{\partial \vartheta_x}{\partial y^*}\frac{\partial y^*}{\partial y} = \left(2\vartheta_0 - 2\vartheta_0 y^*\right)\frac{1}{\delta}$$

Then

$$\tau_w = \left[\frac{2\mu\vartheta_0\left(1-y^*\right)}{\delta}\right]_{y^*=0} = \frac{2\mu\vartheta_0}{\delta}$$

From equation (9.190) we have

$$\tau_w = \frac{1}{b}\frac{dF_D}{dx} = \frac{2\mu\vartheta_0}{\delta}$$

Then

$$F_D \frac{dF_D}{dx} = \frac{2\mu b\vartheta_0}{\delta}\left(\frac{2}{15}\right)\rho b\vartheta_0^2\delta = \frac{4\mu b^2\vartheta_0^3}{15}$$

Integrating this expression, we get

$$\int_0^L F_D \frac{dF_D}{dx}dx = \int_0^L \frac{4\mu b^2\vartheta_0^3}{15}dx$$

$$\frac{F_D^2}{2} = \frac{4\mu b^2\vartheta_0^3 L}{15}$$

$$F_D = \sqrt{\frac{8\mu b^2\vartheta_0^3 L}{15}}$$

Then the drag coefficient for one side of the plate as defined in equation (9.185) becomes

$$C_D \equiv \frac{F_D}{\frac{1}{2}\rho\vartheta_0^2 bL} = \frac{\sqrt{\frac{8\mu b^2\vartheta_0^3 L}{15}}}{\frac{1}{2}\rho\vartheta_0^2 bL} = \frac{1.461}{\sqrt{\frac{\rho\vartheta_0 L}{\mu}}} = \frac{1.461}{\sqrt{Re_L}}$$

Then

$$F_D = \frac{1.461}{\sqrt{Re_L}}\frac{1}{2}\rho\vartheta_0^2 bL \quad \text{and} \quad F_D = \frac{2}{15}\rho b\vartheta_0^2\delta$$

Equating these last two expressions, we get

$$\frac{\delta}{L} = \frac{5.477}{\sqrt{Re_L}}$$

and it follows that

$$\frac{\delta}{x} = \frac{5.477}{\sqrt{Re_x}}$$

For the skin friction coefficient C_f, we have from the definition

$$\frac{C_f}{2} = \frac{\tau_w}{\rho\vartheta_0^2} = \frac{2\mu\vartheta_0}{\delta}\frac{1}{\rho\vartheta_0^2} = \frac{2\mu}{5.477x}\frac{\sqrt{Re_x}}{\rho\vartheta_0}$$

$$C_f = \frac{0.730}{\sqrt{Re_x}}$$

(b) In order to estimate the rate of entropy generation in this boundary layer based on the incompressible Newtonian fluid model, we must first apply the first law of thermodynamics in order to assess the rate of dissipation of kinetic energy of the fluid in the boundary layer. To do this we employ the control volume shown in Figure 9.22. Since there is no pressure gradient in this steady flow and since the flow is also adiabatic with no shaft work transfer, the first law reduces to

$$0 = (h_{in} - h_{out}) + \left(\frac{\vartheta_{in}^2}{2} - \frac{\vartheta_{out}^2}{2}\right)$$

If we now substitute the enthalpy constitutive relation into this expression, we get

$$0 = c\left(T_{in} - T_{out}\right) + v\cancel{\left(P_{in} - P_{out}\right)} + \left(\frac{\vartheta_{in}^{\,2}}{2} - \frac{\vartheta_{out}^{\,2}}{2}\right)$$

$$T_{out} - T_{in} = \frac{1}{2c}\left(\vartheta_{in}^{\,2} - \vartheta_{out}^{\,2}\right)$$

It must be remembered that the kinetic energy terms appearing in this expression are the mass flow rate averaged values over the entry and exit ports. For the entry port the averaging process is trivial since the flow rate is constant over this port, but for the exit port the velocity varies according to the parabolic velocity profile given above. Then

$$\dot{m}\left(\vartheta_{out}^{\,2}\right)_{ave} = \rho b\delta\vartheta_0\left(\vartheta_{out}^{\,2}\right)_{ave} = \rho b\int_0^{\delta}\vartheta_x^{\,3}dy$$

$$\left(\vartheta_{out}^{\,2}\right)_{ave} = \frac{1}{\delta\vartheta_0}\int_0^{\delta}\vartheta_x^{\,3}dy$$

where for the parabolic velocity profile

$$\vartheta_x^{\,3} = \vartheta_0^{\,3}\left[8\left(\frac{y}{\delta}\right)^3 - 12\left(\frac{y}{\delta}\right)^4 + 6\left(\frac{y}{\delta}\right)^5 - \left(\frac{y}{\delta}\right)^6\right]$$

If we change variables by letting $y^* = y/\delta$, we have

$$\int_0^{\delta}\vartheta_x^{\,3}dy = \delta\int_0^{1}\vartheta_x^{\,3}dy^*$$

Substituting for ϑ_x^3 and integrating, we get

$$\int_0^{\delta}\vartheta_x^{\,3}dy = \frac{16}{35}\delta\vartheta_0^{\,3}$$

and

$$\left(\vartheta_{out}^{\,2}\right)_{ave} = \frac{1}{\delta\vartheta_0}\int_0^{\delta}\vartheta_x^{\,3}dy = \frac{1}{\delta\vartheta_0}\frac{16}{35}\delta\vartheta_0^{\,3} = \frac{16}{35}\vartheta_0^{\,2}$$

Then the temperature increase becomes

$$T_{out} - T_{in} = \frac{1}{2c}\left(\vartheta_{in}^{\,2} - \vartheta_{out}^{\,2}\right) = \frac{1}{2c}\left(\vartheta_0^{\,2} - \frac{16}{35}\vartheta_0^{\,2}\right) = \frac{1}{c}\frac{19}{70}\vartheta_0^{\,2}$$

From the second law, we have

$$\dot{S}_{gen} = \dot{m}c\left(s_{out} - s_{in}\right) = \dot{m}c\ln\frac{T_{out}}{T_{in}} = \rho c\dot{V}\ln\left(1 + \frac{T_{out} - T_{in}}{T_{in}}\right)$$

$$\dot{S}_{gen} = \rho cb\delta\vartheta_0\ln\left(1 + \frac{\vartheta_0^{\,2}}{cT_{in}}\frac{19}{70}\right)$$

Thus the rate of entropy generation varies linearly with the boundary layer thickness. Then for a boundary layer of length ℓ, we have

$$\dot{S}_{gen} = \frac{5.477\ell\rho c\vartheta_0}{\sqrt{Re_\ell}}\ln\left(1 + \frac{\vartheta_0^{\,2}}{cT_{in}}\frac{19}{70}\right)$$

Thus, for the flat plate, the rate of entropy generation varies as the square root of the length of the boundary layer.

(c) From these results, it appears that the error associated with the use of the parabolic velocity profile introduces an error of approximately 12 percent. For example,

$$\left|\frac{\delta_{Blasius}-\delta_{parabolic}}{\delta_{Blasius}}\right| = \left|1-\frac{\delta_{parabolic}}{\delta_{Blasius}}\right| = \left|1-\frac{5.477}{4.90}\right| = 0.12$$

Perhaps more importantly, the parabolic velocity profile gives the proper dependence on x for the growth of the boundary layer, namely, the square root of x. There are other analytical forms for the velocity profile that give even greater accuracy, but the method of employing them is precisely the same as that above.

Example 9E.10: As shown in Figure 9E.10a, a flat plate is immersed in a uniform flow of air with a velocity $\vec{v}_0$ and zero pressure gradient. The plate is porous with a very large number of uniformly-spaced small holes drilled through it. Air flows through these holes in a direction normal to the plate with a velocity $\vec{v}_{wall}$ that is the same everywhere, independent of the values of x and y.

(a) Determine the velocity profile of the air for this flow geometry.

(b) Find an expression for the boundary layer thickness of the air flowing over the plate for which the outer limit of the boundary layer is defined as that value of y for which $\vec{v}_x = 0.99\vec{v}_0$.

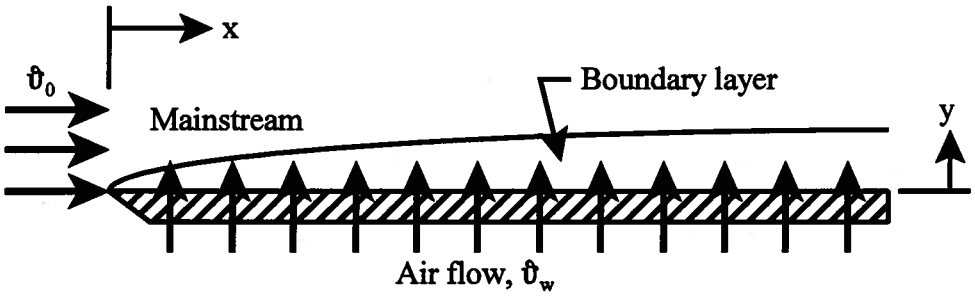

Figure 9E.10a

Solution: (a) We first note that the boundary condition $\vec{v}_y = 0$ at $y = 0$ does not hold in this case even though the boundary condition $\vec{v}_x = 0$ at $y = 0$ does hold. Thus we cannot use the Blasius solution to describe the flow in this case, and it will be necessary to solve the boundary layer equations specifically for this geometry. We further note that $\vec{v}_y = \vec{v}_{wall} =$ constant everywhere. Then $\partial \vec{v}_y/\partial x = 0$ and from continuity

$$\frac{\partial v_x}{\partial x} + \frac{\partial v_y}{\partial y} = 0$$

Then it follows that $\vec{v}_x = \vec{v}_x(y)$. Then the momentum equation, equation (9.156), becomes

$$\rho\left(\frac{\partial v_x}{\partial t} + v_x\frac{\partial v_x}{\partial x} + v_y\frac{\partial v_x}{\partial y}\right) = -\frac{\partial P}{\partial x} + \mu\frac{\partial^2 v_x}{\partial y^2}$$

$$v_y\frac{\partial v_x}{\partial y} = \frac{\mu}{\rho}\frac{\partial^2 v_x}{\partial y^2} = \nu\frac{\partial^2 v_x}{\partial y^2}$$

$$\therefore v_{wall}\frac{dv_x}{dy} = \frac{\mu}{\rho}\frac{d^2 v_x}{dy^2}$$

where we have made use of the fact that the y-component of velocity is $\vec{v}_{wall}$ everywhere and that the x-component of velocity is a function of y only. We have also introduced the kinematic viscosity, ν. The solution of this second order, ordinary differential equation must satisfy the boundary conditions

$$(1) \quad v_x = 0 \quad \text{at} \quad y = 0$$

$$(2) \quad v_x = v_0 \quad \text{at} \quad y \to \infty$$

The solution of the differential equation is of the form

$$\vartheta_x = Ae^{my} + B$$

Then

$$\frac{d\vartheta_x}{dy} = Ame^{my}$$

$$\frac{d^2\vartheta_x}{dy^2} = Am^2e^{my}$$

Then substituting these expressions into the original differential equation, we get

$$Ame^{my} = \frac{\nu}{\vartheta_{wall}} Am^2e^{my}$$

$$\therefore m = \frac{\vartheta_{wall}}{\nu}$$

Then

$$\vartheta_x = Ae^{\frac{\vartheta_{wall}y}{\nu}} + B$$

From the second boundary condition, it is apparent that only negative values of ϑ_{wall} are allowable if the solution is to remain bounded as we move to the outer edge of the boundary layer where $y \to \infty$. This means that there is suction under the plate. (As we shall see shortly, this is a means of controlling the behavior of the boundary layer.) Applying the second boundary condition, we get the result that $B = \vartheta_0$. Then

$$\vartheta_x = Ae^{\frac{\vartheta_{wall}y}{\nu}} + \vartheta_0$$

Applying the first boundary condition, we get

$$0 = A + \vartheta_0$$

$$\therefore A = -\vartheta_0$$

Then the solution becomes

$$\frac{\vartheta_x}{\vartheta_0} = 1 - e^{\frac{\vartheta_{wall}y}{\nu}} \qquad \vartheta_{wall} < 0$$

(b) The boundary layer thickness is given by

$$\left(\frac{\vartheta_x}{\vartheta_0}\right)_{y=\delta} = 0.99 = 1 - e^{\frac{\vartheta_{wall}\delta}{\nu}}$$

$$\therefore e^{\frac{\vartheta_{wall}\delta}{\nu}} = 0.01$$

$$\frac{\vartheta_{wall}\delta}{\nu} = \ln 0.01$$

$$\frac{\vartheta_{wall}\delta}{\nu} = -4.605$$

Then the boundary layer thickness becomes

$$\delta = -\frac{4.605\nu}{\vartheta_{wall}}$$

Hence, the boundary layer has the same thickness at all locations on the plate, and for a given value of the kinematic viscosity ν, i.e., a given fluid, the thickness of the boundary layer is determined solely by the suction velocity ϑ_{wall}.

Thus, we now have at our disposal a means of controlling the thickness of the boundary layer. The problem is that for a given mainstream velocity, as the boundary layer becomes thinner with an increase in suction velocity, the fluid shear and the skin friction increase. Thus boundary layer suction may not be all that worthwhile as a means of reducing skin friction drag. However, the real reasons that boundary layer suction is of interest are: (1) that it delays separation of the boundary layer from the solid surface thereby reducing profile drag; and (2) that it exerts a stabilizing influence on the laminar flow thereby delaying the onset of the transition to turbulent flow. These are two important flow phenomena that we shall consider in greater detail shortly, but suffice it to say at this point that boundary layer suction is in fact used in some thermal-fluid systems to control the flow configuration. Figures 9E.10b and 9E.10c (from L. Prandtl, *Essentials of Fluid Dynamics*, Hafner Publishing Co., New York, 1952, p.143) show just how dramatic the effect can be.

Figure 9E.10b Flow in a Channel with a Sudden Enlargement

Notice in Figure 9E.10b that the flow is separated from the wall in the enlarged section of the channel, but when boundary layer suction is introduced in the portion of the channel where the enlargement occurs, the flow re-attaches to the wall as shown in Figure 9E.10c.

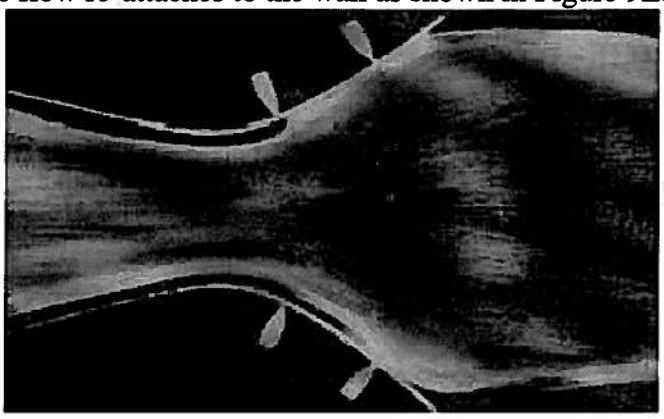

Figure 9E.10c Flow in a Channel with a Sudden Enlargement and Suction at the Wall

9.10 Turbulent Flow

Up to the present time we have been considering flows that are described as laminar in that any perturbation to the flow due to some infinitesimal disturbance is damped out by the action of viscosity. However, we would intuitively expect that if the disturbance became sufficiently large, the flow field could assume another character. As mentioned previously, the experiments of Osborne Reynolds confirmed that this is indeed the case. The Reynolds number provides a good measure of this possibility since it represents the ratio of inertia forces to viscous forces. Thus, at large values of the Reynolds number, we would expect the inertia forces to dominate the flow with the viscous forces exerting little influence on the flow field. At these high Reynolds numbers, perturbations to the flow are no longer subject to the damping action of viscosity. It is now possible, then, for these perturbations to grow in magnitude and thereby destroy the laminar nature of the flow. Such flows are termed *turbulent*, and in fact, most flows commonly encountered in thermal-fluids engineering practice are of this type in which an irregular fluctuation (mixing or eddying motion) is superimposed on the average mainstream flow.

As shown schematically in Figure 9.25, the velocity continually fluctuates about some average value in a manner such that the amplitude of this fluctuation is, in general, of the same order of magnitude as the velocity itself. Not only does the velocity at one point in the flow field fluctuate with time, but also the velocity varies in an irregular fashion from point to point at a particular instant in time. Due to this irregular nature of the velocity, the paths of motion of the fluid particles are highly random which results in an extensive mixing of the fluid and a significant enhancement of the transport of momentum and energy between the fluid and the solid surfaces that bound it. In fact, the effects produced by this mixing motion are such that the viscosity and the thermal conductivity of the fluid appear to have been increased by several orders of magnitude. Unfortunately, the fluctuations in the velocity are so complex that they render the problem inaccessible to mathematical treatment which makes the modeling of turbulent flow one of the major challenges of thermal-fluids engineering.

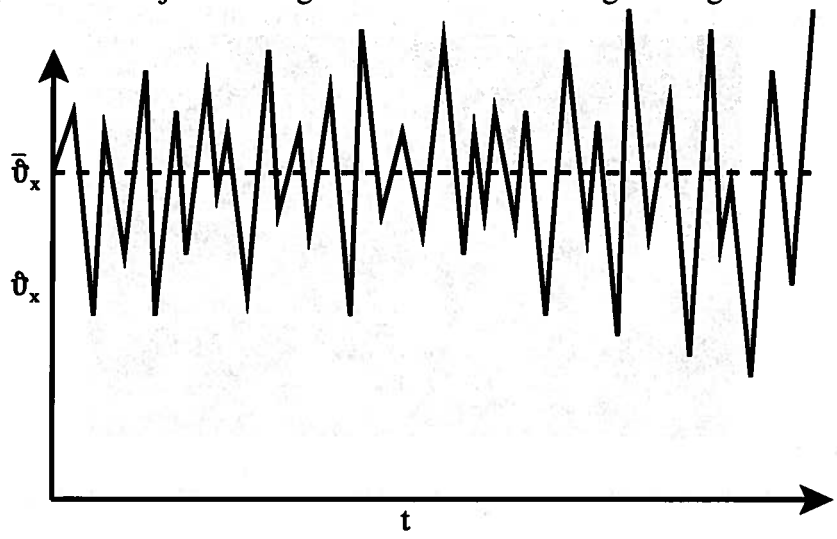

Figure 9.25 Instantaneous Velocity of Fluid in Turbulent Flow at Some Point in Space

The random nature of the motion of the fluid that prevails in turbulent flow fields is similar to that which prevails in the motion of the molecules that make up any physical body. In principle, we could describe the behavior of a macroscopic body by specifying the initial values

of the coordinates and velocities of all the molecules and then integrating the equations of motion for each molecule. This determines the coordinates and velocity of every molecule as a function of time and thereby describes the behavior of the body composed of these molecules. However, since the number of particles making up such a body is incredibly large, the method described is virtually impossible in practice. The resolution of this dilemma lies in the complex and irregular nature of the motion of the molecules themselves. It follows that after a sufficiently long period of time the velocities and coordinates of the molecules assume all possible values so that the effect of the initial conditions is smoothed out and disappears. This condition then permits the use of statistical mechanics to describe the behavior of a macroscopic body in terms of its microscopic components. The situation in turbulent flow is similar to that described above with the fluid particles serving as the analog of the molecules of the body. It follows then that the theory of turbulent flow must be of a statistical nature. Several attempts have been made in this direction; however, to date no complete quantitative theory has been developed. Nevertheless, several important worthwhile results have been deduced using a technique similar to that described below.

At any point in a three-dimensional, fully developed turbulent flow field, the fluid velocity varies with respect to both time and direction. The *instantaneous* velocities and pressure are $\vartheta_{x,i}$, $\vartheta_{y,i}$, $\vartheta_{z,i}$, and P_i while the *time averages* of these quantities are ϑ_x, ϑ_y, ϑ_z, and P where

$$\vartheta_x = \frac{1}{\theta}\int_{t_0}^{t_0+\theta} \vartheta_{x,i}\,dt, \quad \vartheta_y = \frac{1}{\theta}\int_{t_0}^{t_0+\theta} \vartheta_{y,i}\,dt, \quad \vartheta_z = \frac{1}{\theta}\int_{t_0}^{t_0+\theta} \vartheta_{z,i}\,dt, \quad P = \frac{1}{\theta}\int_{t_0}^{t_0+\theta} P_i\,dt \qquad (9.205)$$

By virtue of the equations (9.205) it is possible to separate a turbulent flow into a *mean motion* described by (9.205) and into a *fluctuating* or *eddying motion* which represents the amount of fluctuation of the instantaneous quantity from the average quantity. Thus, if ϑ_x', ϑ_y', ϑ_z', and P' denote the fluctuating components, we have

$$\vartheta_{x,i} = \vartheta_x + \vartheta_x', \quad \vartheta_{y,i} = \vartheta_y + \vartheta_y', \quad \vartheta_{z,i} = \vartheta_z + \vartheta_z', \quad P_i = P + P' \qquad (9.206)$$

It should be pointed out that the mean values are to be taken over a sufficiently long interval of time, θ, so that they are completely independent of time for a steady flow. Thus, it follows that

$$\overline{\vartheta_x'} = \frac{1}{\theta}\int_{t_0}^{t_0+\theta} \vartheta_x'\,dt = 0, \quad \overline{\vartheta_y'} = \frac{1}{\theta}\int_{t_0}^{t_0+\theta} \vartheta_y'\,dt = 0, \quad \overline{\vartheta_z'} = \frac{1}{\theta}\int_{t_0}^{t_0+\theta} \vartheta_z'\,dt = 0, \quad \overline{P'} = \frac{1}{\theta}\int_{t_0}^{t_0+\theta} P_i\,dt = 0 \qquad (9.207)$$

That is, the time average of each of the fluctuating components is zero. By analogy to equations (9.207), the mean square of the velocity fluctuations is defined as

$$\overline{\vartheta_x'^2} = \frac{1}{\theta}\int_{t_0}^{t_0+\theta} \vartheta_x'^2\,dt, \quad \overline{\vartheta_y'^2} = \frac{1}{\theta}\int_{t_0}^{t_0+\theta} \vartheta_y'^2\,dt, \quad \overline{\vartheta_z'^2} = \frac{1}{\theta}\int_{t_0}^{t_0+\theta} \vartheta_z'^2\,dt \qquad (9.208)$$

The turbulent shear components (The reason for this name will become apparent shortly.) are

$$\overline{\vartheta_x'\vartheta_y'} = \frac{1}{\theta}\int_{t_0}^{t_0+\theta} \vartheta_x'\vartheta_y'\,dt, \quad \overline{\vartheta_y'\vartheta_z'} = \frac{1}{\theta}\int_{t_0}^{t_0+\theta} \vartheta_y'\vartheta_z'\,dt, \quad \overline{\vartheta_x'\vartheta_z'} = \frac{1}{\theta}\int_{t_0}^{t_0+\theta} \vartheta_x'\vartheta_z'\,dt \qquad (9.209)$$

Note that when the mean flow is in one direction, e.g. the x-direction, the mean velocities in the other two directions (y and z) are zero but the fluctuating quantities defined in equations (9.208) and (9.209) are all finite, including those in the y- and z-directions.

Even though the flow is turbulent, the Navier-Stokes equation is still applicable if the instantaneous values of the velocity and pressure are used. For an incompressible Newtonian fluid the relevant component equations are equations (9.67). We shall now show the form that the Navier-Stokes equation takes for the turbulent flow field. For example in the absence of body forces the x-component of the Navier-Stokes equation becomes

$$\rho\left(\frac{\partial \vartheta_{x,i}}{\partial t}+\vartheta_{x,i}\frac{\partial \vartheta_{x,i}}{\partial x}+\vartheta_{y,i}\frac{\partial \vartheta_{x,i}}{\partial y}+\vartheta_{z,i}\frac{\partial \vartheta_{x,i}}{\partial z}\right)=-\frac{\partial P_i}{\partial x}+\mu\left(\frac{\partial^2 \vartheta_{x,i}}{\partial x^2}+\frac{\partial^2 \vartheta_{x,i}}{\partial y^2}+\frac{\partial^2 \vartheta_{x,i}}{\partial z^2}\right) \tag{9.210}$$

and the continuity equation, equation (9.70) becomes

$$\frac{\partial \vartheta_{x,i}}{\partial x}+\frac{\partial \vartheta_{y,i}}{\partial y}+\frac{\partial \vartheta_{z,i}}{\partial z}=0 \tag{9.211}$$

Notice that the convective terms in equation (9.210) can be written

$$\vartheta_{x,i}\frac{\partial \vartheta_{x,i}}{\partial x}+\vartheta_{y,i}\frac{\partial \vartheta_{x,i}}{\partial y}+\vartheta_{z,i}\frac{\partial \vartheta_{x,i}}{\partial z}=\frac{\partial\left(\vartheta_{x,i}\right)^2}{\partial x}+\frac{\partial \vartheta_{x,i}\vartheta_{y,i}}{\partial y}+\frac{\partial \vartheta_{x,i}\vartheta_{z,i}}{\partial z} \tag{9.212}$$

Substituting equation (9.212) into equation (9.210) and collecting like terms, we obtain

$$\rho\frac{\partial \vartheta_{x,i}}{\partial t}=-\frac{\partial P_i}{\partial x}+\frac{\partial}{\partial x}\left(\mu\frac{\partial \vartheta_{x,i}}{\partial x}-\rho\vartheta_{x,i}{}^2\right)+\frac{\partial}{\partial y}\left(\mu\frac{\partial \vartheta_{x,i}}{\partial y}-\rho\vartheta_{x,i}\vartheta_{y,i}\right)+\frac{\partial}{\partial z}\left(\mu\frac{\partial \vartheta_{x,i}}{\partial z}-\rho\vartheta_{x,i}\vartheta_{z,i}\right) \tag{9.213}$$

Now substitute in equation (9.213) the appropriate value for the instantaneous velocity given by equations (9.206). Form the time average in the resulting equation term by term taking into account the following rules in which f and g are two dependent variables whose mean values (denoted by the superscript bar) are to be formed. Let s denote any one of the independent variables x, y, z and t. Then,

$$\overline{\bar{f}}=\bar{f},\quad \overline{f+g}=\bar{f}+\bar{g},\quad \overline{\bar{f}\cdot g}=\bar{f}\cdot\bar{g},\quad \overline{\frac{\partial f}{\partial s}}=\frac{\partial \bar{f}}{\partial s},\quad \overline{\int f ds}=\int \bar{f} ds \tag{9.214}$$

In performing the time averages, we make use of the relations (9.207). For example, making the substitution $\vartheta_{x,i}=\vartheta_x+\vartheta_x'$ in the first term of (9.214), we obtain

$$\frac{\partial \vartheta_{x,i}}{\partial t}=\frac{\partial \vartheta_x}{\partial t}+\frac{\partial \vartheta_x'}{\partial t} \tag{9.215}$$

Taking the time average, we get

$$\overline{\frac{\partial \vartheta_{x,i}}{\partial t}}=\overline{\frac{\partial \vartheta_x}{\partial t}+\frac{\partial \vartheta_x'}{\partial t}}=\overline{\frac{\partial \vartheta_x}{\partial t}}+\overline{\frac{\partial \vartheta_x'}{\partial t}}=\frac{\partial}{\partial t}\overline{\vartheta_x}+\frac{\partial}{\partial t}\overline{\vartheta_x'}=\frac{\partial \vartheta_x}{\partial t} \tag{9.216}$$

Applying this technique to each of the other terms, we obtain

$$\overline{\frac{\partial P_i}{\partial x}}=\frac{\partial P}{\partial x} \tag{9.217}$$

$$\overline{\mu\frac{\partial \vartheta_{x,i}}{\partial x}-\rho\vartheta_{x,i}{}^2}=\mu\frac{\partial \vartheta_x}{\partial x}-\rho\vartheta_x{}^2-\rho\overline{\vartheta_x'^2} \tag{9.218}$$

$$\overline{\mu\frac{\partial \vartheta_{x,i}}{\partial y}-\rho\vartheta_{x,i}\vartheta_{y,i}}=\mu\frac{\partial \vartheta_x}{\partial y}-\rho\vartheta_x\vartheta_y-\rho\overline{\vartheta_x'\vartheta_y'} \tag{9.219}$$

$$\overline{\mu\frac{\partial \vartheta_{x,i}}{\partial z}-\rho\vartheta_{x,i}\vartheta_{z,i}}=\mu\frac{\partial \vartheta_x}{\partial z}-\rho\vartheta_x\vartheta_z-\rho\overline{\vartheta_x'\vartheta_z'} \tag{9.220}$$

Substituting equations (9.217) through (9.220) into equation (9.213), we obtain

$$\rho\left(\frac{\partial \vartheta_x}{\partial t}+\vartheta_x\frac{\partial \vartheta_x}{\partial x}+\vartheta_y\frac{\partial \vartheta_x}{\partial y}+\vartheta_z\frac{\partial \vartheta_x}{\partial z}\right)$$
$$=-\frac{\partial P}{\partial x}+\mu\left(\frac{\partial^2 \vartheta_x}{\partial x^2}+\frac{\partial^2 \vartheta_x}{\partial y^2}+\frac{\partial^2 \vartheta_x}{\partial z^2}\right)-\frac{\partial \rho\overline{\vartheta_x'^2}}{\partial x}-\frac{\partial \rho\overline{\vartheta_x'\vartheta_y'}}{\partial y}-\frac{\partial \rho\overline{\vartheta_x'\vartheta_z'}}{\partial z} \tag{9.221}$$

with similar equations for the y- and z-directions.

Comparing equation (9.221) with equations (9.67), we see that for turbulent flow, the Navier-Stokes equation is satisfied provided the mean velocity is used and three additional terms involving the fluctuation components are included in each component equation. These three additional terms have the units of stress and are referred to as the Reynolds stresses in honor of Osborne Reynolds who first derived them. It is customary to group these terms with the viscous terms in the Navier-Stokes equation. In all, there are six independent Reynolds stresses:

three normal stresses $-\rho\overline{\vartheta_x'^2}$, $-\rho\overline{\vartheta_y'^2}$, $-\rho\overline{\vartheta_z'^2}$;

and three shear stresses, $-\rho\overline{\vartheta_x'\vartheta_y'}$, $-\rho\overline{\vartheta_x'\vartheta_z'}$, $-\rho\overline{\vartheta_y'\vartheta_z'}$.

The result of this grouping is that the velocity fluctuations can be regarded as responsible for producing an increase in the shear stress in the fluid.

While the appearance of these Reynolds stresses in the Navier-Stokes equation seems to lend mathematical credence to the notion that they are stresses, we have not yet presented a physical interpretation to confirm this notion. On the one hand, we need to show that physically they are responsible for the transfer of momentum due to turbulence, and on the other hand, we need to show that they affect the flow in much the same manner as the viscous stresses. In this regard, Prandtl in 1925 proposed the following very simple model of turbulence based upon the similarity between the random nature of turbulence and the random nature of molecular motion.

Consider the case of a two-dimensional, parallel turbulent flow in which the average velocity varies only from streamline to streamline. The principal direction of flow is assumed parallel to the x-axis with $\vartheta_y = 0$, $\vartheta_z = 0$, and $\vartheta_x = \vartheta_x(y)$ with $d\vartheta_x/dy > 0$. Then there exists in the flow a velocity profile something like that shown in Figure 9.26.

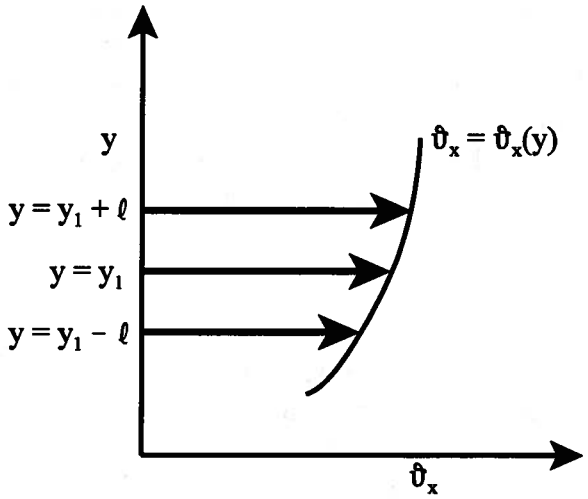

Figure 9.26 Velocity Profile in Turbulent Flow

As the fluid passes along the solid wall that bounds it, a fluid particle traverses some distance in both the x- and y-directions while retaining its momentum parallel to x. Focusing our attention on the plane $y = y_1$, we note that the fluid particle that comes from a layer $(y_1 - \ell)$, and therefore has $\vartheta_y' > 0$, carries with it velocity $\vartheta_x(y_1 - \ell)$ and is displaced transversely a distance ℓ known as the *Prandtl mixing length*. The fluid particle now has an average velocity that is smaller than the average velocity of other fluid particles at its new location. This gives rise to a negative component ϑ_x' in layer y_1 given by

$$\vartheta_x' = \vartheta_x(y_1 - \ell) - \vartheta_x(y_1) = -\ell\left(\frac{d\vartheta_x}{dy}\right)_{y=y_1} \tag{9.222}$$

The transverse component ϑ_y' can be determined from the assumption that two fluid particles that enter the layer at the plane $y = y_1$ from opposite sides approach one another with relative velocity $2\ell d\vartheta_x/dy$ and that this gives rise to transverse fluctuation velocities of the same order of magnitude as the longitudinal fluctuation velocities. Thus

$$\vartheta_y' \sim \ell\left(\frac{d\vartheta_x}{dy}\right)_{y=y_1} \tag{9.223}$$

A similar argument can be applied to a fluid particle that enters the layer from above with $\vartheta_y' < 0$ only now $\vartheta_x' > 0$. Then the product of the two velocities associated with the turbulence is always negative and the relevant Reynolds stress becomes

$$-\rho\overline{\vartheta_x'\vartheta_y'} = \rho\ell^2\left(\frac{d\vartheta_x}{dy}\right)^2 \tag{9.224}$$

Equation (9.224) bears a striking similarity to equation (9.13) with the mixing length playing a role analogous to the mean free path and the fluid particles analogous to the molecules of a gas. Thus momentum transport by eddying particles of fluid is analogous to momentum transport by molecular motion.

One must be careful not to push this analogy too far, however, as there are distinct differences in the underlying physics that limit its validity. In the kinetic theory model, molecules travel a clear path with no interactions occurring between collisions whereas the fluid particles do exchange momentum with surrounding particles during their movement from one location to another. Thus the mixing length is not as well-defined as the mean free path. In addition, with the exception of rarefied gases, the mean free path of the molecules is small compared to typical distances over which the velocity gradient can be viewed as non-linear whereas in the turbulent flow, the size of the typical eddy, as yet undefined, is on the same order as the mixing length ℓ. Nonetheless, this simple model has met with considerable success, particularly for simple shear flows as in the case of turbulent flow in a pipe or turbulent flow over a flat plate.

Equation (9.224) enables us to write the total shear stress in the fluid as the sum of the laminar shear stress and the turbulent or Reynolds shear stress, viz.

$$\tau = \tau_{laminar} + \tau_{turbulent} \tag{9.225}$$

which for two-dimensional flow is

$$\tau = \mu\frac{d\vartheta_x}{dy} - \rho\overline{\vartheta_x'\vartheta_y'} = \mu\frac{d\vartheta_x}{dy} + \mu_T\frac{d\vartheta_x}{dy} \tag{9.226}$$

where μ_T is the *apparent* increase in the viscosity, called the *eddy viscosity*, due to the turbulence in the flow. Since it depends upon the velocity fluctuations which are characteristic of the particular flow field, the eddy viscosity is a property of the flow and must not be regarded as a fluid characteristic like the shear viscosity. It may even vary over the spatial region occupied by the flow. Equation (9.226) can also be written in the form

$$\tau = \rho(\nu + \varepsilon_M)\frac{d\vartheta_x}{dy} \tag{9.227}$$

where ε_M is the *eddy diffusivity* of momentum analogous to the momentum diffusivity characterized by the kinematic viscosity ν. In dimensionless form, the eddy diffusivity is written ε^+ where

$$\tau = \rho\nu\left(1 + \frac{\varepsilon_M}{\nu}\right)\frac{d\vartheta_x}{dy} = \rho\nu\varepsilon^+\frac{d\vartheta_x}{dy} \tag{9.228}$$

9.10.1 Eddies and the Structure of Turbulent Flow

Although eddies are the fundamental reason for enhanced transfer of momentum and energy in turbulent flow, the concept of the "eddy" is not sharply defined. Basically, an eddy of size l represents some sort of coherent motion with a characteristic velocity of $\hat{v}_x(l)$ over this length scale. The characteristic frequency of the eddy is of the order of $\hat{v}_x(l)/l$. Then the irregular motion of turbulent flow can be thought of as a superposition of eddies of different sizes on the mean flow. The process of eddy formation is central to the transport process and can be thought of in the following way. The largest eddies have the largest amplitudes and appear first with a characteristic length l_0 that is of the same order of magnitude as the characteristic length of the flow L. These large eddies have a characteristic velocity $\hat{v}_l$ that is comparable to the mean velocity of the flow $\hat{v}_0$. The characteristic Reynolds number of these large eddies is $Re_l = \hat{v}_l l\rho/\mu$ which is of the same order of magnitude as the Reynolds number of the mean flow Re_L. Since this Reynolds number is typically very large in turbulent flow, the effects of viscosity in these large eddies is relatively small and the motion of these eddies can be modeled as inviscid and can be described by the Euler equation. Since an inviscid fluid possesses no dissipation mechanism, it follows that there is no appreciable dissipation of kinetic energy in the large eddies.

However, the large eddies tend to be unstable so they break up into small eddies, thereby transferring kinetic energy from the large eddies into these small eddies in a manner independent of the viscosity of the fluid. These small eddies undergo a further break-up resulting in a transfer of kinetic energy into still smaller eddies. Thus, by means of a practically dissipationless cascade process, momentum and energy pass from the large eddies to the small eddies. In this model, the small eddies, which correspond to high frequencies, participate in the turbulent flow with much smaller amplitudes. They contain only a small part of the total kinetic energy of the fluid, and, therefore, may be regarded as a fine detailed structure superimposed on the large turbulent eddies. It follows that for distances large compared with l, the variation of the fluctuation velocity component is given by the variation in the velocities of the large eddies, namely $\hat{v}_l$. Over distances small compared with l, the fluctuation velocity component is determined by the small eddies and is therefore small compared with $\hat{v}_l$.

Throughout this cascade process, the Reynolds number characteristic of the eddies is decreasing as the characteristic size of the eddies decreases. This process continues until the Reynolds number becomes so small that the viscous effects become the dominant mechanism for dissipating the kinetic energy.The kinetic energy dissipated in this manner ultimately appears as an increase in the stored thermal energy of the fluid. In order to maintain a steady state in the flow field, it is of course necessary to have some external energy source present to continually supply energy to the large eddies. For the case of an incompressible fluid, this energy is supplied by the flow work transfer to the fluid as manifested in the pressure drop in the direction of the average flow.

Although the dissipation is ultimately due to the viscosity, the rate of dissipation is limited by the first step in the cascade. Then its order of magnitude can be determined only by those quantities which characterize the large eddies, namely the fluid density ρ, the dimension l, and the velocity $\hat{v}_l$. The kinetic energy of the large eddies scales according to $\hat{v}_l^2$. Then if ξ represents the rate of energy transfer from the large eddies to the small eddies, it should scale according to the product of the kinetic energy and the frequency of the large eddies, viz.

$$\xi \sim \hat{v}_l^2\left(\frac{\hat{v}_l}{l}\right) \sim \frac{\hat{v}_l^3}{l}$$

which is independent of the viscosity as confirmed by experiment.

In our discussion, we have taken the eddy diffusivity ε_M to be the embodiment of the turbulence. Then if the eddy diffusivity is to characterize the properties of the turbulent flow, its order of magnitude must also be determined by ρ, ϑ_l, and l as per the above discussion. According to equation (9.228), the eddy diffusivity ε_M must have the same dimensions as the kinematic viscosity ν, namely (length)^2/time. The only quantity with these dimensions that can be formed from the combination ρ, ϑ_l, and l is the product $l\vartheta_l$. Then

$$\varepsilon_M \sim l\vartheta_l \tag{9.229}$$

In point of fact, equation (9.229) gives only the manner in which the eddy diffusivity scales with the characteristics of the large eddies. There is a numerical factor of considerable magnitude that would need to be included in equation (9.229) in order to determine the magnitude of the eddy diffusivity. From equation (9.229) the ratio of the eddy diffusivity to the ordinary kinematic viscosity is

$$\frac{\varepsilon_M}{\nu} \sim \frac{l\vartheta_l}{\nu} = Re_l \tag{9.230}$$

so that this ratio scales as the Reynolds number of the large eddies. In light of the large numerical factor in equation (9.229), equation (9.230) is more appropriately written

$$\frac{\varepsilon_M}{\nu} \sim \frac{Re_l}{Re_{critical}} \tag{9.231}$$

where $Re_{critical}$ is that critical value of Reynolds number for which the transition from laminar to turbulent flow occurs. Equation (9.231) shows that for $Re_l << Re_{critical}$, the eddy diffusivity is insignificant and the shear viscosity dominates; consequently, equation (9.227) reduces to the customary laminar flow relation. On the other hand, for $Re_l >> Re_{critical}$, the eddy diffusivity dominates the flow; consequently, under these conditions it is quite often possible to neglect the laminar contribution entirely.

By now it should be obvious that the primary objective of the analysis of turbulent flow is the determination of the eddy diffusivity (or equivalently, the mixing length) that characterizes the flow, preferably in the form ε^+ given by equation (9.228). Once ε^+ is known, the Navier-Stokes equation can be solved to give the average velocity field and the shear stress at the wall. To effect such a solution it is necessary that the boundary conditions be specified. The boundary conditions to be satisfied by the mean velocity components are identical to those of laminar flow, namely all velocity components must vanish at the wall. In addition, all fluctuation velocity components must vanish at the wall which implies that the fluctuation components are very small in the immediate neighborhood of the wall. It follows, then, that immediately adjacent to the wall the only stresses of any consequence are the viscous stresses of laminar flow. Thus in turbulent flow there exists a very thin layer next to the wall that can be modeled as a simple laminar shear flow. In this thin layer known as the *laminar sublayer*, the viscous forces dominate the inertia forces; consequently, there is no turbulence in the laminar sublayer. Any perturbations that occur are quickly damped out by the viscosity. It follows, then, that in this simple shear layer $\varepsilon_M << \nu$ or equivalently $\varepsilon^+ \sim 1$. The velocity profile in this region is a linear one similar to equation (9.4). In spite of the fact that the laminar sublayer is so thin, it plays a significant role in determining the shear at the wall, and hence the viscous drag on the wall, as well as being the major resistance to heat transfer. The shear stress is constant in the laminar sublayer because of the linear velocity profile typical of simple shear flows. Then $\tau = \tau_w$ and equation (9.228) becomes

$$\tau_w = \rho\nu\varepsilon^+ \frac{d\vartheta_x}{dy} = \rho\nu\varepsilon^+ \frac{d\vartheta_x}{dy}$$

$$\frac{\tau_w}{\rho} = \varepsilon^+\nu \frac{d\vartheta_x}{dy} \tag{9.232}$$

The term on the left-hand side of equation (9.232) has the dimensions of a velocity squared. Then we can define a pseudo-velocity, ϑ^*, known as the friction velocity such that

$$\vartheta^* = \sqrt{\frac{\tau_w}{\rho}} \tag{9.233}$$

Then with the aid of equation (9.233), equation (9.232) can be written in dimensionless form, viz.

$$\vartheta^{*2} = \varepsilon^+ \nu \frac{d\vartheta_x}{dy}$$

$$\vartheta^* = \varepsilon^+ \nu \frac{d\left(\vartheta_x / \vartheta^*\right)}{dy} = \varepsilon^+ \nu \frac{d\vartheta^+}{dy} \tag{9.234}$$

$$\varepsilon^+ = \frac{d\left(\vartheta^* y / \nu\right)}{d\vartheta^+} = \frac{dy^+}{d\vartheta^+}$$

where we have introduced the dimensionless distance from the wall, y^+, and the dimensionless velocity, ϑ^+, such that

$$y^+ = \frac{y\vartheta^*}{\nu} \qquad \vartheta^+ = \frac{\vartheta_x}{\vartheta^*} \tag{9.235}$$

From equation (9.235) it can be seen that the quantity y^+ is like a Reynolds number. In the laminar sublayer where $\varepsilon^+ \sim 1$, equation (9.234) becomes

$$\frac{d\vartheta^+}{dy^+} = 1 \tag{9.236}$$

which can be integrated with the boundary condition $\vartheta^+ = 0$ at $y^+ = 0$ to give the linear velocity profile that we expected, viz.

$$\vartheta^+ = y^+ \tag{9.237}$$

which has been shown by experiment to be valid for $y^+ < 5$.

Adjacent to the laminar sublayer is a transitional region known as the *buffer layer*. In the buffer layer the velocity fluctuations are large enough so that the turbulent stresses are comparable to the viscous stresses. The buffer layer provides a smooth transition from the laminar sublayer next to the wall to the *fully turbulent layer* located far from the wall. In this third region, the actual turbulent boundary layer, the Reynolds stresses completely dominate the flow so that $\varepsilon_M >> \nu$ or $\varepsilon^+ >> 1$. In the fully turbulent layer, the shear stress is equal to the Reynolds stress. Then from equation (9.224), we have

$$\tau = \tau_{turbulent} = -\rho\overline{\vartheta_x' \vartheta_y'} = \rho\ell^2\left(\frac{d\vartheta_x}{dy}\right)^2$$

$$\sqrt{\frac{\tau}{\rho}} = \ell\left(\frac{d\vartheta_x}{dy}\right) \tag{9.238}$$

Based upon the experimental evidence, Prandtl suggested that the shear stress could be modeled as being constant across the laminar sublayer, the buffer layer, and the fully turbulent layer as shown schematically in Figure 9.27.

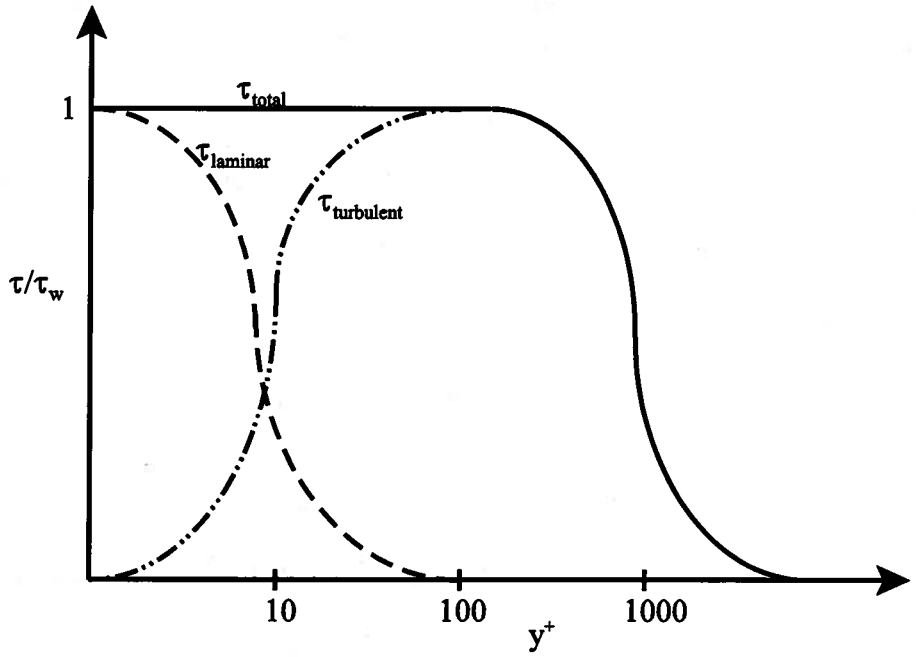

Figure 9.27 Shear Stress Distribution in Turbulent Flow

This is known as the "law of the wall" since the shear stress appearing in equation (9.238) is actually the shear stress at the wall. Then equation (9.238) becomes

$$\sqrt{\frac{\tau_w}{\rho}} = \vartheta^* = \ell\left(\frac{d\vartheta_x}{dy}\right) \tag{9.239}$$

where we have made use of equation (9.233). Prandtl then suggested that the mixing length is proportional to the distance from the wall consistent with our description of the turbulence given above. This suggestion is well supported by the experimental evidence. Then equation (9.239) becomes

$$\vartheta^* = \kappa y \frac{d\vartheta_x}{dy} \tag{9.240}$$

where the constant of proportionality, κ, known as the von Karman constant, is to be determined from the experimental data. Then if we re-arrange equation (9.240), we get

$$d\left(\vartheta_x/\vartheta^*\right) = d\vartheta^+ = \frac{1}{\kappa}\frac{dy}{y} = \frac{1}{\kappa}\frac{dy^+}{y^+} \tag{9.241}$$

Equation (9.241) can be integrated to give

$$\vartheta^+ = \frac{1}{\kappa}\ln y^+ + C \tag{9.242}$$

where the constant of integration, C, is to be determined from the experimental data as shown in Figure 9.28 for both flow in a circular conduit as well as flow over a flat plate.

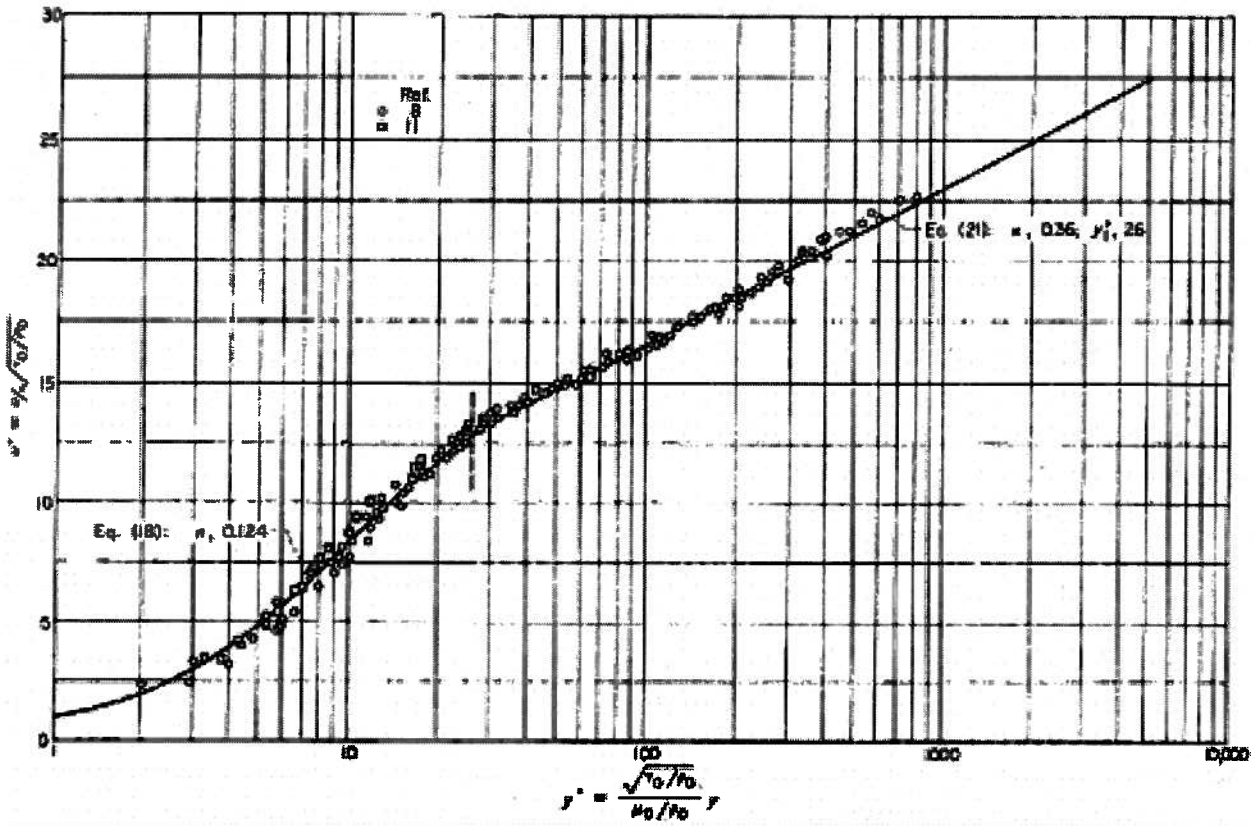

Figure 9.28 Generalized Velocity Distribution for Turbulent Flow
(From Figure 1, NACA Technical Report 1210, *Analysis of Turbulent Heat Transfer, Mass Transfer, and Friction in Smooth Tubes at High Prandtl and Schmidt Numbers*, R. G. Deissler, 1954.)

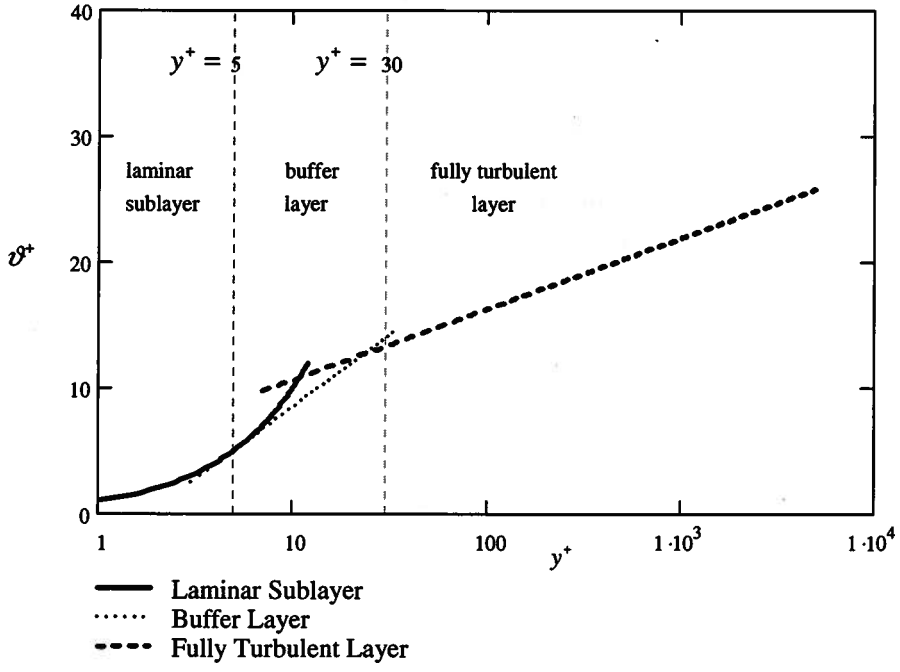

Figure 9.29 Velocity Profiles in Turbulent Boundary Layer

The values that fit the data best are $\kappa = 0.41$ and $C = 5.0$. Then equation (9.242) becomes

$$\vartheta^+ = 2.44 \ln y^+ + 5.0 \tag{9.243}$$

where equation (9.243) is most accurate for $y^+ \geq 30$. In the buffer layer, $5 \leq y^+ < 30$, the velocity profile is best represented by

$$\vartheta^+ = 5 \ln y^+ - 3.05 \tag{9.244}$$

However, as shown in Figure 9.29, this correlation introduces only a small correction to equation (9.243) so it is often neglected. It must be kept in mind that the shear at the wall completely dominates the velocity profile for turbulent flow.

The general structure of turbulent flow discussed above holds for both internal and external flows with some relatively minor differences in each case. Now that we have established the velocity profiles for turbulent flow in the neighborhood of a solid wall, we can use them to determine the characteristics of some turbulent flow geometries, both internal and external, that are important in thermal-fluids engineering.

9.10.2 Turbulent Internal Flows

For obvious reasons, the vast majority of the research in turbulent internal flows has been devoted to studies of flow in a circular conduit. Following this example, we shall consider this case in greater detail than any other. For these internal flows, events at the wall so dominate the flow that even though the flows are driven by a pressure gradient in each case, the velocity profiles are essentially coincident with those developed above for the case of zero pressure gradient. For fully-developed turbulent flow in a circular conduit, the boundary layer extends across the cross-sectional area. The flow consists of a laminar sublayer, a buffer layer, and a fully-turbulent core.

In the laminar sublayer, the velocity profile is the linear one given in equation (9.237) which is valid up to $y^+ < 5$. In order to gain a sense of magnitude of the dimensions of this laminar sublayer in the case of fully-developed turbulent flow in a circular conduit, let us estimate its thickness, δ_L.

$$y^+ = 5$$

$$\frac{\vartheta^* \delta_L}{\nu} = 5$$

$$\frac{\delta_L}{\nu}\sqrt{\frac{\tau_w}{\rho}} = 5 \tag{9.245}$$

where we have made use of the definition of the friction velocity, equation (9.233). The shear stress at the wall is given by equation (9.130). Then

$$\tau_w = \left(\frac{r}{2}\right)_{r=R}\left(\frac{\partial P}{\partial z}\right)_{r=R} = \frac{D}{4}\frac{\Delta P}{L} \tag{9.246}$$

From equation (9.140)

$$\frac{\Delta P}{L} = \frac{\rho f}{D}\left(\frac{\vartheta_{ave}^{\ 2}}{2}\right) \tag{9.247}$$

Substituting equation (9.247) into (9.246), we get

$$\tau_w = \rho \frac{f}{8} \vartheta_{ave}^{\ 2}$$

$$\frac{\tau_w}{\rho} = \frac{f}{8} \vartheta_{ave}^{\ 2} \tag{9.248}$$

Then substituting equation (9.248) into equation (9.245), we get

$$\frac{\vartheta^* \delta_L}{\nu} = \frac{\vartheta_{ave} \delta_L}{\nu} \sqrt{\frac{f}{8}} = 5$$

$$\frac{\delta_L}{D} \frac{\vartheta_{ave} D}{\nu} \sqrt{\frac{f}{8}} = \frac{\delta_L}{D} Re_D \sqrt{\frac{f}{8}} = 5 \tag{9.249}$$

$$\frac{\delta_L}{D} = \frac{5}{Re_D \sqrt{\frac{f}{8}}}$$

We have not yet developed a means of determining the friction factor for turbulent flow. However, for the purposes of an estimate, suppose that the laminar friction factor given in equation (9.141) is still valid for Reynolds numbers close to the laminar-turbulent transition. Then for $Re_D = 4000$, we have

$$f = \frac{64}{Re_D} = \frac{64}{4000} = 0.016 \tag{9.250}$$

and

$$\frac{\delta_L}{D} = \frac{5}{Re_D \sqrt{\frac{f}{8}}} = \frac{5}{4000 \sqrt{\frac{0.016}{8}}} = 0.02795 \tag{9.251}$$

A common size for a circular conduit is $D = 25$ mm. Then

$$\delta_L = 0.02795 D = 0.02795 (0.025 \text{ m}) \approx 0.7 \text{ mm} \tag{9.252}$$

Clearly the laminar sublayer is quite thin and in fact gets thinner as the Reynolds number increases. It is possible, then, that the asperities on the conduit wall due to casting defects in the case of cast iron pipe or due to scale formation on the wall due to the corrosive nature of a fluid are actually large enough to extend through the laminar sublayer. These asperities can then affect the flow by triggering further turbulence or produce additional friction in the flow. For this reason we then divide our study of turbulent flow in a circular conduit into two domains: (1) flow in a conduit considered hydraulically smooth because the inherent roughness of the conduit wall is much less than the thickness of the laminar sublayer as might be the case for flow in a drawn metal tube or a plastic pipe, and (2) flow in conduits whose walls are inherently so rough that the size of the asperities on the wall are of the same order of magnitude as the thickness of the laminar sublayer.

9.10.2.1 Turbulent Flow in Hydraulically Smooth Conduits: For hydraulically smooth conduits, von Karman proposed what Prandtl called a "middle law" for which the difference between the maximum velocity, ϑ_{max}, found at the centerline of the conduit and the velocity at the distance $y = R - r$ from the wall of the conduit is the product of the friction velocity ϑ^* and a universal function g of the ratio y/r. Then

$$\vartheta_{max} - \vartheta_x (y) = \vartheta^* g \left(\frac{y}{r} \right) \tag{9.253}$$

If we use equation (9.243) for the universal function g, we have

$$\frac{\vartheta_x}{\vartheta^*} = 2.44 \ln \frac{y \vartheta^*}{\nu} + 5 = 2.44 \ln \frac{(R - r) \vartheta^*}{\nu} + 5 \tag{9.254}$$

If we now evaluate equation (9.254) at the centerline of the conduit, we have

$$\frac{\vartheta_{max}}{\vartheta^*} = 2.44 \ln \frac{R \vartheta^*}{\nu} + 5 \tag{9.255}$$

If we now subtract equation (9.254) from equation (9.255), we have

$$\frac{\vartheta_{max}-\vartheta_x}{\vartheta^*}=2.44\ln\frac{R}{R-r} \tag{9.256}$$

which is now known as the *universal defect law* rather than the middle law. Note that by defining the velocity profile in this manner, we have forced the velocity profile to assume the value ϑ_{max} at the centerline with the condition for symmetry, $d\vartheta_x/dr = 0$, satisfied at the centerline as well.

If we now compute the average velocity, ϑ_{ave}, for this flow geometry using equation (9.256) as the velocity profile, we have

$$\vartheta_{ave}=\frac{\dot{V}}{A_c}=\frac{1}{\pi R^2}\left[\int_0^R \vartheta_x 2\pi r dr\right]=\frac{1}{\pi R^2}\left[\int_0^R \vartheta_{max}2\pi r dr-\int_0^R \vartheta^*\left\{2.44\ln R-2.44\ln(R-r)\right\}2\pi r dr\right]$$

$$\vartheta_{ave}=\vartheta_{max}-\frac{3}{2}(2.44)\vartheta^* \tag{9.257}$$

Combining equations (9.257), (9.255), (9.233) and (9.248), we get

$$2.44\ln\frac{Re_D}{2}\sqrt{\frac{f}{8}}+5-\frac{3}{2}(2.44)=\sqrt{\frac{f}{8}}$$

$$\frac{1}{\sqrt{f}}=0.8623\ln\left(Re_D\sqrt{f}\right)-1.0200 \tag{9.258}$$

Equation (9.258) is traditionally presented using the base 10 for the logarithm. Then

$$\frac{1}{\sqrt{f}}=1.9856\log_{10}\left(Re_D\sqrt{f}\right)-1.0200 \tag{9.259}$$

The result of equation (9.259) is based upon measurements of the velocity profile in the neighborhood of the wall from which the velocity in the center of the conduit is inferred. Prandtl, together with von Karman, and Nikuradse, decided to improve upon this result by using velocity data actually determined at the center of the conduit. Based on these experimental measurements, the average velocity derived in equation (9.257) becomes

$$\vartheta_{ave}=\vartheta_{max}-4.07\vartheta^* \tag{9.260}$$

Then equation (9.259) becomes

$$\frac{1}{\sqrt{f}}=2.0\log_{10}\left(Re_D\sqrt{f}\right)-0.8 \tag{9.261}$$

which is limited by the experimental data to $3 \times 10^3 < Re_D < 3 \times 10^6$.

Thus, the effects of the fluid viscosity and the turbulence of the flow are manifest in the friction factor used to determine the pressure drop over a given length of conduit according to equation (9.140). Unfortunately, equation (9.261) is a transcendental equation that is rather awkward to use. It is necessary to first guess at a value of f which can be substituted on the right-hand side of equation (9.261) to solve for a new value of f. The process is repeated until the values of f converge.

In an effort to provide the friction factor data in a more tractable form, H. Blasius in 1911 made a critical survey of the then existing experimental results and arranged them in dimensionless form consistent with Reynolds law of similarity. He presented his survey in the form of the coefficient of skin friction, C_f. Thus,

$$C_f=\frac{f}{4}=\frac{0.0791}{Re_D^{0.25}}$$

$$f=\frac{0.316}{Re_D^{0.25}} \tag{9.262}$$

Subsequent experiments have shown that the validity of this correlation is limited to $3 \times 10^3 < Re_D < 10^5$. More recently, Petukov has suggested that the available data can be better correlated by

$$f = (0.790 \ln Re_D - 1.64)^{-2} \tag{9.263}$$

in the range $10^4 < Re_D < 5 \times 10^6$.

9.10.2.2 Turbulent Flow in Hydraulically Smooth Non-circular Conduits: As an example of the case of turbulent flow in a non-circular conduit, consider the familiar geometry of flow between infinite parallel flat plates as shown in Figure 9.9. If in this case we take $y^* = a - y$, we can write the velocity profile of equation (9.243) in the form

$$\frac{\vartheta_x}{\vartheta^*} = 2.44 \ln \frac{(a-y)\vartheta^*}{\nu} + 5 \tag{9.264}$$

Following the procedure used in the case of a circular conduit, we compute the average velocity ϑ_{ave} according to

$$\vartheta_{ave} = \frac{1}{a}\int_0^a \vartheta_x d(a-y) = -\frac{1}{a}\int_a^0 \vartheta_x dy = -\frac{1}{a}\int_a^0 \vartheta^* \left[2.44 \ln \frac{(a-y)\vartheta^*}{\nu} + 5 \right] dy$$

$$\vartheta_{ave} = \vartheta^* \left[2.44 \ln \frac{a\vartheta^*}{\nu} + 2.561 \right] \tag{9.265}$$

From equations (9.233) and (9.248) we have

$$\frac{\vartheta_{ave}}{\vartheta^*} = \sqrt{\frac{8}{f}} = 2.44 \ln \frac{a\vartheta^*}{\nu} + 2.561 \tag{9.266}$$

where we have substituted equation (9.265). Since the hydraulic diameter for this geometry is $D_h = 4a$, we can write

$$\frac{a\vartheta^*}{\nu} = \frac{Re_{D_h}}{4}\sqrt{\frac{f}{8}} \tag{9.267}$$

Then we can substitute equation (9.268) into (9.266) to get

$$\frac{1}{\sqrt{f}} = 0.86233 \ln\left(Re_{D_h}\sqrt{f}\right) - 1.1874$$

$$\frac{1}{\sqrt{f}} = 1.9856 \log_{10}\left(Re_{D_h}\sqrt{f}\right) - 1.1874 \tag{9.268}$$

Since equation (9.268) is nearly identical to equation (9.258), we conclude that the dominance of the events in the neighborhood of the wall is so strong, the friction factor data obtained for circular conduits can be applied to non-circular conduits if the diameter D is replaced by the hydraulic diameter $D_h = 4A_c/\wp$ where $\wp$ is the wetted perimeter and A_c is the cross-sectional area. This is in distinct contrast to the case of laminar flow where it was necessary to develop a unique solution of the Navier-Stokes equation for each geometry. The error associated with this replacement is on the order of 10 percent which is adequate accuracy for design purposes.

Before moving on to take up the matter of rough circular conduits, it is worth reflecting for a moment on what we have just accomplished in describing this incredibly complex thermal-fluids phenomenon that we call turbulence. Based upon the randomness of the events in turbulent flow, we proposed a statistical model that we used in the Navier-Stokes equation to identify the effect of the turbulence on the viscous behavior of the fluid. Without solving the Navier-Stokes equation with these new effects included, we then proposed a simple model, based upon the kinetic theory

of gases, to describe these new effects, the Reynolds stresses. We then identified three different regions in the turbulent flow field based upon the degree to which these effects manifest themselves. For each region, we were able to present physical arguments for the nature of the velocity profile in that region. We then made experimental measurements of these velocity profiles, and from the empirical correlations of these data, we were able to determine the effects of both the viscosity and the turbulence embodied in the friction factor. With the aid of the friction factor data we are now able to determine the pressure drop for turbulent flow in a smooth circular conduit. Interestingly enough, we accomplished all this without ever solving the Navier-Stokes equation.

9.10.2.2 Fully-developed Turbulent Flow in Hydraulically Rough Conduits: Despite which relation is used for the friction coefficient, it must be remembered that equations (9.261), (9.262), and (9.263) apply to smooth tubes only. Drawn metallic tubing is considered to be smooth when it is new; however, after it has been in service for sometime, the internal surface of the tube becomes quite rough due to the formation of scale deposits. Furthermore, the inner wall of "standard" pipe is generally quite rough even when new. Since the average roughness of these surfaces is large enough to penetrate through the laminar sublayer, it is worthwhile to develop relationships similar to equations (9.261), (9.262), and (9.263) which will be valid for "rough" tubes. To do this we must formulate a method for determining the degree of roughness of the inner tube wall. The average height of the roughness projections is denoted by k_s, while the radius of the tube is taken to be the average distance from the tube centerline to the inner wall. Therefore, the relative roughness of the tube wall is given by k_s/R. In deriving a general expression for the velocity distribution in rough tubes, Prandtl proposed that the dimensionless distance from the wall y^+ be replaced by the relative roughness y/k_s.

Following this suggestion, in 1933 Johann Nikuradse (1894 - 1979), another student of Prandtl, performed an elaborate set of experiments in which he glued grains of sand, sifted according to size which he denoted by k_s, to the inner walls of otherwise smooth tubes. Nikuradse found from his data that for values of the relative roughness in the range $15 \le R/k_s \le 507$, the velocity profile for large values of the Reynolds number can be written

$$\frac{\vartheta_x}{\vartheta^*} = 2.5 \ln \frac{y}{k_s} + 8.5 \tag{9.269}$$

Computing the average velocity by integrating this profile over the cross-sectional area of the tube, Nikuradse obtained

$$\frac{\vartheta_{ave}}{\vartheta^*} = 2.5 \ln \frac{R}{k_s} + 4.75 \tag{9.270}$$

Von Karman then substituted this result into the combined equations (9.233) and (9.248). Then

$$\frac{1}{\sqrt{f}} = 2.03 \log_{10} \frac{R}{k_s} + 1.68 \tag{9.271}$$

Following this example, Nikuradse found that his friction factor data could be best correlated by

$$f = \left[2.0 \log_{10} \left(\frac{R}{k_s} \right) + 1.74 \right]^{-2} \tag{9.272}$$

This correlation holds only in the "fully rough" regime at large values of the Reynolds number in excess of the value for which

$$Re_{D_h} = \frac{200}{\frac{k_s}{D_h}\sqrt{f}} \tag{9.273}$$

Notice that in the "fully rough" regime, the friction factor is independent of the Reynolds number.

Between the "fully rough" regime bound by equation (9.273) and the laminar flow regime bound by equation (9.141) there is the "transition" regime. For this regime, in 1939 Colebrook combined equation (9.272) and equation (9.261) into a single expression that is the accepted correlation for friction factors for turbulent flow in circular conduits using D and non-circular conduits using D_h. The resulting transcendental equation,

$$\frac{1}{\sqrt{f}} = -2.0\log_{10}\left(\frac{k_s}{3.7D_h} + \frac{2.51}{Re_{D_h}\sqrt{f}}\right) \tag{9.274}$$

proved to be rather inconvenient to use at the time. To help simplify the design process, in 1944 Lewis Ferry Moody (1880 - 1953) plotted the correlations for all three regimes (laminar, fully rough, and transition) on a single graph of friction factor, f, versus Reynolds number, Re_D. This graph has come to be known as the "Moody Diagram" or the "Moody Chart" in honor of its author. Prior to the advent of programmable calculators and personal computers, this was a very important tool for the thermal-fluids engineer in the design of fluid piping systems. Figure 9.30 is the most common form of the Moody Diagram and is presented here more for its historical interest than for its utility since the computational power of computers now facilitates the use of the correlation equation itself.

More recently, Zigrang and Sylvester[5] proposed an explicit correlation of friction factor data that covers all regimes and lends itself more readily to design of turbulent flow systems than the Moody Diagram, viz.

$$f = \left\{-2.0\log_{10}\left[\frac{\left(k_s/D\right)}{3.7} - \frac{4.518}{Re_{D_h}}\log_{10}\left(\left[\frac{\left(k_s/D\right)}{3.7}\right]^{1.11} + \frac{6.9}{Re_{D_h}}\right)\right]\right\}^{-2} \tag{9.275}$$

In order to use the various correlations of friction factor data or the Moody Diagram for thermal-fluids design, it is necessary to have information regarding the equivalent sand grain roughness k_s of conduits fabricated from various materials by various means. Table 9.5 is just such a compilation of data from various sources. The data of Table 9.5, together with the correlations of equations (9.272) and (9.275), can be used most effectively if we make use of Nikuradse's definition of the dimensionless sand grain size k_s^+.

$$k_s^+ = \frac{\vartheta_{ave} k_s}{\nu}\sqrt{\frac{f}{8}} \tag{9.276}$$

The data for the friction factor f can then be classified according to the value of k_s^+:

$$\begin{aligned} &0 < k_s^+ \le 5 && \text{hydraulically smooth} \\ &5 < k_s^+ < 60 && \text{transitionally rough} \\ &60 < k_s^+ && \text{fully rough, } f \text{ independent of } Re_{D_h} \end{aligned} \tag{9.277}$$

The only problem with using this classification is that the friction factor and the average velocity appear as parameters, and they are often the information we seek.

---

[5] Zigrang, D. J. and Sylvester, N. D., "A Review of Explicit Friction Factor Equations," *Trans. ASME, J. of Energy Resources Technology*, 107, 280-283 (1985).

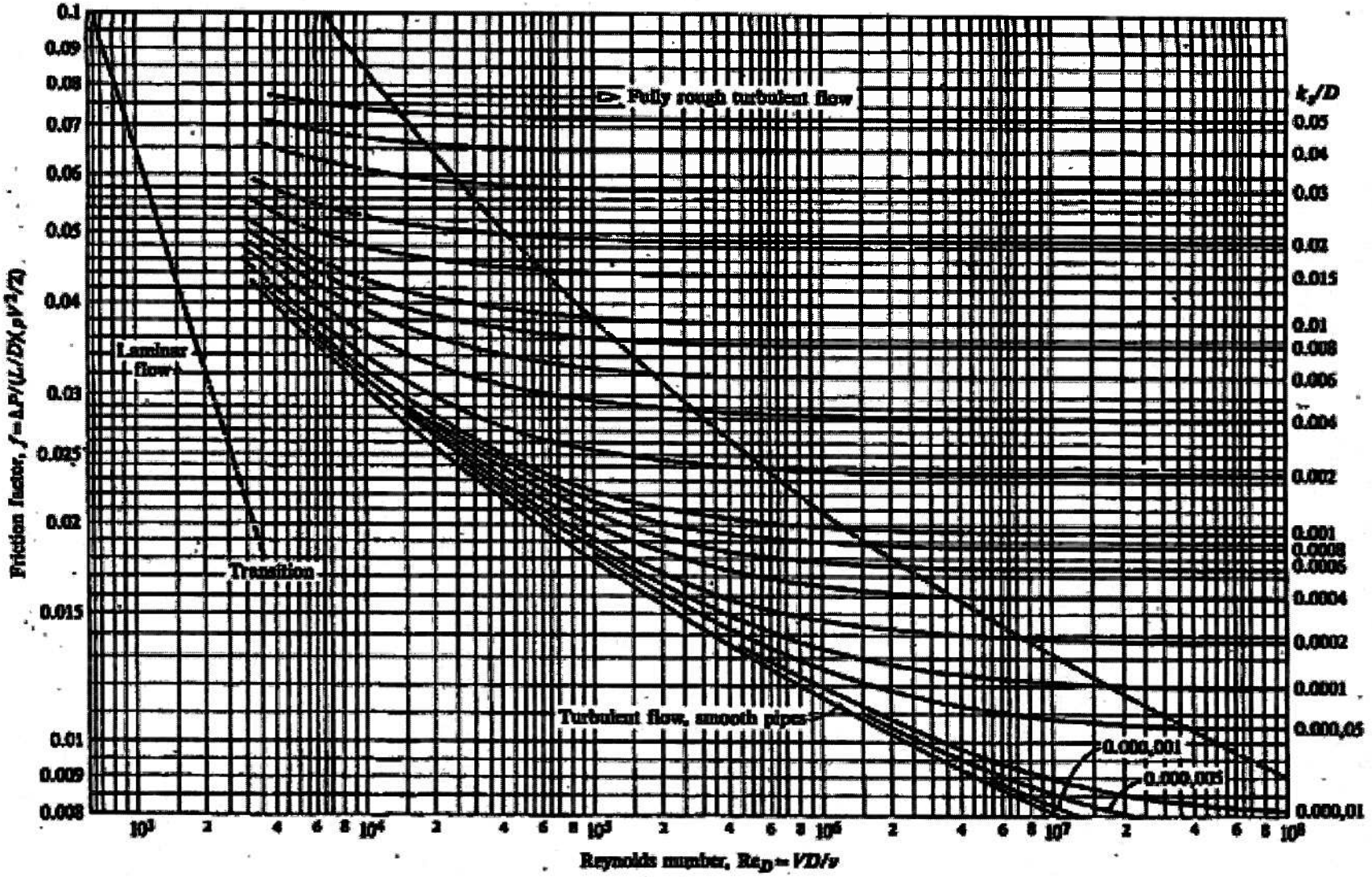

Figure 9.30 Friction Factors for Flow in Circular and Non-circular Conduits
[from Moody, L. F., "Friction Factors for Pipe Flow," *Trans. ASME*, 66, 671-684 (1944)]

Table 9.5 Roughness, k_s, of Various Pipe Configurations

Pipe Configuration	k_s (mm)
Asphalt coated cast iron	0.12
Bituminous lined cast iron	0.0025
Brass	0.0015
Cast iron	0.25
Cement lined cast iron	0.0025
Cement-asbestos	0.3-3
Centrifugally spun cast iron	0.0031
Clay	0.3-3
Commercial steel	0.046
Concrete	0.3-3
Copper	0.0015
Corrugated steel	0.9-9
Drawn tubing	0.0015
Galvanized surface	0.06-0.25
Glass	0.0015
Lead	0.0015
Plastic	0.0015
PVC	Smooth
Riveted steel	0.9-9
Sewer brick	0.3-3
Tin	0.0015
Wood stave	0.18-0.9
Wrought iron	0.046

Source: Johnson, R. W.(editor), *The Handbook of Fluid Dynamics*, CRC Press, Boca Raton, 1998, p. 5-67.

Example 9E.11: As shown in Figure 9E.11, very large cistern is filled with water of density $\rho = 10^3$ kg/m^3 to a depth of $h = 10$ m. Because the water level in the cistern is maintained at a constant level by a well, the water flows from the cistern at a constant rate through a commercial steel pipe of circular cross-section with a diameter of $D = 2.5$ cm and a length of $L =$ 100 m.

(a) Estimate the volumetric flow rate of water from the cistern by modeling the fluid as inviscid.

(b) Estimate the volumetric flow rate of water from the cistern by modeling the fluid as a viscous fluid with a viscosity of $\mu = 8.67 \times 10^{-4}$ kg/m sec.

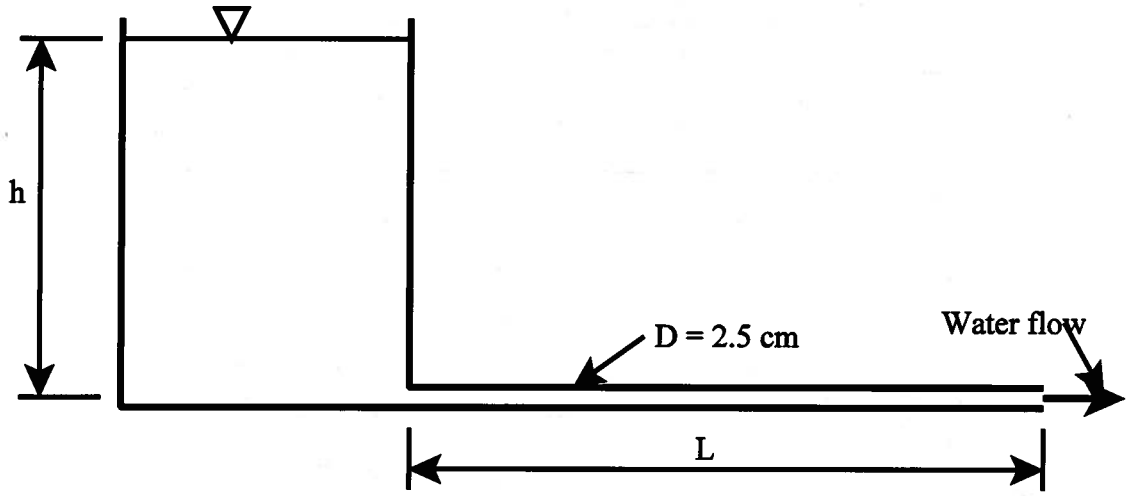

Figure 9E.11

Solution: (a) We begin the solution by assuming that the flow in the discharge pipe is inviscid flow, but we recognize that this is the simplest of all approximations for this flow. This approximation does provide a convenient starting place, however, for more complex models. Consider a streamline that runs from the free surface to the discharge of the pipe. The Bernoulli equation for this streamline is given by

$$\frac{P_1}{\rho}+\frac{\vartheta_1^2}{2}+gz_1=\frac{P_2}{\rho}+\frac{\vartheta_2^2}{2}+gz_2$$

Since $\vartheta_1 = 0$ and $P_1 = P_2 = P_{atm}$, we can write

$$\frac{\vartheta_2^2}{2}=g\left(z_1-z_2\right)=gh$$

$$\vartheta_2=\sqrt{2gh}=\sqrt{2\left(9.81\ \text{m/sec}^2\right)(10\ \text{m})}=14.07\ \text{m/sec}$$

Then the volumetric flow rate for this inviscid fluid model becomes

$$\dot{V}=A_c\vartheta_2=\frac{\pi D^2}{4}\vartheta_2=\frac{\pi(0.025\text{m})^2}{4}(14.07\ \text{m/sec})=6.907\ \text{x}\ 10^{-3}\ \text{m}^3/\text{sec}$$

(b) If we now take viscosity into account, we can use the above calculation to estimate the Reynolds number of the flow.

$$Re_D=\frac{\vartheta D\rho}{\mu}=\frac{(14.07\ \text{m/sec})(0.025\ \text{m/sec})\left(10^3\ \text{kg/m}^3\right)}{8.67\ \text{x}\ 10^{-4}\ \text{kg/m sec}}=4.057\ \text{x}\ 10^5$$

Although we know that the effect of viscosity will be to reduce the velocity of flow considerably, the flow does appear from this estimate to be clearly turbulent. Then from equation (9.140), we have

$$\Delta P=\rho f\left(\frac{L}{D}\right)\left(\frac{\vartheta_{ave}^2}{2}\right)$$

$$\vartheta_{ave}=\sqrt{\left(\frac{\Delta P}{\rho}\right)\left(\frac{D}{L}\right)\left(\frac{2}{f}\right)}$$

The pressure of the water at the inlet to the pipe is given by simple hydrostatics. Then

$$\Delta P = (P_{atm} + \rho g h) - P_{atm} = \rho g h$$

$$\vartheta_{ave} = \sqrt{\left(\frac{\rho g h}{\rho}\right)\left(\frac{D}{L}\right)\left(\frac{2}{f}\right)} = \sqrt{(gh)\left(\frac{D}{L}\right)\left(\frac{2}{f}\right)}$$

We know all of these quantities except for the friction factor f. From Table 9.5, we have for commercial steel pipe, $k_s = 0.046$ mm. Then $k_s/D = (0.046 \text{ mm})/(25 \text{ mm}) = 1.84 \times 10^{-3}$. As a first approximation to f, we can assume that the flow is fully rough since this gives a value of f that is independent of the Reynolds number which we do not yet know. From equation (9.272) we have

$$f = \left[2.0 \log_{10}\left(\frac{R}{k_s}\right) + 1.74\right]^{-2}$$

$$f = \left[2.0 \log_{10}\left(\frac{2}{1.84 \times 10^{-3}}\right) + 1.74\right]^{-2} = 0.0164$$

Then

$$\vartheta_{ave} = \sqrt{(9.81 \text{ m/sec}^2)(10 \text{ m})\left(\frac{0.025 \text{ m}}{100 \text{ m}}\right)\left(\frac{2}{0.0164}\right)} = 1.73 \text{ m/sec}$$

and

$$Re_D = \frac{\rho \vartheta_{ave} D}{\mu} = \frac{(10^3 \text{ kg/m}^3)(1.73 \text{ m/sec})(0.025 \text{ m})}{8.67 \times 10^{-4} \text{ kg/m sec}} = 4.987 \times 10^4$$

Based on the new value for the velocity, the flow is still clearly turbulent. The question now is whether it is "fully-rough" as we had assumed. From equation (9.273), the boundary between transition flow and "fully-rough" is

$$Re_D = \frac{200}{\sqrt{f}\left(k_s/D\right)} = \frac{200}{(0.0164)\left(1.84 \times 10^{-3}\right)} = 6.628 \times 10^6$$

Since the Reynolds number is well below this value, we are in the transition region for which equation (9.272) does not hold. Then

$$f = \left\{-2.0 \log_{10}\left[\frac{\left(k_s/D\right)}{3.7} - \frac{4.518}{Re_{D_h}} \log_{10}\left(\left[\frac{\left(k_s/D\right)}{3.7}\right]^{1.11} + \frac{6.9}{Re_{D_h}}\right)\right]\right\}^{-2}$$

$$f = \left\{-2.0 \log_{10}\left[\frac{\left(1.84 \times 10^{-3}\right)}{3.7} - \frac{4.518}{4.987 \times 10^4} \log_{10}\left(\left[\frac{\left(1.84 \times 10^{-3}\right)}{3.7}\right]^{1.11} + \frac{6.9}{4.987 \times 10^4}\right)\right]\right\}^{-2}$$

$$f = 0.02616$$

Since this new value of the friction factor is considerably greater than the value of $f = 0.0164$ that we computed above, we must re-calculate the average velocity. Thus

$$\vartheta_{ave} = \sqrt{(9.81 \text{ m/sec}^2)(10 \text{ m})\left(\frac{0.025 \text{ m}}{100 \text{ m}}\right)\left(\frac{2}{0.02616}\right)} = 1.37 \text{ m/sec}$$

and with this value of the velocity, the Reynolds number becomes

$$Re_D = \frac{\vartheta_{ave} D \rho}{\mu} = \frac{(1.37 \text{ m/sec})(0.025 \text{ m})(10^3 \text{ kg/m}^3)}{8.67 \text{ x } 10^{-4} \text{ kg/m sec}} = 3.949 \text{ x } 10^4$$

Then the new value for the friction factor becomes

$$f = \left\{ -2.0 \log_{10} \left[\frac{(1.84 \text{ x } 10^{-3})}{3.7} - \frac{4.518}{3.949 \text{ x } 10^4} \log_{10} \left(\left[\frac{(1.84 \text{ x } 10^{-3})}{3.7} \right]^{1.11} + \frac{6.9}{3.949 \text{ x } 10^4} \right) \right] \right\}^{-2}$$

$$f = 0.02684$$

Then the new value of the velocity becomes

$$\vartheta_{ave} = \sqrt{(9.81 \text{ m/sec}^2)(10 \text{ m}) \left(\frac{0.025 \text{ m}}{100 \text{ m}} \right) \left(\frac{2}{0.02684} \right)} = 1.35 \text{ m/sec}$$

and the process has converged. Then the volumetric flow rate becomes

$$\dot{V} = A_c \vartheta_{ave} = \frac{\pi D^2}{4} \vartheta_{ave} = \frac{\pi (0.025 \text{ m})^2}{4} (1.35 \text{ m/sec}) = 6.636 \text{ x } 10^{-4} \text{ m}^3/\text{sec}$$

Thus, by neglecting the viscosity, we obtain a volumetric flow rate that is approximately an order of magnitude greater than the estimate that takes the fluid viscosity into account. Notice also that the turbulent viscous flow analysis requires a trial and error solution that does converge after two trials.

9.10.2.3 Velocity Profile Power Law: Let us return for a moment to equation (9.248). If we now substitute into that expression the result from equation (9.262), we get

$$\tau_w = \frac{0.316}{8} \frac{\rho \vartheta_{ave}^{\ 2}}{Re_D^{1/4}} = 0.0395 \rho \vartheta_{ave}^{7/4} \nu^{1/4} D^{-1/4} \tag{9.278}$$

From equation (9.278), it is apparent that the flow resistance in turbulent flow is proportional to the 1.75 power of the velocity as Hagen's data in 1854 suggested for large values of the flow velocity (large values of the Reynolds number). (See Section 9.9.1.5 and Figure 9.8.) If we substitute equation (9.239) into equation (9.278) and rearrange the terms, we get

$$\left(\frac{\vartheta_{ave}}{\vartheta^*} \right)^{7/4} = \frac{1}{0.0395} \left(\frac{\vartheta^* D}{\nu} \right)^{1/4}$$

$$\frac{\vartheta_{ave}}{\vartheta^*} = 6.3379 \left(\frac{\vartheta^* D}{\nu} \right)^{1/7} \tag{9.279}$$

Equation (9.279) is the first appearance of any kind of a power law for the velocity profile in turbulent flow. Using a power law such as equation (9.279), it can be shown that over a reasonable range of exponents n the mean bulk velocity ϑ_{ave} is approximately 80 percent of the maximum velocity in the tube ϑ_{max}. Then

$$\vartheta_{ave} \approx 0.80 \vartheta_{max} \tag{9.280}$$

Then substituting equation (9.280) into equation (9.279), we get

$$\frac{\vartheta_{max}}{\vartheta^*} = 7.924 \left(\frac{\vartheta^* D}{\nu} \right)^{1/7} = 8.747 \left(\frac{\vartheta^* R}{\nu} \right)^{1/7} \tag{9.281}$$

We now assume that equation (9.281) is valid for any distance y, from the tube wall, not just for the tube centerline where $y = R$. Then equation (9.281) assumes the form

$$\frac{\vartheta_x}{\vartheta^*} = 8.747\left(\frac{\vartheta^* y}{\nu}\right)^{1/7} \tag{9.282}$$

Thus we have succeeded in deriving the *power velocity profile law* from the Blasius friction formula [cf. Equation (9.262)]. Since the Blasius formula is valid only over a limited range of Reynolds numbers, we would expect the 1/7- power velocity distribution law to be similarly restricted.

Encouraged by the result of equation (9.282), Nikuradse conducted an extensive experimental study of the velocity profiles in smooth pipes over a much larger range of Reynolds numbers ($4 \times 10^3 \le Re_D \le 3.2 \times 10^6$) than those that define the limits of the Blasius formula. He found that the results could be correlated by means of the empirical relation

$$\frac{\vartheta_x}{\vartheta_{max}} = \left(\frac{y}{R}\right)^{1/n} = \left(1 - \frac{r}{R}\right)^{1/n} \tag{9.283}$$

where the value of n in the exponent was a function of the Reynolds number. At the lowest value of Reynolds number studied, $n = 6$ and at the highest value of Reynolds number $n = 10$. Although the power velocity profile law is provides a convenient closed form description of the velocity profile for turbulent flow in a pipe, it does have its physical limitations. It predicts infinite velocity gradient at the pipe wall and, hence, cannot be used to evaluate the wall shear stress. Furthermore, it does not produce zero slope at the centerline of the pipe, so it fails to show symmetry about the centerline. Nevertheless, the power velocity profile law does have some utility.

Recalling that the average velocity for flow in a pipe of radius R is defined as

$$\vartheta_{ave} = \frac{\int_0^R \rho \vartheta_x 2\pi r dr}{\rho \pi R^2} \tag{9.284}$$

we can use the empirical velocity profile of equation (9.283) to show that in turbulent flow

$$\frac{\vartheta_{ave}}{\vartheta_{max}} = \frac{2n^2}{(n+1)(2n+1)} \tag{9.285}$$

Table 9.6 shows that as the value of n increases, the ratio of the average velocity to the maximum velocity approaches one. Thus, we conclude that as the Reynolds number of the flow increases, the velocity profile becomes "flatter." Although it applies only to flows at Reynolds numbers of approximately $Re_D = 10^5$, the value $n = 7$ is commonly used as a representative value in equation (9.285).

Table 9.6 Ratio of Average Velocity to Mean Velocity for Turbulent Flow in a Pipe

n	6	7	8	9	10
$\vartheta_{ave}/\vartheta_{max}$	0.791	0.817	0.837	0.852	0.865

9.10.2.4 Turbulent Flow in the Entry Region of a Circular Conduit: Example 9E.11 has not really addressed the issue of the development of the turbulent velocity profile in the entry

region of the conduit. As we saw in the case of laminar flow, there is an entry region for each of these internal flows in which the influence of the viscosity makes itself known across the cross-section of the conduit. Over the distance of the entry length, the boundary layer that forms on the wall at the entrance grows until the boundary layer completely fills the conduit. For the case of turbulent flow, the boundary layer grows more rapidly than in the laminar flow case and the entry length is much shorter.

For the case of turbulent flow in fully-rough circular conduits, Zhiqing[6] combined equations (9.281) and (9.282) to form a power law for the velocity profile in the entry region. He proposed a simple velocity profile in the form

$$\frac{\vartheta_x}{\vartheta_{max}} = \begin{cases} \left(\frac{y}{\delta}\right)^{1/7} & \text{for } 0 \le y \le \delta \\ 1 & \text{for } \delta \le y \le R \end{cases} \tag{9.286}$$

$$\frac{\vartheta_{ave}}{\vartheta_{max}} = 1 - \frac{1}{4}\left(\frac{\delta}{R}\right) + \frac{1}{15}\left(\frac{\delta}{R}\right)^2 \tag{9.287}$$

where δ is the boundary layer thickness which varies with the axial coordinate x according to

$$\frac{x}{D_h Re_{D_h}^{1/4}} = 1.4309\left(\frac{\delta}{R}\right)^{5/4}\left[1 + 0.1577\left(\frac{\delta}{R}\right) - 0.1793\left(\frac{\delta}{R}\right)^2 - 0.0168\left(\frac{\delta}{R}\right)^3 + 0.0064\left(\frac{\delta}{R}\right)^4\right] \tag{9.288}$$

The dimensionless pressure drop defined in equation (9.114) then becomes

$$\left(\Delta P^*\right)_{entry} = \left(\frac{\vartheta_{max}}{\vartheta_{ave}}\right)^2 - 1 \tag{9.289}$$

The hydrodynamic entry length for turbulent flow in a fully-rough circular conduit is then given by

$$\left(\frac{L_{entry}}{D_h}\right)_{turbulent} = 1.359 Re_{D_h}^{1/4} \tag{9.290}$$

By way of comparison, consider two flows in a circular conduit with a Reynolds number of 2300. One of the flows enters a smooth conduit in a laminar fashion while the other enters a fully-rough conduit in a fully-developed turbulent state. In the laminar case, according to equation (9.149), the flow requires approximately 128.8 diameters to become fully-developed Hagen-Poiseuille flow with a parabolic velocity profile while in the turbulent case, according to equation (9.290), the flow requires only 9.4 diameters to become fully-developed turbulent flow with a velocity profile given by equation (9.286). This is clear evidence of the enhanced momentum transport that results from the eddy diffusivity.

9.10.3 Piping Systems

In complex thermal-fluid systems, the working fluid is usually transferred from one system component to another through a piping system consisting of lengths of pipe and various fittings such as elbows, tees, unions, and valves that join these lengths of pipe together. Usually, but not always, the flow in these piping systems is turbulent flow, and these piping systems represent one of the most common applications of the concepts presented in the previous section. In all piping systems, in order to maintain steady flow of the working fluid, it is necessary to provide sufficient flow work transfer in order overcome the viscous dissipation that occurs in the

---

[6] Zhiqing, W., "Study on Correction Coefficients of Laminar and Turbulent Entrance Region Effects in Round Pipe," *Appl. Math. Mech.*, (3/3): 433-446, 1982

various elements of the piping system. This is usually accomplished by means of some sort of pumping apparatus, and in the design of these systems, it is the responsibility of the thermal-fluids engineer to specify the requirements that must be met by this device. In the present section, we shall describe the methods by which the thermal-fluids engineer can determine these requirements.

9.10.3.1 Total Head Loss: Consider the case of a circular conduit of varying cross-section oriented as shown in Figure 9.31. Let us apply the first law of thermodynamics in the form of equation (8.34) to the control volume shown in Figure 9.31.

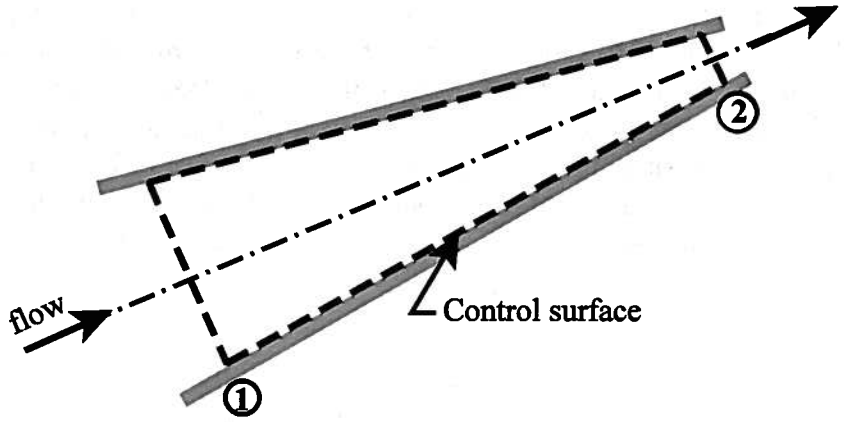

Figure 9.31 Flow in a Circular Conduit of Varying Cross-section

According to equation (8.34), we have

$$\frac{d}{dt}\int_{CV}\rho\left(u+\frac{\vartheta^2}{2}+gz\right)dV=\dot{Q}-\dot{W}_{shear}-\int_{CS}\rho\left(u+\frac{P}{\rho}+\frac{\vartheta^2}{2}+gz\right)\left(\vec{\vartheta}\cdot\vec{n}\right)dA \tag{9.291}$$

In the present case we are interested in steady, adiabatic flow of an incompressible fluid. Through the action of viscosity, there is a shear stress exerted on the lateral surface of the control volume, but since the mass points at this location are not in motion, $\dot{W}_{shear}=0$. Then equation (9.291) becomes

$$\cancel{\frac{d}{dt}\int_{CV}\rho\left(u+\frac{\vartheta^2}{2}+gz\right)dV}=\cancel{\dot{Q}}-\cancel{\dot{W}_{shear}}-\int_{CS}\rho\left(u+\frac{P}{\rho}+\frac{\vartheta^2}{2}+gz\right)\left(\vec{\vartheta}\cdot\vec{n}\right)dA$$

$$\int_{A_2}\rho\vartheta\left(u+\frac{P}{\rho}+\frac{\vartheta^2}{2}+gz\right)dA-\int_{A_1}\rho\vartheta\left(u+\frac{P}{\rho}+\frac{\vartheta^2}{2}+gz\right)dA=0$$

$$\dot{m}\left(u_2-u_1\right)+\dot{m}\left(\frac{P_2}{\rho}-\frac{P_1}{\rho}\right)+\dot{m}g\left(z_2-z_1\right)+\int_{A_2}\rho\vartheta_2\frac{\vartheta_2^2}{2}dA-\int_{A_1}\rho\vartheta_1\frac{\vartheta_1^2}{2}dA=0 \tag{9.292}$$

Then

$$\dot{m}\left(\frac{P_1}{\rho}-\frac{P_2}{\rho}\right)+\dot{m}g\left(z_1-z_2\right)+\int_{A_2}\rho\vartheta_1\frac{\vartheta_1^2}{2}dA-\int_{A_1}\rho\vartheta_2\frac{\vartheta_2^2}{2}dA=\dot{m}\left(u_2-u_1\right) \tag{9.293}$$

The left-hand side of equation (9.293) is the sum of the rate of flow work transfer (the first term) and the net rate of change of gravitational potential energy and the net rate of change of the kinetic energy of the flow. The right-hand side of equation (9.293) is the rate of increase of stored thermal energy of the flow as a consequence of the viscous dissipation in the control volume. If the flow could be modeled as inviscid and, hence, reversible, the right-hand side of equation (9.293) would vanish. In reality, this is not the case so the right-hand side of equation (9.293) represents the rate at which energy must be supplied to the flow (per unit mass flow rate) by the pumping device in order to maintain steady flow conditions.

For historical reasons that originated with the earliest days of the design of municipal water supply systems, the left-hand side of equation (9.293) is known as the total head loss of the flow denoted by the symbol $h_{l,total}$. It is the quantity that must be determined in order to specify the pumping requirements. In evaluating the head loss, the kinetic energy terms are somewhat more troublesome than the other terms in that the velocity of the fluid at the port varies over the port area. This means that the integral for the kinetic energy term must be evaluated in each case. It would be considerably more convenient if we could use the average velocity instead. This can be accomplished by introducing the *kinetic energy coefficient*, α, defined as

$$\int_A \rho v_x \frac{v_x^2}{2} dA = \alpha \dot{m} \frac{v_{ave}^2}{2}$$

$$\alpha = \frac{\int_A \rho v_x^3 dA}{\dot{m} v_{ave}^2} \tag{9.294}$$

For the laminar flow case, we can use equation (9.133) for the velocity profile. Then

$$\alpha = \frac{\int_0^R \rho \left[2v_{ave}\left(1-\frac{r^2}{R^2}\right)\right]^3 2\pi r dr}{\left(\rho v_{ave}\pi R^2\right) v_{ave}^2} = \frac{16}{R^2}\int_0^R \left(1-\frac{r^2}{R^2}\right)^3 r dr = 2 \tag{9.292}$$

where R is the radius of the conduit. For the turbulent flow case, we can use equation (9.283).

$$\alpha = \frac{\int_0^R \rho \left[v_{max}\left(1-\frac{r}{R}\right)^{1/n}\right]^3 2\pi r dr}{\left(\rho v_{ave}\pi R^2\right) v_{ave}^2} = \left(\frac{v_{max}}{v_{ave}}\right)^3 \frac{2n^2}{(3+n)(3+2n)} \tag{9.293}$$

Table 9.7 shows the values of α for the typical values of n. Recall that n is a function of Reynolds number so α, too, is a function of Reynolds number. However, we observe from Table 9.7 that the dependence of α on n, and by inference on Reynolds number, is rather weak. Moreover, the values of α are only slightly greater than one so that in the case of turbulent flow, α can be taken to be unity with minimal error, particularly in light of the fact that the kinetic energy terms in the expression for total head loss are small compared to the flow work transfer term.

Table 9.7 Dependence of the Kinetic Energy Coefficient on the Value of n

n	6	7	8	9	10
α	1.077	1.058	1.046	1.037	1.031

Then the expression for the total head loss becomes

$$h_{l,total} = \left(\frac{P_1}{\rho} + \alpha_1 \frac{(\vartheta_{ave})_1^2}{2} + gz_1 \right) - \left(\frac{P_2}{\rho} + \alpha_2 \frac{(\vartheta_{ave})_2^2}{2} + gz_2 \right) \tag{9.294}$$

Thus the task of determining the pumping requirements for a piping system becomes one of evaluating equation (9.294). To aid in this process, the total head loss can be rewritten in a slightly different, but equivalent form.

$$h_{l,total} = \left(\frac{P_1}{\rho} - \frac{P_2}{\rho} \right) + \left(\alpha_1 \frac{(\vartheta_{ave})_1^2}{2} - \alpha_2 \frac{(\vartheta_{ave})_2^2}{2} \right) + (gz_1 - gz_2) \tag{9.295}$$

For a unit mass flow rate, the terms on the right-hand side of equation (9.295) represent respectively, the flow work transfer, the change in kinetic energy, and the change in gravitational potential energy of the flow. Of these, the flow work transfer, which embodies the viscous dissipation, typically dominates.

The total head loss is typically divided into two components, one due to the effects of viscous dissipation in the lengths of pipe of constant cross-sectional area in the piping system, the other due to viscous dissipation in the fittings and valves in the system. Since piping systems commonly have extremely long lengths of piping in total (a total length of kilometers is not unusual), this component of the head loss can be quite large so it is referred to as the major head loss, denoted by the symbol $h_{l,major}$. The other component due to the fittings and valves is usually the smaller of the two so it is referred to as the minor head loss, denoted by the symbol $h_{l,minor}$ with a minor head loss contribution from each fitting and valve. Then the total head loss for a piping system with N fittings and valves is given by

$$h_{l,total} = h_{l,major} + \sum_i^N (h_{l,minor})_i = \left(\frac{P_1}{\rho} - \frac{P_2}{\rho} \right) + \left(\alpha_1 \frac{(\vartheta_{ave})_1^2}{2} - \alpha_2 \frac{(\vartheta_{ave})_2^2}{2} \right) + (gz_1 - gz_2) \tag{9.296}$$

We now determine the form for each of the two head loss terms.

9.10.3.2 Major Head Loss: To determine the form for the major head loss term, we consider a special case for which we know the head loss. In particular, consider the case of fully developed turbulent flow of an incompressible fluid in a horizontal conduit of constant cross-sectional area. For this flow configuration, $\alpha_1 = \alpha_2 \approx 1$ and the second term on the right-hand side of equation (9.296) vanishes since the average velocity remains unchanged. Furthermore, for a horizontal conduit, the third term also vanishes. Then for a pipe of diameter D and length L carrying a flow with an average velocity ϑ_{ave}, only the pressure terms remain and the major head loss can be calculated with the aid of equation (9.140), viz.

$$h_{l,major} = \left(\frac{P_1}{\rho} - \frac{P_2}{\rho} \right)_{piping} = f \left(\frac{L}{D} \right) \left(\frac{\vartheta_{ave}^2}{2} \right) \tag{9.297}$$

where the friction factor must be determined from the Reynolds number of the flow. For laminar flow in a conduit of circular with $Re_D \leq 2100$, the friction factor is given by equation (9.141), viz.

$$f = \frac{64}{Re_D} \tag{9.298}$$

For laminar flow in conduits of non-circular cross-section, the hydraulic diameter must be used in evaluating the Reynolds number and the friction factor can then be determined from Table 9.3.

For turbulent flow in smooth pipes of either circular or non-circular cross-section, the friction factor can be determined from equation (9.263), viz.

$$f = (0.790 \ln Re_D - 1.64)^{-2} \tag{9.299}$$

with the hydraulic diameter used in the evaluation of the Reynolds number.
For rough pipes, the friction factor can be determined from equation (9.275) and the data of Table 9.5, viz.

$$f = \left\{ -2.0 \log_{10} \left[\frac{(k_s/D)}{3.7} - \frac{4.518}{Re_{D_h}} \log_{10} \left(\left[\frac{(k_s/D)}{3.7} \right]^{1.11} + \frac{6.9}{Re_{D_h}} \right) \right] \right\}^{-2} \tag{9.300}$$

9.10.3.3 Minor Head Loss: For the minor head loss, the necessary information, with a few exceptions, is usually provided by the manufacturer of the component of interest. There are two methods of reporting the data. In one approach, the minor head loss is taken to depend on the kinetic energy of the flow in a manner similar to the major head loss term, viz.

$$(h_{l,minor})_i = K_i \frac{\vartheta_{ave}^{\ 2}}{2} \tag{9.301}$$

where the value of K_i is specific to the component at hand. In the second approach, the minor head loss is evaluated by an expression more closely analogous to the one used in the evaluation of the major head loss with the relevant head loss data expressed in terms of equivalent lengths of straight pipe of the same diameter as the component, viz.

$$(h_{l,minor})_i = f \frac{(L_e)_i}{D} \frac{\vartheta_{ave}^{\ 2}}{2} \tag{9.302}$$

Equations (9.301) and (9.302) each have their advantages and disadvantages and are used with about equal frequency in thermal-fluids engineering practice. In this discussion, we shall use equation (9.301) simply because it provides a sharper contrast between the major and minor head loss terms.

In the following discussion, we present values of the head loss coefficient K_i for a select number of components under turbulent flow conditions. These data are a small sample of the information available in the thermal-fluids engineering literature and are drawn primarily from the comprehensive compilation by R. D. Blevins, *Applied Fluid Dynamics Handbook*, Krieger Publishing Co., Malabar, FL, 1992, Chapter 6. The list of components for which data are presented here includes pipe entrances, enlargements and contractions in pipe cross-sections, and standard fittings.

Pipe Entrances:

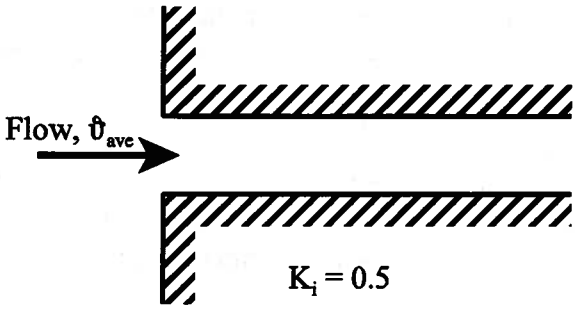

Figure 9.32a Minor Head Loss Coefficient for Square-Edged Entrance

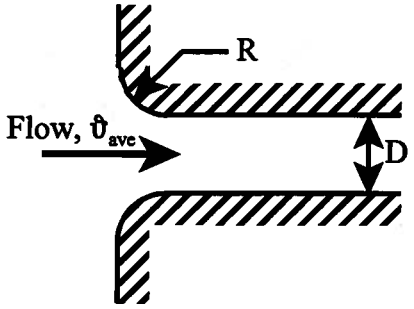

R/D	K_i
0.00	0.50
0.01	0.43
0.02	0.36
0.03	0.31
0.04	0.26
0.05	0.22
0.06	0.20
0.08	0.15
0.12	0.09
0.16	0.06
>0.16	0.03

Figure 9.32b Minor Head Loss Coefficient for Rounded Entrance

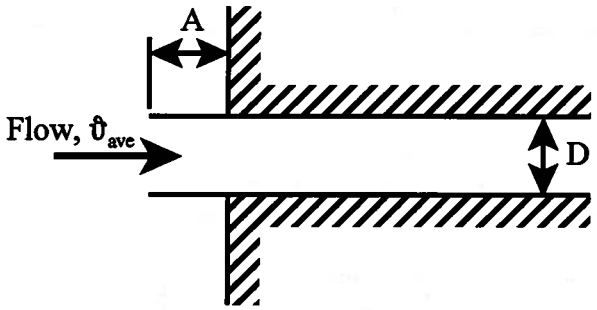

A/D	K_i
0.001	0.63
0.010	0.68
0.100	0.86
0.500	1.00
>0.500	1.00

Figure 9.32c Minor Head Loss Coefficient for Sharp-edged Re-entrant Entrance

Abrupt Enlargements and Contractions:

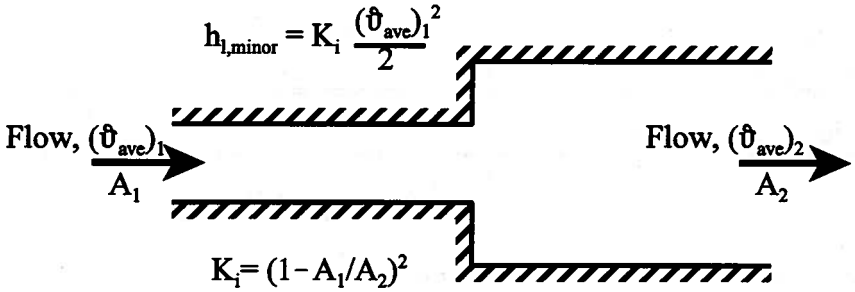

Figure 9.24a Minor Head Loss Coefficient for Abrupt Enlargement

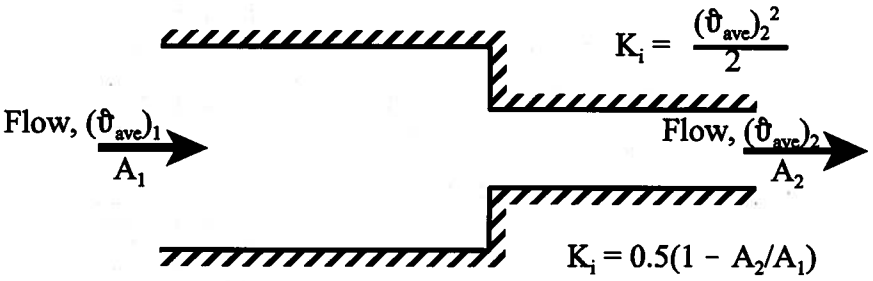

Figure 9.24b Minor Head Loss Coefficient for Abrupt Contraction

Table 9.8 Minor Head Loss Coefficients for Various Fittings and Valves

Valve or Fitting	Nominal Diameter of Fitting, cm					
	2.5	5.0	10	15	20	25
Globe valve, fully open						
Screwed	9	7	5.5			
Flanged	12	9	6	6	5.5	5.5
Gate valve, fully open						
Screwed	0.24	0.18	0.13			
Flanged		0.35	0.16	0.11	0.08	0.06
Foot valve, fully open	0.08 for all sizes					
Swing check valve, fully open						
Screwed	3.0	2.3	2.1			
Flanged	2.0 for all sizes					
Angle valve, fully open						
Screwed	4.5	2.1	1.0			
Flanged		2.4	2.1	2.1	2.1	2.1
Regular elbow, 90°						
Screwed	1.5	1.0	0.65			
Flanged	0.42	0.37	0.31	0.28	0.26	0.25
Long-radius elbow, 90°						
Screwed	0.75	0.4	0.25			
Flanged		0.3	0.22	0.18	0.15	0.14

Source: M. Kutz, *Mechanical Engineers Handbook*, John Wiley, New York, 1998, Table 40.10, p.1321.

Table 9.9 Dimensions for Steel Pipe (American National Standards Institute, ANSI B36.10)

Nominal Size	Pipe OD (in)	Schedule No.	Wall Thkness (in)	ID (in)	Flow Area (in^2)
1/4	0.540	40	0.088	0.364	0.104
		80	0.119	0.302	0.072
3/8	0.675	40	0.091	0.493	0.191
		80	0.126	0.423	0.141
1/2	0.840	40	0.109	0.622	0.304
		80	0.147	0.546	0.234
3/4	1.050	40	0.113	0.824	0.533
		80	0.154	0.742	0.432
1	1.315	40	0.133	1.049	0.864
		80	0.179	0.957	0.719
1-1/4	1.660	40	0.140	1.380	1.50
		80	0.191	1.278	1.28
1-1/2	1.900	40	0.145	1.610	2.04
		80	0.200	1.500	1.77
2	2.375	40	0.154	2.067	3.36
		80	0.218	1.939	2.95
2-1/2	2.875	40	0.203	2.469	4.79
		80	0.276	2.323	4.24
3	3.500	40	0.216	3.068	7.39
		80	0.300	2.900	6.60
4	4.50	40	0.237	4.026	12.73
		80	0.337	3.826	11.50
6	6.625	40	0.280	6.065	28.89
		80	0.432	5.761	26.07
8	8.625	30	0.277	8.071	51.16
		40	0.322	7.981	50.03
		80	0.500	7.625	45.66
10	10.75	30	0.307	10.136	80.69
		40	0.365	10.020	78.85
		XS	0.500	9.750	74.66
		80	0.593	9.564	71.84
12	12.75	30	0.330	12.090	114.8
		ST	0.375	12.000	113.1
		40	0.406	11.938	111.9
		XS	0.500	11.750	108.4
		80	0.687	11.376	71.84

Table 9.9 Notes: Nominal Pipe Sizes (NPS) 1/8 through 12 are known by their nominal diameters in inches. SI standards have not been established as of this writing. The nominal diameter does not indicate a true dimension. All sizes of pipe with NPS 1/8 through NPS 12 have a standardized outside diameter (OD) regardless of Schedule Number or weight. This OD was originally selected so that pipe with a standard wall thickness would have an inside diameter approximately equal to the nominal pipe size. As the Schedule Number or weight changes to accommodate higher working pressures, the wall thickness changes; however, wall thickness affects the inside diameter only. The thicker the wall, the smaller the inside diameter.

In the past, pipe was produced basically in three weights: standard (ST), extra strong (XS), and double extra strong (XXS). In recent years the American National Standards Institute (ANSI) assigned schedule numbers to classify wall thickness for different pressure applications. For NPS1/8 through NPS 10, Schedule 40 is identical with standard weight (ST) pipe. Schedule 80 is identical with extra strong (XS) pipe in nominal NPS 1/8 through NPS 8. Schedules 40 and 80 can vary greatly from standard (ST) and extra strong (XS) pipe in the larger diameters. See ANSI B 36.10.

Useful conversion factors for Table 9.8: To convert from inches to meters, multiply by 2.54×10^{-2}. To convert from $(inches)^2$ to $(meters)^2$ multiply by 6.456×10^{-4}.

In an attempt to establish some correspondence between SI units and the outdated engineering units, "diametre nominel" (DN) has been set as the metric equivalent of Nominal Pipe Sizes (NPS) according to Table 9.10.

Table 9.10 Metric Equivalents (DN) of Nominal Pipe Sizes (NPS)

NPS	⅛	¼	⅜	½	¾	1	1¼	1½	2	2½	3	4	6	8	10	12
DN	6	8	10	15	20	25	32	40	50	65	80	10	15	20	25	30

9.10.3.4 Analysis of Piping Systems: The application of equation (9.296) to a given piping system to determine the pumping requirements embodied in the total head loss is not as straightforward as it might seem on the surface. The difficulty lies in the fact that in a given physical situation, the data for the various head loss terms in equation (9.296) usually depend upon the Reynolds number of the flow, but the Reynolds number depends upon flow velocity which often is not known at the outset. Thus, the analysis of piping systems often requires an iterative procedure in which the thermal-fluids engineer must first guess at a trial solution and then iterate to find the true solution. In the analysis of piping systems there are four different possible situations that present themselves depending upon the information that is known at the outset. We now describe these four different scenarios and offer a plan for approaching each one.

1. *L, D, and $\dot{m}$ (or $\dot{V}$) are known but ΔP is unknown:* In this scenario, the layout of the piping system and the necessary flow rate have been proscribed by the physical configuration of the other systems being connected by the piping. The pump necessary to deliver the working fluid at the specified flow rate must be determined. The dimensions, both length and diameter, of the pipe required together with the fittings and valves necessary to accomplish the connections are known from the piping layout. The performance characteristics of the connecting systems specify the flow rate, either the mass flow rate or the volumetric flow rate. From this information, the flow velocity and the Reynolds number can be determined. Then the friction factor for the pipe and the minor head loss coefficients for the fittings and valves can be determined from the data presented above. Finally, the total head loss and, hence, the pumping requirements can be determined from equation (9.296).

2. *ΔP, $\dot{m}$ (or $\dot{V}$), and D are known but L is unknown:* This scenario is typical of the case in which one of the systems connected by the piping is to be relocated, and it is necessary to determine the length of the new piping configuration to aid in the siting of the component. From the flow rate and the diameter of the pipe, the flow velocity and, hence, the Reynolds number can be determined. From this result and the pressure drop for the configuration, the total head loss can be determined from equation (9.296) and the friction factor can be determined from the correlations. Then equation (9.297) can be solved for the new length of the piping.

3. *ΔP, L, and D are known but $\dot{m}$ (or $\dot{V}$) is unknown:* In this scenario, a pumping device and a piping system exist, and the objective is to determine whether this combination is adequate to meet the flow rate requirement of some other system connected to it. This situation is a bit more complicated than those previously considered since the flow rate and, hence, the flow velocity are unknown. Thus, the Reynolds number is unknown so the friction factor cannot be determined. Without the friction factor, the flow rate cannot be determined. Thus we are faced with making an educated guess at the final result that can then be iterated to obtain the true solution for the flow rate. Two approaches are available to make the "educated guess." In the first approach, the total head loss can be set to zero. Then equation (9.296) can be solved to find the

flow velocity in the absence of friction. This velocity can be used to calculate a Reynolds number that can be used in the appropriate friction factor correlation to obtain a friction factor that can, in turn, be used in equation (9.297) to obtain the new estimate of the major head loss. The new estimate of the minor head loss can be made with the frictionless estimate of the velocity. These estimates of the two head loss contributions can now be used in equation (9.296) to obtain a new estimate of the velocity. This new estimate of velocity that now includes frictional effects can be used to obtain a new estimate of the friction factor, and the whole calculation process can be repeated until the solution for the velocity converges, typically in two iterations. When convergence is obtained, the flow rate can be readily calculated.

In the second approach, the effect of friction can be assumed to be that of the "fully rough" frictional limit for which the friction factor is independent of the Reynolds number [cf. Equation (9.272)]. This estimate of friction factor can be used in equation (9.297) to estimate the velocity provided the minor head loss term is small and that the pressure drop is entirely due to pipe friction. This estimate of velocity can be used to determine a value for Reynolds number that can be used to estimate a new value for the friction factor. The calculation process is then repeated until convergence on the correct value of velocity results.

4. *ΔP, L, and $\dot{m}$ (or $\dot{V}$) are known but D is unknown:* In this scenario, a given pumping device is to be used to pump an incompressible fluid at a predetermined flow rate over a known distance. The diameter of pipe necessary to achieve this is to be determined. This case is similar to case 3 above in that an iterative solution is required because the flow velocity necessary to establish the Reynolds number is unknown. Begin the iterative solution by assuming frictionless flow with zero head loss. Then solve equation (9.296) to determine the flow velocity. Use this flow velocity and the flow rate to determine the "educated guess" at the diameter and the Reynolds number. This estimate of the diameter is the lower bound. Use this Reynolds number to determine the friction factor and then use this friction factor to determine the major head loss from equation (9.297). The minor head loss can be determined from the frictionless velocity and the data for the fittings and valves. Use these results in equation (9.296) to determine a new velocity and subsequently a new Reynolds number. Repeat the analysis as before. Convergence is rapid.

The following examples illustrate the application of the methods of analysis of piping systems.

Example 9E.12: An air impact wrench such as the ones used by NASCAR pit crews to remove the lug nuts from the wheels of race cars, requires a volumetric flow rate of $\dot{V} = 5.4$ CFM at a minimum supply pressure of $P_{supply} = 40$ psi ($\dot{V} = 2.5485 \times 10^{-3}$ m^3/sec at $P_{supply} = 3.77 \times 10^5$ N/m^2) at a temperature of 60 F (288.89 K). The air is supplied through a smooth walled hose with a nominal pipe size of NPS 3/8 and a length of 30 m. It is necessary to determine the pressure drop ΔP through this hose to insure that there is sufficient pressure at the tool for normal operation. The inlet pressure to the hose from the air compressor is P_{inlet}.

For air under these conditions $\mu = 2.0149 \times 10^{-5}$ kg/m sec and $R = 287$ J/kg K.

Solution: This is an example of case 1 above. Let us assume that the flow can be modeled as incompressible even though the working fluid is a gas. We will need to check this later. From Table 9.9 and the conversion factor given in the footnote, the flow area of this "pipe" is

$$A = 0.191 \text{ in}^2 = (0.191 \text{ in}^2)(6.456 \times 10^{-4} \text{ m}^2/\text{in}^2) = 1.2331 \times 10^{-4} \text{ m}^2.$$

Then from continuity, the velocity of flow is

$$\vartheta = \frac{\dot{V}}{A} = \frac{2.5485 \text{ x } 10^{-2} \text{ m}^3/\text{sec}}{1.2331 \text{ x } 10^{-4} \text{ m}^2} = 20.667 \text{ m/sec}$$

This is well below a Mach number of 0.3 since the speed of sound in air under these conditions is on the order of 350 m/sec. Thus we are justified in assuming that the flow can be modeled as incompressible. We need to calculate the density of the air before we can calculate the Reynolds number. Then

$$\rho = \frac{P}{RT} = \frac{3.7711 \text{ x } 10^5 \text{ N/m}^2}{(287 \text{ J/kg K})(288.89 \text{ K})} = 4.5484 \text{ kg/m}^3$$

$$Re = \frac{(20.667 \text{ m/sec})(1.2522 \text{ x } 10^{-2} \text{ m})(4.5484 \text{ kg/m}^3)}{2.0149 \text{ x } 10^{-5} \text{ kg/m sec}} = 58,419$$

For this value of Reynolds number for flow in a smooth tube, we can use equation (9.263) to calculate the friction factor, viz.

$$f = (0.790 \ln Re - 1.64)^{-2} = [0.790 \ln(58,419) - 1.64]^{-2} = 0.020231$$

Then from the Darcy-Weisbach Law

$$\Delta P = \rho f \left(\frac{L}{D}\right)\frac{\vartheta_{ave}^{\ 2}}{2} = (4.5484 \text{ kg/m}^3)(0.020)\left(\frac{30 \text{ m}}{1.2522 \text{ x } 10^{-2} \text{ m}}\right)\frac{(20.667 \text{ m/sec})^2}{2}$$

$$\Delta P = 4.7082 \text{ x } 10^4 \text{ N/m}^2$$

Since the discharge pressure from a typical compressor used to provide compressed air to power these tools is on the order of $P_{inlet} = 7.908 \text{ x } 10^5 \text{ N/m}^2$, this pressure drop is only about five percent of the available pressure. Thus a hose of 30 m in length is acceptable for this application.

Example 9E.13: For the tool described in Example 9E.12, determine the maximum length of compressed air hose L_{max} that could be used if the pressure at inlet to the hose is $P_{inlet} = 7.908 \text{ x } 10^5 \text{ N/m}^2$ and $P_{supply} = 3.77 \text{ x } 10^5 \text{ N/m}^2$ is the minimum pressure at the tool that will still permit the tool to operate.

Solution: This is an example of case 2 described above. The volume flow rate specified by the operational requirements of the tool, $\dot{V} = 2.5485 \text{ x } 10^{-3} \text{ m}^3/\text{sec}$, is the same as Example 9E.12. The pressure required at the tool is $P_{supply} = 3.77 \text{ x } 10^5 \text{ N/m}^2$. The inlet pressure to the hose is $P_{inlet} = 7.908 \text{ x } 10^5 \text{ N/m}^2$. Then the maximum allowable pressure drop is

$$\Delta P_{max} = P_{inlet} - P_{supply} = 7.908 \text{ x } 10^5 \text{ N/m}^2 - 3.771 \text{ x } 10^5 \text{ N/m}^2 = 4.137 \text{ x } 10^5 \text{ N/m}^2$$

Since the inside diameter of the hose is the same as Example 9E.12, the velocity and the Reynolds number are the same as those calculated in that example. Thus the friction factor is also the same. Then from the Darcy-Weisbach Law

$$L_{max} = \frac{2D\Delta P_{max}}{\rho f \vartheta_{ave}^{\ 2}} = \frac{2(1.2522 \text{ x } 10^{-2} \text{ m})(4.137 \text{ x } 10^5 \text{ N/m}^2)}{(4.5484 \text{ kg/m}^3)(0.020)(20.667 \text{ m/sec})^2} = 266.65 \text{ m}$$

Example 9E.14: A young child has an aquarium that holds 30 gallons of water. At 8.33 lbm/gal, the weight of the water alone is 250 lbm. Since the child herself weighs only 45 lbm, this tank is hardly something for her to lift when the water needs changing. To draw the dirty water out of the tank she uses a siphon with a geometry as shown in Figure 9E.14. We wish to estimate the maximum flow rate through the smooth-walled siphon tube (I.D. = 8 mm) for the geometry shown taking into account viscous effects. The water can be modeled as an incompressible fluid with a density $\rho = 1000 \text{ kg/m}^3$ and a viscosity of $\mu = 8.67 \text{ x } 10^{-4} \text{ kg/m sec}$. How does this flow rate estimate compare with that for the case in which viscosity is neglected?

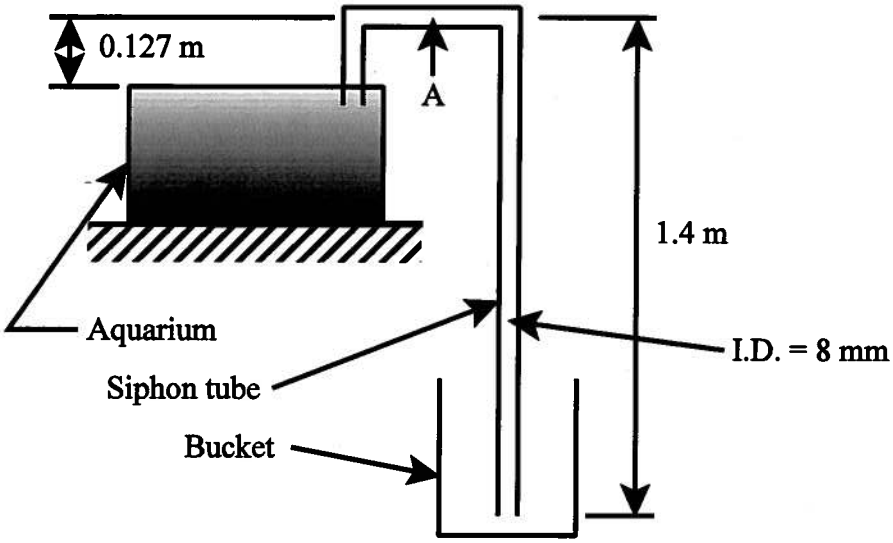

Figure 9E.14 Aquarium Siphon

Solution: The total head loss for this geometry is given by equation (9.296), viz.

$$h_{l,total} = h_{l,major} + \sum_{i}^{N}\left(h_{l,minor}\right)_i = \left(\frac{P_1}{\rho} - \frac{P_2}{\rho}\right) + \left(\alpha_1 \frac{(\vartheta_{ave})_1^2}{2} - \alpha_2 \frac{(\vartheta_{ave})_2^2}{2}\right) + (gz_1 - gz_2)$$

The major head loss is given by equation (9.297)

$$h_{l,major} = f\left(\frac{L}{D}\right)\left(\frac{\vartheta_{ave}^{\,2}}{2}\right)$$

and the minor head loss is given by

$$h_{l,minor} = K_1 \frac{\vartheta_{ave}^{\,2}}{2}$$

where K_1 is the head loss coefficient for the re-entrant entrance of the submerged inlet to the siphon tube. If we take location 1 to the free surface of the water in the aquarium, the inlet velocity is effectively zero, and if we also assume turbulent flow (to be checked later), $\alpha_2 = 1$, the total head loss becomes

$$f\left(\frac{L}{D}\right)\frac{\vartheta_{ave}^{\,2}}{2} + K_1\frac{\vartheta_{ave}^{\,2}}{2} + \frac{\vartheta_{ave}^{\,2}}{2} = \left(\frac{P_1}{\rho} - \frac{P_2}{\rho}\right) + g\left(z_1 - z_2\right)$$

But $P_1 = P_2 = P_{atm}$. Then

$$g\left(z_1 - z_2\right) = \left[f\left(\frac{L}{D}\right) + K_1 + 1\right]\frac{\vartheta_{ave}^{\,2}}{2}$$

If we assume that the siphon tube is submerged to a depth of one tube diameter, Figure 9.32c shows that $K_1 = 1.0$. The difficulty that we now face is that in order to evaluate the friction factor, we need to determine the Reynolds number, but the velocity is as yet unknown. We can make a first guess at the velocity by assuming $f = 0$ in the above expression and solve for ϑ_{ave}. Then

$$\vartheta_{ave} = \sqrt{g\left(z_1 - z_2\right)} = \sqrt{\left(9.81\ \text{m/sec}^2\right)\left(1.4\ \text{m} - 0.127\ \text{m} - 0\right)} = 3.534\ \text{m/sec}$$

Then for this value of velocity, the Reynolds number is

$$Re = \frac{\vartheta_{ave} D \rho}{\mu} = \frac{(3.534\ \text{m/sec})(0.008\ \text{m})\left(1000\ \text{kg/m}^3\right)}{8.67\ \text{x}\ 10^{-4}\ \text{kg/m sec}} = 32{,}609$$

From equation (9.299), the friction factor is

$$f = (0.790 \ln Re - 1.64)^{-2} = [0.790 \ln(32{,}609) - 1.64]^{-2} = 0.023$$

We can now use this value of f to calculate a new value of ϑ_{ave}. Then

$$\vartheta_{ave} = \left[\frac{2g(z_1 - z_2)}{f\left(\frac{L}{D}\right) + K_1 + 1}\right]^{1/2} = \left[\frac{2(9.81 \text{ m/sec}^2)(1.273 \text{ m})}{0.023\left(\frac{1.527 \text{ m}}{0.008 \text{ m}}\right) + 1 + 1}\right]^{1/2} = 1.977 \text{ m/sec}$$

The new value of Reynolds number is

$$Re = \frac{\vartheta_{ave} D \rho}{\mu} = \frac{(1.977 \text{ m/sec})(0.008 \text{ m})(1000 \text{ kg/m}^3)}{8.67 \text{ x } 10^{-4} \text{ kg/m sec}} = 18{,}242$$

and the new friction factor is

$$f = (0.790 \ln Re - 1.64)^{-2} = [0.790 \ln(18{,}242) - 1.64]^{-2} = 0.0267$$

The third iteration on the velocity gives

$$\vartheta_{ave} = \left[\frac{2g(z_1 - z_2)}{f\left(\frac{L}{D}\right) + K_1 + 1}\right]^{1/2} = \left[\frac{2(9.81 \text{ m/sec}^2)(1.273 \text{ m})}{0.0268\left(\frac{1.527 \text{ m}}{0.008 \text{ m}}\right) + 1 + 1}\right]^{1/2} = 1.874 \text{ m/sec}$$

and the third iteration on the Reynolds number gives

$$Re = \frac{\vartheta_{ave} D \rho}{\mu} = \frac{(1.874 \text{ m/sec})(0.008 \text{ m})(1000 \text{ kg/m}^3)}{8.67 \text{ x } 10^{-4} \text{ kg/m sec}} = 17{,}292$$

and the third iteration on the friction factor gives

$$f = (0.790 \ln Re - 1.64)^{-2} = [0.790 \ln(17{,}292) - 1.64]^{-2} = 0.0272$$

and finally the velocity is

$$\vartheta_{ave} = \left[\frac{2g(z_1 - z_2)}{f\left(\frac{L}{D}\right) + K_1 + 1}\right]^{1/2} = \left[\frac{2(9.81 \text{ m/sec}^2)(1.273 \text{ m})}{0.0272\left(\frac{1.527 \text{ m}}{0.008 \text{ m}}\right) + 1 + 1}\right]^{1/2} = 1.864 \text{ m/sec}$$

Then the flow rate is

$$\dot{V} = A\vartheta_{ave} = \pi \frac{(0.008 \text{ m})^2}{4}(1.864 \text{ m/sec}) = 9.37 \text{ x } 10^{-5} \text{ m}^3/\text{sec}$$

$$\dot{m} = \rho A \vartheta_{ave} = \rho \dot{V} = (1000 \text{ kg/m}^3)(9.37 \text{ x } 10^{-5} \text{ m}^3/\text{sec}) = 0.0937 \text{ kg/sec}$$

For the inviscid case

$$\vartheta_{ave} = \sqrt{2g(z_1 - z_2)} = \sqrt{2(9.81 \text{ m/sec}^2)(1.4 \text{ m} - 0.127 \text{ m} - 0)} = 4.998 \text{ m/sec}$$

$$\dot{V} = A\vartheta_{ave} = \pi \frac{(0.008 \text{ m})^2}{4}(4.997 \text{ m/sec}) = 2.5118 \text{ x } 10^{-4} \text{ m}^3/\text{sec}$$

$$\dot{m} = \rho \dot{V} = (1000 \text{ kg/m}^3)(2.5118 \text{ x } 10^{-4} \text{ m}^3/\text{sec}) = 0.251 \text{ kg/sec}$$

Thus the effect of viscosity reduces the maximum flow rate substantially, by a factor of 2.68.

Example 9E.15: A pumping station for a municipal water system delivers water to a holding reservoir. The pumping station consists of a pump fitted with a globe valve on its discharge followed by a length of pipe of 1250 m followed by a second globe valve at the holding reservoir. The pump characteristics are expressed in terms of the total head loss that it can pump against, in this case $h_{l,total} = 550$ m^2/sec^2, and the volumetric flow rate at that head loss, in this case $\dot{V} = 200$ m^3/hr. The pipe and fittings are made of cast iron, but for a pump of this size, the diameter of the pipe is likely to be large enough that the asperities due to the casting process will be so small relative to the pipe diameter that the pipe can be modeled as smooth. For the water: $\rho = 10^3$ kg/m^3 and $\mu = 10^{-3}$ kg/m sec. Determine the pipe diameter (flanged) appropriate for this pumping station.

Solution: In this case, we have the total head loss so we can write

$$h_{l,total} = \left[f\left(\frac{L}{D}\right) + \sum_{i=1}^{2} K_i \right] \frac{\vartheta_{ave}^{\ 2}}{2}$$

The difficulty is that we need the velocity, as yet unknown, to determine the friction factor used in this equation to solve for the pipe diameter. Thus we are faced with making an educated guess at the velocity (or the pipe diameter) to start an iterative solution. To avoid excessive head losses, these water pumping systems typically use flow velocities such that $\vartheta_{ave} \leq 8$ m/sec. Then as a first try, let us assume $\vartheta_{ave} = 5$ m/sec. Then from continuity

$$D = \sqrt{\frac{4\dot{V}}{\pi \vartheta_{ave}}} = \sqrt{\frac{4(200 \text{ m}^3/\text{hr})}{\pi (3600 \text{ sec/hr})(5 \text{ m/sec})}} = 0.119 \text{ m}$$

From Table 9.10, this is midway between the 4 in and 6 in NPS. Let us choose the larger since this will reduce the velocity and enable us to stay within the typical range for velocity. Then from Table 9.9, $D = 6.0625$ in $= 0.154$ m. and the Reynolds number becomes

$$Re = \frac{\vartheta_{ave} D \rho}{\mu} = \frac{4\dot{V}\rho}{\pi D \mu} = \frac{4(200 \text{ m}^3/\text{hr})(1000 \text{ kg/m}^3)}{\pi (3600 \text{ sec/hr})(0.154 \text{ m})(10^{-3} \text{ kg/m sec})} = 4.5932 \text{ x } 10^5$$

Then the friction factor becomes

$$f = (0.790 \ln Re - 1.64)^{-2} = 0.0133$$

The average velocity is

$$\vartheta_{ave} = \frac{\dot{V}}{A} = \frac{4\dot{V}}{\pi D^2} = \frac{4(200 \text{ m}^3/\text{hr})}{\pi (3600 \text{ sec/hr})(0.154 \text{ m})^2} = 2.983 \text{ m/sec}$$

Then using this result and the data in Table 9.8 for a fully open globe valve for 6 NPS pipe, we get

$$h_{l,total} = \left[f\left(\frac{L}{D}\right) + \sum_{i=1}^{2} K_i \right] \frac{\vartheta_{ave}^{\ 2}}{2} = \left[0.0133\left(\frac{1250 \text{ m}}{0.154 \text{ m}}\right) + 2(6) \right] \frac{(2.983 \text{ m/sec})^2}{2} = 533.7 \text{ m}^2/\text{sec}^2$$

This value of the total head loss is within three percent of the specifications for this pump which is probably within the error limits of the measurements of pump characteristics. Thus the design pipe size for this pumping station would be 6 NPS.

9.10.3.5 Pump Characteristics: Thus far in our discussion of the analysis of piping systems, we have stated that the objective of the analysis is to determine the pumping requirements for the system, but we have not yet explained what those characteristics might be. The object of the pump is to provide the flow work transfer necessary to overcome the total head loss of the piping

system downstream of the pump discharge. Then if we establish a control volume coincident with the walls of the pump and apply the first law to the control volume, we obtain for steady flow operation of the pump

$$\dot{Q}-\dot{W}_{shaft}+\sum_{in}\left[\dot{m}\left(u+\frac{P}{\rho}+\frac{\vartheta^2}{2}+gz\right)\right]_{in}-\sum_{out}\left[\dot{m}\left(u+\frac{P}{\rho}+\frac{\vartheta^2}{2}+gz\right)\right]_{out}=0 \qquad (9.303)$$

Typically, a pump for an incompressible fluid operates in an adiabatic manner. There simply is insufficient residence time of the fluid in the device to establish any significant heat transfer that would enable the fluid to approach thermal equilibrium with the device. Then equation (9.303) becomes

$$\begin{aligned} -\dot{W}_{shaft}&=\dot{m}\left[\left(u_{out}-u_{in}\right)+\left(\frac{P_{out}}{\rho}-\frac{P_{in}}{\rho}\right)+\left(\frac{\vartheta_{out}^{\ 2}}{2}-\frac{\vartheta_{in}^{\ 2}}{2}\right)+g\left(z_{out}-z_{in}\right)\right] \\ -\dot{W}_{shaft}&=\dot{m}\left[c\left(T_{out}-T_{in}\right)+\left(\frac{P_{out}}{\rho}-\frac{P_{in}}{\rho}\right)+\left(\frac{\vartheta_{out}^{\ 2}}{2}-\frac{\vartheta_{in}^{\ 2}}{2}\right)+g\left(z_{out}-z_{in}\right)\right] \end{aligned} \qquad (9.304)$$

where we have substituted the energy constitutive relation for the incompressible fluid model.

On the right-hand side of equation (9.304), the second term in the square brackets represents the flow work transfer associated with the transfer of the fluid into and out of the pump. This is the reason for the existence of the pump, i.e., to make the outlet pressure of the fluid higher than the inlet pressure of the fluid so that the higher outlet pressure can subsequently be used to drive the flow through the frictional elements (lengths of pipe, fittings, and valves) downstream of the pump. Thus this second term is positive. The third and fourth terms, the kinetic and gravitational potential energy, respectively, are usually small compared with the flow work terms and are often neglected.

On the other hand, the first term in the square brackets on the right-hand side of equation (9.304) represents the increase in stored energy of the fluid due to the irreversible operation of the pump resulting from the viscous behavior of the fluid. This can be seen most easily by applying the second law to the control volume, viz.

$$\begin{aligned} \sum_j\left(\frac{\dot{Q}}{T}\right)_j+\dot{m}\left(s_{in}-s_{out}\right)+\dot{S}_{gen}&=0 \\ \dot{S}_{gen}=-\dot{m}\left(s_{in}-s_{out}\right)&=\dot{m}c\ln\left(\frac{T_{out}}{T_{in}}\right) \end{aligned} \qquad (9.305)$$

where we have substituted the entropy constitutive relation for the incompressible fluid model. Since the rate of entropy generation will be positive for irreversible operation, the temperature of the fluid, and, hence ,the stored thermal energy, will increase as the fluid passes through the irreversible pump. Thus, like the second term, the first term is also positive for irreversible operation. Clearly, for reversible operation this term is zero.

The net result of these two major energy contributions to the flow is that the shaft power must be negative, i.e., into the pump and, hence, the fluid stream. It follows that the shaft power input to the pump is greater in magnitude for irreversible operation than for reversible operation. Then we can define a pump efficiency η to be

$$\eta=\frac{\left(\dot{W}_{shaft}\right)_{reversible}}{\left(\dot{W}_{shaft}\right)_{irreversible}}=\frac{\dot{m}\left[\left(\frac{P_{out}}{\rho}-\frac{P_{in}}{\rho}\right)+\left(\frac{\vartheta_{out}^{\ 2}}{2}-\frac{\vartheta_{in}^{\ 2}}{2}\right)+g\left(z_{out}-z_{in}\right)\right]}{\left(\dot{W}_{shaft}\right)_{irreversible}} \qquad (9.306)$$

In the pump industry, the numerator in equation (9.306) is usually referred to as the fluid power and the denominator is referred to as the brake horsepower or shaft power of the drive motor. A typical value for the efficiency of a centrifugal pump is 75 percent.

If we divide the numerator of equation (9.306) by the mass flow rate, we get an expression for the change in stored mechanical energy of the flow through the pump per unit mass which is known as the total dynamic head of the pump, viz.

$$h_{pump} = \left(\frac{P_{out}}{\rho} - \frac{P_{in}}{\rho} \right) + \left(\frac{\vartheta_{out}^{\ 2}}{2} - \frac{\vartheta_{in}^{\ 2}}{2} \right) + g\left(z_{out} - z_{in} \right) \tag{9.307}$$

Note that equation (9.307) also represents the reversible shaft power added to the flow per unit mass flow rate. If we now subtract equation (9.307) from equation (9.296), we get an expression for the total net head loss for the piping system including the pumping device, viz.

$$h_{l,major} + \sum_{i}^{N} \left(h_{l,minor} \right)_i - h_{pump} = \left(\frac{P_1}{\rho} - \frac{P_2}{\rho} \right) + \left(\alpha_1 \frac{\vartheta_1^{\ 2}}{2} - \alpha_2 \frac{\vartheta_2^{\ 2}}{2} \right) + g\left(z_1 - z_2 \right) \tag{9.308}$$

where plane 1 refers to the pump inlet and plane 2 refers to the farthest plane of the piping system.

In thermal-fluids engineering practice, the total dynamic head of the pump is usually not the expression given in equation (9.307). In the early days of municipal water systems, the flow was usually driven by gravity alone rather than by mechanical pumps. Based upon this historical practice that dates back to the nineteenth century when the fluid mechanics of water supply systems were first being developed on a rational basis, the term "pump head" usually refers to equation (9.307) divided by the acceleration of gravity g. Then

$$H_{pump} = \frac{h_{pump}}{g} = \left(\frac{P_{out}}{\rho g} - \frac{P_{in}}{\rho g} \right) + \left(\frac{\vartheta_{out}^{\ 2}}{2g} - \frac{\vartheta_{in}^{\ 2}}{2g} \right) + \left(z_{out} - z_{in} \right) \tag{9.309}$$

which has the units of meters, the height of a column of water that caused the flow. The total head loss then becomes

$$H_{l,total} = \frac{h_{l,total}}{g} = f\left(\frac{L}{D} \right) \frac{\vartheta_{ave}^{\ 2}}{2g} + \sum_{i}^{N} K_i \frac{\vartheta_{ave}^{\ 2}}{2g} = \left(\frac{P_1}{\rho g} - \frac{P_{in}}{\rho g} \right) + \left(\frac{\vartheta_{out}^{\ 2}}{2g} - \frac{\vartheta_{in}^{\ 2}}{2g} \right) + \left(z_{out} - z_{in} \right) \tag{9.310}$$

which has the units of meters.

The pump characteristics that are usually most useful in the design of piping systems are the volumetric flow rate, $\dot{V}$ (m^3/hr) and the total dynamic head, H_{pump} (m). There are other pump performance characteristics that are useful, but we shall delay our discussion of these until Chapter 15.

9.10.3.6 Piping Networks: Thus far we have considered only those piping systems for which the components are arranged in series fashion. However, in thermal-fluids engineering practice, it is common to encounter piping networks in which the various components are arranged in both series and parallel configurations simultaneously. The analysis of such configurations can be accomplished by applying the techniques of network analysis except the components in this case are non-linear. In piping networks, all parallel branches have the same pressure drop but different flow rates depending upon the elements that they contain. All elements arranged in series have the same flow rate but different pressure drops depending upon their individual head loss terms.

Example 9E.16: The piping system shown in plan view in Figure 9E.16 consists of two parallel circuits flowing water between two manifolds. The two circuits are in the same horizontal plane. Circuit A is fabricated from 4 NPS cast iron pipe with a flanged globe valve

used to shut off the flow if necessary. Circuit B is fabricated from the same cast iron pipe as circuit A and contains a pump that delivers a volume flow rate of $\dot{V} = 125$ m^3/hr at a head of 33 m. For the water: $\rho = 10^3$ kg/m^3 and $\mu = 10^{-3}$ kg/m sec. Determine the volumetric flow rate of the two circuits together.

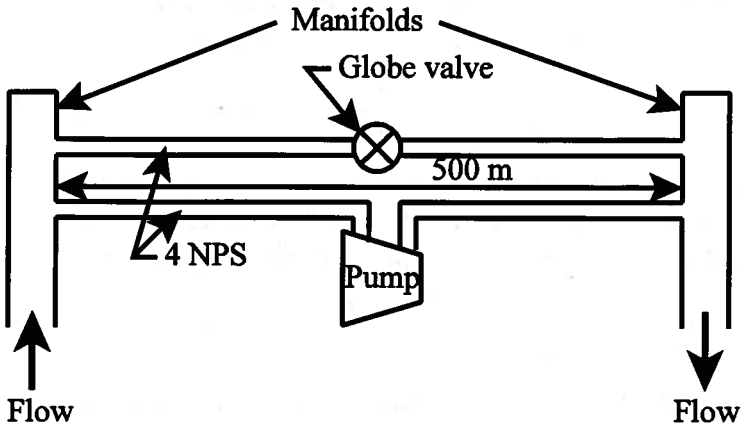

Figure 9E.16 Parallel Piping System (Plan View)

Solution: The pressure drops for the two circuits shown in Figure 9E.16 are the same since they are connected in parallel to the same manifolds. Let the circuit with the pump be circuit A. For this circuit the pressure drop is given by

$$\frac{P_1}{\rho g} - \frac{P_2}{\rho g} = \left[f\left(\frac{L}{D}\right) + K_1 \right] \frac{\vartheta_A^{\,2}}{2g} - H_{pump}$$

where K_1 is the loss coefficient for the entrance to the pipe assumed to be square edged. The flow velocity in circuit A can be determined by the pump through-put (volumetric flow rate). Then for pipe size 4 NPS, $D = 4.026$ in $= 0.1023$ m and $A = 12.73$ in$^2 = 8.2185 \times 10^{-3}$ m^2.

$$\vartheta_A = \frac{\dot{V}}{A} = \frac{\left(125 \text{ m}^3/\text{hr}\right)}{\left(3600 \text{ sec/hr}\right)\left(8.2185\ 10^{-3} \text{ m}^2\right)} = 4.225 \text{ m/sec}$$

Then the Reynolds number for the flow in circuit A is

$$Re_A = \frac{\vartheta_A D \rho}{\mu} = \frac{(4.225 \text{ m/sec})(0.1023 \text{ m})\left(1000 \text{ kg/m}^3\right)}{10^{-3} \text{ kg/m sec}} = 4.3222 \times 10^5$$

For cast iron pipe, Table 9.5 gives $k_s = 0.25$ mm. Then $k_s/D = 2.4438 \times 10^{-6}$ and the friction factor is given by equation

$$f = \left\{ -2.0 \log_{10} \left[\frac{\left(k_s/D\right)}{3.7} - \frac{4.518}{Re_{D_h}} \log_{10} \left(\left[\frac{\left(k_s/D\right)}{3.7} \right]^{1.11} + \frac{6.9}{Re_{D_h}} \right) \right] \right\}^{-2}$$

$$f = \left\{ -2.0 \log_{10} \left[\frac{\left(2.44 \times 10^{-6}\right)}{3.7} - \frac{4.518}{4.32 \times 10^5} \log_{10} \left(\left[\frac{\left(2.44 \times 10^{-6}\right)}{3.7} \right]^{1.11} + \frac{6.9}{4.32 \times 10^5} \right) \right] \right\}^{-2}$$

$$f = 0.0136$$

Then the pressure drop becomes

$$P_1 - P_2 = \left[f\left(\frac{L}{D}\right) + K_1 \right] \frac{\vartheta_A^{\,2} \rho}{2} - H_{pump} \rho g$$

$$P_1 - P_2 = \left[0.0136\left(\frac{500 \text{ m}}{0.1023 \text{ m}}\right) + 0.5 \right] \frac{(4.225 \text{ m/sec})^2 (10^3 \text{ kg/m}^3)}{2} - (33 \text{ m})(10^3 \text{ kg/m}^3)(9.81 \text{ m/sec}^2)$$

$$P_1 - P_2 = 2.7401 \text{ x } 10^5 \text{ N/m}^2$$

Then for circuit B, in order to determine the velocity, we need to have the friction factor which requires the Reynolds number; however, we cannot compute the Reynolds number until we have the velocity. Thus, an iterative solution is required. We then assume as a first estimate that $f_B = f_A$ so that the velocity becomes

$$\vartheta_B = \sqrt{\frac{2(P_1 - P_2)}{\rho\left[f\left(\frac{L}{D}\right) + K_1 + K_2 \right]}} = \sqrt{\frac{2(2.7401 \text{ x } 10^5 \text{ N/m}^2)}{(10^3 \text{ kg/m}^3)\left[0.0136\left(\frac{500 \text{ m}}{0.1023 \text{ m}}\right) + 6 + 0.5 \right]}} = 2.7404 \text{ m/sec}$$

Using this value of velocity we can compute a new value of Reynolds number and a new friction factor. After two iterations we arrive at the result

$$\vartheta_B = 2.637 \text{ m/sec} \quad \text{and} \quad Re = 2.6976 \text{ x } 10^5$$

Then the total flow rate for this parallel circuit becomes

$$\dot{V}_{total} = \dot{V}_A + \dot{V}_B = (\vartheta_A + \vartheta_B) A = (4.225 \text{ m/sec} + 2.637 \text{ m/sec})(8.2185 \text{ x } 10^{-3} \text{ m}^2)$$

$$\dot{V}_{total} = 0.056395 \text{ m}^3/\text{sec} = 203.02 \text{ m}^2/\text{hr}$$

9.10.4 Turbulent External Flows

As we have already discussed in Section 9.9.2.2, in the vicinity of the sharp leading edge of a smooth flat plate, viscous damping ensures that the flow in the boundary layer is laminar even if the flow in the mainstream is turbulent. However, as the laminar boundary layer grows in thickness as the flow proceeds downstream, the flow eventually reaches a location where the characteristic amplitude of the fluctuations inherent in the flow has become so large the viscous forces are no longer able to damp out these disturbances. At this point, the flow in the boundary layer becomes unstable and undergoes a transition to turbulent flow that continues over the remaining length of the plate. In point of fact, the transition from laminar to turbulent flow in the boundary layer is not a sharp one. What happens is that there is a transition region at the end of the laminar region where the laminar boundary layer tries to continue its growth but is constantly being broken up by the instability that derives from the limited damping capabilities of the fluid. Because of this continual destruction and recreation process, transition from laminar to turbulent flow in the boundary layer occurs over a region of the flow rather than at a definite location on the plate. In this transition region, shear stress at the wall increases and the velocity profile undergoes changes in shape as the fully turbulent boundary layer tries to establish itself. Once this occurs, the turbulent boundary layer grows at a much faster rate than that in the laminar region. Of course, as we have already seen in the case of turbulent internal flows, there is a laminar sublayer imbedded in this now fully turbulent boundary layer.

Experimental measurements of this transition phenomenon for a flat plate with zero pressure gradient have reported a range of values of the local Reynolds number at which the transition occurs, typically $6 \times 10^4 < Re_{x,transition} < 5 \times 10^5$. Since these data usually have been obtained in laboratory settings where the conditions are precisely controlled, some investigators believe that these data are artificially high. Kays and Crawford (W. M. Kays and M. E. Crawford, *Convective Heat and Mass Transfer*, 2nd edition, McGraw-Hill, N. Y., 1980, Chapter 10) argue that the results obtained from viscous stability theory might be more appropriate in practice where conditions are not quite so closely controlled, viz. $Re_{x,transition} = 60{,}000$. The location of the transition can also be expressed in terms of the momentum thickness. From equation (9.199),

$$x = \frac{\theta\sqrt{Re_x}}{0.664} \tag{9.311}$$

where θ is the momentum thickness and then

$$Re_{x,transition} = \frac{\vartheta_x x}{\nu} = \frac{\vartheta_x \theta \sqrt{Re_{x,transition}}}{0.664\nu}$$

$$0.664\sqrt{Re_{x,transition}} = \frac{\vartheta_x \theta}{\nu} = Re_{\theta,transition} \tag{9.312}$$

$$Re_{\theta,transition} = 162.65$$

Figure 9.31 shows the fluctuating nature of the outer part of a turbulent boundary layer on a flat plate 3.3 m long suspended in a wind tunnel. Streaklines from a smoke wire near the sharp leading edge are illuminated by a vertical slice of light. (A streamline is the locus of points that are everywhere tangent to the instantaneous velocity vector and cannot be observed directly by

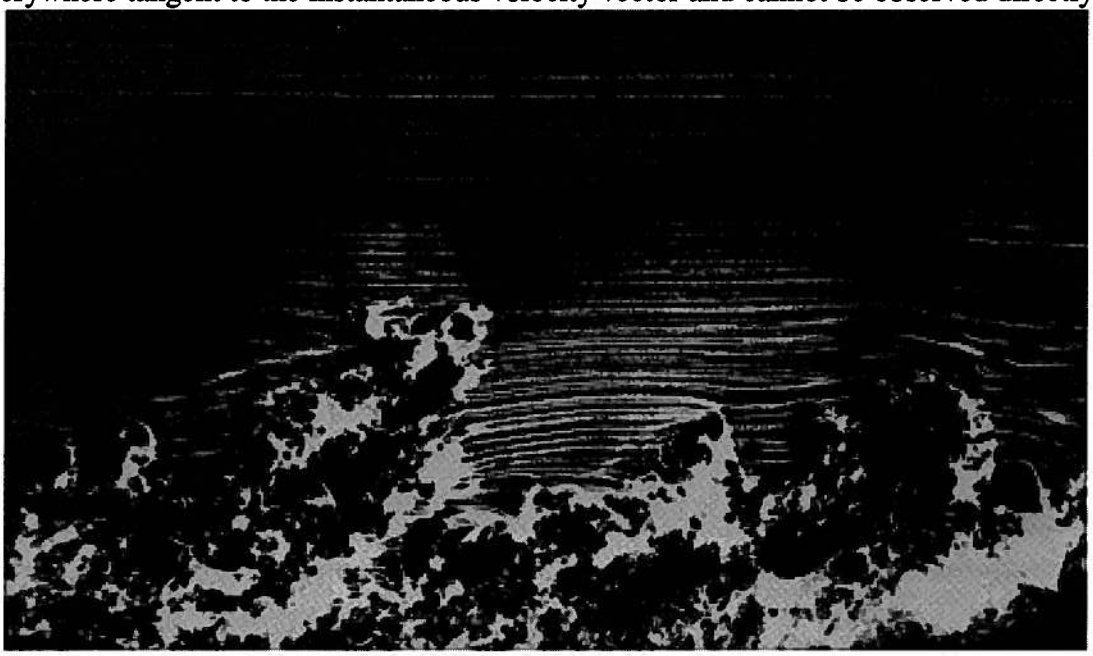

Figure 9.31 Side View of a Turbulent Boundary Layer on a Flat Plate, $Re_\theta = 3500$
(From Figure 157, p. 92 of *An Album of Fluid Motion* by M. Van Dyke, Parabolic Press, Stanford, CA, 1982.)

flow visualization. A pathline is the trajectory of a fluid particle expressed as a function of position and time and is obtained by injecting a dye or some other indicator and observing continuously or photographing with a long exposure time. A streakline is the locus at any instant of all fluid particles that have at some previous time passed through a fixed point in the flow and is obtained by injecting an indicator continuously and observing or photographing instantaneously. In steady flow, all three "lines" are identical, but in unsteady flow, the streamlines, streaklines, and pathlines are all different so that care must be exercised in interpreting the images obtained by various methods of flow visualization. In Figure 9.31, outside the turbulent boundary layer where the flow is steady, the streaklines are identical with the streamlines.) The Reynolds number of the flow in the photograph of Figure 9.31is 3500 as determined by using the momentum thickness as the characteristic length. According to the criterion expressed in equation (9.312), the flow of Figure 9.31 clearly is well into the turbulent regime.

Despite the seemingly chaotic nature of the flow field shown in Figure 9.31, there really is a structure to it. Figure 9.32 shows an image of the laminar sublayer of a turbulent boundary layer on a flat wall. The image was created by introducing a suspension of aluminum particles in a stream of water. The lower portion of the image shows the streaks that result when the sublayer is viewed normal to the wall while the upper portion of the image is a simultaneous side view of the boundary layer formed with the aid of a mirror. The laminar sublayer is clearly evident as is the fully turbulent outer layer.

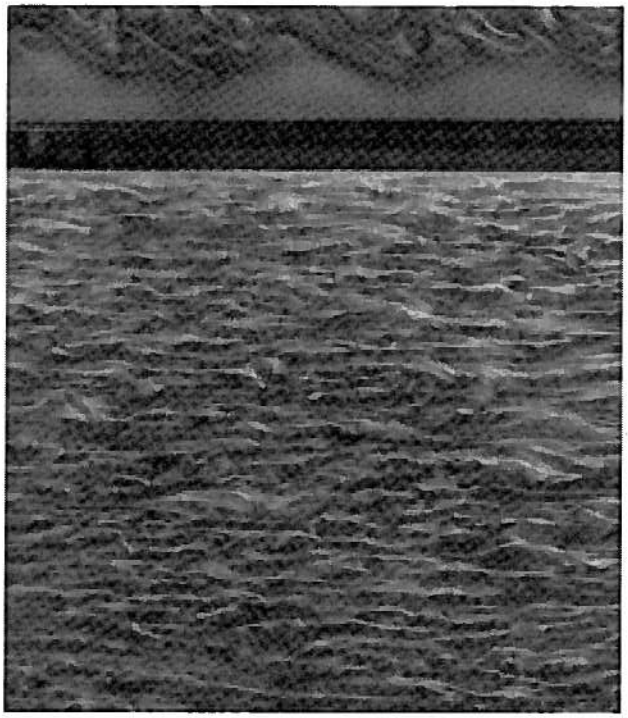

Figure 9.32 Laminar Sublayer of a Turbulent Boundary Layer
(From Figure 159, p. 93 of *An Album of Fluid Motion* by M. Van Dyke, Parabolic Press, Stanford, CA, 1982.)

In internal flows, we focused our interest on the pressure drop required to drive the flow. In contrast, for external flows we are interested in the shear stress that acts on the surface. It is this shear stress that is responsible for the "skin friction drag" experienced by the object. For external flows, the flow is usually driven by the flow external to the boundary layer rather than being driven by a pressure drop in the direction of the flow.

In an attempt to describe the boundary layer on the surface of an object immersed in a flow, we are led to an interesting application of the power velocity profile law developed in Section 9.10.2.2. In that section we showed that the data for the velocity profile in the turbulent boundary layer can be fit approximately with a 1/7th power law. In the analysis of the flow over a flat plate, Von Karman has suggested, in the interests of simplicity, that the similarity solution for the turbulent boundary layer that results for such an external flow can be written in the form

$$\frac{\vartheta_x}{\vartheta_\infty} = \left(\frac{y}{\delta}\right)^{1/7} \tag{9.313}$$

where δ is the bounday layer thickness. Although in the present case we are dealing with the flow over a flat plate, we now borrow some results from turbulent flow in a circular conduit. Recall from equation (9.248) that the shear stress at the wall for turbulent flow in a circular conduit was related to the friction factor by

$$\tau_s = \frac{f}{8}\rho\vartheta_{ave}^{\ 2} \tag{9.314}$$

In 1911 Blasius fit all the data then available for the friction factor for turbulent flow in a circular conduit by the expression

$$f = 0.3164\left(\frac{\vartheta_{ave}D}{\nu}\right)^{-1/4} \tag{9.315}$$

Combining equations (9.314) and (9.315), we get

$$\tau_s = 0.03955\rho\vartheta_{ave}^{\ 7/4}\nu^{1/4}D^{-1/4} \tag{9.316}$$

If we rewrite this result in terms of the radius R of the conduit and recognize that for turbulent flow in this geometry $\vartheta_{ave} = 0.8\vartheta_{max}$, we get

$$\tau_s = 0.0225\rho\vartheta_{max}^{\ 7/4}\left(\frac{\nu}{R}\right)^{1/4} \tag{9.317}$$

Applying equation (9.317) to the case of the flat plate in turbulent flow, we obtain

$$\frac{\tau_s}{\rho\vartheta_\infty^{\ 2}} = 0.0225\left(\frac{\nu}{\vartheta_\infty\delta}\right)^{1/4} \tag{9.318}$$

In our prior discussion of the momentum thickness, we derived the result [equation (9.202)]

$$\tau_s = \rho\vartheta_\infty^{\ 2}\frac{d\theta}{dx} \tag{9.319}$$

where θ is the displacement thickness given by equation (9.197), viz.

$$\theta = \int_0^\delta \frac{\vartheta_x}{\vartheta_\infty}\left(1 - \frac{\vartheta_x}{\vartheta_\infty}\right)dy \tag{9.320}$$

Substituting equation (9.313) into equation (9.320) and carrying out the integration, we get

$$\theta = \frac{7}{72}\delta \tag{9.321}$$

Substituting this result into equation (9.319), we obtain a differential equation for the boundary layer thickness based upon the 1/7th power law similarity solution of equation (9.313), viz.

$$\frac{7}{72}\frac{d\delta}{dx} = 0.0225\left(\frac{\nu}{\vartheta_\infty \delta}\right)^{1/4} \tag{9.322}$$

Integrating equation (9.322) from the leading edge of the plate to the location x, we get

$$\int_0^\delta \delta^{-1/4} d\delta = \frac{0.23143\nu^{1/4}}{\vartheta_\infty^{1/4}} \int_0^x dx$$

$$\delta(x) = 0.37x\left(\frac{\vartheta_\infty x}{\nu}\right)^{-1/5} \tag{9.323}$$

Then from equation (9.321) we get

$$\theta(x) = 0.036x\left(\frac{\vartheta_\infty x}{\nu}\right)^{-1/5} \tag{9.324}$$

We can express the local shear stress on the surface of an object in an external flow in non-dimensional form by defining the local skin friction coefficient C_{fx} as

$$C_{fx} = \frac{\tau_s}{\frac{1}{2}\rho \vartheta_\infty^{\,2}} \tag{9.325}$$

Combining equation (9.325) with equation (9.319), we get

$$C_{fx} = 2\frac{d\theta}{dx} \tag{9.326}$$

Differentiating equation (9.319) and substituting the result into equation (9.326), we get an expression for the local skin friction coefficient on a flat plate, viz.

$$C_{fx} = 0.0576\left(\frac{\vartheta_\infty x}{\nu}\right)^{-1/5} = 0.0576 Re_x^{-1/5} \tag{9.327}$$

Then

$$\frac{C_{fx}}{2} = 0.0288 Re_x^{-1/5}$$

but the experimental data have been found to be better represented by changing the constant slightly so that

$$\frac{C_{fx}}{2} = 0.0296 Re_x^{-1/5} \tag{9.328}$$

which is the commonly accepted correlation in the literature for the local skin friction coefficient for turbulent flow over a smooth flat plate (one side).

The total drag force F_D on one side of a flat plate of length L and width b can be determined by integrating the shear stress on the surface over the area of the plate, viz.

$$F_D = \int_0^L \tau_s b dx \tag{9.329}$$

which is usually expressed in dimensionless form as the drag coefficient C_D such that

$$C_D = \frac{F_D}{\frac{1}{2}\rho \vartheta_\infty^{\,2} bL} = \int_0^1 C_f d\left(\frac{x}{L}\right) \tag{9.330}$$

Substituting equation (9.328) into equation (9.330), we get

$$C_D = 0.0592\int_0^1 Re_x^{-1/5} d\left(\frac{x}{L}\right) = 0.0592\int_0^1 \left(\frac{\vartheta_\infty \rho x}{\mu}\right)^{-1/5} d\left(\frac{x}{L}\right)$$

$$C_D = 0.0592\left(\frac{5}{4}\right)\left(\frac{1}{L}\right)^{1/5}\left(\frac{\vartheta_\infty \rho}{\mu}\right)^{-1/5}\int_0^1 \left(\frac{x}{L}\right)^{-1/5} d\left(\frac{x}{L}\right) \qquad (9.331)$$

$$C_D = 0.074 Re_L^{-1/5}$$

After equations (9.328) and (9.331) had been developed, Prandtl pointed out that they were actually derived on the assumption that the turbulent boundary layer started at the leading edge of the plate. Clearly, this is not the case since there exists a laminar region over a considerable portion of the leading edge even in the case for which the free stream flow is turbulent. The friction force over this leading edge is then considerably less than if the boundary layer had been turbulent from the outset. Prandtl suggested that the turbulent friction force from the leading edge to the to the point of the laminar-turbulent transition be replaced by the laminar friction force over this region. If we use the Blasius solution, equation (9.204), for the laminar region, the integration of the shear stress over the surface of the plate takes on a different form., viz.

$$C_D = \frac{1}{L}\left[\int_0^{x_{transition}} (C_{fx})_{laminar}\, dx + \int_{x_{transition}}^{L} (C_{fx})_{turbulent}\, dx\right]$$

$$C_D = \frac{1}{L}\left[\int_0^{x_{transition}} 0.664 Re_x^{-1/2} dx + \int_{x_{transition}}^{L} 0.0592 Re_x^{-1/5}\right]$$

$$C_D = \frac{\mu}{\vartheta_\infty \rho L}\left[\int_0^{Re_{x,transition}} 0.664 Re_x^{-1/2} d(Re_x) + \int_{Re_{x,transition}}^{Re_L} 0.0592 Re_x^{-1/5} d(Re_x)\right]$$

where we have changed the variable of integration from x to Re_x for simplicity. Carrying out the integration and rearranging the result, we get

$$C_D = 1.328\left(Re_{x,tr}\right)^{-1/2}\left(\frac{Re_{x,tr}}{Re_L}\right) + 0.074 Re_L^{-1/5}\left[1 - \left(\frac{Re_{x,tr}}{Re_L}\right)^{4/5}\right] \qquad (9.332)$$

Of course, the difficulty in applying equation (9.332) in practice is that the transition from laminar to turbulent is not sharply defined because of the continual creation and destruction of the turbulent boundary layer in the transition region. This due in part to the level of turbulence in the free stream. Lacking any other information, it is common practice to assume that the laminar-turbulent transition occurs at a transition Reynolds number of $Re_{x,tr} = 5 \times 10^5$.

When the Reynolds number becomes extremely large, $Re_L > 10^7$, the laminar portion of the boundary layer becomes insignificant. Then using data obtained specifically for this situation and employing the momentum integral approach used above, there results

$$\frac{C_{fx}}{2} = 0.0131 Re_x^{-1/7} \qquad (9.333)$$

and

$$C_D = 0.031 Re_L^{-1/7} \qquad (9.334)$$

The foregoing analysis applies to the case of a smooth flat plate. For the rough flat plate there is no analysis except for the case of the fully rough flat plate for which Mills and Hang [Mills, A. F. and Xu Hang, "On the Skin Friction Coefficient for a Fully Rough Flat Plate," *J. Fluids Engineering*, 105, 364-365, (1983)] suggest

$$C_{fx} = \left(3.476 + 0.707 \ln \frac{x}{k_s} \right)^{-2.46} \quad \text{for} \quad 150 < \frac{x}{k_s} < 1.5 \text{ x } 10^7 \tag{9.335}$$

and

$$C_D = \left(2.635 + 0.618 \ln \frac{L}{k_s} \right)^{-2.57} \quad \text{for} \quad 150 < \frac{L}{k_s} < 1.5 \text{ x } 10^7 \tag{9.336}$$

where as described in section 9.10.2.2 k_s is the average height of the roughness projections with typical values given in Table 9.5.

Example 9E.17: The trailer part of a tractor-trailer highway transport for hauling freight is basically a large box mounted on wheels. The largest size trailer presently allowed on U.S. interstate highways has a length of $L = 16$ m, a width of $W = 2.6$ m, and a height of $H = 2.9$ m. Estimate the engine power required to overcome the just skin friction drag on the trailer alone for a vehicle traveling at a speed of $\vartheta = 100$ km/hr (27.778 m/sec).

For air: $\rho = 1.189$ kg/m^3 and $\mu = 1.825 \text{ x } 10^{-5}$ kg/m sec

Solution: We can model the surfaces of the box of the trailer as flat plates. Then the Reynolds number based upon the length of the box is

$$Re_L = \frac{\vartheta L \rho}{\mu} = \frac{(27.778 \text{ m/sec})(16 \text{ m})(1.189 \text{ kg/m}^3)}{1.825 \text{ x } 10^{-5} \text{ kg/m sec}} = 2.8956 \text{ x } 10^7$$

For a Reynolds number this large, the laminar portion of the boundary layer can be neglected. Then the drag coefficient can be evaluated from equation (9.334), viz.

$$C_D = 0.031 Re_L^{-1/7} = 0.031 \left(2.8956 \text{ x } 10^7 \right)^{-1/7} = 0.08591$$

For a typical side of width b and length L, the drag force is

$$F_D = C_D \left[\frac{1}{2} \rho \vartheta_\infty^2 bL \right] = (0.08591) \left[\frac{1}{2} (1.189 \text{ kg/m}^3)(27.778 \text{ m/sec})^2 bL \right] = (34.409 \text{ N/m}^2) bL$$

In estimating the drag due to skin friction, we consider only the two vertical sides and the top of the box since the bottom has a number of structural elements and the axle assemblies that affect the character of the flow in this region. Then for the top $b = 2.6$ m and $L = 16$ m, and

$$(F_D)_{top} = (39.409 \text{ N/m}^2)(2.6 \text{ m})(16 \text{ m}) = 1639.4 \text{ N}$$

For each of the sides, $b = 2.9$ m and $L = 16$ m, and

$$(F_D)_{side} = (39.409 \text{ N/m}^2)(2.9 \text{ m})(16 \text{ m}) = 1828.6 \text{ N}$$

Then the total skin friction drag for the two sides and the top is

$$(F_D)_{total} = (F_D)_{top} + 2(F_D)_{side} = (1639.4 \text{ N}) + 2(1828.6 \text{ N}) = 5296.6 \text{ N}$$

Then the power required to overcome just this component of the drag is given by

$$\wp = (F_D)_{total} \vartheta = (5296.6 \text{ N})(27.778 \text{ N}) = 147.13 \text{ kW} = 197.22 \text{ hp}$$

As we shall see in section 9.11 this is only a fraction of the total drag on the vehicle. A substantial portion of the total drag is associated with the wake of the vehicle.

9.11 Drag

9.11.1 Drag on a Cylinder Immersed in a Flow of an Inviscid Fluid: d'Alembert's Paradox

Perhaps the most dramatic manifestation of the effect of fluid viscosity on the motion of a fluid is evidenced in the production of a drag force acting on bodies immersed in a flowing fluid. (In this discussion of drag we shall make frequent reference to the flow past a cylinder with the axis of the cylinder oriented normal to the direction of the flow since this flow configuration embodies many of the features central to the phenomenon of drag.) If the fluid possessed no viscosity, i.e., were inviscid, there would be no drag. Figure 9.33 shows a physical simulation of a steady, uniform flow of an inviscid incompressible fluid past a cylinder. (The precise manner in which this simulation was achieved is interesting in its own right since it involved the use of a viscous fluid, but since the details are not essential to the present discussion, the reader is referred to the reference from which Figure 9.33 was taken.) The streamlines of the steady flow are visualized by injecting dye into the flow. Note the nearly perfect symmetry of the streamlines.

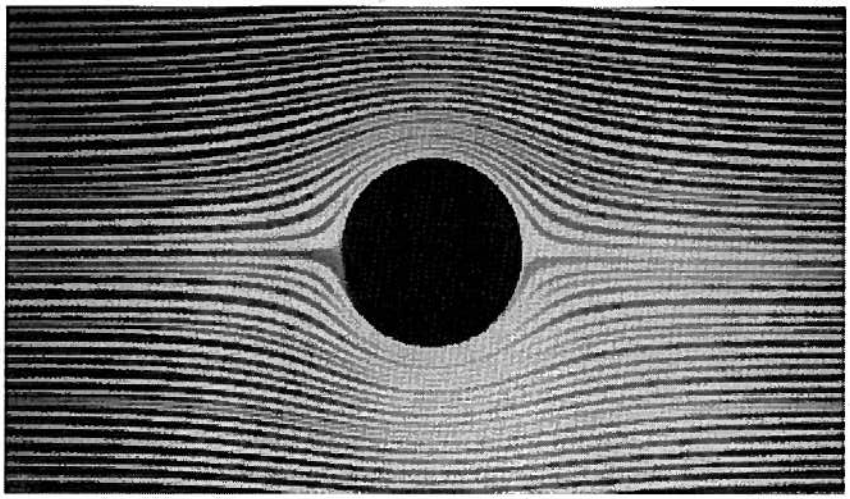

Figure 9.33 Simulation of Flow of an Inviscid Fluid Around a Cylinder
(From Figure 1, p. 8 of *An Album of Fluid Motion* by M. Van Dyke, Parabolic Press, Stanford, CA, 1982.)

As the flow encounters the obstacle represented by the cylinder, the flow in the neighborhood of the cylinder must accelerate in accordance with the continuity equation since a portion of the flow area is taken up by the cylinder. This causes the streamlines to "bunch up" near the surface. The closer together the streamlines, the faster the flow. Clearly, from Figure 9.33 it is apparent that the location of maximum fluid velocity lies at the equator, a position on the surface of the cylinder oriented at an angle 90° to the direction of the free stream. Thus as the fluid travels up the forward facing portion of the cylinder, it accelerates until it reaches its maximum velocity at the equator and then decelerates as it proceeds down the rearward facing portion of the cylinder, eventually reaching the free stream velocity at the rear of the cylinder. (See Figure 9.34.)

From inviscid flow theory, it can be shown that the magnitude of the local velocity $\vec{v}_\theta$ of the fluid on the *surface* of the cylinder is given by

$$\left|\vec{v}_\theta\right| = 2v_\infty \sin\theta \tag{9.337}$$

where ϑ_∞ is the free stream velocity upstream of the cylinder. (The "no-slip" boundary condition does not hold in this case since the fluid is being modeled as inviscid.)

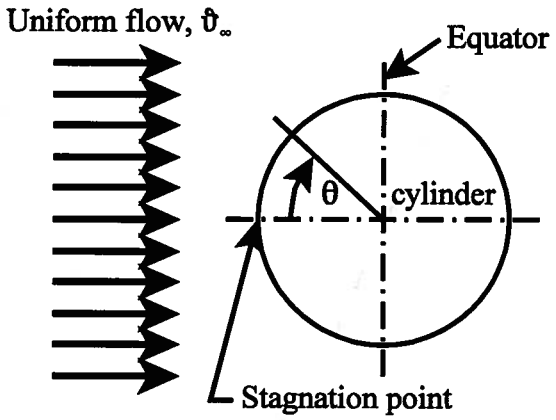

Figure 9.34 Cylinder in Uniform Cross-flow

Since the flow is inviscid and, hence, reversible, the distribution of pressure on the surface of the cylinder is given by the Bernoulli equation

$$\frac{P_\infty}{\rho}+\frac{\vartheta_\infty^{\,2}}{2}=\frac{P_\theta}{\rho}+\frac{\vartheta_\theta^{\,2}}{2} \tag{9.338}$$

If we combine equations (9.337) and (9.338) and solve for P_θ, we get

$$\begin{aligned}\frac{P_\theta}{\rho}+\frac{(2\vartheta_\infty\sin\theta)^2}{2}&=\frac{P_\infty}{\rho}+\frac{\vartheta_\infty^{\,2}}{2}\\ P_\theta&=P_\infty+\frac{\rho\vartheta_\infty^{\,2}}{2}\left(1-4\sin^2\theta\right)\end{aligned} \tag{9.339}$$

There are two observations that can be made from equation (9.339): (1) the pressure on the surface of the cylinder decreases as the flow moves up the forward facing portion ($0 \le \theta \le \pi/2$) and increases as the flow moves down the rearward facing portion ($\pi/2 \le \theta \le \pi$), and (2) the pressure distribution over the surface of the cylinder is symmetric with respect to the forward facing portion and the rearward facing portion with the minimum pressure at the equator. The pressure distribution can be expressed in dimensionless form as the pressure coefficient C_P, viz.

$$C_P=\frac{P_\theta-P_\infty}{\frac{1}{2}\rho\vartheta_\infty^{\,2}}=1-4\sin^2\theta \tag{9.340}$$

This distribution is shown in Figure 9.35. The symmetry of the pressure distribution means that if we integrate the x-component of it over the entire surface of the cylinder to determine the x-component of the net force exerted on the cylinder by the flow, the result is zero. There is no net force; hence, there is no drag on the cylinder.

$$2\int_0^\pi \frac{P_\theta-P_\infty}{\frac{1}{2}\rho\vartheta_\infty^{\,2}}R\cos\theta d\theta=2\int_0^\pi\left(1-4\sin^2\theta\right)R\cos\theta d\theta=\left[2R\sin\theta\right]_0^\pi-8R\left[\frac{\sin^3\theta}{3}\right]_0^\pi=0 \tag{9.341}$$

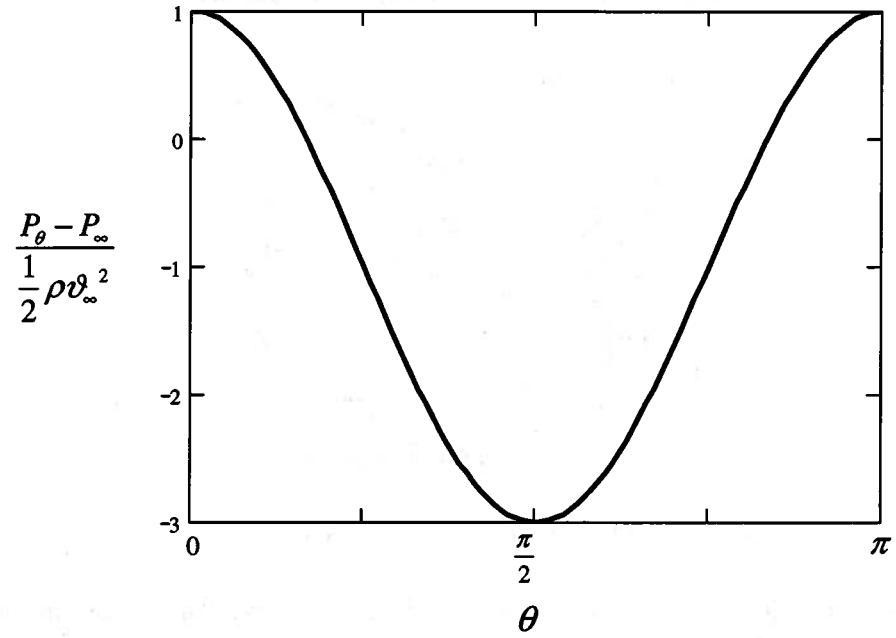

Figure 9.35 Pressure Distribution Over the Surface of a Cylinder Immersed in an Inviscid Flow

In the early days of the study of fluid mechanics, it was thought that this analysis would lead to the correct value of the drag force. When it did not, it was considered a paradox which eventually became known as *d'Alembert's paradox*. In light of our present knowledge of the behavior of fluids and the role that viscosity plays in the development of drag, the result hardly seems paradoxical. In fact, if the result *had* predicted a drag force for the flow of an *inviscid* fluid around a cylinder, that would have been a true paradox! In any case, the name is still used today for historical reasons. It should be noted that this result of zero drag for an inviscid flow applies only to the case of steady flow. If the flow is unsteady, a drag results even for the inviscid model.

9.11.2 The Influence of the Pressure Gradient: Separation of the Flow from the Surface

From our study of the flow of a viscous fluid over a flat plate, we know that in the case of a cylinder with a viscous flow normal to its axis, a boundary layer will develop on the surface of the cylinder beginning from the stagnation point and working its way over the forward facing portion, growing in thickness as the flow progresses toward the equator. As we have discussed before, the flow outside the boundary layer behaves as though it were inviscid and satisfies the Bernoulli equation. All of the influence of viscosity is confined to the boundary layer by definition. For the flat plate the fluid velocity at the outer edge of the boundary layer was the free stream velocity, but in the case of the cylinder, the situation is quite different.

On the cylinder, the boundary layer is quite thin, and the flow velocity at the outer edge of this thin layer is not the free stream velocity but is in fact the velocity that results from the inviscid behavior described above in Section 9.11.1; namely, acceleration of the flow over the forward facing portion and deceleration over the rearward facing portion of the cylinder. Most importantly, as predicted by the Bernoulli equation, the effect of this continual change in the local velocity causes the pressure on the curved surface of the cylinder (actually the pressure on the outer edge of the boundary layer on the curved surface of the cylinder) also to change in the

direction of flow. Since the pressure *across* the boundary layer is constant, this results in a pressure gradient in the boundary layer *in the direction of flow*. This pressure gradient can exert a profound influence on the behavior of the boundary layer and produce a notable difference in the growth of the boundary layer on the curved surface of a cylinder compared with the growth of the boundary layer on a flat plate for which the pressure did not change in the direction of the flow.

This behavior can be illustrated rather simply by writing the Bernoulli equation in differential form for the flow outside the boundary layer, viz.

$$\vartheta_x \frac{d\vartheta_x}{dx} = -\frac{1}{\rho}\frac{dP}{dx} \tag{9.342}$$

where ϑ_x is the local velocity just outside the boundary layer at its outermost edge which changes with x. From equation (9.342), it is apparent that as the flow accelerates in the x-direction, the pressure must decrease, and, conversely, as the flow decelerates, the pressure must increase. Inside the boundary layer, the boundary layer equations must be satisfied on the surface of the object immersed in the flow. At the surface, the boundary conditions of no slip and zero flow through the surface result in

$$\vartheta_x = 0 \quad \text{and} \quad \vartheta_y = 0 \quad \text{at} \quad y = 0 \tag{9.343}$$

Then *at the surface*, equation (9.167) becomes

$$\begin{gathered} \cancel{\vartheta_x}\frac{\partial \vartheta_x}{\partial x} + \cancel{\vartheta_y}\frac{\partial \vartheta_x}{\partial y} = -\frac{1}{\rho}\frac{dP}{dx} + \frac{\mu}{\rho}\frac{\partial^2 \vartheta_x}{\partial y^2} \\ \left(\frac{\partial^2 \vartheta_x}{\partial y^2}\right)_{y=0} = \frac{1}{\mu}\frac{dP}{dx} \end{gathered} \tag{9.344}$$

Thus the pressure gradient established by the flow outside the boundary layer determines the curvature of the velocity profile at the surface.

The situation is similar in many respects to the case of planar Couette flow with a pressure gradient as depicted in Figure 9.15. In the general case of an external flow of a viscous fluid over a surface, there are three cases of interest:

1. Zero pressure gradient: $\dfrac{dP}{dx} = 0$ and $\left(\dfrac{\partial^2 \vartheta_x}{\partial y^2}\right)_{y=0} = 0$

In this case, the forward drag of the fluid in the external flow at the outer edge of the boundary layer is sufficient to overcome the retarding drag (shear stress) exerted on the fluid by the surface, and the boundary layer grows as the flow progresses down stream. The flow over a flat plate is an example of this. For the flat plate, note from Figure 9.21 as well as equation (9.176) and the data of Table 9.4 that, indeed, the curvature of the velocity profile derived by Blasius is zero at the surface. This is shown schematically in Figure 9.36a.

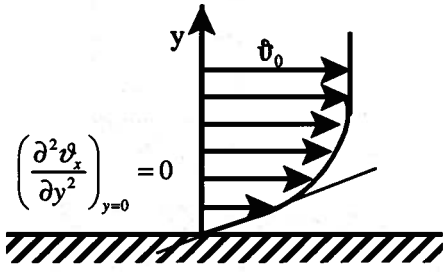

Figure 9.36a Schematic Representation of Velocity Profile with Zero Pressure Gradient

2. Favorable pressure gradient: $\frac{\partial P}{\partial x} < 0$ and $\left(\frac{\partial^2 v_x}{\partial y^2}\right)_{y=0} < 0$

In this case there are two factors that help to overcome the retarding drag of the surface on the fluid in the boundary layer: the forward drag exerted by the fluid in the external flow at the edge of the boundary layer and the favorable net forward "pressure forces" within the boundary layer. These boundary layers tend to be thinner than the boundary layers that develop without a pressure gradient. For this case, the velocity profile has negative curvature at the wall as shown in Figure 9.36b. Flow over the forward facing portion of a cylinder is an example of a boundary layer with a favorable pressure gradient.

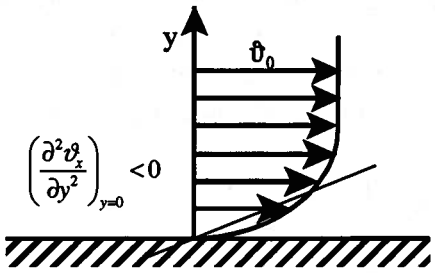

Figure 9.36b Schematic Representation of Velocity Profile with Favorable Pressure Gradient

3. Adverse pressure gradient: $\frac{\partial P}{\partial x} > 0$ and $\left(\frac{\partial^2 v_x}{\partial y^2}\right)_{y=0} > 0$

In this case there are two factors attempting to *retard* the flow in the boundary layer: the retarding drag of the surface and the adverse net "pressure forces" within the boundary layer which are acting against the direction of the flow. If the forward drag of the fluid in the external flow at the edge of the boundary layer is sufficiently large, it can overcome these retarding influences and the boundary layer will continue to grow in the direction of flow; however, if the drag of the external flow is not sufficiently large, the retarding influences dominate and the flow attempts to reverse direction in response to these retarding influences. It is this latter phenomenon that ultimately causes the boundary layer to separate from the surface. For this case, the velocity profile has negative curvature at the wall as shown in Figure 9.36c. A necessary, but not sufficient, condition for flow reversal is when the velocity gradient at the wall becomes negative. When flow reversal occurs, the velocity profile itself has negative slope at the wall. Flow over the rearward facing portion of a cylinder is an example of flow with an adverse pressure gradient.

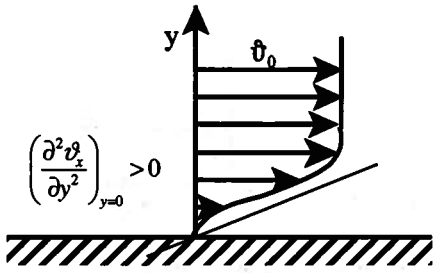

Figure 9.36c Schematic Representation of Velocity Profile with Adverse Pressure Gradient

The latter two conditions above are operative in the case of the cylinder in cross flow. As described in equation (9.340) and shown graphically in Figure 9.35, the flow accelerates over the forward facing portion of the cylinder and the pressure decreases in continuous fashion up to the equator according to the Bernoulli equation. This produces a negative (favorable) pressure gradient in the boundary layer on the forward facing portion. The pressure attains its minimum value at the equator and the pressure gradient reverses sign as the fluid decelerates down the backward facing portion. The question then becomes one of determining where the boundary layer separates from the surface of the cylinder.

Meksyn[7] developed a solution for the boundary layer equation for flow over a cylinder. He assumed that the pressure at the surface of the cylinder could be predicted from the results of the case of an inviscid fluid flowing under the same conditions as the viscous fluid. Following the example of Blasius and other early investigators, he defined a similarity parameter η and a stream function ψ such that

$$\eta = y\sqrt{\frac{2\vartheta_\infty}{\nu\gamma}}\sin(\pi-\theta) \tag{9.345}$$

where θ is defined in Figure 9.34 and

$$\gamma = 2R + \left(R + y + \frac{R^2}{R+y}\right)\cos(\pi-\theta) \tag{9.346}$$

where R is the radius of the surface of the cylinder and y is measured normal to it, and

$$\psi = \sqrt{2\nu\vartheta_\infty\gamma}\,\phi(\eta,\gamma) \tag{9.347}$$

Then the boundary layer equation, equation (9.167), becomes

$$\phi''' + \phi''\phi + \lambda(1-\phi) = 0 \tag{9.348}$$

where the primes denote derivatives with respect to η and

$$\lambda = -\frac{\cos(\pi-\theta)}{\sin^2\left[\dfrac{\pi-\theta}{2}\right]} \tag{9.349}$$

Then the velocity profile at any location defined by θ is

$$\frac{\vartheta_x}{\vartheta_\infty} = \phi'\left[2\sin(\pi-\theta)\right] \tag{9.350}$$

The analysis parallels that for the flat plate and equation (9.348) must be solved numerically in a fashion similar to equation (9.176). Comparison of the results of such a numerical solution with the experimental observations for the velocity profile reveal excellent agreement.

The local coefficient of friction f can be determined from the shear stress on the surface which, in turn, can be determined from the velocity gradient at the surface. Meksyn showed that the coefficient of friction is given by

$$f = 16\sqrt{\frac{\nu}{2R\vartheta_\infty}}\,\phi''(0)\sin^2\frac{\pi-\theta}{2}\cos\frac{\pi-\theta}{2} \tag{9.351}$$

which agrees well with the experimental data. Equation (9.351) is valid up to the point of separation which occurs when the velocity gradient and, hence, the value of f becomes zero. From equation (9.351), separation should occur approximately when $\theta = 95°$. Measured values of the location of the point of separation fall in the range of $85° < \theta < 105°$, depending upon the Reynolds number.

---

[7] Meksyn, D. "The laminar boundary layer equations: I Motion of an elliptic and circular cylinders [sic]," *Proc. Royal Society of London, Series A*, vol. 192, No. 1031,1948, pp. 545-567.

Figure 9.37 shows a circular cylinder in crossflow with a value of Reynolds number of $Re_D = 2000$. The flow visualization is revealed by the introduction of air bubbles in water. The separation of the boundary layer is clearly evident in the photograph as is the turbulent wake.

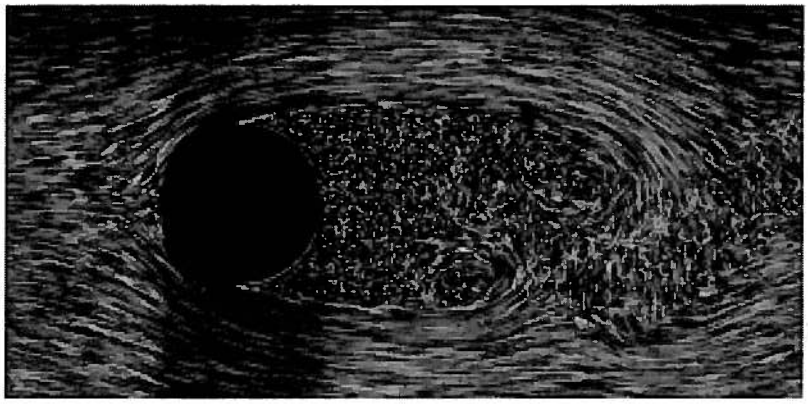

Figure 9.37 Laminar Flow Around Circular Cylinder, $Re_D = 2000$
(From Figure 47, p. 31 of *An Album of Fluid Motion* by M. Van Dyke, Parabolic Press, Stanford, CA, 1982.)

Measurements of the pressure in the wake of a cylinder with $Re_D = 2000$ show that the pressure is essentially uniform across the wake (cf. Figure 9.38 for data at higher values of the Reynolds number) with a pressure coefficient of approximately $C_P \approx -1$ where [cf. Equation (9.340)]

$$C_P = \frac{P_\theta - P_\infty}{\frac{1}{2}\rho \vartheta_\infty^{\,2}} \approx -1 \tag{9.352}$$

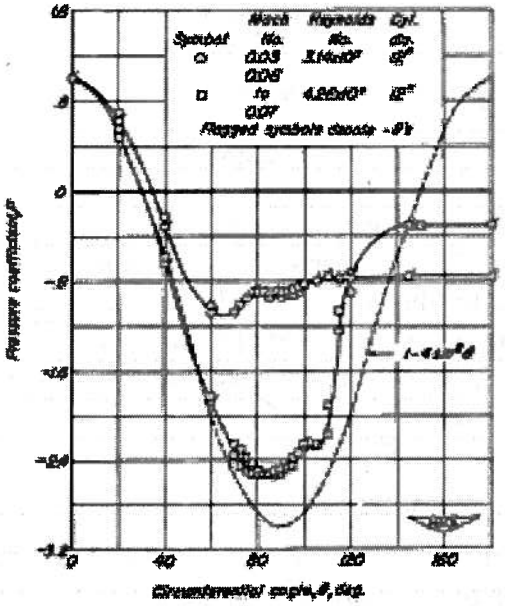

Figure 9.38 Pressure Coefficient for a Cylinder in Crossflow
(From NACA Tech. Note 2960, *Drag of Circular Cylinders for a Wide Range of Reynolds Numbers and Mach Numbers*, F. E. Gowen and E. W. Perkins, 1953, Figure 5.)

Since the pressure varies up to the point of separation according to equation (9.340), it follows that the integration of the pressure distribution over the entire surface of the cylinder yields a net force acting in the direction of flow. This force is a major portion of the drag force that acts on the cylinder. The other contribution to the drag force is, of course, the skin friction resulting from the shear stress at the surface of the cylinder which can be calculated from equation (9.351).

The boundary layer on the surface of the cylinder exhibits a behavior that might not be expected at first glance; namely, as the flow undergoes a transition from laminar to turbulent, the turbulent boundary layer proves to be more stable than the laminar boundary layer and the phenomenon of separation is delayed to a point further along the surface than occurs in laminar flow. Figure 9.39a shows a laminar flow over a convex surface with separation occurring near the apex of the curvature. Figure 9.39b shows a turbulent flow over the same convex surface as Figure 9.39a. In the turbulent case, the boundary layer is thicker than the laminar case, but the boundary layer remains attached far downstream of the point of separation observed in the laminar case.

Figure 9.39a Laminar Flow Past a Convex Surface

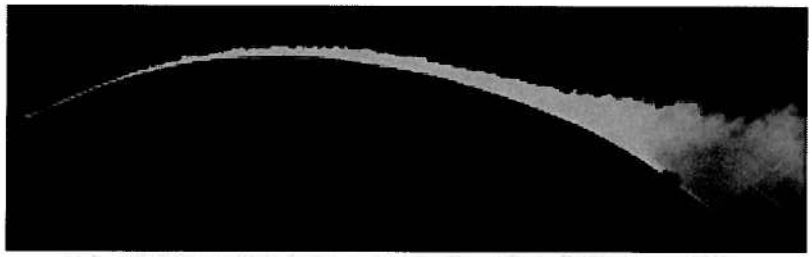

Figure 9.39b Turbulent Flow Past a Convex Surface
(From Figure 156, p. 91 of *An Album of Fluid Motion* by M. Van Dyke, Parabolic Press, Stanford, CA, 1982.)

In the case of flow about a circular cylinder, the observations of Figure 9.39 imply that the wake behind the cylinder will be smaller in turbulent flow than in laminar flow; consequently, wake drag is dramatically reduced in the turbulent case. This phenomenon is shown quite dramatically for the case of flow past a sphere in Figure 9.40. A trip wire has been used to trigger the laminar/turbulent transition in the boundary layer in Figure 9.40b. Note the substantial difference in the size of the wake for the turbulent flow case shown in Figure 9.40b compared with the laminar flow case of Figure9.40a. The small wake in the turbulent case leads to a significant reduction in the drag. We shall return to this point a bit later, but suffice it to say here that this reduction in drag under turbulent flow conditions has implications of considerable practical importance.

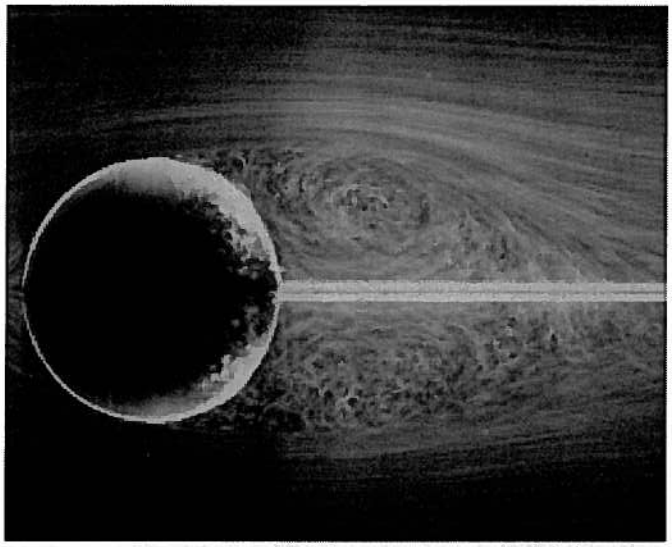

Figure 9.40a Mean Flow Past a Sphere, Re_D = 15,000
(From Figure 56, p. 34 of *An Album of Fluid Motion* by M. Van Dyke, Parabolic Press, Stanford, CA, 1982.)

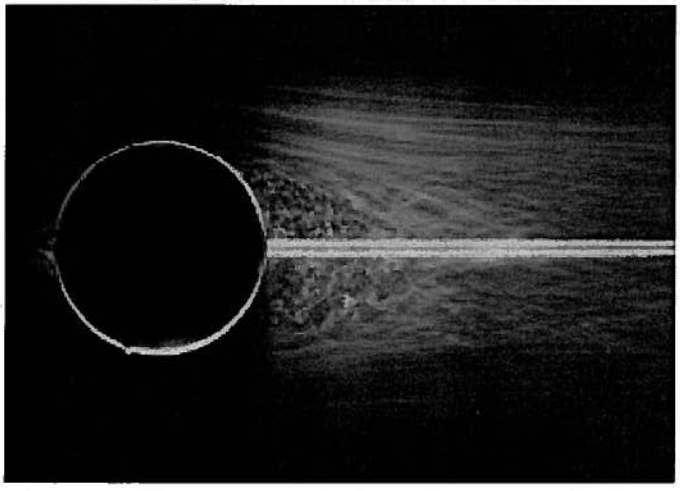

Figure 9.40b Mean Flow Past a Sphere, Re_D = 30,000,
with Boundary Layer Trip Wire Forward of Equator
(From Figure 58, p. 35 of *An Album of Fluid Motion* by M. Van Dyke, Parabolic Press, Stanford, CA, 1982.)

The behavior of the drag for a smooth cylinder of diameter D and length L in crossflow over a wide range of values of the Reynolds number is summarized in Figure 9.41 where the drag coefficient C_D is given by

$$C_D = \frac{F_D}{\frac{1}{2}\rho \vartheta_\infty^{\,2} DL} \tag{9.353}$$

Note the dramatic change in drag coefficient in the range $3.5 \times 10^5 < Re_D < 6 \times 10^5$.

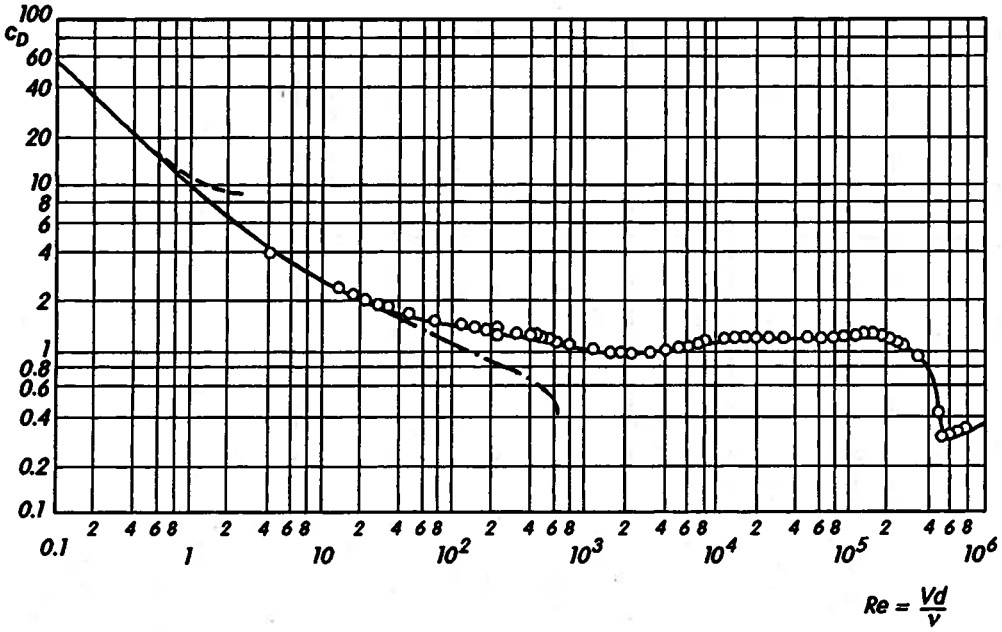

Figure 9.41 Drag Coefficient of a Smooth Cylinder in Crossflow
(From *Boundary Layer Theory*, H. Schlichting and K. Gertsen, Springer, 8th Ed., 2003, Figure 1.12, p. 19. Circles indicate experimental data.)

There are several different flow regimes that can be identified in Figure 9.40, each of which embodies a unique characteristic of the flow that arises not only in the case of flow around a cylinder, but in the flow around other blunt bodies as well. Following the example of Schlichting and Gertsen (H. Schlichting and K. Gertsen, *Boundary Layer Theory*, Springer, 8th Ed., 2003, p. 22; and R. D. Blevins, *Applied Fluid Dynamics Handbook*, Krieger Publishing Co., Malabar, FL, 1992, p. 340.), these are summarized in Table 9.10.

Table 9.10 Flow Regimes for a Circular Cylinder in Crossflow

Reynolds Number Regime	Flow Regime	Illustration	Flow Characteristic	Strouhal Number, Sr	Drag Coefficient, C_D
$0 < Re_D < 5$	creeping flow	Figure 9.42	steady with no wake	NA	$C_D = \frac{8\pi}{Re_D(2.002 - \ln Re_D)}$
$5 < Re_D < 40$	vortex pairs in wake	Figure 9.43	steady symmetric separation	NA	$12.8 > C_D > 1.59$
$40 < Re_D < 90$	onset of Karman vortex street		laminar but unstable wake	NA	$1.59 > C_D > 1.3$
$90 < Re_D < 400$	pure Karman vortex street	Figure 9.44	laminar Karman vortex street	$0.14 < Sr < 0.21$	$1.3 > C_D > 1.17$
$400 < Re_D < 1.3 \times 10^5$	subcritical regime	Figure 9.37	laminar boundary layer with fully turbulent vortex street	$Sr = 0.21$	$C_D \approx 1.17$
$1.3 \times 10^5 < Re_D < 3.5 \times 10^6$	critical regime		transition from laminar to turbulent boundary layer with narrow wake	no organized frequency	$1.17 > C_D > 0.3$
$3.5 \times 10^6 < Re_D$	supercritical regime		re-establishment of turbulent vortex street	$0.25 < Sr < 0.30$	$0.3 < C_D < 0.8$

The Strouhal number appearing in Table 9.10 is the dimensionless frequency of the vortices shed by the cylinder after the boundary layer separates in various flow regimes. In certain regimes, these vortices are stable and are commonly visible. For example, they show quite clearly in satellite views of flows in the atmosphere and in the oceans.
(For example, see http://daac.gsfc.nasa.gov/CAMPAIGN_DOCS/OCDST/vonKarman_vortices.html)
The Strouhal number for a cylinder of diameter D immersed in a flow of velocity ϑ is given by

$$Sr = \frac{fD}{\vartheta} \tag{9.354}$$

where f is now the frequency of oscillation of the vortices in units of Hertz.

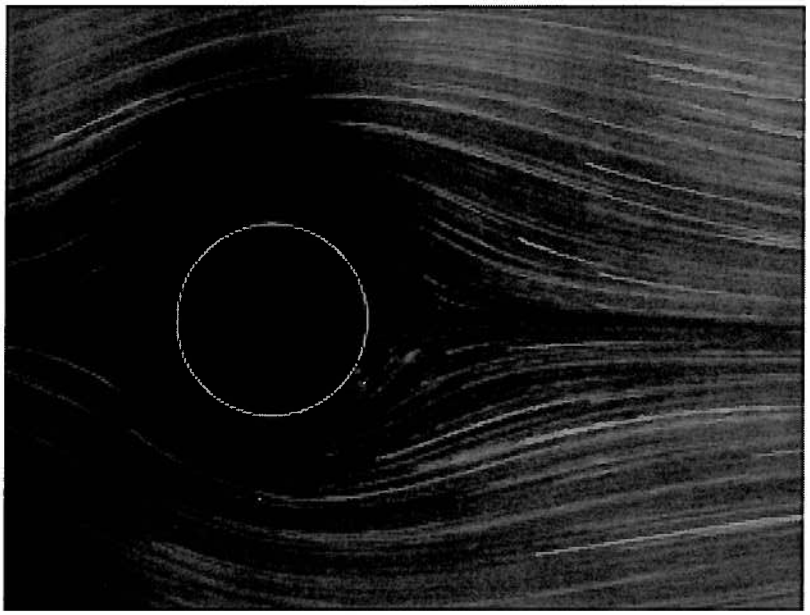

Figure 9.42 Creeping Flow Around a Circular Cylinder, $Re_D = 1.54$
(From Figure 24, p. 20 of *An Album of Fluid Motion* by M. Van Dyke, Parabolic Press, Stanford, CA, 1982.)

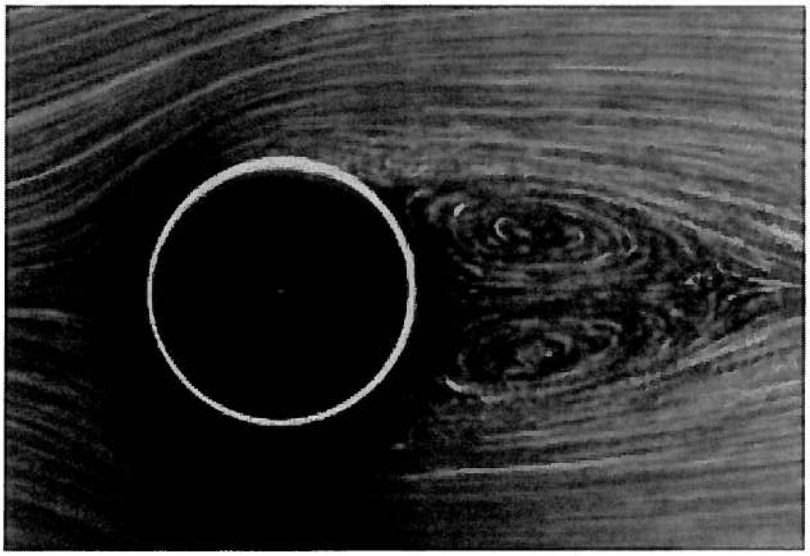

Figure 9.43 Flow Around a Circular Cylinder, $Re_D = 26$.
Note Twin Fixed Föppl Vortices in Wake.
Upper Vortex Rotates Clockwise; Lower Vortex Rotates Counterclockwise.
(From Figure 42, p. 28 of *An Album of Fluid Motion* by M. Van Dyke, Parabolic Press, Stanford, CA, 1982.)

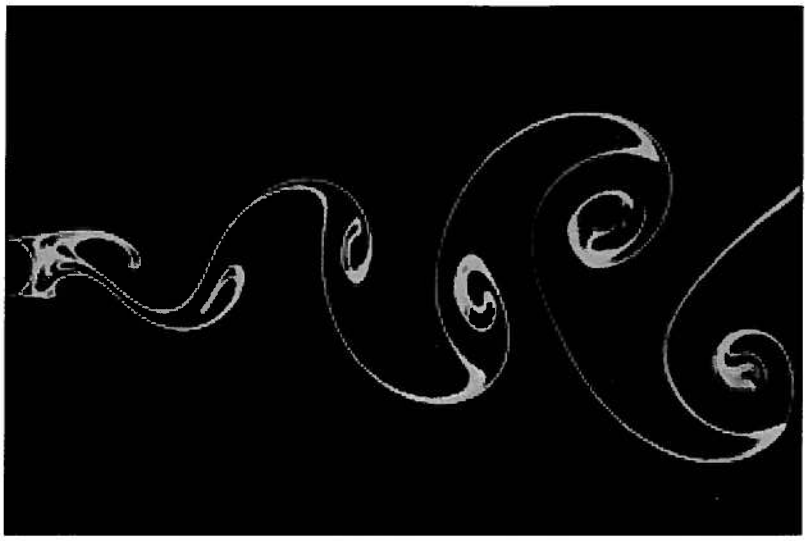

Figure 9.44 Flow Around a Circular Cylinder, $Re_D = 140$.
Note Well-developed Karman Vortex Street
(From Figure 94, p. 56 of *An Album of Fluid Motion* by M. Van Dyke, Parabolic Press, Stanford, CA, 1982.)

At this point in our discussion, it should be apparent that there are two contributions to the drag on a stationary object immersed in a flowing fluid (or conversely, an object moving through a stationary fluid): (1) skin friction drag due to the shear stress acting on the surface of the object as a consequence of the viscosity of the fluid, and (2) wake drag due to separation of the boundary layer as a consequence of the pressure gradient in the direction of flow imposed on the boundary layer by the "inviscid" flow external to the boundary layer. If we wish to reduce the drag on an object, there is little that we can do to reduce the skin friction component. Even the few changes that can be made may not be worth the effort since this component is the smaller of the two. However, there is a great deal that we can do to reduce wake drag. This is one of the principle objectives of the field of aerodynamics.

In their evolutionary process, fish long ago discovered that one of the principle changes that they could make to reduce the energy expended in swimming while increasing speed markedly, was to alter their body shapes so that the pressure gradient on the downstream portion of their bodies was much smaller in magnitude than the pressure gradient on the upstream portion of their bodies. The result is the characteristic shape of fish that we have all observed in nature. This aerodynamic shape is imitated in the cross-section of aircraft wings. There is one important difference between fish and airfoils. The purpose of the airfoil is to produce a lift force to keep the aircraft in the air while at the same time minimizing the drag force on the wing. This requires the airfoil cross-section to be a asymmetric rather than symmetric as most fish are.

Airfoil design is the result of a good deal of analysis and considerable wind tunnel testing using the principles of dimensional analysis set forth in Chapter 10. The National Advisory Committee for Aeronautics (NACA), the predecessor of the current National Aeronautics and Space Administration (NASA), pioneered the design of aircraft wing sections in the United States in the early part of the 20th century. Many of these early designs are in use to this day. Figure 9.45 shows the streamline flow around one such airfoil shape (NACA 64A015). No separation is evident in this photograph.

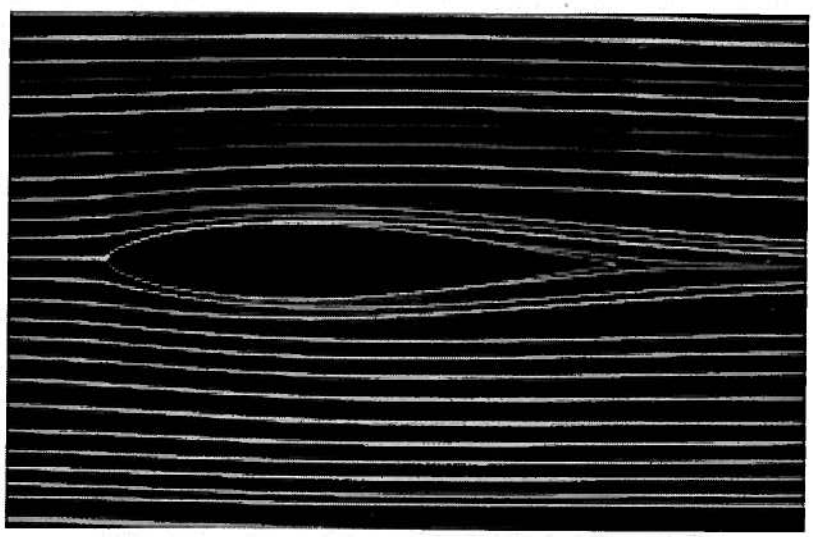

Figure 9.45 Symmetric Plane Flow About NACA Airfoil 64A015 ($Re_L = 7000$)
(From Figure 23, p. 19 of *An Album of Fluid Motion* by M. Van Dyke, Parabolic Press, Stanford, CA, 1982.)

As streamlined and aerodynamic as these airfoil designs may be, the flow about them can be made to separate as evidenced in Figure 9.46. This is usually done by changing the orientation of the airfoil to the principal direction of flow. This maneuver is known as changing the angle of attack. Note the separation of the flow on the upper surface near the trailing edge. The result of this separation is an increase in drag and a loss of lift. The wing on a typical aircraft contains control surfaces known as *flaps* located in the region where the flow is separating in Figure 9.46. The purpose of the flaps is to increase or decrease the drag and lift of the wing during take-off and landing.

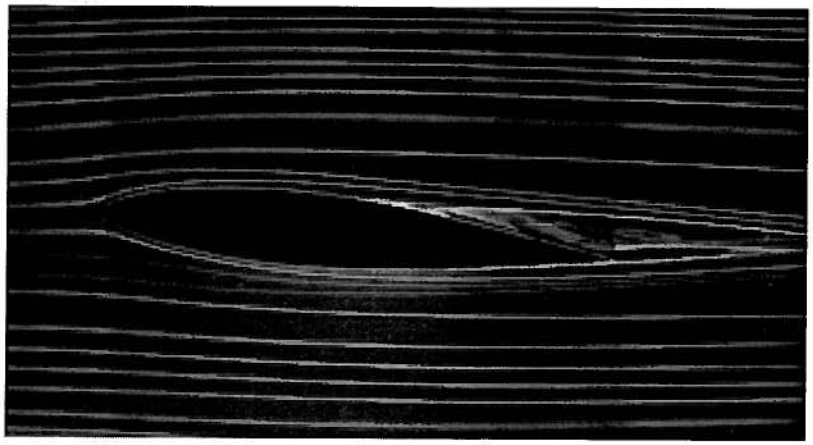

Figure 9.46 Flow About NACA Airfoil 64A015 at an Angle of Attack of 5° ($Re_L = 7000$)
(From Figure 34, p. 25 of *An Album of Fluid Motion* by M. Van Dyke, Parabolic Press, Stanford, CA, 1982.)

As the angle of attack is increased, the point of separation on the upper surface of the wing moves further and further forward until it finally reaches the nose of the wing. (See Figure 9.47.) At this angle of attack, the flow over the upper surface is comprised almost entirely of low-velocity eddy flow. The wing is then said to be "stalled," and the lift of the wing drops

precipitously even though the flow on the underside of the wing is relatively unchanged. In effect, at the stall angle, the wing is about as effective a lifting surface as a flat plate at the same angle of attack. Clearly, stall is an operating condition to be avoided except during landing when it can be used to advantage to return the aircraft to the ground.

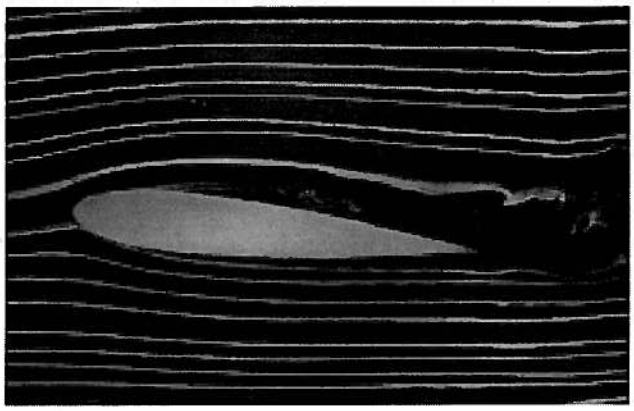

Figure 9.47 Flow About NACA 64A015 Airfoil at Angle of Attack Near Stall
(From Figure 72, p. 41 of *An Album of Fluid Motion* by M. Van Dyke, Parabolic Press, Stanford, CA, 1982.)

Aircraft are not the only vehicles employing aerodynamics to improve performance. Automobiles have shown a trend throughout their history of improving aerodynamics (reducing drag) to improve performance. (See Figure 9.48.) This trend has become more important in recent years as automotive manufacturers have begun employing wind tunnel testing to an ever greater degree in an attempt to improve fuel economy to the highest possible levels for a given body style. Drag coefficients have reached their lowest values ever ($C_D \approx 0.3$) as thermal-fluid engineers in the automotive industry strive for the greatest possible fuel economy. One manufacturer has even resorted to covering the under-carriage with a "belly pan" covered with turbulence promoters in an effort to minimize this contribution to vehicle drag. One danger in this process is that as drag is reduced, lift can improve to the point that it becomes difficult to prevent the vehicle from becoming an aircraft and becoming airborne. Thermal-fluid engineers then work to decrease drag while at the same time maintaining negative lift (down-force) to keep the vehicle on the road, particularly during cornering.

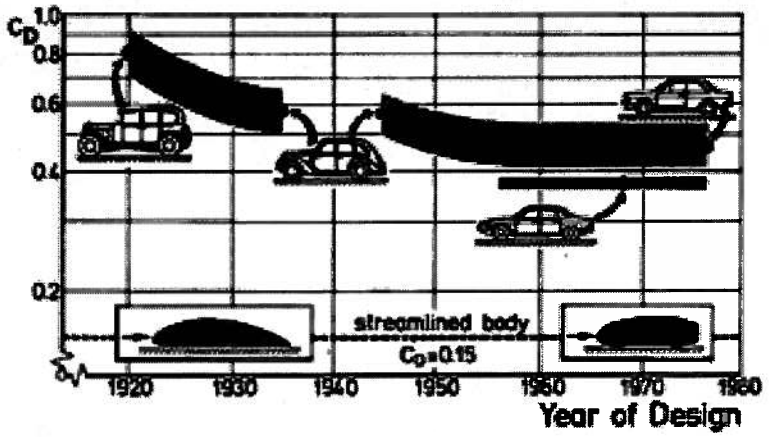

Figure 9.48 Historical Trend of Aerodynamic Drag of the Automobile
(From *Applied Fluid Dynamics Handbook*, R. D. Blevins, Krieger Publishing Co., Malabar, FL, 1992, Fig. 10-32, p. 348.)

PROBLEMS

9.1 The flow of an inviscid fluid around a circular cylinder of radius a centered on the origin is given by, in polar coordinates,

$$\vartheta_r = \vartheta_\infty\left(1-\frac{a^2}{r^2}\right)\cos\theta \quad \text{and} \quad \vartheta_\theta = -\vartheta_\infty\left(1+\frac{a^2}{r^2}\right)\sin\theta$$

where ϑ_∞ is the free stream velocity, a constant.

(a) Check that these forms satisfy the correct boundary condition on the surface of the cylinder and find the velocity at large distances from the cylinder.

(b) Express the pressure on the surface of the cylinder as a pressure coefficient, C_P and sketch the variation of C_P around the cylinder. Note that in this case

$$C_P = \frac{P-P_\infty}{\frac{1}{2}\rho\vartheta_\infty{}^2}$$

where P is the local pressure and P_∞ is the free stream pressure.

(c) Find the maximum speed of the flow over the surface of the cylinder.

9.2 Figure 9P.2 shows a cross-section through the gap between two solid surfaces (which is independent of the direction perpendicular to the page). The fluid flowing in the gap is inviscid and the effect of gravity is negligible.

(a) Sketch the pressure and velocity distribution along the centerline of the gap and along the upper and lower walls.

(b) A short pulse of dye is injected by a rake of probes so that it initially marks a line of fluid particles at AA. Sketch the change in shape of this line of particles as it convects downstream.

Figure 9P.2 Flow in a Gap Between Two Curved Surfaces

9.3 As shown in Figure 9P.3, a viscous, incompressible fluid is flowing in a laminar fashion between two infinite parallel plates.

(a) Starting with the Navier-stokes equation in Cartesian coordinates, show that steady, laminar, incompressible flow of a Newtonian fluid between two parallel plates satisfies the expression

$$\mu\frac{d^2u}{dy^2} = \frac{dP}{dx}$$

Deduce that, if the plates are separated by distance T, the volumetric flow rate per unit width is given by

$$\dot{V} = \frac{T^3}{12\mu}\left|\frac{dP}{dx}\right|$$

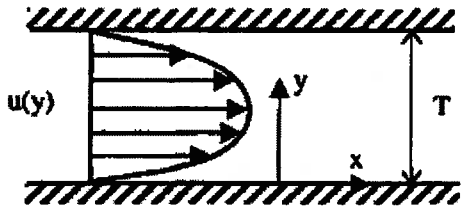

Figure 9P.3 Plane Poiseuille Flow

(b) A horizontal crack forms across a wall of thickness $L = 1$ m separating two tanks containing water at 20° C. The water surface on one side of the wall is 3m higher than that on the other. The crack is 0.01mm wide and is completely submerged. Find the leakage per unit width of the wall, assuming that the flow is laminar. ($\mu_{water} = 1\text{x}10^3$ kg/m sec)

9.4 As shown in Figure 9P.4 below, a Couette flow configuration consists of two infinite parallel plates separated by a gap of height $2h$. The gap is filled with two layers of fluid comprised of two immiscible, incompressible fluids A and B with densities ρ_A and ρ_B ($\rho_B = 0.8\ \rho_A$), respectively, and viscosities μ_A and μ_B ($\mu_B = 0.5\mu_A$), respectively. The two fluid layers are of equal thickness h. The flow of the fluids between the plates is induced by the motion of the bottom plate with constant velocity ϑ_0 relative to the top plate. The pressure gradient in the x-direction is zero.

(a) Derive an expression for the fully-developed velocity profile $\vartheta(y)$ in the gap. Use the coordinate scheme shown in Figure 9P.4. On a carefully proportioned sketch, show this profile. Pay particular attention to the magnitude of the fluid velocity at the midplane of the gap relative to the magnitude of the velocity ϑ_0 of the bottom plate.

For parts (b), (c), and (d), neglect any effects at the edges of the plates.

(b) Derive an expression for the total mass flow rate of fluid for a gap of width b measured normal to the plane of Figure 9P.4.

(c) If the width of the plates is b and the length is L, derive an expression for the power necessary to drive the bottom plate at the constant velocity ϑ_0 relative to the top plate.

(d) If the width of the plates is b and the length is L, derive an expression for the rate of entropy generation in the gap.

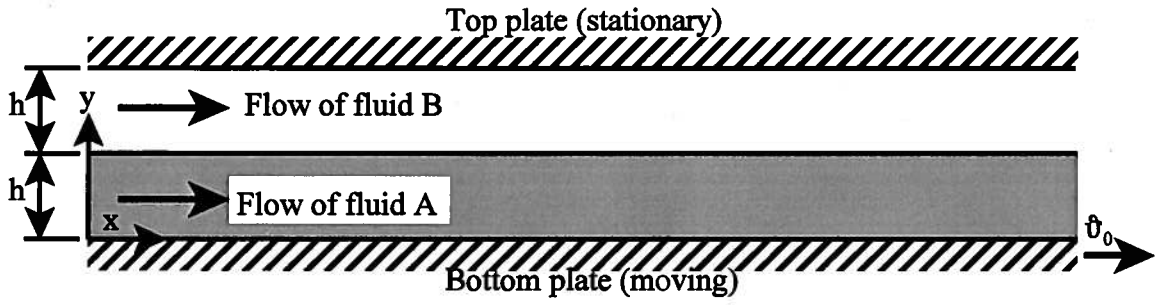

Figure 9P.4 Couette Flow of Two Immiscible, Incompressible Fluids

5. The analysis of Section 9.9.1.4 can be applied to the case of a 'stepped bearing" shown diagrammatically below. The pressures at the left and right hand ends on the bearings may be taken as atmospheric, P_a, (which can be taken as the pressure datum).

(a) Show that, for the flow rates to match in the two parts of the bearing, that the pressure at the step is given by P^* where

$$P^* = \frac{6\mu U(H-h)}{\frac{h^3}{L_1}+\frac{H^3}{L_2}}$$

(Hint: Use a frame of reference moving with the bearing.)

(b) Hence show that the bearing is capable of sustaining a load given by

$$F = \frac{P^*(L_1+L_2)}{2}$$

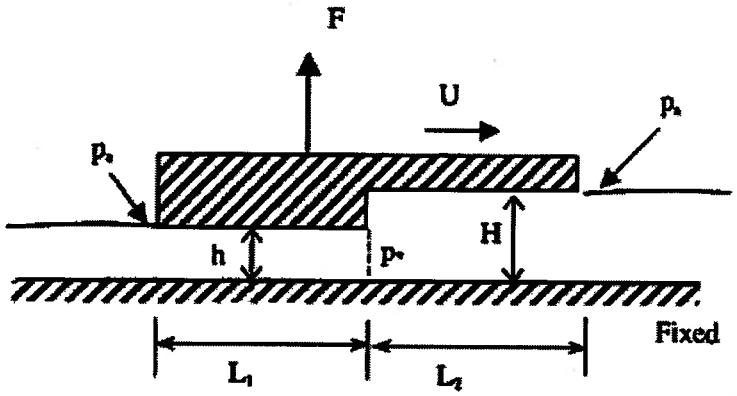

Figure 9P.5 Stepped Bearing

9.6 A viscous liquid flows between two concentric cylinders of radii R_1, R_2 where $R_1 < R_2$. The inner cylinder is at rest and the outer moves parallel to the common axis at speed U. Assuming that the pressure at inlet and outlet to the pipe is atmospheric, show that the velocity profile in the pipe is given by

$$\vartheta(r) = \frac{U}{\ln\left(\frac{R_2}{R_1}\right)}\ln\left(\frac{r}{R_1}\right)$$

9.7 The velocity in the laminar boundary layer on a flat plate in an unbounded stream is often modeled by the form

$$\vartheta = \frac{\vartheta_\infty}{2}\left[3\frac{y}{\delta}-\left(\frac{y}{\delta}\right)^3\right] \quad \text{for} \quad 0 \le y \le \delta \quad \text{and} \quad \vartheta = \vartheta_\infty \quad \text{for} \quad y \ge \delta$$

where ϑ_∞ is the free stream velocity and δ the height of the edge of the boundary layer above the plate. This form is assumed to be valid at each value of x along the length of the plate with δ varying with x.

(a) Explain why the static pressure is approximately uniform throughout the flow and sketch ϑ as a function of y.

(b) Using the result derived in Chapter 9 for mass flow in the boundary layer, find the vertical displacement of the streamline that passes the plate leading edge at a height h in terms of δ.

(c) Again using results from Chapter 9, calculate the total drag force per unit width on the upper side of the plate and the boundary layer thickness at the trailing edge for a plate of length L = 1 m in a stream with a uniform velocity ϑ_∞ of 5 m/sec.

The fluid properties are: $\nu = 1.0 \times 10^{-3}$ m^2/sec and $\rho = 10^3$ kg/m^3

9.8 Water flows through a sudden expansion in a pipe shown in Figure 9P.8. The flow separates from the sharp rim of the smaller pipe, enclosing an almost stagnant region, before mixing in a turbulent manner over a short distance to form a uniform stream at (3).

(a) Explain why the pressure in the stagnant regions marked (a) & (c) on the diagram should be approximately uniform at the same value as that in the region (b).

(b) By applying conservation of mass and conservation of momentum to the control volume shown (because of the short length of (2)-(3), the effect of shear stress on the walls of the larger pipe can be neglected), show that

$$P_{01} - P_{03} = \left(P_1 + \rho\frac{\vartheta_1^2}{2}\right) - \left(P_3 + \rho\frac{\vartheta_3^2}{2}\right) = K\frac{1}{2}\rho\vartheta_1^2$$

where P_{01} and P_{03} are by definition the stagnation pressures at locations (1) and (3), respectively, and $K = \left(1 - \frac{A_1}{A_3}\right)^2$ and where A_1 and A_3 are the cross-sectional areas of inlet and exit.

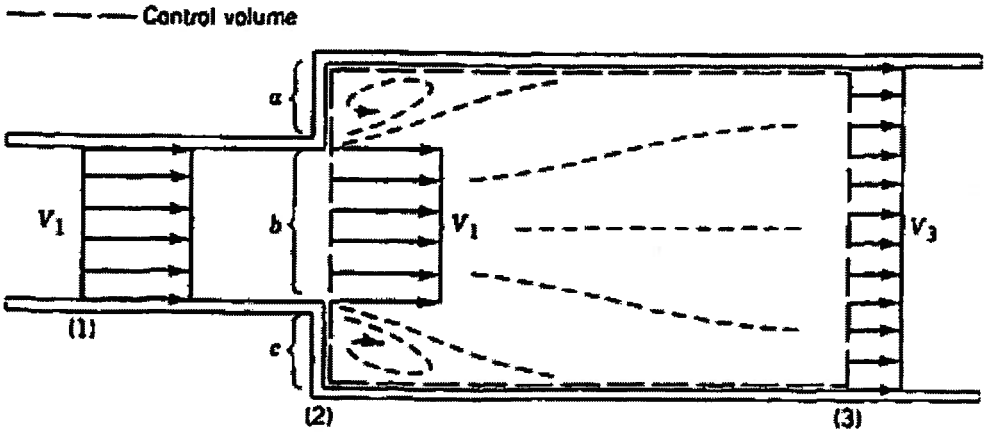

Figure 9P.8 Sudden Expansion

9.9 As shown in Figure 9P.9, two parallel streams of an incompressible fluid each having the same static pressure P_A and a velocity profile that is uniform come together at the location AA′. The two streams mix over a short distance due to the turbulence generated by the unstable shear layer between them.

(a) Assuming that viscous shear stress on the solid surfaces can be neglected, calculate the velocity and static pressure at location BB′, where the mixing is complete.

(b) What is the "loss" of mechanical energy due to the mixing? Where does this energy go?

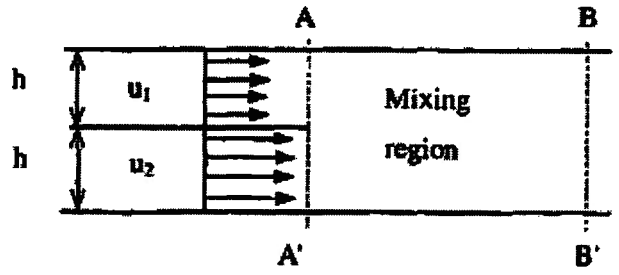

Figure 9P.9 Mixing Streams

9.10 A simple hydrostatic thrust bearing is shown in the Figure 9P.10. Unlike slider bearings, this type of bearing can support a load under static (no motion) conditions. The lubricant is supplied under pressure and fills the recessed region at essentially the supply pressure P_s. The lubricant then slowly flows out between the rotor and the stator as its pressure decreases to atmospheric pressure. Such bearings are useful for supporting very large thrust loads of rotating machinery even under low-speed conditions. The load is determined primarily by the supply pressure that can be maintained in the recess.

For a fixed flow rate of lubricant, the pressure P_s depends upon the film thickness h. Hence, if the lubricant pump flow rate is fixed, the film thickness will decrease as the load F is increased. On the other hand, if a given film thickness must be maintained as the load increases, the lubricant flow rate must then be increased.

In the present analysis, the lubricant is incompressible with density ρ and viscosity μ. The rotor rotates slowly enough that inertial effects can be neglected. Furthermore, we seek a solution for the steady-flow velocity field that is axially symmetric so that $\partial/\partial\theta = 0$ and for which $P = P(r)$. Also the forces due to shear in the radial direction are assumed negligible. That is, the only shear of consequence is due to relative motion of the rotor and stator, and the fluid is in solid body rotation about the z-axis.

(a) Starting with the Navier-Stokes equation and the continuity equation in cylindrical coordinates, show that the r-component equation reduces to

$$\mu\frac{\partial^2 v_r}{\partial z^2} = \frac{\partial P}{\partial r}$$

Similarly, show that the θ-component equation reduces to

$$\frac{\partial^2 v_\theta}{\partial z^2} = 0$$

Also show that the z-component equation vanishes.

(b) Show that

$$v_\theta = r\omega\frac{z}{h}$$

and show that for $b > r > a$,

$$v_r = \frac{1}{2\mu}\frac{dP}{dr}\left(z^2 - hz\right)$$

(c) Show that the volumetric flow rate in the radial direction is given by

$$\dot{V} = \frac{\pi r h^3}{6\mu}\frac{dP}{dr} = \frac{\pi h^3 (P_s - P_{atm})}{6\mu \ln\left(\frac{b}{a}\right)}$$

(d) From the expression for the volumetric flow rate, show that since the pressure is a function of r only, the pressure distribution is given by

$$\frac{P_s - P}{P_s - P_{atm}} = \frac{\ln\left(\frac{r}{a}\right)}{\ln\left(\frac{b}{a}\right)}$$

and sketch the pressure distribution in the oil film on the P-r plane.

(e) Show that the load carrying capability of the bearing is F where

$$F = \frac{\pi\left(b^2 - a^2\right)\left(P_s - P_{atm}\right)}{2\ln\left(\frac{b}{a}\right)}$$

(f) Develop an expression for the frictional torque in the bearing due to fluid friction.

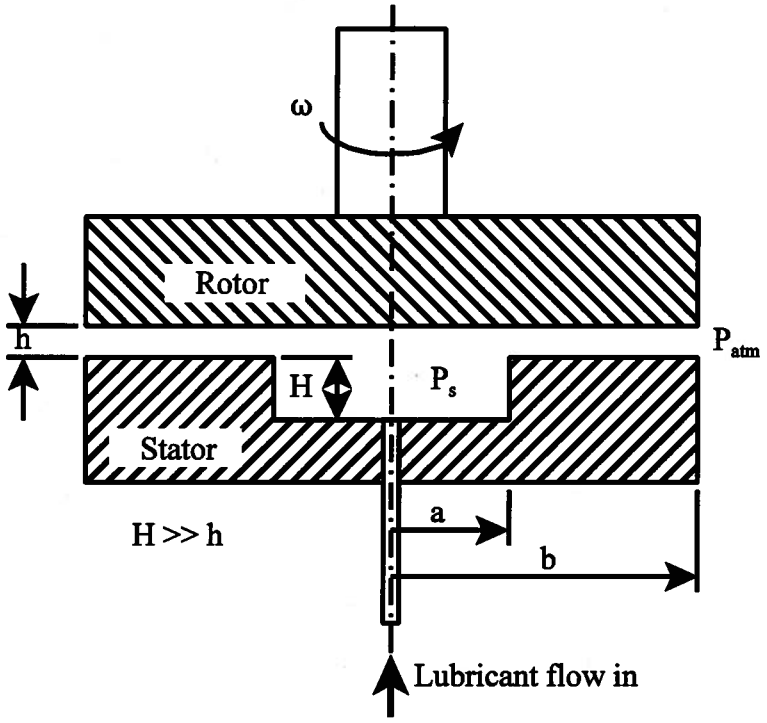

Figure 9P.10 Hydrostatic Thrust Bearing

9.11 A viscosity pump is a simple device for pumping viscous fluids such as lubricating oil. As shown in Figure 9P.11, a typical pump consists of a rotating element of radius R called the rotor mounted in a housing called the stator. These two elements are separated by a narrow gap of dimension h. In operation, oil flows into the gap through the inlet port and is swept around the housing to the outlet port by the viscous drag of the oil acting on the rotor. As a result, the pressure of the oil at the outlet port is higher than the pressure of the oil at the inlet port. In a typical design, $h << R$.

(a) Neglect any leakage due to flow directly from the outlet port to the inlet port and due to flow around the ends of the rotor and determine the following performance parameters as function of the volumetric flow rate through a pump of dimension b normal to the plane of the sketch:

(1) pressure rise in the pump, P_{out} -P_{in}
(2) torque on the rotor, T
(3) shaft power required to run the pump, $\hat{W}_{shaft}$
(4) efficiency of the pump, η

(b) For a pump of dimension $R = 2$ cm with an angular velocity of $\omega = 1000$ rpm and pressure rise $P_{out} - P_{in} = 4 \times 10^5$ N/m^2, determine the maximum value of the gap dimension h for which the flow in the gap between the rotor and stator can be modeled as Couette flow between two infinite flat plates with a maximum error of one percent. Determine the Reynolds number for this flow which will remain laminar if the Reynolds number in the gap is less than the critical value of $Re_{crit} = 1500$ where

$$Re = \frac{\hat{v}_{ave} h \rho}{\mu}$$

where the density of the oil is $\rho = 883$ kg/m^3 and its viscosity is $\mu = 5030 \times 10^{-4}$ kg/m sec.

(c) The oil for which the properties are given above enters the pump ($b = 3$ cm) at a temperature of $T_{in} = 300$ K. For the conditions determined in part (b) above, estimate the temperature at exit and calculate the rate of entropy generation in the oil if $c = 1900$ J/kg K for the oil.

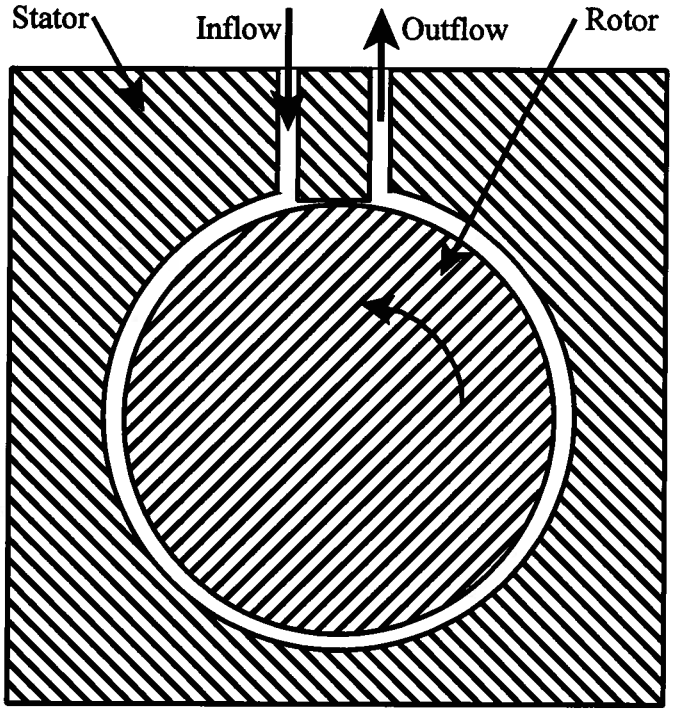

Figure 9P.11 Viscosity Pump

9.12 As shown in Figure 9P.12, a circular disk of radius R is immersed in a fluid of density ρ and viscosity μ. By means of applying a constant force F, the disk is forced down at velocity $\hat{v}_0(t)$ onto a flat parallel surface. At any instant of time, the separation of the surfaces is $h(t)$. The motion of the disk is sufficiently slow so that the acceleration and kinetic energy of the fluid can be neglected. The outward viscous flow of the fluid between the surfaces can then be assumed to have the same velocity distribution as a fully developed two-dimensional laminar flow.

(a) Formulate an expression for the pressure distribution in the fluid as a function of the radius r with the boundary condition $P(R) = 0$. Express the result in terms of r, μ, $\hat{v}_0$, and h.

(b) Calculate the force F in terms of the same variables.

(c) Find the time t required for the disk to move within a distance h of the lower surface. Assume that for the purposes of this calculation, $h(0) = \infty$.

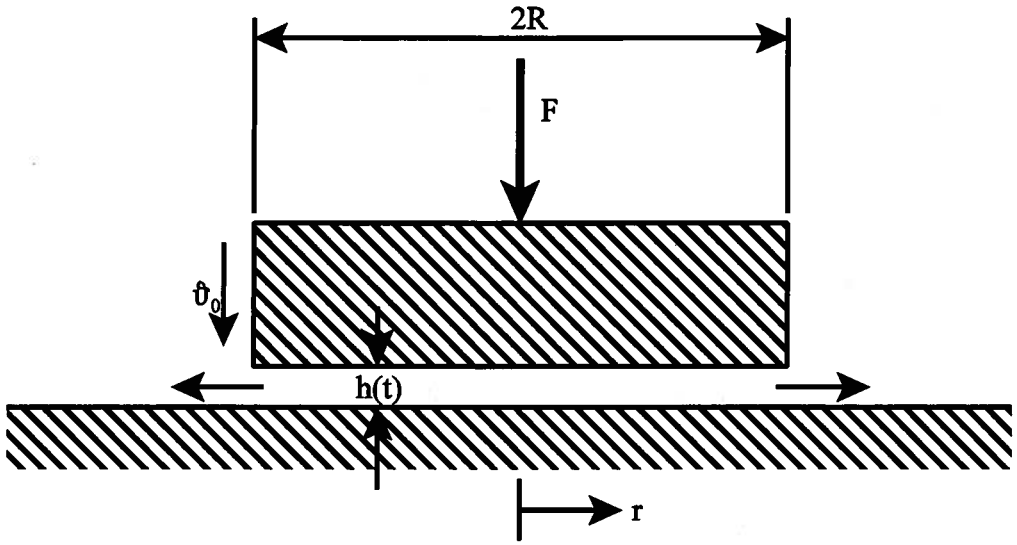

9.13 Figure 9P.13 shows a simple water distribution system. The system is fed by a reservoir connected to a plenum of negligible dimensions by a pipe of diameter $D_1 = 0.5$ m and length $L_1 = 150$ m. Branching out from the plenum is a horizontal pipe of diameter $D_2 = 0.10$ m and length $L_2 = 100$ m and another pipe of diameter $D_3 = 0.15$ m and length $L_3 = 150$ m inclined at an angle of 30° above the horizontal plane. The fourth pipe connected to the plenum is also horizontal and consists of two pipes connected in series. The pipe connected to the plenum is of diameter $D_4 = 0.20$ m and length $L_4 = 100$ m. At its outlet, it is joined to another pipe of diameter $D_5 = 0.10$ m and length $L_5 = 100$ m. The junction of pipes 4 and 5 is a sudden contraction with loss coefficient $K_c = 0.3$ based upon the kinetic energy of the smaller diameter, $(\hat{v}_{ave})_5^2/2$. Find the height of the free surface of the water in the supply reservoir so that the velocity of the water at the outlet of pipe 5 is $(\hat{v}_{ave})_5 = 20$ m/sec.

For water: density $\rho = 1000$ kg/m^3, viscosity $\mu = 10^{-3}$ kg/m sec.

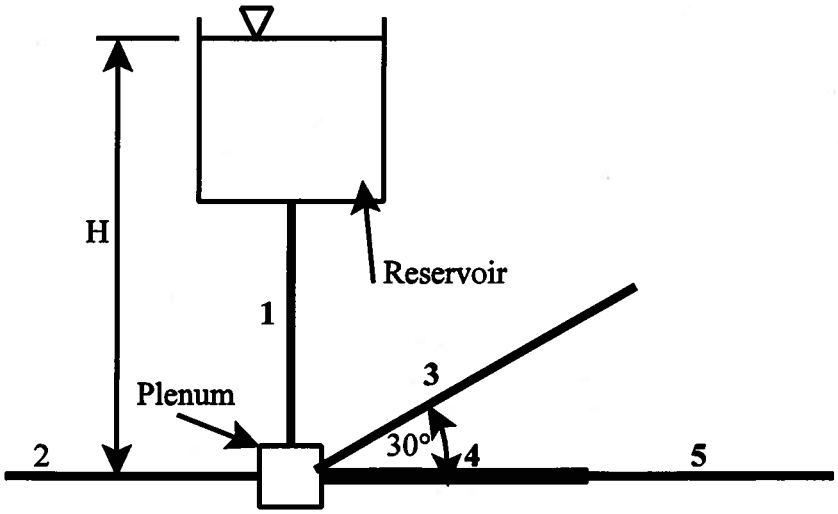

Figure 9P.14 Water Distribution System

9.14 In the cleanup of oil spills from oil tankers on large bodies of water, the oil floats on the surface of the water and is swept into a containment pond by large booms mounted on the bow of another ship. A moving vertical belt, much like that of a belt sander, is used to transport the oil from the water into barges in which it can be processed for safe disposal. In a particular application, it is observed that the belt picks up a layer of oil of thickness h. The belt moves upward with a velocity $\vec{v}$ and the oil has viscosity μ and density ρ.

(a) Estimate the net volume flow rate $\dot{V}$ of oil per unit of width of the belt.

(b) Determine the minimum belt velocity necessary to have a net flow of oil upward, and, hence, to keep the fluid on the belt.

(c) For a fixed belt velocity, what thickness h maximizes the volumetric flow rate?

9.15 As shown in Figure 9P.15, a solid cylinder of mass M, length L, and diameter D is falling in a fluid-filled cylinder of diameter $d = D + 2c$ and length ℓ. The fluid can be modeled as a Newtonian fluid with density ρ and viscosity μ. The solid cylinder is made of material with density ρ_s. The ratios c/D and L/ℓ are very small. The solid cylinder has reached terminal velocity $\vec{v}$ in its descent.

(a) Specify the conditions under which the flow of the fluid in the gap between the two cylinders can be modeled as flow between infinite parallel flat plates.

(b) Using the model of part (a) above, determine the terminal velocity in terms of the geometric parameters and the properties specified.

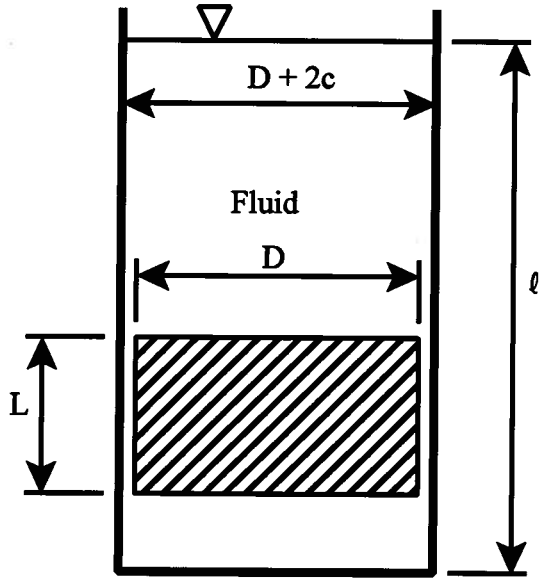

Figure 9P.15 Falling Cylinder

9.16 (a) Sketch the streamlines over the two (two-dimensional) bodies shown in Figure 9P.16 when they are inserted into a uniform ideal, *inviscid* flow from left to right. (The nose of the streamlined body is circular with the same radius as the cylinder). Mark on the sketch the regions of highest and lowest static pressure.

(b) By considering the likely size of any adverse pressure gradients in these ideal flows, explain why the drag on the streamlined body is much less than that on the cylinder for flow at high Reynolds number of a viscous fluid over them from left to right.

(c) Which body will have the least drag for low Reynolds Number flow (i.e. Re << 1)?

cylinder

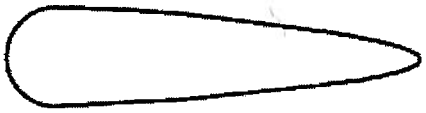

streamlined body

Figure 9P.16 Objects Immersed in a Flowing Fluid

9.17 The measured drag coefficient for a sphere as a function of Reynolds number is as shown in Figure 9P.17a.

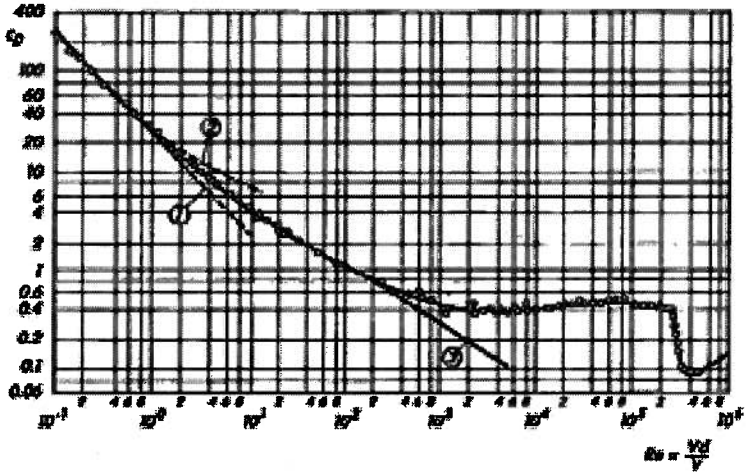

Figure 9P.17a Drag Coefficient for Spheres

(a) Explain why you would expect the drag coefficient to be proportional to Re^{-1} for low values of Re.

(b) Explain why there is a pronounced dip in the value of C_D at high values of Re.

(c) The following table gives typical speeds and sizes of balls used in various sports. Assuming that the kinematic viscosity $\nu = \mu/\rho$ of air is 1.5 x 10^5 m^2/sec, calculate typical Reynolds numbers for the various sports.

	Golf	Cricket	Soccer	Tennis	Baseball
U (m/sec)	70	40	16	50	45
D (m)	0.043	0.068	0.19	0.064	0.075

(d) The effect of surface roughness (defined as the ratio of roughness height to diameter) on C_D is shown in Figure 9P.17b for a particular Reynolds number range. Explain why roughness has this effect.

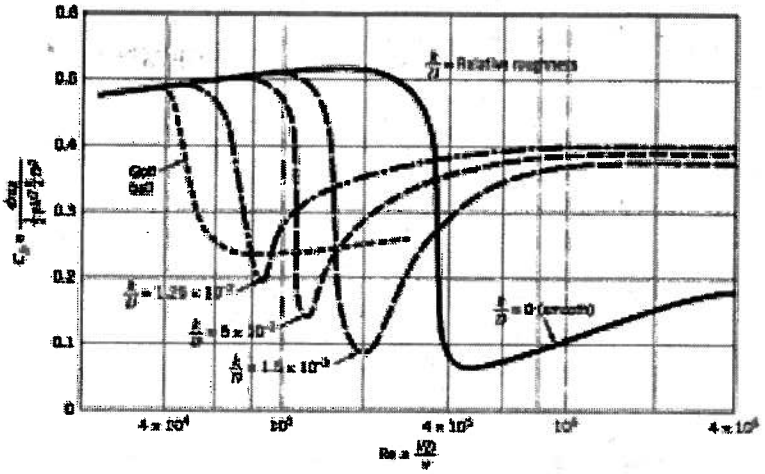

Figure 9P.17b Effect of Surface Roughness on Drag Coefficient for Spheres

9.18 The blood circulatory system in the human body consists of a large diameter vessel ($D = 25$ mm), the aorta, that carries the oxygenated blood away from the heart to the tissues of the body through a continually branching network of vessels that finally become the capillaries ($d = 8$ μm). In this particular problem we are concerned with the behavior of the first branch of the aorta under conditions of extreme cardiac output due to maximal exercise. As shown in plan view in Figure 9P.18, the circular, **smooth-walled** aorta branches into two identical circular, **smooth-walled** vessels of equal diameter with equal blood flow rates.

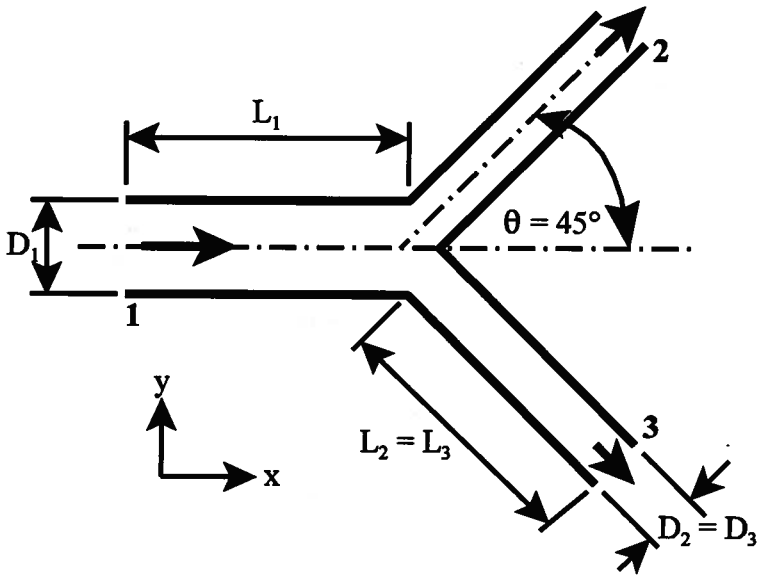

Figure 9P.18 Plan View of Branch in Human Aorta

For this geometry, the aorta and its branches can be modeled as rigid tubes with:

$$D_1 = 0.025 \text{ m}, \quad A_2 = A_3 = \frac{\sqrt{2}}{2} A_1, \quad L_1 = 5D_1, \quad L_2 = L_3 = 5D_2, \quad \dot{V}_1 = 4.167 \text{ x } 10^{-4} \text{ m}^3/\text{sec}$$

The minor head loss due to the branch is given by

$$h_m = \frac{1}{2} \rho v_1^2 K_{12} \quad \text{where} \quad K_{12} = 0.28$$

Although, in general, blood is a non-Newtonian fluid due to the presence of proteins and cellular materials suspended in it, for the purposes here, we can model the blood as a Newtonian fluid with the following properties:

$$\rho = 1050 \text{ kg/m}^3 \quad \text{and} \quad \mu = 3.5 \text{ x } 10^{-3} \text{ kg/m sec}$$

(a) Using the energy equation for fully-developed flow with the major and minor head loss terms included, calculate the pressure drop ΔP between locations 1 and 2 and between locations 1 and 3 for the case in which $P_1 = 1.13 \text{ x } 10^5 \text{ N/m}^2$.

(b) The tissues surrounding this branch must exert a force on the branch itself to keep it from moving within the body. What is the x-component of this force, F_x? Note the sign convention in the sketch above.

(c) What is the y-component of the restraining force, F_y?

9.19 (a) Figure 9P.19 shows a water distribution system from a lower reservoir to two reservoirs at higher level. If the stagnation pressures delivered by the pump to pipes 2 and 3 are equal, show that

$$v_2^2 = \frac{f_3\left(\frac{L_3}{d_3}\right)v_3^2 + 2g(y_3 - y_2)}{f_2\left(\frac{L_2}{d_2}\right)}$$

where v_2 and v_3 are the velocities of the flow in pipes 2 and 3.

(b) Find the total flow rate through the pump, V_{pump}, when that through the pipe 3 is $V_3 = 0.115 \text{ m}^3/\text{sec}$.

(c) Find the rise in stagnation pressure across the pump and the power required, assuming that the pump is adiabatic and reversible. (Ignore all losses except those caused by pipe friction.) The density of water is $\rho = 995 \text{ kg/m}^3$.

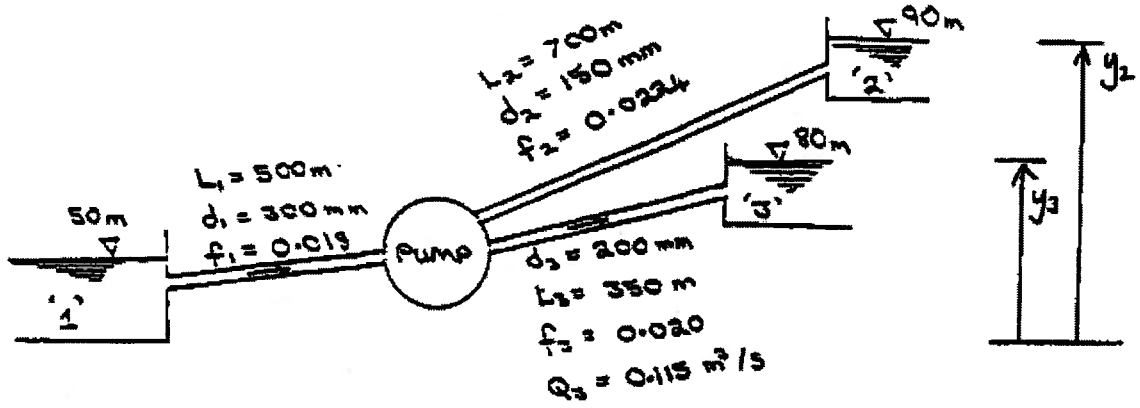

Figure 9.20 Water Distribution Network

9.20 Consider the case of air flowing at a steady rate through a horizontal pipe of constant cross-sectional area. The fully-developed flow configuration is such that the bulk mean temperature of the air is constant at $T_{air} = 27$ C all along the flow direction. At point **A** the pressure is $P_A = 3$ bar and the bulk mean velocity is $v_A = 160$ m/sec. At point **B** the pressure is $P_B = 2$ bar. The temperature of the pipe wall is $T_{wall} = 43$ C. (1 bar = 10^5 N/m^2)

(a) Calculate the bulk mean velocity v_B at **B**.

(b) Calculate $\dot{Q}/\dot{m}$, the heat transfer rate per unit mass flow rate of air between points **A** and **B**.

(c) Assuming that the flow is from **A** to **B**, calculate the rate of entropy generation per unit mass flow rate. Suggest a physical cause for the irreversibility, and comment on the validity of the assumption that the flow is from **A** to **B**.

9.21 Air at a pressure of $P_{atm} = 10^5$ N/m^2 and a temperature of $T_{atm} = 20$ C flows along a flat plate whose dimensions are length L and width b. The undisturbed velocity of the air upstream of the leading edge of the plate is $\vartheta_0 = 10$ m/sec. As a result of the action of the viscosity of the air, the air in the neighborhood of the plate is slowed and a boundary layer develops and grows in thickness downstream of the leading edge. At $L = 145$ mm downstream from the leading edge of the plate the boundary layer thickness is $\delta = 2.3$ mm. The velocity profile in the boundary layer at this location is

$$\frac{\vartheta}{\vartheta_0} = \frac{3}{2}\frac{y}{\delta} - \frac{1}{2}\left(\frac{y}{\delta}\right)^2$$

where y is measured normal to the plate. Determine the x-component (horizontal) force per unit of width required to hold the plate stationary if the air can be modeled as incompressible. Note: Only the upper face of the flat plate is exposed to the air flow.

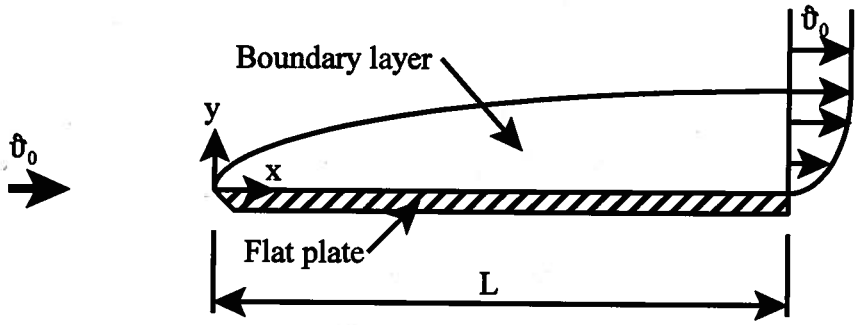

9.22 A "dead-weight" pressure gage tester is a device used to calibrate Bourdon-tube pressure gages. The device shown in Figure 9P.22 consists of a cylinder with a closely fitting piston. The volume between the piston face and the cylinder head is filled with hydraulic oil. Attached to the piston is a pan upon which various masses are placed. By adjusting the mass for a known piston diameter, any desired pressure may be obtained in the oil. In a typical design, the piston uses no piston rings in order to minimize solid friction that would lead to erroneous calibrations. As a consequence, there is some leakage of oil from the cylinder volume to the atmosphere past the piston which causes the piston to descend under the influence of gravity and the viscous drag of the oil in the gap.

In a particular design, the piston diameter is $D = 10$ mm and its length is $L = 70$ mm. The radial clearance is $h = 0.03$ mm, and the oil has a viscosity of $\mu_{oil} = 0.5$ kg/m sec. Atmospheric pressure is $P_{atm} = 10^5$ N/m^2 and $g = 9.81$ m/sec^2.

(a) Assuming no leakage of oil, determine the combined mass of the piston, weights, and pan necessary to produce a pressure of $P_{oil} = 1.5 \times 10^6$ N/m^2 in the oil.

(b) Since the gap thickness is much smaller than the radius of the piston, we can model the leakage of the oil in the gap as a one-dimensional flow as the piston moves. Starting with the Navier-Stokes equations for this one-dimensional flow, show that if we neglect the effect of

gravity in comparison with the viscous effects, the fully-developed laminar velocity profile in the gap is given by

$$v_x = \frac{v_0 y}{h} + \frac{1}{2\mu_{oil}}\left(\frac{dP}{dx}\right)\left(y^2 - yh\right)$$

where μ_{oil} is the viscosity of the oil, h is the gap thickness, v_0 is the velocity of the piston (Note that this value is negative.), and dP/dx is the pressure gradient in the flow.

(c) Show that as a result of the pressure gradient, the volumetric flow of oil past the piston per unit depth b measured normal to the plane of the figure (Note that $b = \pi D$.) is

$$\frac{\dot{V}}{b} = \frac{v_0 h}{2} - \frac{1}{12\mu_{oil}}\left(\frac{dP}{dx}\right)h^3$$

(d) For the mass determined in part (a) above, determine the rate of descent of the piston if drag due to the shear stress acting on the surface of the piston can be neglected.

(e) Calculate the drag force on the piston due to the shear stress acting on the surface of the piston as a result of viscous flow of oil in the gap. How does this compare with the normal force due to the pressure of the oil acting on the face of the piston?

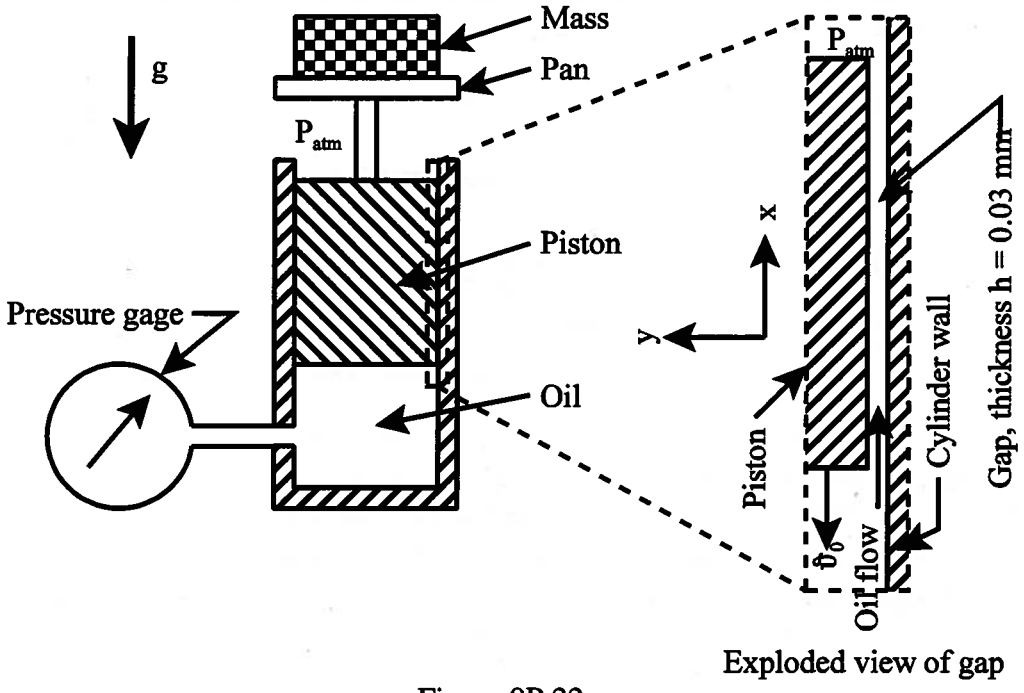

Figure 9P.22

9.23 As shown in Figure 9P.23, a method of coating photographic film with emulsion is to pass the film stock at constant velocity through a bath of liquid emulsion and withdraw the film in the vertical direction. As the film passes through the bath, one side of it becomes coated with liquid emulsion. (The other side is coated with a non-wetting agent that prevents the photographic emulsion from sticking to the film.) Gravity causes the liquid emulsion to drain down, but the continuous motion of the film keeps the liquid emulsion from running off completely. (**Note that the coordinate axes are not in their usual orientation.**)

The film velocity through the bath is v_0; the thickness of the liquid emulsion layer on the film is h; the density of the liquid emulsion is ρ; and the viscosity of the liquid emulsion is μ.

Model the liquid emulsion as a Newtonian fluid. Furthermore, model the flow of the emulsion as a fully developed laminar flow with zero pressure gradient in the x-direction. The viscosity of air is small relative to that of the liquid emulsion.

There are two ways of developing an analysis of this physical situation: one has the coordinate axes attached to the film; the other has the coordinate axes fixed in the room where the film is being coated. Both coordinate schemes are inertial coordinate systems, but they will give different answers for the velocity profile. State which coordinate scheme is to be used in your analysis.

(a) For your coordinate scheme, specify the appropriate boundary conditions at the film/liquid emulsion interface, $y = 0$, and at the liquid emulsion/air interface, $y = h$.

(b) Write the complete expression for the x-component of the Navier-Stokes equation and show that for this physical situation it simplifies to

$$0 = \rho g_x + \mu \frac{\partial^2 \vartheta_x}{\partial y^2}$$

where ϑ_x is the velocity component in the x-direction in your coordinate scheme. In the simplification process, give a reason for the elimination of each term that is dropped from the full form of the Navier-Stokes equation.

(c) Use the simplified Navier-Stokes equation to derive an expression for the velocity profile in the liquid emulsion layer, $\vartheta = \vartheta(x, y)$.

(d) Derive an expression for the shear stress exerted on the film by the liquid emulsion layer, and determine the drag per unit length on the film of width b due to the emulsion layer.

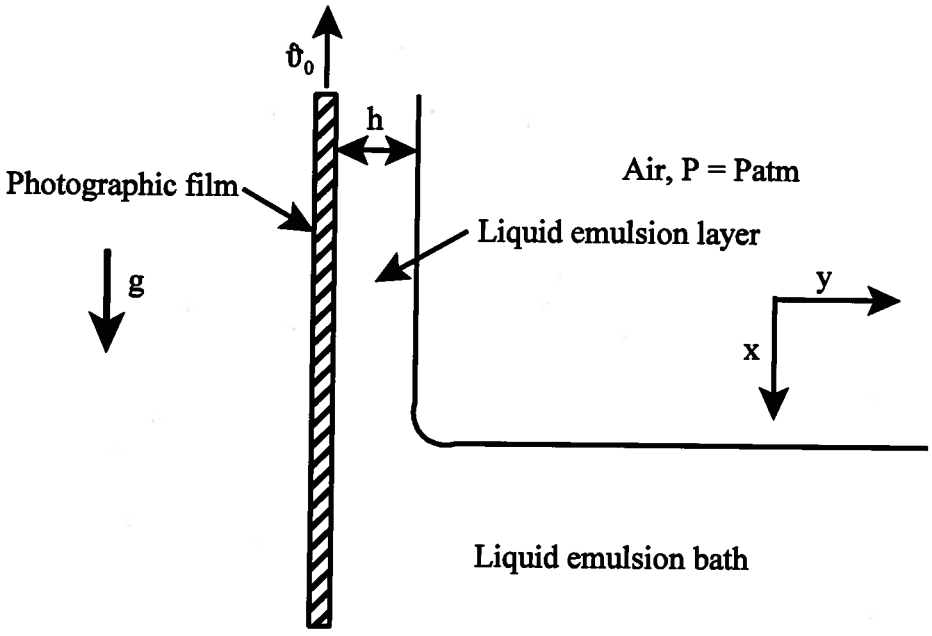

Figure 9P.23

9.24 As shown in Figure 9P.24, a crude oil reservoir in the Bluebell field of northern Utah is being tapped by drilling a well through the natural rock formation in which it is trapped. The reservoir is located 3,000 m below the surface. The pressure in the reservoir at the time the well is drilled is $P_0 = 13.5 \times 10^7$ N/m^2. The viscosity of this light crude oil is $\mu_{oil} = 4 \times 10^{-3}$ kg/m-sec

and its density is ρ_{oil} = 860 kg/m^3. The flow pipe inside the well casing has an inside diameter of 10 cm with a relative roughness of 1 x 10^{-3}.

(a) Estimate the initial volumetric flow rate of oil from this well using the reservoir pressure as the driving pressure to pump the oil to the surface where P_{atm} = 10^5 N/m^2.

(b) If the crude oil is allowed to discharge straight up into the atmosphere in the form of a jet (a "gusher") when it reaches the surface, what is the maximum possible height of the gusher?

(c) This method of using the natural pressure of the oil in the reservoir to pump the oil to the surface is called the "primary recovery". Of course, as the oil is drawn from the reservoir, the pressure in the reservoir will drop and the flow rate will decrease. At what value of the reservoir pressure will the flow rate at the surface decrease to zero?

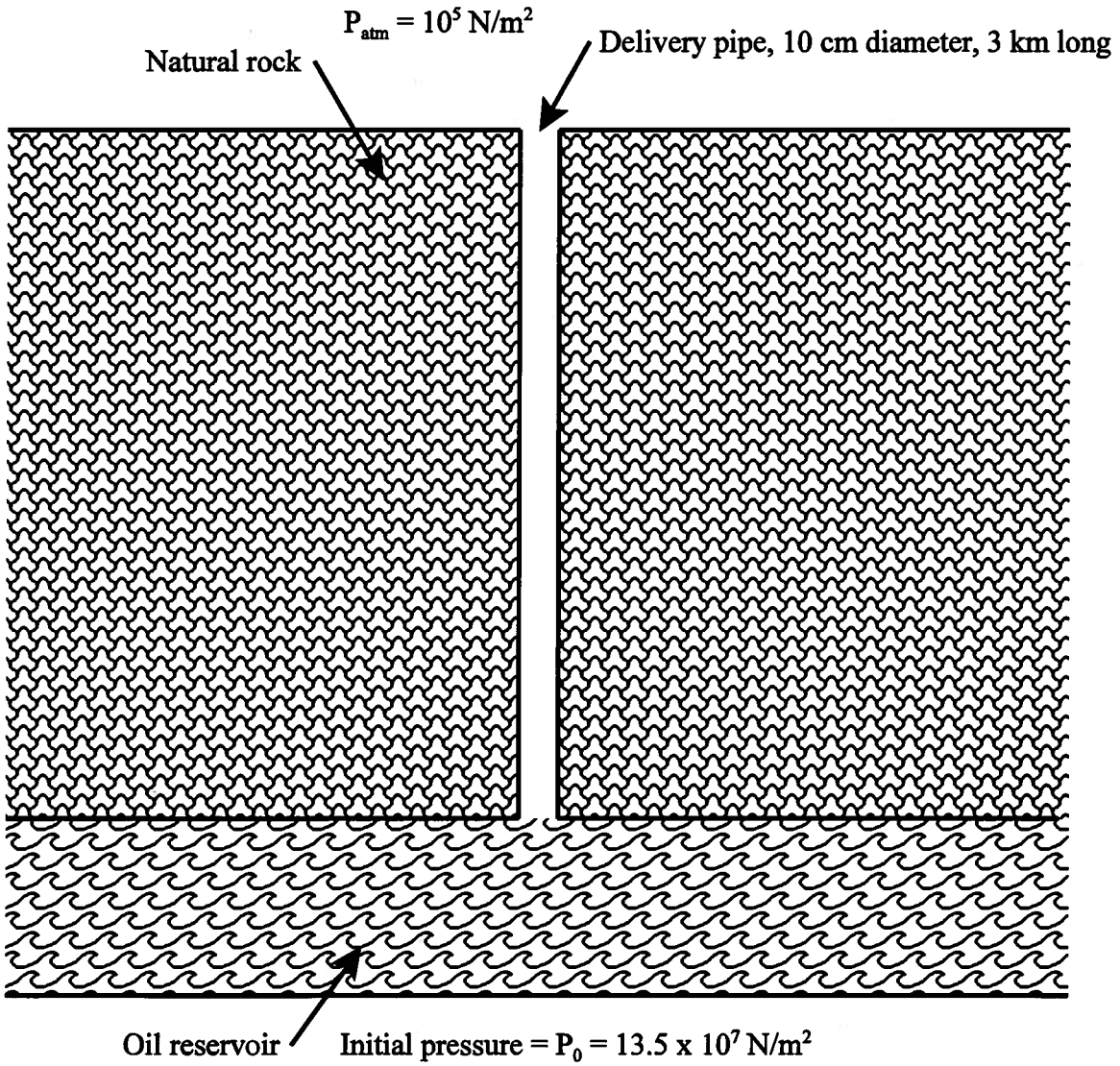

9.25 As shown in Figure 9P.25, a large cistern discharges through a smooth-walled circular pipe with a diameter of D = 10 cm and a length of L = 100 m. The pipe is fitted with a globe valve that is used to regulate the flow rate from the cistern. The water level in the cistern is maintained at a constant value of 30 m above the centerline of the attached pipe.

Determine the maximum volumetric flow rate from the discharge end of the pipe. Include the losses due to the square-edged entrance to the pipe, the globe valve, and the friction of the pipe wall in your analysis. The following data will be useful:

For a square-edged entrance:

$$(h_{lm})_{entrance} = K_1 \frac{\hat{v}_{ave}^{\,2}}{2}$$

where $K_1 = 0.5$ and $\hat{v}_{ave}$ is the average velocity of flow in the pipe.

For a globe valve in the fully-open position:

$$(h_{lm})_{\substack{globe \\ valve}} = K_2 \frac{\hat{v}_{ave}^{\,2}}{2}$$

where $K_2 = 4.1$ and $\hat{v}_{ave}$ is the average velocity of flow in the pipe to which the valve is attached.

For water: $\rho = 1000$ kg/m^3, $\mu = 1 \times 10^{-3}$ kg/m sec
For gravity: $g = 9.81$ m/sec^2

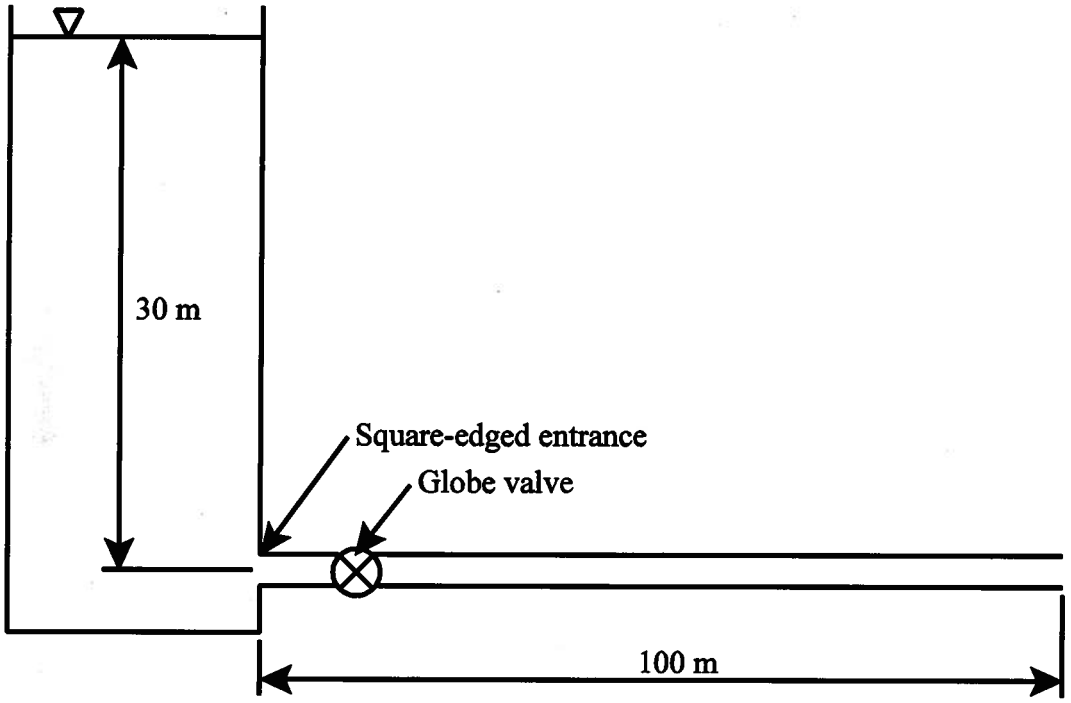

9.26 It has been proposed to construct an inclined tube viscometer as shown in Figure 9P.26. The inclined tube is connected to an infinite supply of the incompressible fluid of density ρ whose viscosity μ is to be measured. In operation, a beaker is to be placed at the discharge end of the tube and the time necessary to collect a fixed volume of the fluid is to be recorded. From these data, the viscosity can be determined.

(a) For the parameters shown in the sketch, show that for certain conditions (which you must specify), the continuity equation in cylindrical coordinates reduces to

$$\frac{1}{r}\frac{\partial}{\partial r}(r\hat{v}_r) = 0$$

and use this result to show that there is only one velocity component $\hat{v}_z = \hat{v}_z(r)$ of consequence.

(b) Using the arguments that you have put forth in part (a) above, show that the relevant form of the Navier-Stokes equation reduces to

$$\frac{1}{r}\frac{\partial}{\partial r}(r\tau)=\frac{d}{dz}(P-\rho gz\sin\theta)$$

where τ is the shear stress and

$$\tau=\mu\left(\frac{\partial \vartheta_z}{\partial r}\right)$$

(c) For the case in which the pressure is atmospheric at both ends of the tube, use the result of part (b) above to derive an expression for the time Δt required to collect a volume V_0 of fluid.

(d) This device cannot be used for just any fluid. What are the conditions that must be satisfied in order for this method to be valid? Express your result in numerical format.

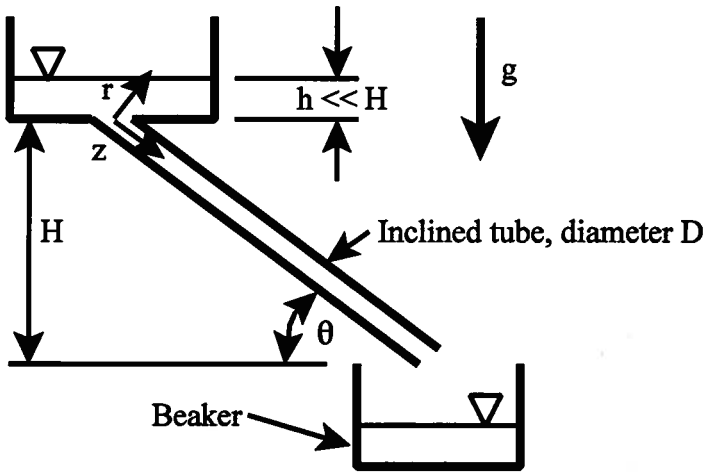

Figure 9P.26

9.27 Consider the case of two concentric tubes for which the radius of the inside wall of the outer tube is R and the radius of the outer wall of the inner tube is κR where $\kappa < 1$. A viscous fluid with viscosity μ flows in a laminar fashion in the annulus between the two tubes.

(a) Show that for fully developed flow in the annulus, the velocity profile is given by

$$\vartheta_z=\frac{(P_1-P_2)R^2}{4\mu L}\left[1-\left(\frac{r}{R}\right)^2-\frac{1-\kappa^2}{\ln\left(1/\kappa\right)}\ln\left(\frac{R}{r}\right)\right]$$

where P_1 is the pressure at some location and P_2 is the pressure at some location a distance L downstream.

(b) Show that the average velocity in the annulus is given by

$$\vartheta_{ave}=\frac{(P_1-P_2)R^2}{8\mu L}\left[\frac{1-\kappa^4}{1-\kappa^2}-\frac{1-\kappa^2}{\ln\left(1/\kappa\right)}\right]$$

(c) Show that the maximum velocity in the flow is given by

$$\vartheta_{max} = \frac{(P_1 - P_2)R^2}{4\mu L}\left[1 - \lambda^2\left(1 - \ln\lambda^2\right)\right]$$

where

$$\lambda^2 = \frac{1}{2}\frac{1-\kappa^2}{\ln\left(1/\kappa\right)}$$

(d) Sketch the velocity profile in the annulus and label ϑ_{ave} and ϑ_{max}.

(e) Show that the physical situation reduces to flow between parallel plates (plane Poiseuille flow) when

$$\frac{R - \kappa R}{R} \ll 1$$

What is the value of the above ratio for a one percent error associated with the plane Poiseuille flow approximation to the annulus configuration?

9.28 As shown in Figure 9P.28, a viscous fluid is trapped between two parallel infinite flat plates. The plates are separated by a uniform gap of h = 10 mm and are inclined at an angle of 45° to the horizontal. The upper plate moves at a constant velocity of ϑ_0 = 1.5 m/sec relative to the bottom plate, counter to the direction of the fluid flow. The gage pressures at points A and B are P_A = 250 x 10^3 N/m^2 and P_B = 80 x 10^3 N/m^2.

(a) Determine the velocity distribution $\vartheta_x(y)$ of the fluid in the gap.

(b) Determine the shear stress distribution $\tau_{yx}(y)$ in the gap.

(c) Determine the average fluid velocity ϑ_{ave} in the gap.

(d) Determine the maximum fluid velocity ϑ_{max} in the gap and its location.

(e) Determine the power per unit area $\wp$ that must be supplied to the upper plate in order to maintain its velocity constant.

For the fluid: ρ = 1260 kg/m^3 and μ = 0.9 kg/m sec

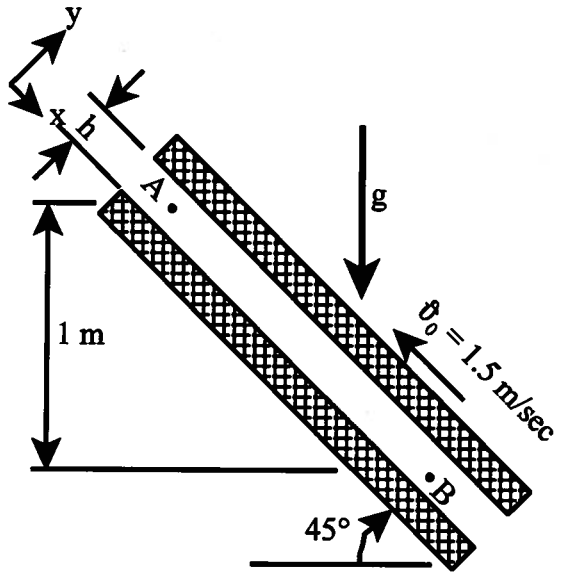

Figure 9P.28

9.29 Consider the boundary layer on a flat plate shown schematically in the sketch below.

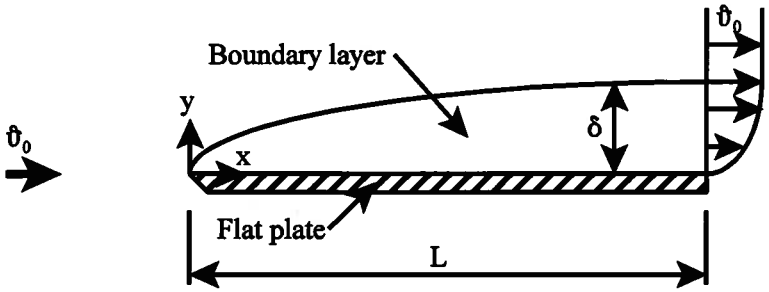

The analysis of this boundary layer can be analyzed in approximate fashion by postulating the form of the velocity distribution in the boundary layer and applying the momentum deficit concept of von Karman. One such velocity profile is given by

$$\vartheta_x = \vartheta_0 \sin\left(\frac{\pi}{2}\frac{y}{\delta}\right)$$

where ϑ_0 is the free stream velocity and $\delta = \delta(x)$ gives the thickness of the boundary layer at any location x measured from the leading edge.

(a) Show that this velocity profile satisfies the no-slip boundary condition at the surface of the plate as well as the requirement that the velocity at the outer edge of the boundary layer must be the free stream velocity, ϑ_0.

(b) Use the momentum integral relation, equation (9.202),

$$\tau_w = \rho \vartheta_0^2 \frac{d\theta}{dx}$$

where θ is the momentum thickness of equation (9.197), viz.

$$\theta = \int_0^\delta \frac{\vartheta_x}{\vartheta_0}\left(1 - \frac{\vartheta_x}{\vartheta_0}\right) dy$$

Together with the definition of the shear stress at the wall

$$\tau_w = \mu\left(\frac{d\vartheta_x}{dy}\right)_{y=0}$$

to show that the friction coefficient C_f for this velocity profile is given by

$$C_f \equiv \frac{\tau_w}{\frac{1}{2}\rho\vartheta_0^2} = \frac{0.655}{\sqrt{Re_x}}$$

(c) Calculate the total drag force for one side of a plate of length L and width b.

(d) Show that the thickness of the boundary layer at any location x for this assumed velocity profile is substantially larger than the corresponding boundary layer thickness for the Blasius profile. How can this be true and yet the difference between the friction coefficients for these two profiles be so small?

9.30 MEMS technology is used to fabricate a heat exchanger from silicon for a micro-turbine system. Air at a temperature of T_{air} = 600 C flows through the passages of the heat exchanger at velocities low enough to be modeled as an incompressible fluid. A design decision has set the

Reynolds number for the flow at $Re_{Dh} = 1000$. The flow channel dimensions are: $H = 2$ mm, $W = 1$ mm, and $L = 1$ m. The thermal-fluid characteristics of the air are:

$\rho_{air} = 0.3988$ kg/m^3 $\quad \mu_{air} = 3.9771 \times 10^{-5}$ kg/m sec $\quad c_p = 1003$ J/kg K $\quad c_v = 716$ J/kg K

(a) Calculate the velocity of the air and show that this velocity results in a Mach number that is less than $M = 0.3$ which is the requirement for the incompressible flow model.

(b) Calculate the pressure drop ΔP for this flow passage. Use the friction factor correlations for laminar flow in a non-circular conduit found in Table 9.3.

9.31 The aorta is the largest blood vessel in the human body with a diameter of $D = 25$ mm. For a person standing erect, the axis of the aorta is vertical, and depending upon the height of the individual, the length of the aorta is approximately $L = 0.5$ m. The volumetric flow rate through the aorta is $\dot{V} = 4.167 \times 10^{-4}$ m^3/sec. The thermal-fluid characteristics of the blood are:

$$\rho = 1050 \text{ kg/m}^3 \quad \text{and} \quad \mu = 3.5 \times 10^{-3} \text{ kg/m sec}$$

(a) Calculate the Reynolds number in the aorta. Is the flow laminar or turbulent?

(b) Blood proteins and fat globules (drink a milkshake or eat a Krispy Kreme) suspended in the blood may actually be able to damp out disturbances in the flow so that the flow is able to remain laminar at values of the Reynolds number in the transition region $2100 < Re_D < 10^4$. In fact, one can advance a teleological argument that the flow wants to remain laminar for two reasons: (1) to reduce the pressure drop in the flow and thereby impose a lower workload on the pump (heart); and (2) to minimize the mechanical damage that might occur to the fragile red cells and platelets as a result of the turbulence if it were allowed to form. Assuming that the flow is fully developed, calculate the pressure drop in the aorta for the two flow regimes. For the turbulent flow case, evaluate the friction factor from the Petukov correlation of equation (9.263), viz.

$$f = \left(0.7904 \ln Re_D - 1.64\right)^{-2}$$

How do the pressure drops compare? Does the first part of the teleological argument hold?

(c) If the flow is not fully developed, estimate the pressure drop for the two regimes.